Mathematical Problems in Engineering

Stochastic Process Theory and Its Applications

Lead Guest Editor: Wenguang Yu
Guest Editors: Shuanming Li, Ming Zhou, and Zhimin Zhang

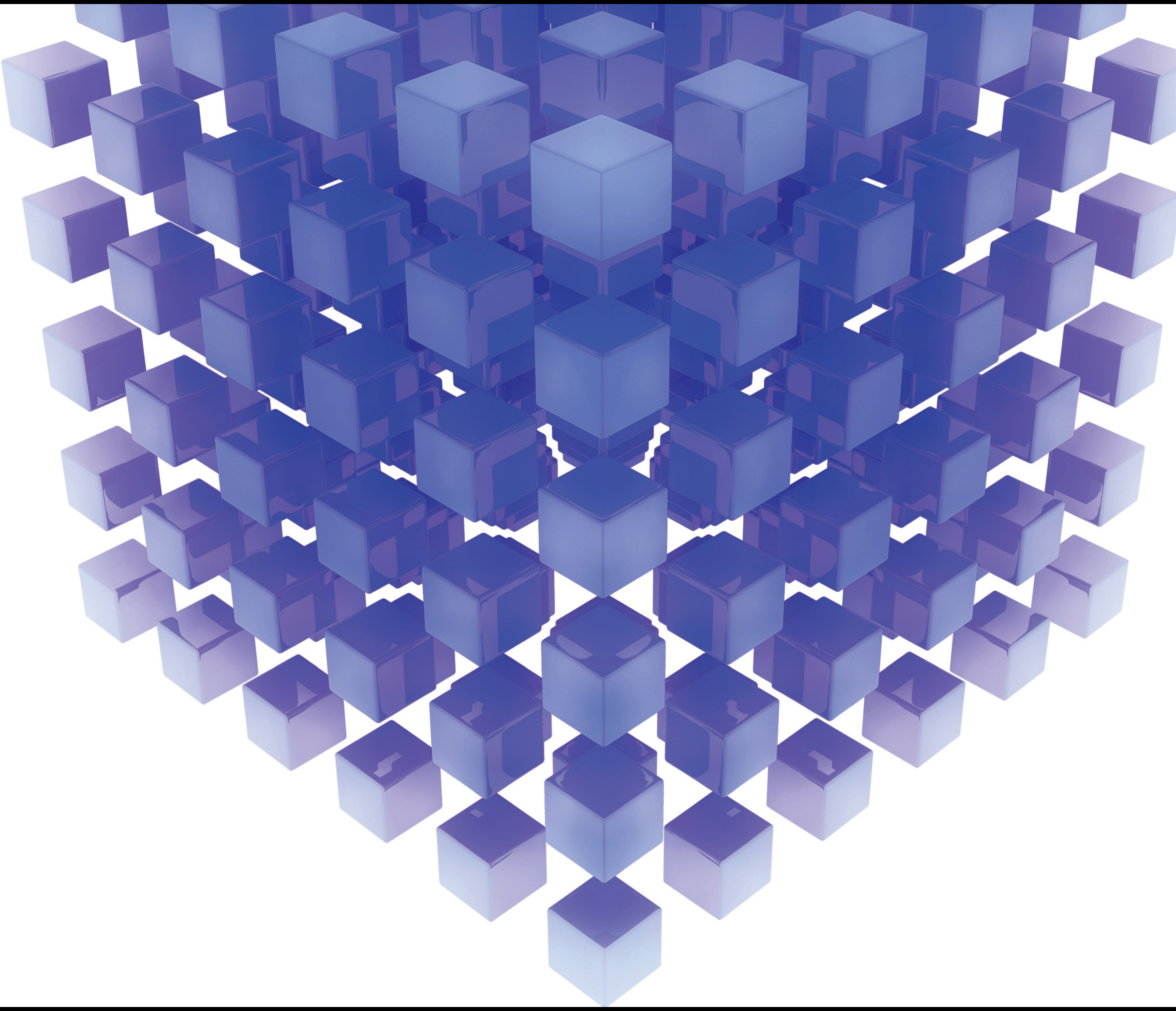

Stochastic Process Theory and Its Applications

Mathematical Problems in Engineering

Stochastic Process Theory and Its Applications

Lead Guest Editor: Wenguang Yu
Guest Editors: Shuanming Li, Ming Zhou, and Zhimin Zhang

Paolo Boscariol, Italy
Daniela Boso, Italy
Guillermo Botella-Juan, Spain
Abdesselem Boulkroune, Algeria
Boulaïd Boulkroune, Belgium
Fabio Bovenga, Italy
Francesco Braghin, Italy
Ricardo Branco, Portugal
Julien Bruchon, France
Matteo Bruggi, Italy
Michele Brun, Italy
Maria Elena Bruni, Italy
Maria Angela Butturi, Italy
Bartłomiej Błachowski, Poland
Dhanamjayulu C, India
Raquel Caballero-Águila, Spain
Filippo Cacace, Italy
Salvatore Caddemi, Italy
Zuowei Cai, China
Roberto Caldelli, Italy
Francesco Cannizzaro, Italy
Maosen Cao, China
Ana Carpio, Spain
Rodrigo Carvajal, Chile
Caterina Casavola, Italy
Sara Casciati, Italy
Federica Caselli, Italy
Carmen Castillo, Spain
Inmaculada T. Castro, Spain
Miguel Castro, Portugal
Giuseppe Catalanotti, United Kingdom
Alberto Cavallo, Italy
Gabriele Cazzulani, Italy
Fatih Vehbi Celebi, Turkey
Miguel Cerrolaza, Venezuela
Gregory Chagnon, France
Ching-Ter Chang, Taiwan
Kuei-Lun Chang, Taiwan
Qing Chang, USA
Xiaoheng Chang, China
Prasenjit Chatterjee, Lithuania
Kacem Chehdi, France
Peter N. Cheimets, USA
Chih-Chiang Chen, Taiwan
He Chen, China
Kebing Chen, China
Mengxin Chen, China
Shyi-Ming Chen, Taiwan
Xizhong Chen, Ireland
Xue-Bo Chen, China
Zhiwen Chen, China
Qiang Cheng, USA
Zeyang Cheng, China
Luca Chiapponi, Italy
Francisco Chicano, Spain
Tirivanhu Chinyoka, South Africa
Adrian Chmielewski, Poland
Seongim Choi, USA
Gautam Choubey, India
Hung-Yuan Chung, Taiwan
Yusheng Ci, China
Simone Cinquemani, Italy
Roberto G. Citarella, Italy
Joaquim Ciurana, Spain
John D. Clayton, USA
Piero Colajanni, Italy
Giuseppina Colicchio, Italy
Vassilios Constantoudis, Greece
Enrico Conte, Italy
Alessandro Contento, USA
Mario Cools, Belgium
Gino Cortellessa, Italy
Carlo Cosentino, Italy
Paolo Crippa, Italy
Erik Cuevas, Mexico
Guozeng Cui, China
Mehmet Cunkas, Turkey
Giuseppe D'Aniello, Italy
Peter Dabnichki, Australia
Weizhong Dai, USA
Zhifeng Dai, China
Purushothaman Damodaran, USA
Sergey Dashkovskiy, Germany
Adiel T. De Almeida-Filho, Brazil
Fabio De Angelis, Italy
Samuele De Bartolo, Italy
Stefano De Miranda, Italy
Filippo De Monte, Italy

Antoine Grall, France
George A. Gravvanis, Greece
Fabrizio Greco, Italy
David Greiner, Spain
Jason Gu, Canada
Federico Guarracino, Italy
Michele Guida, Italy
Muhammet Gul, Turkey
Dong-Sheng Guo, China
Hu Guo, China
Zhaoxia Guo, China
Yusuf Gurefe, Turkey
Salim HEDDAM, Algeria
ABID HUSSANAN, China
Quang Phuc Ha, Australia
Li Haitao, China
Petr Hájek, Czech Republic
Mohamed Hamdy, Egypt
Muhammad Hamid, United Kingdom
Renke Han, United Kingdom
Weimin Han, USA
Xingsi Han, China
Zhen-Lai Han, China
Thomas Hanne, Switzerland
Xinan Hao, China
Mohammad A. Hariri-Ardebili, USA
Khalid Hattaf, Morocco
Defeng He, China
Xiao-Qiao He, China
Yanchao He, China
Yu-Ling He, China
Ramdane Hedjar, Saudi Arabia
Jude Hemanth, India
Reza Hemmati, Iran
Nicolae Herisanu, Romania
Alfredo G. Hernández-Diaz, Spain
M.I. Herreros, Spain
Eckhard Hitzer, Japan
Paul Honeine, France
Jaromir Horacek, Czech Republic
Lei Hou, China
Yingkun Hou, China
Yu-Chen Hu, Taiwan
Yunfeng Hu, China
Can Huang, China
Gordon Huang, Canada
Linsheng Huo, China
Sajid Hussain, Canada
Asier Ibeas, Spain
Orest V. Iftime, The Netherlands
Przemyslaw Ignaciuk, Poland
Giacomo Innocenti, Italy
Emilio Insfran Pelozo, Spain
Azeem Irshad, Pakistan
Alessio Ishizaka, France
Benjamin Ivorra, Spain
Breno Jacob, Brazil
Reema Jain, India
Tushar Jain, India
Amin Jajarmi, Iran
Chiranjibe Jana, India
Łukasz Jankowski, Poland
Samuel N. Jator, USA
Juan Carlos Jáuregui-Correa, Mexico
Kandasamy Jayakrishna, India
Reza Jazar, Australia
Khalide Jbilou, France
Isabel S. Jesus, Portugal
Chao Ji, China
Qing-Chao Jiang, China
Peng-fei Jiao, China
Ricardo Fabricio Escobar Jiménez, Mexico
Emilio Jiménez Macías, Spain
Maolin Jin, Republic of Korea
Zhuo Jin, Australia
Ramash Kumar K, India
BHABEN KALITA, USA
MOHAMMAD REZA KHEDMATI, Iran
Viacheslav Kalashnikov, Mexico
Mathiyalagan Kalidass, India
Tamas Kalmar-Nagy, Hungary
Rajesh Kaluri, India
Jyotheeswara Reddy Kalvakurthi, India
Zhao Kang, China
Ramani Kannan, Malaysia
Tomasz Kapitaniak, Poland
Julius Kaplunov, United Kingdom
Konstantinos Karamanos, Belgium
Michal Kawulok, Poland

Francisco J. Martos, Spain
Elio Masciari, Italy
Paolo Massioni, France
Alessandro Mauro, Italy
Jonathan Mayo-Maldonado, Mexico
Pier Luigi Mazzeo, Italy
Laura Mazzola, Italy
Driss Mehdi, France
Zahid Mehmood, Pakistan
Roderick Melnik, Canada
Xiangyu Meng, USA
Jose Merodio, Spain
Alessio Merola, Italy
Mahmoud Mesbah, Iran
Luciano Mescia, Italy
Laurent Mevel, France
Constantine Michailides, Cyprus
Mariusz Michta, Poland
Prankul Middha, Norway
Aki Mikkola, Finland
Giovanni Minafò, Italy
Edmondo Minisci, United Kingdom
Hiroyuki Mino, Japan
Dimitrios Mitsotakis, New Zealand
Ardashir Mohammadzadeh, Iran
Francisco J. Montáns, Spain
Francesco Montefusco, Italy
Gisele Mophou, France
Rafael Morales, Spain
Marco Morandini, Italy
Javier Moreno-Valenzuela, Mexico
Simone Morganti, Italy
Caroline Mota, Brazil
Aziz Moukrim, France
Shen Mouquan, China
Dimitris Mourtzis, Greece
Emiliano Mucchi, Italy
Taseer Muhammad, Saudi Arabia
Ghulam Muhiuddin, Saudi Arabia
Amitava Mukherjee, India
Josefa Mula, Spain
Jose J. Muñoz, Spain
Giuseppe Muscolino, Italy
Marco Mussetta, Italy
Hariharan Muthusamy, India
Alessandro Naddeo, Italy
Raj Nandkeolyar, India
Keivan Navaie, United Kingdom
Soumya Nayak, India
Adrian Neagu, USA
Erivelton Geraldo Nepomuceno, Brazil
AMA Neves, Portugal
Ha Quang Thinh Ngo, Vietnam
Nhon Nguyen-Thanh, Singapore
Papakostas Nikolaos, Ireland
Jelena Nikolic, Serbia
Tatsushi Nishi, Japan
Shanzhou Niu, China
Ben T. Nohara, Japan
Mohammed Nouari, France
Mustapha Nourelfath, Canada
Kazem Nouri, Iran
Ciro Núñez-Gutiérrez, Mexico
Wlodzimierz Ogryczak, Poland
Roger Ohayon, France
Krzysztof Okarma, Poland
Mitsuhiro Okayasu, Japan
Murat Olgun, Turkey
Diego Oliva, Mexico
Alberto Olivares, Spain
Enrique Onieva, Spain
Calogero Orlando, Italy
Susana Ortega-Cisneros, Mexico
Sergio Ortobelli, Italy
Naohisa Otsuka, Japan
Sid Ahmed Ould Ahmed Mahmoud,
Saudi Arabia
Taoreed Owolabi, Nigeria
EUGENIA PETROPOULOU, Greece
Arturo Pagano, Italy
Madhumangal Pal, India
Pasquale Palumbo, Italy
Dragan Pamučar, Serbia
Weifeng Pan, China
Chandan Pandey, India
Rui Pang, United Kingdom
Jürgen Pannek, Germany
Elena Panteley, France
Achille Paolone, Italy

George A. Papakostas, Greece
Xosé M. Pardo, Spain
You-Jin Park, Taiwan
Manuel Pastor, Spain
Pubudu N. Pathirana, Australia
Surajit Kumar Paul, India
Luis Payá, Spain
Igor Pažanin, Croatia
Libor Pekař, Czech Republic
Francesco Pellicano, Italy
Marcello Pellicciari, Italy
Jian Peng, China
Mingshu Peng, China
Xiang Peng, China
Xindong Peng, China
Yuexing Peng, China
Marzio Pennisi, Italy
Maria Patrizia Pera, Italy
Matjaz Perc, Slovenia
A. M. Bastos Pereira, Portugal
Wesley Peres, Brazil
F. Javier Pérez-Pinal, Mexico
Michele Perrella, Italy
Francesco Pesavento, Italy
Francesco Petrini, Italy
Hoang Vu Phan, Republic of Korea
Lukasz Pieczonka, Poland
Dario Piga, Switzerland
Marco Pizzarelli, Italy
Javier Plaza, Spain
Goutam Pohit, India
Dragan Poljak, Croatia
Jorge Pomares, Spain
Hiram Ponce, Mexico
Sébastien Poncet, Canada
Volodymyr Ponomaryov, Mexico
Jean-Christophe Ponsart, France
Mauro Pontani, Italy
Sivakumar Poruran, India
Francesc Pozo, Spain
Aditya Rio Prabowo, Indonesia
Anchasa Pramuanjaroenkij, Thailand
Leonardo Primavera, Italy
B Rajanarayan Prusty, India
Krzysztof Puszynski, Poland
Chuan Qin, China
Dongdong Qin, China
Jianlong Qiu, China
Giuseppe Quaranta, Italy
DR. RITU RAJ, India
Vitomir Racic, Italy
Carlo Rainieri, Italy
Kumbakonam Ramamani Rajagopal, USA
Ali Ramazani, USA
Angel Manuel Ramos, Spain
Higinio Ramos, Spain
Muhammad Afzal Rana, Pakistan
Muhammad Rashid, Saudi Arabia
Manoj Rastogi, India
Alessandro Rasulo, Italy
S.S. Ravindran, USA
Abdolrahman Razani, Iran
Alessandro Reali, Italy
Jose A. Reinoso, Spain
Oscar Reinoso, Spain
Haijun Ren, China
Carlo Renno, Italy
Fabrizio Renno, Italy
Shahram Rezapour, Iran
Ricardo Riaza, Spain
Francesco Riganti-Fulginei, Italy
Gerasimos Rigatos, Greece
Francesco Ripamonti, Italy
Jorge Rivera, Mexico
Eugenio Roanes-Lozano, Spain
Ana Maria A. C. Rocha, Portugal
Luigi Rodino, Italy
Francisco Rodríguez, Spain
Rosana Rodríguez López, Spain
Francisco Rossomando, Argentina
Jose de Jesus Rubio, Mexico
Weiguo Rui, China
Rubén Ruiz, Spain
Ivan D. Rukhlenko, Australia
Dr. Eswaramoorthi S., India
Weichao SHI, United Kingdom
Chaman Lal Sabharwal, USA
Andrés Sáez, Spain

Yong (Aaron) Tan, United Kingdom
Marco Antonio Taneco-Hernández, Mexico
Lu Tang, China
Tianyou Tao, China
Hafez Tari, USA
Alessandro Tasora, Italy
Sergio Teggi, Italy
Adriana del Carmen Téllez-Anguiano, Mexico
Ana C. Teodoro, Portugal
Efstathios E. Theotokoglou, Greece
Jing-Feng Tian, China
Alexander Timokha, Norway
Stefania Tomasiello, Italy
Gisella Tomasini, Italy
Isabella Torcicollo, Italy
Francesco Tornabene, Italy
Mariano Torrisi, Italy
Thang nguyen Trung, Vietnam
George Tsiatas, Greece
Le Anh Tuan, Vietnam
Nerio Tullini, Italy
Emilio Turco, Italy
Ilhan Tuzcu, USA
Efstratios Tzirtzilakis, Greece
FRANCISCO UREÑA, Spain
Filippo Ubertini, Italy
Mohammad Uddin, Australia
Mohammad Safi Ullah, Bangladesh
Serdar Ulubeyli, Turkey
Mati Ur Rahman, Pakistan
Panayiotis Vafeas, Greece
Giuseppe Vairo, Italy
Jesus Valdez-Resendiz, Mexico
Eusebio Valero, Spain
Stefano Valvano, Italy
Carlos-Renato Vázquez, Mexico
Martin Velasco Villa, Mexico
Franck J. Vernerey, USA
Georgios Veronis, USA
Vincenzo Vespri, Italy
Renato Vidoni, Italy
Venkatesh Vijayaraghavan, Australia
Anna Vila, Spain
Francisco R. Villatoro, Spain
Francesca Vipiana, Italy
Stanislav Vítek, Czech Republic
Jan Vorel, Czech Republic
Michael Vynnycky, Sweden
Mohammad W. Alomari, Jordan
Roman Wan-Wendner, Austria
Bingchang Wang, China
C. H. Wang, Taiwan
Dagang Wang, China
Guoqiang Wang, China
Huaiyu Wang, China
Hui Wang, China
J.G. Wang, China
Ji Wang, China
Kang-Jia Wang, China
Lei Wang, China
Qiang Wang, China
Qingling Wang, China
Weiwei Wang, China
Xinyu Wang, China
Yong Wang, China
Yung-Chung Wang, Taiwan
Zhenbo Wang, USA
Zhibo Wang, China
Waldemar T. Wójcik, Poland
Chi Wu, Australia
Qiuhong Wu, China
Yuqiang Wu, China
Zhibin Wu, China
Zhizheng Wu, China
Michalis Xenos, Greece
Hao Xiao, China
Xiao Ping Xie, China
Qingzheng Xu, China
Binghan Xue, China
Yi Xue, China
Joseph J. Yame, France
Chuanliang Yan, China
Xinggang Yan, United Kingdom
Hongtai Yang, China
Jixiang Yang, China
Mijia Yang, USA
Ray-Yeng Yang, Taiwan

Contents

Contents

Contents

Hindawi
Mathematical Problems in Engineering
Volume 2021, Article ID 2839726, 6 pages
https://doi.org/10.1155/2021/2839726

Research Article

The Pareto-Optimal Stop-Loss Reinsurance

Haiyan You [1] and Xiaoqing Zhou [2]

[1]*School of Science, Shandong Jianzhu University, Jinan 250101, China*
[2]*School of Mathematical Sciences, Shandong Normal University, Jinan 250014, China*

Correspondence should be addressed to Haiyan You; yhy@sdjzu.edu.cn

Received 10 February 2020; Accepted 14 March 2020; Published 30 January 2021

Guest Editor: Wenguang Yu

Reinsurance plays a role of a stabilizer of the insurance industry and can be an effective tool to reduce the risk for the insurer. This paper aims to provide the optimal reinsurance design associated with the stop-loss reinsurance under the criterion of value-at-risk (VaR) risk measure. In this paper, the probability levels in the VaRs used by the both reinsurance parties are assumed to be different and the optimality results of reinsurance are derived by minimizing linear combination of the VaRs of the cedent and the reinsurer. The optimal parameter values of the stop-loss reinsurance policy are formally derived under the expectation premium principle.

1. Introduction

Reinsurance is an effective risk management tool that enables an insurer to reduce the underwriting risk. An insurer must conduct the classical trade off between the risk retained and the premium paid to the reinsurer. Generally speaking, the more risks you have to transfer, the more you will pay. In order to balance the relationship between the risk retained and the reinsurance premium, the academics started the research of the optimal reinsurance problem. Arrow [1] first studied the reinsurance problem and showed that the stop-loss reinsurance was optimal by using the criterion of maximizing the expected utility of the terminal wealth. Heerwaarden et al. and Gollier and Schlesinger [2, 3] give the same conclusion under the second degree stochastic dominance and showed that the stop-loss reinsurance was optimal. Young [4] generalized Arrow's result by considering Wang's premium principle. Recently, the optimal reinsurance problem has been revisited under different risk measures. Cai and Tan [5] derived explicitly the optimal retained level of a stop-loss reinsurance minimizing the value-at-risk (VaR) and conditional tail expectation (CTE) of the insurer's total loss under the expected premium principle. Cai et al. [6] derived the optimal ceded loss functions among the class of increasing convex loss functions. Tan et al. [7] give 17 kinds of reinsurance premium principles and studied the optimal quota-share reinsurance and the optimal stop-loss reinsurance under the criterions of VaR and CTE. Cheung [8] provided a geometric approach to re-examine the optimal reinsurance problems studied in [6] and generalized the results by studying the VaR minimization problem with Wang's premium principle. Chi and Tan [9] analyzed the VaR-based and conditional-value-at-risk (CVaR)-based optimal reinsurance models over different classes of ceded loss functions with increasing generality. Chi [10] showed that the layer reinsurance is always optimal under both the VaR and CVaR criteria when the reinsurance premium is calculated by a variance related principle. Lu et al. [11] studied the optimal reinsurance under VaR and CTE criteria when the ceded loss functions are increasing concave functions.

As we all know, there are two parties in a reinsurance contract, an insurer and a reinsurer. They have conflicting interests. Borch [12] studied the optimal quota-share reinsurance and the optimal stop-loss reinsurance from the both sides of the reinsurance under the optimization criterion of maximizing the product of the expected utility functions of the two parties' terminal wealth. Borch [13] showed reinsurance policy which is very attractive to the insurer may not be optimal for the reinsurer and it might be unacceptable for the reinsurer. Since then, the study of the optimal reinsurance opened a new direction. Cai et al. and Fang and Qu [14, 15] obtained the sufficient conditions for the optimal reinsurance contract by studying the joint survival probability and the joint profitable probability of the two parties. Cai et al. [16] used the convex combination of the VaRs of the cedent and the reinsurer as the object function to research the optimal reinsurance policies. Based on the criterion of VaR under the different confidence levels, Jiang et al. [17] studied pareto-optimal reinsurance strategies and gave the optimal forms. Lo [18] discussed the generalized problems of [16] by using the Neyman–Pearson approach. Cai et al. [19] studied pareto-optimality of reinsurance arrangements under general model settings and obtained the explicit forms of the pareto-optimal reinsurance contracts under tail-value-at-risk (TVaR) measure and the expected value premium principle. By geometric approach, Fang et al. [20] studied pareto-optimal reinsurance policies under general premium principles and gave the explicit parameters of the optimal ceded loss functions under Dutch premium principle and Wang's premium principle. Lo and Tang [21] characterized the set of pareto-optimal reinsurance policies analytically and visualized the insurer-reinsurer trade-off structure geometrically.

It is interesting to notice that most optimal forms of reinsurance in these cited papers are stop-loss reinsurance contracts. Inspired by these results, we mainly study the stop-loss reinsurance in this paper. We study the optimal form of reinsurance policy by minimizing the convex combination of the VaRs of the cedent and the reinsurer under the expected principle. The rest of the paper is organized as follows. In Section 2, we mainly introduce some preliminary knowledge. In Section 3, we assume that the cedent and the reinsurer have different confidence levels and then discuss the optimal stop-loss reinsurance under the expected principle by the optimization problem. In Section 4, we give numerical examples. In Section 5, we conclude the paper.

2. VaR-Based Optimal Reinsurance Model

In this section, we establish the framework of the optimal stop-loss reinsurance model-based VaR risk measure. Let the total loss for an insurer over a period of time be X, where X is a nonnegative random variable and defined in the probability space $(\Omega, \mathcal{F}, \mathcal{P})$, with distribution function $F_X(x) = \mathbb{P}(X \leq x)$, survival function $S_X(x) = \mathbb{P}\{X > x\}$, mean $E[X] = \mu\,(0 < \mu < \infty)$, and variance $D[X] = \sigma^2 > 0$. In a reinsurance contract, a reinsurer agrees to pay the part of the loss X, denoted by $f(X)$, to the insurer at the end of the contract term, while the insurer will pay a reinsurance premium, denoted by $\pi(f(X))$, to the reinsurer when the contract is signed, where the function $f(x)\,(0 \leq f(x) \leq x)$ is called ceded loss function. Then, the retained loss for the insurer is $I(X) = X - f(X)$, where the function $I(x)$ is called retained loss function.

As we all know, stop-loss reinsurance is optimal in the sense that it gives the lowest variance for the retained risk when the mean is given. In many literature studies, stop-loss reinsurance has been shown to be optimal under certain conditions, such as [1–3]. Therefore, many articles take stop-loss reinsurance as an example to study the reinsurance, for example [5, 7, 14]. In this paper, we study the stop-loss reinsurance, that is to say $f(X) = (X - d)_+$, where the parameter $d \geq 0$ is the retention. Under stop-loss agreement, the total loss of the insurer is

$$T_I = X - f(X) + \pi(f(X)), \tag{1}$$

and the total loss of the reinsurer is

$$T_R = f(X) - \pi(f(X)). \tag{2}$$

In fact, the reinsurance aims to control the risks of the two sides of reinsurance, and this will involve their maximum aggregate loss. The risk measure most often used in practice is simply the Value-at-Risk at a certain level α with $0 < \alpha < 1$, which is the amount that will maximally be lost with probability α. The VaR of a random variable is defined as follows.

Definition 1. The VaR of a nonnegative random variable X at a confidence level α, $0 < \alpha < 1$, is defined as

$$\mathrm{VaR}_\alpha(X) = \inf\{x\colon F_X(x) \geq \alpha\}. \tag{3}$$

The VaR defined by (3) is the maximum loss which is not exceeded at a given probability α. We list several properties of the VaR.

Proposition 1. *For any nonnegative random variable X with the survival function $S_X(x)$, we have the following properties for any $\alpha \in (0, 1)$:*

(1) Translation invariance: $VaR_\alpha(X + c) = VaR_\alpha(X) + c$, $(c \in R)$

(2) Homogeneity: $VaR_\alpha(cX) = c\,VaR_\alpha(X)$, $(c \in R)$

(3) If $h(x)$ is an increasing and left-continuous function, then $VaR_\alpha(h(X)) = h(VaR_\alpha(X))$

Obviously, the insurer and the reinsurer are mutually restricted and even opposed in the interests. This means, a reinsurance policy which is very attractive to the insurer may not be optimal for the reinsurer and it might be unacceptable for the reinsurer. To be fair, we consider the two parties of the reinsurance. Inspired by [17], we study the pareto-optimal reinsurance under the criterion of VaR because it can be expressed by the linear combination of the VaRs of the cedent and the reinsurer. Then, in this paper, we study optimal reinsurance policy by solving the following optimization problem:

$$\min L(f) = \min\left\{\beta\,\mathrm{VaR}_{\alpha_c}(T_I) + (1-\beta)\mathrm{VaR}_{\alpha_r}(T_R)\right\}, \tag{4}$$

where $0 \leq \beta \leq 1$, and the probability levels in the VaRs used by the cedent and the reinsurer are possibly different, say α_c and α_r, respectively.

3. Stop-Loss Reinsurance Optimization

Let $f(x) = (x-d)_+$ denote the ceded function, where $d \geq 0$ is the stop-loss retention; then, the objective function is

$$\begin{aligned} L(f) &= \beta \mathrm{VaR}_{\alpha_c}(T_I) + (1-\beta)\mathrm{VaR}_{\alpha_r}(T_R) \\ &= \beta \mathrm{VaR}_{\alpha_c}(X - f(X) + \pi(f(X))) \\ &\quad + (1-\beta)\mathrm{VaR}_{\alpha_r}(f(X) - \pi(f(X))). \end{aligned} \tag{5}$$

Let $a_c = \mathrm{VaR}_{\alpha_c}(X)$ and $a_r = \mathrm{VaR}_{\alpha_r}(X)$; then, the objective function is

$$\begin{aligned} L(d) &= \beta[a_c - (a_c - d)_+] + (1-\beta)(a_r - d)_+ \\ &\quad + (2\beta - 1)\pi[(X-d)_+], \end{aligned} \tag{6}$$

and the optimization problem is

$$\min_{d\in[0,\infty)} L(d). \tag{7}$$

One of the commonly used principles is the expectation premium principle, that is to say $\pi[(X-d)_+] = (1+\theta)E[(X-d)_+] = (1+\theta)\int_d^\infty S_X(x)\mathrm{d}x$, where $\theta > 0$ is the relative safety loading. In order to get the optimal retention d^*, we give the following results.

Theorem 1. *If $\beta = (1/2)$, we have the following conclusions:*

(1) When $\alpha_r < \alpha_c$, the optimal stop-loss coefficient d^* is arbitrarily in $[0, a_r]$

(2) When $\alpha_r > \alpha_c$, the optimal stop-loss coefficient d^* is arbitrarily in $[a_r, \infty)$

Proof. Specifically, when $\beta = (1/2)$, then the objective function is degraded to $L(d) = (1/2)[a_c - (a_c - d)_+ + (a_r - d)+]$.

(1) When $\alpha_r < \alpha_c$, we can obtain $a_r \leq a_c$ and

$$L(d) = \begin{cases} \frac{1}{2}a_r, & d < a_r, \\ \frac{1}{2}d, & a_r \leq d \leq a_c, \\ \frac{1}{2}a_c, & d > a_c. \end{cases} \tag{8}$$

In conclusion, we have

$$\min_{d\in[0,\infty)} L(d) = \frac{1}{2}a_r, \tag{9}$$

so d^* is any number in $[0, a_r]$.

(2) When $\alpha_r > \alpha_c$, we have $a_r \geq a_c$ and

$$L(d) = \begin{cases} \frac{1}{2}a_r, & d < a_c, \\ \frac{1}{2}(a_c + a_r - d), & a_c \leq d \leq a_r, \\ \frac{1}{2}a_c, & d > a_r. \end{cases} \tag{10}$$

So,

$$\min_{d\in[0,\infty)} L(d) = \frac{1}{2}a_c, \tag{11}$$

and d^* is any number in $[a_r, \infty)$.

We study the situation of $\beta \neq (1/2)$ and accomplish our task by subdividing our considerations into four cases: (1) $\beta > (1/2)$ and $\alpha_r < \alpha_c$; (2) $\beta > (1/2)$ and $\alpha_r > \alpha_c$; (3) $\beta < (1/2)$ and $\alpha_r < \alpha_c$; (4) $\beta < (1/2)$ and $\alpha_r > \alpha_c$.

For convenience, we use the notations:

$$\begin{aligned} \theta_1 &= \frac{1}{1+\theta}, \\ \theta_2 &= \frac{\beta}{(2\beta-1)(1+\theta)}, \\ \theta_3 &= \frac{\beta - 1}{(2\beta-1)(1+\theta)}, \\ d_1^* &= \arg\min_{d\in[0,a_c]} L(d), \\ Q(\beta, a_r, a_c) &= \frac{\beta a_c - (1-\beta)a_r}{2\beta - 1}. \end{aligned} \tag{12}$$

□

Theorem 2. *When $\beta > (1/2)$ and $\alpha_r < \alpha_c$, the optimal stop-loss reinsurance parameters are as follows:*

(1) When $S_X(0) \leq \theta_1$, the optimal stop-loss reinsurance coefficient is given by

$$d^* = \begin{cases} 0, & \mu < \theta_1 Q(\beta, a_r, a_c), \\ 0 \text{ or } \infty, & \mu = \theta_1 Q(\beta, a_r, a_c), \\ \infty, & \mu > \theta_1 Q(\beta, a_r, a_c). \end{cases} \tag{13}$$

(2) When $S_X(a_r) \leq \theta_1 < S_X(0)$, the optimal stop-loss reinsurance coefficient is given by

$$d^* = \begin{cases} S_X^{-1}(\theta_1), & \int_{S_X^{-1}(\theta_1)}^\infty S_X(t)\mathrm{d}t < \theta_1\left[Q(\beta, a_r, a_c) - S_X^{-1}(\theta_1)\right], \\ S_X^{-1}(\theta_1) \text{ or } \infty, & \int_{S_X^{-1}(\theta_1)}^\infty S_X(t)\mathrm{d}t = \theta_1\left[Q(\beta, a_r, a_c) - S_X^{-1}(\theta_1)\right], \\ \infty, & \int_{S_X^{-1}(\theta_1)}^\infty S_X(t)\mathrm{d}t > \theta_1\left[Q(\beta, a_r, a_c) - S_X^{-1}(\theta_1)\right]. \end{cases} \tag{14}$$

(3) *When $S_X(0) \leq \theta_1$, the optimal stop-loss reinsurance coefficient is given by*

$$d^* = \begin{cases} a_r, & \int_{S_X^{-1}(a_r)}^{\infty} S_X(t)\mathrm{d}t < \theta_2(a_c - a_r), \\ a_r \text{ or } \infty, & \int_{S_X^{-1}(a_r)}^{\infty} S_X(t)\mathrm{d}t = \theta_2(a_c - a_r), \\ \infty, & \int_{S_X^{-1}(a_r)}^{\infty} S_X(t)\mathrm{d}t > \theta_2(a_c - a_r). \end{cases} \tag{15}$$

(4) *When $S_X(a_c) < \theta_2 \leq S_X(a_r)$, the optimal stop-loss reinsurance coefficient is given by*

$$d^* = \begin{cases} S_X^{-1}(\theta_2), & \int_{S_X^{-1}(\theta_2)}^{\infty} S_X(t)\mathrm{d}t < \theta_2\left[a_c - S_X^{-1}(\theta_2)\right], \\ S_X^{-1}(\theta_2) \text{ or } \infty, & \int_{S_X^{-1}(\theta_2)}^{\infty} S_X(t)\mathrm{d}t = \theta_2\left[a_c - S_X^{-1}(\theta_2)\right], \\ \infty, & \int_{S_X^{-1}(\theta_2)}^{\infty} S_X(t)\mathrm{d}t > \theta_2\left[a_c - S_X^{-1}(\theta_2)\right]. \end{cases} \tag{16}$$

(5) *When $\theta_2 \leq S_X(a_c)$, the optimal stop-loss reinsurance coefficient is given by $d^* = \infty$.*

Proof. Following (6), the derivative of $L(d)$ with respect to d is

$$L'(d) = \begin{cases} (2\beta - 1)(1 + \theta)\left[\theta_1 - S_X(d)\right], & d < a_r, \\ (2\beta - 1)(1 + \theta)\left[\theta_2 - S_X(d)\right], & a_r < d \leq a_c, \\ -(2\beta - 1)(1 + \theta)S_X(d), & d > a_c. \end{cases} \tag{17}$$

We discuss the following partitions in the entire definition interval for simple calculation.

When $\beta > (1/2)$ and $d > a_c$, it follows from (17) that the derivative of the loss function is denoted by

$$L\prime(d) = -(2\beta - 1)(1 + \theta)S_X(d) < 0. \tag{18}$$

Then, $L(d)$ is decreasing in (a_c, ∞). So, we only need to talk about minimum values on the interval $[0, a_c]$ and compared $L(d_1^*)$ with $L(\infty)$.

When $d \leq a_c$, it follows from (17) that

$$L\prime(d) = \begin{cases} (2\beta - 1)(1 + \theta)\left[\theta_1 - S_X(d)\right], & d < a_r, \\ (2\beta - 1)(1 + \theta)\left[\theta_2 - S_X(d)\right], & a_r < d \leq a_c. \end{cases} \tag{19}$$

Because $\beta > (1/2)$, so $L\prime(d)$ is an increasing function. Meanwhile, $\theta_1 \leq \theta_2$ and $S_X^{-1}(\theta_2) \leq S_X^{-1}(\theta_1)$. Now, let us discuss the following situations in turn:

(1) If $S_X(0) \leq \theta_1$, then $L\prime(0) \geq 0$ and $L\prime(d) \geq 0$ for any $d \in [0, a_c]$. So, $d_1^* = 0$ and the optimal parameter d^* depends on the size of $L(0)$ and $L(\infty)$.

(2) If $S_X(a_r) \leq \theta_1 < S_X(0)$, this is equivalent to $0 < S_X^{-1}(\theta_1) \leq a_r$. When $d < S_X^{-1}(\theta_1)$, we can obtained $L\prime(d) < 0$, otherwise, $L\prime(d) > 0$. This means $d_1^* = S_X^{-1}(\theta_1)$, and finally d^* depends on the relative magnitude between $L(S_X^{-1}(\theta_1))$ and $L(\infty)$.

(3) If $\theta_1 < S_X(a_r) < \theta_2$, this means $S_X^{-1}(\theta_2) < a_r < S_X^{-1}(\theta_1)$. When $d < a_r$, we can obtained $L\prime(d) < 0$; on the contrary, $L\prime(d) > 0$. It shows that $d_1^* = a_r$. So, the optimal parameter d^* is determined by the size of $L(a_r)$ and $L(\infty)$.

(4) If $S_X(a_c) < \theta_2 \leq S_X(a_r)$, this is equivalent to $a_r \leq S_X^{-1}(\theta_2) < a_c$. When $d < S_X^{-1}(\theta_2)$, we can obtain $L\prime(d) < 0$; otherwise, $L\prime(d) > 0$. So, we proved that $d_1^* = S_X^{-1}(\theta_2)$ and d^* depends on the size of $L(d_2)$ and $L(\infty)$.

(5) If $\theta_2 \leq S_X(a_c)$, obviously, $L\prime(a_c) \leq 0$ and $L\prime(d) \leq 0$ for any $d \in [0, a_c]$. This implies that $d^* = \infty$. □

Theorem 3. *When $\beta > (1/2)$ and $\alpha_r > \alpha_c$, the optimal stop-loss reinsurance parameters are as follows:*

(1) *When $S_X(0) \leq \theta_1$, the optimal stop-loss reinsurance coefficient is given by*

$$d^* = \begin{cases} 0, & \mu < \theta_1 Q(\beta, a_r, a_c), \\ 0 \text{ or } \infty, & \mu = \theta_1 Q(\beta, a_r, a_c), \\ \infty, & \mu > \theta_1 Q(\beta, a_r, a_c). \end{cases} \tag{20}$$

(2) *When $S_X(a_c) < \theta_1 < S_X(0)$, the optimal stop-loss reinsurance coefficient is given by*

$$d^* = \begin{cases} S_X^{-1}(\theta_1), & \int_{S_X^{-1}(\theta_1)}^{\infty} S_X(t)\mathrm{d}t < \theta_1\left[Q(\beta, a_r, a_c) - S_X^{-1}(\theta_1)\right], \\ S_X^{-1}(\theta_1) \text{ or } \infty, & \int_{S_X^{-1}(\theta_1)}^{\infty} S_X(t)\mathrm{d}t = \theta_1\left[Q(\beta, a_r, a_c) - S_X^{-1}(\theta_1)\right], \\ \infty, & \int_{S_X^{-1}(\theta_1)}^{\infty} S_X(t)\mathrm{d}t > \theta_1\left[Q(\beta, a_r, a_c) - S_X^{-1}(\theta_1)\right]. \end{cases} \tag{21}$$

(3) *When $\theta_1 \leq S_X(a_c)$, the optimal stop-loss reinsurance coefficient is given by $d^* = \infty$.*

Theorem 4. *When $\beta < (1/2)$ and $\alpha_r < \alpha_c$, the optimal stop-loss reinsurance parameters are as follows:*

(1) *When $S_X(0) \leq \theta_2$ and $S_X(0) \leq \theta_1$, the optimal stop-loss reinsurance coefficient is given by $d^* = a_c$.*

(2) *When $S_X(a_c) < \theta_2 < \theta_1 \leq S_X(0)$ and $S_X(a_r) \notin (\theta_2, \theta_1)$, the optimal stop-loss reinsurance coefficient is given by*

$$d^* = \begin{cases} 0, & \int_0^{a_c} S_X(t)\mathrm{d}t > \theta_1 Q(\beta, a_r, a_c), \\ 0 \text{ or } a_c, & \int_0^{a_c} S_X(t)\mathrm{d}t = \theta_1 Q(\beta, a_r, a_c), \\ a_c, & \int_0^{a_c} S_X(t)\mathrm{d}t < \theta_1 Q(\beta, a_r, a_c). \end{cases} \quad (22)$$

(3) *When $\theta_2 < S_X(a_r) < S_X(0) \leq \theta_1$, the optimal stop-loss reinsurance coefficient is given by $d^* = a_r$.*

(4) *When $\theta_2 < S_X(a_r) < \theta_1 < S_X(0)$, the optimal stop-loss reinsurance coefficient is given by*

$$d^* = \begin{cases} 0, & \int_0^{a_r} S_X(t)\mathrm{d}t > \theta_1 a_r, \\ 0 \text{ or } a_r, & \int_0^{a_r} S_X(t)\mathrm{d}t = \theta_1 a_r, \\ a_r, & \int_0^{a_r} S_X(t)\mathrm{d}t < \theta_1 a_r. \end{cases} \quad (23)$$

(5) *When $\theta_1 \leq S_X(a_r)$ and $\theta_2 \leq S_X(a_c)$, the optimal stop-loss reinsurance coefficient is given by $d^* = 0$.*

Theorem 5. *When $\beta < (1/2)$ and $\alpha_r > \alpha_c$, the optimal stop-loss reinsurance parameters are as follows:*

(1) *When $S_X(0) \leq \theta_1$, the optimal stop-loss reinsurance coefficient is given by $d^* = a_r$.*

(2) *When $\theta_1 < S_X(0)$ and $S_X(a_r) < \theta_3$, the optimal stop-loss reinsurance coefficient is given by*

$$d^* = \begin{cases} 0, & \int_0^{a_r} S_X(t)\mathrm{d}t > \theta_1 Q(\beta, a_r, a_c), \\ 0 \text{ or } a_r, & \int_0^{a_r} S_X(t)\mathrm{d}t = \theta_1 Q(\beta, a_r, a_c), \\ a_r, & \int_0^{a_r} S_X(t)\mathrm{d}t < \theta_1 Q(\beta, a_r, a_c). \end{cases} \quad (24)$$

(3) *When $\theta_3 \leq S_X(a_r)$, the optimal stop-loss reinsurance coefficient is given by $d^* = 0$.*

4. Numerical Examples and Comparison

In this section, we construct two numerical examples to illustrate the reinsurance policy that we derived in the previous sections. Specifically, we assume that the loss variable X follows the exponential distribution with the survival function $S_X(x) = e^{-0.001x}$ for $x > 0$ and the mean $\mu = 1000$. Let the safety loading parameter $\theta = 0.2$. We discuss two examples specified below.

Table 1: $f(x)$ with $\alpha_r < \alpha_c$.

β	The optimal-ceded loss function
$\beta \in [0, 0.5)$	$f(x) = (x - 2995.7)_+$
$\beta = 0.5$	$f(x) = (x - d)_+, \forall d \in [0, a_r]$
$\beta \in (0.5, 1]$	$f(x) = (x - 182.32)_+$

Table 2: $f(x)$ with $\alpha_c < \alpha_r$.

β	The optimal-ceded loss function
$\beta \in [0, 0.5)$	$f(x) = (x - 4605.2)_+$
$\beta = 0.5$	$f(x) = (x - d)_+, \forall d \in [a_r, \infty)$
$\beta \in (0.5, 0.6417]$	$f(x) = 0$
$\beta \in (0.6417, 1]$	$f(x) = (x - 182.32)_+$

Example 1. Assume $\alpha_r = 0.95$ and $\alpha_c = 0.99$. In this case, $a_r = 2995.7$ and $a_c = 4605.2$. The optimal ceded loss functions $f(x)$ are shown in Table 1.

Example 2. Assume $\alpha_c = 0.95$ and $\alpha_r = 0.99$. In this case, $a_c = 2995.7$ and $a_r = 4605.2$. The optimal ceded loss functions $f(x)$ are shown in Table 2.

Remark 1. Following the abovementioned examples, we know that the optimal parameter of the stop-loss reinsurance policy depends on the combining parameter β when the probability levels in the VaRs are used by the both reinsurance differently.

5. Conclusions

Some scholars have shown that the stop-loss reinsurance is the optimal reinsurance policy under the convex combination of the both reinsurance parties. In this paper, we main study the pareto-optimal stop-loss reinsurance policy with the expectation premium principle. We analyze the topic from the following aspects: (1) the optimality results of reinsurance are derived by minimizing linear combination of the VaRs of the cedent and the reinsurer; (2) assuming that the probability levels in the VaRs used by the both reinsurance parties are different. Fortunately, through analysis, we finally derived the optimal parameters for the stop-loss reinsurance.

Data Availability

All data, models, or code generated or used during the study are available from the corresponding author upon request.

Conflicts of Interest

The authors declare that there are no conflicts of interest regarding the publication of this paper.

Acknowledgments

This research was supported by the Natural Science Foundation of Shandong Province (ZR2016JL006).

References

[1] K. J. Arrow, "Uncertainty and the welfare economics of medical care," *American Economic Review*, vol. 53, pp. 941–973, 1963.

[2] A. E. Van Heerwaarden, R. Kaas, and M. Goovaerts, "Optimal reinsurance in relation to ordering of risks," *Insurance: Mathematics and Economics*, vol. 8, no. 1, pp. 261–287, 1989.

[3] C. Gollier and H. Schlesinger, "Arrow's theorem on the optimality of deductibles: a stochastic dominance approach," *Economic Theory*, vol. 7, no. 2, pp. 359–363, 1996.

[4] V. R. Young, "Optimal insurance under Wang's premium principle," *Insurance: Mathematics and Economics*, vol. 25, no. 2, pp. 109–122, 1999.

[5] J. Cai and K. S. Tan, "Optimal retention for a stop-loss reinsurance under the VaR and CTE risk measures," *ASTIN Bulletin*, vol. 37, no. 1, pp. 93–112, 2007.

[6] J. Cai, K. S. Tan, C. Weng, and Y. Zhang, "Optimal reinsurance under VaR and CTE risk measures," *Insurance: Mathematics and Economics*, vol. 43, no. 1, pp. 185–196, 2008.

[7] K. S. Tan, C. Weng, and Y. Zhang, "VaR and CTE criteria for optimal quota-share and stop-loss reinsurance," *North American Actuarial Journal*, vol. 13, no. 4, pp. 459–482, 2009.

[8] K. C. Cheung, "Optimal reinsurance revisited-a geometric approach," *ASTIN Bulletin*, vol. 40, no. 1, pp. 221–239, 2010.

[9] Y. C. Chi and K. S. Tan, "Optimal reinsurance under VaR and CVaR risk measures: a simplified approach," *ASTIN Bulletin*, vol. 41, no. 2, pp. 547–574, 2011.

[10] Y. Chi, "Optimal reinsurance under variance related premium principles," *Insurance: Mathematics and Economics*, vol. 51, no. 2, pp. 310–321, 2012.

[11] Z. Lu, L. Liu, and S. Meng, "Optimal reinsurance with concave ceded loss functions under VaR and CTE risk measures," *Insurance: Mathematics and Economics*, vol. 52, no. 1, pp. 46–51, 2013.

[12] K. Borch, "An attempt to determine the optimum amount of stop-loss reinsurance," *Transactions of the 16th International Congress of Actuaries I*, pp. 597–610, 1960.

[13] K. Borch, "The optimal reinsurance treaty," *ASTIN Bulletin*, vol. 5, no. 2, pp. 293–297, 1969.

[14] J. Cai, Y. Fang, Z. Li, and G. E. Willmot, "Optimal reciprocal reinsurance treaties under the joint survival probability and the joint profitable probability," *Journal of Risk and Insurance*, vol. 80, no. 1, pp. 145–168, 2013.

[15] Y. Fang and Z. Qu, "Optimal combination of quota-share and stop-loss reinsurance treaties under the joint survival probability," *IMA Journal of Management Mathematics*, vol. 25, no. 1, pp. 89–103, 2014.

[16] J. Cai, C. Lemieux, and F. Liu, "Optimal reinsurance from the perspectives of both an insurer and a reinsurer," *ASTIN Bulletin*, vol. 46, no. 3, pp. 815–849, 2016.

[17] W. J. Jiang, J. D. Ren, and Z. Ricardas, "Optimal reinsurance policies under the VaR risk measure when the interests of both the cedent and the reinsurer are taken into account," *Risks*, vol. 5, pp. 1–22, 2017.

[18] A. Lo, "A Neyman-pearson perspective on optimal reinsurance with constraints," *ASTIN Bulletin*, vol. 47, no. 2, pp. 467–499, 2017.

[19] J. Cai, H. Liu, and R. Wang, "Pareto-optimal reinsurance arrangements under general model settings," *Insurance: Mathematics and Economics*, vol. 77, no. 1, pp. 24–37, 2017.

[20] Y. Fang, X. Wang, H. Liu, and T. Li, "Pareto-optimal reinsurance for both the insurer and the reinsurer with general premium principles," *Communications in Statistics-Theory and Methods*, vol. 48, no. 24, pp. 6134–6154, 2019.

[21] A. Lo and Z. Tang, "Pareto-optimal reinsurance policies in the presence of individual risk constraints," *Annals of Operations Research*, vol. 274, no. 1-2, pp. 395–423, 2019.

Hindawi
Mathematical Problems in Engineering
Volume 2020, Article ID 9097321, 8 pages
https://doi.org/10.1155/2020/9097321

Research Article

A Continuous-Time Version of a Delegated Asset Management Problem

Yanan Li,[1] Zengti Li,[2] and Chuanzheng Li[1]

[1] *School of Finance, Capital University of Economics and Business, Beijing 100070, China*
[2] *School of Science, Langfang Normal University, Langfang 065000, China*

Correspondence should be addressed to Chuanzheng Li; 13931239029@163.com

Received 31 March 2020; Accepted 27 September 2020; Published 30 November 2020

Academic Editor: Wenguang Yu

This paper develops a continuous-time model to study the widely used investment mandates in the institutional asset management industry. In this paper, just like He and Xiong (2013), we suppose that the asset management industry has a two-layered incentive structure, and fund families charging investors fixed management fees while compensating individual fund managers based on fund performance. Different from He and Xiong (2013), we suppose that the fund family aims to select an optimal incentive strategy to maximize its terminal benefits, while the fund manager needs to select the optimal effort level and the optimal investment portfolio to maximize his terminal net discounted compensation in a continuous-time model. By using dynamic programming principle and stochastic differential game theory, the optimal strategies and value functions of both sides are derived. At last, numerical studies are provided to illustrate the effects of all the parameters on the optimal strategies. The result reveals that the optimal incentive mechanism will redistribute both the benefit of the fund families and the cost of the fund managers' effort.

1. Introduction

Since professional cooperation plays an important role in making a successful investment, most investors handover their money to security companies, fund companies, or other financial management institutions, and the study of the asset management problem has attracted more and more attention. See [1–5] to name just a few.

In the internal of fund management companies, investment decisions are usually made by the fund manager, and the performance of investment portfolio is closely related to the investment strategy and the fund manager's effort level. So, the principal-agent relationship which affects the investment strategy inevitably exists in the investment process, and it is necessary to consider the investment problem under the principal-agent system.

For agency problems, most of the early literature focuses on discrete time models (for instance, [6–8] or [9] for a book treatment). A continuous-time model is first studied by [10], and it shows that the optimal contract is linear. Then, the work is extended by [11–14]. Nowadays, this kind of problem is usually solved by the stochastic maximum principle or martingale representation theorem. For the former, we can refer to [15–17]; for the latter, we can refer to [18, 19].

Different from the aforementioned models, [20] allows the manager to face investment opportunities in two markets instead of one and develops a discrete time model to study the widely used investment mandates in the institutional asset management industry. In this paper, we establish a continuous-time model based on [20] and find the optimal strategies of both the fund family and the fund manager. There are some differences between our model and the model mentioned in [20]:

(1) The effort level takes its value in an interval in this paper while the effort level is zero or a fixed value in [20]
(2) The returns from the two markets are stochastic processes in this paper while the single period model is considered in [20]

(3) Incentive compatibility constraint which must be satisfied in [20] is not necessary in this paper

Since the model in our paper is different from that in [20] and the method used in [20] does not work anymore, we use the stochastic differential game theory to get the optimal strategies of both the fund family and the fund manager. This tool can also be used for other investment problems under principle agency systems.

This paper is organized as follows. In Section 2, a mathematical formulation of the investment problem in the principle agency system is formulated. In Section 3, the problem with no agency conflicts is considered, and the optimal effort level is derived. Some numerical results are presented in this section to illustrate some comparative statics results. In Section 4, the problem with agency conflicts is considered, and the optimal policies of both the fund family and the fund manager are presented. Numerical analysis is also mentioned in this section to get the effects of all parameters on the optimal strategy. A conclusion is made in Section 5 which includes a comparison of the optimal effort levels with and without agency conflicts.

2. Problem Formulation

This paper embeds the optimal problem into the framework adopted in [20]. Suppose that the fund manager has superior expertise in primary market 1, that is, the effort of the fund manager can affect the gains of market 1. At the same time, he can pursue outside investment opportunity in market 2. The fund family aims to select an optimal incentive strategy to maximize its terminal gains, while the fund manager needs to select the optimal effort level and the optimal investment portfolio to maximize his terminal net discounted compensation. In the following, we will establish the mathematical model of the problem on the probability space $(\Omega, \mathcal{F}, P)$.

Referring to [18], we suppose that the manager's effort level n cannot be observed by the fund family and has a positive effect on the gain of market 1. Derived from [18] and considering a more concrete model, let us assume that $R_1^n(t)$, the gain of market 1 under the fund manager's effort level n, satisfies

$$dR_1^n(t) = R_1^n(t)\left[(r + \mu_1 + n)dt + \sigma_1 dW^1(t)\right], \quad (1)$$

where r represents the risk-free rate, $\mu_1 > 0$ is a constant, and $W^1(t)$ is a standard Brown motion on $(\Omega, \mathcal{F}, P)$. Clearly, the more the manager's efforts, the bigger the drift coefficient of market 1. Suppose that the return of market 2 satisfies

$$dR_2(t) = R_2(t)\left[(r + \mu_2)dt + \sigma_2 dW^2(t)\right], \quad (2)$$

where $\mu_2 > 0$ is a constant, and $W^2(t)$ is a standard Brown motion on $(\Omega, \mathcal{F}, P)$. Denote the correlation coefficient of $W^1(t)$ and $W^2(t)$ by ρ.

The manager will decide his effort level in the beginning and get a compensation from the fund family at the terminal time T. Suppose that the compensation is a function of the terminal benefit of the investment portfolio and denote it by $w(\cdot)$. Clearly, the fund family aims to find the optimal incentive strategy to control the performance of the fund and maximize its terminal net value. At the same time, the fund manager needs to look for the optimal effort level and the optimal investment portfolio to maximize his terminal net discounted compensation (wage or dividend). This is a noncooperative game. We are particularly interested in analyzing the joint implications of these two dimensions.

According to [15], we know that the fund family is in the leading position, and the manager should determine the effort level and the investment strategy according to the fund families' incentive strategy. Therefore, first, we intend to fix the compensation strategy $w(\cdot)$ and get the manager's optimal investment strategy and effort level which are expressed with the help of $w(\cdot)$. Then, we put the manager's optimal strategy into the fund family's optimization problem and get the optimal $w(\cdot)$.

The above analysis tells us that, first, we need to fix the incentive strategy $w(\cdot)$ and consider the manager's optimization problem. Consider the manager's policy $\pi = (b_{1,t}^\pi, b_{2,t}^\pi, n^\pi)$, where $b_{i,t}^\pi$, $i = 1, 2$ represent the capital invested in market i and n^π captures the effort level. Since the manager can invest in market 1, market 2, or risk-free market, by some simple calculations, we can have that the return of the investment portfolio under this policy satisfies

$$dX^\pi(t) = \left(X^\pi(t)r + b_{1,t}^\pi(\mu_1 + n^\pi) + b_{2,t}^\pi\mu_2\right)dt + \sigma^\pi(t)dW(t), \quad (3)$$

where $\sigma^\pi(t) = \sqrt{b_{1,t}^{\pi 2}\sigma_1^2 + b_{2,t}^{\pi 2}\sigma_2^2 + 2\rho b_{1,t}^\pi b_{2,t}^\pi \sigma_1\sigma_2}$, and $W(t)$ is the Brown motion on $(\Omega, \mathcal{F}, P)$.

Let $\{\mathcal{F}_t^W\}_{t\ge 0}$ be the natural filtration generated by $W(t)$. Now, let us give the definition of the manager's admissible control. A control policy $\pi = (b_{1,t}^\pi, b_{2,t}^\pi, n^\pi)$ is said to be admissible if $b_{i,t}^\pi$, $i = 1, 2$ are $\mathcal{F}_t^W$ predictable processes and $n^\pi \ge 0$. We denote the set of all admissible controls by Π. Then, we can establish a mathematical model of the manager's optimization problem.

The manager's objective is finding the optimal effort level and investment policy to maximize his utility of compensation minus his effort cost. That is, the objective of the manager is to maximize

$$J_m^\pi(t, x; w) = E\left[U_m\left(w\left(X^\pi(T)\right)\right) - C\left(n^\pi\right) \mid X^\pi(t) = x\right], \quad (4)$$

over $\pi \in \Pi$. Here, $U_m(\cdot)$ is the manager's utility function, and $C(n)$ is the manager's effort cost under the effort level n. Following the structure imposed in [19], we have

$$C(n) = \int_0^T e^{r(T-t)}\frac{\theta n^2}{2}R_1^n(t)dt, \quad (5)$$

where $\theta > 0$ is the cost parameter of the effort level.

Denote the optimal strategy by π^{w*}, and record the value function as

$$V_m(t, x; w) = \sup\nolimits_{\pi\in\Pi} J_m^\pi(t, x; w) = J_m^{\pi^{*w}}(t, x; w). \quad (6)$$

Next, let us consider the fund families' optimization problem. An incentive policy $w(\cdot)$ is said to be admissible if

$w(\cdot)$ is a continuous increasing function. We denote the set of all admissible controls by $\widehat{\Pi}$. The objective of the fund family is to find the optimal incentive policy to maximize its net benefit. Suppose it is risk neutral, then the objective of the fund family is to maximize

$$J_f^w(t,x) = E\left[X^{\pi^{w*}}(T) - w\left(X^{\pi^{w*}}(T)\right) | X^{\pi^{w*}}(t) = x\right], \quad (7)$$

over $w(\cdot) \in \widehat{\Pi}$. Denote the value function by

$$V_f(t,x) = \sup_{w\in\widehat{\Pi}} J_f^w(t,x). \quad (8)$$

3. The Problem with No Agency Conflicts

Let us consider the case when there are no agency conflicts in this section. That is, the fund manager can get all the benefits from asset management. The result in this section is meaningful since it can be used to solve the manager's optimization problem with agency conflicts.

3.1. Preliminary Result with the Effort Level Fixed. First, let us analyze the optimal investment problem of the manager with the effort level n fixed. Let

$$J^\pi(t,x;n) = E\left[U_m(X^\pi(T;n)) | X^\pi(t;n) = x\right], \quad (9)$$

where $X^\pi(t;n)$ is the process defined in (3) with the effort level n and investment policy $(b_{1,t}^\pi, b_{2,t}^\pi)$.

Define

$$V(t,x;n) = \sup\nolimits_{\pi\in\Pi} J^\pi(t,x;n). \quad (10)$$

According to [21], we know that $V(t,x;n)$ satisfies the HJB equation (Hamilton–Jacobi–Bellman equation):

$$\begin{aligned} -V_t(t,x;n) &= \sup_{\pi\in\Pi}\left\{\left[rx + b_{1,t}^\pi(\mu_1+n) + b_{2,t}^\pi\mu_2\right]V_x(t,x;n) + \frac{\sigma^{\pi 2}}{2}V_{xx}(t,x;n)\right\}, \\ V(T,x;n) &= U_m(x), \end{aligned} \quad (11)$$

where $\sigma^\pi = \sqrt{(b_{1,t}^\pi)^2\sigma_1^2 + (b_{2,t}^\pi)^2\sigma_2^2 + 2\rho b_{1,t}^\pi\sigma_1 b_{2,t}^\pi\sigma_2}$. Without losing generality, let $U_m(x) = (x^p/p)$, $0<p<1$. Suppose that $V(t,x;n) = e^{\beta_0(T-t)}U_m(x)$, where β_0 is a constant. We have

$$\begin{aligned} \beta_0 V(t,x;n) = &\left(rx + b_{1,t}^{n*}(\mu_1+n) + b_{2,t}^{n*}\mu_2\right)V_x(t,x;n) \\ &+ \frac{1}{2}\left(b_{1,t}^{n*2}\sigma_1^2 + b_{2,t}^{n*2}\sigma_2^2 + 2\rho b_{1,t}^{n*}\sigma_1 b_{2,t}^{n*}\sigma_2\right) \\ &\cdot V_{xx}(t,x;n), \end{aligned} \quad (12)$$

where $(b_{1,t}^{n*}, b_{2,t}^{n*})$ is the optimal investment strategy. By some simple calculations, we can get that

$$\beta_0 = \beta_0(n) = Ap\left(\frac{(\mu_1+n)^2}{2\sigma_1^2} + \frac{\mu_2^2}{2\sigma_2^2} - \frac{\rho(\mu_1+n)\mu_2}{\sigma_1\sigma_2}\right) + rp, \quad (13)$$

where $A = (1/((1-p)(1-\rho^2)))$. We can also get the optimal investment strategy and the value function:

$$\begin{aligned} b_{1,t}^{n*} &= \frac{X^*(t;n)\left((\mu_1+n)\sigma_2 - \rho\mu_2\sigma_1\right)}{\sigma_1^2\sigma_2\left(1-\rho^2\right)(1-p)}, \\ b_{2,t}^{n*} &= \frac{X^*(t;n)\left(\mu_2\sigma_1 - \rho(\mu_1+n)\sigma_2\right)}{\sigma_1\sigma_2^2\left(1-\rho^2\right)(1-p)}, \\ V(t,x;n) &= \frac{e^{\beta_0(n)(T-t)}x^p}{p}, \end{aligned} \quad (14)$$

where $X^*(t;n)$ is the return of the fund under the optimal investment strategy.

3.2. The Optimal Effort Level of the Manager. Since on the one hand, the effort made by the manager brings a better performance of market 1, and on the other hand, it produces a cost. Clearly, the net benefit of the manager is determined by the effort level. Since when $n=0$, the marginal utility of the effort is greater than zero, and the marginal cost of the effort is equal to zero; we know that at the beginning, the net benefit increases as the effort level increases. As time goes by, the marginal utility decreases and the marginal cost increases. When the marginal utility equals the marginal cost, the net benefit gets its maximum. Denoting this point by n^*, we have

$$\frac{\partial V(t,x;n)}{\partial n}\Big|_{n=n^*} = \frac{\partial E[C(n)]}{\partial n}\Big|_{n=n^*}. \quad (15)$$

Since the portion invested in market 1 is $b_{1,t}^{n*}$, we have

$$R_1^n(t) = b_{1,t}^{n*}. \quad (16)$$

Then,

$$E\left[R_1^n(t)\right] = E\left[b_{1,t}^{n*}\right] = \frac{(\mu_1+n)\sigma_2 - \rho\mu_2\sigma_1}{\sigma_1^2\sigma_2\left(1-\rho^2\right)(1-p)}E\left[X^*(t;n)\right]. \quad (17)$$

Clearly, $E[R_1^n(t)]$ is finite; then, we can exchange the integration order of $E[C(n)]$ and obtain

$$E[C(n)] = e^{rT}\frac{\theta n^2}{2}\int_0^T e^{-rt}E[R_1^n(t)]\mathrm{d}t$$
$$= \frac{\theta n^2}{2}\frac{(\mu_1+n)\sigma_2-\rho\mu_2\sigma_1}{\sigma_1^2\sigma_2(1-\rho^2)(1-p)}\frac{e^{(B(n)+r)T}-e^{rT}}{B(n)}x, \tag{18}$$

where $B(n) = (((\mu_1+n)^2)/(\sigma_1^2(1-p))) + (\mu_2^2/(\sigma_2^2(1-p)))$.

In the following, we focus on the effects of parameters (such as the risk-free rate and the diffusion rate) on the optimal effort level. Since when $\rho = 0, \mu_1 = \mu_2 = \mu$, and $n\sigma_1 = \sigma_2 = \sigma$, the two markets have the same performance without the effect of the effort made by the fund manager, and we can focus on the effect of the manager's effort. In this case, according to (14), (15), and (18), we can get that the optimal effort level n^* satisfies

$$\beta_0'(n^*)\frac{e^{\beta_0(n^*)(T-t)}x^p}{p} = \theta n^*\frac{(\mu+n^*)}{\sigma^2(1-p)}\frac{e^{(B(n^*)+r)T}-e^{rT}}{B(n^*)}x$$
$$+\frac{\theta(n^*)^2}{2\sigma^2(1-p)}\frac{e^{(B(n^*)+r)T}-e^{rT}}{B(n^*)}x$$
$$+\frac{\theta(n^*)^2}{2}\frac{(\mu+n^*)}{\sigma^2(1-p)}$$
$$\cdot\frac{e^{(B(n^*)+r)T}B'(n^*)(B(n^*)T-1)x}{B(n^*)^2}. \tag{19}$$

Clearly, (19) can define function n^* which depends on the parameters of the financial market. In order to analyze the effects of parameters on the optimal effort level, we use R software to get the graphs of the function for each parameter with other parameters fixed. The results are presented in graphs 1–6 in Figures 1–6.

4. The Problem with Agency Conflicts

In this section, we follow the steps mentioned in Section 2 to get the optimal strategies and the value functions of both sides. For simplicity, we consider the problem under the situation in which $w(\cdot)$ is a power function. That is, $w(x) = kx^q$, $k > 0$, $q > 0$.

4.1. The Optimal Nash Equilibrium Strategy. As mentioned above, first, let us fix the fund family's strategy and the fund manager's effort level. That is, k, q, and n are fixed. Then, the compensation of the fund manager with policy $\pi = (b_{1,t}^\pi, b_{2,t}^\pi, n)$ is

$$J_m^\pi(t,x;n) = E\left[\frac{(kX^\pi(T;n)^q)^p}{p}|X^\pi(0;n)=x\right]. \tag{20}$$

Since this optimization problem is similar with the one solved in Section 3.1, with the same method, we have that the optimal investment strategies are

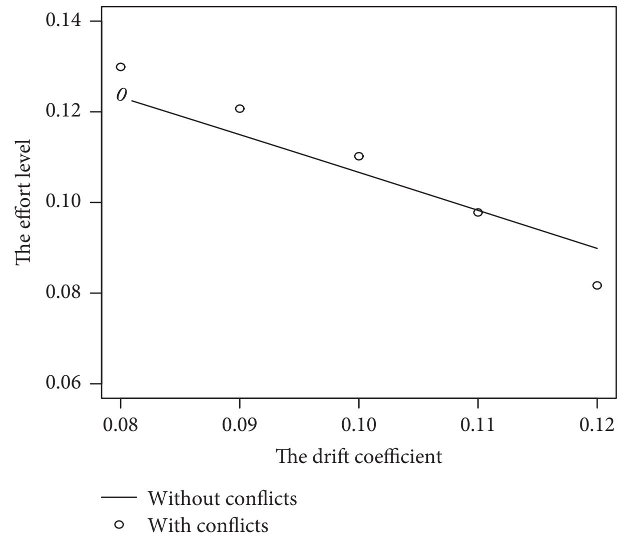

Figure 1: The effect of the drift coefficient on the optimal effort level

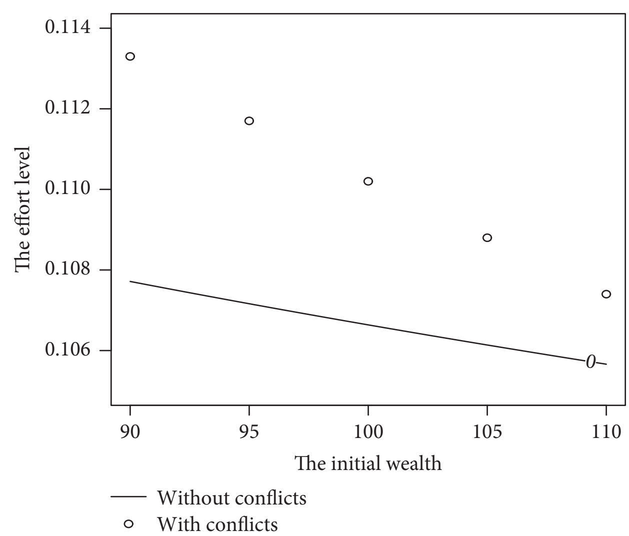

Figure 2: The effect of the initial wealth on the optimal effort level.

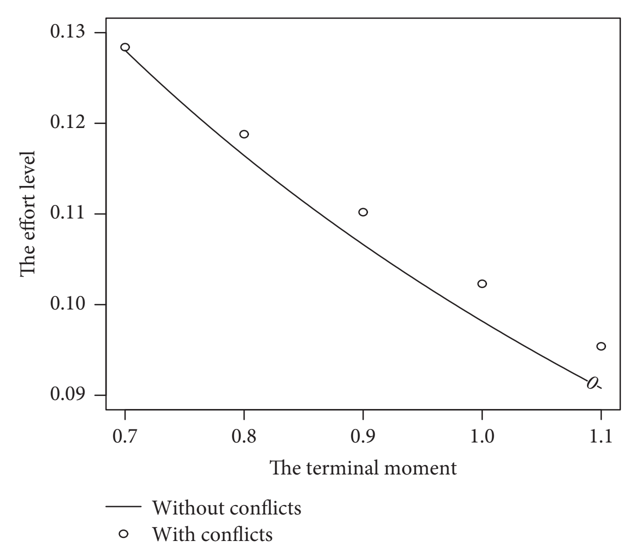

Figure 3: The effect of the terminal moment on the optimal effort level.

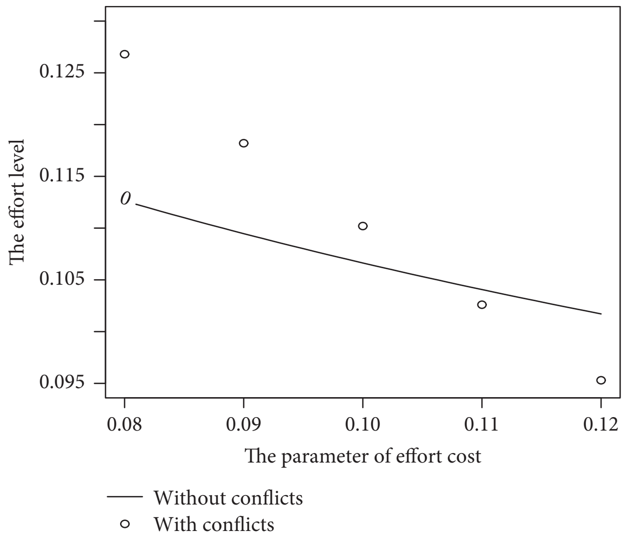

Figure 4: The effect of the effort cost on the optimal effort level.

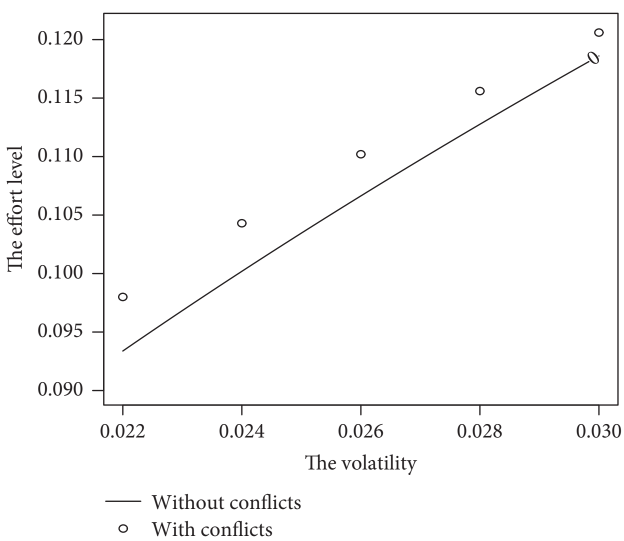

Figure 5: The effect of the volatility on the optimal effort level.

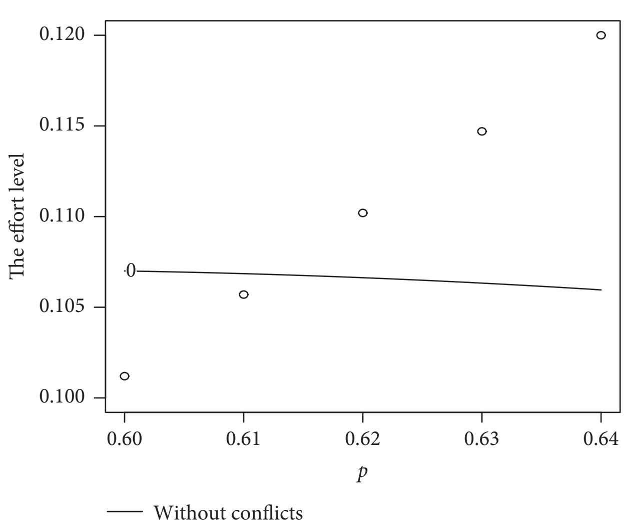

Figure 6: The effect of the risk aversion factor on the optimal effort level.

$$b_{1,t}^{*k,q,n} = \frac{x\left((\mu_1+n)\sigma_2 - \rho\mu_2\sigma_1\right)}{\sigma_1^2\sigma_2\left(1-\rho^2\right)(1-qp)}, \tag{21}$$

$$b_{2,t}^{*k,q,n} = \frac{x\left(\mu_2\sigma_1 - \rho(\mu_1+n)\sigma_2\right)}{\sigma_1^2\sigma_2^2\left(1-\rho^2\right)(1-qp)}, \tag{22}$$

and the value function is

$$V_m(t,x;n) = \sup_{\pi\in\Pi} J_m^{\pi}(t,x;n) = e^{\beta(n)(T-t)}\frac{(kx^q)^p}{p}, \tag{23}$$

where

$$\beta(n) = Apq\left(\frac{(\mu_1+n)^2}{2\sigma_1^2} + \frac{\mu_2^2}{2\sigma_2^2} - \frac{\rho(\mu_1+n)\mu_2}{\sigma_1\sigma_2}\right) + rpq. \tag{24}$$

Clearly, fixing k and q, the optimal effort level n^* satisfies the following equation:

$$\frac{\partial V_m(t,x;n)}{\partial n}\Big|_{n=n^*} = \frac{\partial E[C(n)]}{\partial n}\Big|_{n=n^*}. \tag{25}$$

It is shown from the above analysis that n^* is a function of k and q, and we denote it by $n^*(k,q)$.

Let us suppose that the two parts are all rational, and they will choose their strategy considering the opposite side. Then, if the fund family choose the income policy $k$and$q$, he will confer that the manager will choose the optimal investment strategy

$$\begin{aligned} b_{1,t}^{*k,q} &= b_{1,t}^{*k,q,n^*(k,q)}, \\ b_{2,t}^{*k,q} &= b_{2,t}^{*k,q,n^*(k,q)}, \end{aligned} \tag{26}$$

and the optimal effort level $n^*(k,q)$. Under this strategy, the benefit of the portfolio is

$$\begin{aligned} \mathrm{d}X^{*k,q}(t) = &\left(X^{*k,q}(t)r + b_{1,t}^{*k,q}(\mu_1 + n^*(k,q)) + b_{2,t}^{*k,q}\mu_2\right)\mathrm{d}t \\ &+ \sigma^{*k,q}\mathrm{d}W(t), \end{aligned} \tag{27}$$

where $\sigma^{*k,q} = \sqrt{(b_{1,t}^{*k,q})^2\sigma_1^2 + (b_{2,t}^{*k,q})^2\sigma_2^2 + 2\rho b_{1,t}^{*k,q}b_{2,t}^{*k,q}\sigma_1\sigma_2}$. The fund family's terminal value will be

$$J_f^{k,q}(x) = E\left[X^{*k,q}(T) - k\left(X^{*k,q}(T)\right)^q\right]. \tag{28}$$

Denote the value function by

$$V_f(x) = \sup_{k>0,q>0} J_f^{k,q}(x). \tag{29}$$

4.2. The Effects of Parameters on the Optimal Effort Level and the Compensation Strategy. In this section, we will analyze the effect of parameters on the optimal strategies. Similar to the analysis in Section 3, let us still consider the case when $\rho = 0, \mu_1 = \mu_2 = \mu$, and $\sigma_1 = \sigma_2 = \sigma$. Referring to (21), (22), and (27), we have

$$b_{1,t}^{*k,q} = \frac{X^{*k,q}(t)(\mu+n)}{\sigma^2(1-pq)}, \tag{30}$$

$$b_{2,t}^{*k,q} = \frac{X^{*k,q}(t)\mu}{\sigma^2(1-pq)}, \tag{31}$$

$$dX^{*k,q}(t) = X^{*k,q}(t)\left[\left(r + \frac{\mu^2+(\mu+n)^2}{\sigma^2(1-pq)}\right)dt + \sigma^{*k,q}\right]dW(t), \tag{32}$$

$$d < X^{*k,q} > (t) = \left(\sigma^{*k,q}\right)^2 dt, \tag{33}$$

where $\sigma^{*k,q} = \sigma\sqrt{(b_{1,t}^{*k,q})^2 + (b_{2,t}^{*k,q})^2 + 2\rho b_{1,t}^{*k,q} b_{2,t}^{*k,q}}$, and $n, k,$ and q satisfy (23).

Using Ito's formula, we can obtain that

$$\begin{aligned} dX^{*k,q}(t)^q &= qX^{*k,q}(t)^{q-1}dX^{*k,q}(t) \\ &\quad + \frac{q(q-1)}{2}X^{*k,q}(t)^{q-2}d\langle X^{*k,q}\rangle(t). \end{aligned} \tag{34}$$

Combining with (30)–(33), we can obtain

$$dX^{*k,q}(t)^q = X^{*k,q}(t)^q\left\{\left[\left(r + \frac{(\mu+n)^2+\mu^2}{(1-qp)\sigma^2}\right)q + \frac{q(q-1)((\mu+n)^2+\mu^2)}{2\sigma^2(1-qp)^2}\right]dt + q\sigma^{*k,q}dW(t)\right\}. \tag{35}$$

By some simple calculations, we can obtain that

$$\begin{aligned} E\left[X^{*k,q}(T)^q | X^{*k,q}(0) = x\right] &= \exp\left\{\left\{\left[r + \frac{(\mu+n)^2+\mu^2}{(1-qp)\sigma^2}\right]q + \frac{q(q-1)\left[(\mu+n)^2+\mu^2\right]}{2(1-qp)^2\sigma^2}\right\}T\right\}x^q, \\ E\left[X^{*k,q}(T) | X^{*k,q}(0) = x\right] &= \exp\left\{\left[r + \frac{(\mu+n)^2+\mu^2}{(1-qp)\sigma^2}\right]T\right\}x. \end{aligned} \tag{36}$$

Then, we have

$$E\left[X^{*k,q}(T) - k\left(X^{*k,q}(T)\right)^q\right] = \exp\{[r + B_0(n)]T\}x - k\exp\left\{\left\{[r + B_0(n)]q + \frac{q(q-1)B_0(n)}{2(1-qp)}\right\}T\right\}x^q, \tag{37}$$

where $B_0(n) = (((\mu+n)^2+\mu^2)/((1-qp)\sigma^2))$.

We want to find the optimal $k$and$q$ to maximize (37) under the constraint (23), and $k > 0$and$q > 0$. This is an optimization problem with constraints. This problem seems impossible to be solved explicitly. However, we can easily obtain the numerical solutions by using function donlp2 in software R.

By using R software, the numerical results are illustrated in the following tables.

Table 1 shows that the fund manager's compensation and the effort level all decrease as the drift coefficient increases. Theoretically speaking, according to (23), both the cost of the fund manager's effort and the expected utility of the fund manager's compensation increase with the increase in drift coefficient μ. Furthermore, the effort cost increases at a greater rate than the expected utility of compensation. So, the manager's optimal effort level decreases. This is consistent with the results in Table 1.

The optimal compensation strategy can be affected by the following two aspects:

(1) The drop of the optimal effort level can be inferred by the fund family which leads to a lower compensation

(2) The total benefit increases with the increase in drift coefficient which leads to a higher compensation

According to Table 1, we can see that the drop of the optimal effort level has a greater impact on the optimal compensation.

Table 2 reports that the fund manager's compensation increases as the initial wealth increases. The fund manager's effort level decreases as the initial wealth increases. Clearly, according to (23), both the cost of the fund manager's effort and the expected utility of the fund manager's compensation increase as the initial capital increases. Furthermore, the effort cost increases at a greater rate than the expected utility of compensation. In this situation, the manager's optimal effort level decreases. This is consistent with the results in Table 1.

Table 1: The effect of the drift coefficient on the optimal compensation and the optimal effort level.

μ	k	q	Wage	n
0.08	1.8102	0.8812	104.7603	0.1299
0.09	1.6567	0.8913	100.4070	0.1207
0.10	1.4107	0.9061	91.5460	0.1102
0.11	1.0535	0.9290	75.9769	0.0978
0.12	1.1384	0.7488	35.6902	0.0817

Table 2: The effect of the initial wealth on the optimal compensation and the optimal effort level.

x	k	q	Compensation	n
90	1.5803	0.8976	89.7285	0.1133
95	1.4921	0.9019	90.6894	0.1117
100	1.4107	0.9061	91.5460	0.1102
105	1.3355	0.9101	92.3023	0.1088
110	1.2657	0.9141	92.9645	0.1074

For the optimal compensation strategy, on the one hand, the drop of the optimal effort level can be inferred by the fund family which leads to a lower compensation. On the other hand, the total benefit increases as the initial capital increases. This leads to a higher compensation. According to Table 2, we can see that the increase of the total benefit has a greater impact on the optimal compensation.

As a matter of fact, with the increase of the initial capital, the stability of return on assets is more important to the fund manager than the growth of return on assets. In this situation, the fund manager tends to invest more in risk-free assets and decrease the level of the effort. Considering the following two points:

(1) The decrease of the optimal effort level is due to risk aversion

(2) The increase of the initial capital increases the cost of the fund manager

The fund family will still increase the fund manager's compensation appropriately. This phenomenon can be explained perfectly by the results in Table 2.

The results illustrated in Tables 3–5 can be explained similarly as the one mentioned above.

Table 6 illustrates that the compensation and the effort level of the fund manager all increase along with the decrease of the fund manager's risk aversion level. Clearly, the expected utility of the fund manager's compensation increases as the risk-averse level decreases. In this situation, the manager's optimal effort level increases.

For the optimal compensation policy, on the one hand, the increase of the effort level will raise the fund manager's compensation. On the other hand, the fund manager is more easily satisfied which can be inferred by the fund family. This leads to a lower compensation. According to Table 6, we can see that the increase of the effort level has a greater impact on the optimal compensation.

As a matter of fact, the fund manager with the lower risk-averse level tends to make a greater effort to get a higher Sharp ratio. The fund family can accurately identify the

Table 3: The effect of the terminal time on the optimal compensation and the optimal effort level.

T	k	q	Compensation	n
0.7	1.1975	0.9136	80.4269	0.1284
0.8	1.3170	0.9088	86.5458	0.1188
0.9	1.4107	0.9061	91.5460	0.1102
1.0	1.4555	0.9060	94.4298	0.1023
1.1	1.5044	0.9058	97.4911	0.0954

Table 4: The effect of the effort cost on the optimal compensation and the optimal effort level.

θ	k	q	Compensation	n
0.08	2.6906	0.8626	142.9222	0.1268
0.09	1.9391	0.8845	113.9246	0.1182
0.10	1.4107	0.9061	91.5460	0.1102
0.11	1.0271	0.9278	73.6665	0.1026
0.12	0.7468	0.9497	59.2311	0.0953

Table 5: The effect of the fluctuation coefficient on the optimal compensation and the optimal effort level.

σ^2	k	q	Compensation	n
0.022	1.5008	0.9052	96.9997	0.0980
0.024	1.4475	0.9059	93.8495	0.1043
0.026	1.4107	0.9061	91.5461	0.1102
0.028	1.3528	0.9077	88.4240	0.1156
0.030	1.2935	0.9097	85.3381	0.1206

Table 6: The effect of the risk aversion factor on the optimal compensation and the optimal effort level.

p	k	q	Compensation	n
0.60	0.7942	0.9432	60.9005	0.1012
0.61	1.0608	0.9238	74.6961	0.10
0.62	1.4107	0.9061	91.5460	0.1102
0.63	1.8409	0.8902	111.0353	0.1147
0.64	2.4748	0.8727	137.7054	0.1200

manager's risk preference and speculate that the manager's optimal effort level increases as the risk-averse level decreases and then properly increases the manager's compensation to reward him for the effort.

By using *R* software, the graphs of the optimal effort level changing with parameters with and without agency conflicts are presented in Figures 1–6.

5. Conclusion

According to graphs 1–5, we can see that the optimal effort levels have the same change tendency in the cases with and without agency conflicts. This implies that the manager flourishes if the fund family flourishes. However, the ascending (descending) speed is different because of the effect of agency conflicts. It is shown from graph 6 that the optimal effort levels have the opposite change tendency in two cases. In the case when there are no agency conflicts, the effort level decreases along with the decrease of the fund manager's risk aversion level. In fact, in this case, the fund manager is in the position of the fund family. A decrease of the fund manager's risk aversion level is equivalent to a decrease of the fund family's risk aversion level, which is a relative increase of the fund manager's risk aversion level in the case with agency conflicts. So, the two results in the two cases are consistent.

We can also suppose that the effort level will change with time. In this case, the corresponding HJB equation of the agent optimization problem does not have an explicit solution, which implies that the dynamic programming principle cannot be used any more. Since the martingale representation theorem is usually applied to give a representation of the agent's true continuation value (Sannikov [18], He [19] for example), we can deduce that this problem may also be solved by applying the martingale representation theorem. Anyone interested in this more complex problem can continue to do some research.

Data Availability

The conclusion of this paper is given in the form of an expression with respect to some parameters. No data were used to support this study. The data in the table are selected for the analysis of the influence of each parameter in the expression on the optimal effort level.

Conflicts of Interest

The authors declare that they have no conflicts of interest.

Acknowledgments

This work was partially supported by the National Natural Science Foundation of China (Grant no. 11901404).

References

[1] A. Almazan, K. C. Brown, M. Carlson, and D. A. Chapman, "Why constrain your mutual fund manager?" *Journal of Financial Economics*, vol. 73, no. 2, pp. 289–321, 2004.

[2] M. K. Brunnermeier and L. H. Pedersen, "Market liquidity and funding liquidity," *Review of Financial Studies*, vol. 22, no. 6, pp. 2201–2238, 2009.

[3] P. H. Dybvig, H. K. Farnsworth, and J. N. Carpenter, "Portfolio performance and agency," *Review of Financial Studies*, vol. 23, no. 1, pp. 1–23, 2010.

[4] S. Gervais, A. W. Lynch, and D. K. Musto, "Fund families as delegated monitors of money managers," *Review of Financial Studies*, vol. 18, no. 4, pp. 1139–1169, 2005.

[5] V. Guerrieri and P. Kondor, "Fund managers, career concerns, and asset price volatility," *American Economic Review*, vol. 102, no. 5, pp. 1986–2017, 2012.

[6] S. Ross, "The economic theory of agency: the principal's problem," *American Economic Review*, vol. 63, no. 2, pp. 134–139, 1973.

[7] J. A. Mirrlees, "The optimal structure of incentives and authority within an organization," *The Bell Journal of Economics*, vol. 7, no. 1, pp. 105–131, 1976.

[8] B. Holmstrom, "Moral hazard and observability," *The Bell Journal of Economics*, vol. 10, no. 1, pp. 74–91, 1979.

[9] P. Bolton and M. Dewatripont, *Contract Theory*, MIT Press, Cambridge, UK, 2005.

[10] B. Holmstrom and P. Milgrom, "Aggregation and linearity in the provision of intertemporal incentives," *Econometrica*, vol. 55, no. 2, pp. 303–328, 1987.

[11] H. Schättler and J. Sung, "The first-order approach to the continuous-time principal-agent problem with exponential utility," *Journal of Economic Theory*, vol. 61, no. 2, pp. 331–371, 1993.

[12] H. Schättler and J. Sung, "On optimal sharing rules in discrete-and continuous-time principal-agent problems with exponential utility," *Journal of Economic Dynamics and Control*, vol. 21, no. 2-3, pp. 551–574, 1997.

[13] H. Müller, "The first-best sharing rule in the continuous-time principal-agent problem with exponential utility," *Journal of Economic Theory*, vol. 79, no. 2, pp. 276–280, 1998.

[14] H. M. Müller, "Asymptotic efficiency in dynamic principal-agent problems," *Journal of Economic Theory*, vol. 91, no. 2, pp. 292–301, 2000.

[15] J. Cvitanić, X. Wan, and J. Zhang, "Optimal compensation with hidden action and lump-sum payment in a continuous-time model," *Applied Mathematics and Optimization*, vol. 59, pp. 99–146, 2009.

[16] J. Cvitanić and J. Zhang, *Contract Theory in Continuous Time Models*, Springer-Verlag, Berlin, Germany, 2013.

[17] N. Williams, *On Dynamic Principal-Agent Problems in Continuous Time, Working Paper*, University of Wisconsin, Madison, WI, USA, 2009.

[18] Y. Sannikov, "A continuous-time version of the principal-agent problem," *Review of Economic Studies*, vol. 75, no. 3, pp. 957–984, 2008.

[19] Z. He, "A model of dynamic compensation and capital structure," *Journal of Financial Economics*, vol. 100, no. 2, pp. 351–366, 2011.

[20] Z. He and W. Xiong, "Delegated asset management, investment mandates, and capital immobility," *Journal of Financial Economics*, vol. 107, no. 2, pp. 239–258, 2013.

[21] W. Fleming and H. Soner, *Controlled Markov Processes and Viscosity Solutions*, Springer-Verlag, New York, NY, USA, 1993.

Hindawi
Mathematical Problems in Engineering
Volume 2020, Article ID 1932704, 10 pages
https://doi.org/10.1155/2020/1932704

Research Article

Compound Binomial Model with Batch Markovian Arrival Process

Fang Jin,[1] Chengxun Wu,[1] and Hui Ou[2]

[1]*College of Sciences, Hunan City University, Yiyang 413000, China*
[2]*College of Mathematics and Statistics, Hunan Normal University, Changsha 410081, China*

Correspondence should be addressed to Hui Ou; bt_huiou@hunnu.edu.cn

Received 31 May 2020; Accepted 24 July 2020; Published 28 November 2020

Guest Editor: Wenguang Yu

A compound binomial model with batch Markovian arrival process was studied, and the specific definitions are introduced. We discussed the problem of ruin probabilities. Specially, the recursion formulas of the conditional finite-time ruin probability are obtained and the numerical algorithm of the conditional finite-time nonruin probability is proposed. We also discuss research on the compound binomial model with batch Markovian arrival process and threshold dividend. Recursion formulas of the Gerber–Shiu function and the first discounted dividend value are provided, and the expressions of the total discounted dividend value are obtained and proved. At the last part, some numerical illustrations were presented.

1. Introduction

The compound binomial model is a discrete time analogue of compound Poisson model. In the compound binomial model, the counting process is a binomial process. From the compound binomial model proposed by Gerber [1], a series of papers and books have studied this model (see Gerber [1]; Shiu [2]; Cossette [3]; Wu [4]; Peng et al. [5] and references therein).

As a class of important stochastic point processes, the batch Markovian arrival process (BMAP), proposed by Lucantoni [6], is dense in the class of stationary point processes. BMAP is used to model the stochastic processes in finance, computer, reliability, communication, and inventory conveniently. Particular BMAPs are the batch Poisson arrival process, the Markovian arrival process (MAP), many batch arrival processes with correlated interarrival times and batch sizes, and superpositions of these processes. We note that the MAP, introduced by Neuts [7], includes phase-type (PH) renewal processes and nonrenewal processes such as the Markov modulated Poisson process (MMPP). Like Ahn et al. [8], Eric et al. [9], Artalejo et al. [10], Dong and Liu [11] and many authors have studied the compound Poisson process with MAP.

Inspired by Ahn et al. [8], Badescu et al. [12], Eric et al. [9], Artalejo et al. [10], and Dong and Liu [11], we discuss the compound Binomial model with BMAP. In this model, the counting process is a BMAP, which is a reasonable assumption. For example, an insurance company, which accepts the car insurance policies, might need to deal with several traffic accidents a day. Moreover, in different circumstances, the probability of traffic accident and the claim sizes are of big differences. So it may be more reasonable that the premium rate of car insurance is different in different environments. Therefore, we assume that the premium rate, probability of the claim occurring, and the claim amount are all influenced by the phase process of BMAP. Also, we study the compound binomial model with BMAP and threshold dividend. This study has certain guiding significance in insurance company and shareholders.

This paper is structured as follows: the specific definition of a compound binomial model with BMAP is introduced in Section 2. In Section 3, we discuss the ruin probabilities. Specially, the recursion formulas of the conditional finite-time ruin probability are obtained and the numerical algorithm is proposed. In Section 4, we also discuss research on the compound binomial model with BMAP and threshold dividend. The recursion formulas of the Gerber–Shiu function and the first discounted dividend value are provided, and the explicit expression of the total discounted dividend values are obtained and proved. Finally, we present some numerical examples to illustrate in Section 5.

2. Model

Let $(\Omega, \mathcal{F}, \mathbb{P})$ be a probability space with filtration $\{\mathcal{F}_t\}$ containing all objects defined in this paper. Assume that $\{\mathcal{F}_t\}$ satisfies the usual conditions, i.e., $\{\mathcal{F}_t\}$ is right-continuous and $\mathbb{P}$-complete. At first, we will introduce the compound binomial model and the batch Markovian arrival process.

2.1. Compound Binomial Model. In the compound binomial model, $\{C(n), n = 0, 1, 2, \ldots\}$ denotes the surplus process of an insurer and is given by

$$C(n) = u + t - S(n), \quad n = 0, 1, 2, \ldots, \tag{1}$$

where the initial surplus u is a nonnegative integer, $S(n)$ is the aggregate claim up to time n, which is described by

$$S(n) = X_1\xi_1 + X_2\xi_2 + \cdots + X_n\xi_n, \tag{2}$$

and $S(0) = 0$. In any time period, the probability with only a claim occurrence is $\theta, 0 < \theta \le 1$, and the probability with no claim occurrence is $\lambda = 1 - \theta$. We denote by $\xi_n = 1$ the event where a claim occurs in the time period $(n-1, n]$, and we denote by $\xi_n = 0$ the event where no claim occurs in the time period $(n-1, n]$. The occurrences of claims in different time periods are independent events. $X = \{X_n, t = 1, 2, \ldots\}$ denotes the claim amount that probably occurs at time t, and $X_1, X_2, X_3, \ldots$ are mutually independent, identically distributed (i.i.d.), positive integer-valued random variables, which have a common discrete distribution $P(X = k) = f(k), k = 1, 2, \ldots$. Denote $F(k) = P(X \le k) = \sum_{j=1}^{k} f(j)$ with $F(0) = 0$. And the claim amounts $X = \{X_n, n = 1, 2, \ldots\}$ are independent of $\xi = \{\xi_n, n = 1, 2, \ldots\}$.

2.2. Batch Markovian Arrival Process

Definition 1. Let $E = \{e_1, e_2, \ldots, e_m\}\,(m \ge 1)$. Given a series of $m \times m$ matrixes $D_0 = (d_{ij}^0)$ and $D_k = (d_{ij}^k)\,(k \in \mathbb{N}_+)$ which satisfied the following conditions:

(1) $D_k\,(k \in \mathbb{N}_+)$ are substochastic matrixes

(2) The matrix $I - D_0$ is nonsingular

(3) $P = \sum_{k=0}^{\infty} D_k = (q_{ij})$ is a stochastic matrix, and $q_{ij} = \sum_{k=0}^{\infty} d_{ij}^k$

Then, $(D_0, D_k\,(k \in \mathbb{N}_+))$ is called the numerical characteristic of discrete-time batch Markovian arrival process.

Proposition 1. *Assume that $(D_0, D_k\,(k \in \mathbb{N}_+))$ be the numerical characteristic of discrete-time batch Markovian arrival process. Then,*

(1) $P = \sum_{k=0}^{\infty} D_k$ is a $m \times m$ conservative matrix, and each state is sojourned.

(2) Let $E^* = \{(n, j), n \in \mathbb{N}, e_j \in E\}$ and

$$P^* = \begin{pmatrix} D_0 & D_1 & D_2 & D_3 & \cdots \\ 0 & D_0 & D_1 & D_2 & \cdots \\ 0 & 0 & D_0 & D_1 & \cdots \\ 0 & 0 & 0 & D_0 & \cdots \\ \vdots & \vdots & \vdots & \vdots & \ddots \end{pmatrix}. \tag{3}$$

Then, P^* is a $E^* \times E^*$ conservative matrix, and each state is sojourned.

(3) P and P^* are both regular.

Definition 2. Given the numerical characteristics of batch Markovian arrival process $(D_0, D_k\,(k \in \mathbb{N}_+))$, let $X^* = \{X^*(t), t \in \mathbb{N}\}$ be a stochastic process with transition probability matrix P^* and $X^*(t) = (N(t), J(t))$ be a two-dimensional discrete-time batch Markovian process. Let $\alpha = (\alpha_1, \alpha_2, \ldots, \alpha_m)^T$ be the initial probability distribution vector of X^*, which satisfied $\sum_{j=1}^{m} \alpha_j = 1$. We call X^* as a discrete-time batch Markovian arrival process (DTBMAP); for short, we can denote it as DTBMAP $(\alpha^T, D_0, D_k\,(k \in \mathbb{N}_+))$. $N = \{N(t), t \in \mathbb{N}\}$ is called the counting process and $J = \{J(t), t \in \mathbb{N}\}$ is called the phase process.

The BMAP is one of the most flexible stochastic processes and is defined as a specific Markov chain (MC). More precisely, the BMAP consists of two different processes with discrete state space. One process represents the dynamics of internal state called phase process, and the other process corresponds to the number of events, i.e., the counting process like a binomial process. The phase process is usually modeled by a MC, and the counting process is modulated by the phase process. In fact, Markov-modulated Bernoulli process and discrete-time platoon arrival process, which are specific and subclasses of BMAP, have been utilized to evaluate the information communication systems based on the queueing analysis and finance. BMAP enables one to capture the realistic assumptions as much as possible and provide solutions that practitioners can implement.

2.3. Modified Model. The model we considered in this paper can be described by

$$U(n) = u + \sum_{k=1}^{n} c(k) - \sum_{k=1}^{N(n)} X(k), \quad n = 0, 1, 2, \ldots, \tag{4}$$

where $N(n)$ is the counting process of DTBMAP $(\alpha^T, D_0, D_k\,(k \in \mathbb{N}_+))$ with state space $E^* = \{(n, j), n \in \mathbb{N}, j \in E = \{e_1, e_2, e_3, \ldots, e_m\}\}$. $c(k)$ and $X(k)$, representing the size of the kth premium and claim, respectively, are both dependent on the state of the phase process $J(n)$ of DTBMAP $(\alpha^T, D_0, D_k\,(k \in \mathbb{N}_+))$. That is, given

$J(k) = e_i (\in E)$, $c(k)$ is i.i.d. variable with the common binomial distribution $B(p_i)(p_i \in (0,1], q_i = 1 - p_i)$ and $X(k)$ is i.i.d. positive and integer-valued stochastic series with the mean μ_i and the common distribution $P(X(k) = x) = f_i(x), x = 1, 2, \ldots$. Denote $F_i(k) = P(X(k) \geq x) = \sum_{j=1}^{k} f_i(j)$ with $F_i(0) = 0$. And assume $J(n)$, $N(n), X(n)$, and $c(n)$ are independent.

We should note the following: (1) d_{ii}^0 gives the probability of no state changes without claim arrivals; (2) $d_{ij}^0 (i \neq j)$ gives the probability of state i changes to state j without claim arrivals; (3) $d_{ii}^k (k \in \mathbb{N}_+)$ gives the probability of no state changes with k claims arrival; (4) $d_{ij}^k (i \neq j, k \in \mathbb{N}_+)$ gives the probability of state i changes to state j with k claims arrival. Furthermore, every insurer would want to make a profit. That is, the expected claim size over a single period is strictly inferior to the premium size, i.e.,

$$\sum_{e_i \in E} \sum_{e_j \in E} \sum_{k=0}^{\infty} \alpha_i d_{ij}^k p_j = (1 + \lambda) \sum_{e_i \in E} \sum_{e_j \in E} \sum_{k=1}^{\infty} \alpha_i d_{ij}^k k \mu_j, \tag{5}$$

where $\lambda > 0$ is the safety factor.

Before introducing the main results, we should point out that the DTBMAP is very general. On the one hand, it may represent a renewal process where the interclaim times follow binomial distributions and negative binomial distribution or even discrete-time phase-type distributions. On the other hand, it allows for situations where numbers of claim time and claim size random variables are dependent.

Remark 1. When $E = \{e_1\}, D_0 = p, D_1 = q = 1 - p$, and $D_k = 0 (k \geq 2, k \in \mathbb{N}_+)$, the compound binomial model with DTBMAP $(\alpha^T, D_0, D_k (k \in \mathbb{N}_+))$ degenerates to the compound binomial model. When $E = \{e_1, e_2, \ldots, e_m\} (m \geq 2)$, $D_0 = \operatorname{diag}(p)_{m\times m}, D_1 = \operatorname{diag}(1 - p)_{m\times m}$, and $D_k = 0_{m\times m} (k \geq 2, k \in \mathbb{N}_+)$, then it is the Markov-modulated compound binomial model, a degenerate case of the compound binomial model with DTBMAP $(\alpha^T, D_0, D_k (k \in \mathbb{N}_+))$.

3. Ruin Probability

3.1. Introduction. We define the time of ruin as

$$\tau = \inf\{k \in \mathbb{N}, U(k) < 0\}. \tag{6}$$

If ruin never occurs, $\tau = \infty$. Also, let us define the conditional finite-time ruin probability as

$$\psi(u, n \mid e_i) = P(\tau \leq n \mid J(0) = e_i)(e_i \in E) \tag{7}$$

and conditional finite-time non-ruin probability as

$$\varphi(u, n \mid e_i) = 1 - \psi(u, n \mid e_i)(e_i \in E). \tag{8}$$

Denote

$$\overrightarrow{\varphi}(u, n) = (\varphi(u, n \mid e_1)\varphi(u, n \mid e_2)\varphi(u, n \mid e_3) \cdots \varphi(u, n \mid e_m))_{1\times m}^T. \tag{9}$$

Obviously, we can see that the unconditional finite-time ruin and nonruin probability, $\psi(u, n)$ and $\varphi(u, n)$, can be derived from the conditional ones with following formulas, respectively:

$$\begin{aligned} \psi(u, n) &= \sum_{e_i \in E} \alpha_i \psi(u, n \mid e_i), \\ \varphi(u, n) &= \sum_{e_i \in E} \alpha_i \varphi(u, n \mid e_i) = \alpha^T \overrightarrow{\varphi}(u, n). \end{aligned} \tag{10}$$

For convenience, we also define the infinite-time ones by simply letting $n \longrightarrow \infty$ in our previous conditional or unconditional finite-time ruin or nonruin probabilities. Thus, if we obtain the conditional finite-time ruin probability, all of ruin probabilities of this model are solved.

3.2. Main Result. For convenience, in the next article, we denote

$$\mathbf{h}^j(x) = \left(h_1^j(x) \;\; h_2^j(x) \;\; h_3^j(x) \;\; \cdots \;\; h_m^j(x) \right)_{1\times m}^T, \tag{11}$$

where $h_i^j(x) (i = 1, 2, \ldots, m)$ is a function of x.

Theorem 1. *In the compound binomial model with DTBMAP $(\alpha^T, D_0, D_k (k \in \mathbb{N}_+))$, the conditional finite-time nonruin probabilities satisfy the following recursive formula:*

$$\begin{aligned} \overrightarrow{\varphi}(u, n + 1) = {} & D_0 \times \mathbf{P} \times \overrightarrow{\varphi}(u + 1, n) \\ & + D_0 \times (\mathbf{I} - \mathbf{P}) \times \overrightarrow{\varphi}(u, n) \\ & + \sum_{k=1}^{\infty} D_k \times \mathbf{P} \times \mathbf{h}^1(u.n) \\ & + \sum_{k=1}^{\infty} D_k \times (\mathbf{I} - \mathbf{P}) \times \mathbf{h}^2(u.n), \end{aligned} \tag{12}$$

where $\mathbf{P} = diag(p_1, p_2, \ldots, p_m)$ *and* $I = diag(1, 1, \ldots, 1)$. *Then,*

$$\begin{aligned} h_i^1(u.n) &= \sum_{y=0}^{u} f_i^{*(k)}(y + 1)\varphi(u - y, n \mid e_i), \\ h_i^2(u.n) &= \sum_{y=1}^{u} f_1^{*(k)}(y)\varphi(u - y, n \mid e_1), \end{aligned} \tag{13}$$

where $g^{*(k)}(y)$ represents the kth convolution of $g(y)$. And

$$\begin{gathered} \forall e_i \in E, \varphi(0, 1 \mid e_i) = 1 - \sum_{e_j \in E} d_{ij}^0 - \sum_{e_j \in E} d_{ij}^1 p_j f_j(1), \\ \forall u \in \mathbb{N}, \forall e_i \in E, \varphi(u, 0 \mid e_i) = 1. \end{gathered} \tag{14}$$

Proof. We can separate some possible cases by conditioning on the r.v.'s $J(1), N(1), c(1)$, and $X(1)$. There are possible cases as follows:

(1) No state changes and no claim arrivals
(2) State i changes to state $j (i \neq j)$ and no claim arrivals
(3) No state changes and $k (k \geq 1)$ claims arrival
(4) State i changes to state $j (i \neq j)$ and $k (k \geq 1)$ claims arrival

Then, the following formula can be easily derived by using the formula of full probability and the Markov property. For all $e_i \in E$, we have

$$\begin{aligned}\varphi(u,n+1\mid e_i) &= \sum_{e_j\in E} d_{ij}^0\left[p_j\varphi\left(u+1,n\mid e_j\right)+q_j\varphi\left(u,n\mid e_j\right)\right]\\&+\sum_{e_j\in E}\sum_{k=1}^{\infty} d_{ij}^k\left[p_j\sum_{y=1}^{u+1} f_j^{*(k)}(y)\varphi\left(u+1-y,n\mid e_j\right)+q_j\sum_{y=1}^{u} f_j^{*(k)}(y)\varphi\left(u-y,n\mid e_j\right)\right].\end{aligned} \tag{15}$$

Thus, (12) is derived when we rewrite (15) into the matrix form.

In order to proof the following theorem, some definitions are required to be introduced. Let $V_i(n)=\sum_{l=1}^{N(n)} I_{\{J(l)=e_i\}}$ be the elapsed time by the phase process $J(n)$ in state e_i over the first k periods where $I_A=1$ if A is true and $I_A=0$ if A is false. We also denote $W_i(n)$ the amount of decrease of the surplus process over the first n periods when the phase process $J(n)$ is in state e_i, i.e., $W_i(n)=\sum_{l=1}^{N(n)}(X(l)-c(l))I_{\{J(l)=e_i\}}$. Denote $W(n)$ as the amount of decrease of the surplus process over the first n periods. Furthermore, $X_i(n)$ and $c_i(n)$ are denoted as the nth premium amount and claim size when the phase process $J(n)$ is in state e_i, respectively.

Proposition 2. *The infinite-time ruin probability tends to 0 as initial surplus u tends to ∞.*

Proof. Obviously, we can see $W(n)=\sum_{e_i\in E} W_i(n)$.

Taking the limit as $n\longrightarrow\infty$ of $W(n)/n$ yields

$$\lim_{n\longrightarrow\infty}\frac{W(n)}{n}=\lim_{n\longrightarrow\infty}\sum_{e_i\in E}\frac{W_i(n)}{n}=\sum_{e_i\in E}\lim_{n\longrightarrow\infty}\frac{W_i(n)}{V_i(n)}\times\frac{V_i(n)}{n}. \tag{16}$$

Since $J(n)$ is irreducible and ergodic, it follows that

$$\lim_{n\longrightarrow\infty}\frac{V_i(n)}{n}=\xi_i, \tag{17}$$

where $\xi=(\xi_1,\xi_2,\ldots,\xi_m)$ is the stationary distribution of $J(n)$.

We can easily see that for given $J(n)=e_i$, $X(n)$ and $c(n)$ are both i.i.d. and $W_i(n)$ is distributed as $\sum_{l=1}^{V_i(n)}(X_i(l)-c_i(l))$. Because the phase process $J(n)$ is irreducible, $\lim_{n\longrightarrow\infty} V_i(n)=\infty$:

$$\begin{aligned}\lim_{n\longrightarrow\infty}\frac{W_i(n)}{V_i(n)}&=\lim_{n\longrightarrow\infty}\frac{\sum_{l=1}^{V_i(n)}(X_i(l)-c_i(l))}{V_i(n)}\\&=\lim_{n\longrightarrow\infty}\frac{\sum_{l=1}^{n}(X_i(l)-c_i(l))}{n}=\lim_{n\longrightarrow\infty}\frac{L_i(n)}{n}.\end{aligned} \tag{18}$$

where $L_i(n)=\sum_{l=1}^{n}(X_i(l)-c_i(l))$. Therefore, $\{L_i(n)\}$ is a random walk for $e_i\in E$ and from the strong law of large numbers, we can find $\forall e_i\in E$:

$$\lim_{n\longrightarrow\infty}\frac{L_i(n)}{n}=E\left[X_i(l)-c_i(l)\right]=\mu_i-p_i. \tag{19}$$

By combining (16) to (19), we can obtain that

$$\lim_{n\longrightarrow\infty}\frac{W(n)}{n}=\sum_{e_i\in E}\alpha_i(\mu_i-p_i). \tag{20}$$

Equation (20) and the safety loading condition imply that $\lim_{n\longrightarrow\infty} W(n)=-\infty$ and thus ensure that $\max_{n\in\mathbb{N}} W(n)$ is finite. Consequently,

$$\lim_{n\longrightarrow\infty}\psi(u)=\lim_{n\longrightarrow\infty}P\left(\max_{n\in\mathbb{N}} W(n)>u\right)=0. \tag{21}$$

Theorem 2. *In the compound binomial model with DTBMAP $(\alpha^T, D_0, D_k(k\in\mathbb{N}_+))$, the numerical algorithm proposed to obtain the conditional finite-time nonruin probabilities is as follows:*

Fix $\varphi(u\mid e_i)=1$ for $u=n,n+1,n+2,\ldots$ and $e_i\in E$.

Find $\varphi(u\mid e_i)$ for $u=0,1,2,\ldots,n$ and $e_i\in E$ by solving the following system of $m\times n$ equations with $m\times n$ unknown parameters:

$$\begin{aligned}\varphi(u\mid e_i)&=\sum_{e_j\in E} d_{ij}^0\left[p_j\varphi\left(u+1\mid e_j\right)+q_j\varphi\left(u\mid e_j\right)\right]\\&+\sum_{e_j\in E}\sum_{k=1}^{\infty} d_{ij}^k\left[\sum_{y=1}^{u+1} p_j f_j(y)\varphi\left(u+1-y\mid e_j\right)+\sum_{y=1}^{u} q_j f_j(y)\varphi\left(u-y\mid e_j\right)\right].\end{aligned} \tag{22}$$

Proof. First, by conditioning, respectively, on the random variables $J(1), N(1), c(1)$, and $X(1)$, four cases probably occurred. And from the stationarity of the surplus process, we can find

$$\varphi(u \mid e_i) = \sum_{e_j \in E} d_{ij}^0 \left[p_j \varphi(u+1 \mid e_j) + q_j \varphi(u \mid e_j) \right] + \sum_{e_j \in E} \sum_{k=1}^{\infty} d_{ij}^k \left[\sum_{y=1}^{u+1} p_j f_j(y) \varphi(u+1-y \mid e_j) + \sum_{y=1}^{u} q_j f_j(y) \varphi(u-y \mid e_j) \right], \tag{23}$$

for $e_i \in E$ and $u \in \mathbb{N}$. Given that $\varphi(u \mid e_i) = 1$ for $u = n, n+1, n+2, \ldots$ and $e_i \in E$, we must solve the system of $m \times n$ equations-$m \times n$ unknown parameters given by equation (23) for $u = 0, 1, 2, \ldots, n$ and $e_i \in E$.

4. Compound Binomial Model with BMAP and Dividend

In this section, we will embed a threshold dividend strategy in the compound binomial model with BMAP $(\alpha^T, D_0, D_k (k \in \mathbb{N}_+))$. First, we will introduce the specific description of this model.

4.1. Description. Based on the compound binomial model with BMAP $(\alpha^T, D_0, D_k (k \in \mathbb{N}_+))$, we can define the compound binomial model with BMAP $(\alpha^T, D_0, D_k (k \in \mathbb{N}_+))$ and threshold dividend strategy. The surplus process of an insurer is given by

$$\begin{cases} V(n) = \left\{ c(n) - \sum_{k=N(n-1)}^{N(n)} X(k), b \right\}, & n \in \mathbb{N}_+; \\ V(0) = u. \end{cases} \tag{24}$$

where $N(n), c(n)$, and $X(n)$ are entirely the same as the description in model (4). $b\,(>0)$ is the dividend threshold, i.e., if the surplus of an insurer is greater than b, the exceed part will pay out as dividend to the shareholders and if the surplus of an insurer is smaller than b, nothing is needed to do. And we should point out the assumption that the dividend is paid out after the premium is received and claims are paid out.

Similarly, we define the ruin time of this model as

$$\tau_b = \inf\{k \in \mathbb{N}, V(k) < 0\}. \tag{25}$$

If ruin never occurs, $\tau_b = \infty$.

4.2. Gerber–Shiu Function. The Gerber–Shiu function, also called expected discounted penalty function, was first introduced by Gerber–Shiu [1]. Many papers and books have studied it.

Definition 3. The Gerber–Shiu function is defined by

$$m(u) = E\left[v^{\tau_b} w\left(U(\tau_b - 1), |U(\tau_b)|\right) I_{\{\tau_b < \infty\}} \,\middle|\, U(0) = u \right], \tag{26}$$

where $v \in (0, 1]$ is the discount factor, $w(\cdot,\cdot)$: $\mathbb{N}_+ \times \mathbb{N}_+ \longrightarrow \mathbb{N}$ is a binary function, and $U(\tau_b - 1)$ represents the surplus before ruin. $|U(\tau_b)|$ represents the deficit at ruin, and $I(A)$ is the indicator function of an event A taking value 1 whenever the event A occurs and 0 when it does not.

The Gerber–Shiu function plays an important role in risk theory. When $w(\cdot,\cdot) \equiv 1$ and $v = 1$, the Gerber–Shiu function changes to the ruin probability. When $w(x, y) = x$, it changes to the discounted surplus before ruin time. When $w(x, y) = y$, it changes to the discounted deficit at ruin. Studying on the Gerber–Shiu function can understand this model more deeply and enable to properly handle the operations of an insurance company.

To solve the problem, we denote some auxiliary functions. Denote the conditional Gerber–Shiu function as

$$m(u \mid e_i) = E\left[v^{\tau_b} w\left(U(\tau_b - 1), |U(\tau_b)|\right) I_{\{\tau_b < \infty\}} \,\middle|\, U(0) = u, J(0) = e_i \right], \tag{27}$$

and denote

$$\mathbf{m}(u) = \left(m(u \mid e_1) m(u \mid e_2) m(u \mid e_3) \cdots m(u \mid e_m)\right)_{1\times m}^T. \tag{28}$$

We can easily see that

$$m(u) = \sum_{e_i \in E} \alpha_i m(u \mid e_i) = \alpha^T \mathbf{m}(u). \tag{29}$$

Thus, we can solve the Gerber–Shiu function $m(u)$ by solving $m(u \mid e_i)$. Next, we will derive the solution of $m(u \mid e_i)$.

Theorem 3. *In the compound binomial model with DTBMAP $(\alpha^T, D_0, D_k (k \in \mathbb{N}_+))$ and dividend threshold b, the conditional Gerber–Shiu functions satisfy the following recursive formula.*

For $u = 0, 2, \ldots, b-1$,

$$\mathbf{m}(u) = vD_0 \times \mathbf{P} \times \mathbf{m}(u+1) + vD_0 \times (\mathbf{I} - \mathbf{P}) \times \mathbf{m}(u) + v\sum_{k=1}^{\infty} D_k \times \mathbf{P} \times \mathbf{h}^3(u) + v\sum_{k=1}^{\infty} D_k \times (\mathbf{I} - \mathbf{P}) \times \mathbf{h}^4(u), \tag{30}$$

where

$$h_i^3(u)=\sum_{y=1}^{u} f_i^{*(k)}(y+1)m(u-y\mid e_i)+\sum_{y=1}^{\infty} f_i^{*(k)}(y+1+u)w(u,y),$$
$$h_i^4(u)=\sum_{y=0}^{u} f_1^{*(k)}(y)m(u-y\mid e_1)+\sum_{y=1}^{\infty} f_1^{*(k)}(y+u)w(u,y), \tag{31}$$

and for $u=b,b+1,\ldots,$

$$\mathbf{m}(u)=\nu D_0\times\mathbf{m}(b)+\nu\sum_{k=1}^{\infty}D_k\times\mathbf{P}\times\mathbf{h}^5(u)+\nu\sum_{k=1}^{\infty}D_k\times(\mathbf{I}-\mathbf{P})\times\mathbf{h}^6(u), \tag{32}$$

where

$$h_i^5(u)=\sum_{y=0}^{u-b} f_i^{*(k)}(y+1)m(b\mid e_i)+\sum_{y=u-b+1}^{u} f_i^{*(k)}(y+1)m(u-y\mid e_i)+\sum_{y=1}^{\infty} f_i^{*(k)}(y+1+u)w(u,y),$$
$$h_i^6(u)=\sum_{y=1}^{u-b} f_i^{*(k)}(y)m(b\mid e_i)+\sum_{y=u-b+1}^{u} f_i^{*(k)}(y)m(u-y\mid e_i)+\sum_{y=1}^{\infty} f_i^{*(k)}(y+u)w(u,y). \tag{33}$$

Proof. Similarly, by conditioning on $J(1),N(1),c(1)$, and $X(1)$, we can derive that for $u=b,b+1,\ldots,$

$$\begin{aligned}
m(u\mid e_i)&=\sum_{e_j\in E}d_{ij}^0\left[p_jm(b|e_j)+q_jm(b|e_j)\right]\\
&\quad+\sum_{e_j\in E}\sum_{k=1}^{\infty}d_{ij}^k\Bigg\{\sum_{y=1}^{\infty}p_jf_j^{*(k)}(y)\left[m(b\mid e_j)I_{\{u+1-y>b\}}+m(u+1-y\mid e_j)I_{\{0\le u+1-y\le b\}}+w(u,y-u-1)I_{\{u+1-y<0\}}\right]\\
&\quad+\sum_{y=1}^{\infty}q_jf_j^{*(k)}(y)\left[m(b\mid e_j)I_{\{u-y>b\}}+m(u-y\mid e_j)I_{\{0\le u-y\le b\}}+w(u,y-u)I_{\{u-y<0\}}\right]\Bigg\}\\
&=\sum_{e_j\in E}d_{ij}^0m(b\mid e_j)+\sum_{e_j\in E}\sum_{k=1}^{\infty}d_{ij}^kp_j\left\{\sum_{y=0}^{u-b}f_j^{*(k)}(y+1)m(b\mid e_j)+\sum_{y=u-b+1}^{u}f_j^{*(k)}(y+1)m(u-y\mid e_j)+\sum_{y=1}^{\infty}f_j^{*(k)}(y+1+u)w(u,y)\right\}\\
&\quad+\sum_{e_j\in E}\sum_{k=1}^{\infty}d_{ij}^kq_j\left\{\sum_{y=1}^{u-b}f_j^{*(k)}(y)m(b\mid e_j)+\sum_{y=u-b+1}^{u}f_j^{*(k)}(y)m(u-y\mid e_j)+\sum_{y=1}^{\infty}f_j^{*(k)}(y+u)w(u,y)\right\}.
\end{aligned} \tag{34}$$

But for $u=0,2,\ldots,b-1$,

$$m(u\mid e_i)=\sum_{e_j\in E}d_{ij}^0\left[p_jm(u+1\mid e_j)+q_jm(u\mid e_j)\right]+\sum_{e_j\in E}\sum_{k=1}^{\infty}d_{ij}^k\left[\sum_{y=1}^{u+1}p_jf_j(y)m(u+1-y\mid e_j)+\sum_{y=1}^{u}q_jf_j(y)m(u-y\mid e_j)\right]. \tag{35}$$

Rewrite the abovementioned equations into matrix, and we can derive the theorem.

Remark 2. When we want to calculate $m(u\mid e_i)$, we can perform the following:

> Choose $u=0,1,2,\ldots,b$; then, we can derive an equation system containing $m(b+1)$ equations with $m(b+1)$ unknown numbers. The solutions of the equation system are just $m(u\mid e_i), e_i\in E, u=0,1,2,\ldots,b$.
>
> $m(u\mid e_i), e_i\in E, u\ge b+1$, can be calculated by (32).

4.3. Discounted Dividend Value. For the risk model with dividend, we are also interested in the expected discounted dividend value of all dividends up to the ruin time in general. Especially in shareholders' standpoint, the dividend value is the aim and the only focus thing. So, we will discuss research on the expected discounted dividend value of all dividends up to the ruin time. Let $\gamma\,(0<\gamma\le 1)$ denote the discounted factor, $B_1(u\,|\,e_i)$ denote the expected discounted dividend value of the first dividend under the conditions $V(0)=u$ and $J(0)=e_i$, $B_1(u\,|\,e_i)$ denote the expected discounted dividend value of all dividends up to the ruin time under the conditions $V(0)=u$ and $J(0)=e_i$, and $B(u)$ denote the expected discounted dividend value of all dividends up to the ruin time under the conditions $V(0)=u$.

Theorem 4. *In the compound binomial model with DTBMAP $(\alpha^T, D_0, D_k\,(k\in\mathbb{N}_+))$ and dividend threshold b, we have*

(1) $B_1(u\,|\,e_i)=\gamma(u-b)$ for $e_i\in E$ and $u>b$.

(2) For $e_i\in E$,

$$B_1(b\,|\,e_i)=\gamma\sum_{e_j\in E}d_{ij}^0\left[p_j+q_jB_1\left(b\,|\,e_j\right)\right]+\gamma\sum_{e_j\in E}\sum_{k=1}^{\infty}d_{ij}^k\left[\sum_{y=1}^{u+1}p_jf_j(y)B_1\left(u+1-y\,|\,e_j\right)+\sum_{y=1}^{u}q_jf_j(y)B_1\left(u-y\,|\,e_j\right)\right]. \quad (36)$$

(3) $D_1(u\,|\,e_i)$, for $e_i\in E$ and $u<b$, satisfied the following recursive formula:

$$\mathbf{B}_1(u)=\gamma D_0\times\mathbf{P}\times\mathbf{B}_1(u+1)+\gamma D_0\times(\mathbf{I}-\mathbf{P})\times\mathbf{B}_1(u)+\gamma\sum_{k=1}^{\infty}D_k\times\mathbf{P}\times\mathbf{h}^7(u)+\gamma\sum_{k=1}^{\infty}D_k\times(\mathbf{I}-\mathbf{P})\times\mathbf{h}^8(u), \quad (37)$$

where

$$\begin{aligned}\mathbf{B}_1(u)&=\left(B_1(u\,|\,e_1)B_1(u\,|\,e_2)B_1(u\,|\,e_3)\cdots B_1(u\,|\,e_m)\right)_{1\times m}^T,\\ h_i^7(u)&=\sum_{y=1}^{u}f_1^{*(k)}(y+1)B_1(u-y\,|\,e_1),\\ h_i^8(u)&=\sum_{y=0}^{u}f_1^{*(k)}(y)B_1(u-y\,|\,e_1).\end{aligned} \quad (38)$$

Theorem 5. *In the compound binomial model with DTBMAP $(\alpha^T, D_0, D_k\,(k\in\mathbb{N}_+))$ and dividend threshold b, we have*

(1) $B(u\,|\,e_i)=\gamma(u-b)+\gamma B(b\,|\,e_i)$ for $e_i\in E$ and $u>b$.

(2) $B(u\,|\,e_i)$, $e_i\in E$, and $u\le b$ satisfied the following expression:

$$\mathscr{B}=\mathscr{A}^{-1}\mathscr{V}, \quad (39)$$

$$\begin{pmatrix}B(0)\\B(1)\\B(2)\\\vdots\\B(b)\end{pmatrix}=\begin{pmatrix}A_{00}&A_{01}&A_{02}&\cdots&A_{0b}\\A_{10}&A_{11}&A_{12}&\cdots&A_{1b}\\A_{20}&A_{21}&A_{22}&\cdots&A_{2b}\\\vdots&\vdots&\vdots&\ddots&\vdots\\A_{b0}&A_{b1}&A_{b2}&\cdots&A_{bb}\end{pmatrix}^{-1}\begin{pmatrix}v_1(0)\\v_1(1)\\v_1(2)\\\vdots\\v_1(b)\end{pmatrix}, \quad (40)$$

where

$$B(i)=\left(B(i\,|\,e_1)B(i\,|\,e_2)B(i\,|\,e_3)\cdots B(i\,|\,e_m)\right)_{1\times m}^T. \quad (41)$$

For $i=0,1,2,\ldots,b-1$,

$$\begin{aligned}v_1(i)&=\begin{pmatrix}0&0&0&\cdots&0\end{pmatrix}_{1\times m}^T,\\ v_1(b)&=\left(-\gamma\sum_{e_j\in E}d_{1j}^0p_j-\gamma\sum_{e_j\in E}d_{2j}^0p_j\right.\\&\qquad\left.-\gamma\sum_{e_j\in E}d_{3j}^0p_j\cdots-\gamma\sum_{e_j\in E}d_{mj}^0p_j\right)_{1\times m}^T,\end{aligned} \quad (42)$$

and $A_{sl}\,(s=0,1,\ldots,b,\,l=0,1,\ldots,b)$ is a series of $m\times m$ matrixes:

(1) $s+2\le l$, $A_{sl}=0_{m\times m}$

(2) $s+1=l$, $A_{sl}=(a_{ij})_{m\times m}$,

$$a_{ij}=\gamma d_{ij}^0p_j. \quad (43)$$

(3) $s=l$,

$$\begin{aligned}&s\ne b, A_{sl}=\left(b_{ij}\right)_{m\times m},\\ &\quad b_{ij}=\begin{cases}\gamma\left(q_id_{ii}^0+p_id_{ii}^1f_i(1)\right)-1, & i=j;\\ \gamma\left(q_jd_{ij}^0+p_jd_{ij}^1f_j(1)\right), & i\ne j.\end{cases}\\ &s=b, A_{bb}=\left(\widetilde{b}_{ij}\right)_{m\times m},\\ &\quad \widetilde{b}_{ij}=\begin{cases}\gamma\left(d_{ii}^0+p_id_{ii}^1f_i(1)\right)-1, & i=j;\\ \gamma\left(d_{ij}^0+p_jd_{ij}^1f_j(1)\right), & i\ne j.\end{cases}\end{aligned} \quad (44)$$

(4) $s>l$, $A_{sl}=(c_{ij})_{m\times m}$,

$$c_{ij}=\gamma\sum_{k=1}^{\infty}d_{ij}^k\left(p_jf_j^{*(k)}(s+1-l)+q_jf_j^{*(k)}(s-l)\right). \quad (45)$$

Proof. Similar to the method of the previous theorem, we can obtain a series of equations. Then, we can rewrite the equation system into matrix as follows:

$$\mathscr{A}\mathscr{B} = \mathscr{V}, \tag{46}$$

Hence, to prove this theorem, the most important thing is to prove that $\mathscr{A}$ is nonsingular.

It can be easily seen that since $f_j(x)$ is a probability distribution function, $\forall k = 1, 2, \ldots, m$ and $\forall e_j \in E$,

$$\sum_{x=1}^{\infty} f_j^{*k}(x) = 1. \tag{47}$$

In each r row, we can write $r = sn + l$.

(1) When $s \neq b$, we can see

$$\begin{aligned}
&\sum_{s>l}\sum_{e_j\in E}\sum_{k=1}^{\infty}\gamma d_{rj}^{k}\left(p_j f_j^{*(k)}(s+1-l) + q_j f_j^{*(k)}(s-l)\right) + \sum_{e_j\in E}\gamma\left(q_j d_{rj}^{0} + p_j d_{rj}^{1} f_j(1)\right) + \sum_{e_j\in E}\gamma d_{rj}^{0} p_j \\
&\quad = \sum_{e_j\in E}\left[\sum_{s>l}\sum_{k=1}^{\infty} d_{rj}^{k}\left(p_j f_j^{*(k)}(s+1-l) + q_j f_j^{*(k)}(s-l)\right) + \left(q_j d_{rj}^{0} + p_j d_{rj}^{1} f_j(1)\right) + d_{rj}^{0} p_j\right] \\
&\quad = \gamma \sum_{e_j\in E}\left[\sum_{s>l}\sum_{k=1}^{\infty} d_{rj}^{k}\left(p_j f_j^{*(k)}(s+1-l) + q_j f_j^{*(k)}(s-l)\right) + d_{rj}^{0} + p_j d_{rj}^{1} f_j(1)\right] \\
&\quad \leq \gamma \sum_{e_j\in E}\left[\sum_{k=1}^{\infty}\left[\sum_{s>l} d_{rj}^{k}\left(p_j f_j^{*(k)}(s+1-l) + p_j f_j^{*(k)}(1) + q_j f_j^{*(k)}(s-l)\right)\right] + d_{rj}^{0}\right] \\
&\quad = \gamma \sum_{e_j\in E}\left[\sum_{k=1}^{\infty}\left[\sum_{s>l} d_{rj}^{k}\left(p_j\left(f_j^{*(k)}(s+1-l) + f_j^{*(k)}(1)\right) + q_j f_j^{*(k)}(s-l)\right)\right] + d_{rj}^{0}\right] \\
&\quad \leq \gamma \sum_{e_j\in E}\left[\sum_{k=1}^{\infty}\left[\sum_{s>l} d_{rj}^{k}\left(p_j + q_j\right)\right] + d_{rj}^{0}\right] \\
&\quad = \gamma \sum_{e_j\in E}\sum_{k=0}^{\infty} d_{rj}^{k}.
\end{aligned} \tag{48}$$

Because $P = \sum_{k=0}^{\infty} D_k = (q_{ij})$ is a stochastic matrix, we can derive that

$$\sum_{e_j\in E}\sum_{k=0}^{\infty} d_{rj}^{k} = 1, \forall e_r \in E. \tag{49}$$

So by combining (48) with (49) we can derive

$$\begin{aligned}
&\sum_{s>l}\sum_{e_j\in E}\sum_{k=1}^{\infty}\gamma d_{rj}^{k}\left(p_j f_j^{*(k)}(s+1-l) + q_j f_j^{*(k)}(s-l)\right) \\
&\quad + \sum_{e_j\in E}\gamma\left(q_j d_{rj}^{0} + p_j d_{rj}^{1} f_j(1)\right) + \sum_{e_j\in E}\gamma d_{rj}^{0} p_j \leq \gamma.
\end{aligned} \tag{50}$$

Inequality (50) can be written into

$$\begin{aligned}
&\sum_{s>l}\sum_{e_j\in E}\sum_{k=1}^{\infty}\gamma d_{rj}^{k}\left(p_j f_j^{*(k)}(s+1-l) + q_j f_j^{*(k)}(s-l)\right) \\
&\quad + \sum_{e_j\neq e_r}\gamma\left(q_j d_{rj}^{0} + p_j d_{rj}^{1} f_j(1)\right) + \sum_{e_j\in E}\gamma d_{rj}^{0} p_j \\
&\quad \leq \gamma - \gamma\left(q_r d_{rr}^{0} + p_r d_{rr}^{1} f_r(1)\right) \\
&\quad \leq 1 - \gamma\left(q_r d_{rr}^{0} + p_r d_{rr}^{1} f_r(1)\right) \\
&\quad = \left|\gamma\left(q_r d_{rr}^{0} + p_r d_{rr}^{1} f_r(1)\right) - 1\right|.
\end{aligned} \tag{51}$$

That is,

$$\sum_{e_j\in E} a_{rj} + \sum_{e_j\neq e_r} b_{rj} + \sum_{e_j\in E} c_{rj} \leq \left|b_{rr}\right|. \tag{52}$$

(2) When $s = b$, by using the same method, we can also obtain

$$\begin{aligned}
&\sum_{s>l}\sum_{e_j\in E}\sum_{k=1}^{\infty}\gamma d_{rj}^{k}\left(p_j f_j^{*(k)}(s+1-l) + q_j f_j^{*(k)}(s-l)\right) \\
&\quad + \sum_{e_j\neq e_r}\gamma\left(d_{rj}^{0} + p_j d_{rj}^{1} f_j(1)\right) + \sum_{e_j\in E}\gamma d_{rj}^{0} p_j \\
&\quad \leq \gamma - \gamma\left(d_{rr}^{0} + p_r d_{rr}^{1} f_r(1)\right) \\
&\quad \leq 1 - \gamma\left(d_{rr}^{0} + p_r d_{rr}^{1} f_r(1)\right) \\
&\quad = \left|\gamma\left(d_{rr}^{0} + p_r d_{rr}^{1} f_r(1)\right) - 1\right|.
\end{aligned} \tag{53}$$

That is,

$$\sum_{e_j\in E} a_{rj} + \sum_{e_j\neq e_r} \widetilde{b}_{rj} + \sum_{e_j\in E} c_{rj} \leq \left|\widetilde{b}_{rr}\right|. \tag{54}$$

Inequality (52) and inequality (54) lead to that the absolute value of diagonal (the rth element in the rth row) is

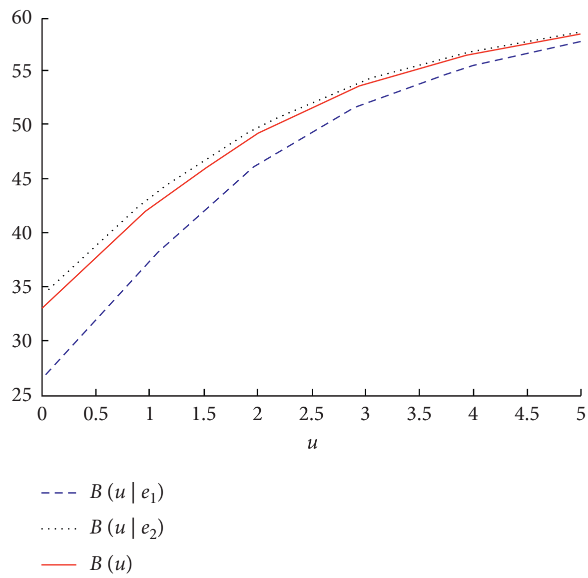

Figure 1: Value of all dividends $p_1 = 2/3$ and $p_2 = 3/4$.

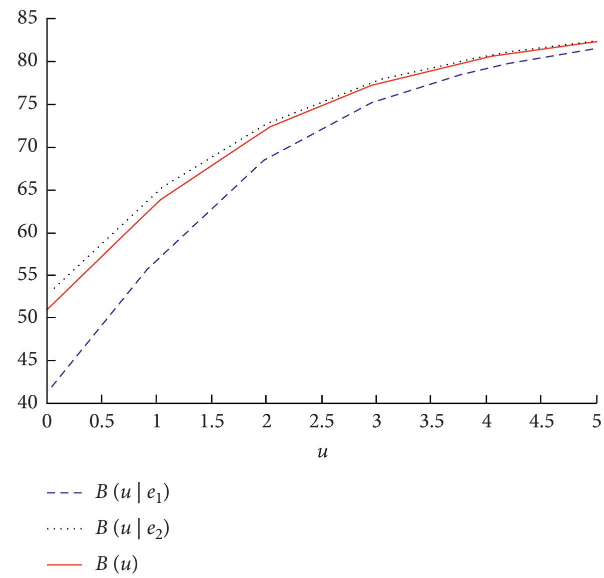

Figure 2: Value of all dividends $p_1 = 3/4$ and $p_2 = 3/4$.

greater than the sum of others in this row. For r being a arbitrary, $\mathscr{A}$ is a (row) strictly diagonally dominant matrix. Hence, $\mathscr{A}$ is nonsingular, which leads to the result.

5. Numerical illustration

Example 1. Let $\gamma = 1, b = 5, E = \{e_1, e_2\}$, and $\alpha = (5/6, 1/6)^T$. The matrixes are given as follows:

$$D_0 = \begin{pmatrix} 3/4 & 1/16 \\ 1/2 & 1/18 \end{pmatrix},$$
$$D_1 = \begin{pmatrix} 1/16 & 1/16 \\ 2/9 & 1/36 \end{pmatrix}, \quad (55)$$
$$D_2 = \begin{pmatrix} 1/32 & 1/32 \\ 1/6 & 1/36 \end{pmatrix}.$$

When $k \geq 3$, we let $D_k = \mathbf{0}_{2\times 2}$. And assume $f_1(1) = 3/4$, $f_1(2) = 1/4$, $f_2(1) = 2/3$, and $f_2(2) = 1/3$. Then, $f_1^{*(2)}(2) = 9/16$, $f_1^{*(2)}(3) = 3/8$, $f_1^{*(2)}(4) = 1/16$, $f_2^{*(2)}(2) = 4/9$, $f_2^{*(2)}(3) = 4/9$, $f_2^{*(2)}(4) = 1/9$, $\mu_1 = 5/4$, and $\mu_2 = 4/3$. From it, we can see that e_1 is a "good" state, but e_2 is a "bad" state. Our example is structured in order to differentiate the "good "state and "bad" state, so we can see the difference between $B(u|e_1)$ and $B(u|e_2)$. When we let $p_1 = 2/3$ and $p_2 = 3/4$, we can obtain the expected dividend value of all dividends up to the ruin time by using Theorem 5. All results are shown in Figure 1.

In order to reflect the effect of each factor, we let $p_1 = 3/4, p_2 = 3/4$; $p_1 = 3/4, p_2 = 4/5$; and $p_1 = 4/5$, $p_2 = 3/4$, respectively, for comparison. The results of the situations $p_1 = 3/4, p_2 = 3/4$; $p_1 = 3/4, p_2 = 4/5$; and $p_1 = 4/5, p_2 = 3/4$ are shown in Figures 2–4, respectively.

Combining all results, we can analyze the following:

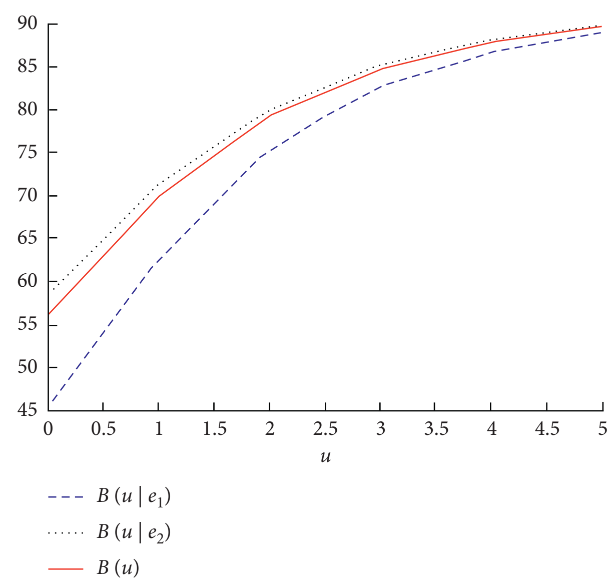

Figure 3: Value of all dividends $p_1 = 3/4$ and $p_2 = 4/5$.

(1) $B(u)$ is gradually increased with the increase of initial surplus u

(2) For a given e_i, $B(u \mid e_i)$ is gradually increased with the increase of initial surplus u

(3) When the initial surplus u is more and more big, the difference between $B(u|e_1)$ and $B(u|e_2)$ is more and more small

(4) For e_1 is a "good" state and e_2 is a "bad" state, $B(u|e_1)$ is larger than $B(u|e_2)$ when u is equal

(5) $B(u)$ is larger than $B(u|e_2)$, but smaller than $B(u|e_1)$ when initial surplus u is equal

(6) The safety factor is larger and the expected dividend value of all dividends up to the ruin time is larger when initial surplus u is equal

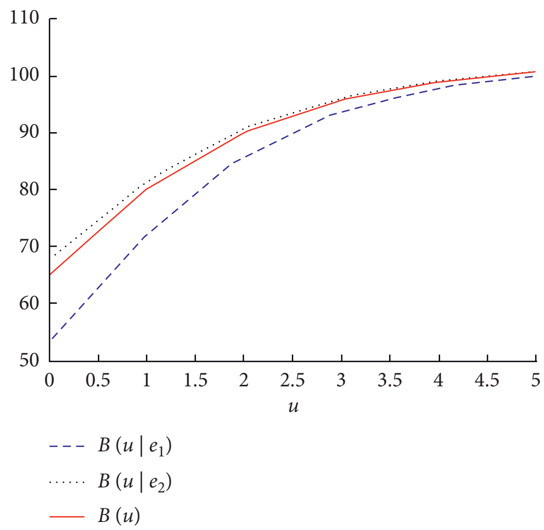

FIGURE 4: Value of all dividends $p_1 = 4/5$ and $p_2 = 3/4$.

Data Availability

The data used to support the findings of this study are currently under embargo while the research findings are commercialized. Requests for data, 6 months after publication of this article, will be considered by the corresponding author.

Conflicts of Interest

The authors declare that they have no conflicts of interest.

Acknowledgments

This work was supported by theNational Natural Science Foundation (No. 11701175), the Hunan Natural Science Foundation (No. 2019JJ50024), and the Hunan Philosophy and Social Science Foundation (Nos. 17YBQ020 and 17YBA291).

References

[1] H. U. Gerber, "Mathematica l fun with the compound binomial process," *Astin Bulletin*, vol. 18, no. 2, pp. 161–168, 1988.

[2] E. Shiu, "The probability of eventual ruin in the compound binomial model," *Astin Bulletin*, vol. 19, no. 2, pp. 179–190, 1989.

[3] H. Cossette, D. Landriault, and E. Marceau, "Ruin probabilities in the compound markov binomoal model," *Scandinavian Actuarial Journal*, vol. 2003, no. 4, pp. 301–323, 2003.

[4] H. Wu, J. Tan, and X. Yang, "The expected present value of dividends in the compound binomial model with a constant dividend barrier," *Mathmatics in Economics*, pp. 41–46, 2010.

[5] X. Peng, W. Su, and W. Su, "On a perturbed compound Poisson risk model under a periodic threshold-type dividend strategy," *Journal of Industrial & Management Optimization*, vol. 16, no. 4, pp. 1967–1986, 2020.

[6] D. M. Zhang, "The BMAP/G/1 queue: a tutorial," in *Models and Techniques for Performance Evaluation of Computer and Communication Systems*, pp. 330–358, Springer-Verlag, Berlin, Germany, 1993.

[7] M. F. Neuts, *Structured Stochastic Matrices of M/G/1-type and Their Applications*, Marcel Dekker, New York, NY, USA, 1989.

[8] S. Ahn and A. L. Badescu, "On the analysis of the Gerber-Shiu discounted penalty function for risk processes with Markovian arrivals," *Insurance: Mathematics and Economics*, vol. 41, no. 2, pp. 234–249, 2007.

[9] C. K. Eric, C. David Landriaultb, and L. B. Andrei, "On a generalization of the risk model with markovian claim arrivals," *Stochastic Models*, vol. 27, no. 3, pp. 407–430, 2011.

[10] R. J. Artalejo, Q. M. Gmez-Corral, and y. Antonio, "Markovian arrivals in stochastic modelling: a survey and some new results," *Statistics and Operations Research Transactions*, vol. 34, no. 2, pp. 101–156, 2012.

[11] H. Dong and Z.-m. Liu, "On a risk model with Markovian arrivals and tax," *Applied Mathematics-A Journal of Chinese Universities*, vol. 27, no. 2, pp. 150–158, 2012.

[12] A. L. Badescu, S. Drekic, and D. Landriault, "Analysis of a threshold dividend strategy for a MAP risk model," *Scandinavian Actuarial Journal*, vol. 2007, no. 4, pp. 227–247, 2007.

Hindawi
Mathematical Problems in Engineering
Volume 2020, Article ID 3984924, 13 pages
https://doi.org/10.1155/2020/3984924

Research Article

A Blockchain Prediction Model on Time, Value, and Purchase Based on Markov Chain and Queuing Theory in Stock Trade

Wenjuan Lian, Qi Fan, Bin Jia, and Yongquan Liang

College of Computer Science & Engineering, Shandong University of Science and Technology, Qingdao, Shandong 266590, China

Correspondence should be addressed to Bin Jia; jiabin@sdust.edu.cn

Received 18 March 2020; Accepted 8 June 2020; Published 9 November 2020

Academic Editor: Juan. P. Amezquita-Sanchez

With the continuous development of the blockchain, it has brought a subversive impact on the blossom of all fields with its characteristics of decentralization, trust-free, and tampering, especially in the financial field. It is of great significance to research the application of blockchain technology in the financial field. As an important part of the financial market, stock has the crucial influence, and the combination of stock and blockchain is becoming a growing trend. In recent years, many studies have focused on the prediction of the stock value, but they have not fully considered the combination of time, value, and purchase. To solve the above problem, we propose a preemption queuing model for multipriority service objects in the blockchain financial architecture according to different service priority. Meanwhile, a queuing-based resource scheduling model is established by using the Markov chain to find the optimal solution. The method in this paper can greatly improve the efficiency of the system and provide a basis for future scientific research in the healthy and sustainable development of the securities industry.

1. Introduction

The cash stock market is the most popular and active capital market in the world. The rise of stocks is directly influenced by national policies. The stock market is also the engine and booster of national economic development. According to statistics, nowadays, it is an era of the national stock speculation. At present, China has more than 100 million investors in the stock market, and people pay more attention to the stock industry. However, due to the process of traditional asset management, such as equity and securities that take a long time, there is an increase in the intermediate business cost, transaction fee, information fraud, disclosure, etc. Moreover, it is managed by different intermediaries, which not only increases the transaction cost of assets, but also causes the problem of certificate falsification. The emergence of the blockchain provides a solution for it, which can upgrade securities trading to the automatic execution of intelligent contracts. Since it allows payments to be finished without any bank or any intermediary, the blockchain can be used in various financial services such as digital assets, remittance, and online payment [1]. Through P2P trading transmission, it not only saves the intermediate process and reduces the cost and loss, but also guarantees the private security of trading information and changes the trading efficiency of the stock market. In addition, the Markov chain can select a decision-making from the available set of actions based on the observed state at each moment. At the same time, the system can make new decisions based on the observed newcome states. Markov chain can be used to conduct the dynamic optimization of the resource scheduling scheme in the stock trading process, and the optimal resource scheduling scheme can be found to ensure the timeliness of the transaction.

In 2008, Satoshi Nakamoto proposed an electronic cash system for bitcoin, which could be implemented through peer-to-peer (P2P) technology, allowing online payments to be initiated directly by one party to another without going through any financial institution [2]. This leads to the concept of "blockchain." The blockchain is one of the hot technologies, which appeared in the last decade and brought a lot of promise with it [3]. As the underlying key technology and infrastructure of bitcoin, the blockchain has attracted great attention from academia and industries. A blockchain, originally blockchain [4], is a growing list of records, called blocks, which are linked and secured by using cryptography [5]. Each block contains a cryptographic hash of the previous block [6], a timestamp, and transaction data. A blockchain is a decentralized, distributed, and public digital ledger that is used to record transactions across many computers so that any involved record cannot be altered retroactively, without the alteration of all subsequent blocks [7]. Blockchain technology has the key characteristics, such as decentralization, persistence, anonymity, and audibility. Blockchain can work in a decentralized environment and be realized by multiple core technologies such as the integrated password hash, the digital signature (based on asymmetric encryption), and the distributed consensus mechanism. Based on a distributed P2P network, blockchain technology combines consensus mechanism, smart contract, and privacy protection with the open source software to ensure the continuity and security of each node in the distributed database. These can make information instant verifiable and traceable, but it is difficult to change and revoke. Thus, blockchain technology is a set of private, efficient, safe, and shared value systems. Blockchain can serve not only to save the operating costs of the companies, but also to retrench the potential legal fees arose from disputes which could have been avoided [8]. In December 2013, Vitalik proposed Ethereum, a blockchain platform, which could realize digital currency transactions based on ether currency. Simultaneously, this platform can also provide a complete programming language to write a smart contract [9]. It is the first time that an intelligent contract is applied to the blockchain. Because the blockchain allows payments to be completed without any bank or agency, it could be used in various financial services [10, 11]. Besides, blockchain technology is applied in other scenarios, such as smart contracts [12], public services [13], Internet of Things (IoT) [14], reputation systems [15], and security services [16]. However, further work still needs to explore the full capabilities of the blockchain and where it can be adopted.

Markov chain was proposed by Andrey A. Markov, a Russian mathematician. It refers to the random transitioning process from one state space to another state space. This process requires memory-less properties. The probability distribution of the next state can only be determined by the current state, which has nothing to do with the original state or the Markov process before the transition. The probability function of a Markov chain is a random process generated by two interrelated mechanisms. One is a potential Markov chain with a finite number of states, and the other is a set of random functions. At discrete instants of time, the process is assumed to be in some state, and observation is generated by the random function corresponding to the current state [17]. Markov chain is a powerful mathematical tool that is widely used to capture random transitions between different states of a system. Since the complexity of the model can be greatly reduced by utilizing the properties of the Markov chain, it has been widely used in many time model sequences and became one of the most widely applied algorithms. Cerqueti et al. optimized the Markov chain according to the application scenario [18]. And, Li et al. studied the limit theorem of the Markov chain function in the environment of single infinite Markovian systems [19]. Markov chain has been widely used for prediction in other fields, such as parallel computing [20], data modeling [21], information freshness [22], robotic surveillance [23], and transformer health estimation [24].

In the model construction, Ma et al. [25] proposed a preemptive multipriority queuing model, but it did not analyze high-priority data. Li et al. [26] studied the queuing theory of blockchain mining based on nodes and designed a Markov batch service queuing system with two different service stages. However, the existing research studies did not fully consider the resource utilization in the queuing process. In order to solve the above problem, we propose a blockchain-enabled queuing model based on service priority. Although the queuing model in our scheme is built under Poisson's hypothesis, our analysis method will inspire a series of potential studies for the queuing theory in the blockchain system.

To the best of our knowledge, this paper proposes creatively a set of theoretical methods and prototyping based on the blockchain tactics and the Markov chain model and attempts to apply it in the stock trading. By doing a lot of market investigation and reading plentiful references, aiming at some deficiencies of existing methods, we proposed a multipriority prediction model in the blockchain based on the Markov chain and queuing theory. Compared with the previous approaches, our proposed method and model has the following advantages:

(i) Combining queuing theory with the blockchain: this paper creatively proposes a queuing model of multipriority service object preemption based on the blockchain scenario.

(ii) Appling the Markov chain to integrated forecast of the stock trading market: according to the three basic principles of stock trading, the priority of the service object is divided. The different priority service objects in the scenario are also discussed.

(iii) The resource scheduling model of the queuing system is established by using the Markov chain and the blockchain, and the optimal solution of resource scheduling is found by adopting the above model.

In the following sections, we will analyze and summarize the principle and basic knowledge of the Markov chain and the queuing theory. Through the analysis of the Markov chain and the blockchain, it is not difficult to find that they belong to the chain structure. Therefore, by combining the queuing model with blockchain technology, this paper proposes a new stock trading method based on the blockchain. Section 2 mainly presents the work related to the blockchain, Markov chain, and queuing theory. Section 3 introduces the theoretical knowledge of the Markov chain and queuing theory. Section 4 establishes a queuing model with priority based on the blockchain. Section 5 uses the Markov chain to schedule resources for the queuing model. Section 7 concludes this paper. The method proposed in this paper optimizes and improves the stock trading, which can shorten the settlement time and improve the liquidity of funds.

2. Related Work

The development of the blockchain is been explored, and its application scenarios have been expanded from a single electronic virtual currency trading system to the other wider fields. Today some of the largest financial institutions in the world, including central banks, major commercial banks, and stock exchanges, have launched ambitious projects to use the blockchain in both wholesale and retail applications [27]. They were committed to applying blockchain technology to real-world production environments and realizing the ultimate goals of high efficiency and low consumption. The security of the blockchain has always been one of the hotspots, and many researchers have made a host of contributions to this problem [28–30]. In other applications, in 2017, Li et al. proposed a payment method based on credit, which can be used for the fast and frequent transactions. Their work also provided an optimal pricing strategy for the Stackelberg game based on credit loans [31]. Due to the lack of some comprehensive literature reviews on the development of decentralized consensus mechanisms in the blockchain network, in 2018, Wang et al. provided a systematic vision of the organization of the blockchain network, and they also made a comprehensive review of the self-organizing strategies of each node in the blockchain backbone network from the perspective of game theory [32]. In the same year, Hussein et al. proposed a data-sharing system based on the blockchain, which makes full use of the invariance and autonomy of the blockchain to meet the challenges of access control and sensitive data processing [33]. In 2019, Andoni et al. demonstrated that the blockchain can get over the technical difficulties of identification and its potential disadvantages. Then, they introduced the current development prospects of the blockchain into industrial projects and entrepreneurial firms in brief. Finally, they discussed the challenges and market obstacles that blockchain technology needs to conquer and proved its commercial feasibility [34]. In order to achieve safe and fair payment of outsourcing services without relying on the third party, Zhang et al. proposed BCPay, which was a fair payment framework of cloud computing outsourcing services based on the blockchain [35].

So far, the research for the blockchain has obtained many important advances, but an army of optimization theory of blockchain systems is anticipated, for example, developing and promoting a slice of mathematical models (e.g., Markov processes, queuing theory, and game models), to provide performance analysis and method improvement, and to set up useful relations among key factors or basic parameters. Kasahara and Kawahara pour attention into applying queuing theory into the processing of transaction confirmation bitcoins, and they gave some interesting ideas and useful simulations for inspiring future research. In their works, Kasahara and Kawahara assumed that the transaction confirmation times follow a continuous probability distribution function. The queuing theory was used to analyze the transaction confirmation time of the blockchain. They modeled the bitcoin transaction confirmation process as a priority queuing system with batch services and derived the average transaction confirmation time [36]. The blockchain is maintained and updated by modeling the mining process with a queuing system. In the model, they considered the joint distribution of the number of transactions in the system and the running service time and obtained the average transaction validation time at last [37]. In 2018, Li et al. designed a Markov batch service queuing system with two different service stages, which can well express the process of mining and establishing a new block [25]. In addition, there are some research studies about the queuing model to apply to the blockchain. In 2019, Ricci et al. proposed a framework that includes the machine learning and queuing theory model to describe the delay experienced in bitcoin transactions, which related transaction delays to the time between every two block validations [38]. Memon et al. built a model that uses queuing theory to simulate the blockchain and verified the designed blockchain model by simulating two-month transactions using actual statistics from bitcoin and Ethereum [39].

3. Preliminaries

3.1. Markov Chain. Markov chain is a discrete Markov process with time and state parameters. Because the time learned by the general Markov process is infinite, the time is a continuous variable, and its value is also continuous. An infinite partition can be made between two adjacent values. Meanwhile, the time parameter of the Markov chain is discrete, and the state of the Markov chain is also finite. When one state can be listed, the future state is solely related to the current state, and it has nothing to do with the previous state.

For instance, consider a discrete-time stochastic process, $\{X^n, n = 0, 1, 2 \ldots\}$; here, its value is a finite or countable set of S, which is the state space of the process, and a state space is the collection of all possible states that contain the Markov chain.

The finite-dimensional distributions of the process are shown as follows:

$$P\left\{X^0 = i_0, \ldots, X^n = j\right\}, \quad i_0, \ldots, j \in S, n \geq 0, \tag{1}$$

where the set S is the state space of the process and the value $X^n \in S$ is the state of the process at the time n. The probability distribution uniquely determines the probability of all events in the process. Therefore, if the finite-dimensional distributions of two random processes are equal, their distributions are equal:

$$P\left\{X^{n+1} = j \mid X^0, \ldots, X^n\right\} = P\left\{X^{n+1} = j \mid X^n\right\}. \tag{2}$$

The stochastic process on the countable set S and $X = \{X^n \colon n \geq 0\}$ is a Markov chain, for any $i, j \in S$ and $n \geq 0$:

$$P\left\{X^{n+1} = j \mid X^n = i\right\} = P_{ij}, \tag{3}$$

where P_{ij} is the probability of a Markov chain moving from state i to state j. Obviously,

$$P_{ij} \geq 0, \quad \sum_{i=0}^{\infty} P_{ij} = 1, j = 0, 1, \ldots. \tag{4}$$

(i) Condition (1), called the Markov property, means that at any time$n$, the conditional distribution of the next state X^{n+1} is independent of the past state $X^0, \ldots, X^{n-1}$. That is to say, the future state is independent of the past state and is dependent on the present state.

(ii) Condition (2) simply says that the transition probabilities do not depend on the time parameter; the Markov chain is "time homogeneous." If the transition probabilities were functions of time, the process X^n would be a nontime-homogeneous Markov chain [40].

P_{ij} is a matrix that consists of the transition probability:

$$P = \begin{bmatrix} P_{00} & P_{01} & \cdots \\ P_{10} & P_{11} & \cdots \\ \vdots & \vdots & \vdots \end{bmatrix}. \tag{5}$$

This process is called the transition probability matrix.

To describe the finite-dimensional distribution of stochastic processes is a basic problem in analyzing the structure of stochastic processes. The finite-dimensional distribution of X^n is determined by its initial probability distribution X^0 and transition probability.

Assuming that the transition probability and the initial probability of the Markov chain X^n are P_{ij} and $\alpha_i = P\{X^0 = i\}$, respectively, for any $i_0, \ldots, i_n \in S$ and $n \geq 0$, we can get the following formula:

$$P\left\{X^0 = i_0, \ldots, X^n = i_n\right\} = \alpha_{i_0} P_{i_0, i_1} \ldots P_{i_{n-1}, i_n}. \tag{6}$$

P_{ij} is defined as the probability of the process through n steps from state i to state j. In particular, $P_{ij}^1 = P_{ij}$,

$$P^n = \underbrace{PP \ldots P}_{n}. \tag{7}$$

The Chapman–Kolmogorov equation can be obtained by the multiplication property of the matrix $P^{m+n} = P^m p^n$, for $m, n \geq 1$:

$$P_{ij}^{m+n} = \sum_{k \in S} p_{ik}^m p_{kj}^n, \quad i, j \in S. \tag{8}$$

Then,

$$P_{ij}^{n+1} = \sum_{k \in S} p_{ik}^n p_{kj}^1 = \sum_{k \in S} p_{ik}^n p_{kj} = \left[P^{n+1}\right]_{ij}. \tag{9}$$

Here, they are established for all nonnegative integers n.

The state transition of the Markov chain can be expressed as a graph, called the transition graph, as shown in Figure 1. And, each edge in the graph is assigned a transition probability. The concepts of "reachable" and "connected" can be introduced through the transition graph.

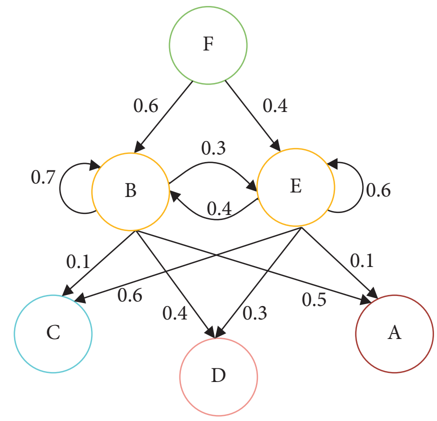

Figure 1: Markov chain on the graph.

3.2. Queuing Theory. Queuing theory, known as a random service system as well, originated from the research on the telephone trunk line in the early 20th century. Queuing theory is widely used in service systems, especially in communication systems, transportation systems, computer storage systems, production management systems, and so on. The queuing process is shown in Figure 2.

Using Kendall's representation method [41], a queuing process is usually represented by A/B/C/X/Y. Among them, "A" represents the random distribution of customers arriving at the system, "B" expresses the distribution type of the service time in the service center, "C" indicates the number of the service center, "X" shows the capacity of the queue, and "Y" reveals the queuing rule. The queuing system mainly has three important performance indicators, and they are queue length, waiting time, and service center workload.

Queuing system with priority has many applications in real life. Priority is a kind of rules separated from service rules, which is the VIP (very important person) system advocated by many merchants in marketing. The queuing system is divided into two types according to their priority, as shown in Figure 3.

4. Priority-Based Queuing Modeling

The blockchain application architecture in this paper is a distributed communication network that is composed of multiple users, in which one user is randomly spread over any position. The set of users is $U = \{u \in U, u = 1, 2, \ldots, m\}$, and the users do not affect each other. Users are represented by nodes in the network, and the connections between every two nodes are irregular. As we can see in Figure 4, the AB chain starts at node A, but the state transition occurs at node X to form a second chain AC. These two chains end at node B and node C, respectively. In Section 5 of this paper, we will use the Markov theory to calculate the transition probability at node X.

In the actual scenario, it is assumed that all users can generate transactions and blocks, where user-generated transaction sets are represented by $\xi = \{t \in \xi, t = 1, 2, \ldots, T\}$ and the user-generated block sets are represented by $\sigma = \{b \in \sigma, b = 1, 2, \ldots, B\}$.

According to the working process of the blockchain, we creatively propose a priority-based stock trading prediction

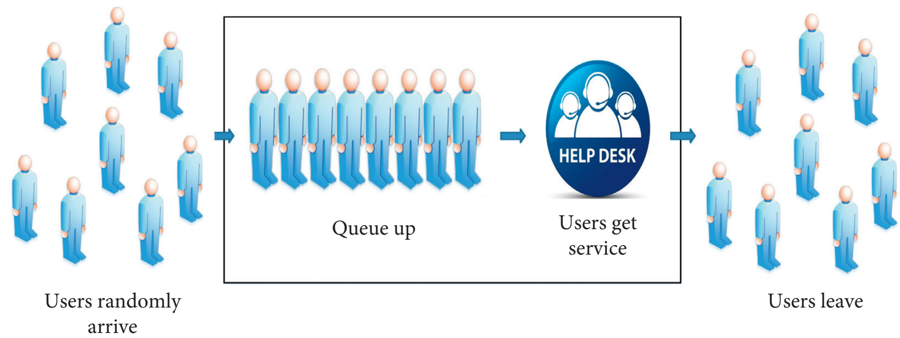

Figure 2: Queuing process of the queuing system.

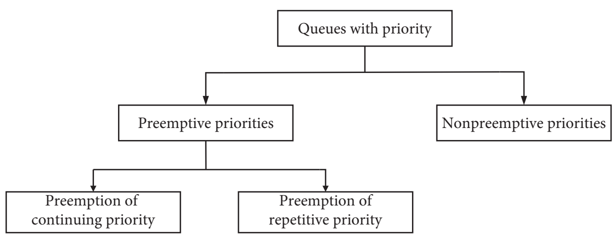

Figure 3: Classification of priority queuing.

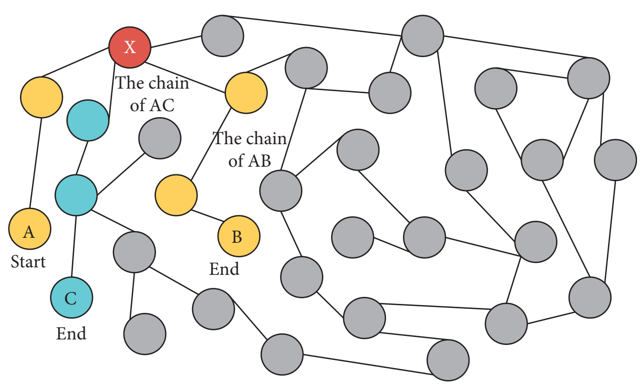

Figure 4: Random distribution of the user and transfer process of status.

model. In stock trading, the model is processed according to three basic principles as follows: the value priority principle, the transaction time priority principle, and the quantity priority principle.

(i) The principle of the value priority: when the value is higher, the priority is higher. The calculation of the value is as follows:

$$W_{\text{value}} = W_p \times W_q, \quad (10)$$

where W_p represents the transaction univalence, W_q indicates the transaction quantity, and W_{value} is the total value of the traded stock.

(ii) The principle of transaction time priority: for the same value declaration, the earlier submission time is preferred.

(iii) The principle of the quantity priority: when the purchase quantity is more, the priority is higher.

The above three principles interact with each other. Users with a high transaction value have higher priority than users with a lower value. However, if the transaction value of two users is equal, it will queue according to the transaction time sequence. And, if two users submit the same value at the same time, they sort according to the third principle. This is a typical queuing problem by priority.

In this section, in order to solve the above problems, we design a queue model with priority based on the blockchain framework. The model is divided into two phases, i.e., the block generation phase and the chain establishment phase. In the block generation phase, when the data flow arrives, it needs to enter and queue in an infinite waiting room. According to the queuing rules, the system divides it into the high-priority data flow and the low-priority data flow, and then it waits to be assembled into blocks. The chain establishment is that the newly generated blocks are concatenated into a blockchain. The queue and establishment model of a blockchain is shown in Figure 5. Since the built blockchain also involves the consensus mechanism of the blockchain, the required time in this stage is related to the consensus in the network, and there is network delay in the consensus process. Each consensus mechanism takes a different amount of time. In this paper, we do not discuss it. Here, we apply ET (establishment time of the blockchain) to represent the required time to build a blockchain. By the above two stages, we can derive the average waiting time and average queue length of all data streams with different priorities in a blockchain.

The priority-based queuing model is regarded as an $M/M/N/m$ queuing model with three types of users, where the first "M" represents that the arrival process is the Poisson process, the second "M" means that the service time obeys exponential distribution, "N" is the N channels, and "m" is the m users. When the data flow arrives, it will select the free channel for transmission, and the system processes the business submitted by users according to three kinds of priorities. Therefore, it can be considered as an $M/M/N/m$ queuing model with three types of users. Assuming that the arrival rates of the three priorities are $\lambda_1, \lambda_2^{k=1}$, and $\lambda_2^{k=2}$, respectively, we will analyze the three different types of priority data flow.

In this model, the transmission time of the high-priority and low-priority data flow in a channel is $(1/\mu_1)$ and T_{tk}, T_ω

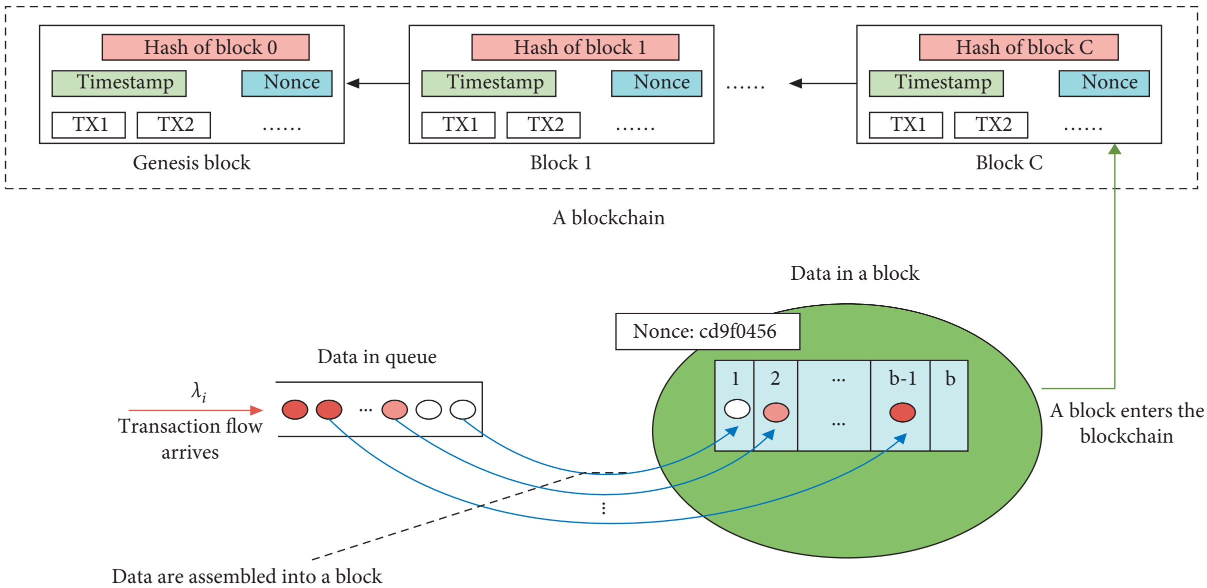

Figure 5: Queue and establishment model of a blockchain.

is the average wait time of high-priority data flow, ω is the average quantity of data flow, and $\partial_{k,j}^{\eta}$ and $\psi_{k,j}^{\eta}$ are the arrival rate and effective service time of low-priority data flow in the channel η with priority k, respectively.

In the $M/M/N/m$ queuing model, each channel can transmit high-priority and low-priority data flow. Here, according to the k value, the low-priority data flow is classified into two categories. The high-priority data flow receives service firstly, and the data flow of the same priority follows the scheduling strategy of the first come first serve (FCFS); the low-priority flow can access the channel only after the high-priority data flow to complete the data transfer. When the high-priority data flow reappears, the low-priority data flow must suspend the data transmission or switch to another channel. The specific transmission process is exhibited in Figure 6. In addition, we assume that all the random variables defined above are independent of each other.

4.1. High-Priority Data Flow. Since the high-priority data flow receives the service firstly, the queuing time of the high-priority data flow is the service time of the same priority data flow.

Based on the analysis of the queuing model above, we assume that b represents the sequence number of blocks and C represents the number of blocks generated by the data flow $(b < C)$. If $\rho = (\lambda_1/(\mu_1 + \sum_{k=1}^{2} \mu_2^k))$ (where ρ is the average quantity of the high-priority data flow model), then the average quantity of data flow to process and the average service time of the high-priority data flow can be described as follows:

$$\omega_1 = \frac{\lambda_1}{\mu_1}\left(\frac{1}{(1-\rho)^2}\right)\left(1 + \frac{\lambda_1}{\mu_1}\left(\frac{1}{1-\rho}\right)\right)^{-1}, \tag{11}$$

$$E\left[X_p^{\eta}\right] = \frac{1}{\mu_1}\left(\frac{1}{(1-\rho)^2}\right)\left(1 + \frac{\lambda_1}{\mu_1}\left(\frac{1}{1-\rho}\right)\right)^{-1} + \sum_{b=0}^{C} ET. \tag{12}$$

We can obtain the probability that a high-priority data flow occupies the busy channel, and the probability is as follows:

$$\alpha_p^{\eta} = \lambda_1 E\left[X_p^{\eta}\right]. \tag{13}$$

The average queue length of data flow in the channel can be expressed as follows:

$$l_\eta = \frac{p_{\eta 0}\rho_\eta \rho_{\eta m}}{m!\left(1-\rho_{\eta m}\right)^2} + \rho_\eta, \tag{14}$$

where $p_{\eta 0} = \left[\sum_{n=0}^{m-1} (\rho_\eta/n!) + (\rho_\eta/m!(1-\rho_{\eta m}))\right]^{-1}$ and $\rho_\eta = m\rho_m$.

4.2. Low-Priority Data Flow. The model belongs to the multiserver system in queuing theory. When the priority has been introduced into the model, it became difficult to deal with. To quantitatively analyze the multiservice flow and multichannel model with priority, the dimension reduction method is adopted to process it. The processing of low-priority data flow depends on the amount of high-priority data flow. When there is no high-priority data flow in the model, all channels transmit low-priority data flow. When the amount of high-priority data flow is more than 0, the remaining channels transmit low-priority data flow; when the amount of high-priority data flow is N, there is no channel to transmit low-priority data flow.

In the model, we set k as the priority of the data flow, the value of k is 1 or 2, and n is the interrupted number. The service time of the low-priority data flow in the channel η is X_k^{η}. Then, the busy degree of the channel is as follows:

$$\nu = \sum_{k=1}^{2}\sum_{i=1}^{n} \nu_{k,i}, \tag{15}$$

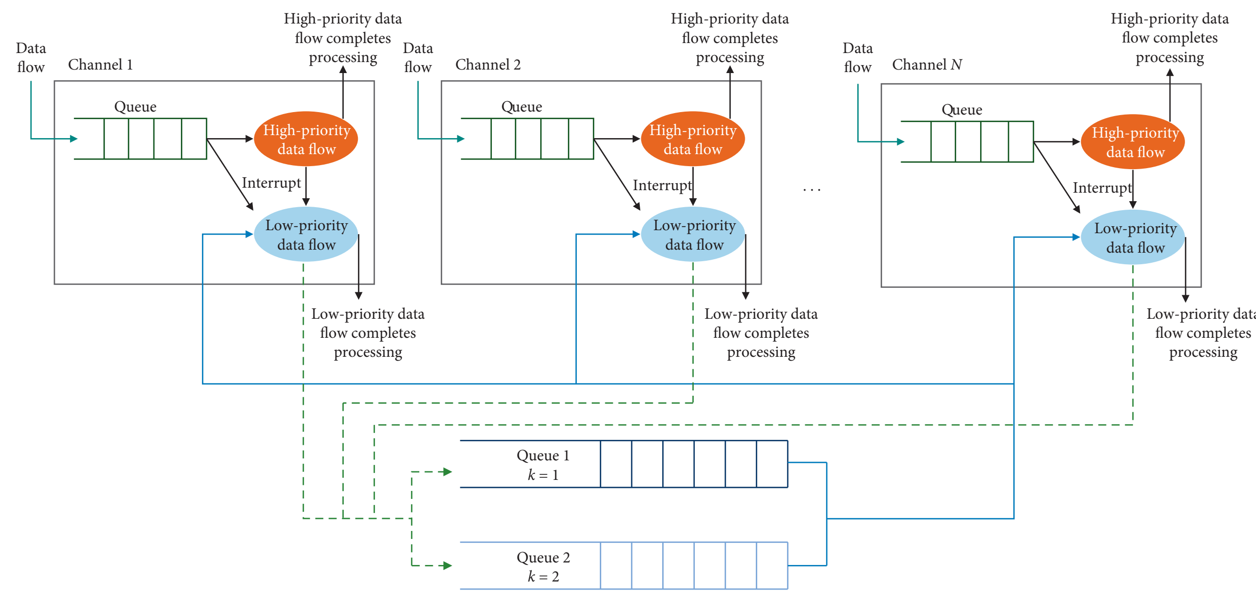

FIGURE 6: Priority-based queuing system model.

where $\nu_{k,i}$ is the probability of the channel busy level caused by data flow with priority k and interrupted number i.

During the data transfer, the process is likely to be interrupted for several times. We consider the traffic of channel η, and then the average data transmission time of data flow can be expressed as follows:

$$E[T_{tk}] = \sum_{i=1}^{n} E[T_{\omega k}]\Pr(n), \tag{16}$$

where

$$E[T_{\omega k}] = E\left[X_k^\eta\right] + \sum_{i=1}^{n} E\left[D_{k,i}^\eta\right], \tag{17}$$

$$\Pr(n) = \left(1 - p_{k,n}^\eta\right)\prod_{i=0}^{n-1} p_{k,n}^n, \tag{18}$$

in which $D_{k,i}^\eta$ is the time delay when the data flow is interrupted in the channel η and $p_{k,n}^\eta$ is the probability of the data that is interrupted again in the current channel. Substituting (17) and (18) into (16), we can gain the following formula:

$$E[T_{tk}] = E\left[X_k^\eta\right] + \sum_{j=1}^{n}\left[\left(\sum_{i=1}^{n} E\left[D_{k,i}^\eta\right]\left(1 - p_{k,n}^\eta\right)\prod_{i=0}^{n-1} p_{k,n}^\eta\right)\right]. \tag{19}$$

The service time can be calculated as follows:

$$E\left[\partial_{k,j}^\eta\right] = \left(\sum_{n=1}^{M}\left(E\left[\psi_{k,i}^\eta\right]\right)^{-1}\right)^{-1}. \tag{20}$$

In the stop-and-wait situation, when $k = 1$, the waiting time of the data flow can be computed as follows:

$$E\left[A_{1,i}^\eta\right] = E\left[X_p^\eta\right] + \lambda_2^{k=1} E\left[A_{1,i}^\eta\right] E\left[X_p^\eta\right] + \sum_{b=0}^{C} ET. \tag{21}$$

On the right of the equal sign of (21), the first item represents the average service time of the high-priority data flow that caused the interruption, and the second item represents the average service time of the newly arrived high-priority data flow within the waiting time.

Through (21), we can obtain the following formula:

$$E\left[A_{1,i}^\eta\right] = \frac{E\left[X_p^\eta\right] + \sum_{b=0}^{C} ET}{1 - \lambda_2^{k=1} E\left[X_p^\eta\right]}. \tag{22}$$

Similarly, when $k = 2$, the waiting time is computed as follows:

$$\begin{aligned} E\left[A_{2,i}^\eta\right] &= E\left[X_p^\eta\right] + \lambda_2^{k=2} E\left[A_{2,i}^\eta\right] E\left[T_{\omega 1}\right] \\ &\quad + \sum_{j=0}^{n} \partial_{1,j}^\eta E\left[A_{2,i}^\eta\right] E\left[\psi_{1,j}^\eta\right] + \sum_{b=0}^{C} ET. \end{aligned} \tag{23}$$

On the right of the equal sign of (23), the first item represents the average service time of the high-priority data flow that caused the interruption, the second item represents the average service time of the newly arrived high-priority data flow, and the third item reveals the average service time of the arrived $k = 2$ data flow during the wait time. Through (22), we get the following:

$$E\left[A_{2,i}^\eta\right] = \frac{E\left[A_{2,i}^\eta\right] + \sum_{b=0}^{C} ET}{1 - \lambda_2^{k=2} E\left[X_p^\eta\right] - \sum_{j=0}^{n} \partial_{1,j}^\eta E\left[\psi_{1,j}^\eta\right]}. \tag{24}$$

The average remaining service time of the current data flow in the channel η can be expressed as follows:

$$E\left[V_t^\eta\right] = \frac{1}{2}\lambda_1 E\left[E\left(X_P^\eta\right)^2\right] + \frac{1}{2}\sum_{k=1}^{2}\sum_{j=0}^{n}\sum_{\eta-1}^{M}\lambda_2^k\partial_{k,j}^\eta E\left[\left(\psi_{k,j}^\eta\right)^2\right] + \sum_{b=0}^{C} ET. \tag{25}$$

The interruptible queuing model in the paper can apply to the stock deal. When the data flow reaches, the model will deal with the data flow according to its priority (in Figure 7). The proposed method in this paper can greatly improve the efficiency of the queuing model and meet the relevant needs in the trade.

5. Markov Chain Model

Markov chain is a mathematical model to describe the state transition of complex systems. The multistage decision process problem can be solved by adopting the model. However, the state of the process must satisfy the nonaftereffect property. The nonaftereffect property is only related to the state of the phase, and it is irrelevant to the previous state. The queuing process is dynamic and meets the above conditions, so it conforms to the requirements of the Markov chain application. Moreover, when an army of users arrive at the model for queuing, the model needs to spread them out the other queues. Meanwhile, the resource scheduling needs to meet the demands as shown in Figure 8. Therefore, the application of the Markov chain theory can solve the problem of resource allocation in the queuing model.

5.1. Model Building. In this paper, we apply $F(s)$ to represent the state of the model, and $\{F(s); s \in S\}$ is a random process; the state vector distribution $\chi = \{\chi_1, \chi_2, \chi_3, \ldots\}$ represents the probability of each state at the current moment. P_{ij} constitutes the probability transition matrix Λ. The formula of state distribution vector at the time n is as follows:

$$\chi(\mathrm{n}) = \chi_{(n)}\Lambda, \tag{26}$$

where x corresponding to $\max(\chi_x)$ is to predict the most possible state of state transition at the time n. In order to calculate the load degree of the server, we divide the occupancy rate of the model, and the specific partition function is as follows:

$$\mathrm{level}(x) = \frac{\mathrm{load}(x)}{100}. \tag{27}$$

We suppose the current time is t, the node o is overloaded, and the state of node o at the time t is L_t. To make the model achieve efficiently, data flow needs to be migrated. For the first d moments $(d < t)$, the load transfer sequence is $L_1, L_2, \ldots L_d$. From this transition sequence, the occurrence time of state transition $i \longrightarrow j$ in adjacent moments are denoted as C_{ij} and P_{ij} is the transition probability from state i to state j, which can also be obtained as follows:

$$P_{ij} = \begin{cases} \dfrac{C_{ij}}{\sum C}, & C_{ij} \neq 0, \\ 0, & C_{ij} = 0. \end{cases} \tag{28}$$

From the state transition probability, we can obtain the transition probability matrix of the Markov chain.

In addition, we supposed that $f(n)$ represents the total expected reward at the end of the process when the model is in the state $F(n) = i$ and r_{ij} represents the corresponding reward for moving from state $F(n) = i$ to the next state $F(n+1) = j$, then we can gain the following equation:

$$f(i, \pi_n) = \sum_{j=1}^{n} P_{ij}r_{ij} + \sum_{j=1}^{n} P_{ij}f_{n+1}(i, \pi_{n+1}) \quad i = 1, 2, \ldots, \tag{29}$$

where π_n represents the sequence $\{\zeta_n, \zeta_{n+1}, \ldots\}$ of the decision rule and ζ is from the n-th period to the end of the process. $\pi_n = (\zeta_n, \pi_{n+1})$, where ζ_n is the decision rule in the n-th period. We assume that

$$q(i) = \sum_{j=1}^{n} P_{ij}r_{ij}, \quad i = 1, 2, \ldots, m, \tag{30}$$

where $q(i)$ is the expected cost of a transition from the state i, namely, it is the expected cost of the state i.

The above two equations are based on solving the dynamic resource scheduling problem. In order to study the instantaneous behavior of the Markov chain, it is necessary to employ the Z-transform analysis method, which can transform the differential equations into the corresponding ordinary equations. The original function and its Z-transformation can be converted into each other. By the application of Z-transformation, the formula (30) from [42] can solve the resource scheduling problem:

$$n\nu + f_i = q_i + \sum_{j=1}^{n} P_{ij}\left[(n-1)\nu + f_i\right], \quad i = 1, 2, \ldots, m, n\nu + f_i = q_i + \sum_{j=1}^{n} P_{ij}f_i, \quad i = 1, 2, \ldots, m. \tag{31}$$

5.2. Resource Scheduling Algorithm Based on Markov Chain. The specific algorithm is shown in Algorithm 1. We apply Algorithm 1 to discover the optimal solution of resource scheduling and distribute the data flow in the blockchain queuing model to reduce the waiting time of data flow in the waiting room. It not only improves the processing efficiency of the blockchain network, but also meets the demand of the stock trades.

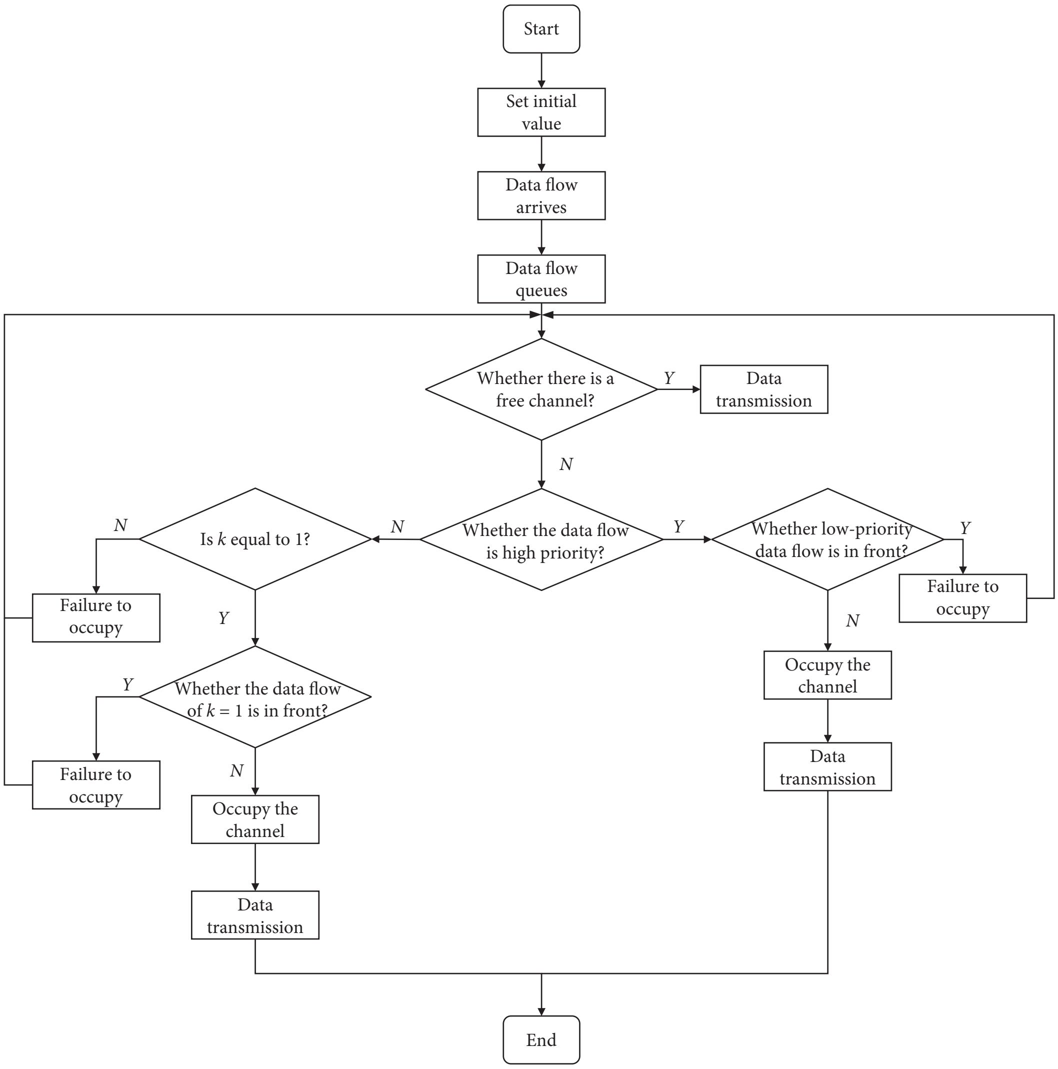

Figure 7: Priority-based queuing model flowchart.

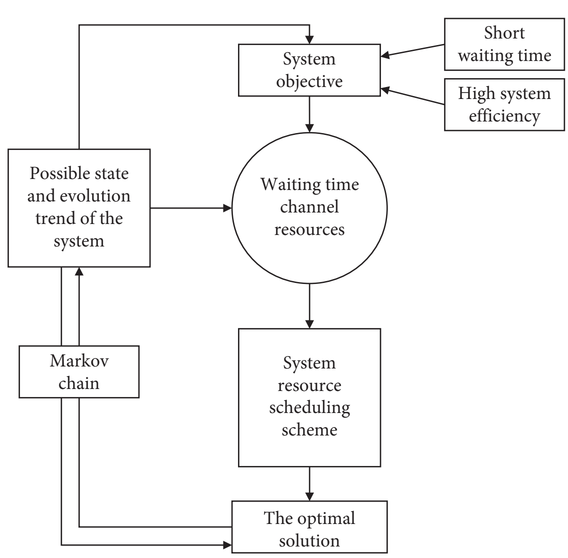

Figure 8: Solving the logical relation of system resource scheduling by using the Markov chain.

Input: state $F(s)$, $s \in S$, π
Output: final strategy π_n
(1) Define $q(i)$, P_{ij}, and r_{ij}
(2) for $i = 0$ to m do
(3) $\quad d^k_{(i)} = \zeta_n(i)$
(4) $\quad$ for $n = 0$ to N do
(5) $\qquad nv + f_i = q_i + \sum_{j=1}^{n} P_{ij}[(n-1)v + f_i], nv + f_i = q_i + \sum_{j=1}^{n} P_{ij} f_i$
(6) $\qquad M \longleftarrow \max(q_i^{\zeta_{n+1}(i)} + \sum_{j=1}^{m} P_{ij}^{\xi_{n+1}(i)} f_j^{(n)} - f_i)$
(7) $\qquad$ if $\pi_n = \pi_{n+1}$, then
(8) $\qquad\quad$ return π_n
(9) $\qquad$ else
(10) $\qquad\quad n = n + 1$

Algorithm 1: Resource scheduling algorithm.

6. Experiment

The queuing model with three channels is considered in our experiment. The arrival process of the three kinds of priority data flow is Poisson arrival process, and their arrival rates are λ_1, $\lambda_2^{k=1}$, and $\lambda_2^{k=2}$, respectively. Their service time follows an exponential distribution. Here, data transmission is simulated in three aspects, they are throughput, delay, and channel utilization.

6.1. Data Simulation. First of all, we set the simulation parameters as follows: $E[X_p^n] = E[X_p] = 20$, $\lambda_1 = \lambda_2^{k=1} = \lambda_2^{k=2} = 0.01$. Then, we set up 1000 accounts, with the number of transactions for each account that is randomly distributed between 1 and 100, and the value of each transaction that is randomly distributed between 1 and 1000. The arrival time of transaction for each account is random as well. The statistics of transaction quantity and transaction price of all accounts are shown in Table 1.

According to Table 1, the transaction quantity and transaction price of the accounts are evenly distributed. We sorted the accounts into three priorities based on the three principles mentioned above.

6.2. Performance Index. In this paper, we also use throughput, delay, and channel utilization as the indicators to measure the queuing model. Then, the queuing model proposed in this paper is compared with the queuing model based on FCFS.

6.2.1. Throughput. Throughput is to measure a system's ability in handling issues, requests, and transactions per unit of time, and it also is an important indicator to measure the system's concurrency. Here, we apply TPS (transaction per second) to represent it. The throughput in the blockchain application refers to that the total number of transactions written into the blockchain divided by the time from transaction issuance to transaction confirmation. The formula is as follows:

$$\mathrm{TPS}_{\Delta_T} = \frac{\mathrm{TransactionSum}_{\Delta T}}{T}, \tag{32}$$

where ΔT is the time interval between the transaction issuance and the block confirmation, and it is the block time as well, and $\mathrm{TransactionSum}_{\Delta T}$ is the number of transactions included in the block during this time interval. The throughput's comparison of the two queuing models is shown in Figure 9.

It can be seen that when $T < 10$ s, the throughput of the FCFS-based queuing model is greater than the M/M/N/m queuing model with priority. At the beginning, there was much influx of data flow. The FCFS queuing model processes data flow in the light of "come first, be served first," and there is needless to process data flow according to priority. Therefore, the throughput of the FCFS queuing model is higher than the M/M/N/m queuing model. However, as time goes on, Markov theory is applied to schedule resources in the M/M/N/m queuing model, which improves the efficiency of queuing and reduces the waiting time of data flow. So, throughput of the model can be increased. In summary, the throughput of the M/M/N/m queuing model is generally higher than the FCFS queuing model.

6.2.2. Delay. In networks, delay includes sending delay, propagation delay, processing delay, and queuing delay. Here, we define the delay indicator as follows:

$$\mathrm{delay} = T_{\mathrm{send}} + T_{\mathrm{deal}} + T_{\mathrm{receive}} + T_{\mathrm{queue}}, \tag{33}$$

where T_{send} is the block-sending delay; T_{deal} is the processing delay; T_{receive} is the transmission delay that the block reaches the next node; T_{queue} is the queuing waiting delay of the data flow. The delay comparison between the two queuing models is shown in Figure 10.

Since the transmission delay and propagation delay of the data flow simulated in this paper are the same, the differences between the two models focus on processing and queuing. When the running time is less than one minute, the delay of the FCFS model is smaller. This is because the high-priority data flow of the M/M/N/m queuing model preempts the channel, and it results in a higher delay of the low-priority data stream. When the running time is longer, as the throughput of the M/M/N/m queuing model increases, the processing capacity of the model also enhances accordingly. Thus, the processing delay of the M/M/N/m queuing model

Table 1: Quantity and price of transactions in the accounts.

Quantity	Price		
	1–350	351–660	661–1000
1–33	87	134	119
34–66	124	91	104
67–100	103	126	112
Total	314	351	335

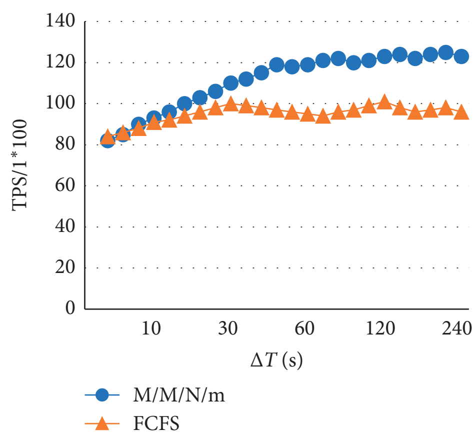

Figure 9: Comparison of throughput between two queuing models.

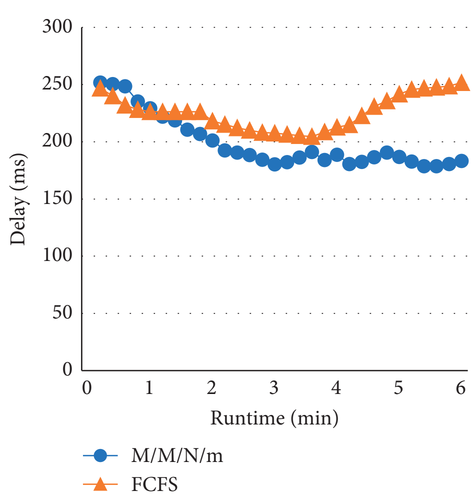

Figure 10: Comparison of delay between two queuing models.

decreases. In addition, Markov theory is applied to schedule resources in the M/M/N/m queuing model, which improves the queuing efficiency of the model. Hence, the queuing delay also is continuously reduced. In summary, the overall delay of the M/M/N/m queuing model is less than the FCFS model.

6.2.3. Channel Utilization. Channel utilization refers to the ratio of the time T_{work} to the total time T_{all} when the channel is in the state of transmitting data, namely,

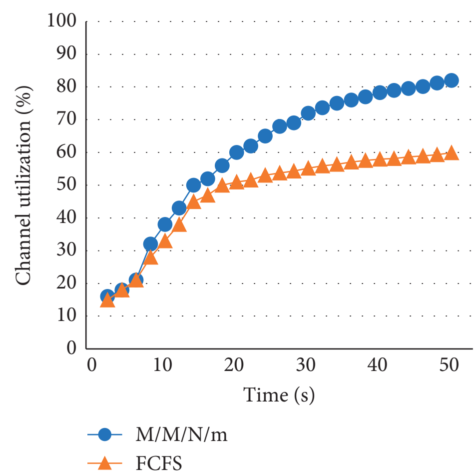

Figure 11: Comparison of channel utilization between two queuing models.

$$\eta_{\text{channel}} = \frac{T_{\text{work}}}{T_{\text{all}}}. \tag{34}$$

Apparently, we hope that the channel utilization is higher. The comparison of channel utilization for the two queuing models is shown in Figure 11.

We find that the channel occupancy rate of the M/M/N/m queuing model is generally higher than the FCFS model. The channel occupancy of the FCFS model is basically maintained at 60%, while the channel occupancy of the M/M/N/m queuing model is higher than 80%. Moreover, the channel occupancy of the M/M/N/m queuing model increases faster than the FCFS model.

In conclusion, the performance of the M/M/N/m queuing model is better than the FCFS model, and the former can better meet the performance requirement of the blockchain application system, reduce the data waiting time, and improve the efficiency of the block.

7. Conclusion

In this paper, we built a multipriority stock trading model based on the Markov chain for blockchain application and deduce the transmission time expression of data flow with different types of priority. We map the priority of service to multiple channels and establish the multichannel data transmission model of the multiservice data flow with priority guarantee. Moreover, applying queuing theory, we analyze the parameters of the multiservice and multichannel model with priority in the blockchain scenario, such as average queue length and average waiting time. In addition, this paper studies the dynamic optimization of resource scheduling in the queuing model by employing the Markov chain, which provides theory and method support for practical application in the future and maximizes the usage of resources in our model. Experiments show that the model proposed in this paper has better performance in three important indicators, i.e., the throughput, the delay, and the channel utilization. So our model improves the efficiency of stock purchase in blockchain application and reduces the waste of resources, which will better meet the current market demand. The methods reported here will open up avenues for further research in the financial field.

Data Availability

The data used to support the findings of this study are included within the article.

Conflicts of Interest

The authors declare that they have no conflicts of interest.

Acknowledgments

This work was supported by the National Key Research and Development Program of China (2017YFC0804406) and the Scientific Research Foundation of the Shandong University of Science and Technology for Recruited Talents (0104060511314).

References

[1] Z. Zheng, S. Xie, H. N. Dai, X. Chen, and H. Wang, “Blockchain challenges and opportunities: a survey,” *International Journal of Web and Grid Services*, vol. 14, no. 4, pp. 352–375, 2018.

[2] S. Nakamoto, “Bitcoin: a peer-to-peer electronic cash system,” 2008, https://bitcoin.org/bitcoin.pdf.

[3] Q. E. Abbas and J. Sung-Bong, “A survey of blockchain and its applications,” in *Proceedings of the 2019 International Conference on Artificial Intelligence in Information and Communication (ICAIIC)*, February 2019.

[4] E. Staff, “Blockchains: the great chain of being sure about things,” *The Economist*, vol. 18, 2015.

[5] J. Brito and A. Castillo, *Bitcoin: A Primer for Policymakers*, Mercatus Center at George Mason University, Arlington, VA, USA, 2013.

[6] A. Narayanan, J. Bonneau, E. Felten et al., *Bitcoin and Cryptocurrency Technologies: A Comprehensive Introduction*, Princeton University Press, Princeton, NJ, USA, 2016.

[7] S. Armstrong, “Move over bitcoin, the blockchain is only just getting started,” *Wired*, 2016, https://www.wired.co.uk/article/unlock-the-blockchain.

[8] S. Kesharwani, M. P. Sarkar, and S. Oberoi, “Impact of blockchain technology and 5G/IoT on supply chain management and trade finance,” *Cybernomics*, vol. 1, no. 1, pp. 18–20, 2019.

[9] V. Buterin, “Ethereum: a next-generation smart contract and decentralized application platform,” 2014, https://github.com/ethereum/wiki/wiki/English-White-Paper.

[10] G. W. Peters, E. Panayi, and A. Chapelle, “Trends in cryptocurrencies and blockchain technologies: a monetary theory and regulation perspective,” *The Journal of Financial Perspectives*, vol. 3, no. 3, 2015.

[11] G. Foroglou and A. L. Tsilidou, “Further applications of the blockchain,” in *Proceedings of the 12th Student Conference on Managerial Science and Technology*, Athens, Greece, May 2015.

[12] A. Kosba, A. Miller, E. Shi et al., “Hawk: the bblockchain model of cryptography and privacy-preserving smart contracts,” in *Proceedings of the 2016 IEEE Symposium on Security and Privacy (SP)*, pp. 839–858, IEEE, San Jose, CA, USA, May 2016.

[13] B. W. Akins, J. L. Chapman, and J. M. Gordon, “A whole new world: income tax considerations of the bitcoin economy,” *Pittsburg Tax Review*, vol. 12, no. 1, pp. 24–56, 2015.

[14] Y. Zhang and J. Wen, “An IoT electric business model based on the protocol of bitcoin,” in *Proceedings of the 8th International Conference on Intelligence in Next Generation Networks*, pp. 184–191, IEEE, Paris, France, February 2015.

[15] M. Sharples and J. Domingue, “The blockchain and kudos: a distributed system for educational record, reputation and reward,” in *Proceedings of the 11th European Conference on Technology Enhanced Learning (EC-TEL)*, pp. 490–496, Springer, Lyon, France, September 2016.

[16] C. Noyes, “BitAV: fast anti-malware by distributed blockchain consensus and feed forward scanning,” 2016, https://arxiv.org/abs/1601.01405.

[17] S. E. Levinson, L. R. Rabiner, and M. M. Sondhi, “An introduction to the application of the theory of probabilistic functions of a Markov process to automatic speech recognition,” *Bell System Technical Journal*, vol. 62, no. 4, pp. 1035–1074, 1983.

[18] R. Cerqueti, P. Falbo, and C. Pelizzari, “Relevant states and memory in Markov chain bootstrapping and simulation,” *European Journal of Operational Research*, vol. 256, no. 1, pp. 163–187, 2017.

[19] Zh. Li, M. Huang, X. Meng, and X. Ge, “The limit theorems for function of Markov chains in the environment of single infinite Markovian systems,” vol. 2020, Article ID 8175723, 11 pages, 2020.

[20] W. Zhang, W. Li, C. Zhang, and T. Zhao, “Parallel computing solutions for Markov chain spatial sequential simulation of categorical fields,” *International Journal of Digital Earth*, vol. 12, no. 5, pp. 566–582, 2019.

[21] G. Mastrantonio and G. Calise, “Hidden Markov model for discrete circular-linear wind data time series,” *Journal of Statistical Computation and Simulation*, vol. 86, no. 13, pp. 2611–2624, 2016.

[22] G. D. Nguyen, S. Kompella, C. Kam, and J. E. Wieselthier, “Information freshness over a Markov channel: the effect of channel state information,” *Ad Hoc Networks*, vol. 86, pp. 63–71, 2019.

[23] M. George, S. Jafarpour, and F. Bullo, “Markov chains with maximum entropy for robotic surveillance,” *IEEE Transactions on Automatic Control*, vol. 64, no. 4, pp. 1566–1580, 2019.

[24] S. Milosavljevic and A. Janjic, “Integrated transformer health estimation methodology based on Markov chains and evidential reasoning,” *Mathematical Problems in Engineering*, vol. 2020, Article ID 7291749, 12 pages, 2020.

[25] B. Ma, S. G. Cheng, and X. Z. Xie, “PRP M/G/m queuing theory spectrum handoff model based on classified secondary users,” *Journal of Electronics & Information Technology*, vol. 40, no. 8, pp. 1963–1970, 2018.

[26] Q. L. Li, J. Y. Ma, and Y. X. Chang, "Blockchain queue theory," in *Proceedings of the International Conference on Computational Social Networks*, Springer, Shanghai, China, pp. 25–40, December 2018.
[27] D. Yermack, "Blockchain technology's potential in the financial system," in *Proceedings of the 2019 Financial Market's Conference*, Amelia Island, FL, USA, May 2019.
[28] J. Li, J. Wu, and L. Chen, "Block-secure: blockchain based scheme for secure P2P cloud storage," *Information Sciences*, vol. 465, pp. 219–231, 2018.
[29] Y. Qian, Y. Jiang, J. Chen et al., "Towards decentralized IoT security enhancement: a blockchain approach," *Computers & Electrical Engineering*, vol. 72, pp. 266–273, 2018.
[30] N. Kshetri, "Blockchain's roles in strengthening cybersecurity and protecting privacy," *Telecommunications Policy*, vol. 41, no. 10, pp. 1027–1038, 2017.
[31] Z. Li, J. Kang, R. Yu et al., "Consortium blockchain for secure energy trading in industrial internet of things," *IEEE Transactions on Industrial Informatics*, vol. 14, no. 8, pp. 3690–3700, 2017.
[32] W. Wang, D. T. Hoang, P. Hu et al., "A survey on consensus mechanisms and mining strategy management in blockchain networks," *IEEE Access*, vol. 7, pp. 22328–22370, 2019.
[33] A. F. Hussein, N. ArunKumar, G. Ramirez-Gonzalez, E. Abdulhay, J. M. R. S. Tavares, and V. H. C. De Albuquerque, "A medical records managing and securing blockchain based system supported by a genetic algorithm and discrete wavelet transform," *Cognitive Systems Research*, vol. 52, pp. 1–11, 2018.
[34] M. Andoni, V. Robu, D. Flynn et al., "Blockchain technology in the energy sector: a systematic review of challenges and opportunities," *Renewable and Sustainable Energy Reviews*, vol. 100, pp. 143–174, 2019.
[35] Y. Zhang, R. H. Deng, X. Liu, and D. Zheng, "Blockchain based efficient and robust fair payment for outsourcing services in cloud computing," *Information Sciences*, vol. 462, pp. 262–277, 2018.
[36] S. Kasahara and J. Kawahara, "Priority mechanism of bitcoin and its effect on transaction-confirmation process," 2016, https://arxiv.org/abs/1604.00103.
[37] Y. Kawase and S. Kasahara, "Transaction-confirmation time for bitcoin: a queueing analytical approach to blockchain mechanism," in *Proceedings of the International Conference on Queueing Theory and Network Applications*, pp. 75–88, Springer, Qinhuangdao, China, August 2017.
[38] S. Ricci, E. Ferreira, D. S. Menasche, A. Ziviani, J. E. Souza, and A. B. Vieira, "Learning bBlockchain delays," *ACM Sigmetrics Performance Evaluation Review*, vol. 46, no. 3, pp. 122–125, 2019.
[39] R. Memon, J. Li, and J. Ahmed, "Simulation model for blockchain systems using queuing theory," *Electronics*, vol. 8, no. 2, p. 234, 2019.
[40] R. Serfozo, *Basics of Applied Stochastic Processes*, Springer Science & Business Media, Berlin, Germany, 2009.
[41] D. G. Kendall, "Some problems in the theory of queues," *Journal of the Royal Statistical Society: Series B (Methodological)*, vol. 13, no. 2, pp. 151–173, 1951.
[42] W. Wang, M. Liu, and L. Wang, "The dynamic optimal method of emergency resources deployment planning based on markov decision processes," *Acta Scientiarum Naturalium Universitatis Nankaiensis*, vol. 43, no. 3, pp. 18–23, 2010.

Hindawi
Mathematical Problems in Engineering
Volume 2020, Article ID 5830245, 10 pages
https://doi.org/10.1155/2020/5830245

Research Article

Some State-Specific Exit Probabilities in a Markov-Modulated Risk Model

Jingchao Li [1,2] and Shuanming Li [3]

[1] College of Mathematics and Statistics, Shenzhen University, Nanhai Ave 3688, Shenzhen 518060, Guangdong, China
[2] Shenzhen Key Laboratory of Advanced Machine Learning and Applications, Shenzhen University, Shenzhen 518060, Guangdong, China
[3] Centre for Actuarial Studies, Department of Economics, University of Melbourne, Parkville 3010, VIC, Australia

Correspondence should be addressed to Jingchao Li; jingchaoli@szu.edu.cn

Received 28 March 2020; Accepted 21 July 2020; Published 20 October 2020

Academic Editor: Alessandro Lo Schiavo

In this paper, we study some state-specific one-sided exit probabilities in a Markov-modulated risk process including the probability that ruin occurs without or with the surplus visiting certain states; the probability that ruin occurs without or with a claim occurring in certain states; the probability that the surplus attains a target level without or with visiting certain states; and the probability that the surplus attains a target level without or with a claim occurring in certain states. We also investigate the corresponding two-sided first exit probabilities without (or with) the surplus visiting certain states or without (or with) claims occurring in certain states. All these probabilities can be expressed elegantly in terms of some modified matrix scale functions which are easily computable.

1. Introduction

In this paper, we consider a Markov-modulated risk model which has been studied by a number of authors since the important paper proposed by Asmussen [1]. In such a model, both the claim amounts and the claim arrivals are influenced by an external environment process which we denote by $\{J(t),\ t \geq 0\}$. For example, it is well known that the weather or climate conditions have impacts on automobile, property, and casualty insurance claims. This process is assumed to be a homogeneous, irreducible, and recurrent Markov process on a finite state space $E = \{1, 2, \ldots, m\}$. The process has intensity matrix $\mathbf{A} = (\alpha_{i,j})_{i,j=1}^{m}$, with $\alpha_{i,i} := -\alpha_i$ for $i \in E$, and has stationary distribution $\overrightarrow{\boldsymbol{\pi}} = (\boldsymbol{\pi}_1, \boldsymbol{\pi}_2, \ldots, \boldsymbol{\pi}_m)$.

Let $N(t)$ denote the number of claims occurring in $(0, t]$. If $J(s) = i$ for all s in a small interval $(t, t+h]$, then $N(t+h) - N(t)$ represents the number of claims occurring in that interval and has a Poisson distribution with parameter $\lambda_i\,(>0)$. The process $\{N(t),\ t \geq 0\}$ is a Markov-modulated Poisson process, and it can also be viewed as a Poisson process with its parameter driven by the external environment process $\{J(t),\ t \geq 0\}$.

Given that $J(t) = i$, we assume that individual claim amounts have distribution function F_i and probability density function f_i, with Laplace transform $\widehat{f}_i(s) = \int_0^\infty e^{-sx} f_i(x)\mathrm{d}x$ and finite mean $\mu_i\,(i \in E)$.

Then, the surplus process $\{U(t),\ t \geq 0\}$ in our Markov-modulated risk model is given by

$$U(t) = u + \sum_{i=1}^{m} \int_0^t I(J(s) = i)\mathrm{d}U_i(s), \quad t \geq 0, \qquad (1)$$

where $u \geq 0$ is the initial surplus and I is the indication function, and for $i \in E$, let $\{U_i(t)\}_{t\geq 0}$ be the surplus process in the classical risk model with premium rate c_i, Poisson parameter λ_i, and individual claim amount distribution F_i. The positive loading condition is also assumed to hold, i.e.,

$$\sum_{i=1}^{m} \boldsymbol{\pi}_i \left(c_i - \lambda_i \mu_i\right) > 0. \tag{2}$$

We next define $T_u = \inf\{t \geq 0, U(t) < 0\}$ to be the time of ruin, with $T_u = \infty$ if $U(t) \geq 0$ for all $t \geq 0$, and

$$\psi_i(u) = \mathrm{P}\left(T_u < \infty \mid J(0) = i\right), \quad i \in E, \tag{3}$$

to be the probability of ruin given that initial environment state i.

Let $N_u := N(T_u)$ be the number of claims and $S_u := S(T_u) = \sum_{n=1}^{N(T_u)} X_n$ be the aggregate claims by the time of ruin, respectively, where X_n is the amount of the nth claim. Now, T_u, N_u, and S_u can be decomposed as

$$\begin{aligned} T_u &= \sum_{l=1}^{m} T_{u,l}, \\ N_u &= \sum_{l=1}^{m} N_{u,l}, \\ S_u &= \sum_{l=1}^{m} S_{u,l}, \end{aligned} \tag{4}$$

where $T_{u,l}$ is the duration that the surplus process spends in state $l \in E$ until the time of ruin, $N_{u,l}$ is the number of claims that occur in state l until the time of ruin, and $S_{u,l}$ is the aggregate claims that occur in state l until the time of ruin.

For $1 \leq l_1 < l_2 < \cdots < l_k \leq m$, let $E_k = \{l_1, l_2, \ldots, l_k\} \subset E$ be a substate space. We define

$$\begin{aligned} T_{u,E_k} &= \sum_{j=1}^{k} T_{u,l_j}, \\ N_{u,E_k} &= \sum_{j=1}^{k} N_{u,l_j}, \\ S_{u,E_k} &= \sum_{j=1}^{k} S_{u,l_j}, \end{aligned} \tag{5}$$

to be duration that the surplus spent in substate space $E_k = \{l_1, l_2, \ldots, l_k\}$, the number of claims occurred in E_k, and the aggregate claims occurred in E_k, respectively, by the time of ruin. In particular, if $E_k = E$, then T_{u,E_k}, N_{u,E_k}, and S_{u,E_k} recover T_u, N_u, and S_u; if $k = 1$ and $E_k = \{l\}$, then T_{u,E_k}, N_{u,E_k}, and S_{u,E_k} simplify to $T_{u,l}, N_{u,l}$, and $S_{u,l}$, respectively.

The Markov-modulated risk models have been studied extensively in the literature. References include the studies of Asmussen et al. [2]; Bäuerle [3]; Schmidli [4]; Snoussi [5]; Lu and Li [6]; Lu [7]; Ng and Yang [8]; and Li and Lu [9]; and Li and Lu [10]. An excellent review paper of the Markov-modulated Poisson process is the paper by Fischer and Meier-Hellstern [11]. Li et al. [12] study the distributions of T_u and N_u for a risk model with Markovian arrival process (MAP). In the study by Li et al. [13], the one-sided exit time (time of ruin or the first hitting time), the number of claims, and the aggregate claims by the exit time are decomposed into m components, respectively, according to the underlying Markov state. Joint Laplace transforms and probability generating functions of all these decomposed quantities are analyzed via matrix scale functions and matrix analysis methods. The motivation of our work is that the insurer would consider a collection of similar conditions as a whole and risk information based on the subset of states would be helpful for insurers to better understand and control their risks for a particular subset of interest and make strategic and contingency plans accordingly.

In this paper, we investigate some state-specific one-sided and two-sided first exit probabilities using several versions of the matrix scale functions for the risk model. To the best knowledge of the authors, this is the first paper to study exit probabilities of the subset of states by using different forms of the matrix scale functions. We start in Section 2 by defining these modified or dimension-reduced matrix scale functions for the Markov-modulated risk model as well as for the classical risk model. We study the probability of ruin without the surplus visiting the state-state space E_k and the probability of ruin without claims occurring in E_k in Sections 3 and 4, respectively. The probability of reaching a target level without the surplus visiting E_k and the probability of reaching a target level without claims occurring in E_k are discussed in Sections 5 and 6, respectively. In Section 7, we study the corresponding two-sided first exit probabilities without the surplus visiting E_k or without claims occurring in E_k. Some numerical examples are demonstrated in Section 8.

2. Notation and Preliminaries

We define the following $m \times m$ matrices:

$$\begin{aligned} \mathbf{c} &= \operatorname{diag}(c_1, c_2, \ldots, c_m), \\ \boldsymbol{\lambda} &= \operatorname{diag}(\lambda_1, \lambda_2, \ldots, \lambda_m), \\ \mathbf{f}(x) &= \operatorname{diag}(f_1(x), f_2(x), \ldots, f_m(x)), \\ \mathbf{F}(x) &= \operatorname{diag}(F_1(x), F_2(x), \ldots, F_m(x)) \\ &= \mathbf{I} - \overline{\mathbf{F}}(x), \\ \mathbf{I} &= \operatorname{diag}(1, 1, \ldots, 1). \end{aligned} \tag{6}$$

Let $E_k = \{l_1, l_2, \ldots, l_k\} \subset E$ and for any $m \times m$ matrix $\mathbf{X} = (x_{i,j})_{i,j \in E}$, we define the following four matrices:

$$\begin{aligned} \mathbf{X}_{11} &= \left(x_{i,j}\right)_{i,j \in E_k}, \\ \mathbf{X}_{22} &= \left(x_{i,j}\right)_{i,j \in E/E_k}, \\ \mathbf{X}_{12} &= \left(x_{i,j}\right)_{i \in E_k, j \in E/E_k}, \\ \mathbf{X}_{21} &= \left(x_{i,j}\right)_{i \in E/E_k, j \in E_k}. \end{aligned} \tag{7}$$

Here, $\mathbf{X}_{22}$ is an $(m-k) \times (m-k)$ matrix obtained by deleting the l_i-th row and the l_i-th column of $\mathbf{X}$, for $i \in E_k$. We remark that if $E_k = E$, then $\mathbf{X}_{11} = \mathbf{X}$ and $\mathbf{X}_{22} = \mathbf{X}_{12} = \mathbf{X}_{21} = \varnothing$.

2.1. Matrix Scale Function and Its Modified and Dimension-Reduced Versions. In this section, we define a matrix-form scale function and its several modified or reduced forms which play important roles in the rest of the paper.

Definition 1. Define $\mathbf{W}(u)$ to be a matrix function such that

$$\begin{aligned}\widehat{\mathbf{W}}(s) &= \int_0^\infty e^{-su}\mathbf{W}(u)\mathrm{d}u \\ &= [\mathbf{B}(s)]^{-1},\end{aligned} \tag{8}$$

where

$$\mathbf{B}(s) = s\mathbf{I} - \mathbf{c}^{-1}(\boldsymbol{\lambda} - \mathbf{A}) + \mathbf{c}^{-1}\boldsymbol{\lambda}\widehat{\mathbf{f}}(s). \tag{9}$$

Here, $\mathbf{W}(u)$ is called the matrix-form scale function for the Markov-modulated risk model with $\mathbf{W}(0) = \lim_{s\longrightarrow\infty} s\widehat{\mathbf{W}}(s) = \lim_{s\longrightarrow\infty} s[\mathbf{B}(s)]^{-1} = \mathbf{I}$. A similar matrix-form scale function can be found in Li et al.'s study [13].

Definition 2. Define $\mathbf{W}_{11}(u)$ and $\mathbf{W}_{22}(u)$ to be a $k\times k$ matrix function and an $(m-k)\times(m-k)$ matrix function, respectively, such that

$$\begin{aligned}\widehat{\mathbf{W}}_{11}(s) &= \int_0^\infty e^{-su}\mathbf{W}_{11}(u)\mathrm{d}u \\ &= [\mathbf{B}_{11}(s)]^{-1}, \\ \widehat{\mathbf{W}}_{22}(s) &= \int_0^\infty e^{-su}\mathbf{W}_{22}(u)\mathrm{d}u \\ &= [\mathbf{B}_{22}(s)]^{-1},\end{aligned} \tag{10}$$

where

$$\begin{aligned}\mathbf{B}_{11}(s) &= s\mathbf{I}_{11} - \mathbf{c}_{11}^{-1}(\boldsymbol{\lambda}_{11} - \mathbf{A}_{11}) + \mathbf{c}_{11}^{-1}\boldsymbol{\lambda}_{11}\widehat{\mathbf{f}}_{11}(s), \\ \mathbf{B}_{22}(s) &= s\mathbf{I}_{22} - \mathbf{c}_{22}^{-1}(\boldsymbol{\lambda}_{22} - \mathbf{A}_{22}) + \mathbf{c}_{22}^{-1}\boldsymbol{\lambda}_{22}\widehat{\mathbf{f}}_{22}(s).\end{aligned} \tag{11}$$

Remark 1

(1) $\mathbf{W}_{11}(u)$ and $\mathbf{W}_{22}(u)$ are called reduced matrix-form scale functions for the Markov-modulated risk model with

$$\begin{aligned}\mathbf{W}_{11}(0) &= \lim_{s\longrightarrow\infty} s\widehat{\mathbf{W}}_{11}(s) \\ &= \lim_{s\longrightarrow\infty} s[\mathbf{B}_{11}(s)]^{-1} \\ &= \mathbf{I}_{11},\end{aligned} \tag{12}$$

and similarly, $\mathbf{W}_{22}(0) = \mathbf{I}_{22}$.

(2) If $E_k = E$, then $\mathbf{W}_{11} = \mathbf{W}(u)$; if $E_k = \varnothing$, then $\mathbf{W}_{22} = \mathbf{W}(u)$.

(3) If $E_k = \{i\}$, then $\mathbf{B}_{11}(s) = s - (\lambda_i + \alpha_i)/c_i + \lambda_i\widehat{f}_i(s)/c_i$, and $\mathbf{W}_{11}(u) = \eta_{\alpha_i}(u)$ is the α_i-scale function defined in the next section for the classical risk model.

(4) For $E_k \subset E$, it follows from the matrix generalization of Rouche's Theorem (De Smit [14] or Li and Ren [15]) that $\mathrm{Det}[\mathbf{B}_{11}(s)] = 0$ has k roots with positive real parts, say $\rho_{11,1}, \rho_{11,2}, \ldots, \rho_{11,k}$. Similarly, $\mathrm{Det}[\mathbf{B}_{22}(s)] = 0$ has $m-k$ roots with positive real parts, say $\rho_{22,1}, \rho_{22,2}, \ldots, \rho_{22,m-k}$.

Definition 3. For $E_k = \{l_1, l_2, \ldots, l_k\} \subset E$, we define $\mathbf{V}(u, E_k)$ to be an $m\times m$ matrix function such that

$$\begin{aligned}\widehat{\mathbf{V}}(s; E_k) &= \int_0^\infty e^{-su}\mathbf{V}(u; E_k)\mathrm{d}u \\ &= [\mathbf{B}(s; E_k)]^{-1},\end{aligned} \tag{13}$$

where

$$\mathbf{B}(s; E_k) = s\mathbf{I} - \mathbf{c}^{-1}(\boldsymbol{\lambda} - \mathbf{A}) + \mathbf{c}^{-1}\boldsymbol{\lambda}\left(\mathbf{I} - \mathbf{I}_{E_k}\right)\widehat{\mathbf{f}}(s), \tag{14}$$

where $\mathbf{I}_{E_k}$ is an $m\times m$ diagonal matrix with the i-th entry being 1, for $i \in E_k$, and all other entries being zeros.

Remark 2

(1) $\mathbf{V}(u; E_k)$ is called a modified matrix scale function for the Markov-modulated risk model with

$$\begin{aligned}\mathbf{V}(0; E_k) &= \lim_{s\longrightarrow\infty} s\widehat{\mathbf{V}}(s; E_k) \\ &= \lim_{s\longrightarrow\infty} s[\mathbf{B}(s; E_k)]^{-1} \\ &= \mathbf{I}.\end{aligned} \tag{15}$$

(2) If $E_k = \varnothing$, then $\mathbf{V}(u; \varnothing) = \mathbf{W}(u)$.

(3) For $E_k \subset E$, it follows from the matrix generalization of Rouche's Theorem (De Smit [14] or Li and Ren [15]) that $\mathrm{Det}[\mathbf{B}(s; E_k)] = 0$ has m roots with positive real parts, say $\rho_1(E_k), \rho_2(E_k), \ldots, \rho_m(E_k)$.

To evaluate the matrix scale functions $\mathbf{W}(u), \mathbf{W}_{11}(u), \mathbf{W}_{22}(u)$, and $\mathbf{V}(u; E_k)$, we need to make assumptions about the claim size distributions. If we assume that each $\widehat{f}_i(s)$ is a rational function, then we can show that each element of $\widehat{\mathbf{W}}(s) = [\mathbf{B}(s)]^{-1} = \mathbf{B}^*(s)/\mathrm{Det}[\mathbf{B}(s)]$ is a rational function which is readily inverted to obtain $\mathbf{W}(u)$ by partial fractions. The same are true for $\mathbf{W}_{11}(u), \mathbf{W}_{22}(u)$, and $\mathbf{V}(u; E_k)$.

2.2. Scale Function in the Classical Risk Model. Let $\eta_\alpha(u)$ with $\eta_\alpha(0) = 1$ be a function such that its Laplace transform $\widehat{\eta}_\alpha(s) = \int_0^\infty e^{-su}\eta_\alpha(u)\mathrm{d}u$ is given by

$$\widehat{\eta}_\alpha(s) = \frac{1}{s - (\lambda+\alpha)/c + \lambda\widehat{f}(s)/c}. \tag{16}$$

Remark 3

(i) $\eta_\alpha(u)$ is called the α-scale function (apart from a multiplicative constant) in the classical risk model with premium rate c, Poisson arrival rates λ, and claim amounts density $f(x)$.

(ii) Chan et al. [16] show that $\eta_\alpha(u)$ has the form of

$$\eta_\alpha(u) = \frac{e^{\rho(\alpha)u} - \Psi_\alpha(u)}{1 - \Psi_\alpha(0)}, \quad u \geq 0, \tag{17}$$

where $\Psi_\alpha(u)$ has three different forms and $\rho = \rho(\alpha)$ with $\rho(0) = 0$ is the unique positive solution of the following generalized Lundberg's equation:

$$\lambda + \alpha - cs = \lambda \hat{f}(s). \tag{18}$$

In particular, if $\alpha = 0, \Psi_0(u) = \psi(u)$ simplifies to the ruin probability for the classical risk model and $\eta_0(u) = (1 - \psi(u))/(1 - \psi(0))$.

(iii) If we replace c by c_k, replace λ by λ_k, replace $f(x)$ by $f_k(x)$, and replace α by α_k, then we write $\eta_\alpha(u)$ as $\eta_{\alpha_k}(u)$ and write $\rho = \rho(\alpha)$ as $\rho_k = \rho_k(\alpha_k)$, for $k = 1, 2, \ldots, m$.

3. Probability of Ruin without the Surplus Visiting States in E_k

First, we define for $i \in E$,

$$\begin{aligned}\psi_i(u; E_k) &= P(T_u < \infty, J(t) \notin E_k, 0 \leq t \leq T_u \mid J(0) = i) \\ &= P\left(T_u < \infty, T_{u,E_k} = 0 \mid J(0) = i\right),\end{aligned} \tag{19}$$

to be the probability of ruin without the external environmental Markov process visiting the substate space E_k prior to ruin.

Remark 4

(1) It follows from the definition above that $\psi_i(u; E_k) = 0$ if $i \in E_k$.

(2) $\psi_i(u; \{k\})$ is the probability of ruin without the surplus visiting state k, for $k \neq i$, given $J(0) = i$.

(3) $\psi_i(u; E\backslash\{E_k\})$ is the probability of ruin with the surplus ever visiting every state in E_k.

(4) $\psi_i(u; E\backslash\{i\})$ is the probability of ruin with the surplus only visiting the initial state i.

(5) If $E_k = \varnothing$, then $\psi_i(u; \varnothing) = \psi_i(u)$ is the probability of ruin given that the initial state is i.

Conditioning on the events that may occur in an infinitesimal interval, we can obtain the following IDE for $\psi_i(u; E_k)$:

$$\begin{aligned}c_i\psi_i'(u; E_k) &= \lambda_i\psi_i(u; E_k) - \lambda_i \int_0^u \psi_i(u - x; E_k) f_i(x)\mathrm{d}x \\ &\quad - \lambda_i\overline{F}_i(u) - \sum_{j=1, j\notin E_k}^{m} \alpha_{i,j}\psi_j(u; E_k), \quad i \in E\backslash\{E_k\}.\end{aligned} \tag{20}$$

Let $\vec{\boldsymbol{\psi}}(u; E_k) = (\psi_i(u; E_k), i \in E\backslash\{E_k\})^\top$ be an $(m-k) \times 1$ column vector. Equation (20) can be rewritten in matrix form as

$$\begin{aligned}\vec{\boldsymbol{\psi}}'(u; E_k) &= \mathbf{c}_{22}^{-1}(\boldsymbol{\lambda}_{22} - \mathbf{A}_{22})\vec{\boldsymbol{\psi}}(u; E_k) \\ &= -\mathbf{c}_{22}^{-1}\boldsymbol{\lambda}_{22}\left[\int_0^u \mathbf{f}_{22}(x)\vec{\boldsymbol{\psi}}(u - x; E_k)\mathrm{d}x + \overline{\mathbf{F}}_{22}(u)\vec{1}\right].\end{aligned} \tag{21}$$

Denote $\hat{\vec{\boldsymbol{\psi}}}(s; E_k) = \int_0^\infty e^{-su}\vec{\boldsymbol{\psi}}(u; E_k)\mathrm{d}u$. Taking Laplace transforms of both sides of equation (21) gives

$$\mathbf{B}_{22}(s)\hat{\vec{\boldsymbol{\psi}}}(s; E_k) = \vec{\boldsymbol{\psi}}(0; E_k) - \mathbf{c}_{22}^{-1}\boldsymbol{\lambda}_{22}\hat{\overline{\mathbf{F}}}_{22}(s)\vec{1}, \tag{22}$$

where $\mathbf{B}_{22}(s) = s\mathbf{I}_{22} - \mathbf{c}_{22}^{-1}(\lambda_{22} - \mathbf{A}_{22}) + \mathbf{c}_{22}^{-1}\lambda_{22}\hat{\mathbf{f}}_{22}(s)$. Use the same arguments as in the study by Li et al. [13] to find $\vec{\boldsymbol{\psi}}(0; E_k)$. Let $\vec{\mathbf{q}}_{22,i}^\top$ be a $1 \times (m-k)$ row vector such that $\vec{\mathbf{q}}_{22,i}^\top\mathbf{B}_{22}(\rho_{22,i}) = \vec{0}^\top$, for $i = 1, 2, \ldots, m-k$. Setting $s = \rho_{22,i}$ and left-multiplying both sides of (22) by the vector $\vec{\mathbf{q}}_{22,i}^\top$, we have

$$\begin{aligned}\vec{0}^\top &= \vec{\mathbf{q}}_{22,i}^\top\mathbf{B}_{22}\left(\rho_{22,i}\right)\hat{\vec{\boldsymbol{\psi}}}\left(\rho_{22,i}; E_k\right) \\ &= \vec{\mathbf{q}}_{22,i}^\top\vec{\boldsymbol{\psi}}(0; E_k) - \vec{\mathbf{q}}_{22,i}^\top\mathbf{c}_{22}^{-1}\boldsymbol{\lambda}_{22}\hat{\overline{\mathbf{F}}}_{22}\left(\rho_{22,i}\right)\vec{1}, \\ &\qquad i = 1, 2, \ldots, m-k.\end{aligned} \tag{23}$$

Since $\mathbf{c}_{22}, \lambda_{22}$, and $\overline{\mathbf{F}}_{22}(u)$ are all diagonal matrixes,

$$\begin{aligned}\vec{\mathbf{q}}_{22,i}^\top\vec{\boldsymbol{\psi}}(0; E_k) &= \vec{\mathbf{q}}_{22,i}^\top\mathbf{c}_{22}^{-1}\boldsymbol{\lambda}_{22}\hat{\overline{\mathbf{F}}}_{22}\left(\rho_{22,i}\right)\vec{1} \\ &= \vec{\mathbf{q}}_{22,i}^\top\mathbf{c}_{22}^{-1}\boldsymbol{\lambda}_{22}\int_0^\infty e^{-\rho_{22,i}u}\overline{\mathbf{F}}_{22}(x)\mathrm{d}x\vec{1} \\ &= \int_0^\infty e^{-\rho_{22,i}u}\vec{\mathbf{q}}_{22,i}^\top\overline{\mathbf{F}}_{22}(x)\mathrm{d}x\mathbf{c}_{22}^{-1}\boldsymbol{\lambda}_{22}\vec{1}.\end{aligned} \tag{24}$$

In matrix form, we have

$$\vec{\boldsymbol{\psi}}(0; E_k) = \int_0^\infty e^{-x\boldsymbol{\Theta}_{22}}\overline{\mathbf{F}}_{22}(x)dx\mathbf{c}_{22}^{-1}\boldsymbol{\lambda}_{22}\vec{1}, \tag{25}$$

where $\boldsymbol{\Theta}_{22} = \mathbf{q}_{22}^{-1}\rho_{22}\mathbf{q}_{22}$, $\boldsymbol{\rho}_{22} = \mathrm{diag}(\rho_{22,1}, \rho_{22,2}, \ldots, \rho_{22,m-k})$, and

$$\mathbf{q}_{22} = \left(\vec{\mathbf{q}}_{22,1}, \vec{\mathbf{q}}_{22,2}, \ldots, \vec{\mathbf{q}}_{22,m-k}\right)^\top, \tag{26}$$

with $\vec{\mathbf{q}}_{22,i}^\top$ being a $1 \times (m-k)$ row vector such that $\vec{\mathbf{q}}_{22,i}^\top\mathbf{B}_{22}(\rho_{22,i}) = \vec{0}^\top$, for $i = 1, 2, \ldots, m-k$.

3.1. Explicit Expression in terms of the Dimension-Reduced Matrix Scale Function. Rearranging (22) gives

$$\hat{\vec{\boldsymbol{\psi}}}(s; E_k) = [\mathbf{B}_{22}(s)]^{-1}\left[\vec{\boldsymbol{\psi}}(0; E_k) - \mathbf{c}_{22}^{-1}\boldsymbol{\lambda}_{22}\hat{\overline{\mathbf{F}}}_{22}(s)\vec{1}\right], \tag{27}$$

as the Laplace transform of $\mathbf{W}_{22}(u)$ is $[\mathbf{B}_{22}(s)]^{-1}$; then, by inverting (27), it gives

$$\begin{aligned}\vec{\psi}(u;E_k) &= \mathbf{W}_{22}(u)\vec{\psi}(0;E_k)\\ &\quad - \int_0^u \mathbf{W}_{22}(u-x)\overline{\mathbf{F}}_{22}(x)\mathrm{d}x\mathbf{c}_{22}^{-1}\boldsymbol{\lambda}_{22}\vec{1}\\ &= \int_0^\infty \mathbf{R}_{22}(u,x)\overline{\mathbf{F}}_{22}(x)\mathrm{d}x\mathbf{c}_{22}^{-1}\boldsymbol{\lambda}_{22}\vec{1}, \quad u>0,\end{aligned} \tag{28}$$

where $\mathbf{W}_{22}(u)$ is the modified matrix version of the scale function defined in Section 2 and

$$\mathbf{R}_{22}(u,x) = \begin{cases}\mathbf{W}_{22}(u)e^{-\boldsymbol{\Theta}_{22}x} - \mathbf{W}_{22}(u-x), & 0\le x\le u,\\ \mathbf{W}_{22}(u)e^{-\boldsymbol{\Theta}_{22}x}, & x>u.\end{cases} \tag{29}$$

Remark 5

(1) Following the same reasoning, we have

$$\begin{aligned}\vec{\psi}(u;E\backslash E_k) &= \int_0^\infty \mathbf{R}_{11}(u,x)\overline{\mathbf{F}}_{11}(x)\mathrm{d}x\mathbf{c}_{11}^{-1}\boldsymbol{\lambda}_{11}\vec{1}, \quad u>0,\\ \vec{\psi}(0;E\backslash E_k) &= \int_0^\infty e^{-x\boldsymbol{\Theta}_{11}}\overline{\mathbf{F}}_{11}(x)\mathrm{d}x\mathbf{c}_{11}^{-1}\boldsymbol{\lambda}_{11}\vec{1},\end{aligned} \tag{30}$$

where $\mathbf{W}_{11}(u)$ is the dimension-reduced matrix scale function defined in Section 2, and

$$\begin{aligned}\mathbf{R}_{11}(u,x) &= \begin{cases}\mathbf{W}_{11}(u)e^{-\boldsymbol{\Theta}_{11}x} - \mathbf{W}_{11}(u-x), & 0\le x\le u,\\ \mathbf{W}_{11}(u)e^{-\boldsymbol{\Theta}_{11}x}, & x>u,\end{cases}\\ \boldsymbol{\Theta}_{11} &= \mathbf{q}_{11}^{-1}\rho_{11}\mathbf{q}_{11},\\ \rho_{11} &= \mathrm{diag}\left(\rho_{11,1},\rho_{11,2},\ldots,\rho_{11,k}\right),\\ \mathbf{q}_{11} &= \left(\vec{\mathbf{q}}_{11,1},\vec{\mathbf{q}}_{11,2},\ldots,\vec{\mathbf{q}}_{11,m-k}\right)^\top,\end{aligned} \tag{31}$$

with $\vec{\mathbf{q}}_{11,i}^\top$ being a $1\times k$ row vector such that $\vec{\mathbf{q}}_{11,i}^\top\mathbf{B}_{11}(\rho_{11,i}) = \vec{0}^\top$, for $i=1,2,\ldots,k$.

(2) In particular, we have

$$\psi_i(0;E\backslash\{i\}) = \frac{\lambda_i}{c_i}\int_0^\infty e^{-\rho_i u}\overline{F}_i(u)\mathrm{d}u, \tag{32}$$

where ρ_i is the unique positive solution of

$$\lambda_i + \alpha_i - c_i s = \lambda_i\hat{f}_i(s), \quad i=1,2,\ldots,m. \tag{33}$$

Equation (30) reduces to the following for $u>0$:

$$\begin{aligned}\psi_i(u;E\backslash\{i\}) &= \eta_{\alpha_i}(u)\psi_i(0;E\backslash\{i\})\\ &\quad - \frac{\lambda_i}{c_i}\int_0^u \eta_{\alpha_i}(u-x)\overline{F}_i(x)\mathrm{d}x, \quad i=1,2,\ldots,m,\end{aligned} \tag{34}$$

where $\psi_i(u;E\backslash\{i\})$ is the probability of ruin with the surplus only visiting the initial state i.

3.2. Exponential Claim Distributions. We assume that $f_i(x) = \boldsymbol{\beta}_i e^{-\boldsymbol{\beta}_i x}$ with $\boldsymbol{\beta}_i>0, x>0, i\in E$, i.e., $\mathbf{f}(x) = \boldsymbol{\beta}e^{-\boldsymbol{\beta}x}$, with $\boldsymbol{\beta} = \mathrm{diag}(\boldsymbol{\beta}_1,\boldsymbol{\beta}_2,\ldots,\boldsymbol{\beta}_m)$. Differentiating equation (21), we obtain a 2nd-order matrix differential equation as follows:

$$\begin{aligned}&\vec{\psi}''(u;E_k) + \left[\boldsymbol{\beta}_{22} - \mathbf{c}_{22}^{-1}(\boldsymbol{\lambda}_{22}-\mathbf{A}_{22})\right]\vec{\psi}'(u;E_k)\\ &\quad + \mathbf{c}_{22}^{-1}\boldsymbol{\beta}_{22}\mathbf{A}_{22}\vec{\psi}(u;E_k) = \vec{0},\end{aligned} \tag{35}$$

with $\lim_{u\longrightarrow\infty}\vec{\psi}(u;E_k) = \vec{0}$ and $\lim_{u\longrightarrow 0}\vec{\psi}(u;E_k) = \vec{\psi}(0;E_k)$. The solution to this matrix differential equation is

$$\vec{\psi}(u;E_k) = e^{-\mathbf{R}u}\vec{\psi}(0;E_k), \quad u>0, \tag{36}$$

where $\vec{\psi}(0;E_k)$ is given in (25) and $\mathbf{R}$ is an $(m-k)\times(m-k)$ matrix satisfying the following equation:

$$\mathbf{R}^2 - \left[\boldsymbol{\beta}_{22} - \mathbf{c}_{22}^{-1}(\boldsymbol{\lambda}_{22}-\mathbf{A}_{22})\right]\mathbf{R} + \mathbf{c}_{22}^{-1}\boldsymbol{\beta}_{22}\mathbf{A}_{22} = 0. \tag{37}$$

Remark 6

(i) The solution to (37) is not unique, and the one whose eigenvalues have positive real parts is our $\mathbf{R}$

(ii) A study of approaches to solve quadratic matrix equations is conducted in Higham and Kim [17]

In particular, if $m=2$ and $E_1=\{2\}$, then it follows from equation (36) that

$$\psi_1(u;\{2\}) = e^{-R_1 u}\psi_1(0;\{2\}), \quad u>0, \tag{38}$$

where R_1 is the positive solution of the following quadratic equation:

$$c_1 s^2 - [c_1\beta_1 - (\lambda_1+\alpha_1)]s - \beta_1\alpha_1 = 0, \tag{39}$$

and $\psi_1(0;\{2\})$ is given by (32) as follows:

$$\begin{aligned}\psi_1(0;\{2\}) &= \frac{\lambda_1}{c_1}\int_0^\infty e^{-\rho_1 x}\overline{F}_1(x)\mathrm{d}x\\ &= \frac{\lambda_1}{c_1}\int_0^\infty e^{-\rho_1 x}e^{-\beta_1 x}\mathrm{d}x\\ &= \frac{\lambda_1}{c_1(\rho_1+\beta_1)},\end{aligned} \tag{40}$$

with ρ_1 satisfying equation $\lambda_1+\alpha_1-c_1 s = \lambda_1\hat{f}_1(s)$. We comment that $-\rho_1$ is the negative solution to equation (39).

4. Probability of Ruin without a Claim Occurring in States in E_k

For $E_k = \{l_1,l_2,\ldots,l_k\}$ and for $i\in E$, let

$$\chi_i(u;E_k) = \mathrm{P}\left(T_u<\infty, N_{u,E_k}=0 \mid J(0)=i\right) \tag{41}$$

be the probability of ruin without a claim occurring in E_k by the time of ruin given that $J(0)=i$.

Remark 7

(1) $\chi_i(u;\{k\})$ is the probability of ruin without a claim occurring in state k, for $k\in E$, given $J(0)=i$

(2) $\chi_i(u;E\backslash\{E_k\})$ is the probability of ruin with claims occurring in states in E_k

(3) $\chi_i(u;E\backslash\{i\})$ is the probability of ruin with claims only occurring when the process is in the state i

(4) If $E_k=\varnothing$, then $\chi_i(u;\varnothing)$ recovers the ruin probability $\psi_i(u)$

(5) Note that $\chi_i(u;E_k)-\psi_i(u;E_k)$ is the probability of ruin with the surplus visiting E_k, but without claims occurring in E_k

Conditioning on the events that may occur in an infinitesimal interval, we can obtain the following IDE for $\chi_i(u;E_k)$:

$$\begin{aligned}c_i\chi_i'(u;E_k)&=\lambda_i\chi_i(u;E_k)-\sum_{j=1}^{m}\alpha_{i,j}\chi_j(u;E_k)\\&\quad-\lambda_i\int_0^u\chi_i(u-x;E_k)f_i(x)\mathrm{d}x-\lambda_i\overline{F}_i(u),\quad i\notin E_k,\\c_i\chi_i'(u;E_k)&=\lambda_i\chi_i(u;E_k)-\sum_{j=1}^{m}\alpha_{i,j}\chi_j(u;E_k),\quad i\in E_k.\end{aligned}\tag{42}$$

Let $\overrightarrow{\chi}(u;E_k)=(\chi_i(u;E_k);i\in E)^\top$ be an $m\times 1$ column vector. In the matrix form, we have

$$\begin{aligned}\overrightarrow{\boldsymbol{\chi}}'(u;E_k)&=\mathbf{c}^{-1}(\boldsymbol{\lambda}-\mathbf{A})\overrightarrow{\boldsymbol{\chi}}(u;E_k)-\mathbf{c}^{-1}\boldsymbol{\lambda}\left(\mathbf{I}-\mathbf{I}_{E_k}\right)\\&\quad\cdot\int_0^u\mathbf{f}(x)\overrightarrow{\boldsymbol{\chi}}(u-x;E_k)\mathrm{d}x-\mathbf{c}^{-1}\boldsymbol{\lambda}\left(\mathbf{I}-\mathbf{I}_{E_k}\right)\overline{\mathbf{F}}(u)\overrightarrow{1}.\end{aligned}\tag{43}$$

Taking Laplace transforms of both sides of (43), we have

$$\mathbf{B}(s;E_k)\widehat{\overrightarrow{\boldsymbol{\chi}}}(s;E_k)=\overrightarrow{\boldsymbol{\chi}}(0;E_k)-\mathbf{c}^{-1}\boldsymbol{\lambda}\left(\mathbf{I}-\mathbf{I}_{E_k}\right)\widehat{\overline{\mathbf{F}}}(s)\overrightarrow{1},\tag{44}$$

where $\mathbf{B}(s;E_k)=s\mathbf{I}-\mathbf{c}^{-1}(\lambda-\mathbf{A})+\mathbf{c}^{-1}\lambda(\mathbf{I}-\mathbf{I}_{E_k})\widehat{\mathbf{f}}(s)$. Then,

$$\begin{aligned}\overrightarrow{\boldsymbol{\chi}}(0;E_k)&=\int_0^\infty e^{-x\boldsymbol{\Theta}_{E_k}}\overline{\mathbf{F}}(x)\mathrm{d}x\mathbf{c}^{-1}\boldsymbol{\lambda}\left(\mathbf{I}-\mathbf{I}_{E_k}\right)\overrightarrow{1},\\\overrightarrow{\boldsymbol{\chi}}(u;E_k)&=\mathbf{V}(u;E_k)\overrightarrow{\boldsymbol{\chi}}(0;E_k)\\&\quad-\int_0^u\mathbf{V}(u-x;E_k)\overline{\mathbf{F}}(x)\mathrm{d}x\mathbf{c}^{-1}\boldsymbol{\lambda}\left(\mathbf{I}-\mathbf{I}_{E_k}\right)\overrightarrow{1}\\&=\int_0^\infty\mathbf{R}(u,x;E_k)\overline{\mathbf{F}}(x)\mathrm{d}x\mathbf{c}^{-1}\boldsymbol{\lambda}\left(\mathbf{I}-\mathbf{I}_{E_k}\right)\overrightarrow{1},\end{aligned}\tag{45}$$

where $\mathbf{V}(u;E_k)$ is a modified matrix scale function defined in Section 2. And,

$$\begin{aligned}\mathbf{R}(u,x;E_k)&=\begin{cases}\mathbf{V}(u;E_k)e^{-x\boldsymbol{\Theta}_{E_k}}-\mathbf{V}(u-x;E_k), & 0\le x\le u,\\\mathbf{V}(u;E_k)e^{-x\boldsymbol{\Theta}_{E_k}}, & x>u,\end{cases}\\\boldsymbol{\Theta}_{E_k}&=\left[\mathbf{Q}_{E_k}\right]^{-1}\operatorname{diag}(\rho_1(E_k),\rho_2(E_k),\ldots,\rho_m(E_k))\mathbf{Q}_{E_k},\\\mathbf{Q}_{E_k}&=\left(\overrightarrow{\mathbf{q}}_{E_k,1},\overrightarrow{\mathbf{q}}_{E_k,2},\ldots,\overrightarrow{\mathbf{q}}_{E_k,m}\right)^\top,\end{aligned}\tag{46}$$

with $\overrightarrow{\mathbf{q}}^\top_{E_k,i}$ being a $1\times m$row vector such that $\overrightarrow{\mathbf{q}}^\top_{E_k,i}\mathbf{B}(\rho_i(E_k);E_k)=\overrightarrow{0}^\top$, for $i=1,2,\ldots,m$.

If we assume claim amounts are exponentially distributed, i.e., $\mathbf{f}(x)=\boldsymbol{\beta}e^{-\boldsymbol{\beta}x}$, with $\boldsymbol{\beta}=\operatorname{diag}(\boldsymbol{\beta}_1,\boldsymbol{\beta}_2,\ldots,\boldsymbol{\beta}_m)$, then by differentiating equation (43), we can obtain a 2nd-order matrix differential equation for $\overrightarrow{\chi}(u;E_k)$ whose solution is given by

$$\overrightarrow{\boldsymbol{\chi}}(u;E_k)=e^{-\Delta u}\overrightarrow{\boldsymbol{\chi}}(0;E_k),\quad u>0,\tag{47}$$

where Δ is the solution to the following quadratic matrix equation:

$$\boldsymbol{\Delta}^2-\left[\boldsymbol{\beta}-\mathbf{c}^{-1}(\boldsymbol{\lambda}-\mathbf{A})\right]\boldsymbol{\Delta}+\mathbf{c}^{-1}\boldsymbol{\beta}\left(\boldsymbol{\lambda}\mathbf{I}_{E_k}-\mathbf{A}\right)=0.\tag{48}$$

We remark that the solutions to the equation above is not unique and the one with positive eigenvalues is our Δ.

5. Probability of Hitting a Target Level without the Surplus Ever Visiting States in E_k

For $u\le b$, let $T_u^b=\min(t\ge 0,U(t)=b)$ be the first time when the surplus reaches level b. We define

$$\psi_{i,j}(u,b;E_k)=\mathrm{P}\left(J(t)\notin E_k,J\left(T_u^b\right)=j,0\le t\le T_u^b\mid J(0)=i\right),\quad i,j\notin E_k,\tag{49}$$

to be the probability of hitting a target level b at state j without the surplus ever visiting substate space E_k, given that the initial state is $i\notin E_k$.

Remark 8

(1) $\psi_{i,j}(u,b;\varnothing)$ is the probability of hitting a target level b at state j given that the initial state is i

(2) $\psi_{i,j}(u,b;E\backslash\{i,j\})$ is the probability of hitting a target level b at state j from the initial state i without the surplus visiting any other states

By conditioning on the events that may occur in an infinitesimal interval, we obtain the following IDE:

$$\begin{aligned}\boldsymbol{\psi}'(u,b;E_k)&=\mathbf{c}_{22}^{-1}(\boldsymbol{\lambda}_{22}-\mathbf{A}_{22})\boldsymbol{\psi}(u,b;E_k)\\&\quad-\mathbf{c}_{22}^{-1}\boldsymbol{\lambda}_{22}\int_0^\infty\mathbf{f}_{22}(y)\boldsymbol{\psi}(u-y;b;E_k)\mathrm{d}x,\end{aligned}\tag{50}$$

where $\boldsymbol{\psi}(u,b;E_k)=(\psi_{i,j}(u,b;E_k);i,j\in E\backslash\{E_k\})$ is an $(m-k)\times(m-k)$ matrix.

The following three properties are satisfied by $\boldsymbol{\psi}_{i,j}$:

Property 1: $\psi_{i,j}(b,b;E_k) = I(i=j)$

Property 2: $\psi_{i,j}(u,b;E_k)$ is a function of $(b-u)$

Property 3: $\psi_{i,j}(u,b;E_k) = \sum_{l\notin E_k}\psi_{i,l}(u,b_1;E_k)\psi_{l,j}(b_1,b;E_k)$, for $u \le b_1 \le b$

This shows that $\boldsymbol{\psi}(u,b;E_k)$ must have the following form:

$$\boldsymbol{\psi}(u,b;E_k) = e^{-\Gamma_{22}(b-u)}, \quad u \le b, \tag{51}$$

where Γ_{22} is an $(m-k)\times(m-k)$ matrix and all of its eigenvalues must have positive real parts. It can be showed by substituting (51) into (50) that Γ_{22} satisfies a matrix equation as follows:

$$\Gamma_{22} + \mathbf{c}_{22}^{-1}\boldsymbol{\lambda}_{22}\int_0^\infty \mathbf{f}_{22}(x)e^{-\Gamma_{22}x}\mathrm{d}x - \mathbf{c}_{22}^{-1}(\boldsymbol{\lambda}_{22} - \mathbf{A}_{22}) = 0, \tag{52}$$

with the following solution:

$$\Gamma_{22} = \mathbf{H}_{22}\rho_{22}\mathbf{H}_{22}^{-1}, \tag{53}$$

where $\mathbf{H}_{22} = (\overrightarrow{\mathbf{h}}_{22,1}, \overrightarrow{\mathbf{h}}_{22,2}, \ldots, \overrightarrow{\mathbf{h}}_{22,m-k})$, $\boldsymbol{\rho}_{22} = \mathrm{diag}(\rho_{22,1}, \rho_{22,2}, \ldots, \rho_{22,m-k})$, and $\rho_{22,1}, \rho_{22,2}, \ldots, \rho_{22,m-k}$ are the $(m-k)$ distinct roots of $\mathrm{Det}[\mathbf{B}_{22}(s)] = 0$. The column vector $\overrightarrow{\mathbf{h}}_{22,i}$ is that $\mathbf{B}_{22}(\rho_{22,i})\overrightarrow{\mathbf{h}}_{22,i} = \overrightarrow{0}$.

In particular, for $E_k = E\backslash\{i\}$, the result in (51) simplifies to

$$\psi_{i,i}(u,b;E\backslash\{i\}) = e^{-\rho_i(b-u)}, \quad u \le b, \tag{54}$$

which is the probability of hitting a target level b at state i from the initial state i without the surplus visiting any other states.

6. Probability of Hitting a Target Level without a Claim Occurring in States in E_k

For $u \le b$, define $\chi_{i,j}(u,b;E_k)$ to be the probability of hitting a target level b at state $j \in E$ without a claim occurring in states in E_k, given that the initial state is $i \in E$.

Remark 9

(1) $\chi_{i,j}(u,b;\varnothing) = \psi_{i,j}(u,b;\varnothing)$ is the probability of hitting a target level b at state j given that the initial state is i

(2) $\chi_{i,j}(u,b;E)$ is the probability of hitting a target level b at state j from the initial state i without any claim occurring

(3) $\chi_{i,j}(u,b;E\backslash\{k\})$ is the probability of hitting a target level b at state j from the initial state i with claims occurring only in state k

Using the same arguments as in the previous section, we have for $u \le b$,

$$\begin{aligned} c_i\chi_{i,j}'(u,b;E_k) &= \lambda_i\chi_{i,j}(u,b;E_k) - \sum_{k=1}^m \alpha_{i,k}\chi_{k,j}(u,b;E_k) \\ &\quad - \lambda_i\int_0^\infty \chi_{i,j}(u-x,b;E_k)f_i(x)\mathrm{d}x, \quad i \notin E_k \\ c_i\chi_{i,j}'(u,b;E_k) &= \lambda_i\chi_{i,j}(u,b;E_k) - \sum_{k=1}^m \alpha_{i,k}\chi_{k,j}(u,b;E_k), \quad i \in E_k. \end{aligned} \tag{55}$$

This is written in matrix form as

$$\begin{aligned} \boldsymbol{\chi}'(u,b;E_k) &= \mathbf{c}^{-1}(\boldsymbol{\lambda} - \mathbf{A})\boldsymbol{\chi}(u,b;E_k) \\ &= -\mathbf{c}^{-1}\boldsymbol{\lambda}\left[\mathbf{I} - \mathbf{I}_{E_k}\right]\int_0^\infty \mathbf{f}(x)\boldsymbol{\chi}(u-x;b;E_k)\mathrm{d}x, \end{aligned} \tag{56}$$

where $\boldsymbol{\chi}(u,b;E_k) = (\chi_{i,j}(u,b;E_k); i,j \in E)$ is an $m\times m$ matrix. Clearly, $\chi_{i,j}(u,b;E_k)$ has the same three properties as for $\boldsymbol{\psi}_{i,j}(u,b;E_k)$ stated in Section 5, and we have

$$\boldsymbol{\chi}(u,b;E_k) = e^{-\Gamma_{E_k}(b-u)}, \quad u \le b, \tag{57}$$

where Γ_{E_k} is an $m\times m$ matrix and all of its eigenvalues must have positive real parts and Γ_{E_k} satisfies an matrix equation with the following solution:

$$\Gamma_{E_k} = \mathbf{H}_{E_k}\rho(E_k)\mathbf{H}_{E_k}^{-1}, \tag{58}$$

where $\mathbf{H}_{E_k} = (\overrightarrow{\mathbf{h}}_{E_k,1}, \overrightarrow{\mathbf{h}}_{E_k,2}, \ldots, \overrightarrow{\mathbf{h}}_{E_k,m})$, $\rho(E_k) = \mathrm{diag}(\rho_1(E_k), \rho_2(E_k), \ldots, \rho_m(E_k))$, and $\rho_1(E_k), \rho_2(E_k), \ldots, \rho_m(E_k)$ are the m distinct roots of $\mathrm{Det}[\mathbf{B}(s;E_k)] = 0$. The column vector $\overrightarrow{\mathbf{h}}_{E_k,i}$ is that $\mathbf{B}(\rho_i(E_k);E_k)\overrightarrow{\mathbf{h}}_{E_k,i} = \overrightarrow{0}$.

In particular, when $E_k = E$, then equations (55) and (56) simplify to

$$\boldsymbol{\chi}'(u,b;E) = \mathbf{c}^{-1}(\boldsymbol{\lambda} - \mathbf{A})\boldsymbol{\chi}(u,b;E), \tag{59}$$

with the following solution:

$$\boldsymbol{\chi}(u,b;E) = e^{\mathbf{c}^{-1}(\mathbf{A}-\boldsymbol{\lambda})(b-u)}, \quad u \le b. \tag{60}$$

7. Two-Sided First Exit Probabilities

In Sections 3–6, we have studied the one-sided exit probability without the surplus visiting states in E_k or without a claim occurring in states in E_k. In this section, we aim to investigate the corresponding two-sided first exit probabilities.

7.1. Probability of Hitting a Target Level prior to Ruin without the Process Visiting States in E_k. For $0 \le u \le b$ and $i,j \in E$, we define

$$\xi_{i,j}(u,b;E_k) = \mathrm{P}\Big(T_u^b < T_u, J\big(T_u^b\big) = j, \\ J(t) \notin E_k, 0 \le t < T_u^b \mid J(0) = i\Big), \tag{61}$$

to be the probability of reaching b in state j with neither ruin occurring nor the process visiting states in E_k, given that the initial state is i. Clearly, we have the following cases:

(1) $\xi_{i,j}(u,b;E_k) = 0$, if $i \in E_k$ or $j \in E_k$

(2) $\xi_{i,j}(b,b;E_k) = I(i=j)$, if $i, j \notin E_k$

(3) If $E_k = \varnothing$, then $\xi_{i,j}(u,b;\varnothing) = \xi_{i,j}(u,b)$ is the probability of reaching b in state j prior to ruin given that $J(0) = i$

Let $\boldsymbol{\xi}(u,b;E_k) = (\xi_{i,j}(u,b;E_k); i,j \in E\backslash\{E_k\})$ be an $(m-k)\times(m-k)$ matrix. Using the same arguments as in Section 3, we can show that $\xi(u,b;E_k)$ satisfies the following matrix-form IDE:

$$\begin{aligned}\boldsymbol{\xi}'(u,b;E_k) &= \mathbf{c}_{22}^{-1}(\boldsymbol{\lambda}_{22} - \mathbf{A}_{22})\boldsymbol{\xi}(u;E_k) \\ &= -\mathbf{c}_{22}^{-1}\boldsymbol{\lambda}_{22}\int_0^u \mathbf{f}_{22}(x)\boldsymbol{\xi}(u-x;E_k)\mathrm{d}x, \quad 0 \le u < b,\end{aligned} \tag{62}$$

with the boundary condition $\boldsymbol{\xi}(b,b;E_k) = \mathbf{I}$. It can be shown by using the Laplace transform method that $\mathbf{W}_{22}(u)$ satisfies the IDE in (62) for $0 \le u < \infty$, we conclude by noting that $\boldsymbol{\xi}(b,b;E_k) = \mathbf{I}$ that

$$\boldsymbol{\xi}(u,b;E_k) = \mathbf{W}_{22}(u)\left[\mathbf{W}_{22}(b)\right]^{-1}, \quad 0 \le u \le b. \tag{63}$$

7.2. Probability of Ruin without the Surplus Hitting a Certain Level b and without Visiting States in E_k. For $0 \le u \le b$ and $i \in E$, we define

$$\tau_i(u,b;E_k) = \mathrm{P}\Big(T_u < T_u^b, J(t) \notin E_k, 0 \le t < T_u \mid J(0) = i\Big), \tag{64}$$

to be the probability of ruin without the surplus reaching b and without the process visiting states in E_k, given that the initial state is i. Clearly, we have the following cases:

(1) $\tau_i(u,b;E_k) = 0$, if $i \in E_k$

(2) $\tau_i(b,b;E_k) = 0$, if $i \in E$

(3) $\tau_i(u,b;E\backslash\{i\})$ is the probability of ruin without the surplus hitting a certain level b and without state change from the initial state i prior to ruin

(4) If $E_k = \varnothing$, then $\tau_i(u,b;\varnothing) = \tau_{i,j}(u,b)$ is the probability of ruin without the surplus reaching b prior to ruin given that $J(0) = i$

By considering whether or not the surplus has reached b prior to ruin, we have the following formula:

$$\psi_i(u;E_k) = \tau_i(u,b;E_k) + \sum_{j\notin E_k}\xi_{i,j}(u,b;E_k)\psi_j(b;E_k), \\ i \notin E_k. \tag{65}$$

In the matrix form, we have

$$\overrightarrow{\boldsymbol{\psi}}(u;E_k) = \overrightarrow{\boldsymbol{\tau}}(u,b;E_k) + \boldsymbol{\xi}(u,b;E_k)\overrightarrow{\boldsymbol{\psi}}(b;E_k), \tag{66}$$

where $\overrightarrow{\boldsymbol{\tau}}(u,b;E_k) = (\tau_{i,j}(u,b;E_k), i \in E\backslash\{E_k\})^\top$. This together with (63) gives

$$\overrightarrow{\boldsymbol{\tau}}(u,b;E_k) = \overrightarrow{\boldsymbol{\psi}}(u;E_k) - \mathbf{W}_{22}(u)\left[\mathbf{W}_{22}(b)\right]^{-1}\overrightarrow{\boldsymbol{\psi}}(b;E_k), \\ 0 \le u \le b. \tag{67}$$

7.3. Probability of Hitting a Certain Level prior to Ruin without Claims Occurring in States in E_k. For $0 \le u \le b$ and $i, j \in E$, we define $\eta_{i,j}(u,b;E_k)$ to be the probability of the surplus reaching b in state j without ruin occurring and without claims occurring in states in E_k, given that $J(0) = i$. Clearly, we have the following cases:

(1) $\eta_{i,j}(b,b;E_k) = I(i=j)$, if $i, j \in E$

(2) If $E_k = \varnothing$, then $\eta_{i,j}(u,b;\varnothing) = \xi_{i,j}(u,b)$ is the probability of reaching b in state j prior to ruin given that $J(0) = i$

Let $\boldsymbol{\eta}(u,b;E_k) = (\eta_{i,j}(u,b;E_k); i,j \in E)$ be an $m \times m$ matrix. Using the same arguments as in Section 5, we can show that $\boldsymbol{\eta}(u,b;E_k)$ satisfies the following matrix-form IDE:

$$\begin{aligned}\boldsymbol{\eta}'(u,b;E_k) &= \mathbf{c}^{-1}(\boldsymbol{\lambda} - \mathbf{A})\boldsymbol{\eta}(u,b;E_k) \\ &= -\mathbf{c}^{-1}\boldsymbol{\lambda}\left[\mathbf{I} - \mathbf{I}_{E_k}\right]\int_0^u \mathbf{f}(x)\boldsymbol{\eta}(u-x,b;E_k)\mathrm{d}x, \\ &\qquad 0 \le u < b,\end{aligned} \tag{68}$$

with the boundary condition $\boldsymbol{\eta}'(b,b;E_k) = \mathbf{I}$.

Using the Laplace transform method, we can show that $\mathbf{V}(u;E_k)$ satisfies IDE in (68) for $0 \le u < \infty$. This together with $\boldsymbol{\eta}(b,b;E_k) = \mathbf{I}$ shows

$$\boldsymbol{\eta}(u,b;E_k) = \mathbf{V}(u;E_k)\left[\mathbf{V}(b;E_k)\right]^{-1}, \quad 0 \le u \le b. \tag{69}$$

7.4. Probability of Ruin without Hitting a Certain Level b and without Claims Occurring in E_k. For $0 \le u \le b$ and $i \in E$, we define

$$\zeta_i(u,b;E_k) = \mathrm{P}\Big(T_u < T_u^b, N_{u,E_k} = 0 \mid J(0) = i\Big) \tag{70}$$

to be the probability of ruin without the surplus reaching b and without claims occurring in any state in E_k given $J(0) = i$. Clearly, $\zeta_i(b,b;E_k) = 0$.

By considering whether or not the surplus has reached b prior to ruin, we have the following formula:

$$\chi_i(u;E_k) = \zeta_i(u,b;E_k) + \sum_{j\in E}\eta_{i,j}(u,b;E_k)\chi_j(b;E_k), \\ i \in E. \tag{71}$$

Table 1: The probability of hitting the target level b prior to ruin without the process visiting certain states.

	$b=15$	$b=20$
$\xi_1(u,b;2)$		
$u=0$	0.001469	0.000196
$u=1$	0.002983	0.000398
$u=5$	0.017706	0.002362
$u=10$	0.133386	0.017793
$\xi_2(u,b;1)$		
$u=0$	0.001132	$1.04995*10^{-6}$
$u=1$	0.000069	$2.29747*10^{-6}$
$u=5$	0.001106	0.000037
$u=10$	0.033274	0.001107

Table 2: The probability of ruin without the surplus hitting a certain level b and without visiting certain states.

	$b=15$	$b=20$	$b=\infty$
$\tau_1(u,b;2)$			
$u=0$	0.534610	0.534611	0.534611
$u=1$	0.335676	0.335677	0.335677
$u=5$	0.052166	0.052175	0.052175
$u=10$	0.005026	0.005091	0.005092
$\tau_2(u,b;1)$			
$u=0$	0.338813	0.338813	0.338813
$u=1$	0.243436	0.243436	0.243436
$u=5$	0.064873	0.064876	0.064876
$u=10$	0.012343	0.012422	0.012423

In the matrix form, we have

$$\vec{\boldsymbol{\chi}}(u;E_k)=\vec{\boldsymbol{\zeta}}(u,b;E_k)+\boldsymbol{\eta}(u,b;E_k)\vec{\boldsymbol{\chi}}(b;E_k), \tag{72}$$

where $\vec{\boldsymbol{\zeta}}(u,b;E_k)=(\zeta_{i,j}(u,b;E_k),i\in E)^{\top}$. This together with (69) gives

$$\vec{\boldsymbol{\zeta}}(u,b;E_k)=\vec{\boldsymbol{\chi}}(u;E_k)-\mathbf{V}(u;E_k)\left[\mathbf{V}(b;E_k)\right]^{-1}\vec{\boldsymbol{\chi}}(b;E_k), \quad 0\le u\le b. \tag{73}$$

8. Numerical Illustrations

In this section, we give some numerical results of the probabilities that we have defined in previous sections. We consider two-state Markov-Modulated risk model with intensity matrix as follows:

$$\mathbf{A}=\begin{pmatrix}-\frac{1}{4} & \frac{1}{4}\\ \frac{3}{4} & -\frac{3}{4}\end{pmatrix}, \tag{74}$$

and $\boldsymbol{\pi}=(\pi_1,\pi_2)=(3/4,1/4)$. Further assume that claims follow exponential distributions with the following densities:

Table 3: The probability of ruin without hitting a certain level b and without claims occurring in certain states with initial state 1.

	$b=15$	$b=20$	$b=\infty$
$\zeta_1(u,b;1)$			
$u=0$	0.054230	0.054231	0.054231
$u=1$	0.039444	0.039444	0.039444
$u=5$	0.011029	0.011038	0.011038
$u=10$	0.002152	0.002245	0.002247
$\zeta_1(u,b;2)$			
$u=0$	0.363240	0.363242	0.363242
$u=1$	0.264192	0.264195	0.264195
$u=5$	0.073910	0.073934	0.073934
$u=10$	0.014803	0.015044	0.015049

$$\begin{aligned}f_1(x)&=e^{-x},\\ f_2(x)&=0.5e^{-0.5x},\\ &x>0.\end{aligned} \tag{75}$$

Other parameters are set as $\lambda_1=1,\lambda_2=2/3$, $c_1=4/3$, and $c_2=5/3$, so that positive loading condition holds true. Then, we have expressions for the probability of ruin without the surplus process visiting certain states and the probability of ruin without a claim occurring in certain states:

$$\begin{aligned}
\psi_1(u;2) &= 0.5346e^{-0.4654u},\\
\psi_2(u;1) &= 0.3388e^{-0.3306u},\\
\chi_1(u,1) &= 0.0542e^{-0.3184u},\\
\chi_1(u,2) &= 0.3632e^{-0.3184u},\\
\chi_2(u,1) &= 0.5817e^{-0.4183u},\\
\chi_2(u,2) &= 0.2064e^{-0.4183u}.
\end{aligned} \tag{76}$$

Table 1 shows the probability of hitting a target level prior to ruin without the process visiting certain states. Table 2 shows the probability of ruin without the surplus hitting a certain level b and without visiting certain states. Table 3 gives the probability of ruin without hitting a certain level b and without claims occurring in certain states with initial states 1.

We can see from Table 1 that the probability of hitting a target level prior to ruin without the process visiting certain states increases as initial surplus u increases and but decreases as target level b increases. As the target level increases, it is less likely for surplus process to hit that target level prior to ruin. Table 2 illustrates that the probability of ruin without the surplus hitting a certain level b and without visiting certain states does not change much as the target level changes, but only when initial surplus level is higher, the difference is slightly more obvious. This is because when initial surplus is small, ruin is more likely to occur at an earlier stage. In addition, Table 3 shows that the probability of ruin without hitting a claim occurring in certain states with different initial states performs a similar pattern as shown in Table 2 for similar reasons. At last, when b goes to infinity in Table 2, probabilities become probabilities of ruin without the surplus visiting certain states, and when b goes to infinity in Table 3, probabilities are probabilities of ruin without claims occurring in certain states with initial states 1.

9. Concluding Remarks

In this paper, we study, for a Markov-modulated risk model, some states-specific one-sided exit probabilities and two-sided first exit probabilities. These probabilities can be expressed in terms of a modified or a dimension-reduced matrix scale function.

Further research includes the expression of joint and/or marginal Laplace transforms of state-specific occupation time (the duration that the surplus is between an interval and in substate space E_k by the time of ruin or other exit times) and the number and the aggregate claims occurred during the state-specific occupation time in terms of the matrix-scale functions defined in this paper.

Data Availability

No data were used to support the findings of this study.

Conflicts of Interest

The authors declare that they have no conflicts of interest.

Acknowledgments

Jingchao Li acknowledges the support from the National Natural Science Foundation of China (project no. 11601344) and Shenzhen Peacock Program (project no. 000417).

References

[1] S. Asmussen, "Risk theory in a Markovian environment," *Scandinavian Actuarial Journal*, vol. 1989, no. 2, pp. 69–100, 1989.
[2] S. Asmussen, A. Frey, T. Rolski, and V. Schmidt, "Does Markov-modulation increase the risk?" *ASTIN Bulletin*, vol. 25, no. 1, pp. 49–66, 1995.
[3] N. Bäuerle, "Some results about the expected ruin time in Markov-modulated risk models," *Insurance: Mathematics and Economics*, vol. 18, no. 2, pp. 119–127, 1996.
[4] H. Schmidli, "Estimation of the Lundberg coefficient for a Markov modulated risk model," *Scandinavian Actuarial Journal*, vol. 1997, no. 1, pp. 48–57, 1997.
[5] M. Snoussi, "The severity of ruin in Markov-modulated risk models," *Bulletin of the Swiss Association of Actuaries*, vol. 1, pp. 31–43, 2002.
[6] Y. Lu and S. Li, "On the probability of ruin in a Markov-modulated risk model," *Insurance: Mathematics and Economics*, vol. 37, no. 3, pp. 522–532, 2005.
[7] Y. Lu, "On the severity of ruin in a Markov-modulated risk model," *Scandinavian Actuarial Journal*, vol. 2006, no. 4, pp. 183–202, 2006.
[8] A. C. Y. Ng and H. Yang, "On the joint distribution of surplus before and after ruin under a Markovian regime switching model," *Stochastic Processes and Their Applications*, vol. 116, no. 2, pp. 244–266, 2006.
[9] S. Li and Y. Lu, "Moments of the dividend payments and related problems in a Markov-modulated risk model," *North American Actuarial Journal*, vol. 11, no. 2, pp. 65–76, 2007.
[10] S. Li and Y. Lu, "The decompositions of the discounted penalty functions and dividends-penalty identity in a Markov-modulated risk model," *ASTIN Bulletin*, vol. 38, no. 1, pp. 53–71, 2008.
[11] W. Fischer and K. Meier-Hellstern, "The Markov-modulated Poisson process (MMPP) cookbook," *Performance Evaluation*, vol. 18, no. 2, pp. 149–171, 1993.
[12] J. Li, D. C. M. Dickson, and S. Li, "Some ruin problems for the MAP risk model," *Insurance: Mathematics and Economics*, vol. 65, pp. 1–8, 2015.
[13] J. Li, D. C. M. Dickson, and S. Li, "Analysis of some ruin-related quantities in a Markov-modulated risk model," *Stochastic Models*, vol. 32, no. 3, pp. 351–365, 2016.
[14] J. H. A. De Smit, "The queue GI/M/s with customers of different types or the queue GI/Hm/s," *Advances in Applied Probability*, vol. 15, no. 2, pp. 392–419, 1983.
[15] S. Li and J. Ren, "The maximum severity of ruin in a perturbed risk process with Markovian arrivals," *Statistics & Probability Letters*, vol. 83, no. 4, pp. 993–998, 2013.
[16] B. Chan, H. U. Gerber, and E. S. W. Shiu, "On a classical risk model with a constant dividend barrier," *North American Actuarial Journal*, vol. 10, no. 2, pp. 133–139, 2006.
[17] N. J. Higham and H. M. Kim, "Numerical analysis of a quadratic matrix equation," *IMA Journal of Numerical Analysis*, vol. 20, no. 4, pp. 499–519, 2000.

Hindawi
Mathematical Problems in Engineering
Volume 2020, Article ID 3042543, 10 pages
https://doi.org/10.1155/2020/3042543

Research Article

On a Discrete Markov-Modulated Risk Model with Random Premium Income and Delayed Claims

Changwei Nie,[1] Mi Chen,[1,2] and Haiyan Liu [1,2]

[1] *College of Mathematics and Informatics, Fujian Normal University, Fuzhou 350117, China*
[2] *Fujian Provincial Key Laboratory of Mathematical Analysis and Its Applications, Fuzhou 350117, China*

Correspondence should be addressed to Haiyan Liu; rain6397@163.com

Received 26 March 2020; Accepted 10 August 2020; Published 20 October 2020

Guest Editor: Wenguang Yu

In this paper, a discrete Markov-modulated risk model with delayed claims, random premium income, and a constant dividend barrier is proposed. It is assumed that the random premium income and individual claims are affected by a Markov chain with finite state space. The model proposed is an extension of the discrete semi-Markov risk model with random premium income and delayed claims. Explicit expressions for the total expected discounted dividends until ruin are obtained by the method of generating function and the theory of difference equations. Finally, the effect of related parameters on the total expected discounted dividends are shown in several numerical examples.

1. Introduction

The study of dividend strategies for the insurance risk model was first proposed by De Finetti [1], and he found that the optimal strategy must be a barrier strategy in the studied discrete time model. Since then, many scholars have tried to work out the dividend problems under more general and more realistic model assumptions, for example, Claramunt et al. [2], Zhou [3], Landriault [4], Gerber et al. [5], Chen et al. [6], Chen and Yuen [7], and Peng et al. [8, 9].

In practice, insurance claims may be delayed for various reasons. Yuen and Guo [10] considered a reasonable claim structure that includes two types of independent claims, namely, main claims and by-claims, but the occurrence of by-claims may be delayed. For example, for a catastrophe such as an earthquake or a rainstorm, it is very likely that there exist other insurance claims after the immediate ones. From then on, the related issues about a risk process with such time-correlated claims have been studied by many authors. Li and Wu [11] calculated the total expected discounted dividends up to the time of ruin in a discrete time risk model with delayed claims and a constant dividend barrier. Other risk models involving delayed claims were studied by Xiao and Guo [12], Bao and Liu [13], Zhou et al. [14], Yuen et al. [15], Liu and Zhang [16], Deng et al. [17], and the references therein.

As an extension of the classical risk model, the risk model with random premium income has attracted a great deal of attention during the last few years. Boikov [18] generalized the classical risk model to the case where the premium process is determined by a compound Poisson process. Bao [19] extended the classical risk model to the case where the premium income process is a Poisson process and studied the expected discounted penalty at ruin. Assuming that the aggregate premium process is modeled as a compound Poisson process, Zou et al. [20] studied the expected discounted penalty function and optimal dividend strategy for a risk model with interclaim-dependent claim sizes. For the risk models with random premium income, one can also see [21–24] for more details.

Markov-modulated risk model where the surplus process is affected by an environmental Markov chain is a quite important model which attributed to the structural changes in conditions of economic, politic, or social, etc. Zhu and Yang [25] considered some ruin problems in a Markov regime-switching risk model where dividends were paid out according to a certain threshold strategy depending on the underlying Markovian environment process. Chen et al. [26]

studied the survival probability for a discrete semi-Markov risk model, which assumes individual claims are influenced by a Markov chain with finite state space. Yuen et al. [27] investigated the expected penalty functions for a discrete semi-Markov risk model with randomized dividends. Other related works can be found in Lu and Li [28], Diko and Usábel [29], Chen et al. [30], Huo et al. [31], etc.

In the discrete time risk model with random premium income, the authors often assumed that the random premium income follows a binomial process with a certain parameter, which means that the premium received in each period is a sequence of independent variables with the same Bernoulli distribution. In this paper, we propose a discrete time risk model where the random premium process and the individual claims are all influenced by a Markov chain. The model proposed in this paper is an extension of the discrete semi-Markov risk model with paying dividends and delayed claims. As mentioned in Chen et al. [26], the discrete semi-Markov risk model includes several existing risk models such as the compound binomial model and the compound Markov binomial model as special cases. So the discrete model studied in this paper is quite general. The explicit expressions for the expected discounted dividends until ruin are obtained for the model.

The outline of this paper is as follows. In Section 2, we introduce the model of this paper, including various parameters and notations. In Section 3, explicit expressions for the total expected discounted dividends until ruin are obtained by the method of generating function and the theory of difference equations. In Section 4, numerical examples are provided to illustrate the impact of the related parameters on the total expected discounted dividends.

2. Problem Formulation

We first recall the discrete time risk model with delayed claims that are studied by Yuen and Guo [10]. Denote the discrete time period by $t = 0, 1, 2, \ldots$, and assume that premiums are received with a constant premium rate of 1 in each time period. The probability of a main claim occurring in any time period is p $(0 < p < 1)$, and the probability of no main claim is $q = 1 - p$. Each main claim causes a by-claim, the probability that the main claim and by-claim occurs in the same period is θ, or the occurrence of by-claim is delayed to next time period with probability $1 - \theta$. Suppose that $\{\xi_k, k = 1, 2, \ldots\}$ be a sequence of Bernoulli random variables with $\mathbb{P}(\xi_k = 1) = p$ and $\mathbb{P}(\xi_k = 0) = 1 - p$, describing whether or not a main claim occurs in the k-th time period, and $\{\eta_k, k = 1, 2, \ldots\}$ be another sequence of Bernoulli random variables with $\mathbb{P}(\eta_k = 1) = \theta$ and $\mathbb{P}(\eta_k = 0) = 1 - \theta$, describing whether or not the k-th by-claim occurs simultaneously with its corresponding main claim. Let $\{X_k, k = 1, 2, \ldots\}$ be the independent and identically distributed (i.i.d.) main claims amounts and $\{Y_k, k = 1, 2, \ldots\}$ be the independent and identically distributed (i.i.d.) by-claims amounts. Then the total amount of the main claims and by-claims until the end of t-th time period are given by

$$\begin{aligned} S_t^X &= \sum_{k=1}^{t} \xi_k X_k, \quad t = 1, 2, \ldots, \\ S_1^Y &= \xi_1 \eta_1 Y_1, \\ S_t^Y &= \sum_{k=1}^{t} \xi_k \eta_k Y_k + \sum_{k=2}^{t} \xi_{k-1} (1 - \eta_{k-1}) Y_{k-1}, \quad t = 2, 3, \ldots. \end{aligned} \tag{1}$$

Hence, the surplus process for an insurance company is described as follows:

$$S(t) = u + t - S_t^X - S_t^Y, \tag{2}$$

where u is the initial surplus of the insurance company.

Now we introduce the risk model with delayed claims, a constant dividend barrier, and random premium income. We assume that premium income and dividends occur at the beginning of the period, and each claim occurs at the end of the period. If the surplus is above a constant barrier b, then the excess is paid out as a dividend. In addition, if the initial surplus $u > b$, $u - b$ is paid out as a dividend immediately. Denote by Z_k the amount of premium received in the k-th time period. Then the surplus process at the end of t-th time period of the risk model with delayed claims, a constant dividend barrier, and random premium income can be expressed as

$$U(t) = u + \sum_{k=1}^{t} Z_k - S_t^X - S_t^Y - \sum_{k=0}^{t} d_k, \tag{3}$$

where d_k is the amount of dividend paid out in the k-th period with $d_0 = \max\{u - b, 0\}$ and $\sum_{k=1}^{0} Z_k = 0$.

In this paper, we assume that $\{J_k, k = 0, 1, \ldots\}$ is a Markov chain with the state space $M = \{1, \ldots, r\}$, and its transition matrix is written as $\mathbf{P} = (p_{ij})_{i,j\in M}$, where $p_{ij} = \mathbb{P}(J_{k+1} = j \mid J_k = i, J_t, t \leq k - 1)$. Furthermore, the distributions of premium income, main claims, and by-claims that depend on the Markov chain are defined as follows:

$$\begin{aligned} q_{ij}(l) &= \mathbb{P}\left(Z_t = l \,\middle|\, J_t = j, J_{t-1} = i, J_k, Z_k, k \leq t - 1\right), \quad l = 0, 1, \\ g_{ij}(n) &= \mathbb{P}\left(X_t = n \,\middle|\, J_t = j, J_{t-1} = i, J_k, X_k, k \leq t - 1\right), \quad n = 1, 2, \ldots, \\ f_{ij}(m) &= \mathbb{P}\left(Y_t = m \,\middle|\, J_t = j, J_{t-1} = i, J_k, Y_k, k \leq t - 1\right), \quad m = 1, 2, \ldots. \end{aligned} \tag{4}$$

For simplicity, this article only considers the case of $M = \{1, 2\}$. In addition, we agree that $\sum_{i=1}^{2} \sum_{j=1}^{2} q_{ij}(1) \neq 0$; otherwise, there must be no premium income in any period. Define $T_{u,b} = \inf\{k \geq 1 \colon U(k) < 0\}$ to be the ruin time of model (3) and the one-period discount factor is $0 < v \leq 1$. Then the total expected discounted dividends until ruin given the initial surplus u and initial state i are defined as follows:

$$V_i(u,b) = E\left[\sum_{k=0}^{T_{u,b}} v^k d_k \,\middle|\, U(0) = u, J_0 = i\right], \quad i = 1,2. \tag{5}$$

The rest of this paper is devoted to obtain the explicit expressions of $V_i(u,b)$ for calculation purposes.

3. The Total Expected Discounted Dividends $V_i(u,b)$

In order to obtain the explicit expressions of the total expected discounted dividends, we need to consider the scenario that the by-claim induced by the main claim is delayed to the next period (see Yuen and Guo [10]). According to this scenario, we define a complementary surplus process as follows:

$$U_1(t) = u + \sum_{k=1}^{t} Z_k - S_t^X - S_t^Y - \sum_{k=0}^{t} d_k - YI_{(t\geq 1)}, \tag{6}$$

where I_A is the indicator function of event A, Y is a random variable following the same probability function with $\{Y_k,\ k = 1,2,\ldots\}$ and is independent of all other claim amounts random variables X_i and Y_j for all i and j. The total expected discounted dividends of the complementary surplus process until ruin are denoted by $V_{1,i}(u,b)$.

Based on the condition of premium income, claims, and dividends, the following equations can be obtained by using the law of total probability for the first period.

For $u = 0,1,\ldots,b$,

$$\begin{aligned} V_i(u,b) &= vq\sum_{j=1}^{2} p_{ij}q_{ij}(0)V_j(u,b) + vp\theta\sum_{j=1}^{2}\sum_{m+n\leq u} p_{ij}q_{ij}(0)g_{ij}(m)f_{ij}(n)V_j(u-m-n,b) \\ &\quad + vq\sum_{j=1}^{2} p_{ij}q_{ij}(1)V_j(u+1,b) + vp\theta\sum_{j=1}^{2}\sum_{m+n\leq u+1} p_{ij}q_{ij}(1)g_{ij}(m)f_{ij}(n)V_j(u+1-m-n,b) \\ &\quad + vp(1-\theta)\sum_{j=1}^{2}\sum_{m=1}^{u} p_{ij}q_{ij}(0)g_{ij}(m)V_{1,j}(u-m,b) \\ &\quad + vp(1-\theta)\sum_{j=1}^{2}\sum_{m=1}^{u+1} p_{ij}q_{ij}(1)g_{ij}(m)V_{1,j}(u+1-m,b), \quad i = 1,2, \end{aligned} \tag{7}$$

$$V_{1,i}(0,b) = vq\sum_{j=1}^{2} p_{ij}q_{ij}(1)f_{ij}(1)V_j(0,b), \quad i = 1,2, \tag{8}$$

and for $u = 1,\ldots,b$,

$$\begin{aligned} V_{1,i}(u,b) &= vq\sum_{j=1}^{2}\sum_{l=1}^{u} p_{ij}q_{ij}(0)f_{ij}(l)V_j(u-l,b) + vq\sum_{j=1}^{2}\sum_{l=1}^{u+1} p_{ij}q_{ij}(1)f_{ij}(l)V_j(u+1-l,b) \\ &\quad + vp\theta\sum_{j=1}^{2}\sum_{m+n+l\leq u} p_{ij}q_{ij}(0)g_{ij}(m)f_{ij}(n)f_{ij}(l)V_j(u-m-n-l,b) \\ &\quad + vp\theta\sum_{j=1}^{2}\sum_{m+n+l\leq u+1} p_{ij}q_{ij}(1)g_{ij}(m)f_{ij}(n)f_{ij}(l)V_j(u+1-m-n-l,b) \\ &\quad + vp(1-\theta)\sum_{j=1}^{2}\sum_{m+l\leq u} p_{ij}q_{ij}(0)g_{ij}(m)f_{ij}(l)V_{1,j}(u-m-l,b) \\ &\quad + vp(1-\theta)\sum_{j=1}^{2}\sum_{m+l\leq u+1} p_{ij}q_{ij}(1)g_{ij}(m)f_{ij}(l)V_{1,j}(u+1-m-l,b), \quad i = 1,2. \end{aligned} \tag{9}$$

According to the barrier dividend strategy, for $u = b+1, \ldots$, we have

$$V_i(u,b) = u - b + V_i(b,b), \quad i = 1,2,$$
$$V_{1,i}(u,b) = u - b + V_{1,i}(b,b), \quad i = 1,2. \tag{10}$$

From (7) and (9), $V_{1,i}(u,b)$ can be rewritten as

$$V_{1,i}(u,b) = \sum_{l=1}^{u} V_i(u-l,b) \sum_{j=1}^{2} p_{ij} f_{ij}(l), \quad i = 1,2. \tag{11}$$

This result can also be obtained from model (6) as

$$V_{1,i}(u,b) = E\left[V_i(u-Y,b)\right] = \sum_{l=1}^{u} V_i(u-l,b) \sum_{j=1}^{2} p_{ij} f_{ij}(l), \quad i = 1,2. \tag{12}$$

Substituting (8) into (7), we get

$$\begin{aligned} V_i(0,b) &= vq \sum_{j=1}^{2} p_{ij} q_{ij}(0) V_j(0,b) + vq \sum_{j=1}^{2} p_{ij} q_{ij}(1) V_j(1,b) \\ &\quad + v^2 pq(1-\theta) \sum_{j=1}^{2} p_{ij} q_{ij}(1) g_{ij}(1) \sum_{k=1}^{2} p_{jk} q_{jk}(1) f_{jk} \cdot (1) V_k(0,b), \quad i = 1,2. \end{aligned} \tag{13}$$

Similarly, substituting (11) into (7), we have

$$\begin{aligned} V_i(u,b) &= vq \sum_{j=1}^{2} p_{ij} q_{ij}(0) V_j(u,b) + vq \sum_{j=1}^{2} p_{ij} q_{ij}(1) V_j(u+1,b) \\ &\quad + vp \sum_{j=1}^{2} \sum_{m+n \le u} p_{ij} h_{ij}^X(m) V_j(u-m-n,b) \cdot \left[\theta f_{ij}(n) + (1-\theta) \sum_{k=1}^{2} p_{jk} f_{jk}(n)\right], \\ &\quad u = 1,2,\ldots,b,\ i = 1,2, \end{aligned} \tag{14}$$

where $h_{ij}^X(m) = q_{ij}(0) g_{ij}(m) + q_{ij}(1) g_{ij}(m+1)$ with $g_{ij}(0) = 0$, $m = 0,1,2,\ldots$.

To obtain the explicit expressions of $V_i(u,b)$, we define new functions $W_i(u)$ as follows:

$$\begin{aligned} W_i(0) &= vq \sum_{j=1}^{2} p_{ij} q_{ij}(0) W_j(0) + vq \sum_{j=1}^{2} p_{ij} q_{ij}(1) W_j(1) \\ &\quad + v^2 pq(1-\theta) \sum_{j=1}^{2} p_{ij} q_{ij}(1) g_{ij}(1) \sum_{k=1}^{2} p_{jk} q_{jk}(1) f_{jk} \cdot (1) W_k(0), \quad i = 1,2. \end{aligned} \tag{15}$$

$$\begin{aligned} W_i(u) &= vq \sum_{j=1}^{2} p_{ij} q_{ij}(0) W_j(u) + vq \sum_{j=1}^{2} p_{ij} q_{ij}(1) W_j(u+1) \\ &\quad + vp \sum_{j=1}^{2} \sum_{m+n \le u} p_{ij} h_{ij}^X(m) W_j(u-m-n) \cdot \left[\theta f_{ij}(n) + (1-\theta) \sum_{k=1}^{2} p_{jk} f_{jk}(n)\right], \\ &\quad u \in \mathbb{N}_+,\ i = 1,2. \end{aligned} \tag{16}$$

We use $\widetilde{h}_{ij}^X(s)$, $\widetilde{f}_{ij}(s)$, and $\widetilde{W}_i(s)$ to represent the generating functions of $h_{ij}^X(k)$, $f_{ij}(k)$, and $W_i(k)$, respectively. Multiplying both sides of (15) and (16) by s^{u+1}, next summing over u from 0 to ∞ gives

$$\begin{aligned} \frac{s}{v} \widetilde{W}_i(s) &= sq \sum_{j=1}^{2} p_{ij} q_{ij}(0) \widetilde{W}_j(s) + q \sum_{j=1}^{2} p_{ij} q_{ij}(1) \left(\widetilde{W}_j(s) - W_j(0)\right) \\ &\quad + sp \sum_{j=1}^{2} p_{ij} \widetilde{W}_j(s) \widetilde{h}_{ij}^X(s) \left[\theta \widetilde{f}_{ij}(s) + (1-\theta) \sum_{k=1}^{2} p_{jk} \widetilde{f}_{jk}(s)\right] \\ &\quad + svpq(1-\theta) \sum_{j=1}^{2} p_{ij} q_{ij}(1) g_{ij}(1) \sum_{k=1}^{2} p_{jk} q_{jk}(1) f_{jk}(1) W_k(0), \quad i = 1,2. \end{aligned} \tag{17}$$

For the convenience of the following derivations, we define

$$\begin{aligned}
\widetilde{e}_1(s) &= q\sum_{j=1}^{2} p_{1j}q_{1j}(1)W_j(0) - svpq(1-\theta)\sum_{j=1}^{2} p_{1j}q_{1j}(1)g_{1j}(1)\sum_{k=1}^{2} p_{jk}q_{jk}(1)f_{jk}(1)W_k(0),\\
\widetilde{e}_2(s) &= q\sum_{j=1}^{2} p_{2j}q_{2j}(1)W_j(0) - svpq(1-\theta)\sum_{j=1}^{2} p_{2j}q_{2j}(1)g_{2j}(1)\sum_{k=1}^{2} p_{jk}q_{jk}(1)f_{jk}(1)W_k(0),\\
\widetilde{e}_{ij}(s) &= qp_{ij}q_{ij}(1) + s\left[qp_{ij}q_{ij}(0) + pp_{ij}\widetilde{h}_{ij}^{X}(s)\left(\theta\widetilde{f}_{ij}(s) + (1-\theta)\sum_{k=1}^{2} p_{jk}\widetilde{f}_{jk}(s)\right)\right], \quad i,j=1,2.
\end{aligned} \tag{18}$$

Now, (17) can be written as

$$\begin{cases}
\left(\widetilde{e}_{11}(s) - \dfrac{s}{v}\right)\widetilde{W}_1(s) + \widetilde{e}_{12}(s)\widetilde{W}_2(s) = \widetilde{e}_1(s),\\
\widetilde{e}_{21}(s)\widetilde{W}_1(s) + \left(\widetilde{e}_{22}(s) - \dfrac{s}{v}\right)\widetilde{W}_2(s) = \widetilde{e}_2(s).
\end{cases} \tag{19}$$

Simplifying the above equation yields

$$\begin{aligned}
&\left[\left(\widetilde{e}_{11}(s) - \frac{s}{v}\right)\left(\widetilde{e}_{22}(s) - \frac{s}{v}\right) - \widetilde{e}_{12}(s)\widetilde{e}_{21}(s)\right]\widetilde{W}_1(s)\\
&\quad = \widetilde{e}_1(s)\left(\widetilde{e}_{22}(s) - \frac{s}{v}\right) - \widetilde{e}_2(s)\widetilde{e}_{12}(s).
\end{aligned} \tag{20}$$

To facilitate the following derivation, denote

$$\begin{aligned}
a_i(0) &= qp_{ii}q_{ii}(1),\\
a_i(1) &= qp_{ii}q_{ii}(0) + pp_{ii}h_{ii}^{X}(0)\left[\theta f_{ii}(0) + (1-\theta)\sum_{k=1}^{2} p_{ik}f_{ik}(0)\right] - \frac{1}{v},\\
a_i(k) &= pp_{ii}\sum_{n=0}^{k-1} h_{ii}^{X}(k-1-n)\left[\theta f_{ii}(n) + (1-\theta)\sum_{k=1}^{2} p_{ik}f_{ik}(n)\right], \quad k=2,3,\ldots, i=1,2,\\
b_{ij} &= vpq(1-\theta)\sum_{k=1}^{2} p_{ik}q_{ik}(1)g_{ik}(1)p_{kj}q_{kj}(1)f_{kj}(1), \quad i,j=1,2,\\
f_k &= \sum_{n=0}^{k}\left[a_1(n)a_2(k-n) - e_{12}(n)e_{21}(k-n)\right],\\
g_k^{(1)} &= \sum_{n=0}^{k} W_1(n)f_{k-n},\\
h_k^{(1)} &= e_1(0)a_2(k) + e_1(1)a_2(k-1) - e_2(0)e_{12}(k) - e_2(1)e_{12}(k-1), \quad k\in\mathbb{N},
\end{aligned} \tag{21}$$

where $e_i(k)$ and $e_{ij}(k)$ are the coefficients of s^k on functions $\widetilde{e}_i(s)$ and $\widetilde{e}_{ij}(s)$. In addition, $a_i(-1)=0, e_{ij}(-1)=0$, $i,j=1,2$.

Comparing the coefficients of s^k in both sides of (20), we get $g_k^{(1)} = h_k^{(1)}$, $k\in\mathbb{N}$. So we have

$$\sum_{n=0}^{k} W_1(n)f_{k-n} = h_k^{(1)}, \quad k\in\mathbb{N}. \tag{22}$$

In a similar way, we obtain that

$$\sum_{n=0}^{k} W_2(n)f_{k-n} = h_k^{(2)}, \quad k\in\mathbb{N}, \tag{23}$$

where $h_k^{(2)} = -e_1(0)e_{21}(k) - e_1(1)e_{21}(k-1) + e_2(0)a_1(k) + e_2(1)a_1(k-1)$.

From (22) and (23), we know that f_k play a decisive role in the value of $\{W_i(k), k \in \mathbb{N}, i = 1, 2\}$. So we discuss the values of f_k in the following lemma.

Lemma 1. *If $f_0 = 0$, then $f_1 \neq 0$.*

Proof. Note that

$$f_0 = e_{11}(0)e_{22}(0) - e_{12}(0)e_{21}(0),$$
$$f_1 = e_{11}(0)\left[e_{22}(1) - \frac{1}{v}\right] + e_{22}(0)\left[e_{11}(1) - \frac{1}{v}\right] - e_{21}(0)e_{12}(1) - e_{12}(0)e_{21}(1). \quad (24)$$

If $f_0 = 0$, we can derive $f_1 \neq 0$ by using reduction to absurdity. Assuming $f_1 = 0$ yields

$$\begin{aligned} e_{11}(0) &= 0, \\ e_{22}(0) &= 0, \\ e_{21}(0)e_{12}(1) &= 0, \\ e_{21}(1)e_{12}(0) &= 0, \end{aligned} \quad (25)$$

where $e_{11}(0) = qp_{11}q_{11}(1)$ means $q_{11}(1) = 0$, and $e_{22}(0) = qp_{22}q_{22}(1)$ means $q_{22}(1) = 0$.

Since $f_0 = 0$, we get $e_{21}(0)e_{12}(0) = 0$. Note that $\sum_{i=1}^{2}\sum_{j=1}^{2} q_{ij}(1) \neq 0$, there are only two situations:

(i) If $e_{12}(0) = 0$ and $e_{21}(0) \neq 0$, we have

$$e_{12}(1) = qp_{12}q_{12}(0) + pp_{12}h_{12}^{X}(0) \cdot \left[\theta f_{12}(0) + (1-\theta)\sum_{k=1}^{2} p_{12}f_{12}(0)\right] = 0, \quad (26)$$

which means $q_{12}(0) = 0$, and $e_{12}(0) = 0$ yields $q_{12}(1) = 0$. The result $\sum_{l=0}^{1} q_{12}(l) \neq 1$ is obviously not in agreement with reality, so there is no such situation.

(ii) If $e_{21}(0) = 0$ and $e_{12}(0) \neq 0$, we can derive in a similar way that $\sum_{l=0}^{1} q_{21}(l) \neq 1$, which is also not realistic. The proof is complete.

In order to obtain the explicit expressions of $V_i(u, b)$, we shall distinguish two cases.

(1) If $f_0 \neq 0$, equations (22) and (23) yield

$$W_i(k) = \frac{1}{f_0}\left[h_k^{(i)} - \sum_{n=0}^{k-1} W_i(n) f_{k-n}\right], \quad i = 1, 2,\ k \in \mathbb{N}_+. \quad (27)$$

Denote

$$\begin{aligned} \xi_k^{(1)} &= e_{11}(0)a_2(k) - b_{11}a_2(k-1) - e_{21}(0)e_{12}(k) + b_{21}e_{12}(k-1), \\ \eta_k^{(1)} &= e_{12}(0)a_2(k) - b_{12}a_2(k-1) - e_{22}(0)e_{12}(k) + b_{22}e_{12}(k-1), \\ \xi_k^{(2)} &= e_{21}(0)a_1(k) - b_{21}a_1(k-1) - e_{11}(0)e_{21}(k) + b_{11}e_{21}(k-1), \\ \eta_k^{(2)} &= e_{22}(0)a_1(k) - b_{22}a_1(k-1) - e_{12}(0)e_{21}(k) + b_{12}e_{21}(k-1). \end{aligned} \quad (28)$$

Note that $h_k^{(i)}$ can be rewritten as

$$h_k^{(i)} = \xi_k^{(i)} W_1(0) + \eta_k^{(i)} W_2(0), \quad i = 1, 2,\ k \in \mathbb{N}, \quad (29)$$

which are determined by $W_1(0)$ and $W_2(0)$, and we can see from (27) that $\{W_1(k), W_2(k)\}_{k\in\mathbb{N}_+}$ is also determined by the initial values $W_1(0)$ and $W_2(0)$. Therefore, apart from a multiplicative constant, the solution of (15) and (16) is unique. For $j = 1, 2$, we set $\{C_{1j}(k), C_{2j}(k)\}$ to be the linearly independent particular solutions of (15) and (16) with initial conditions $C_{ij}(0) = I_{(i=j)}$. Then the general solution of (15) and (16) is given by

$$W_i(u) = \sum_{j=1}^{2} W_j(0)C_{ij}(u), \quad u \in \mathbb{N},\ i = 1, 2. \quad (30)$$

The same procedure may be easily adapted to obtain the solutions of (13) and (14), that is,

$$V_i(u, b) = \sum_{j=1}^{2} V_j(0, b)C_{ij}(u), \quad i = 1, 2,\ u = 0, 1, \ldots, b+1. \quad (31)$$

Let

$$\begin{aligned} \vec{\mathbf{V}}(u, b) &= (V_1(u, b), V_2(u, b))^T, \\ \mathbf{C}(u) &= (C_{ij}(u))_{i,j=1,2}, \\ \vec{1} &= (1, 1)^T. \end{aligned} \quad (32)$$

Rewriting (31) into matrix form as follows:

$$\vec{\mathbf{V}}(u, b) = \mathbf{C}(u)\vec{\mathbf{V}}(0, b), \quad i = 1, 2,\ u = 0, 1, \ldots, b+1. \quad (33)$$

Combining (33) with the boundary condition $\vec{\mathbf{V}}(b+1, b) = \vec{1} + \vec{\mathbf{V}}(b, b)$, we get

$$\vec{\mathbf{V}}(0,b) = [\mathbf{C}(b+1) - \mathbf{C}(b)]^{-1}\vec{1}, \tag{34}$$

which in turn yields that

$$\vec{\mathbf{V}}(u,b) = \mathbf{C}(u)[\mathbf{C}(b+1) - \mathbf{C}(b)]^{-1}\vec{1}, \quad u = 0,1,\ldots,b. \tag{35}$$

(2) If $f_0 = 0$, Lemma 1 guarantees that $f_1 \neq 0$. Based on (22) and (23), we get $W_i(0) = (1/f_1)h_1^{(i)}$, $i = 1,2$, and

$$W_i(k) = \frac{1}{f_1}\left[h_{k+1}^{(i)} - \sum_{n=0}^{k-1} W_i(n) f_{k+1-n}\right], \quad i = 1,2,\ k \in \mathbb{N}_+. \tag{36}$$

Define

$$\mathbf{J}_1 = \begin{pmatrix} \xi_1^{(1)} - f_1 & \eta_1^{(1)} \\ \xi_1^{(2)} & \eta_1^{(2)} - f_1 \end{pmatrix}, \quad \vec{\mathbf{W}}(0) = (W_1(0), W_2(0))^T, \quad \vec{0} = (0,0)^T. \tag{37}$$

We obtain that

$$\mathbf{J}_1 \vec{\mathbf{W}}(0) = \vec{0}. \tag{38}$$

Let

$$\mathbf{D}_0 = \begin{pmatrix} e_{22}(0) & -e_{12}(0) \\ -e_{21}(0) & e_{11}(0) \end{pmatrix}, \quad \mathbf{E} = \begin{pmatrix} \dfrac{1}{v} - e_{11}(1) & -e_{12}(1) \\ -e_{21}(1) & \dfrac{1}{v} - e_{22}(1) \end{pmatrix}. \tag{39}$$

Because of $\mathbf{J}_1 = \mathbf{D}_0\mathbf{E}, \mathbf{D}_0 \neq 0, |\mathbf{D}_0| = f_0 = 0$ and $|\mathbf{E}| > 0$, we have $\text{rank}(\mathbf{J}_1) = \text{rank}(\mathbf{D}_0) = 1$. Equation (38) shows that only one of $W_1(0)$ and $W_2(0)$ is free variable. Assuming that $W_1(0)$ is the free variable without loss of generality, then we know that $\{W_1(k), W_2(k)\}_{k\in\mathbb{N}_+}$ is determined by the initial value $W_1(0)$. Set $\{W_1^{(1)}(u), W_2^{(1)}(u), u \in \mathbb{N}\}$ to be the linearly independent particular solution of (15) and (16) with initial conditions $W_1^{(1)}(0) = 1$, and then the general solution of (15) and (16) is of the form:

$$(W_1(u), W_2(u)) = W_1(0)\left(W_1^{(1)}(u), W_2^{(1)}(u)\right), \quad u \in \mathbb{N}. \tag{40}$$

Therefore, the solution of (13) and (14) is given by

$$(V_1(u,b), V_2(u,b)) = V_1(0,b)\left(W_1^{(1)}(u), W_2^{(1)}(u)\right), \quad u = 0,1,\ldots,b+1. \tag{41}$$

Combining the above equation with $V_1(b+1,b) = 1 + V_1(b,b)$ gives

$$V_1(0,b) = \left[W_1^{(1)}(b+1) - W_1^{(1)}(b)\right]^{-1}. \tag{42}$$

So we have

$$(V_1(u,b), V_2(u,b)) = \left[W_1^{(1)}(b+1) - W_1^{(1)}(b)\right]^{-1} \cdot \left(W_1^{(1)}(u), W_2^{(1)}(u)\right), \quad u = 0,1,\ldots,b. \tag{43}$$

To sum up, the main result of this paper is as follows. □

Theorem 1. *For any given dividend barrier $b \in \mathbb{N}_+$ and initial surplus $u = 0,1,\ldots,b$, the total expected discounted dividends until ruin satisfies the following explicit expression:*

$$\vec{\mathbf{V}}(u,b) = \begin{cases} \mathbf{C}(u)[\mathbf{C}(b+1) - \mathbf{C}(b)]^{-1}\vec{1}, & f_0 \neq 0, \\ \left[W_1^{(1)}(b+1) - W_1^{(1)}(b)\right]^{-1}\left(W_1^{(1)}(u), W_2^{(1)}(u)\right), & f_0 = 0, \end{cases} \tag{44}$$

where $\mathbf{C}(u) = (C_{ij}(u))_{i,j=1,2}$ with $C_{ij}(0) = I_{(i=j)}$ and $C_{ij}(k) = (1/f_0)[\xi_k^{(i)} I_{\{j=1\}} + \eta_k^{(i)} I_{\{j=2\}} - \sum_{n=0}^{k-1} C_{ij}(n) f_{k-n}]$, 2 $k \in \mathbb{N}_+$, $i,j = 1,2$; $W_1^{(1)}(0) = 1, W_2^{(1)}(0) = 0, W_i^{(1)}(k) = (1/f_1)[\xi_{k+1}^{(i)} - \sum_{n=0}^{k-1} W_i^{(1)}(n) f_{k+1-n}]$, $k \in \mathbb{N}_+$, $i = 1,2$.

4. Numerical Simulation

In this section, we use several examples to illustrate the conclusions of $f_0 \neq 0$ in Section 3 and explain the impact of u, b, v, p, and θ on the total expected discounted dividends. In the following numerical examples, the transition

Table 1: The distribution of premium income.

l	$q_{11}(l)$	$q_{12}(l)$	$q_{21}(l)$	$q_{22}(l)$
0	1/10	2/9	1/6	0
1	9/10	7/9	5/6	1

Table 2: The distribution of main claim.

n	$g_{11}(n)$	$g_{12}(n)$	$g_{21}(n)$	$g_{22}(n)$
1	13/16	3/4	5/6	1
2	1/8	1/4	0	0
3	1/16	0	1/6	0
≥4	0	0	0	0

Table 3: Values of $V_i(u,b)$ when $v = 0.93$.

	i	$b=0$	$b=1$	$b=2$	$b=3$	$b=4$	$b=5$	$b=6$	$b=7$	$b=8$
$u=0$	1	2.7495	2.6384	2.4991	2.2867	2.0104	1.7367	1.4871	1.2678	1.0786
	2	3.0406	2.9996	2.8248	2.5835	2.2715	1.9625	1.6805	1.4327	1.2188
$u=1$	1	3.7495	3.5290	3.3566	3.0723	2.7009	2.3331	1.9977	1.7031	1.4488
	2	4.0406	4.0274	3.7846	3.4606	3.0428	2.6290	2.2513	1.9193	1.6328
$u=2$	1	4.7495	4.5290	4.3473	3.9821	3.5001	3.0231	2.5884	2.2066	1.8771
	2	5.0406	5.0274	4.7007	4.2965	3.7781	3.2645	2.7956	2.3835	2.0277
$u=3$	1	5.7495	5.5290	5.3473	4.9066	4.3112	3.7225	3.1867	2.7164	2.3107
	2	6.0406	6.0274	5.7007	5.2055	4.5783	3.9566	3.3887	2.8892	2.4580
$u=4$	1	6.7495	6.5290	6.3473	5.9066	5.1856	4.4744	3.8288	3.2631	2.7756
	2	7.0406	7.0274	6.7007	6.2055	5.4603	4.7208	4.0440	3.4483	2.9337
$u=5$	1	7.7495	7.5290	7.3473	6.9066	6.1856	5.3283	4.5553	3.8807	3.3003
	2	8.0406	8.0274	7.7007	7.2055	6.4603	5.5906	4.7916	4.0867	3.4773

Table 4: Values of $V_i(u,b)$ when $v = 0.95$.

	i	$b=0$	$b=1$	$b=2$	$b=3$	$b=4$	$b=5$	$b=6$	$b=7$	$b=8$
$u=0$	1	3.0651	3.1731	3.2602	3.2280	3.0292	2.7687	2.4935	2.2277	1.9819
	2	3.3921	3.6103	3.6819	3.6419	3.4173	3.1235	2.8130	2.5132	2.2360
$u=1$	1	4.0651	4.1265	4.2627	4.2236	3.9637	3.6227	3.2625	2.9148	2.5932
	2	4.3921	4.7233	4.8039	4.7500	4.4569	4.0736	3.6688	3.2778	2.9162
$u=2$	1	5.0651	5.1265	5.3592	5.3184	4.9918	4.5622	4.1086	3.6706	3.2656
	2	5.3921	5.7233	5.7831	5.7131	5.3603	4.8994	4.4126	3.9424	3.5075
$u=3$	1	6.0651	6.1265	6.3592	6.3342	5.9470	5.4349	4.8941	4.3722	3.8898
	2	6.3921	6.7233	6.7831	6.6872	6.2730	5.7339	5.1644	4.6142	4.1052
$u=4$	1	7.0651	7.1265	7.3592	7.3342	6.8909	6.2966	5.6691	5.0641	4.5051
	2	7.3921	7.7233	7.7831	7.6872	7.2082	6.5892	5.9353	5.3032	4.7183
$u=5$	1	8.0651	8.1265	8.3592	8.3342	7.8909	7.2077	6.4869	5.7934	5.1534
	2	8.3921	8.7233	8.7831	8.6872	8.2082	7.5049	6.7616	6.0422	5.3762

probability matrix of Markov chain is set to be $\begin{pmatrix} 0.7 & 0.3 \\ 0.2 & 0.8 \end{pmatrix}$, the distribution of premium income is shown in Table 1, the distribution of main claim is shown in Table 2, and we assume that the distribution of by-claim is the same as main claim.

Example 1. In this example, we set $p = 0.25$ and $\theta = 0.3$. The results of $V_i(u,b)$ for $v = 0.93, 0.95, 0.97$ are listed in Tables 3–5, respectively. We can see that the expected discounted dividends are gradually increasing with the increase of the initial surplus u or one-period discount factor v. Given the initial surplus u, set the optimal dividend boundary b^* be the boundary value which maximizes the expected discounted dividends $V_i(u,b)$. From Table 3, it is easy to see that $b^* = 0$ when $v = 0.93$. Tables 4 and 5 show that $b^* = 2$ when $v = 0.95$ and $b^* = 4$ when $v = 0.97$. The results in this example imply that it would be better to pay dividends earlier when the discount factor v is smaller.

Example 2. In this example, we take $v = 0.95$, $b = 8$, and $\theta = 0.3$ and investigate the effect of p on the expected discounted dividends $V_i(u,b)$. It can be seen from Table 6 that the expected discounted dividends are a decreasing function of p, and the result is in accordance with the fact.

Table 5: Values of $V_i(u,b)$ when $v = 0.97$.

	i	$b=0$	$b=1$	$b=2$	$b=3$	$b=4$	$b=5$	$b=6$	$b=7$	$b=8$
$u=0$	1	3.4458	3.9036	4.4567	4.9317	5.0810	5.0235	4.8360	4.5801	4.2966
	2	3.8163	4.4453	5.0289	5.5564	5.7232	5.6582	5.4469	5.1587	4.8394
$u=1$	1	4.4458	4.9370	5.6744	6.2860	6.4775	6.4044	6.1654	5.8391	5.4777
	2	4.8163	5.6693	6.3918	7.0582	7.2693	7.1866	6.9183	6.5522	6.1466
$u=2$	1	5.4458	5.9370	6.9269	7.6922	7.9298	7.8409	7.5483	7.1489	6.7064
	2	5.8163	6.6693	7.4579	8.2241	8.4681	8.3714	8.0589	7.6324	7.1600
$u=3$	1	6.4458	6.9370	7.9269	8.8545	9.1369	9.0361	8.6991	8.2386	7.7287
	2	6.8163	7.6693	8.4579	9.2962	9.5667	9.4566	9.1034	8.6217	8.0881
$u=4$	1	7.4458	7.9370	8.9269	9.8545	10.1930	10.0848	9.7090	9.1950	8.6258
	2	7.8163	8.6693	9.4579	10.2962	10.5815	10.4572	10.0664	9.5338	8.9438
$u=5$	1	8.4458	8.9370	9.9269	10.8545	11.1930	11.0854	10.6735	10.1082	9.4821
	2	8.8163	9.6693	10.4579	11.2962	11.5815	11.4388	11.0106	10.4282	9.7831

Table 6: Values of $V_i(u,b)$ when $v = 0.95, b = 8$, and $\theta = 0.3$.

	i	$p=0.05$	$p=0.10$	$p=0.15$	$p=0.20$	$p=0.25$	$p=0.30$	$p=0.40$	$p=0.50$
$u=0$	1	8.8392	6.6890	4.8048	3.2247	1.9819	1.0907	0.2202	0.0250
	2	9.1448	7.0774	5.1970	3.5635	2.2360	1.2551	0.2627	0.0307
$u=1$	1	9.6611	7.5912	5.6875	4.0016	2.5932	1.5145	0.3523	0.0479
	2	9.9655	7.9947	6.1201	4.4017	2.9162	1.7408	0.4222	0.0595
$u=2$	1	10.4853	8.4901	6.5824	4.8166	3.2656	2.0094	0.5327	0.0863
	2	10.6805	8.7312	6.8512	5.0866	3.5075	2.1997	0.6087	0.1030
$u=3$	1	11.2369	9.2628	7.3470	5.5332	3.8898	2.5039	0.7512	0.1456
	2	11.4095	9.4604	7.5651	5.7595	4.1052	2.6877	0.8413	0.1712
$u=4$	1	11.9809	9.9978	8.0648	6.2146	4.5051	3.0202	1.0216	0.2383
	2	12.1553	10.1900	8.2728	6.4317	4.7183	3.2124	1.1328	0.2781
$u=5$	1	12.7585	10.7568	8.8011	6.9170	5.1534	3.5870	1.3640	0.3842
	2	12.9415	10.9558	9.0143	7.1396	5.3762	3.7960	1.5035	0.4462

Table 7: Values of $V_i(u,b)$ when $v = 0.95, b = 8$, and $p = 0.25$.

	i	$\theta=0$	$\theta=0.2$	$\theta=0.4$	$\theta=0.6$	$\theta=0.8$	$\theta=1$
$u=0$	1	2.0822	2.0141	1.9509	1.8920	1.8370	1.7855
	2	2.3755	2.2807	2.1930	2.1117	2.0361	1.9656
$u=1$	1	2.6327	2.6059	2.5810	2.5578	2.5361	2.5158
	2	2.9512	2.9274	2.9055	2.8854	2.8669	2.8499
$u=2$	1	3.2963	3.2755	3.2559	3.2374	3.2197	3.2029
	2	3.5201	3.5114	3.5038	3.4971	3.4914	3.4864
$u=3$	1	3.9092	3.8961	3.8836	3.8715	3.8599	3.8487
	2	4.1132	4.1077	4.1029	4.0989	4.0955	4.0927
$u=4$	1	4.5186	4.5095	4.5008	4.4924	4.4844	4.4767
	2	4.7226	4.7196	4.7172	4.7150	4.7133	4.7119
$u=5$	1	5.1637	5.1567	5.1500	5.1436	5.1374	5.1313
	2	5.3776	5.3766	5.3758	5.3753	5.3749	5.3747

Example 3. In this example, we discuss the impact of θ on the expected discounted dividends $V_i(u,b)$. Let $v = 0.95$, $b = 8$, and $p = 0.25$, The values of $V_i(u,b)$ are shown in Table 7. It is easy to see that the expected discounted dividends $V_i(u,b)$ gradually decrease with the increase of θ, and the effect of θ on $V_i(u,b)$ is decreasing with respect to the initial surplus u.

Data Availability

No data were used to support this study.

Conflicts of Interest

The authors declare that they have no conflicts of interest.

Acknowledgments

This work was supported by the National Natural Science Foundation of China (nos. 11701088 and 11701087), the Natural Science Foundation of Fujian Province (nos. 2018J05003 and 2019J01673), the Shandong Provincial Natural Science Foundation (no. ZR2018MG002), the

Program for Innovative Research Team in Science and Technology in Fujian Province University, and the grant "Probability and Statistics: Theory and Application (no. IRTL1704)" from Fujian Normal University.

References

[1] B. De Finetti, "Su un'impostazione alternativa della teoria collettiva del rischio," *Transactions of the XVth International Congress of Actuaries*, vol. 2, pp. 433–443, 1957.

[2] M. M. Claramunt, M. Marmol, and A. Alegre, "A note on the expected present value of dividends with a constant barrier in the discrete time model," *Bulletin of the Swiss Association of Actuaries*, vol. 2, pp. 149–159, 2003.

[3] X. Zhou, "On a classical risk model with a constant dividend barrier," *North American Actuarial Journal*, vol. 9, no. 4, pp. 95–108, 2005.

[4] D. Landriault, "Constant dividend barrier in a risk model with interclaim-dependent claim sizes," *Insurance: Mathematics and Economics*, vol. 42, no. 1, pp. 31–38, 2008.

[5] H. U. Gerber, E. S. W. Shiu, and H. Yang, "An elementary approach to discrete models of dividend strategies," *Insurance: Mathematics and Economics*, vol. 46, no. 1, pp. 109–116, 2010.

[6] M. Chen, X. Peng, and J. Guo, "Optimal dividend problem with a nonlinear regular-singular stochastic control," *Insurance: Mathematics and Economics*, vol. 52, no. 3, pp. 448–456, 2013.

[7] M. Chen and K. C. Yuen, "Optimal dividend and reinsurance in the presence of two reinsurers," *Journal of Applied Probability*, vol. 53, no. 2, pp. 554–571, 2016.

[8] X. Peng, L. Bai, and J. Guo, "Optimal control with restrictions for a diffusion risk model under constant interest force," *Applied Mathematics & Optimization*, vol. 73, no. 1, pp. 115–136, 2016.

[9] X. Peng, W. Su, and Z. Zhang, "On a perturbed compound Poisson risk model under a periodic threshold-type dividend strategy," *Journal of Industrial & Management Optimization*, vol. 16, no. 4, pp. 1967–1986, 2020.

[10] K. C. Yuen and J. Y. Guo, "Ruin probabilities for time-correlated claims in the compound binomial model," *Insurance: Mathematics and Economics*, vol. 29, no. 1, pp. 47–57, 2001.

[11] J.-Z. Li and R. Wu, "The Gerber-Shiu discounted penalty function for a compound binomial risk model with by-claims," *Acta Mathematicae Applicatae Sinica, English Series*, vol. 31, no. 1, pp. 181–190, 2015.

[12] Y. Xiao and J. Guo, "The compound binomial risk model with time-correlated claims," *Insurance: Mathematics and Economics*, vol. 41, no. 1, pp. 124–133, 2007.

[13] Z. H. Bao and H. Liu, "The compound binomial risk model with delayed claims and random income," *Mathematical and Computer Modelling*, vol. 55, no. 3-4, pp. 1315–1323, 2012.

[14] J. Zhou, X. Mo, H. Ou, and X. Yang, "Expected present value of total dividends in the compound binomial model with delayed claims and random income," *Acta Mathematica Scientia*, vol. 33, no. 6, pp. 1639–1651, 2013.

[15] K. C. Yuen, J. Li, and R. Wu, "On a discrete-time risk model with delayed claims and dividends," *Risk and Decision Analysis*, vol. 4, no. 1, pp. 3–16, 2013.

[16] C. L. Liu and Z. M. Zhang, "On a discrete risk model with delayed claims and a randomized dividend strategy," *Advances in Difference Equations*, vol. 2015, no. 1, pp. 1–14, Article ID 284, 2015.

[17] Y. Deng, J. Liu, Y. Huang, M. Li, and J. Zhou, "On a discrete interaction risk model with delayed claims and stochastic incomes under random discount rates," *Communications in Statistics—Theory and Methods*, vol. 47, no. 23, pp. 5867–5883, 2018.

[18] A. V. Boikov, "The Cramer–Lundberg model with stochastic premium process," *Theory of Probability & Its Applications*, vol. 47, no. 3, pp. 489–493, 2003.

[19] Z.-H. Bao, "The expected discounted penalty at ruin in the risk process with random income," *Applied Mathematics and Computation*, vol. 179, no. 2, pp. 559–566, 2006.

[20] W. Zou, J.-W. Gao, and J.-H. Xie, "On the expected discounted penalty function and optimal dividend strategy for a risk model with random incomes and interclaim-dependent claim sizes," *Journal of Computational and Applied Mathematics*, vol. 255, pp. 270–281, 2014.

[21] H. Yang and Z. Zhang, "On a class of renewal risk model with random income," *Applied Stochastic Models in Business and Industry*, vol. 25, no. 6, pp. 678–695, 2009.

[22] Z. Zhang and H. Yang, "On a risk model with stochastic premiums income and dependence between income and loss," *Journal of Computational and Applied Mathematics*, vol. 234, no. 1, pp. 44–57, 2010.

[23] M. Jacobsen, "The time to ruin in some additive risk models with random premium rates," *Journal of Applied Probability*, vol. 49, no. 4, pp. 915–938, 2012.

[24] W. G. Yu, "Randomized dividends in a discrete insurance risk model with stochastic premium income," *Mathematical Problems in Engineering*, vol. 2013, Article ID 579534, 9 pages, 2013.

[25] J. Zhu and H. Yang, "Ruin theory for a Markov regime-switching model under a threshold dividend strategy," *Insurance: Mathematics and Economics*, vol. 42, no. 1, pp. 311–318, 2008.

[26] M. Chen, K. C. Yuen, and J. Guo, "Survival probabilities in a discrete semi-Markov risk model," *Applied Mathematics and Computation*, vol. 232, pp. 205–215, 2014.

[27] K. C. Yuen, M. Chen, and K. P. Wat, "On the expected penalty functions in a discrete semi-Markov risk model with randomized dividends," *Journal of Computational and Applied Mathematics*, vol. 311, pp. 239–251, 2017.

[28] Y. Lu and S. M. Li, "On the severity of ruin in a Markov-modulated risk model," *Scandinavian Actuarial Journal*, vol. 2006, no. 4, pp. 183–202, 2006.

[29] P. Diko and M. Usábel, "A numerical method for the expected penalty-reward function in a Markov-modulated jump-diffusion process," *Insurance: Mathematics and Economics*, vol. 49, no. 1, pp. 126–131, 2011.

[30] M. Chen, J. Guo, and X. Wu, "Expected discounted dividends in a discrete semi-Markov risk model," *Journal of Computational and Applied Mathematics*, vol. 266, no. 2, pp. 1–17, 2014.

[31] H. Huo, X. Zou, and X. Guo, "The risk probability criterion for discounted continuous-time Markov decision processes," *Discrete Event Dynamic Systems*, vol. 27, no. 4, pp. 675–699, 2017.

Hindawi
Mathematical Problems in Engineering
Volume 2020, Article ID 7037602, 13 pages
https://doi.org/10.1155/2020/7037602

Research Article

Some Properties of Bifractional Bessel Processes Driven by Bifractional Brownian Motion

Xichao Sun[1], **Rui Guo**[2], **and Ming Li**[3,4]

[1]*Department of Mathematics, College of Science, Bengbu University, 1866 Caoshan Rd., Bengbu 233030, China*
[2]*College of Information Science and Technology, Donghua University, 2999 North Renmin Rd., Songjiang, Shanghai 201620, China*
[3]*Ocean College, Zhejiang University, Zhejiang 310012, China*
[4]*Shanghai Key Laboratory of Multidimensional Information Processing, East China Normal University, No. 500 Dong-Chuan Road, Zhongshan, Shanghai 200241, China*

Correspondence should be addressed to Ming Li; ming_lihk@yahoo.com

Received 1 May 2020; Accepted 24 September 2020; Published 19 October 2020

Academic Editor: Wenguang Yu

Let $(B = \{(B_t^1, \ldots, B_t^d)\}_{t\geq 0})$ be a d-dimensional bifractional Brownian motion and $R_t = \sqrt{(B_t^1)^2 + \cdots + (B_t^d)^2}$ be the bifractional Bessel process with the index $(2\mathrm{HK} \geq 1)$. The Itô formula for the bifractional Brownian motion leads to the equation $(R_t = \sum_{i=1}^d \int_0^t (B_s^i/R_s)\mathrm{d}B_s^i + \mathrm{HK}(d-1)\int_0^t (s^{2\mathrm{HK}-1}/R_s)\mathrm{d}s)$. In the Brownian motion case $(K=1)$ and $(H=(1/2))$, $(X_t \coloneqq \sum_{i=1}^d \int_0^t (B_s^i/R_s)\mathrm{d}B_s^i, \quad d\geq 1)$ is a Brownian motion by Lévy's characterization theorem. In this paper, we prove that process X_t is not a bifractional Brownian motion unless $(K=1)$ and $(H=(1/2))$. We also study some other properties and their application of this stochastic process.

1. Introduction

Given $H \in (0,1)$ and $K \in [0,1]$, the bifractional Brownian motion with the indices H and K is a mean zero Gaussian process $B = \{B_t^{H,K}, t\geq 0\}$ such that $B_0^{H,K} = 0$ and

$$E\left[B_s^{H,K} B_t^{H,K}\right] = R(t,s) \coloneqq \frac{1}{2^K}\left[\left(t^{2H} + s^{2H}\right)^K - |t-s|^{2\mathrm{HK}}\right], \tag{1}$$

for all $(s,t\geq 0)$. This process was first introduced by Houdré and Villa [1]. More works for bifractional Brownian motion and their application can be found in [2–10] and the references therein. Clearly, the process is a fractional Brownian motion with Hurst the parameter H when $K=1$. Particularly, the process is a Brownian motion when $(K=1)$ and $(H=(1/2))$. Since $(B_t^{H,K})$ is neither a Markov process nor a semimartingale unless $(K=1)$ and $(H=(1/2))$, a lot of powerful techniques from classical stochastic analysis are not available to deal with it. As the generalization of the fractional Brownian motion, the bifractional Brownian motion also admits Hölder paths and self-similarity, but its increments are not stationary.

Let $B = (B^1, \ldots, B^d)$ be a d-dimensional bifractional Brownian motion with the index $(\mathrm{HK}\geq (1/2))$. That is to say, each component of B is an independent one-dimensional bifractional Brownian motion with the index $(\mathrm{HK}\geq (1/2))$. Let R_t be the bifractional Bessel process defined by $R_t = \sqrt{(B_t^1)^2 + \cdots + (B_t^d)^2}$.

There is an extensive literature on this process for the standard Brownian motion case $(K=1$ and $H=(1/2))$ and the fractional Brownian motion case $(K=1)$ (see [11–15]). For $(d\geq 2, \mathrm{HK} > (1/2))$, by the Itô formula for the bifractional Brownian motion, we have (see Alós et al. [16] and Es-Sebaiy and Tudor [3])

$$R_t = \sum_{i=1}^d \int_0^t \frac{B_s^i}{R_s}\mathrm{d}B_s^i + \mathrm{HK}(d-1)\int_0^t \frac{s^{2\mathrm{HK}-1}}{R_s}\mathrm{d}s, \tag{2}$$

and for $d=1$ and $(\mathrm{HK}\geq (1/2))$, one also has

$$\left|B_t^{H,K}\right| = \int_0^t \operatorname{sign}\left(B_s^{H,K}\right)\mathrm{d}B_s^{H,K} + \mathrm{HK}\int_0^t \delta\left(B_s^{H,K}\right)s^{2\mathrm{HK}-1}\mathrm{d}s, \tag{3}$$

where stochastic integrals are interpreted in the divergence sense and δ denotes the Dirac delta function. When $K = 1$ and $H = (1/2)$, the process

$$X_t = \begin{cases} \int_0^t \operatorname{sign}\left(B_s^{H,K}\right)\mathrm{d}B_s^{H,K}, & d = 1, \\ \sum_{i=1}^{d}\int_0^t \frac{B_s^i}{R_s}\mathrm{d}B_s^i, & d \geq 2 \end{cases} \tag{4}$$

is a standard Brownian motion by Lévy's characterization theorem. Given $K = 1$, the fractional Brownian motion case was researched by Hu and Nualart [11]. So, it is natural and interesting to research the process $X = \{X_t, t \geq 0\}$ for more general H and K. Since there is no characterization as convenient as Lévy's characterization theorem for general bifractional Brownian motion, to prove a stochastic process is a bifractional Brownian motion or not is difficult. The method used here is essentially based on Hu and Nualart [11] and Shen et al. [17]. It is not difficult to find that the bifractional Brownian motion has the nonavailability of convenient stochastic integral representations and more complexity of dependence structures than an fractional Brownian motion and a subfractional Brownian motion. Therefore, it seems interesting to study bifractional Bessel processes driven by bifractional Brownian motions.

The rest of the paper is organized as follows. In Section 2, we present some preliminaries for the bifractional Brownian motion. In Section 3, some properties to the process $\int_0^t \operatorname{sign}(B_t^{H,K})\mathrm{d}B_t^{H,K}$ are studied. In Section 4, we consider the process $(\sum_{i=1}^d \int_0^t (B_s^i/R_s)\mathrm{d}B_s^i)$ with $d \geq 2$. In Section 5, we consider the local time and Tanaka formula of the process $\int_0^t \operatorname{sign}(B_t^{H,K})\mathrm{d}B_t^{H,K}$.

2. Preliminaries

In this paper, we assume that $((1/2) < \mathrm{HK} < 1)$ is arbitrary but fixed and let $B = \left\{B_t^{H,k}, \quad 0 \leq t \leq T\right\}$ be a bifractional Brownian motion with the index H and K, which is defined on the complete probability space $(\Omega, \mathcal{F}, \text{and}\, P)$. One can construct a stochastic calculus of variations with respect to the bifractional Brownian motion $B^{H,k}$ by the Malliavin calculus method (see Alòs et al. [16] and Nualart [18]). We next recall the basic definitions and results for this calculus.

Bifractional Brownian motion $B^{H,k}$ satisfies the estimates:

$$2^{-K}|t-s|^{2\mathrm{HK}} \leq E\left[\left(B_t - B_s\right)^2\right] \leq 2^{1-K}|t-s|^{2\mathrm{HK}}. \tag{5}$$

One can write its covariance as follows:

$$R(t,s) = R_1(t,s) + R_2(t,s), \tag{6}$$

where

$$\begin{aligned} R_1(t,s) &= \frac{1}{2^K}\left[\left(s^{2H} + t^{2H}\right)^K - \left(s^{2\mathrm{HK}} + t^{2\mathrm{HK}}\right)\right], \\ R_2(t,s) &= \frac{1}{2^K}\left[t^{2\mathrm{HK}} + s^{2\mathrm{HK}} - |t-s|^{2\mathrm{HK}}\right]. \end{aligned} \tag{7}$$

Therefore,

$$\begin{aligned} \frac{\partial^2}{\partial t\,\partial s}R_1(t,s) &= 4H^2K(K-1)2^{-K}t^{2H-1}s^{2H-1}\left(t^{2H} + s^{2H}\right)^{K-2}, \\ \frac{\partial^2}{\partial t\,\partial s}R_2(t,s) &= 2(2\mathrm{HK}-1)\mathrm{HK}|t-s|^{2\mathrm{HK}-2}. \end{aligned} \tag{8}$$

Since R_1 is of the class $C^2([0,T]^2)$ and $(\partial^2/\partial t\,\partial s)R_1(t,s)$ is always negative, R_1 is the distribution function and has $(\partial^2/\partial t\,\partial s)R_1(t,s)$ for density. R_2 is the distribution function with density $(\partial^2/\partial r\,\partial s)R_1(t,s) = 2(2\mathrm{HK}-1)\mathrm{HK}|t-s|^{2\mathrm{HK}-2}$ and belongs to $L^1([0,T]^2)$. It follows that there exist two positive constants $c_{H,K}$ and $C_{H,K}$ which satisfy

$$c_{H,K}|t-s|^{2\mathrm{HK}-2} \leq \left|\frac{\partial^2}{\partial t\,\partial s}R(t,s)\right| \leq C_{H,K}|t-s|^{2\mathrm{HK}-2}. \tag{9}$$

Denote

$$\phi(t,s) = (2\mathrm{HK}-1)\mathrm{HK}|t-s|^{2\mathrm{HK}-2}, \quad \text{for}\, s,t \geq 0. \tag{10}$$

As a Gaussian process of $B^{H,k}$, we can construct a stochastic calculus of variations with respect to this process. Suppose that $\mathcal{H}$ is the completion of the space $\mathcal{E}$ which is generated by $\left\{1_{[0,T]}, t \in [0,T]\right\}$ with respect to the following inner product:

$$\left\langle 1_{[0,s]}, 1_{[0,t]}\right\rangle_{\mathcal{H}} = R(s,t). \tag{11}$$

Then, $\varphi \in \mathcal{E} \mapsto B(\varphi)$ is an isometry from $\mathcal{E}$ to the Gaussian space generated by B which can be extended to $\mathcal{H}$. We can write this Hilbert space $\mathcal{H}$ as follows:

$$\mathcal{H} = \left\{\varphi\colon\ [0,T] \longrightarrow \mathbb{R} \,|\, \|\varphi\|_{\mathcal{H}} < \infty\right\}, \tag{12}$$

where $\|\varphi\|_{\mathcal{H}}^2 := \int_0^T \varphi(s)\varphi(r)\phi(s,r)\mathrm{d}s\mathrm{d}r$. We can define the spaces of measurable functions as follows:

$$|\mathcal{H}| = \left\{\varphi\colon\ [0,T] \longrightarrow \mathbb{R} \,|\, \|\varphi\|_{|\mathcal{H}|} < \infty\right\}, \tag{13}$$

where

$$\|\varphi\|_{|\mathcal{H}|}^2 := \int_0^T\int_0^T |\varphi(s)\|\varphi(r)|\phi(s,r)\mathrm{d}s\mathrm{d}r < \infty. \tag{14}$$

It is easy to see that $\mathcal{E}$ is dense in $|\mathcal{H}|$ and $|\mathcal{H}|$ is a Banach space. Suppose that $\mathcal{S}$ is the set of smooth functional

$$F = f\left(B^{H,K}(\varphi_1), B^{H,K}(\varphi_2), \ldots, B^{H,K}(\varphi_2)\right), \tag{15}$$

where $f \in C_b^\infty(\mathbb{R}^n)$ and $\varphi_i \in \mathcal{H}$. The Malliavin derivative D of the above functional F is given as follows:

$$\mathrm{DF} = \sum_{j=1}^{n} \frac{\partial f}{\partial x_j} \left(B^{H,K}(\varphi_1), B^{H,K}(\varphi_2), \ldots, B^{H,K}(\varphi_n) \right) \varphi_j. \tag{16}$$

The derivative operator D is a closable operator from space $L^2(\Omega)$ into space $L^2(\Omega;\mathscr{H})$. We denote $\mathbb{D}^{1,2}$, the closure of $\mathscr{S}$, with respect to norm

$$\|F\|_{1,2} := \sqrt{E|F|^2 + E\|\mathrm{DF}\|_{\mathscr{H}}^2}. \tag{17}$$

The divergence integral δ is the adjoint operator of D. $\delta(u)$ can be defined by the duality relationship:

$$E[F\delta(u)] = E\langle DF, u\rangle_{\mathscr{H}}, \tag{18}$$

for any $u \in \mathbb{D}^{1,2}$. For any $u \in \mathbb{D}^{1,2}$, one has $(\mathbb{D}^{1,2} \subset \mathrm{Dom}(\delta))$ and

$$\begin{aligned} E\left[\delta(u)^2\right] &= E\|u\|_{\mathscr{H}}^2 + E\int_{[0,T]^4} D_\xi u_r D_\eta u_s \phi(\xi,s)\phi(\eta,r)\mathrm{d}s\mathrm{d}r\mathrm{d}\xi\mathrm{d}\eta \\ &\le E\|u\|_{|\mathscr{H}|}^2 + E\int_{[0,T]^4} \left|D_\xi u_r\right|\left|D_\eta u_s\right| \phi(\xi,s)\phi(\eta,r)\mathrm{d}s\mathrm{d}r\mathrm{d}\xi\mathrm{d}\eta, \end{aligned} \tag{19}$$

where

$$\delta(u) = \int_0^T u_s \mathrm{d}B_s^{H,K}, \tag{20}$$

expressing the Skorokhod integral of a process u.

3. Case of One Dimension

We study the stochastic process $X = \{X_t, \quad t \ge 0\}$ defined by

$$X_t = \int_0^t \mathrm{sign}\left(B_s^{H,K}\right) \mathrm{d}B_s^{H,K}. \tag{21}$$

If $K = 1$ and $H = (1/2)$, X_t is a standard Brownian motion from Levý's characterization theorem. It is then natural to study any parameter H and K. Next, we first prove X is an HK-self-similar process for any $\mathrm{HK} \ge (1/2)$.

Proposition 1. *The stochastic process $X = \{X_t, \quad t \ge 0\}$ is HK-self-similar.*

Proof. Together with the HK-self-similarity property of the bifractional Brownian motion and Tanaka formula (4), for any $a > 0$, one can obtain

$$\begin{aligned} X_{\mathrm{at}} &= \left|B_{\mathrm{at}}^{H,K}\right| - \mathrm{HK}\int_0^{at} \delta\left(B_s^{H,K}\right) B_s^{2\mathrm{HK}-1} \mathrm{d}s \\ &= \left|B_{\mathrm{at}}^{H,K}\right| - \mathrm{HK}\int_0^{t} \delta\left(B_{\mathrm{au}}^{H,K}\right) (\mathrm{au})^{2\mathrm{HK}-1} a\mathrm{d}u \\ &\overset{d}{=} a^{\mathrm{HK}}\left|B_{\mathrm{t}}^{H,K}\right| - \mathrm{HK}a^{2\mathrm{HK}}\int_0^{t} \delta\left(a^{\mathrm{HK}} B_u^{H,K}\right) (u)^{2\mathrm{HK}-1} \mathrm{d}u \\ &= a^{\mathrm{HK}} X_t, \end{aligned} \tag{22}$$

where $\overset{d}{=}$ denotes that both stochastic processes have the same distributions. This proof is completed.

For stochastic process $\mathrm{sign}(B_t^{H,K})$, we first obtain the Wiener chaos expansion. Let I_n be the multiple Wiener integral of the stochastic process $B^{H,K}$. □

Proposition 2. *For any $t \ge 0$, one can obtain*

$$\mathrm{sign}\left(B_t^{H,K}\right) = \sum_{m=0}^{\infty} b_{2m+1} I_{2m+1}(1), \tag{23}$$

where

$$b_{2m+1} = \frac{2(-1)^m}{(2m+1)\sqrt{2\pi t}^{(2m+1)\mathrm{HK}} m! 2^m}. \tag{24}$$

Proof. For $\varepsilon > 0$, we denote

$$\begin{aligned} p_\varepsilon(y) &= \frac{1}{\sqrt{2\pi\varepsilon}} e^{-(y^2/2\varepsilon)}, \\ f_\varepsilon(y) &= 2\int_{-\infty}^{y} p_\varepsilon(z)\mathrm{d}z - 1, \quad y \in \mathbb{R}. \end{aligned} \tag{25}$$

Then,

$$p_{t^{2\mathrm{HK}}}(y) = \frac{1}{\sqrt{2\pi}t^{\mathrm{HK}}} \exp\left(-\frac{y^2}{2t^{2\mathrm{HK}}}\right), \quad x \in \mathbb{R}, \tag{26}$$

which is a density function of the bifractional Brownian motion $B_t^{H,K}$ and $f_\varepsilon(B_t^{H,K}) \longrightarrow \mathrm{sign}(B_t^{H,K})$ in $L^2(\Omega)$ as $\varepsilon \longrightarrow 0$. By Stroock's formula, one can obtain

$$f_\varepsilon\left(B_t^{H,K}\right) = \sum_{m=0}^{\infty} a_m^\varepsilon(t) \int_{0<s_1<\cdots<s_n<t} \mathrm{d}B_{s_1}^{H,K}, \ldots, \mathrm{d}B_{s_n}^{H,K}, \tag{27}$$

where

$$\begin{aligned} a_m^\varepsilon(t) &= E\left[D^m\left(f_\varepsilon\left(B_t^{H,K}\right)\right)\right] = 2E\left[p_\varepsilon^{(m-1)}\left(B_t^{H,K}\right)\right] \\ &= 2(-1)^{m-1} \frac{\partial^{m-1}}{\partial z^{m-1}} E\left[p_\varepsilon\left(B_t^{H,K} - z\right)\right]\Big|_{z=0} \\ &= 2(-1)^{m-1} p_{\varepsilon+t^{2\mathrm{HK}}}^{(m-1)}(0). \end{aligned} \tag{28}$$

As $\varepsilon \longrightarrow 0$, by taking the limit of (27) in the space $L^2(\Omega)$, one can obtain

$$\operatorname{sign}\left(B_t^{H,K}\right) = \sum_{m=0}^{\infty} a_n(t) \int_{0<s_1<\cdots<s_n<t} \mathrm{d}B_{s_1}^{H,K}, \ldots, \mathrm{d}B_{s_n}^{H,K}, \tag{29}$$

where $a_m(t) = \lim_{\varepsilon\longrightarrow 0} a_m^{\varepsilon}(t) = 2(-1)^{m-1} p_{t^{2\mathrm{HK}}}^{(n-1)}(0)$, which implies

$$a_m(t) = \begin{cases} 0, & n = 2k, \\ \dfrac{2(-1)^k (2k)!}{\sqrt{2\pi}\, t^{nH} k! 2^k}, & n = 2k+1. \end{cases} \tag{30}$$

The proof is completed.

In this paper, the notation $F \asymp G$ implies that there are two positive constants c_1 and c_2 such that

$$c_1 G(x) \leq F(x) \leq c_2 G(x), \tag{31}$$

where C denotes a generic positive constant and F and G have the common domain. □

Proposition 3. *The random variable sign$(B_t^{H,K})$ belongs to the Sobolev–Watanabe space $\mathbb{D}^{\alpha,2}$ for any $t \geq 0$ and $\alpha < (1/2)$.*

Proof. By Stirling's formula

$$\lim_{k\longrightarrow\infty} \frac{k!}{k^{(k+(1/2))} e^{-k}} = \sqrt{2\pi}, \tag{32}$$

we have

$$\begin{aligned} E\left[I_{2m+1}(b_{2m+1})\right]^2 &= (2m+1)! \langle b_{2m+1}, b_{2k+1} \rangle_{\mathscr{H}^{\otimes 2m+1}} \\ &= \frac{(2m+1)! 4 \left(t^{2\mathrm{HK}}\right)^{2m+1}}{(2m+1)^2 2\pi t^{(2m+1)2\mathrm{HK}} \left(m! 2^m\right)^2} \\ &\asymp \mathrm{Cm}^{-3/2}. \end{aligned} \tag{33}$$

The proof is completed. □

Proposition 4. *For any $t \geq 0$, one has*

$$\int_0^t \operatorname{sign}\left(B_s^{H,K}\right) \mathrm{d}B_s^{H,K} = \sum_{m=1}^{\infty} c_m I_{2m}(h_{2m}), \tag{34}$$

where $c_m = (-1)^{m-1} (\sqrt{2\pi}\,(2m-1)(m-1)! 2^{m-2})^{-1}$ and

$$h_{2m}(B_1, \ldots, B_{2m}) = \left(B_1 \vee B_2 \vee \cdots \vee B_{2m}\right)^{-(2m-1)\mathrm{HK}}. \tag{35}$$

The above proposition is the chaos expansion of $\int_0^t \operatorname{sign}(B_t^{H,K}) \mathrm{d}B_t^{H,K}$ and implies the following result, which can be proved by the method similar to Proposition 3.

Proposition 5. *For any $\alpha < (1/2)$ and $t \geq 0$, the random variable $\int_0^t sign(B_s^{H,K}) dB_s^{H,K}$ belongs to the Sobolev–Watanabe space $\mathbb{D}^{\alpha,2}$. Now, we consider the stochastic process X:*

$$\rho(n) := E\left[\left(X_{a+1} - X_a\right)\left(X_{n+1} - X_n\right)\right], \tag{36}$$

where $(0 < a \leq n)$.

Definition 1. We say a stochastic process $(X_t)_{t\geq 0}$ is long-range dependent (resp. short-range dependent) if for each $a > 0$,

$$\sum_{n\geq a} |\rho(n)| = \infty, \quad \left(\text{resp.} \sum_{n\geq a} |\rho(n)| < \infty\right). \tag{37}$$

Theorem 1. *The stochastic process X of (21) is short-range dependent. Before proving this theorem, a lemma given by Yan et al. [9] is stated.*

Lemma 1. *Let $(0 \leq r < s)$ and $(0 < HK < 1)$, one defines*

$$\rho_{r,s}^2 := s^{2\mathrm{HK}} r^{2\mathrm{HK}} - \mu^2, \tag{38}$$

where $\mu = E(B_s^{H,K} B_r^{H,K})$. Then, we have

$$\rho_{r,s}^2 \asymp (s-r)^{2\mathrm{HK}} r^{2\mathrm{HK}}. \tag{39}$$

Remark 1. The proof of estimate (39) uses the following two inequalities:

$$(1+x)^{\alpha} \leq 1 + \left(2^{\alpha} - 1\right) x^{\alpha}, \quad 0 \leq x,\ \alpha \leq 1, \tag{40}$$

$$(u+v-1)^K \leq u^K + v^K - 1 \leq (u+v-1)^K + (uv)^K, \quad (0 \leq K \leq 1), \tag{41}$$

where $0 \leq u, v \leq 1$ and $u + v \geq 1$. It is not difficult to prove inequality (40), which is stronger than the well-known inequality

$$(1+x)^{\alpha} \leq 1 + \alpha x^{\alpha} \leq 1 + x^{\alpha}, \tag{42}$$

because $(2^{\alpha} - 1 \leq \alpha)$ for all $(0 \leq \alpha \leq 1)$.

Proof of Theorem 1. For $0 < a < k$, one can obtain

$$\begin{aligned}
\rho(k) &= E\left[\int_a^{a+1} \operatorname{sign}\left(B_t^{H,K}\right) dB_t^{H,K} \int_k^{k+1} \operatorname{sign}\left(B_t^{H,K}\right) dB_t^{H,K}\right] \\
&= \int_a^{a+1}\int_k^{k+1} \phi(t,s) E\left(\operatorname{sign} B_s^{H,K} \operatorname{sign} B_t^{H,K}\right) dsdt + \int_a^{a+1}\int_k^{k+1}\int_0^s\int_0^t \phi(s,u)\phi(t,v) E\left[\delta\left(B_s^{H,K}\right)\delta\left(B_t^{H,K}\right)\right] dudvdsdt \\
&= \int_a^{a+1}\int_k^{k+1} \phi(t,s) E\left(\operatorname{sign} B_s^{H,K} \operatorname{sign} B_t^{H,K}\right) dsdt + 4(\mathrm{HK})^2 \int_a^{a+1}\int_k^{k+1} \psi_1(s,t)\psi_2(s,t) E\left[\delta\left(B_s^{H,K}\right)\delta\left(B_t^{H,K}\right)\right] dsdt \\
&= \int_a^{a+1}\int_k^{k+1} \phi(t,s) E\left(\frac{B_s^{H,K}}{\left|B_s^{H,K}\right|}\frac{B_t^{\mathrm{HK}}}{\left|B_t^{\mathrm{HK}}\right|}\right) dsdt + 4(\mathrm{HK})^2 \int_a^{a+1}\int_n^{n+1} \psi_1(s,t)\psi_2(s,t) E\left[\delta\left(B_s^{H,K}\right)\delta\left(B_t^{H,K}\right)\right] dsdt \\
&\asymp \int_a^{a+1}\int_k^{k+1} E\left(\frac{B_s^{H,K}}{\left|B_s^{H,K}\right|}\frac{B_t^{\mathrm{HK}}}{\left|B_t^{\mathrm{HK}}\right|}\right)\phi(t,s) dsdt \\
&\quad + 4(\mathrm{HK})^2 \int_a^{a+1}\int_k^{k+1} E\left[\delta\left(B_s^{H,K}\right)\delta\left(B_t^{H,K}\right)\right]\cdot\left[s^{2\mathrm{HK}-1} + (t-s)^{2\mathrm{HK}-1}\right]\left[t^{2\mathrm{HK}-1} + (t-s)^{2\mathrm{HK}-1}\right] dsdt \\
&\equiv a_k + b_k.
\end{aligned} \tag{43}$$

Now, we only need to estimate a_k and b_k. For a_k, by the orthogonal decomposition,

$$B_t^{H,K} \stackrel{d}{=} \frac{\theta_H(s,t)}{\theta_H(s,s)} B_s^{H,K} + \beta_{s,t}\mathcal{N}, \tag{44}$$

where

$$\beta_{s,t}^2 = \frac{\rho_{s,t}^2}{s^{2\mathrm{HK}}}, \tag{45}$$

in which $\mathcal{N} \in N(0,1)$ independent of $B_s^{H,K}$. Set

$$\lambda_{s,t} = \frac{\theta_H(s,t)}{\beta_{s,t} s^{2\mathrm{HK}}} = \frac{1/2^K\left[\left(t^{2H} + s^{2H}\right)^K - |t-s|^{2\mathrm{HK}}\right]}{s^{\mathrm{HK}}\rho_{s,t}}. \tag{46}$$

Since

$$\left(1 + x^{2H}\right)^K - (1-x)^{2\mathrm{HK}} \sim x^{2\mathrm{HK}}, \tag{47}$$

$x \longrightarrow 0$. By Lemma 1, we obtain

$$\lambda_{s,t} = \frac{\theta_H(s,t)}{\beta_{s,t} s^{2\mathrm{HK}}} \sim C_H t^{-\mathrm{HK}}, \tag{48}$$

as $t \longrightarrow \infty$ and $s \in (0,1)$, which implies

$$\begin{aligned}
E\left(\frac{B_s^{H,K} B_t^{H,K}}{\left|B_s^{H,K}\right|\left|B_t^{H,K}\right|}\right) &= E\left(\frac{B_s^{H,K}\left(\lambda_{s,t} B_s^{H,K} + \mathcal{N}\right)}{\left|B_1^{H,K}\right|\left|\lambda_{s,t} B_s^{H,K} + \mathcal{N}\right|}\right), \\
&= E\left(\frac{B_1^{H,K}\left(s^{H,K}\lambda_{s,t} B_1^{H,K} + \mathcal{N}\right)}{\left|B_1^{H,K}\right|\left|s^{H,K}\lambda_{s,t} B_1^{H,K} + \mathcal{N}\right|}\right) \\
&= O\left(t^{-\mathrm{HK}}\right).
\end{aligned} \tag{49}$$

So, the term a_k behaves as $k^{2\mathrm{HK}-3} o\left(k^{-\mathrm{HK}}\right)$. Now, we evaluate the second term b_n. For $s < t$, using Lemma 1, one can obtain

$$\begin{aligned}
E\left[\delta\left(B_s^{H,K}\right)\delta\left(B_t^{H,K}\right)\right] &= \int_{R^2} h(y,z)\delta(y)\delta(z) dydz = h(0,0) \\
&= \frac{1}{2\pi\rho_{t,s}} \asymp s^{-\mathrm{HK}}(t-s)^{-\mathrm{HK}},
\end{aligned} \tag{50}$$

where $h(y,z)$ is the density function of $\left(B_s^{H,K}, B_t^{H,K}\right)$. So,

$$\begin{aligned}
b_k &= \frac{4(\mathrm{HK})^2}{2\pi}\int_a^{a+1}\int_k^{k+1} \frac{\left[s^{2\mathrm{HK}-1} + (t-s)^{2\mathrm{HK}-1}\right]\left[t^{2\mathrm{HK}-1} + (t-s)^{2\mathrm{HK}-1}\right]}{\left[(\mathrm{st})^{\mathrm{HK}} - (1/4)\left(\left(1/2^K\right)\left[\left(t^{2H} + s^{2H}\right)^K - |t-s|^{2\mathrm{HK}}\right]\right)^2\right]^{(1/2)}} dsdt \\
&\asymp \int_a^{a+1}\int_k^{k+1} \frac{\left[(a+1)^{2\mathrm{HK}-1} + (k+1)^{2\mathrm{HK}-1}\right](k-a-1)^{2\mathrm{HK}-1}}{\left[(\mathrm{ak})^{\mathrm{HK}} - (1/4)\left(\left(1/2^K\right)\left[\left((k+1)^{2H} + (a+1)^{2\mathrm{HK}}\right)^K - |k-a|^{2\mathrm{HK}}\right]\right)^2\right]^{(1/2)}} dsdt \\
&\asymp k^{3\mathrm{HK}-3}.
\end{aligned} \tag{51}$$

The proof is completed. □

4. Case of Multidimension

We now consider the d-dimensional bifractional Brownian motion $B = \{(B_t^1, \ldots, B_t^d)\}_{t\geq 0}$ with the index $\mathrm{HK} \geq (1/2)$, which implies the components $(B^i, \quad i = 1, \ldots, d)$ are independent bifractional Brownian motions with the same index $\mathrm{HK} \geq (1/2)$. As in Section 2, we can define the derivative and divergence operators, D^i and δ^i, with respect to each component B^i. Suppose that $(\mathbb{D}_i^{1,p}(\mathscr{H}))$ are the associated Sobolev spaces. Similarly, $(\mathbb{L}_{\mathrm{HK},i}^{1,p})$ denotes the set of processes u in $(\mathbb{D}_i^{1,p}(|\mathscr{H}|))$ which satisfies

$$|u|^p_{\mathbb{L}^{1,p}_{\mathrm{HK},i}} := E\left[|u|^p_{L^{(1/\mathrm{HK})}([0,T])}\right] + E\left[\left\|D^i u\right\|^p_{L^{(1/\mathrm{HK})}([0,T]^2)}\right] < \infty. \tag{52}$$

Let

$$R_t = |B_t| = \sqrt{\left(B_t^1\right)^2 + \cdots + \left(B_t^d\right)^2} \tag{53}$$

be a bifractional Bessel process. In the following, we research the stochastic process:

$$X_t = \sum_{i=1}^d \int_0^t \frac{B_s^i}{R_s} dB_s^i. \tag{54}$$

The next theorem can be proved similar to Es-Sebaiy and Tudor [3].

Theorem 2. *Let $B_t = (B_t^1, B_t^2, \ldots, B_t^d)$ be a d-dimensional bifractional Brownian motion with $(2HK > 1)$ and f be a function of class $C^2(\mathbb{R}^d)$. Then,*

$$f(B_t) = f(0) + \sum_{i=1}^d \int_0^t \frac{\partial f}{\partial x_i}(B_s) dB_s^i + \mathrm{HK} \sum_{i=1}^d \int_0^t \frac{\partial^2 f}{\partial x_i^2}(B_s) s^{2\mathrm{HK}-1} ds. \tag{55}$$

The following proposition gives an integral representation for bifractional Bessel processes and can be proved along the lines of the proof of Proposition 5.2. in Guerra and Nualart [19].

Proposition 6. *Suppose that $R = \{R_t\}_{t\geq 0}$ is a bifractional Bessel process associated to the d-dimensional bifractional Brownian motion with index $HK > (1/2)$. For each $(i = 1, \ldots, d)$, one can obtain $\{(B_s^i/R_s)\}_{s\in[0,T]} \in \mathbb{L}_{H,i}^{(1,1/HK)}$ and*

$$R_t = \sum_{i=1}^d \int_0^t \frac{B_s^i}{R_s} dB_s^i + \mathrm{HK}(d-1) \int_0^t \frac{B_s^{2\mathrm{HK}-1}}{R_s} ds. \tag{56}$$

Proof

Step1. We prove $\int_0^t (B_s^i/R_s) dB_s^i$ are well defined which only proves $\{(B_s^i/R_s)\}_{s\in[0,T]} \in \mathbb{L}_{\mathrm{HK},i}^{(1,1/\mathrm{HK})}$ for each $(i = 1, \ldots, d)$. Since $|B_s^i/R_s| \leq 1$ for each $(i = 1, \ldots, d)$, one can obtain

$$E \int_0^T \left|\frac{B_s^i}{R_s}\right|^{(1/\mathrm{HK})} ds < \infty, \quad i = 1, \ldots, d. \tag{57}$$

Together with the definition of the derivative operator and the self-similarity of the bifractional Brownian motion, one can obtain

$$\begin{aligned} E \int_0^T \int_0^T \left| D_s^i \left(\frac{B_r^i}{R_r}\right)\right|^{(1/\mathrm{HK})} ds dr &= \int_0^T rE \left|\frac{1}{R_r} - \frac{\left(B_r^i\right)^2}{R_r^3}\right|^{(1/\mathrm{HK})} dr \\ &\leq \int_0^T rE\left[R_r^{-(1/\mathrm{HK})}\right] dr = \mathrm{TE}\left[R_1^{-(1/\mathrm{HK})}\right] = C \int_0^\infty \frac{1}{(2\pi)^{(d/2)}} e^{-(u^2/2)} u^{d-1-(1/\mathrm{HK})} du < \infty, \end{aligned} \tag{58}$$

since $(d - 1 - (1/\mathrm{HK}) > -1)$. So, the integral $\int_0^t (B_s^i/R_s) dB_s^i$ is well defined since $\{(B_s^i/R_s)\}_{s\in[0,T]} \in \mathbb{L}_{H,K,i}^{(1,1/\mathrm{HK})}$ for each $(i = 1, \ldots, d)$.

Step 2. We now prove (56). Note that $f: \mathbb{R}^d \longrightarrow \mathbb{R}$ is defined by

$$f(x) = \sqrt{x_1^2 + \cdots + x_d^2}, \tag{59}$$

which is not differentiable at the origin. So, we cannot apply the Itô formula (55) to f. But, if one considers the square of the bifractional Bessel process

$$R_t^2 = \left(B_t^1\right)^2 + \cdots + \left(B_t^d\right)^2, \tag{60}$$

then one can apply the Itô formula (55), and we have

$$R_t^2 = 2 \sum_{i=1}^d \int_0^t B_s^i dB_s^i + \mathrm{HK} d t^{2\mathrm{HK}}. \tag{61}$$

Set

$$g_\varepsilon(y) = \begin{cases} \dfrac{3}{8}\sqrt{\varepsilon} + \dfrac{3}{4\sqrt{\varepsilon}} y - \dfrac{1}{8\varepsilon\sqrt{\varepsilon}} y^2, & y < \varepsilon, \\ \sqrt{x}, & y \geq \varepsilon. \end{cases} \tag{62}$$

For any $\varepsilon > 0$, $g_\varepsilon(y) \in C^2(\mathbb{R})$, and $\lim_{\varepsilon\longrightarrow 0} g_\varepsilon(y) = \sqrt{y}$ for any $x \geq 0$. Applying (55) to $g_\varepsilon(R_t^2)$, we obtain

$$g_\varepsilon\left(R_t^2\right) = \frac{3}{8}\sqrt{\varepsilon} + \sum_{i=1}^{d} \mathrm{I}(i,\varepsilon) + \mathrm{II}(\varepsilon) + \mathrm{III}(\varepsilon), \tag{63}$$

where

$$\begin{aligned} \mathrm{I}(i,\varepsilon) &:= \int_0^t \left[1_{\{R_s^2<\varepsilon\}} \frac{1}{2\sqrt{\varepsilon}}\left(3 - \frac{R_s^2}{\varepsilon}\right) + 1_{\{R_s^2 \geq \varepsilon\}} \frac{1}{R_s}\right] B_s^i \mathrm{d}B_s^i, \\ \mathrm{II}(\varepsilon) &:= \mathrm{HK}(d-1)\int_0^t 1_{\{R_s^2\geq\varepsilon\}} \frac{1}{R_s} B^{2\mathrm{HK}-1}\mathrm{d}s, \\ \mathrm{III}(\varepsilon) &:= \mathrm{HK}\int_0^t 1_{\{R_s^2<\varepsilon\}} \frac{1}{2\sqrt{\varepsilon}}\left[3d - (d+2)\frac{R_s^2}{\varepsilon}\right] B^{2\mathrm{HK}-1}\mathrm{d}. \end{aligned} \tag{64}$$

Together with $\int_0^t (s^{2\mathrm{HK}-1}/R_s) < \infty$ a.s. and the bounded convergence theorem, one can obtain

$$\lim_{\varepsilon\longrightarrow 0} \mathrm{II}(\varepsilon) = (d-1)\mathrm{HK}\int_0^t \frac{1}{R_s} s^{2\mathrm{HK}-1}\mathrm{d}s. \tag{65}$$

For the third term, by the substituting $u = (\rho/s^{H,K})$ and Fubini's theorem, we can obtain

$$\begin{aligned} 0 \leq E(\mathrm{III}(\varepsilon)) &\leq \frac{3\mathrm{HKd}}{2\sqrt{\varepsilon}} \int_0^t P\left\{R_s^2 < \varepsilon\right\} s^{2\mathrm{HK}-1}\mathrm{d}s \\ &\leq \frac{3\mathrm{HKd}}{2\sqrt{\varepsilon}} \int_0^t P\left\{\left(B_s^1\right)^2 + \left(B_s^2\right)^2 < \varepsilon\right\} s^{2\mathrm{HK}-1}\mathrm{d}s \\ &= \frac{3\mathrm{HKd}}{2\sqrt{\varepsilon}} \int_0^t \left[\int_0^{2\pi}\int_0^{\sqrt{\varepsilon}} \frac{\rho}{2\pi s^{2\mathrm{HK}}} e^{-\left(\rho^2/2B_s^{2\mathrm{HK}}\right)} \mathrm{d}\rho \mathrm{d}\theta\right] s^{2\mathrm{HK}-1}\mathrm{d}s \\ &\leq \frac{3d}{2\sqrt{\varepsilon}} \int_0^{\sqrt{\varepsilon}} \left(\int_{\frac{\rho}{t^{HK}}}^{\infty} \frac{1}{u} e^{-\left(u^2/2\right)}\mathrm{d}u\right)\rho \mathrm{d}\rho, \end{aligned} \tag{66}$$

that is,

$$\lim_{\varepsilon\longrightarrow 0} E(|\mathrm{III}(\varepsilon)|) = 0. \tag{67}$$

Finally, we show that

$$\lim_{\varepsilon\longrightarrow 0} \mathrm{I}(i,\varepsilon) = \int_0^t \frac{B_s^i}{R_s}\mathrm{d}B_s^i \tag{68}$$

in $L^{(1/\mathrm{HK})}(\Omega)$. We have

$$\begin{aligned} A(\varepsilon) &:= E\left[\int_0^T \left|1 - \frac{R_s}{2\sqrt{\varepsilon}}\left(3 - \frac{R_s^2}{\varepsilon}\right)\right|^{(1/\mathrm{HK})} \left|\frac{B_s^i}{R_s}\right|^{(1/\mathrm{HK})} 1_{\{R_s^2<\varepsilon\}}\mathrm{d}s\right] \\ &\leq \int_0^T P\left\{R_s^2 < \varepsilon\right\}\mathrm{d}s \leq \int_0^T P\left\{\left(B_s^1\right)^2 + \left(B_s^2\right)^2 < \varepsilon\right\}\mathrm{d}s \\ &= \int_0^T \left[\int_0^{2\pi}\int_0^{\sqrt{\varepsilon}} \rho \frac{1}{2\pi B^{2\mathrm{HK}}} e^{-\left(\rho^2/2B^{2\mathrm{HK}}\right)}\mathrm{d}\rho\mathrm{d}\theta\right]\mathrm{d}s \longrightarrow 0, \end{aligned} \tag{69}$$

as $\varepsilon \longrightarrow 0$. On the other hand, one can obtain

$$\begin{aligned} B(\varepsilon) &:= E\left[\int_0^T\int_0^T \left|D_B^i\left(\left(\frac{B_r^i}{R_r} - \frac{B_r^i}{2\sqrt{\varepsilon}}\left(3 - \frac{R_r^2}{\varepsilon}\right)\right)1_{\{R_r^2<\varepsilon\}}\right)\right|^{(1/\mathrm{HK})}\mathrm{d}s\mathrm{d}r\right] \\ &= \int_0^T rE\left[\left|\left(\frac{1}{R_r} - \frac{\left(B_r^i\right)^2}{R_r^3}\right) - \frac{3}{2\sqrt{\varepsilon}} + \frac{R_r^2 + 2\left(B_r^i\right)^2}{2\varepsilon\sqrt{\varepsilon}}\right|^{(1/\mathrm{HK})} 1_{\{R_r^2<\varepsilon\}}\right]\mathrm{d}r \\ &\leq \int_0^T rE\left[\left|\frac{1}{R_r} + \frac{3}{2\sqrt{\varepsilon}} + \frac{3R_r^2}{2\varepsilon\sqrt{\varepsilon}}\right|^{(1/\mathrm{HK})} 1_{\{R_r^2<\varepsilon\}}\right]\mathrm{d}r \\ &\leq 4^{\frac{1}{\mathrm{HK}}}\int_0^T E\left[\left|R_1\right|^{-(1/\mathrm{HK})} 1_{\{R_1^2<(\varepsilon/r^{2\mathrm{HK}})\}}\right]\mathrm{d}r. \end{aligned} \tag{70}$$

The distribution of $(B_1^1,\ldots,B_1^d)$ in spherical coordinates yields

$$\int_0^T E\left[\left|R_1\right|^{-(1/\mathrm{HK})} 1_{\{R_1<(\sqrt{\varepsilon}/r^{\mathrm{HK}})\}}\right]dr \leq C_{d,H,K}\int_0^T\int_0^{(\sqrt{\varepsilon}/r^{\mathrm{HK}})} e^{-\left(u^2/2l\right)} u^{d-1-(1/\mathrm{HK})}\mathrm{d}u\mathrm{d}r, \tag{71}$$

where $C_{d,H,K} > 0$ is a constant which depends on H, K, and d.

For any $r \in [0, T]$,

$$\int_0^{(\sqrt{\varepsilon}/r^{\mathrm{HK}})} e^{-(u^2/2l)} u^{d-1-(1/\mathrm{HK})} \mathrm{d}u \longrightarrow 0, \quad \varepsilon \longrightarrow 0,$$
$$\int_0^{(\sqrt{\varepsilon}/r^{\mathrm{HK}})} e^{-(u^2/2l)} u^{d-1-(1/\mathrm{HK})} \mathrm{d}u \le \int_0^{\infty} e^{-(u^2/2l)} u^{d-1-(1/\mathrm{HK})} \mathrm{d}u < \infty. \quad (72)$$

We have

$$\lim_{\varepsilon \longrightarrow 0} \int_0^T E\left[\left|R_1\right|^{-(1/\mathrm{HK})} 1_{\{R_1 < (\sqrt{\varepsilon}/r^{\mathrm{HK}})\}}\right] \mathrm{d}r = 0, \quad (73)$$

by the bounded convergence theorem, that is,

$$\lim_{\varepsilon \longrightarrow 0} B(\varepsilon) = 0. \quad (74)$$

This proves the desired convergence (68), and the proposition follows. □

Proposition 7. *Stochastic process X which is given by (54) is HK-self-similar.*

Proof. Set $a > 0$. Together with the HK-self-similarity property of the bifractional Brownian motion and (56), we can obtain

$$\begin{aligned} X_{\mathrm{at}} &= R_{\mathrm{at}} - \mathrm{HK}(d-1) \int_0^{at} \frac{B_s^{2\mathrm{HK}-1}}{R_s} \mathrm{d}s \\ &= R_{\mathrm{at}} - \mathrm{HK}(d-1) a^{2\mathrm{HK}} \int_0^t \frac{u^{2\mathrm{HK}-1}}{R_{\mathrm{au}}} \mathrm{d}u \\ &\overset{d}{=} a^{\mathrm{HK}} R_t - \mathrm{HK}(d-1) a^H \int_0^t \frac{u^{2\mathrm{HK}-1}}{R_u} \mathrm{d}u = a^{\mathrm{HK}} X_t. \end{aligned} \quad (75)$$

For $h \in \mathscr{H}^{\otimes n}$, we denote

$$I_{i_1,\ldots,i_k}(h) = \int_{0<s_1,\ldots,s_k<t} h(s_1,\ldots,s_k) \mathrm{d}B_{s_1}^{i_1}, \ldots, \mathrm{d}B_{s_n}^{i_n}, \quad 1 \le i_1,\ldots,i_k \le d. \quad (76)$$

□

Theorem 3. *Suppose f_j: $\mathbb{R}^d \longrightarrow \mathbb{R}$, $j = 1, 2, \ldots, d$ are with polynomial growth and smooth functions. Then, the stochastic process $Z_t = \sum_{j=1}^d \int_0^t f_j(B_s) dB_s^j$ has the following chaos expansion:*

$$Z_t = \sum_{j=1}^d \sum_{k=1}^{\infty} \sum_{1 \le i_1,\ldots,i_i \le d} I_{i_1,\ldots,i_k,\mathrm{ji}}\left(g_{i_1,\ldots,i_n}^j(B_1,\ldots,B_{k+1})\right), \quad (77)$$

where

$$g_{i_1,\ldots,i_k}^j(B_1,\ldots,B_{k+1}) = \frac{(-1)^n (B_1 \vee \cdots \vee B_{i+1})^{-\mathrm{kHK}}}{(2\pi)^{(d/2)}} \times \int_{\mathbb{R}^d} \left[\frac{\partial^k}{\partial y_{i_1},\ldots,\partial y_{i_k}} e^{-(|y|^2/2)}\right] f_i\left(y (B_1 \vee \cdots \vee B_{k+1})^{\mathrm{HK}}\right) \mathrm{d}y. \quad (78)$$

Proof. For each $(j = 1, 2, \ldots, d)$, using Stroock's formula, we can obtain

$$f_j(B_s) = \sum_{k=0}^{\infty} \sum_{1 \le i_1,\ldots,i_k \le d} \frac{1}{k!} I_{i_1,\ldots,i_n}\left(f_{i_1,\ldots,i_n}^i(s) 1_{[0,s]}^{\otimes n}\right), \quad (79)$$

where

$$\begin{aligned} f_{i_1,\ldots,i_k}^j(s) &= E\left(D^{i_1},\ldots,D^{i_n}\left(f_j(B_s)\right)\right) \\ &= E\left(\frac{\partial^n f_j}{\partial z_{i_1},\ldots,\partial z_{i_k}}(B_s)\right) \\ &= \frac{1}{\left(2\pi \mathrm{lB}^{2\mathrm{HK}}\right)^{(d/2)}} \int_{\mathbb{R}^d} \frac{\partial^n f_i}{\partial z_{i_1},\ldots,\partial z_{i_n}}(z) e^{-(|z|^2/2s^{2\mathrm{HK}})} dz \\ &= \frac{(\sqrt{l})^{-n} B^{-\mathrm{nH}}}{(2\pi)^{(d/2)}} \int_{\mathbb{R}^d} \frac{\partial^k f_i}{\partial z_{i_1},\ldots,\partial z_{i_n}}\left(y B^{H,K}\right) e^{-(|y||^2/2)} \mathrm{d}y \\ &= \frac{(-1)^n B^{-\mathrm{nH}}}{(2\pi)^{(d/2)}} \int_{\mathbb{R}^d} f_j\left(y B^{H,K}\right)\left[\frac{\partial^n}{\partial z_{i_1},\ldots,\partial z_{i_n}} e^{-(|y||^2/2)}\right] \mathrm{d}y. \end{aligned} \quad (80)$$

So,

$$\begin{aligned} Z_t &= \sum_{j=1}^d \int_0^t f_j(B_s) \mathrm{d}B_s^j, \\ &= \sum_{i=1}^d \sum_{k=0}^{\infty} \sum_{1 \le i_1,\ldots,i_n \le d} I_{i_1,\ldots,i_k,i}\left(\mathrm{symm}\left(f_{i_1,\ldots,i_k}^i(s)\right) 1_{[0,s]}^{\otimes n} 1_{[0,t]}(s)\right) \\ &= \sum_{i=1}^d \sum_{k=0}^{\infty} \sum_{1 \le i_1,\ldots,i_n \le d} I_{i_1,\ldots,i_n,i}\left(f_{i_1,\ldots,i_k}^i(B_1 \vee \cdots \vee B_{k+1}) \prod_{j=1}^{k+1} 1_{[0,t]}(B_j)\right). \end{aligned} \quad (81)$$

This completes the proof.

Let $f_j(x) = (x_j/\sqrt{x_1^2 + \cdots + x_d^2})$; then, $f_j(tx) = f_j(x)$. So, for such f_j, one can obtain

$$g^{j}_{i_1,\ldots,i_k}(B_1,\ldots,B_{k+1}) = \frac{(-1)^k(\sqrt{l})^{-k}(B_1\vee\cdots\vee B_{k+1})^{-\mathrm{kHK}}}{(2\pi)^{(d/2)}} \times \int_{\mathbb{R}^d}\left[\frac{\partial^k}{\partial y_{i_1}\cdots\partial y_{i_n}}e^{-(|y|^2/2)}\right]f_j(y)\mathrm{d}y. \tag{82}$$

Then, (B_t^j/R_t) can be denoted by

$$\frac{B_t^j}{R_t} = \sum_{k=0}^{\infty}\sum_{1\le i_1,\ldots,i_n\le d}\frac{(-1)^k(t)^{-\mathrm{kHK}}}{(2\pi)^{(d/2)}} \times \int_{\mathbb{R}^d}\left[\frac{\partial^n}{\partial y_{i_1},\ldots,\partial y_{i_n}}e^{-(|y|^2/2)}\right]f_j(y)\mathrm{d}y\int_{\{0<s_1<\cdots<s_k<t\}}\mathrm{d}B^{i_1}_{s_1},\ldots,\mathrm{d}B^{i_n}_{s_k}, \tag{83}$$

and the chaos expansion of $\int_0^t (B_B^i/R_s)\mathrm{d}B_s^i$ is

$$\int_0^t \frac{B_s^i}{R_s}\mathrm{d}B_s^i = \sum_{n=1}^{\infty}\sum_{1\le j_1,\ldots,j_k\le d}\frac{(-1)^k}{(2\pi)^{(d/2)}}\int_{\mathbb{R}^d}\left[\frac{\partial^k}{\partial y_{j_1},\ldots,\partial y_{j_n}}e^{-\frac{|y|^2}{2}}\right]f_i(y)\mathrm{d}y \times \int_{\{0<s_1,\ldots,s_n,s_{k+1}<t\}}(s_1\vee\cdots\vee s_{k+1})^{-\mathrm{kHK}}\mathrm{d}B^{j_1}_{s_1},\ldots,\mathrm{d}B^{j_n}_{s_k}\mathrm{d}B^{i}_{s_{k+1}}. \tag{84}$$

The theorem is proved. □

Theorem 4. *The stochastic process X is short-range dependent.*

Proof. Let

$$\rho_k = E\left[\sum_{i=1}^d\int_0^1\frac{B_s^i}{|B_s|}\mathrm{d}B_s^i\sum_{i=1}^d\int_k^{k+1}\frac{B_s^i}{|B_s|}\mathrm{d}B_s^i\right]. \tag{85}$$

For every $K\ge 1$, by the formula, we can decompose ρ_k as

$$\begin{aligned}\rho_k &= \sum_{i,j=1}^d\int_0^1\int_k^{k+1}E\left(\frac{B_s^iB_t^j}{|B_s||B_t|}\right)\phi(t,s)\mathrm{d}s\mathrm{d}t + \sum_{i,j=1}^d\int_0^1\int_k^{k+1}\int_0^t\int_0^B\phi(s,u)\phi(t,v)E\left(D_v^j\left(\frac{B_s^i}{|B_s|}\right)D_u^i\left(\frac{B_t^j}{|B_t|}\right)\right)\mathrm{d}u\mathrm{d}v\mathrm{d}s\mathrm{d}t\\ &\equiv \rho_{k,1}+\rho_{k,2}.\end{aligned} \tag{86}$$

For $\rho_{k,1}$, one can use the decomposition

$$B_t \overset{d}{=} \frac{\theta_H(s,t)}{\theta_H(s,s)}B_s + \beta_{s,t}\mathcal{N}, \tag{87}$$

where

$$\beta_{s,t}^2 = \frac{\rho_{s,t}^2}{s^{2\mathrm{HK}}}, \tag{88}$$

where $\mathcal{N}$ is independent of B_s and is denoted as ad-dimensional standard normal random variable. By Lemma 13 in [11],

$$\begin{aligned}E\left(\frac{\langle B_s,B_t\rangle}{|B_s||B_t|}\right) &= E\left(\frac{\langle B_s,\lambda_{s,t}B_s+\mathcal{N}\rangle}{|B_s||\lambda_{s,t}B_s+\mathcal{N}|}\right)\\ &= E\left(\frac{\langle B_1,s^{H,K}\lambda_{s,t}B_1+\mathcal{N}\rangle}{|B_s||s^{H,K}\lambda_{s,t}B_1+\mathcal{N}|}\right)\\ &= s^{H,K}\lambda_{s,t}E\left(\frac{|B_1|^2|\mathcal{N}|^2-\langle B_1,\mathcal{N}\rangle^2}{|B_s||\mathcal{N}|^3}\right)+O\left(t^{-\mathrm{HK}}\right).\end{aligned} \tag{89}$$

Thus,

$$E\left(\frac{\langle B_s, B_t\rangle}{|B_s\|B_t|}\right)\asymp s^{\mathrm{HK}}t^{-\mathrm{HK}}, \tag{90}$$

which implies that the term $\rho_{k,1}$ behaves as k^{H-3}.

For $\rho_{k,2}$, one has

$$\begin{aligned}
\rho_{k,2} &= (\mathrm{HK})^2\sum_{i,j=1}^{d}\int_0^1\int_k^{k+1}E\left(\left(\frac{\delta_{ij}}{|B_s|}-\frac{B_s^iB_s^j}{|B_s^{H,K}|^3}\right)\left(\frac{\delta_{ij}}{|B_t|}-\frac{B_t^iB_t^j}{|B_t|^3}\right)\right)\psi_1(s,t)\psi_2(s,t)\mathrm{d}s\mathrm{d}t\\
&= (\mathrm{HK})^2\int_0^1\int_k^{k+1}E\left(\frac{d}{|B_s\|B_t|}-\frac{|B_s|^2}{|B_s|^3|B_t|}-\frac{|B_t|^2}{|B_s\|B_t|^3}+\frac{\langle B_s,B_t\rangle^2}{|B_s|^3|B_t|^3}\right)\psi_1(s,t)\psi_2(s,t)\mathrm{d}s\mathrm{d}t\\
&= (\mathrm{HK})^2\int_0^1\int_n^{n+1}E\left(\frac{\langle B_s,B_t\rangle^2}{|B_s|^3|B_t|^3}+\frac{d-2}{|B_s\|B_t|}\right)\psi_1(s,t)\psi_2(s,t)\mathrm{d}s\mathrm{d}t.
\end{aligned} \tag{91}$$

Since

$$E\left(\frac{\langle B_s,B_t\rangle^2}{|B_s|^3|B_t|^3}+\frac{d-2}{|B_s\|B_t|}\right), \tag{92}$$

behaves as $Mt^{-\mathrm{HK}}$ as $t\longrightarrow\infty$, where

$$M=E\left(\frac{\langle B_1,\mathcal{N}\rangle^2}{|B_1|^3|\mathcal{N}|^3}+\frac{d-2}{|B_1\|\mathcal{N}|}\right)>0. \tag{93}$$

We see that the term $\rho_{k,2}$ also behaves as $k^{\mathrm{HK}-3}$, and the theorem follows. □

5. The Local Times of $\int_0^t \operatorname{sign}(B_s^{H,K})\mathrm{d}B_s^{H,K}$

Now, we consider the local times of the stochastic process $X=\{X_t,\quad t\geq 0\}$ defined by

$$X_t=\int_0^t \operatorname{sign}\left(B_s^{H,K}\right)\mathrm{d}B_s^{H,K}. \tag{94}$$

Lemma 2. *Let* $((1/2)<HK<1)$. *Then, for all* $t\geq 0$, *we have*

$$\operatorname{sign}\left(B_t^{H,K}\right)D_tX(t)\geq 0,\ \text{a.s.} \tag{95}$$

Proof. Using the Itô formula, one can obtain

$$\begin{aligned}
X(t)^2 &= 2\int_0^t X_s\operatorname{sign}\left(B_s^{H,K}\right)\mathrm{d}B_s^{H,K}+2\int_0^t\operatorname{sign}\left(B_s^{H,K}\right)D_sX_s\mathrm{d}s,\\
\sigma(t)\equiv E(X(t))^2 &= 2E\int_0^t\operatorname{sign}\left(B_s^{H,K}\right)D_sX_s\mathrm{d}s\\
&=\int_0^t\int_0^s E\left[\operatorname{sign}\left(B_s^{H,K}\right)\operatorname{sign}\left(B_s^{H,K}\right)\right]\phi(s,u)\mathrm{d}u\mathrm{d}s,
\end{aligned} \tag{96}$$

and note that the function $t\longrightarrow\sigma(t)$ is increasing since

$$E\left[\operatorname{sign}\left(B_s^{H,K}\right)\operatorname{sign}\left(B_u^{H,K}\right)\right]=\sum_{m=1}^{\infty}\frac{4(2m)!\left(\left(1/2^K\right)\left[\left(t^{2H}+s^{2H}\right)^K-|t-s|^{2\mathrm{HK}}\right]\right)^{2m+1}}{(2m+1)^2 2\pi\left(k!2^k\right)^2(\mathrm{su})^{2m+1}}. \tag{97}$$

So,

$$E\int_{t_0}^t\operatorname{sign}\left(B_s^{H,K}\right)D_sX_s\mathrm{d}s\geq 0 \tag{98}$$

for all $t\geq t_0\geq 0$. Now, let us prove $(\operatorname{sign}(B_t^{H,K})D_sX(t)\geq 0)$, a.s. We only need to show that

$$\int_{t_0}^t\operatorname{sign}\left(B_s^{H,K}\right)D_sX_s\mathrm{d}s,\quad 0\leq t\leq T \tag{99}$$

is nondecreasing. Let

$$\begin{aligned}
V_{t_0}(t) &= \int_{t_{t_0}}^t\operatorname{sign}\left(B_s^{H,K}\right)D_sX_s\mathrm{d}s,\quad 0\leq t_0\leq t,\\
\Phi(x) &= 1_{x<0},\\
\Phi_\varepsilon &\in C^2(R),\\
I &= \Phi\left(V_{t_0}(t)\right),\\
I_\varepsilon &= \Phi_\varepsilon\left(V_{t_0}(t)\right),
\end{aligned} \tag{100}$$

where $\Phi_\varepsilon(x)=0$ for $x>\varepsilon$ and $\Phi_\varepsilon(x)=1$ for $x<\varepsilon$. Thus, one can obtain

$$\begin{aligned} \mathrm{I}D_s I_\varepsilon &= 0, \\ I \cdot V_{t_0}(t) &\leq 0. \end{aligned} \tag{101}$$

So, for all $t \geq t_0 \geq 0$, one can obtain

$$\begin{aligned} E\left[\mathrm{IV}_{t_0}(t)\right] &= E\int_{t_0}^{t} I\mathrm{sign}\left(B_s^{H,K}\right)D_s X_s \mathrm{d}s \\ &= \lim_{\varepsilon\longrightarrow 0} E\int_{t_0}^{t} II_\varepsilon \mathrm{sign}\left(B_s^{H,K}\right)D_s X_s \mathrm{d}s \\ &\geq E\int_{t_0}^{t} I\mathrm{sign}\left(B_s^{H,K}\right)D_s X_s \mathrm{d}s \geq 0, \end{aligned} \tag{102}$$

which implies that $I = 0$ and $V_{t_0}(t) \geq 0$. Therefore,

$$\int_{t_0}^{t} \mathrm{sign}\left(B_s^{H,K}\right)D_s X_s \mathrm{d}s, \quad 0 \leq t \leq T \tag{103}$$

is nondecreasing. This completes the proof. □

Theorem 5. *Let the stochastic process $X = \{X_t, t \geq 0\}$ be defined by*

$$X_t = \int_0^t \mathrm{sign}\left(B_s^{H,K}\right)\mathrm{d}B_s^{H,K}, \tag{104}$$

and let Φ: $R^+ \longrightarrow R$ be a convex function with polynomial growth. Then, there is a continuous increasing process A^Φ which satisfies

$$\Phi(X_t) = \Phi(0) + \int_0^t D^-(X_s)\mathrm{sign}\left(B_s^{H,K}\right)\mathrm{d}B_s^{H,K} + \frac{1}{2}A_t^\Phi, \tag{105}$$

where $D^-\Phi$ denotes the left-hand derivative of Φ.

Proof. If $\Phi \in C^2$, then this is the Itô formula, and

$$A_t^\Phi = \int_0^t \Phi''(X_s)\mathrm{sign}\left(B_s^{H,K}\right)D_s X_s \mathrm{d}s, \tag{106}$$

together with Lemma 2, implies that the stochastic process A^Φ is increasing.

Now, let $\Phi \notin C^2$. For $x \in R$ and $\varepsilon > 0$, one sets

$$\begin{aligned} p_\varepsilon(x) &= \frac{1}{\sqrt{2\pi\varepsilon}}e^{-(1/2\varepsilon)x^2}, \\ \Phi_\varepsilon(x) &= \int_R p_\varepsilon(x-y)\Phi(y)\mathrm{d}y. \end{aligned} \tag{107}$$

It is easy to see that $\Phi_\varepsilon \in C^2$ and has polynomial growth. So, for all $\varepsilon > 0$, there exists a continuous increasing process A^{Φ_ε} such that

$$\begin{aligned} \Phi_\varepsilon(X_t) &= \Phi_\varepsilon(0) + \int_0^t \Phi_\varepsilon'(X_s)\mathrm{sign}\left(B_s^{H,K}\right)\mathrm{d}B_s^{H,K} + \frac{1}{2}A_t^{\Phi_\varepsilon}, \\ A_t^{\Phi_\varepsilon} &= \int_0^t \Phi_\varepsilon''(X_s)\mathrm{sign}\left(B_s^{H,K}\right)D_s X_s \mathrm{d}s \\ &= \int_R \Phi_\varepsilon''(x)\left(\int_0^t \delta(X_s - x)\right)\left(\mathrm{sign}\left(B_s^{H,K}\right)\right)D_s X_s \mathrm{d}s\mathrm{d}x. \end{aligned} \tag{108}$$

Note that

$$\lim_{\varepsilon\downarrow 0}\Phi_\varepsilon(x) = \Phi(x), \lim_{\varepsilon\downarrow 0}\Phi_\varepsilon'(x) = D^-\Phi(x), \tag{109}$$

and one can obtain as $\varepsilon \longrightarrow 0$

$$\int_0^t \Phi_\varepsilon'(X_s)\mathrm{sign}\left(B_s^{H,K}\right)\mathrm{d}B_s^{H,K} \longrightarrow \int_0^t D^-(X_s)\mathrm{sign}\left(B_s^{H,K}\right)\mathrm{d}B_s^{H,K}, \tag{110}$$

in probability. So, A^{Φ_ε} converges to a stochastic process A^Φ which, as a limit of increasing stochastic processes, is itself an increasing stochastic process and

$$\Phi(X_t) = \Phi(0) + \int_0^t D^-(X_s)\mathrm{sign}\left(B_s^{H,K}\right)\mathrm{d}B_s^{H,K} + \frac{1}{2}A_t^\Phi, \tag{111}$$

where A^Φ can be chosen to be a.s. continuous. The proof is completed. □

Corollary 1. *For the process $X_t = \int_0^t \mathrm{sign}(B_s^{H,K})dB_s^{H,K}$ and all $x \in R$, there exists a local time $\mathscr{L}^x(X)$ such that*

$$\left|X_t - x\right| = |x| + \int_0^t \mathrm{sign}(X_s - x)\mathrm{d}X_s + \mathscr{L}_t^x(X). \tag{112}$$

Proof. Note that the left derivative of the function $\Phi(y) = (y-x)^+$ is equal to $1_{x,\infty}(y)$. By Theorem 5, one can obtain

$$(X_t - x)^+ = (-x)\vee 0 + \int_0^t 1_{X_s > x}\mathrm{sign}\left(B_s^{H,K}\right)\mathrm{d}B_s^{H,K} + \frac{1}{2}A^+, \tag{113}$$

where A^+ is a continuous increasing stochastic process. Similarly, there exists a continuous increasing stochastic process A^- which satisfies

$$(X_t - x)^- = (x)\vee 0 + \int_0^t 1_{X_s > x}\mathrm{sign}\left(B_s^{H,K}\right)\mathrm{d}B_s^{H,K} + \frac{1}{2}A^-. \tag{114}$$

Therefore, one can obtain

$$X_t = \int_0^t \mathrm{sign}\left(B_s^{H,K}\right)\mathrm{d}B_s^{H,K} + \frac{1}{2}\left(A^+ + A^-\right), \tag{115}$$

which implies that $A^+ = A^-$ a.s. and we set $\mathscr{L}_x^x(X) = A_t^+$. This completes the proof.

Combining this corollary with Es-Sebaiy and Tudor [3], we can obtain the following results. □

Corollary 2. *Suppose that $\mathscr{L}^x(X)$ is the local time of the process X and $\mathscr{L}^x(B^{H,K})$ is the weighted local time of the bifractional Brownian motion $B^{H,K}$ defined by*

$$\mathscr{L}_t^x\left(B^{H,K}\right) = 2\mathrm{HK}\int_0^t \delta\left(B^{H,K} - x\right)s^{2\mathrm{HK}-1}\mathrm{d}s. \tag{116}$$

Then, we have

$$\mathscr{L}_t^x(X) - \mathscr{L}_t^x\left(B^{H,K}\right) = \left|X_t - x\right| - \left|B^{H,K} - x\right| + 2\int_0^t 1_{\{X_s \le x\}}\mathrm{sign}\left(B_s^{H,K} - x\right)\mathrm{d}B_s^{H,K}. \tag{117}$$

Proof. By the Tanaka formula, one can obtain

$$\begin{aligned}\left|X_t - x\right| - \left|B^{H,K} - x\right| &= \mathscr{L}_t^x(X) - \mathscr{L}_t^x\left(B^{H,K}\right)\\ &\quad + \int_0^t \mathrm{sign}\left(X_s - x\right)\mathrm{sign}\left(B_s^{H,K} - x\right)\mathrm{d}B_s^{H,K} - \int_0^t \mathrm{sign}\left(B_s^{H,K} - x\right)\mathrm{d}B_s^{H,K}\\ &= \mathscr{L}_t^x(X) - \mathscr{L}_t^x\left(B^{H,K}\right) + \int_0^t \left[\mathrm{sign}\left(X_s - x\right) - 1\right]\mathrm{sign}\left(B_s^{H,K} - x\right)\mathrm{d}B_s^{H,K}\\ &= \mathscr{L}_t^x(X) - \mathscr{L}_t^x\left(B^{H,K}\right) - 2\int_0^t 1_{\{X_s \le x\}}\mathrm{sign}\left(B_s^{H,K} - x\right)\mathrm{d}B_s^{H,K},\end{aligned} \tag{118}$$

which implies that (117) holds. □

Corollary 3. *For any $t \ge 0$ and $x \in R$, we have*

$$\mathscr{L}_t^x(X) = \int_0^t \delta(X(s) - x)\mathrm{sign}\left(B_s^{H,K}\right)D_s X_s \mathrm{d}s. \tag{119}$$

Moreover, let Φ: $R^+ \longrightarrow R$ be a convex function with polynomial growth; one can obtain the following Itô–Tanaka formula:

$$\Phi(X(t)) = \Phi(0) + \int_0^t D^- \Phi\left(X_s\right)\mathrm{sign}\left(B_s^{H,K}\right)\mathrm{d}B_s^{H,K} + \frac{1}{2}\int_R \mathscr{L}_t^x(X)\mu_\Phi \mathrm{d}x, \tag{120}$$

where $D^-\Phi$ denotes the left derivative of Φ and signed measure μ_Φ which is defined by

$$\mu_\Phi([a,b]) = D^-\Phi(b) - D^-\Phi(a), \quad a < b,\ a, b \in R. \tag{121}$$

Finally, one can prove that the local time of the process

$$\sum_{i=1}^d \int_0^t \frac{B_s^i}{R_s}\mathrm{d}B_s^i, \quad d \ge 2 \tag{122}$$

exists by the same method and can obtain the similar results.

6. Conclusions

This paper presents theorems and propositions associated with respect to the stochastic process $R_t = \sqrt{(B_t^1)^2 + \cdots + (B_t^d)^2}$, where $B = \{(B_t^1, \ldots, B_t^d)\}_{t\ge 0}$ is a d-dimensional bifractional Brownian motion and $(2\mathrm{HK} \ge 1)$. Since there is no Lévy's characterization theorem for a general bifractional Brownian motion, to prove whether a stochastic process

$$X_t := \sum_{i=1}^a \int_0^t \frac{B_s^i}{R_s}\mathrm{d}B_s^i, \quad d \ge 1 \tag{123}$$

is a bifractional Brownian motion or not is difficult. Theorems 1 and 4 prove X_t is short-range dependent in one-dimensional case and multidimensional case, respectively. Theorem 5 considers the local times of the stochastic process of X_t in one-dimensional case. Theorem 2 gives the the following chaos expansion of the stochastic process $Z_t = \sum_{i=1}^d \int_0^t f_i(B_s)\mathrm{d}B_s^i$. Moreover, significance results associated with the above theorem are given.

Data Availability

All the data generated during this study are included within this article.

Conflicts of Interest

The authors declare that they have no conflicts of interest.

Authors' Contributions

All the authors contributed equally and significantly in writing this paper. All the authors read and approved the final manuscript.

Acknowledgments

Xichao Sun acknowledges the National Natural Science Foundation of China (11971101 and 11426036), Natural Science Foundation of Anhui Province (1808085MA02), and Quality Engineering of Anhui Education (2018jyxm0497 and 2020zdxsjg214). Ming Li acknowledges the National Natural Science Foundation of China under grant nos. 61672238, 61272402, and 61070214.

References

[1] C. Houdré and J. Villa, "An example of infinite dimensional quasi-helix," in *Stochastic Models (Mexico City, 2002)*, pp. 195–201, American Mathematical Society, 2003American Mathematical Society, Providence, RI, USA, Contemporary Mathematics, 336.

[2] S. Aazizi and K. Es-Sebaiy, "Berry-Ess'een bounds and almost sure CLT for the quadratic variation of the bifractional Brownian motion," *Random Operators and Stochastic Equations*, vol. 24, pp. 1–13, 2012.

[3] K. Es-Sebaiy and C. A. Tudor, "Multidimensional bifractional Brownian motion: itô and Tanaka formulas," *Stochastics and Dynamics*, vol. 7, no. 3, pp. 366–388, 2007.

[4] J. Guo, "Stochastic current of bifractional brownian motion," *Journal of Applied Mathematics*, vol. 2014, Article ID 762484, 10 pages, 2014.

[5] Y. Jiang and Y. Wang, "Self-intersection local times and collision local times of bifractional Brownian motions," *Science in China Series A: Mathematics*, vol. 52, no. 9, pp. 1905–1919, 2009.

[6] I. Kruk, F. Russo, and C. A. Tudor, "Wiener integrals, Malliavin calculus and covariance measure structure," *Journal of Functional Analysis*, vol. 249, no. 1, pp. 92–142, 2007.

[7] F. Russo and C. A. Tudor, "On bifractional Brownian motion," *Stochastic Processes and Their Applications*, vol. 116, no. 5, pp. 830–856, 2006.

[8] C. A. Tudor and Y. Xiao, "Sample path properties of bifractional Brownian motion," *Bernoulli*, vol. 13, no. 4, pp. 1023–1052, 2007.

[9] L. Yan, B. Gao, and J. Liu, "The Bouleau-Yor identity for a bifractional Brownian motion," *Stochastics*, vol. 86, no. 3, pp. 382–414, 2014.

[10] X. Yu, X. Sun, and L. Yan, "Solving a stochastic heat equation driven by a bi-fractional noise," *Boundary Value Problems*, vol. 2016, no. 1, 2016.

[11] Y. Hu and D. Nualart, "Some processes associated with fractional Bessel processes," *Journal of Theoretical Probability*, vol. 18, no. 2, pp. 377–397, 2005.

[12] X. Peng, W. Su, W. Su, and Z. Zhang, "On a perturbed compound Poisson risk model under a periodic threshold-type dividend strategy," *Journal of Industrial & Management Optimization*, vol. 16, no. 4, pp. 1967–1986, 2020.

[13] J. Pitman and M. Yor, "Bessel processes and infinitely divisible laws," in *Lecture Notes in Mathematics*Springer, Berlin, Germany, 1981.

[14] D. Revuz and M. Yor, *Continuous Martingales and Brownian Motion*, Springer, Berlin, Germany, 3rd edition, 1999.

[15] M. Yor, *Some Aspects of Brownian Motion. Part II: Some Recent Martingale Problems*, Birkhäuser, Basel, Switzerland, 1997.

[16] E. Alòs, O. Mazet, and D. Nualart, "Stochastic calculus with respect to Gaussian processes," *The Annals of Probability*, vol. 29, no. 2, pp. 766–801, 2001.

[17] G. Shen, C. Chen, and L. Yan, "Remarks on sub-fractional bessel processes," *Acta Mathematica Scientia*, vol. 31, no. 5, pp. 1860–1876, 2011.

[18] D. Nualart, *Malliavin Calculus and Related Topics*, Springer, New York, NY, USA, 2nd edition, 2006.

[19] J. M. E. Guerra and D. Nualart, "The $(1/H)$ variation of the divergence integral with respect to the fractional Brownian motion for $H > (1/2)$ and fractional Bessel processes," *Stochastic Processes and Their Applications*, vol. 115, pp. 91–115, 2005.

Hindawi
Mathematical Problems in Engineering
Volume 2020, Article ID 5369879, 17 pages
https://doi.org/10.1155/2020/5369879

Research Article

Basket Credit Derivative Pricing in a Markov Chain Model with Interacting Intensities

Kangquan Zhi,[1] **Jie Guo**,[2] **and Xiaosong Qian**[3]

[1]*Center for Financial Engineering, Soochow University, Suzhou 215006, China*
[2]*School of Mathematics and Physics, Suzhou University of Science and Technology, Suzhou 215009, China*
[3]*School of Mathematical Sciences and Center for Financial Engineering, Soochow University, Suzhou 215006, China*

Correspondence should be addressed to Kangquan Zhi; zhikangquan96@163.com

Received 18 June 2020; Accepted 20 September 2020; Published 17 October 2020

Academic Editor: Wenguang Yu

In this paper, we propose a Markov chain model to price basket credit default swap (BCDS) and basket credit-linked note (BCLN) with counterparty and contagion risks. Suppose that the default intensity processes of reference entities and the counterparty are driven by a common external shock as well as defaults of other names in the contracts. The stochastic intensity of the external shock is a Cox process with jumps. We derive recursive formulas for the joint distribution of default times and obtain closed-form premium rates for BCDS and BCLN. Numerical experiments are performed to show how the correlated default risks may affect the premium rates.

1. Introduction

The market for credit derivatives has experienced rapid development during the past decades until the international financial crisis in 2008, which was mainly due to the underestimation of the correlated default risk. Since then, more and more research studies focus on the basket credit derivative pricing. Basket credit default swap (BCDS) and basket credit-linked notes (BCLNs) are two popular multiname credit derivatives, which can reduce the adverse impact of reference assets' defaults on financial institutions. A BCDS is designed to transfer the credit exposure of fixed income products between two parties with N reference entities. The issuer of the contract is the protection seller, and the investor is the protection buyer. A BCDS will have a premium rate and maturity date, and the maturity depends on the performance of reference entities and the counterparty. A BCLN is a note paying an enhanced coupon to investors for bearing the credit risk of N reference entities. The issuer of the note is the protection buyer, and the investor is the protection seller. A BCLN will have a coupon rate, maturity date, and par value just like a standard bond. However, the maturity depends on the performance of the reference entities and the counterparty.

The reduced-form models are widely used to price credit derivatives. In a reduced-form model, there are mainly three approaches to model the default correlation: copula, conditional independence, and contagion. In the copula approach, the joint distribution of the default times is constructed by combining marginal distributions of the individual by a copula function, see Li [1], Schőnbucher and Schubert [2], Brigo and Capponi [3], and Jean-David [4]. The conditional independence approach assumes that the default intensities are conditionally independent under the given filtration, see Wang and Garleanu [5], Giesecke [6], and Liang et al. [7]. In the contagion approach, the default intensity of one entity is affected not only by systematic factors but also by the default of other entities in the contract, see Jarrow and Yu [8], Zheng and Jiang [9], and Dong and Wang [10].

In this paper, we focus on the pricing of basket credit derivatives (BCDS and BCLN). In the existing literature, different approaches in pricing BCDS and BCLN have been developed. Hull and White [11] developed two fast procedures for valuing kth-to-default swaps. Walker [12] studied counterparty risk in BCDS valuation by using a four-state Markov process that includes contagion effects. Yu [13] gave the Monte Carlo method for pricing basket CDS. Frey and Backhaus [14] considered reduced-form models for portfolio credit risk with interacting default intensities. Zheng and Jiang [9] proposed a factor contagion model for the basket CDS pricing. Wu [15] explored a reasonable coupon rate for basket credit-linked notes (BCLN) with the issuer default risk. Herbertsson et al. [16] valued kth-to-default swap spreads in a tractable shot noise model. Wang et al. [17] proposed a model for pricing a basket CDS with the negative correlation between prepayment and default under the bottom-up framework. Li and Li [18] used a type of dynamic copula method to characterize the dependence structure between financial assets and price basket default swaps. Esfahanipour and Jahanbin [19] proposed a heuristic algorithm for pricing of basket default swaps. Dong et al. [20] studied the kth-to-default basket swap under a correlated regime-switching hazard process model. Guo et al. [21] employed an intensity-based credit risk model with regime switching to consider the valuation of basket CDS in a homogeneous portfolio. The previous work did not combine internal contagion and external shock, which is a Cox process. In addition, they seldom obtained the closed-form solutions. In this paper, we propose a model that combines internal contagion and random external shock. Our model is not only applicable to BCDS pricing but also to BCLN. Furthermore, we derive the closed-form solution which is not easy for the complex structure of the default as the numerical analysis can be done very smoothly.

Leung and Kwok [22] presented a Markov chain model to price single-name CDS; the default intensities of the reference entity and counterparty were affected by an external shock. Inspired by Leung and Kwok [22], we present a more general model to study basket credit derivatives with interacting default intensities, which are driven by an external shock as well as defaults of other names in the contracts. We get recursive formulas for the unconditional distribution of default times through ingenious construction of the infinitesimal generator matrix and obtain closed-form premium rates for basket credit default swap and basket credit-linked notes.

The paper is organized as follows. In Section 2, we give the construction of interacting default intensities and derive the joint distribution of default times by solving a system of ordinary differential equations. In Section 3, we calculate the premium rates of kth-to-default CDS and kth-to-default CLN with the counterparty risk. Numerical results are presented to show how the correlated default risks affect the premium rates in Section 4. At last, we conclude the paper.

2. Markov Chain Model with Interacting Intensities

In this section, we construct a reduced-form model with stochastic default intensities by a Markov chain. Consider a complete filtered probability space $(\Omega, \mathcal{G}, \{\mathcal{G}_t\}_{0\le t\le T}, P)$, where P is a martingale measure and $\{\mathcal{G}_t\}_{t\ge 0}$ is filtration satisfying the usual conditions. Our model includes a basket credit derivative and an external shock. The basket credit derivative includes N reference entities, a counterparty, and an investor. Let R_i represent the ith reference entity with default time τ_{R_i} for $i \in I = \{1, 2, \dots, N\}$, C be the counterparty with default time τ_C, S be the external shock with arrival time τ_S, and $\mathcal{L} = \{R_1, R_2, \dots, R_N, C, S\}$ be the set which contains all of the names in the model. Assume that τ_S is independent of τ_C and τ_{R_i} $(i \in I)$. The default process of our model is given by

$$\mathbf{H}_t = \left(H_t^{R_1}, H_t^{R_2}, \dots, H_t^{R_N}, H_t^C, H_t^S \right), \tag{1}$$

where

$$\begin{cases} H_t^{R_i} = \mathbf{1}_{\left\{\tau_{R_i} \le t\right\}}, & i \in I, \\ H_t^C = \mathbf{1}_{\{\tau_C \le t\}}, \\ H_t^S = \mathbf{1}_{\{\tau_S \le t\}}, \end{cases} \tag{2}$$

and $\mathbf{1}_{\{\tau \le t\}}$ is the indicator function. $\mathbf{H}_t$ is a finite-state Markov chain with state space $O = \{0, 1\}^{N+2}$.

The macroeconomic variables are described by a stochastic process $\Psi = (\Psi_t)_{0\le t\le T}$. An investor can get the historical information of the macroeconomic variables and the default status of all names in our model at time t. The filtration $(\mathcal{G}_t)_{t\ge 0}$ is given by

$$\mathcal{G}_t = \mathcal{F}_t^{\Psi} \vee \mathcal{H}_t^{R_1} \vee \mathcal{H}_t^{R_2} \vee \cdots \vee \mathcal{H}_t^{R_N} \vee \mathcal{H}_t^{C} \vee \mathcal{H}_t^{S}, \tag{3}$$

where

$$\begin{cases} \mathcal{F}_t^{\Psi} = \sigma\left(\Psi_s \colon 0 \le s \le t\right), \\ \mathcal{H}_t^{C} = \sigma\left(H_s^C \colon 0 \le s \le t\right), \\ \mathcal{H}_t^{S} = \sigma\left(H_s^S \colon 0 \le s \le t\right), \\ \mathcal{H}_t^{R_i} = \sigma\left(H_s^{R_i} \colon 0 \le s \le t\right), & i \in I, \end{cases} \tag{4}$$

and G_t is the σ-field generated by $\mathcal{F}_t^{\Psi} \cup \mathcal{H}_t^{R_1} \cup \mathcal{H}_t^{R_2} \cup \cdots \cup \mathcal{H}_t^{R_N} \cup \mathcal{H}_t^{C} \cup \mathcal{H}_t^{S}$. The martingale default intensities of the reference entities and counterparty are, respectively, defined by $\lambda^{R_i}(\Psi_t, \mathbf{H}_t)$ $(i \in I)$ and $\lambda^C(\Psi_t, \mathbf{H}_t)$, which satisfy the property that

$$\begin{cases} H_t^C - \displaystyle\int_0^{t\wedge\tau_C} \lambda^C(\Psi_s, \mathbf{H}_s) \mathrm{d}s, \\ H_t^{R_i} - \displaystyle\int_0^{t\wedge\tau_{R_i}} \lambda^{R_i}(\Psi_s, \mathbf{H}_s) \mathrm{d}s, & i \in I, \end{cases} \tag{5}$$

are $\{\mathcal{G}_t\}$-martingales.

The arrival of the external shock is modeled by a Cox process with stochastic intensity λ_t^S. Before the shock S happens, the default intensities of $\lambda_t^{R_i}$ $(i \in I)$ and λ_t^C are, respectively, assumed to be $a_t^{R_i}$ and a_t^C, where $a_t^{R_i}$ and a_t^C are some deterministic functions of t. When the shock S happens, $\lambda_t^{R_i}$ and λ_t^C jump to $\alpha_{R_i}^S a_t^{R_i}$ and $\alpha_C^S a_t^C$, respectively, where nonnegative constants $\alpha_{R_i}^S$ and α_C^S denote the effects from the external shock to reference entities and the counterparty. Depending on whether $\alpha_{R_i}^S$ and α_C^S are greater than 1 or not, the densities λ^{R_i} and λ^C can jump upward or downward. Besides, two kinds of contagion risks are considered in our model. One is the contagion effects between reference entities, and the other one is the contagion effects from reference entities to the counterparty. If reference entity i defaults, the default intensities of other reference entities and the counterparty jump to $\alpha_{R_j}^{R_i} a_t^{R_j}$ $(j \neq i)$ and $\alpha_C^{R_i} a_t^C$, respectively, where $\alpha_{R_j}^{R_i}$ and $\alpha_C^{R_i}$ are nonnegative constants. We do not consider the contagion effects from the counterparty to reference entities because the credit derivative would be terminated if the counterparty defaulted first. In summary, the default intensities of reference entities and the counterparty can be expressed as follows:

$$\begin{aligned}
\lambda_t^{R_i} &= a_t^{R_i}\left[\left(\alpha_{R_i}^S - 1\right) I_{\tau_S \le t} + 1\right] \prod_{j \in I \setminus \{i\}} \left[\left(\alpha_{R_i}^{R_j} - 1\right) I_{\tau_{R_j} \le t} + 1\right], \\
&\qquad \alpha_{R_i}^S, \alpha_{R_i}^{R_j} \ge 0, i,\ j \in I \text{ and } i \neq j, \\
\lambda_t^C &= a_t^C\left[\left(\alpha_C^S - 1\right) I_{\tau_S \le t} + 1\right] \prod_{i \in I} \left[\left(\alpha_C^{R_i} - 1\right) I_{\tau_{R_i} \le t} + 1\right], \\
&\qquad \alpha_C^S, \alpha_C^{R_i} \ge 0, i \in I.
\end{aligned} \tag{6}$$

We assume that the simultaneous defaults or shock cannot happen in the model for the sake of simplicity. In this paper, we consider basket credit derivatives with N reference entities, and the state space O of $\mathbf{H}_t$ is 2^{N+2} dimensions. Let $\psi^S = (\lambda_t^S)_{t \in [0,T]}$, and conditional on the given state ψ^S, the infinitesimal generator matrix of $\mathbf{H}_t$ is $\Lambda_{[\psi^S]}(t) \triangleq (\Lambda_{\mathrm{H} \times \mathrm{H}'}(t) \mid \psi^S)_{2^{N+2} \times 2^{N+2}}$, where $\mathrm{H}, \mathrm{H}' = (H^{R_1}, \ldots, H^{R_N}, H^C, H^S) \in O$represent the states of the Markov chain $\mathbf{H}_t$. The conditional transition probability matrix $P(0, t \mid \psi^S) \triangleq (P_{\mathrm{H} \times \mathrm{H}'}(0, t \mid \psi^S))_{2^{N+2} \times 2^{N+2}}$ is governed by the following forward Kolmogorov equation:

$$\frac{\mathrm{d} P\left(0, t \mid \psi^S\right)}{\mathrm{d} t} = P\left(0, t \mid \psi^S\right) \Lambda_{[\psi^S]}(t), \quad t \ge 0, \tag{7}$$

with $P(0, 0 \mid \psi^S) = E$, and E is the unit matrix. Because the default states and the shock are absorbing states for the Markov chain $\mathbf{H}_t$, the matrix $\Lambda_{[\psi^S]}(t)$ is upper triangular, and the conditional transition probabilities $P(0, t \mid \psi^S)$ can be solved successively in a sequential manner.

To describe the generator matrix $\Lambda_{[\psi^S]}(t) = (\Lambda_{\mathrm{H} \times \mathrm{H}'}(t) \mid \psi^S)_{2^{N+2} \times 2^{N+2}}$, we introduce some auxiliary notations as follows:

(i) H^{R_M} represents the state that only reference entities in set $M \subset I$ defaulted. Here, $\mathrm{H}^{R_M} = (H^{R_1}, \ldots, H^{R_N}, H^C, H^S) = (\overset{N}{\frown 0, \ldots, 1}, \ldots, 0, 0, 0)$, where $H^{R_i} =_n 1$ for all $i \in M$. Especially, $\mathrm{H}^{R_\phi} = (\frown 0, \ldots, 0, 0, 0)$ represents the state that no reference entity defaults.

(ii) H^C represents the state that only the counterparty defaulted.
Here, $\mathrm{H}^C = (H^{R_1}, \ldots, H^{R_N}, H^C, H^S) = (\overset{N}{\frown 0, \ldots}, 0, 1, 0)$.

(iii) H^S represents the state that only the external shock arrived.
Here, $\mathrm{H}^S = (H^{R_1}, \ldots, H^{R_N}, H^C, H^S) = (\overset{N}{\frown 0, \ldots}, 0, 0, 1)$.

(iv) $\mathrm{H}^{R_M \cup C}$ represents the state that reference entities in set $M \subset I$ and the counterparty C defaulted.
Here, $\mathrm{H}^{R_M \cup C} = (H^{R_1}, \ldots, H^{R_N}, H^C, H^S) = (\overset{N}{\frown 0, \ldots, 1}, \ldots, 0, 1, 0)$, where $H^{R_i} = 1$ for all $i \in M$.

(v) $\mathrm{H}^{R_M \cup S}$ represents the state that reference entities in set $M \subset I$ defaulted, and the external shock S happened.
Here, $\mathrm{H}^{R_M \cup S} = (H^{R_1}, \ldots, H^{R_N}, H^C, H^S) = (\overset{N}{\frown 0, \ldots, 1}, \ldots, 0, 0, 1)$, where $H^{R_i} = 1$ for all $i \in M$.

(vi) $\mathrm{H}^{R_M \cup C \cup S}$ represents the state that reference entities in set $M \subset I$ and the counterparty C both defaulted, and the external shock S happened.
Here, $\mathrm{H}^{R_M \cup C \cup S} = (H^{R_1}, \ldots, H^{R_N}, H^C, H^S) = (\overset{N}{\frown 0, \ldots, 1}, \ldots, 0, 1, 1)$, where $H^{R_i} = 1$ for all $i \in M$.

(vii) $\Lambda_{\mathrm{H}}(t) \triangleq \Lambda_{\mathrm{H} \times \mathrm{H}}(t)$ for $\mathrm{H} \in O$ are elements on the diagonal of the matrix $\Lambda_{[\psi^S]}(t)$, which represent the intensities that the Markov chain $\mathbf{H}_t$ remains at states H.

(viii) $P_{\mathrm{H}}(0, t \mid \psi^S) \triangleq P_{\mathrm{H}^{R_\phi} \times \mathrm{H}}(0, t \mid \psi^S)$ represents the conditional probability that Markov chain $\mathbf{H}_t$ transfers from the initial state H^{R_ϕ} to state H during $[0, t]$. It is the first line of the conditional transition probability matrix $P(0, t \mid \psi^S)$ and can be used to present the joint distributions of default times during $[0, t]$.

Firstly, we calculate the conditional transition probabilities that none of the reference entities defaults during $[0, t]$. The corresponding states of $\mathbf{H}_t$ are H^{R_ϕ} and H^S. The corresponding elements in the infinitesimal generator matrix $\Lambda_{[\psi^S]}(t)$ are as follows:

$$\begin{array}{c}
\\ \mathrm{H}^{R_\phi} \\ \vdots \\ \mathrm{H}^S \\ \vdots
\end{array}
\begin{array}{c}
\begin{array}{cccccccccc}
\mathrm{H}^{R_\phi} & \mathrm{H}^{R_{\{1\}}} & \cdots & \mathrm{H}^{R_{\{N\}}} & \mathrm{H}^C & \mathrm{H}^S & \cdots & \mathrm{H}^{R_{\{i\}} \cup S} & \cdots & \mathrm{H}^{C \cup S} \cdots
\end{array} \\
\begin{pmatrix}
\Lambda_{\mathrm{H}^{R_\phi}} & a_t^{R_1} & \cdots & a_t^{R_N} & a_t^C & \lambda_t^S & \cdots & 0 & \cdots & 0 & \cdots \\
\vdots & \vdots & \vdots & \vdots & \vdots & \vdots & \vdots & \vdots & \vdots & \vdots & \vdots \\
0 & 0 & \cdots & 0 & 0 & \Lambda_{\mathrm{H}^S} & \cdots & \alpha_{R_i}^S a_t^{R_i} & \cdots & \alpha_C^S a_t^C & \cdots \\
\vdots & \vdots & \vdots & \vdots & \vdots & \vdots & \vdots & \vdots & \vdots & \vdots & \vdots
\end{pmatrix}
\end{array}. \tag{8}$$

In the $\mathrm{H}^{R_\varnothing}$-row of the generator matrix $\Lambda_{[\psi^S]}(t)$, the positive elements represent the transition intensities from state $\mathrm{H}^{R_\varnothing}$ to other states by one jump. Because the cases of simultaneous defaults or shock are not examined here, the possible positive elements in this row are $a_t^{R_i}\ (i \in I)$, a_t^C, or λ_t^S. Noting that the elements on the diagonal of the generator matrix $\Lambda_{[\psi^S]}(t)$ are the sum of all other elements in the row multiplied with -1, we can get the first element $\Lambda_{\mathrm{H}^{R_\phi}}$ of the $\mathrm{H}^{R_\varnothing}$-row as follows:

$$\Lambda_{\mathrm{H}^{R_\phi}}(t) = -\left[\sum_{i\in I} a_t^{R_i} + a_t^C + \lambda_t^S\right]. \tag{9}$$

Because the generator matrix $\Lambda_{[\psi^S]}(t)$ is upper diagonal, $\Lambda_{\mathrm{H}^{R_\phi}}(t)$ is the only nonzero element in the H^{R_ϕ}-column.

In the H^S-row of the generator matrix $\Lambda_{[\psi^S]}(t)$, the positive elements represent the transition intensities from state H^S to other states by one jump. By (6), the positive elements in the H^S-row are $\alpha^S_{R_i} a_t^{R_i}\ (i \in I)$ and $\alpha^S_C a_t^C$. Summing these positive elements and multiplying the sum with -1, we get the diagonal element in this row as follows:

$$\Lambda_{\mathrm{H}^S}(t) = -\left[\sum_{i\in I} \alpha^S_{R_i} a_t^{R_i} + \alpha^S_C a_t^C\right]. \tag{10}$$

In the H^S-column of the generator matrix $\Lambda_{[\psi^S]}(t)$, the positive elements represent the transition intensities from other states to state H^S by one jump. The only possible state which can jump to H^S is H^{R_ϕ}. So, the nonzero elements in the H^S-column are λ_t^S and $\Lambda_{\mathrm{H}^S}(t)$.

By forward Kolmogorov equation (7), we have

$$\begin{cases} \dfrac{\mathrm{d}P_{\mathrm{H}^{R_\phi}}\left(0,t \mid \psi^S\right)}{\mathrm{d}t} = P_{\mathrm{H}^{R_\phi}}\left(0,t \mid \psi^S\right)\Lambda_{\mathrm{H}^{R_\phi}}(t), \\[2ex] \dfrac{\mathrm{d}P_{\mathrm{H}^S}\left(0,t \mid \psi^S\right)}{\mathrm{d}t} = P_{\mathrm{H}^{R_\phi}}\left(0,t \mid \psi^S\right)\lambda_t^S + P_{\mathrm{H}^S}\left(0,t \mid \psi^S\right)\Lambda_{\mathrm{H}^S}(t). \end{cases} \tag{11}$$

It is easy to obtain the solutions of the above equations as follows:

$$\begin{cases} P_{\mathrm{H}^{R_\phi}}\left(0,t \mid \psi^S\right) = e^{\int_0^t \Lambda_{\mathrm{H}^{R_\phi}}(u)\mathrm{d}u}, \\ P_{\mathrm{H}^S}\left(0,t \mid \psi^S\right) = e^{\int_0^t \Lambda_{\mathrm{H}^S}(u)\mathrm{d}u} \displaystyle\int_0^t \lambda_u^S e^{-\int_0^u \Lambda_{\mathrm{H}^S}(r)\mathrm{d}r} P_{\mathrm{H}^{R_\phi}}\left(0,u \mid \psi^S\right)\mathrm{d}u. \end{cases} \tag{12}$$

Secondly, we calculate the conditional transition probabilities that only one reference entity defaults during $[0,t]$. The corresponding states of $\mathbf{H}_t$ are $\mathrm{H}^{R_{\{i\}}}$ and $\mathrm{H}^{R_{\{i\}}\cup S}$ for $i \in I$. The corresponding elements in the infinitesimal generator matrix $\Lambda_{[\psi^S]}(t)$ are as follows:

$$\begin{array}{c} \\ \mathrm{H}^{R_\phi} \\ \vdots \\ \mathrm{H}^S \\ \vdots \\ \mathrm{H}^{R_{\{i\}}} \\ \vdots \\ \mathrm{H}^{R_{\{i\}}\cup S} \\ \vdots \end{array} \begin{array}{c} \begin{array}{ccccccccccccc} \cdots & \mathrm{H}^{R_{\{i\}}} & \cdots & \mathrm{H}^{R_{\{i,j\}}} & \cdots & \mathrm{H}^{R_{\{i\}}\cup C} & \cdots & \mathrm{H}^{R_{\{i\}}\cup S} & \cdots & \mathrm{H}^{R_{\{i,j\}}\cup S} & \cdots & \mathrm{H}^{R_{\{i\}}\cup C\cup S} & \cdots \end{array} \\ \left(\begin{array}{ccccccccccccc} \cdots & a_t^{R_i} & \cdots & 0 & \cdots & 0 & \cdots & 0 & \cdots & 0 & \cdots & 0 & \cdots \\ \vdots & \vdots & \vdots & \vdots & \vdots & \vdots & \vdots & \vdots & \vdots & \vdots & \vdots & \vdots & \vdots \\ \cdots & 0 & \cdots & 0 & \cdots & 0 & \cdots & \alpha^S_{R_i} a_t^{R_i} & \cdots & 0 & \cdots & 0 & \cdots \\ \vdots & \vdots & \vdots & \vdots & \vdots & \vdots & \vdots & \vdots & \vdots & \vdots & \vdots & \vdots & \vdots \\ \cdots & \Lambda_{\mathrm{H}^{R_{\{i\}}}} & \cdots & \alpha^{R_i}_{R_j} a_t^{R_j} & \cdots & \alpha^{R_i}_C a_t^C & \cdots & \lambda_t^S & \cdots & 0 & \cdots & 0 & \cdots \\ \vdots & \vdots & \vdots & \vdots & \vdots & \vdots & \vdots & \vdots & \vdots & \vdots & \vdots & \vdots & \vdots \\ \cdots & 0 & \cdots & 0 & \cdots & 0 & \cdots & \Lambda_{\mathrm{H}^{R_{\{i\}}\cup S}} & \cdots & \alpha^S_{R_j}\alpha^{R_i}_{R_j} a_t^{R_j} & \cdots & \alpha^S_C\alpha^{R_i}_C a_t^C & \cdots \\ \vdots & \vdots & \vdots & \vdots & \vdots & \vdots & \vdots & \vdots & \vdots & \vdots & \vdots & \vdots & \vdots \end{array}\right) \end{array}. \tag{13}$$

In the $\mathrm{H}^{R_{\{i\}}}$-row of the generator matrix $\Lambda_{[\psi^S]}(t)$, the positive elements represent the transition intensities from state $\mathrm{H}^{R_{\{i\}}}$ to other states by one jump. There are three possible scenarios: a single reference entity defaults, counterparty defaults, or external shock happens. The positive elements in this row are $\alpha^{R_i}_{R_j} a_t^{R_j}\ (j \in I\backslash\{i\})$ and $\alpha^{R_i}_C a_t^C$ by (6) and λ_t^S if external shock happens. The diagonal element in this row is as follows:

$$\Lambda_{\mathrm{H}^{R_{\{i\}}}}(t) = -\left[\sum_{j\subset I\backslash\{i\}} \alpha^{R_i}_{R_j} a_t^{R_j} + \alpha^{R_i}_C a_t^C + \lambda_t^S\right]. \tag{14}$$

In the $\mathrm{H}^{R_{\{i\}}}$-column of the generator matrix $\Lambda_{[\psi^S]}(t)$, the positive elements represent the transition intensities from other states to state $\mathrm{H}^{R_{\{i\}}}$ by one jump. The only possible state which can jump to $\mathrm{H}^{R_{\{i\}}}$ is H^{R_ϕ}. So, the nonzero elements in the H^{R_i}-column are $a_t^{R_i}$ and the diagonal element $\Lambda_{\mathrm{H}^{R_{\{i\}}}}(t)$.

In the $\mathrm{H}^{R_{\{i\}}\cup S}$-row of the generator matrix $\Lambda_{[\psi^S]}(t)$, the positive elements represent the transition intensities from state $\mathrm{H}^{R_{\{i\}}\cup S}$ to other states by one jump. There are two possible scenarios: a single reference entity defaults or counterparty defaults. By (6), the positive elements in this row are $\alpha^S_{R_j}\alpha^{R_i}_{R_j} a_t^{R_j}\ (j \in I\backslash\{i\})$ and $\alpha^S_C\alpha^{R_i}_C a_t^C$. The diagonal element in this row is as follows:

$$\Lambda_{\mathrm{H}^{R_{\{i\}}\cup S}}(t) = -\left[\sum_{j\in I\backslash\{i\}} \alpha^S_{R_j}\alpha^{R_i}_{R_j} a_t^{R_j} + \alpha^S_C\alpha^{R_i}_C a_t^C\right]. \tag{15}$$

In the $\mathrm{H}^{R_{\{i\}}\cup S}$-column of the generator matrix $\Lambda_{[\psi^S]}(t)$, the positive elements represent the transition intensities from other states to state $\mathrm{H}^{R_{\{i\}}\cup S}$ by one jump. The possible states which can jump to $\mathrm{H}^{R_{\{i\}}\cup S}$ are $\mathrm{H}^{R_{\{i\}}}$ and H^S. So, the nonzero elements in the $\mathrm{H}^{R_{\{i\}}\cup S}$-column are $\alpha^S_{R_i} a^{R_i}_t$, λ^S_t, and the diagonal element $\Lambda_{\mathrm{H}^{R_{\{i\}}\cup S}}$.

By forward Kolmogorov equation (7), we have

$$\begin{cases} \dfrac{\mathrm{d}P_{\mathrm{H}^{R_{\{i\}}}}\left(0,t\mid\psi^S\right)}{\mathrm{d}t} = P_{\mathrm{H}^{R_\phi}}\left(0,t\mid\psi^S\right)a^{R_i}_t + P_{\mathrm{H}^{R_{\{i\}}}}\left(0,t\mid\psi^S\right)\Lambda_{\mathrm{H}^{R_{\{i\}}}}(t), \\[2ex] \dfrac{\mathrm{d}P_{\mathrm{H}^{R_{\{i\}}\cup S}}\left(0,t\mid\psi^S\right)}{\mathrm{d}t} = P_{\mathrm{H}^{R_{\{i\}}}}\left(0,t\mid\psi^S\right)\lambda^S_t + P_{\mathrm{H}^S}\left(0,t\mid\psi^S\right)\alpha^S_{R_i}a^{R_i}_t + P_{\mathrm{H}^{R_{\{i\}}\cup S}}\left(0,t\mid\psi^S\right)\Lambda_{\mathrm{H}^{R_{\{i\}}\cup S}}(t), \end{cases} \tag{16}$$

where $P_{\mathrm{H}^{R_\phi}}(0,t\mid\psi^S)$ and $P_{\mathrm{H}^S}(0,t\mid\psi^S)$ are already obtained in (12). It is easy to solve equation (16) as follows:

$$\begin{cases} P_{\mathrm{H}^{R_{\{i\}}}}\left(0,t\mid\psi^S\right) = e^{\int_0^t \Lambda_{\mathrm{H}^{R_{\{i\}}}}(u)\mathrm{d}u}\displaystyle\int_0^t a^{R_i}_u e^{-\int_0^u \Lambda_{\mathrm{H}^{R_{\{i\}}}}(r)\mathrm{d}r} P_{\mathrm{H}^{R_\phi}}\left(0,u\mid\psi^S\right)\mathrm{d}u, \\[2ex] P_{\mathrm{H}^{R_{\{i\}}\cup S}}\left(0,t\mid\psi^S\right) = e^{\int_0^t \Lambda_{\mathrm{H}^{R_{\{i\}}\cup S}}(u)\mathrm{d}u}\left[\displaystyle\int_0^t \lambda^S_u e^{-\int_0^u \Lambda_{\mathrm{H}^{R_{\{i\}}\cup S}}(r)\mathrm{d}r} P_{\mathrm{H}^{R_{\{i\}}}}\left(0,u\mid\psi^S\right)\mathrm{d}u + \displaystyle\int_0^t \alpha^S_{R_i}a^{R_i}_u e^{-\int_0^u \Lambda_{\mathrm{H}^{R_{\{i\}}\cup S}}(r)\mathrm{d}r} P_{\mathrm{H}^S}\left(0,u\mid\psi^S\right)\mathrm{d}u\right]. \end{cases} \tag{17}$$

We can derive all the conditional transition probabilities by the method of mathematical induction. Suppose that we have obtained the conditional transition probabilities that $k-1$ reference entities default during $[0,t]$. For the cases that k reference entities default, the corresponding states of $\mathbf{H}_t$ are H^{R_M} and $\mathrm{H}^{R_M\cup S}$ for $M\subset I$ and $|M|=k$, where $|M|$ is the cardinal number of set M. The corresponding elements in the infinitesimal generator matrix $\Lambda_{[\psi^S]}(t)$ are as follows:

$$\begin{array}{c} \\ \vdots \\ \mathrm{H}^{R_{M\setminus\{i\}}} \\ \vdots \\ \mathrm{H}^{R_{M\setminus\{i\}}\cup S} \\ \vdots \\ \mathrm{H}^{R_M} \\ \vdots \\ \mathrm{H}^{R_M\cup S} \\ \vdots \end{array}
\begin{array}{c} \begin{array}{ccccccccccccc} \cdots & \mathrm{H}^{R_M} & \cdots & \mathrm{H}^{R_{M\cup\{j\}}} & \cdots & \mathrm{H}^{R_M\cup C} & \cdots & \mathrm{H}^{R_M\cup S} & \cdots & \mathrm{H}^{R_{M\cup\{j\}}\cup S} & \cdots & \mathrm{H}^{R_M\cup C\cup S} & \cdots \end{array} \\
\begin{pmatrix} \vdots & \vdots & \vdots & \vdots & \vdots & \vdots & \vdots & \vdots & \vdots & \vdots & \vdots & \vdots & \vdots \\
\cdots & \left(\prod_{j\in M\setminus\{i\}}\alpha^{R_i}_{R_i}\right)a^{R_i}_t & \cdots & 0 & \cdots & 0 & \cdots & 0 & \cdots & 0 & \cdots & 0 & \cdots \\
\vdots & \vdots & \vdots & \vdots & \vdots & \vdots & \vdots & \vdots & \vdots & \vdots & \vdots & \vdots & \vdots \\
\cdots & 0 & \cdots & 0 & \cdots & 0 & \cdots & \left(\prod_{j\in M\setminus\{i\}}\alpha^{R_j}_{R_i}\right)\alpha^S_{R_i}a^{R_i}_t & \cdots & 0 & \cdots & 0 & \cdots \\
\vdots & \vdots & \vdots & \vdots & \vdots & \vdots & \vdots & \vdots & \vdots & \vdots & \vdots & \vdots & \vdots \\
\cdots & \Lambda_{\mathbb{H}^{R_M}} & \cdots & \left(\prod_{i\in M}\alpha^{R_i}_{R_i}\right)a^{R_i}_t & \cdots & \left(\prod_{i\in M}\alpha^{R_i}_C\right)a^C_t & \cdots & \lambda^S_t & \cdots & 0 & \cdots & 0 & \cdots \\
\vdots & \vdots & \vdots & \vdots & \vdots & \vdots & \vdots & \vdots & \vdots & \vdots & \vdots & \vdots & \vdots \\
\cdots & 0 & \cdots & 0 & \cdots & 0 & \cdots & \Lambda_{\mathbb{H}^{R_M\cup S}} & \cdots & \left(\prod_{i\in M}\alpha^{R_i}_{R_i}\right)\alpha^S_{R_j}a^R_t & \cdots & \left(\prod_{i\in M}\alpha^{R_i}_C\right)\alpha^S_C a^R_t & \cdots \\
\vdots & \vdots & \vdots & \vdots & \vdots & \vdots & \vdots & \vdots & \vdots & \vdots & \vdots & \vdots & \vdots \end{pmatrix} \end{array}. \tag{18}$$

In the H^{R_M}-row of the generator matrix $\Lambda_{[\psi^S]}(t)$, the positive elements represent the transition intensities from state H^{R_M} to other states by one jump. There are three possible scenarios: a single reference entity defaults, counterparty defaults, or external shock happens. The positive elements in this row are $(\prod_{i\in M}\alpha^{R_i}_{R_j})a^{R_j}_t$ $(j\in I\setminus M)$ and $(\prod_{i\in M}\alpha^{R_i}_C)a^C_t$ by (7) and λ^S_t if external shock happens. The diagonal element in this row is as follows:

$$\Lambda_{\mathrm{H}^{R_M}}(t) = -\left[\sum_{j\in I\backslash M}\left(\prod_{i\in M}\alpha_{R_j}^{R_i}\right)a_t^{R_j} + \left(\prod_{i\in M}\alpha_C^{R_i}\right)a_t^C + \lambda_t^S\right]. \tag{19}$$

In the H^{R_M}-column of the generator matrix $\Lambda_{[\psi^S]}(t)$, the positive elements represent the transition intensities from other states to state H^{R_M} by one jump. The possible states which can jump to H^{R_M} are $\mathrm{H}^{R_{M\backslash\{i\}}}$ for $i\in M$. So, the nonzero elements in this column are $(\prod_{j\in M\backslash\{i\}}\alpha_{R_i}^{R_j})a_t^{R_i}$ by (6) and the diagonal element $\Lambda_{\mathrm{H}^{R_M}}$.

In the $\mathrm{H}^{R_M\cup S}$-row of the generator matrix $\Lambda_{[\psi^S]}(t)$, the positive elements represent the transition intensities from state $\mathrm{H}^{R_M\cup S}$ to other states by one jump. There are two possible scenarios: a single reference entity defaults or counterparty defaults. By (6), the positive elements in this row are $(\prod_{i\in M}\alpha_{R_j}^{R_i})\alpha_{R_j}^S a_t^{R_j}$ $(j\in I\backslash M)$ and $(\prod_{i\in M}\alpha_C^{R_i})\alpha_C^S a_t^C$. The diagonal element in this row is obtained as follows:

$$\Lambda_{\mathrm{H}^{R_M\cup S}}(t) = -\left[\sum_{j\in I\backslash M}\left(\prod_{i\in M}\alpha_{R_j}^{R_i}\right)\alpha_{R_j}^S a_t^{R_j} + \left(\prod_{i\in M}\alpha_C^{R_i}\right)\alpha_C^S a_t^C\right]. \tag{20}$$

In the $\mathrm{H}^{R_M\cup S}$-column of the generator matrix $\Lambda_{[\psi^S]}(t)$, the positive elements represent the transition intensities from other states to state $\mathrm{H}^{R_M\cup S}$ by one jump. The possible states which can jump to $\mathrm{H}^{R_M\cup S}$ are H^{R_M} and $\mathrm{H}^{R_{M\backslash\{i\}}\cup S}$ $(i\in M)$. So, the nonzero elements in this column are λ_t^S, $(\prod_{j\in M\backslash\{i\}}\alpha_{R_i}^{R_j})\alpha_{R_i}^S a_t^{R_i}$, and the diagonal element $\Lambda_{\mathrm{H}^{R_M\cup S}}$.

By forward Kolmogorov equation (7), we have

$$\begin{cases} \dfrac{\mathrm{d}P_{\mathrm{H}^{R_M}}(0,t\mid\psi^S)}{\mathrm{d}t} = \displaystyle\sum_{i\in M}\left[P_{\mathrm{H}^{R_{M\setminus\{i\}}}}(0,t\mid\psi^S)\left(\prod_{j\in M\setminus\{i\}}\alpha_{R_i}^{R_j}\right)a_t^{R_i}\right] + P_{\mathrm{H}^{R_M}}(0,t\mid\psi^S)\Lambda_{\mathrm{H}^{R_M}}(t), \\ \dfrac{\mathrm{d}P_{\mathrm{H}^{R_M\cup S}}(0,t\mid\psi^S)}{\mathrm{d}t} = \displaystyle\sum_{i\in M}\left[P_{\mathrm{H}^{R_{M\setminus\{i\}}\cup S}}(0,t\mid\psi^S)\left(\prod_{j\in M\setminus\{i\}}\alpha_{R_i}^{R_j}\right)\alpha_{R_i}^S a_t^{R_i}\right] + P_{\mathrm{H}^{R_M}}(0,t\mid\psi^S)\lambda_t^S + P_{\mathrm{H}^{R_M\cup S}}(0,t\mid\psi^S)\Lambda_{\mathrm{H}^{R_M\cup S}}(t), \end{cases} \tag{21}$$

where $P_{\mathrm{H}^{R_{M\backslash\{i\}}}}(0,t\mid\psi^S)$ and $P_{\mathrm{H}^{R_{M\backslash\{i\}}\cup S}}(0,t\mid\psi^S)$ are known by induction. It is easy to get the solutions of equation (21) as follows:

$$\begin{cases} P_{\mathrm{H}^{R_M}}(0,t\mid\psi^S) = e^{\int_0^t\Lambda_{\mathrm{H}^{R_M}}(u)\mathrm{d}u}\displaystyle\sum_{i\in M}\left[\int_0^t\left(\prod_{j\in M\setminus\{i\}}\alpha_{R_i}^{R_j}\right)a_u^{R_i}e^{-\int_0^u\Lambda_{\mathrm{H}^{R_M}}(r)\mathrm{d}r}\times P_{\mathrm{H}^{R_{M\setminus\{i\}}}}(0,u\mid\psi^S)\right]\mathrm{d}u, \\ P_{\mathrm{H}^{R_M\cup S}}(0,t\mid\psi^S) = e^{\int_0^t\Lambda_{\mathrm{H}^{R_M\cup S}}(u)\mathrm{d}u}\left\{\displaystyle\int_0^t\lambda_u^S e^{-\int_0^u\Lambda_{\mathrm{H}^{R_M\cup S}}(r)\mathrm{d}r}P_{\mathrm{H}^{R_M}}(0,u\mid\psi^S)\mathrm{d}u\right. \\ \left.+\displaystyle\sum_{i\in M}\left[\alpha_{R_i}^S\left(\prod_{j\in M\setminus\{i\}}\alpha_{R_i}^{R_j}\right)\int_0^t a_u^{R_i}e^{-\int_0^u\Lambda_{\mathrm{H}^{R_M\cup S}}(r)\mathrm{d}r}\times P_{\mathrm{H}^{R_{M\setminus\{i\}}\cup S}}(0,u\mid\psi^S)\mathrm{d}u\right]\right\}. \end{cases} \tag{22}$$

In order to calculate the unconditional transition probabilities, we need the following proposition.

Proposition 1
(i) $P_{H^{R_M}}(0,t\mid\psi^S)$ contains only one random term $e^{-\int_0^t\lambda_u^S du}$ which is outside the integral symbol; (ii) each term in $P_{H^{R_M\cup S}}(0,t\mid\psi^S)$ contains only one random term $\lambda_u^S e^{-\int_0^u\lambda_r^S dr}$ which is inside the integral symbol.

Proof. We use the induction method to prove this proposition.

(i) Firstly, $|M| = 0$:

$$P_{\mathrm{H}^{R_\phi}}(0,t\mid\psi^S) = e^{\int_0^t\Lambda_{\mathbb{H}^{R_\phi}}(u)\mathrm{d}u} = e^{-\int_0^t\lambda_u^S\mathrm{d}u}e^{-\int_0^t\left(\sum_{i\in I}a_u^{R_i}+a_u^C\right)\mathrm{d}u}. \tag{23}$$

$P_{\mathrm{H}^{R_\phi}}(0,t\mid\psi^S)$ just contains one random term owning the path of λ_t^S.

Secondly, $|M| = 1$:

$$\begin{aligned}P_{\mathrm{H}^{R_{\{i\}}}}\left(0,t\mid\psi^S\right)&=e^{\int_0^t \Lambda_{\mathrm{H}^{R_{\{i\}}}}(u)\mathrm{d}u}\int_0^t a_u^{R_i}e^{-\int_0^u \Lambda_{\mathrm{H}^{R_{\{i\}}}}(r)\mathrm{d}r}P_{\mathrm{H}^{R_\phi}}\left(0,u\mid\psi^S\right)\mathrm{d}u\\&=e^{-\int_0^t\left(\sum_{j\subset I\setminus\{i\}}\alpha_{R_j}^{R_i}a_u^{R_j}+\alpha_C^{R_i}a_u^C+\lambda_u^S\right)\mathrm{d}u}\\&\quad\times\int_0^t a_u^{R_i}e^{\int_0^u\left(\sum_{j\subset I\setminus\{i\}}\alpha_{R_j}^{R_i}a_r^{R_j}+\alpha_C^{R_i}a_r^C+\lambda_r^S\right)\mathrm{d}r}\\&\quad\times e^{-\int_0^u\left(\sum_{i\in I}a_r^{R_i}+a_r^C+\lambda_r^S\right)\mathrm{d}r}\mathrm{d}u\\&=e^{-\int_0^t\lambda_u^S\mathrm{d}u}e^{-\int_0^t\left(\sum_{j\subset I\setminus\{i\}}\alpha_{R_j}^{R_i}a_u^{R_j}+\alpha_C^{R_i}a_u^C\right)\mathrm{d}u}\\&\quad\times\int_0^t a_u^{R_i}e^{\int_0^u\left(\sum_{j\subset I\setminus\{i\}}\alpha_{R_j}^{R_i}a_r^{R_j}+\alpha_C^{R_i}a_r^C\right)\mathrm{d}r}e^{-\int_0^u\left(\sum_{i\in I}a_r^{R_i}+a_r^C\right)\mathrm{d}r}\mathrm{d}u.\end{aligned}\tag{24}$$

$P_{\mathrm{H}^{R_M}}(0,t\mid\psi^S)$ contains one random term $e^{-\int_0^t\lambda_u^S\mathrm{d}u}$ outside the integral.

Assume that (i) holds for $|M|=k-1$. When $|M|=k$,

$$\begin{aligned}P_{\mathrm{H}^{R_M}}\left(0,t\mid\psi^S\right)&=e^{\int_0^t\Lambda_{\mathrm{H}^{R_M}}(u)\mathrm{d}u}\\&\cdot\sum_{i\in M}\left[\int_0^t\left(\prod_{j\in M\setminus\{i\}}\alpha_{R_i}^{R_j}\right)a_u^{R_i}e^{-\int_0^u\Lambda_{\mathrm{H}^{R_M}}(r)\mathrm{d}r}\right.\\&\left.\times P_{\mathrm{H}^{R_{M\setminus\{i\}}}}\left(0,u\mid\psi^S\right)\right]\mathrm{d}u.\end{aligned}\tag{25}$$

In the integral of (25), the only random term $e^{-\int_0^u\lambda_r^S\mathrm{d}r}$ contained in $P_{\mathrm{H}^{R_{M\setminus\{i\}}}}(0,u\mid\psi^S)$ offsets the term $e^{\int_0^u\lambda_r^S\mathrm{d}r}$ in $e^{-\int_0^u\Lambda_{\mathrm{H}^{R_M}}(r)\mathrm{d}r}$. Then, $P_{\mathrm{H}^{R_M}}(0,t\mid\psi^S)$ contains only one random term $e^{-\int_0^t\lambda_u^S\mathrm{d}u}$ from $e^{\int_0^t\Lambda_{\mathrm{H}^{R_M}}(u)\mathrm{d}u}$ outside the integral in (25), and (i) holds for $|M|=k$.

(ii) Firstly, $|M|=0$:

$$\begin{aligned}P_{\mathrm{H}^S}\left(0,t\mid\psi^S\right)&=e^{\int_0^t\Lambda_{\mathrm{H}^S}(u)\mathrm{d}u}\int_0^t\lambda_u^Se^{-\int_0^u\Lambda_{\mathrm{H}^S}(r)\mathrm{d}r}P_{\mathrm{H}^{R_\phi}}\left(0,u\mid\psi^S\right)\mathrm{d}u\\&=e^{\int_0^t\Lambda_{\mathrm{H}^S}(u)\mathrm{d}u}\int_0^t\lambda_u^Se^{-\int_0^u\Lambda_{\mathrm{H}^S}(r)\mathrm{d}r}e^{\int_0^u\Lambda_{\mathrm{H}^{R_\phi}}(r)\mathrm{d}r}\mathrm{d}u\\&=e^{\int_0^t\Lambda_{\mathrm{H}^S}(u)\mathrm{d}u}\int_0^t\lambda_u^Se^{-\int_0^u\lambda_r^S\mathrm{d}r}e^{-\int_0^u\Lambda_{\mathrm{H}^S}(r)\mathrm{d}r}e^{-\int_0^u\left(\sum_{i\in I}a_r^{R_i}+a_r^C\right)\mathrm{d}r}\mathrm{d}u.\end{aligned}\tag{26}$$

$P_{\mathrm{H}^S}(0,t\mid\psi^S)$ contains one random term $\lambda_u^S e^{-\int_0^u \lambda_r^S \mathrm{d}r}$ inside the integral.

Secondly, $|M| = 1$:

$$\begin{aligned}
P_{\mathrm{H}^{R_{\{i\}}\cup S}}\left(0,t\mid\psi^S\right) &= e^{\int_0^t \Lambda_{\mathrm{H}^{R_{\{i\}}\cup S}}(u)\mathrm{d}u}\left[\int_0^t \lambda_u^S e^{-\int_0^u \Lambda_{\mathrm{H}^{R_{\{i\}}\cup S}}(r)\mathrm{d}r} P_{\mathrm{H}^{R_{\{i\}}}}\left(0,u\mid\psi^S\right)\mathrm{d}u + \int_0^t \alpha_{R_i}^S a_u^{R_i} e^{-\int_0^u \Lambda_{\mathrm{H}^{R_{\{i\}}\cup S}}(r)\mathrm{d}r} P_{\mathrm{H}^S}\left(0,u\mid\psi^S\right)\mathrm{d}u\right] \\
&= e^{\int_0^t \Lambda_{\mathrm{H}^{R_{\{i\}}\cup S}}(u)\mathrm{d}u}\Bigg[\int_0^t \lambda_u^S e^{-\int_0^u \lambda_r^S \mathrm{d}r} e^{\int_0^u \left(\sum_{j\subset I\setminus\{i\}} \alpha_{R_j}^{R_i} a_r^{R_j} + \alpha_C^{R_i} a_r^C\right)\mathrm{d}r} e^{-\int_0^u \Lambda_{\mathrm{H}^{R_{\{i\}}\cup S}}(r)\mathrm{d}r} \\
&\quad\times \int_0^u a_r^{R_i} e^{-\int_0^r \left(\sum_{j\subset I\setminus\{i\}} \alpha_{R_j}^{R_i} a_v^{R_j} + \alpha_C^{R_i} a_v^C\right)\mathrm{d}v} e^{\int_0^r \left(\sum_{i\in I} a_v^{R_i} + a_v^C\right)\mathrm{d}v} \mathrm{d}r\,\mathrm{d}u \\
&\quad+ \int_0^t \alpha_{R_i}^S a_u^{R_i} e^{-\int_0^u \Lambda_{\mathrm{H}^{R_{\{i\}}\cup S}}(r)\mathrm{d}r} e^{\int_0^u \Lambda_{\mathrm{H}^S}(r)\mathrm{d}r} \\
&\quad\times \int_0^u \lambda_r^S e^{-\int_0^r \lambda_v^S \mathrm{d}v} e^{-\int_0^r \Lambda_{\mathrm{H}^S}(v)\mathrm{d}v} e^{-\int_0^r \left(\sum_{i\in I} a_v^{R_i} + a_v^C\right)\mathrm{d}v} \mathrm{d}r\,\mathrm{d}u\Bigg].
\end{aligned} \tag{27}$$

The two terms in the right side of (27) contain only one random term $\lambda_u^S e^{-\int_0^u \lambda_r^S \mathrm{d}r}$ (or $\lambda_r^S e^{-\int_0^r \lambda_v^S \mathrm{d}v}$) inside the integral.

Assume that (ii) holds for $|M| = k - 1$. When $|M| = k$,

$$\begin{aligned}
P_{\mathrm{H}^{R_M\cup S}}\left(0,t\mid\psi^S\right) &= e^{\int_0^t \Lambda_{\mathrm{H}^{R_M\cup S}}(u)\mathrm{d}u}\Bigg\{\int_0^t \lambda_u^S e^{-\int_0^u \Lambda_{\mathrm{H}^{R_M\cup S}}(r)\mathrm{d}r} P_{\mathrm{H}^{R_M}}\left(0,u\mid\psi^S\right)\mathrm{d}u \\
&\quad+ \sum_{i\in M}\left[\alpha_{R_i}^S\left(\prod_{j\in M\setminus\{i\}} \alpha_{R_i}^{R_j}\right)\int_0^t a_u^{R_i} e^{-\int_0^u \Lambda_{\mathrm{H}^{R_M\cup S}}(r)\mathrm{d}r} \times P_{\mathrm{H}^{R_{M\setminus\{i\}}\cup S}}\left(0,u\mid\psi^S\right)\mathrm{d}u\right]\Bigg\}.
\end{aligned} \tag{28}$$

By (i), $P_{\mathrm{H}^{R_M}}(0,u\mid\psi^S)$ only contains one random term $e^{-\int_0^u \lambda_r^S \mathrm{d}r}$ which is outside the integral symbol. Then, the first term in $P_{\mathrm{H}^{R_M\cup S}}(0,t\mid\psi^S)$ contains only one random term $\lambda_u^S e^{-\int_0^u \lambda_r^S \mathrm{d}r}$. By induction, each term in $P_{\mathrm{H}^{R_{M\setminus\{i\}}\cup S}}(0,t\mid\psi^S)$ contains only one random term $\lambda_u^S e^{-\int_0^u \lambda_r^S \mathrm{d}r}$ which is in the integral symbol. Then, each term in the sum part of equation (28) contains only one random term $\lambda_u^S e^{-\int_0^u \lambda_r^S \mathrm{d}r}$ in the integral. In summary, (ii) also holds when $|M| = k$.

According to Proposition 1 and Fubini's theorem, we can take the expectation $E_{\psi^S}[\cdot]$ of equation (22) and obtain the unconditional transition probabilities as follows:

$$\begin{cases} P_{\mathrm{H}^{R_M}}(0,t) = e^{\int_0^t -\left(\sum_{j \in I \setminus M} \left(\prod_{i \in M} \alpha_{R_j}^{R_i} \right) a_u^{R_j} + \left(\prod_{i \in M} \alpha_C^{R_i} \right) a_u^C \right) \mathrm{d}u} E_{\psi^S}\left[e^{-\int_0^t \lambda_u^S \mathrm{d}u} \right] \\ \times \sum_{i \in M} \left[\int_0^t \left(\prod_{j \in M \setminus \{i\}} \alpha_{R_i}^{R_j} \right) a_u^{R_i} e^{\int_0^t \left(\sum_{j \in I \setminus M} \left(\prod_{i \in M} \alpha_{R_j}^{R_i} \right) a_r^{R_j} + \left(\prod_{i \in M} \alpha_C^{R_i} \right) a_r^C \right) \mathrm{d}r} \right. \\ \left. \times \left(\frac{P_{\mathrm{H}^{R_{M \setminus \{i\}}}}(0,u)}{E_{\psi^S}\left[e^{-\int_0^u \lambda_r^S dr} \right]} \right) \mathrm{d}u \right], \\ P_{\mathrm{H}^{R_M \cup S}}(0,t) = e^{\int_0^t \Lambda_{\mathrm{H}^{R_{M \cup S}}}(u) \mathrm{d}u} \left\{ \int_0^t E_{\psi^S}\left[\lambda_u^S e^{-\int_0^u \lambda_r^S \mathrm{d}r} \right] e^{\int_0^u \Lambda_{\mathrm{H}^{R_{M \cup S}}}(r) \mathrm{d}r} \right. \\ \times \frac{P_{\mathbb{H}^{R_M}}(0,u)}{E_{\psi^S}\left[e^{-\int_0^t \lambda_u^S \mathrm{d}u} \right]} \\ \left. + \sum_{i \in M} \left[\alpha_{R_i}^S \left(\prod_{j \in M \setminus \{i\}} \alpha_{R_i}^{R_j} \right) \int_0^t a_u^{R_i} e^{-\int_0^u \Lambda_{\mathrm{H}^{R_{M \cup S}}}(r) \mathrm{d}r} \times P_{\mathrm{H}^{R_{M \setminus \{i\}} \cup S}}(0,u) \mathrm{d}u \right] \right\}, \end{cases} \tag{29}$$

where $E_{\psi^S}[\cdot]$ is the expectation taken over the path of $(\lambda_t^S)_{t \in [0,T]}$.

To compute $E_{\psi^S}[e^{-\int_0^t \lambda_u^S \mathrm{d}u}]$ and $E_{\psi^S}[\lambda_t^S e^{-\int_0^t \lambda_u^S \mathrm{d}u}]$, we adopt the affine diffusion process with the jump for λ_t^S as that proposed by Wang and Garleanu [5], which is a special Lévy process. We use Cox process to describe the external shock to obtain the closed-form solutions in this paper. The stochastic differential equation of λ_t^S is given by

$$\mathrm{d}\lambda_t^S = k\left(\theta - \lambda_t^S\right)\mathrm{d}t + \sigma\sqrt{\lambda_t^S}\mathrm{d}Z_t + \Delta J_t, \tag{30}$$

where Z_t is a standard Brownian motion, J_t is a pure jump process, and ΔJ_t denotes the jump of J_t at time t. Here, J_t is taken to be independent of Z_t with jump sizes that are independent and exponentially distributed with mean μ and whose jump times are those of all independent Poisson processes with constant jump arrival rate l. It was shown by Wang and Garleanu [5] that

$$\begin{cases} E_{\psi^S}\left[e^{-\int_0^t \lambda_u^S du} \right] = e^{\alpha(t) + \beta(t)\lambda_0^S}, \\ E_{\psi^S}\left[\lambda_t^S e^{-\int_0^t \lambda_u^S du} \right] = -\left[\overline{\alpha}(t) + \overline{\beta}(t)\lambda_0^S \right] e^{\alpha(t) + \beta(t)\lambda_0^S}, \end{cases} \tag{31}$$

where

$$\alpha(t) = \frac{k\theta(c_1+d_1)}{b_1c_1d_1}\ln\frac{c_1+d_1e^{b_1t}}{c_1+d_1}+\frac{k\theta}{c_1}t$$
$$+\frac{l(a_2c_2-d_2)}{b_2c_2d_2}\ln\frac{c_2+d_2e^{b_2t}}{c_2+d_2}+\left(\frac{l}{c_2}-l\right)t,$$
$$\beta(t) = \frac{1-e^{b_1t}}{c_1+d_1e^{b_1t}},$$
$$\overline{\alpha}(t) = \frac{k\theta(c_1+d_1)}{c_1}\frac{e^{b_1t}}{c_1+d_1e^{b_1t}}+\frac{k\theta}{c_1}$$
$$+\frac{l(a_2c_2-d_2)}{c_2}\frac{e^{b_2t}}{c_2+d_2e^{b_2t}}+\left(\frac{l}{c_2}-l\right)$$
$$\overline{\beta}(t) = \frac{-(k^2+2\sigma^2)e^{b_1t}}{(c_1+d_1e^{b_1t})^2}, \tag{32}$$
$$b_1 = -\sqrt{k^2+2\sigma^2},$$
$$c_1 = \frac{k+\sqrt{k^2+2\sigma^2}}{-2},$$
$$d_1 = \frac{-k+\sqrt{k^2+2\sigma^2}}{-2},$$
$$a_2 = \frac{-k+\sqrt{k^2+2\sigma^2}}{k+\sqrt{k^2+2\sigma^2}},$$
$$b_2 = b_1, d_2 = \frac{d_1+\mu}{c_1},$$
$$c_2 = 1-\frac{\mu}{c_1}.$$

Replacing the conditional expectations in (29) with equation (31), we obtain the unconditional transition probabilities. □

3. Pricing Basket Credit Derivatives

We will compute the fair premium rates of BCDS and BCLN with the counterparty risk in this section. Under the continuous model assumption, the premium rates are paid continuously at a constant rate. We assume that the notional of the BCDS or BCLN is 1, T is the maturity date of the contracts, c_k is the premium rate of kth-to-default credit derivatives, τ_k is the kth default time of reference entities, constant r is the risk-free interest rate, and constant $\rho \in [0,1)$ is the recovery rate.

3.1. kth-to-Default CDS. The cash flow of a kth-to-default CDS is presented in Figure 1.

(i) The protection buyer pays constant premium rate c_k during the life of the kth-to-default CDS

(ii) If the kth default in the pool occurs before the maturity, the protection buyer gives a recovery payoff ρ, and the contract is terminated

The expected cash flow of kth-to-default CDS is as follows (see Zheng and Jiang [9]):

$$E\left[\int_0^T c_k e^{-rs} I_{\tau_k>s} I_{\tau_C>s}\mathrm{d}s\right] = E\left[(1-\rho)e^{-r\tau_k} I_{\tau_k\le T} I_{\tau_C>T}\right], \tag{33}$$

and the premium rate is given by

$$c_k = \frac{E\left[(1-\rho)e^{-r\tau_k} I_{\tau_k\le T} I_{\tau_C>T}\right]}{E\left[\int_0^T e^{-rs} I_{\tau_k>s} I_{\tau_C>s}\mathrm{d}s\right]}. \tag{34}$$

To calculate the premium rate for the kth-to-default CDS, there are two possible scenarios during $[0,t]$: nonoccurrence of the external shock S or occurrence of S. If $k-1$ reference entities have defaulted during $[0,t]$ and another reference entity defaults during $(t,t+\mathrm{d}t]$, the probability of such occurrence is given by

$$Q_k(t)\mathrm{d}t = \sum_{M\subset I,|M|=k-1}\Bigg[P_{\mathrm{H}^{R_M}}(0,t)\left(\sum_{j\in I\backslash M}\left(\prod_{i\in M}\alpha_{R_j}^{R_i}\right)a_t^{R_j}\right)$$
$$+P_{\mathrm{H}^{R_M\cup S}}(0,t)\times\left(\sum_{j\subset I\backslash M}\alpha_{R_j}^{S}\left(\prod_{i\in M}\alpha_{R_j}^{R_i}\right)a_t^{R_j}\right)\Bigg]\mathrm{d}t, \tag{35}$$

where $\sum_{M\subset I,|M|=k-1}[P_{\mathrm{H}^{R_M}}(0,t)(\sum_{j\in I\setminus M}(\prod_{i\in M}\alpha_{R_j}^{R_i})a_t^{R_j})]\mathrm{d}t$ corresponds to nonoccurrence of S and $\sum_{M\subset I,|M|=k-1}[P_{\mathbf{H}^{R_M\cup S}}(0,t)\times(\sum_{j\subset I\setminus M}\alpha_{R_j}^{S}(\prod_{i\in M}\alpha_{R_j}^{R_i})a_t^{R_j})]\mathrm{d}t$ corresponds to the case otherwise. So, the expected present value of the compensation payment paid by the protection seller within $(t,t+\mathrm{d}t]$ is

$$(1-\rho)e^{-rt}Q_k(t)\mathrm{d}t. \tag{36}$$

Over the entire period $[0,T]$, the expected present value of the compensation payment paid by the protection seller is

$$E\left[(1-\rho)e^{-r\tau_k} I_{\tau_k\le T} I_{\tau_C>T}\right] = \int_0^T (1-\rho)e^{-rt}Q_k(t)\mathrm{d}t. \tag{37}$$

The kth-to-default CDS contract will be terminated if more than $k-1$ reference entities default. The corresponding states to continue the contract are H^{R_M} and $\mathrm{H}^{R_M\cup S}(M\subset I, 0\le|M|\le k-1)$. The expected premium payment paid by the protection buyer within $(t,t+\mathrm{d}t]$ is given by

$$c_k e^{-rt}D_k(t)\mathrm{d}t, \tag{38}$$

where

$$D_k(t) = \sum_{M\subset I,0\le|M|\le k-1}\left[P_{\mathrm{H}^{R_M}}(0,t)+P_{\mathrm{H}^{R_M\cup S}}(0,t)\right]. \tag{39}$$

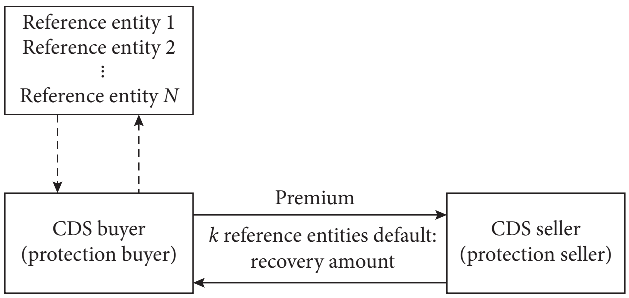

Figure 1: The cash flow of kth-to-default CDS.

Over the entire period $[0, T]$, the expected present value of the premium payment paid by the protection buyer is

$$E\left[\int_0^T c_k e^{-rs} I_{\tau_k > s} I_{\tau_C > s} \mathrm{d}s\right] = c_k \int_0^T e^{-rt} D_k(t)\mathrm{d}t. \qquad (40)$$

By (34), the kth-to-default CDS premium rate is given by

$$c_k = (1-\rho)\frac{\int_0^T e^{-rt} Q_k(t)\mathrm{d}t}{\int_0^T e^{-rt} D_k(t)\mathrm{d}t}. \qquad (41)$$

3.2. kth-to-Default CLN. The cash flow of a kth-to-default CLN is presented in Figure 2.

(i) The protection seller pays a nominal amount at the initial date

(ii) The protection buyer pays constant premium rate c_k during the life of the kth-to-default CLN

(iii) If the kth default in the pool occurs before the maturity, the protection buyer gives a recovery payoff ρ, and the contract is terminated

(iv) If the kth default in the pool does not occur before the maturity, the protection buyer returns the nominal amount

The expected cash flow of the kth-to-default CLN is as follows:

$$1 = E\left[\int_0^T c_k e^{-rs} I_{\tau_k > s} I_{\tau_C > s}\mathrm{d}s + \rho e^{-r\tau_k} I_{\tau_k \le T} I_{\tau_C > T} + e^{-rT} I_{\tau_k > T} I_{\tau_C > T}\right]. \qquad (42)$$

The premium rate is given by

$$c_k = \frac{E\left[1 - \rho e^{-r\tau_k} I_{\tau_k \le T} I_{\tau_C > T} - e^{-rT} I_{\tau_k > T} I_{\tau_C > T}\right]}{E\left[\int_0^T e^{-rs} I_{\tau_k > s} I_{\tau_C > s}\mathrm{d}s\right]}. \qquad (43)$$

Here, the method for calculating the default probabilities is the same as the method for the kth-to-default CDS case.

Over the whole period $[0, T]$, the expected present value of the recovery payment paid by the CLN issuer is

$$E\left[\rho e^{-r\tau_k} I_{\tau_k \le T} I_{\tau_C > T}\right] = \int_0^T \rho e^{-\mathrm{rt}} Q_k(t)\mathrm{d}t, \qquad (44)$$

where

$$Q_k(t)\mathrm{d}t = \sum_{M \subset I, |M| = k-1}\left[P_{\mathrm{H}^{R_M}}(0,t)\left(\sum_{j \in I\setminus M}\left(\prod_{i\in M}\alpha_{R_j}^{R_i}\right)a_t^{R_j}\right) + P_{\mathrm{H}^{R_M \cup S}}(0,t) \times \left(\sum_{j \subset I\setminus M}\alpha_{R_j}^{S}\left(\prod_{i\in M}\alpha_{R_j}^{R_i}\right)a_t^{R_j}\right)\right]\mathrm{d}t. \qquad (45)$$

The expected present value of the premium payment paid by the CLN issuer is

$$E\left[\int_0^T c_k e^{-rs} I_{\tau_k > s} I_{\tau_C > s}\mathrm{d}s\right] = c_k \int_0^T e^{-rt} D_k(t)\mathrm{d}t, \qquad (46)$$

where

$$D_k(t) = \sum_{M \subset I, 0 \le |M| \le k-1}\left[P_{\mathrm{H}^{R_M}}(0,t) + P_{\mathrm{H}^{R_M \cup S}}(0,t)\right]. \qquad (47)$$

The expectation of the payment of nominal amount at maturity of the contract is

$$E\left[e^{-\mathrm{rT}} I_{\tau_k > T} I_{\tau_C > T}\right] = e^{-\mathrm{rT}} D_k(T). \qquad (48)$$

By (43), the kth-to-default CLN premium rate is given by

$$c_k = \frac{1 - \rho\int_0^T e^{-\mathrm{rt}} Q_k(t)\mathrm{d}t - e^{-\mathrm{rT}} D_k(T)}{\int_0^T e^{-\mathrm{rt}} D_k(t)\mathrm{d}t}. \qquad (49)$$

4. Numerical Analysis

In this section, we perform numerical experiments to show how the correlated default risk may affect the premium rates. We will investigate the sensitivity of the premium rates to the parameters of our model.

4.1. kth-to-Default CDS. The parameters of the model are assumed to be

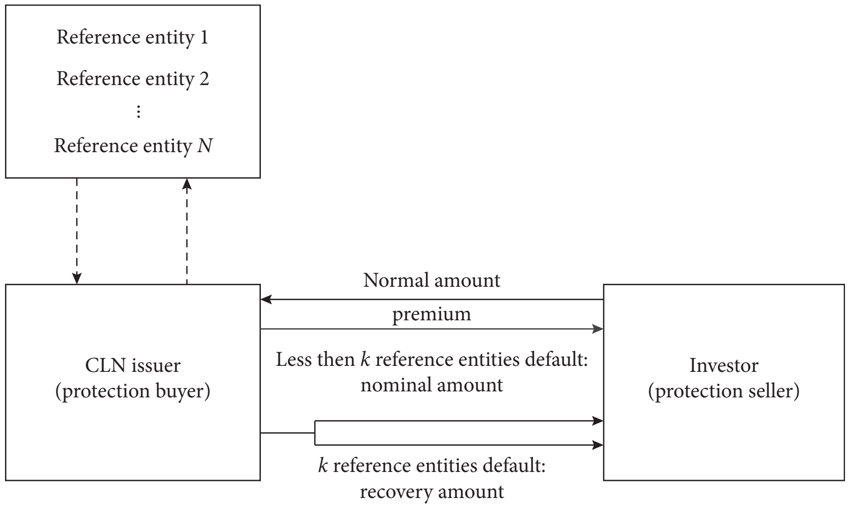

FIGURE 2: The cash flow of the kth-to-default CLN.

$$\begin{gathered}\rho = 0.4,\\ r = 0.04,\\ \alpha_{R_i}^{S} = 1.1,\\ \alpha_{C}^{S} = 1.1,\\ \alpha_{R_j}^{R_i} = 1.1,\\ \alpha_{C}^{R_i} = 1.1,\\ \lambda_0^{S} = 0.05,\\ \sigma = 0.2,\\ k = 0.3,\\ \theta = 0.02,\\ l = 0.3,\\ \mu = 0.15,\\ T = 5.\end{gathered} \tag{50}$$

For convenience of calculation, we assume

$$a_{R_i}(t) = a_C(t) = 0.1. \tag{51}$$

We take a basket CDS with ten reference entities, for example. Table 1 lists the kth-to-default CDS premium rates for $k = 1, \dots, 10$.

The CDS premium rates decrease as k increases because the default probability of k reference entities decreases with increasing of k. Lower default probability leads to lower premium rates. The premium rates tend to 0 with increasing of k.

We analyze the effects of the default correlation on kth-to-default CDS premium rates for $k = 1, 4$.

The numerical calculation shows that the defaults of other reference entities have no effects on the 1st-to-default CDS. The premium rates of kth-to-default CDS have similar trends on the default correlation for $k = 2, 3, \dots, 10$. We just choose immediate number 4 to illustrate the trends.

TABLE 1: The premium rates of the kth-to-default CDS.

kth	Premium rate (%)
1st	60.3724
2nd	28.7716
3rd	17.2977
4th	13.5195
5th	8.3919
6th	4.4503
7th	1.8347
8th	0.4272
9th	0.0565
10th	0.0000009

Figure 3 illustrates that kth-to-default CDS premium rates are increasing functions of $\alpha_{R_i}^{S}$ $(i \in I)$ because the reference entities become more risky with higher $\alpha_{R_i}^{S}$, and a higher default risk leads to a higher premium rate.

Figure 4 illustrates that kth-to-default CDS premium rates are decreasing functions of α_C^S because the counterparty becomes more risky with higher α_C^S, and a higher counterparty risk leads to a lower premium rate.

Figure 5 illustrates that kth-to-default CDS $(k \geq 2)$ premium rates are increasing functions of $\alpha_{R_j}^{R_i}$ $(i \in I, j \in I \setminus \{i\})$ because the reference entities become more risky with high $\alpha_{R_j}^{R_i}$, and a higher default risk leads to a higher premium rate. The contagion risk has no effect on 1th-to-default CDS because the contract will be terminated if any reference entity defaulted.

Figure 6 illustrates that kth-to-default CDS $(k \geq 2)$ premium rates are decreasing functions of $\alpha_C^{R_i}$ $(i \in I)$ because the counterparty becomes more risky with high $\alpha_C^{R_i}$, and a higher counterparty risk leads to a lower premium rate. The contagion risk has no effect on 1st-to-default CDS because the contract will be terminated if any reference entity defaulted.

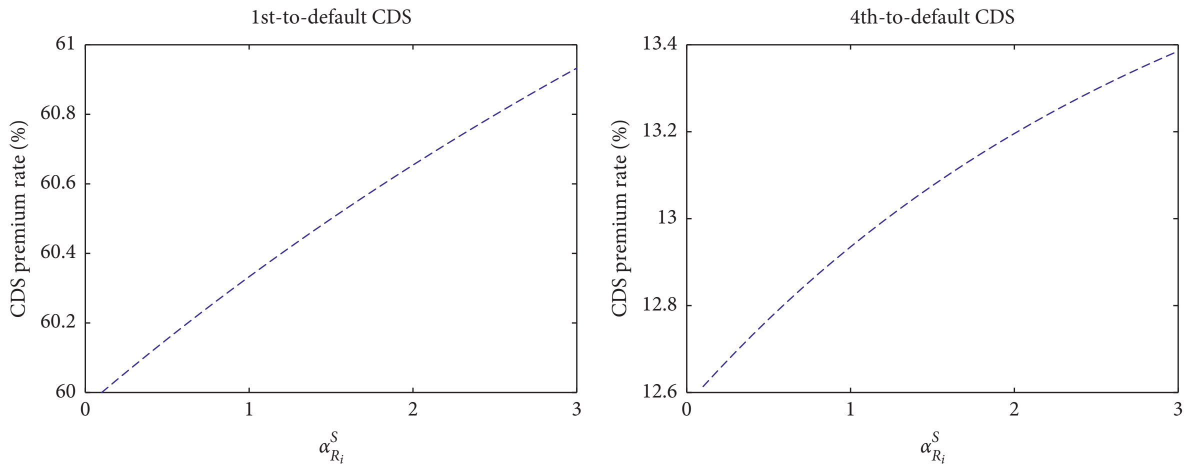

(a)

(b)

Figure 3: The premium rates of the kth-to-default CDS.

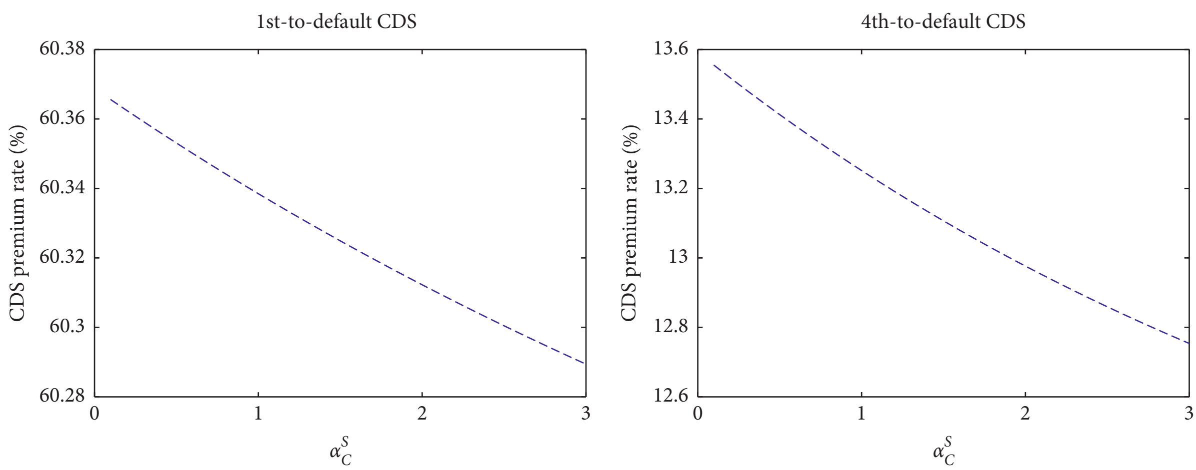

(a)

(b)

Figure 4: The premium rates of the kth-to-default CDS.

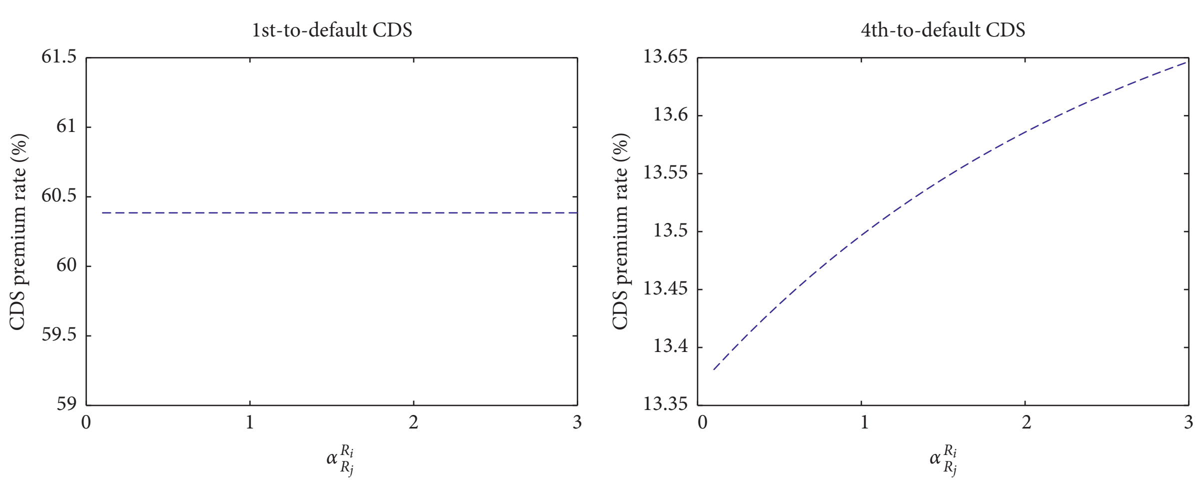

(a)

(b)

Figure 5: The premium rates of the kth-to-default CDS.

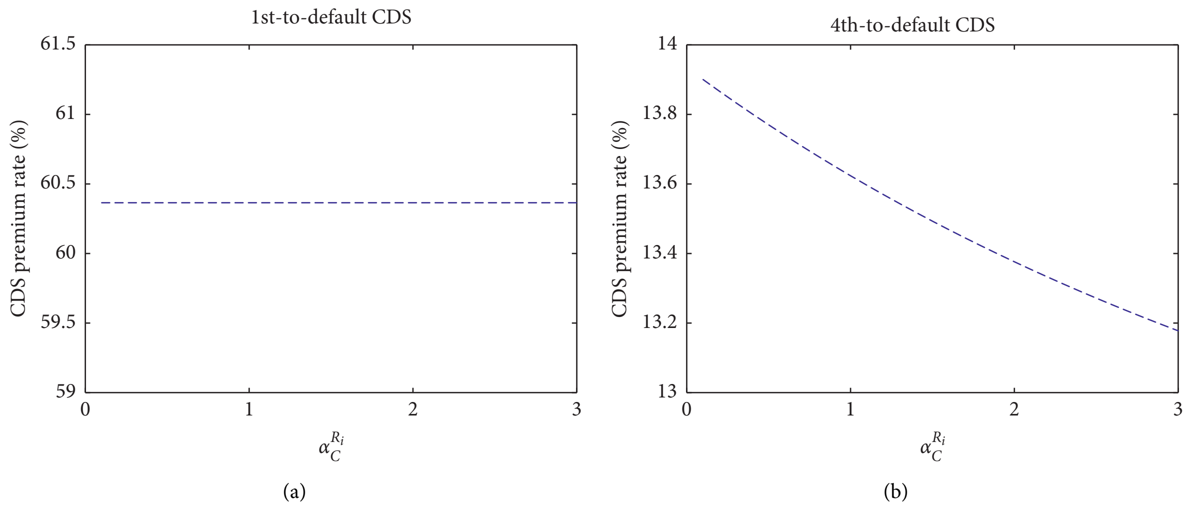

Figure 6: The premium rates of the kth-to-default CDS.

Table 2: The premium rates of the kth-to-default CLN.

kth	Premium rate (%)
1st	64.9980
2nd	33.4078
3rd	21.3288
4th	17.3264
5th	12.6668
6th	8.4503
7th	5.8347
8th	4.9583
9th	4.0034
10th	4.00000853

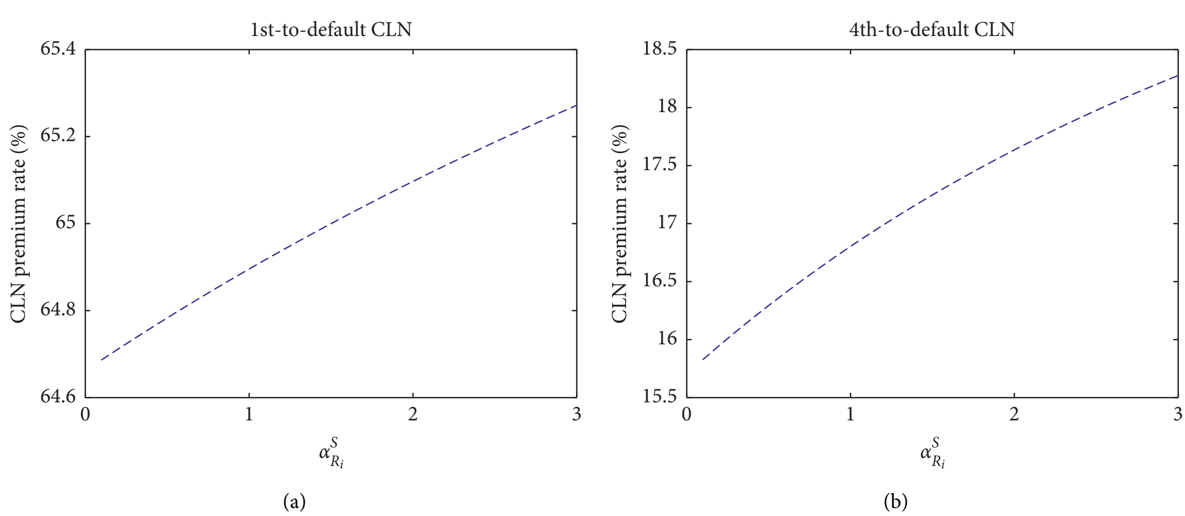

Figure 7: The premium rates of the kth-to-default CLN.

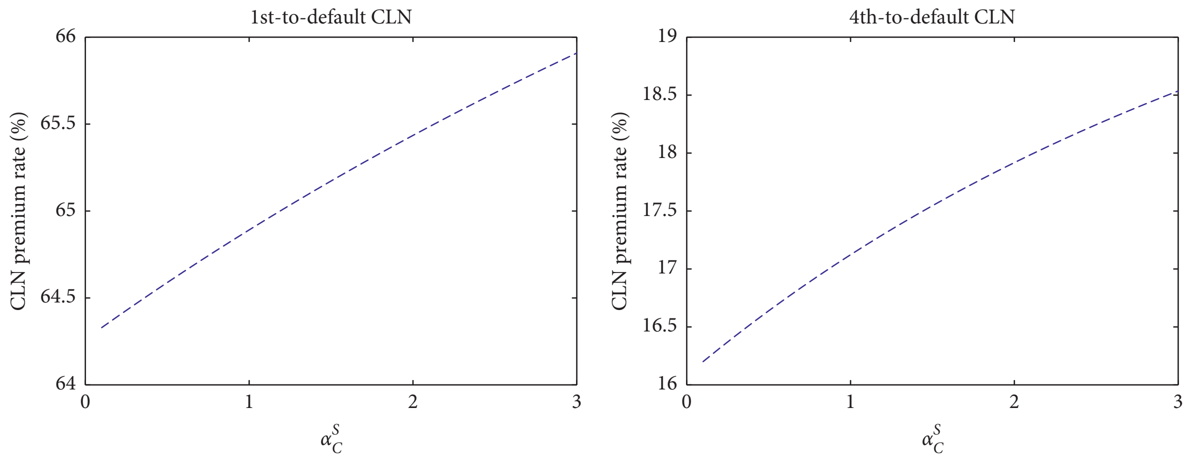

(a) (b)

Figure 8: The premium rates of the kth-to-default CLN.

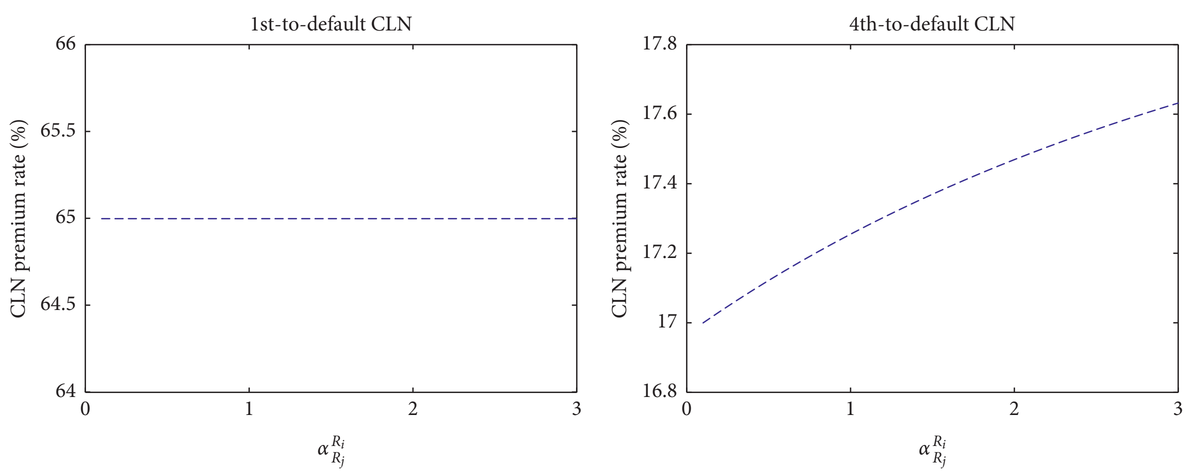

(a) (b)

Figure 9: The premium rates of the kth-to-default CLN.

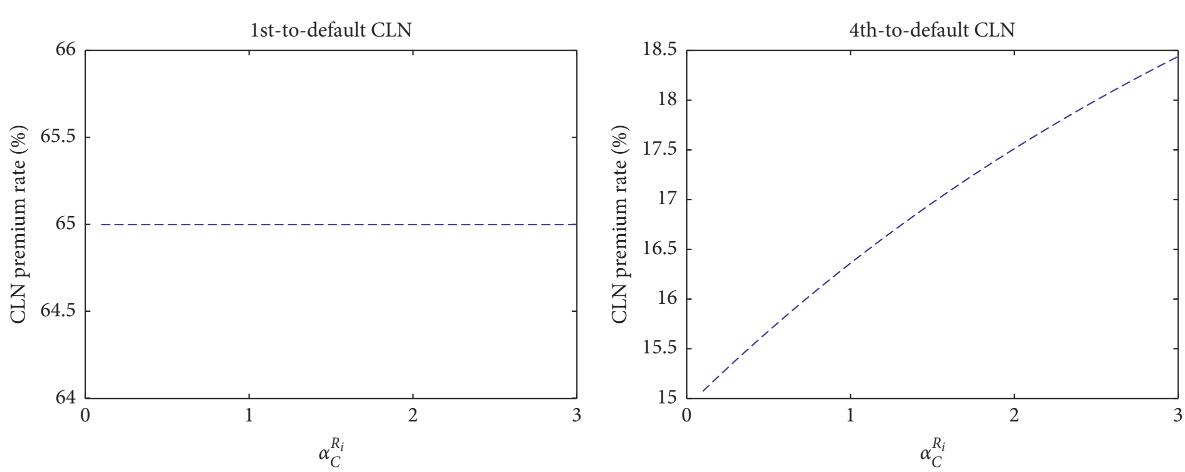

(a) (b)

Figure 10: The premium rates of the kth-to-default CLN.

4.2. kth-to-Default CLN. The parameters of the model are assumed to be

$$\begin{aligned} \rho &= 0.6, \\ r &= 0.04, \\ \alpha_{R_i}^S &= 1.1, \\ \alpha_C^S &= 1.1, \\ \alpha_{R_j}^{R_i} &= 1.1, \\ \alpha_C^{R_i} &= 1.1, \\ \lambda_0^S &= 0.05, \\ \sigma &= 0.2, \\ k &= 0.3, \\ \theta &= 0.02, \\ l &= 0.3, \\ \mu &= 0.15, \\ T &= 5. \end{aligned} \tag{52}$$

For convenience of calculation, we assume

$$a_{R_i}(t) = a_C(t) = 0.1. \tag{53}$$

We take a basket CLN with ten reference entities, for example. Table 2 lists the kth-to-default CLN premium rates for $k = 1, \ldots, 10$.

The premium rates of the BCLN on k have similar trends as the premium rate of BCDS. However, the premium rates tend to the risk-free interest rate with the increase of k.

The effects of the default correlation on kth-to-default CLN premium rates are demonstrated for $k = 1, 4$. The numerical calculation shows that the defaults of other reference entities have no effects on the 1st-to-default CLN. The premium rates of the kth-to-default CLN have similar trends on the default correlation for $k = 2, 3, \ldots, 10$. We just choose immediate number 4 to illustrate the trends.

Figure 7 illustrates that the premium rates of BCLN are increasing functions of $\alpha_{R_i}^S$ $(i \in I)$, which is the same as the BCDS case.

Figure 8 illustrates that kth-to-default CLN premium rates are increasing functions of α_C^S which is different from the BCDS case because the counterparty in the BCLN is the protection buyer.

Figure 9 illustrates that the kth-to-default $(k \geq 2)$ CLN premium rates are increasing functions of $\alpha_{R_j}^{R_i}$ $(i \in I, j \in I \setminus \{i\})$, which is the same as the BCDS case. The contagion risk also has no effect on the 1st-to-default CLN.

Figure 10 illustrates that kth-to-default $(k \geq 2)$ CLN premium rates are increasing functions of $\alpha_C^{R_i}$ $(i \in I)$, which is different from the BCDS case because the counterparty in the BCLN is the protection buyer. The contagion risk also has no effect on the 1st-to-default CLN.

5. Conclusion

In this paper, we use a Markov chain model with interacting intensities to compute the kth-to-default CDS and kth-to-default CLN premium rates. We model the default correlation among the names in the portfolio by an external shock as well as the defaults of other names in the portfolio. By presenting a general infinitesimal generator matrix of $2^{N+2} \times 2^{N+2}$ dimension, we obtain the joint distribution of default times. Then, the formulas of kth-to-default CDS and kth-to-default CLN premium rates are calculated. In numerical analysis, we show that the premium rates decrease as k increases, and the contagion risk does not affect the 1st-to-default premium rate. Our numerical results also show the effects of correlated risks between the counterparty and reference entities on the premium rates. Due to different product structures between BCDS and BCLN, the impacts of the contagion risk on premium rates are different.

Data Availability

The data in this paper can be used publicly.

Conflicts of Interest

The authors declare that they have no conflicts of interest.

Acknowledgments

This work was supported by the National Natural Science Foundation of China (nos. 11671291 and 11901420) and Humanities and Social Science Research Projects in the Ministry of Education (no. 20YJAZH025).

References

[1] D. X. Li, “On default correlation,” *The Journal of Fixed Income*, vol. 9, no. 4, pp. 43–54, 2000.

[2] P. Schőnbucher and D. Schubert, “Copula-dependent defaults in intensity models,” *SSRN Electronic Journal*, vol. 63, Article ID 301968, 2001.

[3] D. Brigo and A. Capponi, “Bilateral counterparty risk valuation with stochastic dynamical models and application to credit default swaps,” Cornell University, Ithaca, NY, USA, 2008, http://arxiv.org/abs/0812.3705.

[4] F. Jean-David, “Recent developments in copula models,” *Econometrics*, vol. 5, no. 3, pp. 34–43, 2017.

[5] D. Wang and N. Gârleanu, “Risk and valuation of collateralized debt obligations,” *Financial Analysts Journal*, vol. 57, no. 1, pp. 41–59, 2001.

[6] K. Giesecke, “A simple exponential model for dependent defaults,” *The Journal of Fixed Income*, vol. 13, no. 3, pp. 74–83, 2003.

[7] X. Liang, G. Wang, and H. Li, “Pricing credit default swaps with bilateral counterparty risk in a reduced form model with Markov regime switching,” *Applied Mathematics and Computation*, vol. 230, pp. 290–302, 2014.

[8] R. A. Jarrow and F. Yu, “Counterparty risk and the pricing of defaultable securities,” *The Journal of Finance*, vol. 56, no. 5, pp. 1765–1799, 2001.

[9] H. Zheng and L. Jiang, "Basket cds pricing with interacting intensities," *Finance and Stochastics*, vol. 13, no. 3, pp. 445–469, 2009.
[10] Y. Dong and G. Wang, "Bilateral counterparty risk valuation for credit default swap in a contagion model using Markov chain," *Economic Modelling*, vol. 40, no. 2, pp. 91–100, 2014.
[11] J. C. Hull and A. D. White, "Valuation of a CDO and an n -th to default CDS without Monte Carlo simulation," *The Journal of Derivatives*, vol. 12, no. 2, pp. 8–23, 2004.
[12] M. B. Walker, "Credit default swaps with counterparty risk: a calibrated markov model," *Journal of Credit Risk*, vol. 2, no. 1, pp. 24–39, 2006.
[13] F. Yu, "Correlated defaults in intensity-based models," *Mathematical Finance*, vol. 17, no. 2, pp. 155–173, 2007.
[14] R. Frey and J. Backhaus, "Pricing and hedging of portfolio credit derivatives with interacting default intensities," *International Journal of Theoretical and Applied Finance*, vol. 11, no. 6, pp. 611–634, 2008.
[15] P.-C. Wu, "Applying a factor copula to value basket credit linked notes with issuer default risk," *Finance Research Letters*, vol. 7, no. 3, pp. 178–183, 2010.
[16] A. Herbertsson, J. Jang, and T. Schmidt, "Pricing basket default swaps in a tractable shot noise model," *Statistics & Probability Letters*, vol. 81, no. 8, pp. 1196–1207, 2011.
[17] T. Wang, J. Liang, and X. Yang, "Pricing for basket cds and lcds," *Modern Economy*, vol. 03, no. 02, pp. 171–178, 2012.
[18] P. Li and Z.-Z. Li, "Change analysis for the dependence structure and dynamic pricing of basket default swaps," *European Financial Management*, vol. 21, no. 4, pp. 646–671, 2013.
[19] A. Esfahanipour and R. Jahanbin, "An application of genetic network programming model for pricing of basket default swaps (bds)," *AUT Journal of Modeling and Simulation*, vol. 49, no. 1, pp. 13–22, 2017.
[20] Y. Dong, K. C. Yuen, and K. Chuen Yuen, "Pricing credit derivatives under a correlated regime-switching hazard processes model," *Journal of Industrial & Management Optimization*, vol. 13, no. 3, p. 1395, 2017.
[21] J. Guo, Y. Dong, and G. Wang, "Basket CDS pricing with default intensities using a regime-switching shot-noise model," *Communications in Statistics - Theory and Methods*, vol. 47, no. 18, pp. 4443–4458, 2018.
[22] K. S. Leung and Y. K. Kwok, "Counterparty risk for credit default swaps: Markov chain interacting intensities model with stochastic intensity," *Asia-Pacific Financial Markets*, vol. 16, no. 3, pp. 169–181, 2009.

Hindawi
Mathematical Problems in Engineering
Volume 2020, Article ID 4613536, 9 pages
https://doi.org/10.1155/2020/4613536

Research Article

A Fourier-Cosine Method for Pricing Discretely Monitored Barrier Options under Stochastic Volatility and Double Exponential Jump

Shoude Huang and **Xunxiang Guo**

School of Economic Mathematics, Southwestern University of Finance and Economics, Chengdu 611130, Si Chuan, China

Correspondence should be addressed to Xunxiang Guo; xguo3@swufe.edu.cn

Received 23 May 2020; Accepted 30 September 2020; Published 13 October 2020

Academic Editor: Wenguang Yu

In this paper, the valuation of the discrete barrier options on the condition that the underlying asset price process follows the GARCH volatility and double exponential jump is studied. We derived an analytical approximation of the characteristic function for the underlying log-asset price. Then, a quasianalytical approximate formula of the price of the discrete barrier option is obtained based the on Fourier-cosine method. Numerical examples show that the Fourier-cosine method is fast and efficient for pricing discrete barrier options compared with the Monte Carlo simulation method. Finally, the influences of some important parameters on the prices of discrete barrier options are studied to further illustrate the rationality of the model.

1. Introduction

Since it was proposed in 1973, the well-known Black-Scholes-Merton (BS) model [1] is often applied in financial industries because the analytic solution of European option under the risk-neutral measure has been obtained by assuming that the underlying price process follows the geometric Brownian motion. In order to hedge and manage the risk, more options were created, such as American options and exotic options. Barrier option is one of the most actively traded exotic options in international financial derivative markets because of lower cost. For example, the gross market value of the Over-the-Counter (OTC) barrier options accounted for a significant proportion in the US foreign exchange option market in 2018. And many participants maintain considerable barrier option portfolios, which call for associated valuation and risk management tools for these securities in foreign exchange markets.

In view of the important role of barrier options, barrier option pricing is a significant problem in the theoretical researches and applications. Under the BS model framework, closed-form solutions for all kinds of European style barrier options have been obtained [2–4]. But many studies have shown that jump exists in the prices of various financial assets, such as stocks and commodities, especially after financial crises or major natural disasters happen, while the above-mentioned literatures did not take jumps into account. Kou and Wang [5] proposed a jump-diffusion model and obtained analytical solution of the European style barrier options using the Laplace transform method, where the jump size is assumed to follow a double exponential distribution.

In financial engineering, the discretely monitored barrier options are becoming a research focus. A growing number of researchers are becoming interested in the valuation of discretely monitored options. Feng and Linetsky [6] proposed the fast Hilbert transform method to obtain the price of the discretely monitored barrier options under Lévy models. Fusai, Germano, and Marazzina [7] utilized Wiener-Hopf factorization to obtain the price of discretely monitored barrier options under exponential Lévy models. Lian, Zhu, Elliott, and Cui [8] proposed a semianalytical solution for the valuation of the discrete barrier options given that the underlying asset price process was driven by a time-dependent Lévy process. Sobhani and Milev [9] presented a Legendre multiwavelets method for pricing discrete double barrier options. Thakoor, Tangman, and Bhuruth [10] proposed a novel spectral method by discretizing the pricing equation of the discrete barrier options whose price process is modelled by the stochastic Alpha Beta Rho (SABR) model. Liu and Zhang [11] proposed a novel jump-diffusion model in present of liquidity risk and derived an approximate solution for the valuation of the discrete barrier options.

Unfortunately, these mentioned models are assumed that the volatility is constant. This is different from the well-known facts of empirical researches such as volatility smile or smirk. To overcome these shortcomings, many researchers proposed stochastic volatility models, among which the popular models are raised by Stein and Stein [12], Heston [13]. But a large number of studies have shown that the square-root process setup of the Heston model does not perform well in applications and cannot describe some of the stylized facts observed from the financial time series. For the past few years, the generalized autoregressive conditional heteroskedasticity (GARCH) model proposed by Nelson [14] has attracted extensive attention. Christoffersen P.et al. [15] and Chourdakis and Dotsis [16] further studied the GARCH model and found that the GARCH model describes the features of observations from the option markets much better than other stochastic volatility models, including the Heston model. In addition, Huang et al. [17] reached the same conclusion after their empirical study on Shanghai Stock Exchange (SSE) 50 ETF option.

In this paper, we focus on the valuation of discretely monitored barrier options under the GARCH volatility and double exponential jump. Since there is no analytical formula for the characteristic function of the underlying asset log-price, a perturbation method is applied to derive an analytical approximation of the characteristic function for the log-price of the underlying asset. Moreover, we obtain an approximate price for the discretely monitored barrier option using the Fourier-cosine method proposed by Fang and Oosterlee [18]. Fourier-cosine method, as an alternative to the fast Fourier transform, was firstly proposed by Fang and Oosterlee. It can improve the speed of pricing and achieve an exponential convergence rate for European options. This method has been widely used in option pricing, such as Fang and Oosterlee [19, 20], Zhang and Geng [21], and Li and Zhang et al. [11]. Finally, some numerical simulations and sensitivity analysis are proposed to explain our results, and some economic implications of these results are discussed to demonstrate some interesting phenomena.

An outline of this paper is as follows. Section 2 sets up an option pricing model based on the GARCH volatility and double exponential jump. The approximation of the characteristic function for the underlying asset log-asset price is derived. And an approximate price for discretely monitored barrier option is also derived in Section 3. Some numerical examples and sensitivity analysis are provided to explain our results in Section 4. We conclude the paper in Section 5.

2. Model Specification

Let $\{\Omega, \mathscr{F}, \{\mathscr{F}_t\}_{0\le t\le T}, \mathbb{Q}\}$ be a complete probability space with a filtration continuous on the right line, where $\mathbb{Q}$ is a risk-neutral probability. The price process of the underlying asset S_t and the process of the volatility v_t are specified under the risk-neutral measure $\mathbb{Q}$ as follows:

$$\frac{dS_t}{S_t} = (r - \lambda m)dt + \sqrt{v_t}dW_{s,t} + \left(e^J - 1\right)dN_t, \quad (1)$$

$$dv_t = k(\theta - v_t)dt + \sigma v_t\left(\rho dW_{s,t} + \sqrt{\left(1-\rho^2\right)}\, dW^{\perp}_{v,t}\right), \quad (2)$$

where $\mathrm{Cov}(dW_{s,t}, dW_{v,t}) = \rho dt$. And k, θ, σ mean the speeds of the mean reversion, long-run volatility, and instantaneous volatility of the process v_t, respectively. N_t is a Poisson process with constant intensity $\lambda, m = E^{\mathbb{Q}}(e^J - 1)$. Jump size J is a random variable and follows an asymmetric double exponential distribution with the density

$$f(J) = p\eta_1 e^{-\eta_1 J}1_{\{J\ge 0\}} + q\eta_2 e^{\eta_2 J}1_{\{J<0\}}, \quad \eta_1 > 1, \eta_2 > 0, \quad (3)$$

where $p, q \le 1, p + q = 1$ are probability of up-move jump and probability of down-move jump, respectively. So we can obtain that $m = p\eta_1/\eta_1 - 1 + q\eta_2/\eta_2 + 1 - 1$.

Let $x_t = \ln S_t/K$. We can transform the equations (1) and (2) into the following equations (4) and (5), respectively:

$$dx_t = \left(r - \lambda m - \frac{v_t}{2}\right)dt + \sqrt{v_t}dW_{s,t} + J dN_t, \quad (4)$$

$$dv_t = k(\theta - v_t)dt + \sigma v_t\left(\rho dW_{s,t} + \sqrt{\left(1-\rho^2\right)}\, dW^{\perp}_{v,t}\right). \quad (5)$$

3. Valuation of Discretely Monitored Barrier Options

In this section, we derived the approximate characteristic function of the underlying log-asset price. Then we obtain the approximate prices of discretely monitored barrier options via the Fourier-cosine method based on the proposed model.

3.1. Derivation of Approximate Characteristic Function. Following Caldana and Fusai [22], the characteristic function of x_T under the risk-neutral $\mathbb{Q}$ is defined by

$$\Phi(x, v, \tau; u) = E^{\mathbb{Q}}\left[e^{iux_T} | tx_t n = qxh, v_t x = 7v\right], \quad (6)$$

where $T \ge t, \tau = T - t, i = \sqrt{-1}$. Then we can obtain the following theorem.

Theorem 1. *Given that the underlying asset price follows the dynamics in equations (1) and (2). The approximate characteristic function for x_T is given by*

$$\Phi(x, v, \tau; u) = \exp(iux + A(u, \tau)v + B(u, \tau)), \tag{7}$$

where

$$\begin{aligned}
A(u,\tau) &= \alpha_0 \frac{1 - e^{-\alpha\tau}}{-\beta_2 + \beta_1 e^{-\alpha\tau}}, \\
B(u,\tau) &= -\frac{1}{2}\theta A(\tau, u) \\
&\quad - \frac{\alpha_3}{\alpha_2}\left[\beta_1 \tau + \ln\left(\frac{-\beta_2 + \beta_1 e^{-\alpha\tau}}{\alpha}\right)\right] \\
&\quad + ((r - \lambda m)iu + \lambda\Lambda(u))\tau - \frac{1}{4}\theta\left(iu + u^2\right)\tau, \\
\alpha_0 &= -\frac{1}{2}\left(iu + u^2\right), \\
\alpha_1 &= \frac{3}{2}\theta^{\frac{1}{2}}\sigma\rho iu - k, \\
\alpha_2 &= \sigma^2\theta, \\
\beta_1 &= \frac{\alpha_1 + \alpha}{2}, \\
\beta_2 &= \frac{\alpha_1 - \alpha}{2}, \\
\alpha &= \sqrt{\alpha_1^2 - 4\alpha_0\alpha_2}, \\
\alpha_3 &= \frac{1}{2}\theta k + \frac{1}{4}\sigma\rho iu\theta^{3/2}.
\end{aligned} \tag{8}$$

Proof. By Feynman-Kac theorem, $\Phi(x, v, \tau; u)$ satisfies the following PIDE:

$$\begin{aligned}
&-\frac{\partial\Phi}{\partial\tau} + \left(r - \frac{1}{2}v - \lambda m\right)\frac{\partial\Phi}{\partial x} + \frac{1}{2}v\frac{\partial^2\Phi}{\partial x^2} \\
&+ k(\theta - v)\frac{\partial\Phi}{\partial v} + \frac{1}{2}\sigma^2 v^2 \frac{\partial^2\Phi}{\partial v^2} \\
&+ \frac{\partial^2\Phi}{\partial x \partial v} v^{3/2}\sigma\rho + \lambda\int_{-\infty}^{+\infty} [\Phi(x + J) - \Phi(x)] f(J)\mathrm{d}J = 0.
\end{aligned} \tag{9}$$

The boundary condition for equation (9) is given by

$$\Phi(x, v, 0; u) = e^{iux_T}. \tag{10}$$

Notice that the integral term in equation (9),

$$\begin{aligned}
&\int_{-\infty}^{+\infty} [\Phi(x + J) - \Phi(x)] f(J)\mathrm{d}J \\
&= \int_{-\infty}^{+\infty} \left[E^{\mathbb{Q}}\left[e^{iu(x+J)}\right] - E^{\mathbb{Q}}\left[e^{iux}\right]\right] f(J)\mathrm{d}J \\
&= \int_{-\infty}^{+\infty} \left[E^{\mathbb{Q}}\left[e^{iux}\left(e^{iuJ} - 1\right)\right]\right] f(J)\mathrm{d}J \\
&= \int_{-\infty}^{+\infty} E^{\mathbb{Q}}\left[e^{iux}\right] E^{\mathbb{Q}}\left[e^{iuJ} - 1\right] f(J)\mathrm{d}J \\
&= \Phi(x, v, \tau; u)\Lambda(u),
\end{aligned} \tag{11}$$

where $\Lambda(u) = p\eta_1/\eta_1 - iu + q\eta_2/\eta_2 + iu - 1$. Equation (9) is very difficult to solve since it is a nonlinear PDE. So we first linearize it approximately. The idea is to approximate $v^{3/2}$, v^2 in the PIDE using Taylor expansions around the long-run mean of variance as follows:

$$v^2 \approx 2\theta v - \theta^2, \tag{12}$$

$$v^{3/2} \approx \frac{3}{2}\theta^{1/2} v - \frac{1}{2}\theta^{3/2}. \tag{13}$$

Substituting equations (11)–(13) into the PDE in equation (9), we have

$$\begin{aligned}
&-\frac{\partial\Phi}{\partial\tau} + \left(r - \frac{1}{2}v - \lambda m\right)\frac{\partial\Phi}{\partial x} + \frac{1}{2}v\frac{\partial^2\Phi}{\partial x^2} \\
&+ k(\theta - v)\frac{\partial\Phi}{\partial v} + \frac{1}{2}\sigma^2\left(2\theta v - \theta^2\right)\frac{\partial^2\Phi}{\partial v^2} \\
&+ \frac{\partial^2\Phi}{\partial x \partial v}\left(\frac{3}{2}\theta^{1/2} v - \frac{1}{2}\theta^{3/2}\right)\sigma\rho + \lambda\Phi(x, v, \tau; u)\Lambda(u) = 0.
\end{aligned} \tag{14}$$

According to Duffie et al. [23], this PDE has an exponential-affine solution of the form

$$\Phi(x, v, \tau; u) = \exp(iux + A(u, \tau) + B(u, \tau)v), \tag{15}$$

with the boundary conditions

$$A(u, 0) = B(u, 0) = 0. \tag{16}$$

Substituting equation (15) into equation (14) yields

$$\begin{aligned}
&-\left(\frac{\partial A}{\partial\tau}v + \frac{\partial B}{\partial\tau}\right) + \left(r - \lambda m - \frac{v}{2}\right)iu + \frac{1}{2}v(iu)^2 \\
&+ k(\theta - v)A + \frac{\sigma^2}{2}\left(2\theta v - \theta^2\right)A^2 \\
&+ \left(\frac{3}{2}\theta^{1/2} v - \frac{1}{2}\theta^{3/2}\right)\sigma\rho iuA + \lambda\Lambda(u) = 0.
\end{aligned} \tag{17}$$

By matching coefficients, we can derive the following two ordinary differential equations (ODEs):

$$\frac{\partial A}{\partial \tau} = \sigma^2\theta A^2 + \left(\frac{3}{2}\theta^{1/2}\sigma\rho i u - k\right)A - \frac{1}{2}\left(iu + u^2\right), \tag{18}$$

$$\frac{\partial B}{\partial \tau} = (r - \lambda m)iu + k\theta A - \frac{1}{2}\sigma^2\theta^2 A^2 - \frac{1}{2}\sigma\rho\theta^{3/2} iuA + \lambda\Lambda(u). \tag{19}$$

Since the ODE (18) is a Riccati equation, its general solution is

$$A(u,\tau) = \alpha_0 \frac{1 - e^{-\alpha\tau}}{-\beta_2 + \beta_1 e^{-\alpha\tau}}, \tag{20}$$

where

$$\begin{aligned} \alpha_0 &= -\frac{1}{2}\left(iu + u^2\right), \\ \alpha_1 &= \frac{3}{2}\theta^{1/2}\sigma\rho i u - k, \\ \alpha_2 &= \sigma^2\theta, \\ \beta_1 &= \frac{\alpha_1 + \alpha}{2}, \\ \beta_2 &= \frac{\alpha_1 - \alpha}{2}, \\ \alpha &= \sqrt{\alpha_1^2 - 4\alpha_0\alpha_2}. \end{aligned} \tag{21}$$

Multiplying $\theta/2$ on both sides of equation (18), and substituting it into equation (19), we can obtain:

$$\begin{aligned} \frac{\partial B}{\partial \tau} &= (r - \lambda m)iu + \left(\frac{1}{2}\theta k + \frac{1}{4}\sigma\rho i u\theta^{3/2}\right)A \\ &\quad - \frac{1}{4}\theta\left(iu + u^2\right) - \frac{\theta}{2}\frac{\partial A}{\partial \tau} + \lambda\Lambda(u). \end{aligned} \tag{22}$$

Integrating on both sides of the above equation, we have the following result:

$$\begin{aligned} B(\tau,u) &= -\frac{1}{2}\theta A(\tau,u) - \frac{\alpha_3}{\alpha_2}\left[\beta_1\tau + \ln\left(\frac{-\beta_2 + \beta_1 e^{-\alpha\tau}}{\alpha}\right)\right] \\ &\quad + ((r - \lambda m)iu + \lambda\Lambda(u))\tau - \frac{1}{4}\theta\left(iu + u^2\right)\tau, \end{aligned} \tag{23}$$

where

$$\alpha_3 = \frac{1}{2}\theta k + \frac{1}{4}\sigma\rho i u\theta^{3/2}. \tag{24}$$

This finished the proof of Theorem 1. □

Remark 1. Once that the analytic expression of the characteristic function has been obtained, the cumulant of $\ln S_T$ can be computed, which will be used in the truncation of the computational domain of option pricing. Following Fang and Oosterlee [18], the n-th cumulant of $\ln S_T$ is given by

$$c_n = \frac{1}{i^n}\frac{\partial^n(\ln\Phi(u))}{\partial u^n}\Big|_{u=0}. \tag{25}$$

3.2. Valuation of Discretely Monitored Barrier Options. It is well known that according to whether the underlying asset price needs to pass or to avoid a certain barrier level to receive a payoff and whether it has the barrier above or below the initial underlying asset price, barrier options can be classified into four cases, i.e., up-and-out option, up-and-in option, down-and-out option, down-and-in option. Without loss of generality, we take knock-out options as an example to illustrate the derivation of pricing formulas of barrier option in this section. The payoff functions are shown in Table 1 for different discretely monitored knock-out barrier options with strike K, barrier level H, and maturity T.

Let $x := \ln(S_{t_{m-1}}/K)$ and $y := \ln(S_{t_m}/K)$, $m = M, M-1, \ldots, 2$. Then the prices of discretely knock up-and-out and down-and-out barrier option, i.e., v_{OU} and v_{OD}, can be expressed as the following recursive formulas:

$$v_{\mathrm{OU}}(x,t_{m-1}) = \begin{cases} c(x,t_{m-1}), & x < h, \\ e^{-r(T-t_{m-1})}\mathrm{Rb}, & x \geq h, \end{cases} \tag{26}$$

$$v_{\mathrm{OD}}(x,t_{m-1}) = \begin{cases} e^{-r(T-t_{m-1})}\mathrm{Rb}, & x \leq h, \\ c(x,t_{m-1}), & x > h, \end{cases} \tag{27}$$

where

$$c(x,t_{m-1}) = e^{-r\Delta t}\int_{\mathbb{R}} v(y,t_m) f(y|x)\,\mathrm{d}y, \tag{28}$$

with

$$v(x,t_0) = e^{-r\Delta t}\int_{\mathbb{R}} v(y,t_1) f(y|x)\,\mathrm{d}y, \tag{29}$$

where $h = \ln H/K$, K is the strike price, T is the maturity, M is the monitoring date and H is the barrier level, Rb is a rebate, r denotes the risk-free interest rate; $v(x,t)$ and $c(x,t)$ are the option value and continuation value at time t, respectively; $f(y|x)$ is the probability density of y given x under the risk-neutral measure $\mathbb{Q}$.

Usually, the probability density function $f(y|x)$ is unknown. Fortunately, Fang and Oosterlee [18] proposed an approximation of the probability density function with a truncated region $[a,b]$ as follows:

$$f(y|x) \approx \frac{2}{b-a}\sum_{k=0}^{N-1'} \mathrm{Re}\left\{\Phi\left(\frac{k\pi}{b-a}\right)e^{ik\pi(x-a/b-a)}\right\}\cos\left(k\pi\frac{y-a}{b-a}\right), \tag{30}$$

where $\sum'$ means the summation whose first term is multiplied by 1/2, $\mathfrak{R}\{\cdot\}$ denotes taking the real part of a complex number. And $\Phi(u)$ is the conditional characteristic function of probability density function $f(y|x)$.

Table 1: Payoff functions for different types of discretely monitored knock-out barrier options.

Option type	Payoff
Up-and-out call	$[(S_T-K)^+-\mathrm{Rb}]1_{\{S_{t_i}<H\}}+\mathrm{Rb}$
Up-and-out put	$[(K-S_T)^+-\mathrm{Rb}]1_{\{S_{t_i}<H\}}+\mathrm{Rb}$
Down-and-out call	$[(S_T-K)^+-\mathrm{Rb}]1_{\{S_{t_i}>H\}}+\mathrm{Rb}$
Down-and-out put	$[(K-S_T)^+-\mathrm{Rb}]1_{\{S_{t_i}>H\}}+\mathrm{Rb}$

t_i is the observation date.

Replacing the $f(y|x)$ in equation (26) with its approximation equation (29) and interchanging summation and integration, the approximation of the continuation value $c(x;t_{m-1})$ can be obtained:

$$\hat{c}(x,t_{m-1})=e^{-r\Delta t}\frac{2}{b-a}\sum_{k=0}^{N-1}\mathfrak{R}'\left\{\Phi\left(\frac{k\pi}{b-a}\right)e^{ik\pi(x-a/b-a)}\right\}V_k(t_m), \tag{31}$$

where

$$V_k(t_m)=\frac{2}{b-a}\int_a^b v(y,t_m)\cos\left(k\pi\frac{y-a}{b-a}\right)\mathrm{d}y. \tag{32}$$

We know that barrier options are equivalent to European options at time $t\in[t_0,t_1]$. So the price of the discrete barrier option at initial time t_0 can be approximated as

$$\hat{v}(x,t_0)=e^{-r\Delta t}\sum_{k=0}^{N-1}\mathfrak{R}'\left\{\Phi\left(\frac{k\pi}{b-a}\right)e^{ik\pi(x-a/b-a)}\right\}V_k(t_1). \tag{33}$$

Now the key point is to obtain the coefficient $V_k(t_m), m=M,M-1,\ldots,1$. For the convenience of later description, we denote:

$$\begin{aligned}
\chi_k(x_1,x_2)&=\int_{x_1}^{x_2}e^x\cos\left(k\pi\frac{x-a}{b-a}\right)dx\\
&=\frac{1}{1+(k\pi b-a)^2}\left[\cos\left(k\pi\frac{x_2-a}{b-a}\right)e^{x_2}-\cos\left(k\pi\frac{x_1-a}{b-a}\right)e^{x_1}+\frac{k\pi}{b-a}\sin\left(k\pi\frac{x_2-a}{b-a}\right)e^{x_2}-\frac{k\pi}{b-a}\sin\left(k\pi\frac{x_1-a}{b-a}\right)e^{x_1}\right],\\
\psi_k(x_1,x_2)&=\int_{x_1}^{x_2}\cos\left(k\pi\frac{x-a}{b-a}\right)\mathrm{d}x\\
&=\begin{cases}\dfrac{b-a}{k\pi}\left[\sin\left(k\pi\dfrac{x_2-a}{b-a}\right)-\sin\left(k\pi\dfrac{x_1-a}{b-a}\right)\right], & k\neq 0,\\ x_2-x_1, & k=0.\end{cases}
\end{aligned} \tag{34}$$

When $m=M$, if $h<0$, we have the following results:

$$V_k(t_M)=\begin{cases}\dfrac{2}{b-a}\mathrm{Rb}\psi_k(h,b), & \text{for up}-\text{and}-\text{out call},\\[2ex] \dfrac{2}{b-a}\left[\mathrm{Rb}\psi_k(a,h)+K\chi_k(0,b)-K\psi_k(0,b)\right], & \text{for down}-\text{and}-\text{out call},\\[2ex] \dfrac{2}{b-a}\left[K\psi_k(a,h)-K\chi_k(a,h)+\mathrm{Rb}\psi_k(h,b)\right], & \text{for up}-\text{and}-\text{out put},\\[2ex] \dfrac{2}{b-a}\left[\mathrm{Rb}\psi_k(a,h)+K\psi_k(h,0)-K\chi_k(h,0)\right], & \text{for down}-\text{and}-\text{out put}.\end{cases} \tag{35}$$

If $h\geq 0$, then we can obtain the following result:

$$V_k(t_M) = \begin{cases} \dfrac{2}{b-a}\left[K\chi_k(0,h) - K\psi_k(0,h) + \mathrm{Rb}\psi_k(h,b)\right], & \text{for up} - \text{and} - \text{out call}, \\ \dfrac{2}{b-a}\left[\mathrm{Rb}\psi_k(a,h) + K\chi_k(h,b) - K\psi_k(h,b)\right], & \text{for down} - \text{and} - \text{out call}, \\ \dfrac{2}{b-a}\left[K\psi_k(a,0) - K\chi_k(a,0) + \mathrm{Rb}\psi_k(h,b)\right], & \text{for up} - \text{and} - \text{out put}, \\ \dfrac{2}{b-a}\mathrm{Rb}\psi_k(a,h), & \text{for down} - \text{and} - \text{out put}. \end{cases} \tag{36}$$

For $m = M-1, M-2, \ldots, 1$, we have the following theorem.

Theorem 2. *For the up-and-out option and down-and-out option, the recurrent coefficients $V_k(t_m)$ can be approximately expressed as follows:*

$$\widehat{V}_k(t_m) = \begin{cases} \widehat{C}_k(a,h,t_m) + e^{-r(T-t_m)}\mathrm{Rb}\dfrac{2}{b-a}\psi_k(h,tb), & \text{up} - \text{and} - \text{out}, \\ e^{-r(T-t_m)}\mathrm{Rb}\dfrac{2}{b-a}\psi_k(a,h) + \widehat{C}_k(h,b,t_m), & \text{down} - \text{and} - \text{out}, \end{cases} \tag{37}$$

where $\widehat{C}_k(x_1,x_2,t_m)$ can be approximately calculated by:

$$\widehat{C}_k(x_1,x_2,t_m) = e^{-r\Delta t}\mathrm{Re}\left\{\sum_{j=0}^{N-1}{}' \Phi\left(\frac{j\pi}{b-a}\right)\widehat{V}_j(t_{m+1})M_{k,j}(x_1,x_2)\right\}, \tag{38}$$

with

$$M_{kj}(x_1,x_2) = \frac{2}{b-a}\int_{x_1}^{x_2} e^{ij\pi(x-a/b-a)}\cos\left(k\pi\frac{x-a}{b-a}\right)\mathrm{d}x. \tag{39}$$

Proof. According to the payoff of discrete barrier options at time T, we can rewrite $v(y,T)$ as follows:

$$v(y,T) = \left[K\alpha(e^y - 1)^+ - \mathrm{Rb}\right]1_{\{y_{t_i} < h\}} + \mathrm{Rb}, \tag{40}$$

where $\alpha = 1$ for call option and $\alpha = -1$ for put option. Then we can obtain the above-mentioned results by the following computations.

For $m = M-1, M-2, \ldots, 1$, we have

$$\begin{aligned} V_k(t_m) &= \frac{2}{b-a}\int_a^b v(y,t_m)\cos\left(k\pi\frac{y-a}{b-a}\right)\mathrm{d}y \\ &= \frac{2}{b-a}\int_a^h v(y,t_m)\cos\left(k\pi\frac{y-a}{b-a}\right)\mathrm{d}y + \frac{2}{b-a}\int_h^b v(y,t_m)\cos\left(k\pi\frac{y-a}{b-a}\right)\mathrm{d}y \\ &= \frac{2}{b-a}\int_a^h c(y,t_m)\cos\left(k\pi\frac{y-a}{b-a}\right)\mathrm{d}y + \frac{2}{b-a}\int_h^b e^{-r(T-t_m)}\mathrm{Rb}\cos\left(k\pi\frac{y-a}{b-a}\right)\mathrm{d}y \\ &= C_k(a,h,t_m) + e^{-r(T-t_m)}\mathrm{Rb}\frac{2}{b-a}\psi_k(h,b). \end{aligned} \tag{41}$$

On the other hand, $c(y,t_m)$ can be approximated by $\widehat{c}(x,t_m)$, where

$$\widehat{c}(x,t_m) = e^{-r\Delta t}\sum_{k=0}^{N-1}{}' \mathrm{Re}\left\{\Phi\left(\frac{k\pi}{b-a}\right)e^{ik\pi(x-a/b-a)}\right\}V_k(t_{m+1}). \tag{42}$$

Table 2: Parameter values for the numerical experiments.

Parameter	r	λ	k	θ	σ	p	η_1	T	S_0	ρ	v_0	H	Rb	η_2
Value	0.05	3	5	0.2	0.7	0.3	10	1	100	−0.5	0.2	120	5	5

Table 3: Comparisons of the CPU time and accuracy for Fourier-cosine method(FC method) and the Monte Carlo simulation (MC Simulation) for pricing discrete up-and-out call barrier options.

M	K	FC method	MC simulation	Abs R.E.
4	90	3.6231	3.6681	1.23
	100	2.8640	2.9086	1.53
	110	2.4709	2.5083	1.49
	cpu time (sec)	1.142	110.952	
12	90	3.5703	3.6003	0.83
	100	3.0630	3.0909	0.90
	110	2.8221	2.8489	0.94
	cpu time (sec)	1.2721	144.136	
26	90	3.5709	3.6128	1.16
	100	3.1584	3.1882	0.93
	110	2.9740	2.9965	0.75
	cpu time (sec)	1.429	136.546	
52	90	3.5815	3.6216	1.10
	100	3.2239	3.2511	0.83
	110	3.0713	3.0892	0.58
	cpu time (sec)	1.492	197.555	
252	90	3.6075	3.6373	0.82
	100	3.3168	3.3343	0.52
	110	3.2021	3.2109	0.27
	cpu time(sec)	1.013	324.363	

Table 4: Comparisons of the CPU time and accuracy for Fourier-cosine method (FC method) and the Monte Carlo simulation(MC Simulation) for pricing discrete up-and-out put barrier options.

M	K	FC method	MC simulation	Abs R.E. (%)
4	90	15.3051	15.2912	0.09
	100	19.2898	19.2349	0.29
	110	23.6405	23.5468	0.04
	cpu time (sec)	1.219	237.383	
12	90	14.3355	14.2995	0.25
	100	17.7990	17.7157	0.47
	110	21.5291	21.4019	0.59
	cpu time (sec)	1.066	289.999	
26	90	13.8651	13.8281	0.27
	100	17.0935	17.0050	0.52
	110	20.5499	20.4138	0.67
	cpu time (sec)	1.099	136.546	
52	90	13.5387	13.5097	0.21
	100	16.6115	16.5350	0.46
	110	19.8893	19.7695	0.61
	cpu time (sec)	1.383	155.311	
252	90	13.0696	13.0470	0.17
	100	15.9276	15.8641	0.40
	110	18.9614	18.8627	0.52
	cpu time (sec)	1.170	113.495	

Substituting the above equation into $C_k(a,h,t_m)$, we can obtain $\widehat{C}_k(a,h,t_m)$ as follows: which is the approximate value of $C_k(a,h,t_m)$:

$$\begin{aligned}\widehat{C}_k(a,h,t_m) &= \frac{2}{b-a}\int_a^h \widehat{c}(y,t_m)\cos\left(k\pi\frac{y-a}{b-a}\right)dy \\ &= e^{-r\Delta t}\Re\left\{\sum_{j=0}^{N-1}\Phi'\left(\frac{j\pi}{b-a}\right)V_j(t_{m+1})\mathscr{M}_{k,j}(a,h)\right\},\end{aligned} \tag{43}$$

where

$$\mathscr{M}_{k,j}(a,h) := \frac{2}{b-a}\int_a^h e^{ij\pi(x-a/b-a)}\cos\left(k\pi\frac{x-a}{b-a}\right)dx. \tag{44}$$

Hence, $V_k(t_m)$ can be recovered from $V_k(t_{m+1})$. Finally, we substitute the approximation $\widehat{V}_k(t_1)$ into equation (28) to calculate the option price $\widehat{v}(x,t_0)$. □

4. Numerical Analysis

4.1. Comparison of the Approximate Solutions against Monte Carlo Simulations. In this section, some numerical examples are performed to show the performance of the Fourier-cosine method for pricing discrete barrier options against its alternative competitor, the Monte Carlo simulation, as a benchmark. We perform numerical examples on the discretely monitored up-and-out call and up-and-out put barrier options. Following Fang and Oosterlee [19], the integration interval [a, b] is chosen as follows:

$$[a,b] = \left[c_1 + a_0 - L\sqrt{c_2+\sqrt{c_4}}, c_1 + a_0 + L\sqrt{c_2+\sqrt{c_4}}\right], \tag{45}$$

with $a_0 = \ln S_0$, $L = 10$ and c_n is the n-th cumulant of $\ln S_T$.

For Monte Carlo method, we use 100,000 numbers of simulations, 200 numbers of time steps. Let $N = 2^{10}$ for Fourier-cosine method. The parameter values are listed in Table 2 for all our numerical examples. The computer used in the experiments equips an Intel Core $i3$ CPU with a 2.53 GHZ processor. And all of our numerical examples were performed using Matlab 2016a.

Our numerical results show that the Fourier-cosine method is fast and accurate for pricing discrete up-and-out barrier options. The absolute relative error (Abs R.E.) and CPU time information, comparing the Fourier-cosine method and the Monte Carlo simulation, are presented in Tables 3 and 4 for pricing discrete up-and-out call and put barrier options. Tables 3 and 4 also compares relative errors between the Fourier-cosine method and the Monte Carlo simulation for pricing discrete up-and-out call and put barrier options and they show that the Fourier-cosine method is significantly faster than Monte Carlo simulation. Furthermore, Tables 3 and 4 compare the pricing accuracy between the two methods across a range of strike prices, and

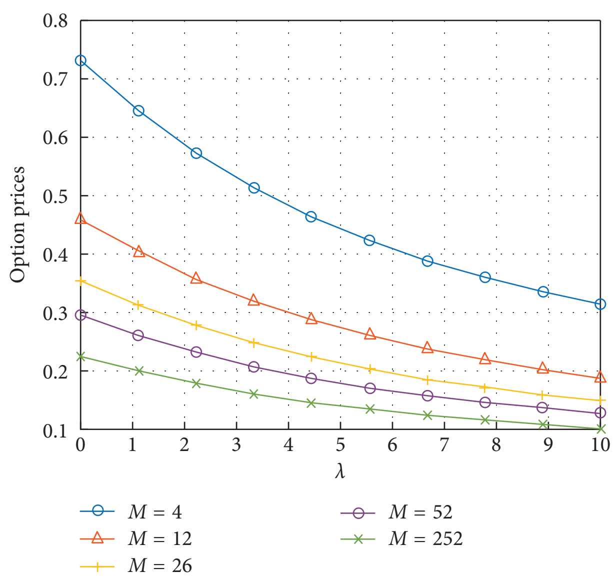

Figure 1: Prices of discrete up-and-out call barrier options with respect to the parameters of λ.

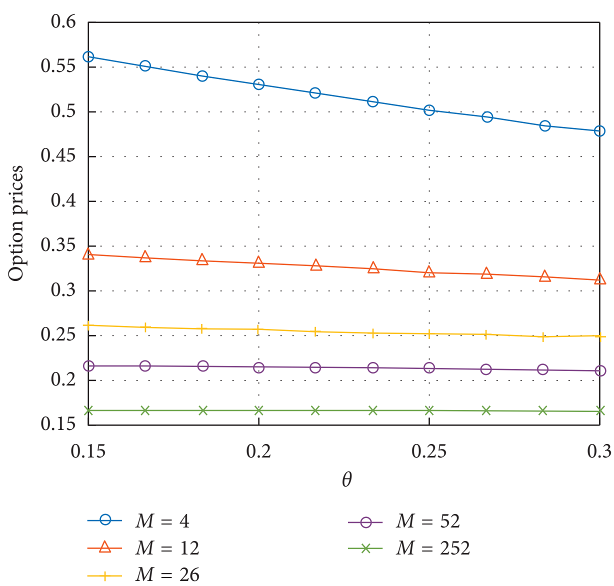

Figure 2: Prices of discrete up-and-out call barrier options with respect to θ.

the relative percentage of price differences of Fourier-cosine method are all less than 1.6%. Therefore, numerical results show that the Fourier-cosine method is accurate and effective.

4.2. Sensitivity Analysis of the Model Parameters. In this section, we will evaluate the impact of parameters on pricing discretely monitored up-and-out call barrier options. We mainly study the effects of the following parameters on the price of discretely monitored up-and-out call barrier options: (*i*) the jump intensity λ, (*ii*) the long-run mean level θ,

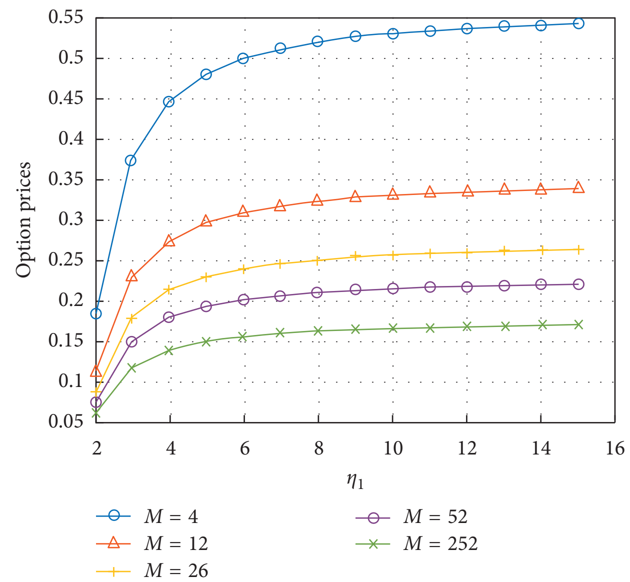

Figure 3: Prices of discrete up-and-out call barrier options with respect to the parameters of η_1.

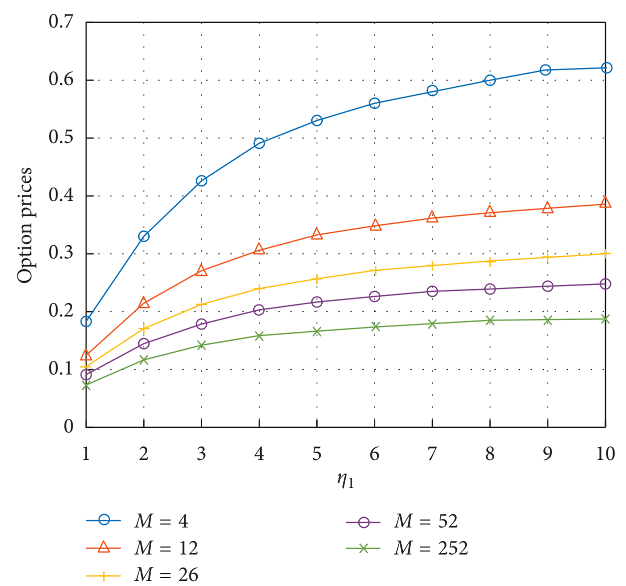

Figure 4: Prices of discrete up-and-out call barrier options with respect to the parameters of η_2.

(*iii*) the reciprocal of the mean for the positive jumps η_1, and (*iv*) the reciprocal of the mean for the negative jumps η_2.

Figures 1 and 2 show the variation trend of the price of the discrete knock up-out call barrier option with respect to the jump intensity λ and the long-run mean level θ, respectively. As shown in Figure 1, a higher jump intensity λ induces a lower price of discrete knock up-out call barrier option. The explanation for this phenomenon is that it makes the underlying asset price process more variable as the jump intensity λ increases. So it makes the underlying asset price more likely to cross the barrier level H at the monitoring dates. Therefore, the price of discrete up-and-out call barrier option is a decreasing function of the jump intensity λ. The implication of Figure 2 can be expressed in the similar way.

Figures 3 and 4 illustrate the effects of the reciprocal of the mean for the positive jumps η_1, and the negative jumps η_2 on the price of discrete knock up-out call barrier option. We can see that the price of discrete knock up-out call barrier option increases with respect to the parameters η_1 and η_2, respectively. The reason is that the probability density function of the underlying log-asset price becomes more leptokurtosis and heavy tails when the parameters η_1 and η_2 increase.

5. Conclusion

This paper proposed an efficient method for the valuating the discrete barrier options when the underlying asset price process is governed by the GARCH volatility and double exponential jump. We utilized Taylor expansion method to derive an analytical approximation of the characteristic function for the underlying log-asset price. Based on Fourier-cosine method, a quasianalytical approximate formula of the price of the discrete barrier is obtained. The Fourier-cosine method is fast and efficient for pricing discrete barrier options compared with Monte Carlo simulation. Finally, the sensitivities of some parameters in the model are provided to explain our results.

Data Availability

The data used to support the findings of this study are available from the corresponding author upon request.

Conflicts of Interest

The authors declare no conflicts of interest.

Acknowledgments

This research was financially supported by the Fundamental Research Funds for the Central Universities JBK2002003, and the authors gratefully acknowledge this support.

References

[1] F. Black and M. Scholes, "The pricing of options and corporate liabilities," *Journal of Political Economy*, vol. 81, no. 3, pp. 637–654, 1973.

[2] R. C. Merton, "Theory of rational option pricing," *The Bell Journal of Economics and Management Science*, vol. 4, no. 1, pp. 141–183, 1973.

[3] D. Rich, "The mathematical foundations of barrier option-pricing theory," *Advances in Futures and Options Research*, vol. 7, pp. 267–311, 1994.

[4] M. Rubinstein and E. Reiner, "Breaking down the barriers," *Risk*, vol. 4, pp. 28–35, 1991.

[5] S. G. Kou and H. Wang, "Option pricing under a double exponential jump diffusion model," *Management Science*, vol. 50, no. 9, pp. 1178–1192, 2004.

[6] L. Feng and V. Linetsky, "Pricing discretely monitored barrier options and defaultable bonds in lvy process models: a fast hilbert transform approach," *Mathematical Finance*, vol. 18, no. 3, pp. 337–384, 2008.

[7] G. Fusai, G. Germano, D. Marazzina, and S. identity, "Spitzer identity, Wiener-Hopf factorization and pricing of discretely monitored exotic options," *European Journal of Operational Research*, vol. 251, no. 1, pp. 124–134, 2016.

[8] G. Lian, S.-P. Zhu, R. J. Elliott, and Z. Cui, "Semi-analytical valuation for discrete barrier options under time-dependent Lévy processes," *Journal of Banking & Finance*, vol. 75, pp. 167–183, 2017.

[9] A. Sobhani and M. Milev, "A numerical method for pricing discrete double barrier option by legendre multiwavelet," *Journal of Computational and Applied Mathematics*, vol. 328, pp. 355–364, 2018.

[10] N. Thakoor, D. Y. Tangman, M. Bhuruth et al., "A spectral approach to pricing of arbitrage-free SABR discrete barrier options," *Computational Economics*, vol. 54, no. 3, pp. 1085–1111, 2019.

[11] Z. Li, W.-G. Zhang, Y.-J. Liu, and Y. Zhang, "Pricing discrete barrier options under jump-diffusion model with liquidity risk," *International Review of Economics & Finance*, vol. 59, pp. 347–368, 2019.

[12] E. M. Stein and J. C. Stein, "Stock price distributions with stochastic volatility: an analytic approach," *Review of Financial Studies*, vol. 4, no. 4, pp. 727–752, 1991.

[13] S. L. Heston, "A closed-form solution for options with stochastic volatility with applications to bond and currency options," *Review of Financial Studies*, vol. 6, no. 2, pp. 327–343, 1993.

[14] D. B. Nelson, "ARCH models as diffusion approximations," *Journal of Econometrics*, vol. 45, no. 1-2, pp. 7–38, 1990.

[15] P. Christoffersen, K. Jacobs, and K. Mimouni, "Volatility dynamics for the S&P500: evidence from realized volatility, daily returns, and option prices," *Review of Financial Studies*, vol. 23, no. 8, pp. 3141–3189, 2010.

[16] K. Chourdakis and G. Dotsis, "Maximum likelihood estimation of non-affine volatility processes," *Journal of Empirical Finance*, vol. 18, no. 3, pp. 533–545, 2011.

[17] Z. Huang, C. Tong, T. Wang et al., "Which volatility model for option valuation in China? empirical evidence from SSE 50 ETF options," *Applied Economics*, vol. 52, no. 17, pp. 1866–1880, 2020.

[18] F. Fang and C. W. Oosterlee, "A novel pricing method for European options based on fourier-cosine series expansions," *SIAM Journal on Scientific Computing*, vol. 31, no. 2, pp. 826–848, 2008.

[19] F. Fang and C. W. Oosterlee, "Pricing early-exercise and discrete barrier options by fourier-cosine series expansions," *Numerische Mathematik*, vol. 114, no. 1, pp. 27–62, 2009.

[20] F. Fang and C. W. Oosterlee, "A fourier-based valuation method for bermudan and barrier options under heston's model," *SIAM Journal on Financial Mathematics*, vol. 2, no. 1, pp. 439–463, 2011.

[21] S. Zhang and J. Geng, "Fourier-cosine method for pricing forward starting options with stochastic volatility and jumps," *Communications in Statistics-Theory and Methods*, vol. 46, no. 20, pp. 9995–10004, 2017.

[22] R. Caldana and G. Fusai, "A general closed-form spread option pricing formula," *Journal of Banking & Finance*, vol. 37, no. 12, pp. 4893–4906, 2013.

[23] D. Duffie, J. Pan, K. Singleton et al., "Transform analysis and asset pricing for affine jump-diffusions," *Econometrica*, vol. 68, no. 6, pp. 1343–1376, 2000.

Hindawi
Mathematical Problems in Engineering
Volume 2020, Article ID 3061298, 16 pages
https://doi.org/10.1155/2020/3061298

Research Article

Pareto-Optimal Reinsurance Revisited: A Two-Stage Optimisation Procedure Approach

Ying Fang,[1] **Lu Wang**,[2] **and Zhongfeng Qu**[3]

[1]*School of Mathematics and Statistics, Shandong Normal University, Jinan 250358, China*
[2]*Caoxian No. 1 Middle School, Heze 274400, China*
[3]*School of Mathematical Sciences, University of Jinan, Jinan 250022, China*

Correspondence should be addressed to Ying Fang; fangying319@163.com

Received 16 June 2020; Accepted 21 July 2020; Published 29 September 2020

Guest Editor: Wenguang Yu

In this paper, based on the Tail-Value-at-Risk (TVaR) measure, we revisit the Pareto-optimal reinsurance policies for the insurer and the reinsurer via a two-stage optimisation procedure. To reduce ex-post moral hazard, we assume that reinsurance contracts satisfy the principle of indemnity and the incentive compatible constraint which have been advocated by Huberman et al. (1983). We show that the Pareto-optimal reinsurance policy exists if the reinsurance premiums can be expressed as an integral form. The proposed class of premium principles encompasses the net premium principle, expected value premium principle, TVaR premium principle, generalized percentile premium principle, and so on. We further use the TVaR premium principle and the expected value premium principle as examples to illustrate the two-stage optimisation procedure by deriving explicitly the Pareto-optimal reinsurance policies. We extend the results by Cai et al. (2017) when the expected value premium principle is replaced by the TVaR premium principle.

1. Introduction

The study of optimal reinsurance design has drawn great interest from both academics and practitioners since the seminal work by Borch [1] and Arrow [2]. There have been many important literatures and conclusions about this problem in the past few decades. For example, by minimizing the variance of the insurer's retained loss, Borch [1] showed that the stop-loss reinsurance is optimal under the expected value premium principle. Arrow [2] obtained that the optimal reinsurance policy is a stop-loss reinsurance strategy when the optimisation criterion is to maximize the expected utility function of the insurer. Both these results have been extended in a number of important directions. For example, Young [3] generalized Arrow's result under Wang's premium principle. Kaluszka [4] generalized Borch's result under mean-variance premium principles. Kaluszka and Okolewski [5] showed that the limited stop-loss and the truncated stop-loss are the optimal contracts under a number of criteria including the maximization of the expected utility, the stability, and the survival probability of the insurer for a fixed reinsurance premium calculated according to the maximal possible claims principle. Cai and Tan [6] developed two new optimisation criteria for deriving the optimal retentions by minimizing the Value-at-Risk (VaR) and the conditional tail expectation (CTE) of the total risk of an insurer. In recent years, VaR and CTE have been used as optimisation criteria to study the optimal reinsurance strategy. For example, by minimizing VaR and CTE of an insurer's total cost, Cai et al. [7] derived the optimal reinsurance strategies in the set of increasing and convex ceded loss functions. The optimal reinsurance strategy depends on the confidence level of risk measurement, and it can be a stop-loss reinsurance strategy, a quota-share reinsurance strategy, or a change-loss reinsurance strategy. Bernard and Tian [8] provided alternative risk transfer mechanisms on the capital market when the optimal reinsurance is arranged under tail risk measures. Cheung [9] gave a geometric approach to revisit the optimal reinsurance problem and generalized the results in [7] by studying the

VaR-minimization problem with Wang's premium principle. Chi and Tan [10] analyzed the VaR- and CVaR-based optimal reinsurance models over different classes of ceded loss functions with increasing generality. However, the above statements only consider the insurer, and from the point of view of the reinsurer, the optimal policy may not be optimal. For example, Vajda [11] showed that the optimal reinsurance strategy is a quota-share reinsurance instead of a stop-loss reinsurance when the optimisation criterion is to minimize the variance of the loss of the reinsurer. Thus, an optimal reinsurance contract for the insurer may not be optimal for the reinsurer and it might be unacceptable for the reinsurer. Then, an interesting question about optimal reinsurance is to design a reinsurance contract so that it considers the interests of both the insurer and the reinsurer.

Borch [1] first studied the optimal reinsurance strategy that consider the interests of both the insurer and the reinsurer. He discussed the optimal quota-share retention and stop-loss retention that maximize the product of the expected utility functions of the two parties' wealth. Kaishev [12] analyzed the optimal reinsurance contracts under which the finite horizon joint survival probability of the two parties is maximized. Under the general reinsurance principles, Cai et al. [13] took maximization of the joint survival probability and the joint profitable probability of both the insurer and the reinsurer as the optimisation criterion to give a sufficient condition of the optimal reinsurance existence. To maximize the joint survival probability of the insurer and the reinsurer, Fang and Qu [14] studied the optimal policy of combination of quota-share reinsurance and stop-loss reinsurance. Fang et al. [15] studied the optimal reinsurance models from the perspective of both the insurer and the reinsurer by minimizing their total costs under the criteria of the loss function which is defined by the joint Value-at-Risk. Cai et al. [16] studied the optimal reinsurance strategy, which was based on the minimum convex combination of the VaR of the insurer and the reinsurer under two types of constraints. Lo [17] discussed the generalized problems in [16] by using the Neyman–Pearson approach. Based on the optimal reinsurance strategy in [16], Jiang et al. [18] proved that the optimal reinsurance strategy is a Pareto-optimal reinsurance policy and gave optimal reinsurance strategies using the geometric method. Cai et al. [19] studied the Pareto optimality of reinsurance arrangements under general model settings and obtained the explicit forms of the Pareto-optimal reinsurance contracts under the TVaR measure and the expected value premium principle. Jiang et al. [20] studied the optimal reinsurance with constraints under the distortion risk measure. By the geometric approach, Fang et al. [21] studied Pareto-optimal reinsurance policies under general premium principles and gave the explicit parameters of the optimal ceded loss functions under the Dutch premium principle and Wang's premium principle. Lo and Tang [22] characterized the set of Pareto-optimal reinsurance policies analytically and visualized the insurer-reinsurer trade-off structure geometrically. Huang and Yin [23] studied two classes of optimal reinsurance models from perspectives of both insurers and reinsurers by minimizing their convex combination where the risk is measured by a distortion risk measure and the premium is given by a distortion premium principle.

In this paper, based on the TVaR measure, we revisit the Pareto-optimal reinsurance policies for the insurer and the reinsurer via a two-stage optimisation procedure which was proposed by Asimit et al. [24]. To reduce ex-post moral hazard, we assume that reinsurance contracts satisfy the principle of indemnity and the incentive compatible constraint which have been advocated by Huberman et al. [25]. We first show that the Pareto-optimal reinsurance policy exists if the reinsurance premiums can be expressed as an integral form such as (10). We emphasize that there are many premium principles which satisfy this property such as the net premium principle, expected value premium principle, TVaR premium principle, and generalized percentile premium principle. Then, we take the TVaR premium principle and the expected value premium principle as examples to illustrate the two-stage optimisation procedure by deriving explicitly the parameters of the Pareto-optimal reinsurance policies.

It is worth noting that the Pareto-optimal reinsurance contracts under the TVaR measure and the expected value premium principle has been obtained in [19]. We reexamine this problem for two reasons. First, it should be emphasized that the results can be achieved by using a different approach based on a two-stage optimisation procedure. Second, and more importantly, the two-stage optimisation procedure is more intuitive and can analyze Pareto-optimal reinsurance policies with other reinsurance premium principles.

The remaining arrangements of this paper are as follows. In Section 2, we introduce some definitions and model formulation and then we show that the Pareto-optimal reinsurance policy exists if the reinsurance premiums can be expressed as an integral form such as (10). Based on the TVaR measure, we obtain the Pareto-optimal policies under the TVaR premium principle and the expected value premium principle in Section 3. In Section 4, we give illustrative numerical examples. Section 5 concludes the paper. Finally, all the proofs are given in the Appendix.

2. Model Formulation

Let X be the amount of loss faced by the insurer in a given time period. Suppose that X is a nonnegative random variable with a distribution function $F_X(x) = \mathrm{P}\{X \leq x\}$ and survival function $S_X(x) = 1 - F_X(x)$. In addition, the value of the right endpoint X_F of the distribution function $F_X(x)$ can be either finite or infinite, where $X_F := \inf\{z: F(z) = 1\}$. Under a reinsurance arrangement, $R(X)$ and $I_R(X)$ represent the ceded loss and the retained loss of the insurer, respectively, where $I_R(X) = X - R(X)$. Functions $R(x)$ and $I_R(x)$ are called the ceded loss function and the retained loss function. The principle of indemnity, which is widely used in insurance and reinsurance, requires the indemnity to be nonnegative and less than the initial loss. Mathematically, we should have $0 \leq R(x) \leq x$. Let $\pi(R(X))$ be the reinsurance premium. Under such a setting, the total losses of the insurer and the reinsurer are $M_R := X - R(X) + \pi(R(X))$ and $N_R := R(X) - \pi(R(X))$, respectively.

In this paper, besides the principle of indemnity, we also assume that reinsurance contracts satisfy the incentive compatible constraint which has been advocated by Huberman et al. [25] to reduce ex-post moral hazard. This means that the more the realized loss, the more paid by both the insurer and the reinsurer. Mathematically, this implies that both the ceded loss function and the retained loss function should be increasing. Therefore, throughout the paper, we assume that the admissible set of ceded loss functions is given by

$$\begin{aligned}\mathscr{F} = \{&R(x)\colon 0 \le R(x) \le x, \text{both } R(x) \\ &\text{and } I_R(x) \text{ are increasing functions}\}.\end{aligned} \tag{1}$$

It was shown by Chi and Tan [10] that all functions $R(x) \in \mathscr{F}$ are Lipschitz continuous and differentiable almost everywhere.

In insurance and finance, risk measures such as VaR and TVaR have been widely used for quantifying risks. Now, we give a brief description of VaR and TVaR measures:

Definition 1 (**VaR**). For a random variable X, VaR is defined as

$$\mathrm{VaR}_p(X) \coloneqq \inf\{\{x \in R\colon \mathrm{P}(X \le x) \ge p\}, \tag{2}$$

where $0 < p < 1$ represents a confidence level of the loss variable X.

Definition 2 (**TVaR**). For a random variable X, TVaR is defined as

$$\begin{aligned}\mathrm{TVaR}_p(X) &\coloneqq \frac{1}{1-p}\int_p^1 \mathrm{VaR}_s(X)\,ds = \mathrm{VaR}_p(X) \\ &\quad + \frac{1}{1-p}E\left(X - \mathrm{VaR}_p(X)\right)_+,\end{aligned} \tag{3}$$

where $0 < p < 1$ represents a confidence level of the loss variable X.

Remark 1

(1) By the definitions of the VaR and the TVaR, distinctly, TVaR_p evaluates the expected loss amount incurred among the worst $(1-p)\%$ scenarios under a confidence level p. Therefore, the TVaR represents a more precise risk measurement than the VaR.

(2) When $1 - p \ge S_X(0)$, we have $\mathrm{VaR}_p(X) = 0$. Therefore, in order to avoid a trivial case, we assume that $1 - p \in (0, S_X(0))$.

In this paper, we assume that the confidence levels of the insurer and the reinsurer are possibly different. Let α_c and α_r denote the confidence levels of the insurer and the reinsurer, respectively. Therefore, the total loss of the insurer and the reinsurer under the TVaR measure is

$$\begin{aligned}\mathrm{TVaR}_{\alpha_c}(M_R) &= \mathrm{VaR}_{\alpha_c}(M_R) + \frac{1}{1-\alpha_c}E\left(M_R - \mathrm{VaR}_{\alpha_c}(M_R)\right)_+, \\ \mathrm{TVaR}_{\alpha_r}(N_R) &= \mathrm{VaR}_{\alpha_r}(N_R) + \frac{1}{1-\alpha_r}E\left(N_R - \mathrm{VaR}_{\alpha_r}(N_R)\right)_+.\end{aligned} \tag{4}$$

Next, we study Pareto-optimal reinsurance policies whereby the risk is measured by the TVaR. For our model, a reinsurance policy with the ceded loss function $R^*(x)$ is called Pareto optimal if there is no other admissible ceded loss function $R \in \mathscr{F}$ such that $\mathrm{TVaR}_{\alpha_c}(M_R) \le \mathrm{TVaR}_{\alpha_c}(M_{R^*})$ and $\mathrm{TVaR}_{\alpha_r}(N_R) \le \mathrm{TVaR}_{\alpha_r}(N_{R^*})$ and at least one of the inequalities is strict. A general approach to identify Pareto-optimal reinsurance policies is to minimize a convex combination of the TVaRs of the two parties. The result can be found in [18–20].

Proposition 1. *All Pareto-optimal reinsurance policies R in $\mathscr{F}$ can be determined by solving the problem:*

$$\min_{R\in\mathscr{F}}\left\{\beta\mathrm{TVaR}_{\alpha_c}(M_R) + (1-\beta)\mathrm{TVaR}_{\alpha_r}(N_R)\right\}, \tag{5}$$

where $\beta \in [0, 1]$.

In view of Proposition 1, throughout the rest of this paper, we only need to determine optimal reinsurance policies by solving the optimisation problem (5). Define

$$V(R) = \beta\mathrm{TVaR}_{\alpha_c}(M_R) + (1-\beta)\mathrm{TVaR}_{\alpha_r}(N_R). \tag{6}$$

Then, by translation invariance and comonotonic additivity of TVaR, we have

$$\begin{aligned}V(R) &= \beta\mathrm{TVaR}_{\alpha_c}(X) - \beta\mathrm{TVaR}_{\alpha_c}(R(X)) \\ &\quad + (1-\beta)\mathrm{TVaR}_{\alpha_r}(R(X)) + (2\beta-1)\pi(R(X)).\end{aligned} \tag{7}$$

Therefore, the optimisation problem (5) becomes

$$\min_{R\in\mathscr{F}} H(R), \tag{8}$$

where

$$\begin{aligned}H(R) &= -\beta\mathrm{TVaR}_{\alpha_c}(R(X)) + (1-\beta)\mathrm{TVaR}_{\alpha_r}(R(X)) \\ &\quad + (2\beta-1)\pi(R(X)).\end{aligned} \tag{9}$$

In this paper, we determine the Pareto-optimal reinsurance policies via a two-stage optimisation procedure which was developed in [24]. The first stage is solving an infinite-dimensional problem, while the second stage becomes a classical constrained optimisation problem. The first stage can be solved as shown in Proposition 1 in [24], and we now present it as a lemma.

Lemma 1. *Let $f(\cdot)$ be a real-valued function defined on $[s_1, s_2]$ with $0 \le s_1 \le s_2 \le 1$. Then,*

$$\begin{aligned}
\min_{R\in\mathcal{F}} \quad & \int_{s_1}^{s_2} f(s)R(\mathrm{VaR}_s(x))\mathrm{d}s, \\
\text{subjectto} \quad & R\big(\mathrm{VaR}_{s_1}(X)\big) = \xi_1, \\
& R\big(\mathrm{VaR}_{s_2}(X)\big) = \xi_2,
\end{aligned} \tag{10}$$

is uniquely solved by

$$R^*(X;\xi_1,\xi_2) = \begin{cases} \big(X - \mathrm{VaR}_{s_1}(X) + \xi_1\big)\wedge\xi_2, & \text{if } f(s) < 0 \text{ for all } s_1 \le s \le s_2, \\ \xi_1 + \big(X - \mathrm{VaR}_{s_2}(X) + \xi_2 - \xi_1\big)_+, & \text{if } f(s) > 0 \text{ for all } s_1 \le s \le s_2, \end{cases} \tag{11}$$

where (ξ_1,ξ_2) *are some constants such that* $0 \le \xi_2 - \xi_1 \le VaR_{s_2}(X) - VaR_{s_1}(X)$.

Note that

$$H(R) = \int_{\alpha_c}^{1} \frac{-\beta}{1-\alpha_c} R(\mathrm{VaR}_s(X))\mathrm{d}s + \int_{\alpha_r}^{1} \frac{1-\beta}{1-\alpha_r} R(\mathrm{VaR}_s(X))\mathrm{d}s + (2\beta-1)\pi(R(X)). \tag{12}$$

By Lemma 1, we know that the Pareto-optimal reinsurance policy exists if the reinsurance premiums $\pi(R(X))$ can be expressed as an integral form such as (10). Next, we give several premium principles which satisfy this property:

(1) Net premium principle: $\pi(X) = E(X)$. Since $R(x)$ is a nondecreasing continuous function, then $\pi(R(X)) = \int_0^1 R(\mathrm{VaR}_s(X))\mathrm{d}s$.

(2) Expected value premium principle: $\pi(X) = (1+\theta)E(X)$, where $\theta \in [0,1]$ is a safety loading coefficient. Therefore, $\pi(R(X)) = (1+\theta)\int_0^1 R(\mathrm{VaR}_s(X))\mathrm{d}s$.

(3) TVaR premium principle: $\pi(X) = (1+\theta/1-\alpha)\int_\alpha^1 \mathrm{VaR}_s(X)\mathrm{d}s$, where $\alpha \in [0,1)$ is a confidence level and $\theta \in [0,1]$ is a safety loading coefficient. Since $R(x)$ is a nondecreasing continuous function, then $\pi(R(X)) = (1+\theta/1-\alpha)\int_\alpha^1 R\ (\mathrm{VaR}_s(X))\mathrm{d}s$.

(4) Generalized percentile premium principle: $\pi(X) = E(X) + \beta\{F_X^{-1}(1-p) - E(X)\}$ with $0 < \beta, p < 1$. Since $F_X^{-1}(1-p) = \mathrm{VaR}_{1-p}(X)$, then $\pi(R(X)) = (1-\beta)E[R(X)] + \beta R(\mathrm{VaR}_{1-p}(X))$.

In the following sections, we take the TVaR premium principle and the expected value premium principle as examples to illustrate the two-stage optimisation procedure.

3. Pareto-Optimal Reinsurance Policy

In this section, we determine the Pareto-optimal reinsurance policies under the TVaR premium principle and the expected value premium principle. The TVaR premium principle was first proposed by Young [26]. It can be viewed as an extended version of the expected value premium principle, that is, letting $\alpha = 0$ gives the expected value premium principle.

3.1. Pareto-Optimal Reinsurance Policies under TVaR Principle. Under the TVaR premium principle, the optimisation problem (8) becomes

$$\min_{R\in\mathcal{F}} H(R), \tag{13}$$

where $H(R) = -\beta\mathrm{TVaR}_{\alpha_c}(R(X)) + (1-\beta)\mathrm{TVaR}_{\alpha_c}(R(X)) + (2\beta-1)(1+\theta)\mathrm{TVaR}_\alpha(R(X))$. From the mathematical point of view, the confidence level α can be larger than confidence levels α_c and α_r. However, α is usually smaller while α_c and α_r are usually larger in practice. So, we assume further $\alpha < \min\{\alpha_c, \alpha_r\}$ to avoid complex and lengthy discussions in this section.

For simplicity, we define the following notations:

$$\begin{aligned}
a &= \mathrm{VaR}_\alpha(X), \\
a_c &= \mathrm{VaR}_{\alpha_c}(X), \\
a_r &= \mathrm{VaR}_{\alpha_r}(X), \\
\xi &= R(\mathrm{VaR}_\alpha(X)), \\
\xi_c &= R\big(\mathrm{VaR}_{\alpha_c}(X)\big), \\
\xi_r &= R\big(VaR_{\alpha_r}(X)\big), \\
m &= \frac{(2\beta-1)(1+\theta)}{1-\alpha} - \frac{\beta}{1-\alpha_c}, \\
n &= \frac{(2\beta-1)(1+\theta)}{1-\alpha} + \frac{1-\beta}{1-\alpha_r}, \\
s(\beta) &= 1 - \frac{\beta-1}{m}, \\
t(\beta) &= 1 - \frac{\beta}{n}.
\end{aligned} \tag{14}$$

Next, we divide our discussion into three cases: ① $a_c < a_r$; ② $a_r < a_c$; ③ $a_c = a_r$. Then, we obtain the following three theorems.

Theorem 1. *Under the condition $a_c < a_r$, the Pareto-optimal reinsurance policies are given as follows:*

(1) *If* $0 \le \beta < 1/2$ *and* $(\beta - 1/1 - \alpha_r) < m$, *then*

$$R^*(x) = \begin{cases} x \wedge \mathrm{VaR}_{s(\beta)}(X), & \text{when } (1+\theta)(1-\alpha_c) > 1-\alpha, \\ x \wedge \mathrm{VaR}_{(\theta+\alpha/1+\theta)}(X), & \text{when } (1+\theta)(1-\alpha_c) \le 1-\alpha. \end{cases} \quad (15)$$

(2) *If* $0 \le \beta < 1/2$ *and* $(\beta - 1/1 - \alpha_r) > m$, *then* $R^*(x) = x$.

(3) *If* $0 \le \beta < 1/2$ *and* $(\beta - 1/1 - \alpha_r) = m$, *then* $R^*(x) = xI_{\{a \le x \le a_r\}} + R(x)I_{\{x > a_r\}}$, *where* $R(x)$ *is any increasing 1-Lipschitz continuous function such that* $R^*(x) \in \mathcal{F}$.

(4) *If* $\beta = 1/2$, *then* $R^*(x) = R(x)I_{\{a \le x \le a_c\}} + u_1 I_{\{x > a_c\}}$, *where* u_1 *is an arbitrary constant in* $[u, a_c - a + u]$, u *is an arbitrary constant in* $[0, a]$, *and* $R(x)$ *is any increasing 1-Lipschitz continuous function such that* $R^*(x) \in \mathcal{F}$.

(5) *If* $1/2 < \beta \le 1$ *and* $m > 0$, *then* $R^*(x) = 0$.

(6) *If* $1/2 < \beta < 1$ *and* $(\beta - 1/1 - \alpha_r) < m < 0$, *then*

$$R^*(x) = \begin{cases} 0, & \text{when } (1+\theta)(1-\alpha_c) \ge 1-\alpha, \\ \left(x - \mathrm{VaR}_{(\theta+\alpha/1+\theta)}(X)\right)_+ \wedge \left(\mathrm{VaR}_{s(\beta)}(X) - \mathrm{VaR}_{(\theta+\alpha/1+\theta)}(X)\right), & \text{when } (1+\theta)(1-\alpha_c) < 1-\alpha. \end{cases} \quad (16)$$

(7) *If* $1/2 < \beta \le 1$ *and* $m < (\beta - 1/1 - \alpha_r)$, *then* $R^*(x) = (x - VaR_{(\theta+\alpha/1+\theta)}(X))_+$.

(8) *If* $1/2 < \beta < 1$ *and* $m = (\beta - 1/1 - \alpha_r)$, *then* $R^*(x) = (x - VaR_{(\theta+\alpha/1+\theta)}(X))_+ I_{\{a \le x \le a_r\}} + R(x)I_{\{x > a_r\}}$, *where* $R(x)$ *is any increasing 1-Lipschitz continuous function such that* $R^*(x) \in \mathcal{F}$.

(9) *If* $1/2 < \beta < 1$ *and* $m = 0$, *then* $R^*(x) = 0$.

(10) *If* $\beta = 1$ *and* $(1+\theta)(1-\alpha_c) = 1-\alpha$, *then* $R^*(x) = R(x)I_{\{x > a_c\}}$, *where* $R(x)$ *is any increasing 1-Lipschitz continuous function such that* $R^*(x) \in \mathcal{F}$.

Theorem 2. *Under the condition* $a_r < a_c$, *the Pareto-optimal reinsurance policies are given as follows:*

(1) *If* $\beta = 0$ *and* $(1+\theta)(1-\alpha_r) = 1-\alpha$, *then* $R^*(x) = xI_{\{a \le x \le a_r\}} + R(x)I_{\{x > a_r\}}$, *where* $R(x)$ *is any increasing 1-Lipschitz continuous function such that* $R^*(x) \in \mathcal{F}$.

(2) *If* $0 \le \beta < 1/2$ *and* $n > (\beta/1 - \alpha_c)$, *then* $R^*(x) = x \wedge VaR_{(\theta+\alpha/1+\theta)}(X)$.

(3) *If* $0 < \beta < 1/2$ *and* $0 < n < (\beta/1 - \alpha_c)$, *then*

$$R^*(x) = \begin{cases} x \wedge \mathrm{VaR}_{(\theta+\alpha/1+\theta)}(X) + \left(x - \mathrm{VaR}_{t(\beta)}(X)\right)_+, & \text{when } (1+\theta)(1-\alpha_r) < 1-\alpha, \\ x, & \text{when } (1+\theta)(1-\alpha_r) \ge 1-\alpha. \end{cases} \quad (17)$$

(4) *If* $0 < \beta < 1/2$ *and* $n = (\beta/1 - \alpha_c)$, *then* $R^*(x) = (x \wedge VaR_{(\theta+\alpha/1+\theta)}(X))I_{\{a \le x \le a_c\}} + R(x)I_{\{x > a_c\}}$, *where* $R(x)$ *is any increasing 1-Lipschitz continuous function such that* $R^*(x) \in \mathcal{F}$.

(5) *If* $0 \le \beta < 1/2$ *and* $n < 0$, *then* $R^*(x) = x$.

(6) *If* $0 < \beta < 1/2$ *and* $n = 0$, *then* $R^*(x) = xI_{\{a \le x \le a_r \text{ or } x > a_c\}} + R(x)I_{\{a_r < x \le a_c\}}$, *where* $R(x)$ *is any increasing 1-Lipschitz continuous function such that* $R^*(x) \in \mathcal{F}$.

(7) *If* $\beta = 1/2$, *then* $R^*(x) = R(x)I_{\{a \le x \le a_r\}} + (x - a_r + u_2) I_{\{x > a_r\}}$, *where* u_2 *is an arbitrary constant in* $[u, a_r - a + u]$, u *is an arbitrary constant in* $[0, a]$, *and* $R(x)$ *is any increasing 1-Lipschitz continuous function such that* $R^*(x) \in \mathcal{F}$.

(8) *If* $1/2 < \beta \le 1$ *and* $n > (\beta/1 - \alpha_c)$, *then* $R^*(x) = 0$.

(9) *If* $1/2 < \beta \le 1$ *and* $0 < n < (\beta/1 - \alpha_c)$, *then*

$$R^*(x) = \begin{cases} \left(x - \mathrm{VaR}_{(\theta+\alpha/1+\theta)}(X)\right)_+, & \text{when } (1+\theta)(1-\alpha_r) \le 1-\alpha, \\ \left(x - \mathrm{VaR}_{t(\beta)}(X)\right)_+, & \text{when } (1+\theta)(1-\alpha_r) > 1-\alpha. \end{cases} \quad (18)$$

(10) *If* $1/2 < \beta \le 1$ *and* $n = (\beta/1 - \alpha_c)$, *then* $R^*(x) = R(x)I_{\{x > a_c\}}$, *where* $R(x)$ *is any increasing 1-Lipschitz continuous function such that* $R^*(x) \in \mathcal{F}$.

Theorem 3. *Under the condition* $a_c = a_r$, *the Pareto-optimal reinsurance policies are given as follows:*

(1) *If* $0 \le \beta < 1/2$, *then*

$$R^*(x) = \begin{cases} x, & \text{when } (1+\theta)(1-\alpha_c) > 1-\alpha, \\ xI_{\{a \le x \le a_c\}} + R(x)I_{\{x > a_c\}}, & \text{when } (1+\theta)(1-\alpha_c) = 1-\alpha, \\ x \wedge \mathrm{VaR}_{(\theta+\alpha/1+\theta)}(X), & \text{when } (1+\theta)(1-\alpha_c) < 1-\alpha, \end{cases} \quad (19)$$

where $R(x)$ is any increasing 1-Lipschitz continuous function such that $R^*(x) \in \mathcal{F}$.

(2) *If $\beta = 1/2$, the objective function is identical to 0 and the problem is trivial.*

(3) *If $1/2 < \beta \le 1$, then*

$$R^*(x) = \begin{cases} 0, & \text{when } (1+\theta)(1-\alpha_c) > 1-\alpha, \\ R(x) I_{\{x>a_c\}}, & \text{when } (1+\theta)(1-\alpha_c) = 1-\alpha, \\ \left(x - \mathrm{VaR}_{(\theta+\alpha/1+\theta)}(X)\right)_+, & \text{when } (1+\theta)(1-\alpha_c) < 1-\alpha, \end{cases} \tag{20}$$

where $R(x)$ is any increasing 1-Lipschitz continuous function such that $R^*(x) \in \mathcal{F}$.

3.2. Pareto-Optimal Reinsurance Policies under Expected Value Principle. In this section, we reexamine an optimal reinsurance problem studied in [19], in which the objective is to find the optimal reinsurance contracts that minimize the TVaR of the total risk exposure under the expected value premium principle. We provide a more intuitive approach to solve the problem by using a two-stage optimisation method. Under the expected value principle, the optimisation problem (5) becomes

$$\min_{R\in\mathcal{F}} \left\{-\beta \mathrm{TVaR}_{\alpha_c}(R(X)) + (1-\beta)\mathrm{TVaR}_{\alpha_r}(R(X)) + (2\beta-1)(1+\theta)E(R(X))\right\}. \tag{21}$$

For simplicity, we define the following notations:

$$\begin{aligned} m_0 &= (2\beta-1)(1+\theta) - \frac{\beta}{1-\alpha_c}, \\ n_0 &= (2\beta-1)(1+\theta) + \frac{1-\beta}{1-\alpha_r}, \\ s_0(\beta) &= 1 - \frac{\beta-1}{m_0}, \\ t_0(\beta) &= 1 - \frac{\beta}{n_0}. \end{aligned} \tag{22}$$

Theorem 4. *Under the condition $a_c < a_r$, the Pareto-optimal reinsurance policies are given as follows:*

(1) *If $0 \le \beta < 1/2$ and $(\beta - 1/1-\alpha_r) < m_0 < 0$, then*

$$R^*(x) = \begin{cases} x \wedge \mathrm{VaR}_{s_0(\beta)}(X), & \text{when } (1+\theta)(1-\alpha_c) > 1, \\ 0, & \text{when } S_X(0) \le \theta^* \text{ and } (1+\theta)(1-\alpha_c) \le 1, \\ x \wedge \mathrm{VaR}_{(\theta/1+\theta)}(X), & \text{when } S_X(0) > \theta^* \text{ and } (1+\theta)(1-\alpha_c) \le 1. \end{cases} \tag{23}$$

(2) *If $0 \le \beta < 1/2$ and $m_0 < (\beta - 1/1-\alpha_r)$, then $R^*(x) = x$.*

(3) *If $0 \le \beta < 1/2$ and $(\beta - 1/1-\alpha_r) = m_0$, then $R^*(x) = xI_{\{x\le a_r\}} + R(x)I_{\{x>a_r\}}$, where $R(x)$ is an increasing 1-Lipschitz continuous function such that $R^*(x) \in \mathcal{F}$.*

(4) *If $\beta = 1/2$, then $R^*(x) = R(x)I_{\{x\le a_c\}} + u_3 I_{\{x>a_c\}}$, where $R(x)$ is an increasing 1-Lipschitz continuous function such that $R^*(x) \in \mathcal{F}$ and $u_3 \in [0, a_c]$.*

(5) *If $1/2 < \beta \le 1$ and $m_0 > 0$, then $R^*(x) = 0$.*

(6) *If $1/2 < \beta < 1$ and $(\beta - 1/1-\alpha_r) < m_0 < 0$, then*

$$R^*(x) = \begin{cases} 0, & \text{when } (1+\theta)(1-\alpha_c) \ge 1, \\ x \wedge \mathrm{VaR}_{s_0(\beta)}(X), & \text{when } S_X(0) \le \theta^* \text{ and } (1+\theta)(1-\alpha_c) < 1, \\ \left(x - \mathrm{VaR}_{(\theta/1+\theta)}(X)\right)_+ \wedge \left(\mathrm{VaR}_{s_0(\beta)}(X) - \mathrm{VaR}_{(\theta/1+\theta)}(X)\right), & \text{when } S_X(0) > \theta^* \text{ and } (1+\theta)(1-\alpha_c) < 1. \end{cases} \tag{24}$$

(7) *If $1/2 < \beta \le 1$ and $m_0 < (\beta - 1/1-\alpha_r)$, then*

$$R^*(x) = \begin{cases} x, & \text{when } S_X(0) \le \theta^*, \\ \left(x - \mathrm{VaR}_{(\theta/1+\theta)}(X)\right)_+, & \text{when } S_X(0) > \theta^*. \end{cases} \tag{25}$$

(8) *If $1/2 < \beta < 1$ and $m_0 = (\beta - 1/1-\alpha_r)$, then*

$$R^*(x) = \begin{cases} xI_{\{x\le a_r\}} + R(x)I_{\{x>a_r\}}, & \text{when } S_X(0) \le \theta^*, \\ \left(x - \mathrm{VaR}_{(\theta/1+\theta)}(X)\right)_+ I_{\{x\le a_r\}} + R(x)I_{\{x>a_r\}}, & \text{when } S_X(0) > \theta^*, \end{cases} \tag{26}$$

where $R(x)$ is an increasing 1-Lipschitz continuous function such that $R^*(x) \in \mathcal{F}$.

(9) *If $1/2 < \beta < 1$ and $m_0 = 0$, then $R^*(x) = 0$.*

(10) *If* $\beta = 1$ *and* $(1+\theta)(1-\alpha_c) = 1$, *then* $R^*(x) = R(x)I_{\{x>a_c\}}$, *where* $R(x)$ *is an increasing 1-Lipschitz continuous function such that* $R^*(x) \in \mathcal{F}$.

Theorem 5. *Under the condition* $a_r < a_c$, *the Pareto-optimal reinsurance policies are given as follows:*

(1) *If* $\beta = 0$ *and* $(1+\theta)(1-\alpha_r) = 1$, *then* $R^*(x) = xI_{\{x\le a_r\}} + R(x)I_{\{x>a_r\}}$, *where* $R(x)$ *is an increasing 1-Lipschitz continuous function such that* $R^*(x) \in \mathcal{F}$.

(2) *If* $0 \le \beta < 1/2$ *and* $n_0 > (\beta/1-\alpha_c)$, *then*

$$R^*(x) = \begin{cases} 0, & \text{when } S_X(0) \le \theta^*, \\ x \wedge \mathrm{VaR}_{(\theta/1+\theta)}(X), & \text{when } S_X(0) > \theta^*. \end{cases} \tag{27}$$

(3) *If* $0 < \beta < 1/2$ *and* $0 < n_0 < (\beta/1-\alpha_c)$, *then*

$$R^*(x) = \begin{cases} x, & \text{when } (1+\theta)(1-\alpha_r) \ge 1, \\ \left(x - \mathrm{VaR}_{t_0(\beta)}(X)\right)_+, & \text{when } S_X(0) \le \theta^* \text{ and } (1+\theta)(1-\alpha_r) < 1, \\ x \wedge \mathrm{VaR}_{(\theta/1+\theta)}(X) + \left(x - \mathrm{VaR}_{t_0(\beta)}(X)\right)_+, & \text{when } S_X(0) > \theta^* \text{ and } (1+\theta)(1-\alpha_r) < 1. \end{cases} \tag{28}$$

(4) *If* $0 < \beta < 1/2$ *and* $n_0 = (\beta/1-\alpha_c)$, *then*

$$R^*(x) = \begin{cases} R(x)I_{\{x>a_c\}}, & \text{when } S_X(0) \le \theta^*, \\ \left\{x \wedge \mathrm{VaR}_{(\theta/1+\theta)}(X)\right\} I_{\{x\le a_c\}} + R(x)I_{\{x>a_c\}}, & \text{when } S_X(0) > \theta^*, \end{cases} \tag{29}$$

where $R(x)$ *is an increasing 1-Lipschitz continuous function such that* $R^*(x) \in \mathcal{F}$.

(5) *If* $0 \le \beta < 1/2$ *and* $n_0 < 0$, *then* $R^*(x) = x$.

(6) *If* $0 < \beta < 1/2$ *and* $n_0 = 0$, *then* $R^*(x) = xI_{\{x\le a_r \text{ or } x>a_c\}} + R(x)I_{\{a_r < x \le a_c\}}$, *where* $R(x)$ *is an increasing 1-Lipschitz continuous function such that* $R^*(x) \in \mathcal{F}$.

(7) *If* $\beta = 1/2$, *then* $R^*(x) = R(x)I_{\{x\le a_r\}} + (x - a_r + u_4)I_{\{x>a_r\}}$, *where* $R(x)$ *is an increasing 1-Lipschitz continuous function such that* $R^*(x) \in \mathcal{F}$ *and* $u_4 \in [0, a_r]$.

(8) *If* $1/2 < \beta \le 1$ *and* $n_0 > (\beta/1-\alpha_c)$, *then* $R^*(x) = 0$.

(9) *If* $1/2 < \beta \le 1$ *and* $0 < n_0 < (\beta/1-\alpha_c)$, *then*

$$R^*(x) = \begin{cases} \left(x - \mathrm{VaR}_{t_0(\beta)}(X)\right)_+, & \text{when } (1+\theta)(1-\alpha_r) \ge 1, \\ x, & \text{when } S_X(0) \le \theta^* \text{ and } (1+\theta)(1-\alpha_r) < 1, \\ \left(x - \mathrm{VaR}_{(\theta/1+\theta)}(X)\right)_+, & \text{when } S_X(0) > \theta^* \text{ and } (1+\theta)(1-\alpha_r) < 1. \end{cases} \tag{30}$$

(10) *If* $1/2 < \beta \le 1$ *and* $n_0 = (\beta/1-\alpha_c)$, *then* $R^*(x) = R(x)I_{\{x>a_c\}}$, *where* $R(x)$ *is an increasing 1-Lipschitz continuous function such that* $R^*(x) \in \mathcal{F}$.

Theorem 6. *Under the condition* $a_c = a_r$, *the Pareto-optimal reinsurance policies are given as follows:*

(1) *If* $0 \le \beta < 1/2$, *then*

$$R^*(x)=\begin{cases} x, & \text{when } (1+\theta)(1-\alpha_c)>1,\\ xI_{\{x\le a_c\}}+R(x)I_{\{x>a_c\}}, & \text{when } (1+\theta)(1-\alpha_c)=1,\\ 0, & \text{when } S_X(0)\le\theta^* \text{ and } (1+\theta)(1-\alpha_c)<1,\\ x\wedge \mathrm{VaR}_{(\theta/1+\theta)}(X), & \text{when } S_X(0)>\theta^* \text{ and } (1+\theta)(1-\alpha_c)<1, \end{cases} \tag{31}$$

where $R(x)$ is an increasing 1-Lipschitz continuous function such that $R^*(x)\in\mathcal{F}$.

(2) If $\beta=1/2$, the objective function is zero and the problem is trivial.

(3) If $1/2<\beta\le 1$, then

$$R^*(x)=\begin{cases} 0, & \text{when } (1+\theta)(1-\alpha_c)>1,\\ R(x)I_{\{x>a_c\}}, & \text{when } (1+\theta)(1-\alpha_c)=1,\\ x, & \text{when } S_X(0)\le\theta^* \text{ and } (1+\theta)(1-\alpha_c)<1,\\ \left(x-\mathrm{VaR}_{(\theta/1+\theta)}(X)\right)_+, & \text{when } S_X(0)>\theta^* \text{ and } (1+\theta)(1-\alpha_c)<1, \end{cases} \tag{32}$$

where $R(x)$ is an increasing 1-Lipschitz continuous function such that $R^*(x)\in\mathcal{F}$.

Remark 1. By comparing our results with those in [19], we would like to point out the relationship between the two articles. First, Cai et al. [19] give the explicit forms of the Pareto-optimal reinsurance contracts under the expected value premium principle by the construction method. In our paper, we use the two-stage optimisation procedure. This technique is intuitive and applicable when the expected value premium principle is replaced by other premium principles. Using this technique, we extend the results in [19] under the TVaR premium principle. Second, under the expected value premium principle, Cai et al. [19] derived the optimal ceded loss functions without considering the relationship between $S_X(0)$ and 1 in their Theorems 1 and 2. However, we discuss the relationship between them and derive different optimal ceded functions from theirs in the case $S_X(0)<1$. By comparison, we find that our result is more reasonable.

4. Numerical Examples

In this section, we give two numerical examples to illustrate the applications of the results obtained in previous sections.

Example 1 (TVaR principle). Assume that the loss variable X is exponentially distributed with the survival function $S_X(x)=e^{-0.001x}$. In this section, we assume $\theta=0.2$ and $\alpha=0.2$; then $a=223.1$. Using the results in Theorems 1, 3, and 3, we have the following cases.

Case 1. $\alpha_c=0.95$ and $\alpha_r=0.99$. In this case, $a=223.1$, $a_c=2995.7$, $a_r=4605.2$, $\mathrm{TVaR}_{\alpha_c}(X)=3995.7$, and $\mathrm{TVaR}_{\alpha_r}(X)=5605.2$. The optimal ceded loss function $R^*(x)$ is shown in Table 1, and the various key values of $R^*(x)$ are shown in Table 2.

From Table 1, we know that the optimal reinsurance policy depends on the combining coefficient β. From Table 2, obviously, with the increase in the weight coefficient β, the loss of the insurer $\mathrm{TVaR}_{\alpha_c}(M_{R^*})$ is decreasing while the loss of the reinsurer $\mathrm{TVaR}_{\alpha_r}(N_{R^*})$ and the mean premium $E(\pi(R^*))$ are increasing, especially more intuitive when $\beta\in(0.5,0.8419)$. Note that we ignore the key values at the endpoints 0.5 and 0.8419 because the Pareto-optimal reinsurance policy at endpoints 0.5 and 0.8419 is uncertain.

Case 2. $\alpha_c=0.99$ and $\alpha_r=0.95$.

In this case, $a=223.1$, $a_c=4605.2$, $a_r=2995.7$, $TVaR_{\alpha_c}(X)=5605.2$, and $\mathrm{TVaR}_{\alpha_r}(X)=3995.7$. The optimal ceded loss function $R^*(x)$ is shown in Table 3, and the various key values of $R^*(x)$ are shown in Table 4.

Case 3. $\alpha_c=\alpha_r=0.95$.

In this case, $a=223.1$, $a_c=a_r=2995.7$, and $\mathrm{TVaR}_{\alpha_c}(X)=\mathrm{TVaR}_{\alpha_r}(X)=3995.7$. The optimal ceded loss function $R^*(x)$ is shown in Table 5, and the various key values of $R^*(x)$ are shown in Table 6.

Remark 2. Under the expected value premium, assume that the loss variable X is exponentially distributed with the survival function $S_X(x)=e^{-0.001x}$ and $\theta=0.2$. Using the results in Theorems 4, 5, and 6 we get the same results as in [19].

Table 1: $R^*(x)$ with $\alpha_c < \alpha_r$ under exponential distribution.

$\beta \in [0, 0.5)$	$R^*(x) = x \wedge 405.5$
$\beta = 0.5$	$R^*(x)$ is unspecified, $223.1 \le x \le 2995.7$ $R^*(x) = u_1,\ x > 2995.7, \forall u_1 \in [223.1, 2995.7]$
$\beta \in (0.5, 0.8419)$	$R^*(x) = ((x - 405.5)_+ \wedge (\mathrm{VaR}_{s(\beta)}(X) - 405.5)), \forall \mathrm{VaR}_{s(\beta)}(X) \in (2995.7, 4605.2)$
$\beta = 0.8419$	$R^*(x) = (x - 405.5)_+, 223.1 \le x \le 4605.2,\ R^*(x)$ is unspecified, $x > 4605.2$
$\beta \in (0.8419, 1]$	$R^*(x) = (x - 405.5)_+$

Table 2: Various key values of $R^*(x)$ with $\alpha_c < \alpha_r$ under exponential distribution.

	$\mathrm{TVaR}_{\alpha_c}(M_{R^*})$	$\mathrm{TVaR}_{\alpha_r}(N_{R^*})$	$E(\pi(R^*))$
$\beta \in [0, 0.5)$	4058	-62.3	467.8
$\beta \in (0.5, 0.8419)$	$(2330.5 \downarrow 1590.5)$	$(1665.2 \uparrow 33214.7)$	$(925 \uparrow 985)$
$\beta \in (0.8419, 1]$	1405.5	4199.7	1000

Table 3: $R^*(x)$ with $\alpha_c > \alpha_r$ under exponential distribution.

$\beta \in [0, 0.1581)$	$R^*(x) = x \wedge 405.5$
$\beta = 0.1581$	$R^*(x) = x \wedge 405.5,\ 223.1 \le x \le 4605.2,\ R^*(x)$ is unspecified, $x > 4605.2$
$\beta \in (0.1581, 0.5)$	$R^*(x) = x \wedge 405.5 + (x - \mathrm{VaR}_{t(\beta)}(X))_+, \forall \mathrm{VaR}_{t(\beta)}(X) \in (2995.7, 4605.2)$
$\beta = 0.5$	$R^*(x)$ is unspecified, $223.1 \le x \le 4605.2$ $R^*(x) = x - 2995.7 + u_2,\ x > 4605.2, \forall u_2 \in [223.1, 2995.7]$
$\beta \in (0.5, 1]$	$R^*(x) = (x - 405.5)_+$

Table 4: Various key values of $R^*(x)$ with $\alpha_c > \alpha_r$ under exponential distribution.

	$\mathrm{TVaR}_{\alpha_c}(M_{R^*})$	$\mathrm{TVaR}_{\alpha_r}(N_{R^*})$	$E((\pi(R^*))$
$\beta \in [0, 0.1581)$	5667.5	-62.3	467.8
$\beta \in (0.1581, 0.5)$	$(4682.5 \downarrow 3133)$	$(122.7 \uparrow 862.7)$	$(482.8 \uparrow 542.8)$
$\beta \in (0.5, 1]$	1405.5	2590.2	1000

Table 5: $R^*(x)$ with $\alpha_c = \alpha_r$ under exponential distribution.

$\beta \in [0, 0.5)$	$R^*(x) = x \wedge 405.5$
$\beta = 0.5$	$R^*(x)$ is unspecified
$\beta \in (0.5, 1]$	$R^*(x) = (x - 405.5)_+$

Table 6: Various key values of $R^*(x)$ with $\alpha_c = \alpha_r$ under exponential distribution.

	$\mathrm{TVaR}_{\alpha_c}(M_{R^*})$	$\mathrm{TVaR}_{\alpha_r}(N_{R^*})$	$E(\pi(R^*))$
$\beta \in [0, 0.5)$	4058	-62.3	467.8
$\beta = 0.5$	$(4058 \downarrow 1405.5)$	$(-62.3 \uparrow 2590.2)$	$(467.8 \uparrow 1000)$
$\beta \in (0.5, 1]$	1405.5	2590.2	1000

Example 2 (expected value premium principle). Assume $\theta = 0.2$ and the loss variable X with the survival function:

$$S_X(x) = \begin{cases} 1, & x < 0, \\ 0.25, & x = 0, \\ 0.75e^{-0.001x}, & x > 0. \end{cases} \tag{33}$$

Using the results in Theorems 4, 5, and 6, we have the following cases.

Case 4. $\alpha_c = 0.95$ and $\alpha_r = 0.99$. In this case, $a_c = 2708.1$, $a_r = 4317.5$, $\mathrm{TVaR}_{\alpha_c}(X) = 3708.1$, and $\mathrm{TVaR}_{\alpha_r}(X) = 5317.5$. The optimal ceded loss function $R^*(x)$ is shown in Table 7, and the various key values of $R^*(x)$ are shown in Table 8.

Case 5. $\alpha_c = 0.99$ and $\alpha_r = 0.95$.

In this case, $a_c = 4317.5$, $a_r = 2708.1$, $\mathrm{TVaR}\alpha_c(X) = 5317.5$, and $\mathrm{TVaR}_{\alpha_r}(X) = 3708.1$. The optimal ceded loss function $R^*(x)$ is shown in Table 9, and the various key values of $R^*(x)$ are shown in Table 10.

Case 6. $\alpha_c = \alpha_r = 0.95$.

In this case, $a_c = a_r = 2708.1$ and $\mathrm{TVaR}_{\alpha_c}(X) = \mathrm{TVaR}_{\alpha_r}(X) = 3708.1$. The optimal ceded loss function $R^*(x)$ is shown in Table 11, and the various key values of $R^*(x)$ are shown in Table 12.

It is worth mentioning that the distribution in Example 2 is not applicable in [19], and it violates the meaning of the ceded loss function. In addition, note that the parameter β and the confidence levels of TVaRs have significant influences on the Pareto-optimal contracts. If β is small, the weight of the reinsurer is larger than the insurer, and then

Table 7: $R^*(x)$ with $\alpha_c < \alpha_r$.

$\beta \in [0, 0.5)$	$R^*(x) = 0$
$\beta = 0.5$	$R^*(x)$ is unspecified, $x \leq 2708.1$ $R^*(x) = u_3,\ x > 2708.1, \forall u_3 \in [0, 2708.1]$
$\beta \in (0.5, 0.84)$	$R^*(x) = \min\{x, \mathrm{VaR}_{s_0(\beta)}(X)\},\ \forall \mathrm{VaR}_{s_0(\beta)}(X) \in (2708.1, 4317.5)$
$\beta = 0.84$	$R^*(x) = x,\ x \leq 4317.5,\ R^*(x)$ is unspecified, $x > 4317.5$
$\beta \in (0.84, 1]$	$R^*(x) = x$

Table 8: Various key values of $R^*(x)$ with $\alpha_c < \alpha_r$.

	$\mathrm{TVaR}_{\alpha_c}(M_{R^*})$	$\mathrm{TVaR}_{\alpha_r}(N_{R^*})$	$E(\pi(R^*))$
$\beta \in [0, 0.5)$	3708.1	0	0
$\beta \in (0.5, 0.84)$	$(1840\downarrow 1088)$	$(1868.1\uparrow 3429.5)$	$(840\uparrow 888)$
$\beta \in (0.84, 1]$	900	4417.5	900

Table 9: $R^*(x)$ with $\alpha_c > \alpha_r$.

$\beta \in [0, 0.1599)$	$R^*(x) = 0$
$\beta = 0.1599$	$R^*(x) = 0,\ x \leq 4317.5$ $R^*(x)$ is unspecified, $x > 4317.5$
$\beta \in (0.1599, 0.5)$	$R^*(x) = (x - \mathrm{VaR}_{t_0(\beta)}(X))_+,\ \forall \mathrm{VaR}_{t_0(\beta)}(X) \in (2708.1, 4317.5)$
$\beta = 0.5$	$R^*(x)$ is unspecified, $x \leq 2708.1$ $R^*(x) = x - 2708.1 + u_4,\ x > 2708.1,\ \forall u_4 \in [0, 2708.1]$
$\beta \in (0.5, 1]$	$R^*(x) = x$

Table 10: Various key values of $R^*(x)$ with $\alpha_c > \alpha_r$.

	$\mathrm{TVaR}_{\alpha_c}(M_{R^*})$	$\mathrm{TVaR}_{\alpha_r}(N_{R^*})$	$E(\pi(R^*))$
$\beta \in [0, 0.1599)$	5317.5	0	0
$\beta \in (0.1599, 0.5)$	$(4329.5\downarrow 2768.1)$	$(188\uparrow 940)$	$(12\uparrow 60)$
$\beta \in (0.5, 1]$	900	2808.1	900

Table 11: $R^*(x)$ with $\alpha_c = \alpha_r$.

$\beta \in [0, 0.5)$	$R^*(x) = 0$
$\beta = 0.5$	$R^*(x)$ is unspecified
$\beta \in (0.5, 1]$	$R^*(x) = x$

Table 12: Various key values of $R^*(x)$ with $\alpha_c = \alpha_r$.

	$\mathrm{TVaR}_{\alpha_c}(M_{R^*})$	$\mathrm{TVaR}_{\alpha_r}(N_{R^*})$	$E(\pi(R^*))$
$\beta \in [0, 0.5)$	3708.1	0	0
$\beta = 0.5$	$(3708.1\downarrow 900)$	$(0\uparrow 2808.1)$	$(0\uparrow 900)$
$\beta \in (0.5, 1]$	900	2808.1	900

the reinsurer bears less losses. Conversely, if β is large, the weight of the insurer is larger than the reinsurer, and then the reinsurer bears more losses. If $\alpha_c < \alpha_r$, which means that the TVaR standard of the reinsurer is higher than the insurer, then the reinsurer bears less losses. If $\alpha_c > \alpha_r$, which means that the TVaR standard of the insurer is higher than the reinsurer, then the reinsurer bears more losses.

5. Conclusion

In this paper, based on the TVaR measure, we show that the Pareto-optimal reinsurance policies must exist for the insurer and the reinsurer under a class of premium principle, such as the net principle, expected value premium principle, TVaR principle, and generalized percentile. Using a two-stage optimisation procedure, we derive explicitly the Pareto-optimal reinsurance policies under the TVaR principle. Since the expected value premium principle can be viewed as a special case of the TVaR principle, then letting $\alpha = 0$ in the TVaR principle gives Pareto-optimal reinsurance policies for the expected value premium principle. We extend the results in [19]. Compared with the method used in [19], using the two-stage optimisation method to derive the Pareto-optimal strategy is simpler and more intuitive. Furthermore, by comparing the results in [19] with ours, Cai et al. [19] derived the optimal ceded loss functions without considering the relationship between $S_X(0)$ and 1, while we discuss the relationship between $S_X(0)$ and 1 and derive different optimal ceded functions from theirs in the case $S_X(0) < 1$.

We also wish to point out that further research on this topic is needed. First, the risk measure TVaR can be generalized to coherent risk measures. Although some papers have been devoted to deriving optimal reinsurance under coherent risk measures, the optimal reinsurance study still lacks of available analyze tools. Since nonlinear expectation is an essential feature of coherent risk measures, maybe we can draw support from nonlinear expectation; research literatures in this regard are [27–31], etc. Second, we can analyze risk with the strategies of dividend and reinsurance. For more references on the dividend, refer to [32–34], etc. Third, in most of the optimal reinsurance problems, it is assumed that the distributions of the insurer's risks are known. However, in practice, only incomplete information on the distributions is available. How to obtain optimal reinsurance contracts with incomplete information is also an interesting topic. An attempt to such a problem is to use the statistical methods. For more references on statistical methods, see, e.g., [35–37]. We hope that these important open problems can be addressed in the future research. We also believe that this article will foster further research in this direction.

Appendix

The proof of Theorem 1.

By (3), the equivalent form of (13) is

$$\min_{R\in\mathcal{F}}\left\{\frac{(2\beta-1)(1+\theta)}{1-\alpha}\int_{\alpha}^{\alpha_c}R(\mathrm{VaR}_s(X))\mathrm{d}s+m\int_{\alpha c}^{\alpha_r}R(\mathrm{VaR}_s(X))\mathrm{d}s+\left(m+\frac{1-\beta}{1-\alpha_r}\right)\int_{\alpha_r}^{1}R(\mathrm{VaR}_s(X))\mathrm{d}s\right\}. \quad \text{(A.1)}$$

(1) If $0\le\beta<1/2$ and $(\beta-1/1-\alpha_r)<m$, by Lemma 1, we get that (A.1) is solved by

$$R^*(X;\xi,\xi_c,\xi_r)=\begin{cases}(X-a+\xi)\wedge\xi_c, & a\le X\le a_c,\\ (X-a_c+\xi_c)\wedge\xi_r, & a_c<X\le a_r,\\ \xi_r, & X>a_r,\end{cases} \quad \text{(A.2)}$$

where $(\xi,\xi_c,\xi_r)\in\mathcal{D}_1$ and $\mathcal{D}_1=\{(\xi,\xi_c,\xi_r)$: $0\le\xi\le a; 0\le\xi_c\le a_c; 0\le\xi_r\le a_r; 0\le\xi_r-\xi_c\le a_r-a_c$; $0\le\xi_c-\xi\le a_c-a; 0\le\xi_r-\xi\le a_r-a\}$. Thus,

$$\begin{aligned}
&\mathrm{TVaR}_{\alpha}(R^*(X;\xi,\xi_c,\xi_r))=\xi+\frac{1}{1-\alpha}\int_a^{a-\xi+\xi_c}S_X(x)\mathrm{d}x+\frac{1}{1-\alpha}\int_{a_c}^{a_c-\xi_c+\xi_r}S_X(x)\mathrm{d}x,\\
&\mathrm{TVaR}_{\alpha_c}((R^*(X;\xi,\xi_c,\xi_r))=\xi_c+\frac{1}{1-\alpha_c}\int_{a_c}^{a_c-\xi_c+\xi_r}S_X(x)\mathrm{d}x,\\
&\mathrm{TVaR}_{\alpha_r}(R^*(X;\xi,\xi_c,\xi_r))=\xi_r.
\end{aligned} \quad \text{(A.3)}$$

Define $H(R^*)=H_1(\xi,\xi_c,\xi_r)$ in this case; then the second-stage optimisation problem is reduced to minimize H_1. Note that $(\partial H_1/\ \partial\xi_r)=1-\beta+[((2\beta-1)(1+\theta)/1-\alpha)-(\beta/1-\alpha_c)]S_X(a_c-\xi_c+\xi_r)$, and it is increasing in ξ_r on $[\xi_c,a_r-a_c+\xi_c]$ since $m<0$.

① When $(1+\theta)(1-\alpha_c)>1-\alpha$, we have $(\partial H_1/\partial\xi_r)|_{\xi_r=\xi_c}<0$. Since $m+(1-\beta/1-\alpha_r)>0$, then we obtain $(\partial H_1/\partial\xi_r)|_{\xi_r=a_r-a_c+\xi_c}>0$. So, H_1 attains its minimum value at $\xi_r^*=VaR_{s(\beta)}(X)-a_c+\xi_c$. Note that

$$\begin{aligned}
H_1(\xi,\xi_c,\xi_r^*)={}&-\beta\xi_c-\frac{\beta}{1-\alpha_c}\int_{a_c}^{\mathrm{VaR}_{s(\beta)}(X)}S_X(x)\mathrm{d}x+(1-\beta)\left(\mathrm{VaR}_{s(\beta)}(X)-a_c+\xi_c\right)\\
&+(2\beta-1)(1+\theta)\left(\xi+\frac{1}{1-\alpha}\left(\int_a^{a-\xi+\xi_c}S_X(x)\mathrm{d}x+\int_{a_c}^{\mathrm{VaR}_{s(\beta)}(X)}S_X(x)\mathrm{d}x\right)\right),
\end{aligned} \quad \text{(A.4)}$$

and $(\partial H_1/\partial\xi_c)=(2\beta-1)[(1+\theta/1-\ \alpha)S_X(a-\xi+\xi_c)-1]$, so $(\partial H_1/\partial\xi_c)$ is increasing in ξ_c on $[\xi,a_c-a+\xi]$. Since $(\partial H_1/\partial\xi_c)|_{\xi_c=a_c-a+\xi}<0$, then H_1 attains its minimum value at $\xi_c^*=a_c-a+\xi$. Furthermore, $(\partial H_1/\partial\xi)=(2\beta-1)\theta<0$ always holds, and so H_1 attains its minimum value at $\xi^*=a$. In conclusion, $R^*(x)=x\wedge\mathrm{VaR}_{s(\beta)}(X)$.

② When $(1+\theta)(1-\alpha_c)\le1-\alpha$, we have $(\partial H_1/\partial\xi_r)|_{\xi_r=\xi_c}\ge0$, so H_1 attains its minimum value at $\xi_r^*=\xi_c$. Note that $H_1(\xi,\xi_c,\xi_r^*)=(1-$

$2\beta)\xi_c + (2\beta - 1)(1 + \theta)(\xi + 1/1 - \alpha \int_a^{a-\xi+\xi_c} S_X(x)\mathrm{d}x)$ and $(\partial H_1/\partial \xi_c) = (2\beta - 1)[(1 + \theta/1- \alpha)S_X(a - \xi + \xi_c) - 1]$; then $(\partial H_1/\partial \xi_c)$ is increasing in ξ_c on $[\xi, a_c - a + \xi]$ since $(\partial H_1/\partial \xi_c)|_{\xi_c=\xi} < 0$ and $(\partial H_1/\partial \xi_c)|_{\xi_c=a_c-a+\xi} \geq 0$.

When $(\partial H_1/\partial \xi_c)|_{\xi_c=a_c-a+\xi} = 0$, then H_1 attains its minimum value at $\xi_c^* = a_c - a + \xi$ and $\xi^* = a$. Therefore, $R^*(x) = x \wedge a_c$.

When $(\partial H_1/\partial \xi_c)|_{\xi_c=a_c-a+\xi} > 0$, H_1 attains its minimum value at $\xi_c^* = \mathrm{VaR}_{(\theta+\alpha/1+\theta)}(X) - a + \xi$ and $\xi^* = a$. Therefore, $R^*(x) = x \wedge \mathrm{VaR}_{(\theta+\alpha/1+\theta)}(X)$.

Note that $\mathrm{VaR}_{(\theta+\alpha/1+\theta)}(X) = a_c$ if $(\partial H_1/\partial \xi_c)|_{\xi_c=a_c-a+\xi} = 0$. Therefore, $R^*(x) = x \wedge \mathrm{VaR}_{(\theta+\alpha/1+\theta)}(X)$ when $(1 + \theta)(1 - \alpha_c) \leq 1 - \alpha$.

(2) If $0 \leq \beta < 1/2$ and $m < (\beta - 1/1 - \alpha_r)$, by Lemma 1, we get that (A.1) is solved by

$$R^*(X; \xi, \xi_c, \xi_r) = \begin{cases} (X - a + \xi) \wedge \xi_c, & a \leq X \leq a_c, \\ (X - a_c + \xi_c) \wedge \xi_r, & a_c < X \leq a_r, \\ X - a_r + \xi_r, & X > a_r, \end{cases} \tag{A.5}$$

where $(\xi, \xi_c, \xi_r) \in \mathscr{D}_1$. Therefore,

$$\begin{aligned} \mathrm{TVaR}_\alpha(R^*(X; \xi, \xi_c, \xi_r)) &= \xi + \frac{1}{1-\alpha}\int_a^{a-\xi+\xi_c} S_X(x)\mathrm{d}x + \frac{1}{1-\alpha}\int_{a_c}^{a_c-\xi_c+\xi_r} S_X(x)\mathrm{d}x + \frac{1}{1-\alpha}\int_{a_r}^{X_F} S_X(x)\mathrm{d}x, \\ \mathrm{TVaR}_{\alpha_c}(R^*(X; \xi, \xi_c, \xi_r)) &= \xi_c + \frac{1}{1-\alpha_c}\int_{a_c}^{a_c-\xi_c+\xi_r} S_X(x)\mathrm{d}x + \frac{1}{1-\alpha_c}\int_{a_r}^{X_F} S_X(x)\mathrm{d}x, \\ \mathrm{TVaR}_{\alpha_r}(R^*(X; \xi, \xi_c, \xi_r)) &= \xi_r + \frac{1}{1-\alpha_r}\int_{a_r}^{X_F} S_X(x)\mathrm{d}x. \end{aligned} \tag{A.6}$$

Then,

$$\begin{aligned} H(R^*) &:= H_2(\xi, \xi_c, \xi_r) \\ &= -\beta\xi_c + (1-\beta)\xi_r + (2\beta - 1)(1+\theta)\xi + m\int_{a_c}^{a_c-\xi_c+\xi_r} S_X(x)\mathrm{d}x \\ &\quad + \frac{(2\beta-1)(1+\theta)}{1-\alpha}\int_a^{a-\xi+\xi_c} S_X(x)\mathrm{d}x + \left(m + \frac{1-\beta}{1-\alpha_r}\right)\int_{a_r}^{X_F} S_X(x)\mathrm{d}x, \end{aligned} \tag{A.7}$$

and H_2 attains its minimum value at $(\xi^*, \xi_c^*, \xi_r^*) = (a, a_c, a_r)$ in this case. Therefore, $R^*(x) = x$.

(3) If $0 \leq \beta < 1/2$ and $m = (\beta - 1/1 - \alpha_r)$, by Lemma 1, we get that (A.1) is solved by

$$R^*(X; \xi, \xi_c, \xi_r) = \begin{cases} (X - a + \xi) \wedge \xi_c, & a \leq X \leq a_c, \\ (X - a_c + \xi_c) \wedge \xi_r, & a_c < X \leq a_r, \\ R(x), & X > a_r, \end{cases} \tag{A.8}$$

where $R(x)$ is an increasing 1-Lipschitz continuous function. Therefore,

$$\mathrm{TVaR}_{\alpha}(R^*(X;\xi,\xi_c,\xi_r)) = \xi + \frac{1}{1-\alpha}\int_a^{X_F} \mathrm{P}(R^*(X;\xi,\xi_c,\xi_r) > x)\mathrm{d}x,$$
$$\mathrm{TVaR}_{\alpha_c}(R^*(X;\xi,\xi_c,\xi_r)) = \xi_c + \frac{1}{1-\alpha_c}\int_{a_c}^{X_F} \mathrm{P}(R^*(X;\xi,\xi_c,\xi_r) > x)\mathrm{d}x, \tag{A.9}$$
$$\mathrm{TVaR}_{\alpha_r}(R^*(X;\xi,\xi_c,\xi_r)) = \xi_r + \frac{1}{1-\alpha_r}\int_{a_r}^{X_F} \mathrm{P}(R^*(X;\xi,\xi_c,\xi_r) > x)\mathrm{d}x.$$

In this case,

$$H(R^*) \coloneqq H_3(\xi,\xi_c,\xi_r)$$
$$= -\beta\xi_c + (1-\beta)\xi_r + (2\beta-1)(1+\theta)\xi + m\int_{a_c}^{a_c-\xi_c+\xi_r} S_X(x)\mathrm{d}x + \frac{(2\beta-1)(1+\theta)}{1-\alpha}\int_a^{a-\xi+\xi_c} S_X(x)\mathrm{d}x, \tag{A.10}$$

and H_3 attains its minimum value at $(\xi^*,\xi_c^*,\xi_r^*) = (a,a_c,a_r)$. Therefore, $R^*(x) = xI_{\{a\le x\le a_r\}} + R(x) I_{\{x>a_r\}}$.

(4) If $\beta = 1/2$, by Lemma 1, we get that (A.1) is solved by

$$R^*(X;\xi,\xi_c,\xi_r) = \begin{cases} R(x), & a \le X \le a_c, \\ (X - a_c + \xi_c)\wedge\xi_r, & a_c < X \le a_r, \\ \xi_r, & X > a_r. \end{cases} \tag{A.11}$$

Then,

$$\mathrm{TVaR}_{\alpha}(R^*(X;\xi,\xi_c,\xi_r)) = \xi + \frac{1}{1-\alpha}\int_a^{X_F} \mathrm{P}(R^*(X;\xi,\xi_c,\xi_r) > x)\mathrm{d}x,$$
$$\mathrm{TVaR}_{\alpha_c}(R^*(X;\xi,\xi_c,\xi_r)) = \xi_c + \frac{1}{1-\alpha_c}\int_{a_c}^{a_c-\xi_c+\xi_r} S_X(x)\mathrm{d}x,$$
$$\mathrm{TVaR}_{\alpha_r}(R^*(X;\xi,\xi_c,\xi_r)) = \xi_r, \tag{A.12}$$
$$H(R^*) \coloneqq H_4(\xi,\xi_c,\xi_r)$$
$$= \frac{1}{2}\xi_c + \frac{1}{2}\xi_r + \frac{1}{2(1-\alpha_c)}\int_{a_c}^{a_c-\xi_c+\xi_r} S_X(x)\mathrm{d}x.$$

It is easy to see that H_4 attains its minimum value at $(\xi^*,\xi_c^*,\xi_r^*) = (\xi,u_1,u_1)$, where $u_1 \in [a,a_c]$. Therefore, $R^*(x) = R(x)I_{\{a\le x\le a_c\}} + u_1 I_{\{x>a_c\}}$.

(5) If $1/2 < \beta \le 1$ and $m > 0$, the coefficients of the three integrals in (A.1) are all positive, obviously $R^*(x) = 0$.

(6) If $1/2 < \beta < 1$ and $(\beta - 1/1 - \alpha_r) < m < 0$, by Lemma 1, we get that (A.1) is solved by

Then,

$$R^*(X;\xi,\xi_c,\xi_r)=\begin{cases}\xi+(X-a_c+\xi_c-\xi)_+, & a\le X\le a_c,\\ (X-a_c+\xi_c)\wedge\xi_r, & a_c<X\le a_r,\\ \xi_r, & X>a_r.\end{cases}\tag{A.13}$$

$$\begin{aligned}H(R^*)&\coloneqq H_5(\xi,\xi_c,\xi_r)\\&=-\beta\xi_c+(1-\beta)\xi_r-\frac{\beta}{1-\alpha_c}\int_{a_c}^{a_c-\xi_c+\xi_r}S_X(x)\mathrm{d}x+(2\beta-1)(1+\theta)\left(\xi+\frac{1}{1-\alpha}\int_{a_c-\xi_c+\xi}^{a_c-\xi_c+\xi_r}S_X(x)\mathrm{d}x\right).\end{aligned}\tag{A.14}$$

Note that $(\partial H_5/\partial\xi_r)=1-\beta+[((2\beta-1)(1+\theta)/1-\alpha)-(\beta/1-\alpha_c)]S_X(a_c-\xi_c+\xi_r)$ is increasing in ξ_r on $[\xi_c,a_r-a_c+\xi_c]$.

① When $(1+\theta)(1-\alpha_c)\ge 1-\alpha$, H_5 attains its minimum value at $(\xi^*,\xi_c^*,\xi_r^*)=(0,0,0)$. Therefore, $R^*(x)=0$.

② When $(1+\theta)(1-\alpha_c)<1-\alpha$, H_5 attains its minimum value at $(\xi^*,\xi_c^*,\xi_r^*)=(0,a_c-\mathrm{VaR}_{(\theta+\alpha/1+\theta)}(X),\mathrm{VaR}_{S(\beta)}(X)-\mathrm{VaR}_{(\theta+\alpha/1+\theta)}(X))$. Therefore, $R^*(x)=(x-\mathrm{VaR}_{(\theta+\alpha/1+\theta)}(X))_+\wedge(\mathrm{VaR}_{S(\beta)}(X)-\mathrm{VaR}_{(\theta+\alpha/1+\theta)}(X))$.

(7) If $1/2<\beta\le 1$ and $m<(\beta-1/1-\alpha_r)$, then (A.1) is solved by

$$R^*(X;\xi,\xi_c,\xi_r)=\begin{cases}\xi+(X-a_c+\xi_c-\xi)_+, & a\le X\le a_c,\\ (X-a_c+\xi_c)\wedge\xi_r, & a_c<X\le a_r,\\ x-a_r+\xi_r, & X>a_r.\end{cases}\tag{A.15}$$

Note that

$$\begin{aligned}H(R^*)&\coloneqq H_6(\xi,\xi_c,\xi_r)\\&=-\beta\xi_c-\frac{\beta}{1-\alpha_c}\int_{a_c}^{a_c-\xi_c+\xi_r}S_X(x)\mathrm{d}x+(1-\beta)\xi_r+(2\beta-1)(1+\theta)\xi+\frac{(2\beta-1)(1+\theta)}{1-\alpha}\int_{a_c-\xi_c+\xi}^{a_c-\xi_c+\xi_r}S_X(x)\mathrm{d}x\\&\quad+(m+1-\beta)\int_{a_r}^{X_F}S_X(x)\mathrm{d}x,\end{aligned}\tag{A.16}$$

then H_6 attains its minimum value at $(\xi^*,\xi_c^*,\xi_r^*)=(0,a_c-\mathrm{VaR}_{(\theta+\alpha/1+\theta)}(X),a_r-\mathrm{VaR}_{(\theta+\alpha/1+\theta)}(X))$. Therefore, $R^*(x)=(x-\mathrm{VaR}_{(\theta+\alpha/1+\theta)}(X))_+$.

(8) If $1/2<\beta<1$ and $m=(\beta-1/1-\alpha_r)$, then (A.1) is solved by

$$R^*(X;\xi,\xi_c,\xi_r)=\begin{cases}\xi+(X-a_c+\xi_c-\xi)_+, & a\le X\le a_c,\\ (X-a_c+\xi_c)\wedge\xi_r, & a_c<X\le a_r,\\ R(x), & X>a_r.\end{cases}\tag{A.17}$$

We obtain $R^*(x)=(x-\mathrm{VaR}_{(\theta+\alpha/1+\theta)}(X))_+I_{\{x\le a_r\}}+R(x)I_{\{x>a_r\}}$.

(9) If $1/2<\beta<1$ and $m=0$, then (A.1) is solved by

$$R^*(X;\xi,\xi_c,\xi_r)=\begin{cases}\xi+(X-a_c+\xi_c-\xi)_+, & a\le X\le a_c,\\ R(x), & a_c<X\le a_r,\\ \xi_r, & X>a_r.\end{cases}\tag{A.18}$$

It is easy to get $\xi_r^*=\xi_c^*=\xi^*=0$, so $R^*(x)=0$.

(10) If $\beta=1$ and $m=0$, then (A.1) is solved by

$$R^*(X;\xi,\xi_c,\xi_r)=\begin{cases}\xi+(X-a_c+\xi_c-\xi)_+, & a\le X\le a_c,\\ R(x), & a_c<X\le a_r,\\ R(x), & X>a_r.\end{cases}\tag{A.19}$$

Obviously, $R^*(X;\xi,\xi_c,\xi_r)$ is independent of ξ_r, and it is easy to get $\xi_c^* = \xi^* = 0$, so $R^*(x) = R(x)I_{\{x>a_c\}}$, where $R(x)$ is an increasing 1-Lipschitz continuous function such that $R^*(x) \in \mathscr{F}$.

The proof of Theorem 2.

By (3), the equivalent form of (13) is

$$\min_{R\in\mathscr{F}}\left\{\frac{(2\beta-1)(1+\theta)}{1-\alpha}\int_{\alpha}^{\alpha_r} R\left(\mathrm{VaR}_s(X)\right)\mathrm{d}s + n\int_{\alpha_r}^{\alpha_c} R\left(\mathrm{VaR}_s(X)\right)\mathrm{d}s + \left(n-\frac{\beta}{1-\alpha_c}\right)\int_{\alpha_c}^{1} R\left(\mathrm{VaR}_s(X)\right)\mathrm{d}s\right. \tag{A.20}$$

Using the same method as the proof of Theorem 1, we can obtain the desired results, so we omit the proof. It is worth noting that $(\xi,\xi_c,\xi_r) \in \mathscr{D}_2$ and $\mathscr{D}_2 = \{(\xi,\xi_c,\xi_r)$: $0\le\xi\le a; 0\le\xi_c\le a_c; 0\le\xi_r\le a_r; 0\le\xi_c-\xi_r\le a_c-a_r; 0\le\xi_c-\xi\le a_c-a; 0\le\xi_r-\xi\le a_r-a\}$.

The proof of Theorem 3.

By (3), the equivalent form of (13) is

$$\min_{R\in\mathscr{F}}\left\{\frac{(2\beta-1)(1+\theta)}{1-\alpha}\int_{\alpha}^{\alpha_c} R\left(\mathrm{VaR}_s(X)\right)\mathrm{d}s + \left[(2\beta-1)\left(\frac{1+\theta}{1-\alpha}-\frac{1}{1-\alpha_c}\right)\right]\int_{\alpha_c}^{1} R\left(\mathrm{VaR}_s(X)\right)\mathrm{d}s\right\}. \tag{A.21}$$

Note that $(\xi,\xi_c) \in \mathscr{D}_3$ and $\mathscr{D}_3 = \{(\xi,\xi_c)$: $0\le\xi\le a; 0\le\xi_c\le a_c; 0\le\xi_c-\xi\le a_c-a\}$. Then, the same technique as used in the proof of Theorem 1 yields the results.

Data Availability

The data used to support the findings of this study are available from the corresponding author upon request.

Conflicts of Interest

The authors declare that they have no conflicts of interest.

Acknowledgments

The research was supported by the Project of the Shandong Province Higher Educational Science and Technology Program (J18KA249) and the Social Science Planning Project of Shandong Province (20CTJJ02).

References

[1] K. Borch, "An attempt to determine the optimum amount of stop loss reinsurance," *Transactions of the 16th International Congress of Actuaries*, vol. 1, pp. 597–610, 1960.

[2] K. J. Arrow, "Uncertainty and the welfare economics of medical care," *American Economic Review*, vol. 53, pp. 941–973, 1963.

[3] V. R. Young, "Optimal insurance under Wang's premium principle," *Insurance: Mathematics and Economics*, vol. 25, no. 2, pp. 109–122, 1999.

[4] M. Kaluszka, "Optimal reinsurance under mean-variance premium principles," *Insurance: Mathematics and Economics*, vol. 28, no. 1, pp. 61–67, 2001.

[5] M. Kaluszka and A. Okolewski, "An extension of arrow's result on optimal reinsurance contract," *Journal of Risk & Insurance*, vol. 75, no. 2, pp. 275–288, 2008.

[6] J. Cai and K. S. Tan, "Optimal retention for a stop-loss reinsurance under the VaR and CTE risk measures," *ASTIN Bulletin*, vol. 37, no. 1, pp. 93–112, 2007.

[7] J. Cai, K. S. Tan, C. Weng, and Y. Zhang, "Optimal reinsurance under VaR and CTE risk measures," *Insurance: Mathematics and Economics*, vol. 43, no. 1, pp. 185–196, 2008.

[8] C. Bernard and W. Tian, "Optimal reinsurance arrangements under tail risk measures," *Journal of Risk and Insurance*, vol. 76, no. 3, pp. 709–725, 2009.

[9] K. C. Cheung, "Optimal reinsurance revisited—a geometric approach," *ASTIN Bulletin*, vol. 40, no. 1, pp. 221–239, 2010.

[10] Y. C. Chi and K. S. Tan, "Optimal reinsurance under VaR and CVaR risk measures: a simplified approach," *ASTIN Bulletin*, vol. 41, pp. 487–509, 2011.

[11] S. Vajda, "Minimum variance reinsurance," *ASTIN Bulletin*, vol. 2, no. 2, pp. 257–260, 1962.

[12] V. K. Kaishev, "Optimal retention levels, given the joint survival of cedent and reinsurer," *Scandinavian Actuarial Journal*, vol. 2004, no. 6, pp. 401–430, 2004.

[13] J. Cai, Y. Fang, Z. Li, and G. E. Willmot, "Optimal reciprocal reinsurance treaties under the joint survival probability and the joint profitable probability," *Journal of Risk and Insurance*, vol. 80, no. 1, pp. 145–168, 2013.

[14] Y. Fang and Z. Qu, "Optimal combination of quota-share and stop-loss reinsurance treaties under the joint survival probability," *IMA Journal of Management Mathematics*, vol. 25, no. 1, pp. 89–103, 2014.

[15] Y. Fang, G. Cheng, and Z. Qu, "Optimal reinsurance for both an insurer and a reinsurer under general premium principles," *AIMS Mathematics*, vol. 5, no. 4, pp. 3231–3255, 2020.

[16] J. Cai, C. Lemieux, and F. Liu, "Optimal reinsurance from the perspectives of both an insurer and a reinsurer," *ASTIN Bulletin*, vol. 46, no. 3, pp. 815–849, 2016.

[17] A. Lo, "A Neyman-Pearson perspective on optimal reinsurance with constraints," *ASTIN Bulletin*, vol. 47, no. 2, pp. 467–499, 2017.

[18] W. J. Jiang, J. D. Ren, and R. Zitikis, "Optimal reinsurance policies under the VaR risk measure when the interests of both the cedent and the reinsurer are taken into account," *Risks*, vol. 5, pp. 1–22, 2017a.

[19] J. Cai, H. Liu, and R. Wang, "Pareto-optimal reinsurance arrangements under general model settings," *Insurance: Mathematics and Economics*, vol. 77, pp. 24–37, 2017.

[20] W. Jiang, H. Hong, and J. Ren, "On Pareto-optimal reinsurance with constraints under distortion risk measures," *European Actuarial Journal*, vol. 8, no. 1, pp. 215–243, 2017b.

[21] Y. Fang, X. Wang, H. Liu, and T. Li, "Pareto-optimal reinsurance for both the insurer and the reinsurer with general premium principles," *Communications in Statistics—Theory and Methods*, vol. 48, no. 24, pp. 6134–6154, 2019.

[22] A. Lo and Z. Tang, "Pareto-optimal reinsurance policies in the presence of individual risk constraints," *Annals of Operations Research*, vol. 274, no. 1-2, pp. 395–423, 2019.

[23] Y. Huang and C. Yin, "A unifying approach to constrained and unconstrained optimal reinsurance," *Journal of Computational and Applied Mathematics*, vol. 360, pp. 1–17, 2019.
[24] A. V. Asimit, A. M. Badescu, and T. Verdonck, "Optimal risk transfer under quantile-based risk measurers," *Insurance: Mathematics and Economics*, vol. 53, no. 1, pp. 252–265, 2013.
[25] G. Huberman, D. Mayers, and C. W. Smith Jr., "Optimal insurance policy indemnity schedules," *The Bell Journal of Economics*, vol. 14, no. 2, pp. 415–426, 1983.
[26] V. R. Young, "Premium principles," in *Encyclopedia of Actuarial Science*, J. Teugels and B. Sundt., Eds., Vol. 3, John Wiley & Sons, Hoboken, NJ, USA, 2004.
[27] C. Hu, "Strong laws of large numbers for sublinear expectation under controlled 1st moment condition," *Chinese Annals of Mathematics, Series B*, vol. 39, no. 5, pp. 791–804, 2018.
[28] C. Hu, "Central limit theorems for sub-linear expectation under the Lindeberg condition," *Journal of Inequalities and Applications*, vol. 2018, no. 1, 2018.
[29] C. Hu, "Weak and strong laws of large numbers for sub-linear expectation," *Communications in Statistics—Theory and Methods*, vol. 49, no. 2, pp. 430–440, 2019.
[30] C. Hu, "Marcinkiewicz-Zygmund laws of large numbers under sublinear expectation," *Mathematical Problems in Engineering*, vol. 2020, Article ID 5050973, 11 pages, 2020.
[31] X. J. Shi, R. L. Ji, and Q. Feng, "Representation of filtration-consistent nonlinear expectation by g-expectation in general framework," *Communications in Statistics-Theory and Methods*, 2020.
[32] Y. Zhao, P. Chen, and H. Yang, "Optimal periodic dividend and capital injection problem for spectrally positive Lévy processes," *Insurance: Mathematics and Economics*, vol. 74, pp. 135–146, 2017.
[33] W. Yu, P. Guo, Q. Wang et al., "On a periodic capital injection and barrier dividend strategy in the compound Poisson risk model," *Mathematics*, vol. 8, no. 4, p. 511, 2020.
[34] X. Peng, W. Su, W. Su, and Z. Zhang, "On a perturbed compound Poisson risk model under a periodic threshold-type dividend strategy," *Journal of Industrial & Management Optimization*, vol. 16, no. 4, pp. 1967–1986, 2020.
[35] H. Y. Wang and Z. Wu, "Eigenvalues of stochastic Hamiltonian systems driven by Poisson process with boundary conditions," *Boundary Value Problems*, vol. 2017, no. 1, 2017.
[36] X. Wang, Y. Song, and L. Lin, "Handling estimating equation with nonignorably missing data based on SIR algorithm," *Journal of Computational and Applied Mathematics*, vol. 326, pp. 62–70, 2017.
[37] Q. Zhao, R. J. Karunamuni, and J. J. Wu, "An empirical classification procedure for nonparametric mixture models," *Journal of the Korean Statistical Society*, vol. 49, pp. 924–952, 2020.

Hindawi
Mathematical Problems in Engineering
Volume 2020, Article ID 1746413, 8 pages
https://doi.org/10.1155/2020/1746413

Research Article

Measurement of Longevity Risk of Life Annuity Based on C-ROSS Framework

Ming Zhao ,[1,2] Ziwen Li,[2] Yinge Cai,[2] and Weiting Li[2]

[1]*Environmental, Social and Governance Institute, Capital University of Economics and Business, Beijing 100070, China*
[2]*School of Finance, Capital University of Economics and Business, Beijing 100070, China*

Correspondence should be addressed to Ming Zhao; zhaoming@cueb.edu.cn

Received 6 June 2020; Accepted 24 July 2020; Published 18 September 2020

Guest Editor: Wenguang Yu

This paper constructs a model to measure longevity risk and explains the reasons for restricting the supply of annuity products in life insurance companies. According to the Lee–Carter Model and the VaR-based stochastic simulation, it can be found that the risk margin of the first type of longevity risk for ignoring the improvement of mortality rate is about 7%, and the risk margin of the second type of longevity risk for underestimating mortality improvement is about 7%. Therefore, the insurer needs to use cohort life table pricing premium and gradually prepares longevity risk capital during the insurance period.

1. Introduction

With the rapid development of the global economy and the improvement of medical skills, the extension of human life span has become an inevitable trend, which has a significant impact on the stability of life insurance companies. The fact that insurance companies cannot effectively manage longevity risk due to extended life expectancy results in the insufficient motivation to provide lifelong annuity, which limits the supply of annuity. There are two aspects in evaluating the longevity risk of the life annuity products: one is to establish a stochastic mortality model to forecast the improvement of mortality, and the other one is to select an appropriate method to measure longevity risk.

There are lots of studies on the stochastic mortality model. Among all, the Lee–Carter model [1], which is based on the hypothesis that the logarithmic mortality is composed by the independent age and periodic effects, is a pioneering one. Because of its easy form, obvious parameter significance, and easy quantitative calculation, this model is widely used by scholars all over the world. Renshaw and Haberman expand the Lee–Carter model by taking the impact of population cohort on mortality into account to improve the scientificity of the model [2]. Also, due to less exposure of the elderly population and abnormal distribution of death, the general model cannot fully reflect the mortality curve of the elderly. Cairns et al. propose the CBD model with two factors to solve this problem [3]. Raftery et al. put forward a method based on Bayesian Hierarchical Model (BHM), taking the average life span data from 1950 to 1995 over the world into BHM to forecast life expectancy [4]. According to the cross-check with an actual statistic, Raftery et al. believe that the model could show an accurate prediction interval. At the same time, domestic scholars have explored the application of stochastic mortality model in China, and the results show that the Lee–Carter model is suitable for China [5–7].

As for longevity risk measurement, Olivieri used the present value of the annuity to measure the longevity risk for insurer [8], whereafter Olivieri and Pitacco further studied the solvency capital requirements of annuity insurance under longevity risk based on a stochastic mortality model [9]. In 2010, Borger compared the risk value (VaR) with the long-lived risk metric under standard deterministic mortality volatility and found out that VaR was more reasonable to apply in measurement. Hari et al. point out that longevity risk exists at both the individual and the general levels [10]. The former refers to the fact that individuals spend more money for the desire of longevity than they have accumulated over a lifetime, which can be reduced by using various pension plans, such as the government's social security pension insurance, the employer's pension for the enterprise, and commercial pension insurance. The overall longevity risk is also called the aggregate longevity risk; that is, the life expectancy exceeds the prediction. In this situation, the budget in the pension plan of the insurance company will exceed the expectation, which will lead to severe debts and cause an economic burden to both government and insurance companies. It is worth noting that we are mainly focusing on the risk of a commercial insurance company. Then, Richards et al. explore the applicability of the stochastic mortality model in different ways, presenting a long-lived risk measurement with a one-year perspective. Antolin proposes a new risk metric that could meet the consistency requirements. Based on Glue VaR, the longevity risk is measured in China's pension system and insurer's survival annuity products.

The structure of this paper is as follows. Section 2 introduces the stochastic mortality model and the method for measuring of longevity risk. Next, Section 3 describes the data features and research scheme. Following this, Section 4 analyses the longevity risk faced by insurers when providing lifelong pension funds. Finally, Section 5 concludes the paper.

2. Longevity Risk Model and Measurement

2.1. Lee–Carter Model. Lee and Carter propose Lee–Carter model, which is superior due to its simple form, obvious practicality of parameters, and convenience for quantitative calculation and is broadly used nowadays. It has become the standard in the US Census Bureau and the United Nations Population Division with good fitting and prediction results. The basic form of the Lee–Carter stochastic mortality model is as follows:

$$\begin{gathered}\ln m_x(t) = \alpha_x + \beta_x \kappa_t + \varepsilon_{x,t},\\ \varepsilon_{x,t} \sim N\left(0, \sigma^2\right).\end{gathered} \tag{1}$$

In the above formula, $m_x(t)$ is the central mortality rate of the x-year-old in year t. Generally, it is as the mortality data in the demographic survey; that is,

$$m_x(t) = \frac{\mathrm{D}(t,x)}{\mathrm{E}(t,x)}, \tag{2}$$

where $\mathrm{D}(t,x)$ is the number of deaths of the x-year population during the entire calendar year t. $\mathrm{E}(t,x)$ is the average number of people aged x, that is, the number of exposures during the calendar year t. Under the assumption that the deadly force is constant, the age-specific mortality rate, used in the actuarial model frequently, has the following approximate relationship with the central mortality rate:

$$q_x(t) = 1 - \exp\left[-m_x(t)\right]. \tag{3}$$

Or, under the assumption that death occurs evenly,

$$q_x(t) = \frac{m_x(t)}{1 + 0.5 m_x(t)}. \tag{4}$$

Lee–Carter Model decomposes the population mortality into three parts: the fixed general level of mortality α_x, the refining trend of mortality over time $\beta_x \kappa_t$, and the random fluctuation term. x, which is independent of time, represents the general level of logarithmic mortality at age x. It can take the average of historical data in the time dimension or the value of the last observation year to reflect the difference of mortality at different ages. The model decomposes the trend of mortality over time into the interactive product of age and time. κ_t indicates the relative intensity of overall mortality in each year and gradually decreases with time, reflecting the continuous improvement of mortality over time. β_x shows the sensitivity of the logarithmic mortality rate of the x-year population towards the change in the overall trend, reflecting the inconsistent rate of decline at different ages. The last one is a random error term that reflects the random fluctuation of mortality rate outside the trend.

To ensure the uniqueness of the results, the Lee–Carter model contains two restrictions:

$$\begin{gathered}\sum_x \beta_x = 1,\\ \sum_t \kappa_t = 0.\end{gathered} \tag{5}$$

At present, the parameter estimation methods for the Lee–Carter model mainly include singular value decomposition (SVD), ordinary least squares (OLS), weighted least squares (WLS), and Poisson log bilinear model (Poisson log-bilinear). The estimation of α_x is not controversial. Generally, it is

$$\alpha_x = \frac{1}{n} \sum_{t=T_1}^{T_n} \ln m_x(t). \tag{6}$$

Or, to increase the impact weight of the latest observations, the estimate is

$$\alpha_x = \ln m_x(T_n). \tag{7}$$

The main difference among the mentioned methods is how to decompose the trend effect into the age factor β_x and the time factor κ_t. Based on the characteristics of the matrix, singular value decomposition (SVD) extracts the main information of trend effect skillfully. The main estimation method is to singly decompose the matrix $\ln m_x(t) - \alpha_x$, which can be obtained as follows:

$$\mathrm{SVD}\left[\ln m_x(t) - \alpha_x\right] = \sum_{i=1}^{r} \rho_i U_{x,i} V_{i,t}, \tag{8}$$

where r is the rank of the matrix $\ln m_x(t) - \alpha_x$ and $\rho_1, \ldots, \rho_2, \ldots, \rho_r$ are the singular values of the matrix from large to small. $U_{x,i}$ and $V_{i,x}$ are, respectively, two singular vectors. Since ρ_1 is much larger than the subsequent eigenvalues, most of the information of the matrix $\ln m_x(t) - \alpha_x$ can be extracted only by taking the first term $U_{x,1}$ and $V_{1,t}$ of two singular vectors, and the matrix is as follows:

$$\ln\left[m_x(t) - \alpha_x\right] \approx \rho_1 U_{x,1} V_{1,t}. \tag{9}$$

Thus, estimates of β_x and κ_t can be obtained:

$$\beta_x = \frac{U_{x,1}}{\sum_x U_{x,1}},$$
$$\kappa_t = \rho_1 V_{1,t} \sum_x U_{x,1}. \tag{10}$$

The fitting effect of the singular value decomposition depends on the efficiency of extracting information from the $\ln m_x(t) - \alpha_x$ matrix. It is generally considered that the method can explain more than 90% of the sum of squares of deviations. After obtaining the estimated values of the parameters, it can be found that α_x and β_x are fixed over time, and the variety of mortality over time is mainly reflected by $\{\kappa_t\}$. The prediction value of future mortality can be obtained by extrapolating $\{\kappa_t\}$. It is believed that $\{\kappa_t\}$ is a random walk with drift or ARIMA process. According to the BIC information criterion, $\{\kappa_t\}$ should be the ARIMA (0, 1, 1) Model with drift term.

2.2. Measurement of Longevity Risk

2.2.1. Method of Pressure Trend. Taking the trend risk of mortality prediction into account, the method of pressure trend gives the extreme situation of the long-term decline of mortality. It then measures the difference of the present value paid by insurance companies between the serious cases and the optimal estimation. For instance, $\{\kappa_t\}$ shows the decreasing trend of mortality in the Lee–Carter model. When using not only ARIMA but also drifting random walk model to predict the value of future κ_T, it is a random variable obeying normal distribution. After taking the expected value of κ_T, we can get the mortality in the middle situation, that is, the optimally estimated mortality. If the risk level is given certainly, after taking the 1-α quantile of κ_T, we can get the critical value of trend mortality under the risk level. The difference between the pressure trend line and the optimal mortality estimate trend line is the possibility of underestimation of the trend mortality. Under the pressure trend method, measuring formula of longevity risk is defined as

$$\text{LRM} = \left(\frac{\ddot{a}_{x:\, w-x}^{z=\phi^{-1}(1-\alpha)}}{\ddot{a}_{x:\, w-x}^{z=0}} \right) \cdot 100\%. \tag{11}$$

Because there is a certain correlation in mortality in different periods, the extreme trend of mortality at each moment in the future will overestimate the risk of longevity to some extent. It can be seen that the method of pressure trend is not based on the VaR, and there is no clear standard for the value of α. Considering that the second quantitative impact study (QIS2) proposes to use the 75% quantile to measure the risk margin, and the European Solvency Regulatory Standard II requires risk margin to be sufficient to ensure that the probability of loss exceeding solvency capital is less than 0.5%, based on which we calculate the margin of longevity risk at 25% and 0.5% risk levels.

2.2.2. Method of Mortality Fluctuation. Method of mortality fluctuation is a standard method required by QIS5 to calculate the marginal risk of longevity. It adjusts for conservative mortality by assuming an immediate downward wave in current and future expected mortality. The formula is defined as follows:

$$q_{x,t}^{\text{shock}} = q_{x,t} \times (1 - f). \tag{12}$$

$q_{x,t}$ is the optimal estimated mortality and f is the mortality adjustment ratio. The formula of the risk margin under this method is

$$\text{LRM} = \left(\frac{\ddot{a}_{x:\, w-x}^{f}}{\ddot{a}_{x:\, w-x}} - 1 \right) \cdot 100\%. \tag{13}$$

According to the requirements of QIS5, f takes 20%, which means that, in the conservative case, a 20% reduction in mortality rate in the future is the best estimate. China's C-ROSS has a distinct demand, that is, for the remaining life insurance period, and different downward ratios are given for each year's mortality. The specific adjustments are as follows.

$$\begin{aligned} -f &= \text{SF} \\ &= \begin{cases} (1-3\%)^t - 1, & 0 < t \le 5, \\ (1-3\%)^5 \times (1-2\%)^{t-5} - 1, & 5 < t \le 10, \\ (1-3\%)^5 \times (1-2\%)^5 \times (1-1\%)^{t-10} - 1, & 10 < t \le 20, \\ (1-3\%)^5 \times (1-2\%)^5 \times (1-1\%)^{10} - 1, & t > 20. \end{cases} \end{aligned} \tag{14}$$

C-ROSS has made minor adjustments to recent mortality rates but major readjustment to long-term rate. Figure 1 shows a comparison of the mortality ratio of the QIS5 and C-ROSS in conservative cases. For QIS5, the mortality ratio f is always 20%, while for C-ROSS, f gradually increases with time, but the increasing trend is slowing down. Within eight years after the evaluation date, the C-ROSS mortality rate is lower than QIS5. After that, the C-ROSS mortality rate becomes higher than QIS5 and remains unchanged at 29.8% after 20 years.

The mortality fluctuation method not only contains the trend risk of mortality in the long-term process but also is a comprehensive measure of the components of longevity risk. Börger points out that the mortality fluctuation method had been underestimating the longevity risk of low age and overestimated the longevity risk of high age longevity [11]. Thus, it is structurally defected. Next, the paper will measure the margin risk of Chinese life annuity products under the QIS5 and C-ROSS standards in the empirical analysis.

2.2.3. Stochastic Simulation Based on VaR and CTE. Widely used in the risk management field, Value at Risk (VaR) embodies the maximum possible loss at a specific level, that is, to ignore the extreme risk at the tail and only consider the maximum loss within a certain probability. Conditional Tail Expectation (CTE) is a conditional expectation in the case of tail extreme risk. It can effectively

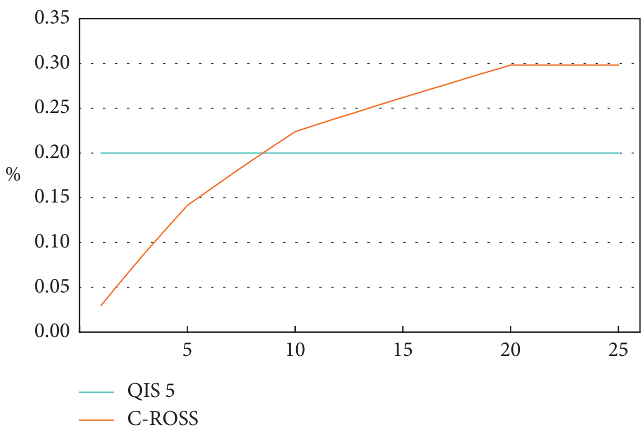

Figure 1: Comparison of mortality ratios between QIS5 and C-ROSS under conservative cases.

describe the extreme risk of the tail and then make up for the deficiency of VaR to some extent. The EU Solvency II requires that the probability of the insurer's loss exceeding its repayment capital should be less than 0.5%, which is a kind of risk regulation based on VaR. At the same time, the Swiss Solvency Test (SST) takes CTE as the standard method of risk measurement. The general expression formulas for VaR and CTE are as follows:

$$\begin{aligned} \mathrm{VaR}_\alpha &= \min\{x \mid F(x) > \alpha\}, \\ \mathrm{CTE}_\alpha &= \mathrm{VaR}_\alpha + \mathrm{E}\big(X - \mathrm{VaR}_\alpha \mid X > \mathrm{VaR}_\alpha\big). \end{aligned} \tag{15}$$

The method based on VaR and CTE needs to measure the loss distribution. However, in reality, due to the complexity of the mortality change and the structural characteristics of the annuity products, the loss distribution can only be fitted by random simulation, based on which the values of VaR and CTE are calculated. Plat uses stochastic simulation to measure the longevity risk of lifelong pensions based on population mortality data of the Dutch, but it had some nonsystemic hazard [12]. Here, the method of Plat is revised to be suitable for China, and it is described by taking the Lee–Carter model as an example. The steps are as follows:

(i) Select a data set with a calendar year from t_L to t_H and age from x_l to x_h, including the number of deaths for each age and the corresponding mid-year population estimates. Then corresponding central mortality rate $m_x(t)$ can be calculated.

(ii) Fit the data in the first step by the Lee–Carter model and find the corresponding parameters in the model.

(iii) Perform a random simulation of the future value of $\{\kappa_t\}$ and obtain a random path of $\{\kappa_t\}$. Then the downward trend in future mortality is calculated.

(iv) Bring the obtained $\{\kappa_t\}$ random path into the normative Lee–Carter model, and add the annual random fluctuation to get a stochastic simulation $\{m_x(t)\}$ of mortality of different ages in each year in the future.

(v) According to the above formula, convert the central mortality rate to the probability of death $\{q_x(t)\}$. Then the simulated life table of a specific cohort can be obtained by taking the death probability value of the corresponding age and year. After that, the lifetime annuity factor $\ddot{a}^{(1)}_{x:\,w-x}$ of the cohort can be calculated.

(vi) Repeat the above 3 to 5 steps for n times; then we can get n stochastic mortality paths; finally find a set of n annuity factors:

$$S = \left\{\ddot{a}^{(j)}_{x:\,w-x}\right\}, \qquad j = 1, 2, \ldots, n. \tag{16}$$

(vii) Select the 1-α quantile of S as s_{VaR_α}, and calculate the conditional tail expectation as s_{CTE_α}. The corresponding longevity risk metric is

$$\begin{aligned} \mathrm{LRM} &= \left(\frac{s_{\mathrm{VaR}_\alpha}}{\ddot{a}_{x:\,w-x}} - 1\right) \cdot 100\%, \\ \mathrm{LRM} &= \left(\frac{s_{\mathrm{CTE}_\alpha}}{\ddot{a}_{x:\,w-x}} - 1\right) \cdot 100\%. \end{aligned} \tag{17}$$

According to the request of EU Solvency II, α is 0.5%. So, the number of simulations is generally required to be at least 1000 times. Performing 30, 000 simulations in an empirical analysis could improve the accuracy of measuring longevity risk.

2.2.4. VaR-Based Stochastic Simulation from One-Year Perspective. The above methods consider changes in mortality during the entire insurance period. Still, unlike other risks faced by insurers, longevity risks are chronic; that is, the mortality rate reduces slowly during a long period until it is completely exposed. Therefore, in the actual operation, the insurer needs to constantly adjust the mortality model according to the new information of mortality and adjust the reserve level correspondingly, leading to two problems: First, how will the mortality model vary with the new mortality data added in the next year? Second, how will the change of the mortality model lead to the change of reserves? From these two problems, Richards proposes a method based on VaR in a one-year period to calculate the marginal longevity risk. The core idea of this method is to assume that there will be adverse fluctuations in the mortality in the next year so that the mortality model and the predicted mortality level will be changed, and then calculate the future cash payment value of the insurance company under the new situation. This paper constructs a one-year VaR-based stochastic simulation method suitable for China. The stimulation could measure the longevity risk of Chinese commercial pension funds, and the steps are as follows:

(i) Select a data set with a calendar year from t_L to t_H and age from x_l to x_h, including the number of deaths for each age and the corresponding mid-year population estimate. Then the corresponding central mortality rate $m_x(t)$ can be calculated.

(ii) Fit the data in the first step using the Lee–Carter model and find the corresponding parameters in the model.

(iii) Perform a random simulation of κ_{t_H+1} to obtain a value of it.

(iv) Bring the obtained stochastic simulation value of κ_{t_H+1} into the normative Lee–Carter model, and add the annual random fluctuation to acquire the age-specific mortality rate for the next year; then get a stochastic simulation $\{m_x(t)\}(t_H+1)$.

(v) Put $\{m_x(t)\}(t_H+1)$. into the data set in the first step, refit the new data set with the Lee–Carter model, and predict the optimal estimate of future mortality $\{m_x(t)\}$.

(vi) According to formula (4), convert the central mortality rate into the probability of death $\{q_x(t)\}$. Then the simulated life table of a specific cohort can be obtained by taking the mortality value of the corresponding age and year. After all, the lifetime annuity factor $\ddot{a}^{(1)'}_{x:\,w-x}$ of the cohort can be calculated.

(vii) Repeat the above 3 to 5 steps n times, get n stochastic mortality paths, and finally obtain a set of n annuity factors:

$$S = \left\{\ddot{a}^{(j)'}_{x:\,w-x}\right\}, \quad j = 1, 2, \ldots, n. \tag{18}$$

(viii) The quantile of 1-α of S is selected as $s_{\mathrm{VaR}'_\alpha}$, and the corresponding longevity risk metric is

$$\mathrm{LRM} = \left(\frac{S_{\mathrm{VaR}'_\alpha}}{\ddot{a}_{x:\,w-x}} - 1\right) \cdot 100\%. \tag{19}$$

The one-year VaR-based stochastic simulation considers the longevity risk in the short term focusing on the possible adverse changes in mortality in the next year and the long-term effects of such changes. This method, which only considers the risk factors of one year, is to split the long-term longevity risk into each year in advance and help the insurance company shorten the long-term hazard from the perspective of operation. It can also test the sensitivity of mortality model towards new data.

3. Comparison of Longevity Risk Measurement

Lee–Carter model, which directly models mortality, reflects the characteristics of mortality more in line with the characteristics of China's population mortality. Based on the mortality predicted by Lee and Carter, we could compare the different outcomes from different measurements of longevity risk. Since China's population mortality statistics are generally up to 90 or 100 years of age, we have used the Kannisto Model to extrapolate the mortality rate of the elderly over 90 years of age. The Kannisto Model has a good effect on the extrapolation of the mortality rate of the elderly population. The specific form of the Kannisto Model is as follows:

$$m_x = \frac{ae^{bx}}{1 + a\left(e^{bx} - 1\right)}. \tag{20}$$

This paper predicted the results of male and female mortality from 60 to 110 years of age using Lee–Carter model and Kannisto model every ten years from 2017 to 2057. It is observed that the projected mortality rate presents a general trend of increasing with age and decreasing with time.

To calculate the longevity risk of life annuity products sold to 60-year-olds in 2017, the benchmark pricing rate is assumed to be 3.5%. The longevity risk is classified into two types. The first type of longevity risk is the longevity risk taken by insurance companies when using the period life table to make a price, regardless of the future mortality decline of the insured cohort. The second type of longevity risk is the longevity risk taken by insurance companies when using the cohort life table to make a price but underestimating the prediction of future cohort mortality. In conclusion, the longevity risk from calculating the period life table belongs to the first type, while that from the cohort life table belongs to the second type.

3.1. *Longevity Risk from the Period Life Table.*

We compared the period life table and the cohort life table of males and females in 2017. At the same time, the confidence interval of trend fluctuation is given under a 99% confidence level of cohort life table based on the pressure trend method. It can be discovered that the period life table only contains the static mortality rate of the current year without considering the decline of the insured mortality rate. The mortality level of the period life table is not only higher than that of the optimal estimation of the cohort life table but also higher than the upper limit of the 99% confidence interval of the cohort life table in the advanced age stage. If the life table is used to make a price for the annuity, the premium level will be lower than the normal level, which leads to the risk of insufficient solvency for the insurance company.

Next, the paper measures the longevity risk faced by insurance companies under the period life table pricing. Table 1 gives the measurement values of longevity risk margin of 60-year-old male and female life annuity under different interest rates. The period life table does not take into account the future mortality decline of the insured cohort. Under the interest rate of 3.5%, the annuity factors of males and females, which are the prices of an annuity product whose annual payment is 1, are 15.5 and 17.1, respectively. But, in fact, the group's future mortality rate should have followed the cohort life table. Under the optimal estimate, the marginal longevity risk is 7.7% for men and 6.7% for women. If the future mortality falls to the lower edge of 99% confidence interval of trend mortality, the extra payments of lifetime annuity products for men and women will reach 17.9% and 13.6% of their premiums. Also, interest rates have significant impacts on the measurement of margin risk. The higher the evaluation interest rate is, the smaller the margin of longevity risk will become and vice versa, which is mainly because the low-interest rate has a less discount effect

Table 1: The first type of longevity risk measure for the pension of 60-year-olds.

	Male			Female		
	2.50%	3.50%	4.50%	2.50%	3.50%	4.50%
Annuity factor	17.2	15.5	14.1	19.2	17.1	15.4
LRM (99% high)	−3.5%	−3.3%	−3.1%	−1.2%	−1.2%	−1.2%
LRM (optimal estimate)	9.0%	7.7%	6.6%	7.9%	6.7%	5.7%
LRM (99% low)	20.9%	17.9%	15.4%	15.9%	13.6%	11.6%

on the difference in the payment due to the variety in mortality in future years. In comparison, high-interest rate has a greater impact.

Figure 2 shows the effect from the initial payment age on marginal longevity risk. It can be seen that, for males and females, when initial payment age changes from 60 to 110, the first type of marginal longevity risk increases first and then decreases, with the initial benefit age, reaching the maximum value of 30.4% for men at 93 years of age and 20.4% for women at 92 years of age. For all ages, the first type of risk influences male pension greater than females. The risk margin of insurance policy with low initial payment age is low, which is mainly due to the long insurance period and the greater discount effect of discount rate on the difference of payment value under different mortality rates. However, the risk margin of the insurance policy with high initial payment age decreases mainly because the longevity risk decreases with the shortening of the policy life. In reality, there is almost no annuity product for people over 90 years of age. Therefore, for insurers, the lower the initial payment age of an annuity product is the smaller risk of the first type they will face.

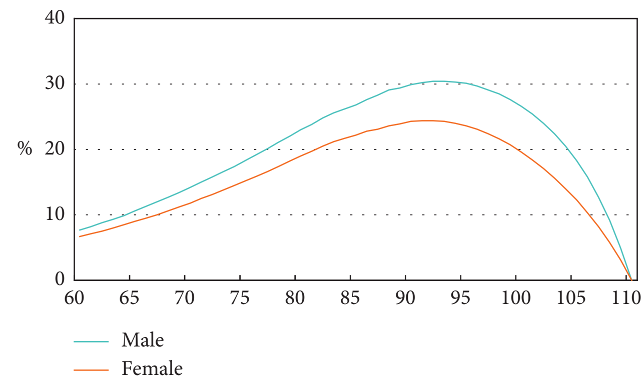

Figure 2: Effect of initial payment age under the first type.

3.2. Longevity Risk from the Cohort Life Table. In reality, insurers can use cohort life table as pricing base to avoid the first type of longevity risk. Still, the second type of longevity risk caused by the uncertainty of future mortality cannot be circumvented. Table 2 shows the risk margin values calculated by different longevity risk measurement methods. It is observed that the risk value level under the pressure trend method significantly affects the risk margin. When α is 0.5%, the marginal longevity risk of male and female life annuities is more than other measures, reaching 9.5% and 6.4%, respectively. When α is 25%, the marginal risk is smaller than the others, which are 2.6% and 1.8%, respectively.

Comparing the results of mortality fluctuation method, the standard of China's C-ROSS longevity risk measurement is more stringent than that of EU QIS5. Specifically, under the intermediate interest rate level, for the life annuity of 60-year-old males, the longevity risk margin is 5.2% under QIS5 standard and 6.6% under C-ROSS standard. For females, the marginal longevity risks measured by QIS5 and C-ROSS are 3.9% and 5.3%, respectively. Similarly, the marginal value of risk measured by C-ROSS is higher than QIS5 at both high-interest and low-interest rates. Therefore, it can be proved that China's second generation of compensation in the declining level of mortality estimate is more conservative.

The stochastic simulation based on VaR and CTE accurately defines the conditional expectation of the maximum loss proportion and tail loss faced by insurers under a specific risk level. It is found that the marginal risk of a male life annuity as a standard is 7.9%, which is higher than that of female life annuity by 5.5%. In other words, to prevent an unexpected drop in mortality, the insurer needs to prepare an additional 7.9% of the premium for the male and 5.5% for the female as the venture capital to reduce the risk of being unable to repay due to insufficient capital to 0.5%, meeting the requirements of the EU for the second generation. The standard marginal risk measure under the criterion is greater with 9% for males and 6.1% for females. After comparing stochastic simulation method with the pressure trend method, it can be seen that the latter focuses on the extreme level of the change in the mortality trend, while it ignores the hedging in the risk of mortality fluctuation in different years. Thus, under the same risk level, the pressure trend method overrates the longevity risk, while the marginal longevity risk brought by stochastic simulation has more practical significance.

At the risk level of 0.5%, the marginal longevity risks of male and female lifelong pensions measured by stochastic simulation method in one-year perspective are 3.8% and 3.3%, respectively, which are smaller than those measured by other ways at the same risk level. The main reason is that VaR method based on one-year perspective focuses on the risk situation of the next year rather than the size of longevity risk in the long-term process. It reflects the additional venture capital that the insurer should prepare for the long-term debt changes in response to mortality change next year. Under this method, the longevity risk in the long-term process is gradually reflected in the insurance period through annual calculation.

Also, through comparing the marginal longevity risk of males and females, it can be seen that, same as the first type of longevity risk, the second one faced by men for lifelong pension is also greater than that of women as well, which is mainly because the current mortality level of men is higher than that of women, and the improvement space and possible fluctuation range in the future are also larger, while the current mortality rate of women is already at a lower level. That is to say, the decreasing mortality rate for females

Table 2: The second type of longevity risk measurement for the pension of 60-year-olds.

	Male			Female		
	2.5%	3.5%	4.5%	2.5%	3.5%	4.5%
Annuity factor	18.8	16.7	15.0	20.7	18.2	16.2
Pressure trend method (0.5%)	11.0%	9.5%	8.2%	7.5%	6.4%	5.6%
Pressure trend method (25%)	2.9%	2.6%	2.3%	2.1%	1.8%	1.5%
Mortality fluctuation method (QIS5)	6.0%	5.2%	4.6%	4.6%	3.9%	3.4%
Mortality fluctuation method (C-ROSS)	7.8%	6.6%	5.6%	6.3%	5.3%	4.5%
Stochastic simulation (VaR 0.5%)	9.4%	7.9%	6.9%	6.5%	5.5%	4.7%
Stochastic simulation (CTE 0.5%)	10.5%	9.0%	7.6%	7.3%	6.1%	5.3%
One-year stochastic simulation (0.5%)	4.4%	3.8%	3.4%	3.8%	3.3%	2.8%

will bring even less impact on its longevity risk. The effect of interest rates on the second type of longevity risk is the same as that of the first type. For all longevity risk measurement methods, the marginal interest rate and longevity risk are inversely proportional.

Overall, stochastic simulation based on VaR and CTE can better measure the longevity risk in the long run. Therefore, the calculation results have more clear practical significance for insurers [13]. The one-year VaR-based stochastic simulation rule decomposes the long-term longevity risk into each year, which can be used by the insurer to deal with the longevity risk in each policy year of the whole insurance period. The pressure trend method and the mortality fluctuation method are easy and convenient. The pressure trend method, which considers the extreme situation of a trend change, overestimates the longevity risk under a specific risk level. However, the adjustment of mortality fluctuation method to the lower limit of mortality fluctuation is relatively rough. From the calculation results of China's actual data, both QIS5 and C-ROSS measurement standards underestimate the longevity risk.

4. Investment Risk Calculation

Another important risk of a lifelong annuity is investment risk. Here, a simple measurement of investment risk is shown. According to the annually disclosed data of insurance funds' operation, the investment yields of China's insurance funds are 3.39%, 5.04%, 6.30%, 7.56%, and 5.66% from 2012 to 2016, respectively. Here, we calculated the risk of loss for the life annuity when the initial payment age is 60, and the actual investment returns are 3.39%, 3.25%, 3%, 2.75%, and 2.5%. The results are shown in Table 3. It is found that when the actual investment yield is lower than the pricing rate of 3.5%, the insurer will face additional losses. When the practical return of investment falls to 3.39%, the excess loss ratios for male and female life annuities are 1.35% and 1.25%, respectively. As the actual return on investment is lower than the pricing rate, the proportion of additional loss increases rapidly. When the actual investment yield drops to 2.5%, the loss rate of a male life annuity is 13.5%, and the loss rate of female life annuity reaches 12.5%, exceeding the level of longevity risk.

Figure 3 shows the risk of loss for life annuities at different initial payment ages when the actual investment yield is lower than the pricing interest rate of 3.39%. It is found that when the initial payment age is lower than 93, the risk of loss for men is higher than that for women. When it is higher than 93, there is almost no gap between men and women. Overall, the risk of investment loss decreases as the initial payment age increases, which is mainly because the older the initial payment age is, the shorter the insurance period and the lower the investment risk we have.

Table 3: Risk of investment loss for the lifelong pension of 60-year-olds.

	Actual return on investment				
	3.39%	3.25%	3.00%	2.75%	2.50%
Male	1.35%	3.11%	6.39%	9.84%	13.48%
Female	1.25%	2.88%	5.92%	9.10%	12.45%

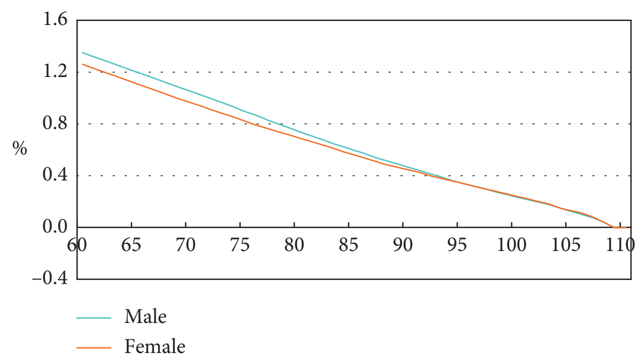

Figure 3: Impact of initial payment age on lifetime annuity investment loss risk.

5. Conclusion

This paper studies the annuity puzzle from the supply perspective, pays attention to the longevity risk faced by insurers, and focuses on the longevity risk measurement. We have established a unified framework of longevity risk measurement, covering population mortality model and longevity risk measurement model. Based on the actual data from China, the differences among diverse mortality models and different longevity risk measurement models were compared, and the longevity risk faced by China's life pension fund was measured.

As for the measurement of longevity risk, different risk measurement methods have their emphasis. The marginal longevity risk based on the stochastic simulation of VaR and CTE is more realistic for insurers. In comparison, the pressure trend method overestimates the longevity risk, while QIS5 and C-ROSS based mortality volatility underestimates the longevity risk. It can be seen that current regulatory requirements cannot fully reflect the longevity risk. The stochastic simulation based on one-year perspective measures the longevity risk from a short-term perspective and its measured value is relatively small, reflecting the impact of the adverse changes in mortality in the next year. This method can shorten long-term longevity risk, so that insurers can gradually establish longevity risk reserve during the insurance period.

Above all, the life annuity insurance faces longevity risk, and the longevity risk scale could have significant impacts on the insurer's solvency. The inability to accurately assess the longevity risk and manage longevity risks has greatly limited the incentives for insurers to provide lifelong pensions. It is recommended to strengthen the study on longevity risk measurement and use the mortality prediction models that are suitable for China's condition and the risk measurement models that could accurately reflect the longevity risk to help the insurers precisely measure the lifelong longevity risk and prepare for the proper management.

Data Availability

The data used to support the findings of this study are from the Human Mortality Database and the China National Bureau of Statistics.

Conflicts of Interest

The authors declare that there are no conflicts of interest regarding the publication of this paper.

Acknowledgments

This work was supported by the Beijing Social Science Foundation of China (no. 19YJC042), the Special Foundation for Basic Scientific Research Business Expenses of Universities Owned by the Municipal Government of Beijing of Capital University of Economics and Business, titled "Research on the Measurement of Longevity Risk of Pension System Considering the Change of Death Pattern."

References

[1] R. D. Lee and L. R. Carter, "Modeling and forecasting U. S. mortality," *Journal of the American Statistical Association*, vol. 87, no. 419, pp. 659–671, 1992.

[2] A. E. Renshaw and S. Haberman, "A cohort-based extension to the Lee-Carter model for mortality reduction factors," *Insurance: Mathematics and Economics*, vol. 38, no. 3, pp. 556–570, 2006.

[3] A. J. Cairns, D. Blake, and K. Dowd, "A two-factor model for stochastic mortality with parameter uncertainty," 2005.

[4] A. E. Raftery, J. L. Chunn, P. Gerland, and H. Ševčíková, "Bayesian probabilistic projections of life expectancy for all countries," *Demography*, vol. 50, no. 3, pp. 777–801, 2013.

[5] M. Zhao and X. J. Wang, "A quantitative comparison of multiple population mortality model on some east asian countries and regions," *Mathematical Problems in Engineering*, vol. 50, 2020.

[6] W. Yu, P. Guo, Q. Wang, G. Guan et al., "On a periodic capital injection and barrier dividend strategy in the compound Poisson risk model," *Mathematics*, vol. 8, no. 4, p. 511, 2020.

[7] X. Peng, S. Wen, W. Su, and Z. Zhang, "On a perturbed compound Poisson risk model under a periodic threshold-type dividend strategy," *Journal of Industrial & Management Optimization*, vol. 16, no. 4, pp. 1967–1986, 2020.

[8] A. Olivieri, "Uncertainty in mortality projections: an actuarial perspective," *Insurance: Mathematics and Economics*, vol. 29, no. 2, pp. 231–245, 2001.

[9] A. Olivieri and E. Pitacco, "Solvency requirements for pension annuities," *Journal of Pension Economics and Finance*, vol. 2, no. 2, pp. 127–157, 2003.

[10] N. Hári, A. De Waegenaere, B. Melenberg, and T. E. Nijman, "Longevity risk in portfolios of pension annuities," *Insurance: Mathematics and Economics*, vol. 42, no. 2, pp. 505–519, 2008.

[11] M. Börger, "Deterministic shock vs. stochastic value-at-risk - an analysis of the Solvency II standard model approach to longevity risk," *Blätter der DGVFM*, vol. 31, no. 2, pp. 225–259, 2010.

[12] R. Plat, "One-year value-at-risk for longevity and mortality," *Insurance: Mathematics and Economics*, vol. 49, no. 3, pp. 462–470, 2011.

[13] J. R. Wilmoth, *Mortality Projections for Japen: A Comparison of Four Methods*, Health & Mortality Among Elderly Populations, New York, NY, USA, 1996.

Hindawi
Mathematical Problems in Engineering
Volume 2020, Article ID 1420618, 9 pages
https://doi.org/10.1155/2020/1420618

Research Article

On the Usefulness of the Logarithmic Skew Normal Distribution for Describing Claims Size Data

E. Gómez–Déniz [1] and E. Calderín-Ojeda [2]

[1] *Department of Quantitative Methods in Economics and Tides Institute, University of Las Palmas de Gran Canaria, Las Palmas de Gran Canaria 35017, Spain*
[2] *Centre for Actuarial Studies, Department of Economics, The University of Melbourne, Melbourne, Australia*

Correspondence should be addressed to E. Calderín-Ojeda; ecalderin@unimelb.edu.au

Received 24 May 2020; Accepted 17 July 2020; Published 18 September 2020

Academic Editor: Łukasz Jankowski

In this paper, the three-parameter skew lognormal distribution is proposed to model actuarial data concerning losses. This distribution yields a satisfactory fit to empirical data in the whole range of the empirical distribution as compared to other distributions used in the actuarial statistics literature. To the best of our knowledge, this distribution has not been used in insurance context and it might be suitable for computing reinsurance premiums in situations where the right tail of the empirical distribution plays an important role. Furthermore, a regression model can be simply derived to explain the response variable as a function of a set of explanatory variables.

1. Introduction

The modelling of large claims is a topic of relevant importance in general insurance and reinsurance, particularly in the field of mathematical risk theory, see, for instance, McNeil [1]; Beirlant and Teugels [2]; Beirlant et al. [3]; and Embrechts et al. [4]. For a comprehensive study about reinsurance, see the recent book of Albrecher et al. [5]. It is our interest to find simple statistical distributions appropriate for modelling both, smaller and medium-size losses with a high frequency and large losses with a low frequency. This is an issue of particular interest in the context of reinsurance and premium calculation principles. In this sense, the classical Pareto distribution [6–8] has been traditionally considered as a suitable claims' size distribution in relation to rating problems. Concerning this, the single parameter Pareto distribution not only has nice statistical properties but also provides a good description of the random behaviour of large losses (e.g., the right tail of the distribution). Particularly, when calculating deductibles and excess-of-loss levels of reinsurance, the simple Pareto distribution has been proved to be convenient (see, for example, [9, 10]). As an alternative to the classical Pareto distribution, other models have been recently introduced in the actuarial literature by Sarabia et al. [11–13] and Ghitany et al. [14].

On the contrary, there exist many situations where the empirical data show slight or marked asymmetry. This is frequently the case, for example, with actuarial and financial data that also have heavy tails reflecting the existence of extreme values. These two features imply that the data cannot be adequately modelled by the Gaussian or normal distribution.

Let g and G, respectively, be the probability density function (pdf) and the cumulative distribution function (cdf) of a symmetric distribution. A random variable Z is said to have a skew distribution if its pdf is given by

$$f_Z(z) = 2g(z)G(\gamma z), \quad -\infty < z < \infty, \ \gamma \in \mathbb{R}. \tag{1}$$

This family of distributions has been widely studied as an extension of the normal distribution via a shape parameter, γ, that accounts for the skewness of the model. When $g(\cdot)$ and $G(\cdot)$ are replaced in (1) by $\phi(z)$ and $\Phi(z)$, i.e., the standard normal density and distribution function, respectively, the resulting model is called the skew normal distribution.

In this paper, special attention is paid to the generalized skew normal density provided in Henze [15] and also studied by Arnold and Beaver [16]. Its pdf is given by

$$f_Z(z) = \frac{\phi(z)\Phi(\gamma_0 + \gamma_1 z)}{\Phi\left(\gamma_0/\left(\sqrt{1+\gamma_1^2}\right)\right)}, \quad -\infty < z < \infty,\ \gamma_0, \gamma_1 \in \mathbb{R}. \tag{2}$$

For multivariate extensions, see for instance Azzalini and Valle [17], Azzalini and Capitanio [18], and Arnold and Beaver [16]. For an exhaustive and comprehensive study of the skew-normal distribution, see the recent book of Azzalini [19].

This paper is organized as follows. In Section 2, the proposed distribution is studied and some interesting properties are given. Numerical applications are provided in Section 3, and conclusions are drawn in Section 4.

2. Modelling the Size of Losses

The basic skew lognormal distribution has been studied by Lin and Stoyanov [20] (see also [19]; Chap. 2, [21–23]). Nevertheless, in this paper, we will pay special attention to the distribution arising from exponentiation of (2) in the following sense: if X is a random variable with density (2), $X \sim f_Z$, we consider a new random variable $Y \sim \exp(X)$. Also, if taking $\gamma_0 = \gamma_1 = \lambda$ and using a linear transformation, we allow for more flexible location and scale parameters in our model. Thus, we get the pdf given by

$$f_{\mu,\sigma,\lambda}(x) = \frac{\phi\left(r_{\mu,\sigma}(x)\right)}{\sigma x}\frac{\Phi\left(\left(1 + r_{\mu,\sigma}(x)\right)\lambda\right)}{\Phi(\lambda_0)}, \quad x > 0, \tag{3}$$

where

$$r_{\mu,\sigma}(x) = \frac{\log x - \mu}{\sigma}, \qquad \lambda_0 = \frac{\lambda}{\sqrt{1+\lambda^2}}. \tag{4}$$

Here, $\lambda \in \mathbb{R}$, $\mu \in \mathbb{R}$, and $\sigma > 0$. Observe that when $\lambda = 0$ expression (3) reduces to the classical lognormal distribution. It can be seen that the parameter λ regulates the shape of the distribution. Furthermore, Lin and Stoyanov [20] established that the distribution has heavy tails and therefore it is a suitable distribution to be incorporated to the wide catalogue of heavy tails (see [5]). Additionally Lin and Stoyanov [20] provided a stochastic representation of this distribution and determined that the distribution can be obtained as the product of two independent random variables, one of which is lognormal and the other one a logarithmic half-normal. Simple calculations show that density (3) can be also written as

$$f_{\mu,\sigma,\lambda}(x) = \frac{\exp\left\{1/2\left(1 + 2r_{\mu,\sigma}(x)\right)\right\}}{\Phi(\lambda_0)} f_Z(z), \tag{5}$$

where $f_Z(z)$ is expression (1) with $z = (1 + r_{\mu,\sigma}(x))$, $\gamma = \lambda$, $g(z) = \phi(z)$, and $G(z) = \Phi(z)$.

It is straightforward to show that the distribution is unimodal with the mode satisfying the equation:

$$\frac{\lambda\phi\left(1 + r_{\mu,\sigma}(z)\right)}{\Phi\left(1 + r_{\mu,\sigma}(z)\right)} = r_{\mu,\sigma}(z) + \sigma. \tag{6}$$

The mean value and the second order moment of the random variable X with density (3), $X \sim \mathrm{LSN}(\mu, \sigma, \lambda)$, are given by

$$E[X] = \frac{\Phi((1+\sigma)\lambda_0)}{\Phi(\lambda_0)}\exp\left\{\mu + \frac{\sigma^2}{2}\right\}, \qquad E\left[X^2\right] = \frac{\Phi((1+2\sigma)\lambda_0)}{\Phi(\lambda_0)}\exp\left\{2\left(\mu + \sigma^2\right)\right\}. \tag{7}$$

Let $F_{\mu,\sigma,\lambda}(x) = \Pr[X \le x]$ denote the cdf of $X \sim \mathrm{LSN}(\mu, \sigma, \lambda)$. By applying directly result B.21 in Azzalini [19], it is not difficult to observe that this cdf is given by

$$\begin{aligned} F_{\mu,\sigma,\lambda}(x) = {} & \Phi\left(r_{\mu,\sigma}(x)\right) + \frac{1}{\Phi(\lambda_0)}\left[T\left(r_{\mu,\sigma}(x), \frac{\lambda_0}{r_{\mu,\sigma}(x)}\right) + T\left(\lambda_0, \frac{r_{\mu,\sigma}(x)}{\lambda_0}\right)\right. \\ & \left. - T\left(r_{\mu,\sigma}(x), \frac{\left(1 + r_{\mu,\sigma}(x)\right)\lambda}{r_{\mu,\sigma}(x)}\right) - T\left(\lambda_0, \frac{\lambda^2 + \left(1+\lambda^2\right)r_{\mu,\sigma}(x)}{\lambda}\right)\right], \end{aligned} \tag{8}$$

which is satisfied whenever $\lambda \neq 0$ and $x > 0$. Here, $T(x, a)$ represents Owen's function (see [24]) given by

$$T(x, a) = \frac{1}{2\pi}\int_0^a \frac{1}{1+t^2}\exp\left\{-\frac{1}{2}x^2\left(1+t^2\right)\right\}dt, \quad a \in \mathbb{R}^+. \tag{9}$$

If $\lambda = 0$, we deal with the standard normal distribution, and $T(x, 0) = 0$. The latter function can be easily computed by using the Mathematica software package.

The Acceptance-Rejection method of simulation can be used to generate random variates from (3). We begin by simulating a value from a lognormal distribution with parameters μ and σ. Then, having chosen an alternative random variable that follows a lognormal probability distribution to simulate from, we define a constant c in the following way:

$$c = \max_x \frac{f_{\mu,\sigma,\lambda}(x)}{g(x)}, \tag{10}$$

where $f_{\mu,\sigma,\lambda}(x)$ is given by (3) and $g(x)$ is the standard lognormal density. The algorithm for simulating a random variate from the LSN distribution is as follows:

(1) Generate a random variate from the lognormal distribution, x_1.
(2) Generate a random number u_1.
(3) If $u_1 \leq \Phi((1 + r_{\mu,\sigma}(x_1))\lambda)$, then set the simulated value from (3) equal to x_1. Otherwise, return to step 1.

By writing μ as

$$\mu = -\frac{\sigma^2}{2} + \log\left[\frac{\theta\,\Phi(\lambda_0)}{\Phi((1+\sigma)\lambda_0)}\right], \tag{11}$$

pdf (3) has mean value equal to $\theta > 0$ and variance provided by

$$\operatorname{var}(X) = \psi_1(\theta)\psi_2(\sigma,\lambda), \tag{12}$$

where

$$\begin{aligned} \psi_1(\theta) &= \theta^2, \\ \psi_2(\sigma,\lambda) &= \frac{\Phi((1+2\sigma)\lambda_0)\left[\Phi(\lambda_0)\right]^2 \exp\{-\sigma^2\}}{\left[\Phi((1+\sigma)\lambda_0)\right]^2} - 1. \end{aligned} \tag{13}$$

Therefore, a regression model can be derived from the LSN distribution. In this model, θ is the mean of the response variable and $\psi_2(\sigma,\lambda)$ can be interpreted as a precision parameter in a way such that, for fixed θ, the larger the value of $\psi_2(\sigma,\lambda)$, the larger the variance of X.

Let us now consider that the random variable X_i is related to a vector of k covariates $\mathbf{y}_i = (y_{1i}, \ldots, y_{ki})'$ associated with the ith observation, where $i = 1, 2 \ldots, n$. This vector assigns a weight of observable features is related to θ_i through a log link function and $\beta = (\beta_1, \ldots, \beta_k)'$ is a vector of regressors with $\beta_j \in \mathbb{R}$ for $j = 1, \ldots, k$. The regression model takes the form

$$\begin{aligned} X_i &\sim \operatorname{LSN}(\theta_i, \sigma, \lambda), \\ \log\theta_i &= \mathbf{y}_i'\boldsymbol{\beta}. \end{aligned} \tag{14}$$

Observe that log link ensures that θ_i falls within the interval $(0, \infty)$.

On the contrary, sometimes it is desirable to deal with a lower value in the range of X by shifting this random variable, say $X - \alpha$ with $\alpha > 0$, and therefore a shifted version of the previous distribution is obtained. In this case, it is convenient to work with the pdf given by

$$f_{\mu,\sigma,\alpha}(x) = \frac{\phi\left(\widetilde{r}_{\mu,\sigma,\alpha}(x)\right)}{\sigma(x-\alpha)}\,\frac{\Phi\left(\left(1+\widetilde{r}_{\mu,\sigma,\alpha}(x)\right)\lambda\right)}{\Phi(\lambda_0)}, \quad x > \alpha, \tag{15}$$

where

$$\widetilde{r}_{\mu,\sigma,\alpha}(x) = \frac{\log(x-\alpha) - \mu}{\sigma}. \tag{16}$$

Figure 1 shows pdf (15) as compared to the Pareto and PAT (Pareto ArcTan distribution) (this generalization of the

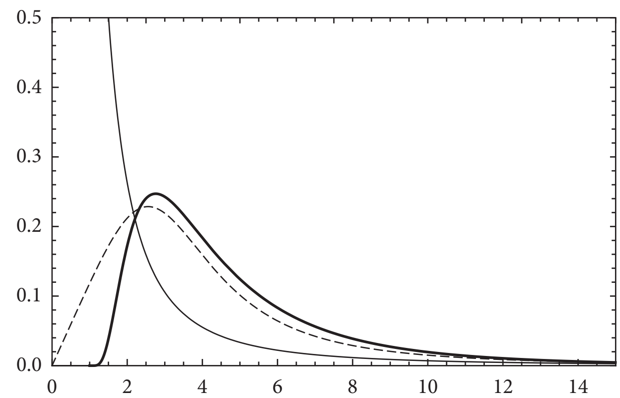

Figure 1: Graph of the Pareto (thin line), PAT (dashed line), and LSN (thick line) with the same mean given by (22).

Pareto distribution was proposed by Gómez-Déniz and Calderín-Ojeda [13]), all of them with the same mean, say (22), and a threshold of $\alpha = 1$. It is discernible that the tail of the LSN density seems larger than those ones of the other models.

By taking

$$\mu = -\frac{\sigma^2}{2} + \log\left[\frac{(\theta-\alpha)\Phi(\lambda_0)}{\Phi((1+\sigma)\lambda_0)}\right], \tag{17}$$

it is guaranteed that (15) has mean equal to $\theta > \alpha$. In this case, for the associated regression model, we will use the link function:

$$\theta_i = \alpha + \exp\{\mathbf{y}_i'\boldsymbol{\beta}\}, \tag{18}$$

which guarantees that θ_i falls within the interval $[\alpha, \infty)$.

It is already known (see Lemma 2 in [25]) that

$$\lim_{z\longrightarrow\infty} \frac{-\ln\Phi(-z)}{z^2} = \frac{1}{2}. \tag{19}$$

Then, it is straightforward to see that if $\lambda < 0$, we have

$$\lim_{x\longrightarrow\infty} \frac{-\ln\Phi\left(1 + r_{\mu,\sigma,\alpha}(x)\right)}{\left[\lambda\left(1 + r_{\mu,\sigma,\alpha}(x)\right)\right]^2} = \frac{1}{2}. \tag{20}$$

This can be used to easily obtain asymptotic values of the pdf given in (15). In fact, if $\lambda < 0$, we have the following approximation:

$$f(x) \approx \frac{\phi\left(r_{\mu,\sigma,\alpha}(x)\right)}{\sigma(x-\alpha)\Phi(\lambda_0)} \exp\left[-\frac{1}{2}\left(\left(1 + r_{\mu,\sigma,\alpha}(x)\right)\lambda\right)^2\right], \quad x > \alpha, \quad x \longrightarrow \infty. \tag{21}$$

3. Empirical Illustrations

In this section, the versatility of the proposed skew lognormal model, as compared with the Pareto distribution and the Pareto ArcTan Distribution [13], is tested using three datasets. The first dataset is the danishuni that can be found in the *R* package CASdatasets collected at *Copenhagen Reinsurance* and comprises 2167 fire losses over the period 1980 to 1990, adjusted for inflation to reflect 1985 values and are expressed in millions of Danish Krone. The second dataset is norfire comprises 9181 fire losses over the period 1972 to 1992 from an unknown Norwegian company. A priority of 500 thousands of Norwegian Krone (NKR) (if this amount is exceeded, the reinsurer becomes liable to pay) was applied to obtain this dataset. The third dataset considers hospital costs in the state of Wisconsin. It can be found in the personal web page of Professor E. Frees. It examines the impact of several predictors on hospital charges obtained from the Office of Health Care Information, Wisconsin's Department of Health and Human Services, in the year 1989. The response variable is the *logarithm of total hospital charges per number of discharges*, and the explanatory variables considered are the *health service area*, *hospital discharge costs*, *the type of payer*, *size of the area population*, *number of hospital beds*, and *average income within the area*. For comparison reasons some alternative distributions have been considered in this paper, their pdf's are provided in Appendix A and B. Some descriptive statistics of the three variables of interest are shown in Table 1.

Parameter estimation for all the models considered in this paper has been carried out by the method of maximum likelihood using Mathematica v.12.0® and also confirmed by using WinRATS v.7.0. Both moments and the maximum likelihood methods are suitable to estimate the vector of parameters of the distribution via sample observations, as shown in Appendix A and B. Codes are available from the authors upon request. For details about software, see Ruskeepaa [26] and Brooks [27].

Since closed expressions are not available for the maximum likelihood estimates and the computation of the global maximum of the logarithm function of the likelihood is not guaranteed, thus it is advisable to use several seed points as the starting value. It is also prudent to use different optimization methods (Newton–Raphson, Broyden–Fletcher–Goldfarb–Sanno, BGGS) (this is an iterative method for solving unconstrained nonlinear optimization problems which can be seen in Broyden [28, 29] and Shanno [30]) that ensure that the same solution is obtained from any of these methods. The standard errors of the estimates can be calculated by inverting the Hessian matrix. In this sense, both Mathematica and WinRats have at least two methods to reach it. The first is to retrieve them from the Cholesky factors (this package is available on the web upon request). The second, faster, is to obtain them by finite differentiation. Furthermore, WinRats package also offers the possibility to directly compute the maximum of the log-likelihood providing the elements of the Fisher information matrix. In fact, for the examples considered in this section, these two packages were used to quickly compute the maximum likelihood estimates. Commands for fitting the skew normal and log-skew normal distributions are also available in stata (see [31]).

Parameter estimates and their standard errors (in brackets), negative of the maximum of the log likelihood function, and AIC for the three datasets considered are shown in Tables 2 and 3. Model assessment is derived through the following information criteria. Negative log likelihood (NLL) is calculated by taking the negative of the value of the log-likelihood evaluated at the ML estimates; Akaike information criterion (AIC) is computed as twice the NLL and evaluated at the ML estimates, plus twice the number of estimated parameters; Consistent Akaike Information Criteria (CAIC), a corrected version of the AIC is proposed by Bozdogan [32] to overcome the tendency of the AIC overestimating the complexity of the underlying model as it lacks the asymptotic property of consistency. In order to calculate the CAIC, a correction factor based on the sample size is used to compensate for the overestimating nature of AIC. The CAIC is defined as twice the NLL plus $k(1+\ln(n))$, where k is the number of free parameters and n refers to the sample size. Note that a model with a lower statistics value is preferred to one with a higher value. All these results are shown in Table 2. Furthermore, we also include the Kolmogorov–Smirnov test (KS) and the Anderson–Darling test (AD) to express the fit of the model to the data in terms of the distribution function. For these statistics, smaller values indicate a better fit of the model to the data. Note that they not only provide a way to measure the fit in terms of distribution functions but also allow us to perform hypothesis testing for model selection purposes. The p value of the test statistics, computed using the Monte Carlo method by using 1000 simulations, is shown in brackets. An extremely small p value may lead to a confident rejection of the null hypothesis that the data comes from the proposed model. It can be seen that LSN distribution is not rejected at the usual significance levels for both tests.

Table 1: Descriptive statistics of the dependent variable.

Data	Mean	Stand. dev.	Minimum	Maximum
Danish	56.339	534.161	1.00	14239
Norwegian	2217.21	7759.97	500.000	465365
Hospital cost (in log scale)	7.94537	0.75167	6.10504	9.64179

Graphs of histogram of the data and superimposed fitted densities are given in Figure 2. As can be seen, the proposed distribution provides a good fit for the empirical data.

In Table 4, the LSN distribution is fitted to the Wisconsin hospital costs' dataset. From left to right the parameter estimates, standard errors (SE), and the corresponding p values calculated based on the t-Wald statistic are displayed. Besides, AIC and BIC values for each model are provided in the last two rows of the table. The estimates of the regressors associated with the explanatory variables, *number of beds* and *income*, are not significant at the usual nominal level.

Finally, in order to choose a model that provides an acceptable description of the loss process for the Danish and Norwegian datasets, we should verify that the population limited expected values, computed numerically by

$$L(x) = E[\min(X, x)] = \int_0^x y\,\mathrm{d}F(y) + x\overline{F}(x), \tag{22}$$

are close to the empirical ones. As is well known, (22) is the expected amount per claim retained by the insured on a policy with a fixed amount deductible of x. In this case, the empirical limited expected value function was calculated based on $E_n(x) = (1/n)\sum_{i=1}^{n}\min(x_i, x)$. Obviously, when x

Table 2: Parameter estimates and their standard errors (in brackets), negative of the maximum of the log likelihood function, and AIC without covariates.

$\hat{\lambda}$	$\hat{\theta}$	$\hat{\sigma}$	$\hat{\alpha}$	NLL	AIC	CAIC	KS	AD
Danish data								
−1.324	3.121	2.075	0.993	3361.486	6730.970	6757.700	0.029	0.001
(0.308)	(0.097)	(0.222)	(0.004)				(0.319)	(0.136)
Norwegian data								
657.218	1894.500	1.239	318.836	20966.835	41941.700	41969.100	0.031	0.001
(18.987)	(43.876)	(0.027)	(9.600)				(0.148)	(0.049)

Table 3: Parameter estimates and standard errors (in brackets) of the homogeneous model together with some measures of model selection for different distributions considered for Wisconsin hospital costs' dataset.

Model	$\hat{\lambda}$	$\hat{\theta}$	$\hat{\sigma}$	$\hat{\alpha}$	NLL	AIC	CAIC	KS	AD
Pareto			3.620	6.000	937.019	1876.040	1881.300	0.345	0.224
			(0.158)					(0.000)	(0.000)
PAT		15.900	647.273	5.307	600.407	1206.330	1222.120	0.846	1.355
		(0.628)	(10.897)	(0.083)				(0.000)	(0.000)
LSN	−3.132	7.941	0.277	2.601	590.134	1188.270	1209.330	0.051	0.004
	(0.338)	(0.031)	(0.007)	(0.123)				(0.492)	(0.260)

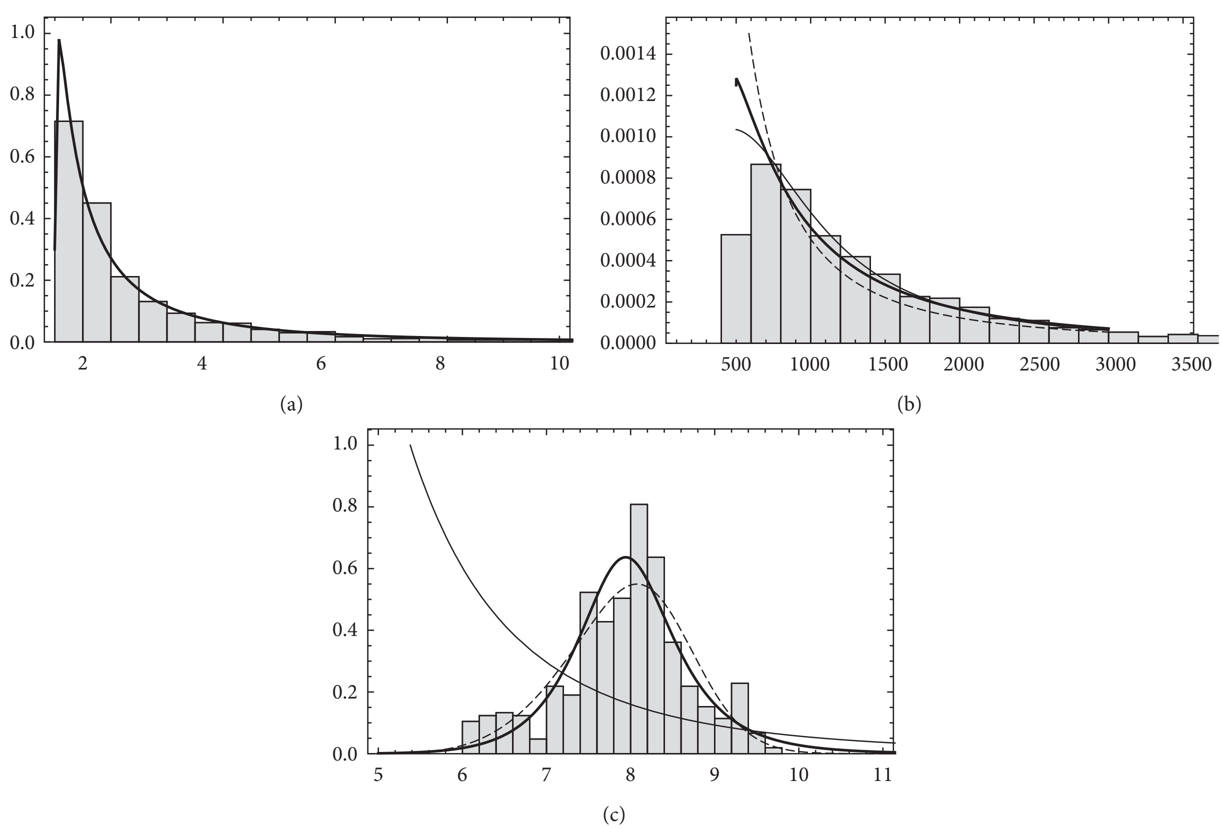

Figure 2: Smooth histogram of the empirical Danish, Norwegian insurance data, and hospital cost (in log scale) as compared to fitted models. Pareto (dashed line), PAT (thin line), and LSN (thick line). (a) Danish insurance loss data. (b) Norwegian insurance loss data. (c) Hospital costs' data.

tends to infinity, $L(x)$ and $E_n(x)$ approach $E(X)$ and the sample mean, respectively.

Table 5 below exhibits the limited expected value for different values of the policy limit x considered for the hospital costs' dataset. It is observed that the values obtained from the LSN distribution adheres closely to the observed empirical limited expected values obtained from the Pareto and PAT distributions. Similarly, in Figure 3, empirical and fitted limited expected value function for this dataset and also for the Danish and Norwegian data are shown. As can

Table 4: Parameter estimates for Wisconsin hospital costs dataset including covariates.

Variable	Estimate	SE	t-Stat.	p value
Hospital discharge costs	0.015	0.002	6.37	0.000
Health service area	0.002	0.001	1.74	0.080
Payer	0.012	0.005	2.43	0.014
Size area population	0.015	0.005	3.10	0.001
Number of beds	−0.010	0.008	−1.20	0.228
Income	0.001	0.005	0.31	0.756
Constant	1.607	0.008	200.32	0.000
α	0.563	0.269	2.09	0.036
λ	−2.974	0.361	−8.21	0.000
σ	0.186	0.014	13.03	0.000
NLL = 564.619				
AIC = 1149.240				
CAIC = 1201.890				

Table 5: :Limited expected value for the different distributions considered and different values of the fixed amount deductible x for hospital costs dataset.

	Limited expected value			
Deductible	Empirical	Pareto	PAT	LSN
6.00	6.00000	6.00000	5.99853	5.99810
6.15	6.14978	6.14346	6.14740	6.14661
6.30	6.29677	6.27480	6.29568	6.29419
6.45	6.44047	6.39529	6.44308	6.44044
6.60	6.58092	6.50605	6.58927	6.58482
6.75	6.71905	6.60806	6.73373	6.72666
6.90	6.85458	6.70218	6.87580	6.86517
7.05	6.98883	6.78918	7.01456	6.99940
7.20	7.11933	6.86973	7.14881	7.12827
7.35	7.24475	6.94442	7.27702	7.25059
7.50	7.36489	7.01380	7.39730	7.36506
7.65	7.47366	7.07833	7.50753	7.47039
7.80	7.57179	7.13843	7.60564	7.56533
7.95	7.65844	7.19450	7.69007	7.64882
8.10	7.73372	7.24686	7.76028	7.72019
8.25	7.79120	7.29582	7.81694	7.77925
8.40	7.83213	7.34167	7.86162	7.82640
8.55	7.86265	7.38465	7.89634	7.86260
8.70	7.88567	7.42498	7.92311	7.88928
8.85	7.90437	7.46287	7.94369	7.90813
9.00	7.91949	7.49850	7.95951	7.92088
9.15	7.93157	7.53205	7.97170	7.92914
9.30	7.94065	7.56367	7.98111	7.93427
9.45	7.94438	7.59349	7.98839	7.93731
9.60	7.94527	7.62165	7.99406	7.93905
9.75	7.94537	7.64826	7.99848	7.94001
9.90	7.94537	7.67342	8.00194	7.94051
10.00	7.94537	7.68945	8.00383	7.94070

be observed, the LSN distribution stays closer to the empirical limited expected values for the three datasets considered.

3.1. Out-of-Sample Validation of LSN Distribution. We are interested now in showing the power of the LSN distribution to predict the number of claims out-of-sample via quantile-quantile plots (QQ-plots) of randomized quantile residuals. For this reason, the dataset `danishuni` is randomly partitioned into two disjoint subsets of different sizes. The first subset (dataset A) is used for fitting the models, whereas the second subset (dataset B) is used for graphing the quantile-quantile plots of the randomized quantile residuals to check for normality. The residuals for the out-of-sample datasets are exhibited in Figure 4 for different in-sample sizes, i.e., size of dataset A. For comparison purposes, we have we have plotted the residuals for the whole dataset (top-left graph)

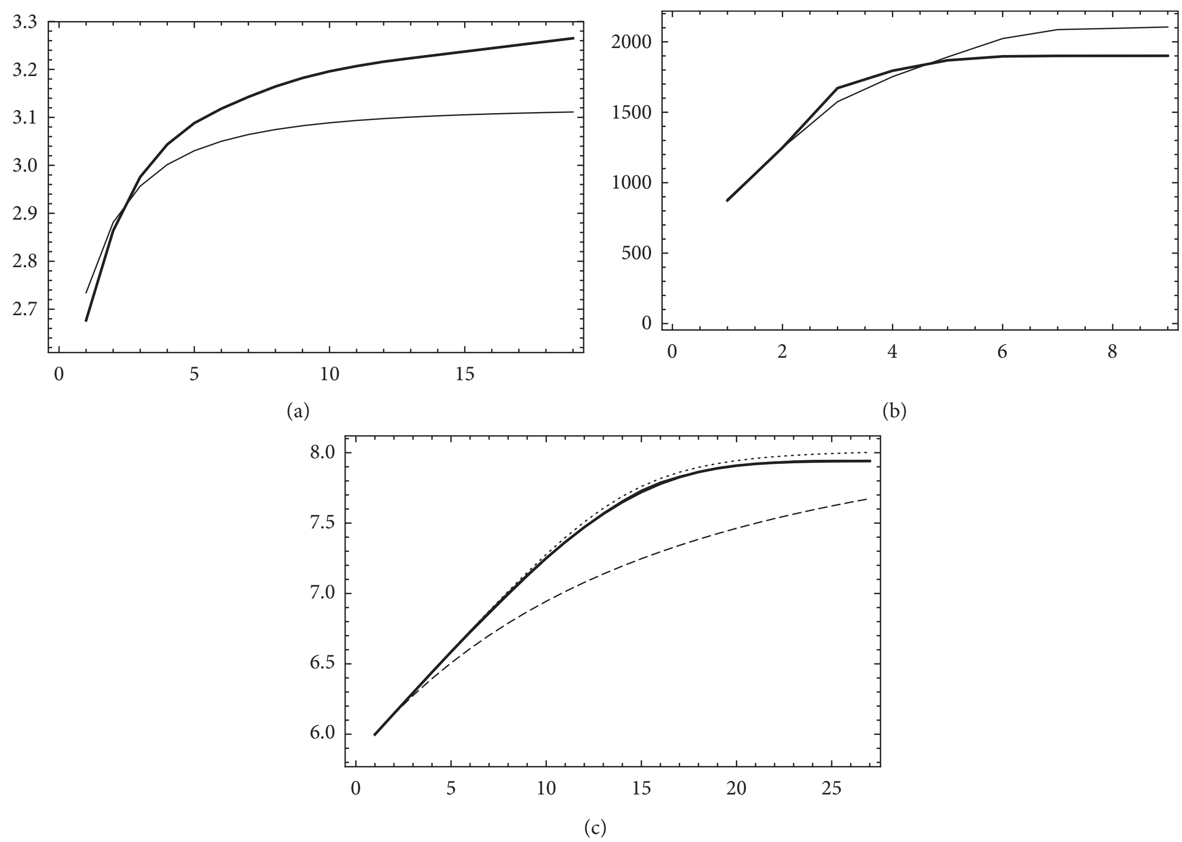

Figure 3: Empirical (thick line) and fitted limited expected values: Pareto distribution (dashed line), PAT distribution (dotted line), and LSN (thin line) for the (a) Danish data, (b) Norwegian data, and (c) hospital cost data.

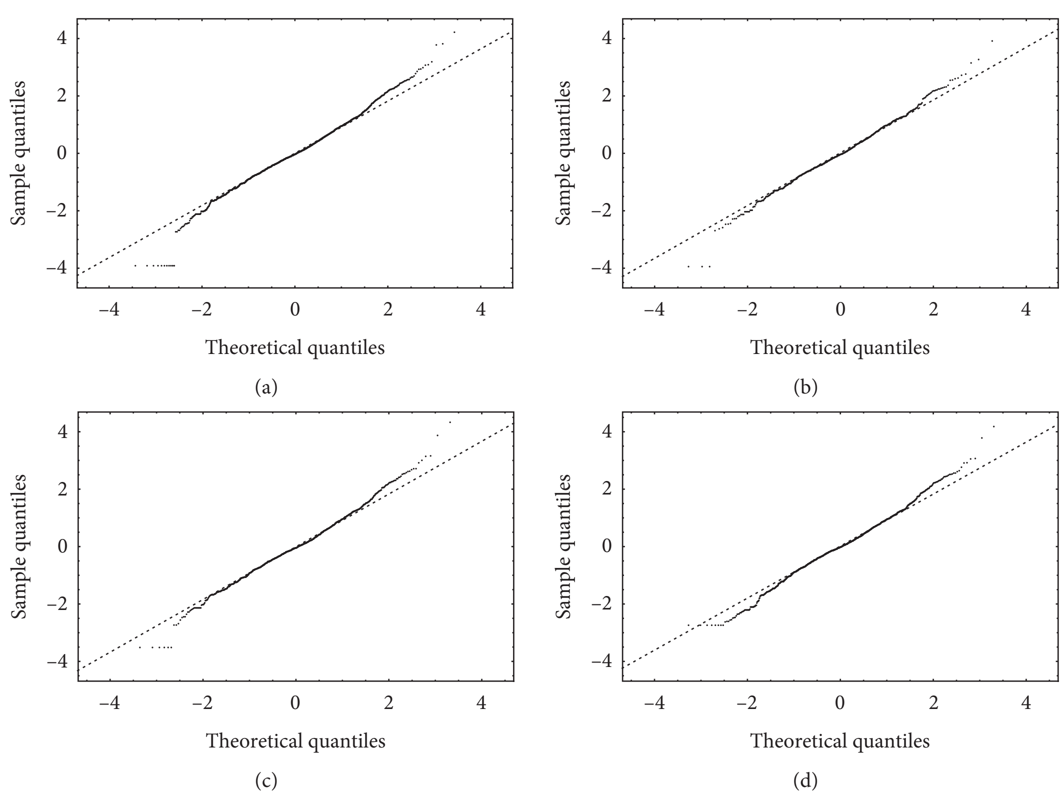

Figure 4: QQ-plots of randomized quantile residuals for the LSN distribution for the whole dataset `danishuni` and different in-sample sizes. (a) Whole dataset size-2167. (b) In-sample size-1500. (c) In-sample size-1000. (d) In-sample size-750.

with sample size 2167. A perfect alignment with the 45° line implies the residuals are normally distributed. It is observable that the residuals for LSN distribution adheres reasonably well to the line throughout the residual distribution. However, for all different in-sample sizes considered, the model tends to overestimate the lower quantiles and underestimate the upper quantiles. In general, the predictive power of the model is acceptable.

4. Conclusions and Extensions

In this paper, the use of the skew lognormal distribution has been proposed as a suitable model for describing claims' size empirical data. To the best of our knowledge, this probabilistic family has not been previously considered in the actuarial literature. The advantages of this distribution are twofold. On the one hand, it includes heavy tails which makes it an interesting model to describe severity data and; on the other hand, the distribution can be rewritten to allow for the incorporation of predictors to explain a response variable.

Finally, it is worthy to point out that the distribution introduced in this paper could be extended to other areas of risk theory. For example, the LSN distribution could be employed as the secondary distribution (the distribution of the claims size) in the compound collective risk model. In particular, this distribution could be used as an approximation of the distribution of the total claims' size instead of the traditionally considered normal distribution. Furthermore, calculation of reinsurance premiums based on this distribution is an issue that deserves to be studied.

Appendix

A. PDF of the Alternative Distributions

The pdf of the classical Pareto and PAT distributions used in this work are given by

$$\begin{aligned} f(x) &= \frac{\sigma\alpha^{\sigma}}{x^{\sigma+1}}, \quad x \geq \alpha,\ \sigma > 0, \\ f(x) &= \frac{1}{\tan^{-1}\sigma}\frac{\sigma\theta x^{\theta-1}\alpha^{\theta}}{\sigma\alpha^{\theta}+x^{2\theta}}, \quad x \geq \alpha,\ \theta > 0,\ \sigma > 0, \end{aligned} \tag{A.1}$$

respectively.

B. Normal Equations

Let us firstly consider the case of the model without covariates and let $\tilde{x} = \{x_1, x_2, \ldots, x_n\}$ be a sample obtained from distribution (3). By denoting $\Theta = (\mu, \sigma, \lambda)$ as the vector of parameters to be estimated, the log-likelihood is proportional to

$$\begin{aligned} \ell(\tilde{x};\Theta) = {} & \sum_{i=1}^{n}\left[\log\Phi\left(\left(1+r_{\mu,\sigma}(x_i)\right)\lambda\right) - \frac{1}{2}r_{\mu,\sigma}(x_i)^2\right] \\ & - n\left[\log\sigma - \log\Phi(\lambda_0)\right]. \end{aligned} \tag{B.1}$$

The required normal equations to compute the maximum likelihood estimates are

$$\begin{aligned} \frac{\partial\ell(\tilde{x};\Theta)}{\partial\mu} &= \sum_{i=1}^{n} r_{\mu,\sigma}(x_i) - \lambda\sum_{i=1}^{n}\frac{\phi\left(\left(1+r_{\mu,\sigma}(x_i)\right)\lambda\right)}{\Phi\left(\left(1+r_{\mu,\sigma}(x_i)\right)\lambda\right)} = 0, \\ \frac{\partial\ell(\tilde{x};\Theta)}{\partial\sigma} &= -\lambda\sum_{i=1}^{n}\frac{r_{\mu,\sigma}(x_i)\phi\left(\left(1+r_{\mu,\sigma}(x_i)\right)\lambda\right)}{\Phi\left(\left(1+r_{\mu,\sigma}(x_i)\right)\lambda\right)} + \sum_{i=1}^{n} r_{\mu,\sigma}(x_i)^2 - n = 0, \\ \frac{\partial\ell(\tilde{x};\Theta)}{\partial\lambda} &= \frac{n\lambda_0\phi(\lambda_0)}{\Phi(\lambda_0)} - \lambda\left(1+\lambda^2\right)\sum_{i=1}^{n}\frac{\left(1+r_{\mu,\sigma}(x_i)\right)\phi\left(\left(1+r_{\mu,\sigma}(x_i)\right)\lambda\right)}{\Phi\left(\left(1+r_{\mu,\sigma}(x_i)\right)\lambda\right)} = 0. \end{aligned} \tag{B.2}$$

Data Availability

The csv data used to support the findings of this study can be found in the R repository CASdatasets and also at https://instruction.bus.wisc.edu/jfrees/jfreesbooks/Regression%20Modeling/BookWebDec2010/data.html.

Conflicts of Interest

The authors declare that they have no conflicts of interest.

Acknowledgments

EGD would like to thank the Ministerio de Economía y Competitividad (project ECO2017-85577-P) for partial support of this work (Ministerio de Economía y Competitividad, Spain).

References

[1] A. McNeil, "Estimating the tails of loss severity distribution using extreme value theory," *ASTIN Bulletin*, vol. 27, no. 1, pp. 117–137, 1988.
[2] J. Beirlant and J. L. Teugels, "Modeling large claims in non-life insurance," *Insurance: Mathematics and Economics*, vol. 11, no. 1, pp. 17–29, 1992.
[3] J. Beirlant, J. Teugels, and P. Vynckier, *Practical Analysis of Extreme Values*, Leuven University Press, Leuven, Belgium, 1996.
[4] P. Embrechts, S. I. Resnick, and G. Samorodnitsky, "Extreme value theory as a risk management tool," *North American Actuarial Journal*, vol. 3, no. 2, pp. 30–41, 1999.

[5] H. Albrecher, J. Beirlant, and J. Teugels, *Reinsurance: Actuarial and Statistical Aspects*, Wiley, Hoboken, NJ, USA, 2017.
[6] B. Arnold, *Pareto Distributions*, International Cooperative Publishing House, Silver Spring, MD, USA, 1983.
[7] V. Brazauskas and R. Serfling, "Favorable estimators for fitting Pareto models: a study using goodness-of-fit measures with actual data," *ASTIN Bulletin*, vol. 33, no. 2, pp. 365–381, 2003.
[8] M. Rytgaard, "Estimation in the Pareto distribution," *ASTIN Bulletin*, vol. 20, no. 2, pp. 201–216, 1990.
[9] A. V. Boyd, "Fitting the truncated Pareto distribution to loss distributions," *Journal of the Staple Inn Actuarial Society*, vol. 31, pp. 151–158, 1988.
[10] A. J. Mata, "Pricing excess of loss reinsurance with reinstatements," *ASTIN Bulletin*, vol. 30, no. 2, pp. 349–368, 2000.
[11] J. M. Sarabia and F. Prieto, "The Pareto-positive stable distribution: a new descriptive model for city size data," *Physica A: Statistical Mechanics and Its Applications*, vol. 388, no. 19, pp. 4179–4191, 2009.
[12] E. Gómez-Déniz and E. Calderín-Ojeda, "A suitable alternative to the Pareto distribution," *Hacettepe Journal of Mathematics and Statistics*, vol. 43, no. 5, pp. 843–860, 2014.
[13] E. Gómez-Déniz and E. Calderín-Ojeda, "Modelling insurance data with the Pareto arctan distribution," *ASTIN Bulletin*, vol. 45, no. 3, pp. 639–660, 2015.
[14] M. Ghitany, E. Gómez-Déniz, and S. Nadarajah, "A new generalization of the Pareto distribution and its application to insurance data," *Journal of Risk and Financial Management (Special Issue: Extreme Values and Financial Risk)*, vol. 11, no. 10, pp. 1–14, 2008.
[15] N. Henze, "A probabilistic representation of the skew-normal distribution," *Scandinavian Journal of Statistics*, vol. 13, no. 4, pp. 271–275, 1986.
[16] B. Arnold and R. Beaver, "Skewed multivariate models related to hidden truncation and/or selective reporting (with discussion)," *Test*, vol. 11, no. 1, pp. 1–54, 2002.
[17] A. Azzalini and A. Valle, "The multivariate skew-normal distribution," *Biometrika*, vol. 83, no. 4, pp. 715–726, 1996.
[18] A. Azzalini and A. Capitanio, "Statistical applications of the multivariate skew normal distribution," *Journal of the Royal Statistical Society: Series B (Statistical Methodology)*, vol. 61, no. 3, pp. 579–602, 1999.
[19] A. Azzalini, *The Skew-Normal and Related Families*, Cambridge University Press, Cambridge, UK, 2013.
[20] G. D. Lin and J. Stoyanov, "The logarithmic skew-normal distributions are moment-indeterminate," *Journal of Applied Probability*, vol. 46, no. 3, pp. 909–916, 2009.
[21] A. Azzalini, D. Cappello, and S. Kotz, "Log-skew-normal and log-skew-t distributions as model for family income data," *Journal of Income Distribution*, vol. 11, pp. 12–20, 2003.
[22] H. Bolfarine, H. W. Gómez, and L. I. Rivas, "The log-bimodal-skew-normal model. A geochemical application," *Journal of Chemometrics*, vol. 25, no. 6, pp. 329–332, 2011.
[23] O. Venegas, H. Bolfarine, D. I. Gallardo, A. Vergara-Fernández, and H. W. Gómez, "A note on the log-alpha-skew-normal model with geochemical applications," *Applied Mathematics & Information Sciences*, vol. 10, no. 5, pp. 1697–1703, 2016.
[24] D. B. Owen, "Tables for computing bivariate normal probabilities," *The Annals of Mathematical Statistics*, vol. 27, no. 4, pp. 1075–1090, 1956.
[25] B. Arnold and G. Lin, "Characterizations of the skew-normal and generalized chi distributions," *Sankhya*, vol. 66, pp. 593–606, 2004.
[26] H. Ruskeepaa, *Mathematica Navigator. Mathematics, Statistics, and Graphics*, Academic Press, Cambridge, MA, USA, Third edition, 2009.
[27] C. Brooks, *RATS Handbook to Accompany Introductory Econometrics for Finance*, Cambridge University Press, Cambridge, UK, 2009.
[28] C. G. Broyden, "A class of methods for solving nonlinear simultaneous equations," *Mathematics of Computation*, vol. 19, no. 92, pp. 577–593, 1965.
[29] C. G. Broyden, "Quasi-Newton methods and their application to function minimisation," *Mathematics of Computation*, vol. 21, no. 99, pp. 368–381, 1967.
[30] D. F. Shanno, "Conditioning of quasi-Newton methods for function minimization," *Mathematics of Computation*, vol. 24, no. 111, pp. 647–657, 1970.
[31] Y. V. Marchenko and M. G. Genton, "A suite of commands for fitting the skew-normal and skew-t models," *The Stata Journal: Promoting Communications on Statistics and Stata*, vol. 10, no. 4, pp. 507–539, 2010.
[32] H. Bozdogan, "Model selection and Akaike's Information Criterion (AIC): the general theory and its analytical extensions," *Psychometrika*, vol. 52, no. 3, pp. 345–370, 1987.

Hindawi
Mathematical Problems in Engineering
Volume 2020, Article ID 8563790, 7 pages
https://doi.org/10.1155/2020/8563790

Research Article

Partial Information Stochastic Differential Games for Backward Stochastic Systems Driven by Lévy Processes

Fu Zhang,[1] **QingXin Meng**,[2] **and MaoNing Tang**[2]

[1]*College of Science, University of Shanghai for Science and Technology, Shanghai 200433, China*
[2]*Department of Mathematics, Huzhou University, Zhejiang 313000, China*

Correspondence should be addressed to QingXin Meng; mqx@zjhu.edu.cn and MaoNing Tang; tmorning@zjhu.edu.cn

Received 20 May 2020; Accepted 15 June 2020; Published 18 September 2020

Guest Editor: Wenguang Yu

In this paper, we consider a partial information two-person zero-sum stochastic differential game problem, where the system is governed by a backward stochastic differential equation driven by Teugels martingales and an independent Brownian motion. A sufficient condition and a necessary one for the existence of the saddle point for the game are proved. As an application, a linear quadratic stochastic differential game problem is discussed.

1. Introduction

Consider a partial information two-person zero-sum stochastic differential game problem, where the system is governed by the following nonlinear backward stochastic differential equation (BSDE), for any $t \in [0,T]$,

$$\begin{aligned} y(t) = \xi + \int_t^T f(s, y(s), q(s), z(s), u_1(t), u_2(t))\mathrm{d}s \\ - \sum_{i=1}^{d} \int_t^T q^i(s)\mathrm{d}W^i(s) - \sum_{i=1}^{\infty} \int_t^T z^i(s)\mathrm{d}H^i(s), \end{aligned} \tag{1}$$

with the cost functional

$$J(u(\cdot)) = E\left[\phi(y(0)) + \int_0^T l(t, y(t), q(t), z(t), u_1(t), u_2(t))\mathrm{d}t\right], \tag{2}$$

where $\{W(t), 0 \le t \le T\}$ is a standard d-dimensional Brownian motion and $H(t) = \{H^i(t)_{i=1}^{\infty}, 0 \le t \le T\}$ are Teugels martingales associated with a Lévy processes $\{L(t), 0 \le t \le T\}$ (see Section 2, for more details). The filtration generated by the underlying Brownian motion W and the Lévy process $\{L(t), 0 \le t \le T\}$ is denoted by $\{\mathcal{F}_t\}_{0 \le t \le T}$. The meaning of variables are given in Assumptions 1 and 2.

In the above, the processes $u_1(\cdot)$ and $u_2(\cdot)$ are open-loop control processes, which present the controls of the two players. Let $U_1 \subset R^{k_1}$ and $U_2 \subset R^{k_2}$ be two given nonempty convex sets. Under many situations, under which the full information $\mathcal{F}_t$ is inaccessible for players, ones can only observe a partial information. For this, an admissible control process $u_i(\cdot)$ for the player i is defined as a $\mathcal{G}_t$-predictable process with values in U_i s.t. $E\int_0^T |u_i(t)|^2 \mathrm{d}t < +\infty$, where $i = 1, 2$. Here, $\mathcal{G}_t \subseteq \mathcal{F}_t$ for all $t \in [0,T]$ is a given subfiltration representing the information available to the controller at time t. For example, we could choose $\mathcal{G}_t = \mathcal{F}_{(t-\delta)^+}$, $t \in [0,T]$, where $\delta > 0$ is a fixed delay of information.

The set of all admissible open-loop controls $u_i(\cdot)$ for the player i is denoted by $\mathcal{A}_i$, $(i = 1, 2)$. $\mathcal{A}_1 \times \mathcal{A}_2$ is called the set of open-loop admissible controls for the players. We denote the strong solution of (1) by $(y^{u_1,u_2}(\cdot), q^{u_1,u_2}(\cdot), z^{u_1,u_2}(\cdot))$, or $(y(\cdot), q(\cdot), z(\cdot))$ if its dependence on admissible control $(u_1(\cdot), u_2(\cdot))$ is clear from context. Then, we call $(y(\cdot), q(\cdot), z(\cdot))$ the state process corresponding to the control process $(\overline{u}_1(\cdot), \overline{u}_2(\cdot))$ and call $(u_1(\cdot), u_2(\cdot); y(\cdot), q(\cdot), z(\cdot))$ the admissible quintuplet.

Roughly speaking, for the zero-sum differential game, Player I seeks control $\overline{u}_1(\cdot)$ to minimize (2), while Player II seeks control $\overline{u}_2(\cdot)$ to maximize (2). Let $(\overline{u}_1(\cdot),\overline{u}_2(\cdot))$ be an optimal open-loop control satisfying

$$J(\overline{u}_1(\cdot),u_2(\cdot)) \le J(\overline{u}_1(\cdot),\overline{u}_2(\cdot)) \le J(u_1(\cdot),\overline{u}_2(\cdot)), \qquad (3)$$

for all admissible open-loop controls $(u_1(\cdot), u_2(\cdot)) \in \mathcal{G}_1 \times \mathcal{G}_2$. We denote this partial stochastic differential game by Problem (P). We refer to $(\overline{u}_1(\cdot), \overline{u}_2(\cdot))$ as an open-loop saddle point of Problem (P). The corresponding strong solution $(\overline{y}(\cdot),\overline{q}(\cdot),\overline{z}(\cdot))$ of (1) is called the saddle state process. Then, $(\overline{u}_1(\cdot),\overline{u}_2(\cdot);\overline{y}(\cdot),\overline{q}(\cdot),\overline{z}(\cdot))$ is called a saddle quintuplet.

Game theory had been an active area of research and a useful tool in many applications, particularly in biology and economic. For the partial information two-person zero-sum stochastic differential games, the objective is to find a saddle point, for which the controller has less information than the complete information filtration $\{\mathcal{F}_t\}_{t\ge 0}$. Recently, An and Øksendal [1] established a maximum principle for stochastic differential games of forward systems with Poisson jumps for the type of partial information in our paper. Moreover, we refer to [2, 3] and the references therein, for more related results on the partial information stochastic differential games.

In 2000, Nualart and Schoutens [4] got a martingale representation theorem for a type of Lévy processes through Teugels martingales, where Teugels martingales are a family of pairwise strongly orthonormal martingales associated with Lévy processes. Later, Nualart and Schoutens [5] proved the existence and uniqueness theory of BSDE driven by Teugels martingales. The above results are further extended to the case for one-dimensional BSDE driven by Teugels martingales and an independent multidimensional Brownian motion by Bahlali et al. [6].

Since the theory of BSDE driven by Teugels martingales and an independent Brownian motion is established, it is natural to apply the theory to the stochastic optimal control problem. Now, the full information stochastic optimal control problem related to Teugels martingales has been in many literatures. For example, the stochastic linear quadratic problem with Lévy processes was studied by Mitsui and Tabata [7]. Motivated by [7], Meng and Tang [8] studied the general full information stochastic optimal control problem for the forward stochastic systems driven by Teugels martingales and an independent multidimensional Brownian motion and proved the corresponding stochastic maximum principle. Furthermore, Tang and Zhang [9] extended [8] to the Backward stochastic systems and obtained the corresponding stochastic maximum principle. For the case of the partial information, in 2012, Bahlali et al. [10] studied the stochastic control problem for forward system and obtained the corresponding stochastic maximum principle. In the meantime, Meng et al. [11] extended [9] to the partial information stochastic optimal control problem of backward stochastic systems and obtained the corresponding optimality conditions. For the recent results about stichastic differential control problems or games, the readers are referred to [12–17] and the references therein.

However, to the best of our knowledge, there is little discussion on the partial information stochastic differential games for the system driven by Teugels martingales and an independent Brownian motion, which motives us to write this paper. The main purpose of this paper is to establish partial information necessary and sufficient conditions for optimality for Problem (P) by using the results in [9]. The results obtained in this paper can be considered as a generalized form of stochastic optimal control problem to the two-person zero-sum case. As an application, a two-person zero-sum stochastic differential game of linear backward stochastic differential equations with a quadratic cost criteria under partial information is discussed and the optimal control is characterized explicitly by the adjoint processes.

The rest of this paper is organized as follows. We introduce useful notations and give needed assumptions in Section 2. Section 3 is devoted to present the sufficient condition for the existence of the optimal control problem. In Section 4, we establish the necessary condition of optimality. In Section 5, a linear quadratic stochastic differential game problem is solved by applying the theoretical results.

2. Preliminaries and Assumptions

Let $(\Omega, F, \{\mathcal{F}_t\}_{0\le t\le T}, P)$ be a complete probability space. The filtration $\{\mathcal{F}_t\}_{0\le t\le T}$ is right-continuous and generated by a d-dimensional standard Brownian motion $\{W(t), 0\le t\le T\}$ and a one-dimensional Lévy process $\{L(t), 0\le t\le T\}$. It is known that $L(t)$ has a characteristic function of the form: $Ee^{i\theta L(t)} = \exp[ia\theta t - 1/2\sigma^2 \theta^2 t + t\int_{R^1}(e^{i\theta x} - 1 - i\theta x I_{\{|x|<1\}})\nu\,(\mathrm{d}x)]$, where $a \in R^1$, $\sigma > 0$ and ν is a measure on R^1 satisfying the following: (i) $\int_{R^1}(1\wedge x^2)\nu(\mathrm{d}x) < \infty$ and (ii) there exists $\varepsilon > 0$ and $\lambda > 0$, s.t. $\int_{R^1/(-\varepsilon,\varepsilon)} e^{\lambda|x}\nu(dx) < \infty$. These settings imply that the random variables $L(t)$ have moments of all orders. We denote by $\{H^i(t), 0\le t\le T\}_{i=1}^{\infty}$ the Teugels martingales associated with the Lévy process $\{L(t), 0\le t\le T\}$. Here, $H^i(t)$ is given by

$$H^i(t) = c_{i,i}Y^{(i)}(t) + c_{i,i-1}Y^{(i-1)}(t) + \cdots + c_{i,1}Y^{(1)}(t), \qquad (4)$$

where $Y^{(i)}(t) = L^{(i)}(t) - E[L^{(i)}(t)]$ for all $i\ge 1$, $L^{(i)}(t)$ are so called power-jump processes with $L^{(1)}(t) = L(t)$, $L^{(i)}(t) = \sum_{0<s\le t}(\Delta L(s))^i$ for $i\ge 2$, and the coefficients $c_{i,j}$ correspond to the orthonormalization of polynomials $1, x, x^2, \cdots$ w.r.t. the measure $\mu(\mathrm{d}x) = x^2\nu(\mathrm{d}x) + \sigma^2\delta_0(\mathrm{d}x)$. The Teugels martingales $\{H^i(t)\}_{i=1}^{\infty}$ are pathwise strongly orthogonal and their predictable quadratic variation processes are given by

$$\langle H^{(i)}(t), H^{(j)}(t)\rangle = \delta_{ij}t. \qquad (5)$$

For more details of Teugels martingales, we invite the reader to consult Nualart and Schoutens [4, 5]. Denote by g the predictable sub-σ field of $\mathcal{B}([0,T]) \times \mathcal{F}$; then, we introduce the following notation used throughout this paper.

In the following, we introduce some basic spaces:

(i) H: a Hilbert space with norm $\|\cdot\|_H$.

(ii) $\langle\alpha,\beta\rangle$: the inner product in R^n, $\forall\alpha$, $\beta\in R^n$.

(iii) $|\alpha| = \sqrt{\langle\alpha,\alpha\rangle}$: the norm of R^n, $\forall\alpha\in R^n$.

(iv) $\langle \mathscr{A}, B\rangle = tr(\mathscr{A}B^T)$: the inner product in $R^{n\times m}$, $\forall \mathscr{A}, B \in R^{n\times m}$.

(v) $|\mathscr{A}| = \sqrt{tr(\mathscr{A}\mathscr{A}^T)}$: the norm of $R^{n\times m}$, $\forall \mathscr{A} \in R^{n\times m}$.

(vi) l^2: the space of all real-valued sequences $x = (x_i)_{i\geq 1}$ satisfying

$$\|x\|_{l^2} \leq \sqrt{\sum_{i=1}^{\infty} x_i^2} < \infty. \tag{6}$$

(vii) $l^2(H)$: the space of all H-valued sequence $f = \{f^i\}_{i\geq 1}$ satisfying

$$\|f\|_{l^2(H)} \leq \sqrt{\sum_{i=1}^{\infty} \left\|f^i\right\|_H^2} < \infty. \tag{7}$$

(viii) $l^2_{\mathscr{F}}(0,T;H)$: the space of all $l^2(H)$-valued and $\mathscr{F}_t$-predictable processes $f = \{f^i(t,\omega), (t,\omega) \in [0,T]\times\Omega\}_{i\geq 1}$ satisfying

$$\|f\|_{l^2_{\mathscr{F}}(0,T,H)} \leq \sqrt{E\int_0^T \sum_{i=1}^{\infty} \left\|f^i(t)\right\|_H^2 dt} < \infty. \tag{8}$$

(ix) $M^2_{\mathscr{F}}(0,T;H)$: the space of all H-valued and $\mathscr{F}_t$-adapted processes $f = \{f(t,\omega), (t,\omega) \in [0,T]\times\Omega\}$ satisfying

$$\|f\|_{M^2_{\mathscr{F}}(0,T;H)} \leq \sqrt{E\int_0^T \|f(t)\|_H^2 dt} < \infty. \tag{9}$$

(x) $S^2_{\mathscr{F}}(0,T;H)$: the space of all H-valued and $\mathscr{F}_t$-adapted càdlàg processes $f = \{f(t,\omega), (t,\omega) \in [0,T]\times\Omega\}$ satisfying

$$\|f\|_{S^2_{\mathscr{F}}(0,T;H)} \leq \sqrt{E\sup_{0\leq t\leq T}\|f(t)\|_H^2 dt} < +\infty. \tag{10}$$

(xi) $L^2(\Omega,\mathscr{F},P;H)$: the space of all H-valued random variables ξ on $(\Omega,\mathscr{F},P)$ satisfying

$$\|\xi\|_{L^2(\Omega,\mathscr{F},P;H)} \leq E\|\xi\|_H^2 < \infty. \tag{11}$$

The coefficients of the state equation (1) and the cost functional (2) are defined as follows:

$$\begin{aligned} \xi &: \Omega \longrightarrow R^n, \\ f &: [0,T]\times\Omega\times R^n\times R^{n\times d}\times l^2(R^n)\times U_1\times U_2 \longrightarrow R^n, \\ l &: [0,T]\times\Omega\times R^n\times R^{n\times d}\times l^2(R^n)\times U_1\times U_2 \longrightarrow R, \end{aligned} \tag{12}$$

$$\phi: \Omega\times R^n \longrightarrow R^1. \tag{13}$$

Throughout this paper, we introduce the following basic assumptions on coefficients (ξ, f, l, ϕ).

Assumption 1. $\xi \in L^2(\Omega,\mathscr{F}_T,P;R^n)$ and the random mapping f is predictable w.r.t. t, Borel measurable w.r.t. other variables, and $f(\cdot,0,0,0,0,0) \in M^2_{\mathscr{F}}(0,T;R^n)$. For almost all $(t,\omega)\in[0,T]\times\Omega$, $f(t,\omega,y,p,z,u_1,u_2)$ is Fréchet differentiable w.r.t. (y,p,z,u_1,u_2) and the corresponding Fréchet derivatives f_y, f_p, f_z, f_{u_1}, and f_{u_2} are continuous and uniformly bounded.

Assumption 2. The random mapping l is predictable w.r.t. t, Borel measurable w.r.t. other variables, and for almost all $(t,\omega)\in[0,T]\times\Omega$, l is Fréchet differentiable w.r.t. (y,p,z,u_1,u_2) with continuous Fréchet derivatives l_y, l_q, l_z, l_{u_1}, and l_{u_2}. The random mapping ϕ is measurable, and for almost all $(t,\omega)\in[0,T]\times\Omega$, ϕ is Fréchet differentiable w.r.t. y with continuous Fréchet derivative ϕ_y. Moreover, for almost all $(t,\omega)\in[0,T]\times\Omega$, there exists a constant C s.t. for all $(p,q,z,u_1,u_2)\in R^n\times R^{n\times d}\times l^2(R^n)\times U_1\times U_2$:

$$\begin{aligned} |l| &\leq C\left(1+|y|^2+|q|^2+|z|^2+|u|_1^2+|u|_2^2\right), \\ |\phi| &\leq C\left(1+|y|^2\right), \\ \left|l_y\right|+\left|l_q\right|+\left|l_z\right|+\left|l_{u_1}\right|+\left|l_{u_2}\right| &\leq C\left(1+|y|+|q|+|z|+\left|u_1\right|+\left|u_2\right|\right), \end{aligned} \tag{14}$$

$$\left|\phi_y\right| \leq C(1+|y|). \tag{15}$$

Under Assumption 1, we can get from Lemma 2.3 in [9] that, for each $(u_1(\cdot),u_2(\cdot))\in\mathscr{A}_1\times\mathscr{A}_2$, system (1) admits a unique strong solution. Furthermore, by Assumption 2 and a priori estimate for BSDE driven by Teugels martingales (see Lemma 3.2 in [9]), it is easy to check that

$$\left|J(u_1(\cdot),u_2(\cdot))\right| < \infty. \tag{16}$$

So, Problem (P) is well defined.

3. A Partial Information Sufficient Maximum Principle

In this section, we want to study the sufficient maximum principle for Problem (P).

In our setting, the Hamiltonian function $H: [0,T]\times R^n\times R^{n\times d}\times l^2(R^n)\times U_1\times U_2\times R^n \longrightarrow R^1$ is of the following form:

$$\begin{aligned} &H(t,y,q,z,u_1,u_2,k) \\ &\quad = \langle k, -f(t,y,q,z,u_1,u_2)\rangle + l(t,y,q,z,u_1,u_2). \end{aligned} \tag{17}$$

The adjoint equation, which fits into system (1) and (2) corresponding to the given admissible quintuplet $((u_1(\cdot),u_2(\cdot)); y(\cdot),q(\cdot),z(\cdot))$, is given by the following forward stochastic differential equation driven by multidimensional Brownian motion W and Teugels martingales $\{H^i\}_{i=1}^{\infty}$:

$$\begin{cases} dk = -H_y(t, y, q, z, u_1, u_2, k)dt \\ -\sum_{i=1}^{d} H_{q^i}(t, y, \overline{q}, z, u_1, u_2, k dW^i(t)) \\ -\sum_{i=1}^{\infty} H_{z^i}(t, y, q, z, u_1, u_2, k dH^i(t)) \\ k(0) = -\phi_y(y(0)). \end{cases} \tag{18}$$

Under Assumptions 1 and 2, the forward stochastic differential equation (18) has a unique solution $k(\cdot) \in \mathcal{G}^2_{\mathcal{F}}(0, T; R^n)$ by Lemma 2.1 in [9].

We now come to a verification theorem for Problem (P).

Theorem 1 (partial information sufficient maximum principle). *Let Assumptions 1 and 2 hold. Let $(\overline{u}_1(\cdot), \overline{u}_2(\cdot); \overline{y}(\cdot), \overline{q}(\cdot), \overline{z}(\cdot))$ be an admissible quintuplet and $\overline{k}(\cdot)$ the unique strong solution of the corresponding adjoint equation (18). Suppose that the Hamiltonian function H satisfies the following conditional maximum principle:*

$$\begin{aligned} &\inf_{u_1 \in U_1} E\left[H\left(t, \overline{y}(t), \overline{q}(t), \overline{z}(t), u_1, \overline{u}_2(t), \overline{k}(t)\right) \Big| G_t\right] \\ &= E\left[H\left(t, \overline{y}(t), \overline{q}(t), \overline{z}(t), \overline{u}_1(t), \overline{u}_2(t), \overline{k}(t)\right) \Big| G_t\right] \\ &= \sup_{u_2 \in U_2} E\left[H\left(t, \overline{y}(t), \overline{q}(t), \overline{z}(t), \overline{u}_1(t), u_2, \overline{k}(t)\right) \Big| G_t\right]. \end{aligned} \tag{19}$$

(i) Suppose that, for all $t \in [0, T]$, $\phi(y)$ is convex in y, and

$$(y, q, z, u_1) \mapsto H\left(t, y, q, z, u_1, \overline{u}_2(t), \overline{k}(t)\right) \tag{20}$$

is convex. Then, for all,

$$J(\overline{u}_1(\cdot), \overline{u}_2(\cdot)) \le J(u_1(\cdot), \overline{u}_2(\cdot)), \tag{21}$$

$$J(\overline{u}_1(\cdot), \overline{u}_2(\cdot)) = \inf_{u_1(\cdot) \in \mathcal{A}_1} J(u_1(\cdot), \overline{u}_2(\cdot)). \tag{22}$$

(ii) Suppose that, for all $t \in [0, T]$, $\phi(y)$ is concave in y, and

$$(y, q, z, u_2) \mapsto H\left(t, y, q, z, \overline{u}_1(t), u_2, \overline{k}(t)\right) \tag{23}$$

is concave. Then, for all $u_2(\cdot) \in \mathcal{A}_2$,

$$J(\overline{u}_1(\cdot), \overline{u}_2(\cdot)) \ge J(\overline{u}_1(\cdot), u_2(\cdot)), \tag{24}$$

$$J(\overline{u}_1(\cdot), \overline{u}_2(\cdot)) = \sup_{u_2(\cdot) \in \mathcal{A}_2} J(\overline{u}_1(\cdot), u_2(\cdot)). \tag{25}$$

(iii) If both cases (i) and (ii) hold (which implies, in particular, that $\phi(y)$ is an affine function), then $(\overline{u}_1(\cdot), \overline{u}_2(\cdot))$ is an open-loop saddle point and

$$\begin{aligned} J(\overline{u}_1(\cdot), \overline{u}_2(\cdot)) &= \sup_{u_2(\cdot) \in \mathcal{A}_2}\left(\inf_{u_1(\cdot) \in \mathcal{A}_1} J(u_1(\cdot), u_2(\cdot))\right) \\ &= \inf_{u_1(\cdot) \in \mathcal{A}_1}\left(\sup_{u_2(\cdot) \in \mathcal{A}_2} J(u_1(\cdot), u_2(\cdot))\right). \end{aligned} \tag{26}$$

Proof

(i) In the following, we consider a stochastic optimal control problem over $\mathcal{G}_1$, where the system is

$$\begin{aligned} y(t) = \xi &+ \int_t^T f(s, y(s), q(s), z(s), u_1(t), \overline{u}_2(t))ds \\ &- \sum_{i=1}^{d} \int_t^T q^i(s)dW^i(s) - \sum_{i=1}^{\infty} \int_t^T z^i(s)dH^i(s), \end{aligned} \tag{27}$$

with the cost functional

$$\begin{aligned} J(u_1(\cdot), \overline{u}_2(\cdot)) = E\Big[\phi(y(0)) \\ + \int_o^T l(t, y(t), q(t), z(t), u_1(t), \overline{u}_2(t))dt\Big]. \end{aligned} \tag{28}$$

Our optimal control problem is to minimize $J(u_1(\cdot), \overline{u}_2(\cdot))$ over $u_1(\cdot) \in \mathcal{A}_1$, i.e., find $\overline{u}_1(\cdot) \in \mathcal{A}_1$ such that

$$J(\overline{u}_1(\cdot), \overline{u}_2(\cdot)) = \inf_{u_1(\cdot) \in \mathcal{A}_1} J(u_1(\cdot), \overline{u}_2(\cdot)). \tag{29}$$

Then, for this case, it is easy to check that the Hamilton is $H(t, y, q, z, u_1, \overline{u}_2(t), k)$, and for the admissible control $\overline{u}_1(\cdot) \in \mathcal{A}_1$, the corresponding sate process and the adjoint process is still $(\overline{y}(t), \overline{q}(t), \overline{z}(t))$ and $\overline{k}(t)$, respectively. And the optimality condition is

$$\begin{aligned} &\inf_{u_1 \in U_1} E\left[H\left(t, \overline{y}(t), \overline{q}(t), \overline{z}(t), u_1, \overline{u}_2(t), \overline{k}(t)\right) \Big| G_t\right] \\ &= E\left[H(t, \overline{y}(t), \overline{q}(t), \overline{z}(t), \overline{u}_1(t), \overline{u}_2(t)) \big| G_t\right]. \end{aligned} \tag{30}$$

Thus, from the partial information sufficient maximum principle for optimal control (see Theorem 1 in [9]), we conclude that $\overline{u}_1(\cdot)$ is the optimal control of the optimal control problem, i.e.,

$$J(\overline{u}_1(\cdot), \overline{u}_2(\cdot)) = \inf_{u_1(\cdot) \in \mathcal{A}_1} J(u_1(\cdot), \overline{u}_2(\cdot)). \tag{31}$$

The proof of (i) is complete.

(ii) This statement can be proved in a similar way as (i).

(iii) If both (i) and (ii) hold, then

$$J(\overline{u}_1(\cdot), u_2(\cdot)) \le J(\overline{u}_1(\cdot), \overline{u}_2(\cdot)) \le J(u_1(\cdot), \overline{u}_2(\cdot)), \tag{32}$$

for any $(u_1(\cdot), u_2(\cdot)) \in \mathcal{A}_1 \times \mathcal{A}_2$, i.e.,

$$\begin{aligned} J(\overline{u}_1(\cdot), \overline{u}_2(\cdot)) &\le \inf_{u_1(\cdot) \in \mathcal{A}_1} J(u_1(\cdot), \overline{u}_2(\cdot)) \\ &\le \sup_{u_2(\cdot) \in \mathcal{A}_2}\left(\inf_{u_1(\cdot) \in \mathcal{A}_1} J(u_1(\cdot), u_2(\cdot))\right). \end{aligned} \tag{33}$$

On the contrary,

$$J(\bar{u}_1(\cdot),\bar{u}_2(\cdot)) \geq \sup_{u_2(\cdot)\in\mathcal{A}_2} J(\bar{u}_1(\cdot),u_2(\cdot)) \geq \inf_{u_1(\cdot)\in\mathcal{A}_1}\left(\sup_{u_2(\cdot)\in\mathcal{A}_2} J(u_1(\cdot),u_2(\cdot))\right). \tag{34}$$

Now, due to the inequality,

$$\inf_{u_1(\cdot)\in\mathcal{A}_1}\left(\sup_{u_2(\cdot)\in\mathcal{A}_2} J(u_1(\cdot),u_2(\cdot))\right) \geq \sup_{u_2(\cdot)\in\mathcal{A}_2}\left(\inf_{u_1(\cdot)\in\mathcal{A}_1} J(u_1(\cdot),u_2(\cdot))\right), \tag{35}$$

we have

$$J(\bar{u}_1(\cdot),\bar{u}_2(\cdot)) = \inf_{u_1(\cdot)\in\mathcal{A}_1}\left(\sup_{u_2(\cdot)\in\mathcal{A}_2} J(u_1(\cdot),u_2(\cdot))\right) = \sup_{u_2(\cdot)\in\mathcal{A}_2}\left(\inf_{u_1(\cdot)\in\mathcal{A}_1} J(u_1(\cdot),u_2(\cdot))\right). \tag{36}$$

The proof of the theorem is completed.

If the control process $(u_1(\cdot),u_2(\cdot))$ is admissible adopted to the filtration $\mathcal{F}_t$, we have the following full information sufficient maximum principle.

Corollary 1. *Suppose that $\mathcal{G}_t = \mathcal{F}_t$. Moreover, suppose that, for all $t \in [0,T]$, the following maximum principle holds:*

$$\begin{aligned}\inf_{u_1\in U_1} H\big(t,\bar{x}(t),\bar{y}(t),\bar{z}(t),u_1,\bar{u}_2(t),\bar{p}(t),\bar{q}(t),\bar{k}(t)\big) &= H\big(t,\bar{x}(t),\bar{y}(t),\bar{z}(t),\bar{u}_1(t),\bar{u}_2(t),\bar{p}(t),\bar{q}(t),\bar{k}(t)\big) \\ &= \sup_{u_2\in U_2} H\big(t,\bar{x}(t),\bar{y}(t),\bar{z}(t),\bar{u}_1(t),u_2,\bar{p}(t),\bar{q}(t),\bar{k}(t)\big).\end{aligned} \tag{37}$$

(i) *Suppose that, for all $t \in [0,T]$, $\phi(y)$ is convex in y and*

$$(x,y,z,u_1) \mapsto H\big(t,x,y,z,u_1,\bar{u}_2(t),\bar{p}(t),\bar{q}(t),\bar{k}(t)\big) \tag{38}$$

is convex. Then, for all $u_1(\cdot) \in \mathcal{A}_1$,

$$J(\bar{u}_1(\cdot),\bar{u}_2(\cdot)) \leq J(u_1(\cdot),\bar{u}_2(\cdot)), \tag{39}$$

$$J(\bar{u}_1(\cdot),\bar{u}_2(\cdot)) = \inf_{u_1(\cdot)\in\mathcal{A}_1} J(u_1(\cdot),\bar{u}_2(\cdot)). \tag{40}$$

(ii) *Suppose that, for all $t \in [0,T]$, $\phi(y)$ is concave in y, and*

$$(x,y,z,u_2) \mapsto H\big(t,x,y,z,\bar{u}_1(t),u_2,\bar{p}(t),\bar{q}(t),\bar{k}(t)\big) \tag{41}$$

is concave. Then, for all $u_2(\cdot) \in \mathcal{A}_2$,

$$J(\bar{u}_1(\cdot),\bar{u}_2(\cdot)) \geq J(\bar{u}_1(\cdot),u_2(\cdot)), \tag{42}$$

$$J(\bar{u}_1(\cdot),\bar{u}_2(\cdot)) = \sup_{u_2(\cdot)\in\mathcal{A}_2} J(\bar{u}_1(\cdot),u_2(\cdot)). \tag{43}$$

(iii) *If both cases (i) and (ii) hold (which implies, in particular, that $\phi(y)$ is an affine function), then $(\bar{u}_1(\cdot),\bar{u}_2(\cdot))$ is an open-loop saddle point based on the information flow $\mathcal{F}_t$ and*

$$J(\bar{u}_1(\cdot),\bar{u}_2(\cdot)) = \sup_{u_2(\cdot)\in\mathcal{A}_2}\left(\inf_{u_1(\cdot)\in\mathcal{A}_1} J(u_1(\cdot),u_2(\cdot))\right) = \inf_{u_1(\cdot)\in\mathcal{A}_1}\left(\sup_{u_2(\cdot)\in\mathcal{A}_2} J(u_1(\cdot),u_2(\cdot))\right). \tag{44}$$

4. Partial Information Necessary Maximum Principle

In this section, we give a necessary maximum principle for Problem (P).

Theorem 2 (a partial information necessary maximum principle). *Under Assumptions 1 and 2, let $(\bar{u}_1(\cdot),\bar{u}_2(\cdot))$ be an optimal control of Problem (P). Suppose that $(\bar{y}(\cdot),\bar{q}(\cdot),\bar{z}(\cdot))$ is the state process of system (1) corresponding to the admissible control $(\bar{u}_1(\cdot),\bar{u}_2(\cdot))$. Let $(\bar{k}(\cdot))$ be the unique solution of the adjoint equation (18) corresponding $(\bar{u}_1(\cdot),\bar{u}_2(\cdot);\bar{y}(\cdot),\bar{q}(\cdot),\bar{z}(\cdot))$. Then, for $i = 1,2$, we have, for all $u_i \in U_i$*

$$\left\langle E\left[H_{u_i}(t) \,\middle|\, \mathcal{G}_t\right], u_i - \bar{u}_i(t)\right\rangle \geq 0, \text{a.s. a.e}, \tag{45}$$

$$H_{u_i}(t) := H_{u_i}\big(t,\bar{y}(t),\bar{q}(t),\bar{z}(t),\bar{u}_1(t),\bar{u}_2(t),\bar{k}(t)\big). \tag{46}$$

Proof. Since $(\bar{u}_1(\cdot),\bar{u}_2(\cdot))$ is a saddle open-loop control, then $(\bar{u}_1(\cdot),\bar{u}_2(\cdot))$ is an open-loop saddle point, i.e.,

$$J(\bar{u}_1(\cdot),u_2(\cdot)) \leq J(\bar{u}_1(\cdot),\bar{u}_2(\cdot)) \leq J(u_1(\cdot),\bar{u}_2(\cdot)). \tag{47}$$

So, we have

$$J_1(\bar{u}_1(\cdot),\bar{u}_2(\cdot)) = \min_{u_1(\cdot)\in\mathcal{A}_1} J_1(u_1(\cdot),\bar{u}_2(\cdot)), \tag{48}$$

$$J_2(\bar{u}_1(\cdot),\bar{u}_2(\cdot)) = \max_{u_2(\cdot)\mathcal{A}_2} J_2(\bar{u}_1(\cdot),u_2(\cdot)). \tag{49}$$

By (48), $\bar{u}_1(\cdot)$ can be regarded as an optimal control of the optimal control problem, where the controlled system is (27) and the cost functional is (28). Then, for this case, it is easy to check that the Hamilton is $H(t,y,q,z,u_1,\bar{u}_2(t),k)$, and for the optimal control $\bar{u}_1(\cdot) \in \mathcal{G}_1$, the corresponding optimal sate process and the adjoint process is still $(\bar{y}(t),\bar{q}(t),\bar{z}(t))$ and $\bar{k}(t)$, respectively. Thus, applying the partial necessary stochastic maximum principle for optimal control problems (see Theorem 2 in [9]), we can obtain (45) for $i = 1$. Similarly, from (49), we can obtain (45) for $i = 2$. The proof is complete.

5. Example: Linear Quadratic Problem

In this section, we will apply our stochastic maximum principles to a linear quadratic problem under partial information, i.e., consider the game problem to the following quadratic cost functional over (u_1,u_2) valued in $R^{m_1} \times R^{m_2}$:

$$
\begin{aligned}
J(u_1(\cdot),u_2(\cdot)) := E\langle M, y(0)\rangle + E\int_0^T &[\langle E(s), y(s)\rangle] \\
&+\sum_{i=1}^{d}\langle F^i(s), q^i(s)\rangle \\
&+\sum_{i=1}^{\infty}\langle G^i(s), z^i(s)\rangle \\
&+\langle N_1(s)u_1(s), u_1(s)\rangle \\
&-\langle N_2(s)u_2(s), u_2(s)\rangle \mathrm{d}s,
\end{aligned}
\tag{50}
$$

where the state process $(y(\cdot), q(\cdot), z(\cdot))$ is the solution to the controlled linear backward stochastic system below:

$$
\begin{cases}
\mathrm{d}y(t) = -\left[\mathscr{A}(t)y(t) + \sum_{i=1}^{d} B^i(t)q^i(t) + \sum_{i=1}^{\infty} C^i(t)z^i(t) + D_1(t)u_1(t) + D_2(t)u_2(t)\right]dt + \sum_{i=1}^{d} q^i(t)\mathrm{d}W^i(t) + \sum_{i=1}^{\infty} z^i(t)\mathrm{d}W^i(t), \\
y(T) = \xi.
\end{cases}
\tag{51}
$$

This problem is denoted by Problem (LQ). To study this problem, we need the assumptions on the coefficients as follows.

Assumption 3. The matrix-valued functions $\mathscr{A}: [0,T] \longrightarrow R^{n\times n}$; $B^i: [0,T] \longrightarrow R^{n\times n}$, $i = 1,2,\cdots,d$; $C^i: [0,T] \longrightarrow R^{n\times n}$, $i = 1,2,\cdots$; $D^i: [0,T] \longrightarrow R^{n\times m_i}$, $i = 1,2$; $E: [0,T] \longrightarrow R^{n\times n}$; $F^i: [0,T] \longrightarrow R^{n\times m}$; $R^n, i = 1,2,\cdots,d$, $G^i: [0,T] \longrightarrow R^n$, $i = 1,2,\cdots$; $N^i: [0,T] \longrightarrow R^{m_i\times m_i}$, $i = 1,2$ and the matrix $M \in R^n$ are uniformly bounded. Moreover, N^i is uniformly positive, i.e., $N^i \geq \delta I$, $(i = 1,2)$ for some positive constant δ.

Assumption 4. There is no further constraint imposed on the control processes; the set all admissible control processes is

$$
\mathscr{A}_1 \times \mathscr{A}_2 = \left\{
\begin{array}{c}
(u_1(\cdot),u_2(\cdot))\colon\ (u_1(\cdot),u_2(\cdot)) \text{ is} \\
G_t - \text{predictable process with values in} \\
R^{m_1}\times R^{m_2} \text{ and } E\int_0^T |u(t)|^2 \mathrm{d}t < \infty
\end{array}
\right\}.
\tag{52}
$$

In what follows, we will utilize the stochastic maximum principle to study the dual representation of the game Problem (LQ).

We first define the Hamiltonian function $H: \Omega\times[0,T]\times R^n\times R^{n\times d}\times l^2(R^n)\times R^{m_1}\times R^{m_2}\times R^n \longrightarrow R^1$ by

$$
\begin{aligned}
&H(t, y, q, z, u_1, u_2, k) \\
&= -\langle k, \mathscr{A}(t)(y) + \sum_{i=1}^{d} B^i(t)q^i \\
&\quad + \sum_{i=1}^{\infty} C^i(t)z^i + D_1(t)u_1 + D_2(t)u_2\rangle \\
&\quad + \langle E(t), y\rangle + \sum_{i=1}^{d}\langle F^i(t), q^i\rangle + \langle N_1(t)u_1, u_1\rangle \\
&\quad + \sum_{i=1}^{\infty}\langle G^i(t), z^i\rangle - \langle N_2(t)u_1, u_1\rangle.
\end{aligned}
\tag{53}
$$

Then, the adjoint equation corresponding to an admissible quintuplet $(u_1(\cdot), u_2(\cdot); y(\cdot), q(\cdot), z(\cdot))$ can be rewritten as

$$
\begin{cases}
\mathrm{d}k(t) = (\mathscr{A}^\top k - E)\mathrm{d}t - \sum_{i=1}^{d}\left((B^i)^\top k - F^i\right)\mathrm{d}W^i - \sum_{i=1}^{\infty}\left((C^i)^\top k - G^i\right)\mathrm{d}H^i, \\
k(0) = -M.
\end{cases}
\tag{54}
$$

Under Assumption 3, for any admissible quintuplet $(u_1(\cdot), u_2(\cdot); y(\cdot), q(\cdot), z(\cdot))$, the adjoint equation (54) has a unique solution $k(\cdot)$ in view of Lemma 2.1 in [9].

It is time to give the dual characterization of the optimal control.

Theorem 3. *Let Assumptions 3 and 4 be satisfied. Then, a necessary and sufficient condition for an admissible quintuplet $(u_1(\cdot), u_2(\cdot); y(\cdot), q(\cdot), z(\cdot))$ to be a saddle quintuplet* *of Problem (LQ) is that the control* $(u_1(\cdot), u_2(\cdot))$ *has the representation*

$$\begin{aligned} u_1(t) &= -\frac{1}{2} N_1^{-1}(t) D_1^*(t) E\left[k(t) \mid \mathcal{G}_t\right], \\ u_2(t) &= \frac{1}{2} N_2^{-1}(t) D_2^*(t) E\left[k(t) \mid \mathcal{G}_t\right], \end{aligned} \tag{55}$$

where $k(\cdot)$ *is the unique solution of the adjoint equation (54) corresponding to the admissible quintuplet* $(u_1(\cdot), u_2(\cdot); y(\cdot), q(\cdot), z(\cdot))$.

Proof. For the necessary part, let $(u_1(\cdot), u_2(\cdot); y(\cdot), q(\cdot), z(\cdot))$ *be an saddle quintuplet; then, by the necessary optimality condition (45) and* $U_i = R^{m_i}$ $(i = 1, 2)$, *we have, a.e., a.s.,*

$$H_{u_i}\left(t, y(t), q(t), z(t), u_1(t), u_2(t), k(t)\right) = 0. \tag{56}$$

Noticing the definition of H in (53), we obtain

$$2N_1(t) u_1(t) + D_1^*(t) E\left[k(t) \mid \mathcal{G}_t\right] = 0, \text{a.e. a.s.}, \tag{57}$$

$$-2N_2(t) u_2(t) + D_2^*(t) E\left[k(t) \mid \mathcal{G}_t\right] = 0, \text{a.e. a.s.} \tag{58}$$

So, the saddle point $(u_1(\cdot), u_2(\cdot))$ has the dual presentation (55).

For the sufficient part, let $(u_1(\cdot), u_2(\cdot); y(\cdot), q(\cdot), z(\cdot))$ be an admissible quintuplet satisfying (55). By the classical technique of completing squares, from (55), we can claim that $(u_1(\cdot), u_2(\cdot); y(\cdot), q(\cdot), z(\cdot))$ satisfies the optimality condition (19) in Theorem 1. Moreover, from Assumptions 3 and 4, it is easy to check that all other conditions in Theorem 1 are satisfied. Hence, $(u_1(\cdot), u_2(\cdot); y(\cdot), q(\cdot), z(\cdot))$ is a saddle quintuplet by Theorem 1.

Data Availability

No data were used to support this study.

Conflicts of Interest

The authors declare that they have no conflicts of interest.

Acknowledgments

This work was supported by the National Natural Science Foundation of China (nos. 11871121 and 11701369) and Natural Science Foundation of Zhejiang Province for Distinguished Young Scholar (no. LR15A010001).

References

[1] T. T. K. An and B. Øksendal, "Maximum principle for stochastic differential games with partial information," *Journal of Optimization Theory and Applications*, vol. 139, no. 3, pp. 463–483, 2008.

[2] B. Øksendal and A. Sulem, "Forward-backward stochastic differential games and stochastic control under model uncertainty," *Journal of Optimization Theory and Applications*, vol. 161, no. 1, pp. 22–55, 2014.

[3] G. Wang and Z. Yu, "A partial information non-zero sum differential game of backward stochastic differential equations with applications," *Automatica*, vol. 48, no. 2, pp. 342–352, 2012.

[4] D. Nualart and W. Schoutens, "Chaotic and predictable representations for lévy processes," *Stochastic Processes and their Applications*, vol. 90, no. 1, pp. 109–122, 2000.

[5] D. Nualart and W. Schoutens, "Backward stochastic differential equations and feynman-kac formula for levy processes, with applications in finance," *Bernoulli*, vol. 7, no. 5, pp. 761–776, 2001.

[6] K. Bahlali, M. Eddahbi, and E. Essaky, "BSDE associated with lévy processes and application to pdie," *Journal of Applied Mathematics and Stochastic Analysis*, vol. 16, no. 1, pp. 1–17, 2003.

[7] K.-I. Mitsui and Y. Tabata, "A stochastic linear-quadratic problem with lévy processes and its application to finance," *Stochastic Processes and their Applications*, vol. 118, no. 1, pp. 120–152, 2008.

[8] Q. X. Meng and M. N. Tang, "Necessary and sufficient conditions for optimal control of stochastic systems associated with lévy processes," *Science China Information Sciences*, vol. 52, no. 11, pp. 1982–1992, 2009.

[9] M. Tang and Q. Zhang, "Optimal variational principle for backward stochastic control systems associated with lévy processes," *Science China Mathematics*, vol. 55, no. 4, pp. 745–761, 2012.

[10] K. Bahlali, N. Khelfallah, and B. Mezerdi, "Optimality conditions for partial information stochastic control problems driven by lévy processes," *Systems & Control Letters*, vol. 61, no. 11, pp. 1079–1084, 2012.

[11] Q. Meng, F. Zhang, and M. Tang, "Maximum principle for backward stochastic systems associated with lévy processes under partial information," in *Proceedings of the 31th Chinese Control Conference*, pp. 1–6, Hefei, China, July 2012.

[12] K. Du and Z. Wu, "Linear-quadratic stackelberg game for mean-field backward stochastic differential system and application," *Mathematical Problems in Engineering*, vol. 2019, Article ID 1798585, 17 pages, 2019.

[13] J. Shi, G. Wang, and J. Xiong, "Leader-follower stochastic differential game with asymmetric information and applications," *Automatica*, vol. 63, pp. 60–73, 2016.

[14] G. Wang, H. Xiao, and J. Xiong, "A kind of lq non-zero sum differential game of backward stochastic differential equation with asymmetric information," *Automatica*, vol. 97, pp. 346–352, 2018.

[15] J. Wu and Z. Liu, "Maximum principle for mean-field zero-sum stochastic differential game with partial information and its applications to finance," *European Journal of Control*, vol. 37, pp. 8–15, 2017.

[16] J. Wu and Z. Liu, "Optimal control of mean-field backward doubly stochastic systems driven by itô-lévy processes," *International Journal of Control*, vol. 93, no. 4, pp. 953–970, 2020.

[17] W. Yu, F. Wang, Y. Huang, and H. Liu, "Social optimal mean field control problem for population growth model," *Asian Journal of Control*, pp. 1–8, 2019.

Hindawi
Mathematical Problems in Engineering
Volume 2020, Article ID 9368346, 20 pages
https://doi.org/10.1155/2020/9368346

Research Article

Optimal Time-Consistent Investment and Reinsurance Strategy Under Time Delay and Risk Dependent Model

Sheng Li [1] and Yong He [2]

[1] School of Economic Mathematics, Southwestern University of Finance and Economics, Chengdu 611130, China
[2] School of Mathematics, Physics and Data Science Chongqing University of Science and Technology, Chongqing 401331, China

Correspondence should be addressed to Sheng Li; 1180202z1002@smail.swufe.edu.cn

Received 26 May 2020; Accepted 16 July 2020; Published 28 August 2020

Guest Editor: Wenguang Yu

In this paper, we consider the problem of investment and reinsurance with time delay under the compound Poisson model of two-dimensional dependent claims. Suppose an insurance company controls the claim risk of two kinds of dependent insurance businesses by purchasing proportional reinsurance and invests its wealth in a financial market composed of a risk-free asset and a risk asset. The risk asset price process obeys the geometric Brownian motion. By introducing the capital flow related to the historical performance of the insurer, the wealth process described by stochastic delay differential equation (SDDE) is obtained. The extended HJB equation is obtained by using the stochastic control theory under the framework of game theory. Under the reinsurance expected premium principle, optimal time-consistent investment and reinsurance strategy and the corresponding value function are obtained. Finally, the influence of model parameters on the optimal strategy is explained by numerical analysis.

1. Introduction

Since insurance companies have been allowed to enter the financial market for investing risk assets, the optimal investment strategy has become an important research topic in recent years. Many literature have studied the maximization of the utility of the terminal wealth or the minimization of the ruin probability of the insurer. Browne [1] uses the surplus process given by the diffusion risk model to study the investment problem of maximizing the utility of the terminal wealth and minimizing the ruin probability of an enterprise and obtains the explicit optimal solution. Hipp and Plum [2] apply the Cramer–Lundberg model to describe the insurance surplus process, based on the assumption that there is only one risky asset in the financial market and the time is discrete; the investment problem is studied. Wang et al. [3] use martingale approach to study the optimal portfolio selection of insurers under the criteria of mean-variance and constant absolute risk aversion utility maximization. For more similar literature, see Liu and Yang [4], Yang and Zhang [5], Wang [3], and Bai and Guo [6].

In addition to market risk, the insurer will also consider insurance risk. It is impossible to avoid insurance risk by investing in bonds and other assets in the market alone. However, reinsurance business provides a way for the insurer to avoid this risk. In recent years, this approach has been widely concerned. Reinsurance business mainly adopts two different forms of insurance: excess-of-loss reinsurance and proportional reinsurance. Promislow and Young [7] first investigate the proportional reinsurance and investment. Bauerle [8] considers proportional reinsurance and investment also, and the optimal explicit solution of the investment-reinsurance problem is obtained under the mean-variance criterion. Zeng and Li [9] also study proportional reinsurance and obtain the efficient frontier of the mean-variance under the multidimensional risky asset model. The stock price in the above model generally follows the geometric Brownian motion; the market price of stock-related risk is constant, but in the real market, stock price may have other characteristics, such as stochastic volatility. Liang et al. [10] used the Ornstein–Uhlenbeck process to characterize the instantaneous return of stocks and obtained the optimal reinsurance and investment strategy. Gu et al. [11] investigate the excess-of-loss reinsurance-investment problem under the constant elasticity variance (CEV) model.

There are two deficiencies in the above literature that deserve further discussion. On the one hand, these literature implicitly assume that all insurance businesses of insurers are independent of each other, so they only study the investment and reinsurance of a single insurance business. However, in the real insurance market, there are often interdependencies between insurance businesses. For example, during the 2019-nCoV, medical claims and death claims often occur together. In order to depict this kind of dependency between different insurance businesses, the risk dependent model is proposed. The main works in this area are as follows. Yuen et al. [12], taking the expected utility maximization of the terminal wealth as the criterion, considered the optimal proportional reinsurance problem with multidimensional risk dependence by using the diffusion approach method. For the detailed process of diffusion approximate to the compound Poisson process, see Gandell [13]. Liang and Yuen [14], under the principle of variance premium, investigated the optimal proportional reinsurance of the Poisson model and diffusion approximation model. Ming et al. [15] derive the explicit expression of the optimal proportional reinsurance under the mean-variance criterion by using stochastic linear quadratic control. Considering the combination of investment and reinsurance, Bi et al. [16] obtains the optimal investment-reinsurance strategy for mean-variance under the diffusion approximation model. Bi and Chen [17], under the criterion of maximizing the expected utility of terminal wealth, arrived at the optimal investment and reinsurance strategies. On the other hand, most of the literature on optimal investment-reinsurance and other optimal control problems focus on time-delay free controlled systems. In fact, financial markets tend to rely on the past, Chang [18] considers the investment and consumption problems related to the return on risk assets and the historical performance. Federico [19] introduces the time-delay state process by considering the capital inflow/outflow related to performance. Peng et al. [20] and Yu et al. [21] study the optimal dividend policy based on observing the information of past time points to determine the behavior of the next moment. In fact, this is a discrete case of time delay. However, the stochastic control problems of systems with time-delay state may be infinite-dimensional in continuous cases; hence, it is difficult to find the analytical solutions. Only in some special cases, it is finite-dimensional and the problem has explicit solution. Elsanosi et al. [22], Øksendal and Sulem [23], and David [24] provide a theoretical basis for solving such problems. Shen and Zeng [25] first introduced the time delay in the investment and insurance problem. They introduced the inflow/outflow of capital in the wealth process of insurer and then depicted the wealth process of insurance companies through the stochastic delay differential equation (SDDE). After that Li [26] and Lai [27] studied the optimal investment-reinsurance problem with time delay under Heston and CEV models, respectively.

Inspired by the above research, this paper combines risk dependence with time delay to consider investment-reinsurance problem. The structure of the rest of this paper is as follows. In Section 2, the financial model framework of this paper is given, assuming that an insurer can invest in a risk-free asset and a risky asset, and in the case of two-dimensional dependent claim compound Poisson model and the introduction of the historical performance of the insurance company, the company's wealth process with time delay is obtained. In Section 3, considering the mean-variance preference criterion, the time-inconsistent optimization problem is defined, and the extended HJB equation is obtained by using the stochastic control theory in the framework of game theory. In Section 4, under the principle of reinsurance expected premium, the explicit solutions of optimal investment and reinsurance strategies and their corresponding value functions are derived. In Section 5, the numerical calculation process of optimal investment and reinsurance strategies are introduced through numerical examples, and the influence of important model parameters on optimal strategy is analyzed. Section 6 concludes this paper.

2. The Model

Suppose that model is based on the probability space $(\Omega, \mathcal{F}, \{\mathcal{F}\}_{t\in[0,T]}, \mathbb{P})$ of information flow which satisfies the general assumptions of right continuity and completeness, where T is a finite constant, representing the operation cycle of an insurance company, and $\{\mathcal{F}\}_{t\in[0,T]}$ is the sum of information available up to time t. All stochastic processes involved in this paper are assumed to adapt to $\{\mathcal{F}\}_{t\in[0,T]}$.

Suppose an insurer has an insurance portfolio business, which is composed of two different insurance businesses, such as medical insurance and death insurance. Suppose that the random variable $\{Y_i, i \geq 1\}$ represents the claim amount of the first type of insurance business; they are independent and have the same distribution function $F_Y(y)$. $\{Z_i, i \geq 1\}$ represents the claim amount of the second type of insurance business; they are independent and have the same distribution function $F_Z(z)$. We assume that if $y \leq 0$, then $F_Y(y) = 0$. Otherwise, $0 < F_Y(y) \leq 1$. And also assume that if $z \leq 0$, then $F_Z(z) = 0$. Otherwise, $0 < F_Z(z) \leq 1$. In addition, their moment generating functions $M_Y(\iota)$ and $M_Z(\iota)$ exist. The cumulative claim process of the two insurance businesses are as follows:

$$\begin{aligned} C_1(t) &= \sum_{i=1}^{\widetilde{N}_1(t)} Y_i, \\ C_2(t) &= \sum_{i=1}^{\widetilde{N}_2(t)} Z_i, \end{aligned} \tag{1}$$

where $\widetilde{N}_1(t)$ and $\widetilde{N}_2(t)$ represent the number of claims for the first and second categories of insurance business up to time t, respectively. And suppose $\{Y_i, i \geq 1\}$, $\{Z_i, i \geq 1\}$, $\{\widetilde{N}_1(t)\}_{t>0}$, and $\{\widetilde{N}_2(t)\}_{t>0}$ are independent of each other.

For different insurance businesses, it is assumed that they are interdependent as follows:

$$\begin{aligned}\widetilde{N}_1(t) &= N_1(t) + N(t),\\ \widetilde{N}_1(t) &= N_2(t) + N(t),\end{aligned} \tag{2}$$

where $N(t)$, $N_1(t)$, and $N_2(t)$ are three independent Poisson processes and the corresponding intensities are λ, λ_1, and λ_2, respectively. Therefore, the total claim amount of these two types of the insurance business is

$$C(t) = C_1(t) + C_2(t) = \sum_{i=1}^{N_1(t)+N(t)} Y_i + \sum_{i=1}^{N_2(t)+N(t)} Z_i. \tag{3}$$

Suppose for arbitrary $\iota \in (0,\zeta)$, $E[Ye^{\iota Y}]$ and $E(Ze^{\iota Z})$ exist. And, for some $\zeta \in (0,\infty]$, there are $\lim_{\iota\longrightarrow\zeta} E[Ye^{\iota Y}] \longrightarrow \infty$ and $\lim_{\iota\longrightarrow\zeta} E[Ze^{\iota Z}] \longrightarrow \infty$.

For convenience of writing, we define

$$\begin{aligned}a_1 &:= E[C_1(t)] = (\lambda+\lambda_1)\mu_{1Y},\\ b_1 &:= \mathrm{Var}\left[C_1^2(t)\right] = (\lambda+\lambda_1)\mu_{2Y},\\ a_2 &:= E[C_2(t)] = (\lambda+\lambda_2)\mu_{1Z},\\ b_2 &:= \mathrm{Var}\left[C_2^2(t)\right] = (\lambda+\lambda_2)\mu_{2Z},\end{aligned} \tag{4}$$

where $\mu_{1Y} = E[Y_i]$, $\mu_{2Y} = E[Y_i^2]$, $\mu_{1Z} = E[Z_i]$, and $\mu_{2Z} = E[Z_i^2]$.

Considering the financial market, it is assumed that assets are traded continuously in time interval $[0,T]$, and tax and transaction costs are not considered. Suppose the insurer can invest its wealth in the financial market composed of a risk-free asset and a risky asset. The risk-free asset price process $\{B(t)\}$ is

$$\begin{cases} \mathrm{d}B(t) = rB(t)\mathrm{d}t, & t \in [0,T],\\ B(0) = 1. \end{cases} \tag{5}$$

The risky asset price process $\{S(t)\}$ is as follows:

$$\begin{cases} \mathrm{d}S(t) = S(t)\left[\alpha_1 \mathrm{d}t + \sigma \mathrm{d}W(t)\right], & t \in [0,T],\\ S(0) = s_0, \end{cases} \tag{6}$$

where r, $\alpha\,(>r)$, and $\sigma\,(>0)$ are constants, representing risk-free interest rate, drift rate, and volatility, respectively. Define $\alpha := \alpha_1 - r$.

As usual, the surplus process from the insurer up to time t is defined as follows:

$$R(t) = R_0 + ct - C(t), \tag{7}$$

where R_0 is the initial surplus and c is the premium rate. In addition, it is assumed that insurance companies can continuously reinsurance insurance business in a certain proportion to control business risk. We denote the retention ratio of categories 1 and 2 insurance business by $q_1(t) \in [0,1]$ and $q_2(t) \in [0,1]$. When the claim occurs, the insurance company pays $q_1(t)Y_i$ or $q_2(t)Z_i$, while the reinsurance company pays $(1-q_1(t))Y_i$ or $(1-q_2(t))Z_i$. Let the reinsurance rate be $\delta(q_1(t), q_2(t))$ at time t.

Let $X(t)$ denote the wealth process of insurance companies at time t, $p_1(t)$ denote the amount of capital invested in the risky asset, and then $X(t) - p_1(t)$ denote the amount of wealth invested in the risk-free asset. The investment-reinsurance strategy $\pi(t) := (p_1(t), q_1(t), q_2(t))$ will be applied by the insurer. Given an investment-reinsurance strategy $\pi(t)$, the wealth process $\{X^\pi(t)\}$ of an insurer satisfies the following stochastic differential equation:

$$\begin{aligned}\mathrm{d}X^\pi(t) = {}&\left[rX^\pi(t) + \alpha p_1(t) + \left(c - \delta\left(q_1(t), q_2(t)\right)\right)\right]\mathrm{d}t\\ &+ \sigma p_1(t)\mathrm{d}W(t) - q_1(t)C_1(t) - q_2(t)\mathrm{d}C_2(t).\end{aligned} \tag{8}$$

Next, we consider the influence of historical performance on the wealth process. Suppose that $f(t, X^\pi(t) - \overline{L}^\pi(t), X^\pi(t) - M^\pi(t))$ represents the inflow/outflow of capital, then the wealth process of insurers with time delay is given by the following stochastic delay differential equation (SDDE):

$$\begin{aligned}\mathrm{d}X^\pi(t) = {}&\left[rX^\pi(t) + \alpha p_1(t) + \left(c - \delta\left(q_1(t), q_2(t)\right)\right)\right]\mathrm{d}t\\ &+ \sigma p_1(t)\mathrm{d}W(t) - f\left(t, X^\pi(t) - \overline{L}^\pi(t), X^\pi(t) - M^\pi(t)\right)\mathrm{d}t\\ &- q_1(t)\mathrm{d}C_1(t) - q_2(t)\mathrm{d}C_2(t).\end{aligned} \tag{9}$$

To make the problem easier to deal with, consider a linear capital inflow/outflow function, that is,

$$\begin{aligned}&f\left(t, X^\pi(t) - \overline{L}^\pi(t), X^\pi(t) - M^\pi(t)\right)\\ &= \gamma_1\left(X^\pi(t) - \overline{L}^\pi(t)\right) + \gamma_2\left(X^\pi(t) - M^\pi(t)\right)\\ &= \gamma_1\left(X^\pi(t) - \frac{L^\pi(t)}{\int_{-h}^0 e^{As}}\mathrm{d}s\right) + \gamma_2\left(X^\pi(t) - M^\pi(t)\right)\\ &= (\gamma_1+\gamma_2)X^\pi(t) - \overline{\gamma}_1 L^\pi(t) - \gamma_2 M^\pi(t),\end{aligned} \tag{10}$$

where $\gamma_1 > 0$ and $\gamma_2 > 0$ are constants, $\overline{\gamma}_1 = \gamma_1/\int_{-h}^0 e^{Au}\mathrm{d}u$. $L^\pi(t) = \int_{-h}^0 e^{Au}X^\pi(t+u)\mathrm{d}u$, $\overline{L}^\pi(t) = L^\pi(t)/\int_{-h}^0 e^{Au}\mathrm{d}u$, and $M^\pi(t) = X^\pi(t-h)$ represent the integrated, average, and point by point delay information of wealth process in time interval $[t-h,t]$. $A\,(\geq 0)$ and $h\,(\geq 0)$ are given average parameters and delay parameters, respectively. Note that $\overline{L}^\pi(t)$ is defined as the weighted average value of wealth process $X^\pi(\cdot)$ in time interval $[t-h,t]$, and the exponential decay factor $e^{Au}\,(u \in [-h,0])$ represents the weight. When $h = 1$, $X^\pi(t) - \overline{L}^\pi(t)$ and $X^\pi(t) - M^\pi(t)$ represent the average gain or loss and absolute gain or loss of wealth of insurers in the last operating cycle. Because the inflow/outflow of capital is closely related to the past performance of the wealth process. If the past performance is good, the company will give part of its earnings to shareholders or give bonuses to the management, which shows the outflow of capital, i.e., $f > 0$. At this time, $X^\pi(t) > \overline{L}^\pi(t)$ and $X^\pi(t) > M^\pi(t)$. On the contrary, if the past performance of the insurance company is not good, the company needs additional financing to achieve the predetermined goal. This shows capital inflow, i.e., $f < 0$ when $X^\pi(t) < \overline{L}^\pi(t)$ and $X^\pi(t) < M^\pi(t)$. Therefore, the function $f(\cdot,\cdot,\cdot)$ considers the average and absolute performance of the wealth process in $[t-h,t]$.

Substituting (10) into (9), the following stochastic delay differential equation (SDDE) is obtained:

$$\begin{cases} \mathrm{d}^{\pi}X(t) = \left[(r-\gamma_1(t)-\gamma_2)X(t)+\overline{\gamma}_1(t)L^{\pi}(t)+\gamma_2 M^{\pi}(t)+\alpha p_1(t)+\left(c-\delta\left(q_1(t),q_2(t)\right)\right)\right]\mathrm{d}t \\ \qquad +\sigma p_1(t)\mathrm{d}W(t)-q_1(t)\mathrm{d}C_1(t)-q_2(t)\mathrm{d}C_2(t), \\ \mathrm{d}L^{\pi}(t) = \left[X^{\pi}(t)-AL^{\pi}(t)-e^{-Ah}M^{\pi}(t)\right]\mathrm{d}t. \end{cases} \tag{11}$$

Furthermore, suppose $X^{\pi}(t)=x_0$, $\forall t\in[-h,0]$, which can be interpreted as that the insurance company has the initial wealth of x_0 at $-h$. There is no business operation during $[-h,0]$, and the wealth has no change. The integrated delay wealth initial value can be calculated to get $L^{\pi}(0)=x_0/A(1-e^{-Ah})$.

Definition 1 (admissible strategy). For any fixed $t\in[0,T]$, an investment-reinsurance strategy $\pi(t)=(p_1(t),q_1(t),q_2(t))$ is said to admissible if (i) $(p_1(t),q_1(t),q_2(t))$ is $\mathscr{F}_t$ progressively measurable, (ii) for $t\in[0,T]$, $q_1(t)\in[0,1]$, $q_2(t)\in[0,1]$, and $E[\int_0^T p_1^2(t)\mathrm{d}t]<0$, and (iii) SDDE (11) has a unique strong solution $X(\cdot)$ such that $E[\sup_{0\le t\le T}|X(t)|^2]<\infty$. Let Π be the set of all admissible investment-reinsurance strategy.

3. Optimization Problem

To take historical operating performance into account, the insurer will focus on both terminal wealth $X^{\pi}(T)$ and historical average operating performance $L^{\pi}(T)$; thus, the following objective function is defined:

$$\begin{aligned} J(t,x,l,m;\widehat{\pi}) &= \sup_{\pi\in\Pi} E_{t,x,l,m}\left[X^{\pi}(T)+\overline{\beta}\overline{L}^{\pi}(T)\right] \\ &\quad -\frac{\omega}{2}\mathrm{Var}_{t,x,l,m}\left[X^{\pi}(T)+\overline{\beta}\overline{L}^{\pi}(T)\right], \end{aligned} \tag{12}$$

where risk aversion coefficient $\omega(>0)$ and delay parameter $\overline{\beta}(\in[0,1])$ are constants. $E_{t,x,l,m}[\cdot]$ and $\mathrm{Var}_{t,x,l,m}[\cdot]$ represent conditional expectation and conditional variance based on $X^{\pi}(t)=x$, $L^{\pi}(t)=l$, and $M^{\pi}(t)=m$, respectively. $\overline{\beta}(\in[0,1])$ is the weight of $\overline{L}^{\pi}(t)$, indicating the degree of terminal wealth affected by historical average performance. If we write $\beta=\overline{\beta}/\int_{-h}^0 e^{Au}\mathrm{d}u$, then $X^{\pi}(t)+\overline{\beta}\overline{L}^{\pi}(t)=X^{\pi}(t)+\beta L^{\pi}(t)$. In addition, according to Chang [18], delay optimal control problem is generally an infinite-dimensional problem. In order to obtain the optimal solution, some additional conditions will be attached. We assume that the value function $V(\cdot)$ is only related to x and l, but $L^{\pi}(t)$ is related to $M^{\pi}(t)$; in order to make $V(\cdot)$ only depend on (t,x,l), the problem can obtain the optimal solution, and we assume the following conditions hold:

$$\begin{aligned} \gamma_2 &= \beta e^{-Ah}, \\ \overline{\gamma}_1 - A\beta &= (r-\gamma_1-\gamma_2+\beta)\beta. \end{aligned} \tag{13}$$

Therefore, this paper aims at the following optimization problems:

$$\begin{aligned} J(t,x,l;\widehat{\pi}) &= \sup_{\pi\in\Pi} E_{t,x,l,m}\left[X^{\pi}(T)+\beta L^{\pi}(T)\right] \\ &\quad -\frac{\omega}{2}\mathrm{Var}_{t,x,l,m}\left[X^{\pi}(T)+\beta L^{\pi}(T)\right] \\ &= E_{t,x,l,m}\left[F\left(X^{\pi}(T)+\beta L^{\pi}(T)\right)\right] \\ &\quad + G\left(E_{t,x,l,m}\left[X^{\pi}(T)+\beta L^{\pi}(T)\right]\right), \end{aligned} \tag{14}$$

where $F(x)=x-\omega/2x^2$ and $G(x)=\omega/2x^2$.

Remark 1

(i) According to Shen and Zeng [25], condition (13) can be regarded as exogenous technical conditions that need to be determined in advance by the insurance company. Firstly, the average delay wealth $\overline{L}^{\pi}(t)$ and point by point delay wealth $M^{\pi}(t)$ are determined by selecting the average parameter A and delay time h. Secondly, it selects the weight β. Finally, it calculates the weight ratios $\gamma_2=\beta e^{-Ah}$ and $\gamma_1=(\beta\int_{-h}^0 e^{Au}\mathrm{d}u/(1+\beta\int_{-h}^0 e^{Au}\mathrm{d}u))(r-\gamma_2+\beta+A)$ of historical performance $X^{\pi}(t)-\overline{L}^{\pi}(t)$ and $X^{\pi}(t)-M^{\pi}(t)$ according to the two assumptions in (13) and adjusts the inflow/outflow of capital accordingly.

(ii) Because there is a nonlinear function of the expectation of the terminal value wealth in the variance term, problem (14) is time inconsistent, which leads to the failure of Bellman's optimal principle. Many works of literature deal with the mean-variance problem by setting a precommitment, so the optimal strategy obtained are time-inconsistent. However, for a rational decision maker, time consistency is often not negligible. Rational decision makers hope that the equilibrium strategy they find is not only optimal at this time but also optimal in the future with the evolution of time, that is to say, the equilibrium strategy is time consistent. Therefore, for problem (14), this paper aims to find the equilibrium strategy.

Definition 2. Consider a control law $\{\widehat{\pi}(t), t \in [0,T]\}$. Choose arbitrarily $\widetilde{\pi} \in \Pi$, $t > 0$, and $\varepsilon > 0$ and define the control law $\widehat{\pi}_\varepsilon$:

$$\pi_\varepsilon(u) = \begin{cases} \widetilde{\pi}, & t \le u < t + \varepsilon, \\ \widehat{\pi}(u), & t + \varepsilon \le u \le T. \end{cases} \tag{15}$$

We call that $\widehat{\pi}$ is an equilibrium strategy if $\lim_{\varepsilon\downarrow 0}\inf (J(t,x,l;\widehat{\pi}) - J(t,x,l;\pi_\varepsilon)/\varepsilon) \ge 0$ for any t and $\widetilde{\pi}$. If the equilibrium strategy $\widehat{\pi}$ exists, the equilibrium value function is defined as $V(t,x,l) = J(t,x,l;\widehat{\pi})$.

According to Definition 2, the equilibrium strategy is time consistent. For simplicity, we denote that $\mathscr{C}^{1,2,1}[0,T] \times \mathbb{R} \times \mathbb{R} = \{\phi(t,x,l) \mid \phi(t,\cdot,\cdot)\}$ is once continuously differentiable on $[0,T]$, $\phi(\cdot,x,\cdot)$ is twice continuously differentiable on $\mathbb{R}$, and $\phi(\cdot,\cdot,l)$ is once continuously differentiable on $\mathbb{R}$. To provide verification theorem and derive conveniently extended HJB equation, for $\forall (t,x,l) \in [0,T] \times \mathbb{R} \times \mathbb{R}$, $\forall \phi \in \mathscr{C}^{1,2,1}([0,T] \times \mathbb{R} \times \mathbb{R})$, and given control law π, we define variational operator as follows:

$$\begin{aligned} \mathscr{L}^\pi \phi(t,x,l) = {} & \phi_t(t,x,l) + \left[(r - \gamma_1 - \gamma_2)x + \overline{\gamma_1} l + \gamma_2 m + \alpha p_1(t) + \left(c - \delta\left(q_1(t), q_2(t)\right)\right)\right]\phi_x(t,x,l) \\ & + \left(x - Al - e^{-Ah} m\right)\phi_l(t,x,l) + \frac{1}{2}\sigma^2 p_1^2(t)\phi_{xx}(t,x,l) \\ & + \lambda_1 E\left[\phi\left(t, x - q_1(t)Y_i, l\right) - \phi(t,x,l)\right] + \lambda_2 E\left[\phi\left(t, x - q_2(t)Z_i, l\right) - \phi(t,x,l)\right] \\ & + \lambda E\left[\phi\left(t, x - q_1(t)Y_i - q_2(t)Z_i, l\right) - \phi(t,x,l)\right]. \end{aligned} \tag{16}$$

The following theorem provides verification for the extended HJB equation in problem (14).

Theorem 1 (verification theorem). *For problem (14), we assume that there exist two real-valued functions $V(t,x,l), g(t,x,l) \in \mathscr{C}^{1,2,1}([0,T] \times \mathbb{R} \times \mathbb{R})$ satisfying the following extended HJB equation:*

$$\begin{cases} \sup_{\pi\in\Pi}\left\{\mathscr{L}^\pi V(t,x,l) - \dfrac{\omega}{2}\mathscr{L}^\pi g^2(t,x,l) + \omega g(t,x,l)\mathscr{L}^\pi g(t,x,l)\right\} = 0, \\ \mathscr{L}^{\widehat{\pi}} g(t,x,l) = 0, \\ \widehat{\pi} = \operatorname{argsup}_{\pi\in\Pi}\left\{\mathscr{L}^\pi V(t,x,l) - \dfrac{\omega}{2}\mathscr{L}^\pi g^2(t,x,l) + \omega g(t,x,l)\mathscr{L}^\pi g(t,x,l)\right\}, \\ V(T,x,l) = x + \beta l, \quad g(T,x,l) = x + \beta l. \end{cases} \tag{17}$$

Then, $J(t,x,l;\widehat{\pi}) = V(t,x,l)$, $E_{t,x,l}[X^{\widehat{\pi}}(T) + \beta L^{\widehat{\pi}}(T)] = g(t,x,l)$, and $\widehat{\pi}$ is an equilibrium investment-reinsurance strategy.

The proof process of Theorem 1 is similar to that of Björk et al. [28], so it is omitted here.

In Definition 1, the policy set Π is allowed to require the reinsurance policy to satisfy the constraint $q_1(t) \in [0,1]$ and $q_2(t) \in [0,1]$. To facilitate the solution, we do not consider this constraint temporarily and record all the policy sets satisfying (i) and (iii) as $\widetilde{\Pi}$. According to the variational operator (16), the extended HJB (17) can be expanded as follows:

$$\begin{cases} \sup_{\pi\in\widehat{\Pi}} \Big\{ V_t(t,x,l) + [(r-\gamma_1(t)-\gamma_2)x + \overline{\gamma_1}(t)l + \gamma_2 m + \alpha p_1(t) + (c-\delta(q_1(t),q_2(t)))]V_x(t,x,l) \\ \quad + \frac{1}{2}\sigma^2 p_1^2(t)\left[V_{xx}(t,x,l) - \omega g_x^2(t,x,l)\right] + \left(x - Al - e^{-Ah}m\right)V_l(t,x,l) + \lambda_1\Big[E[V(t,x-q_1(t)Y_i,l) - V(t,x,l)] \\ \quad - \frac{\omega}{2}E\left[g^2(t,x-q_1(t)Y_i,l) - g^2(t,x,l)\right] + \omega g(t,x,l)E[g(t,x-q_1(t)Y_i,l) - g(t,x,l)]\Big] \\ \quad + \lambda_2\Big[E[V(t,x-q_2(t)Z_i,l) - V(t,x,l)] - \frac{\omega}{2}E\left[g^2(t,x-q_2(t)Z_i,l) - g^2(t,x,l)\right] \\ \quad + \omega g(t,x,l)E[g(t,x-q_2(t)Z_i,l) - g(t,x,l)]\Big] \\ \quad + \lambda\Big[E[V(t,x-q_1(t)Y_i - q_2(t)Z_i,l) - V(t,x,l)] - \frac{\omega}{2}E\left[g^2(t,x-q_1(t)Y_i-q_2(t)Z_i,l) - g^2(t,x,l)\right] \\ \quad - \omega g(t,x,l)E[g(t,x-x-q_1(t)Y_i-q_2(t)Z_i,l) - g(t,x,l)]\Big]\Big\} = 0, \quad t\in[0,T], \\ g_t(t,x,l) + [(r-\gamma_1(t)-\gamma_2)x + \overline{\gamma_1}(t)l + \gamma_2 m + \alpha\widehat{p}_1(t) + (c-\delta(\widehat{q}_1(t),\widehat{q}_2(t)))] \\ g_x(t,x,l) + \frac{1}{2}\sigma^2\widehat{p}_1^2(t)g_{xx}(t,x,l) + \left(x - Al - e^{-Ah}m\right)g_l(t,x,l) + \lambda_1 E[g(t,x-\widehat{q}_1(t)Y_i,l) - g(t,x,l)] \\ + \lambda_2 E[g(t,x-\widehat{q}_2(t)Z_i,l) - g(t,x,l)] + \lambda E[g(t,x-\widehat{q}_1(t)Y_i - \widehat{q}_2(t)Z_i,l) - g(t,x,l)] = 0, \quad t\in[0,T], \\ V(T,x,l) = x + \beta l, \\ g(T,x,l) = x + \beta l. \end{cases} \tag{18}$$

Suppose that the solution of the above extended HJB equation has the following structure:

$$\begin{cases} V(t,x,l) = H_1(t)(x+\beta l) + F_1(t), \\ g(t,x,l) = H_2(t)(x+\beta l) + F_2(t), \end{cases} \tag{19}$$

with the boundary condition $H_1(T) = H_2(T) = 1$ and $F_1(T) = F_2(T) = 0$.

Differentiating V and g with respect to t, x, and l, we obtain

$$\begin{aligned} V_t(t,x,l) &= H_1'(t)(x+\beta l) + F_1'(t), \\ V_x(t,x,l) &= H_1(t), \\ V_l(t,x,l) &= \beta H_1(t), \\ V_{xx}(t,x,l) &= 0, \\ g_t(t,x,l) &= H_2'(t)(x+\beta l) + F_1'(t), \\ g_x(t,x,l) &= H_2(t), \\ g_l(t,x,l) &= \beta H_2(t), \\ g_{xx}(t,x,l) &= 0. \end{aligned} \tag{20}$$

Through simple calculation, we can also obtain

$$\begin{cases} E[V(t,x-q_1(t)Y_i,l) - V(t,x,l)] = -\mu_{1Y}q_1(t)H_1(t), \\ E[V(t,x-q_2(t)Z_i,l) - V(t,x,l)] = -\mu_{1Z}q_2(t)H_1(t), \\ E[V(t,x-q_1(t)Y_i - q_2(t)Z_i,l) - V(t,x,l)] = -\mu_{1Y}q_1(t)H_1(t) - \mu_{1Z}q_2(t)H_1(t), \end{cases}$$
$$\begin{cases} E[g^2(t,x-q_1(t)Y_i,l) - g^2(t,x,l)] = [\mu_{2Y}q_1^2(t) - 2\mu_{1Y}q_1(t)(x+\beta l)]H_2^2(t) - 2\mu_{1Y}q_1(t)H_2(t)F_2(t), \\ E[g^2(t,x-q_2(t)Z_i,l) - g^2(t,x,l)] = [\mu_{2Z}q_2^2(t) - 2\mu_{1Z}q_2(t)(x+\beta l)]H_2^2(t) - 2\mu_{1Z}q_1(t)H_2(t)F_2(t), \\ E[g^2(t,x-q_1(t)Y_i - q_2(t)Z_i,l) - g^2(t,x,l)] = [\mu_{2Y}q_1^2(t) + \mu_{2Z}q_2^2(t) + 2\mu_{1Y}\mu_{1Z}q_1(t)q_2(t) - 2(\mu_{1Y}q_1(t) + \mu_{1Z}q_2(t))(x+\beta l)], \\ H_2^2 - 2(\mu_{1Y}q_1(t) + \mu_{1Z}q_2(t))H_2(t)F_2(t), \end{cases}$$
$$\begin{cases} E[g(t,x-q_1(t)Y_i,l) - g(t,x,l)] = -\mu_{1Y}q_1(t)H_2(t), \\ E[g(t,x-q_2(t)Z_i,l) - g(t,x,l)] = -\mu_{1Z}q_2(t)H_2(t), \\ E[g(t,x-q_1(t)Y_i - q_2(t)Z_i,l) - g(t,x,l)] = -\mu_{1Y}q_1(t)H_2(t) - \mu_{1Z}q_2(t)H_2(t). \end{cases} \tag{21}$$

Putting the above results back into (18), we can arrive at

$$\begin{cases} \sup_{\pi\in\widehat{\Pi}}\left\{H_1'(t)(x+\beta l)+F_1'(t)+\psi(p_1,q_1,q_2)H_1(t)-\frac{\omega}{2}\sigma^2p_1^2(t)H_2^2(t)-\frac{\omega}{2}\left(b_1q_1^2(t)+b_2q_2^2(t)\right)H_2^2(t)-\omega\lambda\mu_{1Y}\mu_{1Z}q_1(t)q_2(t)H_2^2(t)\right\}=0, \\ H_2'(t)(x+\beta l)+F_2'(t)+\psi(p_1,q_1,q_2)H_2(t)=0, \\ H_1(T)=H_2(T)=1, \\ F_1(T)=F_2(T)=0, \end{cases} \tag{22}$$

where

$$\begin{aligned}\psi(p_1,q_1,q_2)=&(r-\gamma_1-\gamma_2+\beta)x+(\overline{\gamma_1}-A\beta)l\\&+\left(\gamma_2-\beta e^{-Ah}\right)m+\alpha p_1(t)\\&+(c-\delta(q_1(t),q_2(t)))-a_1q_1(t)-a_2q_2(t).\end{aligned} \tag{23}$$

According to $\gamma_2=\beta e^{-Ah}$, we have

$$\begin{aligned}\psi(p_1,q_1,q_2)=&(r-\gamma_1(t)-\gamma_2+\beta)x+(\overline{\gamma_1}-A\beta)l+\alpha p_1(t)\\&+(c-\delta(q_1(t),q_2(t)))-a_1q_1(t)-a_2q_2(t).\end{aligned} \tag{24}$$

For the convenience of writing, let

$$\begin{aligned}h(p,q_1,q_2)=&\psi(p,q_1,q_2)H_1(t)-\frac{\omega}{2}\sigma^2p_1^2(t)H_2^2(t)\\&-\frac{\omega}{2}\left(b_1q_1^2(t)+b_2q_2^2(t)\right)H_2^2(t)\\&-\omega\lambda\mu_{1Y}\mu_{1Z}q_1(t)q_2(t)H_2^2(t).\end{aligned} \tag{25}$$

4. Optimal Time-Consistent Strategy

This section assumes that the reinsurance premium rate is calculated by the expected premium principle, i.e.,

$$\delta(q_1(t),q_2(t))=(1+\eta_1)(1-q_1(t))a_1+(1+\eta_2)(1-q_2(t))a_2, \tag{26}$$

where η_1 and η_2 are the reinsurer's safety loading of the insurance business.

Substituting the above formula into (24), we have

$$\begin{aligned}\psi(p_1,q_1,q_2)=&(r-\gamma_1-\gamma_2+\beta)x+(\overline{\gamma_1}-A\beta)l+\alpha p_1(t)\\&+c-a_1(1+\eta_1)\\&-a_2(1+\eta_2)+a_1\eta_1q_1(t)+a_2\eta_2q_2(t).\end{aligned} \tag{27}$$

To facilitate derivation, we rewrite (25) as

$$\begin{aligned}h(p,q_1,q_2)=&\psi(p,q_1,q_2)H_1(t)-\frac{\omega}{2}\sigma^2p_1^2(t)H_2^2(t)\\&-\frac{\omega}{2}\left(b_1q_1^2(t)+b_2q_2^2(t)\right)H_2^2(t)\\&-\omega\lambda\mu_{1Y}\mu_{1Z}q_1(t)q_2(t)H_2^2(t).\end{aligned} \tag{28}$$

Differentiating $h(p,q_1,q_2)$ with respect to p_1, q_1, and q_2, we can derive

$$\begin{cases}\frac{\partial h}{\partial p_1}=\alpha H_1(t)-\omega\sigma^2p_1(t)H_2^2(t),\\ \frac{\partial^2h}{\partial p_1^2}=-\omega\sigma^2H_2^2(t),\\ \frac{\partial^2h}{\partial p_1\partial q_1}=\frac{\partial^2h}{\partial p_1\partial q_2}=0,\\ \frac{\partial h}{\partial q_1}=a_1\eta_1H_1(t)-\omega b_1q_1(t)H_2^2(t)-\omega\lambda\mu_{1Y}\mu_{1Z}q_2(t)H_2^2(t),\\ \frac{\partial h}{\partial q_2}=a_2\eta_2H_1(t)-\omega b_2q_2(t)H_2^2(t)-\omega\lambda\mu_{1Y}\mu_{1Z}q_1(t)H_2^2(t),\\ \frac{\partial^2h}{\partial q_1^2}=-\omega b_1H_2^2(t),\\ \frac{\partial^2h}{\partial q_2^2}=-\omega b_2H_2^2(t),\\ \frac{\partial^2h}{\partial q_1\partial q_2}=-\omega\lambda\mu_{1Y}\mu_{1Z}H_2^2(t).\end{cases} \tag{29}$$

From (29), we obtain the following Hessian matrix:

$$\begin{bmatrix} \frac{\partial^2 h}{\partial p_1^2} & \frac{\partial^2 h}{\partial p_1 \partial q_1} & \frac{\partial^2 h}{\partial p_1 \partial q_2} \\ \frac{\partial^2 h}{\partial p_1 \partial q_1} & \frac{\partial^2 h}{\partial q_1^2} & \frac{\partial^2 h}{\partial q_1 \partial q_2} \\ \frac{\partial^2 h}{\partial p_1 \partial q_2} & \frac{\partial^2 h}{\partial q_1 \partial q_2} & \frac{\partial^2 h}{\partial q_2^2} \end{bmatrix} = -\omega H_2^2(t)\mathbf{B}, \tag{30}$$

where

$$\mathbf{B} = \begin{bmatrix} \sigma^2 & 0 & 0 \\ 0 & b_1 & \lambda\mu_{1Y}\mu_{1Z} \\ 0 & \lambda\mu_{1Y}\mu_{1Z} & b_2 \end{bmatrix}, \tag{31}$$

Lemma 1. *The function $h(p_1, q_1, q_2)$ in (28) is concave with respect to (p_1, q_1, q_2).*

Proof. In order to prove Lemma 1, we only need to prove that the Hessian matrix is negative definite. From (43), we know $H_2(t) \neq 0$, thus $H_2^2(t) > 0$. According to (30), we only need to prove that matrix $\mathbf{B}$ is positive definite.

$\forall \mathbf{C} = (c_1, c_2, c_3) \in \mathbb{R}^3$ and $\mathbf{C} \neq \mathbf{0}$. Let $(\cdot)^{tr}$ denote the transposition of a vector or matrix, then

$$\begin{aligned} \mathbf{C}\cdot\mathbf{B}\cdot\mathbf{C}^{tr} &= c_1^2\sigma^2 + c_2^2 b_1 + c_3^2 b_2 + 2c_2c_3\lambda\mu_{1Y}\mu_{1Z} \\ &= c_1^2\sigma^2 + c_2^2(\lambda_1+\lambda)\mu_{2Y} + c_3^2(\lambda_2+\lambda)\mu_{2Z} + 2c_2c_3\mu_{1Y}\mu_{1Z} \\ &= c_1\sigma^2 + c_2^2\lambda_1 E\left[(Y_i)^2\right] + c_3^2\lambda_2 E\left[(Z_i)^2\right] + \lambda\left[c_2^2 E\left[(Y_i)^2\right] + c_3^2 E\left[(Z_i)^2\right] + 2c_2c_3E[Y_i]E[Y_i]\right] \\ &\geq c_1\sigma^2 + c_2^2\lambda_1 E\left[(Y_i)^2\right] + c_3^2\lambda_2 E\left[(Z_i)^2\right] + \lambda\left[c_2E[Y_i] + c_3E[Z_i]\right]^2 > 0. \end{aligned} \tag{32}$$

So, matrix $\mathbf{B}$ is positive definite.

From (29), we have

$$\begin{cases} \alpha H_1(t) - \omega\sigma^2 p_1(t)H_2^2(t) = 0, \\ a_1\eta_1 H_1(t) - \omega b_1 q_1(t)H_2^2(t) - \omega\lambda\mu_{1Y}\mu_{1Z}q_2(t)H_2^2(t) = 0, \\ a_2\eta_2 H_1(t) - \omega b_2 q_2(t)H_2^2(t) - \omega\lambda\mu_{1Y}\mu_{1Z}q_1(t)H_2^2(t) = 0. \end{cases} \tag{33}$$

By solving the above equations, we can obtain

$$\begin{cases} \widehat{p}_1(t) = \frac{\alpha}{\sigma^2}\frac{H_1(t)}{\omega H_2^2(t)}, \\ \widehat{q}_1(t) = D_1\frac{H_1(t)}{\omega H_2^2(t)}, \\ \widehat{q}_2(t) = D_2\frac{H_1(t)}{\omega H_2^2(t)}, \end{cases} \tag{34}$$

where $D_1 = a_1\eta_1 b_2 - a_2\eta_2\lambda\mu_{1Y}\mu_{1Z}/b_1b_2 - \lambda^2\mu_{1Y}^2\mu_{1Z}^2$ and $D_2 = a_2\eta_2 b_1 - a_1\eta_1\lambda\mu_{1Y}\mu_{1Z}/b_1b_2 - \lambda^2\mu_{1Y}^2\mu_{1Z}^2$.

From Lemma 1, we know that $(\widehat{p}_1(t), \widehat{q}_1(t), \widehat{q}_2(t))$ is the point where function $h(p_1, q_1, q_2)$ takes the maximum value. Putting $(\widehat{p}_1(t), \widehat{q}_1(t), \widehat{q}_2(t))$ into (22), we can obtain

$$\begin{aligned} &H_1'(t)(x+\beta l) + F_1'(t) + \left[(r-\gamma_1-\gamma_2+\beta)x + (\overline{\gamma}_1 - A\beta)l\right]H_1(t) \\ &\quad + \left[c - a_1(1+\eta_1) - a_2(1+\eta_2)\right]H_1(t) + \left[\alpha\widehat{p}_1(t) + a_1\eta_1\widehat{q}_1(t) + a_2\eta_2\widehat{q}_2(t)\right]H_1(t) \\ &\quad - \frac{\omega}{2}\left[\sigma^2\widehat{p}_1^2(t) + \left(b_1\widehat{q}_1^2(t) + b_2\widehat{q}_2^2(t)\right) + 2\lambda\mu_{1Y}\mu_{1Z}\widehat{q}_1(t)\widehat{q}_2(t)\right]H_2^2(t) = 0, \end{aligned} \tag{35}$$

$$\begin{aligned} &H_2'(t)(x+\beta l) + F_2'(t) + \left[(r-\gamma_1-\gamma_2+\beta)x + (\overline{\gamma}_1 - A\beta)l\right]H_2(t) \\ &\quad + \left[\alpha\widehat{p}_1(t) + c - a_1(1+\eta_1) - a_2(1+\eta_2) + a_1\eta_1\widehat{q}_1(t) + a_2\eta_2\widehat{q}_2(t)\right]H_2(t) = 0. \end{aligned} \tag{36}$$

According to

$$\overline{\gamma}_1 - A\beta = (r-\gamma_1-\gamma_2+\beta)\beta, \tag{37}$$

we have

$$(r-\gamma_1-\gamma_2+\beta)x + (\overline{\gamma}_1 - A\beta)l = (r-\gamma_1-\gamma_2+\beta)(x+\beta l). \tag{38}$$

By separating variables of $(x+\beta l)$, we can obtain

$$\begin{cases} H_1'(t) + (r - \gamma_1 - \gamma_2 + \beta)H_1(t) = 0, \\ H_1(T) = 1, \end{cases} \tag{39}$$

$$\begin{cases} H_2'(t) + (r - \gamma_1 - \gamma_2 + \beta)H_2(t) = 0, \\ H_2(T) = 1, \end{cases} \tag{40}$$

$$\begin{cases} F_1'(t) + [c - a_1(1+\eta_1) - a_2(1+\eta_2)]H_1(t) + [\alpha\widehat{p}_1(t) + a_1\eta_1\widehat{q}_1(t) + a_2\eta_2\widehat{q}_2(t)]H_1(t) \\ -\dfrac{\omega}{2}\left[\sigma^2\widehat{p}_1^2(t) + b_1\widehat{q}_1^2(t) + b_2\widehat{q}_2^2(t) + 2\lambda\mu_{1Y}\mu_{1Z}\widehat{q}_1(t)\widehat{q}_2(t)\right]H_2^2(t) = 0, \\ F_1(T) = 0, \end{cases} \tag{41}$$

$$\begin{cases} F_2'(t) + [\alpha\widehat{p}_1(t) + c - a_1(1+\eta_1) - a_2(1+\eta_2) + a_1\eta_1\widehat{q}_1(t) + a_2\eta_2\widehat{q}_2(t)]H_2(t) = 0, \\ F_1(T) = 0. \end{cases} \tag{42}$$

By solving the above equations, we have

$$\begin{cases} H_1(t) = H_2(t) = e^{(r-\gamma_1-\gamma_2+\beta)(T-t)}, \\ F_1(t) = \dfrac{c - a_1(1+\eta_1) - a_2(1+\eta_2)}{r - \gamma_1 - \gamma_2 + \beta}\left[e^{(r-\gamma_1-\gamma_2+\beta)(T-t)} - 1\right] + \dfrac{1}{\omega}\left[a_1\eta_1 D_1 + a_2\eta_2 D_2 - \dfrac{1}{2}b_1 D_1^2 - \dfrac{1}{2}b_2 D_2^2 - \lambda\mu_{1Y}\mu_{1Z}D_1 D_2 + \dfrac{\alpha^2}{2\sigma^2}\right](T-t), \\ F_2(t) = \dfrac{c - a_1(1+\eta_1) - a_2(1+\eta_2)}{r - \gamma_1 - \gamma_2 + \beta}\left[e^{(r-\gamma_1-\gamma_2+\beta)(T-t)} - 1\right] + \dfrac{1}{\omega}\left[a_1\eta_1 D_1 + a_2\eta_2 D_2 + \dfrac{\alpha^2}{\sigma^2}\right](T-t). \end{cases} \tag{43}$$

According to the above discussion, the following proposition can be obtained.

Proposition 1. *For problem (14), the time-consistent investment-reinsurance strategy in set $\widehat{\Pi}$ is as follows:*

$$\begin{cases} \widehat{p}_1(t) = \dfrac{\alpha}{\sigma^2\omega}e^{-(r-\gamma_1-\gamma_2+\beta)(T-t)}, \\ \widehat{q}_1(t) = \dfrac{a_1\eta_1 b_2 - a_2\eta_2\lambda\mu_{1Y}\mu_{1Z}}{\left(b_1 b_2 - \lambda^2\mu_{1Y}^2\mu_{1Z}^2\right)\omega}e^{-(r-\gamma_1-\gamma_2+\beta)(T-t)}, \\ \widehat{q}_2(t) = \dfrac{a_2\eta_2 b_1 - a_1\eta_1\lambda\mu_{1Y}\mu_{1Z}}{\left(b_1 b_2 - \lambda^2\mu_{1Y}^2\mu_{1Z}^2\right)\omega}e^{-(r-\gamma_1-\gamma_2+\beta)(T-t)}. \end{cases} \tag{44}$$

The corresponding equilibrium function is

$$V(t,x,l) = H_1(t)(x + \beta l) + F_1(t), \tag{45}$$

where H and F are given by (43).

Let $t_1 = T - (1/r - \gamma_1 - \gamma_2 + \beta)\ln(D_1/\omega)$ for $\omega \le D_1 \le \omega e^{(r-\gamma_1-\gamma_2+\beta)T}$. Let $t_2 = T - (1/r - \gamma_1 - \gamma_2 + \beta)\ln(D_2/\omega)$ for $\omega \le D_2 \le \omega e^{(r-\gamma_1-\gamma_2+\beta)T}$. For $D_1 < \omega$ ($D_2 < \omega$), we set $t_1 = T$ ($t_2 = T$). And for $D_1 > \omega e^{(r-\gamma_1-\gamma_2+\beta)T}$ ($D_2 > \omega e^{(r-\gamma_1-\gamma_2+\beta)T}$), we set $t_1 = 0$ ($t_2 = 0$). To make sure that the optimal reinsurance strategies satisfy $q_1(t) \in [0,1]$ and $q_2(t) \in [0,1]$, we introduce the following lemma.

Lemma 2. *For λ, μ_{1Y}, μ_{1Z}, a_1, a_2, b_1, and b_2 given in (4), the following inequality holds:*

$$\frac{\lambda\mu_{1Y}\mu_{1Z}a_2}{a_1 b_2} \le \frac{\lambda\mu_{1Y}\mu_{1Z}a_2 + b_1 a_2}{a_1 b_2 + \lambda\mu_{1Y}\mu_{1Z}a_1} \le \frac{b_1 a_2}{\lambda\mu_{1Y}\mu_{1Z}a_1}. \tag{46}$$

Proof. Using Cauchy − Schwarz inequality, we can easily get $b_1 > \lambda\mu_{1Y}\mu_{1Z}$ and $b_2 > \lambda\mu_{1Y}\mu_{1Z}$ and then we can obtain

$$\frac{\lambda\mu_{1Y}\mu_{1Z}a_2}{b_2 a_1} \le \frac{b_1 a_2}{\lambda\mu_{1Y}\mu_{1Z}a_1}. \tag{47}$$

In addition, for any positive number d_1, d_2, d_3, and d_4, if $(d_1/d_2) \le (d_3/d_4)$, then $(d_1/d_2) \le (d_1 + d_3/d_2 + d_4) \le (d_3/d_4)$. In combination with inequality (47), inequality (46) is easily proved.

From Lemma 2, we will investigate the optimal results in the following four cases:

Case 1: $\eta_1 < (\lambda\mu_{1Y}\mu_{1Z}a_2/b_2 a_1)\eta_2$

Case 2: $(\lambda\mu_{1Y}\mu_{1Z}a_2/b_2 a_1)\eta_2 \le \eta_1 < (\lambda\mu_{1Y}\mu_{1Z}a_2 + b_1 a_2/a_1 b_2 + \lambda\mu_{1Y}\mu_{1Z}a_1)\eta_2$

Case 3: $(\lambda\mu_{1Y}\mu_{1Z}a_2 + b_1 a_2/a_1 b_2 + \lambda\mu_{1Y}\mu_{1Z}a_1)\eta_2 \le \eta_1 \le (b_1 a_2/\lambda\mu_{1Y}\mu_{1Z}a_1)\eta_2$

Case 4: $\eta_1 > (b_1 a_2/\lambda\mu_{1Y}\mu_{1Z}a_1)$

Next, the optimal time-consistent strategy $\pi^*(t) = (p_1^*(t), q_1^*(t), q_2^*(t))$ in admissible strategy set Π and the corresponding value function $V(t,x,l)$ are discussed. In order to have a clear classification discussion, it is assumed that $r-\gamma_1-\gamma_2+\beta \geq 0$.

Case 1: in this case, we have $\widehat{q}_1(t) < 0$ and $\widehat{q}_1(t) \geq 0$; thus, $q_1^*(t) = 0$. Let $h_1(p_1,q_2) = h(p_1,0,q_2)$. By substituting $q_1^*(t) = 0$ into (28) and maximizing function $h_1(p_1,q_2)$, we can get the maximum point:

$$\begin{aligned}\widehat{p}_1(t) &= \frac{\alpha}{\omega\sigma^2}e^{-(r-\gamma_1-\gamma_2+\beta)(T-t)},\\ \overline{q}_2(t) &= \frac{a_2\eta_2}{\omega b_2}e^{-(r-\gamma_1-\gamma_2+\beta)(T-t)}.\end{aligned} \tag{48}$$

Let $t_3 = T - (1/r-\gamma_1-\gamma_2+\beta)\ln(\eta_2 a_2/\omega b_2)$. For $0 \leq t \leq t_3$, it is easy to see $\widehat{q}_2(t) \leq 1$, and then we have $\pi^*(t) = (\widehat{p}_1(t), 0, \overline{q}_2(t))$. Putting $(\widehat{p}_1(t), 0, \overline{q}_2(t))$ into (41) and (45), we obtain

$$V(t,x,l) = Q_1(t,x,l) + Q_2(t) + R_1, \tag{49}$$

where

$$\begin{aligned}Q_1(t,x,l) &= e^{(r-\gamma_1-\gamma_2+\beta)(T-t)}(x+\beta l)\\ &\quad+\frac{c-a_1(1+\eta_1)-a_2(1+\eta_2)}{r-\gamma_1-\gamma_2+\beta}\\ &\quad\times\left(e^{(r-\gamma_1-\gamma_2+\beta)(T-t)}-1\right)+\frac{\alpha^2}{2\omega\sigma^2}(T-t),\end{aligned} \tag{50}$$

$$Q_2(t) = \frac{a_2^2\eta_2^2}{2\omega b_2}(T-t), \tag{51}$$

where R_1 is a constant whose value will be determined in a later calculation.

For $t_3 < t \leq T$, we have $\pi^*(t) = (\widehat{p}_1(t), 0, 1)$. Substituting it into (41) and (45), we can obtain

$$V(t,x,l) = Q_1(t,x,l) + Q_3(t) + Q_4(t), \tag{52}$$

where

$$Q_3(t) = \frac{a_2\eta_2}{r-\gamma_1-\gamma_2+\beta}\left(e^{(r-\gamma_1-\gamma_2+\beta)(T-t)}-1\right), \tag{53}$$

$$Q_4(t) = -\frac{\omega b_2}{4(r-\gamma_1-\gamma_2+\beta)}\left(e^{2(r-\gamma_1-\gamma_2+\beta)(T-t)}-1\right). \tag{54}$$

To make the value function $V(t,x,l)$ continuous, let $Q_2(t_3) + R_1 = Q_3(t_3) + Q_4(t_3)$; then,

$$R_1 = Q_3(t_3) + Q_4(t_3) - Q_2(t_3). \tag{55}$$

Case 2: in this case, we have $\widehat{q}_1(t) \geq 0$, $\widehat{q}_2(t) \geq 0$ and $D_1 \leq D_2$, and it is easy to see $t_2 \leq t_1$.

For $0 \leq t \leq t_2$, we have $\widehat{q}_1(t) \leq 1$, $\widehat{q}_2(t) \leq 1$, and thus $\pi^*(t) = (\widehat{p}_1(t), \widehat{q}_1(t), \widehat{q}_2(t))$. Substituting it into (41) and (45), we can derive

$$V(t,x,l) = Q_1(t,x,l) + Q_5(t) + R_2, \tag{56}$$

where

$$\begin{aligned}Q_5(t) &= \frac{1}{\omega}\left(a_1\eta_1 D_1 + a_2\eta_2 D_2 - \frac{1}{2}b_1 D_1^2 - \frac{1}{2}b_2 D_2^2\right.\\ &\quad\left.-\lambda\mu_{1Y}\mu_{1Z}D_1D_2\right)(T-t).\end{aligned} \tag{57}$$

For $t \geq t_2$, we have $\widehat{q}_2(t) \geq 1$, and thus $q_2^*(t) = 1$. Let $h_2(p_1,q_1) = h(p_1,q_1,1)$. Putting $q_2^*(t) = 1$ into (28) and maximizing function $h_2(p_1,q_2)$, we can get the maximum point:

$$\begin{aligned}\widehat{p}_1(t) &= \frac{\alpha}{\omega\sigma^2}e^{-(r-\gamma_1-\gamma_2+\beta)(T-t)},\\ \widetilde{q}_1(t) &= \frac{a_1\eta_1 e^{-(r-\gamma_1-\gamma_2+\beta)(T-t)}-\omega\lambda\mu_{1Y}\mu_{1Z}}{\omega b_1}.\end{aligned} \tag{58}$$

Let $t_4 = T - (1/r-\gamma_1-\gamma_2+\beta)\ln(a_1\eta_1/\omega\lambda\mu_{1Y}\mu_{1Y})$ and $t_5 = T - (1/r-\gamma_1-\gamma_2+\beta)\ln(a_1\eta_1/\omega(b_1+\lambda\mu_{1Y}\mu_{1Z}))$. It is easy to see that $t_4 \leq t_2 \leq t_5$.

For $t_2 < t \leq t_5$, we have $\pi^*(t) = (\widehat{p}_1(t), \widetilde{q}_1(t), 1)$. Inserting it into (41) and (45), we can obtain

$$V(t,x,l) = Q_1(t,x,l) + Q_3(t) + Q_6(t) + Q_7(t) + R_3, \tag{59}$$

where

$$Q_6(t) = \frac{a_1^2\eta_1^2}{2\omega b_1}(T-t) - \frac{\lambda a_1\eta_1\mu_{1Y}\mu_{1Z}}{b_1(r-\gamma_1-\gamma_2+\beta)}\left(e^{(r-\gamma_1-\gamma_2+\beta)(T-t)}-1\right), \tag{60}$$

$$\begin{aligned}Q_7(t) &= \left(\frac{\omega\lambda^2\mu_{1Y}^2\mu_{1Z}^2}{4b_1(r-\gamma_1-\gamma_2+\beta)} - \frac{\omega b_2}{4(r-\gamma_1-\gamma_2+\beta)}\right)\\ &\quad\cdot\left(e^{2(r-\gamma_1-\gamma_2+\beta)(T-t)}\right).\end{aligned} \tag{61}$$

For $t_5 < t \leq T$, we have $\widehat{q}_2(t) > 1$, and thus $\pi^*(t) = (\widehat{p}_1(t), 1, 1)$. Putting it into (41) and (45), we can arrive at

$$V(t,x,l)=Q_1(t,x,l)+Q_3(t)+Q_8(t)+Q_9(t), \quad (62)$$

where

$$Q_8(t)=\frac{a_1\eta_1}{r-\gamma_1-\gamma_2+\beta}\left(e^{(r-\gamma_1-\gamma_2+\beta)(T-t)}-1\right), \quad (63)$$

$$Q_9(t)=-\frac{\omega(b_1+b_2+2\lambda\mu_{1Y}\mu_{1Z})}{4(r-\gamma_1-\gamma_2+\beta)}\left(e^{2(r-\gamma_1-\gamma_2+\beta)(T-t)}-1\right). \quad (64)$$

Let

$$\begin{aligned}Q_5(t_2)+R_2&=Q_3(t_2)+Q_6(t_2)+Q_7(t_2)+R_3,\\ Q_3(t_5)+Q_6(t_5)+Q_7(t_5)+R_3&=Q_3(t_5)+Q_8(t_5)+Q_9(t_5),\end{aligned} \quad (65)$$

then

$$R_3=Q_3(t_5)+Q_8(t_5)+Q_9(t_5)-Q_3(t_5)-Q_6(t_5)-Q_7(t_5), \quad (66)$$

$$\begin{aligned}R_2&=Q_3(t_2)+Q_6(t_2)+Q_7(t_2)+Q_3(t_5)\\&\quad+Q_8(t_5)+Q_9(t_5)-Q_3(t_5)-Q_6(t_5)-Q_7(t_5)-Q_5(t_5).\end{aligned} \quad (67)$$

Case 3: in this case, we have $\hat{q}_1(t)\geq 0$, $\hat{q}_2(t)\geq 0$. And $D_1\geq D_2$, so $t_1\leq t_2$.

For $0\leq t\leq t_1$, we have $\pi^*(t)=(\hat{p}_1(t),\hat{q}_1(t),\hat{q}_2(t))$. Substituting it into (41) and (45), we can obtain

$$V(t,x,l)=Q_1(t,x,l)+Q_5(t)+R_4. \quad (68)$$

For $t\geq t_1$, we have $\hat{q}_1(t)\geq 1$, and thus $q_1^*(t)=1$. Denote by $h_3(p_1,q_2)$ the function $h(p_1,q_1,q_2)$ in (28). By maximizing $h_3(p_1,q_2)$, we derive

$$\begin{aligned}\hat{p}_1(t)&=\frac{\alpha}{\omega\sigma^2}e^{-(r-\gamma_1-\gamma_2+\beta)(T-t)},\\ \tilde{q}_2(t)&=\frac{a_2\eta_2e^{-(r-\gamma_1-\gamma_2+\beta)(T-t)}-\omega\lambda\mu_{1Y}\mu_{1Z}}{\omega b_2}.\end{aligned} \quad (69)$$

Let $t_6=T-(1/r-\gamma_1-\gamma_2+\beta)\ln(a_2\eta_2/\omega\lambda\mu_{1Y}\mu_{1Z})$ and $t_7=T-(1/r-\gamma_1-\gamma_2+\beta)\ln(a_2\eta_2/\omega(b_2+\omega\lambda\mu_{1Y}\mu_{1Z}))$. It is easy to see that $t_6\leq t_1\leq t_7$.

For $t_1<t\leq t_7$, we have $\pi^*(t)=(\hat{p}_1(t),1,\tilde{q}_2(t))$. By substituting it into (41) and (45), we can obtain

$$V(t,x,l)=Q_1(t,x,l)+Q_8(t)+Q_{10}(t)+Q_{11}(t)+R_5, \quad (70)$$

where

$$\begin{aligned}Q_{10}(t)&=\frac{a_2^2\eta_2^2}{2\omega b_2}(T-t)-\frac{\lambda a_2\eta_2\mu_{1Y}\mu_{1Z}}{b_2(r-\gamma_1-\gamma_2+\beta)}\\&\quad\cdot\left(e^{(r-\gamma_1-\gamma_2+\beta)(T-t)}-1\right),\end{aligned} \quad (71)$$

$$\begin{aligned}Q_{11}(t)&=\left(\frac{\omega\lambda^2\mu_{1Y}^2\mu_{1Z}^2}{4b_2(r-\gamma_1-\gamma_2+\beta)}-\frac{\omega b_1}{4(r-\gamma_1-\gamma_2+\beta)}\right)\\&\quad\cdot\left(e^{2(r-\gamma_1-\gamma_2+\beta)(T-t)}\right).\end{aligned} \quad (72)$$

For $t_7<t\leq T$, we have $\pi^*(t)=(\hat{p}_1(t),1,1)$. Putting it into (41) and (45), we can obtain

$$V(t,x,l)=Q_1(t,x,l)+Q_3(t)+Q_8(t)+Q_9(t). \quad (73)$$

Let

$$\begin{aligned}Q_5(t_1)+R_4&=Q_8(t_1)+Q_{10}(t_1)+Q_{11}(t_1)+R_5,\\ Q_8(t_7)+Q_{10}(t_7)+Q_{11}(t_7)+R_5&=Q_3(t_7)+Q_8(t_7)+Q_9(t_7).\end{aligned} \quad (74)$$

We derive

$$R_5=Q_3(t_7)+Q_8(t_7)+Q_9(t_7)-Q_8(t_7)-Q_{10}(t_7)-Q_{11}(t_7), \quad (75)$$

$$\begin{aligned}R_4&=Q_8(t_1)+Q_{10}(t_1)+Q_{11}(t_1)+Q_3(t_7)+Q_8(t_7)\\&\quad+Q_9(t_7)-Q_8(t_7)-Q_{10}(t_7)-Q_{11}(t_7)-Q_5(t_1).\end{aligned} \quad (76)$$

Case 4: in this case, we have $\hat{q}_1(t)\geq 0$ and $\hat{q}_2(t)<0$, and thus $q_2^*(t)=0$. Let $h_4(p_1,q_1)=h(p_1,q_1,q_2)$. By maximizing $h_4(p_1,q_2)$, we arrive at

$$\begin{aligned}\hat{p}_1(t)&=\frac{\alpha}{\omega\sigma^2}e^{-(r-\gamma_1-\gamma_2+\beta)(T-t)},\\ \bar{q}_1(t)&=\frac{a_2\eta_2}{\omega b_2}e^{-(r-\gamma_1-\gamma_2+\beta)(T-t)}.\end{aligned} \quad (77)$$

Let $t_8=T-(1/r-\gamma_1-\gamma_2+\beta)\ln(a_1\eta_1/\omega b_1)$.

For $0 \le t \le t_8$, we have $\pi^*(t) = (\widehat{p}_1(t), \overline{q}_1(t), 0)$. Inserting it into (41) and (45), we can derive

$$V(t,x,l) = Q_1(t,x,l) + Q_{12}(t) + R_6, \tag{78}$$

where

$$Q_{12}(t) = \frac{a_1^2\eta_1^2}{2\omega b_1}(T-t). \tag{79}$$

For $t_8 < t \le T$, we have $\pi^*(t) = (\widehat{p}_1(t), 1, 0)$. Putting it into (41) and (45), we can obtain

$$V(t,x,l) = Q_1(t,x,l) + Q_8(t) + Q_{13}(t), \tag{80}$$

where

$$Q_{13}(t) = -\frac{\omega b_1}{4(r-\gamma_1-\gamma_2+\beta)}\left(e^{2(r-\gamma_1-\gamma_2+\beta)(T-t)} - 1\right). \tag{81}$$

Let

$$Q_{12}(t) + R_6 = Q_8(t) + Q_{13}(t). \tag{82}$$

We have

$$R_6 = Q_8(t) + Q_{13}(t) - Q_{12}(t). \tag{83}$$

From the above discussion, we can get the following theorem.

Theorem 2. *Assuming $r-\gamma_1-\gamma_2+\beta \ge 0$, the optimal time-consistent investment and reinsurance strategies for problem (14) are as follows:*

(i) If Case 1 holds, the optimal investment-reinsurance strategies for model (14) are

$$\left(p_1^*(t), q_1^*(t), q_2^*(t)\right) = \begin{cases} \left(\dfrac{\alpha}{\omega\sigma^2}e^{-(r-\gamma_1-\gamma_2+\beta)(T-t)}, 0, \dfrac{a_2\eta_2}{\omega b_2}e^{-(r-\gamma_1-\gamma_2+\beta)(T-t)}\right), & 0 \le t \le t_3, \\ \left(\dfrac{\alpha}{\omega\sigma^2}e^{-(r-\gamma_1-\gamma_2+\beta)(T-t)}, 0, 1\right), & t_3 < t \le T, \end{cases} \tag{84}$$

and the value function is given by

$$V(t,x,l) = \begin{cases} Q_1(t,x,l) + Q_2(t) + R_1, & 0 \le t \le t_3, \\ Q_1(t,x,l) + Q_3(t) + Q_4(t), & t_3 < t \le T, \end{cases} \tag{85}$$

where $Q_1(t,x,l)$, $Q_2(t)$, $Q_3(t)$, $Q_4(t)$, and R_1 are given by (50)–(55), respectively.

(ii) If Case 2 holds, the optimal investment-reinsurance strategies for model (14) are

$$\left(p_1^*(t), q_1^*(t), q_2^*(t)\right) = \begin{cases} \left(\dfrac{\alpha}{\sigma^2\omega}e^{-(r-\gamma_1-\gamma_2+\beta)(T-t)}, \dfrac{a_1\eta_1 b_2 - a_2\eta_2\lambda\mu_{1Y}\mu_{1Z}}{\left(b_1b_2 - \lambda^2\mu_{1Y}^2\mu_{1Z}^2\right)\omega}e^{-(r-\gamma_1-\gamma_2+\beta)(T-t)}, \right. \\ \left. \cdot\dfrac{a_2\eta_2 b_1 - a_1\eta_1\lambda\mu_{1Y}\mu_{1Z}}{\left(b_1b_2 - \lambda^2\mu_{1Y}^2\mu_{1Z}^2\right)\omega}e^{-(r-\gamma_1-\gamma_2+\beta)(T-t)}, \quad 0 \le t \le t_2, \right) \\ \left(\dfrac{\alpha}{\sigma^2\omega}e^{-(r-\gamma_1-\gamma_2+\beta)(T-t)}, \dfrac{a_1\eta_1 e^{-(r-\gamma_1-\gamma_2+\beta)(T-t)} - \omega\lambda\mu_{1Y}\mu_{1Z}}{\omega b_1}, 1\right), & t_2 < t \le t_5, \\ \left(\dfrac{\alpha}{\sigma^2\omega}e^{-(r-\gamma_1-\gamma_2+\beta)(T-t)}, 1, 1\right), & t_5 < t \le T, \end{cases} \tag{86}$$

and the value function is given by

$$V(t,x,l)=\begin{cases}Q_1(t,x,l)+Q_5(t)+R_2, & 0\le t\le t_2,\\ Q_1(t,x,l)+Q_3(t)+Q_6(t)+Q_7(t)+R_3, & t_2<t\le t_5,\\ Q_1(t,x,l)+Q_3(t)+Q_8(t)+Q_9(t), & t_5<t\le T,\end{cases}\tag{87}$$

where $Q_5(t)$, $Q_6(t)$, $Q_7(t)$, $Q_8(t)$, $Q_9(t)$, R_3, and R_2 are given by (57)–(67), respectively.

(iii) *If Case 3 holds, the optimal investment-reinsurance strategies for model (14) are*

$$\left(p_1^*(t),q_1^*(t),q_2^*(t)\right)=\begin{cases}\left(\dfrac{\alpha}{\sigma^2\omega}e^{-(r-\gamma_1-\gamma_2+\beta)(T-t)},\dfrac{a_1\eta_1b_2-a_2\eta_2\lambda\mu_{1Y}\mu_{1Z}}{\left(b_1b_2-\lambda^2\mu_{1Y}^2\mu_{1Z}^2\right)\omega}e^{-(r-\gamma_1-\gamma_2+\beta)(T-t)},\right.\\ \left.\cdot\dfrac{a_2\eta_2b_1-a_1\eta_1\lambda\mu_{1Y}\mu_{1Z}}{\left(b_1b_2-\lambda^2\mu_{1Y}^2\mu_{1Z}^2\right)\omega}e^{-(r-\gamma_1-\gamma_2+\beta)(T-t)}, \quad 0\le t\le t_1,\right)\\ \left(\dfrac{\alpha}{\sigma^2\omega}e^{-(r-\gamma_1-\gamma_2+\beta)(T-t)},1,\dfrac{a_2\eta_2e^{-(r-\gamma_1-\gamma_2+\beta)(T-t)}-\omega\lambda\mu_{1Y}\mu_{1Z}}{\omega b_2}\right), & t_1<t\le t_7,\\ \left(\dfrac{\alpha}{\sigma^2\omega}e^{-(r-\gamma_1-\gamma_2+\beta)(T-t)},1,1\right), & t_7<t\le T,\end{cases}\tag{88}$$

and the value function is given by

$$V(t,x,l)=\begin{cases}Q_1(t,x,l)+Q_5(t)+R_4, & 0\le t\le t_1,\\ Q_1(t,x,l)+Q_8(t)+Q_{10}(t)+Q_{11}(t)+R_5, & t_1<t\le t_7,\\ t_7<t\le T,\end{cases}\tag{89}$$

where $Q_{10}(t)$, $Q_{11}(t)$, R_5, and R_4 are given by (71)–(76), respectively.

(iv) *If Case 4 holds, the optimal investment-reinsurance strategies for model (14) are*

$$\left(p_1^*(t),q_1^*(t),q_2^*(t)\right)=\begin{cases}\left(\dfrac{\alpha}{\sigma^2\omega}e^{-(r-\gamma_1-\gamma_2+\beta)(T-t)},\dfrac{a_2\eta_2}{\omega b_2}e^{-(r-\gamma_1-\gamma_2+\beta)(T-t)},0\right), & 0\le t\le t_8,\\ \left(\dfrac{\alpha}{\sigma^2\omega}e^{-(r-\gamma_1-\gamma_2+\beta)(T-t)},1,0\right), & t_8<t\le T,\end{cases}\tag{90}$$

and the value function is given by

$$\begin{cases}Q_1(t,x,l)+Q_{12}(t)+R_6, & 0\le t\le t_8,\\ Q_1(t,x,l)+Q_8(t)+Q_{13}(t), & t_8<t\le T,\end{cases}\tag{91}$$

where $Q_{12}(t)$, $Q_{13}(t)$, and R_6 are given by (79)–(83), respectively.

Remark 2. (i) Since

$$\begin{cases}Q_2(t_3)+R_1=Q_3(t_3)+Q_4(t_3),\\ Q_5(t_2)+R_2=Q_3(t_2)+Q_6(t_2)+Q_7(t_2)+R_3,\\ Q_3(t_5)+Q_6(t_5)+Q_7(t_5)+R_3=Q_3(t_5)+Q_8(t_5)+Q_9(t_5),\\ Q_5(t_1)+R_4=Q_8(t_1)+Q_{10}(t_1)+Q_{11}(t_1)+R_5,\\ Q_8(t_7)+Q_{10}(t_7)+Q_{11}(t_7)+R_5=Q_3(t_7)+Q_8(t_7)+Q_9(t_7),\\ Q_{12}(t)+R_6=Q_8(t)+Q_{13}(t),\end{cases}\tag{92}$$

$V(t,x,l)$ is a continuous function for any $(t,x,l)\in[0,T]\times\mathbb{R}\times\mathbb{R}$. Furthermore,

$$\begin{cases} Q_2'(t_3) = Q_3'(t_3) + Q_4'(t_3), \\ Q_5'(t_2) = Q_3'(t_2) + Q_6'(t_2) + Q_7'(t_2), \\ Q_3'(t_5) + Q_6'(t_5) + Q_7'(t_5) = Q_3'(t_5) + Q_8'(t_5) + Q_9'(t_5), \\ Q_5'(t_1) = Q_8'(t_1) + Q_{10}'(t_1) + Q_{11}'(t_1), \\ Q_8'(t_7) + Q_{10}'(t_7) + Q_{11}'(t_7) = Q_3'(t_7) + Q_8'(t_7) + Q_9'(t_7), \\ Q_{12}'(t) = Q_8'(t) + Q_{13}'(t), \end{cases} \tag{93}$$

which includes that $V(t,x,l)$ is a classical solution to the extended HJB (18).

(ii) According to Theorem 2, the investment and reinsurance strategy of the insurer is not directly affected by the average parameter A and the delay time h, but according to (13), the average parameter A and the delay time h have an indirect influence on the investment and reinsurance strategy of insurance companies.

(iii) Note that, in the classification discussion of Theorem 2, in order to make the classification clear, we assume that $r - \gamma_1 - \gamma_2 + \beta \geq 0$. For $r - \gamma_1 - \gamma_2 + \beta < 0$, we can also make a similar discussion.

When $A = h = \beta = \gamma_1 = \gamma_2 = 0$, problem (14) degenerates to the case without time delay.

Corollary 1. *Without time delay, the optimal time-consistent investment and reinsurance policies of problem (14) are as follows:*

(i) If Case 1 holds, the optimal investment-reinsurance strategies for problem (14) are

$$\left(p_1^*(t), q_1^*(t), q_2^*(t)\right) = \begin{cases} \left(\dfrac{\alpha}{\omega\sigma^2} e^{-r(T-t)}, 0, \dfrac{a_2\eta_2}{\omega b_2} e^{-r(T-t)}\right), & 0 \leq t \leq t_3, \\ \left(\dfrac{\alpha}{\omega\sigma^2} e^{-r(T-t)}, 0, 1\right), & t_3 < t \leq T, \end{cases} \tag{94}$$

and the value function is given by

$$V(t,x,l) = \begin{cases} \widetilde{Q}_1(t,x,l) + \widetilde{Q}_2(t) + R_1, & 0 \leq t \leq t_3, \\ \widetilde{Q}_1(t,x,l) + \widetilde{Q}_3(t) + \widetilde{Q}_4(t), & t_3 < t \leq T, \end{cases} \tag{95}$$

where

$$\begin{cases} \widetilde{Q}_1(t,x,l) = e^{r(T-t)}(x + \beta l) + \dfrac{c - a_1(1+\eta_1) - a_2(1+\eta_2)}{r}\left(e^{r(T-t)} - 1\right) + \dfrac{\alpha^2}{2\omega\sigma^2}(T-t), \\ \widetilde{Q}_2(t) = \dfrac{a_2^2\eta_2^2}{2\omega b_2}(T-t), \\ \widetilde{Q}_3(t) = \dfrac{a_2\eta_2}{r}\left(e^{r(T-t)} - 1\right), \\ \widetilde{Q}_4(t) = -\dfrac{\omega b_2}{4r}\left(e^{2r(T-t)} - 1\right), \\ \widetilde{R}_1 = \widetilde{Q}_3(t_3) + \widetilde{Q}_4(t_3) - \widetilde{Q}_2(t_3). \end{cases} \tag{96}$$

(ii) If Case 2 holds, the optimal investment-reinsurance strategies for problem (14) are

$$\left(p_1^*(t), q_1^*(t), q_2^*(t)\right) = \begin{cases} \left(\dfrac{\alpha}{\sigma^2\omega}e^{-r(T-t)}, \dfrac{a_1\eta_1 b_2 - a_2\eta_2\lambda\mu_{1Y}\mu_{1Z}}{\left(b_1 b_2 - \lambda^2\mu_{1Y}^2\mu_{1Z}^2\right)\omega}e^{-r(T-t)}, \dfrac{a_2\eta_2 b_1 - a_1\eta_1\lambda\mu_{1Y}\mu_{1Z}}{\left(b_1 b_2 - \lambda^2\mu_{1Y}^2\mu_{1Z}^2\right)\omega}e^{-r(T-t)}\right), & 0 \le t \le t_2, \\ \left(\dfrac{\alpha}{\sigma^2\omega}e^{-r(T-t)}, \dfrac{a_1\eta_1 e^{-r(T-t)} - \omega\lambda\mu_{1Y}\mu_{1Z}}{\omega b_1}, 1\right), & t_2 < t \le t_5, \\ \left(\dfrac{\alpha}{\sigma^2\omega}e^{-r(T-t)}, 1, 1\right), & t_5 < t \le T, \end{cases} \tag{97}$$

and the value function is given by

$$V(t,x,l) = \begin{cases} \widetilde{Q}_1(t,x,l) + \widetilde{Q}_5(t) + R_2, & 0 \le t \le t_2, \\ \widetilde{Q}_1(t,x,l) + \widetilde{Q}_3(t) + \widetilde{Q}_6(t) + \widetilde{Q}_7(t) + R_3, & t_2 < t \le t_5, \\ \widetilde{Q}_1(t,x,l) + \widetilde{Q}_3(t) + \widetilde{Q}_8(t) + \widetilde{Q}_9(t), & t_5 < t \le T, \end{cases} \tag{98}$$

where

$$\begin{cases} \widetilde{Q}_5(t) = \dfrac{1}{\omega}\left(a_1\eta_1 D_1 + a_2\eta_2 D_2 - \dfrac{1}{2}b_1 D_1^2 - \dfrac{1}{2}b_2 D_2^2 - \lambda\mu_{1Y}\mu_{1Z}D_1 D_2\right)(T-t), \\ \widetilde{Q}_6(t) = \dfrac{a_1^2\eta_1^2}{2\omega b_1}(T-t) - \dfrac{\lambda a_1\eta_1\mu_{1Y}\mu_{1Z}}{b_1 r}\left(e^{r(T-t)} - 1\right), \\ \widetilde{Q}_7(t) = \left(\dfrac{\omega\lambda^2\mu_{1Y}^2\mu_{1Z}^2}{4b_1 r} - \dfrac{\omega b_2}{4r}\right)\left(e^{2r(T-t)}\right), \\ \widetilde{Q}_8(t) = \dfrac{a_1\eta_1}{r}\left(e^{r(T-t)} - 1\right), \\ \widetilde{Q}_9(t) = -\dfrac{\omega\left(b_1 + b_2 + 2\lambda\mu_{1Y}\mu_{1Z}\right)}{4r}\left(e^{2r(T-t)} - 1\right), \\ \widetilde{R}_3 = \widetilde{Q}_3(t_5) + \widetilde{Q}_8(t_5) + \widetilde{Q}_9(t_5) - \widetilde{Q}_3(t_5) - \widetilde{Q}_6(t_5) - \widetilde{Q}_7(t_5), \\ \widetilde{R}_2 = \widetilde{Q}_3(t_2) + \widetilde{Q}_6(t_2) + \widetilde{Q}_7(t_2) + \widetilde{Q}_3(t_5) + \widetilde{Q}_8(t_5) + \widetilde{Q}_9(t_5) - \widetilde{Q}_3(t_5) - \widetilde{Q}_6(t_5) - \widetilde{Q}_7(t_5) - \widetilde{Q}_5(t_2). \end{cases} \tag{99}$$

(iii) *If Case 3 holds, the optimal investment-reinsurance strategies for problem (14) are*

$$\left(p_1^*(t), q_1^*(t), q_2^*(t)\right) = \begin{cases} \left(\dfrac{\alpha}{\sigma^2\omega}e^{-r(T-t)}, \dfrac{a_1\eta_1 b_2 - a_2\eta_2\lambda\mu_{1Y}\mu_{1Z}}{\left(b_1b_2 - \lambda^2\mu_{1Y}^2\mu_{1Z}^2\right)\omega}e^{-r(T-t)}, \dfrac{a_2\eta_2 b_1 - a_1\eta_1\lambda\mu_{1Y}\mu_{1Z}}{\left(b_1b_2 - \lambda^2\mu_{1Y}^2\mu_{1Z}^2\right)\omega}e^{-r(T-t)}\right), & 0 \le t \le t_1, \\ \left(\dfrac{\alpha}{\sigma^2\omega}e^{-r(T-t)}, 1, \dfrac{a_2\eta_2 e^{-r(T-t)} - \omega\lambda\mu_{1Y}\mu_{1Z}}{\omega b_2}\right), & t_1 < t \le t_7, \\ \left(\dfrac{\alpha}{\sigma^2\omega}e^{-r(T-t)}, 1, 1\right), & t_7 < t \le T, \end{cases} \tag{100}$$

and the value function is given by

$$V(t,x,l) = \begin{cases} \widetilde{Q}_1(t,x,l) + \widetilde{Q}_5(t) + R_4, & 0 \le t \le t_1, \\ \widetilde{Q}_1(t,x,l) + \widetilde{Q}_8(t) + \widetilde{Q}_{10}(t) + \widetilde{Q}_{11}(t) + R_5, & t_1 < t \le t_7, \\ t_7 < t \le T, \end{cases} \tag{101}$$

where

$$\begin{cases} \widetilde{Q}_{10}(t) = \dfrac{a_2^2\eta_2^2}{2\omega b_2}(T-t) - \dfrac{\lambda a_2\eta_2\mu_{1Y}\mu_{1Z}}{b_2 r}\left(e^{r(T-t)} - 1\right), \\ \widetilde{Q}_{11}(t) = \left(\dfrac{\omega\lambda^2\mu_{1Y}^2\mu_{1Z}^2}{4b_2 r} - \dfrac{\omega b_1}{4r}\right)\left(e^{2r(T-t)}\right), \\ \widetilde{R}_5 = \widetilde{Q}_3(t_7) + \widetilde{Q}_8(t_7) + \widetilde{Q}_9(t_7) - \widetilde{Q}_8(t_7) - \widetilde{Q}_{10}(t_7) - \widetilde{Q}_{11}(t_7), \\ \widetilde{R}_4 = \widetilde{Q}_8(t_1) + \widetilde{Q}_{10}(t_1) + \widetilde{Q}_{11}(t_1) + \widetilde{Q}_3(t_7) + \widetilde{Q}_8(t_7) + \widetilde{Q}_9(t_7) - \widetilde{Q}_8(t_7) - \widetilde{Q}_{10}(t_7) - \widetilde{Q}_{11}(t_7) - \widetilde{Q}_5(t_1). \end{cases} \tag{102}$$

(iv) *If Case 4 holds, the optimal investment-reinsurance strategies for problem (14) are*

$$\left(p_1^*(t), q_1^*(t), q_2^*(t)\right) = \begin{cases} \left(\dfrac{\alpha}{\sigma^2\omega}e^{-r(T-t)}, \dfrac{a_2\eta_2}{\omega b_2}e^{-r(T-t)}, 0\right), & 0 \le t \le t_8, \\ \left(\dfrac{\alpha}{\sigma^2\omega}e^{-r(T-t)}, 1, 0\right), & t_8 < t \le T, \end{cases} \tag{103}$$

and the value function is given by

$$\begin{cases} \widetilde{Q}_1(t,x,l) + \widetilde{Q}_{12}(t) + R_6, & 0 \le t \le t_8, \\ \widetilde{Q}_1(t,x,l) + \widetilde{Q}_8(t) + \widetilde{Q}_{13}(t), & t_8 < t \le T, \end{cases} \tag{104}$$

where

$$\begin{cases} \widetilde{Q}_{12}(t) = \dfrac{a_1^2\eta_1^2}{2\omega b_1}(T-t), \\ \widetilde{Q}_{13}(t) = -\dfrac{\omega b_1}{4r}\left(e^{2r(T-t)} - 1\right), \\ \widetilde{R}_6 = \widetilde{Q}_8(t) + \widetilde{Q}_{13}(t) - \widetilde{Q}_{12}(t). \end{cases} \tag{105}$$

5. Numerical Simulations

In this section, Example 1 will be used to illustrate the specific numerical calculation process of finding the optimal

Table 1: Optimal time-consistent strategy in $\widehat{\Pi}$.

t	0	1	2	3	4	5	6	7	8
$\widehat{p}_1$	3.8978	4.6503	5.5481	6.6192	7.8971	9.4218	11.2407	13.4109	16.0000
$\widehat{q}_1$	0.4213	0.5026	0.5997	0.7155	0.8536	1.0184	1.2150	1.4496	1.7294
$\widehat{q}_2$	0.6019	0.7181	0.8567	1.0221	1.2194	1.4548	1.7357	2.0708	2.4706

Table 2: Optimal time-consistent strategy in Π.

t	0	1	2	3	4	5	6	7	8
p_1^*	1.9205	2.5032	3.2628	4.2528	5.5433	7.2253	9.4177	12.2753	16.0000
q_1^*	0.4213	0.5026	0.5997	0.4458	0.5577	0.6911	0.8502	1.0000	1.0000
q_2^*	0.6019	0.7181	0.8567	1.0000	1.0000	1.0000	1.0000	1.0000	1.0000

time-consistent strategy, and Example 2 will be used to analyze the influence of important parameters on the optimal time-consistent strategy. Assuming that the claim amount Y_i and Z_i are exponentially distributed with parameters ξ_1 and ξ_2, respectively, then $\mu_{1Y} = 1/\xi_1$, $\mu_{1Z} = 1/\xi_2$, $b_1 = 2(\lambda + \lambda_1)/\xi_1^2$, and $b_2 = 2(\lambda + \lambda_2)/\xi_2^2$.

Example 1. Let $\eta_1 = \eta_2 = 0.7$, $\xi_1 = 2$, $\xi_2 = 3$, $\lambda = 2$, $\lambda_1 = 3$, $\lambda_2 = 5$, $\alpha_1 = 0.5$, $\sigma = 0.2$, $T = 8$, $r = 0.18$, $\beta = 0.1$, $A = 0.15$, and $h = 0.2$ and according to Remark 1, we can calculate $\gamma_1 = 0.0064$ and $\gamma_2 = 0.0970$, and thus $r - \gamma_1 - \gamma_2 + \beta = 0.1765 > 0$. According to the above model parameters, Table 1 can be calculated.

From Table 1, for $t \geq 5$, we have $\widehat{q}_2(t) > 1$. According to the analysis of Theorem 2, it is easy to see that $t_2 = T - (1/r - \gamma_1 - \gamma_2 + \beta)\ln(D_2/\omega) = 2.8762$ and $t_5 = T - (1/r - \gamma_1 - \gamma_2 + \beta)\ln(a_1\eta_1/\ \omega(b_1 + \lambda\mu_{1Y}\mu_{1Z})) = 6.8029$, $t_2 < t \leq t_5$, and hence $q_1^*(t) = a_1\eta_1 e^{-(r-\gamma_1-\gamma_2+\beta)(T-t)} - \omega\lambda\mu_{1Y}\mu_{1Z}/\omega b_1$. For $t_5 < t \leq T$, we have $q_1^*(t) = 1$. So, recalculate Table 1 to obtain Table 2.

Example 2. If there is no special description in this example, the basic parameter values are as follows: $\eta_1 = \eta_2 = 0.7$, $\xi_1 = 2$, $\xi_2 = 3$, $\lambda = 3$, $\lambda_1 = 2$, $\lambda_2 = 4$, $\alpha_1 = 0.5$, $\sigma = 0.2$, $r = 0.18$, $A = 0.1$, $\beta = 0.1$, $h = 0.2$, and $\omega = 0.5$.

Figures 1 and 2 depict the influence of risk aversion parameter ω and delay parameter β on the optimal time-consistent investment strategy. From Figure 1, we can see that the optimal time-consistent investment strategy $p_1(t)$ decreases with the increase of risk aversion parameter ω, that is to say, the higher the risk aversion degree of the insurer is, the less the amount of risk investment will be. Because parameter β includes the information of average parameter A and delay h, it is a comprehensive time-delay parameter, so we only analyze β. Figure 2 shows that the larger the delay parameter β is, the larger the number of investment in risky assets will be. Note that if $\beta = 0$, then the insurer decision-making is only based on the current information, so it may take short-term risk-taking behavior for the immediate possible high return. For $\beta > 0$, when the insurer is making decision, the comprehensive performance in the past period will be taken into account. Insurer focuses on information in a period when making decisions. According to (12), the greater the value of β, the greater the proportion of average

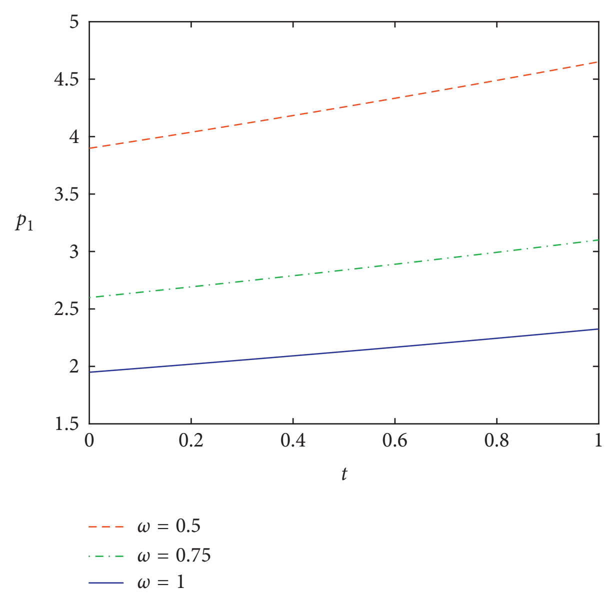

Figure 1: The effect of risk aversion parameter ω on p_1.

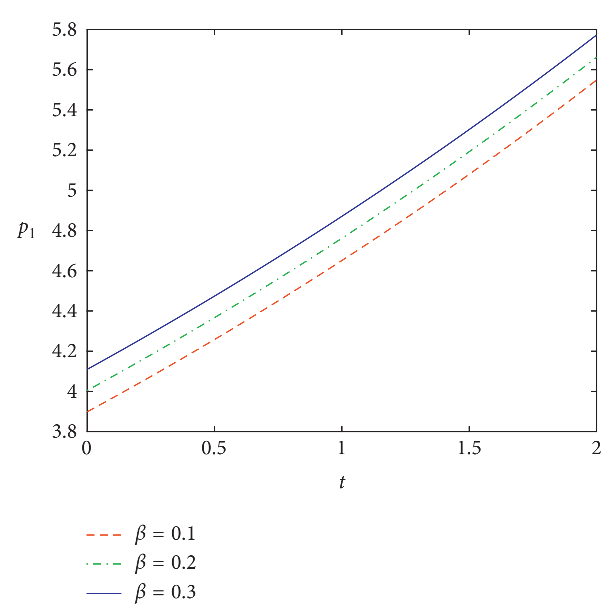

Figure 2: The effect of delay parameter β on p_1.

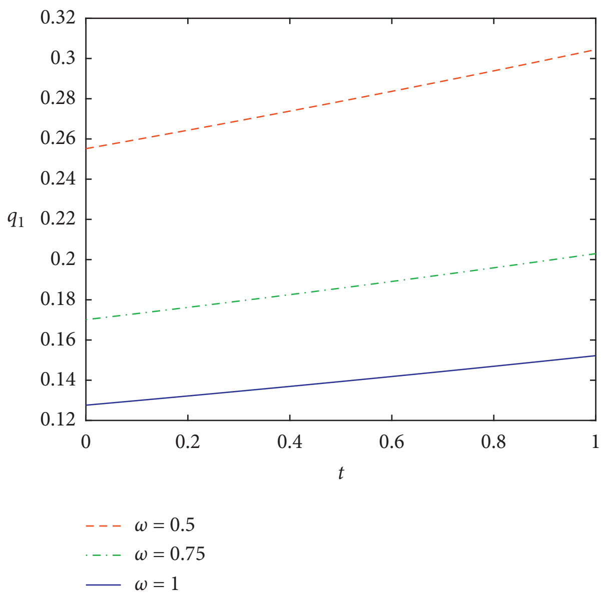

Figure 3: The effect of risk aversion parameter ω on q_1.

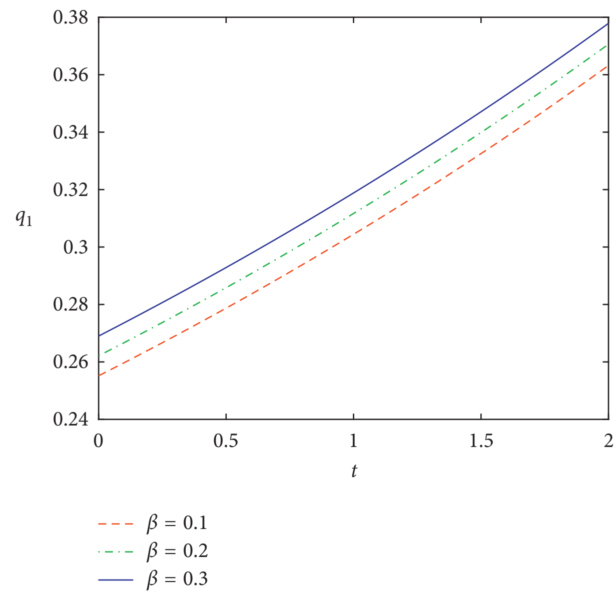

Figure 5: The effect of delay parameter β on q_1.

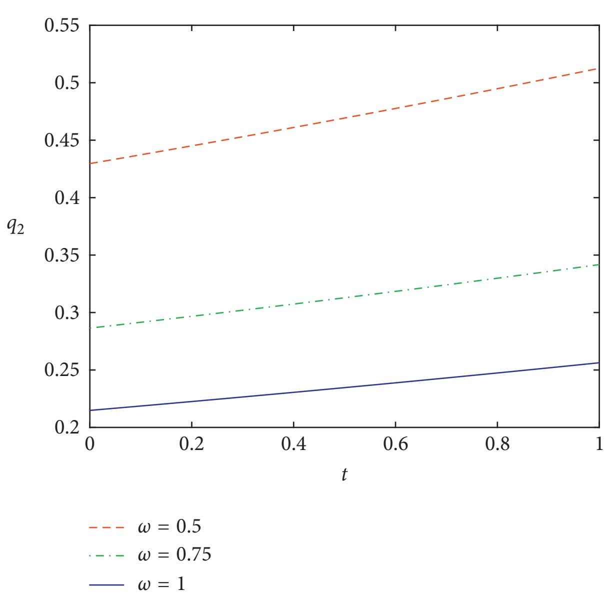

Figure 4: The effect of risk aversion parameter ω on q_2.

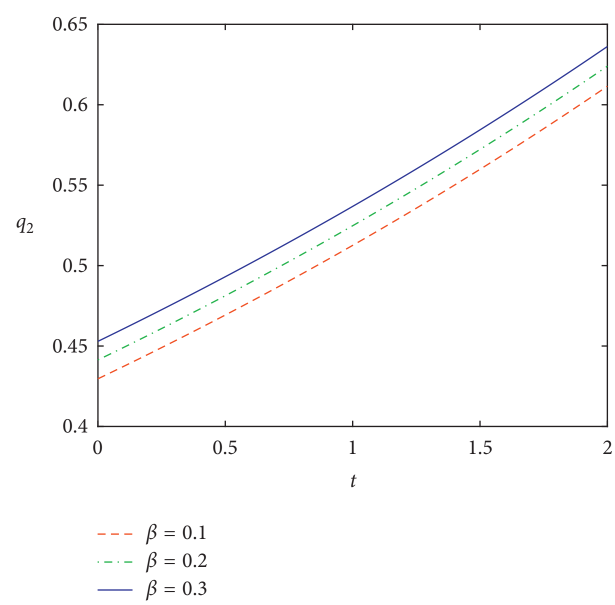

Figure 6: The effect of delay parameter β on q_2.

wealth in performance measurement. That is, the insurer can change the inflow/outflow of the insurer's capital by adjusting the size of the parameter beta, thus changing the risk faced by the insurer. The bigger the beta, the smaller the risk, so the insurer will consider increasing the number of risky assets.

Figures 3–6 depict the influence of risk aversion coefficient ω and delay parameter β on two types of insurance reinsurance. According to Figures 3 and 4, $q_1(t)$ and $q_2(t)$ decrease with respect to ω. The higher the risk aversion degree of the insurer, the more reinsurance he will buy to reduce his risk, so the retention ratio of $q_1(t)$ and $q_2(t)$ will be reduced. Figures 5 and 6 show that the retention ratio $q_1(t)$ $(q_1(t))$ increase with respect to the parameter β. As the impact of β on investment strategy p_1. The larger the β, the stronger the insurer's ability to adjust capital inflow/outflow, that is, the stronger the insurer's risk control ability. To a certain extent, the profitability of the insurer will be stronger, so the insurer will reduce the purchase of reinsurance, and the proportion of reinsurance retention $q_1(t)$ $(q_1(t))$ will increase. This is consistent with economic reality, which the more information investors observe, the more profit they will make.

Figures 7–9 depict the effect of the claim intensity λ_1, λ_2, and λ on reinsurance. In Figure 7, the larger the λ_1 is, the larger the $q_1(t)$ is and the smaller the $q_2(t)$ is. Because the

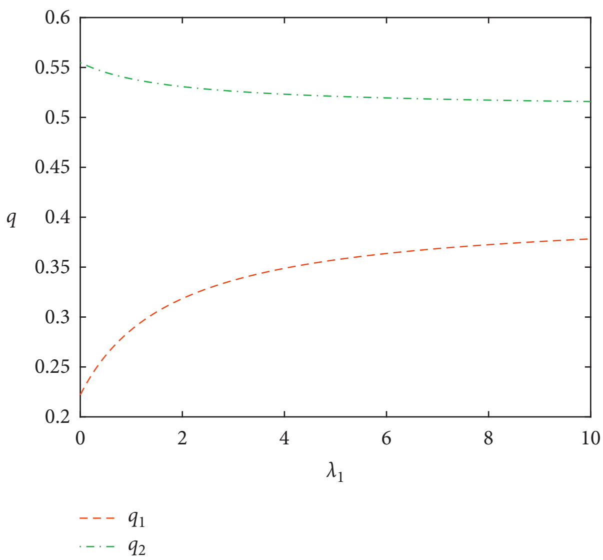

FIGURE 7: The effect of λ_1 on q.

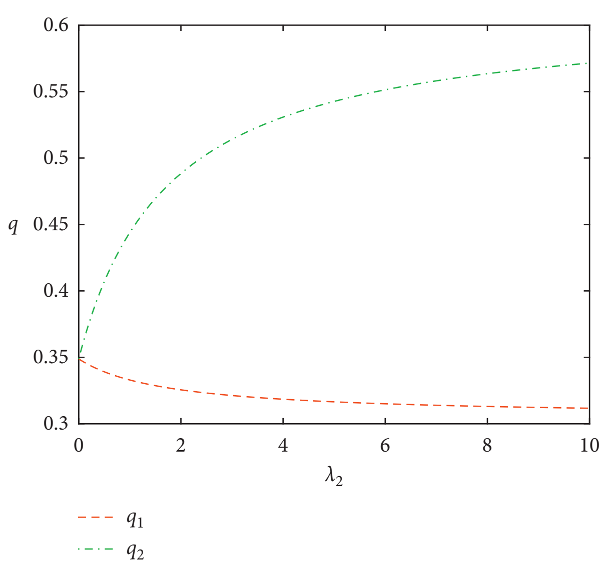

FIGURE 8: The effect of λ_2 on q.

larger the λ_1 is, the greater the expected claim amount of the first type of insurance business will be, so the insurer will purchase more reinsurance for the first type of insurance business and reduce the proportion of retained insurance $q_1(t)$. At this time, λ_2 will remain unchanged, that is, the expected claim amount of the second type of insurance business will remain unchanged. Based on the consideration of constant total risk and more profits, the insurer will increase the retention ratio $q_2(t)$ of reinsurance. A similar analysis can explain why; with the increase of λ_2, $q_1(t)$ decreases and $q_2(t)$ increases in Figures 8 and 9 which shows that the retention ratios $q_1(t)$ and $q_2(t)$ of the two types of insurance businesses decrease with the increase of lambda. Because the larger the lambda is, the greater the expected claim amount of the two types of insurance businesses will be. Therefore, in order to control the risk within a certain

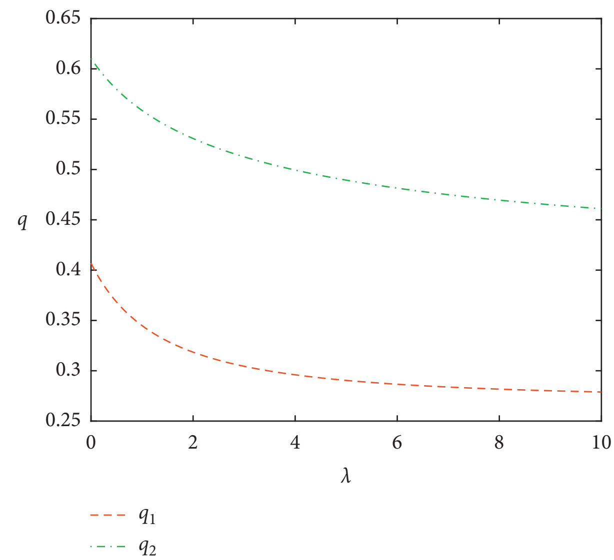

FIGURE 9: The effect of λ on q.

range, the insurer will buy more reinsurance for the two types of insurance businesses and reduce the retention ratio $q_1(t)$ and $q_2(t)$.

6. Conclusion

In this paper, we study the optimal investment-reinsurance problem with delay and risk dependence under the mean-variance preference criterion. Considering the time-delay effect and risk dependence, we obtain the extended HJB equation with delay based on the time delay stochastic control framework and the equilibrium stochastic control method. The results show that the optimal time-consistent investment and reinsurance strategy will be affected by the time delay effect. The larger the capital flow related to the historical business performance, the greater the risk faced by the insurance company. In a prudent attitude, the insurer will reduce the amount invested in a risk asset and reduce the reinsurance retention ratio of all insurance businesses. In addition, risk dependence is linked by common risk shock sources. The greater the risk common shock intensity is, the smaller the reinsurance retention ratio will be. From the numerical analysis results, we can see not only the numerical calculation process of the optimal strategy but also the intuitive verification of the above conclusions.

In this paper, we study the risk assets under geometric Brownian motion. To better simulate the real financial market, the following research will consider the introduction of CEV, Heston, and other stochastic volatility models, Vasicek, CIR, and other stochastic interest rate models.

Data Availability

The data in this paper can be used publicly.

Conflicts of Interest

The authors declare that they have no conflicts of interest.

Acknowledgments

This work was supported by the science and technology research project of Chongqing Education Commission under Grant KJQN201801529 and Doctoral Research Projects for Central Universities under Grant JBK2007190.

References

[1] S. Browne, "Optimal investment policies for a firm with a random risk process: exponential utility and minimizing the probability of ruin," *Mathematics of Operations Research*, vol. 20, no. 4, pp. 937–958, 1995.

[2] C. Hipp and M. Plum, "Optimal investment for insurers," *Insurance: Mathematics and Economics*, vol. 27, no. 2, pp. 215–228, 2000.

[3] Z. Wang, J. Xia, and L. Zhang, "Optimal investment for an insurer: the martingale approach," *Insurance: Mathematics and Economics*, vol. 40, no. 2, pp. 322–334, 2007.

[4] C. S. Liu and H. Yang, "Optimal investment for an insurer to minimize its probability of ruin," *North American Actuarial Journal*, vol. 8, no. 2, pp. 11–31, 2004.

[5] H. Yang and L. Zhang, "Optimal investment for insurer with jump-diffusion risk process," *Insurance: Mathematics and Economics*, vol. 37, no. 3, pp. 615–634, 2005.

[6] L. Bai and J. Guo, "Optimal proportional reinsurance and investment with multiple risky assets and no-shorting constraint," *Insurance: Mathematics and Economics*, vol. 42, no. 3, pp. 968–975, 2008.

[7] S. David Promislow and V. R. Young, "Minimizing the probability of ruin when claims follow brownian motion with drift," *North American Actuarial Journal*, vol. 9, no. 3, pp. 110–128, 2005.

[8] N. Bäuerle, "Benchmark and mean-variance problems for insurers," *Mathematical Methods of Operations Research*, vol. 62, no. 1, pp. 159–165, 2005.

[9] Y. Zeng and Z. Li, "Optimal time-consistent investment and reinsurance policies for mean-variance insurers," *Insurance: Mathematics and Economics*, vol. 49, no. 1, pp. 145–154, 2011.

[10] Z. Liang, K. C. Yuen, and J. Guo, "Optimal proportional reinsurance and investment in a stock market with Ornstein-Uhlenbeck process," *Insurance: Mathematics and Economics*, vol. 49, no. 2, pp. 207–215, 2011.

[11] Z. Liang, K. C. Yuen, and J. Guo, "Optimal control of excess-of-loss reinsurance and investment for insurers under a cev model," *Insurance: Mathematics and Economics*, vol. 51, p. 674, 2012.

[12] K. C. Yuen, Z. Liang, and M. Zhou, "Optimal proportional reinsurance with common shock dependence," *Insurance: Mathematics and Economics*, vol. 64, pp. 1–13, 2015.

[13] J. Grandell, *Aspects of Risk Theory*, Springer-Verlag, New York, NY, USA, 1991.

[14] Z. Liang and K. C. Yuen, "Optimal dynamic reinsurance with dependent risks: variance premium principle," *Scandinavian Actuarial Journal*, vol. 2016, no. 1, pp. 18–36, 2016.

[15] Z. Ming, Z. Liang, and C. Zhang, "Optimal mean-variance reinsurance with common shock dependence," *The Anziam Journal*, vol. 58, no. 2, pp. 162–181, 2016.

[16] J. Bi, Z. Liang, and F. Xu, "Optimal mean-variance investment and reinsurance problems for the risk model with common shock dependence," *Insurance: Mathematics and Economics*, vol. 70, pp. 245–258, 2016.

[17] J. Bi and K. Chen, "Optimal investment-reinsurance problems with common shock dependent risks under two kinds of premium principles," *RAIRO - Operations Research*, vol. 53, no. 1, pp. 179–206, 2019.

[18] M.-H. Chang, T. Pang, and Y. Yang, "A stochastic portfolio optimization model with bounded memory," *Mathematics of Operations Research*, vol. 36, no. 4, pp. 604–619, 2011.

[19] S. Federico, "A stochastic control problem with delay arising in a pension fund model," *Finance and Stochastics*, vol. 15, no. 3, pp. 421–459, 2011.

[20] X. Peng, W. Su, and Z. Zhang, "On a perturbed compound Poisson risk model under a periodic threshold-type dividend strategy," *Journal of Industrial and Management Optimization*, vol. 13, no. 5, pp. 1–20, 2017.

[21] W. Yu, P. Guo, Q. Wang et al., "On a periodic capital injection and barrier dividend strategy in the compound Poisson risk model," *Mathematics*, vol. 8, no. 4, p. 511, 2020.

[22] I. Elsanosi, B. Øksendal, and A. Sulem, "Some solvable stochastic control problems with delay," *Stochastics and Stochastic Reports*, vol. 71, no. 1-2, pp. 69–89, 2000.

[23] B. Øksendal and A. Sulem, "A maximum principle for optimal control of stochastic systems with delay, with applications to finance," 2000.

[24] D. David, "Optimal control of stochastic delayed systems with jumps," 2020.

[25] Y. Shen and Y. Zeng, "Optimal investment-reinsurance strategy for mean-variance insurers with square-root factor process," *Insurance: Mathematics and Economics*, vol. 62, pp. 118–137, 2015.

[26] Y. Lai, "Optimal investment and excess-of-loss reinsurance problem with delay for an insurer under Heston's SV model," *Insurance: Mathematics and Economics*, vol. 61, pp. 181–196, 2015.

[27] Y. Lai and Y. Shao, "Optimal excess-of-loss reinsurance and investment problem with delay and jump-diffusion risk process under the CEV model," *Journal of Computational and Applied Mathematics*, vol. 342, pp. 317–336, 2018.

[28] T. Björk, M. Khapko, and A. Murgoci, "On time-inconsistent stochastic control in continuous time," *Finance and Stochastics*, vol. 21, no. 2, pp. 331–360, 2017.

Hindawi
Mathematical Problems in Engineering
Volume 2020, Article ID 4696941, 12 pages
https://doi.org/10.1155/2020/4696941

Research Article

A Reinsurance and Investment Game between Two Insurers under the CEV Model

Gongliang Zhang,[1] **Shuo Cheng**,[1] **Ziye Li**,[2] **and Ming Cao**[3]

[1]*Management College, Zhongkai University of Agriculture and Engineering, Guangzhou 510225, China*
[2]*School of Mathematics and Statistics, Central China Normal University, Wuhan 430079, China*
[3]*School of Economics and Trade, Guangdong University of Finance, Guangzhou 510519, China*

Correspondence should be addressed to Shuo Cheng; cs_gdut@163.com

Received 1 July 2020; Accepted 18 July 2020; Published 21 August 2020

Guest Editor: Wenguang Yu

In this paper, the problem of nonzero-sum stochastic differential game between two competing insurance companies is considered, i.e., the relative performance concerns. A certain proportion of reinsurance can be taken out by each insurer to control his own risk. Moreover, each insurer can invest in a risk-free asset and risk asset with the price dramatically following the constant elasticity of variance (CEV) model. Based on the principle of dynamic programming, a general framework regarding Nash equilibrium for nonzero-sum games is established. For the typical case of exponential utilization, we, respectively, give the explicit solutions of the equilibrium strategy as well as the equilibrium function. Some numerical studies are provided at last which assist in obtaining some economic explanations.

1. Introduction

As the insurers must invest their wealth in the financial market for wealth management, the most proper investment in the financial market is one of the main problems faced by actuarial practitioners and researchers. In addition, risk management is also an important issue faced by insurance companies. In practice, reinsurance is a significant tool for insurers to diversify risk. Therefore, the optimal reinsurance problem has been widely concerned in the financial and actuarial literature. More and more scholars have studied these problems from different perspectives. Aiming at maximizing the expected terminal wealth utility, Bai and Guo [1] investigated the optimal proportional reinsurance as well as the investment problem of insurers, obtaining the explicit expression of the optimal strategy with the constraint of no-shorting. Mean-variance criterion is also a significant objective function in addition to the minimization of ruin probability as well as utility maximization. Thus, the stochastic dynamic programming method assists in studying the problem of reinsurance and investment with robust optimal excess loss of fuzzy aversion insurer, with jump, obtaining the optimal strategy together with the optimal value function, Li et al. [2].

The studies above assume that risk asset prices are subjected to the geometric Brownian motion (GBM), demonstrating the deterministic volatility exhibited by risk asset prices. However, as mentioned by much empirical evidence, risky assets prices usually exhibit random volatility and the volatility varies with the price of risky assets, Beckers [3] and Campbell [4]. Cox and Ross [5] proposed a constant variance elastic (CEV) process for modeling the underlying stock price about European options to overcome the shortcomings of GBM. The random volatility CEV process of this model naturally expands the GBM and can capture the volatility skewness. At present, the CEV model is generally advocated in the actuarial literature. Li et al. [6] investigated the problem of optimal proportional reinsurance and investment to maximize the product utility of the insurers and the reinsurers, the CEV model. As assumed by Lin and Qian [7], the risky asset price obeys the CEV model. They focused on studying the selection of the optimal time-consistent reinsurance-investment strategy in the compound Poisson risk model. In order to solve the portfolio problem, Zhao and Rong [8] used the CEV process for describing relevant risk assets price. Wang et al. [9] applied a jump diffusion risk process to solve the optimal investment problem for an insurer and a reinsurer under the CEV model.

Besides, nonzero-sum stochastic difference game has many insightful applications in insurance field. Bensoussan et al. [10] established a nonzero-sum stochastic differential game of reinsurance and investment between two competitive insurers affected by systematic risks in a compound Poisson risk model. Deng et al. [11] considered a nonzero-sum stochastic differential game of reinsurance and investment between two CARA insurers with regard to a financier market which involves a defaultable corporate bond. Based on Chen et al. [12], the competition between them is considered as a nonzero-sum stochastic differential game. Hu and Wang [13] investigated the optimal time-consistent investment as well as reinsurance regarding 2 insurance managers with mean variance, and the Nash equilibrium policies and value functions were derived. The study is the first one that focuses on investigating the optimal reinsurance and investment problem with the CEV model under the nonzero-sum stochastic differential game framework.

In this paper, following the framework of Bensoussan et al. [10], a stochastic differential reinsurance and investment game is proposed between two insurers under the CEV model. In our problem setting, the insurers with the classical Cramér–Lundberg diffusion-approximated model are capable of purchasing proportional reinsurance as well as investing in an asset without risk and a risky asset governed by the CEV model. Each insurer aims at finding the equilibrium investment-reinsurance strategy, meanwhile pursuing maximization of expected utility. In line with the setup described above, stochastic control theory assists in formulating, a nonzero-sum game problem between two competitive insurers and obtaining the Hamilton–Jacobi–Bellman (HJB) equation, and the closed-form expressions for equilibrium strategies are obtained. Finally, sensitivity analysis is given in many numerical examples or illustrating the finding.

Our paper contributes to the literature in that the CEV model is introduced into the problem of reinsurance and investment facing two competitive insurers with relative performance concerns. Moreover, this paper has obtained the analytical solutions for the balanced investment-reinsurance strategies; thus, we can analytically examine the influences of the volatility skew on each insurer's equilibrium strategies.

The rest of the paper is divided into five sections. The basic model of the two competitive insurers is introduced in Section 2. The optimal reinsurance-investment problem affected by relative performance concern is formulated in Section 3. We show that this problem is equivalent to the nonzero-sum game between two insurers. Section 4 focuses on deriving the HJB equation under general utility function, followed by obtaining the explicit solutions to Nash equilibrium strategies and the corresponding value functions when both insurers have exponential utilities. Numerical studies are provided in Section 5 in detail for discussing how model parameters affect the equilibrium strategies. Section 6 is the conclusion, together with providing useful reference to future research.

2. Financial Market Model and Assumptions

Models as well as some related basic assumptions are given in the section. As supposed, the financial market harbors the continuous trading of all assets with time, which do not involve transaction costs or taxes. $(\Omega, \mathscr{F}, P)$ refers to an intact probability space with filtration $\{\mathscr{F}_t\}_{t\in[0,T]}$. T denotes a positive finite constant that represents the terminal time. $\mathscr{F}_t$ affects the decision that is made at t, which represents the information available until t, thereby regarding $T-t$ as the horizon at t.

2.1. Surplus Process. Consider a market with two competitive insurers. Following Bensoussan et al. [10], the surplus process of the insurer $k \in \{1,2\}$ is modeled by the standard Cramér–Lundberg diffusion approximation, expressed as $\{R_k(t)\}_{t\geq 0}$. Klugman et al. [14] discussed the diffusion approximation in the insurance models. To be specific, $R_k(t)$ meets the stochastic differential equation (SDE):

$$\mathrm{d}R_k(t) = \left[p_k - \lambda_k \mathbb{E}[\xi_k]\right]\mathrm{d}t + \sqrt{\lambda_k \mathbb{E}\left[\xi_k^2\right]}dB_k(t), \tag{1}$$

where $p_k > 0$ and $\lambda_k > 0$ represent the premium rate and arrival rate of claims, respectively. $\xi_k \neq 0$ refers to a random variable that represents the claim size. $\mathbb{E}[\xi_k^2] < \infty$ and $\{B_k(t)\}_{t\geq 0}$ form a standard Brownian motion, $k = 1, 2$. The correlation between $\{B_1(t)\}_{t\geq 0}$ and $\{B_2(t)\}_{t\geq 0}$ demonstrates the dependence exhibited by two insurers, and $E[\mathrm{d}B_1(t)\mathrm{d}B_2(t)] = \rho\,\mathrm{d}t$, for $\rho \in [-1, 1]$.

2.2. Reinsurance and Investment Opportunities. Supposing we have a reinsurance firm, insurer $k \in \{1,2\}$ is capable of managing his insurance risks via buying proportional reinsurance protection at a premium rate $\iota_k > p_k > 0$. $1 - a_k(t)$ refers to the reinsurance proportion regarding insurer $k \in \{1,2\}$ at time t. $(1 - a_k(t))100\%$ of the claims are born by the reinsurance company and the rest $a_k(t)\%$ comes to insurer k. The reinsurance strategy adopted by insurer $k \in \{1,2\}$ is expressed by $\{a_k(t)\}_{t\geq 0}$, a process of $\mathscr{F}_t$-which can be measured progressively, with value in $[0,1]$. $A_k \triangleq \{a_k(t) : 0 \leq a_k(t) \leq 1,\ t \geq 0\}$ refers to the set of convex reinsurance strategies adopted by insurer k. With reinsurance, the surplus process $\{R_k^{a_k}(t)\}_{t\geq 0}$ regarding insurer $k \in \{1,2\}$ is

$$\begin{aligned}\mathrm{d}R_k^{a_k}(t) &= \left[p_k - (1 - a_k(t))\iota_k - a_k(t)\lambda_k \mathbb{E}[\xi_k]\right]\mathrm{d}t \\ &\quad + a_k(t)\sqrt{\lambda_k \mathbb{E}\left[\xi_k^2\right]}\mathrm{d}B_k(t), \\ &=: \left[m_k + \theta_k a_k(t)\right]\mathrm{d}t + \delta_k a_k(t)\mathrm{d}B_k(t),\end{aligned} \tag{2}$$

where $m_k = p_k - \iota_k < 0$ is the premium difference, $\theta_k = \iota_k - \lambda_k \mathbb{E}[\xi_k]$ is the relative safety loading, and $\delta_k = \sqrt{\lambda_k \mathbb{E}[\xi_k^2]}$ is the volatility of the claim process.

Each insurer, besides buying reinsurance protection, can invest in one bond and one stock. The evolution of price process $S_0(t)$ regarding the bond is based on the ordinary differential equation (ODE):

$$\begin{aligned} dS_0(t) &= rS_0(t)dt, \\ S_0(0) &= 1, \end{aligned} \tag{3}$$

where $r > 0$ represents the risk-free interest rate. The price process $S(t)$ of the stock meets the CEV model:

$$\begin{aligned} dS(t) &= S(t)\left[\mu dt + \sigma S(t)^\beta dW(t)\right], \\ S(0) &= s_0 > 0. \end{aligned} \tag{4}$$

Thereinto, $\mu > r > 0$ means the proper stock rate, β refers to the elasticity parameter, and $\beta \leq 0$ based on Gao [15]. $\sigma S(t)^\beta$ refers to the instantaneous stock volatility. $\{W(t)\}_{t\geq 0}$ is a standard Brownian motion. For notational simplicity, $\{B_k(t) : t \geq 0,\ k = 1, 2\}$ is assumed to be independent of $\{W(t)\}_{t\geq 0}$.

$\{b_k(t)\}_{t\geq 0}$ refers to the $\mathcal{F}_t$-progress which can be measured progressively, and $\{X_k^{\pi_k}(t)\}_{t\geq 0}$ refers to the surplus process regarding insurer k, for $k = 1, 2$, where $b_k(t)$ and $X_k^{\pi_k}(t) - b_k(t)$ denote the amount of money invested in the stock and in the bond, respectively. $B_k \triangleq \{b_k(t) : t \geq 0\}$ as the set of investment strategies adopted by insurer k. A reinsurance-investment strategy of insurer k is then denoted as $\{\pi_k(t)\}_{t\geq 0} \triangleq \{(a_k(t), b_k(t))\}_{t\geq 0} \in A_k \times B_k$. In line with a reinsurance-investment strategy $\pi_k(t)$, the surplus process of insurer k, for $k = 1, 2$, is expressed as

$$\begin{cases} dX_k^{\pi_k}(t) = \left[X_k^{\pi_k}(t) - b_k(t)\right]\dfrac{dS_0(t)}{S_0(t)} + b_k(t)\dfrac{dS(t)}{S(t)} + dR_k^{a_k}(t) \\ \qquad = \left[rX_k^{\pi_k}(t) + m_k + \theta_k a_k(t) + (\mu - r)b_k(t)\right]dt + \delta_k a_k(t) dB_k(t) + \sigma b_k(t) S(t)^\beta dW(t), \\ X_k^{\pi_k}(0) = X_k > 0. \end{cases} \tag{5}$$

We denote by $\Pi_k \triangleq \mathbb{A}_k \times \mathbb{B}_k \subset \mathbb{A}_k \times \mathbb{B}_k$ the set of convex strategies $\pi_k = (a_k, b_k) \in \Pi_k$ of insurer $k \in \{1, 2\}$ satisfying the condition that $0 \leq a_k(t) \leq 1$ and $\mathrm{E}[\int_0^T (b_k(t))^2 dt] < \infty$. We shall refer a strategy $\pi_k \in \Pi_k$ to be an *admissible strategy*. Based on standard stochastic control theory [16], for all $\pi_k = (a_k, b_k) \in \Pi_k$, and for any initial condition $(t, x) \in [0, T] \times R$, the SDE in (5) has a unique strong solution. In this case, we also have

$$E\left[\sup_{0\leq t\leq T}\left|X_k^{\pi_k}(t)\right|^2\right] < \infty, \quad k = 1, 2. \tag{6}$$

3. Optimal Strategies Affected by the Relative Performance Concerns

Suppose that insurer $k \in \{1, 2\}$ involves a utility function U_k which is strictly with a strict concave and a continuous differentiability on $(-\infty, \infty)$. The optimization problem of each insurer lies in optimally selecting a reinsurance-investment strategy $\pi_k \in \Pi_k$, for $k = 1, 2$, for maximizing the expected relative performance utility compared with competitors at the terminal time T. More precisely, we have the following.

Problem 1. The problem of optimal reinsurance as well as investment affected by two competitive insurance companies under the expected utility framework is actually a coupled stochastic optimization problem.

Given the strategy of their competitor $j \in \{1, 2\}$, that is, $\pi_j = (a_j, b_j)$, the objective function, denote as $J_k(t, x_k, x_j, \pi_k(t), \pi_j(t))$, of insurer $k \neq j$ aims at finding an optimal strategy $\pi_k^* \triangleq (a_k^*, b_k^*)$, that is,

$$\max_{\pi_k \in \Pi_k} J_k\left(t, x_k, x_j, \pi_k(t), \pi_j(t)\right) = J_k\left(t, x_k, x_j, \pi_k^*(t), \pi_j^*(t)\right), \tag{7}$$

$$\begin{aligned} &J_k\left(t, x_k, x_j, \pi_k(t), \pi_j(t)\right) \\ &\quad \triangleq E\left[U_k\left((1 - \kappa_k)X_k^{\pi_k}(T) + \kappa_k\left(X_k^{\pi_k}(T) - X_j^{\pi_j}(T)\right)\right)\right. \\ &\qquad \cdot \left.\left|\, X_k^{\pi_k}(t) - \kappa_k X_j^{\pi_j}(t) = x_k - \kappa_k x_j\right.\right] \\ &\quad = E\left[U_k\left(X_k^{\pi_k}(T) - \kappa_k X_j^{\pi_j}(T)\right) \,\middle|\, X_k^{\pi_k}(t) - \kappa_k X_j^{\pi_j}\right. \\ &\qquad \cdot \left.(t) = x_k - \kappa_k x_j\right]. \end{aligned} \tag{8}$$

The parameter $\kappa_k \in [0, 1]$ in (8), for $k = 1, 2$, denotes the sensitivity parameter exhibited by insurer $k\prime$ to his competitor's performance as different insurer generally has different perception of the degree of influence of their competitor's surplus on his strategy, that is, $\kappa_1 \neq \kappa_2$. Problem 1 is a typical example of the nonzero-sum games between two insurers. Consequently, the solution of Problem 1 is the Nash equilibrium regarding the nonzero-sum game between two insurers, where the Nash equilibrium is the strategy $\pi_k^* \triangleq (a_k^*, b_k^*) \in \Pi_k$, such that, for all $\widehat{\pi}_1 \triangleq (\widehat{a}_1, \widehat{b}_1)$ and $\widehat{\pi}_2 \triangleq (\widehat{a}_2, \widehat{b}_2)$,

$$\begin{cases} J_1(t,x_1,x_2,\widehat{\pi}_1,\pi_2^*) \le J_1(t,x_1,x_2,\pi_1^*,\pi_2^*), \\ J_2(t,x_1,x_2,\pi_1^*,\widehat{\pi}_2) \le J_2(t,x_1,x_2,\pi_1^*,\pi_2^*). \end{cases} \tag{9}$$

4. Nash Equilibrium

4.1. General Case. The section focuses on using dynamic programming principle to solve the Nash equilibrium of Problem 1. To this end, the relative surplus process of insurer k is denoted by $Z_k^{\pi_k}(t) \triangleq X_k^{\pi_k}(t) - \kappa_k X_j^{\pi_j}(t)$, for $k=1,2$; hence it follows that

$$\begin{cases} dZ_k^{\pi_k}(t) = \left[rZ_k^{\pi_k}(t) + m_k - \kappa_k m_j + \theta_k a_k(t) - \kappa_k\theta_j a_j(t) + (\mu - r)\left(b_k(t) - \kappa_k b_j(t)\right)\right]dt \\ \qquad + \delta_k a_k(t)dB_k(t) - \kappa_k\delta_j a_j(t)dB_j(t) + \sigma S(t)^\beta\left[b_k(t) - \kappa_k b_j(t)\right]dW(t), \\ Z_k^{\pi_k}(0) = X_k - \kappa_k X_j, \end{cases} \tag{10}$$

where $k \ne j \in \{1,2\}$. Define $V^k(t,z,s)$, for $k=1,2$, to be the value function as follows:

$$V^k(t,z,s) \triangleq \sup_{\pi_k\in\Pi_k} E\left[U_k\left(Z_k^{\pi_k}(T)\right) \mid Z_k^{\pi_k}(t) = z, S(t) = s\right], \tag{11}$$

for $k, j = 1,2$ with $k \ne j$. In addition, let $\Gamma = [0,T) \times \mathbb{R} \times \mathbb{R}$ and $\overline{\Gamma} = [0,T] \times \mathbb{R} \times \mathbb{R}$; for $W^k \in \mathscr{C}^{1,2,2}(\Gamma) \cap \mathscr{C}^0(\overline{\Gamma})$, where $k \ne j \in \{1,2\}$, denote $\mathscr{L}^{\pi_k}$ to be the infinitesimal generator of $Z_k^{\pi_k}$ with an admissible strategy of insurer k, $\pi_k \in \Pi_k$:

$$\begin{aligned} \mathscr{L}^{\pi_k}W^k(t,z,s) \triangleq{}& \mu s W_s^k(t,z,s) + \frac{1}{2}\sigma^2 s^{2\beta+2}W_{ss}^k(t,z,s) + \left[rz + m_k - \kappa_k m_j + \theta_k a_k(t) - \kappa_k\theta_j a_j^*(t)\right. \\ & \left. + (\mu - r)\left(b_k(t) - \kappa_k b_j^*(t)\right)\right]W_z^k(t,z,s) + \frac{1}{2}\left[\delta_k^2 a_k(t)^2 - 2\rho\kappa_k\delta_k\delta_j a_k(t)a_j^*(t)\right] \\ & + \kappa_k^2\delta_j^2 a_j^*(t)^2 + \sigma^2 s^{2\beta}\left(b_k(t)^2 - 2\kappa_k b_k(t)b_j^*(t) + \kappa_k^2 b_j^*(t)^2\right)W_{zz}^k(t,z,s) \\ & + \sigma^2 s^{2\beta+1}\left[b_k(t) - \kappa_k b_j^*(t)\right]W_{zs}^k(t,z,s). \end{aligned} \tag{12}$$

Similar to Theorem 1 proposed by Siu et al. [17] and Theorem 2 proposed by Bensoussan et al. [10], the verification theorem is set forth as follows. Here, the proof is omitted.

Theorem 1. *Let $W^k \in \mathscr{C}^{1,2,2}(\Gamma) \cap \mathscr{C}^0(\overline{\Gamma})$, for $k=1,2$, be the solution of the following Hamilton–Jacobi–Bellman (HJB) equation:*

$$\begin{cases} 0 = W_t^k(t,z,s) + \sup_{\pi_k\in\Pi_k} \mathscr{L}^{\pi_k}W^k(t,z,s), & \text{for } 0 \le t < T, \\ W^k(T,z,s) = U_k(z), \end{cases} \tag{13}$$

and, with regard to the relative surplus process $Z_k^{\pi_k}$ associated with an admissible strategy $\pi_k \in \Pi_k = \mathscr{A}_k \times \mathscr{B}_k$, we have

$$E\left[U_k\left(Z_k^{\pi_k}(T)\right) \mid Z_k^{\pi_k}(t) = z, S(t) = s\right] \le W^k(t,z,s). \tag{14}$$

Denote $\pi_k^* = (a_k^*, b_k^*)$, where $a_k^* \in \mathscr{A}_k$ and $b_k^* \in \mathscr{B}_k$ are given as follows:

$$\begin{aligned} a_k^*(t) \triangleq \arg\max_{a_k\in\mathscr{A}_k}\Big\{&\left[\theta_k a_k(t)\right]W_z^k(t,z,s) + \frac{1}{2} \\ &\cdot \left[\delta_k^2 a_k(t)^2 - 2\rho\kappa_k\delta_k\delta_j a_k(t)a_j^*(t)\right]W_{zz}^k(t,z,s)\Big\}, \end{aligned} \tag{15}$$

$$\begin{aligned} b_k^*(t) \triangleq \arg\max_{b_k\in\mathscr{B}_k}\Big\{&\left[(\mu - r)b_k(t)\right]W_z^k(t,z,s) + \frac{1}{2}\sigma^2 s^{2\beta} \\ &\cdot \left[b_k(t)^2 - 2\kappa_k b_k(t)b_j^*(t)\right]W_{zz}^k(t,z,s) \\ &+ \left[\sigma^2 s^{2\beta+1}b_k(t)\right]W_{zs}^k(t,z,s)\Big\}, \end{aligned} \tag{16}$$

and let $Z_k^{\pi_k^*}$ be the corresponding relative surplus process of insurer k. Then, we have

$$V^k(t,z,s) = \mathrm{E}\left[U_k\left(Z_k^{\pi_k^*}(T)\right) \Big| Z_k^{\pi_k^*}(t) = z, S(t) = s\right] = W^k(t,z,s). \tag{17}$$

Theorem 1 gives the necessary condition for the equilibrium strategy to exist in Problem 1. In the following, we proceed to analyze the sufficient condition which enables the equilibrium strategy to exist.

Assuming that $W_{zz}^k(t,z,s) \neq 0$, for $(t,z,s) \in \Gamma$, the first-order conditions of (15) and (16) give

$$\begin{cases} a_k^*(t) = \left[\left(\rho\kappa_k \frac{\delta_j}{\delta_k} a_j^*(t) - \frac{\theta_k W_z^k(t,z,s)}{\delta_k^2 W_{zz}^k(t,z,s)}\right) \wedge 1\right]^+, \\ b_k^*(t) = \kappa_k b_j^*(t) - \dfrac{(\mu - r) W_z^k(t,z,s)}{\sigma^2 s^{2\beta} W_{zz}^k(t,z,s)} - \dfrac{s W_{zs}^k(t,z,s)}{W_{zz}^k(t,z,s)}. \end{cases} \tag{18}$$

with $a_k^*(t)$, $b_k^*(t)$ expressed in (18), corresponding to HJB equation specific to insurer $k \neq j \in \{1,2\}$ being

$$\begin{aligned} 0 = {} & W_t^k(t,z,s) + \mu s W_s^k(t,z,s) + \left[rz + m_k - \kappa_k m_j - \kappa_k\left(\theta_j - \rho\frac{\delta_j}{\delta_k}\theta_k\right) a_j^*(t)\right] W_z^k(t,z,s) \\ & + \frac{1}{2}\sigma^2 s^{2\beta+2} W_{ss}^k(t,z,s) + \frac{1}{2}\left[\left(1-\rho^2\right)\kappa_k^2 \delta_j^2 a_j^*(t)^2\right] W_{zz}^k(t,z,s) - \frac{1}{2}\left[\frac{\theta_k^2}{\delta_k^2} + \frac{(\mu - r)^2}{\sigma^2 s^{2\beta}}\right] \frac{\left(W_z^k(t,z,s)\right)^2}{W_{zz}^k(t,z,s)} \\ & - \frac{\sigma^2 s^{2\beta+2}\left(W_{zs}^k(t,z,s)\right)^2}{2 W_{zz}^k(t,z,s)} - \frac{(\mu - r) s W_z^k(t,z,s) W_{zs}^k(t,z,s)}{W_{zz}^k(t,z,s)}, \end{aligned} \tag{19}$$

and the terminal condition is

$$W^k(T,z,s) = U_k(z), \quad k = 1,2. \tag{20}$$

Theorem 2 presents the sufficient condition allowing the Nash equilibrium to exist in Problem 1.

Theorem 2. *Assume that $W_{zz}^k(t,z,s) \neq 0$, for $k = 1,2$, where W^k denotes the solution to (19). The Nash equilibrium reinsurance-investment strategy specific to Problem 1 acts as the solution of the coupled system of nonlinear equations as follows:*

$$\begin{cases} a_1^*(t) = \left[\left(\rho\kappa_1 \frac{\delta_2}{\delta_1} a_2^*(t) - \dfrac{\theta_1 W_z^1(t,z,s)}{\delta_1^2 W_{zz}^1(t,z,s)}\right) \wedge 1\right]^+, \\ b_1^*(t) = \kappa_1 b_2^*(t) - \dfrac{(\mu - r) W_z^1(t,z,s)}{\sigma^2 s^{2\beta} W_{zz}^1(t,z,s)} - \dfrac{s W_{zs}^1(t,z,s)}{W_{zz}^1(t,z,s)}, \\ a_2^*(t) = \left[\left(\rho\kappa_2 \frac{\delta_1}{\delta_2} a_1^*(t) - \dfrac{\theta_2 W_z^2(t,z,s)}{\delta_2^2 W_{zz}^2(t,z,s)}\right) \wedge 1\right]^+, \\ b_2^*(t) = \kappa_2 b_1^*(t) - \dfrac{(\mu - r) W_z^2(t,z,s)}{\sigma^2 s^{2\beta} W_{zz}^2(t,z,s)} - \dfrac{s W_{zs}^2(t,z,s)}{W_{zz}^2(t,z,s)}. \end{cases} \tag{21}$$

W^1 *and* W^2 denote the Nash equilibrium functions, subsequently acting as the solutions of the coupled PDEs system as follows:

$$\begin{cases} 0 = W_t^1(t,z,s) + \mu s W_s^1(t,z,s) + \left[rz + m_1 - \kappa_1 m_2 - \kappa_1 \left(\theta_2 - \rho \dfrac{\delta_2}{\delta_1}\theta_1 \right) a_2^*(t) \right] W_z^1(t,z,s) \\ \quad + \dfrac{1}{2}\sigma^2 s^{2\beta+2} W_{ss}^1(t,z,s) + \dfrac{1}{2}\left[\left(1-\rho^2\right)\kappa_1^2\delta_2^2 a_2^*(t)^2 \right] W_{zz}^1(t,z,s) \\ \quad - \dfrac{1}{2}\left[\dfrac{\theta_1^2}{\delta_1^2} + \dfrac{(\mu-r)^2}{\sigma^2 s^{2\beta}} \right] \dfrac{\left(W_z^1(t,z,s)\right)^2}{W_{zz}^1(t,z,s)} - \dfrac{\sigma^2 s^{2\beta+2}\left(W_{zs}^1(t,z,s)\right)^2}{2W_{zz}^1(t,z,s)} - \dfrac{(\mu-r)sW_z^1(t,z,s)W_{zs}^1(t,z,s)}{W_{zz}^1(t,z,s)}, \\ 0 = W_t^2(t,z,s) + \mu s W_s^2(t,z,s) + \left[rz + m_2 - \kappa_2 m_1 - \kappa_2 \left(\theta_1 - \rho \dfrac{\delta_1}{\delta_2}\theta_2 \right) a_1^*(t) \right] W_z^2(t,z,s) \\ \quad + \dfrac{1}{2}\sigma^2 s^{2\beta+2} W_{ss}^2(t,z,s) + \dfrac{1}{2}\left[\left(1-\rho^2\right)\kappa_2^2\delta_1^2 a_1^*(t)^2 \right] W_{zz}^2(t,z,s) \\ \quad - \dfrac{1}{2}\left[\dfrac{\theta_2^2}{\delta_2^2} + \dfrac{(\mu-r)^2}{\sigma^2 s^{2\beta}} \right] \dfrac{\left(W_z^2(t,z,s)\right)^2}{W_{zz}^2(t,z,s)} - \dfrac{\sigma^2 s^{2\beta+2}\left(W_{zs}^2(t,z,s)\right)^2}{2W_{zz}^2(t,z,s)} - \dfrac{(\mu-r)sW_z^2(t,z,s)W_{zs}^2(t,z,s)}{W_{zz}^2(t,z,s)}, \end{cases} \tag{22}$$

and the terminal condition is $W^1(T,z,s) = U_1(z)$; $W^2(T,z,s) = U_2(z)$.

Based on Theorem 2, the existence of Nash equilibrium is equivalent to the solvability of the coupled systems in (21), and the solvability equals that of the coupled PDEs in (22). Bensoussan et al. [10] and Siu et al. [17] mentioned that it was very difficult to establish the general existence of the solution to (22) for any $T > 0$. Nevertheless, for a sufficiently small time $T > 0$, Cauchy–Kowalevski theorem can assisted in establishing the local existence as well as the uniqueness regarding the solution to (22). It is interesting to find that the corresponding coupled equations in (21) and the coupled PDEs in (22) can be explicitly solved, specific to the representative case concerning CARA insurers.

4.2. CARA Insurers. The section pays attention to discussing the constant absolute risk aversion (CARA) insurer $k \in \{1,2\}$ with an exponential utility function:

$$U_k(z) = -\frac{1}{\gamma_k}\exp(-\gamma_k z), \tag{23}$$

where $\gamma_k > 0$ is the risk aversion coefficient of insurer k. Based on Theorem 3, the Nash equilibrium reinsurance-investment strategies and the corresponding equilibrium value functions in Theorem 2 have closed-form solutions specific to the situation involving two CARA insurers.

Theorem 3. *It is assumed that* $\kappa_1\kappa_2 < 1$ *and insurer k, for* $k = 1,2$ *involves an exponential utility function (23) and the relative surplus process* $\left\{Z_k^{\pi_k}(t)\right\}_{t\ge 0}$ *in (10). Then, the solution to the coupled PDE system in (22) is* $V^k(t,z,s)$, *for* $k = 1,2$, *which admits the explicit form as follows:*

$$V^k(t,z,s) = -\frac{1}{\gamma_k}\exp\left\{\left(-\gamma_k z - f^k(t)\right)e^{r(T-t)} + A(t) + B(t)s^{-2\beta}\right\}, \tag{24}$$

$$\begin{aligned} f^k(t) = {} & \frac{\gamma_k\left[m_k - \kappa_k m_j - \kappa_k\left(\theta_j - \rho\left(\delta_j/\delta_k\right)\theta_k\right)a_j^*(t)\right]}{r} \\ & \cdot \left[1 - e^{-r(T-t)}\right] - \frac{\left(1-\rho^2\right)\kappa_k^2\gamma_k^2\delta_j^2 a_j^*(t)^2}{4r} \\ & \times \left[e^{r(T-t)} - e^{-r(T-t)}\right] + \frac{\theta_k^2(T-t)}{2\delta_k^2}e^{-r(T-t)}, \end{aligned} \tag{25}$$

$$A(t) = -\frac{(2\beta+1)(\mu-r)^2}{4r}\left(T - t - \frac{1-e^{-2r\beta(T-t)}}{2r\beta}\right), \tag{26}$$

$$B(t) = -\frac{(\mu-r)^2}{4\sigma^2 r\beta}\left(1 - e^{-2r\beta(T-t)}\right). \tag{27}$$

For $0 \le t \le T$, define

$$\begin{cases} \hat{a}_1(t) \triangleq \dfrac{e^{-r(T-t)}}{1-\rho^2\kappa_1\kappa_2}\left(\dfrac{\rho\kappa_1\theta_2}{\delta_1\delta_2\gamma_2} + \dfrac{\theta_1}{\delta_1^2\gamma_1}\right), \\ \hat{a}_2(t) \triangleq \dfrac{e^{-r(T-t)}}{1-\rho^2\kappa_1\kappa_2}\left(\dfrac{\rho\kappa_2\theta_1}{\delta_1\delta_2\gamma_1} + \dfrac{\theta_2}{\delta_2^2\gamma_2}\right), \end{cases} \tag{28}$$

and then the reinsurance strategy (a_1^*, a_2^*) at equilibrium admits one of the following forms, for $k \neq j \in \{1,2\}$,

(i) If $\widehat{a}_1(t) \geq 0$ and $\widehat{a}_2(t) \geq 0$, then

(a) If $\widehat{a}_1(t) \leq 1$ and $\widehat{a}_2(t) \leq 1$, then $(a_1^*(t), a_2^*(t)) = (\widehat{a}_1(t), \widehat{a}_2(t))$.

(b) If $\widehat{a}_1(t) \leq 1$ and $\widehat{a}_2(t) > 1$, then

$$(a_1^*(t), a_2^*(t)) = \left(\rho\kappa_1\frac{\delta_2}{\delta_1} + \frac{e^{-r(T-t)}\theta_1}{\delta_1^2\gamma_1}, 1\right). \quad (29)$$

(c) If $\widehat{a}_1(t) > 1$ and $\widehat{a}_2(t) \leq 1$, then

$$(a_1^*(t), a_2^*(t)) = \left(1, \rho\kappa_2\frac{\delta_1}{\delta_2} + \frac{e^{-r(T-t)}\theta_2}{\delta_2^2\gamma_2}\right). \quad (30)$$

(d) If $\widehat{a}_1(t) > 1$ and $\widehat{a}_2(t) > 1$, then $(a_1^*(t), a_2^*(t)) = (1,1)$.

(ii) In other cases, the following statements are true:

$$\eta \triangleq \frac{\theta_1\delta_2\gamma_2}{\theta_2\delta_1\gamma_1}, \quad (31)$$

(a) If $\kappa_2\eta \geq -1/\rho$ and $1/\kappa_1\eta \geq -\rho$, then

$$(a_1^*(t), a_2^*(t)) = \left(\left(\frac{e^{-r(T-t)}\theta_1}{\delta_1^2\gamma_1}\right)\wedge 1, \left(\rho\kappa_2\frac{\delta_1}{\delta_2} + \frac{e^{-r(T-t)}\theta_2}{\delta_2^2\gamma_2}\right)^+\right). \quad (32)$$

(b) If $\kappa_2\eta < -1/\rho$ and $1/\kappa_1\eta < -\rho$, then

$$(a_1^*(t), a_2^*(t)) = \left(\left(\rho\kappa_1\frac{\delta_2}{\delta_1} + \frac{e^{-r(T-t)}\theta_1}{\delta_1^2\gamma_1}\right)^+, \frac{e^{-r(T-t)}\theta_2}{\delta_2^2\gamma_2}\wedge 1\right), \quad (33)$$

and the investment amount (b_1^*, b_2^*) at equilibrium is

$$\begin{cases} b_1^*(t) = \dfrac{e^{-r(T-t)}}{1-\kappa_1\kappa_2}\left[\left(\dfrac{1}{\gamma_1} + \dfrac{\kappa_1}{\gamma_2}\right)\left(\dfrac{\mu-r}{\sigma^2 s^{2\beta}} - 2\beta s^{-2\beta}B(t)\right)\right], \\ b_2^*(t) = \dfrac{e^{-r(T-t)}}{1-\kappa_1\kappa_2}\left[\left(\dfrac{1}{\gamma_2} + \dfrac{\kappa_2}{\gamma_1}\right)\left(\dfrac{\mu-r}{\sigma^2 s^{2\beta}} - 2\beta s^{-2\beta}B(t)\right)\right]. \end{cases} \quad (34)$$

Proof. Consider the following Ansatz:

$$W^k(t,z,s) = -\frac{1}{\gamma_k}\exp\left\{\left(-\gamma_k z - f^k(t)\right)e^{r(T-t)} + g(t,s)\right\}, \quad (35)$$

and the boundary condition is $f^k(T) = 0$ and $g(T,s) = 0$.

From fd35(35), we have

$$\begin{aligned} W_t^k &= \left[\left(rz\gamma_k + rf^k\right)e^{r(T-t)} - f_t^k e^{r(T-t)} + g_t\right]W^k, \\ W_s^k &= g_s W^k, \\ W_{ss} &= \left(g_s^2 + g_{ss}\right)W^k, \\ W_z^k &= -\gamma_k e^{r(T-t)}W^k, \\ W_{zz}^k &= \gamma_k^2 e^{2r(T-t)}W^k, \\ W_{zs} &= -\gamma_k e^{r(T-t)}g_s W^k. \end{aligned} \quad (36)$$

Under the notations of (35) and (36), we now derive the corresponding $a_k^*(t)$ and $b_k^*(t)$, for $k = 1,2$. From (15), we can find that the minimizer $a_k(t)$ satisfies

$$\begin{aligned} 0 &= \theta_k W_z^k(t,z,s) + \left[\delta_k^2 a_k - \rho\kappa_k\delta_k\delta_j\widehat{a}_j\right]W_{zz}^k(t,z,s) \\ &= -\theta_k\gamma_k e^{r(T-t)}W^k(t,z,s) \\ &\quad + \left[\delta_k^2 a_k - \rho\kappa_k\delta_k\delta_j\widehat{a}_j\right]\gamma_k^2 e^{2r(T-t)}W^k(t,z,s), \end{aligned} \quad (37)$$

$$\widehat{a}_k = \left(\rho\kappa_k\frac{\delta_j}{\delta_k}\right)\widehat{a}_j + e^{-r(T-t)}\frac{\theta_k}{\delta_k^2\gamma_k}. \quad (38)$$

With (38) in mind, by using the similar method presented by Bensoussan et al. [10], we can derive the corresponding $a_k^*(t)$, for $k = 1,2$; here the details are omitted.

On the other hand, the minimizers b_k^* in (15) are

$$b_k^*(t) = \kappa_k b_j^*(t) + e^{-r(T-t)}\frac{\mu-r}{\sigma^2 s^{2\beta}\gamma_k} + e^{-r(T-t)}\frac{sg_s}{\gamma_k}, \quad (39)$$

yielding (26), where $B(t)$ shall be determined in the following.

Substituting (35) and (36) into (19) yields

$$\begin{aligned} 0 &= rf^k e^{r(T-t)} - f_t^k e^{r(T-t)} + g_t + \frac{1}{2}\sigma^2 s^{2\beta+2}g_{ss} - e^{r(T-t)}\gamma_k \\ &\quad \cdot\left[m_k - \kappa_k m_j - \kappa_k\left(\theta_j - \rho\frac{\delta_j}{\delta_k}\theta_k\right)a_j^*(t)\right] \\ &\quad + \frac{1}{2}e^{2r(T-t)}\left(1-\rho^2\right)\kappa_k^2\gamma_k^2\delta_j^2 a_j^*(t)^2 - \frac{\theta_k^2}{2\delta_k^2} - \frac{(\mu-r)^2}{2\sigma^2 s^{2\beta}} + \mathrm{rsg}_s, \end{aligned} \quad (40)$$

for $j = 1,2$ with $j \neq k$, which can be decomposed into two equations:

$$0 = g_t + \frac{1}{2}\sigma^2 s^{2\beta+2}g_{ss} - \frac{(\mu-r)^2}{2\sigma^2 s^{2\beta}} + \mathrm{rsg}_s, \quad (41)$$

$$\begin{aligned} 0 &= -f_t^k + rf^k - \gamma_k\left[m_k - \kappa_k m_j - \kappa_k\left(\theta_j - \rho\frac{\delta_j}{\delta_k}\theta_k\right)a_j^*(t)\right] \\ &\quad + \frac{1}{2}e^{r(T-t)}\left(1-\rho^2\right)\kappa_k^2\gamma_k^2\delta_j^2 a_j^*(t)^2 - e^{-r(T-t)}\frac{\theta_k^2}{2\delta_k^2}. \end{aligned} \quad (42)$$

To solve (41), we assume that $g(t,s)$ is expressed as

$$g(t,s) = A(t) + B(t)s^{-2\beta}, \tag{43}$$

with the boundary conditions $A(T) = 0$ and $B(T) = 0$. Substituting (43) into (41), we have

$$A_t + \beta(2\beta+1)\sigma^2 B(t) + s^{-2\beta}\left[B_t - 2r\beta B(t) - \frac{(\mu-r)^2}{2\sigma^2}\right] = 0. \tag{44}$$

By matching coefficients, we derive

$$\begin{aligned} &A_t + \beta(2\beta+1)\sigma^2 B(t) = 0,\\ &A(T) = 0, \end{aligned} \tag{45}$$

$$\begin{aligned} &B_t - 2r\beta B(t) - \frac{(\mu-r)^2}{2\sigma^2} = 0,\\ &B(T) = 0. \end{aligned} \tag{46}$$

Solving (45) and (46), we can find that the solutions, $A(t)$ and $B(t)$, admit the forms in (26) and (27), respectively.

Finally, from (42), obviously, $f^k(t)$ is a solution of the linear ODE, which admits the form in (25).

Proof of Theorem 3 is completed. □

5. Numerical Studies

The section focuses on conducting many numerical studies to investigate how model parameters affect the equilibrium reinsurance-investment strategy adopted by the CARA insurers as mentioned in Section 4.2. Except as otherwise specified, the numerical studies will be conducted using the model parameters listed in Table 1.

5.1. Optimal Reinsurance Proportion at Equilibrium. Figures 1 and 2 give a diagram regarding Theorem 3 of $a_k^*(0)$, when $k = 1, 2X \sim f_Z$. Figure 1 illustrates how k' (a parameter of risk aversion) owned by insurer γ_k affects the adopted proportional reinsurance strategy $a_k^*(0)$ in the equilibrium state when the insurers are positively correlated ($\rho = 0.5$) while Figure 2 shows the same influence in the negative correlation ($\rho = -0.5$). Firstly, it is observed that with the increase of γ_k, the insurer + tends to show stronger risk-aversiveness. Hence, a smaller retention level $a_k^*(0)$ is selected for transferring a larger amount of risks to the reinsurer. This is consistent with the strategy of optimal proportional reinsurance without competition. For $a_k^*(0)$ represents the proportion retained by the insurer k during the purchase of proportional reinsurance, the γ_k increase will increase the risk that the insurer k transfers to the reinsurance company. In addition, the condition of $a_k^*(0)$% in Theorem 3 guarantees that $a_k^*(0) \in [0,1]$. This is especially obvious in the influence of η_2 on $a_2^*(0)$. As shown in Figures 1 and 2 when $\rho = 0.5$ and $\rho = -0.5$, respectively.

Table 1: Model parameters.

			Base parameters			
r	μ	σ	β	ρ	T	s
0.05	0.2	0.4	−1	−0.5/0.5	4	10
			Insurer 1			
p_1	ι_1	λ_1	$E[\xi_1]$	$E[\xi_1^2]$	γ_1	κ_1
5	7	0.8	2.5	80	0.1	0.7
			Insurer 2			
p_2	ι_2	λ_2	$E[\xi_2]$	$E[\xi_2^2]$	γ_2	κ_2
3	4	0.5	2	50	0.3	0.5

For illustrating the impact brought about by competition, Figures 1 and 2 also show the influence of the sensitivity parameter $k\prime$ of the insurer κ_k on its proportional reinsurance strategy $a_k^*(0)$, for $k = 1, 2$, when $\kappa_k = 0$, $\kappa_k = 0.3$, and $\kappa_k = 0.7$. The parameter κ_k reflects the dependence gradation of competitors of insurance company k' on the terminal wealth; the higher κ_k causes k to pay more attention than that of its competitors to its performance during the terminal period T. Although purchasing proportional reinsurance is capable of reducing the risk facing insurer k, insurer k is required to pay $(1 - a_k^*(0))\iota_k$ to the reinsurance company for the reinsurance protection fee (see (2)), thereby it has a high cost and declines the terminal value of the insurer compared with the competitor, $X_k^{\pi_k}(T) - \kappa_k X_m^{\pi_m^*}(T)$, for $k \neq m \in \{1,2\}$. As shown in Figure 1, if there is a positive relation between the insurance companies, that is, $\rho = 0.5$, insurer k will prefer to pay less to the reinsurance company, that is, smaller $(1 - a_k^*(0))\iota_k$; thus, the dependence parameter κ_k is increased, also meaning an increase in $a_k^*(0)$. The opposite result appears in the case of negative correlation of insurance companies, that is, $\rho = -0.5$. In this case, based on Figure 2, an increase in the dependency parameter κ_k will cause $a_k^*(0)$ to decrease.

5.2. Optimal Investment at Equilibrium. In Figure 3, the optimal investment strategy adopted by insurer k is positively affected at equilibrium, relying on the expected instantaneous rate of the stocks return μ, which can also be explained as a larger μ leads to a higher expected return of the stock. Thus, $k \in \{1,2\}$ will focus on increasing the investment in the stock.

Figure 4 displays how the elasticity coefficient β affects the optimal investment strategy of insurance company k. As can be seen from the figure, there is an optimistic connection between b_k^* and β. With the decrease of beta coefficient, the insurance company $k \in \{1,2\}$ will reduce the investment in risk assets.

As shown in Figure 5, the optimal investment strategy b_k^* acts as a decreasing function of the interest rate r. The increase in the interest rate r will add the attractiveness of the

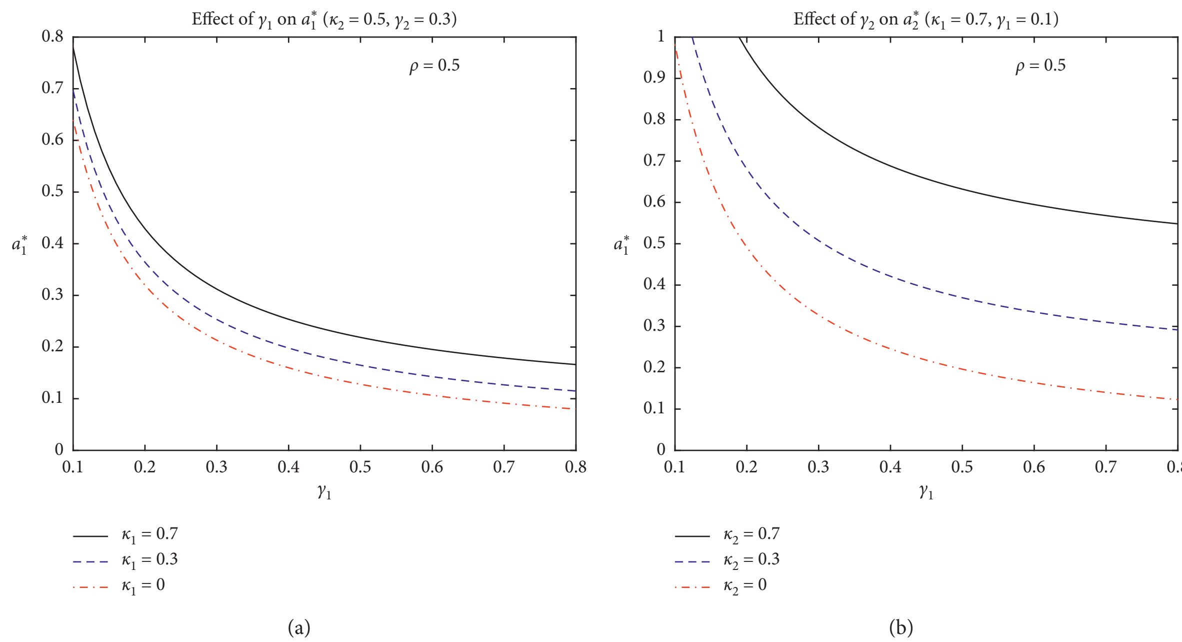

FIGURE 1: Effects of γ_k on a_k^* (0), when $\rho = 0.5$, for $k = 1, 2$.

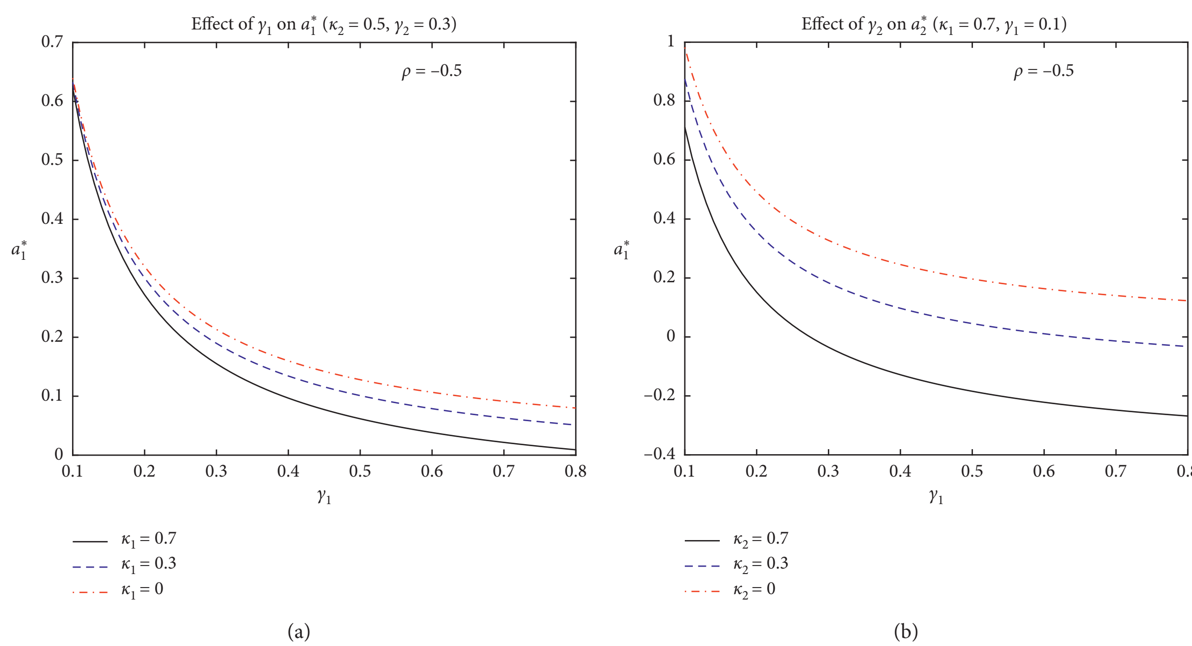

FIGURE 2: Effects of γ_k on a_k^* (0), when $\rho = -0.5$, for $k = 1, 2$.

bond. On that account, insurer $k \in \{1, 2\}$ will pay attention to investing more in the bond.

In addition, Figures 3–5 also capture the effect of competition on the equilibrium investment strategies. In contrast to reinsurance protection, investment in stocks is likely to generate income, so CARA insurance company will increase its exposure to stock S at the terminal time T. Moreover, the presence of competition, which is captured by the sensitivity parameter κ_k, for $k = 1, 2$, induces both CARA insurers to increase their exposure on the stock S.

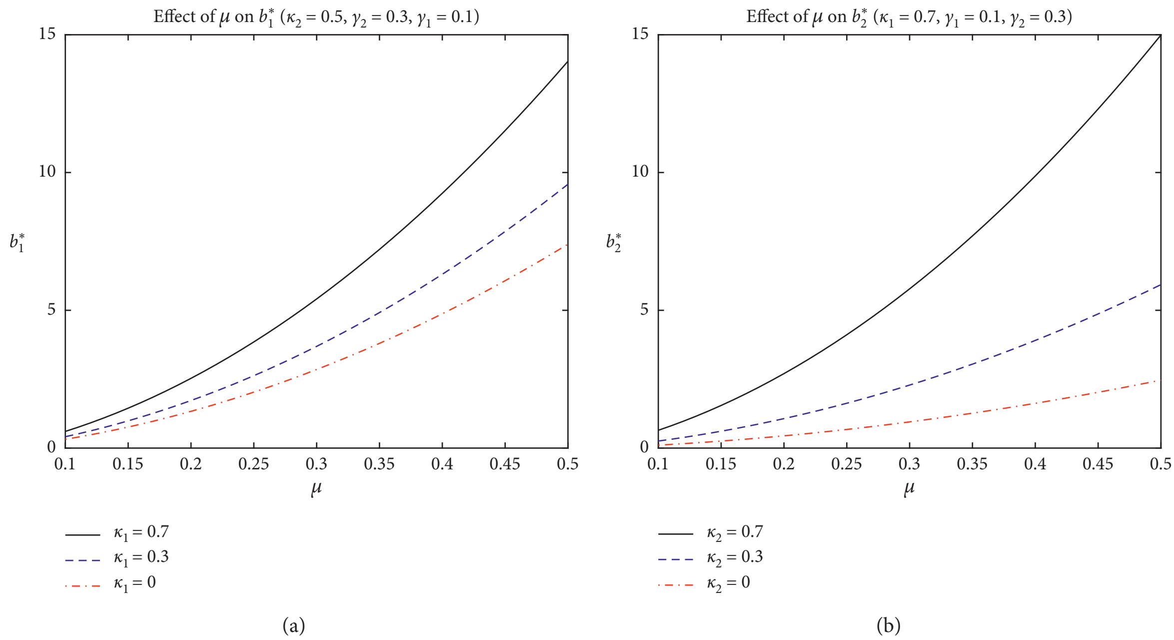

Figure 3: Effects of μ on b_k^* (0), for $k = 1, 2$.

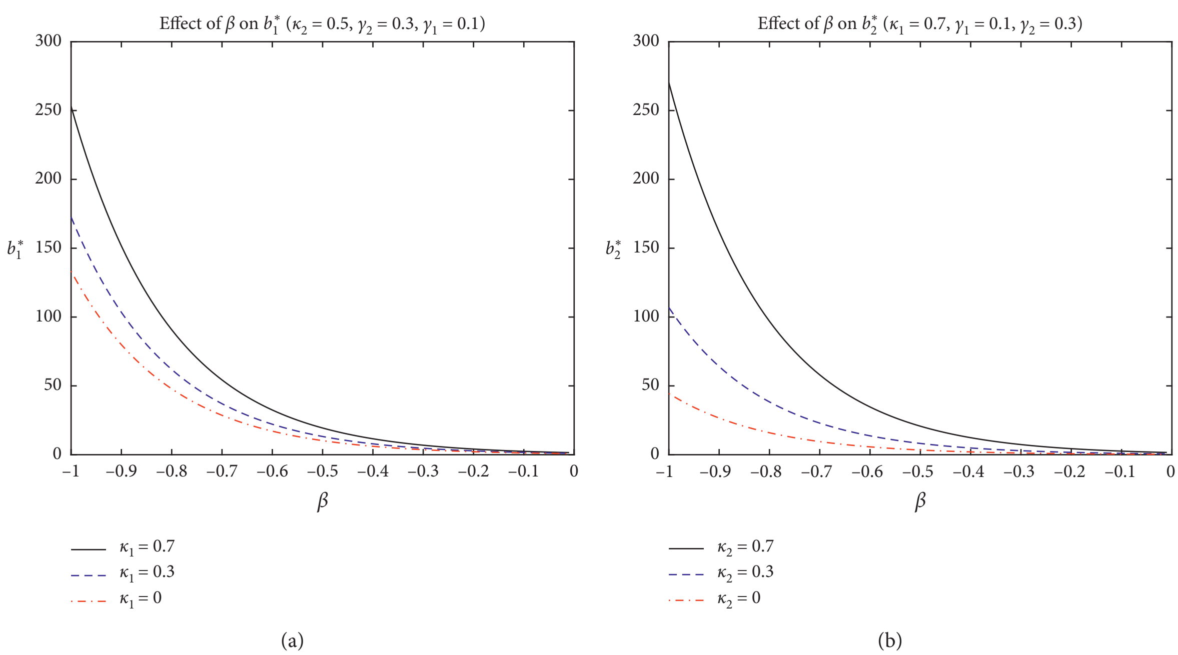

Figure 4: Effects of β on b_k^* (0), for $k = 1, 2$.

6. Conclusion

The paper takes into account the relative performance exhibited by two competitive insurers relying on a nonzero-sum stochastic differential game framework under the CEV model. The dynamic programming principle is applied to solve the Nash equilibrium game, obtaining the optimal reinsurance and investment strategies capable of maximizing the expected utility regarding the relative performance of insurers. We consider two CARA insurers who both have an exponential utility function and give the necessary and sufficient conditions of the equilibrium strategy adaption at the same time. Finally, some numerical studies demonstrate how model parameters affect the equilibrium reinsurance-investment strategies of the CARA insurers.

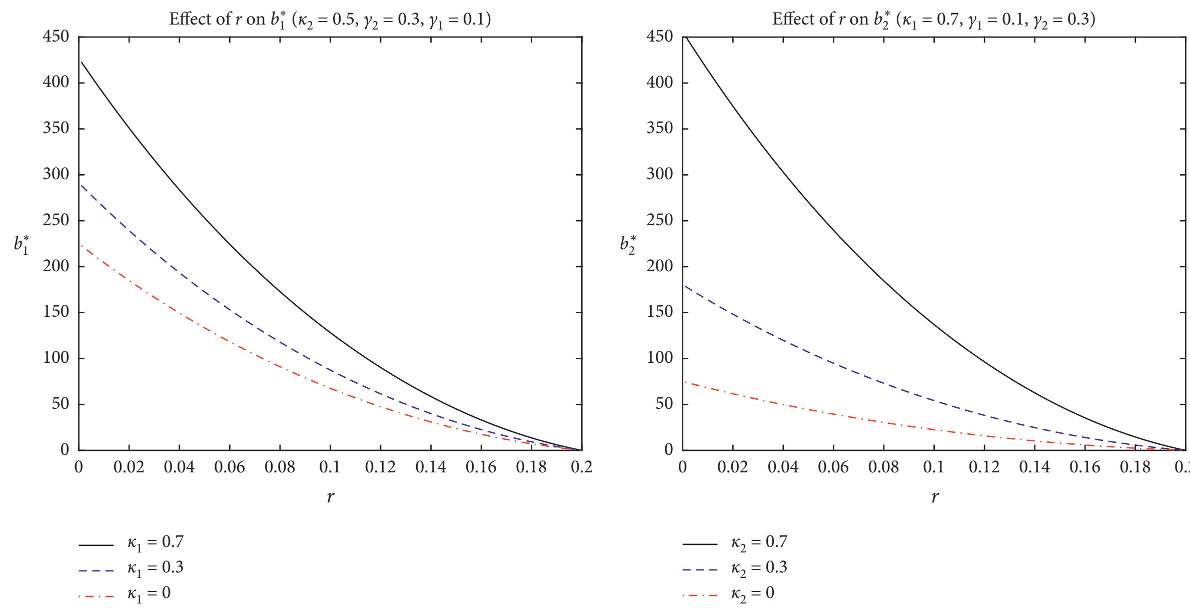

(a) (b)

Figure 5: Effects of r on b_k^* (0), for $k = 1, 2$.

Data Availability

The data used to support the findings of this study are available from the corresponding author upon request.

Conflicts of Interest

The authors declare that there are no conflicts of interest regarding the publication of this paper.

Acknowledgments

This work was supported by the National Natural Science Foundation of China (nos. 71571053 and 71673061); National Social Science Fund of China (no. 17BJY045); Humanities and Social Sciences Project of Ministry of Education of China (no. 18YJC790003); Natural Science Foundation of Guangdong Province (nos. 2015A030310218 and 2016A030313701); Philosophy and Social Science Project of Guangzhou City (nos. 2018GZQN45 and 2018GZYB61); Colleges Innovation and Promotion Project of Education Commission of Guangdong Province (no. 2017WQNCX107); Development of Philosophy and Social Sciences Foundation of Guangzhou (no. 2017GZQN13); and Young Innovative Talents Project of Guangdong Ordinary Universities (nos. 2017WQNCX066 and 2017WQNCX067).

References

[1] L. Bai and J. Guo, "Optimal proportional reinsurance and investment with multiple risky assets and no-shorting constraint," *Insurance: Mathematics and Economics*, vol. 42, no. 3, pp. 968–975, 2008.

[2] D. Li, Y. Zeng, and H. Yang, "Robust optimal excess-of-loss reinsurance and investment strategy for an insurer in a model with jumps," *Scandinavian Actuarial Journal*, vol. 2018, no. 2, pp. 145–171, 2018.

[3] S. Beckers, "The constant elasticity of variance model and its implications for option pricing," *The Journal of Finance*, vol. 35, no. 3, pp. 661–673, 1980.

[4] J. Y. Campbell, "Stock returns and the term structure," *Journal of Financial Economics*, vol. 18, no. 2, pp. 373–399, 1987.

[5] J. C. Cox and S. A. Ross, "The valuation of options for alternative stochastic processes," *Journal of Financial Economics*, vol. 3, no. 1-2, pp. 145–166, 1976.

[6] D. Li, X. Rong, and H. Zhao, "Optimal reinsurance-investment problem for maximizing the product of the insurer's and the reinsurer utilities under a CEV model," *Journal of Computational and Applied Mathematics*, vol. 255, pp. 671–683, 2014.

[7] X. Lin and Y. Qian, "Time-consistent mean-variance reinsurance-investment strategy for insurers under CEV model," *Scandinavian Actuarial Journal*, vol. 2016, no. 7, pp. 646–671, 2016.

[8] H. Zhao and X. Rong, "On the constant elasticity of variance model for the utility maximization problem with multiple risky assets," *IMA Journal of Management Mathematics*, vol. 28, no. 2, pp. 299–320, 2017.

[9] Y. Wang, X. Rong, and H. Zhao, "Optimal investment strategies for an insurer and a reinsurer with a jump diffusion risk process under the CEV model," *Journal of Computational and Applied Mathematics*, vol. 328, pp. 414–431, 2018.

[10] A. Bensoussan, C. C. Siu, S. C. P. Yam, and H. Yang, "A class of non-zero-sum stochastic differential investment and reinsurance games," *Automatica*, vol. 50, no. 8, pp. 2025–2037, 2014.

[11] C. Deng, X. Zeng, and H. Zhu, "Non-zero-sum stochastic differential reinsurance and investment games with default risk," *European Journal of Operational Research*, vol. 264, no. 3, pp. 1144–1158, 2018.

[12] S. Chen, H. Yang, and Y. Zeng, "Stochastic differential games between two insurers with generalized mean-variance

premium principle," *ASTIN Bulletin*, vol. 48, no. 1, pp. 413–434, 2018.

[13] D. Hu and H. Wang, "Time-consistent investment and reinsurance under relative performance concerns," *Communications in Statistics—Theory and Methods*, vol. 47, no. 7, pp. 1693–1717, 2018.

[14] S. A. Klugman, H. H. Panjer, and G. E. Willmot, *Loss Models: From Data to Decisions*, John Wiley & Sons, Hoboken, NJ, USA, 2012.

[15] J. Gao, "Optimal portfolios for DC pension plans under a CEV model," *Insurance: Mathematics and Economics*, vol. 44, no. 3, pp. 479–490, 2009.

[16] H. Pham, *Continuous-Time Stochastic Control and Optimization with Financial Applications*, Springer Science Business Media, Berlin, Germany, 2009.

[17] C. C. Siu, S. C. P. Yam, H. Yang, and H. Zhao, "A class of nonzero-sum investment and reinsurance games subject to systematic risks," *Scandinavian Actuarial Journal*, vol. 2017, no. 8, pp. 670–707, 2017.

Hindawi
Mathematical Problems in Engineering
Volume 2020, Article ID 1583807, 9 pages
https://doi.org/10.1155/2020/1583807

Research Article

Generalization of *h*-Convex Stochastic Processes and Some Classical Inequalities

Hao Zhou,[1] Muhammad Shoaib Saleem ,[2] Mamoona Ghafoor,[2] and Jingjng Li[3]

[1]*Transportation School of Wuhan University of Technology, Wuhan University of Technology, Wuhan 430070, China*
[2]*Department of Mathematics, University of Okara, Okara, Pakistan*
[3]*China Ship Development and Design Center, Wuhan 430064, China*

Correspondence should be addressed to Muhammad Shoaib Saleem; shaby455@yahoo.com

Received 30 April 2020; Revised 21 June 2020; Accepted 30 June 2020; Published 8 August 2020

Academic Editor: Shuanming Li

The field of stochastic processes is essentially a branch of probability theory, treating probabilistic models that evolve in time. It is best viewed as a branch of mathematics, starting with the axioms of probability and containing a rich and fascinating set of results following from those axioms. In probability theory, a convex function applied to the expected value of a random variable is always bounded above by the expected value of the convex function of the random variable. In this paper, the concept of generalized *h*-convex stochastic processes is introduced, and some basic properties concerning generalized *h*-convex stochastic processes are developed. Furthermore, we establish Jensen and Hermite–Hadamard and Fejér-type inequalities for this generalization.

1. Introduction

Stochastic processes are a branch of probability theory, treating probabilistic models that evolve in time [1–3]. It is a branch of mathematics, starting with the axioms of probability and containing a rich and fascinating set of results following from those axioms [4]. Although the results are applicable to many areas [5], they are best understood initially in terms of their mathematical structure and interrelationships [6].

There are various ways to define stochastic monotonicity and convexity for stochastic processes [7], and they are of great importance in optimization, especially in optimal designs, and also useful for numerical approximations when there exist probabilistic quantities in the literature [8]. We also refer [9–12] for detailed survey about the importance and interesting properties of stochastic models.

The idea of convex functions was put forward, and many generalizations were made in this area [13]. h-Convex [14] and ϕ-convex functions [15] are famous generalizations of convex functions. Later, the theory of stochastic processes has developed very rapidly and has found application in a large number of fields. The study on convex stochastic processes was initiated in [16] by B. Nagy in 1974. After that, Nikodem in 1980 introduced the convex stochastic processes in his article [17]. Following this line of investigation, Skowronski described the properties of Jensen-convex and Wright-convex stochastic processes in [18, 19]. Some interesting properties of convex and Jensen-convex processes are also presented in [20, 21]. Assume a Jensen-convex stochastic process $\xi\colon I\times\Omega\longrightarrow\mathbb{R}$ which is mean-square continuous in I, where $I\subseteq\mathbb{R}$ is an interval. Then, for every $a_1, a_2\in I$ $(a_1<a_2)$,

$$\xi\left(\frac{a_1+a_2}{2}\right)\leq\frac{1}{a_2-a_1}\int_{a_1}^{a_2}\xi(u)\mathrm{d}u\leq\frac{\xi(a_1)+\xi(a_2)}{2}\ (a.e.),\quad (1)$$

is known as the Hermite–Hadamard-type inequality for the convex stochastic process [22].

The aim of this paper is to introduce the notion of the generalized h-convex stochastic process and to extend the classical Hermite–Hadamard inequality for convex stochastic processes to generalized h-convex stochastic processes.

2. Novelty and Significance

The study of convex functions makes them special because of their interesting properties as maximum are attained at the boundary point, and moreover, any local minimum is global one. So, this topic of research got the attention of many researchers of different areas because of their enormous applications in optimization theory. As far as convex stochastic processes are concerned, there is a lot of work in the last few decades. In [23], the authors investigated the gradient descent optimality for strongly convex stochastic optimization. A continuous-time financial portfolio selection model with expected utility maximization typically boils down to solve a convex stochastic optimization problem in terms of terminal wealth with budget constraints, see, e.g., [24]. For more details related to this work, see [25–31].

3. Preliminaries

Let (Ω, P) be a probability space. A function $\xi\colon \Omega \longrightarrow \mathbb{R}$ is a random variable if it is -measurable. A function $\xi\colon I \times \Omega \longrightarrow \mathbb{R}$, where $I \subseteq \mathbb{R}$ is an interval, is a stochastic process if for every $t \in I$, the function $\xi(t)$ is a random variable.

The stochastic process $\xi\colon I \times \Omega \longrightarrow \mathbb{R}$ is known as

(1) Stochastically continuous in I if

$$\mu - \lim_{v \longrightarrow v^\circ} \xi(v) = \xi(v^\circ), \tag{2}$$

for all $v^\circ \in I$, where $\mu - \lim$ represents the limit in the probability.

(2) Mean-square continuous in I if

$$\lim_{v \longrightarrow v^\circ} \mathbb{E}\left(\xi(v) - \xi(v^\circ)\right)^2 = 0, \tag{3}$$

for all $v^\circ \in I$, where $\mathbb{E}[\xi(v)]$ represents an expectation value of random variable $\xi(v)$.

Clearly in probability, mean-square continuity implies continuity, but converse is not true.

A stochastic process ξ is known as mean-square differentiable in I if there is a stochastic process ξ' (derivative of ξ) such that

$$\lim_{v \longrightarrow v^\circ} \mathbb{E}\left[\frac{\xi(v) - \xi(v^\circ)}{v - v^\circ} - \xi'(v^\circ)\right]^2 = 0, \tag{4}$$

for every $v^\circ \in I$.

Now, we would like to recall the concept of the mean-square integral. For the definition and basic properties, see [32, 33].

Assume a stochastic process $\xi\colon I \times \Omega \longrightarrow \mathbb{R}$ with $\mathbb{E}[\xi(t)^2] < \infty$. A random variable $\zeta\colon \Omega \longrightarrow \mathbb{R}$ is said to be the mean-square integral of the process ξ on $[a, b]$ if for every normal sequence of partitions of $[a_1, a_2]$, $a_1 = v^\circ < v_1 < \ldots < v_n = a_2$, and for all $\Theta_k \in [v_{k-1}, v_k]$, we have

$$\lim_{n \longrightarrow \infty} \mathbb{E}\left[\left(\sum_{k=1}^{n} \xi(\Theta_k)(v_k - v_{k-1}) - \zeta(.)\right)^2\right] = 0. \tag{5}$$

Then, we write

$$\zeta(.) = \int_a^b \xi(s) \mathrm{d}s\,(a.e). \tag{6}$$

Now, we shall present some definitions and generalizations of the convex stochastic process.

Definition 1 (see [34]). A stochastic process $\xi\colon I \times \Omega \longrightarrow \mathbb{R}$ is known as generalized convex with respect to a bifunction $\eta\colon \xi(I) \times \xi(I) \longrightarrow \mathbb{R}$ if

$$\xi(\alpha u + (1 - \alpha)v) \le \xi(v) + \alpha \eta(\xi(u), \xi(v))\,(a.e), \tag{7}$$

for all $u, v \in I$ and $\alpha \in [0, 1]$.

Definition 2 (see [35]). Let $h\colon (0, 1) \longrightarrow \mathbb{R}$ be a function which is nonnegative and $h \neq 0$. A stochastic process $\xi\colon I \times \Omega \longrightarrow \mathbb{R}$ is said to be h-convex if

$$\xi(\alpha u + (1 - \alpha)v) \le h(\alpha)\xi(u) + h(1 - \alpha)\xi(v)\,(a.e), \tag{8}$$

for every $u, v \in I$ and $\alpha \in (0, 1)$.

Definition 3 (see [15]). The function $\eta\colon \xi(I) \times \xi(I) \longrightarrow \mathbb{R}$ is said to be

(1) Nonnegatively homogeneous if $\eta(\gamma u, \gamma v) = \gamma \eta(u, v)$ for all $u, v \in \mathbb{R}$ and $\gamma \ge 0$

(2) Additive if $\eta(u_1, v_1) + \eta(u_2, v_2) = \eta(u_1 + u_2, v_1 + v_2)$ for all $u_1, u_2, v_1, v_2 \in \mathbb{R}$

Definition 4 (see [14]). A function $h\colon J \longrightarrow \mathbb{R}$, $J \subseteq \mathbb{R}$, is said to be a supermultiplicative function if

$$h(uv) \ge h(u)h(v), \tag{9}$$

for all $u, v \in J$.

Now, we are ready to give our main definition.

Definition 5 (generalized h-convex stochastic process). h and η are fixed like above. We say that a stochastic process $\xi\colon I \times \Omega \longrightarrow$ is called generalized h-convex if

$$\xi(\alpha u + (1 - \alpha)v) \le \xi(v) + h(\alpha)\eta(\xi(u), \xi(v))\,(a.e), \tag{10}$$

for all $u, v \in I$ and $\alpha \in [0, 1]$.

In (10), if we take $\eta(u, v) = u - v$ and $h(\alpha) = \alpha$, we obtain the convex stochastic process. We observe that, by taking $u = v$ in (10), we get

$$h(\alpha)\eta(\xi(u), \quad \xi(u)) \ge 0, \tag{11}$$

for any $u \in I$ and $\alpha \in [0, 1]$, which implies that

$$\eta(\xi(u), \quad \xi(u)) \ge 0, \tag{12}$$

for any $u \in I$. Also, if we take $\alpha = 1$ and $h(1) = 1$ in (10), we get

$$\xi(u) - \xi(v) \leq \eta(\xi(u), \xi(v)), \tag{13}$$

for any $u, v \in I$. (13) obviously implies (12).

We observe that if $\xi\colon I \longrightarrow \mathbb{R}$ is a convex stochastic process and $\eta\colon \xi(I) \times \xi(I) \longrightarrow \mathbb{R}$ is an arbitrary bifunction that satisfies

$$\eta(a, b) \geq a - b, \tag{14}$$

for any $a, b \in I$ and $h(\alpha) \geq \alpha$, then for any $u, v \in I$ and $\alpha \in [0,1]$, we have

$$\begin{aligned}\xi(\alpha u + (1-\alpha)v) &\leq \xi(v) + \alpha(\xi(u) - \xi(v)) \\ &\leq \xi(v) + h(\alpha)\eta(\xi(u), \xi(v)),\end{aligned} \tag{15}$$

showing that ξ is a generalized h-convex stochastic process.

Example 1. Every generalized h-convex function gives an example of a generalized h-convex stochastic process.

Example 2. Let $\xi\colon I \times \Omega \longrightarrow \mathbb{R}$ be a convex stochastic process. For every $k \leq 1$, consider the function

$$\begin{aligned} h_k\colon\ & (0,1) \longrightarrow \mathbb{R}, \\ & x \longmapsto x^k. \end{aligned} \tag{16}$$

Note that $h_k(\alpha) \geq \alpha$ for all $\alpha \in (0,1)$. Also, take $\eta(x, y) = x - y$. Moreover, for every $u, v \in I$ and $\alpha \in (0,1)$, the following inequality is satisfied:

$$\begin{aligned}\xi(\alpha u + (1-\alpha)v) &\leq \alpha\xi(u) + (1-\alpha)\xi(v) \\ &\leq \xi(v) + h_k(\alpha)\eta(\xi(u), \xi(v))\,(a.e).\end{aligned} \tag{17}$$

Then, ξ is a generalized h_k-convex stochastic process.

The paper is organized as follows: in Section 4, we will derive some basic results for the generalized h-convex stochastic process. In Section 5, Jensen-type inequality will be proved, whereas in Section 6, Hermite–Hadamard and Fejér-type inequalities will be established. Finally, in Section 7, we will derive Ostrowski-type inequality for generalized h-convex stochastic processes.

4. Basic Results

Proposition 1. *Consider two generalized h-convex stochastic processes $\xi_1, \xi_2\colon I \times \Omega \longrightarrow \mathbb{R}$ such that*

(1) *If η is additive, then $\xi_1 + \xi_2\colon I \longrightarrow \mathbb{R}$ is η_h-convex stochastic process*

(2) *If η is nonnegatively homogeneous, then for any $\gamma \geq 0$, $\gamma\xi_1\colon I \times \Omega \longrightarrow \mathbb{R}$ is a generalized h-convex stochastic process*

(3) *If ξ_2 is linear, then $\xi_1 \circ \xi_2$ is a generalized h-convex stochastic process*

Proof. The proof of the proposition is straightforward. □

Proposition 2. *If $\xi\colon [a,b] \longrightarrow \mathbb{R}$ is a generalized h-convex stochastic process and $h(\alpha) \leq k$, then we have almost everywhere*

$$\max_{u \in [a,b]} \xi(u) \leq \max\{\xi(b), \xi(b) + k\eta(\xi(a), \xi(b))\}. \tag{18}$$

Proof. For any $u \in [a,b]$, we have $u = \alpha a + (1-\alpha)b$, for some $\alpha \in [0,1]$, and

$$\xi(u) = \xi(\alpha a + (1-\alpha)b). \tag{19}$$

since ξ is a generalized h-convex stochastic process, so

$$\begin{aligned}\xi(u) &\leq \xi(b) + h(\alpha)\eta(\xi(a), \xi(b)) \\ &\leq \max\{\xi(b), \xi(b) + k\eta(\xi(a), \xi(b))\}.\end{aligned} \tag{20}$$

Since u is arbitrary,

$$\max_{u \in [a,b]} \xi(u) \leq \max\{\xi(b), \xi(b) + k\eta(\xi(a), \xi(b))\}. \tag{21}$$

□

5. Jensen-Type Inequality

We will use the next lemma to derive the Jensen-type inequality for the generalized h-convex stochastic process.

Lemma 1. *Assume a generalized h-convex stochastic process $\xi\colon I \times \Omega \longrightarrow \mathbb{R}$. For $u_1, u_2 \in I$ and $\alpha_1 + \alpha_2 = 1$, we have*

$$\xi(\alpha_1 u_1 + \alpha_2 u_2) \leq \xi(u_2) + h(\alpha_1)\eta(\xi(u_2), \xi(u_2))\,(a.e). \tag{22}$$

Also, when $n > 2$ for $u_1, u_2, \ldots, u_n \in I$, $\sum_{i=1}^{n} \alpha_i = 1$, and $T_i = \sum_{j=1} \alpha_j$, the following inequality holds almost everywhere:

$$\begin{aligned}\xi\left(\sum_{i=1}^{n} \alpha_i u_i\right) &= \xi\left(\left(T_{n-1}\sum_{i=1}^{n-1}\frac{\alpha_i}{T_{n-1}}u_i\right) + \alpha_n u_n\right) \\ &\leq \xi(u_n) + h(T_{n-1})\eta\left(\xi\left(\sum_{i=1}^{n-1}\frac{\alpha_i}{T_{n-1}}u_i\right), \xi(u_n)\right).\end{aligned} \tag{23}$$

Theorem 1 *(Jensen-type inequality). Assume a generalized h-convex stochastic process $\xi\colon I \times \Omega \longrightarrow \mathbb{R}$, and let $\eta\colon A \times B \longrightarrow \mathbb{R}$ be nondecreasing, nonnegatively sublinear in the first variable. If $T_i = \sum_{j=1}^{i} \alpha_j$ for $i = 1, 2, \ldots, n$ such that $T_n = 1$, then we have almost everywhere*

$$\xi\left(\sum_{i=1}^{n} \alpha_i u_i\right) \leq \xi(u_n) + \sum_{i=1}^{n-1} h(T)_i \eta_\xi(u_i, u_{i+1}, \ldots, u_n), \tag{24}$$

where

$$\begin{aligned}\eta_\xi(u_i, u_{i+1}, \ldots, u_n) = \eta\big(&\eta_\xi(u_i, u_{i+1}, \ldots, u_{n-1}), \\ &\xi(u_n)\big) \text{ and } \eta_\xi(u) = \xi(u),\end{aligned} \tag{25}$$

for all $u \in I$.

Proof. Since η is nondecreasing, nonnegatively sublinear in the first variable, from Lemma 1, we have

$$\begin{aligned}
\xi\left(\sum_{i=1}^{n}\alpha_i u_i\right) &\leq \xi(u_n) + h(T_{n-1})\eta\left(\xi\left(\sum_{i=1}^{n-1}\frac{\alpha_i}{T_{n-1}}u_i\right),\xi(u_n)\right) = \xi(u_n)\\
&\quad + h(T_{n-1})\eta\left(\xi\left(\frac{T_{n-2}}{T_{n-1}}\sum_{i=1}^{n-2}\frac{\alpha_i}{T_{n-2}}u_i + \frac{\alpha_{n-1}}{T_{n-1}}u_{n-1}\right),\xi(u_n)\right)\\
&\leq \xi(u_n) + h(T_{n-1})\eta\left(\xi(u_{n-1}) + h\left(\frac{T_{n-2}}{T_{n-1}}\right)\times\eta\left(\xi\left(\sum_{i=1}^{n-2}\frac{\alpha_i}{T_{n-2}}u_i\right),\xi(u_{n-1})\right),\xi(u_n)\right)\\
&\leq \xi(u_n) + h(T_{n-1})\eta(\xi(u_{n-1}),\xi(u_n))\\
&\quad + h(T_{n-2})\eta\left(\eta\left(\xi\left(\sum_{i=1}^{n-2}\frac{\alpha_i}{T_{n-2}}u_i\right),\xi(u_{n-1})\right),\xi(u_n)\right) \leq \ldots\\
&\leq \xi(u_n) + h(T_{n-1})\eta(\xi(u_{n-1}),\xi(u_n))\\
&\quad + h(T_{n-2})\eta(\eta(\xi(u_{n-2}),\xi(u_{n-1})),\xi(u_n)) + \ldots\\
&\quad + h(T_1)\eta(\eta(\ldots\eta(\eta(\xi(u_1),\xi(u_2)),\xi(u_3))\ldots)),(\xi(u_{n-1})),(\xi(u_n))\\
&= \xi(u_n) + h(T_{n-1})\eta_\xi(u_{n-1},u_n) + h(T_{n-2})\eta_\xi(u_{n-2},u_{n-1},u_n) + \cdots + h(T_1)\eta_\xi(u_1,u_2,\ldots,u_{n-1},u_n).
\end{aligned} \tag{26}$$

Finally, small calculations yield (26). □

6. Hermite–Hadamard and Fejér-Type Inequalities

Theorem 2. *Assume a mean-square integrable generalized h-convex stochastic process ξ: $[a_1,a_2]\times\Omega\longrightarrow\mathbb{R}$. Then, for any $a_1,a_2\in I$ $(a_1<a_2)$, the following inequality holds almost everywhere:*

$$\begin{aligned}
&\xi\left(\frac{a_1+a_2}{2}\right) - \frac{h(1/2)}{a_2-a_1}\int_{a_1}^{a_2}\eta(\xi(a_1\\
&\quad + a_2 - u),\xi(u))\mathrm{d}u\\
&\leq \frac{1}{a_2-a_1}\int_{a_1}^{a_2}\xi(u)\mathrm{d}u \leq \frac{\xi(a_1)+\xi(a_2)}{2}\\
&\quad + \frac{1}{2}[\eta(\xi(a_1),\xi(a_2))\\
&\quad + \eta(\xi(a_2),\xi(a_1))]\int_0^1 h(\alpha)\mathrm{d}\alpha.
\end{aligned} \tag{27}$$

Proof. Let $x=\alpha a_1+(1-\alpha)a_2$ and $y=(1-\alpha)a_1+\alpha a_2$; then,

$$\begin{aligned}
\xi\left(\frac{a_1+a_2}{2}\right) &= \xi\left(\frac{x+y}{2}\right)\\
&= \xi\left(\frac{1}{2}(\alpha a_1+(1-\alpha)a_2) + \frac{1}{2}((1-\alpha)a_1+\alpha a_2)\right)\\
&\leq \xi((1-\alpha)a_1+\alpha a_2) + h\left(\frac{1}{2}\right)\\
&\quad \times\eta(\xi(\alpha a_1+(1-\alpha)a_2),\xi((1-\alpha)a_1+\alpha a_2)).
\end{aligned} \tag{28}$$

Integrating the above inequality with respect to'α' over $[0,1]$,

$$\begin{aligned}
&\xi\left(\frac{a_1+a_2}{2}\right) \leq \frac{1}{a_2-a_1}\int_{a_1}^{a_2}\xi(u)\mathrm{d}u + \frac{h(1/2)}{a_2-a_1}\int_{a_1}^{a_2}\eta\\
&\quad\cdot(\xi(a_1+a_2-u),\xi(u))\mathrm{d}u\\
&\xi\left(\frac{a_1+a_2}{2}\right) - \frac{h(1/2)}{a_2-a_1}\int_{a_1}^{a_2}\eta(\xi(a_1+a_2-u),\\
&\quad\xi(u))\mathrm{d}u \leq \frac{1}{a_2-a_1}\int_{a_1}^{a_2}\xi(u)\mathrm{d}u.
\end{aligned} \tag{29}$$

Now,

$$\int_{a_1}^{a_2} \xi(u)\mathrm{d}u = (a_2 - a_1)\int_0^1 \xi(\alpha a_1 + (1-\alpha)a_2)\mathrm{d}\alpha$$
$$\leq (a_2 - a_1)\left[\xi(a_2) + \int_0^1 h(\alpha)\eta(\xi(a_1), \xi(a_2))d\alpha\right] \quad (30)$$
$$\frac{1}{a_2 - a_1}\int_{a_1}^{a_2} \xi(u)\mathrm{d}u \leq \xi(a_2) + \int_0^1 h(\alpha)\eta(\xi(a_1), \xi(a_2))\mathrm{d}\alpha.$$

Similarly,

$$\frac{1}{a_2 - a_1}\int_{a_1}^{a_2} \xi(u)\mathrm{d}u \leq \xi(a_1) + \int_0^1 h(\alpha)\eta(\xi(a_2), \xi(a_1))\mathrm{d}\alpha. \quad (31)$$

Adding (30) and (31),

$$\frac{1}{a_2 - a_1}\int_{a_1}^{a_2} \xi(u)\mathrm{d}u \leq \frac{\xi(a_1) + \xi(a_2)}{2} + \frac{1}{2}[\eta(\xi(a_1), \xi(a_2)) + \eta(\xi(a_2), \xi(a_1))]\int_0^1 h(\alpha)\mathrm{d}\alpha. \quad (32)$$

Combining (29) and (32), we get (27). □

Remark 1. If we take $\eta(x, y) = x - y$ and $h(\alpha) = \alpha$, then Theorem 1 reduces to the Hermite–Hadamard inequality for stochastic convexity in [22].

Definition 6 (see [36]). A stochatic process ξ: $[a, b] \longrightarrow \mathbb{R}$ is said to be symmetric with respect to $a + b/2$ on $[a, b]$ if

$$\xi(x) = \xi(a + b - x), \quad (33)$$

for any $a \leq x \leq b$.

Theorem 3. *Assume a generalized h-convex stochastic process ξ_1: $[a_1, a_2] \times \Omega \longrightarrow \mathbb{R}$ with η bounded above on $\xi_1([a_1, a_2]) \times \xi_1([a_1, a_2])$ and a nonnegative function h: $(0, 1) \longrightarrow \mathbb{R}$. Also, suppose that ξ_2: $[a_1, a_2] \longrightarrow \mathbb{R}^+$ is integrable and symmetric about $a_1 + a_2/2$. Then,*

$$\int_{a_1}^{a_2} \xi_1(u)\xi_2(u)\mathrm{d}u \leq \frac{\xi_1(a_1) + \xi_1(a_2)}{2}\int_{a_1}^{a_2} \xi_2(u)\mathrm{d}u + \frac{\eta(\xi_1(a_1), \xi_1(a_2)) + \eta(\xi_1(a_2), \xi_1(a_1))}{2h(a_2 - a_1)} \times \int_{a_1}^{a_2} h(a_2 - u)\xi_2(u)\mathrm{d}u. \quad (34)$$

Proof. By using the definition of the generalized h-stochastic convexity of ξ_1, change of variable, and the assumption that ξ_2 is symmetric about $a_1 + a_2/2$, we have

$$\int_{a_1}^{a_2} \xi_1(u)\xi_2(u,)\mathrm{d}u \leq (a_2 - a_1)\int_0^1 [\xi_1(a_2) + h(\alpha)\eta(\xi_1(a_1), \xi_1(a_2))] \times \xi_2(\alpha a_1 + (1-\alpha)a_2)\mathrm{d}\alpha$$
$$= (a_2 - a_1)\left[\int_0^1 \xi_1(a_2)\xi_2(\alpha a_1 + (1-\alpha)a_2)\mathrm{d}\alpha + \eta(\xi(a_1), \xi(a_2))\int_0^1 h(\alpha)\xi_2(\alpha a_1 + (1-\alpha)a_2)\mathrm{d}\alpha\right], \quad (35)$$

$$\int_{a_1}^{a_2} \xi_1(u,)\xi_2(u,)\mathrm{d}u \leq (a_2 - a_1)\int_0^1 [\xi_1(a_1) + h(\alpha)\eta(\xi_1(a_2), \xi_1(a_1))] \times \xi_2((1-\alpha)a_1 + \alpha a_2)\mathrm{d}\alpha = (a_2 - a_1)\left[\int_0^1 \xi_1(a_1)\xi_2(\alpha a_1 + (1-\alpha)a_2)\mathrm{d}\alpha + \eta(\xi_1(a_2), \xi_1(a_1))\int_0^1 h(\alpha)\xi_2(\alpha a_1 + (1-\alpha)a_2)\mathrm{d}\alpha\right]. \quad (36)$$

Adding (35) and (36), we get

$$2\int_{a_1}^{a_2}\xi_1(u)\xi_2(u)\mathrm{d}u \le (a_2-a_1)(\xi_1(a_1)+\xi_1(a_2))$$
$$\times\int_0^1 \xi_2(\alpha a_1+(1-\alpha)a_2)\mathrm{d}\alpha + (a_2-a_1)(\eta(\xi_1(a_1),\xi_1(a_2)))$$
$$+\eta((\xi_1(a_2),\xi_1(a_1)))\int_0^1 h(\alpha)\xi_2(\alpha a_1+(1-\alpha)a_2)\mathrm{d}\alpha, \quad (37)$$

and by changing the variable $u=\alpha a_1+(1-\alpha)a_2$, we obtain

$$\int_{a_1}^{a_2}\xi_1(u)\xi_2(u)\mathrm{d}u \le \frac{\xi_1(a_1)+\xi_1(a_2)}{2}\cdot\int_{a_1}^{a_2}\xi_2(u)\mathrm{d}u + \frac{\eta(\xi_1(a_1),\xi_1(a_2))+\eta(\xi_1(a_2),\xi_1(a_1))}{2h(a_2-a_1)}\times\int_{a_1}^{a_2}h(a_2-u)\xi_2(u)\mathrm{d}u. \quad (38)$$

□

Theorem 4. *Assume a generalized h-convex stochastic process ξ_1: $[a_1,a_2]\times\Omega \longrightarrow \mathbb{R}$ with η bounded above on $\xi_1([a_1,a_2])\times\xi_1([a_1,a_2])$ and a nonnegative function h: $(0,1)\longrightarrow\mathbb{R}$. Also, suppose that ξ_2: $[a_1,a_2]\longrightarrow\mathbb{R}^+$ is integrable and symmetric about $a_1+a_2/2$. Then,*

$$\xi_1\left(\frac{a_1+a_2}{2}\right)\int_{a_1}^{a_2}\xi_2(u)-h\left(\frac{1}{2}\right)\cdot\int_{a_1}^{a_2}\eta(\xi_1(a_1+a_2-u),\xi(u))\xi_2(u)\mathrm{d}u \le \int_{a_1}^{a_2}\xi(u)\xi_2(u)\mathrm{d}u. \quad (39)$$

Proof. Using the definition of the generalized h-convex stochastic process, change of variable, and the assumption that ξ_2 is symmetric about $a_1+a_2/2$, we get

$$\xi_1\left(\frac{a_1+a_2}{2}\right)=\xi_1\left(\frac{\alpha a_1-\alpha a_1+a_1+a_2+\alpha a_2-\alpha a_2}{2}\right)$$
$$=\xi_1\left(\frac{\alpha a_1+(1-\alpha)a_2+\alpha a_2+(1-\alpha)a_1}{2}\right)$$
$$\le\xi_1(\alpha a_2+(1-\alpha)a_1)+h\left(\frac{1}{2}\right)\times\eta(\xi_1(\alpha a_2+(1-\alpha)a_1),\xi_1(\alpha a_2+(1-\alpha)a_1)). \quad (40)$$

By changing the variable $u=\alpha a_2+(1-\alpha)a_1$, we obtain

$$\xi_1\left(\frac{a_1+a_2}{2}\right)\int_{a_1}^{a_2}\xi_2(u)\mathrm{d}u=\xi_1\left(\frac{a_1+a_2}{2}\right)\cdot\int_0^1\xi_2(\alpha a_2+(1-\alpha)a_1)(a_2-a_1)\mathrm{d}\alpha$$
$$\le\int_0^1\xi_1(\alpha a_2+(1-\alpha)a_1)\xi_2(\alpha a_2+(1-\alpha)a_1)(a_2-a_1)\mathrm{d}\alpha$$
$$+h\left(\frac{1}{2}\right)\int_0^1\eta(\xi_1(\alpha a_1+(1-\alpha)a_2),\xi_1(\alpha a_2+(1-\alpha)a_1))\times\xi_2(\alpha a_2+(1-\alpha)a_1)(a_2-a_1)\mathrm{d}\alpha$$
$$=\int_{a_1}^{a_2}\xi_1(u)\xi_2(u)\mathrm{d}u+h\left(\frac{1}{2}\right)\times\int_{a_1}^{a_2}\eta(\xi_1(a_1+a_2-u),\xi_1(u))\xi_2(u)\mathrm{d}u. \quad (41)$$

□

Corollary 1. *By setting $\eta(x,y)=x-y$ and $h(\alpha)=\alpha$ in (34 and 39) and then combining, we obtain the classical Hermite–Hadamard–Fejér-type inequality as*

$$\xi_1\left(\frac{a_1+a_2}{2}\right)\int_{a_1}^{a_2}\xi_2(u)\mathrm{d}u\le\int_{a_1}^{a_2}\xi_1(u)\xi_2(u)\mathrm{d}u\le\frac{\xi_1(a_1)+\xi_1(a_2)}{2}\cdot\int_{a_1}^{a_2}\xi_2(u)\mathrm{d}u. \quad (42)$$

7. Ostrowski-Type Inequality

In order to prove Ostrowski-type inequality for the generalized h-convex stochastic process, the following lemma is required.

Lemma 2 (see [37]). *Let ξ: $I\times\Omega\longrightarrow\mathbb{R}$ be a stochastic process which is mean-square differentiable on I° and its derivative ξ' be mean-square integrable on $[a_1,a_2]$, where a_1, $a_2\in I$ with $a_1<a_2$; then, the following equality holds:*

$$\xi(u)-\frac{1}{a_2-a_1}\int_{a_1}^{a_2}\xi(v)\mathrm{d}v=\frac{(u-a_1)^2}{a_2-a_1}\cdot\int_0^1\alpha\xi'(\alpha u+(1-\alpha)a_1)\mathrm{d}\alpha-\frac{(a_2-u)^2}{a_2-a_1}\int_0^1\alpha\xi'(\alpha u+(1-\alpha)b_1)\mathrm{d}\alpha\,(a.e.), \quad (43)$$

for each $u\in[a,b]$.

Theorem 5. *Assume a mean-square stochastic process* ξ: $I \times \Omega \longrightarrow \mathbb{R}$ *such that* $\xi\prime$ *(the derivative of* ξ*) is mean-square integrable on* $[a_1, a_2]$*, where* $a_1, a_2 \in I$ *with* $a_1 < a_2$*, and consider a nonnegative function* h: $(0,1) \longrightarrow \mathbb{R}$ *which is supermultiplicative such that, for every* α, $h(\alpha) > \alpha$. *If* $|\xi\prime|$ *is a generalized h-convex stochastic process on* I *and* $|\xi\prime(u)| \leq M$ *for every* u*, then*

$$\left|\xi(u) - \frac{1}{a_2 - a_1}\int_{a_1}^{a_2}\xi(v)\mathrm{d}v\right| \leq M\left[\frac{(u-a_1)^2 + (a_2-u)^2}{a_2 - a_1}\right]\int_0^1 h(y)\mathrm{d}y + \left(\frac{(u-a_1)^2}{a_2-a_1}\eta\left(|\xi\prime(u)|, \left|\xi'(a_1)\right|\right) + \frac{(a_2-u)^2}{a_2-a_1}\eta\left(|\xi'(u)|, \left|\xi'(a_2)\right|\right)\right)\int_0^1 h^2(y)\mathrm{d}y. \tag{44}$$

Proof. By using Lemma 2 and the definition of generalized h-stochastic convexity of $|\xi'|$, we get

$$\begin{aligned}
\left|\xi(u) - \frac{1}{a_2 - a_1}\int_{a_1}^{a_2}\xi(v)\mathrm{d}v\right| &\leq \frac{(u-a_1)^2}{a_2-a_1}\int_0^1 y\left|\xi\prime(yu + (1-y)a_1)\right|\mathrm{d}y \\
&+ \frac{(a_2-u)^2}{a_2-a_1}\int_0^1 y\left|\xi'(yu + (1-y)a_2)\right|\mathrm{d}y \\
&\leq \frac{(u-a_1)^2}{a_2-a_1}\int_0^1 y\left[\left|\xi\prime(a_1)\right| + h(y)\eta\left(|\xi\prime(u)|, \left|\xi\prime(a_1)\right|\right)\right]\mathrm{d}y \\
&+ \frac{(a_2-u)^2}{a_2-a_1}\int_0^1 y\left[\left|\xi\prime(a_2)\right| + h(y)\eta\left(|\xi\prime(u)|, \left|\xi\prime(a_2)\right|\right)\right]\mathrm{d}y \leq M\frac{(u-a_1)^2}{a_2-a_1}\int_0^1 h(y)\mathrm{d}y \\
&+ \frac{(u-a_1)^2}{a_2-a_1}\int_0^1 h^2(y)\eta\left(|\xi\prime(u)|, \left|\xi\prime(a_1)\right|\right)\mathrm{d}y + M\frac{(a_2-u)^2}{a_2-a_1}\int_0^1 h(y)\mathrm{d}y \\
&+ \frac{(a_2-u)^2}{a_2-a_1}\int_0^1 h^2(y)\eta\left(|\xi\prime(u)|, \left|\xi\prime(a_2)\right|\right)\mathrm{d}y \leq M\left[\frac{(u-a_1)^2 + (a_2-u)^2}{a_2-a_1}\right]\int_0^1 h(y)\mathrm{d}y \\
&+ \frac{(u-a_1)^2}{a_2-a_1}\eta\left(|\xi\prime(u)|, \left|\xi\prime(a_1)\right|\right) \times \int_0^1 h^2(y)\mathrm{d}y + \frac{(a_2-u)^2}{a_2-a_1}\eta\left(|\xi\prime(u)|, \left|\xi\prime(a_2)\right|\right)\int_0^1 h^2(y)\mathrm{d}y \\
&= M\left[\frac{(u-a_1)^2 + (a_2-u)^2}{a_2-a_1}\right]\int_0^1 h(y)\mathrm{d}y + \left(\frac{(u-a_1)^2}{a_2-a_1}\eta\left(|\xi\prime(u)|, \left|\xi\prime(a_1)\right|\right)\right. \\
&\left.+ \frac{(a_2-u)^2}{a_2-a_1}\eta\left(|\xi\prime(u)|, \left|\xi\prime(a_2)\right|\right)\right)\int_0^1 h^2(y)\mathrm{d}y.
\end{aligned} \tag{45}$$

□

8. Conclusion

Stochastic processes have many applications in statistics, which obviously lead to lots of other domains, for example, Kolmogorov–Smirnoff test on the equality of distributions [38–40] (the test statistic is derived from a Brownian bridge, which is a Brownian motion conditioned to have certain values at the endpoints of an interval of time). The other applications include sequential analysis [41, 42] (this is the rigorous way you can stop an A/B test dynamically. Stopping rules are obtained by approximating discrete problems with their continuous time analogs, in which the sufficient statistic process follows a stochastic differential equation) and quickest detection [43, 44] (my stock story is that you are using a gold mine which gives you a random amount of gold per day, but at some point, it will get depleted, and you want to know when this happens as quickly as possible. Decision rules are again based on properties of hitting times of random processes). In this paper, we have introduced generalized h-conevex stochastic processes and proved Jensen, Hermite–Hadamard, and Fejér-type inequalities. Our results are applicable because applying the convex function to the expected value of a random variable is always bounded above by the expected value of the convex function of the random variable.

Data Availability

All data required for this research are included within this paper.

Conflicts of Interest

The authors do not have any conflicts of interest.

Authors' Contributions

All authors contributed equally to this paper.

Acknowledgments

This research was supported by the National Natural Science Foundation of China (Grant nos. 11971142, 11871202, 61673169, 11701176, 11626101, and 11601485).

References

[1] S. Ghahramani, *Fundamentals of Probability with Stochastic Process*, Pearson Education India, New York, NY, USA, 2005.

[2] A. Anguraj and R. Kumar, "Existence and uniqueness of mild solution for stochastic partial differential equation with Poisson jumps and delays," *Open Journal of Mathematical Sciences*, vol. 3, no. 1, pp. 343–348, 2019.

[3] A. Kumar, "Optimal control analysis of combined anti-angiogenic and tumor immunotherapy," *Open Journal of Mathematical Sciences*, vol. 3, no. 1, pp. 349–357, 2019.

[4] K. Itô, "On stochastic processes (I)," in *Japanese Journal of Mathematics: Transactions and Abstracts*, vol. 18, pp. 261–301, The Mathematical Society of Japan, Japan, 1941.

[5] H. P. Hong, "Application of the stochastic process to pitting corrosion," *Corrosion*, vol. 55, no. 1, pp. 10–16, 1999.

[6] J. L. Doob, "Stochastic processes depending on a continuous parameter," *Transactions of the American Mathematical Society*, vol. 42, no. 1, p. 107, 1937.

[7] M. Shaked and J. G. Shanthikumar, "Parametric stochastic convexity and concavity of stochastic processes," *Annals of the Institute of Statistical Mathematics*, vol. 42, no. 3, pp. 509–531, 1990.

[8] P. Chen, A. Quarteroni, and G. Rozza, "Stochastic optimal Robin boundary control problems of advection-dominated elliptic equations," *SIAM Journal on Numerical Analysis*, vol. 51, no. 5, pp. 2700–2722, 2013.

[9] A. Bogdanov, S. Chiu, L. U. Gokdere, and J. Vian, "Stochastic optimal control of a servo motor with a lifetime constraint," in *Proceedings of the 45th Ieee Conference on Decision and Control*, IEEE, Berlin, Germany, pp. 4182–4187, 2006.

[10] A. Belloni, L. Piroddi, and M. Prandini, "A stochastic optimal control solution to the energy management of a microgrid with storage and renewables," in *Proceedings of the 2016 American Control Conference (ACC)*, IEEE, Berlin, Germany, pp. 2340–2345, 2016.

[11] S. Haesaert, P. M. Van den Hof, and A. Abate, "Experiment design for formal verification via stochastic optimal control," in *Proceedings of the 2016 European Control Conference (ECC)*, IEEE, Berlin, Germany, pp. 427–432, 2016.

[12] I. Exarchos, E. A. Theodorou, and P. Tsiotras, "Game-theoretic and risk-sensitive stochastic optimal control via forward and backward stochastic differential equations," in *Proceedings of the 2016 IEEE 55th Conference on Decision and Control (CDC)*, IEEE, Berlin, Germany, pp. 6154–6160, 2016.

[13] A. W. Roberts, "Convex functions," in *Handbook of Convex Geometry*, pp. 1081–1104, IEEE, North-Holland, MA, USA, 1993.

[14] S. Varošanec, "On h-convexity," *Journal of Mathematical Analysis and Applications*, vol. 326, no. 1, pp. 303–311, 2007.

[15] M. E. Gordji, M. R. Delavar, and M. D. L. Sen, "On φ-convex functions," *Journal of Mathematical Inequalities*, vol. 10, no. 1, pp. 173–183, 2016.

[16] B. Nagy, "On a generalization of the cauchy equation," *Aequationes Mathematicae*, vol. 10, no. 2-3, pp. 165–171, 1974.

[17] K. Nikodem, "On convex stochastic processes," *Aequationes Mathematicae*, vol. 20, no. 1, pp. 184–197, 1980.

[18] A. Skowronski, "On some properties of j-convex stochastic processes," *Aequationes Mathematicae*, vol. 44, no. 2-3, pp. 249–258, 1992.

[19] A. Skowronski, "On wright-convex stochastic processes," *Aequationes Mathematicae*, vol. 9, pp. 29–32, 1995.

[20] Z. Páles, "Nonconvex functions and separation by power means," *Mathematical Inequalities & Applications*, vol. 3, no. 2, pp. 169–176, 2000.

[21] R. Rasuli, "Intuitionistic fuzzy subgroups with respect to norms (T,S)," *Engineering and Applied Science Letter*, vol. 3, no. 2, pp. 40–53, 2020.

[22] D. Kotrys, "Hermite-hadamard inequality for convex stochastic processes," *Aequationes Mathematicae*, vol. 83, no. 1-2, pp. 143–151, 2012.

[23] A. Rakhlin, O. Shamir, and K. Sridharan, "Making gradient descent optimal for strongly convex stochastic optimization," 2012.

[24] H. Jin, Z. Q. Xu, and X. Y. Zhou, "A convex stochastic optimization problem arising from portfolio selection," *Mathematical Finance*, vol. 18, no. 1, pp. 171–183, 2008.

[25] J. Cvitanic and I. Karatzas, "Convex duality in constrained portfolio optimization," *The Annals of Applied Probability*, vol. 2, no. 4, pp. 767–818, 1992.

[26] H. Kushner and G. Yin, *Stochastic Approximation and Recursive Algorithms and Applications*, Springer, Berlin, Germany, 2nd edition, 2003.

[27] S. Shalev-Shwartz, O. Shamir, N. Srebro, and K. Sridharan, "Stochastic convex optimization," COLT, Berlin, Germany, 2009.

[28] S. Mehmood and G. Farid, "Fractional integrals inequalities for exponentially \(m\)-convex functions," *Open Journal of Mathematical Sciences*, vol. 4, no. 1, pp. 78–85, 2020.

[29] W. Farid, K. M. Awan, K. M. Awan, and A. U. Rehman, "An extension of Petrović's inequality for \(h-\)convex (\(h-\) concave) functions in plane," *Open Journal of Mathematical Sciences*, vol. 3, no. 1, pp. 398–403, 2019.

[30] S. I. Farid, M. Nadeem, and G. Farid, "On caputo fractional derivatives via exponential (sm)-convex functions," *Engineering and Applied Science Letter*, vol. 3, no. 2, pp. 32–39, 2020.

[31] S. Mehmood, G. Farid, K. A. Khan, and M. Yussouf, "New fractional hadamard and fejr-hadamard inequalities

associated with exponentially (hm)-convex functions," *Engineering and Applied Science Letter*, vol. 3, no. 2, pp. 9–18, 2020.

[32] Z. Brzezniak and T. Zastawniak, *Basic Stochastic Processes: A Course through Exercises*, Springer Science & Business Media, Berlin, Germany, 2000.

[33] K. Sobczyk, *Stochastic Differential Equations: with Applications to Physics And Engineering*, Springer Science & Business Media, Berlin, Germany, 2013.

[34] A. V. Skorokhod, "On a generalization of stochastic integral," *Teoriya Veroyatnostei I Ee Primeneniya*, vol. 20, no. 2, pp. 223–238, 1975.

[35] D. Barráez, L. González, N. Merentes, and A. Moros, "On h-convex stochastic processes," *Mathematica Aeterna*, vol. 5, no. 4, pp. 571–581, 2015.

[36] M. R. Delavar and S. S. Dragomir, "On η-convexity," *Mathematical Inequalities & Applications*, vol. 20, no. 1, pp. 203–216, 2017.

[37] L. Gonzales, J. Materano, and M. V. Lopez, "Ostrowski-type inequalities via hconvex stochastic processes," *JP Journal of Mathematical Sciences*, vol. 16, no. 2, pp. 15–29, 2016.

[38] S. Engmann and D. Cousineau, "Comparing distributions: the two-sample anderson-darling test as an alternative to the kolmogorov-smirnoff test," *Journal of Applied Quantitative Methods*, vol. 6, no. 3, pp. 1–17, 2011.

[39] B. B. Bhattacharya, "Two-sample tests based on geometric graphs: asymptotic distribution and detection thresholds," 2015.

[40] R. Dey, "Hypothesis tests with precedence probabilities and precedence-type tests," *Wiley Interdisciplinary Reviews: Computational Statistics*, vol. 10, no. 1, p. e1417, 2018.

[41] D. Siegmund, *Sequential Analysis: Tests and Confidence Intervals*, Springer Science & Business Media, Berlin, Germany, 2013.

[42] P. K. Andersen, O. Borgan, R. D. Gill, and N. Keiding, *Statistical Models Based on Counting Processes*, Springer Science & Business Media, Berlin, Germany, 2012.

[43] A. Delorme, T. Sejnowski, and S. Makeig, "Enhanced detection of artifacts in EEG data using higher-order statistics and independent component analysis," *Neuroimage*, vol. 34, no. 4, pp. 1443–1449, 2007.

[44] P. Dollár, R. Appel, S. Belongie, and P. Perona, "Fast feature pyramids for object detection," *IEEE Transactions on Pattern Analysis and Machine Intelligence*, vol. 36, no. 8, pp. 1532–1545, 2014.

Hindawi
Mathematical Problems in Engineering
Volume 2020, Article ID 3529858, 23 pages
https://doi.org/10.1155/2020/3529858

Research Article

Robust Waveform Design Based on Bisection and Maximum Marginal Allocation Methods with the Concept of Information Entropy

Bin Wang [1] **and Xiaolei Hao** [2]

[1] *School of Electrical and Electronic Engineering, Shijiazhuang Tiedao University, Shijiazhuang, China*
[2] *School of Computer and Communication Engineering, Northeastern University at Qinhuangdao, Qinhuangdao, China*

Correspondence should be addressed to Bin Wang; wangbinneu@qq.com

Received 20 May 2020; Accepted 16 July 2020; Published 6 August 2020

Guest Editor: Wenguang Yu

Cognitive radar can overcome the shortcomings of traditional radars that are difficult to adapt to complex environments and adaptively adjust the transmitted waveform through closed-loop feedback. The optimization design of the transmitted waveform is a very important issue in the research of cognitive radar. Most of the previous studies on waveform design assume that the prior information of the target spectrum is completely known, but actually the target in the real scene is uncertain. In order to simulate this situation, this paper uses a robust waveform design scheme based on signal-to-interference-plus-noise ratio (SINR) and mutual information (MI). After setting up the signal model, the SINR and MI between target and echo are derived based on the information theory, and robust models for MI and SINR are established. Next, the MI and SINR are maximized by using the maximum marginal allocation (MMA) algorithm and the water-filling method which is improved by bisection algorithm. Simulation results show that, under the most unfavorable conditions, the robust transmitted waveform has better performance than other waveforms in the improvement degree of SINR and MI. By comparing the robust transmitted waveform based on SINR criterion and MI criterion, the influence on the variation trend of SINR and MI is explored, and the range of critical value of T_y is found. The longer the echo observation time is, the better the performance of the SINR-based transmitted waveform over the MI-based transmitted waveform is. For the mutual information between the target and the echo, the performance of the MMA algorithm is better than the improved water-filling algorithm.

1. Introduction

Radar uses radio method to find targets and determine their spatial position. However, with the wide application of electromagnetic spectrum, the working environment of radar is more and more complex. The traditional radar has a single transmitting waveform, which is difficult to adapt to the complex and changeable working environment. Cognitive radar is an intelligent radar system concept proposed in recent years. This system can improve the system performance of the radar through using the feedback structure from the receiver to the transmitter to optimize the transmitted waveform based on the recognition of the target and the scene. The whole system forms a closed-loop structure [1]. In view of the leading role of cognitive radar research in the development direction of radar, experts and scholars in various countries have launched research in related fields.

Adaptive waveform design is the key problem in cognitive radar research, which makes cognitive radar transmit the waveform that adapts to the change of environment. In the past decades, many experts and scholars devoted themselves to researching on transmitted waveform to improve the detection and estimation performance of radar system for extended target. In [2], based on information theory, the author proposes a water-filling algorithm to maximize the mutual information between the received radar waveform and the target. The author studies the use of information theory to design the waveform to measure the resonance phenomenon of the extended radar target. For the deterministic target impulse response and the random target impulse response, the radar waveform design problem with waveform energy and duration constraints is solved. The optimal target detection scheme puts as much energy as possible in the maximum target scattering mode to maximize the mutual information between target and the received radar echo. In [3], the authors propose a minimax robust signal processing scheme when the prior knowledge is inaccurate and discuss robust linear filters for signal estimation and signal detection. Related applications and nonlinear methods for robust signal detection and robust estimation are also studied. In [4], considering the uncertainty of the prior information of the radar target in the actual scene, the authors propose a waveform design method based on mutual information to ensure the parameter estimation performance of complex target models. This algorithm is robust to the uncertainty under the layered game model of radar and jammer and can effectively guarantee the parameter estimation performance. In [5], the authors study the relationship between the transmitted waveform and the multitarget mutual information in the two cases of noise only and clutter included according to the maximum mutual information criterion. Compared with the LFM signal, the waveform designed based on the maximum mutual information criterion can make the radar echo contain more information about multiple targets. In [6], the authors derive the convergence of the iterative water-filling algorithm and propose an algorithm that can guarantee its convergence in the presence of various forms of time-varying errors. Simulation results show that under the condition of strong interference, the traditional iterative water-filling algorithm is divergent, but the algorithm in this paper is still convergent. In [7], the authors focus on the transmitted waveform and filter structure of polarimetric radar. The worst-case signal-to-interference-plus-noise ratio is used as the criterion under both a similarity and an energy constraint on the transmit signal. An iterative optimization method for robust design is proposed. In [8], the authors propose a comprehensive theory of matched illumination waveforms for determining extended targets and random extended targets, use signal-to-noise ratio and mutual information as optimization criteria to design matched waveforms, and extensively discuss the waveform design of random targets and known targets with correlated interference based on SNR and MI. In [9], the authors propose a multitarget detection method and adaptive waveform design algorithm for MIMO cognitive radar, which models multitarget detection as multiple hypothesis testing. An adaptive waveform design algorithm based on information theory is proposed. The semidefinite relaxation technique and semidefinite programming are used to solve nonconvex design problems, which improves the efficiency of multiple hypothesis testing. In [10], the authors propose an adaptive orthogonal frequency division multiplexing radar communication waveform design method to improve the efficiency of limited spectrum resources and study the optimization problem of the conditional mutual information between the random target impulse response and the received signal and data information rate for frequency-selective fading channels. In [11], the author investigates the design of orthogonal frequency division multiplexing multiple-input multiple-output radar waveforms with target uncertainty and improves the space-time adaptive processing detection performance of MIMO-OFDM radar in the most unfavorable case. The author proposes a method based on diagonal loading. By using the DL method, the optimization problem can be reduced to a semidefinite programming problem. In [12], the authors propose a robust waveform technique for multistatic cognitive radars in the context of signal-related clutter and derive a new method that directly assumes uncertainty on the radar cross section and Doppler parameter of the clutters. A specific clutter random optimization method using Taylor series approximation is proposed to determine a robust waveform with specific SINR outage constraints. In [13], the authors study the robust waveform design of multiple-input multiple-output cognitive radar and propose a two-step process. First, the covariance matrix of the detection signal is designed. Then, a waveform is synthesized from the obtained covariance matrix. In [14], the authors investigate the design of angle-robust joint transmit waveforms and receive filters for multiple-input multiple-output (MIMO) radars under signal-dependent interference. The method maximizes the output signal-to-interference-plus-noise ratio (SINR) in the most unfavorable case in unknown target angles. Based on rank-relaxed semidefinite programming (SDP) of nonnegative triangular polynomials, a cyclic optimization algorithm is proposed to solve this problem. In [15], the authors extend the traditional Gaussian target response to arbitrary non-Gaussian target distributions, use cognitive radar multiple hypothesis classification algorithms for non-Gaussian targets, and utilize the sparse spectrum of related narrowband target responses. In previous studies, most of them assume that the target spectrum is known. However, the real target spectrum cannot be accurately captured in practice. Even if some researchers consider the uncertainty of target spectrum and use robust technology, the solution process is very complex.

In this paper, we fully consider the uncertainty of the target in practice. Based on the concept of entropy in information theory, we establish robust waveform design model of MI and SINR. Then, we use water-filling method improved by bisection algorithm and maximum marginal allocation algorithm to maximize MI and SINR. Finally, we obtain robust waveforms with better performance than other waveforms. The whole paper is organized as follows. Section 2 is the signal model. Section 3 is the robust waveform design based on MI. Section 4 is the robust waveform design based on SINR. Section 5 gives the search method of Lagrange multipliers based on bisection algorithm. Section 6 introduces the maximum marginal allocation algorithm. Section 7 shows the simulation results and related analysis. Section 8 concludes the whole paper.

2. Signal Model

Assume that the target model is a stationary random process on time interval $[0, T_h]$, with a value 0 outside of $[0, T_h]$. A stationary random process is a random process whose probability distribution at a fixed time and position is the same as that of all times and positions, which means the statistical characteristics of the random process do not change over time.$g(t)$ is a generalized stationary Gaussian random process, whose mathematical expectation and variance are independent of time, and its correlation function is only related to time interval. $a(t)$ is the rectangle window function, and the duration of the window function is T_h. Therefore, $h(t) = g(t)a(t)$ can be constructed, which is a random process with finite duration. Since $g(t)$ is generalized stationary, $h(t)$ is locally stationary in $[0, T_h]$.

$x(t)$ and $h(t)$ represent the transmitted waveform and target, respectively, $c(t)$ denotes clutter, and $n(t)$ represents noise. Suppose that $c(t)$ and $n(t)$ are Gaussian random processes with zero mean value, and the power spectral density is $S_{\mathrm{cc}}(f)$ and $S_{\mathrm{nn}}(f)$, respectively.

The transmitted waveform $x(t)$ and the interference signal $c(t)$ are convolved with the target $h(t)$ to obtain $z(t)$ and $d(t)$, respectively. After the addition of the above two with the noise $n(t)$, the echo $y(t)$ can be obtained after the ideal low-pass filter, and the duration of $y(t)$ is T_y, as shown in Figure 1.

Since the real radar target signal has a finite duration, $h(t)$ is a random process with finite energy, and it is assumed that any sample function of $h(t)$ can be integrated. The Fourier transform of the sample function $h(t)$ is $H(f)$. From Parseval's theorem,

$$E_h = \int_0^{T_h} |h(t)|^2 \mathrm{d}t = \int_{-\infty}^{+\infty} |H(f)|^2 \mathrm{d}f. \tag{1}$$

The energy spectral density of $h(t)$ is

$$\xi_H(f) = E\left[|H(f)|^2\right]. \tag{2}$$

The mean and variance are defined as

$$\begin{aligned} \mu_H(f) &= E[|H(f)|], \\ \sigma_H^2(f) &= E\left[\left|H(f) - \mu_H(f)\right|^2\right]. \end{aligned} \tag{3}$$

In this paper, it is assumed that $\mu_H(f)$ is 0, so the energy spectral density (ESD) and the energy spectral variance (ESV) are equal. ESV describes the average energy of a random process with finite duration and zero mean value.

For the convolution of known signal $x(t)$ with random process $h(t)$, such as $z(t) = x(t) * h(t)$, the output ESV is

$$\sigma_Z^2(f) = \sigma_H^2(f)|X(f)|^2. \tag{4}$$

3. Robust Waveform Design Based on MI

3.1. Derivation of Mutual Information Formula. The mutual information to be researched in this paper is $I(h(t); y(t) \mid x(t))$ between target $h(t)$ and echo $y(t)$ when the transmitted waveform $x(t)$ is known.

Before solving mutual information, the basic knowledge of information theory needs to be introduced. Suppose Y is a discrete random variable with a value range of $R_Y = \{y_1, y_2, y_3, \ldots\ldots\}$, and for each $y \in R_Y$, the probability of $Y = y$ is $P(y)$. The empirical and historical data

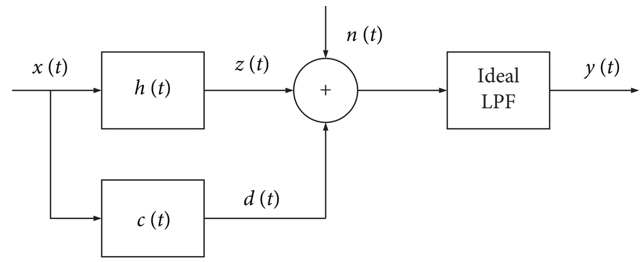

Figure 1: Signal model of random target with finite duration in clutter.

obtained before the experiment of obtaining samples are called prior information. In order to measure the size of the prior information, the self-information of Y is defined as

$$I(y) = -\log P(y). \tag{5}$$

In information theory, the logarithm base 2 is often used, and the unit is Bit. In this paper, for the convenience of calculation, the logarithm base e is used, and the unit is Nat. Therefore, the discrete form and continuous form of information entropy $H(Y)$ are, respectively, as follows:

$$\begin{aligned} H(Y) &= -\sum_{Y \in R_Y} P(y) \ln P(y), \\ H(Y) &= -\int_{-\infty}^{+\infty} P(y) \ln P(y) \mathrm{d}y. \end{aligned} \tag{6}$$

The mutual information between Y and Z is

$$I(Y; Z) = H(Y) - H(Y \mid Z), \tag{7}$$

where Y is the sum of three Gaussian random variables with zero mean value, so it is also a Gaussian random variable with zero mean value. Considering that Z and D are statistically independent, and N is also statistically independent, the variance of Y is as follows:

$$\sigma_Y^2 = \sigma_Z^2 + \sigma_N^2 + \sigma_D^2, \tag{8}$$

where Y is a Gaussian random variable, so $P(y)$ conforms to a normal distribution. Assume that the mean value is μ and the variance is σ, then

$$\begin{aligned} P(y) &= \frac{1}{\sqrt{2\pi\sigma^2}} e^{-(y-\mu)^2/2\sigma^2}, \\ &\int_{-\infty}^{+\infty} P(y) \mathrm{d}y = 1. \end{aligned} \tag{9}$$

So,

$$\begin{aligned} H(Y) &= -\int_{-\infty}^{+\infty} P(y) \ln P(y) \mathrm{d}y = -\int_{-\infty}^{+\infty} P(y) \ln \frac{1}{\sqrt{2\pi\sigma^2}} e^{-(y-\mu)^2/2\sigma^2} \mathrm{d}y \\ &= -\int_{-\infty}^{+\infty} P(y) \left[\ln \frac{1}{\sqrt{2\pi\sigma^2}} + \ln e^{-(y-\mu)^2/2\sigma^2}\right] \mathrm{d}y \\ &= \frac{1}{2} \ln\left(2\pi\sigma^2\right) + \int_{-\infty}^{+\infty} \frac{(y-\mu)^2}{2\sigma^2} \frac{1}{\sqrt{2\pi\sigma^2}} e^{-(y-\mu)^2/2\sigma^2} \mathrm{d}y. \end{aligned} \tag{10}$$

Create a function

$$F(\mu,\sigma)=\int_{-\infty}^{+\infty}\frac{(y-\mu)^2}{2\sigma^2}\frac{1}{\sqrt{2\pi\sigma^2}}e^{-(y-\mu)^2/2\sigma^2}\mathrm{d}y, \quad (11)$$

with known

$$\int_{-\infty}^{+\infty}e^{-y^2}\mathrm{d}y=\sqrt{\pi}. \quad (12)$$

So,

$$\int_{-\infty}^{+\infty}e^{-y^2}y^2\mathrm{d}y=-\frac{1}{2}\int_{-\infty}^{+\infty}yd\left(e^{-y^2}\right)\mathrm{d}y$$
$$=-\frac{1}{2}\left[ye^{-y^2}\right]_{-\infty}^{+\infty}-\frac{1}{2}\int_{-\infty}^{+\infty}e^{-y^2}\mathrm{d}y=\frac{\sqrt{\pi}}{2}. \quad (13)$$

From the abovementioned equation, we can obtain

$$\int_{-\infty}^{+\infty}e^{-y^2}y^2\mathrm{d}y=\frac{\sqrt{\pi}}{2}. \quad (14)$$

Let us replace y with $(y-\mu)/\sqrt{2}\sigma$; it can be calculated by

$$F(\mu,\sigma)=\frac{\sqrt{2}\sigma}{\sqrt{2\pi\sigma^2}}\int_{-\infty}^{+\infty}\frac{(y-\mu)^2}{2\sigma^2}e^{-(y-\mu)^2/2\sigma^2}\mathrm{d}\left(\frac{y-\mu}{\sqrt{2}\,\sigma}\right)$$
$$=\frac{\sqrt{2}\sigma}{\sqrt{2\pi\sigma^2}}\frac{\sqrt{\pi}}{2}=\frac{1}{2}. \quad (15)$$

So,

$$H(Y)=\frac{1}{2}\ln\left(2\pi\sigma^2\right)+\int_{-\infty}^{+\infty}\frac{(y-\mu)^2}{2\sigma^2}\frac{1}{\sqrt{2\pi\sigma^2}}e^{-(y-\mu)^2/2\sigma^2}\mathrm{d}y$$
$$=\frac{1}{2}\ln\left(2\pi\sigma^2\right)+\frac{1}{2}. \quad (16)$$

Because of the nature of information entropy, the constant can be ignored, so the information entropy can be obtained as

$$H(Y)=\frac{1}{2}\ln\left(2\pi\sigma^2\right)=\frac{1}{2}\ln\left[2\pi\left(\sigma_Z^2+\sigma_N^2+\sigma_D^2\right)\right]. \quad (17)$$

Similarly, the conditional entropy $H(Y\mid Z)$ between Y and Z is

$$H(Y\mid Z)=\frac{1}{2}\ln\left[2\pi\left(\sigma_N^2+\sigma_D^2\right)\right]. \quad (18)$$

Mutual information $I(Y;Z)$ can be obtained as

$$I(Y;Z)=H(Y)-H(Y\mid Z)=\frac{1}{2}\ln\left[1+\frac{\sigma_Z^2}{\sigma_N^2+\sigma_D^2}\right]. \quad (19)$$

For the signals defined on the frequency interval $F_k=[f_k,f_k+\Delta f]$, such as $z_k(t)$, $y_k(t)$, $d_k(t)$, and $n_k(t)$, according to the sampling theorem, each signal can be replaced by a series of samples obtained from uniform sampling. Suppose that the sampling frequency of the signal is $2\Delta f$. When Δf is very small, the spectrum $X(f)$, $Z(f)$, $D(f)$, $Y(f)$ is flat in $f\in F_k$ and can be approximated to a constant value. The Gaussian process samples sampled with uniform sampling rate $2\Delta f$ are also statistically independent.

Sample $z_k(t)$ is an independent, identically distributed random variable, with zero mean value and variance σ_Z^2, and the total energy of $z_k(t)$ in the frequency interval F_k is

$$\varepsilon_Z(F_k)=\Delta f\left|X(f_k)\right|^2\sigma_H^2(f_k). \quad (20)$$

The number of sample points is $2T_y\Delta f$, and the energy is uniformly distributed on independent sample points with the same distribution. So, the variance σ_Z^2 of each sample point is

$$\sigma_Z^2=\frac{\varepsilon_Z(F_k)}{2T_y\Delta f}=\frac{\Delta f\left|X(f_k)\right|^2\sigma_H^2(f_k)}{2T_y\Delta f}=\frac{\left|X(f_k)\right|^2\sigma_H^2(f_k)}{2T_y}. \quad (21)$$

The total energy of the clutter process on time interval T_y is

$$\varepsilon_D(F_k)=\Delta f\left|X(f_k)\right|^2S_{\mathrm{cc}}(f_k)T_y. \quad (22)$$

The variance of the clutter process at each sample point is

$$\sigma_D^2=\frac{\varepsilon_D(F_k)}{2T_y\Delta f}=\frac{\Delta f\left|X(f_k)\right|^2S_{\mathrm{cc}}(f_k)T_y}{2T_y\Delta f}=\frac{\left|X(f_k)\right|^2S_{\mathrm{cc}}(f_k)}{2}. \quad (23)$$

Similarly, the total energy of the noise process on time interval T_y is

$$\varepsilon_N(F_k)=S_{\mathrm{nn}}(f_k)T_y\Delta f. \quad (24)$$

Considering that the noise is Gaussian white noise, its power spectral density is a constant in the frequency domain, so

$$\varepsilon_N(F_k)=S_{\mathrm{nn}}(f_k)T_y\Delta f=S_{\mathrm{nn}}(f)T_y\Delta f. \quad (25)$$

The variance of the noise process at each sample point is

$$\sigma_N^2=\frac{\varepsilon_N(F_k)}{2T_y\Delta f}=\frac{S_{\mathrm{nn}}(f)T_y\Delta f}{2T_y\Delta f}=\frac{S_{\mathrm{nn}}(f)}{2}. \quad (26)$$

Substituting σ_Z^2, σ_D^2, and σ_N^2 into formula (19), we get

$$I(Y;Z)=\frac{1}{2}\ln\left[1+\frac{\sigma_Z^2}{\sigma_N^2+\sigma_D^2}\right]$$
$$=\frac{1}{2}\ln\left[1+\frac{\left(\left|X(f_k)\right|^2\sigma_H^2(f_k)\right)/2T_y}{(S_{\mathrm{nn}}(f)/2)+\left(\left(\left|X(f_k)\right|^2S_{\mathrm{cc}}(f_k)\right)/2\right)}\right], \quad (27)$$

that is,

$$I(Y;Z)==\frac{1}{2}\ln\left[1+\frac{\left|X(f_k)\right|^2\sigma_H^2(f_k)}{T_y\left(S_{\mathrm{nn}}(f)+\left|X(f_k)\right|^2S_{\mathrm{cc}}(f_k)\right)}\right]. \quad (28)$$

Within the observation interval T_y, there are statistically independent sample values with the number of $2T_y\Delta f$, so the mutual information of $z_k(t)$ and $y_k(t)$ in the case of known $x_k(t)$ is

$$I\left(y_k(t); z_k(t) \mid x_k(t)\right) = 2T_y\Delta f I(Y;Z), \tag{29}$$

that is,

$$\begin{aligned} &I\left(y_k(t); z_k(t) \mid x_k(t)\right) \\ &\quad = T_y\Delta f \ln\left[1 + \frac{\left|X(f_k)\right|^2 \sigma_H^2(f_k)}{T_y\left(S_{\mathrm{nn}}(f) + \left|X(f_k)\right|^2 S_{\mathrm{cc}}(f_k)\right)}\right]. \end{aligned} \tag{30}$$

Within any frequency interval BW, it is divided into many disjoint intervals, and the interval bandwidth is Δf. When $\Delta f \longrightarrow 0$, the number of intervals is infinite, and the integral expression of mutual information can be obtained as

$$\begin{aligned} &I(y(t); z(t) \mid x(t)) \\ &\quad = T_y\int_{\mathrm{BW}} \ln\left[1 + \frac{|X(f)|^2\sigma_H^2(f)}{T_y\left(S_{\mathrm{nn}}(f) + |X(f)|^2 S_{\mathrm{cc}}(f)\right)}\right]\mathrm{d}f. \end{aligned} \tag{31}$$

3.2. Robust Water-Filling Waveform. In previous studies on waveform design, it is assumed that the prior information of the target spectrum is completely known. However, in actual scene, the real target spectrum cannot be captured with complete precision. It is assumed that the target spectrum exists in an uncertain range δ, which is defined by the known upper and lower bounds, that is,

$$H(f) \in \delta \Rightarrow \{l_k \le H(f_k) \le u_k, k = 1, 2, 3 \ldots\ldots\}, \tag{32}$$

where f_k is the sampling frequency, and for each sampling point, there is an upper bound and a lower bound. The confidence band of the target spectrum can be determined by spectrum estimation, so the upper and lower bounds of the estimated waveform spectrum are reasonable. In this paper, the upper and lower bounds are determined according to the uniform distribution function, which refers to the fact that the range of upper and lower bound is the random number consistent with uniform distribution within $[0, |H(f)|]$. So, the difference value of the spectrum corresponding to each sampling frequency may be different between the upper and lower bounds. The greater the difference between the upper and lower bounds of the uncertainty range is, the greater the uncertainty of the target spectrum is. For each specific target spectrum, there is an optimal transmitted waveform. However, the real target spectrum varies in the range of uncertainty, so in this paper, we adopt the maximin robust waveform design scheme.

For this, we first introduce the concept of robustness. Robustness is a term used in statistics to describe the insensitivity of control systems to perturbation of characteristics or parameters. In general, a robust signal processing scheme may not perform as well under nominal conditions as the optimal scheme under nominal conditions, but its overall performance will be good or acceptable relative to the defined feature categories. To achieve this, we must first specify a metric for the overall performance of a solution, which relates to a class of allowable conditions at the time of input. In many cases, a widely used and effective measure is the worst performance of a solution under certain input conditions. Obviously, if it performs well under most unfavorable condition, we can say that the given scheme is robust. Therefore, we propose the best performance scheme in the worst case, which is maximin robust scheme. The worst-case performance of this solution will be acceptable, which refers to the best performance that can be achieved under the most adverse conditions. So, this is not going to be very much lower than the optimal solution in the nominal case.

In the process of designing the robust transmitted waveform based on MI and SINR, the most unfavorable situation is the lower bound of the uncertainty range of the target waveform spectrum, that is, the lower bound of $H(f)$. Assume the real energy spectral density is $|H(f)|^2$, the upper bound is $\sigma_{\mathrm{U}}^2(f)$, and the lower bound is $\sigma_{\mathrm{L}}^2(f)$:

$$\begin{aligned} &\mathrm{MI}\left(\left|X^{\max\min}(f)\right|^2, \sigma_{\mathrm{U}}^2(f)\right)\Big|_{\int_{\mathrm{BW}}\left|X^{\max\min}(f)\right|^2 \mathrm{d}f \le E_x} \\ &\ge \mathrm{MI}\left(\left|X^{\max\min}(f)\right|^2, \sigma_{\mathrm{H}}^2(f)\right)\Big|_{\int_{\mathrm{BW}}\left|X^{\max\min}(f)\right|^2 \mathrm{d}f \le E_x} \\ &\ge \mathrm{MI}\left(\left|X^{\max\min}(f)\right|^2, \sigma_{\mathrm{L}}^2(f)\right)\Big|_{\int_{\mathrm{BW}}\left|X^{\max\min}(f)\right|^2 \mathrm{d}f \le E_x} \\ &\ge \mathrm{MI}\left(|X(f)|^2, \sigma_{\mathrm{L}}^2(f)\right)\Big|_{\int_{\mathrm{BW}}|X(f)|^2 \mathrm{d}f \le E_x}. \end{aligned} \tag{33}$$

To solve the formula,

$$\max \left\{\min_{H(f)\in\delta} \mathrm{MI}\left(|X(f)|^2, \sigma_{\mathrm{L}}^2(f)\right) \Big|_{\int_{\mathrm{BW}}|X(f)|^2 \mathrm{d}f \le E_x}\right\}, \tag{34}$$

that is,

$$\begin{aligned} &\max \quad T_y\int_{\mathrm{BW}} \ln\left[1 + \frac{|X(f)|^2\sigma_{\mathrm{L}}^2(f)}{T_y\left(S_{\mathrm{nn}}(f) + |X(f)|^2 S_{\mathrm{cc}}(f)\right)}\right]\mathrm{d}f \\ &\text{s.t.} \quad \int_{\mathrm{BW}} |X(f)|^2 \mathrm{d}f \le E_x \end{aligned}. \tag{35}$$

The following function is established by using the Lagrange multiplier method:

$$L\left(|X(f)|^2,\lambda\right) = T_y\int_{\mathrm{BW}} \ln\left[1+\frac{|X(f)|^2\sigma_{\mathrm{L}}^2(f)}{T_y\left(S_{\mathrm{nn}}(f)+|X(f)|^2S_{\mathrm{cc}}(f)\right)}\right]\mathrm{d}f - \lambda\left(\int_{\mathrm{BW}}|X(f)|^2\mathrm{d}f - E_x\right). \tag{36}$$

After removing the integral sign and constant, it is equivalent to maximizing the function $l(|X(f)|^2)$ with the energy spectrum $|X(f)|^2$ of transmitted waveform, which can be expressed by the following equation:

$$l\left(|X(f)|^2\right) = T_y\ln\left[1+\frac{|X(f)|^2\sigma_{\mathrm{L}}^2(f)}{T_y\left(S_{\mathrm{nn}}(f)+|X(f)|^2S_{\mathrm{cc}}(f)\right)}\right] - \lambda|X(f)|^2. \tag{37}$$

The above-given formula is too complicated, so we adopt the method of symbol substitution to simplify the formula. Let $|X(f)|^2 = x$, $\sigma_{\mathrm{L}}^2(f) = h$, $S_{\mathrm{cc}}(f) = c$, $S_{\mathrm{nn}}(f) = n$, and $T_y = t$; then, equation (37) becomes

$$l(x) = t\ln\left[1+\frac{hx}{t(cx+n)}\right] - \lambda x. \tag{38}$$

Derive $l(x)$ to x as follows:

$$\frac{\mathrm{d}(l(x))}{\mathrm{d}x} = t\frac{1}{1+(hx/t(cx+n))}\frac{ht(cx+n)-htcx}{t^2(cx+n)^2} - \lambda. \tag{39}$$

Let $A = T_y/\lambda$, and set the derivative function to zero to find stagnation point, so

$$\frac{hnt}{[hx+t(n+cx)](cx+n)} - \frac{t}{A} = 0, \tag{40}$$

that is,

$$\left(hc+tc^2\right)x^2 + (hn+2tcn)x + tn^2 - hnA = 0. \tag{41}$$

Then,

$$x = \frac{-(hn+2tcn) \pm \sqrt{(hn+2tcn)^2 - 4(hc+tc^2)(tn^2-hnA)}}{2(hc+tc^2)}. \tag{42}$$

Leaving out the minus sign, we can get

$$x = -\frac{n(h+2tc)}{2c(h+tc)} + \sqrt{\frac{h^2n^2+4Anch^2+4Ahntc^2}{4(hc+tc^2)^2}}. \tag{43}$$

Let

$$d = \frac{tn}{h},$$
$$r = \frac{n(h+2tc)}{2c(h+tc)}, \tag{44}$$
$$s = \frac{nh}{c(h+tc)}.$$

Then,

$$x = -r + \sqrt{r^2 + s(A-d)}. \tag{45}$$

Since the power spectrum density of the transmitted signal is nonnegative, the robust waveform can be expressed as

$$\left|X^{\max\min}(f)\right|^2 = \max\left[-R(f) + \sqrt{R^2(f)+S(f)(A-D(f))}, 0\right], \tag{46}$$

where

$$D(f) = \frac{T_yS_{\mathrm{nn}}(f)}{\sigma_{\mathrm{L}}^2(f)},$$
$$R(f) = \frac{S_{\mathrm{nn}}(f)\left(\sigma_{\mathrm{L}}^2(f)+2T_yS_{\mathrm{cc}}(f)\right)}{2S_{\mathrm{cc}}(f)\left(\sigma_{\mathrm{L}}^2(f)+T_yS_{\mathrm{cc}}(f)\right)}, \tag{47}$$
$$S(f) = \frac{S_{\mathrm{nn}}(f)\sigma_{\mathrm{L}}^2(f)}{S_{\mathrm{cc}}(f)\left(\sigma_{\mathrm{L}}^2(f)+T_yS_{\mathrm{cc}}(f)\right)}.$$

A can be obtained from the following energy constraints:

$$\text{s.t.} \quad \int_{\mathrm{BW}} \max\left[-R(f) + \sqrt{R^2(f)+S(f)(A-D(f))}, 0\right]\mathrm{d}f \le E_x. \tag{48}$$

3.3. First-Order Taylor Approximation. Assume that

$$\left|X^{\max\min}(f)\right|^2 = -R(f) + \sqrt{R^2(f)+S(f)(A-D(f))}. \tag{49}$$

Taylor's first-order approximation is the first two terms of Taylor expansion:

$$f(x) = f'(x_0)x + f(x_0). \tag{50}$$

Let $A - D(f) = x$, $R(f) = r$, and $S(f) = s$; then,

$$\left|X^{\max\min}(f)\right|^2 = -r + \sqrt{r^2 + s(A-d)}. \tag{51}$$

Derive $|X^{\max\min}(f)|^2$ to x as follows:

$$\frac{\mathrm{d}\left|X^{\max\min}(f)\right|^2}{\mathrm{d}x} = \frac{s}{2\sqrt{r^2+sx}}. \tag{52}$$

Taylor's expansion at $x_0 = 0$ is

$$\left.\frac{\mathrm{d}\left|X^{\max\min}(f)\right|^2}{\mathrm{d}x}\right|_{x=0} = \frac{s}{2r} = \frac{nh/(c(h+tc))}{(n(h+2tc))/(c(h+tc))} = \frac{h}{h+2tc}. \tag{53}$$

Let

$$b = \frac{h}{h+2tc}. \tag{54}$$

Then,

$$\left|X^{\max\min}(f)\right|^2 = bx, \tag{55}$$

that is,

$$\left|X^{\max\min}(f)\right|^2 = B(f)(A - D(f)), \tag{56}$$

where

$$B(f) = \frac{\sigma_{\mathrm{L}}^2(f)}{\sigma_{\mathrm{L}}^2(f) + 2T_y S_{\mathrm{cc}}(f)}. \tag{57}$$

4. Robust Waveform Design Based on SINR

It can be seen from the signal model in Figure 1 that

$$y(t) = z(t) + d(t) + n(t). \tag{58}$$

The definition of SINR is the ratio of the useful signal power in the echo to the power of the interference signal plus the noise signal:

$$\mathrm{SINR} = \int_{\mathrm{BW}} \frac{\sigma_Z^2(f)}{S_{\mathrm{nn}}(f) + \sigma_D^2(f)} \mathrm{d}f, \tag{59}$$

where

$$\begin{aligned} \sigma_Z^2(f) &= |X(f)|^2 \sigma_{\mathrm{H}}^2(f), \\ \sigma_D^2(f) &= |X(f)|^2 S_{\mathrm{cc}}(f). \end{aligned} \tag{60}$$

So,

$$\mathrm{SINR} = \int_{\mathrm{BW}} \frac{|X(f)|^2 \sigma_{\mathrm{H}}^2(f)}{S_{\mathrm{nn}}(f) + |X(f)|^2 S_{\mathrm{cc}}(f)} \mathrm{d}f. \tag{61}$$

Similarly, from the above derivation of MI robust waveform, it can be seen that, for SINR, the spectrum corresponding to each sampling frequency still has upper and lower bounds:

$$\begin{aligned} &\mathrm{SINR}\left(\left|X^{\max\min}(f)\right|^2, \sigma_{\mathrm{U}}^2(f)\right)\Big|_{\int_{\mathrm{BW}} |X^{\max\min}(f)|^2 \mathrm{d}f \le E_x} \\ &\ge \mathrm{SINR}\left(\left|X^{\max\min}(f)\right|^2, \sigma_{\mathrm{H}}^2(f)\right)\Big|_{\int_{\mathrm{BW}} |X^{\max\min}(f)|^2 \mathrm{d}f \le E_x} \\ &\ge \mathrm{SINR}\left(\left|X^{\max\min}(f)\right|^2, \sigma_{\mathrm{L}}^2(f)\right)\Big|_{\int_{\mathrm{BW}} |X^{\max\min}(f)|^2 \mathrm{d}f \le E_x} \\ &\ge \mathrm{SINR}\left(|X(f)|^2, \sigma_{\mathrm{L}}^2(f)\right)\Big|_{\int_{\mathrm{BW}} |X(f)|^2 \mathrm{d}f \le E_x}. \end{aligned} \tag{62}$$

The problem of optimizing the SINR can be expressed as

$$\begin{aligned} &\max \quad \int_{\mathrm{BW}} \frac{|X(f)|^2 \sigma_{\mathrm{L}}^2(f)}{S_{\mathrm{nn}}(f) + |X(f)|^2 S_{\mathrm{cc}}(f)} \mathrm{d}f \\ &\text{s.t.} \quad \int_{\mathrm{BW}} |X(f)|^2 \mathrm{d}f \le E_x \end{aligned}. \tag{63}$$

The following function is established by using the Lagrange multiplier method:

$$\begin{aligned} L\left(|X(f)|^2, \lambda\right) = &\int_{\mathrm{BW}} \frac{|X(f)|^2 \sigma_{\mathrm{L}}^2(f)}{S_{\mathrm{nn}}(f) + |X(f)|^2 S_{\mathrm{cc}}(f)} \mathrm{d}f \\ &- \lambda\left(\int_{\mathrm{BW}} |X(f)|^2 \mathrm{d}f - E_x\right). \end{aligned} \tag{64}$$

After removing the integral sign and constant, it is equivalent to maximizing the function $l(|X(f)|^2)$ with the energy spectrum $|X(f)|^2$ of the transmitted waveform, which can be expressed by the following equation:

$$l\left(|X(f)|^2\right) = \frac{|X(f)|^2 \sigma_{\mathrm{L}}^2(f)}{S_{\mathrm{nn}}(f) + |X(f)|^2 S_{\mathrm{cc}}(f)} - \lambda |X(f)|^2. \tag{65}$$

The above formula is too complicated, so we take the method of symbol substitution to simplify the formula. Let $|X(f)|^2 = x$, $\sigma_{\mathrm{L}}^2(f) = h$, $S_{\mathrm{cc}}(f) = c$, $S_{\mathrm{nn}}(f) = n$, and $T_y = t$; then, the above equation becomes

$$l(x) = \frac{hx}{cx + n} - \lambda x. \tag{66}$$

Derive $l(x)$ to x as follows:

$$\frac{\mathrm{d}(l(x))}{\mathrm{d}x} = \frac{h(cx + n) - hcx}{(cx + n)^2} - \lambda. \tag{67}$$

We let $A = \sqrt{1/\lambda}$ and set the derivative function to zero to find stagnation point, so

$$\frac{nh}{(cx + n)^2} = \frac{1}{A^2}, \tag{68}$$

that is,

$$c^2 x^2 + 2cnx + n^2 - nhA^2 = 0. \tag{69}$$

Then,

$$x = \frac{-2cn \pm \sqrt{4c^2 n^2 - 4c^2 (n^2 - nhA^2)}}{2c^2}. \tag{70}$$

Leaving out the minus sign, we get

$$x = -\frac{n}{c} + \sqrt{\frac{4nhA^2 c^2}{4c^4}} = \frac{A\sqrt{nh} - n}{c}. \tag{71}$$

Set

$$\begin{aligned} d &= \sqrt{\frac{n}{h}}, \\ b &= \frac{\sqrt{nh}}{c}. \end{aligned} \tag{72}$$

Then,

$$x = b(A - d). \tag{73}$$

Since the power spectrum density of the transmitted signal is nonnegative, the robust waveform can be expressed as

$$\left|X^{\max\min}(f)\right|^2 = \max[B(f)(A - D(f)), 0], \tag{74}$$

where

$$D(f) = \sqrt{\frac{S_{\mathrm{nn}}(f)}{\sigma_{\mathrm{L}}^2(f)}},$$
$$B(f) = \frac{\sqrt{S_{\mathrm{nn}}(f)\sigma_{\mathrm{L}}^2(f)}}{S_{\mathrm{cc}}(f)}. \tag{75}$$

A can be obtained from the following energy constraints:

$$\text{s.t.} \quad \int_{\mathrm{BW}} \max[B(f)(A - D(f)), 0]\mathrm{d}f \le E_x. \tag{76}$$

5. Search of Lagrange Multipliers Based on Bisection Algorithm

The abovementioned robust transmitted waveform based on SINR and MI has been obtained as

$$\left|X^{\max\min}(f)\right|^2 = \max[B(f)(A - D(f)), 0], \tag{77}$$

where $B(f)$, A, and $D(f)$ have different values based on different criteria, and $A = 1/\lambda$ based on SINR, $A = T_y/\lambda$ based on MI. As for how to find the value of A, this paper adopts successive bisection algorithm to search it.

The idea of bisection algorithm is continuous split in half, which is a very classic algorithm. We suppose that $[a, b]$ is the closed interval over the real number field, and define the interval sequence as follows: $[a_n, b_n]$, $a_0 = a$, and $b_0 = b$. And for any natural number n, $[a_{n+1}, b_{n+1}]$ is equal to $[a_n, c_n]$ or $[c_n, b_n]$, where c_n is the midpoint of $[a_n, b_n]$. When using bisection algorithm to search approximation, the data should be arranged in order of size.

Examples are given to illustrate the realization process of bisection algorithm, such as using bisection algorithm to find the zero point of the function. Set the function $f(x) = x^4 + x - 1$. Because the function is continuous, and $f(0) < 0$, $f(1) > 0$, the function must have zero point in the interval $[0, 1]$. Now, use bisection algorithm to find the zero point, take the midpoint 0.5 of interval $[0, 1]$, and get $f(0.5) < 0$. Therefore, we can narrow down the range of interval. Next, take the midpoint 0.75 of interval $[0.5, 1]$, and continue to compare $f(0.75)$ with 0, until the error is within the allowable range; then, we can consider this point as the zero point of the function. Figure 2 shows a flowchart of bisection algorithm.

The principle used to search Lagrange multiplier A is similar. Find the value interval of A, take the midpoint, substitute in to find $|X^{\max\min}(f)|^2$, and compare the relationship between $\int_{\mathrm{BW}}|X^{\max\min}(f)|^2\mathrm{d}f$ and E_x. Make successive approximation by bisection algorithm and assume the allowable error is *eps*, until $|\int_{\mathrm{BW}}|X^{\max\min}(f)|^2\mathrm{d}f - E_x| \le \mathrm{eps}$, and it can be considered that A meets the condition.

In this paper, the scope of A is shown as follows:

$$A_{\min} = \min[D(f)],$$
$$A_{\max} = \frac{E_x}{\mathrm{BW}\min[B(f)]} + \max[D(f)]. \tag{78}$$

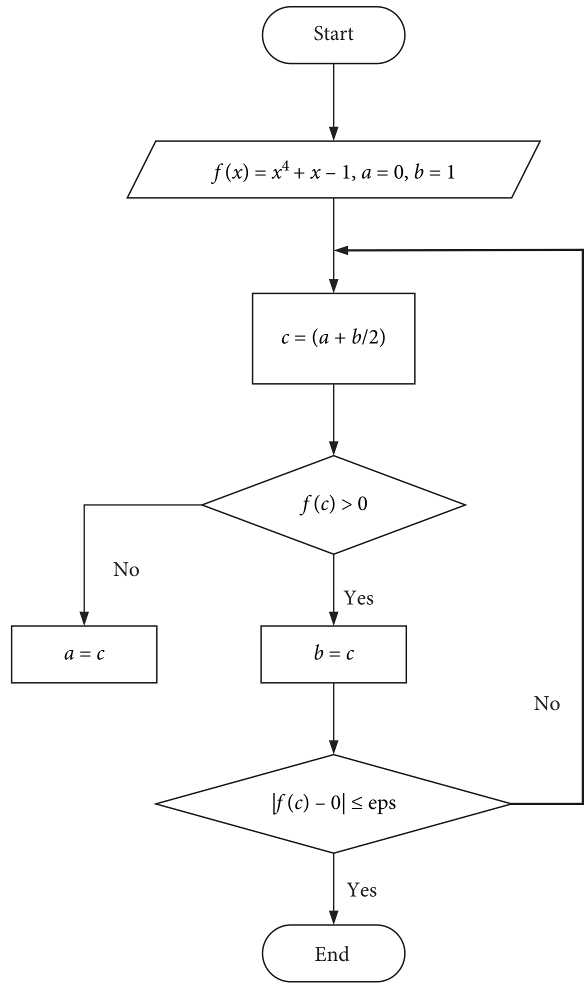

Figure 2: Flowchart of bisection algorithm.

Let $a_0 = A_{\min}$ and $b_0 = A_{\max}$. By using the energy constraint, the value of the optimal A can be approached step by step.

6. Maximum Marginal Allocation

The amount of a certain resource is limited. If resources are invested in a variety of activities, the problem of how to allocate resources to achieve the optimal total effect will arise. This is resource allocation problem. We can regard the energy allocation of transmitted waveform as a resource allocation problem, which solves the optimization problem of a single constraint. That is, how to allocate the energy of transmitted waveform to achieve the most effective result under the condition of energy constraint.

As for how to allocate the energy of the transmitted waveform in a certain frequency band, we can regard it as a multistage decision process of dynamic programming. In each stage, a decision needs to be made on the allocation of energy. The finite energy E_x is allocated to different f_k to maximize the overall mutual information or signal-to-interference-plus-noise ratio.

The integral form of mutual information is discretized to obtain

$$\mathrm{MI} = T_y \sum_{k=1}^{N} \ln\left[1 + \frac{\left|X(f_k)\right|^2 \sigma_{\mathrm{L}}^2(f_k)}{T_y\left(S_{\mathrm{nn}}(f_k) + \left|X(f_k)\right|^2 S_{\mathrm{cc}}(f_k)\right)}\right]\Delta f. \tag{79}$$

Similarly,

$$\mathrm{SINR} = \sum_{k=1}^{N} \frac{\left|X(f_k)\right|^2 \sigma_{\mathrm{L}}^2(f_k)}{S_{\mathrm{nn}}(f_k) + \left|X(f_k)\right|^2 S_{\mathrm{cc}}(f_k)}\Delta f, \tag{80}$$

where

$$f_k = k\Delta f, \qquad \Delta f = \frac{\mathrm{BW}}{N}. \tag{81}$$

The above formula is too complex, and we adopt the method of symbol substitution to simplify the formula. Let

$$\begin{aligned} x(k) &= \left|X(f_k)\right|^2, \\ \alpha_1(k) &= \frac{T_y S_{\mathrm{cc}}(f_k)}{\sigma_{\mathrm{L}}^2(f_k)}, \\ \alpha_2(k) &= \frac{S_{\mathrm{cc}}(f_k)}{\sigma_{\mathrm{L}}^2(f_k)}, \\ \beta_1(k) &= \frac{T_y S_{\mathrm{nn}}(f_k)}{\sigma_{\mathrm{L}}^2(f_k)}, \\ \beta_2(k) &= \frac{S_{\mathrm{nn}}(f_k)}{\sigma_{\mathrm{L}}^2(f_k)}. \end{aligned} \tag{82}$$

So, MI and SINR can be abbreviated as

$$\begin{aligned} \mathrm{MI} &= T_y \sum_{k=1}^{N} \ln\left[1 + \frac{x(k)}{\alpha_1(k)x(k) + \beta_1(k)}\right]\Delta f, \\ \mathrm{SINR} &= \sum_{k=1}^{N} \frac{x(k)}{\alpha_2(k)x(k) + \beta_2(k)}\Delta f. \end{aligned} \tag{83}$$

Energy constraint is

$$\sum_{k=1}^{N} x(k) = \frac{E_x}{\Delta f} = X_{\max}. \tag{84}$$

Under the above energy constraints, we seek the maximization of

$$\sum_{k=1}^{N} f(x(k), k), \tag{85}$$

where

$$\begin{aligned} f_{\mathrm{MI}}(x(k), k) &= \ln\left[1 + \frac{x(k)}{\alpha_1(k)x(k) + \beta_1(k)}\right], \\ f_{\mathrm{SINR}}(x(k), k) &= \frac{x(k)}{\alpha_2(k)x(k) + \beta_2(k)}. \end{aligned} \tag{86}$$

The minimum energy distribution unit is defined as ε_0, and the number of energy components is defined as P.

So,

$$\begin{aligned} X_{\max} &= P\varepsilon_0, \\ 0 \le x(k) &\le X_{\max}, \end{aligned} \tag{87}$$

$x(k)$ can be selected in set $\{0, \varepsilon_0, 2\varepsilon_0, 3\varepsilon_0, \ldots\ldots, P\varepsilon_0\}$. The core idea of MMA algorithm is to allocate the energy of ε_0 in each step and allocate all the energy after step P. When ε_0 is set to be very small, P is very large, and the energy allocated in each step will have a tiny impact. We choose the serial number k corresponding to the impact that maximizes mutual information to allocate, so that each step is optimal, so as to achieve the purpose of the overall optimal.

In the first step, for any $k \ne j$, if $f(\varepsilon_0, j) > f(\varepsilon_0, k)$, it is optimal for $k = j$. Let $x(j) = \varepsilon_0$, and assign a unit of energy to it. Since the first step has already allocated a share of the energy, in the second step, for $k = j$, we compare the edge increase by $f(2\varepsilon_0, j) - f(\varepsilon_0, j)$. So, $\{f(\varepsilon_0, 1), f(\varepsilon_0, 2), \ldots\ldots, f(\varepsilon_0, j-1), f(2\varepsilon_0, j) - f(\varepsilon_0, j), f(\varepsilon_0, j+1), \ldots\ldots, f(\varepsilon_0, N)\}$. The second step is to find the maximum value in the above set and assign a unit of energy to it. Similarly, after step P, all the energy is allocated, that is,

$$\begin{aligned} x(k) &= a_k\varepsilon_0, \ (k = 1, 2, \ldots\ldots, N), \\ \sum_{k=1}^{N} a_k &= P. \end{aligned} \tag{88}$$

The flowchart is shown in Figure 3.

In order to understand the algorithm of MMA, an example is given. For example, the frequency domain is discretized into four components ($N = 4$). Let $X_{\max} = 5$, which is $x(1) + x(2) + x(3) + x(4) = 5$. To maximize M,

$$M = f(x(1), 1) + f(x(2), 2) + f(x(3), 3) + f(x(4), 4) \tag{89}$$

According to the different criteria MI and SINR, M can be divided into

$$\begin{aligned} M_1 &= \sum_{k=1}^{4} \ln\left[1 + \frac{x(k)}{\alpha_1(k)x(k) + \beta_1(k)}\right], \\ M_2 &= \sum_{k=1}^{4} \frac{x(k)}{\alpha_2(k)x(k) + \beta_2(k)}. \end{aligned} \tag{90}$$

Let $\varepsilon_0 = 1$, so with total energy $X_{\max} = 5$, you can distribute 0, 1, 2, 3, 4, or 5 units of energy to $x(1)$, $x(2)$, $x(3)$, or $x(4)$.

The corresponding values of $f_{\mathrm{MI}}(x(k), k)$ and $f_{\mathrm{SINR}}(x(k), k)$ are shown in Tables 1 and 2, when initial allocation of energy. The underlined value is the maximum marginal growth at this time.

Taking mutual information as an example, the realization process of MMA algorithm is illustrated. When the initial energy is allocated by Table 1, for $k = 1, 2, 3, 4$, $f_{\mathrm{MI}}(x(k), k)$ is 0.0708, 0.0793, 0.0880, 0.0969, respectively. Find the maximum value 0.0969 and allocate a unit of energy

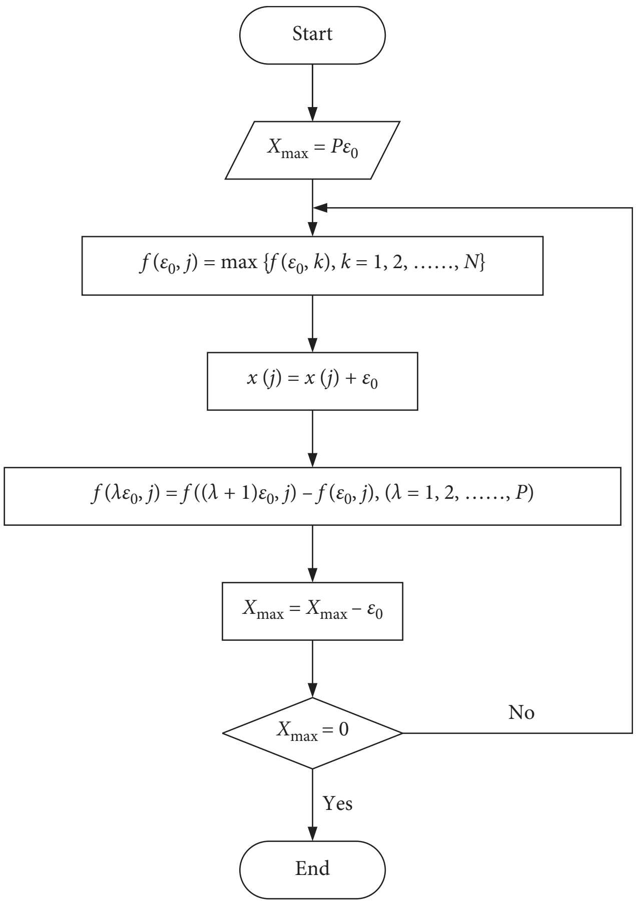

Figure 3: Flowchart of MMA algorithm.

Table 1: $f_{MI}(x(k), k)$ corresponding to different $x(k)$.

	$k = 1$	$k = 2$	$k = 3$	$k = 4$
$x(k) = 0$	0	0	0	0
$x(k) = 1$	0.0708	0.0793	0.0880	0.0969
$x(k) = 2$	0.0892	0.0998	0.1108	0.1219
$x(k) = 3$	0.0977	0.1092	0.1212	0.1334
$x(k) = 4$	0.1025	0.1147	0.1272	0.1400
$x(k) = 5$	0.1057	0.1182	0.1311	0.1443

Table 2: $f_{SINR}(x(k), k)$ corresponding to different $x(k)$.

	$k = 1$	$k = 2$	$k = 3$	$k = 4$
$x(k) = 0$	0	0	0	0
$x(k) = 1$	0.7337	0.8248	0.9200	1.0177
$x(k) = 2$	0.9329	1.0495	1.1714	1.2966
$x(k) = 3$	1.0258	1.1543	1.2888	1.4270
$x(k) = 4$	1.0795	1.2150	1.3568	1.5026
$x(k) = 5$	1.1146	1.2546	1.4012	1.5519

to $k = 4$. When the second energy is allocated by Table 3, the key is the marginal growth when $k = 4$. Find the maximum value 0.0880 and allocate a unit of energy to $k = 3$. Similarly, the next steps are the same. Tables 4–6 summarize the final energy distribution. In the end, the maximum mutual information is 0.3600 and two parts of energy are allocated to $k = 4$, and one part of energy is allocated to all the other parts, which is

$$x(1) = x(2) = x(3) = \varepsilon_0, x(4) = 2\varepsilon_0. \quad (91)$$

7. Simulation Results and Analysis

7.1. SINR and MI in Three Cases. The power spectral density of noise is

$$S_{nn}(f) = 1. \quad (92)$$

The frequency range is $[-0.5, 0.5]$, and the number of sampling points is $N = 256$. The energy range of the transmitted waveform is $[1, 10]$. It is assumed that the upper and lower bounds of the uncertainty range of the target spectrum conform to the uniform distribution on $[0, |H(f)|]$.

As can be seen from Figure 4, the target spectrum is mainly concentrated around the frequency of −0.2 and 0.4 and is less subject to clutter interference around 0.2. Therefore, the energy distribution of the transmitted waveform is mainly concentrated around −0.2, 0.2, and 0.4, so that a larger mutual information or signal-to-interference-plus-noise ratio can be obtained, so as to obtain better target estimation performance.

Under the three conditions including known target spectrum, known target spectrum lower bound (worst case), and known target spectrum upper bound (best case), and energy from 1 to 10 is allocated to the transmitted waveform, we compare the size of SINR.

From the above Figures 5–7, we can conclude that the SINR obtained from the upper bound waveform and the optimal waveform is very close when the target spectrum is known or under the most favorable case (upper bound). When the target spectrum is known, the SINR obtained from the optimal waveform is larger, and under the most favorable case (upper bound), the SINR obtained from the upper bound waveform is larger. However, in real scenarios, the real target spectrum cannot be captured with complete precision. In the worst case (lower bound), the SINR is the largest by using the robust waveform, and the difference is more significant than the other two waveforms.

Similarly, the comparison on MI is similar under three conditions including the known target spectrum, the known target spectrum lower bound (the worst case), and the known target spectrum upper bound (the best case).

From Figures 8–10, we can still conclude that when the target spectrum is known or under the most favorable case (upper bound), the MI obtained by the upper bound waveform is very close to that obtained by the optimal waveform. However, in the worst case (lower bound), the maximum MI is obtained by using the robust waveform, and the difference is more significant than by the other two waveforms. Therefore, the robust waveform design scheme based on SINR and MI can improve the performance of radar system under the most unfavorable condition.

Table 3: The marginal value of $f_{\mathrm{MI}}(x(k), k)$ after the first energy allocation.

	$k = 1$	$k = 2$	$k = 3$	$k = 4$
$x(k) = 0$	0	0	0	0
$x(k) = 1$	0.0708	0.0793	0.0880	0.0250
$x(k) = 2$	0.0892	0.0998	0.1108	0.0365
$x(k) = 3$	0.0977	0.1092	0.1212	0.0431
$x(k) = 4$	0.1025	0.1147	0.1272	0.0474
$x(k) = 5$	0.1057	0.1182	0.1311	—

Table 4: The marginal value of $f_{\mathrm{MI}}(x(k), k)$ after the second energy allocation.

	$k = 1$	$k = 2$	$k = 3$	$k = 4$
$x(k) = 0$	0	0	0	0
$x(k) = 1$	0.0708	0.0793	0.0228	0.0250
$x(k) = 2$	0.0892	0.0998	0.0332	0.0365
$x(k) = 3$	0.0977	0.1092	0.0392	0.0431
$x(k) = 4$	0.1025	0.1147	0.0431	0.0474
$x(k) = 5$	0.1057	0.1182	—	—

Table 5: The marginal value of $f_{\mathrm{MI}}(x(k), k)$ after the third energy allocation.

	$k = 1$	$k = 2$	$k = 3$	$k = 4$
$x(k) = 0$	0	0	0	0
$x(k) = 1$	0.0708	0.0205	0.0228	0.0250
$x(k) = 2$	0.0892	0.0299	0.0332	0.0365
$x(k) = 3$	0.0977	0.0354	0.0392	0.0431
$x(k) = 4$	0.1025	0.0389	0.0431	0.0474
$x(k) = 5$	0.1057	—	—	—

Table 6: Final energy allocation.

Step	$k = 1$	$k = 2$	$k = 3$	$k = 4$	f_{MI}
1				ε_0	0.0969
2			ε_0		0.1849
3		ε_0			0.2642
4	ε_0				0.3350
5				ε_0	0.3600
	ε_0	ε_0	ε_0	$2\varepsilon_0$	—

7.2. Effect of T_y on SINR and MI. When $T_y = 0.01$, the energy distribution of transmitted waveform calculated based on SINR criterion and MI criterion and the resulting mutual information comparison are shown in Figure 11.

It can be seen that in the three cases, the mutual information is all largest based on MI criterion.

However, when $T_y = 1$, the transmitted waveform energy distribution based on SINR criterion and MI criterion is obtained, and the resulting mutual information comparison is shown in Figure 12.

At this time, the mutual information obtained based on the SINR criterion is the largest.

For signal-to-interference-plus-noise ratio, the comparison based on SINR and MI criteria is similar.

It can be inferred from Figures 13 and 14 that when T_y is large, the SINR criterion is better than the MI criterion, but when T_y is small, the MI criterion is better than the SINR criterion, in which, for signal to interference noise ratio, SINR is better than MI in the most unfavorable case.

For this, we select one of the three cases and allocate certain energy to verify the influence of the size of T_y on SINR and MI. For example, we select the robust transmitted waveform under the most unfavorable condition and allocate 5 units of energy.

Since the formula of SINR is independent of T_y, the value of SINR is constant with respect to the independent variable T_y based on the SINR criterion. From Figure 15, it can be seen that the SINR criterion is always better than the MI criterion at the most worst case, while in the other two cases, the SINR criterion is better when T_y is large, and the MI criterion is better when T_y is small. At this time, there is a critical value of T_y. In the parameters assumed in this paper, the critical value is around 0.1.

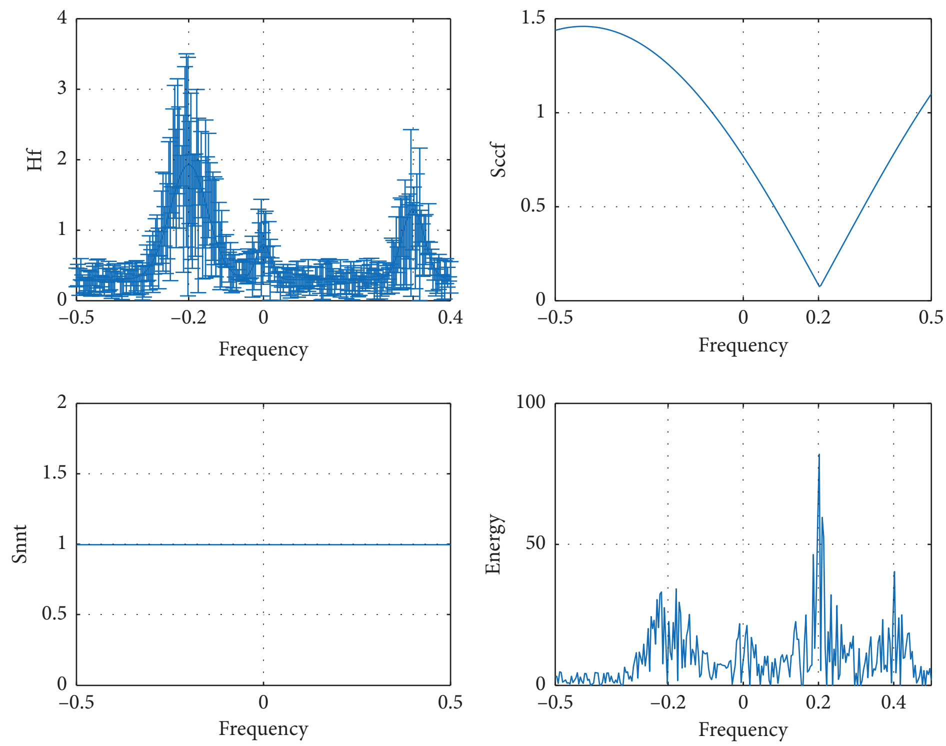

Figure 4: (a) Target spectrum, (b) clutter spectrum, (c) noise spectrum, and (d) transmitted waveform spectrum.

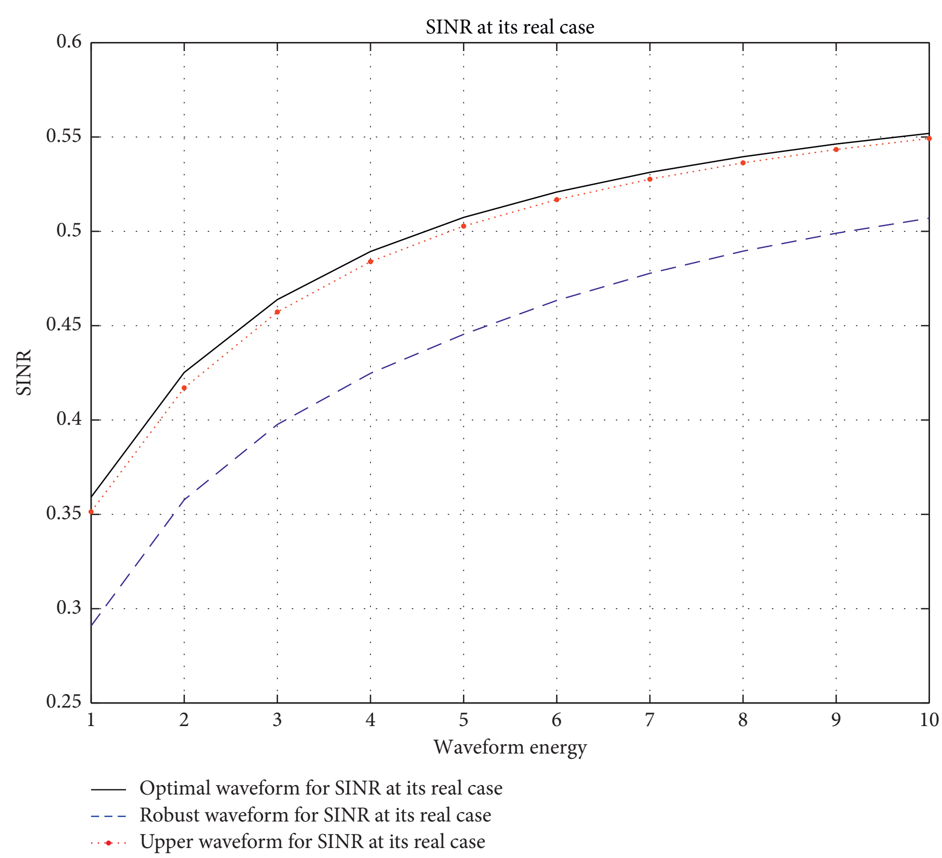

Figure 5: SINR of three waveforms when the real target spectrum is known.

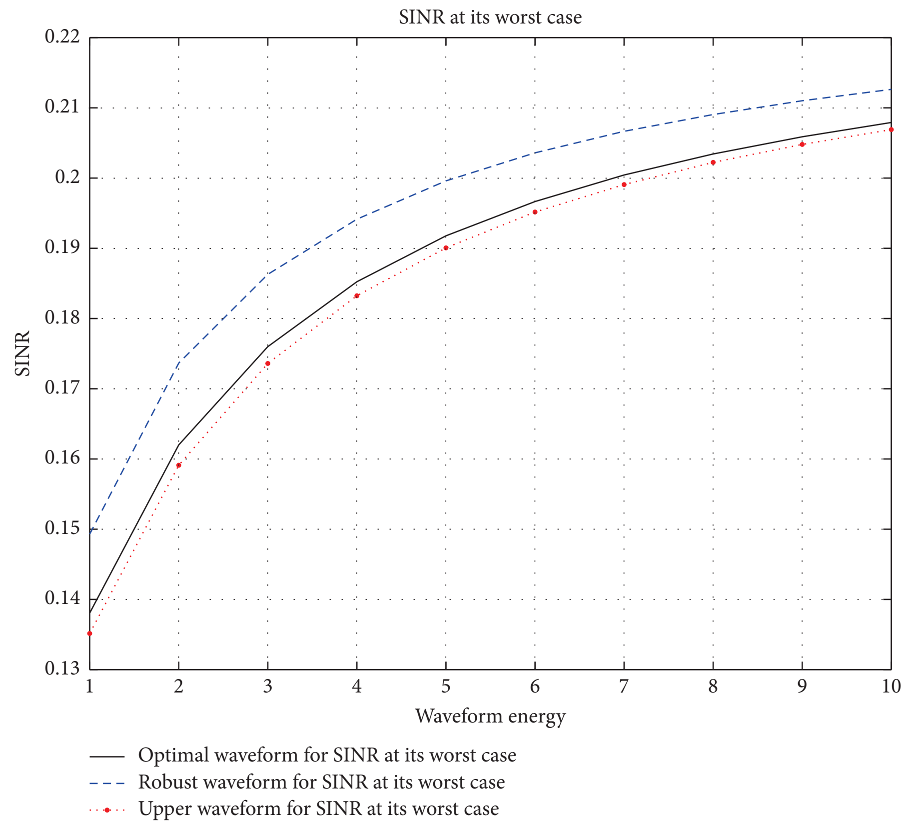

Figure 6: SINR of the three waveforms under the most unfavorable condition.

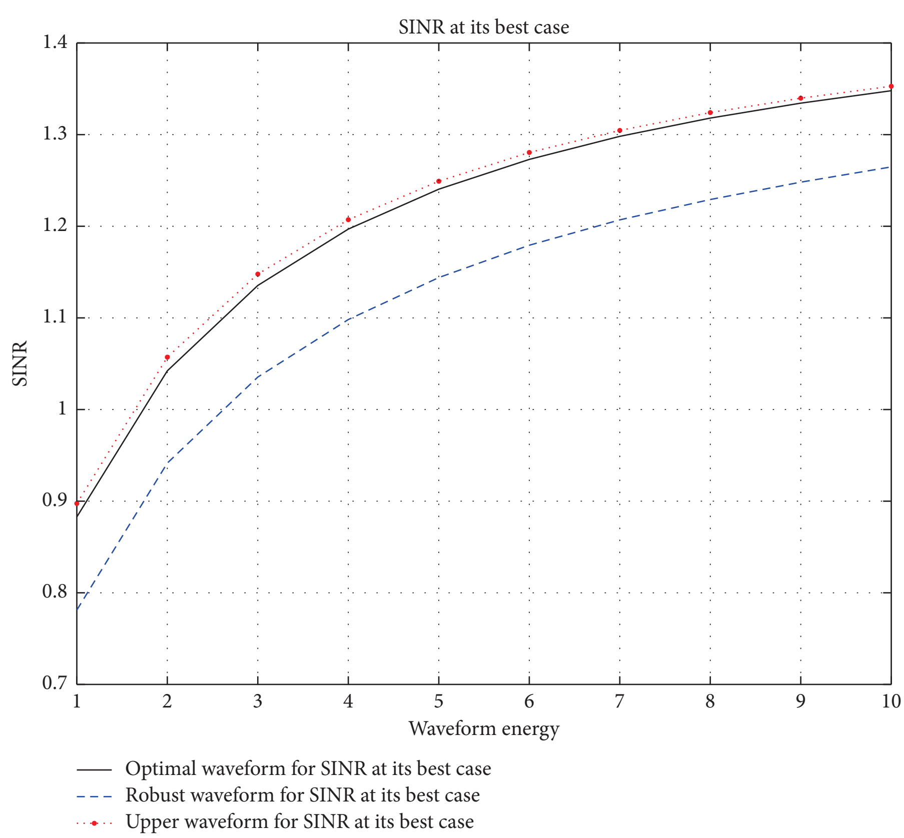

Figure 7: SINR of the three waveforms under the most favorable condition.

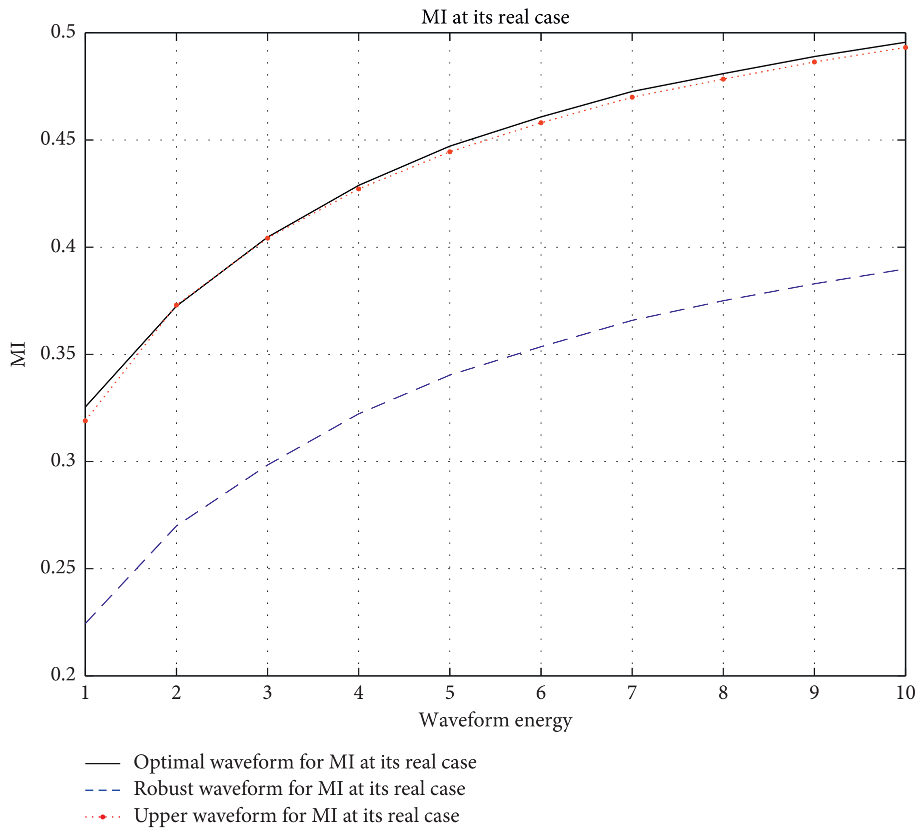

Figure 8: MI of the three waveforms when the real target spectrum is known.

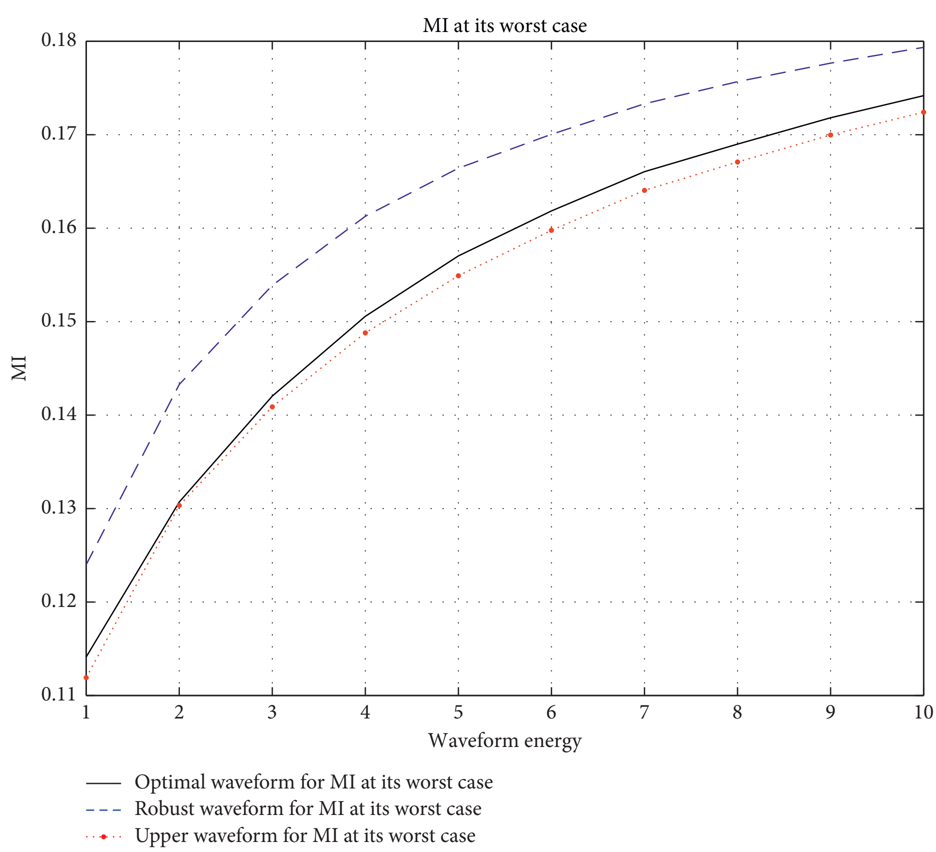

Figure 9: MI of the three waveforms under the most unfavorable condition.

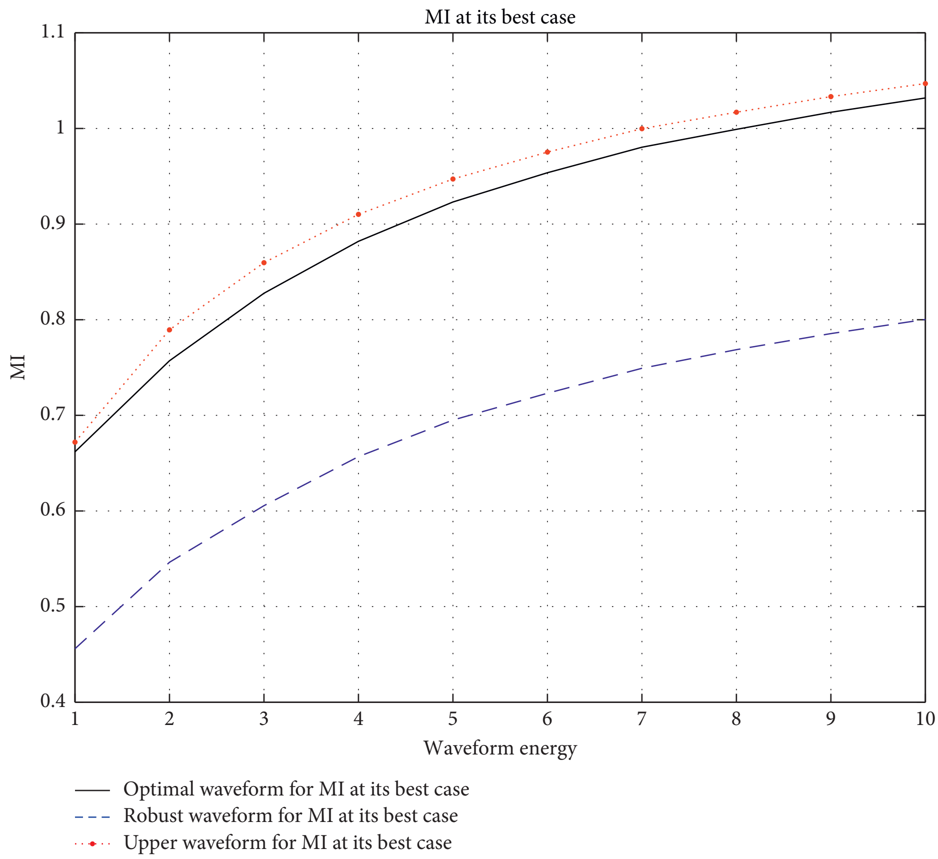

FIGURE 10: MI of the three waveforms under the most favorable condition.

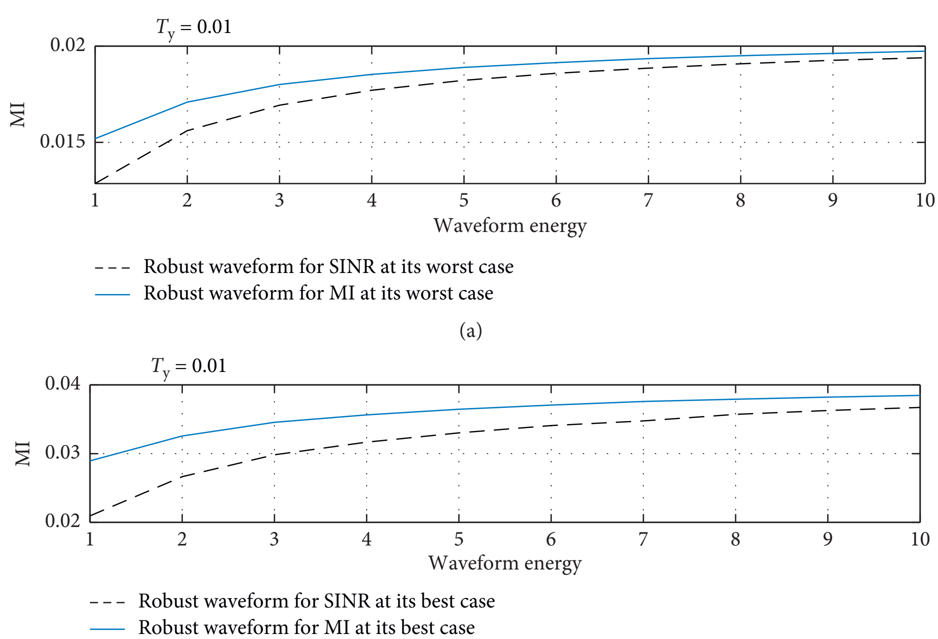

(a)

(b)

FIGURE 11: Continued.

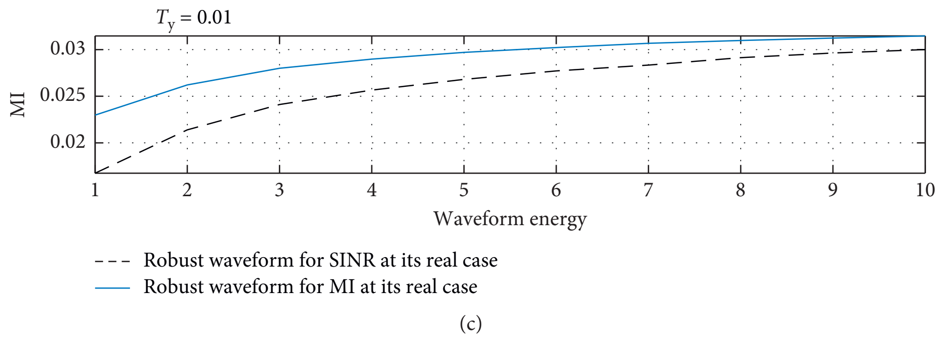

Figure 11: Comparison of MI under three conditions when $T_y = 0.01$. (a) Comparison of MI at its worst case. (b) Comparison of MI at its best case. (c) Comparison of MI at its real case.

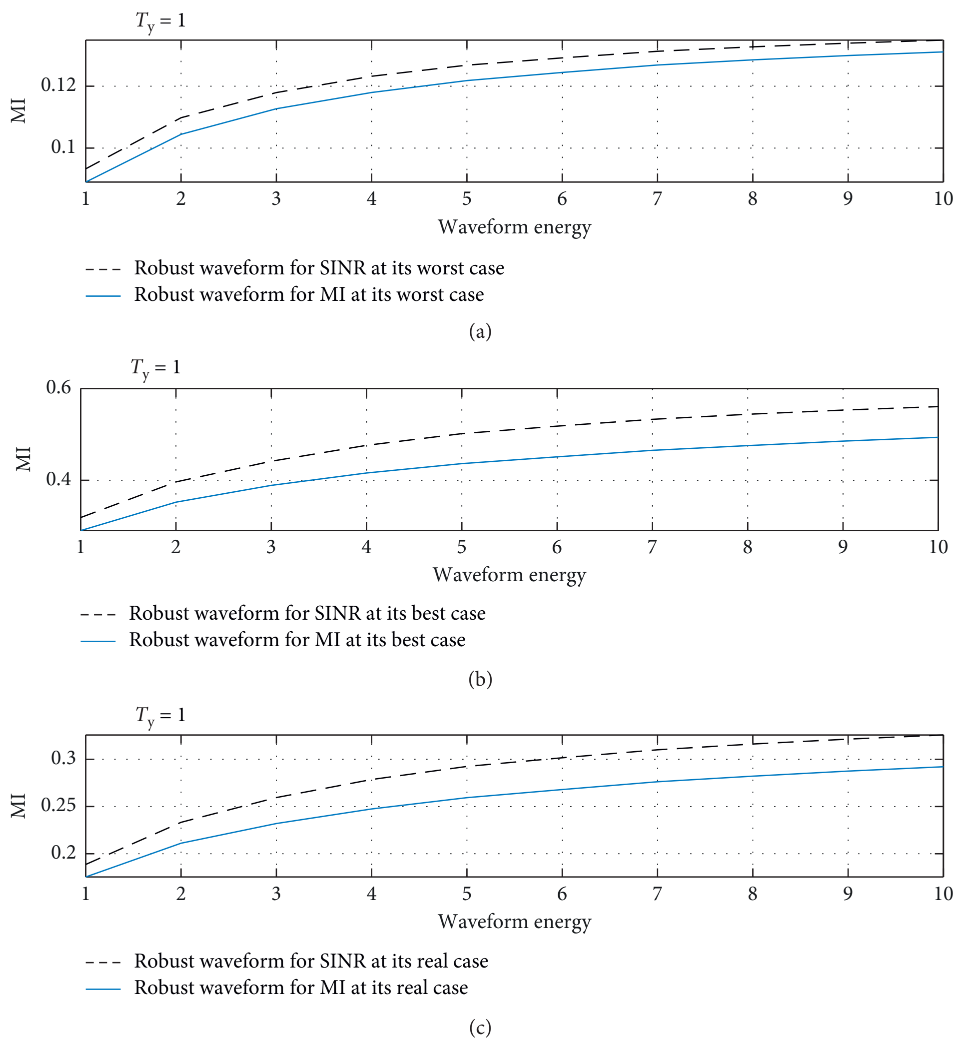

Figure 12: Comparison of MI under three conditions when $T_y = 1$. (a) Comparison of MI at its worst case. (b) Comparison of MI at its best case. (c) Comparison of MI at its real case.

According to Figures 16 and 17, in three cases, when T_y is large, it is better based on SINR criterion, and when T_y is small, it is better based on MI criterion. At this time, the critical value is still around 0.1.

7.3. Comparison of Two Water-Filling Algorithms and MMA. In the case of fixed energy constraint of 10 and $P = 1000$ in MMA algorithm, the energy distribution and SINR of the transmitted waveform obtained by the three methods are shown in Figures 18 and 19.

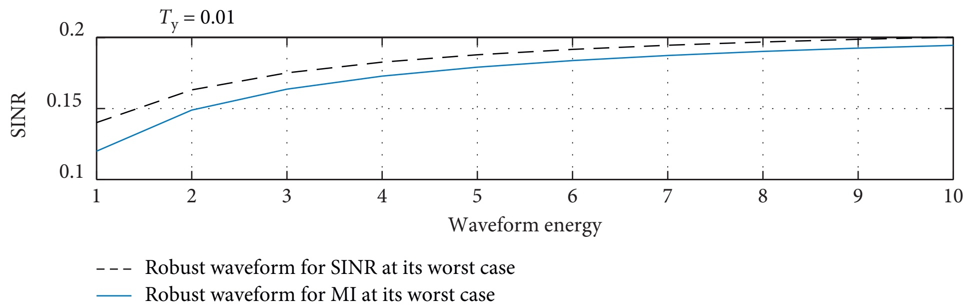

(a)

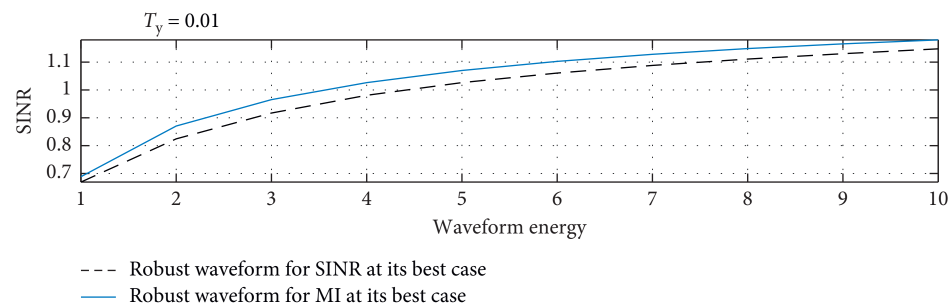

(b)

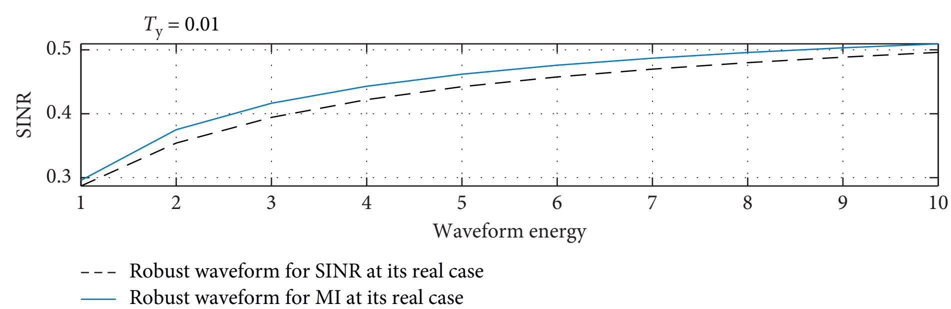

(c)

Figure 13: Comparison of SINR under three conditions when $T_y = 0.01$. (a) Comparison of SINR at its worst case. (b) Comparison of SINR at its best case. (c) Comparison of SINR at its real case.

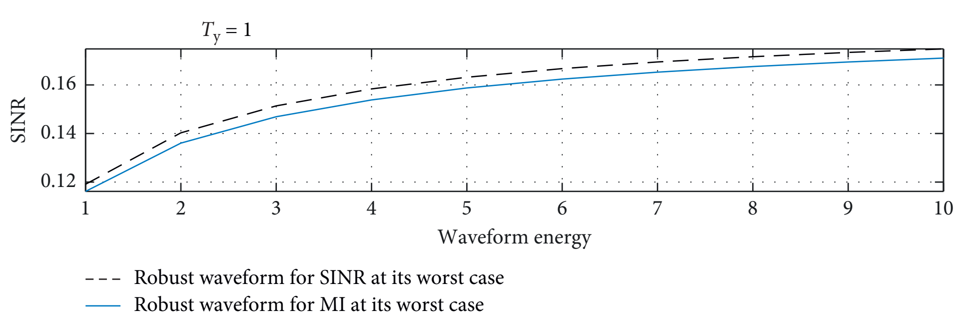

(a)

Figure 14: Continued.

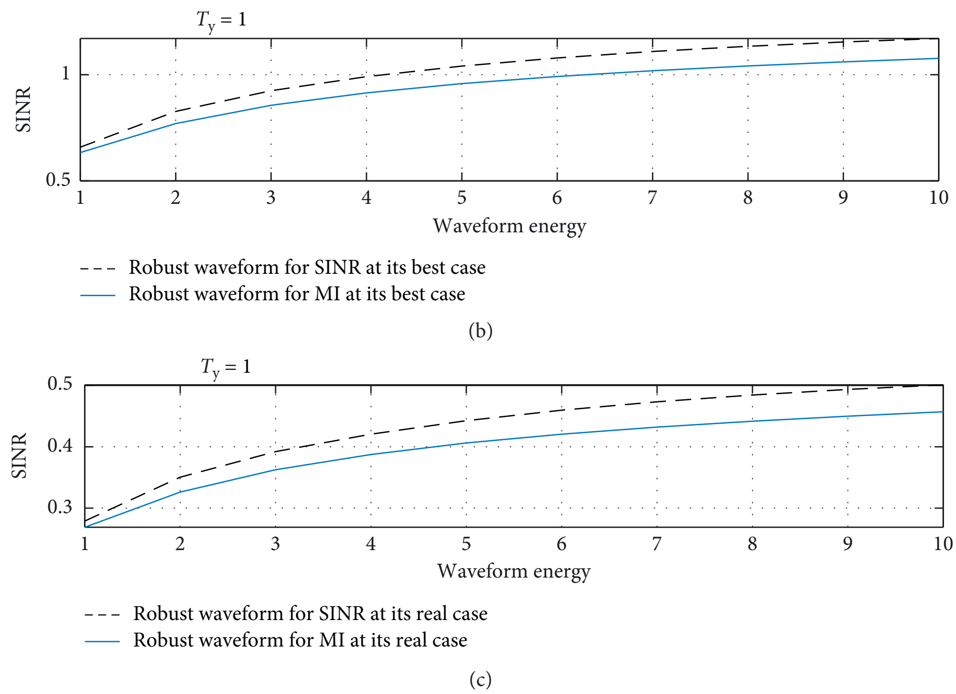

Figure 14: Comparison of SINR under three conditions when $T_y = 1$. (a) Comparison of SINR at its worst case. (b) Comparison of SINR at its best case. (c) Comparison of SINR at its real case.

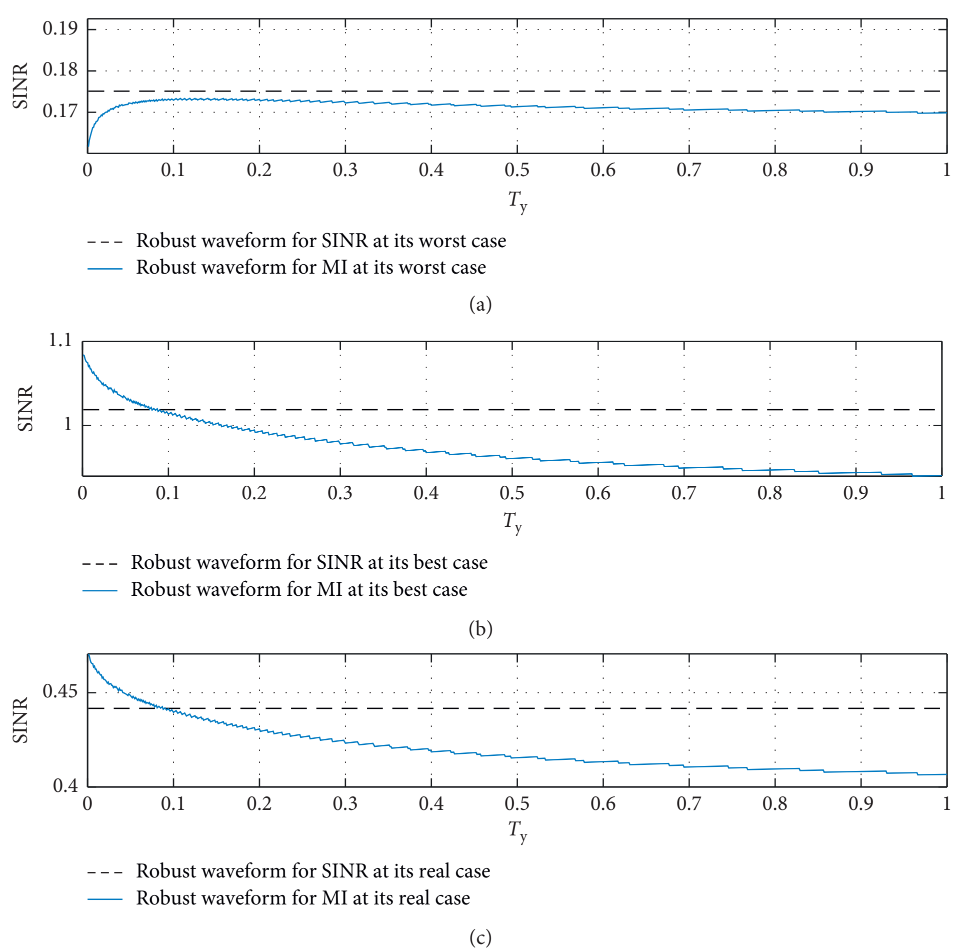

Figure 15: Comparison of SINR under three conditions with the change of T_y. (a) Comparison of SINR at its worst case. (b) Comparison of SINR at its best case. (c) Comparison of SINR at its real case.

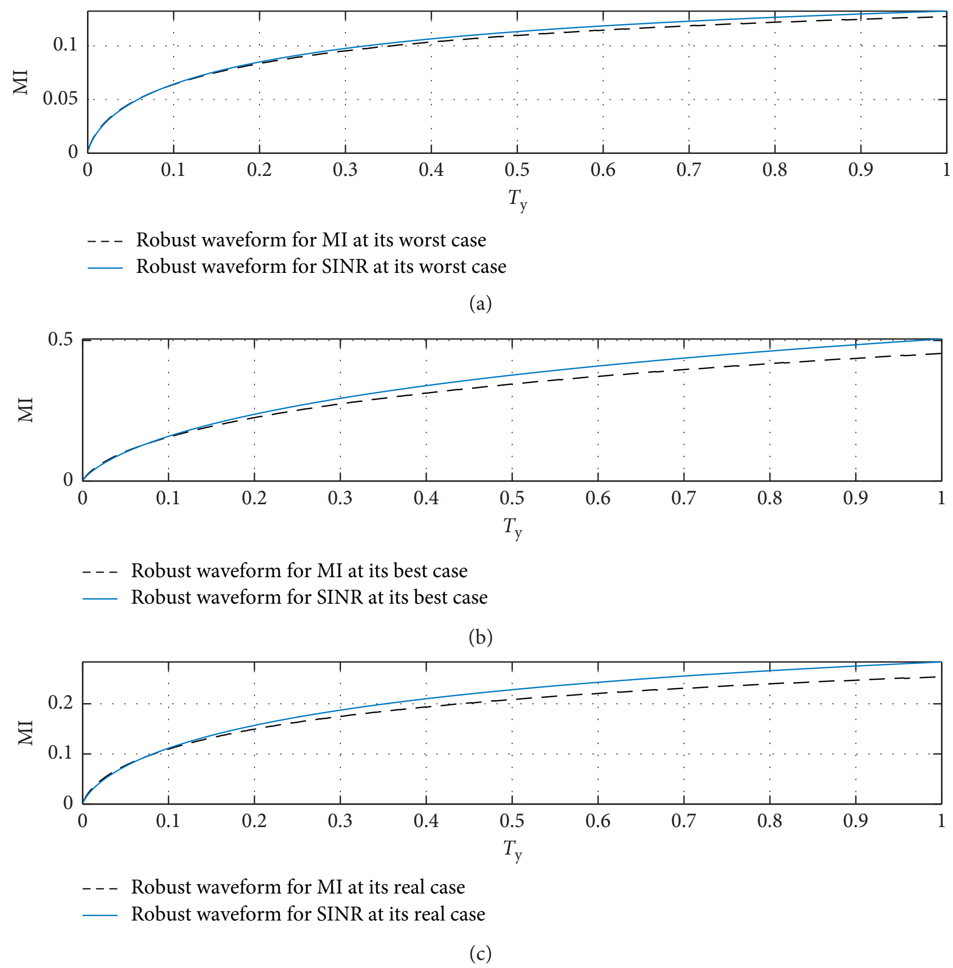

Figure 16: Comparison of MI under three conditions with the change of T_y. (a) Comparison of MI at its worst case. (b) Comparison of MI at its best case. (c) Comparison of MI at its real case.

It can be seen from Figures 18 and 19 that the energy distribution of the transmitted waveform obtained by the three methods is very close, and the energy distribution at the frequency of −0.2, 0.2, and 0.4 is relatively large. Moreover, the signal-to-interference-plus-noise ratio obtained by the three methods almost coincides with each other, so there is not much difference in the performance. In terms of simulation time, the MMA algorithm is greater than the general water-filling algorithm than the bisection water-filling algorithm.

In the case that the fixed energy constraint is 10, $T_y = 10$, and $P = 1000$ in MMA algorithm, the energy distribution and MI of the transmitted waveform obtained by the three methods are shown in the following figures.

It can be seen from Figures 20 and 21 that in terms of energy distribution of transmitted waveform, the two water-filling algorithms distribute the energy more intensively around the frequency of −0.2, while the MMA algorithm distributes the energy in a large number of frequency bands, mainly around −0.2, 0.2, and 0.4. Furthermore, the mutual information obtained by MMA algorithm is significantly larger than that obtained by the two water-filling algorithms. In terms of simulation time, the general water-filling algorithm is longer than the MMA algorithm than the Bisection water-filling algorithm. It can be seen that the use of bisection algorithm to search Lagrange multiplier improves the time performance, while the MMA algorithm is more effective in improving the mutual information between echo and target.

8. Conclusions

This paper studies the transmitted waveform design of cognitive radar. Cognitive radar can obtain information by interacting with the environment and improve the transmitted waveform through by sensing change of the surrounding environment. Most previous researches are based on known a priori information of target and environment. In this paper, considering the uncertainty of target in the real scenario, the robust waveform design technology based on signal-to-interference-plus-noise ratio and mutual information is adopted, and two methods to maximize the performance of MI and SINR are proposed. Firstly, the signal model is established, signal-to-interference-plus-noise ratio and the mutual information between the target and the echo are derived,

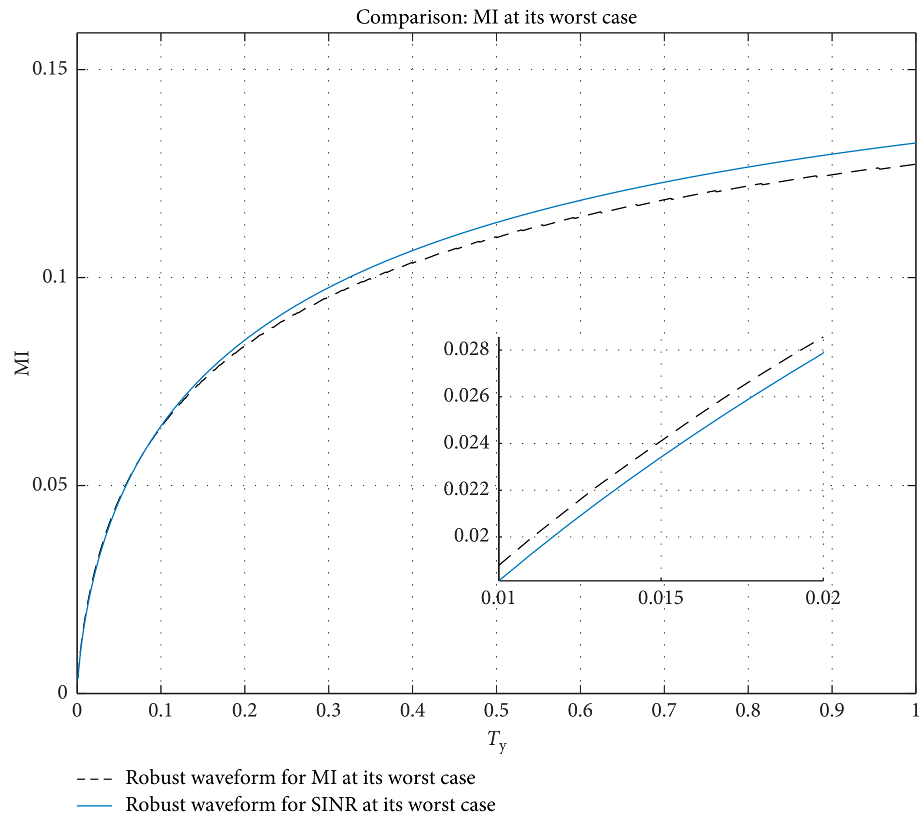

Figure 17: Comparison of MI under the most worst condition with the change of T_y.

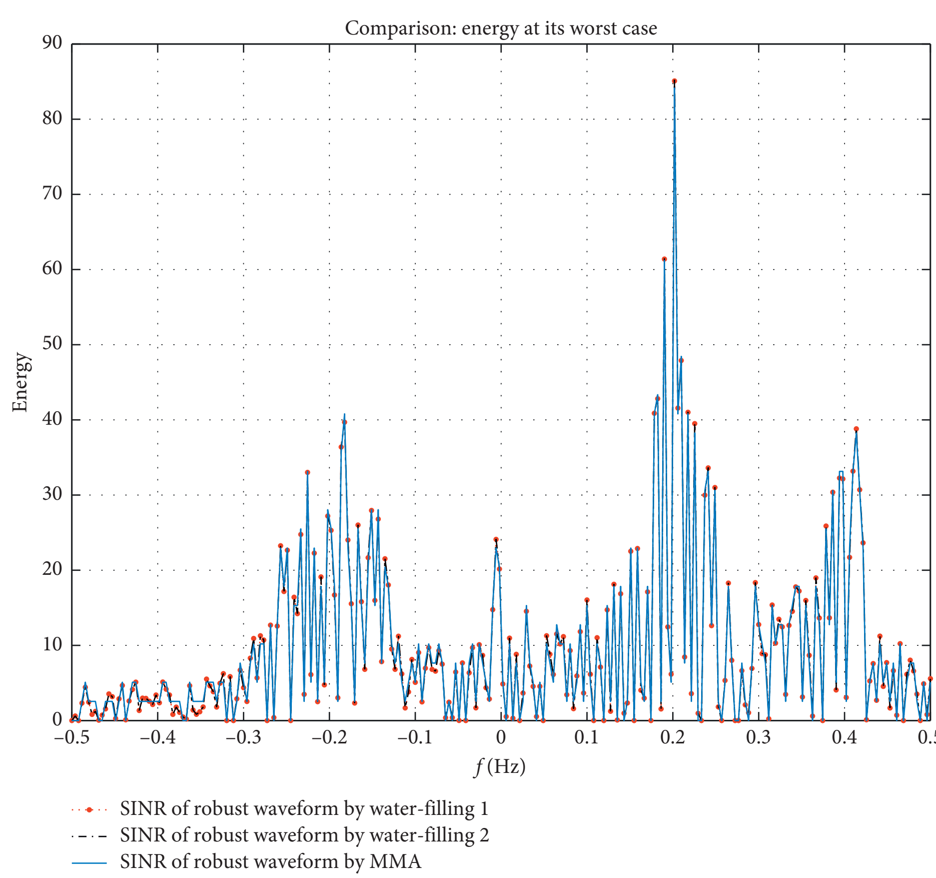

Figure 18: Energy distribution comparison of three SINR-based algorithms for transmitted waveform.

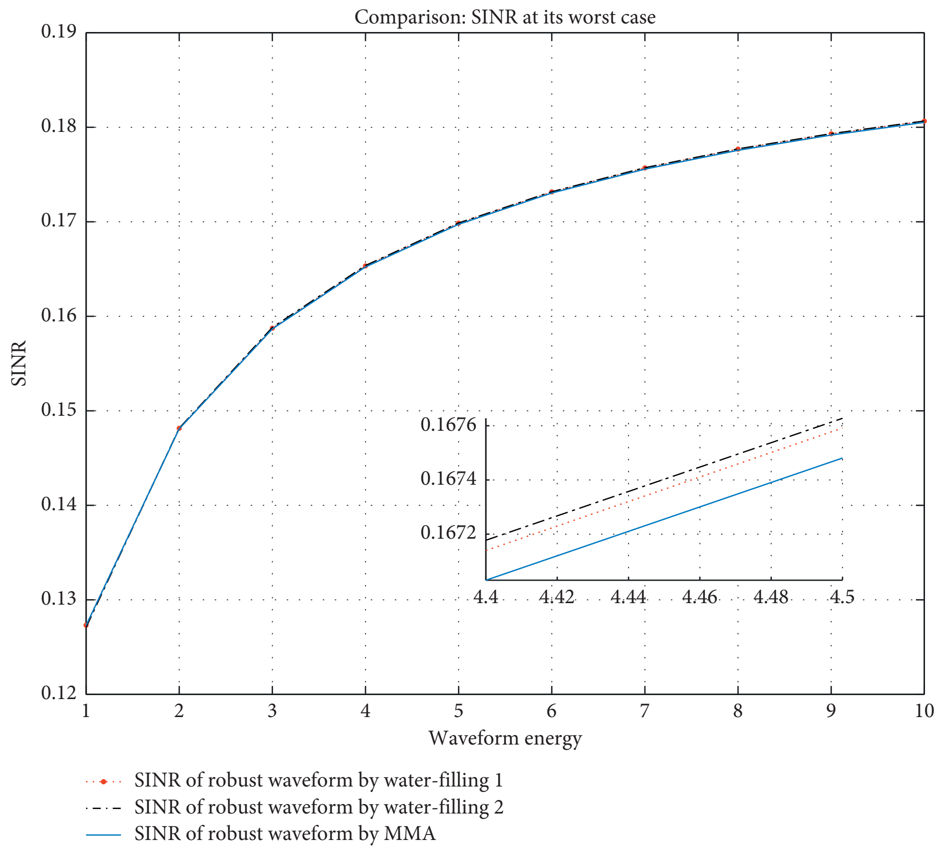

Figure 19: Comparison of SINR of three algorithms.

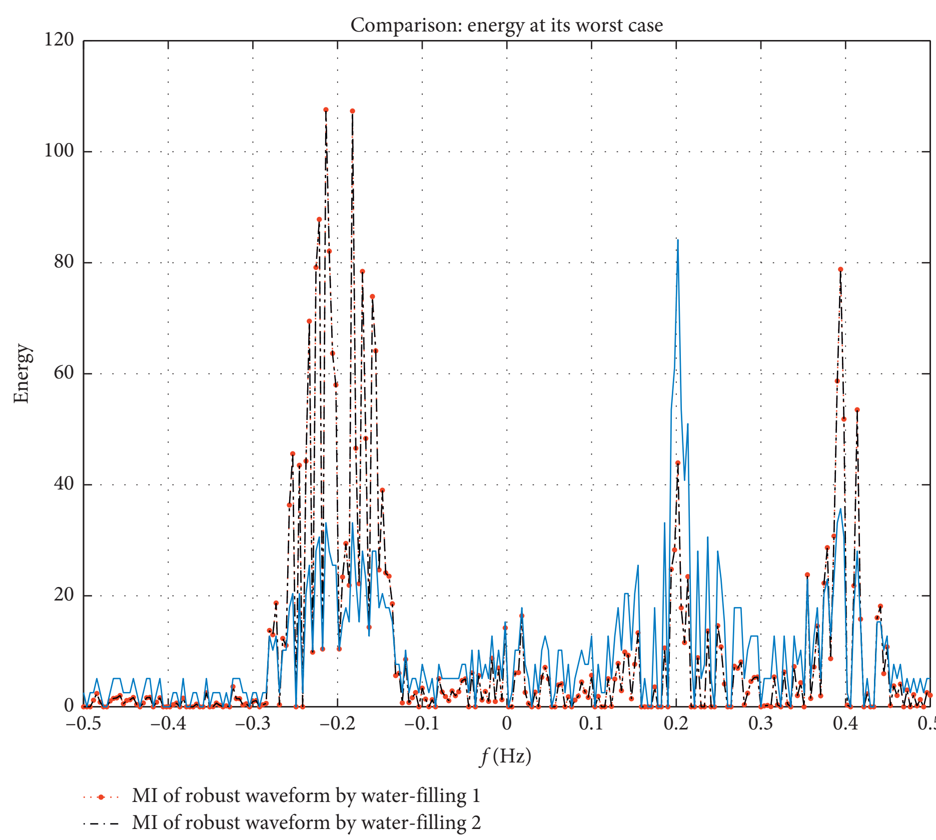

Figure 20: Energy distribution comparison of three MI-based algorithms for transmitted waveform.

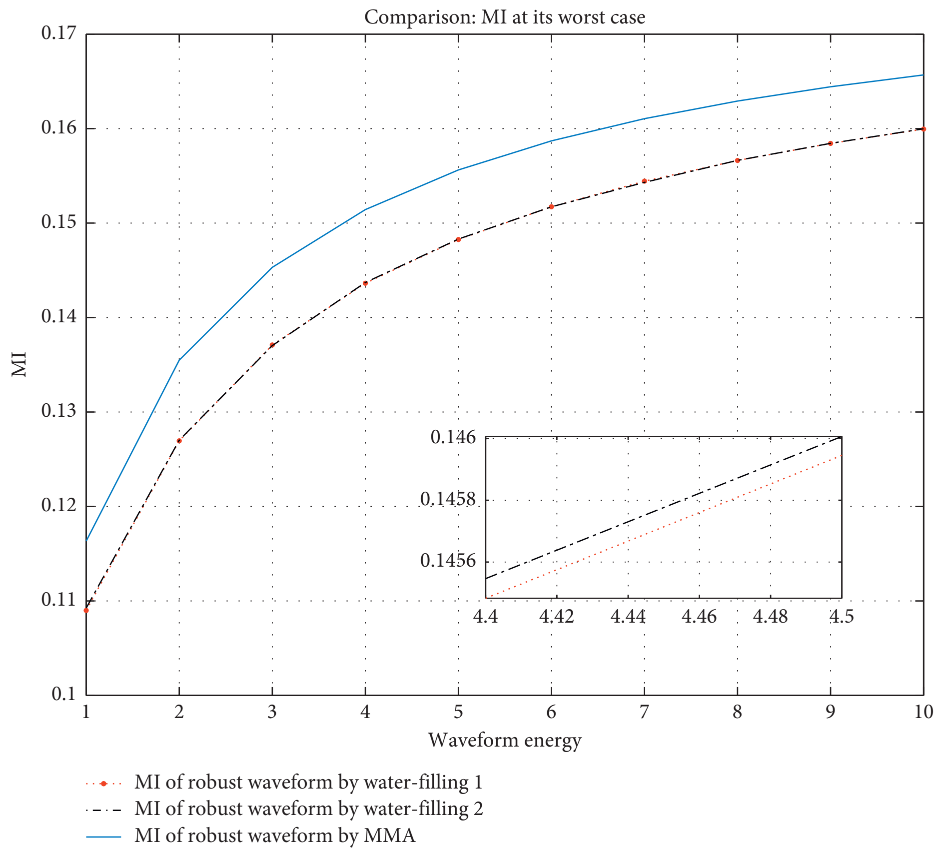

Figure 21: Comparison of MI of three algorithms.

and the robust signal model with upper and lower bounds is established. Then, based on the maximization of MI and SINR, two algorithms are proposed to solve the optimal robust transmitted waveform under the most unfavorable conditions. The traditional water-filling algorithm is improved and the time performance is promoted by using bisection algorithm when searching Lagrange multiplier. The maximum marginal allocation algorithm is introduced to maximize SINR and MI by selecting the optimal allocation of energy at each stage. Under known target spectrum, known target spectrum lower bound (worst case), and known target spectrum upper bound (best case), we simulate and compare the SINR and MI of several waveforms, respectively, and conclude that robust waveforms can improve the performance of the radar system in the most unfavorable situations. This paper also explores the effect of echo observation time on SINR and MI. Simulation results show that there is a critical value for the impact of echo observation time on transmitted waveforms based on different criteria. When the echo observation time is short, the MI-based transmitted waveform is better and when the echo observation time is long, the SINR-based transmitted waveform is more excellent. Finally, the advantages and disadvantages of MMA and two water-filling algorithms are compared, and the results show that the time performance of searching Lagrange multiplier is improved by using bisection algorithm, and the MMA algorithm is more effective in improving the mutual information between echo and target. In terms of signal-to-interference-plus-noise ratio, the time performance of the water-filling algorithm improved by bisection algorithm is better than that of MMA algorithm, but the SINR obtained by several algorithms has little difference. In terms of mutual information, the time performance of the water-filling algorithm improved by bisection algorithm is better than that of MMA algorithm, but MMA algorithm has the largest MI. In the future, we will deeply explore the principle of the influence of echo observation time on SINR and MI or optimize the time performance of MMA algorithm.

Data Availability

All data used to support the findings of this study are included within the article.

Conflicts of Interest

The authors declare that there are no conflicts of interest regarding the publication of this paper.

Acknowledgments

This work was supported by the Natural Science Foundation of Hebei Province (no. F2018501051).

References

[1] S. Haykin, "Cognitive radar: a way of the future," *IEEE Signal Processing Magazine*, vol. 23, no. 1, pp. 30–40, 2006.

[2] M. R. Bell, "Information theory and radar waveform design," *IEEE Transactions on Information Theory*, vol. 39, no. 5, pp. 1578–1597, 1993.

[3] S. A. Kassam and H. V. Poor, "Robust techniques for signal processing: a survey," *Proceedings of the IEEE*, vol. 73, no. 3, pp. 433–481, 1985.

[4] B. Wang, X. Chen, S. Li, F. Xin, and J. Wang, "Robust waveform design based on jammer games in cognitive radar," in *Proceedings of the 2018 10th International Conference on Communications, Circuits and Systems (ICCCAS)*, pp. 195–198, Chengdu, China, December 2018.

[5] L. Wang, H. Wang, and M. Chen, "Cognitive radar waveform design for multiple targets based on information theory," in *Proceedings of the 2016 CIE International Conference on Radar (RADAR)*, pp. 1–5, Guangzhou, China, October 2016.

[6] M. Hong and A. Garcia, "Averaged iterative water-filling algorithm: robustness and convergence," *IEEE Transactions on Signal Processing*, vol. 59, no. 5, pp. 2448–2454, 2011.

[7] X. Cheng, A. Aubry, D. Ciuonzo, A. De Maio, and X. Wang, "Robust waveform and filter bank design of polarimetric radar," *IEEE Transactions on Aerospace and Electronic Systems*, vol. 53, no. 1, pp. 370–384, 2017.

[8] R. A. Romero, J. Bae, and N. A. Goodman, "Theory and application of SNR and mutual information matched illumination waveforms," *IEEE Transactions on Aerospace and Electronic Systems*, vol. 47, no. 2, pp. 912–927, 2011.

[9] L. Wang, W. Zhu, Y. Zhang, Q. Liao, and J. Tang, "Multi-target detection and adaptive waveform design for cognitive MIMO radar," *IEEE Sensors Journal*, vol. 18, no. 24, pp. 9962–9970, 2018.

[10] Y. Liu, G. Liao, J. Xu, Z. Yang, and Y. Zhang, "Adaptive OFDM integrated radar and communications waveform design based on information theory," *IEEE Communications Letters*, vol. 21, no. 10, pp. 2174–2177, 2017.

[11] H. Wang, "Robust waveform design for MIMO–OFDM-based STAP in the presence of target uncertainty," *IET Radar, Sonar & Navigation*, vol. 12, no. 9, pp. 1021–1027, 2018.

[12] G. Rossetti and S. Lambotharan, "Robust waveform design for multistatic cognitive radars," *IEEE Access*, vol. 6, pp. 7464–7475, 2018.

[13] L. Wang, Y. Zhang, Q. Liao, and J. Tang, "Robust waveform design for multi-target detection in cognitive MIMO radar," in *Proceedings of the 2018 IEEE Radar Conference (RadarConf18)*, pp. 116–120, Oklahoma City, OK, USA, April 2018.

[14] W. Zhu and J. Tang, "Robust design of transmit waveform and receive filter for colocated MIMO radar," *IEEE Signal Processing Letters*, vol. 22, no. 11, pp. 2112–2116, 2015.

[15] Z. Rui, Z. Bo, L. Lin, Z. Xiaofen, and J. Bin, "Improved waveform design for non-Gaussian target classification in cognitive radar," in *Proceedings of the IET International Radar Conference 2015*, pp. 1–4, Hangzhou, China, October 2015.

Hindawi
Mathematical Problems in Engineering
Volume 2020, Article ID 8978504, 13 pages
https://doi.org/10.1155/2020/8978504

Research Article

A Hybrid Forecasting Model for Nonstationary and Nonlinear Time Series in the Stochastic Process of CO_2 Emission Trading Price Fluctuation

Shanglei Chai,[1] Mo Du ,[2] Xi Chen,[3] and Wenjun Chu[1]

[1]*School of Business, Shandong Normal University, 88 Wenhua Road, Jinan 250014, China*
[2]*School of Accounting, Shandong Youth University of Political Science, 31699 East Jingshi Road, Licheng District, Jinan 250103, China*
[3]*Department of Management Engineering, School of Economics &Management, Xidian University, Xi'an 710071, China*

Correspondence should be addressed to Mo Du; dumo1977@163.com

Received 16 June 2020; Accepted 16 July 2020; Published 4 August 2020

Guest Editor: Wenguang Yu

Predicting CO_2 emission prices is an important and challenging task for policy makers and market participants, as carbon prices follow a stochastic process of complex time series with nonstationary and nonlinear characteristics. Existing literature has focused on highly precise point forecasting, but it cannot correctly solve the uncertainties related to carbon price datasets in most cases. This study aims to develop a hybrid forecasting model to estimate in advance the maximum or minimum loss in the stochastic process of CO_2 emission trading price fluctuation. This model can granulate raw data into fuzzy-information granular components with minimum (Low), average (R), and maximum (Up) values as changing space-description parameters. Furthermore, it can forecast carbon prices' changing space with Low, R, and Up as inputs to support a vector regression. This method's feasibility and effectiveness is examined using empirical experiments on European Union allowances' spot and futures prices under the European Union's Emissions Trading Scheme. The proposed FIG-SVM model exhibits fewer errors and superior performance than ARIMA, ARFIMA, and Markov-switching methods. This study provides several important implications for investors and risk managers involved in trading carbon financial products.

1. Introduction

Since the launch of the European Union's Emissions Trading Scheme (EU ETS), carbon dioxide (CO_2) emission certificates have been cultivated as a scarce resource. Furthermore, EU allowances (EUAs) have been actively traded in spot and its derivative future markets as a new class of financial assets. Consequently, reinforced carbon price signals coupled with complementary policies can effectively mitigate the costs of global carbon emissions. With carbon markets' rapid growth, carbon prices have become more volatile due to the influence of many potential fundamentals, which are drivers that have led to drastic changes in carbon prices. Irregular and unexpected price fluctuations have increased the risk in the carbon market, which affects participants' confidence and emission-mitigation targets [1]. Therefore, it is essential to understand carbon prices' dynamics and establish a scientific carbon price-forecasting model, as predicting carbon prices is useful for reducing market risk [2]. This study aims to predict EUA prices in an effort to not only assist entities regulated under the EU ETS in managing risk but also benefit policy makers concerned with this pricing mechanism.

Meanwhile, a scientific prediction tool in the investment field can help speculators seek short-term arbitrage opportunities from volatility trades and develop efficient investment strategies in the carbon market. Given the significance of scientific prediction models, many studies have presented several methods to forecast carbon prices and this literature is commonly divided into two strands [3]. First, the literature forecasts carbon prices in the context of classic statistical methods, including the ARIMA, GARCH, VAR, and Markov-switching models [4–7]. These typically manifest as a parameterisation or linearity, and most of their estimation processes use the maximum likelihood method. In this case, the time-series variables must obey an assumption of normal distribution or the sample observation must be sufficiently long. However, carbon prices in practice do not possess linear characteristics or may not be generally predictable in a linear manner [8–10]. Chevallier [9] detects the strong nonlinearities existing in carbon prices' fluctuations to indicate that a nonparametric forecasting model can substantially reduce prediction errors. Arouri et al. [8] capture the asymmetry and nonlinearity of carbon prices and confirm the necessity of establishing a nonlinear carbon price-prediction model. To achieve a better nonlinear approximation, empirical studies on carbon prices' forecasting have increasingly built a second strand of the literature using computational intelligence techniques [3,11–18]. These primarily refer to the artificial neural network, fuzzy logic, evolutionary algorithm, support vector machine (SVM), and hybrid models, which exploit the advantages of the intelligence algorithm and statistical models. Some early studies preferred to use the neural network for carbon price forecasting, with favourable results [11, 12]. Although the neural network exhibits a good nonlinear approximation ability, it is prone to fall into local optimum, overtraining and undertraining, and has poor generalisability. Therefore, the neural network exhibits certain limitations in applying a replicated time series.

Support vector machines (SVM) as proposed by Cortes and Vapnik [19] differ from traditional learning theory, in which SVM obeys the principle of structural rather than empirical risk minimisation, and thus, it exhibits good generalisability. Given this advantage, this method has been used in carbon prices forecasting issues to demonstrate a higher robustness than other methods [14, 15, 17, 18]. A common, noteworthy feature of these papers is that a variety of hybrid models are constructed using SVM and such traditional time-series analysis methods as ARIMA, GARCH, and empirical mode decomposition, among others. The empirical results suggest that a hybrid model performs well in nonstationary and nonlinear time-series analyses, and especially in forecasting carbon prices. Unlike the previously mentioned studies which primarily predict the EU carbon market, some studies have predicted the emerging carbon market in China [3, 13, 20]. Despite the different topics investigated, these papers reach the same conclusion, in which hybrid models have a higher forecasting accuracy than benchmark models.

Although many have studied the previously mentioned time-series models for point forecasting with high precision in numerical calculations, these may not be absolutely essential for relevant real-world information users. For example, it is more suitable for stock investors to predict the changing space for future stock prices and thus make profits from them, rather than providing some specific numbers for stock price. This is because the fluctuations in stock price forecasting help investors make reasonable decisions to seize arbitrage opportunities. The same principle applies to the carbon market, as it is similar to the stock market. Thus, precision is not an absolutely necessary condition for human thinking or reasoning, so the range of trusted variation of time series is satisfactory for some decision makers [21]. In addition, previous studies on carbon price forecasting mainly focus on point forecasting, but point forecasting in most cases cannot correctly solve the uncertainties related to carbon price datasets [22]. On the contrary, changing space predictions can quantify the influence of uncertain factors on the results so that the original value is within the prediction interval determined by the upper and lower limits of the interval. Therefore, it is highly significant for most investors to make changing space predictions of carbon prices in practical application rather than point forecasting, the latter of which has highly precise numerical values.

Consequently, this study aims to develop a novel carbon prices' changing space forecasting model to make up for previous point forecasting methods. It compensates for a lack of point forecasting by using the original data that must be processed through fuzzy information granulation (FIG) as first proposed by Zadeh [23]. This useful tool provides appropriate solutions in developing a fast-space forecasting model for complex time-series process with nonstationary and nonlinear characteristics [21]. Furthermore, studies increasingly use information granulation to process complicated time-series data to improve prediction accuracy [24–28]. Each information granule represents the fuzziness and uncertainty of a certain period. The granulated data can be analysed after the original data is preprocessed using FIG and then forecasts can be conducted.

We consider this motivation in developing fast-changing space predictors—and not point predictions—using a FIG-SVM model in this paper, with the following primary contributions to existing studies. First, the input scales for SVM can be reduced by FIG and therefore forecasting efficiency may be improved. This method granulates time-series carbon prices into Low, R, and Up categories to rapidly predict the possible minimum, average, and maximum of complicated time-series. Second, our proposed FIG-SVM model can forecast carbon prices' changing space using a novel framework with minor errors and good generalisability. The experimental results demonstrate its superiority to the other benchmark models, such as the ARIMA, ARFIMA, and Markov-switching models. Third, a credible approach to carbon prices' changing space forecasting is more helpful to some decision makers in carbon markets rather than the point-forecasting method commonly used in the existing literature. This provides several important implications for speculators to catch arbitrage opportunities and also provides some early warnings for policy makers to manage volatility risks arising from carbon markets. In addition, this study contributes to the general development of stochastic process theory, and its applications in the following aspects are shown in Figure 1. We provide theoretical models and empirical conclusions to carbon price stochastic process of complex time series with nonstationary and nonlinear characteristics.

The remainder of this study is structured as follows. Section 2 gives a detailed introduction of the FIG-SVM

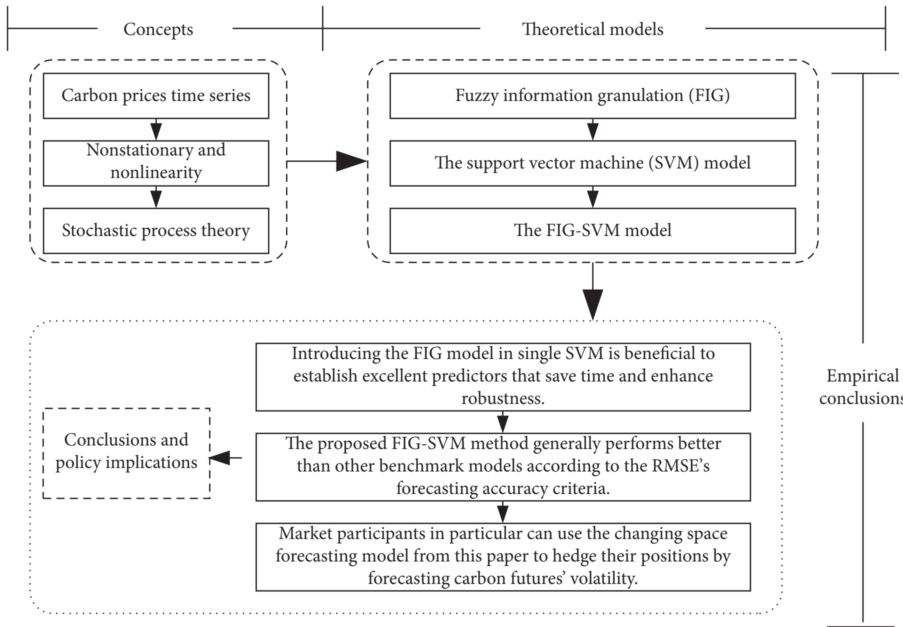

Figure 1: The contributions to stochastic process theory and its applications.

model. Section 3 illustrates some statistical characteristics of EUA data and essential testing results. Section 4 displays some valuable results from our proposed FIG-SVM model. Finally, the conclusion is set forth in Section 5.

2. Methodology

2.1. Fuzzy Information Granulation (FIG). Granular computing has become a general platform to construct, describe, and process information granules. It aims to discover an efficient system dealing with granulation in complex time series issues and has become a rapidly growing research field [29, 30]. As carbon prices follow a stochastic process of complex time series with the inherent nonlinear and nonstationary characteristics [3, 31], it is necessary to granulate its information. The granulating process divides large amounts of complex information into several blocks according to their own characteristics, with each block defined as an information granule. Therefore, complex issues in a large-scale time series can be decomposed into simple ones by removing some irrelevant information.

Suppose that $X = \{x_1, x_2, \ldots x_n\}$ denotes a given time series of carbon prices and p $(1 \leq p \leq n)$ refers to time windows' number that determine the essential information retaining ability. The fuzzification process creates a convex fuzzy subset G that can logically describe X. The formula is shown below:

$$g \overset{\Delta}{=} (x \,\text{is}\, G) \,\text{is}\, \lambda, \tag{1}$$

where λ is the probability of x belonging to the subset G. Subsequently, if the changing space of future carbon prices is considered as an information granule, a model can be constructed to forecast this changing space for a future period. This model can better assist investors in making reasonable decisions compared to those based on points forecasting with numerical values. This paper adopts the triangular membership function proposed by Pedrycz and Vukovich [32]:

$$T(x; a, m, b) = \begin{cases} 0, & x \leq a, \\ \dfrac{x-a}{m-a}, & a < x < m, \\ \dfrac{x-b}{m-b}, & m \leq x < b, \\ 0, & x \geq b, \end{cases} \tag{2}$$

where a, m, and b are the scalar parameters, corresponding to three variables Low, R, and Up for single window, which are obtained by granulation. The variable Low, R, and Up, respectively, represent the minimum, average, and maximum value of the time series change in the window.

For a given time series $Y = \{Y_i, \ldots, Y_n\}$, a proper triangular granule $T(a, m, b)$ can be constructed by an optimization technique as follows:

$$\max_{a,m,b} \sum_{Y_i \in Y} \frac{T(Y_i; a, m, b)}{\text{measure}\,(Supp(T(a, m, b)))}, \tag{3}$$

where $\text{measure}\,(\text{Supp}\,(\text{T}))$ is the measure of support of $T(a, m, b)$ while $T(Y_i)$ is the membership degree of Y_i:

$$T(Y_i; a, m, b) = \begin{cases} \dfrac{x-a}{m-a}, & x < m, \\ \dfrac{x-b}{m-b}, & x \geq m. \end{cases} \tag{4}$$

As for how to obtain an proper granule, we can solve the optimization equation (3) by minimizing the denominator measure (Supp (T)) and maximizing the numerator $T(Y_i)$ to acquire a high specificity of the granule that contain enough empirical information.

2.2. The Support Vector Machine (SVM) Model. As a machine-learning method based on statistical theory, SVM has been used to successfully address nonlinear classifications and regressions [19]. In this study, we focus on the SVM model in regression and forecasting for time series. Suppose that $T = \{(x_1, y_1), \ldots (x_l, y_l)\}$ is a training set of time series data, where x_i and y_i refer to input and output variables. They are defined by a regression model as follows:

$$y = f(x_i) = (w \cdot x_i) + b, \tag{5}$$

where w is the weight vector and b is the threshold. We can solve the optimization problem as follows to estimate w and b:

$$\begin{aligned} \min \quad & \frac{1}{2}\|w\|^2 + C\sum_{i=1}^{l}(\xi_i + \xi_i^*) \\ \text{s.t.} \quad & (w \cdot x_i + b) - y_i \le \varepsilon + \xi_i \\ & y_i - (w \cdot x_i + b) \le \varepsilon + \xi_i^* \\ & \xi_i^{(*)} \ge 0, \quad i = 1, \ldots, l, \end{aligned} \tag{6}$$

where $\|w\|^2$ is regularization term, C is punishment coefficient, ξ_i and ξ_i^* are slack variables, and ε is insensitive loss coefficient.

Due to the limited computing power of linear functions, nonlinear SVM becomes an extension for complicated time-series forecasting issues. In order to get the nonlinear SVM, it is essential to perform a transformation as $\phi\colon R^n \longrightarrow H, x_i \longrightarrow \phi(x)$, making$K(x, x') = \phi(x) \cdot \phi(x)'$, where H denotes the high-dimensional feature space obtained by mapping the original space x and $K(x, x')$ is a kernel function. In constructing a nonlinear SVM, the decision function takes the following form:

$$y = f(x_i) = \sum_{i=1}^{l}(\alpha_i - \alpha_i^*)K(x_i, x) + b, \tag{7}$$

where α and α^* are Lagrange multipliers and b is the nonzero intercept.

2.3. The FIG-SVM Model. Ruan et al. [21] mentioned two challenges in using normal SVM models. First, the original data are often complex and characterised by noise and outliers in some real-world applications, which may disturb the normal SVM's performance in classifications or regressions. Second, a class imbalance problem may occur when training imbalanced data. Furthermore, most of the normal SVM classifiers with balanced class distribution assumptions or equal misclassification costs may produce models biased toward a majority class that exhibit weak performance towards a minority class. In summary, problems with noise and imbalances may affect the SVM model's accuracy and efficiency, a topic of much recent attention.

To deal with this issue, Lin and Wang [33] apply fuzzy theory to reduce impacts of noises and the results show that it performs well. Following their study of fuzzy SVM, we develop a novel FIG-SVM model for nonstationary and nonlinear time series prediction. This model can decompose large-scale complex time-series issues into some simpler problems to be handled independently. The original data are firstly extracted with partition sets in order to train and test. Next, the training data are granulated by the FIG method as Low, R, and Up. These granules are then integrated into SVM as input variables to select the optimal parameter pairs. After getting proper granules and selecting optimal SVM parameters, we can input the testing data in the FIG-SVM model to forecast the changing space of carbon prices time series.

3. Data

3.1. Data Description. We use three time-series datasets, comprised of European Union allowances' spot prices and future prices most heavily traded under the EU ETS, with daily frequencies. These prices are benchmarks of the most frequent EUA exchanges executed in the European Union's carbon markets. All original carbon pricing data are derived from European Energy Exchange's website (http://www.eex.com). Analysing carbon prices from different trading products of the spot and future markets allows us to compare different time series to investigate the proposed forecasting model's general applicability and robustness.

Substantial research has examined the modelling of carbon prices prior to the 2008 financial crisis to demonstrate that carbon prices peaked in mid-2008 [34–37], or just before the global financial crisis occurred. However, the carbon prices after this period exhibit an opposite trend, in which they sharply decline for various reasons. We investigate the price variations in the postcrisis era, which has demonstrated no such additional collapse, by choosing a carbon price time-series sample spanning 2009 to 2019. We select a dataset of EUA spot prices from 16 January 2009 to 22 March 2019, with 2,443 observations. Our EUA futures prices consist of two datasets: DEC18, which spans 26 March 2012 to 17 December 2018 and includes 1,705 observations; and DEC19, which spans 26 March 2012 to 26 March 26 2019, with 1,771 observations. The basic changing trends of these time series are illustrated in Figures 2–4.

Figure 2 plots the time variations of the EUA spot prices in our studied sample interval and displays the continuous EUA spot returns' volatility as computed by $r_t = \ln(p_t) - \ln(p_{t-1})$. Clearly, the EUA spot prices' time series does not appear to be stationary; meanwhile, it exhibits violent fluctuations, decreasing by 53.65% from €12.32 on 16 January 2009 to €5.71 on 4 December 2012. This sharp decrease can be explained by some fundamentals, such as macroeconomic [38] or policy factors [39], among others. Furthermore, it increases by approximately 338%, from €5.71 on 4 December 2012 to €25.01 on 22 January 2019.

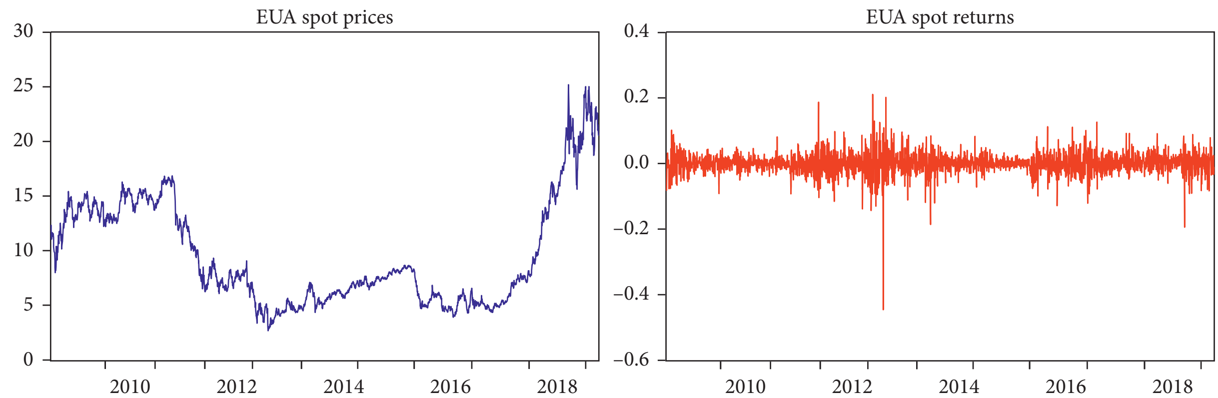

Figure 2: The time series of EUA spot prices and returns.

Regarding the EUA futures prices and returns from the DEC18 and DEC19 datasets, Figures 3 and 4 exhibit patterns of change similar to the EUA spot prices. This phenomenon occurs given the truth that these related markets have released some common information to investors. The correlation coefficient of spot prices and futures prices is significantly higher than 0.9; therefore, these series show a strong comovement while responding to the arrival of new common information.

Moreover, two noteworthy important features can be observed among the EUA spot and futures returns, plotted in Figures 2–4. On the one hand, the returns time series tendency towards volatility appears in bunches because information comes in clutters. This is because carbon returns' volatility is affected by previous values, and this is a persistent characteristic. Therefore, the time series future values can be easily forecast based on carbon returns' volatility. On the other hand, the most compelling feature is the leverage or asymmetric effect discovered early in financial markets according to the previous literature, a phenomenon that also exists in the carbon market [40, 41]. Clearly, carbon spot and future returns exhibit higher volatility when prices decrease than increase given an asymmetric response. This phenomenon appears in the form of negative impact arising from bad news, which may cause the increase in volatility to be greater than a positive impact from good news.

Table 1 presents the study's statistical indicators. The minimum and maximum values reveal that the changing range of daily EUA spot and futures prices is significantly large. Moreover, the huge intraday losses of spot and futures markets are obvious, with maximum losses of 44.66% in the EUA spot market, 36.38% in the DEC18 futures market, and 34.12% in the DEC19 futures market. Therefore, it is essential to establish a scientific changing space-forecasting model for carbon prices. Furthermore, the coefficients of skewness and kurtosis exhibit a leptokurtic characteristic, and the returns on the EUA spot market and futures market are both negatively skewed. Revenues are significantly and negatively skewed which is attributed to the risk associated with high prices. From a distribution perspective, the carbon prices and returns are not normally distributed, but are characterised by "heavy-tailed" and "high-kurtosis" properties.

The result of Jarque–Bera test suggests that the "normally distributed" hypothesis can be rejected at any significance level, which is consistent with most prior studies [42–45]. This evidence suggests that forecasting the changing space of EUA spot and future prices is of great significance to risk managers and policy makers in carbon markets. As we have discovered some complicated statistics exist in carbon prices and returns series, the extra but essential tests are then performed to precisely determine these time series' nonstationary and nonlinear characteristics.

3.2. Nonstationary and Nonlinear Data Tests. This study adopts some classical time-series test methods to confirm the existence of nonstationary and nonlinear characteristics in carbon prices. First, it is necessary to test whether these time series are nonstationary. The augmented Dickey–Fuller (ADF) and Phillips–Perron tests are most commonly used in the existing literature based on the basic principle of unit root tests for nonstationary. Table 2 shows the ADF test result in Panel A and Phillips–Perron test result in Panel B, respectively. They demonstrate that EUA spot prices and futures prices are not stationary at the 1%, 5%, and 10% significance levels.

However, these tests are not sufficiently convincing under abnormal circumstances. The traditional unit root test method can only identify the existence of unit roots in time series containing intercept or trend items and cannot identify the unit roots if breakpoints exist in the time series. If the stationary time series contains breakpoints, it is highly likely that a null hypothesis to accept nonstationarity will be obtained by the ADF or Phillips–Perron tests, distorting the test results; specifically, we should consider a case with structural breakpoints.

Prior literature indicates that the fluctuation of carbon prices has breakpoints, and the carbon prices' structure changes before and after these breakpoints [46, 47]. When these structural breakpoints exist in carbon prices, the power of conventional unit root tests as previously mentioned is unstable. Therefore, it is essential to use a breakpoint unit root test to examine the nonstationarity of this study's carbon price time series. Panel C in Table 2 lists the nonstationary breakpoint unit root test results, using a breakpoint ADF test for EUA spot and futures prices.

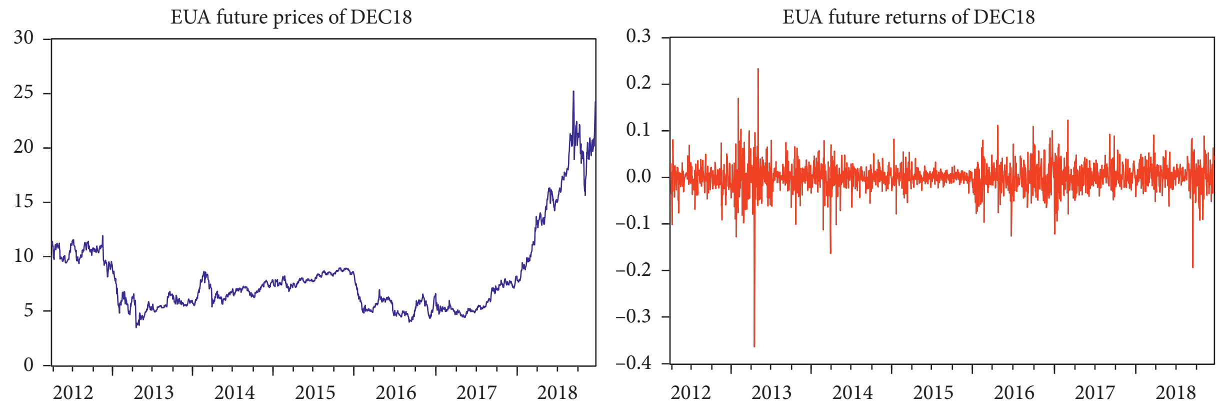

Figure 3: The time series of EUA future prices and returns for DEC18 contracts.

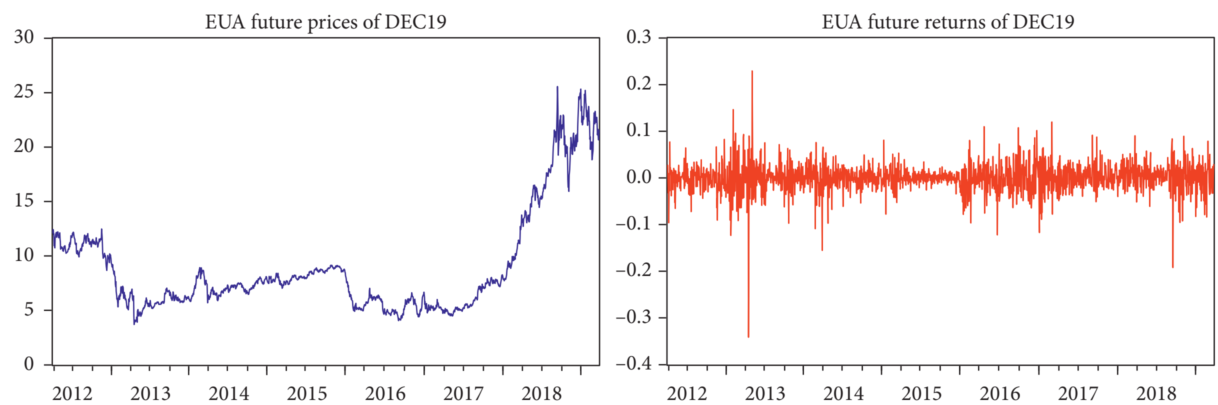

Figure 4: The time series of EUA future prices and returns for DEC19 contracts.

Table 1: Summary statistics of the EUA prices' and returns' time series.

	EUA spot		EUA futures—DEC18		EUA futures—DEC19	
	Prices	Returns	Prices	Returns	Prices	Returns
Mean	9.5310	0.0002	8.1587	0.0005	8.9314	0.0003
Median	7.5950	0.0000	7.1150	0.0011	7.4400	0.0011
Maximum	25.1900	0.2106	25.2400	0.2334	25.5600	0.2292
Minimum	2.6800	−0.4466	3.4800	−0.3638	3.7100	−0.3412
Std. dev.	4.8402	0.0329	3.8572	0.0319	4.7028	0.0311
Skewness	0.9405	−0.9881	1.9159	−0.9703	1.7496	−0.8960
Kurtosis	3.0575	20.4610	6.4729	17.4954	5.3223	15.7228
Jarque–Bera	360.3567	31419.3800	1898.8660	15185.5700	1300.7370	12174.6200

These results show that each of time series has a unit root; thus, we should accept the nonstationary hypothesis. This study's breakpoint ADF test adopts an innovational outlier (IO) model by assuming that the breakpoint process is gradual and an exogenous shock follows the same dynamic process. Two structural breakpoints were found on 5 September 2017 and 15 January 2018, according to a selection method that maximised the t-statistic of the intercept term's breakpoint.

Moreover, it is also important to test the EUA spot and futures prices' nonlinear characteristics. Our nonlinearity test of the time series adopts the Brock–-Decher–Scheikman test method used by Zhu et al. [17]; with two to six embedding dimensions. Table 3 presents the nonlinearity test results and demonstrates that our studied sample data are not linear. Our findings are consistent with those of other studies determining that the carbon prices time series follow a nonlinear process [8, 9, 10, 17].

This nonlinearity test leads us to conclude that carbon prices cannot be linearly predicted using traditional models, as this will lead to distortions once the linear model is established for nonlinear data. To deal with this issue, we apply an SVM model developed through statistical learning theory in a nonlinear regression estimation. Furthermore, a structural risk-minimisation principle is adopted for the function estimation by minimising the upper boundary of some generalisation errors [48]. This method can also create favourable effects in resisting the overfitting problem, which

Table 2: The ADF test, Phillips–Perron test, and Breakpoint ADF test results for nonstationary time series.

	EUA spot	EUA futures—DEC18	EUA futures—DEC19
Panel A: ADF test			
t-statistic	−0.8185	0.8239	−0.2305
Prob.	0.8132	0.9945	0.9321
Critical values:			
1%	−3.4328	−3.4340	−3.4338
5%	−2.8625	−2.8630	−2.8630
10%	−2.5673	−2.5676	−2.5676
Panel B: Phillips–Perron test			
Adj. t-Statistic	−0.6770	1.6015	0.1372
Prob.	0.8505	0.9995	0.9684
Critical values:			
1%	−3.4328	−3.4340	−3.4338
5%	−2.8625	−2.8630	−2.8630
10%	−2.5673	−2.5676	−2.5676
Panel C: Breakpoint ADF test			
t-Statistic	−3.1497	−4.3648	−3.8930
Prob.	0.6151	0.2706	0.5113
Critical values:			
1%	−5.1497	−5.7114	−5.7114
5%	−4.6106	−5.1550	−5.1550
10%	−4.3073	−4.8610	−4.8610

Table 3: The Brock–Decher–Scheikman (BDS) test results for nonlinear time series.

Dimension	EUA spot		EUA futures—DEC18		EUA futures—DEC19	
	BDS statistic	Prob.	BDS statistic	Prob.	BDS statistic	Prob.
2	0.1974	0.0000	0.1994	0.0000	0.2006	0.0000
3	0.3357	0.0000	0.3391	0.0000	0.3416	0.0000
4	0.4320	0.0000	0.4366	0.0000	0.4403	0.0000
5	0.4987	0.0000	0.5046	0.0000	0.5095	0.0000
6	0.5445	0.0000	0.5519	0.0000	0.5579	0.0000

may create imprecise and unsatisfactory forecasting. So far, the application of SVM to nonlinear regression estimation problems has become one of the most successful technical cases.

4. Empirical Results

4.1. Extracting Sample Data. We divide the entire dataset into two subsets to test the proposed forecasting model's validity in light of Alizadeh et al. 's [49] study. The first two-thirds of the total sample data were selected as a dataset to train our model and obtain the optimal parameter estimation. The last one-third of all sample were utilized as a testing set to forecast the future carbon prices based on the established model. Table 4 reports the details of the partitioned data set.

4.2. Fuzzy Information Granulation (FIG). We use the fuzzy granulation model as proposed in Section 2.1 to granulate the original data, which divides a complicated problem into some simpler ones to be handled by our proposed granular computing technique. This basic process consists of four steps, as illustrated in Figure 5.

These four steps will granulate the original time series of carbon prices into the following granules: Low (minimum), R (average), and Up (maximum). First, Low is generated by granulating the relatively small values of each window, which can denote the minimum values of original data changes. Second, R is generated from the average values of each granulated window, indicating the major dominant of original data changes. Third, Up is produced from the larger values of each granulated window, denoting the maximum values of the original data changes.

The three variables—Low, R, and Up—are obtained after the fuzzy granulation process for each window, as Figure 6 illustrates. These variables, respectively, correspond to the three parameters of a, m, and b in the triangular fuzzy granulation presented in equation (2). The normal SVM input size decreases for the carbon prices' time series after granulation, which may improve forecasting efficiency. Therefore, the FIG theory is successfully incorporated into a normal SVM model to develop time saving, robust predictors. The proposed hybrid FIG-SVM model can produce results with a good fit in a shorter time, which is advantageous for large scale, nonstationary, and nonlinear time series.

4.3. The Parameter Optimization. The model's generalisability can only be tested after obtaining a trained model with appropriate parameters. It is necessary to strive for selecting

Table 4: The division results of training set and testing set of the total sample.

Carbon prices		Size	Date
EUA spot	Sample set	2443	January 16, 2009-March 22, 2019
	Training set	1629	January 16, 2009-January 13, 2016
	Testing set	814	January 14, 2016-March 22, 2019
EUA futures—DEC18	Sample set	1705	March 26, 2012-December 17, 2018
	Training set	1137	March 26, 2012-September 27, 2016
	Testing set	568	September 28, 2016-December 17, 2018
EUA futures—DEC19	Sample set	1771	March 26, 2012-March 26, 2019
	Training set	1181	March 26, 2012-November 28, 2016
	Testing set	590	November 29, 2016-March 26, 2019

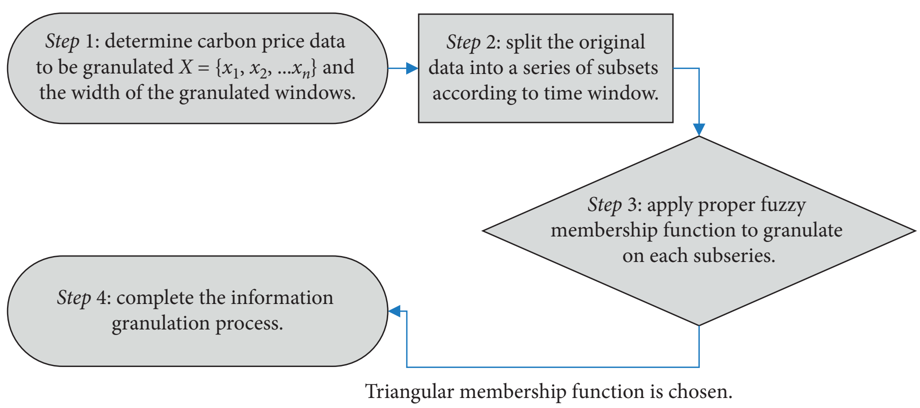

Figure 5: The basic steps of FIG on the original time series.

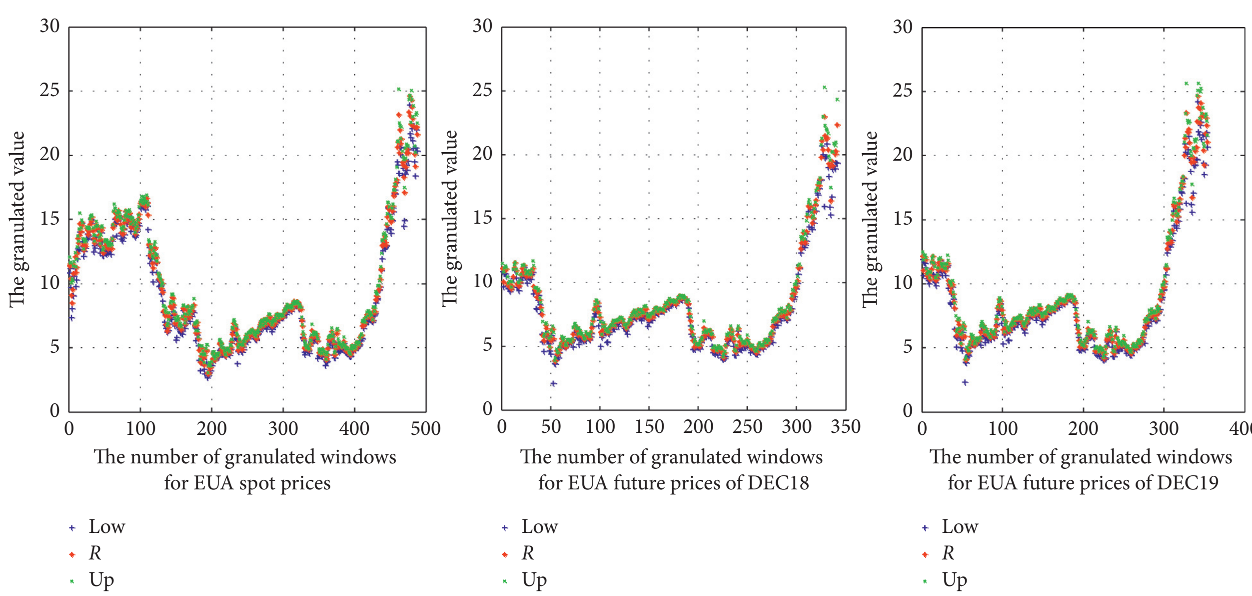

Figure 6: The granulation results for the original EUA spot and futures prices time series.

optimal SVM parameters because it greatly affects the quality of support machine regression for prediction. This selection process involves two crucial parameter pairs: the penalty parameter c and kernel parameter g (abbreviated for c-g). While no internationally recognised or unified method exists in the optimal parameter selection process for SVM, a more common method involves calculating c-g parameter pairs within a given scope. For example, a training set for a selected c-g parameter pairs is taken as an original dataset, and a crossvalidating K-fold crossvalidation method (K-CV) is applied to obtain the training accuracy of the dataset under the selected c-g parameter pairs. Finally, the selected c-g parameter pairs achieving maximum precision in the training set is taken as the best parameters for SVM model.

However, an unexpected issue may occasionally occur, in which multiple pairs of c-g may correspond to the maximum precision. This study's method to address this issue involves selecting the parameter pairs with the smallest c to attain the maximum precision. If multiple pairs of g correspond to the smallest c, the first c-g parameter we searched is selected as the best one. This is due to the following facts. The penalty parameter that is too high will lead to overlearning, or specifically, the training and testing sets exhibit very high and very low accuracies, respectively, or generalisability decreases. Therefore, the smaller penalty parameter is considered as a more reasonable selection in all the c-g parameter pairs that can achieve the highest verification accuracy. Table 5 displays the crossvalidation results for optimising SVM parameters.

The Low parameter in the EUA spot prices' time series can be taken as an example to explain the SVM for regression prediction process in detail. The optimal parameter combination under the crossvalidation condition is obtained as the relaxation parameter $c = 1$ and the kernel parameter $g = 0.0055$. Figure 7 illustrates the optimisation parameter-selection results for the Low parameters. The left and right panels display the contour map and the 3D view, respectively, which verify that the SVMs' parameters significantly impact their regression results. The other optimal parameter-searching processes for R and Up in the EUA spot and futures prices' time series yield similar results, which are omitted here for brevity.

4.4. Predict the Low (Minimum), R (Average), and up (Maximum). After obtaining the proper granules for Low (minimum), R (average), and Up (maximum) and selecting the optimal c-g parameter pairs for SVM, we input these into the SVM model to predict the possible ranges of change for the next window. Next, we take the EUA spot prices here as an example to demonstrate our proposed FIG-SVM results. Figure 8 illustrates the fitting results of the Low, R, and Up fuzzy particles for the EUA spot prices. The *predict Low*, *predict R*, and *predict Up* time series depict the predicted values of the Low, R, and Up fuzzy particles, which are close to the *original Low*, *original R* and *original Up* time series exhibiting the actual values of the Low, R, and Up fuzzy particles, respectively.

The results indicate that the proposed FIG-SVM forecasting model performs well in the case involving EUA spot prices. We further validate this method's effectiveness by conducting more experiments on the other two time series. With the same settings and the same granulation window, we obtain the results from our proposed FIG-SVM model for the Low, R, and Up granules in the cases of DEC18 and DEC19 futures prices. These experimental results all exhibit predicted values that approximate real values. This indicates that the normal SVM model combined with a developed FIG method can produce well-fit performances for predicting carbon prices time series with complex characteristics.

Table 5: The SVM parameters' optimisation results.

Carbon prices		Best c	Best g
EUA spot	Low	1	0.0055
	R	2.8284	0.0055
	Up	64	0.0442
EUA futures—DEC18	Low	2	0.0625
	R	1	0.0313
	Up	64	0.0625
EUA futures—DEC19	Low	1	0.0625
	R	4	0.0884
	Up	181	0.0039

4.5. Forecasting Performance Measures. We use ARIMA, ARFIMA, and Markov-switching method as benchmarks to compare the proposed FIG-SVM forecasting model's prediction capacity against other widely used forecasting approaches. As for evaluation criterion, we choose the root mean square error (RMSE) given by

$$\mathrm{RMSE} = \sqrt{\frac{1}{N}\sum_{t=1}^{n}\left(\hat{y}_t - y_t\right)^2}. \tag{8}$$

The formula represents the extent to which the predicted value of our proposed model deviates from actual data. The predicted value is going to be more consistent with the actual value, as the RMSE gets smaller.

Table 6 reveals that the proposed FIG-SVM forecasting model decreases prediction errors by 40.06%, 33.88%, and 25.49% compared to the traditional ARIMA model to calculate the EUA spot, DEC18, and DEC19 futures time series, respectively. Moreover, our model performs better than the other forecasting models as ARFIMA and Markov switching. From this perspective, the proposed FIG-SVM forecasting model can produce a well-fit performance, which verifies the effectiveness of the FIG-SVM model to forecast complicated time series with the characteristics of nonstationarity and nonlinearity.

4.6. Carbon Prices Changing Space Forecasting. After obtaining the FIG-SVM training predictors, the testing data are used to forecast the changing space of carbon prices' time series and evaluate the forecast performance. As Table 7 indicates, SVM can be used to make regression predictions for the Low, R, and Up fuzzy granulations to obtain the parameters of Low, R, and Up within five trading days, respectively.

We then verified the FIG-SVM model predictions' effectiveness by testing whether the carbon prices in the next five days changed within the range of the previous prediction. We compared this with the previous five trading days to investigate the overall trends in carbon pricing changes. The results reveal that the predicted range of carbon prices' changes in the next five days is accurate. Moreover, the EUA spot price indicates a downward trend in the following five days compared with the previous five days. However, opposite results occur in cases of EUA futures price changes, while the DEC18 and DEC19 carbon prices

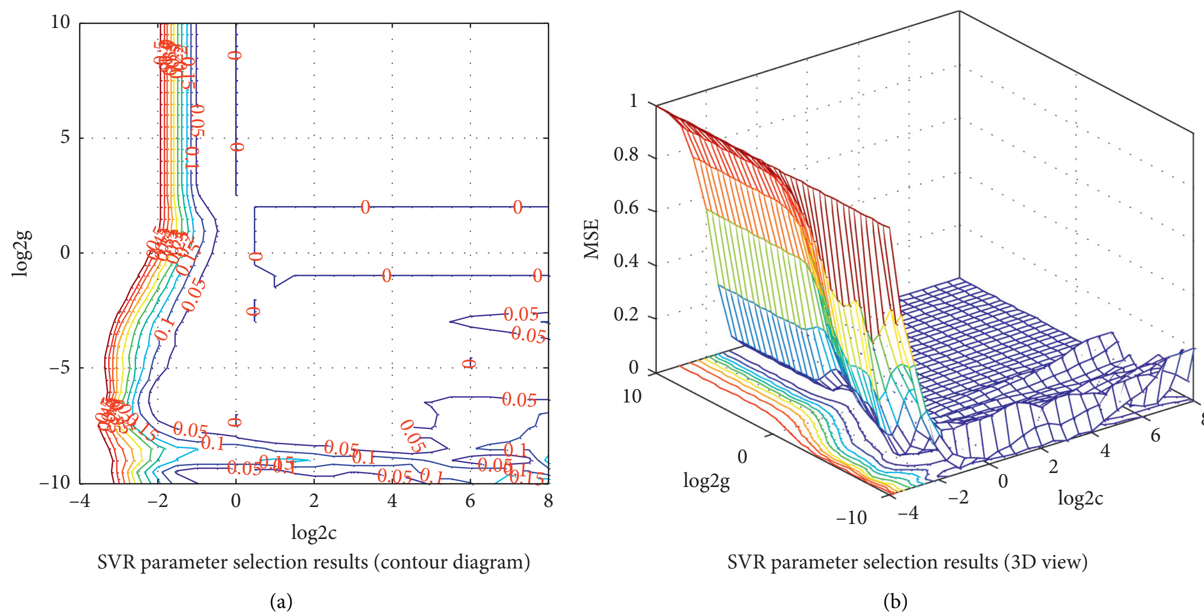

FIGURE 7: The parameter selection results for Low (minimum) value of the EUA spot prices. (a) SVR parameter selection results (contour diagram). (b) SVR parameter selection results (3D view).

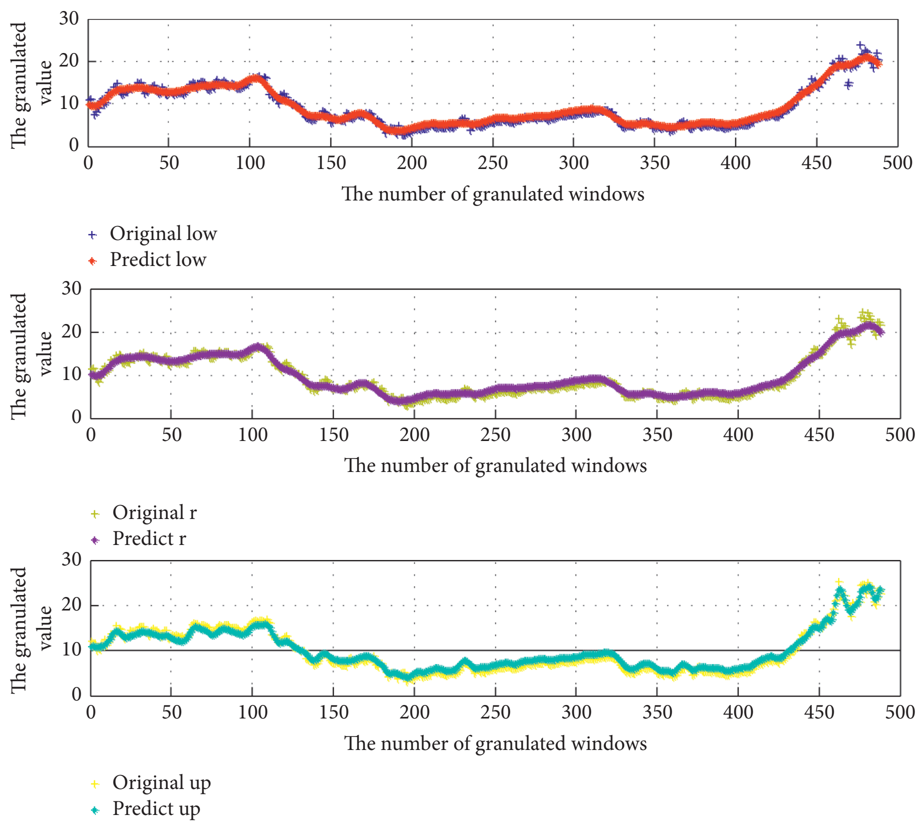

FIGURE 8: The prediction results for the Low, R, and Up of the EUA spot prices.

Table 6: The comparison results of the proposed FIG-SVM model with traditional forecasting models.

Forecasting models	EUA spot	EUA futures—DEC18	EUA futures—DEC19
Panel A: Root Mean Square Error (RMSE)			
ARIMA	0.031879	0.031678	0.030991
ARFIMA	0.031872	0.031690	0.030940
Markov-switching	0.031856	0.031577	0.030878
FIG-SVM	0.019108	0.020945	0.023091
Panel B: Error Reduction (%)			
FIG-SVM/ARIMA	40.06	33.88	25.49
FIG-SVM/ARFIMA	40.05	33.91	25.37
FIG-SVM/Markov-switching	40.02	33.67	25.22

Table 7: The changing space forecasting results for EUA spot and future prices.

Carbon prices	The original data						Changing space
EUA spot	Date	2019/3/11	2019/3/12	2019/3/13	2019/3/14	2019/3/15	Actual changing space
	Price	22.18	22.22	22.16	22.61	22.35	[Low,R,Up] = [20.57,21,21.71]
	Date	2019/3/18	2019/3/19	2019/3/20	2019/3/21	2019/3/22	Predicted changing space
	Price	21.71	21	21.52	20.82	20.57	[Low,R,Up] = [18.79,19.89,22.60]
EUA futures—DEC18	Date	2018/12/3	2018/12/4	2018/12/5	2018/12/6	2018/12/7	Actual changing space
	Price	20.64	20.73	19.68	19.99	20.3	[Low,R,Up] = [20.16,21.47,23.37]
	Date	2018/12/10	2018/12/11	2018/12/12	2018/12/13	2018/12/14	Predicted changing space
	Price	20.86	20.16	21.47	22.32	23.37	[Low,R,Up] = [16.66,19.38,23.88]
EUA futures—DEC19	Date	2019/2/18	2019/2/19	2019/2/20	2019/2/21	2019/2/22	Actual changing space
	Price	20.02	20.2	20.47	18.82	18.93	[Low,R,Up] = [19.25,21.28,22.28]
	Date	2019/2/25	2019/2/26	2019/2/27	2019/2/28	2019/3/1	Predicted changing space
	Price	19.25	19.67	21.28	21.69	22.28	[Low,R,Up] = [17.05,17.86,23.66]

exhibit upward trends in the following five days compared with the previous five days.

5. Conclusions

In this paper, the data of EUA spot prices and futures prices for DEC18 and DEC19 from 2009 to 2019 are examined for changing space forecasting of carbon prices. Since the launch of the European Union ETS, its rules have changed significantly from the first stage of 2005–2007 to the third stage of 2013–2020. The first stage is a pilot period, and the second stage is related to stricter emission caps because some industrialized countries have already committed to binding emission targets. The third stage has undergone some specific changes. Under the influence of different rules, the carbon prices in different stages of the EU emission trading system may change significantly. From a new perspective, this paper proposes a model that can predict the fluctuation space of carbon prices, which is of great significance to investors and policy makers involved in carbon market trading. It helps them to understand the changing laws of carbon prices and establish an effective carbon price stabilization mechanism. Furthermore, it can avoid carbon market risks and therefore enhance the activity of carbon trading participants. Some conclusions are drawn as follows.

First, we provide a changing space-forecasting model for carbon prices, which existing studies of carbon price forecasting have neglected. Prior literature has focused on a point prediction method for carbon prices, although relatively few works have forecast the changing space for carbon prices' time series. In fact, changing space forecasting is more important in practical investment applications, as investors can decide to buy a call or put options according to the predicted changing space. Moreover, investors can estimate the maximum or minimum loss or return in advance according to the Low, R, and Up fuzzy granulations. This article provides several important implications for investors and risk managers involved in trading carbon financial products. Market participants in particular can use the changing space forecasting model from this article to hedge their positions by forecasting carbon futures' volatility.

Second, we develop an integrated FIG-SVM approach for changing space forecasting, which builds a foundation to solve decision-making problems. Introducing the FIG model in single SVM is beneficial to establish excellent predictors that save time and enhance robustness. The granulation method produces Low (minimum), R (average), and Up (maximum) granules from carbon prices' time series. It can decompose large-scale complex time series issues into some simpler problems to be handled independently. Thus, the FIG method improves the prediction efficiency by reducing the complexity of the data and retaining the inherent essential information.

Third, we compare the forecasting performances between the proposed FIG-SVM model and traditional ARIMA, ARFIMA, and Markov-switching models in the context of carbon prices changing space forecasting. The empirical experimental results reveal that the proposed FIG-SVM method generally performs better than other benchmark models according to the RMSE's forecasting accuracy criteria. We prove the FIG-SVM model's feasibility and effectiveness in forecasting the changing space of carbon prices with some complicated characteristics of nonstationary and nonlinearity.

Although this paper provides the previously mentioned contributions, other issues still remain for further study. The complex changes and fluctuations in carbon prices is a nonlinear, dynamic system problem characterised by randomness, significant noise, and strong nonlinearity, among other chaotic characteristics. Such a system tends to exhibit unstable increases and decreases, resulting in a high concentration of risk. Therefore, the chaotic nonlinear dynamic system model is one alternative to analyse the characteristics of market price behaviour. This may lead to a new direction in studying the essential characteristics of carbon prices' fluctuation. An additional important issue pertains to China's well-known carbon-trading system, which has rapidly developed among emerging markets in recent years. However, the relevant literature is insufficient and must be further strengthened in the future.

Data Availability

The data used to support the findings of this study are available from the corresponding author upon request.

Conflicts of Interest

The authors declare that they have no conflicts of interest.

Acknowledgments

This work was supported by the National Natural Science Foundation of China (nos. 71704098, 71974154, and 71701115) and Natural Science Foundation of Shandong Province (nos. ZR2016GQ03, ZR2017QG003, and ZR2017MF058).

References

[1] Z. H. Feng, Y. M. Wei, and K. Wang, "Estimating risk for the carbon market via extreme value theory: an empirical analysis of the EU ETS," *Applied Energy*, vol. 99, pp. 97–108, 2012.

[2] Y. Zhang and Y. Wei, "An overview of current research on EU ETS: evidence from its operating mechanism and economic effect," *Applied Energy*, vol. 87, pp. 1804–1814, 2010.

[3] W. Sun and C. Zhang, "Analysis and forecasting of the carbon price using multi—resolution singular value decomposition and extreme learning machine optimized by adaptive whale optimization algorithm," *Applied Energy*, vol. 231, pp. 1354–1371, 2018.

[4] E. Benz and S. Trück, "Modeling the price dynamics of CO_2 emission allowances," *Energy Economics*, vol. 31, no. 1, pp. 4–15, 2009.

[5] A. K. Dhamija, S. S. Yadav, and P. K. Jain, "Forecasting volatility of carbon under EU ETS: a multi-phase study," *Environmental Economics and Policy Studies*, vol. 19, pp. 299–335, 2017.

[6] C. García-Martos, J. Rodríguez, and M. J. Sánchez, "Modelling and forecasting fossil fuels, CO2 and electricity prices and their volatilities," *Applied Energy*, vol. 101, pp. 363–375, 2013.

[7] M. E., Sanin, F. Violante, and M. Mansanet-Bataller, "Understanding volatility dynamics in the EU ETS market," *Energy Policy*, vol. 82, pp. 321–331, 2015.

[8] M. E. H. Arouri, F. Jawadi, and D. K. Nguyen, "Nonlinearities in carbon spot-futures price relationships during phase II of the EU ETS," *Economic Modelling*, vol. 29, no. 3, pp. 884–892, 2012.

[9] J. Chevallier, "Nonparametric modeling of carbon prices," *Energy Economics*, vol. 33, no. 6, pp. 1267–1282, 2011.

[10] B. J. Lutz, U. Pigorsch, and W. Rotfuß, "Nonlinearity in cap-and-trade systems: the EUA price and its fundamentals," *Energy Economics*, vol. 40, pp. 222–232, 2013.

[11] G. S. Atsalakis, "Using computational intelligence to forecast carbon prices," *Applied Soft Computing*, vol. 43, pp. 107–116, 2016.

[12] X. Fan, S. Li, and L. Tian, "Chaotic characteristic identification for carbon price and an multi-layer perceptron network prediction model," *Expert Systems with Applications*, vol. 42, pp. 3945–3952, 2015.

[13] M. Han, L. Ding, X. Zhao, and W. Kang, "Forecasting carbon prices in the Shenzhen market, China: the role of mixed-frequency factors," *Energy*, vol. 171, pp. 69–76, 2019.

[14] J. Zhang, D. Li, Y. Hao, and Z. Tan, "A hybrid model using signal processing technology, econometric models and neural network for carbon spot price forecasting," *Journal of Cleaner Production*, vol. 204, pp. 958–964, 2018.

[15] B. Zhu, D. Han, P. Wang, Z. Wu, T. Zhang, and Y. Wei, "Forecasting carbon price using empirical mode decomposition and evolutionary least squares support vector regression," *Applied Energy*, vol. 191, pp. 521–530, 2017.

[16] B. Zhu and Y. Wei, "Carbon price forecasting with a novel hybrid ARIMA and least squares support vector machines methodology," *Omega*, vol. 41, pp. 517–524, 2013.

[17] B. Zhu, S. Ye, P. Wang, K. He, T. Zhang, and Y. Wei, "A novel multiscale nonlinear ensemble leaning paradigm for carbon price forecasting," *Energy Economics*, vol. 70, pp. 143–157, 2018.

[18] J. Zhu, P. Wu, H. Chen, J. Liu, and L. Zhou, "Carbon price forecasting with variational mode decomposition and optimal combined model," *Physica AStatistical Mechanics and its Applications*, vol. 519, pp. 140–215, 2019.

[19] C. Cortes and V. N. Vapnik, "Support vector networks," *Machine Learning*, vol. 20, no. 3, pp. 273–297, 1995.

[20] Y. Song, T. Liu, D. Liang, Y. Li, and X. Song, "A fuzzy stochastic model for carbon price prediction under the effect of demand-related policy in China's carbon market," *Ecological Economics*, vol. 157, pp. 253–265, 2019.

[21] J. Ruan, X. Wang, and Y. Shi, "Developing fast predictors for large-scale time series using fuzzy granular support vector machines," *Applied Soft Computing*, vol. 13, no. 9, pp. 3981–4000, 2013.

[22] C. Tian and Y. Hao, "Point and interval forecasting for carbon price based on an improved analysis-forecast system," *Applied Mathematical Modelling*, vol. 79, pp. 126–144, 2020.

[23] L. A. Zadeh, "Fuzzy sets and information granularity," *Advances in Fuzzy Set Theory and Application*, vol. 1, pp. 3–18, 1979.

[24] M. Y. Chen and B. T. Chen, "A hybrid fuzzy time series model based on granular computing for stock price forecasting," *Information Sciences*, vol. 294, pp. 227–241, 2015.

[25] Y. He, Y. Yan, X. Wang, and C. Wang, "Uncertainty forecasting for streamflow based on support vector regression method with fuzzy information granulation," *Energy Procedia*, vol. 158, pp. 6189–6194, 2019.

[26] O. Hryniewicz and K. Kaczmarek, "Bayesian analysis of time series using granular computing approach," *Applied Soft Computing Journal*, vol. 47, pp. 644–652, 2016.

[27] W. Lu, X. Chen, W. Pedrycz, X. Liu, and J. Yang, "Using interval information granules to improve forecasting in fuzzy time series," *International Journal of Approximate Reasoning*, vol. 57, pp. 1–18, 2015.
[28] L. Wang, X. Liu, and W. Pedrycz, "Effective intervals determined by information granules to improve forecasting in fuzzy time series," *Expert Systems with Applications*, vol. 40, no. 14, pp. 5673–5679, 2013.
[29] B. Huang, Y. L. Zhuang, and H. X. Li, "Information granulation and uncertainty measures in interval-valued intuitionistic fuzzy information systems," *European Journal of Operational Research*, vol. 231, no. 1, pp. 162–170, 2013.
[30] W. Pedrycz, "Allocation of information granularity in optimization and decision-making models: towards building the foundations of Granular Computing," *European Journal of Operational Research*, vol. 232, no. 1, pp. 137–145, 2014.
[31] Y. Huang and Z. He, "Carbon price forecasting with optimization prediction method based on unstructured combination," *Science of the Total Environment*, vol. 725, no. 10, p. 138350, 2020.
[32] W. Pedrycz and G. Vukovich, "Feature analysis through information granulation and fuzzy sets," *Pattern Recognition*, vol. 35, no. 4, pp. 825–834, 2002.
[33] C. F. Lin and S. D. Wang, "Training algorithms for fuzzy support vector machines with noisy data," *Pattern Recognition Letters*, vol. 25, no. 14, pp. 1647–1656, 2004.
[34] J. Chevallier, "Carbon futures and macroeconomic risk factors: a view from the EU ETS," *Energy Economics*, vol. 31, no. 4, pp. 614–625, 2009.
[35] G. Daskalakis, D. Psychoyios, and R. N. Markellos, "Modeling CO_2 emission allowance prices and derivatives: evidence from the european trading scheme," *Journal of Banking and Finance*, vol. 33, pp. 1230–1241, 2009.
[36] M. Mansanet-Bataller, J. Chevallier, M. Hervé-Mignucci, and E. Alberola, "EUA and sCER phase II price drivers: unveiling the reasons for the existence of the EUA-sCER spread," *Energy Policy*, vol. 39, pp. 1056–1069, 2011.
[37] D. Rittler, "Price discovery and volatility spillovers in the European Union emissions trading scheme: a high-frequency analysis," *Journal of Banking & Finance*, vol. 36, pp. 774–785, 2012.
[38] N. Koch, S. Fuss, G. Grosjean, and O. Edenhofer, "Causes of the EU ETS price drop: recession, CDM, renewable policies or a bit of everything?-new evidence," *Energy Policy*, vol. 73, pp. 676–685, 2014.
[39] Q. Tu and J. L. Mo, "Coordinating carbon pricing policy and renewable energy policy with a case study in China," *Computers & Industrial Engineering*, vol. 113, pp. 294–304, 2017.
[40] K. R. French, G. W. Schwert, and R. F. Stambaugh, "Expected stock returns and volatility," *Journal of Financial Economics*, vol. 19, pp. 3–29, 1987.
[41] D. B. Nelson, "Conditional Heteroskedasticity in asset returns: a new approach," *Econometrica*, vol. 59, no. 2, pp. 347–370, 1991.
[42] J. Chevallier, "Modelling risk premia in CO_2 allowances spot and futures prices," *Economic Modelling*, vol. 27, pp. 717–729, 2010.
[43] F. G. Kalantzis and N. T. Milonas, "Analyzing the impact of futures trading on spot price volatility: evidence from the spot electricity market in France and Germany," *Energy Economics*, vol. 36, pp. 454–463, 2013.
[44] G. S. Uddin, J. A. Hernandez, S. J. H. Shahzad, and A. Hedström, "Multivariate dependence and spillover effects across energy commodities and diversification potentials of carbon assets," *Energy Economics*, vol. 71, pp. 35–46, 2018.
[45] S. Viteva, Y. V. Veld-Merkoulova, and K. Campbell, "The forecasting accuracy of implied volatility from ECX carbon options," *Energy Economics*, vol. 45, pp. 475–484, 2014.
[46] J. Chevallier, "Detecting instability in the volatility of carbon prices," *Energy Economics*, vol. 33, no. 1, pp. 99–110, 2011.
[47] X. P. Tan and X. Y. Wang, "Dependence changes between the carbon price and its fundamentals: a quantile regression approach," *Applied Energy*, vol. 190, pp. 306–325, 2017.
[48] V. N. Vapnik, "An overview of statistical learning theory," *IEEE Transactions on Neural Networks*, vol. 10, no. 5, pp. 988–999, 1999.
[49] A. H. Alizadeh, C.-Y. Huang, and S. Van Dellen, "A regime switching approach for hedging tanker shipping freight rates," *Energy Economics*, vol. 49, pp. 44–59, 2015.

Hindawi
Mathematical Problems in Engineering
Volume 2020, Article ID 4343629, 9 pages
https://doi.org/10.1155/2020/4343629

Research Article

An Optimal Portfolio Problem of DC Pension with Input-Delay and Jump-Diffusion Process

Weixiang Xu and Jinggui Gao

College of Mathematics and Systems Science, Shandong University of Science and Technology, Qingdao 266590, China

Correspondence should be addressed to Jinggui Gao; jingguigao@126.com

Received 5 June 2020; Accepted 10 July 2020; Published 31 July 2020

Guest Editor: Wenguang Yu

In this paper, an optimal portfolio control problem of DC pension is studied where the time interval between the implementation of investment behavior and its effectiveness (hereafter input-delay) is particularly focused. There are two assets available for investment: a risk-free cash bond and a risky stock with a jump-diffusion process. And the wealth process of the pension fund is modeled as a stochastic delay differential equation. To secure a comfortable retirement life for pension members and also avoid excessive risk, the fund managers in this paper aim to minimize the expected value of quadratic deviations between the actual terminal fund scale and a preset terminal target. By applying the stochastic dynamic programming approach and the match method, the optimal portfolio control problem is solved and the closed-form solution is obtained. In addition, an algorithm is developed to calculate the numerical solution of the optimal strategy. Finally, we have performed a sensitivity analysis to explore how the managers' preset terminal target, the length of input-delay, and the jump intensity of risky assets affect the optimal investment strategy.

1. Introduction

In recent decades, the analysis and optimal control of pension investment strategy have become a hot topic as people have paid more attention on the security of retirement life. There are two major ways to manage pension funds [1]. One is the DB (defined-benefit) plans, whose pension is predetermined, and the financial risk is borne by the sponsor of the plan; the other is the DC (defined-contribution) schemes, whose contributions are preset and benefits determined by the returns on fund's portfolio. Compared to the DB pension plan, the advantage of DC plans is to transfer longevity risk and financial risk from the sponsor to the member. Due to the development of stock market and a fact that the population ageing is threatening the solvability of Pay-as-you-go public pension systems, the management of pensions is increasingly leaning towards DC plans rather than DB schemes [2, 3].

The stochastic optimal control theory has been extensively used to obtain the optimal investment strategy of DC pension. In [4], the stochastic optimal dynamic programming method was applied by Merton (1969) to solve the portfolio problem. In [5], with the salary risk and the inflation risk considered, the optimal investment proportion for DC pension in the stochastic interest framework was obtained by the help of the stochastic dynamic programming approach. In [6], an optimal asset allocation problem for DC pension was investigated where the price process of risky assets followed the Heston model, and the optimization problem was then solved via the stochastic dynamic programming method. It is worth noting that the price processes of risky assets have been described as a continuous process in the above literature.

In fact, emergencies such as Corona Virus Disease 2019, plunge in oil prices, policy intervention, and so on will cause that the price processes of the risky assets discontinuous and have jumps [7]. However, the sudden jumps in the price process of available assets could not be described by Brownian motion. To cope with the jumps, scholars gradually pay attention to the jump-diffusion model. In [8], an optimal portfolio policy and consumption problem was proposed under the environment where the price process of the stock was modeled as a log-normal jump-diffusion process. Their optimal portfolio fraction and optimal consumption were obtained with the help of the stochastic dynamic programming method. In [9], an optimal precommitment and equilibrium investment strategies problem was presented for DC pension, where the dynamics of the risky asset was modeled as a jump-diffusion process. The precommitment strategy was then found by the stochastic dynamic programming approach, while the equilibrium strategy was derived under the framework of game theory. In [10], Walter Mudzimbabwe investigated an optimal portfolio policy problem of DC pension under a special case of the market environment in [9], and he obtained the optimal numerical solution by applying the stochastic dynamic programming method and the bisection method. In [10], the impacts of the jump intensity and jump amplitude on the optimal portfolio policies were displayed. In [11], an optimal consumption and portfolio strategy problem was analyzed where the CPI, interest rate, index bonds and stocks were both modeled as jump-diffusion processes. And their optimal fraction of consumption and investment strategy was obtained by adopting the stochastic dynamic programming approach. Lately, in [12], taking into account that the reserve level of an insurance company can only be observed at discrete time points, periodic capital injection and barrier dividend strategy was considered in the compound Poisson risk model. The explicit expression of the Gerber–Shiu function in [12] was derived by means of the integral and differential method, and the expected discounted capital injection function and the expected discounted dividend function was derived on condition that the observation interval and claim amount are exponentially distributed.

The current international financial situation is changing rapidly, leading to the inevitable time interval from knowing the change in the economic situation to formulating the relevant investment strategies and, finally, the investment strategy taking effect [13]. To deal with the time interval, the optimal portfolio problem with delay was gradually focused by scholars. This can be found in [13–15]. In [14], an optimal portfolio and consumption problem was considered where the dynamics of the risky asset is modeled as a stochastic delay differential equation whose coefficients vary according to a stochastic factor. And their problem was solved by applying a dynamic programming approach. In [15], the wealth process of the insurer was modeled as a stochastic delay differential equation under which an optimal reinsurance and portfolio problem with jump-diffusion was investigated. The closed-form expression for the optimal strategy was then obtained by solving the derived HJB equation. For investors, with the time interval between the implementation of investment behavior and its effect (hereafter the input-delay) considered, the obtained optimal investment strategy will be more in line with the actual investment environment so that the investment risk can be reduced. Therefore, it is necessary to consider input-delay in solving the investment portfolio problem. In [13], the portfolio problem with input-delay was studied to maximize the expected return and the explicit expression of the optimal solution is obtained by applying the maximum principle. In terms of the optimal investment strategy for DC pension, affected by the input-delay, the duration that the investment behavior actually plays a role (hereafter acting duration) is shorter than the nominal management duration of DC pension (hereafter management duration). Thus, the fund manager of DC pension should formulate the optimal portfolio fraction with input-delay considered to make sure that the managers' preset terminal target could be achieved within the acting duration. However, one seldom studies the optimal asset allocation for DC pension with input-delay put into consideration.

In the optimal asset allocation problem of DC pension, scholars commonly aim to maximize the expected utility of terminal wealth [1, 5, 16, 17]. Especially, to satisfy the basic requirement of fund members' retirement life, in [18], a minimum guarantee of the final wealth was calculated where the date of members' death was considered as a constant. Their objective was to maximize the expected utility of the final wealth exceeding the guarantee. A similar form of the objective in [18] can be found in [3, 19]. In this circumstance, a large positive value of difference also means excessive risks, which may be unacceptable to some fund members. In [20], with the mortality considered, the managers aimed to minimize the accumulated deviations between a benefit outgo target and the actual benefit outgo during the whole distribution period and their optimal solution was obtained by applying the variational inequality method.

In this paper, we consider an optimal portfolio problem for DC pension with input-delay and jump-diffusion process. The financial market consists of a risk-free cash bond and a risky stock. During the nominal management duration of DC pension, the pension members are required to provide continuous contribution to managers. Fund managers invest pension wealth into available assets so that the pension fund scale is affected by the investment return. We assume that the pension fund is fully invested in cash bond after members' retirement (i.e., after the terminal time) and converted into annuities.

To obtain the numerical solution of the optimal investment strategies in the above situation, the main contributions of this paper are listed as follows:

(i) Put into consideration both the input-delay (i.e., the time interval between the implementation of investment behavior and its effectiveness) and the jump-diffusion process. The dynamics of DC pension fund is modeled as a stochastic delay differential equation (SDDE).

(ii) A target of the terminal fund scale (hereafter the preset terminal target) is calculated with the mortality and the inflation considered. It reflects the required fund scale at retirement time to maintain high standard retirement life for members. To secure a comfortable retirement life for fund members while avoiding excessive risk, the goal in our model is to minimize the expected value of quadratic deviation between the actual terminal fund and the preset terminal target.

(iii) An optimization algorithm is given for calculating the numerical solution of the optimal strategy with input-delay. Meanwhile, sensitivity analysis is performed to show the impact of the preset terminal target, the length of input-delay, and jump intensity on the optimal investment strategies.

The remainder of this paper is organized as follows. In Section 2, we introduce the price processes of available assets and model the dynamics of the pension fund as a SDDE. In Section 3, the optimal asset allocation problem of DC pension with input-delay and jump-diffusion process is presented. In Section 4, the stochastic dynamic programming approach and the match method are applied to solve the optimization problem. An algorithm is developed to obtain the numerical solution of the optimal strategies. In Section 5, the numerical simulation and sensitivity analysis are provided.

2. The Financial Market

In this section, the financial market environment is introduced under which the optimization problem is proposed. We consider two financial assets available for investment: a risk-free cash bond and a single risky stock.

As in [10], the instantaneous risk-free rate of the cash bond is assumed to be a constant in this paper. Thus the price process of cash bond can be described by the following:

$$\mathrm{d}M(t) = rM(t)\mathrm{d}t, \quad M(0) = M_0, \tag{1}$$

where $M(t)$ describes the price of risk-free cash bond at t and $M(0)$ indicates the initial price of risk-free cash bond. $t \in [0, T]$ and T is a given positive finite constant denoting the investment time horizon of DC pension plan. r denotes the instantaneous risk-free interest rate.

In this paper, the jumping behavior of stock is focused and described as a compound Poisson process. Thus, the stochastic dynamics of stock can be expressed by a jump-diffusion process:

$$\mathrm{d}S(t) = S(t)\left[c\mathrm{d}t + \sigma\mathrm{d}W(t) + \mathrm{d}\sum_{i=1}^{N(t)} V_i\right], \quad S(0) = S_0, \tag{2}$$

where $S(t)$ is the price of stock at time t and $S(0)$ represents the initial price of stock. c and σ are the expected return and the volatility of the stock, respectively. In order to capture the features of the real market, we assume that $c > r$ [21]. As in [10], all processes and random variables are assumed to be defined on a filtered probability space (Ω, F, P). $\{W(t), t \geq 0\}$ denotes a standard Brownian motion. $\sum_{i=1}^{N(t)} V_i$ is a compound Poisson process to describe the jumping behavior of stock. $N(t)$ is a Poisson process with jump intensity λ. $V_i (i = 1, \ldots, N(t))$ are *i.i.d* variables denoting the jump amplitude with mean $\mu_v = E(V_i)$ and variance $\sigma_v^2 = \mathrm{Var}(V_i)$. Considering that the occurrence of Brownian motion and jump-diffusion process is independent, we assume that $W(t)$, $N(t)$, and $V_i (i = 1, \ldots, N(t))$ are mutually independent.

We consider the investment fraction in stock as the control variable. The short sale of the financial assets (the cash bond and stock) is both permitted, so the admissible range of the investment fraction in stock (Π) is not restricted, i.e., $\Pi = (-\infty, +\infty)$ [20]. In this paper, the pension members are required to provide continuous contribution during the nominal management duration of DC pension.

Then, based on the dynamics of available assets, the stochastic dynamics of the pension fund can be written by the following stochastic differential equation (SDE):

$$\begin{aligned}\mathrm{d}X(t) &= [X(t) - X(t)\pi(t)]\frac{\mathrm{d}M(t)}{M(t)} + X(t)\pi(t)\frac{\mathrm{d}S(t)}{S(t)} \\ &\quad + l(t)\mathrm{d}t, \quad X(0) = X_0,\end{aligned} \tag{3}$$

where $t \in [0, T]$. $X(t)$ represents the fund scale of DC pension at time t and $X(0)$ is the initial pension fund scale. $l(t)$ means the contribution rate at t. $\pi(t)$ is the investment fraction in stock at t, with $\pi(t) \in \Pi$.

From the investment behavior, the optimal asset allocation problem of DC pension can be regarded as a sort of optimal investment strategy problem. In optimal investment strategy problems, SDE with a similar composition to SDE (3) is commonly used to describe the wealth process, especially the dynamic of pension fund scale. This can be found in [19, 22–25]. However, considering the time interval between the implementation of investment behavior and its effect, the acting duration of investment behavior is shorter than the nominal management duration of DC pension. Therefore, in order to make sure that the preset terminal target could be achieved within the acting duration, the fund manager should formulate the optimal portfolio fraction with input-delay considered. Thus, we introduce the input-delay into SDE (3). The input-delay is denoted as τ which is an exogenous variable determined in advance. Then, the investment strategy that acts at a time t is actually the investment strategy carried out at time $t - \tau$. Correspondingly, the actual amount invested in stock and cash bond at t is $X(t - \tau)\pi(t - \tau)$ and $X(t) - X(t - \tau)\pi(t - \tau)$. Therefore, we have the following:

$$X(t) = X_0 + l(t)\mathrm{d}t, \quad t \in [0, \tau). \tag{4}$$

The dynamics of the pension fund in $[\tau, T]$ could be rewritten as a SDDE as follows:

$$\begin{aligned}\mathrm{d}X(t) &= [X(t)r + X(t-\tau)\pi(t-\tau)(c - r) + l(t)]\mathrm{d}t \\ &\quad + X(t-\tau)\pi(t-\tau)\sigma\mathrm{d}W(t) \\ &\quad + X(t-\tau)\pi(t-\tau)\mathrm{d}\sum_{i=1}^{N(t)} V_i, \quad t \in [\tau, T].\end{aligned} \tag{5}$$

3. The Optimization Problem

3.1. The Preset Terminal Target. In DC plans, there is a principal-agent relationship between pension members and managers. In this paper, we assume that managers preset a target of the terminal fund scale which reflects the required wealth at retirement time to maintain high standard retirement life for members. Since the value of the preset terminal target directly affects the optimal proportion in different assets, its formulation has become a key part of the optimal portfolio control problem. In this paper, we present the calculation of the terminal target with both the mortality credit and the inflation considered.

$$L_0 = \int_0^{\infty} \mathrm{NP} \cdot e^{gs} e^{-rs} {}_s p_{x_0+T} \mathrm{d}s, \tag{6}$$

where L_0 represents the preset terminal target of the pension fund. NP is an exogenous variable which means the requirement benefit outgo per unit of time to maintain a high standard retirement life at time T. g denotes the inflation. ${}_s p_{x_0+T}$ is an actuarial symbol which means the conditional probability that a person is alive at the age $x_0 + T$ and still alive at $x_0 + T + s$. The De Moivre Model in [26] is introduced in this paper to describe the force of mortality function and calculate ${}_s p_{x_0+T}$.

$$\mu(x) = \frac{1}{\omega - x}, \tag{7}$$

where $\mu(x)$ is the force of mortality function at the age of x. ω is the maximum age of an alive person.

Then, we have the following:

$$\begin{aligned} L_0 &= \int_0^{\infty} \mathrm{NP} \cdot e^{gs} e^{-rs} {}_s p_{x_0+T} \mathrm{d}s \\ &= \int_0^{\infty} \mathrm{NP} \cdot e^{(g-r)s} e^{-\int_0^s \mu(x_0+T+v)\mathrm{d}v} \mathrm{d}s \\ &= \frac{\mathrm{NP}}{r-g}\left(1 + \frac{1}{\omega - x_0 - T}\right). \end{aligned} \tag{8}$$

3.2. The Optimal Portfolio Control Problem (OPCP). The comfortable retirement life of fund members would lose guarantee when the value of the actual terminal fund is much lower than the preset terminal target. Conversely, if the value of the actual terminal fund scale is much higher than the target, the fund members will bear excessive risk. Therefore, the absolute deviation between the value of the actual terminal fund scale and the preset terminal target should not be too large. For the sake of simplicity, the goal of the optimal asset allocation problem in this paper is decided as minimizing the expected value of quadratic deviation between the actual terminal fund scale and the preset terminal target, i.e.,

$$\min_{\pi(t-\tau)\in\Pi} \mathrm{E}\left\{\left[X(T) - L_0\right]^2\right\}. \tag{9}$$

Due to the existence of input-delay, the duration for carrying out an investment strategy and the duration of its effect are $[0, T-\tau]$ and $[\tau, T]$, respectively. Then, we have $t \in [\tau, T]$ in (9).

Then, the optimal portfolio control problem for DC pension with input-delay and jump-diffusion process (OPCP) can be expressed by the following equation:

$$(\mathrm{OPCP}): \begin{cases} \min\limits_{\pi(t-\tau)\in\Pi}, & \mathrm{E}\left\{\left[X(T) - L_0\right]^2\right\}, \\ \text{s.t.}, & (4), \end{cases} \tag{10}$$

where $t \in [\tau, T]$.

4. The Optimal Solution and Optimization Algorithm

4.1. The Optimal Solution of OPCP. In this paper, we define the value function as follows:

$$H(t,x) = \min_{\pi(t-\tau)\in\Pi} \mathrm{E}\left\{\left[X(T) - L_0\right]^2 \mid X(t) = x\right\}, \tag{11}$$

where $H(t,x)$ is assumed to be at least twice continuously differentiable in x and once in t.

In order to derive the HJB equation for (OPCP), based on [27], we decompose the SDDE (5) into continuous changes $d_{(\mathrm{cont})}X(t)$ and discontinuous changes $d_{(\mathrm{jump})}X(t)$. From SDDE (5), $d_{(\mathrm{cont})}X(t)$ and $d_{(\mathrm{jump})}X(t)$ can be expressed by the following:

$$\begin{aligned} \mathrm{d}_{(\mathrm{cont})}X(t) = {} & [X(t)r + X(t-\tau)\pi(t-\tau)(c-r) + l(t)]\mathrm{d}t \\ & + X(t-\tau)\pi(t-\tau)\sigma \mathrm{d}W(t), \end{aligned} \tag{12}$$

while

$$\mathrm{d}_{(\mathrm{jump})}X(t) = X(t-\tau)\pi(t-\tau)\mathrm{d}\sum_{i=1}^{N(t)} V_i. \tag{13}$$

Thus, the dynamics of $H(t,x)$ can also be decomposed into continuous changes and jump changes as follows:

$$\begin{aligned} \mathrm{d}_{(\mathrm{cont})}H(t,X(t)) \simeq {} & H_t(t,X(t))\mathrm{d}t \\ & + H_x(t,X(t))\mathrm{d}_{(\mathrm{cont})}X(t) + \frac{1}{2}H_{xx}(t,X(t)) \\ & \left(\mathrm{d}_{(\mathrm{cont})}X(t)\right)^2, \\ \mathrm{d}_{(\mathrm{jump})}H(t,X(t)) = {} & \left[H\left(t, X(t) + X(t-\tau)\pi(t-\tau)V_1\right)\right. \\ & \left. - H(t,X(t))\right]\mathrm{d}N(t). \end{aligned} \tag{14}$$

Then, we have the following:

$$\begin{aligned} \mathrm{d}H(t,X(t)) &= \mathrm{d}_{(\mathrm{cont})}H(t,X(t)) + \mathrm{d}_{(\mathrm{jump})}H(t,X(t)) \\ &= H_t(t,X(t))\mathrm{d}t + H_x(t,X(t))\mathrm{d}_{(\mathrm{cont})}X(t) \\ &\quad + \frac{1}{2}H_{xx}(t,X(t))\left(\mathrm{d}_{(\mathrm{cont})}X(t)\right)^2 \\ &\quad + \left[H\left(t, X(t) + X(t-\tau)\pi(t-\tau)V_1\right)\right. \\ &\quad \left. - H(t,X(t))\right]\mathrm{d}N(t). \end{aligned} \tag{15}$$

Therefore, the HJB equation for (OPCP) can be derived and expressed as follows:

$$0=\min_{\pi(t-\tau)\in\Pi}\Big\{H_t+H_x[X(t)r+X(t-\tau)\pi(t-\tau)(c-r)+l(t)]+\frac{1}{2}H_{xx}X^2(t-\tau)\pi^2(t-\tau)\sigma^2+\lambda\mathrm{E}[H(t,X(t)+X(t-\tau)\pi(t-\tau)V_1)-H(t,X(t))]\Big\}. \tag{16}$$

With the boundary condition of the value function

$$H(T,x)=(x-L_0)^2, \tag{17}$$

we try a form of the value function

$$H(t,x)=P(t)x^2+Q(t)x+R(t), \tag{18}$$

where $P(T)=1$, $Q(T)=-2L_0$, $R(T)=L_0^2$. $P(t)$, and $R(t)$ are both positive while $Q(t)$ is negative.

Then, we can derive that

$$\begin{aligned}H_t&=P_t(t)x^2+Q_t(t)x+R_t(t),\\ H_x&=2P(t)x+Q(t),\\ H_{xx}&=2P(t).\end{aligned} \tag{19}$$

Combining (16), (18), and (19), the HJB equation can be rewritten as follows:

$$\begin{aligned}0=\min_{\pi(t-\tau)\in\Pi}\Big\{&P_t(t)X^2(t)+Q_t(t)X(t)+2P(t)X(t)\\&[X(t)r+X(t-\tau)\pi(t-\tau)(c-r)+l(t)]\\&+R_t(t)+Q(t)[X(t)r+X(t-\tau)\pi(t-\tau)(c-r)\\&+l(t)]+P(t)X^2(t-\tau)\pi^2(t-\tau)\sigma^2\\&+2\lambda P(t)X(t)X(t-\tau)\pi(t-\tau)V_1\\&+\lambda Q(t)X(t-\tau)\pi(t-\tau)V_1\\&+\lambda P(t)X^2(t-\tau)\pi^2(t-\tau)V_1^2\Big\}.\end{aligned} \tag{20}$$

By the match method, we transform (20) into the following form:

$$\begin{aligned}0=\min_{\pi(t-\tau)\in\Pi}\Bigg\{&\left[X(t-\tau)\sqrt{(\sigma^2+\lambda V_1^2)P(t)}\,\pi(t-\tau)+\frac{(c-r+\lambda V_1)(2X(t)P(t)+Q(t))}{2\sqrt{(\sigma^2+\lambda V_1^2)P(t)}}\right]^2\\&+P_t(t)X^2(t)+Q_tX(t)+R_t(t)+2P(t)X(t)l(t)+Q(t)l(t)\\&+2P(t)rX^2(t)+Q(t)rX(t)-\frac{(c-r+\lambda V_1)^2(2X(t)P(t)+Q(t))^2}{4(\sigma^2+\lambda V_1^2)P(t)}\Bigg\}.\end{aligned} \tag{21}$$

Thus, the solution of the HJB equation can be described as follows:

$$\pi^*(t-\tau)=-\frac{(c-r+\lambda V_1)(2X(t)P(t)+Q(t))}{2(\sigma^2+\lambda V_1^2)P(t)X(t-\tau)},\quad t\in[\tau,T]. \tag{22}$$

Combining with (21) and (22), we obtain the following:

$$\begin{aligned}0=&P_t(t)X^2(t)+Q_tX(t)+R_t(t)+2P(t)rX^2(t)+Q(t)rX(t)\\&+2P(t)X(t)l(t)+Q(t)l(t)-\frac{(c-r+\lambda V_1)^2}{4(\sigma^2+\lambda V_1^2)}\\&\cdot\left[4X^2(t)P(t)+\frac{Q^2(t)}{P(t)}+4X(t)Q(t)\right].\end{aligned} \tag{23}$$

Letting the coefficient of the quadratic factor be zero in (23), we get the following ordinary differential equation related to $P(t)$:

$$\begin{cases}P_t(t)+P(t)(2r+k)=0,\\ P(T)=1,\end{cases} \tag{24}$$

where $k=-(c-r+\lambda V_1)^2/(\sigma^2+\lambda V_1^2)$.

Letting the coefficient of the linear factor be zero in (23), the following ordinary differential equation related to $Q(t)$ is obtained:

$$\begin{cases}Q_t(t)+Q(t)(r+k)+2P(t)l(t)=0,\\ Q(T)=-2L_0.\end{cases} \tag{25}$$

Through the separating variables method and the constant variation method, we can easily obtain the solution of (24) and (25), i.e.,

$$\begin{aligned}P(t)&=e^{(2r+k)(T-t)},\\ Q(t)&=-2\left[\int_t^T e^{(3r+2k)(T-t)}l(s)\mathrm{d}s+L_0\right]e^{-(r+k)(T-t)}.\end{aligned} \tag{26}$$

Since $P(t),Q(t)$ are enough to describe $\pi^*(t-\tau)$ in (22), we omit the calculations of $R(t)$ here. Substituting the obtained $P(t)$ and $Q(t)$ into (22), then we have the following:

$$\pi^*(t-\tau) = \frac{c-r+\lambda V_1}{\sigma^2+\lambda V_1^2}\Bigg\{-X(t) + \left[\int_t^T e^{(3r+2k)(T-s)} l(s)\mathrm{d}s + L_0\right] e^{-(3r+2k)(T-t)}\Bigg\}\frac{1}{X(t-\tau)}, \tag{27}$$

where $t \in [\tau, T]$.

Through the closed-form of the optimal investment strategy in (27), we learn that the manager will formulate the current optimal portfolio fraction ($\pi^*(t)$) based on the current state ($X(t)$) and the effect generated by previous strategies (i.e.,$X(t+\tau)$). It is obvious that our result is different from previous research results once the input-delay is not 0.

4.2. An Optimization Algorithm for OPCP. To obtain the numerical solution of the optimal investment strategy and show its sample trajectory, in this paper, an algorithm (OPCPA) is developed, and the split-step algorithm (see [28] for details) is adopted to calculate the numerical solution of (27). The detailed design procedure of OPCPA is as follows:

Step 1: set the value of the parameters (r, c, σ, λ, μ_v, σ_v, T, X_0, $l(t)$, τ, g, x_0, ω, NP) and give the distribution function of the jump amplitude (V).

Step 2: let $t = 0$, $h = 0.01$.

Step 3: calculate $\pi^*(t)$ by (4), (5) and (27).

Step 4: substitute the obtained $\pi^*(t)$ into (5) and combine with the split-step algorithm to give a numerical approximation of $X(t+\tau+h)$. Let $t = t+h$.

Step 5: if $0 \le t \le \tau$, return to Step 3; else if $\tau < t < T-\tau$, substitute $X(t)$ and $X(t+\tau)$ into (27) to calculate $\pi^*(t)$ and return to Step 4; else if $t > T-\tau$, go to Step 6.

Step 6: draw the sample trajectory of the optimal investment strategy where $t \in [0, T-\tau]$.

5. Numerical Simulation

In this section, a numerical simulation is performed to demonstrate the effectiveness of our model. Consider a DC pension with $T = 20$ (years). The pension contribution rate is assumed to be constant $l(t) = 0.15$. The other parameters are $X_0 = 1$(ten thousand dollars), $r = 0.02$, $c = 0.065$, $\sigma = 0.4$, $\lambda = 0.1$, $\mu_v = 0.1$, $\sigma_v = 0.4$, $\tau = 0.2$, $g = 0.015$, $x_0 = 35$, $\omega = 110$, NP $= 0.03122$. As in [9], we assume that the jump amplitude of stock is simulated with log-normal distribution, i.e.,

$$V_i = R_i - 1, \qquad \ln R_i \sim N\left(\mu, \theta^2\right), \qquad i = 1, 2, 3, \ldots, \tag{28}$$

where $\mu = 2\ln(1+\mu_v) - 1/2\ln(1+2\mu\, v+\sigma_v^2)$, $\theta^2 = \ln(1+2\mu_v+\sigma_v^2) - 2\ln(1+\mu_v)$.

From the expression of the optimal investment strategy in (27), in addition to the parameters of the market model, we know that the optimal investment strategy carried out at time t is also dependent on the pension fund at t and the pension fund at $t+\tau$. We adopt the OPCPA algorithm to simulate the evolution process of the pension fund and the trajectory of the optimal investment strategy.

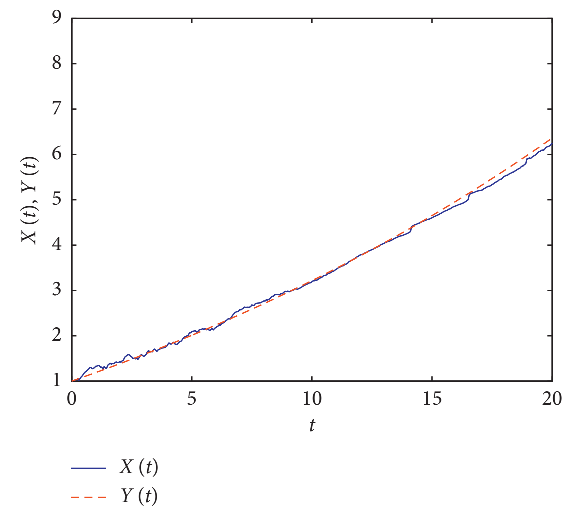

Figure 1: $X(t)$ is the pension fund scale at t; $Y(t)$ represents the cumulative process of investing all of the pension fund in a risk-free asset with instantaneous interest rate δ. $l(t) = 0.15$, $r = 0.02$, $c = 0.065$, $\sigma = 0.4$, $\lambda = 0.1$, $\mu_v = 0.1$, $\sigma_v = 0.4$, $\tau = 0.2$, $g = 0.015$, $x_0 = 35$, $\omega = 110$, NP $= 0.03122$.

With step length $h = 0.05$, we perform numerical simulation in two parts: simulating the trajectory of optimal investment strategy and the accumulation process of DC pension fund; sensitivity analysis including the impact of managers' preset terminal target, the length of input-delay, and jump intensity on the optimal investment strategies.

In order to facilitate the observation of the evolution process of the actual fund scale, we assume that the preset terminal target is the value of a risk-free asset at time T. The value of the risk-free asset at time t can be expressed as $Y(t) = X_0 \cdot e^{\delta t} + \int_0^t l(s)e^{\delta(t-s)}\mathrm{d}s$, $Y(T) = L_0$ and $Y(0) = X_0$. The dynamics of $Y(t)$ describes the cumulative process of investing all of the pension fund in a risk-free asset with an instantaneous interest rate δ. Combining with (8), we have $\delta = 0.035$. In the numerical simulation, we will compare the evolution process of $Y(t)$ with $X(t)$.

Figure 1 shows the evolution process of pension fund under the obtained optimal investment strategy in our model. Due to the input-delay, the duration of carrying out investment strategy is $[0, T-\tau]$ while the duration of its effect is $[\tau, T]$. The results show a relatively larger increase of fund scale in the first two years and a relatively gentle increase in the later stage. From Figure 1, we know that the optimal investment strategy obtained via our model can satisfy the manager's goal; that is, the DC pension fund scale is close to the managers' preset terminal target at the terminal moment.

Figure 2 shows the trajectory of the optimal investment strategy obtained in our model. The duration of carrying out the optimal investment strategies is $[0, T-\tau]$. It is clear that $\pi^*(t)$ presents a wave-like decline over time. The relatively high proportion investing in stock in the initial stage has

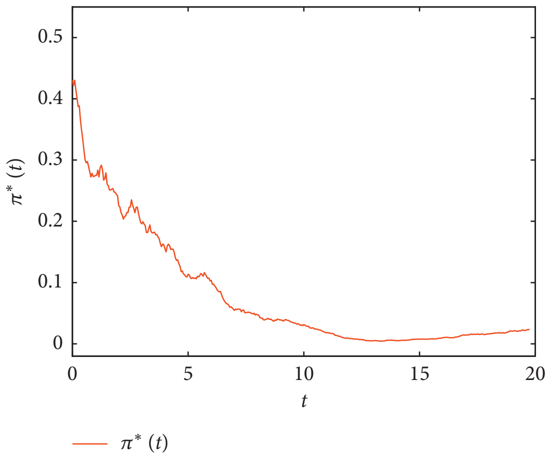

FIGURE 2: The optimal investment fraction in stock obtained in our model. $l(t) = 0.15$, $r = 0.02$, $c = 0.065$, $\sigma = 0.4$, $\lambda = 0.1$, $\mu_v = 0.1$, $\sigma_v = 0.4$, $\tau = 0.2$, $g = 0.015$, $x_0 = 35$, $\omega = 110$, NP = 0.03122.

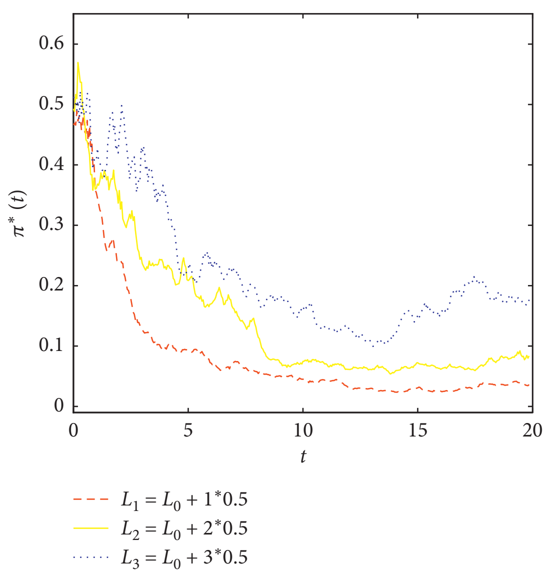

FIGURE 3: The impact of managers' preset terminal target on the optimal investment strategy $\pi^*(t)$. $l(t) = 0.15$, $r = 0.02$, $c = 0.065$, $\sigma = 0.4$, $\lambda = 0.1$, $\mu_v = 0.1$, $\sigma_v = 0.4$, $\tau = 0.1$, $g = 0.015$, $x_0 = 35$, $\omega = 110$, $NP = 0.03122$. $L_i\,(i = 1, 2, 3)$ represents the level of the different preset terminal target.

resulted in a significant increase of pension fund, which has led to less demand for stock in the later stages to avoid unnecessary risks.

Figure 3 shows the impact of the managers' preset terminal target on the optimal investment fraction in stock. The results show that increasing the preset terminal target (L_0) increases the optimal investment fraction in stock. This result is in line with reality. The higher the preset terminal target, the more the stock needed to significantly increase the pension fund scale and meet the preset terminal target.

Figure 4 shows the effect of the length of input-delay on the optimal investment fraction in stock. The results show that the longer the length of input-delay, the higher the

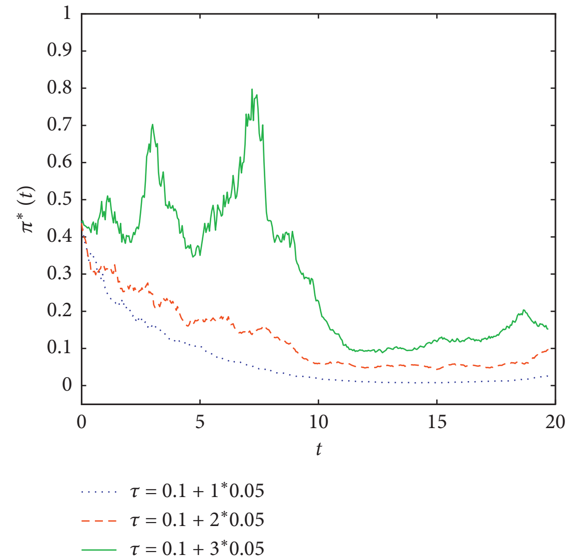

FIGURE 4: The impact of the length of input-delay τ on optimal investment strategy $\pi^*(t)$. $l(t) = 0.15$, $r = 0.02$, $c = 0.065$, $\sigma = 0.4$, $\lambda = 0.1$, $\mu_v = 0.1$, $\sigma_v = 0.4$, $g = 0.015$, $x_0 = 35$, $\omega = 110$, NP = 0.03122.

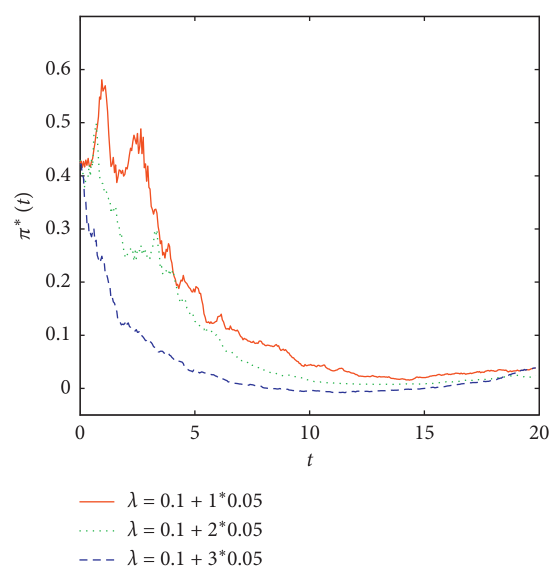

FIGURE 5: The impact of the jump intensity λ on an optimal investment strategy. $l(t) = 0.15$, $r = 0.02$, $c = 0.065$, $\sigma = 0.4$, $\mu_v = 0.1$, $\sigma_v = 0.4$, $\tau = 0.1$, $g = 0.015$, $x_0 = 35$, $\omega = 110$, NP = 0.03122.

optimal investment proportion in stock. Due to the existence of input-delay, the acting duration of investment behavior is $[\tau, T]$. Increasing the length of input-delay reduces the length of acting duration. In this situation, the investment proportion of stock should be increased to meet the managers' preset terminal target at the terminal time.

Figure 5 shows the influence of the jump intensity of stock on optimal investment proportion in stock. From Figure 5, we know that the increasing jump intensity decreases the optimal investment proportion in stock. Large λ implies great uncertainty of financial market and also unknown risk that fund members have to bear, that is, the great investment risk. Therefore, in this circumstance, the proportion invested in stock should be reduced to avoid unknown great risk.

6. Conclusion

In this paper, we studied an optimal DC pension plan, where the input-delay is considered and the price process of the risky asset is modeled as a jump-diffusion process. Due to the input-delay, the accumulation process of DC pension fund is expressed as a SDDE. Considering the principal-agent relationship between pension members and managers, we present the calculation of a terminal target with both the mortality credit and the inflation included, which reflects the required fund scale at the terminal time to provide high standard retirement life for members. To secure a comfortable retirement life for pension members and avoid excessive risk, the management goal of our model is to minimize the expected value of the quadratic deviations between the actual terminal fund and the preset terminal target. In order to solve the optimal portfolio control problem, the stochastic dynamic programming method is adopted. Then, the closed-form solution of the resulting HJB equation is obtained by applying the match method. In addition, an algorithm is given in this paper to calculate the numerical solution of the optimal investment strategy. With the help of the optimization algorithm, we simulated the trajectory of the optimal investment strategy and the accumulation process of the DC pension under the optimal strategy. The results show that our model could satisfy the management goal. And we also conducted a sensitivity analysis to explore the impact of the preset terminal target, the length of the input-delay and the jump intensity of stock on the optimal investment strategy.

Our findings show that the increasing preset terminal target increases the optimal investment proportion of stock to satisfy the management goal. The longer the length of input-delay, the shorter the acting duration of investment behavior, the larger the optimal investment fraction of stock to improve the performance of pension fund in a shorter duration and managers should decrease the proportion of investing in stock when jump intensity of stock is high to avoid unknown great risk.

Data Availability

No data were used to support this study.

Conflicts of Interest

The authors declare that they have no conflicts of interest.

Acknowledgments

This work was supported by the Natural Science Foundation of Shandong Province, China (Grant no. ZR2015FM014), Postdoctoral Science Foundation of China (Grant no. 2015M572060), and Postdoctoral Science Foundation of Qingdao, China.

References

[1] P. Battocchio and F. Menoncin, "Optimal pension management in a stochastic framework," *Insurance: Mathematics and Economics*, vol. 34, no. 1, pp. 79–95, 2004.

[2] G. Guan and Z. Liang, "Optimal management of DC pension plan under loss aversion and value-at-risk constraints," *Insurance: Mathematics and Economics*, vol. 69, pp. 224–237, 2016.

[3] Y. Dong and H. Zheng, "Optimal investment of DC pension plan under short-selling constraints and portfolio insurance," *Insurance: Mathematics and Economics*, vol. 85, pp. 47–59, 2019.

[4] R. C. Merton, "Lifetime portfolio selection under uncertainty: the continuous-time case," *The Review of Economics and Statistics*, vol. 51, no. 3, pp. 247–257, 1969.

[5] P. Battocchio and F. Menoncin, "Optimal portfolio strategies with stochastic wage income: the case of a defined contribution pension plan," Discussion Papers (IRES-Institut de Recherches Economiques et Sociales), Noisy-le-Grand, France, 2002.

[6] J. Ma, H. Zhao, and X. Rong, "Optimal investment strategy for a DC pension plan with mispricing under the Heston model," *Communications in Statistics-Theory and Methods*, vol. 49, no. 13, pp. 3168–3183, 2020.

[7] M. Li, Y. Deng, Y. Huang, and H. Ou, "Optimal strategies for an ambiguity-averse insurer under a jump-diffusion model and defaultable risk," *Mathematical Problems in Engineering*, vol. 2020, Article ID 6207805, 20 pages, 2020.

[8] F. B. Hanson and J. J. Westman, "Optimal consumption and portfolio control for jump-diffusion stock process with log-normal jumps," in *Proceedings of the 2002 American Control Conference (IEEE Cat. No. CH37301)*, Anchorage, AK, USA, May 2002.

[9] J. Sun, Z. Li, and Y. Zeng, "Precommitment and equilibrium investment strategies for defined contribution pension plans under a jump-diffusion model," *Insurance: Mathematics and Economics*, vol. 67, pp. 158–172, 2016.

[10] W. Mudzimbabwe, "A simple numerical solution for an optimal investment strategy for a DC pension plan in a jump diffusion model," *Journal of Computational and Applied Mathematics*, vol. 360, pp. 55–61, 2019.

[11] C. I. Nkeki, "Optimal pension fund management in a jump-diffusion environment: theoretical and empirical studies," *Journal of Computational and Applied Mathematics*, vol. 330, pp. 228–252, 2018.

[12] W. Yu, P. Guo, Q. Wang et al., "On a periodic capital injection and barrier dividend strategy in the compound Poisson risk model," *Mathematics*, vol. 8, no. 4, p. 511, 2020.

[13] L. Li, *Study on Mean-Variance Portfolio Selection with Time Delay*, Shandong University, Jinan, China, 2016.

[14] L. Li and H. Mi, "Optimal investment and consumption with stochastic factor and delay," *The ANZIAM Journal*, vol. 61, no. 1, pp. 99–117, 2019.

[15] Q. Zhang and P. Chen, "Optimal reinsurance and investment strategy for an insurer in a model with delay and jumps," *Methodology and Computing in Applied Probability*, vol. 22, no. 2, pp. 777–801, 2020.

[16] J. Gao, "Stochastic optimal control of DC pension funds," *Insurance: Mathematics and Economics*, vol. 42, no. 3, pp. 1159–1164, 2008.

[17] H. Chang, C. Wang, Z. Fang, and D. Ma, "Defined contribution pension planning with a stochastic interest rate and mean-reverting returns under the hyperbolic absolute risk

aversion preference," *IMA Journal of Management Mathematics*, vol. 31, no. 2, pp. 167–189, 2020.

[18] J.-F. Boulier, S. Huang, and G. Taillard, "Optimal management under stochastic interest rates: the case of a protected defined contribution pension fund," *Insurance: Mathematics and Economics*, vol. 28, no. 2, pp. 173–189, 2001.

[19] G. Guan and Z. Liang, "Optimal management of DC pension plan in a stochastic interest rate and stochastic volatility framework," *Insurance: Mathematics and Economics*, vol. 57, pp. 58–66, 2014.

[20] L. He and Z. Liang, "Optimal assets allocation and benefit outgo policies of DC pension plan with compulsory conversion claims," *Insurance: Mathematics and Economics*, vol. 61, pp. 227–234, 2015.

[21] D. Li, X. Rong, H. Zhao, and B. Yi, "Equilibrium investment strategy for DC pension plan with default risk and return of premiums clauses under CEV model," *Insurance: Mathematics and Economics*, vol. 72, pp. 6–20, 2017.

[22] J. Gao, "Optimal portfolios for DC pension plans under a CEV model," *Insurance: Mathematics and Economics*, vol. 44, no. 3, pp. 479–490, 2009.

[23] Q.-P. Ma, "On "optimal pension management in a stochastic framework" with exponential utility," *Insurance: Mathematics and Economics*, vol. 49, no. 1, pp. 61–69, 2011.

[24] P. Wang and Z. Li, "Robust optimal investment strategy for an AAM of DC pension plans with stochastic interest rate and stochastic volatility," *Insurance: Mathematics and Economics*, vol. 80, pp. 67–83, 2018.

[25] X. Zhang and X. Zheng, "Optimal investment-reinsurance policy with stochastic interest and inflation rates," *Mathematical Problems in Engineering*, vol. 2019, Article ID 5176172, 14 pages, 2019.

[26] H.-P. Kohler and I. V. Kohler, "Frailty modeling for adult and old age mortality: the application of a modified de moivre hazard function to sex differentials in mortality," *Demographic Research*, vol. 3, no. 1, 2000.

[27] F. Hanson, *Applied Stochastic Processes and Control for Jump-Diffusions: Modeling, Analysis, and Computation*, Society for Industrial and Applied Mathematics, Philadelphia, PA, USA, 2007.

[28] Y. Qiu, Z. Wang, and Y. Qin, "Split-step algorithm for nonlinear stochastic delay differential equations with jumps," *Journal of East China University of Science and Technology (Natural Science Edition)*, vol. 40, p. 816, 2014.

Hindawi
Mathematical Problems in Engineering
Volume 2020, Article ID 3561089, 12 pages
https://doi.org/10.1155/2020/3561089

Research Article

Threshold Estimation for a Spectrally Negative Lévy Process

Honglong You and Chuncun Yin

School of Statistics, Qufu Normal University, Jining, Shandong 273165, China

Correspondence should be addressed to Honglong You; youhonglong815@163.com

Received 11 June 2020; Accepted 7 July 2020; Published 30 July 2020

Guest Editor: Wenguang Yu

Consider a spectrally negative Lévy process with unknown diffusion coefficient and Lévy measure and suppose that the high frequency trading data is given. We use the techniques of threshold estimation and regularized Laplace inversion to obtain the estimator of survival probability for a spectrally negative Lévy process. The asymptotic properties are given for the proposed estimator. Simulation studies are also given to show the finite sample performance of our estimator.

1. Introduction

In actuarial science, it is an important topic to consider the ruin probability for some risk models. There are some methods for this topic, for example, the integro-differential equation technique, renewal theory, Laplace transform, martingale theory, and so on. For details, see the monograph of Asmussen and Albrecher [1]. These methods heavily depend on the knowledge of the risk model, which are usually unknown in practice. It is also known that explicit formula for the ruin probability is usually not available when we have no precise information on the risk model. In order to overcome this difficulty, many researchers have done a large amount of work and obtained lots of nice results. Some authors have considered the approximations, upper and lower bounds of the ruin probability. See, for example, Dufresne and Gerber [2], Veraverbeke [3], Dermitzakis and Politis [4], and Li et al. [5]. Others have been contributed to semiparametric and nonparametric estimation of the ruin probability. See, for example, Croux and Veraverbeke [6], Frees [7], Mnatsakanov et al. [8], Pitts [9], Politis [10], You et al. [11], and Zhang et al. [12].

In practical situations, to get the data is much easier than to obtain the precise information on the risk model. In financial market, high frequency trading exists and a lot of high frequency trading data can be used to make statistical inference of the law of financial market. Using the data, we can estimate the survival probability by some statistical methods. In our work, we assume that the high frequency data is from n discrete time observations with step h_n. The asymptotic framework is that n tends to infinity and h_n tends to zero while nh_n tends to infinity. See, Comte and Genon-Catalot [13, 14]. For an insurance company, if the surplus has lots of small fluctuations, we assume that the surplus may be described by Lévy process. Our work will consider the survival probability for Lévy process. There are also some nice results for the ruin probability in Lévy process. For example, Zhang and Yang [15] have proposed a nonparametric estimator of ruin probability for pure jump Lévy process by Fourier (inversion) transform. The method of Zhang and Yang [15] has also been used by Shimizu and Zhang [16] to study the Gerber–Shiu function for Lévy subordinator. You and Cai [17] and Cai et al. [18] have constructed an estimator for the survival probability in a spectrally negative Lévy risk model by the regularized Laplace inversion technique. In the paper, we will use a threshold technique to study the survival probability. Mancini [19], Mancini [20], Shimizu [21], and Shimizu [22] have proposed the threshold technique for identifying the times when jumps larger than a suitably defined threshold occurred. Given a discrete record of observations, the technique may separate the contributions of the diffusion part and jump part of the risk model. Therefore, we can obtain more accurate data for the jump part of the risk model by the threshold technique. In this paper, we will give an estimator of the survival probability by the threshold technique and the regularized Laplace inversion technique. Our method will calculate the survival probability more accurately for a spectrally negative Lévy risk model.

Here is a brief outline of this paper. We will introduce our risk model and define the survival probability in Section 2. In Section 3, we will construct an estimator of survival probability for our risk model. Section 4 gives the asymptotic properties of the estimators. In Section 5, we will do some simulations to show the finite sample size performance of the estimators. Finally, some conclusions are given in Section 6. All the technical proofs are presented in Appendix.

2. Preliminaries

2.1. Risk Model. Let

$$Y_t = ct + \sigma W_t - J_t, \quad t \geq 0 \tag{1}$$

be a spectrally negative Lévy process, where $c > 0$, $\sigma > 0$, and $W = \{W_t, t \geq 0\}$ is a standard Brownian motion; $J = \{J_t, t \geq 0\}$ is a subordinator; Suppose that W and J are independent of each other.

The Laplace exponent of $Y = \{Y_t, t \geq 0\}$ is denoted by

$$\begin{aligned}\psi_Y(s) &= \frac{1}{t}\ln\left(\mathbf{E}\left[e^{sY_t}\right]\right)\\ &= cs + \frac{1}{2}\sigma^2 s^2 - \int_0^\infty \left(1 - e^{-sx}\right)\nu(\mathrm{d}x), \quad s > 0,\end{aligned} \tag{2}$$

where ν is a Lévy measure and satisfies $\int_0^\infty (1 \wedge x)(\mathrm{d}x) < \infty$.

Let $u > 0$ be the initial surplus of an insurance company. The surplus at time t is given by

$$U_t = u + Y_t = u + ct + \sigma W_t - J_t, \quad t \geq 0, \tag{3}$$

where c is the rate of premium; σ represents the diffusion coefficient; and J and W denote the cumulative claims amount and a diffusion process.

2.2. Survival Probability. The infinite-time horizon survival probability $\Phi(u)$ is defined as follows:

$$\Phi(u) = 1 - \mathbf{P}\left(\inf_{0 \leq t < \infty} U_t \leq 0 \,\middle|\, U_0 = u\right). \tag{4}$$

In [23], Huzak et al. have given the following Pollaczek–Khinchin type formula for the survival probability,

$$\Phi(u) = \left(1 - \frac{\mu_1}{c}\right)\sum_{i=0}^\infty \rho^i \left(G^{(i+1)*} * H^{(i)*}\right)(u), \quad u > 0, \tag{5}$$

where $\mu_1 = \int_0^\infty x\nu(\mathrm{d}x)$, $H(x) = (1/\mu_1)\int_0^x \nu(y, \infty)\mathrm{d}y$ and G is determined by the Laplace transform

$$\int_0^\infty e^{-sx}\mathrm{d}G(x) = \frac{c}{c + (\sigma^2/2)s}. \tag{6}$$

By (5), the Laplace transform of $\Phi(u)$ is given by

$$\begin{aligned}\mathscr{L}_\Phi(s) &= \int_0^\infty e^{-su}\Phi(u)\mathrm{d}u\\ &= \frac{c - \mu_1}{cs + (\sigma^2/2)s^2 - \int_0^\infty \left(1 - e^{-sx}\right)\nu(\mathrm{d}x)}, \quad s > 0.\end{aligned} \tag{7}$$

3. Estimation of Survival Probability

In our work, we assume that σ and ν are unknown. In order to estimate $\Phi(u)$, we need to estimate the Laplace transform of $\Phi(u)$. Now, let us rewrite (7) as follows:

$$\mathscr{L}_\Phi(s) = \frac{1 - \rho}{(1/c)\psi_Y(s)}, \quad s > 0, \tag{8}$$

where $\rho = \mu_1/c$ and $\psi_Y(s) = cs + (1/2)\sigma^2 s^2 - \int_0^\infty (1 - e^{-sx})\nu(\mathrm{d}x)$.

Suppose that a discrete sample $Y^n = \{Y_{t_i^n} \mid t_i^n = ih_n; i = 0, 1, 2, \ldots, n\}$ can be observed. Let $Z_i = Y_{t_i^n} - Y_{t_{i-1}^n}$ and $h_n = t_i^n - t_{i-1}^n > 0$. Our interest is to estimate $\Phi(u)$ by a sample $\{Z_1, Z_2, \ldots, Z_n\}$.

3.1. A Threshold Estimator of $\mathscr{L}_\Phi(s)$. In this part, we will construct an estimator of $\mathscr{L}_\Phi(s)$. If we can estimate ρ and $\psi_Y(s)$ in (8), the estimator of $\mathscr{L}_\Phi(s)$ will be given by a plug-in device. By You and Cai [17], an estimator of $\psi_Y(s)$ has been given by

$$\widehat{\psi}_Y(s) = \frac{1}{h_n}\left(\frac{1}{n}\sum_{k=1}^n e^{sZ_k} - 1\right), \quad s > 0. \tag{9}$$

Now, the following work is to estimate $\rho = \mu_1/c$. By Shimizu [21, 22], we introduce the filter which is defined by

$$\begin{aligned}\mathscr{D}_k^n &:= \left\{\omega \in \Omega; \left(ch_n - Z_k\right) > h_n^b\right\},\\ \mathscr{C}_k^n &:= \left\{\omega \in \Omega; \left(ch_n - Z_k\right) \leq h_n^b\right\},\end{aligned} \tag{10}$$

where b is a positive constant.

In Shimizu [21], the author assumed that $J = \{J_t, t \geq 0\}$ is a compound Poisson process. When $b \in (0, (1/2))$, it is easy to judge a jump occurred if $(ch_n - Z_k) > h_n^b$. As a result, $(ch_n - Z_k)$ can be an approximation of the jump size when $(ch_n - Z_k) > h_n^b$ and $h_n \longrightarrow 0$.

When $J = \{J_t, t \geq 0\}$ is a compound Poisson process, we can give the following estimator of ρ:

$$\widehat{\rho} = \frac{1}{cnh_n}\sum_{k=1}^n \left(ch_n - Z_k\right)\mathbf{I}_{\mathscr{D}_k^n}. \tag{11}$$

If $J = \{J_t, t \geq 0\}$ has possibly a infinite number of jumps in each finite time interval, we still choose $\widehat{\rho}$ as an estimator of ρ.

Finally, by (8), (9), and (11), an estimator of $\mathscr{L}_\Phi(s)$ is given by

$$\widehat{\mathscr{L}}_\Phi(s) = \frac{1 - \widehat{\rho}}{(1/c)\widehat{\psi}_Y(s)}, \quad s > 0. \tag{12}$$

3.2. A Regularized Laplace Inversion Technique. In [24], Chauveau et al. have given the following regularized Laplace inversion technique.

Definition 1. Let $m>0$ be a constant. The regularized Laplace inversion L_m^{-1}: $L^2(0,\infty) \longrightarrow L^2(0,\infty)$. is given by

$$L_m^{-1} g(t) = \frac{1}{\pi^2}\int_0^\infty \int_0^\infty \Psi_m(y) y^{-1/2} e^{-tvy} g(v) \mathrm{d}v\, \mathrm{d}y, \quad (13)$$

for a function $g \in L^2(0,\infty)$ and $t \in (0,\infty)$, where

$$\Psi_m(y) = \int_0^{a_m} \cosh(\pi x)\cos(x \log y)\mathrm{d}x, \quad (14)$$

and $a_m = \pi^{-1}\cosh^{-1}(\pi m) > 0$.

By Definition 1, the regularized Laplace inversion technique is available for any $L^2(0,\infty)$ functions. According to the proof of Proposition 3.3 in You and Cai [17], we know that $\widehat{\mathscr{L}}_\Phi(s) \notin L^2(0,\infty)$. In order to apply Definition 1, we must amend $\widehat{\mathscr{L}}_\Phi(s)$.

Let $\Phi_\theta(u)$: $= e^{-\theta u}\Phi(u)$ for arbitrary fixed $\theta>0$. Obviously, we have

$$\mathscr{L}_{\Phi_\theta}(s) = \mathscr{L}_\Phi(s+\theta), \quad s>0. \quad (15)$$

Therefore, we will give an estimator of $\mathscr{L}_{\Phi_\theta}(s)$ as follows:

$$\widehat{\mathscr{L}}_{\Phi_\theta}(s) \coloneqq \widehat{\mathscr{L}}_\Phi(s+\theta) = \frac{1-\widehat{\rho}}{(1/c)\widehat{\psi_Y}(s+\theta)}, \quad s>0. \quad (16)$$

By Definition 1, we can construct an estimator of $\Phi(u)$ as follows:

$$\widehat{\Phi}_m(u) = e^{\theta u}\mathscr{L}_m^{-1}\widehat{\mathscr{L}}_{\Phi_\theta}(s), \quad u>0,\ \theta>0, \quad (17)$$

for suitable $m>0$.

4. Asymptotic Property of Estimators

In this section, we will study the asymptotic property for those estimators which are proposed in Section 3. In [17], You and Cai have given the asymptotic normality and consistency of $\widehat{\psi}_Y(s)$. The following work will consider the asymptotic property of $\widehat{\rho}$, $\widehat{\mathscr{L}}_{\Phi_\theta}(s)$, and $\widehat{\Phi}_m$.

If $J=\{J_t, t\geq 0\}$ is a compound Poisson process, we will give the following Theorems 1 and 2.

Let $J_t = \sum_{j=1}^{N_t}\gamma_j$, where $N=\{N_t, t\geq 0\}$ is a Poisson process with constant intensity λ. The random variables $\gamma_1, \gamma_2, \gamma_3, \ldots$ are *i.i.d.* and independent of N. Let $\mu_\gamma = E[\gamma_1] < \infty$, $\sigma_\gamma^2 = E[\gamma_1^2] - \mu_\gamma^2 < \infty$, and $\mathscr{L}_\gamma(s) = E[e^{-s\gamma_1}]$.

Theorem 1. *Suppose that the net profit condition $c>\lambda\mu_\gamma$ hold. If $b\in(0,(1/2))$, $\theta>0$, $\lim_{n\longrightarrow\infty}h_n = 0$, $\lim_{n\longrightarrow\infty}nh_n = \infty$, and $\lim_{n\longrightarrow\infty}nh_n^{1+\beta} = 0$ for some $\beta\in(0,1)$, then for $n\longrightarrow\infty$, we have*

$$\widehat{\rho} - \rho \xrightarrow{P} 0, \quad (18)$$

$$\sqrt{nh_n}(\widehat{\rho}-\rho) \xrightarrow{D} \mathscr{N}\left(0, \frac{1}{c^2}\lambda\left(\mu_\gamma^2+\sigma_\gamma^2\right)\right), \quad (19)$$

$$\sqrt{nh_n}\left(\widehat{\mathscr{L}}_{\Phi_\theta}(s) - \mathscr{L}_{\Phi_\theta}(s)\right) \xrightarrow{D} \mathscr{N}\left(0, \frac{\lambda\left(\mu_\gamma^2+\sigma_\gamma^2+\sigma^2\right)}{\psi_Y^2(s+\theta)} + \frac{\mu_\gamma^2\psi_Y(2s+2\theta)}{\psi_Y^4(s+\theta)}\right). \quad (20)$$

Theorem 2. *Suppose that $\Phi(u)$ has the first derivative $g(u)$ such that $g(u)$ is of the polynomial growth and the conditions of Theorem 1 are satisfied. Then, for $m=\sqrt{nh_n/\log(nh_n)}$, $u>0$ and any constant $B>0$, we have*

$$\left\|\widehat{\Phi}_m - \Phi\right\|_B^2 = O_P\left(\frac{1}{\log(nh_n)}\right), \quad n\longrightarrow\infty. \quad (21)$$

Now, we consider that the process J contains lots of small jumps, i.e., an infinite number of jumps in each finite time interval. Theorem 3 will give the consistency for $\widehat{\rho}$ and $\widehat{\mathscr{L}}_{\Phi_\theta}(s)$.

Theorem 3. *Suppose that the net profit condition $c>\mu_1$ hold. If $b\in(0,(1/4))$, $h_n\longrightarrow 0$, $nh_n\longrightarrow\infty$, and $nh_n^{1+\beta}\longrightarrow 0$ for some $\beta\in(0,1)$ as $n\longrightarrow\infty$, then*

$$\widehat{\rho} - \rho \xrightarrow{P} 0, \quad (22)$$

$$\widehat{\mathscr{L}}_{\Phi_\theta}(s) - \mathscr{L}_{\Phi_\theta}(s) \xrightarrow{P} 0. \quad (23)$$

Theorem 4. *Suppose that $\Phi(u)$ has the first derivative $g(u)$ such that $g(u)$ is of the polynomial growth and the conditions of Theorem 3 are satisfied. Then, for $u>0$, $m>0$, and $B>0$, we have*

$$\left\|\widehat{\Phi}_m - \Phi\right\|_B^2 \leq m^2 o_P(1) + a_m, \quad n\longrightarrow\infty, \quad (24)$$

where $a_m = O(1/\log m)$ as $m\longrightarrow\infty$.

5. Simulation

In this section, we will give some simulation studies to show the performance of our estimator with finite samples. The work is based on MATLAB. We do not pretend to find an optimal threshold function for each considered model.

We assume that the Lévy measure is given by $\nu(\mathrm{d}x) = \lambda(1/\eta)e^{-(1/\eta)x}\mathrm{d}x$, then J is a compound Poisson process where the Poisson intensity is λ and the individual claim sizes are exponentially distributed with mean η.

The survival probability is given by

$$\Phi(u) = 1 - \frac{r_1 + (1/\eta) + \left(2\lambda\eta/\sigma^2\right)}{r_1-r_2}e^{r_1 u} - \frac{r_2 + (1/\eta) + \left(2\lambda\eta/\sigma^2\right)}{r_2-r_1}e^{r_2 u}, \quad (25)$$

where $r_2<r_1<0$ are negative roots of the following equation

$$\frac{1}{2}\sigma^2 s + c - \frac{\lambda}{s+(1/\eta)} = 0. \quad (26)$$

We take $c=\lambda=10$, $\eta=1/2$, $\sigma=5$, $b=1/4$, and $h_n = n^{-4/5}$. Then, $\mu_1 = \lambda\eta = 5$ and $\rho = \mu_1/c = 0.5$.

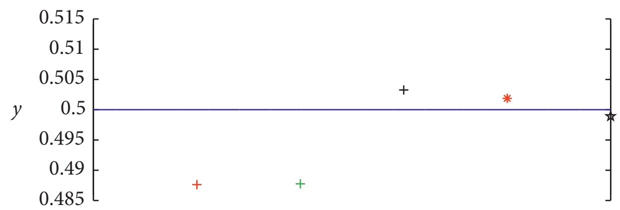

Figure 1: $\widehat{\rho}$ with sample sizes $n = 1000$, 5000, 8000, 10000, and 30000.

Table 1: The data of $\widehat{\rho}$ and its errors.

Sample sizes	The data of $\widehat{\rho}$	The actual data of ρ	Errors
$n = 1000$	0.4878	0.5	0.0122
$n = 5000$	0.4876	0.5	0.0124
$n = 8000$	0.5033	0.5	0.0033
$n = 10000$	0.5019	0.5	0.0019
$n = 30000$	0.4989	0.5	0.0011

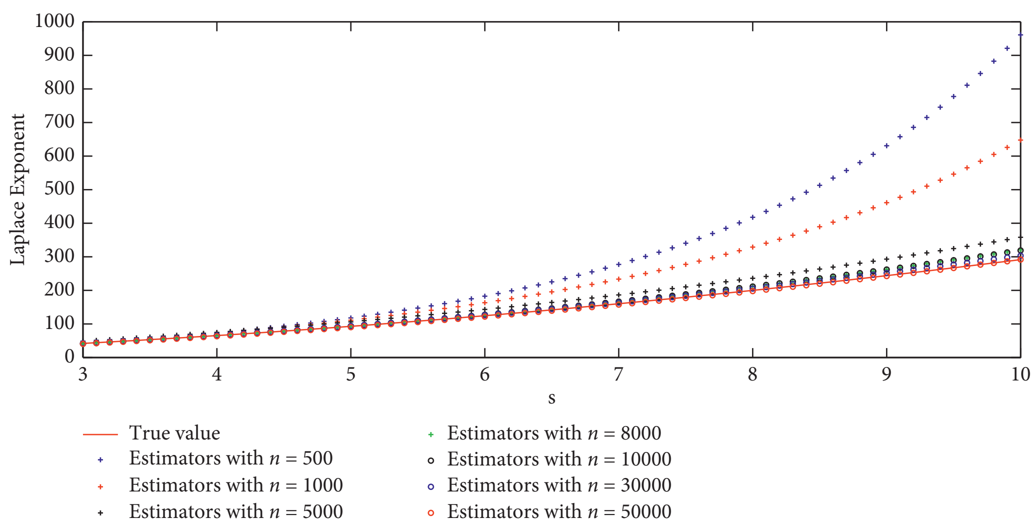

Figure 2: The estimator of ψ_Y with sample sizes $n = 500$, 1000, 5000, 8000, 10000, 30000, and 50000.

First of all, we consider $\widehat{\rho}$. In Figure 1, we plot the mean points with sample sizes $n = 1000, 5000, 8000, 10000$, and 30000, which are computed based on 5000 simulation experiments.

In Table 1, we give the data of $\widehat{\rho}$ and its errors with sample sizes $n = 1000, 5000, 8000, 10000$, and 30000.

Now, we consider the estimator of ψ_Y. In Figure 2, we plot the mean points with sample sizes $n = 500, 1000, 5000, 8000, 10000, 30000$, and 50000, which are computed based on 5000 simulation experiments.

Next, we consider the estimator of $\mathscr{L}_{\Phi_\theta}$ with $\theta = 0.075$. In Figure 3, we plot the mean points with sample sizes $n = 5000, 10000, 30000, 50000$, and 80000, which are computed based on 5000 simulation experiments.

By Figure 3, the estimator $\widehat{\mathscr{L}}_{\Phi_\theta}$ is very close to the actual data of $\mathscr{L}_{\Phi_\theta}$ as $n \geq 30000$. Thus, we will use the same method as of Cai et al. [18] and You and Cai [17] to simulate $\Phi(u)$. In order to improve computational efficiency, we define

$$\Phi_p(u) = \left(e^{u\theta}/\pi^2\right) \int_0^\infty \int_0^\infty e^{-usy} \left(\widehat{\mathscr{L}}_{\Phi_\theta}(s)\right)_{n_0} \Psi_p(y) y^{-1/2} \mathrm{d}s\, \mathrm{d}y, \tag{27}$$

where $(\widehat{\mathscr{L}}_{\Phi_\theta}(s))_{n_0} = 1 - (1/cn_0 h_{n_0}) \sum_{k=1}^{n_0} (ch_{n_0} - Z_k)\mathbf{I}_{\mathscr{D}_k^{n_0}} / (1/ch_{n_0})((1/n_0)\sum_{k=1}^{n_0} e^{sZ_k} - 1)$,

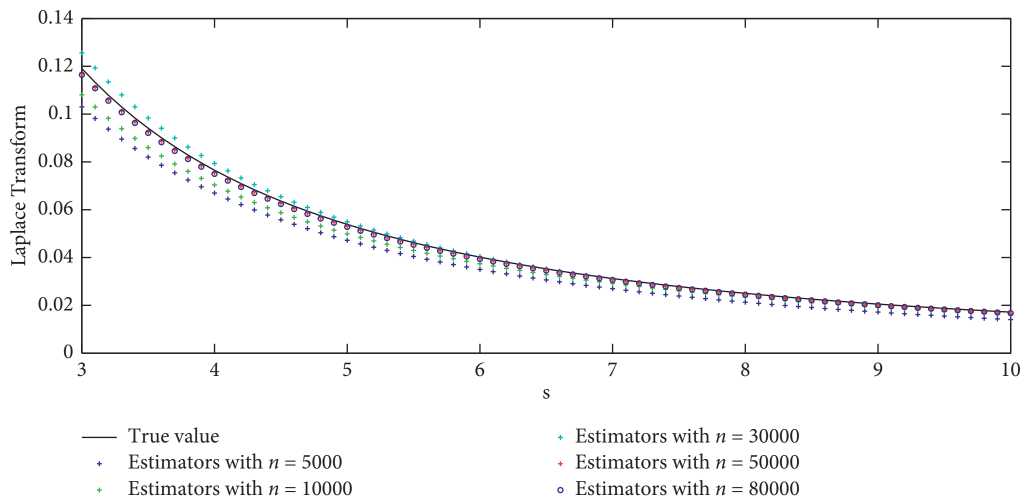

FIGURE 3: The estimator of $\mathscr{L}_{\Phi_\theta}$ with sample sizes $n = 5000$, 10000, 30000, 50000, and 80000.

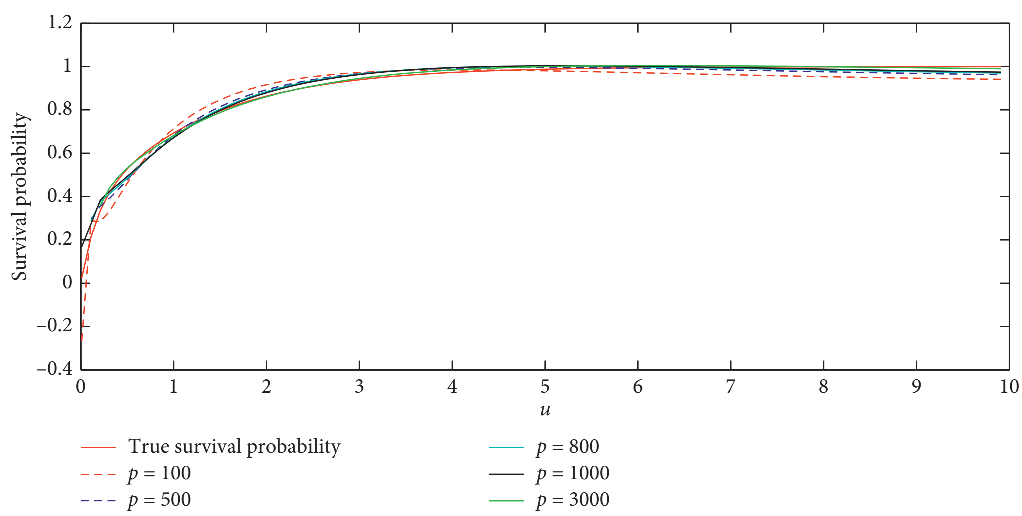

FIGURE 4: True curve and mean curves with sample size $n = 30000$ and $p = 100, 500, 800, 1000,$ and 3000.

$\Psi_p(y) = \int_0^{a_p} \cosh(\pi x)\cos(x\log(y))dx$ and $a_p = \pi^{-1}\cosh^{-1}(\pi p) > 0$, and $n_0 = 30000$.

Now, we will show the performance of $\Phi_p(u)$.

In Figure 4, we plot the mean points with sample sizes $n = 30000$ and $p = 100, 500, 800, 1000,$ and 3000, which are computed based on 5000 simulation experiments.

6. Conclusion

In this paper, we use the threshold estimation technique and regularized Laplace inversion technique to construct an estimator of survival probability for a spectrally negative Lévy process. The rate of convergence for the estimator is a logarithmic rate. We adopt a method which is proposed in Cai et al. [18] to improve the speed in simulated calculation. The further work is to improve the speed of convergence for the estimator. We will combine the threshold estimation technique with the Fourier transform (inversion) technique, Fourier cosine series expansion method, and Laguerre series expansion method to construct an estimator of survival probability. These methods can be referred to Zhang and Hu [12, 25], Zhang and Su [26, 27], Yu et al. [28], and so on. We hope some further studies will be performed for the risk model with the barrier or threshold dividend strategy. See, e.g., Peng et al. [29] and Yu et al. [30]. The Gerber–Shiu function and the aggregate dividends up to ruin will be estimated by some statistical methods.

Appendix

The proof of Theorem 1

Proof. First of all, we have

$$\begin{aligned}
\sqrt{nh_n}(\widehat{\rho}-\rho) &= \sqrt{nh_n}\left(\frac{1}{cnh_n}\sum_{k=1}^{n}(ch_n-Z_k)I_{\mathscr{D}_k^n}-\frac{\lambda\mu_\gamma}{c}\right)\\
&= \sqrt{nh_n}\left(\frac{1}{cnh_n}\sum_{k=1}^{n}(ch_n-Z_k)I_{\mathscr{D}_k^n}-\frac{1}{cnh_n}\sum_{k=1}^{n}\mu_\gamma I_{\{\Delta_i^n N\geq 2\}}+\frac{1}{cnh_n}\sum_{k=1}^{n}\mu_\gamma I_{\{\Delta_i^n N\geq 2\}}-\frac{\lambda\mu_\gamma}{c}\right)\\
&= \frac{1}{c\sqrt{nh_n}}\sum_{k=1}^{n}(ch_n-Z_k)I_{\mathscr{D}_k^n}I_{\{\Delta_i^n N=0\}}+\frac{1}{c\sqrt{nh_n}}\sum_{k=1}^{n}\left((ch_n-Z_k)I_{\mathscr{D}_k^n}-\mu_\gamma\right)I_{\{\Delta_i^n N\geq 2\}}\\
&\quad+\sqrt{nh_n}\left(\frac{1}{cnh_n}\sum_{k=1}^{n}(ch_n-Z_k)I_{\mathscr{D}_k^n}I_{\{\Delta_k^n N=1\}}-\frac{\lambda\mu_\gamma}{c}\right)\\
&\quad+\sqrt{nh_n}\left(\frac{1}{cnh_n}\sum_{k=1}^{n}\mu_\gamma I_{\{\Delta_k^n N\geq 2\}}\right).
\end{aligned} \tag{A.1}$$

Let us now deal with the first term of (A.1),

$$\begin{aligned}
&P\left(\frac{1}{c\sqrt{nh_n}}\sum_{k=1}^{n}(ch_n-Z_k)I_{\mathscr{D}_k^n}I_{\{\Delta_i^n N=0\}}\neq 0\right)\\
&\quad\leq P\left(\cup_{k=1}^{n}\left\{(ch_n-Z_k)>h_n^b,\Delta_k^n N=0\right\}\right)\\
&\quad\leq P\left(\sup_k(ch_n-Z_k)I_{\{\Delta_k^n N=0\}}>h_n^b\right)\\
&\quad\leq P\left(\sup_k\left|\sigma\left(W_{t_k^n}-W_{t_{k-1}^n}\right)\right|>h_n^b\right)\\
&\quad\leq \sum_k P\left(\left|\sigma\left(W_{t_k^n}-W_{t_{k-1}^n}\right)\right|>h_n^b\right).
\end{aligned} \tag{A.2}$$

By Proposition 3.2 and Corollary 3.3 in Mancini [19],

$$\sum_k P\left(\left|\sigma\left(W_{t_k^n}-W_{t_{k-1}^n}\right)\right|>h_n^b\right)\leq n2e^{-h_n^{2b}/2\sigma^2 h_n}=2ne^{-h_n^{(2b-1)}/2\sigma^2}. \tag{A.3}$$

Because of $b\in 0(0,(1/2))$, $2ne^{-h_n^{(2b-1)}/2\sigma^2}\longrightarrow 0$ as $n\longrightarrow\infty$.

Thus, the first term tends to zero in probability.

The second term of (A.1) tends to zero in probability, since

$$\begin{aligned}
&P\left(\frac{1}{c\sqrt{nh_n}}\sum_{k=1}^{n}\left((ch_n-Z_k)I_{\mathscr{D}_k^n}-\mu\right)I_{\{\Delta_i^n N\geq 2\}}\neq 0\right)\\
&\quad\leq P\left(\cup_{k=1}^{n}\{\Delta_i^n N\geq 2\}\right)\\
&\quad\leq O\left(nh_n^2\right).
\end{aligned} \tag{A.4}$$

Therefore, we only need to compute the limit in distribution of the third term of (A.1).

By Mancini [19], we know $P\lim_{n\longrightarrow\infty}I_{\mathscr{D}_k^n}=P\lim_{n\longrightarrow\infty}I_{\{\Delta_k^n N=1\}}$, then

$$\begin{aligned}
&d\lim_{n\longrightarrow\infty}\sqrt{nh_n}\left(\frac{1}{cnh_n}\sum_{k=1}^{n}(ch_n-Z_k)I_{\mathscr{D}_k^n}I_{\{\Delta_k^n N=1\}}-\frac{\lambda\mu}{c}\right)\\
&\quad= d\lim_{n\longrightarrow\infty}\sqrt{nh_n}\left(\frac{1}{cnh_n}\sum_{k=1}^{n}\left[\gamma_k-\sigma\left(W_{t_k^n}-W_{t_{k-1}^n}\right)\right]I_{\{\Delta_k^n N=1\}}-\frac{\lambda\mu}{c}\right).
\end{aligned} \tag{A.5}$$

Because the random variables γ, N, and W are independent to each other and γ_k are *i.i.d*, we have (A.5) that tends to $\mathscr{N}(0,(\lambda(\mu_\gamma^2+\sigma_\gamma^2)/c^2))$ in distribution as $n\longrightarrow\infty$. Thus, we can obtain (19). By (19) and Slutsky's Theorem, it is easy to obtain (18).

Next, by (7) and (16), we have

$$\begin{aligned}
&\sqrt{nh_n}\left(\widehat{\mathscr{L}}_{\Phi_\theta}(s)-\mathscr{L}_{\Phi_\theta}(s)\right)\\
&\quad= \sqrt{nh_n}\left(\frac{\widehat{\rho}}{(1/c)\widehat{\psi}_Y(s+\theta)}-\frac{\rho}{(1/c)\psi_Y(s+\theta)}\right)\\
&\quad= \sqrt{nh_n}\,\frac{\widehat{\rho}\left(\psi_Y(s+\theta)-\widehat{\psi}_Y(s+\theta)\right)+\widehat{\psi}_Y(s+\theta)(\widehat{\rho}-\rho)}{(1/c)\widehat{\psi}_Y(s+\theta)\psi_Y(s+\theta)}.
\end{aligned} \tag{A.6}$$

By Slutsky's Theorem, (11), (9), and (A.6), we have

$$\begin{aligned}
\sqrt{nh_n}\left(\widehat{\mathscr{L}}_{\Phi_\theta}(s)-\mathscr{L}_{\Phi_\theta}(s)\right) &= \sqrt{nh_n}\,\frac{\rho\left(\psi_Y(s+\theta)-\widehat{\psi}_Y(s+\theta)\right)+\psi_Y(s+\theta)\left(\widehat{\rho}-\rho\right)}{(1/c)\left(\psi_Y(s+\theta)\right)^2}+o_P(1)\\
&= \sqrt{nh_n}\,\frac{\psi_Y(s+\theta)\left(\left(\sum_{k=1}^n\left(ch_n-Z_k\right)I_{\mathscr{D}_k^n}/cnh_n\right)-\rho\right)}{(1/c)\left(\psi_Y(s+\theta)\right)^2}\\
&= -\sqrt{nh_n}\,\frac{\rho\left(((1/n)\sum_{k=1}^n e^{(s+\theta)Z_k}-1/h_n)-\psi_Y(s+\theta)\right)}{(1/c)\left(\psi_Y(s+\theta)\right)^2}+o_P(1)\\
&= \sqrt{nh_n}\sum_{k=1}^n\frac{\psi_Y(s+\theta)\left(\left(ch_n-Z_k\right)I_{\mathscr{D}_k^n}/cnh_n\right)-\rho\left(e^{(s+\theta)Z_k}-1\right)/nh_n}{(1/c)\left(\psi_Y(s+\theta)\right)^2}+o_P(1)\\
&= \frac{1}{\sqrt{nh_n}}\sum_{k=1}^n\frac{\psi_Y(s+\theta)\left[\left(ch_n-Z_k\right)I_{\mathscr{D}_k^n}\right]-\rho c\left[e^{(s+\theta)Z_k}-1\right]}{\left(\psi_Y(s+\theta)\right)^2}\\
&\quad+o_P(1).
\end{aligned} \tag{A.7}$$

By $P\lim_{n\longrightarrow\infty}I_{\mathscr{D}_k^n}=P\lim_{n\longrightarrow\infty}I_{\{\Delta_k^n N=1\}}$,

$$\begin{aligned}
&d\lim_{n\longrightarrow\infty}\frac{1}{\sqrt{nh_n}}\sum_{k=1}^n\frac{\psi_Y(s+\theta)\left[\left(ch_n-Z_k\right)I_{\mathscr{D}_k^n}\right]-\rho c\left[e^{(s+\theta)Z_k}-1\right]}{\left(\psi_Y(s+\theta)\right)^2}\\
&\quad=d\lim_{n\longrightarrow\infty}\frac{1}{\sqrt{nh_n}}\sum_{k=1}^n\frac{\psi_Y(s+\theta)\left[\left(ch_n-Z_k\right)I_{\Delta_k^n N=1}\right]-\rho c\left[e^{(s+\theta)Z_k}-1\right]}{\left(\psi_Y(s+\theta)\right)^2}.
\end{aligned} \tag{A.8}$$

By the independent property of γ, N, W, and $\gamma_1,\gamma_2,\gamma_3,\ldots,\gamma_n$,

$$\begin{aligned}
&\sqrt{nh_n}\left(\widehat{\mathscr{L}}_{\Phi_\theta}(s)-\mathscr{L}_{\Phi_\theta}(s)\right)\\
&\quad\xrightarrow{D}\mathscr{N}\left(0,\frac{\lambda\left(\mu_\gamma^2+\sigma_\gamma^2+\sigma^2\right)}{\psi_Y^2(s+\theta)}+\frac{\mu_\gamma^2\psi_Y(2s+2\theta)}{\psi_Y^4(s+\theta)}\right).
\end{aligned} \tag{A.9}$$

In order to prove Theorem 2, we need the following Lemma 1 (see Theorem 3.2 in [24]). □

Lemma 1. *Suppose that for a function $f\in L^2(0,\infty)$ with the derivative f', $\int_0^\infty[t(t^{1/2}f(t))']^2t^{-1}dt<\infty$, then*

$$\left\|\mathscr{L}_n^{-1}\mathscr{L}_f-f\right\|=O\left((\log n)^{-1/2}\right),\quad(n\longrightarrow\infty). \tag{A.10}$$

The proof of Theorem 2

Proof. Using (17),

$$\begin{aligned}
\left\|\widehat{\Phi}_m-\Phi\right\|_B^2&\le e^{2\theta B}\left\|\widehat{\Phi}_m e^{-\theta u}-\Phi_\theta\right\|_B^2\\
&\le 2e^{2\theta B}\left\{\left\|\mathscr{L}_m^{-1}\widehat{\mathscr{L}}_{\Phi_\theta}-\mathscr{L}_m^{-1}\mathscr{L}_{\Phi_\theta}\right\|^2+\left\|\mathscr{L}_m^{-1}\mathscr{L}_{\Phi_\theta}-\Phi_\theta\right\|^2\right\}.
\end{aligned} \tag{A.11}$$

Let $\Phi_\theta'=g_\theta$. Because $g(u)$ satisfies the polynomial growth,

$$\begin{aligned}
\int_0^\infty\left[x\left(\sqrt{x}\,\Phi_\theta(x)\right)'\right]^2(1/x)\mathrm{d}x&\lesssim\int_0^\infty\Phi_\theta^2(x)\mathrm{d}x+\int_0^\infty x^2g_\theta^2(x)\mathrm{d}x\\
&=\left\|\Phi_\theta\right\|^2+\int_0^\infty x^2\left[g(x)e^{-\theta x}-\theta\Phi(x)e^{-\theta x}\right]^2\mathrm{d}x\\
&\lesssim\left\|\Phi_\theta\right\|^2+\int_0^\infty x^2g^2(x)e^{-2\theta x}\mathrm{d}x+\int_0^\infty x^2\Phi^2(x)e^{-2\theta x}\mathrm{d}x\\
&\lesssim\left\|\Phi_\theta\right\|^2+\int_0^\infty x^2e^{-2\theta x}\left(M^2+1\right)\mathrm{d}x\\
&<\infty.
\end{aligned} \tag{A.12}$$

By Lemma 1,

$$\left\|\mathscr{L}_m^{-1}\mathscr{L}_{\Phi_\theta}-\Phi_\theta\right\|^2=O\left(\frac{1}{\log m}\right),\quad m\longrightarrow\infty. \tag{A.13}$$

By (7), (12), (15), and (16), we have

$$\left\|\widehat{\mathscr{L}}_{\Phi_\theta}-\mathscr{L}_{\Phi_\theta}\right\|^2=\int_0^\infty\left(\frac{(\rho-1)\left((1/c)\widehat{\psi}_Y(s+\theta)-(1/c)\psi_Y(s+\theta)\right)}{(1/c)\widehat{\psi}_Y(s+\theta)(1/c)\psi_Y(s+\theta)}+\frac{(\rho-\widehat{\rho})}{(1/c)\widehat{\psi}_Y(s+\theta)}\right)^2\mathrm{d}s. \tag{A.14}$$

Using the proof of Propositions 2.3 and 2.4 in You and Cai [17], the right-hand side in (A.14) is bounded by

$$\frac{2}{(1-\widehat{\rho})^2}I_1+\frac{2(\widehat{\rho}-\rho)^2}{(1-\widehat{\rho})^2}I_2, \tag{A.15}$$

where

$$\begin{aligned}I_1&=\int_0^\infty\frac{1}{c^2}\frac{\left(\widehat{\psi}_Y(s+\theta)-\psi_Y(s+\theta)\right)^2}{(s+\theta)^4}\mathrm{d}s,\\ I_2&=\int_0^\infty\frac{1}{(s+\theta)^2}\mathrm{d}s<\infty.\end{aligned} \tag{A.16}$$

By Theorem 1, it follows that

$$I_1=O_P\left(\frac{1}{nh_n}\right), \tag{A.17}$$

$$\frac{2}{(1-\widehat{\rho})^2}=O_P(1), \tag{A.18}$$

$$\frac{2(\widehat{\rho}-\rho)^2}{(1-\widehat{\rho})^2}=O_P\left(\frac{1}{nh_n}\right), \tag{A.19}$$

as $n\longrightarrow\infty$.

Combining (A.15) and (A.17)–(A.19) yields

$$\left\|\widehat{\mathscr{L}}_{\Phi_\theta}-L_{\Phi_\theta}\right\|^2=O_P\left(\frac{1}{nh_n}\right),\quad n\longrightarrow\infty. \tag{A.20}$$

By $L_m^{-1}\le\sqrt{\pi}m$ in Chauveau et al. [24], (A.13), and (A.20), we have

$$\left\|\widehat{\Phi}_{m(n)}-\Phi\right\|_B^2=O_P\left(\frac{m^2}{nh_n}\right)+O_P\left(\frac{1}{\log m}\right). \tag{A.21}$$

With an optimal $m=\sqrt{nh_n/\log nh_n}$, balancing the right-hand two terms in (A.21), the order becomes $O_P\left((\log nh_n)^{-1}\right)$. □

The proof of Theorem 3

Proof. Since $J=J_1+J_2$ and (11),

$$\begin{aligned}\widehat{\rho}-\rho&=\frac{\sum_{k=1}^n(ch_n-Z_k)I_{\mathscr{D}_k^n}}{cnh_n}-\frac{\mu_1}{c}\\ &\le\frac{\sum_{k=1}^n\left(\Delta_k^nJ_1-\sigma\left(W_{t_k^n}-W_{t_{k-1}^n}\right)\right)I_{\left\{\left|\Delta_k^nJ_1-\sigma\left(W_{t_k^n}-W_{t_{k-1}^n}\right)\right|>(1/2)h_n^b\right\}}}{cnh_n}-\frac{E[J_{11}]}{c}\\ &+\frac{\sum_{k=1}^n\left(\Delta_k^nJ_1-\sigma\left(W_{t_k^n}-W_{t_{k-1}^n}\right)\right)\left(I_{\mathscr{D}_k^n}-I_{\left\{\left|\left(\Delta_k^nJ_1-\sigma W_{t_k^n}-W_{t_{k-1}^n}\right)\right|>(1/2)h_n^b\right\}}\right)}{cnh_n}\\ &+\frac{\sum_{k=1}^n\Delta_k^nJ_2}{cnh_n}-\frac{E[J_{21}]}{c}\\ &+\frac{\sum_{k=1}^n\Delta_k^nJ_2I_{\mathscr{C}_k^n}}{cnh_n}.\end{aligned} \tag{A.22}$$

Let us consider the second term of (A.22),

$$\begin{aligned}
&\frac{\sum_{k=1}^{n}\left(\Delta_k^n J_1-\sigma\left(W_{t_k^n}-W_{t_{k-1}^n}\right)\right)I_{\mathscr{D}_k^n}}{cnh_n}\\
&-\frac{\sum_{k=1}^{n}\left(\Delta_k^n J_1-\sigma\left(W_{t_k^n}-W_{t_{k-1}^n}\right)\right)I_{\left\{\left|\Delta_k^n J_1-\sigma\left(W_{t_k^n}-W_{t_{k-1}^n}\right)\right|>(1/2)h_n^b\right\}}}{cnh_n}\\
&\le\frac{\sum_{k=1}^{n}\left(\Delta_k^n J_1-\sigma\left(W_{t_k^n}-W_{t_{k-1}^n}\right)\right)I_{\left\{\left|\Delta_k^n J_1-\sigma\left(W_{t_k^n}-W_{t_{k-1}^n}\right)\right|+\left|\Delta_k^n J_2\right|>h_n^b\right\}}}{cnh_n}\\
&-\frac{\sum_{k=1}^{n}\left(\Delta_k^n J_1-\sigma\left(W_{t_k^n}-W_{t_{k-1}^n}\right)\right)I_{\left\{\left|\Delta_k^n J_1-\sigma\left(W_{t_k^n}-W_{t_{k-1}^n}\right)\right|>(1/2)h_n^b\right\}}}{cnh_n}\\
&\le\frac{\sum_{k=1}^{n}\left(\Delta_k^n J_1-\sigma\left(W_{t_k^n}-W_{t_{k-1}^n}\right)\right)I_{\left\{\left|\Delta_k^n J_2\right|>\left(h_n^b/2\right)\right\}}}{cnh_n}\\
&\le\frac{\sum_{k=1}^{n}\left|\Delta_k^n J_1\right|I_{\left\{\left|\Delta_k^n J_2\right|>\left(h_n^b/2\right)\right\}}}{cnh_n}+\frac{\sum_{k=1}^{n}\left|\sigma\left(W_{t_k^n}-W_{t_{k-1}^n}\right)\right|I_{\left\{\left|\Delta_k^n J_2\right|>\left(h_n^b/2\right)\right\}}}{cnh_n}
\end{aligned} \tag{A.23}$$

By the Paul Lévy law for the modulus of continuity of Brownian motion's path (Vondraček and Shreve [31], p.114, Theorem 9.25) implies that

$$\lim_{h_n\longrightarrow 0}\sup_{k\in\{1,2,\ldots,n\}}\frac{\left|\left(W_{t_k^n}-W_{t_{k-1}^n}\right)\right|}{\sqrt{h_n\ln\left(1/h_n\right)}}\le 1,\ \text{a.s.} \tag{A.24}$$

We have

$$\begin{aligned}
&\frac{\sum_{k=1}^{n}\left|\sigma\left(W_{t_k^n}-W_{t_{k-1}^n}\right)I_{\left\{\left|\Delta_k^n J_2\right|>\left(h_n^b/2\right)\right\}}\right|}{cnh_n}\\
&\le\sqrt{h_n\ln\left(\frac{1}{h_n}\right)}\ \frac{\sum_{k=1}^{n}I_{\left\{\left|\Delta_k^n J_2\right|>\left(h_n^b/2\right)\right\}}}{cnh_n}\xrightarrow{P}0,
\end{aligned} \tag{A.25}$$

since

$$\begin{aligned}
&\sqrt{h_n\ln\left(\frac{1}{h_n}\right)}\ \frac{1}{h_n}P\left(\left(\Delta_k^n J_2\right)^2>\frac{h_n^{2b}}{4}\right)\le\sqrt{h_n\ln\left(\frac{1}{h_n}\right)}\ \frac{1}{h_n}\ \frac{E\left[\left(\Delta_k^n J_2\right)^2\right]}{h_n^{2b}/4}\\
&=4\sigma^2\frac{\sqrt{h_n\ln\left(1/h_n\right)}}{h_n^{2b}}\longrightarrow 0,
\end{aligned} \tag{A.26}$$

as $n\longrightarrow\infty$ and $b\in(0,(1/4))$.

Moreover,

$$\begin{aligned}
&P\left(\frac{\sum_{k=1}^{n}\left|\Delta_k^n J_1\right|I_{\left\{\left|\Delta_k^n J_2\right|>\left(h_n^b/2\right)\right\}}}{cnh_n}\neq 0\right)\\
&=P\left(\frac{\sum_{k=1}^{n}\left|\sum_{j=1}^{\Delta_k N}\gamma_j\right|I_{\left\{\left|\Delta_k^n J_2\right|>\left(h_n^b/2\right)\right\}}}{cnh_n}\neq 0\right)\\
&\le P\left(\bigcup_{k=1}^{n}\left\{\Delta_k N\neq 0,\left(\Delta_k^n J_2\right)^2>h_n^{2b}\right\}\right)\\
&\le nP\left(\Delta_1 N\neq 0\right)\frac{E\left[\left(\Delta_k^n J_2\right)^2\right]}{h_n^{2b}}\\
&=nO\left(h_n\right)\frac{\sigma^2(1)h_n}{h_n^{2b}}\longrightarrow 0,
\end{aligned} \tag{A.27}$$

since for $\forall\beta>0$, $nh_n^{1+\beta}\longrightarrow 0$.

Now, let us consider the last term of the right-hand side of (A.22):

$$\frac{\sum_{k=1}^{n}\Delta_k^n J_2 I_{\mathscr{C}_k^n}}{cnh_n}=\frac{\sum_{k=1}^{n}\Delta_k^n J_2 I_{\{|ch_n-Z_k|\le h_n^b,|\Delta_k^n J_2|>2h_n^b\}}}{cnh_n}+\frac{\sum_{k=1}^{n}\Delta_k^n J_2 I_{\{|ch_n-Z_k|\le h_n^b,|\Delta_k^n J_2|\le 2h_n^b\}}}{cnh_n}\le\frac{\sum_{k=1}^{n}\Delta_k^n J_2 I_{\left\{\left|\Delta_k^n J_1+\Delta_k^n J_2-\sigma\left(W_{t_k^n}-W_{t_{k-1}^n}\right)\right|\le h_n^b,|\Delta_k^n J_2|>2h_n^b\right\}}}{cnh_n}+\frac{\sum_{k=1}^{n}\Delta_k^n J_2 I_{\left\{\left|\Delta_k^n J_1+\Delta_k^n J_2-\sigma\left(W_{t_k^n}-W_{t_{k-1}^n}\right)\right|\le h_n^b,|\Delta_k^n J_2|\le 2h_n^b\right\}}}{cnh_n}. \tag{A.28}$$

In fact, if

$$\left|\Delta_k^n J_1+\Delta_k^n J_2-\sigma\left(W_{t_k^n}-W_{t_{k-1}^n}\right)\right|\le h_n^b,\ |\Delta_k^n J_2|>2h_n^b, \tag{A.29}$$

then

$$2h_n^b-\left|\Delta_k^n J_1-\sigma\left(W_{t_k^n}-W_{t_{k-1}^n}\right)\right|<|\Delta_k^n J_2|-\left|\Delta_k^n J_1-\sigma\left(W_{t_k^n}-W_{t_{k-1}^n}\right)\right|\le\left|\Delta_k^n J_1+\Delta_k^n J_2-\sigma\left(W_{t_k^n}-W_{t_{k-1}^n}\right)\right|\le h_n^b, \tag{A.30}$$

so that

$$|\Delta_k^n J_1|>\frac{1}{2}h_n^b \text{ or } \left|\sigma\left(W_{t_k^n}-W_{t_{k-1}^n}\right)\right|>\frac{1}{2}h_n^b, \tag{A.31}$$

since a.s., for small h_n, $I_{\left\{|\sigma(W_{t_k^n}-W_{t_{k-1}^n})|>(1/2)h_n^b\right\}}=0$, for all $k=1,2,..,n$, then

$$P\left(\frac{\sum_{k=1}^{n}|\Delta_k^n J_2| I_{\left\{\left|\Delta_k^n J_1+\Delta_k^n J_2-\sigma\left(W_{t_k^n}-W_{t_{k-1}^n}\right)\right|\le h_n^b,|\Delta_k^n J_2|>2h_n^b\right\}}}{cnh_n}\ne 0\right)\le P\left(\bigcup_{k=1}^{n}\left\{|\Delta_k^n J_2|>2h_n^b,\Delta_k^n N\ne 0\right\}\right)\le nP(\Delta_k^n N\ne 0)\frac{E\left[(\Delta_k^n J_2)^2\right]}{4h_n^{2b}}=nO\left(h_n^2\right)\frac{4\sigma^2(1)}{h_n^{2b}}\longrightarrow 0, \tag{A.32}$$

as $n\longrightarrow\infty$, since $b\in(0,(1/4))$.

Now, let us consider the term:

$$P\lim_{h_n\longrightarrow 0}\frac{\sum_{k=1}^{n}\Delta_k^n J_2 I_{\left\{\left|\Delta_k^n J_1+\Delta_k^n J_2-\sigma\left(W_{t_k^n}-W_{t_{k-1}^n}\right)\right|\le h_n^b,|\Delta_k^n J_2|\le 2h_n^b\right\}}}{cnh_n}\le P\lim_{h_n\longrightarrow 0}\frac{\sum_{k=1}^{n}\Delta_k^n J_2 I_{\{|\Delta_k^n J_2|\le 2h_n^b\}}}{cnh_n}. \tag{A.33}$$

Because Y_t is a spectrally negative Lévy process, for any $\delta>0$, we have

$$0\le\frac{\sum_{k=1}^{n}\Delta_k^n J_2 I_{\{|\Delta_k^n J_2|\le 2h_n^b\}}}{cnh_n}\le\frac{\sum_{k=1}^{n}\int_{t_{k-1}^n}^{t_k^n}\left[\int_{|x|\le\delta+2h_n^b}x[\mu(\mathrm{d}s,\mathrm{d}x)-\nu(\mathrm{d}x)\mathrm{d}s]-h_n\int_{\delta+2h_n^b<x\le 1}x\nu(\mathrm{d}x)\right]}{cnh_n}\le\frac{\sum_{k=1}^{n}\int_{t_{k-1}^n}^{t_k^n}\int_{|x|\le\delta+2h_n^b}x\mu(\mathrm{d}s,\mathrm{d}x)}{cnh_n}, \tag{A.34}$$

since δ is arbitrary, we can conclude that $P\lim_{n\longrightarrow\infty}(\sum_{k=1}^{n}\Delta_k^n J_2 I_{\{|\Delta_k^n J_2|\le 2h_n^b\}}/cnh_n)=0$, as $E[\sum_{k=1}^{n}\int_{t_{k-1}^n}^{t_k^n}\int_{|x|\le\delta+2h_n^b}x\mu(ds,dx)/cnh_n]=E[\int_0^{h_n}\int_{|x|\le\delta+2h_n^b}x\mu(\mathrm{d}s,\mathrm{d}x)]/ch_n=(1/c)\int_{|x|\le\delta+2h_n^b}x\nu(\mathrm{d}x)\longrightarrow 0,\ \delta\longrightarrow 0, n\longrightarrow\infty$.

By the law of large number, we know that the first term and thirst term of (A.22) are convergence to zero in probability.

By (7), (16), (22), Theorem 1, and continuous mapping theorem, it is easy to obtain (23).

Therefore, we obtain the result of Theorem 3. □

The proof of Theorem 4

Proof. By (17), we have

$$\left\|\widehat{\Phi}_m-\Phi\right\|_B^2\le e^{2\theta B}\left\|\widehat{\Phi}_m e^{-\theta u}-\Phi_\theta\right\|_B^2\le 2e^{2\theta B}\left\{\left\|\mathscr{L}_m^{-1}\widehat{\mathscr{L}}_{\Phi_\theta}-\mathscr{L}_m^{-1}\mathscr{L}_{\Phi_\theta}\right\|^2+\left\|\mathscr{L}_m^{-1}\mathscr{L}_{\Phi_\theta}-\Phi_\theta\right\|^2\right\}. \tag{A.35}$$

By the proof of Theorem 2, we may conclude that

$$a_m = \left\| \mathscr{L}_m^{-1} \mathscr{L}_{\Phi_\theta} - \Phi_\theta \right\|^2 = O\left(\frac{1}{\log m}\right), \quad m \longrightarrow \infty, \tag{A.36}$$

$$\begin{aligned} &\left\| \widehat{\mathscr{L}}_{\Phi_\theta} - \mathscr{L}_{\Phi_\theta} \right\|^2 \\ &= \int_0^\infty \left(\frac{(\rho - 1)\left((1/c)\widehat{\psi}_Y(s+\theta) - (1/c)\psi_Y(s+\theta)\right)}{(1/c)\widehat{\psi}_Y(s+\theta)(1/c)\psi_Y(s+\theta)} \right. \\ &\quad \left. + \frac{(\rho - \widehat{\rho})}{(1/c)\widehat{\psi}_Y(s+\theta)} \right)^2 ds \\ &\leq \frac{2}{(1-\widehat{\rho})^2} I_1 + \frac{2(\widehat{\rho} - \rho)^2}{(1-\widehat{\rho})^2} I_2, \end{aligned} \tag{A.37}$$

where

$$\begin{aligned} I_1 &= \int_0^\infty \frac{1}{c^2} \frac{\left(\widehat{\psi}_Y(s+\theta) - \psi_Y(s+\theta)\right)^2}{(s+\theta)^4} ds, \\ I_2 &= \int_0^\infty \frac{1}{(s+\theta)^2} ds < \infty. \end{aligned} \tag{A.38}$$

By Theorem 3 and continuous mapping theorem, it follows that

$$\left\| \widehat{\mathscr{L}}_{\Phi_\theta} - L_{\Phi_\theta} \right\|^2 = o_P(1), \quad n \longrightarrow \infty. \tag{A.39}$$

Combining $L_m^{-1} \leq \sqrt{\pi} m$ in Chauveau et al. [24], (A.36), and (A.39), we have

$$\left\| \widehat{\Phi}_m - \Phi \right\|_B^2 \leq m^2 o_P(1) + a_m, \tag{A.40}$$

as $n \longrightarrow \infty$. □

Data Availability

The data used to support the findings of this study are available from the corresponding author upon request.

Conflicts of Interest

The authors declare that they have no conflicts of interest.

Acknowledgments

The authors were supported by the Postdoctoral Science Foundation of China (Grant no. 2018M642634) and the National Natural Science Foundation of China (Grant no. 11571198).

References

[1] S. Asmussen and H. Albrecher, *Ruin Probabilities*, World Scientific, Singapore, 2nd edition, 2010.
[2] F. Dufresne and H. U. Gerber, "Risk theory for the compound Poisson process that is perturbed by diffusion," *Insurance: Mathematics and Economics*, vol. 10, no. 1, pp. 51–59, 1991.
[3] N. Veraverbeke, "Asymptotic estimates for the probability of ruin in a Poisson model with diffusion," *Insurance: Mathematics and Economics*, vol. 13, no. 1, pp. 57–62, 1993.
[4] V. Dermitzakis and K. Politis, "Asymptotics for the moments of the time to ruin for the compound Poisson model perturbed by diffusion," *Methodology and Computing in Applied Probability*, vol. 13, no. 4, pp. 749–761, 2011.
[5] S. Li, C. S. Zhang, and R. Wu, "Ruin estimates of diffusion models under constant interest rate," *Chinese Journal of Applied Probability and Statisties*, vol. 19, no. 1, pp. 79–84, 2003.
[6] K. Croux and N. Veraverbeke, "Nonparametric estimators for the probability of ruin," *Insurance: Mathematics and Economics*, vol. 9, no. 2-3, pp. 127–130, 1990.
[7] E. W. Frees, "Nonparametric estimation of probability of ruin," *Astin Bulletin*, vol. 16, no. 3, pp. 81–90, 1986.
[8] R. Mnatsakanov, L. L. Ruymgaart, and F. H. Ruymgaart, "Nonparametric estimation of ruin probabilities given a random sample of claims," *Mathematical Methods of Statistics*, vol. 17, no. 1, pp. 35–43, 2008.
[9] S. M. Pitts, "Nonparametric estimation of compound distributions with applications in insurance," *Annals of the Institute of Statistical Mathematics*, vol. 46, no. 3, pp. 537–555, 1994.
[10] K. Politis, "Semiparametric estimation for non-ruin probabilities," *Scandinavian Actuarial Journal*, vol. 2003, no. 1, pp. 75–96, 2003.
[11] H. You, J. Guo, and J. Jiang, "Interval estimation of the ruin probability in the classical compound Poisson risk model," *Computational Statistics and Data Analysis*, vol. 144, Article ID 106890, 2020.
[12] Z. Zhang, H. Yang, and H. Yang, "On a nonparametric estimator for ruin probability in the classical risk model," *Scandinavian Actuarial Journal*, vol. 2014, no. 4, pp. 309–338, 2014.
[13] F. Comte and V. Genon-Catalot, "Nonparametric estimation for pure jump Lévy processes based on high frequency data," *Stochastic Processes and Their Applications*, vol. 119, no. 12, pp. 4088–4123, 2009.
[14] F. Comte and V. Genon-Catalot, "Estimation for Lévy processes from high frequency data within a long time interval," *The Annals of Statistics*, vol. 39, no. 2, pp. 803–837, 2011.
[15] Z. Zhang and H. Yang, "Nonparametric estimate of the ruin probability in a pure-jump Lévy risk model," *Insurance: Mathematics and Economics*, vol. 53, no. 1, pp. 24–35, 2013.
[16] Y. Shimizu and Z. Zhang, "Estimating Gerber-Shiu functions from discretely observed Lévy driven surplus," *Insurance: Mathematics and Economics*, vol. 74, pp. 84–98, 2017.
[17] H. You and C. Cai, "Nonparametric estimation for a spectrally negative Lévy process based on high frequency data," *Journal of Computational and Applied Mathematics*, vol. 345, pp. 196–205, 2019.
[18] C. Cai, N. Chen, and H. You, "Nonparametric estimation for a spectrally negative Lévy risk process based on low-frequency observation," *Journal of Computational and Applied Mathematics*, vol. 328, pp. 432–442, 2018.
[19] C. Mancini, "Estimation of the characteristics of the jumps of a general Poisson-diffusion model," *Scandinavian Actuarial Journal*, vol. 2004, no. 1, pp. 42–52, 2004.
[20] C. Mancini, "Non-parametric threshold estimation for models with stochastic diffusion coefficient and jumps," *Scandinavian Journal of Statistics*, vol. 36, no. 2, pp. 270–296, 2009.
[21] Y. Shimizu, "A new aspect of a risk process and its statistical inference," *Insurance: Mathematics and Economics*, vol. 44, no. 1, pp. 70–77, 2009.

[22] Y. Shimizu, "Functional estimation for Lévy measures of semimartingales with Poissonian jumps," *Journal of Multivariate Analysis*, vol. 100, no. 6, pp. 1073–1092, 2009.

[23] M. Huzak, M. Perman, H. Š rma, and Z. Vondraček, "Ruin probabilities for general perturbed risk processes," *The Annals of Applied Probability*, vol. 14, no. 3, pp. 1378–1397, 2004.

[24] D. E. Chauveau, A. C. M. Vanrooij, and F. H. Ruymgaart, "Regularized inversion of noisy Laplace transforms," *Advances in Applied Mathematics*, vol. 15, no. 2, pp. 186–201, 1994.

[25] Z. Zhang and H. Yang, "Nonparametric estimation for the ruin probability in a Lévy risk model under low-frequency observation," *Insurance: Mathematics and Economics*, vol. 59, pp. 168–177, 2014.

[26] Z. Zhang and W. Su, "Estimating the Gerber-Shiu function in a Lévy risk model by Laguerre series expansion," *Journal of Computational and Applied Mathematics*, vol. 346, pp. 133–149, 2019.

[27] Z. Zhang and W. Su, "A new efficient method for estimating the Gerber-Shiu function in the classical risk model," *Scandinavian Actuarial Journal*, vol. 2018, no. 5, pp. 426–449, 2018.

[28] W. Yu, Y. Yong, G. Guan, Y. Huang, W. Su, and C. Cui, "Valuing guaranteed minimum death benefits by cosine series expansion," *Mathematics*, vol. 7, no. 9, p. 835, 2019.

[29] X. Peng, W. Su, W. Su, and Z. Zhang, "On a perturbed compound Poisson risk model under a periodic threshold-type dividend strategy," *Journal of Industrial & Management Optimization*, vol. 16, no. 4, pp. 1967–1986, 2020.

[30] W. Yu, P. Guo, Q. Wang et al., "On a periodic capital injection and barrier dividend strategy in the compound Poisson risk model," *Mathematics*, vol. 8, no. 4, p. 511, 2020.

[31] I. Vondraček and S. F. Shreve, *Brownian Motion and Stochastic Calculus*, Springer, New York, NY, USA, 1999.

Hindawi
Mathematical Problems in Engineering
Volume 2020, Article ID 1430105, 4 pages
https://doi.org/10.1155/2020/1430105

Research Article

G-SIRS Model with Logistic Growth and Nonlinear Incidence

Ping He [1,2] **and Defei Zhang** [2]

[1] *Department of Mathematics, Anhui Normal University, Wuhu 241000, China*
[2] *Department of Mathematics, Honghe University, Mengzi 661199, China*

Correspondence should be addressed to Defei Zhang; zhdefei@163.com

Received 8 June 2020; Accepted 30 June 2020; Published 28 July 2020

Guest Editor: Wenguang Yu

We present the stochastic SIRS model in the G-expectation space as follows: $\mathrm{d}X(t) = [rX(1-(X/K)) - (\beta XY/(1+\alpha Y)) + \delta Z]\mathrm{d}\langle B\rangle(t) + \overline{\sigma}_1 X\mathrm{d}B(t)$, $\mathrm{d}Y(t) = [(\beta XY/(1+\alpha Y)) - (\rho+\vartheta+c)Y]\mathrm{d}\langle B\rangle(t) + \overline{\sigma}_2 Y\mathrm{d}B(t)$, $\mathrm{d}Z(t) = [cY - (\mu+\delta)Z]\mathrm{d}\langle B\rangle(t) + \overline{\sigma}_3 Z\mathrm{d}B(t)$, where $\overline{\sigma}_1, \overline{\sigma}_2, \overline{\sigma}_3$ are three intensities of the G-Brownian motion and disturb the three variables, and $B(1)$ follows G-Normal distribution, namely, $B(1) \sim \mathcal{N}(0, [\underline{\pi}^2, \overline{\pi}^2])$. For any initial condition $(X(0), Y(0), Z(0)) \in D^*$, we prove the new model admits a unique solution $(X(t), Y(t), Z(t))$ for $t \geq 0$ and the solution $(X(t), Y(t), Z(t))$ satisfies $v(\omega: (X(t), Y(t), Z(t)) \in R_+^3, t \geq 0) = 1$.

1. Introduction

Liu [1] presented the SIRS model without random perturbation as follows:

$$\begin{cases} \mathrm{d}X(t) = \left[rX\left(1-\dfrac{X}{K}\right) - \dfrac{\beta XY}{1+\alpha Y} + \delta Z\right]\mathrm{d}t, \\ \mathrm{d}Y(t) = \left[\dfrac{\beta XY}{1+\alpha Y} - (\rho+\vartheta+\gamma)Y\right]\mathrm{d}t, \\ \mathrm{d}Z(t) = [\gamma Y - (\mu+\delta)Z]\mathrm{d}t, \end{cases} \tag{1}$$

where $X(t)$ reflects the susceptible number, $Y(t)$ is the infected number, and $Z(t)$ denotes the recovered number at time t. Model (1) took into account logistic growth and nonlinear incidence. The parameters $(\alpha, \beta, \rho, \vartheta, K, \gamma, \delta, \mu)$ in model (1) have practical significance, please refer to reference [1].

The possible region of (1) is $\{(X, Y, Z) \in R_+^3: X + Y + Z \leq K\} = D^*$. The basic reproduction number for system (1) is $\mathfrak{R}_0 = (\beta K/(\rho+\vartheta+\gamma))$.

In the actual environment, various diseases are disturbed by random factors, and there are many models that reflect this stochastic phenomenon, for example, [2–6]. Rajasekar and Pitchaimani [7] assumed this random interference is described by three independent Wiener processes. Specifically, they proposed the following SIRS model:

$$\begin{cases} \mathrm{d}X(t) = \left[rX\left(1-\dfrac{X}{K}\right) - \dfrac{\beta XY}{1+\alpha Y} + \delta Z\right]\mathrm{d}t + \sigma_1 X\mathrm{d}W_1(t), \\ \mathrm{d}Y(t) = \left[\dfrac{\beta XY}{1+\alpha Y} - (\rho+\vartheta+\gamma)Y\right]\mathrm{d}t + \sigma_2 Y\mathrm{d}W_2(t), \\ \mathrm{d}Z(t) = [\gamma Y - (\mu+\delta)Z]\mathrm{d}t + \sigma_3 Z\mathrm{d}W_3(t). \end{cases} \tag{2}$$

Peng in [8, 9] constructed the interesting G-Brownian motion in nonlinear expectation space, see [10]. Many important properties on G-Brownian motion were investigated, for example, [11]. As far as we know, there is no research on model (1) in the nonlinear expectation space. Some notations and concepts used in this paper are similar to those in references [11, 12].

2. G-SIRS Model

We consider the stochastic SIRS model in the G-expectation space and propose the G-SIRS model (GSIRSM for short) as follows:

$$\begin{cases} dX(t) = \left[rX\left(1 - \frac{X}{K}\right) - \frac{\beta XY}{1+\alpha Y} + \delta Z\right] d\langle B\rangle(t) + \overline{\sigma}_1 X dB(t), \\ dY(t) = \left[\frac{\beta XY}{1+\alpha Y} - (\rho + \vartheta + \gamma)Y\right] d\langle B\rangle(t) + \overline{\sigma}_2 Y dB(t), \\ dZ(t) = [\gamma Y - (\mu + \delta)Z] d\langle B\rangle(t) + \overline{\sigma}_3 Z dB(t), \end{cases} \tag{3}$$

where $\overline{\sigma}_1, \overline{\sigma}_2, \overline{\sigma}_3$ are three intensities of the G-Brownian motion, which disturb the three variables, and $B(t)$ satisfies $B(1) \sim \mathcal{N}(0, [\underline{\pi}^2, \overline{\pi}^2])$, $\widehat{\mathbb{E}}[B(1)^2] = \overline{\pi}^2$, $\widehat{\mathbb{E}}[-B(1)^2] = -\underline{\pi}^2$. Note that model (3) has nonlinear incidence. We denote $v(c) = \inf_{P\in\mathcal{Q}} E_P[1_c]$ and $V(c) = \sup_{P\in\mathcal{Q}} E_P[1_c]$, where $\widehat{\mathbb{E}}[\cdot] = \sup_{P\in\mathcal{Q}} E_P[\cdot]$.

It is very important to prove that the solution (X, Y, Z) of model (3) is of global existence and is nonnegative. We first show system (3) is global and positive. Many asymptotic properties of this system (3) deserve further investigation in the future.

Theorem 1. *$\forall (X(0), Y(0), Z(0)) \in D^*$ and $t \ge 0$, $(X(t), Y(t), Z(t))$ in (3) are unique and satisfy*

$$v\left(\omega: (X(t), Y(t), Z(t)) \in R_+^3, t \in [0, +\infty)\right) = 1. \tag{4}$$

Proof. Since the coefficients of (3) are locally Lipschitz continuous, then $\forall (X(0), Y(0), Z(0)) \in D^*$, there exists a local solution $(X(t), Y(t), Z(t))$ on $t \in [0, \lambda_e)$ quasi surely (q.s.), where λ_e represents the explosion time. To show $\lambda_e = +\infty$ q.s., we prove $(X(t), Y(t), Z(t))$ does not explode to infinity in a finite time. Suppose $k_0 > 1$ is large enough such that (s.t) $(X(0), Y(0), Z(0))$ lies in the interval $[(1/k_0), k_0]^3$. For $k \ge k_0$, define

$$\lambda_k = \inf\left\{t \in [0, \lambda_e): X(t) \notin \left(\frac{1}{k}, k\right) \text{ or } Y(t) \notin \left(\frac{1}{k}, k\right) \text{ or } Z(t) \notin \left(\frac{1}{k}, k\right)\right\}, \tag{5}$$

where λ_k is increasing as $k \longrightarrow \infty$. We have $\lambda_\infty = \lim_{k\longrightarrow\infty} \lambda_k$, therefore $\lambda_\infty \le \lambda_e$ quasi surely. Suppose we guarantee that $\lambda_\infty = \infty$ q.s., then $\lambda_e = \infty$ and $v(\omega: (X(t), Y(t), Z(t)) \in R_+^3) = 1$ q.s. If we assume $0 < V(\lambda_\infty < +\infty)$, then there exists a pair of constants $\chi > 0$ and $\varepsilon \in (0, 1)$ s.t.

$$V(\lambda_\infty \le \chi) \ge v(\lambda_\infty \le \chi) \ge \varepsilon. \tag{6}$$

Then, $\exists k_1 \ge k_0$ s.t.

$$V(\Pi_k) := V(\lambda_k \le \chi) \ge \varepsilon, \quad \text{for all } k \ge k_1. \tag{7}$$

Set a function $U_1: R_+^3 \longrightarrow R_+$ by

$$U_1(X, Y, Z) = (X - \ln X) + (Y - \ln Y) + (Z - \ln Z) - 3. \tag{8}$$

We note the function $g(x):\ = (x - \ln x) - 1 \ge 0$ for any $x > 0$. Using the G-Ito lemma for the function U_1, we get

$$\begin{aligned} dU_1 &= \frac{\partial U_1}{\partial x} dX + \frac{\partial U_1}{\partial y} dY + \frac{\partial U_1}{\partial z} dZ \\ &\quad + \frac{1}{2}\left[\frac{\partial^2 U_1}{\partial x^2}(dX)^2 + \frac{\partial^2 U_1}{\partial y^2}(dY)^2 + \frac{\partial^2 U_1}{\partial z^2}(dZ)^2\right] \\ &= \left(1 - \frac{1}{X}\right) dX + \left(1 - \frac{1}{Y}\right) dY + \left(1 - \frac{1}{Z}\right) dZ \\ &\quad + \frac{1}{2}\left[\overline{\sigma}_1^2 + \overline{\sigma}_2^2 + \overline{\sigma}_3^2\right] d\langle B\rangle(t) \\ &=: \mathscr{L}U_1 d\langle B\rangle(t) + \Theta(X, Y, Z) dB(t), \end{aligned} \tag{9}$$

where

$$\begin{aligned} \mathscr{L}U_1 &= (X - 1)\left[\left(\frac{rK - rX}{K}\right) - \frac{\beta Y}{1+\alpha Y}\right] + \frac{\delta(X-1)Z}{X} \\ &\quad + (Y - 1)\left[\frac{\beta X}{1+\alpha Y} - (\rho + \vartheta + \gamma)\right] \\ &\quad + \frac{(Z-1)\gamma Y}{Z} - (Z - 1)(\mu + \delta) + \frac{1}{2}\sum_{i=1}^{3} \overline{\sigma}_i^2 \\ &= \left(r + \frac{r}{K}\right) X - \frac{r}{K} X^2 - \frac{\beta X}{1+\alpha Y} + \frac{\beta Y}{1+\alpha Y} \\ &\quad - \rho Y - \vartheta Y - \frac{\gamma}{Z} Y - \frac{\delta}{X} Z - \mu Z \\ &\quad - r + \rho + \vartheta + \gamma + \mu + \delta + \frac{1}{2}\sum_{i=1}^{3} \overline{\sigma}_i^2, \\ \Theta(X, Y, Z) &= \overline{\sigma}_1^2 (X - 1) + \overline{\sigma}_2^2 (Y - 1) + \overline{\sigma}_3^2 (Z - 1). \end{aligned} \tag{10}$$

We note that the region $D^* = \{X + Y + Z \le K\}$ and all the parameters are positive, then we have

$$\begin{aligned} \mathscr{L}U_1 &\le \left(r + \frac{r}{K}\right) X + \frac{\beta Y}{1+\alpha Y} + \rho + \vartheta + \gamma + \mu + \delta + \frac{1}{2}\sum_{i=1}^{3} \overline{\sigma}_i^2 \\ &\le \left(r + \frac{r}{K}\right) X + \beta Y + \rho + \vartheta + \gamma + \mu + \delta + \frac{1}{2}\sum_{i=1}^{3} \overline{\sigma}_i^2 \\ &\le \Lambda K + \rho + \vartheta + \gamma + \mu + \delta + \frac{1}{2}\sum_{i=1}^{3} \overline{\sigma}_i^2, \end{aligned} \tag{11}$$

where $\Lambda = :\ \max\{(r + (r/K)), \beta\}$. We denote

$$\mathrm{C} = \Lambda K + \rho + \vartheta + \gamma + \mu + \delta + \frac{1}{2}\sum_{i=1}^{3}\overline{\sigma}_i^2. \quad (12)$$

Therefore,

$$\begin{aligned} \mathrm{d}U_1 &=: \mathscr{L}U_1 \mathrm{d}\langle B\rangle(t) + \Theta(X,Y,Z)\mathrm{d}B(t) \\ &\le \mathrm{C}\mathrm{d}\langle B\rangle(t) + \Theta(X,Y,Z)\mathrm{d}B(t). \end{aligned} \quad (13)$$

Integrate (13) from 0 to $\lambda_k \wedge \chi$,

$$\begin{aligned} &U_1(X(\lambda_k\wedge\chi), Y(\lambda_k\wedge\chi), Z(\lambda_k\wedge\chi)) \\ &\quad \le U_1(X(0),Y(0),Z(0)) + \mathrm{C}\cdot\langle B\rangle(\lambda_k\wedge\chi) \\ &\quad + \int_0^{\lambda_k\wedge\chi}\Theta(X(t),Y(t),Z(t))\mathrm{d}B(t), \end{aligned} \quad (14)$$

and take the G-expectation,

$$\begin{aligned} &\widehat{\mathbb{E}}[U_1(X(\lambda_k\wedge\chi), Y(\lambda_k\wedge\chi), Z(\lambda_k\wedge\chi))] \\ &\le U_1(X(0),Y(0),Z(0)) + \mathrm{C}\cdot\widehat{\mathbb{E}}[\langle B\rangle(\lambda_k\wedge\chi)] \\ &= U_1(X(0),Y(0),Z(0)) + \mathrm{C}\cdot\overline{\pi}^2\cdot(\lambda_k\wedge\chi). \end{aligned} \quad (15)$$

Note the set $\Pi_k(\omega)\colon = \{\omega\colon \lambda_k(\omega)\le\chi\}$ and (7), then $V(\Pi_k(\omega))\ge\varepsilon$ for all $k\ge k_1$. We see that the definition of λ_k, then for every$\omega\in\Pi_k(\omega)$, there exist at least $X(\lambda_k(\omega))$ or $Y(\lambda_k(\omega))$ or $Z(\lambda_k(\omega))$ equals to k or $(1/k)$. For example, if $X(\lambda_k(\omega)) = k$ or $X(\lambda_k) = (1/k)$, then $U_1(X(\lambda_k), Y(\lambda_k), Z(\lambda_k)) = k - 1 - \ln k + Y(\lambda_k) - 1 - \ln Y(\lambda_k) + Z(\lambda_k) - 1 + \ln Z(\lambda_k) \ge k - 1 - \ln k$, or $U_1(X(\lambda_k), Y(\lambda_k), Z(\lambda_k)) = (1/k) - 1 + \ln k + Y(\lambda_k) - 1 - \ln Y(\lambda_k) + Z(\lambda_k) - 1 + \ln Z(\lambda_k) \ge (1/k) - 1 + \ln k$. Thus,

$$U_1(X(\lambda_k), Y(\lambda_k), Z(\lambda_k)) \ge \min\left\{\frac{1}{k} - 1 + \ln k, k - 1 - \ln k\right\}. \quad (16)$$

From (7) and (14)–(16), we have

$$\begin{aligned} &\widehat{\mathbb{E}}\left[I_{\Pi_k(\omega)}U_1(X(\lambda_k), Y(\lambda_k), Z(\lambda_k))\right] \\ &= \widehat{\mathbb{E}}\left[I_{\Pi_k(\omega)}U_1(X(\lambda_k\wedge\chi), Y(\lambda_k\wedge\chi), Z(\lambda_k\wedge\chi))\right] \\ &\le U_1(X(0),Y(0),Z(0)) + \mathrm{C}\cdot\widehat{\mathbb{E}}\left[I_{\Pi_k(\omega)}\langle B\rangle(\lambda_k\wedge\chi)\right] \\ &\le U_1(X(0),Y(0),Z(0)) + \mathrm{C}\cdot\overline{\pi}^2\cdot\chi < +\infty, \end{aligned} \quad (17)$$

$$\begin{aligned} &\widehat{\mathbb{E}}\left[I_{\Pi_k(\omega)}U_1(X(\lambda_k), Y(\lambda_k), Z(\lambda_k))\right] \\ &\quad \ge \widehat{\mathbb{E}}\left[\left(\frac{1}{k} + \ln k - 1\right)\wedge(k - 1 - \ln k)\cdot I_{\Pi_k(\omega)}\right] \\ &= \left[\left(\frac{1}{k} + \ln k - 1\right)\wedge(k - 1 - \ln k)\right]\cdot\widehat{\mathbb{E}}\left[I_{\Pi_k(\omega)}\right] \\ &= \left[\left(\frac{1}{k} + \ln k - 1\right)\wedge(k - 1 - \ln k)\right]\cdot V(\Pi_k(\omega)) \\ &\quad \ge \left[\left(\frac{1}{k} + \ln k - 1\right)\wedge(k - 1 - \ln k)\right]\cdot\varepsilon. \end{aligned} \quad (18)$$

Therefore, from inequalities (17) and (18), we have

$$\begin{aligned} &\left[\left(\frac{1}{k} + \ln k - 1\right)\wedge(k - 1 - \ln k)\right]\cdot\varepsilon \\ &\quad \le \widehat{\mathbb{E}}\left[I_{\Pi_k(\omega)}U_1(X(\lambda_k), Y(\lambda_k), Z(\lambda_k))\right] < +\infty. \end{aligned} \quad (19)$$

Letting $k \longrightarrow \infty$, we find out inequality (19) is a contradiction. Thus, $V(\lambda_\infty < +\infty) = 0$, namely, $v(\lambda_\infty = +\infty) = 1$ and $v(\omega\colon (X(t), Y(t), Z(t)) \in R_+^3, t \ge 0) = 1$. □

3. Discussion

Although the endemic equilibrium for (1) exists, the endemic equilibrium of the stochastic versions (2) and (3) do not exist. From stochastic stability of Has'minskii [13], Rajasekar and Pitchaimani [7] exemplified that system (2) admits an ergodic stationary distribution. However, in the G-expectation space, we first need to obtain the new ergodic stationary distribution theorem similar to the theory of Has'minskii and use it to show the ergodic property for G-system (3). We also hope to discuss the disease is extinct for a long time in model (3). We need to find sufficient conditions for extinction of the disease for (3). However, because of the lack of a theorem which is similar to Theorem 1.16 in [14], we cannot get the corresponding results immediately for G-system (3). We will investigate the existence of ergodic stationary distribution and the sufficient conditions of extinction for G-stochastic system (3) in the future research. By the way, some more realistic and impulsive perturbations models, as well as a nonautonomous case for system (3) are also worth continuing to probe. In addition, numerical simulations for the system will be further investigated.

Data Availability

No data were used to support this study.

Conflicts of Interest

The authors declare that they have no conflicts of interest.

Acknowledgments

This work was funded by Foundations (nos. 11761028, 2015HB061, 2014HB0204, and 2018JS480) and Joint Project of Local Universities.

References

[1] J. Liu, "Hopf bifurcation analysis for an SIRS epidemic model with logistic growth and delays," *Journal of Applied Mathematics and Computing*, vol. 50, no. 1-2, pp. 557–576, 2016.

[2] Y. Bin, C. Yongli, W. Kai, and W. Weiming, "Global threshold dynamics of a stochastic epidemic model incorporating media coverage," *Advances in Differential Equations*, vol. 2018, no. 1, p. 462, 2018.

[3] Q. Liu, D. Jiang, N. Shi, T. Hayat, and A. Alsaedi, "Stationary distribution and extinction of a stochastic SIRS epidemic model with standard incidence," *Physica A: Statistical Mechanics and Its Applications*, vol. 469, pp. 510–517, 2017.

[4] X.-B. Zhang, S. Chang, Q. Shi, and H.-F. Huo, "Qualitative study of a stochastic SIS epidemic model with vertical transmission," *Physica A: Statistical Mechanics and Its Applications*, vol. 505, pp. 805–817, 2018.
[5] Z. Cao, W. Feng, X. Wen, and L. Zu, "Dynamical behavior of a stochastic SEI epidemic model with saturation incidence and logistic growth," *Physica A: Statistical Mechanics and Its Applications*, vol. 523, pp. 894–907, 2019.
[6] W. Yu, F. Wang, Y. Huang, and H. Liu, "Social optimal mean field control problem for population growth model," *Asian Journal of Control*, vol. 21, 2019.
[7] S. P. Rajasekar and M. Pitchaimani, "Ergodic stationary distribution and extinction of a stochastic SIRS epidemic model with logistic growth and nonlinear incidence," *Applied Mathematics and Computation*, vol. 377, Article ID 125143, 2020.
[8] S. Peng, "*G*-expectation, *G*-Brownian motion and related stochastic calculus of Itô type," *Stochastic Analysis and Applications*, Springer, Berlin, Germany, pp. 541–567, 2007.
[9] S. Peng, *Nonlinear Expectations and Stochastic Calculus under Uncertainty*, Springer, Berlin, Germany, 2019.
[10] S. Peng, "Survey on normal distributions, central limit theorem, Brownian motion and the related stochastic calculus under sublinear expectations," *Science in China Series A: Mathematics*, vol. 52, no. 7, pp. 1391–1411, 2009.
[11] F. Hu, Z. Chen, and D. Zhang, "How big are the increments of *G*-Brownian motion?" *Science China Mathematics*, vol. 57, no. 8, pp. 1687–1700, 2014.
[12] Z. Chen, "Strong laws of large numbers for sub-linear expectations," *Science China Mathematics*, vol. 59, no. 5, pp. 945–954, 2016.
[13] R. Has'minskii, *Stochastic Stability of Differential Equations*, Sijthoff and Noordhoff, Alphen aan den Rijn, Netherlands, 1980.
[14] Y. A. Kutoyants, *Statistical Inference for Ergodic Diffusion Processes*, Springer-Verlag, London, UK, 2004.

Hindawi
Mathematical Problems in Engineering
Volume 2020, Article ID 1603509, 25 pages
https://doi.org/10.1155/2020/1603509

Research Article

Estimation of Tail Risk and Moments Using Option Prices with a Novel Pricing Model under a Distorted Lognormal Distribution

Yan Chen,[1] Ya Cai,[2] and Chengli Zheng[2]

[1]*School of Mathematics and Statisctics, Central China Normal University, Wuhan, China*
[2]*School of Economics and Business Administration, Financial Engineering Research Center, Central China Normal University, Wuhan, China*

Correspondence should be addressed to Chengli Zheng; zhengchengli168@163.com

Received 29 May 2020; Accepted 15 June 2020; Published 20 July 2020

Guest Editor: Wenguang Yu

Risk measures based on the trading option prices in the market are forward-looking, such as VIX. We propose a new method combining distorted lognormal distribution with interpolation to price options accurately and then estimate tail risk. Our method can price the option of any strikes between the maximum and the minimum value of strikes in the real market, which reduces the instability and inaccuracy of using the limited option to measure the risk. In addition, our novel method treats the underlying asset price as a stochastic indicator rather than a fixed indicator as described in previous research studies for risk measurement. Moreover, even if the available sample size is very small, we can measure the risk stably and precisely after interpolation. Finally, the empirical test results of SP500 market show that this method has good performance, especially for the option markets with sparse strikes.

1. Introduction

Risk measure is always being regarded as one of the most important parts for risk management. To quantify the risk well, the future distribution of the risk must be characterized, which involves forecasting and is difficult. The traditional method is based on the assumption that the history has a habit of repeating itself. So, the historical time series are used to estimate the risk measures. This method is backward-looking, which will never contain information about future.

To solve this problem, people turn to options market. Derivative markets are viewed as forward-looking markets because the prices of the derivative instruments traded in those markets incorporate the market participants' perception of future market changes, which is extra information compared to those from stock markets. As a publicly traded market, the options market including stock options and index options can bring all the opinions about the future information of investors together. So, the options market can be exploited to compute the risk measures of their underlying assets. The standard approach is to determine the volatility of a stock or a stock index that is implied by today's market prices of traded options.

The VIX volatility index is one of the application methods of option price. It is disseminated by the Chicago Board Options Exchange (CBOE) following the results of Whaley [1] and has attracted much attention in recent years. The index is computed from current price on a wide range of out-of-the-money European style call and put options written on the SP500 equity index, and it is built to serve as a model-free option-implied return volatility measure for the SP500 index over the coming 30 days, expressed in annualized percentage terms. VIX captures attention from the real market, and it is even labeled "fear gauge" and routinely cited by the media when describing current market conditions or "investor sentiment." Besides the popularity in practice, VIX is increasingly used in financial economics, especially it provides a model-free measurement of the expected value of the SP500 return variation under the risk-neutral (Q probability) measure. Hence, the VIX embodies a model-free market volatility forecast. The literature about VIX can be classified in three main directions. One direction is about the forecast power of variation in the VIX for future realized return volatility. For example, Jiang and Tian [2] thought that the information content of the VIX volatility forecast is superior to alternative implied volatility measures as well as forecasts based on historical volatility. The second direction emphasizes the fact that the VIX measure is constructed directly from observed option prices so it is bound to incorporate any pricing of variance risk that may be embedded in the market prices. Thus, VIX does not represent a pure estimator of future return volatility for the underlying asset because it includes compensation for variance risk as well. Instead, the wedge between regular time series forecasts for volatility, developed under the actual or objective (P probability) measure, and the VIX, representing the risk-neutral return volatility forecast, may be interpreted as a market volatility risk premium (see, e.g., Bondarenko [3]; Bollerslev et al. [4]; and Carr and Wu [5] and their extensions Todorov [6] and Todorov and Bollerslev [7]). The third one is about seeking to draw inference regarding the stochastic properties of the underlying market return volatility process directly from the high-frequency behavior of the VIX (see Todorov and Tauchen [8] and Jiang and Tian [9]). Andersen et al. [10] considered a novel Corridor Implied Volatility index (CX) based on a range of strikes with high-frequency data including jumps and asymmetries. For more information about model-free volatility indices, see Gonzalez-Perez [11].

Besides research on VIX, there are some others using the ideas behind this kind of model-free estimation from options. Linders et al., [12] proposed a novel group of herd behavior indices (HIX), which are model-free and risk-neutral, derived from available option data from the market. Their numerical illustration showed that the HIX based on the Dow Jones is identical to the CIX from Dhaene et al., [13], which further demonstrated that model-free estimation is an appropriate approach to calculate the HIX. Related empirical research studies are limited and need to be further explored.

This idea of model-free estimation based on options data is very important and contributes to reduce model error dramatically. However, their applications are based on the options market, where the number of options traded are limited. Usually, the strikes of options are located mainly close to the strike of at-the-money option, and the options with strikes far from that are less, even sparse. However, when this model-free method is applied, the options used mainly are those out-of-the-money options with strikes far from that of at-the-money option. Moreover, there are not enough options traded in some markets, such as China; the size of samples of data is very small. Both of the above cases will lead to non-negligible computation errors of risk measurement.

The second problem of the current method to compute risk measures is attributable to range estimation of risk measures. Andersen et al., [14] thought that some extreme options value with strikes on the tails might be noises and will make the estimation of risk to be not correct and not stable. To make it robust, the corridor method is developed, discarding the data of tails and only considering a range of strikes. Dhaene et al., [13] have the similar idea of range when building their downside heard behavior indices (DHIX). In fact, because the trading options cannot cover all ranges of strikes from zero to infinity, current risk measures based on market data are all within the strike range from the minimum to the maximum in the real market. The ranges of those measures are consistent with the fixed range of strikes, including Andersen et al. [14] and Linders et al. [12]. But the real range of risk measures must be built on the range of underlying assets, which is a stochastic process, so the range must be random, too. Apparently, it is not suitable to describe risk features with a fixed range and there are differences between the two ranges of fixed and random. Therefore, the current method (proposed by VIX, Andersen et al. [14] and Linders et al. [12]) cannot deal with this problem well because they only used the option prices traded in the market and measure risk on a fixed range of strikes.

To make some improvements on above problems, we propose a new method based on distorted lognormal distribution and interpolation in this paper. Firstly, according to the characteristics of market price of options, we introduce a distorted variable to traditional lognormal distribution of underlying asset. This distorted variable is the function of the strikes, and it makes the options price of market to fit very well. Through market data, the distorted variables of options traded in the market can be estimated, and then using interpolation, all the distorted variables of arbitrary strikes between the minimum strike to maximum strike in the real market can be obtained, and then the prices of all the options (with or without options traded in the real market) can be computed well. This method can enlarge the size of samples of data from limited traded options, which will make the computation of risk measures more precise and robust. To test validation of our method, we decrease the size of samples gradually. And we present the whole equations for risk measures under the stochastic range using this method; it shows that our new method can solve the second problem very well. The empirical results show that the differences between the two ranges of fixed and random can be very big.

Besides the traditional risk measure such as volatility which is computed on the whole range from zero to infinity and their corridor versions, we also consider the computations of tail risk, including left tail and right tail, and their range versions, discarding the extreme points of the tails. The empirical results from SP500 market show that our novel method of distorted lognormal distribution combined with interpolation is very good, especially for the option markets with sparse strikes.

The rest of the paper is arranged as follows. In Section 2, the idea of distorted lognormal distribution will be introduced, and the empirical estimations of distorted variables and their interpolations will be presented. In Section 3, we will use this method to compute moments and tail risk estimations, compared with the current traditional method; especially, the stochastic ranges are treated for three different kinds of range moments and tail risk. Section 4 concludes the paper.

2. Distorted Lognormal Distributions

Precise option price is the basis of computing risk measurement with the model-free estimation. But many empirical results (see, e.g., MacBeth and Merville [15]; Gultekin et al. [16]; and Long and Officer [17]) show that the traditional B-S-M model mispriced the options, sometimes undervalued options and sometimes overvalued options out of the money or in the money. So, we think this is one kind of investing psychology or behavior. The investors prefer to adjust subjective probability according to the moneyness. This makes the final equilibrium market prices vary with the moneyness, which may be the source of the puzzle of volatility smiles or smirks. So, we describe this adjustment of probability by a parameter $m = m(\lambda)$, which varies with the moneyness $\lambda = K/S_0$. We can view that the market distorts the probability with the moneyness. The idea of distorting the normal distribution has been accepted and developed gradually to fit the "spike and fat tail" distribution better (see, e.g., Hamada and Sherris [18]; Godin et al. [19]; Labuschagne and Offwood [20]; Gerber and Shiu [21]; and Xiao-nan et al. [22]). Specifically, we assume that the distortion function is as follows:

$$f(S_T) = \frac{e^{m(\lambda)S_T}}{E[e^{m(\lambda)S_T}]}, \tag{1}$$

where S_T is the price of underlying asset at the time T and E means expectation. Then, we can use this distortion function to options pricing.

2.1. Theoretical Approach. In this section, we will explain how to define distorted variables of $m(\lambda)$ for a call option and $q(\lambda)$ for a put option. Given the price of a call and of a put as a function of K, σ, r, T, S_0, and m. Now we consider the option pricing model based on the distortion function as equation (1). For simplicity, we only consider to distort the lognormal distribution here.

Under the traditional assumptions, an underlying stock price S follows the stochastic process as follows:

$$\frac{\mathrm{d}S}{S} = r\mathrm{d}t + \sigma\,\mathrm{d}B, \tag{2}$$

where B is a Brownian motion under risk-neutral probability measure Q, r is the risk-free rate, and σ is the constant volatility of S. So, we have

$$S_T = S_0 e^{(r-\sigma^2/2)T+\sigma\sqrt{T}x}, \tag{3}$$

where $x \sim N(0,1)$ with a probability distribution as

$$p(x) = \frac{1}{\sqrt{2\pi}} e^{-x^2/2}. \tag{4}$$

Here, we just distort the probability of x directly with weight function as

$$f(x) = \frac{e^{m}}{E[e^{mx}]} = e^{mx-(m^2/2)}. \tag{5}$$

$m(\lambda)$ is omitted as m, briefly. So, the probability Q is transformed to Q^*, and $p(x)$ is distorted to $p^*(x)$ as

$$p^*(x) = f(x)p(x) = e^{mx-(m^2/2)}\frac{1}{\sqrt{2\pi}}e^{-x^2/2} = \frac{1}{\sqrt{2\pi}}e^{-(x-m)^2/2}. \tag{6}$$

Obviously, it still follows a normal distribution. Based on this normal distribution, we can get the closed solution for European options easily.

For European call:

$$\begin{aligned} c_0^* &= E^{Q^*}\left[(S_T-K)1_{S_T>K}\right]e^{-rT} \\ &= e^{-rT}\int_{S_T>K}(S_T-K)1_{S_T>K}p^*(x)\mathrm{d}x \\ &= S_0 e^{m\sigma\sqrt{T}}N(d_1^*) - Ke^{-rT}N(d_2^*), \end{aligned} \tag{7}$$

where

$$d_1^* = -\frac{(\log(K/S_0)-(r-\sigma^2/2)T)}{\sigma\sqrt{T}} + \sigma\sqrt{T} + m, \tag{8}$$

$$d_2^* = d_1^* - \sigma\sqrt{T}. \tag{9}$$

Apparently, when $m = 0$, equation (7) is transformed into the traditional B-S-M model. We can estimate $m(\lambda)$ from the real market data of call options, and then we can price for call options by (7).

Here, it is further illustrated that this distorted method can solve the problem of volatility smiles and smirks, which is described as follows:

$$\begin{aligned} c_0(\widehat{\sigma}, K) &= \overline{c_0}, \\ \widehat{\sigma} &= c_0^{-1}(\overline{c_0}, K), \end{aligned} \tag{10}$$

where $c_0(\widehat{\sigma}, K)$ is the price based on the traditional B-S-M model, $\overline{c_0}$ is the price in the real market, and $\widehat{\sigma}$ is the implied volatility. For the same underlying assets with the same S_0, T, r, but different strike price K, the implied volatility $\widehat{\sigma}$ varies with strike price K, which means the traditional B-S-M model does not work in the real market. Here, we show that our new model (equation (7)) can value the options well and solve the problem of volatility smiles and smirks. We suppose that our price is the same as the real market price:

$$\overline{c_0} = c_0^*, \tag{11}$$

and guess the shape of $m(\lambda)$ through the shape of volatility smiles and smirks, and then we compute the implied volatility as follows:

$$\widehat{\sigma} = c_0^{-1}(c_0^*, K). \tag{12}$$

According to the shapes of volatility smiles and smirks reported, there are some kinds of distortion function that can be chosen, such as logistic, exponential, quadric, and their composite shapes. Here, we just show an example with quadric function as

$$m(\lambda) = a(\lambda-1)^2 1_{\lambda>1} + b(\lambda-1)^2 1_{\lambda\le 1}. \tag{13}$$

Equation (13) means m is zero at $\lambda = 1$ and is asymmetrical around $\lambda = 1$. To show the volatility smiles and smirks, we use an example. We suppose that

$S_0 = 100, T = 1, r = 0.05$, and $\lambda = 0.25$, and we select proper value for parameters a and b in equation (13). Figure 1 shows the example of $m(\lambda)$; Figures 2 and 3 show the corresponding volatility smile and smirk from equation (12).

For European put, we denote distortion as $q(\lambda)$ because we think it is different from that of call options. At this situation, we can get the closed solution for European put options easily.

$$\begin{aligned} p_0^* &= E^{Q^*}\left[(K - S_T)1_{S_T < K}\right]e^{-rT} \\ &= e^{-rT}\int_{S_T < K}(K - S_T)1_{S_T < K}p^*(x)\mathrm{d}x \\ &= Ke^{-rT}N(-d_2^*) - S_0 e^{q\sigma\sqrt{T}}N(-d_1^*), \end{aligned} \tag{14}$$

where the definitions of d_1^* and d_2^* are the same as equations (8) and (9)fd9.

$$\begin{aligned} d_1^* &= -\frac{(\log(K/S_0) - (r - \sigma^2/2)T)}{\sigma\sqrt{T}} + \sigma\sqrt{T} + q, \\ d_2^* &= d_1^* - \sigma\sqrt{T}. \end{aligned} \tag{15}$$

Apparently, when $q = 0$, equation (14) is transformed into the traditional B-S-M model.

Similarly, we can estimate $q(\lambda)$ from the real market data of put options, and then we can price the put options by equation (14). And we show volatility smiles and smirks with put option similarly. We still use quadric function as

$$q(\lambda) = a(\lambda - 1)^2 1_{\lambda > 1} + b(\lambda - 1)^2 1_{\lambda \le 1}. \tag{16}$$

Equation (16) means q is zero at $\lambda = 1$ and is asymmetrical around $\lambda = 1$. To show the volatility smiles and smirks, we still use the example with $S_0 = 100, T = 1, r = 0.05$, and $\lambda = 0.25$, and we select proper value for parameter a and b in equation (16). Figure 4 shows the example of $q(\lambda)$; Figures 5 and 6 show the corresponding volatility smile and smirk from equation (12). To show a little difference, here we show left smirk in Figure 6, while in Figure 3, we show a right smirk.

So, we show that our distorted method can explain the puzzle of volatility smiles and smirks well with simulation examples theoretically. To show that this method can be good in practice, we will use the real market data to fit in next section.

2.2. Practice. We now consider a date with options available on the SP500 index and all the maturity shorter than 3 years.

We collect all data about options whose underlying asset is SP500 index. The whole data are collected from the Reuters database. The data period starts from the date of Feb 7, 2017, so the Current date is Feb 7, 2017. We have 2666 types of prices of European options, half of which are calls and the others are puts. The maturity of options listed in Table 1 has 11 types and each maturity corresponds to a different risk-free rate r (%). On that day, the close price of SP500 index is 2293, which means $S_0 = 2293$, and the volatility $\sigma = 0.125$.

The scatter graph of options market price with different moneyness is shown in Figure 7. The basic descriptive

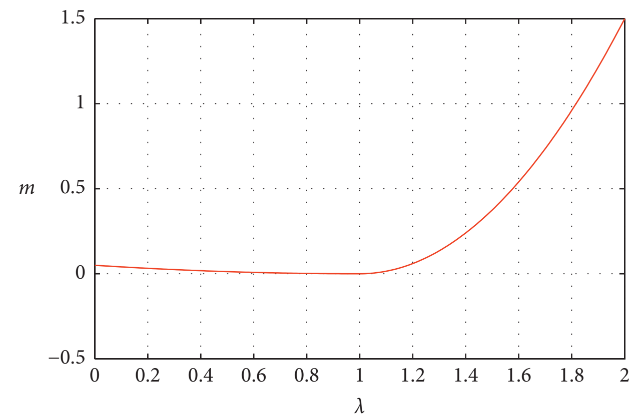

Figure 1: $m(\lambda)$ with $a = 1.5$, $b = 0.05$.

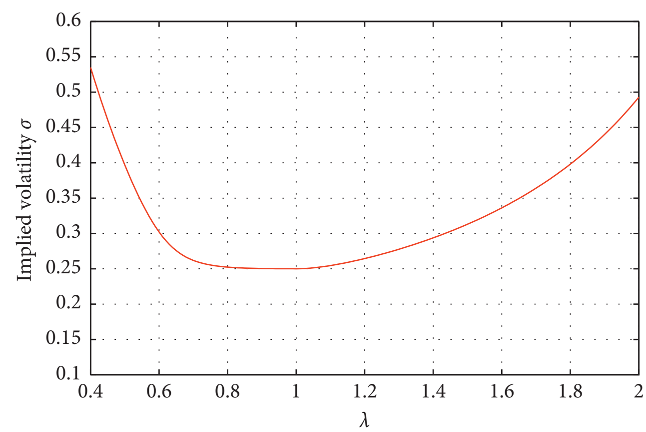

Figure 2: Volatility smile with $a = 1.5$ and $b = 0.05$.

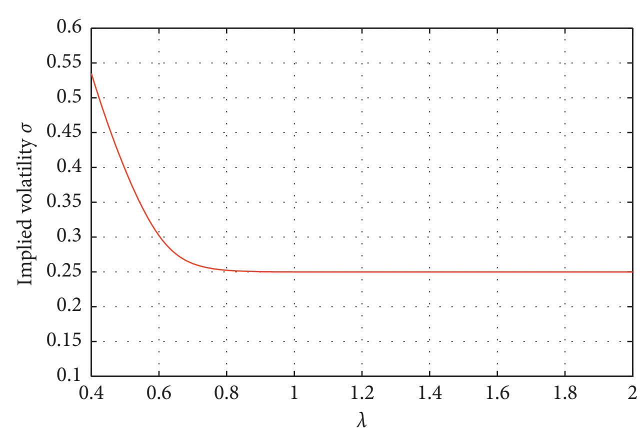

Figure 3: Volatility smirk with $a = 0$ and $b = 0.05$.

statistics are listed in Table 2. From Table 2, we can see that the moneyness λ in the real market changes around in the interval of $[0.035, 1.55]$. Its mean and median values are lower than 1 and the kurtosis can be nearly approximate to that of normal distribution. Both the market prices of calls and puts are right-skewness distributions, which means the market is more likely to be optimistic, especially for the puts market due to its significantly high kurtosis. Surely, the basic

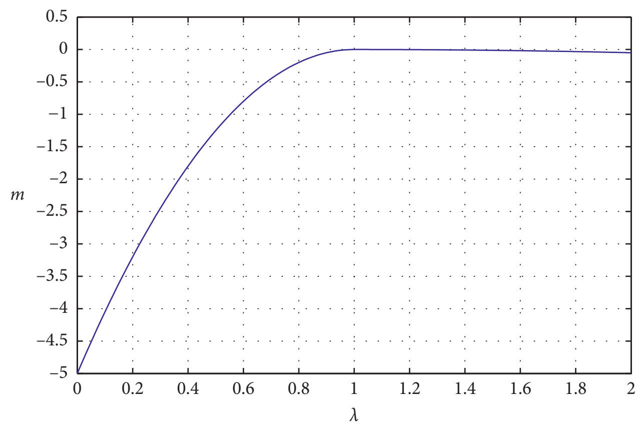

Figure 4: $q(\lambda)$ with $a = -0.05$ and $b = -5$.

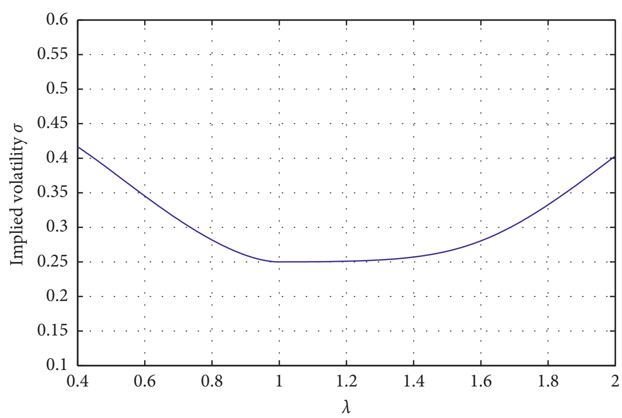

Figure 5: Volatility smile with $a = -0.05$ and $b = -5$.

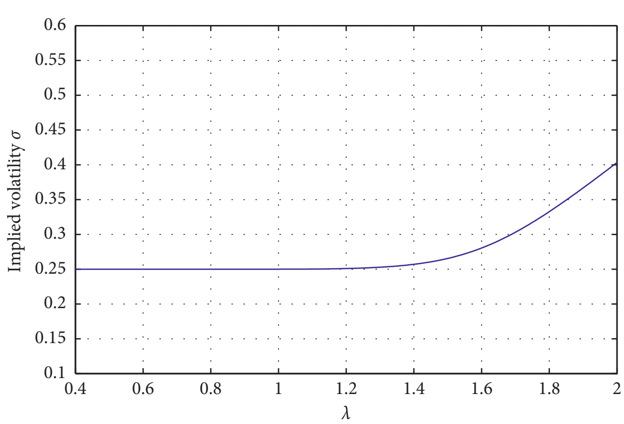

Figure 6: Volatility smirk with $a = -0.05$ and $b = 0$.

descriptive statistics show a little difference among different maturities; here we omit them. In Table 2, cp_0 means a mixture of all the put and call options.

Now, we represent the theoretical $m(\lambda)$ (for calls) and $q(\lambda)$ (for puts); for each strike, we solve for the exact value of λ so that the market price of the option matches the model price. We assume that our option pricing model based on distorted lognormal distributions is reasonable and equals the real market price:

$$c_0^*(m(\lambda)) = \overline{c_0}, \tag{17}$$

and then by using equation (17), we can estimate $m(\lambda)$ for calls as

$$m(\lambda) = c_0^{*-1}(\overline{c_0}). \tag{18}$$

Similarly, we can estimate $q(\lambda)$ for puts as

$$q(\lambda) = p_0^{*-1}(\overline{p_0}). \tag{19}$$

We call $m(\lambda)$ estimated from real market implied m and $q(\lambda)$ implied q. Then, we get all the implied m and q at all the 11 types of maturities T. Figures 8 and 9 show the scatter graphs for all the implied m and q with different moneyness at all 11 types of maturities T; the basic descriptive statistics are listed in Table 3. From Figures 8 and 9, it can be seen that the implied m and q at different maturities T varying with the moneyness λ have the similar trend, which means that the relationship between these two variables can be described by the same kind of function. We can find that the shapes of q are almost the same as we guessed in Figure 4; we can find a function similar to equation (13) to fit them well. But the shapes of m are not the same as we guessed in Figure 1, only similar; they are more complicated, with a big convex around $\lambda = 1$ (see Figures 9 and 10). Figures 10 and 11 show the relationship between implied m (or q) and the moneyness λ at maturities $T = 0.28$. If we can find suitable functions to fit them very well, we can use the method of distorted lognormal distribution we proposed to all the prices of options with all the strikes from zero to $+\infty$ (or big enough), whether they are traded in the real market or not. Then, we can use these options to compute the moments and tail risk measures more precisely. However, we cannot find a good function to fit them well, which may be our work in future. So, we use another method—interpolation—to extend the number of strikes. Though the interpolation cannot extend the range of strikes outside of the range of real market, it can enlarge the number of strikes inside that range, where there are no options traded in the real market. As we know, the number of options traded in the market is limited.

The method of interpolation will be useful for the markets where there are not enough options. To verify this, we narrow the number of samples and then make interpolation treatment. Figures 10 and 11 show the original data and their interpolations. The interpolation method here chosen is spline. The blue dot is the original data, there are 63 points for maturity $T = 0.28$, and the red curve denotes interpolation. We can see that even for SP500 options market, the points are not enough, especially for the right side where λ is high. For some option markets, such as some single stock-based option market and Chinese options market, there are not enough options traded, which will be similar to Figure 12. In Figure 12, we decrease the number of samples by deleting part of points. From Figures 12(a)–12(d), the number of samples decreases and becomes more and more sparse. Here, we do not delete the first and the last

Table 1: Some basic data.

T	0.03	0.1	0.2	0.28	0.35	0.6	0.85	0.95	1.35	1.87	2.87
r	0.50	0.51	0.53	0.53	0.57	0.66	0.75	0.78	0.926	1.11	1.42
σ	0.125										
S_0	2293										

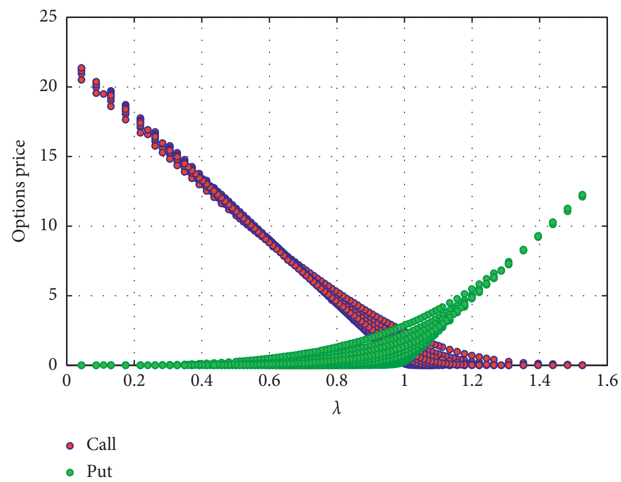

Figure 7: Options market price with different λ.

Table 2: Descriptive statistics of options.

	Max	Min	Mean	Median	Std	Skewness	Kurtosis
λ	1.53	0.04	0.79	0.81	0.26	−0.27	3.05
cp_0	2136.45	0.05	311.49	92.63	431.86	1.65	5.27
c_0	2136.45	0.05	536.67	440.35	489.98	0.90	3.19
p_0	1225.40	0.05	86.32	7.60	177.71	3.30	15.71

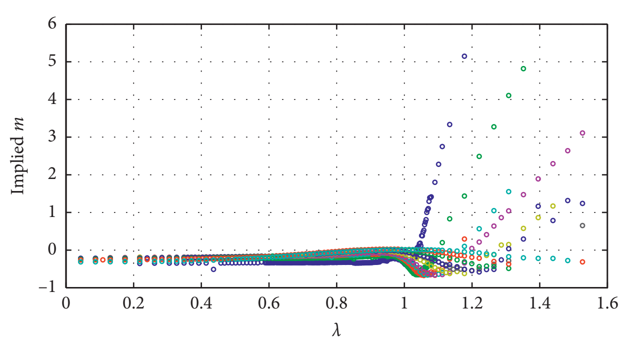

Figure 8: Implied m with different λ for all maturities.

original points to hold the same range of strikes. In the real market, that will not be the truth. For the traditional method, to replicate risk measures by options, enough samples are very important, especially for tail risk. In case of Figure 12(d), there are only 12 points; if we compute the tail risk, there are only one or two points that can be used, and the result may be very bad. Our interpolation method can overcome this problem.

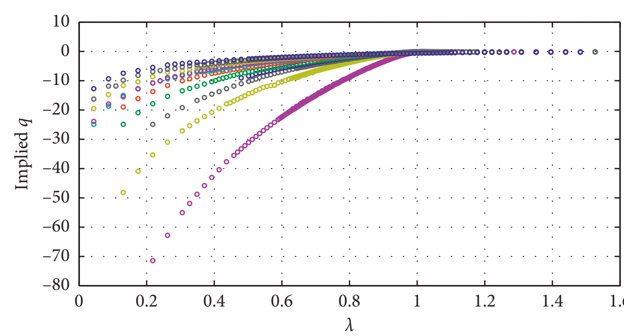

Figure 9: Implied q with different λ for all maturities.

In the next section, we will use this method to price the options and apply these prices to compute moments and tail risks.

3. Applications to Moments and Tail Risk Estimation

In this section, we will use the methods suggested by Andersen et al. [14] and LDS (2014, 2015) to construct moments and tail risk measures via options with a range of strike prices, and for comparison, we will use the pricing model we proposed to compute them.

3.1. Theory. Firstly, we will explain how to compute $E[f(S)]$ with f twice differential as a function of the prices of the options and approximation for the finite number of strikes available.

Table 3: Descriptive statistics of m and q.

T	Call (m)						Put (q)					
	Max	Min	Mean	Std	Skewness	Kurtosis	Max	Min	Mean	Std	Skewness	Kurtosis
0.03	5.15	−0.51	−0.17	0.58	5.46	39.50	−0.27	−71.41	−10.4	11.5	−2.02	8.69
0.1	4.82	−0.65	−0.17	0.54	6.99	56.60	−0.09	−48.17	−4.79	6.64	−3.09	15.90
0.2	0.30	−0.67	−0.21	0.17	−1.48	4.78	−0.05	−24.93	−3.34	4.34	−2.37	9.67
0.28	1.55	−0.66	−0.16	0.33	2.79	15.12	−0.06	−9.05	−2.62	2.65	−0.80	2.41
0.35	3.11	−0.66	−0.01	0.63	3.28	14.05	−0.08	−24.90	−4.01	4.98	−1.84	6.79
0.6	1.17	−0.62	−0.14	0.25	2.30	14.18	−0.11	−18.97	−3.02	3.70	−1.95	7.40
0.85	0.65	−0.54	−0.16	0.15	0.87	11.16	−0.13	−24.92	−3.30	4.22	−2.47	10.97
0.95	1.32	−0.58	−0.11	0.29	3.21	15.62	−0.15	−23.90	−3.01	4.04	−2.58	11.36
1.35	0.02	−0.48	−0.14	0.12	−0.71	3.47	−0.17	−19.52	−2.55	3.29	−2.82	12.63
1.87	0.03	−0.37	−0.13	0.10	0.01	1.74	−0.19	−16.26	−2.41	2.82	−2.43	10.20
2.87	0.02	−0.31	−0.13	0.11	−0.23	1.60	−0.27	−12.72	−1.84	2.04	−2.87	13.29

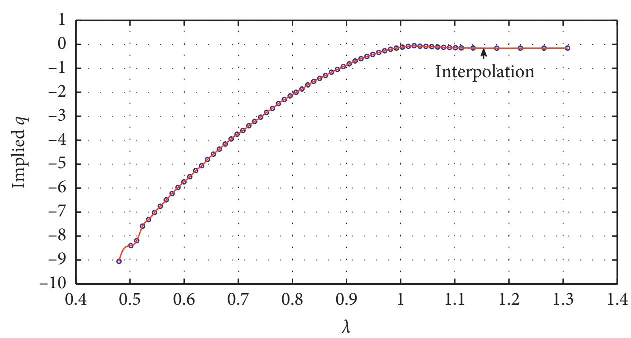

Figure 10: Implied q with different λ for $T = 0.28$.

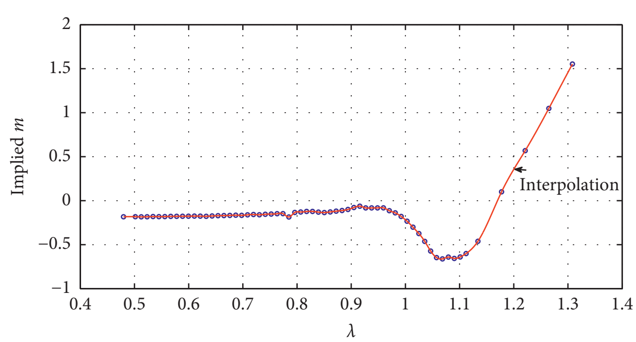

Figure 11: Implied m with different λ for $T = 0.28$.

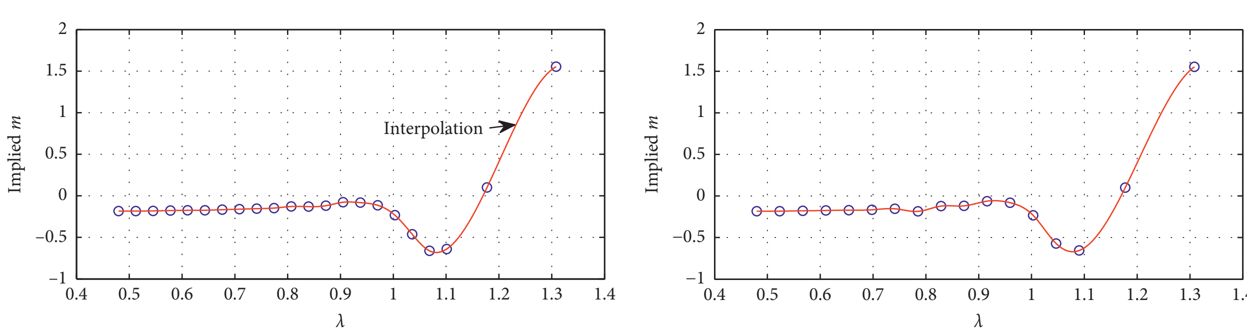

(a)

(b)

Figure 12: Continued.

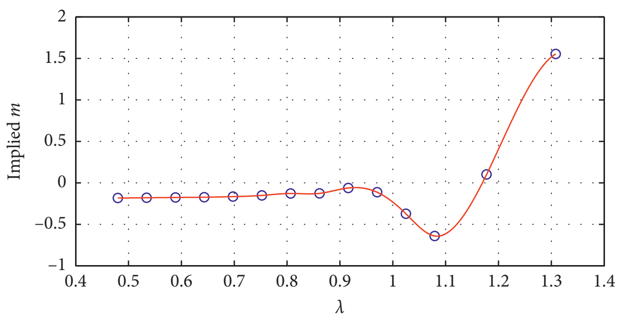

(c)

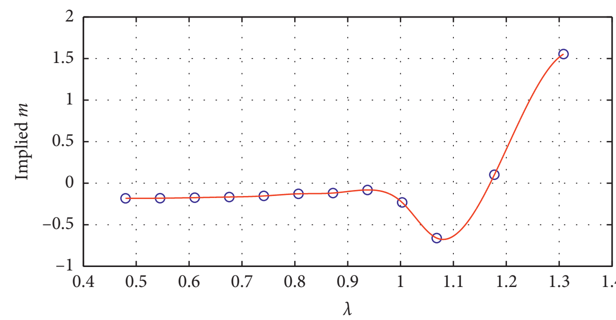

(d)

FIGURE 12: Interpolation under different situations ($T = 0.28$).

We will use the same approach as the paper on corridor VIX [14] or on HIX [23, 24]. This approach is from the idea of Carr and Madan [25].

From Carr and Madan [25], for any twice continuously differentiable function $f(x)$, it can be expressed as follows:

$$f(x) = f(F) + f'(F)(x-F) + \int_F^{\infty} f''(v)(x-v)^+ \mathrm{d}v + \int_0^F f''(v)(v-x)^+ \mathrm{d}v. \tag{20}$$

Linders et al. [12] used this to express the swap rate $E[f(S/(E[S]))]$ with $F = 1$, as follows:

$$\begin{aligned} E\left[f\left(\frac{S}{E[S]}\right) - f(1)\right] &= E\left[\int_1^{\infty} f''(v)\left(\frac{S}{E[S]} - v\right)^+ \mathrm{d}v + \int_0^1 f''(v)\left(v - \frac{S}{E[S]}\right)^+ \mathrm{d}v\right] \\ &= \frac{1}{(E[S])^2}\left(\int_{E[S]}^{\infty} f''\left(\frac{K}{E[S]}\right)E[(S-K)^+]\mathrm{d}K + \int_0^{E[S]} f''\left(\frac{K}{E[S]}\right)E[(K-S)^+]\mathrm{d}K\right) \\ &= \frac{e^{rT}}{(E[S])^2}\left(\int_{E[S]}^{\infty} f''\left(\frac{K}{E[S]}\right)C[K]\mathrm{d}K + \int_0^{E[S]} f''\left(\frac{K}{E[S]}\right)P[K]\mathrm{d}K\right), \end{aligned} \tag{21}$$

where $C[K] = E[(S-K)^+]e^{-rT}$ and $P[K] = E[(K-S)^+]e^{-rT}$. Equation (21) means that for any twice continuously differentiable function $f(x)$, its expectation can be expressed as the integral of European puts and calls at different strikes. Because the options market is looking forward, they can react with the information more actively for the future than the underlying assets markets, so we can use this method to construct some kind of measures in a way of model-free estimation to forecast the market more precisely.

Apparently, equation (21) requires that there must exist options with all the strikes from 0 to infinity continuously. However, only some of them exist in the real options market with limited discrete strikes. To deal with this problem, Linders et al. [12] used the composite trapezoidal rule; they approximated formula (21) as follows:

$$E\left[f\left(\frac{S}{E[S]}\right) - f(1)\right] \approx \frac{e^{rT}}{(E[S])^2}\left(\sum_{i=-l}^{h} f''\left(\frac{K_i}{E[S]}\right)Q[K_i]\Delta K_i - \frac{f''(K_0/E[S])}{2}\left(\frac{E[S]-K_0}{E[S]}\right)^2\right), \tag{22}$$

where

$$\Delta K_i = \begin{cases} K_{-l+1} - K_{-l}, & \text{if } i = -l, \\ \dfrac{K_{i+1} - K_{i-1}}{2}, & \text{if } i = -l+1, \ldots, h-1, \\ K_h - K_{h-l}, & \text{if } i = h, \end{cases}$$

$$Q[K_i] = \begin{cases} P[K_i], & \text{if } K_i < K_0, \\ \dfrac{C[K_i] + P[K_i]}{2}, & \text{if } K_i = K_0, \\ C[K_i], & \text{if } K_i > K_0, \end{cases} \tag{23}$$

Throughout the whole paper, we will assume that there are only a finite number of European options with maturity T. In particular, for the underlying asset (SP500 index), the strikes of the traded puts and calls are denoted by $K_i, i = -l, -l+1, \ldots, h-1, h$, with

$$0 = K_{-l} < \cdots < K_{-1} < K_0 \leq E[S] < K_1 < K_2 < K_h < K_{h+1}, \tag{24}$$

where $K_{h+1} = F_S^{-1}(1)$ is assumed to be finite. In reality, the underlying asset and call option based in it have unknown upward potential. For discrete approximation, here a finite upper bound can be chosen arbitrarily large. Note that as long as there is at least one strike K for which the prices $C[K]$ and $P[K]$ are traded, the forward rate $E[S]$ can be computed in model-free way using the put-call parity. In practical situations, we follow the methodology proposed in Chicago Board Options Exchange [26] to determine the forward rate of the SP500 index:

$$E[S] = e^{rT}\left(C[K^*] - P[K^*]\right) + K^*, \tag{25}$$

with

$$K^* = \arg \min_{K \in \{K_{-l}, \ldots, K_{h-1}\}} |C[K] - P[K]|. \tag{26}$$

Now we use this method to estimate some kinds of measures.

Example 1. Estimation of $E[S^\theta]$.

The first is to estimate moments of $E[S^\theta]$.

When $\theta = 1$, $E[S]$ can be estimated.

When $\theta = 2$, $f''(K_i/E[S]) = 2$, we have

$$\begin{aligned} E\left[\left(\frac{S}{E[S]}\right)^2 - 1\right] &= \frac{\mathrm{Var}[S]}{(E[S])^2} \\ &\approx \frac{2e^{rT}}{(E[S])^2}\left(\sum_{i=-l}^{h} Q[K_i]\,\Delta K_i\right) \\ &\quad - \left(\frac{E[S] - K_0}{E[S]}\right)^2. \end{aligned} \tag{27}$$

When $\theta = 3$, $f''(K_i/E[S]) = 6K_i/E[S]$, we have

$$\begin{aligned} E\left[\left(\frac{S}{E[S]}\right)^3 - 1\right] &\approx \frac{e^{rT}}{(E[S])^3}\left(\sum_{i=-l}^{h} 6K_i Q[K_i]\Delta K_i\right) \\ &\quad - \frac{6K_0}{E[S]}\left(\frac{E[S] - K_0}{E[S]}\right)^2. \end{aligned} \tag{28}$$

Example 2. Estimation of range of variance $R\mathrm{Var}(S)$.

In the real market, the extreme situations are not stable; this means that the options price with extreme strikes may not be good to estimate the variance, so these extreme strike situations must be discarded. Andersen et al. [14] used this method to replicate implied volatility; they called it Corridor Implied Volatility Index, or CX, and through the empirical test, they proved that this CX is more robust than the ordinary Implied Volatility Index (VIX). In fact, the basic theory they considered is as follows:

$$\begin{aligned} E\left[\left(f\left(\frac{S}{E[S]}\right) - f(1)\right)1_{S\in[K_\alpha,K_\beta]}\right] &= E\left[\int_1^\infty f''(\nu)\left(\frac{S}{E[S]} - \nu\right)^+ 1_{S\in[K_\alpha,K_\beta]}\mathrm{d}\nu\right] + E\left[\int_0^1 f''(\nu)\left(\nu - \frac{S}{E[S]}\right)^+ 1_{S\in[K_\alpha,K_\beta]}\mathrm{d}\nu\right] \\ &= \frac{1}{(E[S])^2}\left(\int_{E[S]}^\infty f''\left(\frac{K}{E[S]}\right)E\left[(S-K)^+ 1_{S\in[K_\alpha,K_\beta]}\right]\mathrm{d}K + \int_0^{E[S]} f''\left(\frac{K}{E[S]}\right)E\left[(K-S)^+ 1_{S\in[K_\alpha,K_\beta]}\right]\mathrm{d}K\right) \\ &= \frac{e^{rT}}{(E[S])^2}\left(\int_{E[S]}^\infty f''\left(\frac{K}{E[S]}\right)C_R[K]\mathrm{d}K + \int_0^{E[S]} f''\left(\frac{K}{E[S]}\right)P_R[K]\mathrm{d}K\right), \end{aligned} \tag{29}$$

where $C_R[K] = E[(S-K)^+ 1_{S\in[K_\alpha,K_\beta]}]e^{-rT}$ and $P_R[K] = E[(K-S)^+ 1_{S\in[K_\alpha,K_\beta]}]e^{-rT}$; apparently, $C_R[K]$ and $P_R[K]$ are not options in the real market, so they cannot use equation (22) to approximate $E[(f(S/E[S]) - f(1))1_{S\in[K_\alpha,K_\beta]}]$ with the real market prices of options. The real reason of this problem is that $1_{S\in[K_\alpha,K_\beta]}$ is stochastic. To solve this problem, they substitute it with $1_{K\in[K_\alpha,K_\beta]}$, which is not stochastic. This is an approximation method. Then, equation (29) transforms to

$$E\left[\left(f\left(\frac{S}{E[S]}\right)-f(1)\right)1_{S\in[K_\alpha,K_\beta]}\right]\approx E\left[\left(f\left(\frac{S}{E[S]}\right)-f(1)\right)1_{K\in[K_\alpha,K_\beta]}\right]$$
$$=E\left[\left(f\left(\frac{S}{E[S]}\right)-f(1)\right)\right]1_{K\in[K_\alpha,K_\beta]}. \tag{30}$$

Using equation (21), we have

$$E\left[f\left(\frac{S}{E[S]}\right)-f(1)\right]1_{K\in[K_\alpha,K_\beta]}=\frac{e^{rT}}{(E[S])^2}\left(\int_{E[S]}^{\infty}f''\left(\frac{K}{E[S]}\right)C[K]\mathrm{d}K+\int_0^{E[S]}f''\left(\frac{K}{E[S]}\right)P[K]\mathrm{d}K\right)1_{K\in[K_\alpha,K_\beta]}, \tag{31}$$

where $C[K]=E[(S-K)^+]e^{-rT}$ and $P[K]=E[(K-S)^+]e^{-rT}$. If $K_\alpha<E[S]<K_\beta$, then equation (31) will be

$$E\left[\left(f\left(\frac{S}{E[S]}\right)-f(1)\right)\right]1_{K\in[K_\alpha,K_\beta]}=\frac{e^{rT}}{(E[S])^2}\left(\int_{E[S]}^{K_\beta}f''\left(\frac{K}{E[S]}\right)C[K]\mathrm{d}K+\int_{K_\alpha}^{E[S]}f''\left(\frac{K}{E[S]}\right)P[K]\mathrm{d}K\right). \tag{32}$$

It only considers the range without the left and right tails and can be replicated both by call and put options which are out of the money. The Corridor Implied Volatility Index of Andersen et al. [14] is one of the special cases of this situation.

In most of situations, people only consider the downside risk, especially for the left tail; many risk measures are created to quantify the risk of this tail, such as Value at Risk (VaR) and Average Value at Risk (TVaR). Similarly, their calculations need to estimate the risk-neutral density (RND), which will be not forward-looking. Because the second derivatives for VaR and TVaR are zero, we cannot replicate them by options prices as the method we proposed here. We can consider the moments higher than first order, such as second and third moments of tail, to quantify the risk of this tail. Using equation (32), moments of tails can be quantified by replicating with options.

If $K_\alpha<K_\beta<E[S]$, then equation (32) will be

$$E\left[\left(f\left(\frac{S}{E[S]}\right)-f(1)\right)\right]1_{K\in[K_\alpha,K_\beta]}=\frac{e^{rT}}{(E[S])^2}\int_{K_\alpha}^{K_\beta}f''\left(\frac{K}{E[S]}\right)P[K]\mathrm{d}K. \tag{33}$$

It only considers the left tail and can be replicated only by put options which are out of the money.

If $E[S]<K_\alpha<K_\beta$, then equation (31) will be

$$E\left[\left(f\left(\frac{S}{E[S]}\right)-f(1)\right)\right]1_{K\in[K_\alpha,K_\beta]}=\frac{e^{rT}}{(E[S])^2}\int_{K_\alpha}^{K_\beta}f''\left(\frac{K}{E[S]}\right)C[K]\mathrm{d}K. \tag{34}$$

It only considers the right tail and can be replicated only by call options which are out of the money.

For these three kinds of risk measures, we can compute arbitrary moments of them, except the first-order moment.

For the same reason, to calculate the moments through real options market, approximation by discretization must be done. Then using equation(22), equation (31) can be approximated by discretization as follows:

$$E\left[\left(f\left(\frac{S}{E[S]}\right)-f(1)\right)\right]1_{K\in[K_\alpha,K_\beta]}\approx\frac{2e^{rT}}{(E[S])^2}\left(\sum_{i=-l_\alpha}^{h_\beta}f''\left(\frac{K_i}{E[S]}\right)Q[K_i]\,\Delta K_i-\left(\frac{E[S]-K_0}{E[S]}\right)^2\right), \tag{35}$$

where $K_{-l_\alpha}\geq K_\alpha$ and $K_{h_\beta}\leq K_\beta$. $K_\alpha=F_S^{-1}(\alpha)$, and $K_\beta=F_S^{-1}(\beta)$; we only need to choose proper α and β to make the results stable or robust. That is a problem, not only because of selection of α and β, but also because of the calculation of the quantile of S, which means we need to estimate the risk-neutral density (RND) of S, which is not easy. How to solve this problem? Firstly, we try to determine K_α by a fixed proportion of $E[S]$ under the standard log-normal assumption simply, such as $K_\alpha=k_sE[S]$. And k_s can be chosen based on

$$k_s=\frac{F_{S^B}^{-1}(\alpha)}{E^B[S]}, \tag{36}$$

where B refers to geometrical Brownian motion.

But, we find it is not good. Figure 13 shows k_s with the confidence α. From this figure, we can find that even when confidence is approaching zero, k_s is still higher than 0.8. From Table 2, we can see that the median value of $\lambda=0.81$, which means this method will lose a large part of information of the options market.

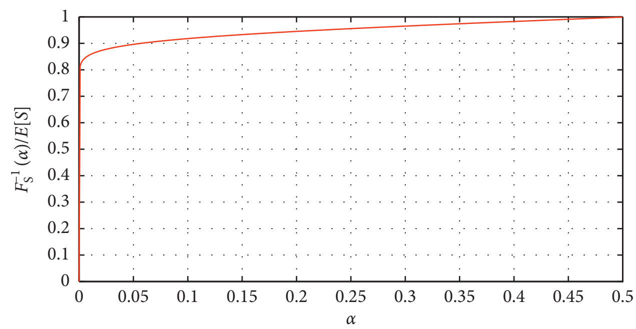

Figure 13: k with the confidence α.

To avoid this difficulty, Andersen et al. [14] proposed a good method. They adopted the approach of Andersen and Bonarenko [27]. It builds on the fact that option prices reflect tail moments. The left and right tail moments of a positive random variable, x with strictly positive density $f(x)$ for all $x > 0$, are given by

$$\begin{aligned} LT(K) &= \int_0^K (K-x) f(x) \mathrm{d}x, \\ RT(K) &= \int_K^\infty (x-K) f(x) \mathrm{d}x, \end{aligned} \tag{37}$$

and then they define the ratio statistic, $R(K)$, as an indicator of how far in the tail a given point, K, is located within the support of x:

$$R(K) = \frac{LT(K)}{LT(K) + RT(K)}. \tag{38}$$

$R(K)$ is akin to a cumulative density function or CDF as it is increasing on $(0, \infty)$ with $R(0) = 0$ and $R(\infty) = 1$. So, for a given percentile, q, in the range of the $R(K)$ function, we can get the quotient, K_q, as

$$K_q = R^{-1}(q), \quad \text{for any } q \in [0,1]. \tag{39}$$

Let $f(x)$ denote the risk-neutral density for SP500 forward price at maturity $T = 1/12$, or one month, and K be the strike price of European style put and call options; we have

$$R(K) = \frac{P(K)}{P(K) + C(K)}. \tag{40}$$

The ratio statistic is computed only from put and call prices. Hence, if the range is located where option prices may be extracted reliably, $R(K)$ can be computed without estimation of risk-neutral density. Here, we can borrow this method to determine the K_α, K_β. After considering the market liquidity, we can settle the 2% truncation level for the tails. That is,

$$\begin{aligned} K_\alpha &\geq R^{-1}(0.02), \\ K_\beta &\leq R^{-1}(0.98). \end{aligned} \tag{41}$$

Utilizing this method, we can compute the moments via replicating options prices in the real market. However, the options traded are limited, and these computations may not be so good. And all of the range moments are just approximations as shown in equation (30); it will have big error. To solve these two problems, we propose the alternative approach in the next section.

3.2. Alternative Approach. As mentioned above, the options traded in the real market are limited; especially, for some extreme strikes, it will be sparse. Using the limited options to replicate the risk measures will lead to errors. And when calculating the range moments, the method of approximations as shown in equation (30) is not convincing. In this section, we will propose some methods to solve these two problems.

In the first section, we propose a novel method to evaluate the options well. It shows that the weight function can be fitted very well. So, for the first problem, we can use the method of distorted lognormal distribution to get all $m(\lambda)$ and $q(\lambda)$, from the limited options traded in the real market. Then, we use interpolation to get enough points of $m(\lambda)$ and $q(\lambda)$ between the minimum and maximum of λ. Based on this, we can get all the prices of call and put options with these strikes (λ). Then, we can use equation (21) to compute the risk measures precisely.

In fact, in equation (21), the options $Q[K]$ are supposed to be existing in the real market with price $\overline{Q}[K]$, and by using the implied volatility equation, we have

$$\overline{Q}[K] = Q[\widehat{\sigma}, K], \tag{42}$$

where $Q[\widehat{\sigma}, K]$ is $C[\widehat{\sigma}, K]$ for call options and $P[\widehat{\sigma}, K]$ for put options. Then, equation (20) transforms into

$$E\left[f\left(\frac{S}{E[S]}\right) - f(1)\right] = \frac{e^{rT}}{(E[S])^2}\left(\int_{E[S]}^\infty f''\left(\frac{K}{E[S]}\right) C[\widehat{\sigma}, K] \mathrm{d}K + \int_0^{E[S]} f''\left(\frac{K}{E[S]}\right) P[\widehat{\sigma}, K] \mathrm{d}K\right). \tag{43}$$

This means that equation (43) is the function of implied volatility of different options with all the strikes. Because we do not have the real traded prices for options with all the strikes, we can approximate equation (43) well. Here, we remember that if $m(\lambda)$ and $q(\lambda)$ can be obtained, we can use them to price all the options with all the strikes. Namely, we assume that the price of our new price model can fit the market prices well, so we can offer the option prices for strikes that are not traded in the real market:

$$\overline{Q}[K] = Q[\widehat{\sigma}, K] = Q^*[\sigma, K]. \tag{44}$$

So, equation (43) can be rewritten as

$$E\left[f\left(\frac{S}{E[S]}\right) - f(1)\right] = \frac{e^{rT}}{(E[S])^2}\left(\int_{E[S]}^{\infty} f''\left(\frac{K}{E[S]}\right)C^*[\sigma, K]\mathrm{d}K + \int_0^{E[S]} f''\left(\frac{K}{E[S]}\right)P^*[\sigma, K]\mathrm{d}K\right). \tag{45}$$

$C^*[\sigma, K]$ and $P^*[\sigma, K]$ are from our new pricing model equations (7) and (14). Using this method, we can compute equation (45) smoothly with integral. In fact, if the points by interpolation are enough, equation (22) is still a good approximation to (45):

$$E\left[f\left(\frac{S}{E[S]}\right) - f(1)\right] \approx \frac{e^{rT}}{(E[S])^2}\left(\sum_{i=-l}^{h} f''\left(\frac{K_i}{E[S]}\right)Q^*[K_i]\,\Delta K_i - \frac{f''(K_0/E[S])}{2}\left(\frac{E[S] - K_0}{E[S]}\right)^2\right). \tag{46}$$

Moreover, denote $K = \lambda S_0$; then, we have

$$\begin{aligned} E\left[f\left(\frac{S}{E[S]}\right) - f(1)\right] &= \frac{e^{rT}}{(E[S])^2}\left(\int_{E[S]/S_0}^{\infty} f''\left(\frac{\lambda S_0}{E[S]}\right)C^*[\sigma, \lambda S_0]\mathrm{d}\lambda S_0 + \int_0^{E[S]/S_0} f''\left(\frac{\lambda S_0}{E[S]}\right)P^*[\sigma, \lambda S_0]\mathrm{d}\lambda S_0\right) \\ &= \frac{e^{rT}S_0^2}{(E[S])^2}\left(\int_{E[S]/S_0}^{\infty} f''\left(\frac{\lambda S_0}{E[S]}\right)C_\lambda^*[\sigma, \lambda]\mathrm{d}\lambda + \int_0^{E[S]/S_0} f''\left(\frac{\lambda S_0}{E[S]}\right)P_\lambda^*[\sigma, \lambda]\mathrm{d}\lambda\right), \end{aligned} \tag{47}$$

where

$$C_\lambda^*[\sigma, \lambda] = e^{m\sigma\sqrt{T}}N(d_1^*) - \lambda e^{-rT}N(d_2^*), \tag{48}$$

$$P_\lambda^*[\sigma, \lambda] = \lambda e^{-rT}N(-d_2^*) - e^{q\sigma\sqrt{T}}N(-d_1^*), \tag{49}$$

and the definitions of d_1^* and d_2^* are

$$\begin{aligned} d_1^* &= -\frac{(\log(\lambda) - (r - \sigma^2/2)T)}{\sigma\sqrt{T}} + \sigma\sqrt{T} + q, \\ d_2^* &= d_1^* - \sigma\sqrt{T}. \end{aligned} \tag{50}$$

We can see that equations (48) and (49) are the functions of λ, $m(\lambda)$ and $q(\lambda)$.

For the second problem, we can still solve it using our novel method of distorted lognormal distribution. In equation (29),

$$E\left[\left(f\left(\frac{S}{E[S]}\right) - f(1)\right)1_{S\in[K_\alpha, K_\beta]}\right] = \frac{e^{rT}}{(E[S])^2}\left(\int_{E[S]}^{\infty} f''\left(\frac{K}{E[S]}\right)C_R[K]\mathrm{d}K + \int_0^{E[S]} f''\left(\frac{K}{E[S]}\right)P_R[K]\mathrm{d}K\right), \tag{51}$$

where $C_R[K] = E[(S-K)^+1_{S\in[K_\alpha, K_\beta]}]e^{-rT}$ and $P_R[K] = E[(K-S)^+1_{S\in[K_\alpha, K_\beta]}]e^{-rT}$.

Because $C_R[K]$ and $P_R[K]$ are not options in the real market, we cannot use equation (22) to approximate $E[(f(S/E[S]) - f(1))1_{S\in[K_\alpha, K_\beta]}]$ with the real market prices of options. The papers before [14, 24] use a nonstochastic indicator $1_{K\in[K_\alpha, K_\beta]}$ to take the place of the stochastic indicator $1_{S\in[K_\alpha, K_\beta]}$. Using our method, we can calculate them easily:

$$E\left[\left(f\left(\frac{S}{E[S]}\right)-f(1)\right)1_{S\in[K_\alpha,K_\beta]}\right]=\frac{e^{rT}}{(E[S])^2}\left(\int_{E[S]}^{\infty}f''\left(\frac{K}{E[S]}\right)C_R^*[K]\mathrm{d}K+\int_0^{E[S]}f''\left(\frac{K}{E[S]}\right)P_R^*[K]\mathrm{d}K\right), \tag{52}$$

where

$$\begin{aligned}
C_R^*[K] &= E^{Q*}\left[(S-K)^+1_{[S\in K_\alpha,K_\beta]}\right]e^{-rT}\\
&= E^{Q*}\left[(S-K)1_{S\in[K_\alpha,K_\beta]}1_{K<K_\alpha}\right]e^{-rT}+E^{Q*}\left[(S-K)1_{S\in[K,K_\beta]}1_{K_\alpha<K<K_\beta}\right]e^{-rT}\\
&= E^{Q*}\left[(S-K)\left(1_{S>K_\alpha}-1_{S>K_\beta}\right)\right]1_{K<K_\alpha}e^{-rT}+E^{Q*}\left[(S-K)\left(1_{S>K}-1_{S>K_\beta}\right)\right]1_{K_\alpha<K<K_\beta}e^{-rT}\\
&= E^{Q*}\left[(S-K_\alpha+K_\alpha-K)1_{S>K_\alpha}-\left(S-K_\beta+K_\beta-K\right)1_{S>K_\beta}\right]e^{-rT}1_{K<K_\alpha}+E^{Q*}\\
&\quad\cdot\left[(S-K)1_{S>K}-\left(S-K_\beta+K_\beta-K\right)1_{S>K_\beta}\right]e^{-rT}1_{K_\alpha<K<K_\beta}\\
&=\left(C^*[K_\alpha]-C^*\left[K_\beta\right]+(K_\alpha-K)e^{-rT}N[-d(m,K_\alpha)]-\left(K_\beta-K\right)e^{-rT}N\left[-d\left(m,K_\beta\right)\right]\right)1_{K<K_\alpha}\\
&\quad+\left(C^*[K]-C^*\left[K_\beta\right]-\left(K_\beta-K\right)e^{-rT}N\left[-d\left(m,K_\beta\right)\right]\right)1_{K_\alpha<K<K_\beta},
\end{aligned} \tag{53}$$

$$\begin{aligned}
P_R^*[K] &= E^{Q*}\left[(K-S)^+1_{S\in[K_\alpha,K_\beta]}\right]e^{-rT}\\
&= E^{Q*}\left[(K-S)1_{S\in[K_\alpha,K_\beta]}1_{K>K_\beta}\right]e^{-rT}+E^{Q*}\left[(K-S)1_{S\in[K_\alpha,K]}1_{K_\alpha<K<K_\beta}\right]e^{-rT}\\
&= E^{Q*}\left[(K-S)\left(1_{S<K_\beta}-1_{S<K_\alpha}\right)\right]1_{K>K_\beta}e^{-rT}+E^{Q*}\left[(K-S)\left(1_{S<K}-1_{S<K_\alpha}\right)\right]1_{K_\alpha<K<K_\beta}e^{-rT}\\
&= E^{Q*}\left[\left(K_\beta-S+K-K_\beta\right)1_{S<K_\beta}-(K_\alpha-S+K-K_\alpha)1_{S<K_\alpha}\right]e^{-rT}1_{K>K_\beta}+E^{Q*}\\
&\quad\cdot\left[(K-S)1_{S<K}-(K_\alpha-S+K-K_\alpha)1_{S<K_\alpha}\right]e^{-rT}1_{K_\alpha<K<K_\beta}\\
&=\left(P^*\left[K_\beta\right]-P^*[K_\alpha]+\left(K-K_\beta\right)e^{-rT}N\left[d\left(q,K_\beta\right)\right]-(K-K_\alpha)e^{-rT}N[d(q,K_\alpha)]\right)1_{K>K_\beta}\\
&\quad+\left(P^*[K]-P^*[K_\alpha]-(K-K_\alpha)e^{-rT}N[d(q,K_\alpha)]\right)1_{K_\alpha<K<K_\beta},
\end{aligned} \tag{54}$$

where $C^*[K]$ and $P^*[K]$ are from equations (7) and (14), and

$$\begin{aligned}
d(m,K) &= \frac{(\log(K/S_0)-(r-\sigma^2/2)T)}{\sigma\sqrt{T}}-m,\\
d(q,K) &= \frac{(\log(K/S_0)-(r-\sigma^2/2)T)}{\sigma\sqrt{T}}-q.
\end{aligned} \tag{55}$$

As we show that our novel distorted method can price the options very well, all $C^*[K]$, $P^*[K]$, $d(m,K)$, and $d(q,K)$ at arbitrary strikes between $K_{\min}$ and $K_{\max}$ of the real market (which corresponds to $\lambda_{\min},\lambda_{\max}$) can be calculated precisely. We do not need to use the approximation equation (30) any more. Similarly, we can get different situations of range moments, including tail moments as equations (32) and (34):

If $K_\alpha<K_\beta<E[S]$, then equation (52) transforms to

$$\begin{aligned}
E\left[\left(f\left(\frac{S}{E[S]}\right)-f(1)\right)1_{S\in[K_\alpha,K_\beta]}\right] &= \frac{e^{rT}}{(E[S])^2}\left(\int_{K_\alpha}^{K_\beta}f''\left(\frac{K}{E[S]}\right)\left(P^*[K]-P^*[K_\alpha]-(K-K_\alpha)e^{-rT}N[d(q,K_\alpha)]\right)\mathrm{d}K\right.\\
&\quad+\int_{K_\beta}^{E[S]}f''\left(\frac{K}{E[S]}\right)\left(P^*\left[K_\beta\right]-P^*[K_\alpha]+\left(K-K_\beta\right)e^{-rT}N\left[d\left(q,K_\beta\right)\right]\right.\\
&\quad\left.\left.-(K-K_\alpha)e^{-rT}N[d(q,K_\alpha)]\right)\mathrm{d}K\right).
\end{aligned} \tag{56}$$

This situation is to measure the risk of the left tail; it can be replicated by a series of put options out of the money.

If $K_\alpha < E[S] < K_\beta$, then equation (53) transforms to

$$E\left[\left(f\left(\frac{S}{E[S]}\right) - f(1)\right)1_{S\in[K_\alpha,K_\beta]}\right] = \frac{e^{rT}}{(E[S])^2}\left(\int_{E[S]}^{K_\beta} f''\left(\frac{K}{E[S]}\right)\left(C^*[K] - C^*[K_\beta] - (K_\beta - K)e^{-rT}N[-d(m,K_\beta)]\right)\mathrm{d}K + \int_{K_\alpha}^{E[S]} f''\left(\frac{K}{E[S]}\right)\left(P^*[K] - P^*[K_\alpha] - (K-K_\alpha)e^{-rT}N[d(q,K_\alpha)]\right)\mathrm{d}K\right). \tag{57}$$

This situation is to measure the risk of the middle without left and right tails; it can be replicated by a series of put and call options out of the money.

If $E[S] < K_\alpha < K_\beta$, then equation (53) transforms to

$$E\left[\left(f\left(\frac{S}{E[S]}\right) - f(1)\right)1_{S\in[K_\alpha,K_\beta]}\right] = \frac{e^{rT}}{(E[S])^2}\left(\int_{E[S]}^{K_\alpha} f''\left(\frac{K}{E[S]}\right)\left(C^*[K_\alpha] - C^*[K_\beta] + (K_\alpha - K)e^{-rT}N[-d(m,K_\alpha)] - (K_\beta - K)e^{-rT}N[-d(m,K_\beta)]\right)\mathrm{d}K + \int_{K_\alpha}^{K_\beta} f''\left(\frac{K}{E[S]}\right)\left(C^*[K] - C^*[K_\beta] + (K_\beta - K)e^{-rT}N[-d(m,K_\beta)]\right)\mathrm{d}K\right). \tag{58}$$

This situation is to measure the risk of the right tail; it can be replicated by a series of call options out of the money.

Compared with equations (32) and (34), the results with stochastic indicator are different. The first difference is that the integral terms are different. The integral terms with stochastic indicator have some adjustment items. The second difference is the integral interval. For the tail moments, the intervals with stochastic indicator are bigger than those with nonstochastic indicator. So, we can expect that the final results of numerical calculation of moments may be different.

We can compute the integral of these equations by MATLAB. Surely, if there are enough interpolation points (here we have 3000 points), we can use approximation method of equation (22). Similarly, equation (52) can be approximated by discretization as follows:

$$E\left[\left(f\left(\frac{S}{E[S]}\right) - f(1)\right)1_{S\in[K_\alpha,K_\beta]}\right] \approx \frac{2e^{rT}}{(E[S])^2}\left(\sum_{i=-l_\alpha}^{h_\beta} f''\left(\frac{K_i}{E[S]}\right)Q_R^*[K_i]\,\Delta K_i - \left(\frac{E[S]-K_0}{E[S]}\right)^2\right), \tag{59}$$

where

$$Q_R^*[K_i] = \begin{cases} P_R^*[K_i], & \text{if } K_i < K_0, \\ \dfrac{C_R^*[K_i] + P_R^*[K_i]}{2}, & \text{if } K_i = K_0, \\ C_R^*[K_i], & \text{if } K_i > K_0, \end{cases} \tag{60}$$

and ΔK_i and other variables have the same definitions as that of Section 3.1.

In next section, we will use the real data of SP options market to calculate the moments and tail risk and compare these different methods mentioned here.

3.3. Comparison. In this section, we will utilize the real data of SP options market to calculate the moments and tail risk and compare these different methods mentioned here. We compare three kinds of approaches to compute two moments of risks with 3 pairs of ranges.

The three kinds of approaches are as follows: the first approach is to replicate risk measures by limited options traded in the market, used by current papers (see [14, 24]); the second approach is to replicate risk measures by enough interpolation points through our novel distorted lognormal distribution; these two methods are based on the nonstochastic indicator $1_{K\in[K_\alpha,K_\beta]}$. Here, we call the first method NSO (nonstochastic indicator with original data) and call the second method NSDI (nonstochastic indicator with distorted and interpolation data). And the third approach is to replicate risk measures by enough interpolation points through our novel distorted lognormal distribution based on the stochastic indicator $1_{S\in[K_\alpha,K_\beta]}$. We call the third method SDI (stochastic indicator with distorted and interpolation data).

The two moments are for $(S/E[S])^\theta$ with $\theta = 2, 3$. We choose three pairs of range $[K_\alpha, K_\beta]$ through changing $[\alpha,\beta] = \{[0, 1], [0.02.0.98]\}$, $\{[0, 0.1], [0.02, 0.1]\}$, $\{[0.90, 1.0], [0.90, 0.98]\}$. Here, $[\alpha,\beta] = [0, 1]$ means calculations will be done by all the options traded in the market without discarding the extreme strikes of the tails. This situation can be viewed as a special case of range risk measures. The range $[K_{\min}, K_{\max}]$ is the maximum range of strikes for the options traded in the real market. $[\alpha,\beta] = [0.02, 0.98]$ means calculations will be done by some of the options with discarding 2% of the extreme strikes of the both tails. According to Andersen et al. [14], this range will make the risk measures more stable.

The second pair of range $[\alpha,\beta] = \{[0, 0.1], [0.02, 0.1]\}$ is for the left tail risk without and with discarding 2% of the extreme strikes of the left tail.

The third pair of range $[\alpha,\beta] = \{[0.9, 1.0], [0.9, 0.98]\}$ is for the right tail risk without and with discarding 2% of the extreme strikes of the right tail.

We want to check if discarding 2% of the extreme strikes can make the risk measure to be more stable. $[\alpha,\beta] = [0.02, 0.10]$will be replicated by some of the put options out of the money with discarding 2% of the extreme strikes of the left tail to make it stable. The right tail risk will be replicated by some of the call options out of the money with discarding 2% of the extreme strikes of the right tail to make it stable.

Besides these situations, to show that our interpolation methods are good for markets with sparse options, we decrease the number of the samples and then compute those risk measures again. The method to decrease is as follows: $\mathrm{mod}(N, k) = 0$. For example, there are $N = 12$ samples; $\mathrm{mod}(12, 2) = 0$ means only 6 samples are left, and they are $2, 4, 6, 8, 10, 12$; $\mathrm{mod}(12, 6) = 0$ means only 2 samples are left, and they are $6, 12$. Here, we will take $k = 1, 2, \ldots, 6$. We can see that the number of samples decreases to $1/k$ of original data. With k increasing, when $k = 6$ or $k = 5$, it will be very sparse, and there are not enough samples to finish the calculations, especially for the tail risk.

The data are the same as those in Section 2.2, and we use the method of Section 2 to estimate $m(\lambda)$ and $q(\lambda)$, and then we use the interpolation method to get all the points of $m(\lambda)$ and $q(\lambda)$ between $\lambda_{\min}$ and $\lambda_{\max}$. We will get 3000 points, which is enough.

Firstly, we compute $(S/E[S])^\theta$ with $\theta = 2$. To be convenient, we denote

$$\rho_{[\alpha,\beta]} = \sqrt{E\left[\left(\left(\frac{S}{E[S]}\right)^2 - 1\right)1_{S\in\left[K_\alpha,K_\beta\right]}\right]}. \tag{61}$$

We compute all $\rho_{[\alpha,\beta]}$ with different situations for all the 11 maturities. Here, we only show results of $T = 0.28$ as an example because the results for the other maturities are similar.

Table 4 shows the results of $\rho_{[0,1]}$ and its truncated range $\rho_{[0.02,0.98]}$ with three approaches NSO, NSDI, and SDI and 6 kinds of number of samples ($k = 1, 2, \ldots, 6$). It shows that NSO > NSDI > SDI. NSO > NSDI is expected because the former is coarser than the latter. NSDI > SDI can be explained too. They have the same integral interval, but there is a negative adjustment of integral term for SDI because of the truncated tails. For $\rho_{[0,1]}$, there are still truncated tails with the range of $[K_{\min}, K_{\max}]$. For $\rho_{[0.02,0.98]}$, the range is smaller, so difference between NSDI and SDI is bigger (theoretically, with the narrowing of range, this difference will increase first and then decrease to zero from equation (52)). This means that the risks of this kind (with $K_\alpha < E[S] < K_\beta$) can be overvalued by fixed indicator methods (NSO and NSDI), relative to the stochastic indicator method (SDI). From Table 4, it shows that the distorted and interpolation methods (NSDI and SDI) are more stable than the traditional method (NSO) through different samples from $k = 1$ to $k = 6$. And the range moments $\rho_{[0.02,0.98]}$ are more stable than $\rho_{[0,1]}$.

Table 5 shows the results of $\rho_{[0,0.1]}$ and its truncated range $\rho_{[0.02,0.1]}$ with three approaches NSO, NSDI, and SDI and 6 kinds of number of samples ($k = 1, 2, \ldots, 6$). It shows that NSO > NSDI < SDI. NSO > NSDI is the same as Table 4. NSDI < SDI is different from Table 4. It may be explained by the bigger integral interval because of the truncated tail effect (see equation (56)). For $\rho_{[0,0.1]}$, there are still truncated tails with range of $[K_{\min}, K_{0.1}]$. This means that the risks of this kind (with $K_\alpha < K_\beta < E[S]$) can be undervalued by fixed indicator methods (NSO and NSDI), relative to the stochastic indicator method (SDI). From Table 5, it shows that the distorted and interpolation methods (NSDI and SDI) are more stable than the traditional method (NSO) through different samples from $k = 1$ to $k = 6$. For NSO, when $k = 6$, its number of samples is too small, only one, so that $\rho_{[\alpha,\beta]}$ cannot be calculated well (we only show it with zero here). And the range moments $\rho_{[0.02,0.1]}$ are more stable than $\rho_{[0,0.1]}$.

Table 6 shows the results of $\rho_{[0.9,1]}$ and its truncated range $\rho_{[0.90,0.98]}$ with three approaches NSO, NSDI, and SDI and 6 kinds of number of samples ($k = 1, 2, \ldots, 6$). The results are almost the same as Table 5. Table 5 shows the left tail, and Table 6 shows the right tail. Theoretically, they must be similar. But it shows differences and unstability for NSO; sometimes they are even bigger than NSDI. This is because of the number of samples. For maturity $T = 0.28$, there are only 63 samples for strikes and only a small part of them at the right tail; for $k = 1$, there are only 6 and 4 samples for $\rho_{[0.9,1]}$ and $\rho_{[0.90,0.98]}$, respectively. So, the results are unstable and incorrect. This shows that our distorted and interpolation method is better than the traditional method. The other results are similar to Table 5, such as NSDI < SDI, and the range moments $\rho_{[0.90,0.98]}$ are more stable than $\rho_{[0.9,1]}$.

The results for the other maturities T are similar to $T = 0.28$. To show this, we present the results in Figures 14–16 for three pairs of ranges, respectively. These three figures are outcomes calculated from the original data without decreasing ($k = 1$). We can see that for range

TABLE 4: Second range moment for $T = 0.28$.

k	$\rho_{[0,1]}$ NSO	NSDI	SDI	$\rho_{[0.02,0.98]}$ NSO	NSDI	SDI
1	0.0762	0.0761	0.0760	0.0713	0.0707	0.0574
2	0.0765	0.0759	0.0757	0.0720	0.0706	0.0574
3	0.0773	0.0761	0.0759	0.0725	0.0707	0.0575
4	0.0780	0.0754	0.0748	0.0743	0.0704	0.0575
5	0.0907	0.0877	0.0877	0.0766	0.0709	0.0579
6	0.0806	0.0755	0.0744	0.0777	0.0707	0.0575

TABLE 5: Second range moment for $T = 0.28$: left tail.

k	$\rho_{[0,0.1]}$ NSO	NSDI	SDI	$\rho_{[0.02,0.1]}$ NSO	NSDI	SDI
1	0.0410	0.0409	0.0586	0.0331	0.0321	0.0459
2	0.0423	0.0407	0.0584	0.0351	0.0321	0.0459
3	0.0365	0.0404	0.0582	0.0275	0.0317	0.0457
4	0.0334	0.0405	0.0584	0.0252	0.0319	0.0459
5	0.0428	0.0407	0.0583	0.0385	0.0324	0.0461
6	0	0.0404	0.0581	0	0.0317	0.0457

TABLE 6: Second range moment for $T = 0.28$: right tail.

k	$\rho_{[0.9,1]}$ NSO	NSDI	SDI	$\rho_{[0.9,0.98]}$ NSO	NSDI	SDI
1	0.0181	0.0183	0.0387	0.0139	0.0136	0.0187
2	0.0157	0.0183	0.0386	0.0113	0.0137	0.0189
3	0.0142	0.0191	0.0390	0.0080	0.0139	0.0190
4	0	0.0174	0.0369	0	0.0141	0.0190
5	0.0283	0.0170	0.0365	0.0267	0.0144	0.0198
6	0	0.0164	0.0359	0	0.0140	0.0189

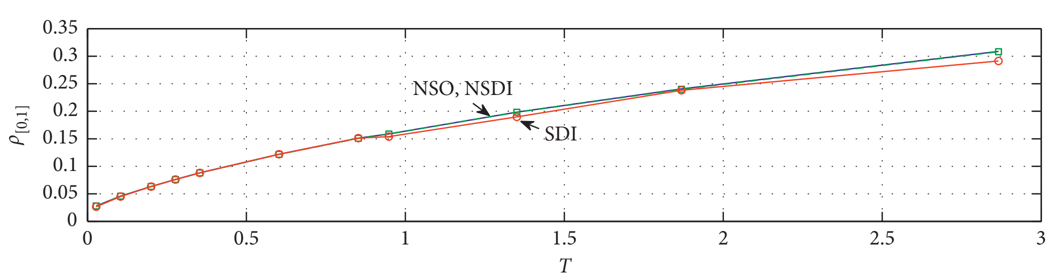

(a)

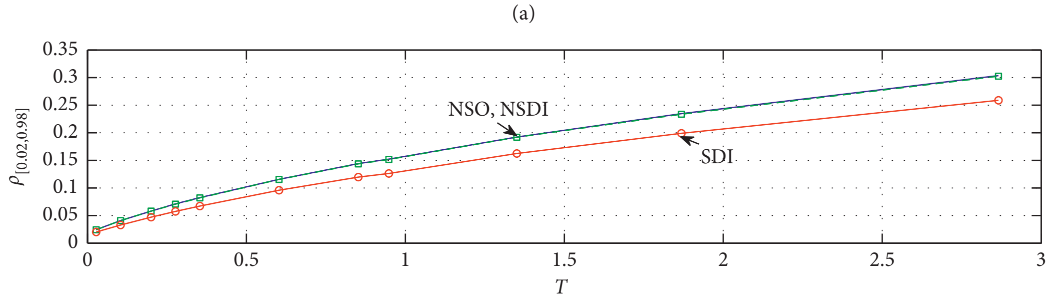

(b)

FIGURE 14: $\rho_{[0,1]}$ and $\rho_{[0.02,0.98]}$ with different T.

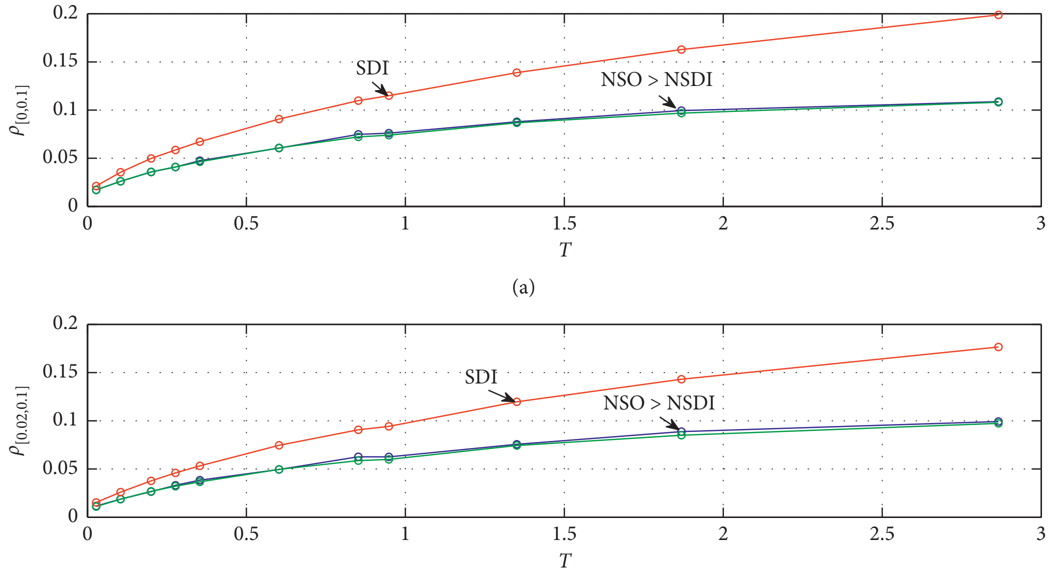

Figure 15: $\rho_{[0,0.1]}$ and $\rho_{[0.02,0.1]}$ with different T.

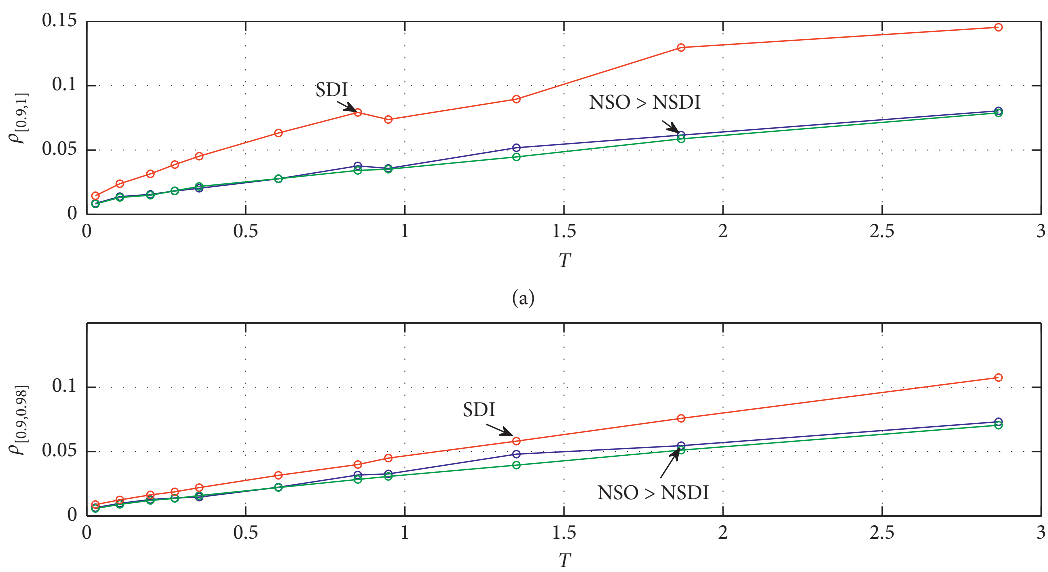

Figure 16: $\rho_{[0.9,1]}$ and $\rho_{[0.9,0.98]}$ with different T.

moment of type of $K_\alpha < E[S] < K_\beta$, NSO > NSDI > SDI; however, for the other types of tail risk, NSO > NSDI < SDI. Because the difference between NSO and NSDI is small, the curves in the figures are overlapped to one curve. For right tail, there are errors because of the limited samples and the nonrational market data at the extreme tail, and it performs better after being truncated (see Figure 16).

To elaborate the influence of size of samples on $\rho_{[\alpha,\beta]}$ with different T, we put all the results of different k in the same figure to compare them. Figures 17 and 18 show the influence of size of samples on $\rho_{[0,1]}$ and its truncated $\rho_{[0.02,0.98]}$. We can see from $k = 1$ to $k = 6$ that the influence of size of samples is weak. We attribute this result to the relatively large sample size between this interval. And it is clear that using the distorted and interpolation method (DI) is more sensitive to the size k because this method will enlarge the effect of some extreme extraordinary value when the size of the samples is small. After truncated, they are better (see Figure 18). However, there is still an abnormal point for distorted and interpolation method (DI) in the figure. It is the second point for maturity $T = 0.1$. And we will see that this strange point exists in all the range moments when

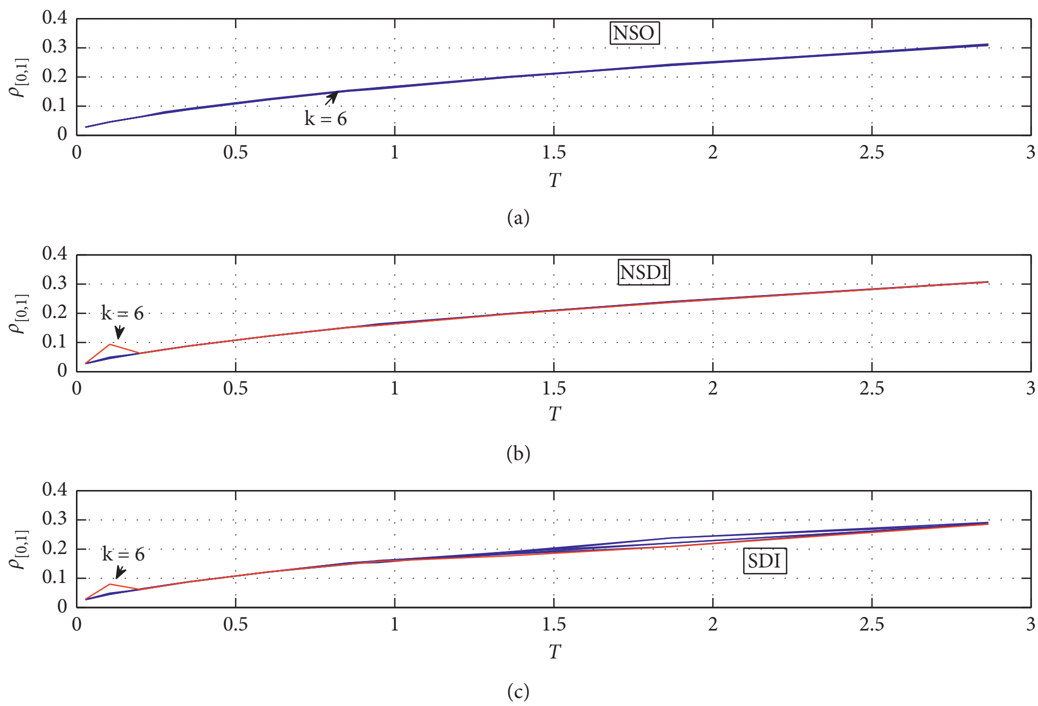

Figure 17: Influence of size of samples on $\rho_{[0,1]}$ with different T.

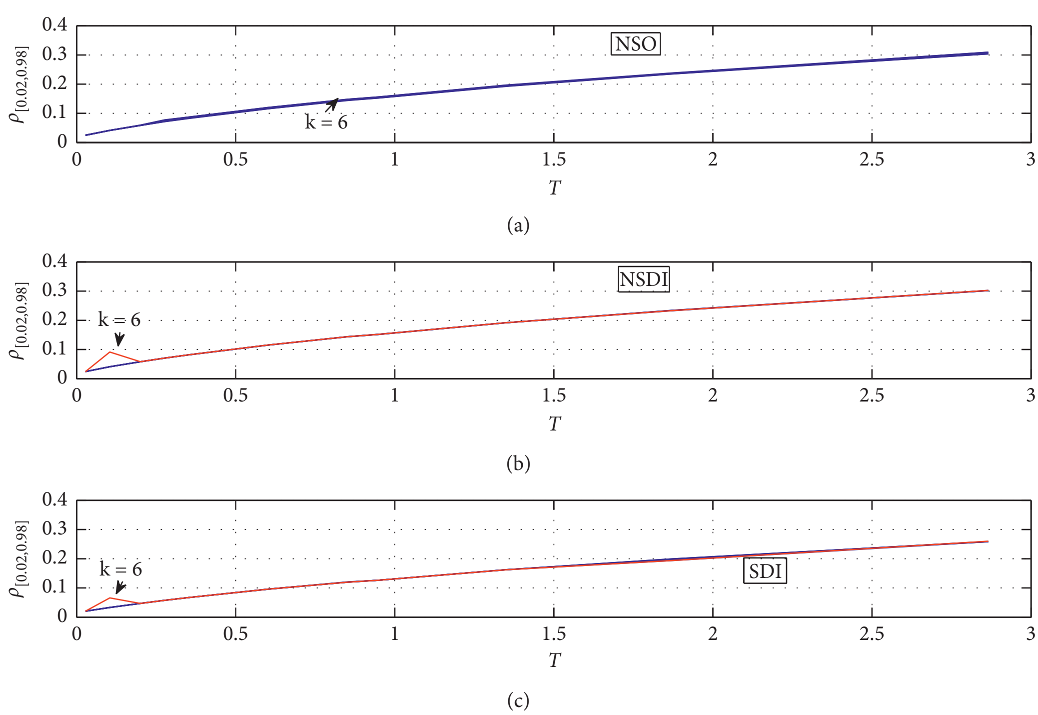

Figure 18: Influence of size of samples on $\rho_{[0.02,0.98]}$ with different T.

considering the right tail risk. Finally, we try to seek the reason for it. Figure 19 shows the right tail of call options price for $T = 0.1$. It shows that there are extraordinary points from points A to B, especially for point C. As mentioned before, we know that if $\rho_{[\alpha,\beta]}$ involved the right tail, it will depend on the call options out of the money heavily. If there are extraordinary points in some sparse area, interpolation method will amplify the negative effect of these

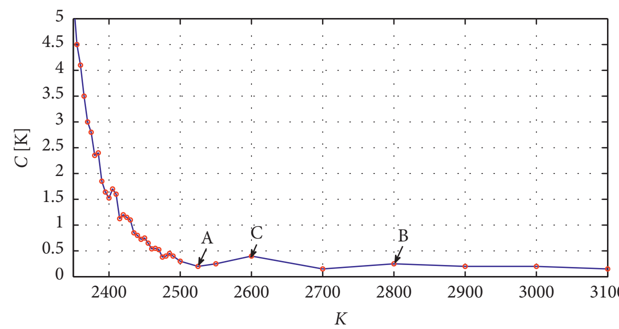

Figure 19: Extraordinary value of call options price for $T = 0.1$.

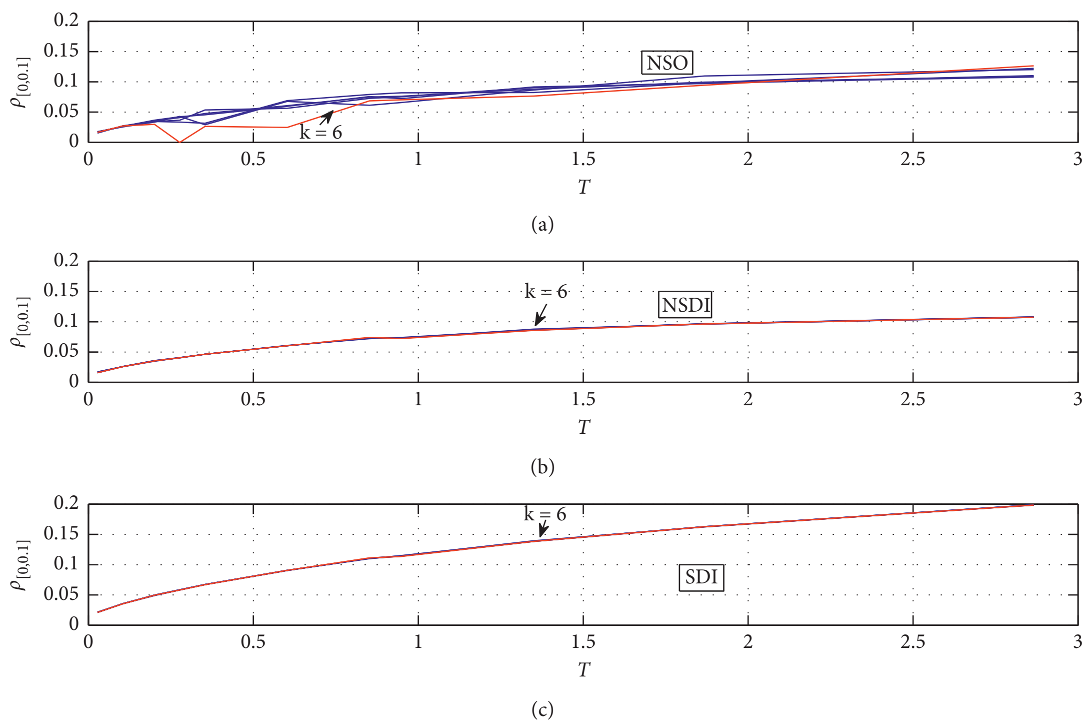

Figure 20: Influence of size of samples on $\rho_{[0,0.1]}$ with different T.

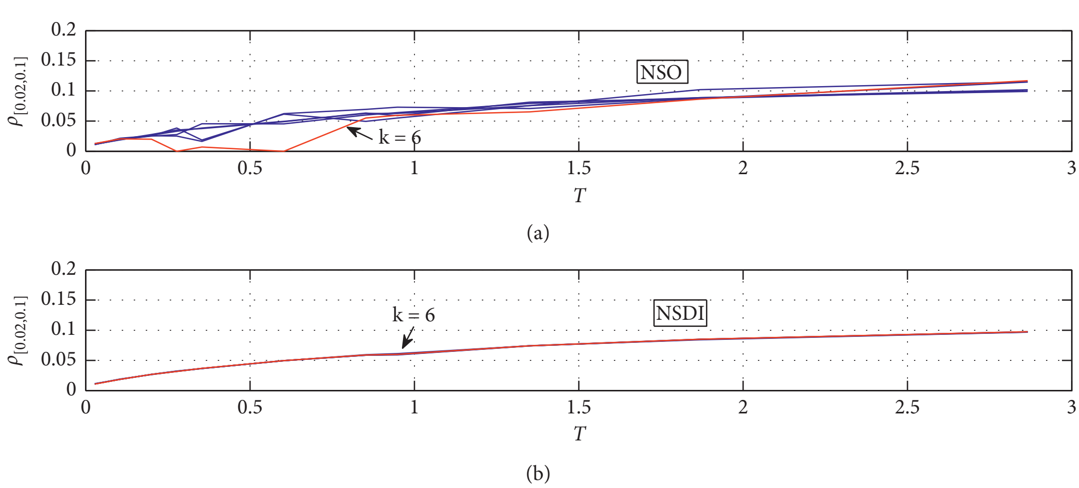

Figure 21: Continued.

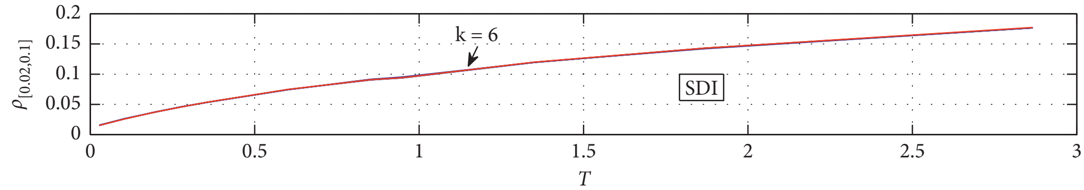

(c)

Figure 21: Influence of size of samples on $\rho_{[0.02,0.1]}$ with different T.

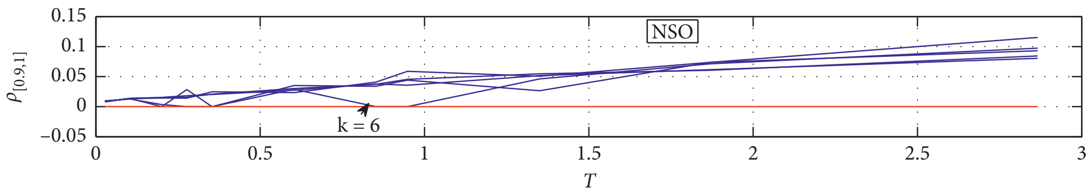

(a)

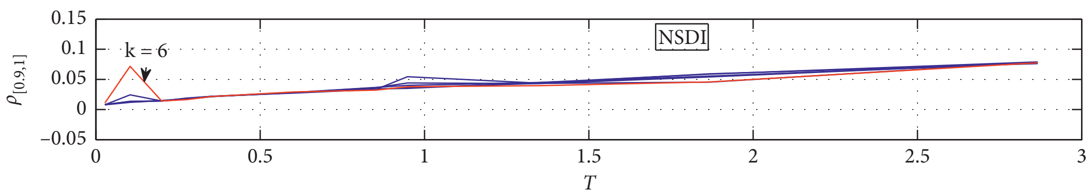

(b)

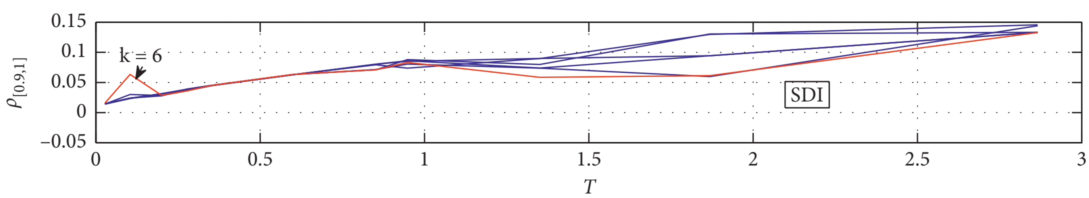

(c)

Figure 22: Influence of size of samples on $\rho_{[0.9,1]}$ with different T.

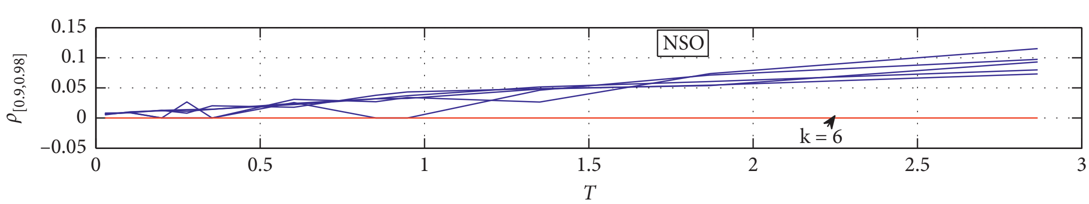

(a)

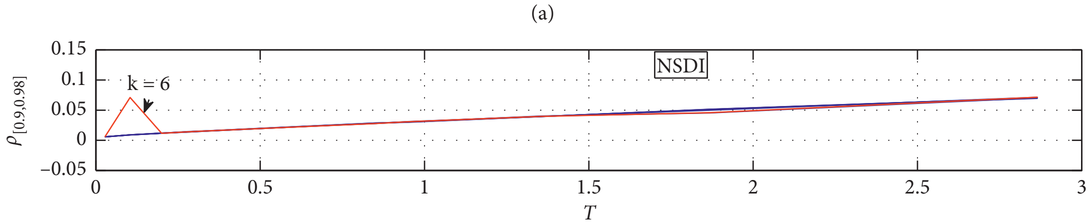

(b)

Figure 23: Continued.

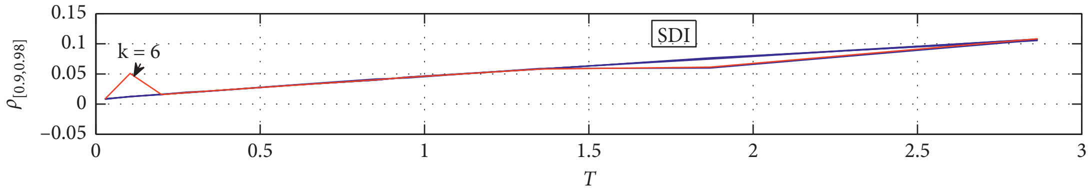

(c)

Figure 23: Influence of size of samples on $\rho_{[0.9,0.98]}$ with different T.

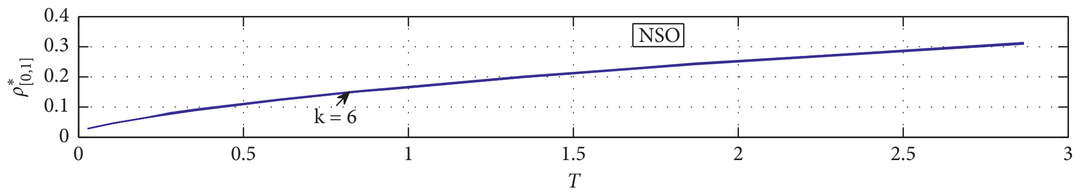

(a)

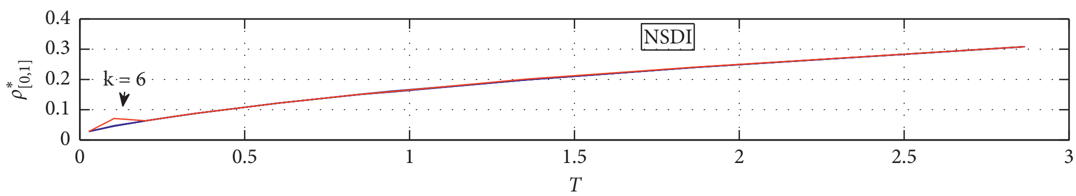

(b)

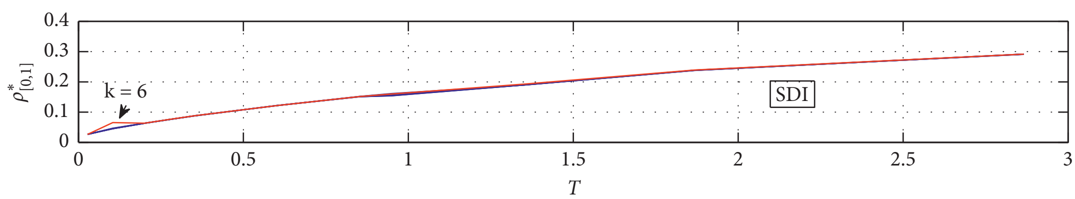

(c)

Figure 24: Influence of size of samples on $\rho^*_{[0,1]}$ with different T.

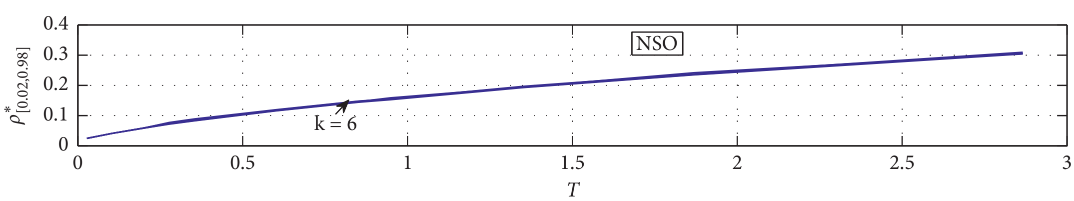

(a)

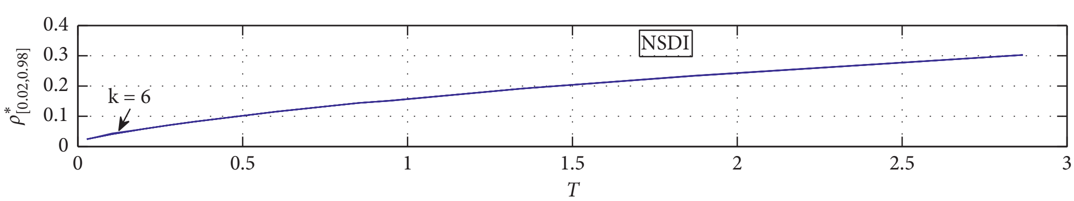

(b)

Figure 25: Continued.

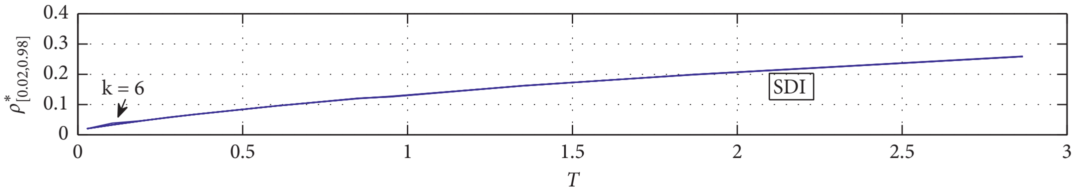

(c)

Figure 25: Influence of size of samples on $\rho^*_{[0.02,0.98]}$ with different T.

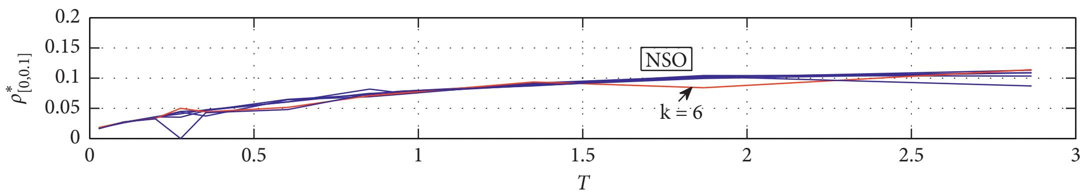

(a)

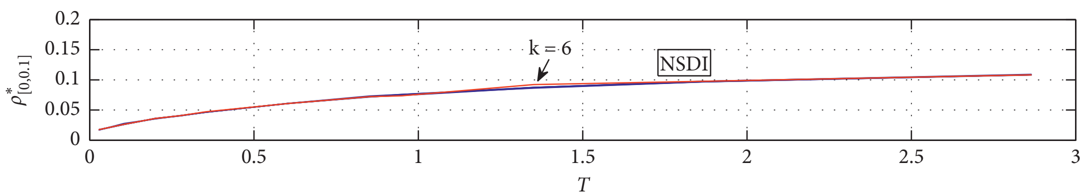

(b)

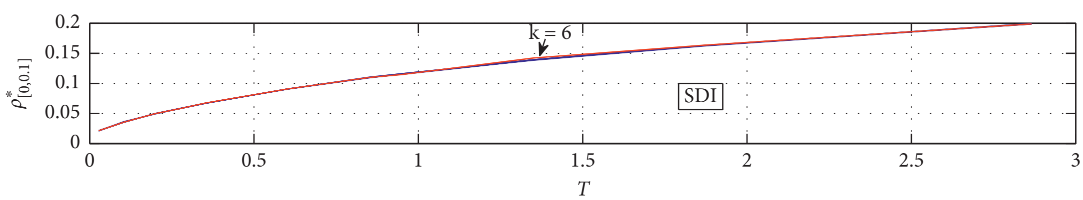

(c)

Figure 26: Influence of size of samples on $\rho^*_{[0,0.1]}$ with different T.

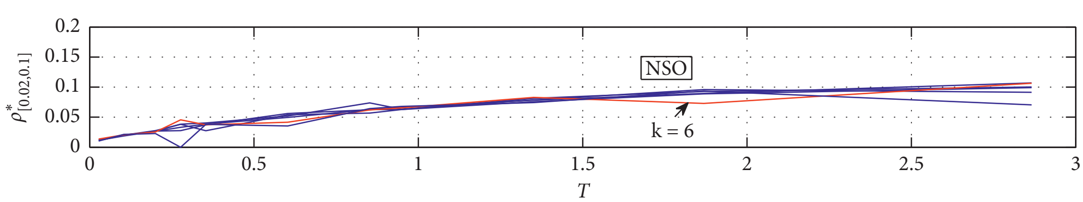

(a)

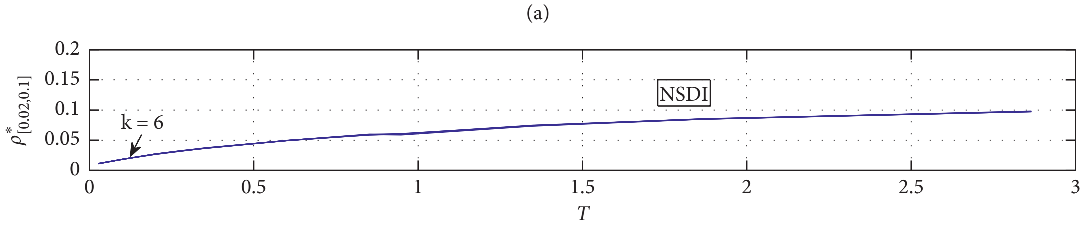

(b)

Figure 27: Continued.

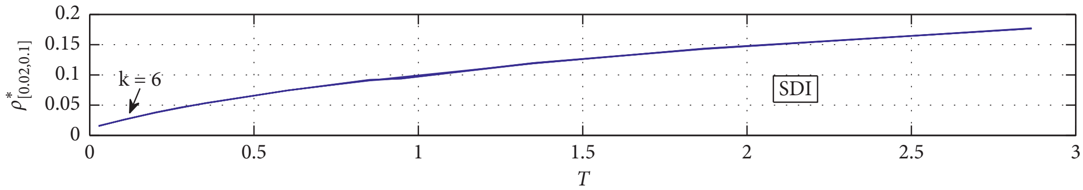

(c)

Figure 27: Influence of size of samples on $\rho^*_{[0.02,0.1]}$ with different T.

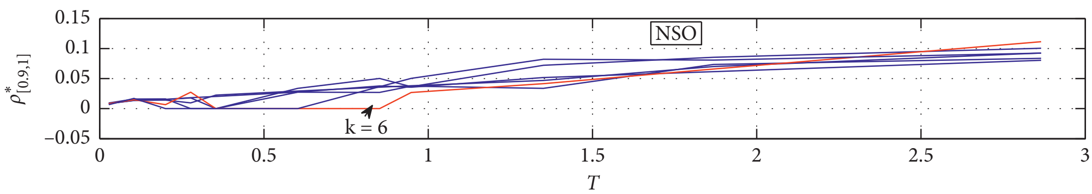

(a)

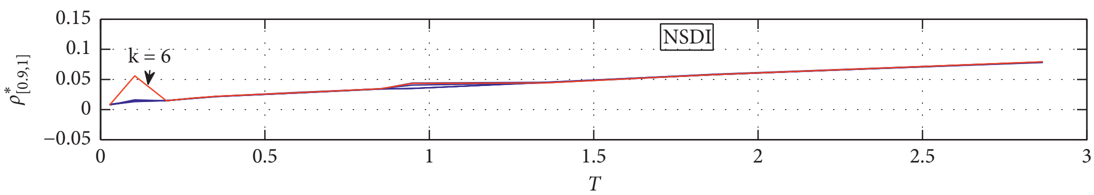

(b)

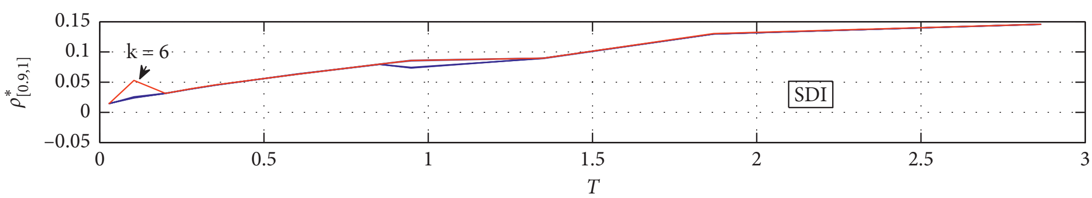

(c)

Figure 28: Influence of size of samples on $\rho^*_{[0.9,1]}$ with different T.

extraordinary points; especially, for the situation there are several samples. Here Figures 17 and 18 show consistent performance.

Figures20 and21 show the influence of size of samples on $\rho_{[0,0.1]}$ and its truncated $\rho_{[0.02,0.1]}$. We can see from $k = 1$ to $k = 6$ that the influence of size of samples is very small for the distorted and interpolation method (DI), especially for truncated situations. That means that the distorted and interpolation method (DI) is better and the truncated method is better.

Figures 22 and 23 show the influence of size of samples on $\rho_{[0.9,1]}$ and its truncated $\rho_{[0.9,0.98]}$. They show the same results, except for points of maturity $T = 0.1$ because of the same reason we have explained.

Besides observing the influences of size of samples on $\rho_{[\alpha,\beta]}$, we check the influences of range length of $[\alpha, \beta]$ on $\rho_{[\alpha,\beta]}$ simultaneously. We narrow the size of samples by $\bmod(N, k) = 0$ while reserving the first and the last point of the original data to hold the length of the range of $[\alpha, \beta]$. Then, we calculate all the range moments, denoted by $\rho^*_{[\alpha,\beta]}$.

Figures 24 and 25 show the influence of size of samples on $\rho^*_{[0,1]}$ and its truncated $\rho^*_{[0.02,0.98]}$. Figures 26 and 27 show the influence of size of samples on $\rho^*_{[0,0.1]}$ and its truncated $\rho^*_{[0.02,0.1]}$. Figures 28 and 29 show the influence of size of samples on $\rho^*_{[0.9,1]}$ and its truncated $\rho^*_{[0.9,0.98]}$.

From these figures, we can conclude that (1) the distorted and interpolation method (DI) is better than the traditional one (NSO), and they are more stable while the size of samples is decreasing; (2) the truncated versions are more stable than their nontruncated versions; (3) the length of range of strikes has influence on moments, especially for tail moments; and (4) the effect of extraordinary value points at the extreme tail still exists, though it is smaller. To offset this effect, the extraordinary value points must be deleted before calculations.

Secondly, we compute $(S/E[S])^\theta$ with $\theta = 3$. To be convenient, we denote $\rho3_{[\alpha,\beta]} = \sqrt{E[((S/E[S])^3 - 1)1_{S\in[K_\alpha,K_\beta]}]}$. We compute all $\rho3_{[\alpha,\beta]}$ with different situations for all the 11 maturities and find that the results are similar to $\rho_{[\alpha,\beta]}$. The only difference is that the results of $\rho_{[\alpha,\beta]}$ are more sensitive to extraordinary value points because when $\theta = 3$, the weights

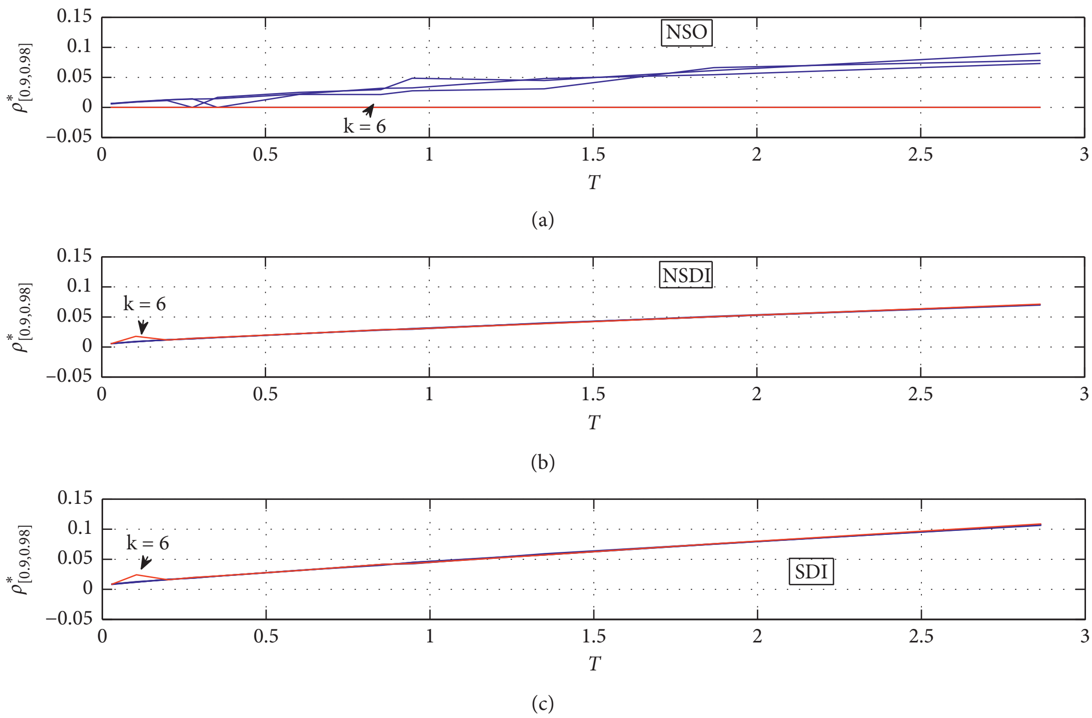

Figure 29: Influence of size of samples on $\rho^*_{[0.9,0.98]}$ with different T.

$f''(K_i/E[S]) = 6(K_i/E[S])$ are not constant anymore; it depends on the strike K. Here, we do not show the details.

4. Conclusions

From the discussions, including the tables and figures, we can conclude that

(1) The distorted and interpolation method (DI) is better than the traditional one (NSO) because they are more stable when the size of samples decreases through different sparse samples from $k = 1$ to $k = 6$. This result is compatible with our theoretical analysis. As the foundation of model-free estimation, precise option price is important, and distorted lognormal distribution makes an important contribution to it. Furthermore, we interpolate the strikes of market trading options and then increase the available data for model estimation in a reasonable way, so the model error is reduced and more stable.

(2) The method to compute the moments with stochastic indicator is apparently different from that with nonstochastic indicator; the risks of this kind(with $K_\alpha < E[S] < K_\beta$) can be overvalued by fixed indicator methods (NSO and NSDI), relative to the stochastic indicator method (SDI), and the risks of this kind (with $K_\alpha < K_\beta < E[S]$) can be undervalued by fixed indicator methods (NSO and NSDI), relative to the stochastic indicator method (SDI). That is to say, the moments calculated by fixed indicator will always be underestimated or overestimated, and the stochastic indicator method is more appropriate.

(3) The truncated version is more stable than nontruncated version. Truncation means that there is a market without serious extreme situations, so we can get stable and smooth computation result easily.

(4) The length of range of strikes has influence on moments, especially for tail moments. As for the left tail risk and the right tail risk, we can get more stable results with the narrowing of range, which is consistent with truncated cases.

(5) The effect of extraordinary value points at the extreme tail still exists, though it is smaller. It is evident that sparsity of data in extraordinary area will enlarge the negative effect of these extraordinary points. So, if we want to offset this effect, the extraordinary value points must be deleted before calculations. So, if we want to get a better calculation of risk measure, we must (1) have more samples in the real market; (2) have the length of range of strikes as long as possible; (3) delete the extraordinary value points before calculations; (4) use range moments by discarding some of strikes at the tail (in fact, if we have deleted the extraordinary value points before calculations, range moments are not required); (5) use a stochastic indicator to calculate the range moments of risk rather than a fixed one; and (6) use the distorted and interpolation method to estimate option prices of all the strikes between the range of $[K_{\min}, K_{\max}]$.

Our future work is to explore a better way to fit the distorted functions $m(\lambda)$ and $q(\lambda)$ well so that we can extend the range of strikes to $(0, +\infty)$ and can compute the risk measures more precisely and then do more works based on this.

Data Availability

The data used to support the findings of this study are deposited at the Reuters database.

Conflicts of Interest

The authors declare that they have no conflicts of interest regarding the publication of this paper.

Acknowledgments

This study was supported by the Humanities and Social Science Planning Fund from Ministry of Education (16YJAZH078), the Fundamental Research Funds for the Central Universities of China (grant nos. CCNU19TS062, CCNU19A06043, and CCNU19TD006), and the Raising Initial Capital for High-Level Talents of Central China Normal University (30101190001).The authors also greatly appreciate Prof. Carole Bernard, from Grenoble Ecole de Management, France, for her useful discussions and comments.

References

[1] R. E. Whaley, "Derivatives on market volatility: hedging tools long overdue," *The Journal of Derivatives*, vol. 1, no. 1, pp. 71–84, 1993.

[2] G. J. Jiang and Y. S. Tian, "The model-free implied volatility and its information content," *Review of Financial Studies*, vol. 18, no. 4, pp. 1305–1342, 2005.

[3] O. Bondarenko, "Variance trading and market price of variance risk," *Journal of Econometrics*, vol. 180, no. 1, pp. 81–97, 2014.

[4] T. Bollerslev, G. Tauchen, and H. Zhou, "Expected stock returns and variance risk premia," *Review of Financial Studies*, vol. 22, no. 11, pp. 4463–4492, 2009.

[5] P. Carr and L. Wu, "Variance risk premiums," *The Review of Financial Studies*, vol. 22, no. 3, pp. 1311–1341, 2008.

[6] V. Todorov, "Variance risk-premium dynamics: the role of jumps," *Review of Financial Studies*, vol. 23, no. 1, pp. 345–383, 2010.

[7] V. Todorov and T. Bollerslev, "Jumps and betas: a new framework for disentangling and estimating systematic risks," *Journal of Econometrics*, vol. 157, no. 2, pp. 220–235, 2010.

[8] V. Todorov and G. Tauchen, "Activity signature functions for high-frequency data analysis," *Journal of Econometrics*, vol. 154, no. 2, pp. 125–138, 2010.

[9] G. J. Jiang and Y. S. Tian, "Extracting model-free volatility from option prices: an examination of the VIX index," *The Journal of Derivatives*, vol. 14, no. 3, pp. 35–60, 2007.

[10] T. G. Andersen, O. Bondarenko, and M. T. Gonzalez-Perez, "Uncovering novel features of equity-index return dynamics via corridor implied volatility," Available at SSRN 1787528, 2012.

[11] M. T. Gonzalez-Perez, "Model-free volatility indexes in the financial literature: a review," *International Review of Economics & Finance*, vol. 40, pp. 141–159, 2015.

[12] D. Linders, J. Dhaene, and W. Schoutens, "Option prices and model-free measurement of implied herd behavior in stock markets," *International Journal of Financial Engineering*, vol. 2, no. 02, p. 1550012, 2015.

[13] J. Dhaene, J. Dony, M. Forys, D. Linders, and W. Schoutens, "FIX: the fear indexmeasuring market fear," in *Topics in Numerical Methods for Finance*, pp. 37–55, Springer, Berlin, Germany, 2012a.

[14] T. G. Andersen, O. Bondarenko, and M. T. Gonzalez-Perez, "Exploring return dynamics via corridor implied volatility," *Review of Financial Studies*, p. hhv033, 2015.

[15] J. D. MacBeth and L. J. Merville, "An empirical examination of the Black-Scholes call option pricing model," *The Journal of Finance*, vol. 34, no. 5, pp. 1173–1186, 1979.

[16] N. B. Gultekin, R. J. Rogalski, and S. M. Tinic, "Option pricing model estimates: some empirical results," *Financial Management*, pp. 58–69, 1982.

[17] D. M. Long and D. T. Officer, "The relation between option mispricing and volume in the black-scholes option model," *Journal of Financial Research*, vol. 20, no. 1, pp. 1–12, 1997.

[18] M. Hamada and M. Sherris, "Contingent claim pricing using probability distortion operators: methods from insurance risk pricing and their relationship to financial theory," *Applied Mathematical Finance*, vol. 10, no. 1, pp. 19–47, 2003.

[19] F. Godin, S. Mayoral, and M. Morales, "Contingent claim pricing using a normal inverse Gaussian probability distortion operator," *Journal of Risk and Insurance*, vol. 79, no. 3, pp. 841–866, 2012.

[20] C. C. Labuschagne and T. M. Offwood, "Pricing exotic options using the Wang transform," *The North American Journal of Economics and Finance*, vol. 25, pp. 139–150, 2013.

[21] H. U. Gerber and E. S. Shiu, ""Martingale approach to pricing perpetual American options," *ASTIN Bulletin*," *The Journal of the IAA*, vol. 24, no. 2, pp. 195–220, 1994.

[22] S. Xiao-nan, W. Wei, and W. Wen-sheng, "Valuing power options under a regime-switching model," *Journal of East China Normal University (Natural Science)*, vol. 2013, no. 6, p. 32, 2013.

[23] J. Dhaene, D. Linders, W. Schoutens, and D. Vyncke, "The herd behavior index: a new measure for the implied degree of co-movement in stock markets," *Insurance: Mathematics and Economics*, vol. 50, no. 3, pp. 357–370, 2012b.

[24] J. Dhaene, D. Linders, W. Schoutens, and D. Vyncke, "A multivariate dependence measure for aggregating risks," *Journal of Computational and Applied Mathematics*, vol. 263, pp. 78–87, 2014.

[25] P. Carr and D. Madan, "Optimal positioning in derivative securities," *Quantitative Finance*, vol. 1, no. 1, pp. 19–37, 2001.

[26] C. B. O. Exchange, "VIX CBOE volatility index," *White Paper*, 2003, http://www.cboe.com.

[27] T. G. Andersen and O. Bondarenko, "Dissecting the Pricing of Equity Index Volatility," *Northwestern University and University of Illinois*, Chicago, IL, USA, 2010, http://www.cboe.com.

Hindawi
Mathematical Problems in Engineering
Volume 2020, Article ID 2767231, 11 pages
https://doi.org/10.1155/2020/2767231

Research Article

Stable Portfolio Selection Strategy for Mean-Variance-CVaR Model under High-Dimensional Scenarios

Yu Shi, Xia Zhao, Fengwei Jiang, and Yipin Zhu

School of Statistics and Information, Shanghai University of International Business and Economics, Shanghai 201620, China

Correspondence should be addressed to Xia Zhao; zhaoxia-w@163.com

Received 29 April 2020; Accepted 29 May 2020; Published 15 July 2020

Guest Editor: Wenguang Yu

This paper aims to study stable portfolios with mean-variance-CVaR criteria for high-dimensional data. Combining different estimators of covariance matrix, computational methods of CVaR, and regularization methods, we construct five progressive optimization problems with short selling allowed. The impacts of different methods on out-of-sample performance of portfolios are compared. Results show that the optimization model with well-conditioned and sparse covariance estimator, quantile regression computational method for CVaR, and reweighted L_1 norm performs best, which serves for stabilizing the out-of-sample performance of the solution and also encourages a sparse portfolio.

1. Introduction

Mean-risk models are widely used and play an important role in financial risk management. The classical and revolutionary work is mean-variance (MV) optimization model proposed by Markowitz [1], in which variance is used to measure risk. Afterwards, more and more researchers are devoted to the study of this field. Kolm et al. [2] review the development, challenges, and trends of MV optimization problems in recent six decades. Considering different risk measures focus on different characteristics of risk, some risk measures other than variance are incorporated into the mean-risk framework. For example, Konno and Yamazaki [3] and Ogryczak and Ruszczynski [4] use absolute deviation and semideviation to measure risk, respectively, and construct mean-risk model for portfolio selection. Value-at-Risk (VaR) and Conditional Value-at-Risk (CVaR) have been employed as the risk measure to conduct asset allocation (see Consigli [5], Alexander and Baptista [6], Xu et al. [7], and Quaranta and Zaffaroni [8] for more details).

Since different risk measures delineate different information of risk, the combination of two risk measures is used to control risk in mean-risk models. For instance, Konno et al. [9] and Konno and Suzuki [10] construct mean-absolute deviation-skewness model and mean-variance-skewness model, respectively, in which the skewness is indicative of unidirectional movement (bearish or bullish) of the stock market. Robert and Philip [11] propose a mean-variance-skewness-kurtosis portfolio optimization model and show that higher-order moments of return can significantly change optimal portfolio construction. Roman et al. [12] construct an optimization model based on mean-variance-CVaR criterion, in which variance and CVaR are combined to obtain a range of balanced solutions that are generally discarded by both mean-variance and mean-CVaR models. Additionally, the personal preference between variance and CVaR of the decision-maker can be considered. Gao et al. [13] extend it to dynamic scenario in financial field and Shi et al. [14] give the discussion in insurance investment under regulatory constraints. However, the study of the stability of optimal strategy's out-of-sample performance is ready to explore under mean-variance-CVaR criterion. Thus, the adaptability of optimal investment strategy in practice is questionable, especially in high-dimensional scenarios (dimensionality of assets is comparable to or even larger than the number of observations). Here, we will study this problem from the point of view of model-solving procedure.

To solve mean-variance-CVaR optimization problem, the computation of variance and CVaR for portfolios is a central and fundamental work. For variance term, estimating covariance matrix of the return variables of assets is necessary. Generally, sample covariance matrix is a good estimator when sample size is large sufficiently. But under high-dimensional scenarios, it usually delivers the presence of poor out-of-sample performance (see, e.g., Green and Hollifield [15]; Chopra and Ziemba [16]; DeMiguel et al. [17]). To deal with such instable out-of-sample performance, researchers make various contributions. Based on different thresholding function, thresholding covariance matrix estimator is one of the mainstreams of improving sample covariance matrix by considering sparsity (e.g., Tibshirani [18]; Bickel and Levin'a [19]; Cai et al. [20]). Moreover, to guarantee the presence of a convex optimization problem, Rothman et al. [21] propose the positive definite sparse covariance estimator (PDSCE). While considering the property of well condition, Ledoit and Wolf [22] propose an estimator of covariance matrix as a linear combination of sample covariance and identity matrix. Maurya [23] develops a well-conditioned and sparse estimator of covariance matrix in high-dimensional setting. This estimator has the properties of well-conditioned, sparsity, and positive definite; especially, the property of positive definite guarantees a convex optimization problem and it performs better than several other popular methods used in literatures (e.g., graphical lasso in Friedman et al. [24], PDSCE in Rothman [21], and Bickel and Levin'a thresholding estimator in Bickel and Levin'a [19]).

For CVaR item, Rockafeller and Uryasev [25, 26] calculate CVaR through a convex programming problem, which pave the way of portfolio selection with CVaR under nonnormal assumption. Bassett et al. [27] bridge the gap between quantile regression and calculation of CVaR without distribution assumption of returns. However, it has also been investigated that the out-of-sample performance is unstable in mean-CVaR model (see Lim et al. [28], Takeda and Kanamori [29], and Kondor et al. [30] for more details). A popular way to make mean-CVaR model stable is regularization technique which can lead to a sparse portfolio simultaneously. Xu et al. [7] incorporate penalty function into mean-CVaR model under the large scale sample scenarios to get a sparse portfolio. Gao and Wu [31] combine penalty function and variance item to improve the out-of-sample performance of mean-CVaR model. Additionally, regularization method has wide applications in constructing mean-variance model to find stable optimal portfolios with better out-of-sample performance. For example, Brodie et al. [32] reformulate classical Markowitz's mean-variance model as a constrained least-squares regression problem. They add a L_1-regularization term to the objective function and show that this penalty regularizes the optimization problem and encourages sparse portfolios. Other works about regularization technique used in mean-variance or mean-CVaR model to promote stable solutions can be seen in literatures (e.g., Gotoh and Takeda [33] and Fastrich et al. [34]).

Motivated by the above discussion, in this paper, we try to find portfolios with more stable out-of-sample performance for mean-variance-CVaR model under high-dimensional scenarios. Five progressive optimization problems are designed carefully based on mean-variance-CVaR criteria through combining two estimators for covariance matrix, two computing methods for CVaR, and two penalty functions in different ways. Simulation is conducted to compare the out-of-sample performance of portfolios obtained from these optimization problems and the impact of underlying methods on optimal strategy is analyzed. Based on the historical data from the constituent stocks in Shanghai Stock Exchange 50 Index, an empirical study is considered.

The remaining of this paper is organized as follows. Section 2 describes the related methods used in this paper. Section 3 shows the optimization problems we formulate based on the mean-variance-CVaR criterion. Section 4 provides simulation and result comparisons. An empirical study is carried out in Section 5. Finally, Section 6 concludes the paper.

2. Methods

In this section, we will briefly introduce risk measures used in this paper, their estimating methods, and some regularization methods. Suppose that we have the opportunity to invest in p assets with returns X_k, $k = 1, 2, \ldots, p$. Let $\mathbf{X} = (X_1, X_2, \ldots, X_p)'$ represent return vector with weight vector $\boldsymbol{\beta} = (\beta_1, \beta_2, \ldots, \beta_p)'$, in which β_k is the portfolio allocation weight for X_k. Thus, the total return is $Y = \mathbf{X}'\boldsymbol{\beta}$.

2.1. Variance. Variance describes the degree of dispersion of a random variable and hence can measure the fluctuation of investment return. Here, we use $\mathscr{V}(\mathbf{X}'\boldsymbol{\beta})$ to denote the variance of a portfolio return variable Y since $Y = \mathbf{X}'\boldsymbol{\beta}$, and $\mathscr{V}(\mathbf{X}'\boldsymbol{\beta})$ can be expressed as

$$\mathscr{V}(\mathbf{X}'\boldsymbol{\beta}) = \sum_{k=1}^{p}\sum_{j=1}^{p}\beta_k\beta_j\sigma_{kj} = \boldsymbol{\beta}'\boldsymbol{\Sigma}\boldsymbol{\beta}, \tag{1}$$

where $\boldsymbol{\Sigma} = (\sigma_{kj})_{p\times p}$ is the covariance matrix of X and σ_{kj} is the covariance of X_k and X_j.

Generally, $\boldsymbol{\Sigma}$ is estimated by sample covariance matrix (called as classical estimator); that is, $\widehat{\boldsymbol{\Sigma}}_c = (\widehat{\sigma}_{kj})_{p\times p}$ and $\widehat{\sigma}_{kj} = (1/n-1)\sum_{i=1}^{n}(x_{ki}-\overline{x}_k)(x_{ji}-\overline{x}_j)$ denote the sample covariance of X_k and X_j, where n is the sample size.

Since the well-conditioned and sparse estimator proposed by Maurya [23], noted as $\widehat{\boldsymbol{\Sigma}}_w$, has been proved its superiority of property. Therefore, in this paper, we employ the well-conditioned and sparse estimator $\widehat{\boldsymbol{\Sigma}}_w$ directly. Following the notation in Maurya [23], we have

$$\widehat{\boldsymbol{\Sigma}}_w(\lambda_1, \tau_1) = \operatorname{argmin}_{\boldsymbol{\Sigma}=\boldsymbol{\Sigma}^T}\left(\left\|\boldsymbol{\Sigma} - \widehat{\boldsymbol{\Sigma}}_c\right\|_2^2 + \lambda_1\|\boldsymbol{\Sigma}^-\|_1 + \tau_1\sum_{k=1}^{p}(\sigma_i(\boldsymbol{\Sigma}) - \overline{\sigma}_{\boldsymbol{\Sigma}})^2\right), \tag{2}$$

where $\boldsymbol{\Sigma}^{-} = \boldsymbol{\Sigma} - \boldsymbol{\Sigma}^{+}$ and $\boldsymbol{\Sigma}^{+}$ denote a diagonal matrix with the same diagonal as $\boldsymbol{\Sigma}$, $\sigma_i(\boldsymbol{\Sigma})$ is the ith largest eigenvalue of matrix $\boldsymbol{\Sigma}$, and $\overline{\sigma}_{\boldsymbol{\Sigma}}$ is the mean of eigenvalues of $\boldsymbol{\Sigma}$, and the way to identify the best pair (λ_1, τ_1) can also be found in Maurya [23].

2.2. CVaR. For financial assets or portfolio, VaR refers to the greatest possible loss over specific holding period, at a certain confidence level $100(1-\alpha)\%, \alpha \in (0,1)$. If the cumulative distribution function for return Y is F, VaR can be defined as

$$\mathrm{VaR}_{1-\alpha} = -F^{-1}(\alpha). \tag{3}$$

As we know, compared with VaR, a key advantage of CVaR is that CVaR satisfies the four coherence axioms of Artzner et al. [35], whereas VaR is not coherent. The definition of CVaR is as follows:

$$\mathrm{CVaR}_{1-\alpha} = E\left[-Y \mid -Y \geq \mathrm{VaR}_{1-\alpha}\right]. \tag{4}$$

Evidently, $\mathrm{CVaR}_{1-\alpha}$, the conditional expectation of losses exceeding $\mathrm{VaR}_{1-\alpha}$, is more informative about the tail of the distribution than $\mathrm{VaR}_{1-\alpha}$. Two popular ways to compute CVaR without distribution constraints have been employed recently. The first one is a linear programming model for optimizing CVaR proposed by Rockafellar and Uryasev [25, 26], generally called as Rockafellar–Uryasev's approximation. They have proved that CVaR can be calculated by solving a convex optimization problem. In other words, CVaR can be formulated as

$$\mathrm{CVaR}^{1}_{1-\alpha} = \min_{\boldsymbol{\beta},\xi} \xi + \alpha^{-1} E\left[-\mathbf{X}'\boldsymbol{\beta} - \xi\right]^{+}, \tag{5}$$

where ξ is the αth quantile of Y. This method has been widely used in many literatures (e.g., Roman et al. [12], Lim et al. [28], and Gao and Wu [31]).

The second way is quantile regression method proposed in Bassett et al. [27]. Xu et al. [7] have proved that it has faster computational speed compared with Rockafellar–Uryasev's approximation method. According to Bassett et al. [27], the CVaR of a portfolio return Y could be calculated by

$$\mathrm{CVaR}^{2}_{1-\alpha} = \alpha^{-1} \min_{\xi} E\left[\rho_\alpha (Y - \xi)\right] - E[Y], \tag{6}$$

where ξ is the αth quantile of Y and $\rho_\alpha(u) = u(\alpha - I(u<0))$ is the check function, in which $I(\cdot)$ is an indicator function that takes on the value one whenever its argument is true and zero otherwise.

Since $Y = \mathbf{X}'\boldsymbol{\beta}$, we can have $Y = X_1 - \sum_{j=2}^{p}(X_1 - X_j)\beta_j$ under the constraint $\mathbf{1}'\boldsymbol{\beta} = 1$. Let $\widetilde{X_j} = X_1 - X_j$ $(j = 2, 3, \ldots, p)$, we can convert equation (6) into

$$\mathrm{CVaR}^{2}_{1-\alpha} = \alpha^{-1} \min_{\beta,\xi} E\left[\rho_\alpha\left(X_1 - \sum_{j=2}^{p} \widetilde{X_j}\beta_j - \xi\right)\right] - E\left[\mathbf{X}'\boldsymbol{\beta}\right]. \tag{7}$$

2.3. Regularization Method. To encourage a stable and sparse solution in optimization problem, penalty item $\mathrm{Pen}(\cdot)$ is frequently used, which is regarded as regularization method. $\mathrm{Pen}(\cdot)$ is a general penalty function that allows shrinking the components in $\boldsymbol{\beta}$ to zero. In this paper, we focus on smoothly clipped absolute deviation (SCAD) penalty proposed by Fan et al. [36] and reweighted L_1 norm penalty proposed by Emmanuel et al. [37], since they have oracle properties.

The SCAD penalty is formulated as follows:

$$\lambda \sum_{k=1}^{p} \mathrm{Pen}_1(\beta_k) = \sum_{k=1}^{p} \left\{ \lambda|\beta_k| I\left(|\beta_k| \leq \lambda\right) + \frac{-\beta_k^2 + 2\zeta\lambda|\beta_k| - \lambda^2}{2(\zeta - 1)} I\left(\lambda < |\beta_k| \leq \zeta\lambda\right) + \frac{(\zeta+1)\lambda^2}{2} I\left(|\beta_k| > \zeta\lambda\right) \right\}, \tag{8}$$

where $\zeta\,(\zeta < 2)$ and λ are tuning parameters. It is well known that SCAD is continuous and singular at the origin, penalizes large coefficients equally, and has no bias, and the reweighted L_1 norm is as follows:

$$\lambda \sum_{k=1}^{p} \mathrm{Pen}_2(\beta_k) = \lambda \sum_{k=1}^{p} \omega_k |\beta_k|, \tag{9}$$

where λ is a tuning parameters and the value of ω_k can be identified by iteration method based on the value of $|\beta_k|$. Reweighed L_1 norm has a better out-of-sample performance compared with L_1 norm penalty [34], since it gives every component in $\boldsymbol{\beta}$ a corresponding weight so that the penalization is more accurate.

3. Model Formation

Motivated by Roman et al. [12], we consider the following mean-variance-CVaR model:

$$\mathscr{P}_{\mathrm{mvc}}: \begin{cases} \min\limits_{\boldsymbol{\beta}} & \eta \mathscr{V}(\mathbf{X}'\boldsymbol{\beta}) + (1-\eta)\mathrm{CVaR}_{1-\alpha} \\ \text{s.t.} & \begin{array}{l} \mathbf{1}'\boldsymbol{\beta} = 1 \\ E\left[\mathbf{X}'\boldsymbol{\beta}\right] = \mu_0, \end{array} \end{cases} \tag{10}$$

where $0 \leq \eta \leq 1$ is a weighting parameter, which represents the attitude that investors hold towards the two risk measures and hence balances the importance of them.

Remark 1. Letting $\eta = 0$ or $\eta = 1$, respectively, the above optimization problem is reduced to the mean-CVaR model or mean-variance model.

Remark 2. Different from Roman et al. [12], in this paper, we incorporate the variance term and CVaR term into the objective function of optimization model simultaneously and short selling is allowed.

3.1. Optimization Problems. In this section, we present the following five optimization problems based on different methods of calculating variance, CVaR, and different regularization methods in order to obtain optimal portfolio for $\mathscr{P}_{\mathrm{mvc}}$.

To illustrate clearly, we outline the optimization problems in Table 1. Here, "$\sqrt{}$" means the underlying method is incorporated in the corresponding optimization problem. For example, the second row tells us that the classical estimation $\widehat{\mathbf{\Sigma}}_c$ of variance term and Rockafellar–Uryasev's approximation $\mathrm{CVaR}^1_{1-\alpha}$ for CVaR term are used in problem $\mathscr{P}_1$.

Mathematically, optimization problems can be written in the following forms:

$$
\begin{aligned}
&\mathscr{P}_1: \begin{cases} \min\limits_{\boldsymbol{\beta},\xi} & \eta\boldsymbol{\beta}'\widehat{\mathbf{\Sigma}}_c\boldsymbol{\beta} + (1-\eta)\left(\xi + \alpha^{-1}E\left[-\mathbf{X}'\boldsymbol{\beta} - \xi\right]^{+}\right) \\ \text{s.t.} & \begin{array}{l} \mathbf{1}'\boldsymbol{\beta} = 1 \\ E\left[\mathbf{X}'\boldsymbol{\beta}\right] = \mu_0, \end{array} \end{cases} \\
&\mathscr{P}_2: \begin{cases} \min\limits_{\boldsymbol{\beta},\xi} & \eta\boldsymbol{\beta}'\widehat{\mathbf{\Sigma}}_w\boldsymbol{\beta} + (1-\eta)\left(\xi + \alpha^{-1}E\left[-\mathbf{X}'\boldsymbol{\beta} - \xi\right]^{+}\right) \\ \text{s.t.} & \begin{array}{l} \mathbf{1}'\boldsymbol{\beta} = 1 \\ E\left[\mathbf{X}'\boldsymbol{\beta}\right] = \mu_0, \end{array} \end{cases} \\
&\mathscr{P}_3: \begin{cases} \min\limits_{\boldsymbol{\beta},\xi} & \eta\boldsymbol{\beta}'\widehat{\mathbf{\Sigma}}_w\boldsymbol{\beta} + (1-\eta)\alpha^{-1}E\left[\rho_\alpha\left(X_1 - \sum_{j=2}^{p}\widetilde{X_j}\beta_j - \xi\right)\right] \\ \text{s.t.} & E\left[\mathbf{X}'\boldsymbol{\beta}\right] = \mu_0, \end{cases} \\
&\mathscr{P}_4: \begin{cases} \min\limits_{\boldsymbol{\beta},\xi} & \eta\boldsymbol{\beta}'\widehat{\mathbf{\Sigma}}_w\boldsymbol{\beta} + (1-\eta)\alpha^{-1}E\left[\rho_\alpha\left(X_1 - \sum_{j=2}^{p}\widetilde{X_j}\beta_j - \xi\right)\right] + \lambda\sum_{i=1}^{p}\mathrm{Pen}_1\left(\beta_i\right) \\ \text{s.t.} & E\left[\mathbf{X}'\boldsymbol{\beta}\right] = \mu_0, \end{cases} \\
&\mathscr{P}_5: \begin{cases} \min\limits_{\boldsymbol{\beta},\xi} & \eta\boldsymbol{\beta}'\widehat{\mathbf{\Sigma}}_w\boldsymbol{\beta} + (1-\eta)\alpha^{-1}E\left[\rho_\alpha\left(X_1 - \sum_{j=2}^{p}\widetilde{X_j}\beta_j - \xi\right)\right] + \lambda\sum_{i=1}^{p}\mathrm{Pen}_2\left(\beta_i\right) \\ \text{s.t.} & E\left[\mathbf{X}'\boldsymbol{\beta}\right] = \mu_0. \end{cases}
\end{aligned} \tag{11}
$$

Why do we design such five optimization problems in the foregoing way? In $\mathscr{P}_1$, the classical method of variance term and Rockafellar–Uryasev's approximation for CVaR term are used to find the solution. To construct $\mathscr{P}_2$, we replace the classical estimator $\widehat{\mathbf{\Sigma}}_c$ in the variance term in $\mathscr{P}_1$ with $\widehat{\mathbf{\Sigma}}_w$, and the CVaR part remains the same so that we could find if $\widehat{\mathbf{\Sigma}}_w$ could mitigate the instability. Further, we replace $\mathrm{CVaR}^1_{1-\alpha}$ in $\mathscr{P}_2$ with $\mathrm{CVaR}^2_{1-\alpha}$ to get $\mathscr{P}_3$, so that the difference between the two computational methods for CVaR could be compared. In $\mathscr{P}_3 - \mathscr{P}_5$, $\mathbf{1}'\boldsymbol{\beta} = 1$ can be absorbed into the CVaR item based on quantile regression method. To examine the performance of SCAD and reweighted L_1 norm penalty function, we design $\mathscr{P}_4$ and $\mathscr{P}_5$, in which quantile computational method for CVaR is used because of the convenience of selecting tuning parameter in penalty function and faster computational speed [7]. Through such progressive problem design, we can figure out the performance of different methods and find the most effective one in our setting.

Remark 3. The estimation methods used in $\mathscr{P}_1$ for variance and CVaR are the same as that in Roman et al. [12].

Remark 4. If $\eta = 0$, $\mathscr{P}_4$ degenerates into the model in Xu et al. [7]. However, the constraint $E[\mathbf{X}'\boldsymbol{\beta}] = \mu_0$ is missing in their paper. According to Bassett et al. [27], the $E[\mathbf{X}'\boldsymbol{\beta}]$ item in CVaR part (see (7)) in objective function can be neglected only under the constraint that the expected return of portfolio is a constant.

Table 1: Methods in optimization problems.

	$\widehat{\Sigma}_c$	$\widehat{\Sigma}_w$	$\mathrm{CVaR}^1_{1-\alpha}$	$\mathrm{CVaR}^2_{1-\alpha}$	Pen_1	Pen_2
$\mathscr{P}_1$	√		√			
$\mathscr{P}_2$		√	√			
$\mathscr{P}_3$		√		√		
$\mathscr{P}_4$		√		√	√	
$\mathscr{P}_5$		√		√		√

3.2. Selection of Tuning Parameter. For $\mathscr{P}_4$ and $\mathscr{P}_5$, we need to search the best tuning parameter for penalty item.

In $\mathscr{P}_4$, the nonnegative regularization parameter λ drives the relevance of the SCAD penalty and ζ is a tuning parameter belonging to SCAD penalty. Here, we search the best pair $\boldsymbol{\theta} = (\lambda, \zeta)'$ over two-dimension grids following the criterion mentioned in the following. Motivated by Lee et al. [38] and Wang et al. [39], we use the modified Bayesian Information Criterion as follows:

$$\widehat{\boldsymbol{\theta}} = \mathrm{argmin}_{\boldsymbol{\theta}} \ln \left\{ \eta \cdot \widehat{\boldsymbol{\beta}} \widehat{\boldsymbol{\Sigma}}_w \widehat{\boldsymbol{\beta}} + (1-\eta)\alpha^{-1} \sum_{i=1}^{n} \rho_\alpha \left(x_{i,1} - \sum_{j=2}^{p} \widetilde{x}_{i,j} \widehat{\beta}_{j,\boldsymbol{\theta}} - \widehat{\xi}_{\boldsymbol{\theta}} \right) \right\} + \mathrm{d}f \cdot \frac{\ln n}{2n} \cdot \ln p, \tag{12}$$

where $x_{1,1}, x_{2,1}, \ldots, x_{n,1}$ are random samples of X_1, $\widetilde{x}_{1,j}, \widetilde{x}_{2,j}, \ldots, \widetilde{x}_{n,j}$ are random samples of $\widetilde{X}_j$ for $j = 2, 3, \ldots, p$, and $\mathrm{d}f$ is the effective dimension of fitting model. Additionally, $\mathrm{d}f = |\mathscr{E}|$ indicates the number of points in the set $\mathscr{E}$ with $\mathscr{E} = \{ j: \widehat{\beta}_{j,\theta} \neq 0, 2 \le j \le p \}$. Furthermore, the iterative algorithm for conducting $\mathscr{P}_4$ can be seen in Wu and Liu [40].

In $\mathscr{P}_5$, λ is the nonnegative regularization parameter and $\omega_k, k = 1, 2, \ldots, p$ is the tuning parameter in reweighted L_1 norm penalty. For $\boldsymbol{\omega} = (\omega_1, \omega_2, \ldots, \omega_p)'$, we apply the following iterative procedure for every given λ to change the weighting parameter ω_k dynamically and adaptively [37].

(1) Let the iteration count be h. For any given $\boldsymbol{\omega}^{(h)}$, we solve the problem $\mathscr{P}_5$, which gives the solution $\widehat{\boldsymbol{\beta}}^{(h)}$. If the stopping criteria are satisfied, for example, compared with every component in $\widehat{\boldsymbol{\beta}}^{(h-1)}$, the maximum change does not exceed some small constant, we stop the iteration. Otherwise, go to Step (2).

(2) Use $\widehat{\boldsymbol{\beta}}^{(h)}$ to construct the new weighting parameter $\omega_k^{(h+1)} = 1/(|\widehat{\beta}_k^{(h)}| + \varepsilon)$, where ε can be a small positive number and let $h = h + 1$. Go to Step (1).

Finally, here, $\boldsymbol{\theta} = (\lambda, \omega_1, \omega_2, \ldots, \omega_p)'$ can be searched by iteration based on the modified Bayesian Information Criterion equation (12).

4. Simulation and Discussion

4.1. Data Generation. To evaluate the out-of-sample performance of these five portfolio optimization problems, the dataset is generated by simulation approach with parameters being estimated from real historical price data of stock index.

4.1.1. Construction of Return Variable. Following the idea in Lim et al. [28], the random returns are captured by a hybrid distribution with multivariate normal distribution and exponential distribution. So all assets might suffer a perfectly correlated exponential-tail loss in a small probability. Let z be the exponential random variable with parameter q and we set $q = 10$ for simplicity. So the return variable is constructed as follows:

$$\mathbf{X} \sim B(\tau)(z\mathbf{1} + \mathbf{c}) + (1 - B(\tau))N, \tag{13}$$

where $B(\tau)$ is the Bernoulli random variable with parameter τ, N follows multivariate normal distribution with mean vector $\widetilde{\boldsymbol{\mu}}$ and covariance matrix $\widetilde{\boldsymbol{\Sigma}}$, and $\mathbf{c} = (c_1, c_2, \ldots, c_p)'$ with $c_k = \widetilde{\mu}_k - \sqrt{\widetilde{\Sigma}_{kk}}/2$, where $\widetilde{\Sigma}_{kk}$ is the k-th diagonal element of the matrix $\widetilde{\boldsymbol{\Sigma}}$. The parameter τ controls the tail loss of the distribution.

4.1.2. Determination of Parameter Values. We choose 142 stocks which in Shanghai Stock Exchange Constituent (SSEC) index download the data from Joinquant Data platform. The sample period spans from Jan 3, 2015, to Dec 31, 2015. We calculate the daily yield return and estimate their mean return vector $\widetilde{\boldsymbol{\mu}} = (\mu_1, \mu_2, \ldots, \mu_p)'$ and covariance matrix $\widetilde{\boldsymbol{\Sigma}}$. (Note that the 180 constituent stocks in SSEC are always changing in the sample period, since the sample is adjusted every half year; therefore, we choose 142 stocks which continuously stay in the index over the period.)

4.1.3. Data Generation. As we know, when the dimensionality of assets is comparable to the number of observations, the data set belongs to high-dimensional scenarios. Therefore, in order to simulate a high-dimensional data set, we set the size of n close to $p = 142$. Letting $n = 150$ and $\tau = 0.05$, we simulate 101 groups of data, one group as in-sample data, and 100 group as out-of-sample data.

4.2. Optimization Results. In this section, we will calculate simulation results based on the five optimization problems, respectively, and give the comparisons from the point view of the out-of-sample performance. Without loss of generality, we set $\mu_0 = 0.01$. All the calculations follow three steps:

Step 1: calculate the weight of assets in portfolio selection model with different $\eta = 0, 0.25, 0.5, 0.75$, and 1 for in-sample data.

Step 2: based on the weights in Step 1, we calculate the variance, CVaR with 0.95 confidence level, and expected return for other 100 groups of out-of-sample data.

Step 3: summarize their mean value and standard deviation for every case. For example, under the case of $\mathscr{P}_1$ at $\eta = 1$, the mean value and the standard deviation for 100 values of CVaR are calculated to be 10.0812 and (0.9708), respectively.

Steps 1 and 2 mean that we hold the optimal portfolio generated from in-sample data in the out-of-sample period, in which the data follow the same distribution as in-sample data. Therefore, if the optimal portfolio is stable, the performance of portfolio in 100 groups of out-of-sample data should be similar, and hence, we calculate the standard deviation in Step 3 to measure the similarity of the performance in 100 groups.

The results are shown in Table 2.

From Table 2, the following results are concluded:

(1) Compared $\mathscr{P}_1$ with $\mathscr{P}_2$–$\mathscr{P}_5$, the mean for 100 values of variance, CVaR in $\mathscr{P}_1$ are larger, which means that the risks of portfolios in out-of-sample data get out of control and the expected returns are also higher. This is consistent with the truth of "high risk; high return." The inherent reason is that sample covariance estimator lost its theoretical support (Law of Large Numbers) in high-dimensional scenarios.

(2) Compared $\mathscr{P}_2$ with $\mathscr{P}_1$, we can find that all the counterparts in $\mathscr{P}_2$ decrease, which tells that the use of well-conditioned and sparse estimator ($\widehat{\mathbf{\Sigma}}_w$) could control the risk significantly and improves the stability of solutions' out-of-sample performance as well. When $\eta = 0$, the model is reduced to mean-CVaR model, whose solution is irrelevant to the estimation of $\mathbf{\Sigma}$, so the values of CVaR and expected return should remain the same. The data in Table 2 really illustrate this fact.

(3) The results in $\mathscr{P}_2$ and $\mathscr{P}_3$ share identical in-sample optimal portfolio values and out-of-sample performance. This means that the impact of Rockafellar–Uryasev's approximation and quantile regression method of CVaR on the solution of optimization problem shows no significant difference under our setting.

(4) The values in $\mathscr{P}_4$ further become smaller than ones in $\mathscr{P}_3$, which says that the use of SCAD penalty technique can improve the stability and the risk-controlling ability for out-of-sample performance.

(5) Compared $\mathscr{P}_5$ with $\mathscr{P}_4$, the values of variance and CVaR in $\mathscr{P}_5$ show a slight decrease, which means that the reweighted L_1 norm penalty contributes to a more stable out-of-sample performance than SCAD penalty, even though the improvement is fractional.

(6) Bigger η represents a higher proportion for variance item in objective function. Since variance is a more conservative risk measure compared with CVaR, generally, bigger η results in a more conservative portfolio with relative low-risk index and expected return in out-of-sample analysis. The values in $\mathscr{P}_4$ and $\mathscr{P}_5$ show this trend well. But others fail, which may attribute to the instable out-of-sample performance.

Table 2: Out-of-sample performance of $\mathscr{P}_1$–$\mathscr{P}_5$.

		$\eta = 1$	$\eta = 0.75$	$\eta = 0.5$	$\eta = 0.25$	$\eta = 0$
$\mathscr{P}_1$	Variance	5.0235 (0.3525)	4.6044 (0.3281)	4.3821 (0.3163)	4.2897 (0.3111)	4.9986 (0.3121)
	CVaR	10.0812 (0.9708)	9.2110 (0.9307)	8.7280 (0.9299)	8.5244 (0.9324)	9.9947 (0.9786)
	Exp return	0.2389 (0.4227)	0.2076 (0.3950)	0.1996 (0.3855)	0.2205 (0.3894)	0.31 (0.4571)
$\mathscr{P}_2$	Variance	1.3405 (0.1919)	1.5978 (0.2613)	1.9141 (0.3365)	2.3783 (0.4369)	5.1578 (0.9564)
	CVaR	2.5983 (0.2618)	3.0591 (0.3213)	3.6541 (0.3635)	4.5752 (0.4496)	9.9947 (0.9786)
	Exp return	0.1939 (0.1226)	0.1817 (0.1438)	0.1974 0.1729)	0.1690 (0.2176)	0.31 (0.4571)
$\mathscr{P}_3$	Variance	1.3405 (0.1919)	1.5978 (0.2613)	1.9141 (0.3365)	2.3783 (0.4369)	5.1578 (0.9564)
	CVaR	2.5983 (0.2618)	3.0591 (0.3213)	3.6541 (0.3635)	4.5752 (0.4496)	9.9947 (0.9786)
	Exp return	0.1939 (0.1226)	0.1817 (0.1438)	0.1974 (0.1729)	0.1690 (0.2176)	0.31 (0.4571)
$\mathscr{P}_4$	Variance	1.1758 (0.0837)	1.1934 (0.0815)	1.2232 (0.0795)	1.2782 (0.0802)	1.2769 (0.0764)
	CVaR	2.4739 (0.25	2.4997 (0.2670)	2.5401 (0.2751)	2.6587 (0.2882)	2.6631 (0.2867)
	Exp return	0.0772 (0.1092)	0.0816 (0.1112)	0.0925 (0.1148)	0.0962 (0.1215)	0.0917 (0.1199)
$\mathscr{P}_5$	Variance	1.1223 (0.0769)	1.1632 (0.0769)	1.1830 (0.0744)	1.2094 (0.0738)	1.2274 (0.0705)
	CVaR	2.3334 (0.2407)	2.4151 (0.2570)	2.4395 (0.2625)	2.4956 (0.2770)	2.5304 (0.2750)
	Exp return	0.08499 (0.1026)	0.0852 (0.1071)	0.0917 (0.1092)	0.0956 (0.1142)	0.0976 (0.1145)

To analyze the stability of out-of-sample performance in $\mathscr{P}_1$–$\mathscr{P}_5$ easily, we draw the scatter diagram for each optimization problem at $\eta = 0.5$. For the convenience of comparison, we give the following graphical design. First, $\mathscr{P}_1$, $\mathscr{P}_2$, and $\mathscr{P}_3$ share the same coordinate system (see Figure 1), and the diagrams of $\mathscr{P}_2$ and $\mathscr{P}_3$ are identical, so we draw them in one diagram. Second, to give a vivid comparison, we zoom in the coordinate scale and draw the diagrams of $\mathscr{P}_3$ and $\mathscr{P}_4$; see Figure 2. The coordinate scale is further amplified in Figure 3 for the diagrams of $\mathscr{P}_4$ and $\mathscr{P}_5$.

From Figure 1, we can find that the points in (b) are in lower risk positions and more concentrative, which means that the portfolio generated from $\mathscr{P}_2$ (or $\mathscr{P}_3$) has a better risk-controlling ability and more similar performance in 100 groups of out-of-sample data sets. Thus, the well-conditioned and sparse estimator $\widehat{\mathbf{\Sigma}}_w$ helps to stabilize the out-of-sample performance and control the risk better. This is consistent with result (2) from Table 2.

From Figures 2 and 3, we can conclude that penalty items also help to stabilize the out-of-sample performance

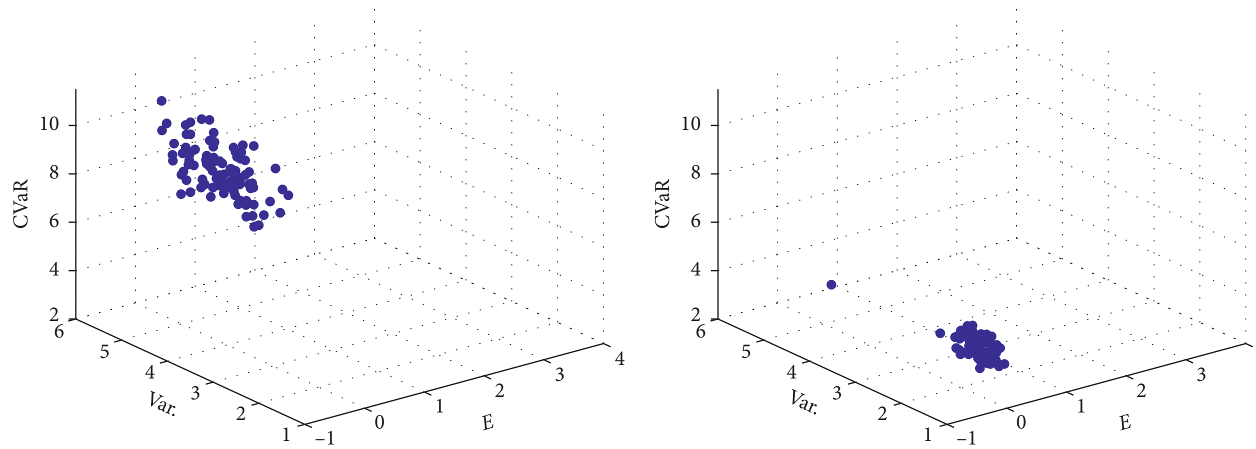

(a) (b)

Figure 1: Out-of-sample performance of $\mathscr{P}_1$–$\mathscr{P}_3$ ($\eta = 0.5$). (a) Performance of $\mathscr{P}_1$; (b) performance of $\mathscr{P}_2$ or $\mathscr{P}_3$.

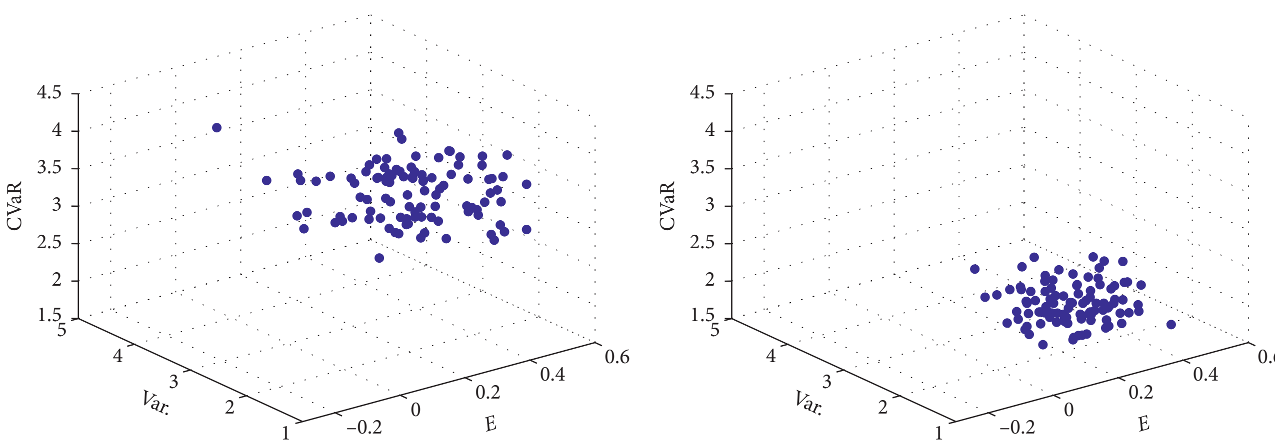

(a) (b)

Figure 2: Out-of-sample performance of $\mathscr{P}_3$–$\mathscr{P}_4$ ($\eta = 0.5$). (a) Performance of $\mathscr{P}_3$; (b) performance of $\mathscr{P}_4$.

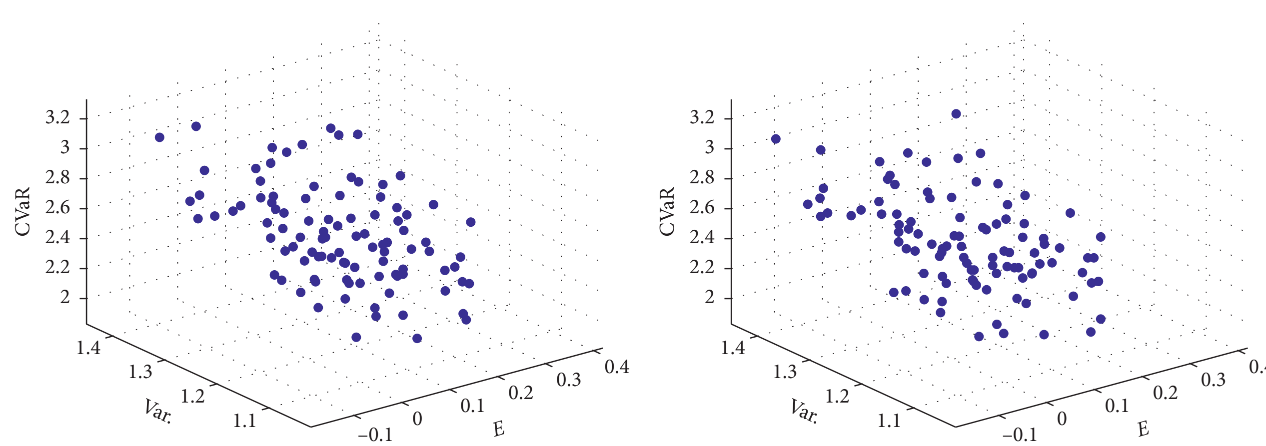

(a) (b)

Figure 3: Out-of-sample performance of $\mathscr{P}_4$–$\mathscr{P}_5$ ($\eta = 0.5$). (a) Performance of $\mathscr{P}_4$; (b) performance of $\mathscr{P}_5$.

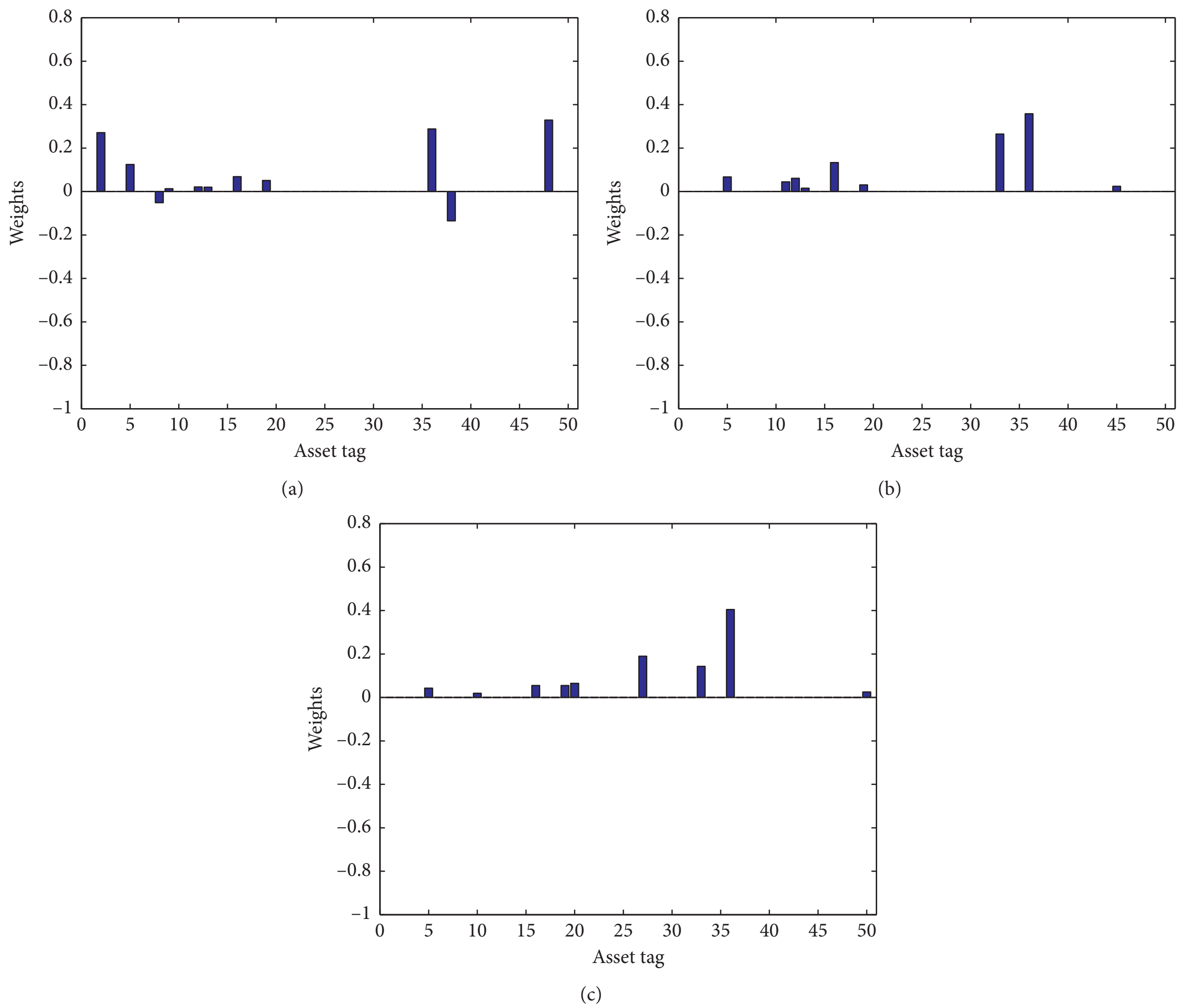

Figure 4: Portfolio strategy of $\mathscr{P}_5$ under different η. (a) Portfolio of $\mathscr{P}_5$ ($\eta = 0$), (b) portfolio of $\mathscr{P}_5$ ($\eta = 0.5$), and (c) portfolio of $\mathscr{P}_5$ ($\eta = 1$).

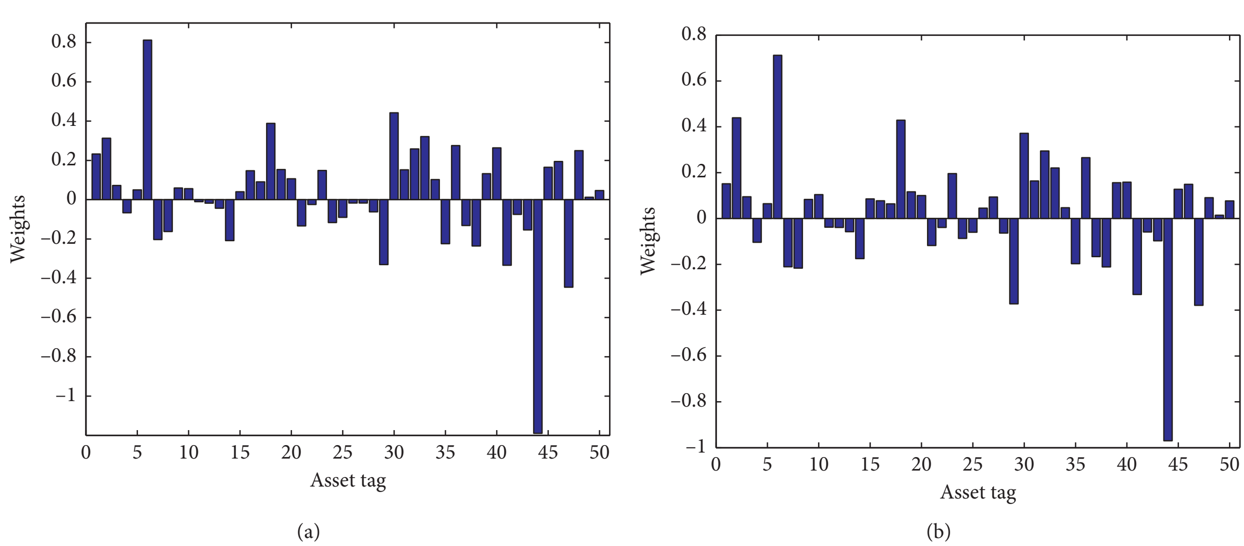

Figure 5: Continued.

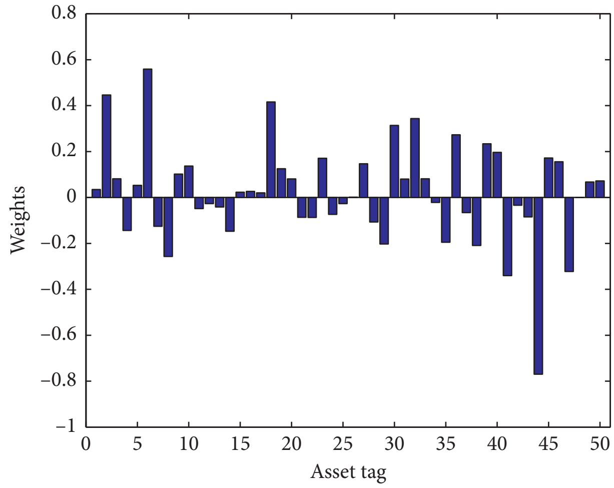

(c)

Figure 5: Portfolio strategy of $\mathscr{P}_1$ under different η. (a) Portfolio of $\mathscr{P}_1$ ($\eta = 0$), (b) portfolio of $\mathscr{P}_1$ ($\eta = 0.5$), and (c) portfolio of $\mathscr{P}_1$ ($\eta = 1$).

Table 3: Out-of-sample performance of portfolios.

	$\eta = 0$		$\eta = 0.5$		$\eta = 1$		EW
	$\mathscr{P}_1$	$\mathscr{P}_5$	$\mathscr{P}_1$	$\mathscr{P}_5$	$\mathscr{P}_1$	$\mathscr{P}_5$	
Variance	3.609	1.674	3.326	1.937	3.158	1.986	2.787
CVaR	3.836	2.998	3.998	3.210	3.827	3.187	3.985
Avg return	0.006	0.061	−0.059	0.075	−0.065	0.0380	0.017

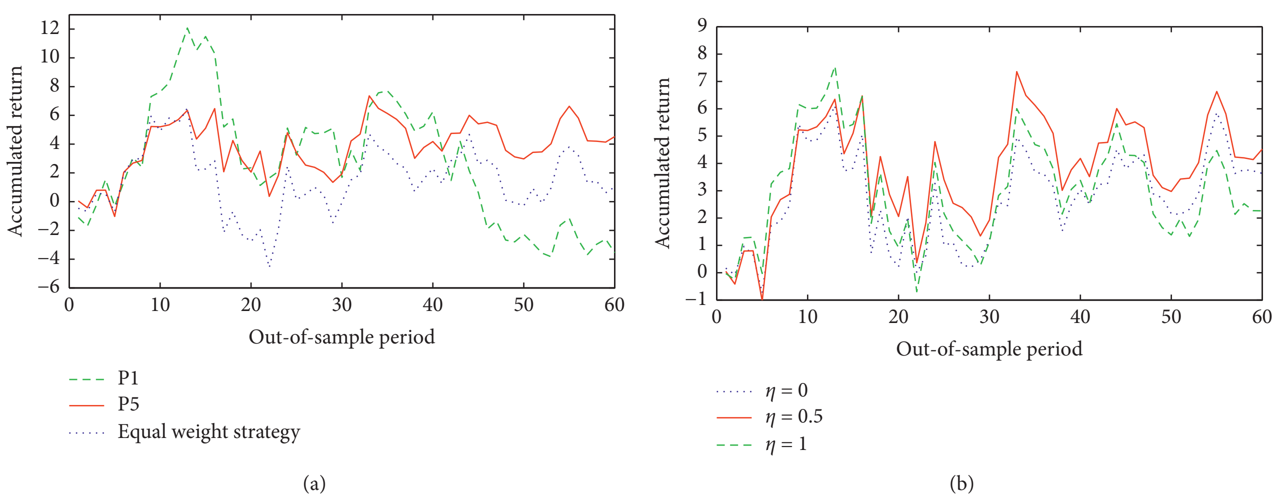

Figure 6: Accumulated return in out-of-sample period. (a) Different model with $\eta = 0.5$. (b) Model $\mathscr{P}_5$ with different η.

significantly and the reweighted L_1 norm penalty performs a little bit better than SCAD penalty under our settings. This is consistent with results (4) and (5) from Table 2.

5. Empirical Study

Suppose that an investor intends to track a stock index in a financial market allowing short selling. Through the Joinquant Data platform, we select daily data of the constituent stocks in Shanghai Stock Exchange 50 (SSE 50) Index from Jun 11, 2018, to Dec 11, 2018. The reason why we choose data in a period of half a year elaborates as follows. The constituent stocks in SSE 50 change every half year or so, and keeping them as a group in an index apparently influences the dependency structure of assets, which further affects the optimal investment strategy. Therefore, when an investor intends to track SSE 50, it is reasonable to get the data in which the same 50 stocks always stay in SSE 50.

Then, we tag the 50 stocks from No. 1 to No. 50. After calculating, we obtain 124 observations of daily logarithm yield return, including 64 in-sample data spanning from Jun 11, 2018, to Sept 10, 2018, and 60 out-of-sample data spanning from Sept 11, 2018, to Dec 11, 2018. Here, we can find that the dimensionality of in-sample data meets the requirement of high-dimensional scenarios because $p = 50$ and $n = 64$ are comparable.

Since $\mathscr{P}_5$ outperforms $\mathscr{P}_1$–$\mathscr{P}_4$ from Section 4, we calculate the optimal portfolios based on $\mathscr{P}_5$ in formula (13) and show the results in Figure 4. The parameter η is supposed to be 0, 0.5, and 1, respectively, and the target return μ_0 is set to be the average value of the return data of 50 stocks. Considering the idea in this paper is illuminated by the pioneering work of Roman et al. [12], we further conduct the corresponding analysis from $\mathscr{P}_1$ for comparison and the results are shown in Figure 5. It can be easily found that portfolios from $\mathscr{P}_5$ are much more sparse and can avoid extreme investment action, which will be more applicable to the practice of finance.

Next, we observe the out-of-sample performance of the portfolios. There is evidence that equal weight (EW) strategy cannot be defeated by many portfolio methods consistently (DeMiguel et al. [17]). We also add EW strategy into comparison here. The variance, $\mathrm{CVaR}_{0.95}$, and average return of the portfolios are calculated, respectively; see Table 3. The accumulated returns of the portfolios in out-of-sample period are displayed in Figure 6.

From Table 3 and Figure 6(a), we can conclude that the portfolio generated from $\mathscr{P}_5$ has the highest terminal return and can control the risk robustly over the period, since it has a relatively slight fluctuation and avoids extreme losses and outperforms the EW strategy basically. However, the portfolio generated from $\mathscr{P}_1$ is unstable even compared with EW strategy and ends up with the lowest return in spite of being dominate at the beginning. Figure 6(b) also tells us that $\eta = 0.5$ in $\mathscr{P}_5$ will have a more promising terminal return compared with the case only considering CVaR ($\eta = 0$) or variance ($\eta = 1$).

6. Conclusion

In this paper, we have constructed five progressive optimization problems to figure out a relatively better way to conduct mean-variance-CVaR portfolio selection model in high-dimension scenarios. Specifically, two covariance matrix estimators (classical estimator and well-conditioned and sparse estimator), two estimation methods for CVaR (Rockafellar–Uryasev's approximation and quantile regression), and two penalty functions (SCAD and reweighted L_1 norm) have been considered and different combinations of them have been used for the formulation of optimization problems. The data for simulation is generated from a hybrid distribution with multivariate normal distribution and exponential distribution. Moreover, the correlation matrix and mean vector of the multivariate normal distribution are estimated from real data. The simulation studies show that the well-conditioned and sparse estimator and penalty item devote to alleviate poor out-of-sample performance significantly and the reweighted L_1 norm penalty has a slight superiority. Additionally, we find that the classical optimization methods for mean-variance-CVaR model in Roman et al. [12] may result in poor out-of-sample performance under high-dimension scenarios. An empirical study has been conducted based on the data of constituent stocks in SSE 50. The results solidify the foregoing findings. Therefore, we suggest to combine well-conditioned and sparse covariance estimator, quantile regression computational method for CVaR, and reweighted L_1 norm for portfolio optimization under mean-variance-CVaR criterion, since the fragile out-of-sample performance could be effectively mitigated.

The study in this paper focuses on the high-dimensional setting, where n is just a little bit greater than p. An extension of this study under a more extremely high-dimensional scenario in which $p > n$ would also be interesting. Moreover, it is noteworthy to further stabilize the out-of-sample performance by controlling the fragile brought by mean item. We will explore these problems in the following study.

Data Availability

The data used to support the findings of this study are available from the corresponding author upon request.

Conflicts of Interest

The authors declare that they have no conflicts of interest.

Acknowledgments

This work was partially supported by National Natural Science Foundation of China under Grant nos. 71671104 and 11971301, Key Project of National Social Science of China under Grant no. 16AZD019, and Incubation Group Project of Financial Statistics and Risk Management of SDUFE.

References

[1] H. Markowitz, "Portfolio selection," *The Journal of Finance*, vol. 7, no. 1, pp. 77–91, 1952.

[2] P. N. Kolm, R. Tütüncü, and F. J. Fabozzi, "60 years of portfolio optimization: practical challenges and current trends," *European Journal of Operational Research*, vol. 234, no. 2, pp. 356–371, 2014.

[3] H. Konno and H. Yamazaki, "Mean-absolute deviation portfolio optimization model and its applications to tokyo stock market," *Management Science*, vol. 37, no. 5, pp. 519–531, 1991.

[4] W. Ogryczak and A. Ruszczyński, "From stochastic dominance to mean-risk models: semideviations as risk measures," *European Journal of Operational Research*, vol. 116, no. 1, pp. 33–50, 1999.

[5] G. Consigli, "Tail estimation and mean-VaR portfolio selection in markets subject to financial instability," *Journal of Banking & Finance*, vol. 26, no. 7, pp. 1355–1382, 2002.

[6] G. J. Alexander and A. M. Baptista, "Economic implications of using a mean-var model for portfolio selection: a comparison

with mean-variance analysis," *Journal of Economic Dynamics and Control*, vol. 26, no. 7-8, pp. 1159–1193, 2002.
[7] Q. Xu, Y. Zhou, C. Jiang, K. Yu, and X. Niu, "A large CVaR-based portfolio selection model with weight constraints," *Economic Modelling*, vol. 59, pp. 436–447, 2016.
[8] A. G. Quaranta and A. Zaffaroni, "Robust optimization of conditional value at risk and portfolio selection," *Journal of Banking & Finance*, vol. 32, no. 10, pp. 2046–2056, 2008.
[9] H. Konno, H. Shirakawa, and H. Yamazaki, "A mean-absolute deviation-skewness portfolio optimization model," *Annals of Operations Research*, vol. 45, no. 1, pp. 205–220, 1993.
[10] H. Konno and K.-i. Suzuki, "A mean-variance-skewness portfolio optimization model," *Journal of the Operations Research Society of Japan*, vol. 38, no. 2, pp. 173–187, 1995.
[11] C. S. Robert and A. H. Philip, "On the direction of preference for moments of higher order than the variance," *The Journal of Finance*, vol. 35, no. 4, pp. 915–919, 1980.
[12] D. Roman, K. Darby-Dowman, and G. Mitra, "Mean-risk models using two risk measures: a multi-objective approach," *Quantitative Finance*, vol. 7, no. 4, pp. 443–458, 2007.
[13] J. Gao, Y. Xiong, and D. Li, "Dynamic mean-risk portfolio selection with multiple risk measures in continuous-time," *European Journal of Operational Research*, vol. 249, no. 2, pp. 647–656, 2016.
[14] Y. Shi, X. Zhao, and X. Yan, "Optimal asset allocation for a mean-variance-CVaR insurer under regulatory constraints," *American Journal of Industrial and Business Management*, vol. 09, no. 07, pp. 1568–1580, 2019.
[15] R. C. Green and B. Hollifield, "When will mean-variance efficient portfolios be well diversified?" *The Journal of Finance*, vol. 47, no. 5, pp. 1785–1809, 1992.
[16] V. K. Chopra and W. T. Ziemba, "The effect of errors in means, variances, and covariances on optimal portfolio choice," *The Journal of Portfolio Management*, vol. 19, no. 2, pp. 6–11, 1993.
[17] V. DeMiguel, L. Garlappi, and R. Uppal, "Optimal versus naive diversification: how inefficient is the 1/NPortfolio strategy?" *Review of Financial Studies*, vol. 22, no. 5, pp. 1915–1953, 2009.
[18] R. Tibshirani, "Regression shrinkage and selection via the lasso," *Journal of the Royal Statistical Society: Series B (Methodological)*, vol. 58, no. 1, pp. 267–288, 1996.
[19] P. J. Bickel and E. Levina, "Covariance regularization by thresholding," *The Annals of Statistics*, vol. 36, no. 6, pp. 2577–2604, 2008.
[20] T. T. Cai, M. Yuan, D. Giannone, and I. Loris, "Adaptive covariance matrix estimation through block thresholding," *The Annals of Statistics*, vol. 40, no. 4, pp. 2014–2042, 2012.
[21] A. J. Rothman, "Positive definite estimators of large covariance matrices," *Biometrika*, vol. 99, no. 3, pp. 733–740, 2012.
[22] O. Ledoit and M. Wolf, "A well-conditioned estimator for large-dimensional covariance matrices," *Journal of Multivariate Analysis*, vol. 88, no. 2, pp. 365–411, 2004.
[23] A. Maurya, "A well conditioned and sparse estimate of covariance and inverse covariance matrix using a joint penalty," *The Journal of Machine Learning Research*, vol. 17, no. 130, pp. 1–28, 2016.
[24] J. Friedman, T. Hastie, and R. Tibshirani, "Sparse inverse covariance estimation with the graphical lasso," *Biostatistics*, vol. 9, no. 3, pp. 432–441, 2008.
[25] R. T. Rockafellar and S. Uryasev, "Conditional Value-at-Risk for general loss distributions," *Journal of Banking & Finance*, vol. 26, no. 7, pp. 1443–1471, 2002.
[26] R. T. Rockafellar and S. Uryasev, "Optimization of conditional value-at-risk," *The Journal of Risk*, vol. 2, no. 3, pp. 21–41, 2000.
[27] G. W. Bassett, R. Koenker, and G. Kordas, "Pessimistic portfolio allocation and Choquet expected utility," *Journal of Financial Econometrics*, vol. 2, no. 4, pp. 477–492, 2004.
[28] A. E. B. Lim, J. G. Shanthikumar, and G.-Y. Vahn, "Conditional value-at-risk in portfolio optimization: coherent but fragile," *Operations Research Letters*, vol. 39, no. 3, pp. 163–171, 2011.
[29] A. Takeda and T. Kanamori, "A robust approach based on conditional value-at-risk measure to statistical learning problems," *European Journal of Operational Research*, vol. 198, no. 1, pp. 287–296, 2009.
[30] I. Kondor, S. Pafka, and G. Nagy, "Noise sensitivity of portfolio selection under various risk measures," *Journal of Banking & Finance*, vol. 31, no. 5, pp. 1545–1573, 2007.
[31] J. J. Gao and W. P. Wu, "Sparse and multiple risk measures approach for data driven mean-CVaR portfolio optimization model," in *Optimization and Control for Systems in the Big-Data Era: Theory and Applications*, Springer, Berlin, Germany, 2017.
[32] J. Brodie, I. Daubechies, C. De Mol, D. Giannone, and I. Loris, "Sparse and stable Markowitz portfolios," *Proceedings of the National Academy of Sciences*, vol. 106, no. 30, pp. 12267–12272, 2009.
[33] J.-Y. Gotoh and A. Takeda, "On the role of norm constraints in portfolio selection," *Computational Management Science*, vol. 8, no. 4, pp. 323–353, 2011.
[34] B. Fastrich, S. Paterlini, and P. Winker, "Constructing optimal sparse portfolios using regularization methods," *Computational Management Science*, vol. 12, no. 3, pp. 417–434, 2015.
[35] P. Artzner, F. Delbaen, J.-M. Eber, and D. Heath, "Coherent measures of risk," *Mathematical Finance*, vol. 9, no. 3, pp. 203–228, 1999.
[36] J. Fan, J. Zhang, and K. Yu, "Vast portfolio selection with gross-exposure constraints," *Journal of the American Statistical Association*, vol. 107, no. 498, pp. 592–606, 2012.
[37] J. C. Emmanuel, B. W. Michael, and P. B. Stephen, "Enhancing sparsity by reweighted l1 minimization," *Journal of Fourier Analysis and Applications*, vol. 14, pp. 877–905, 2008.
[38] E. R. Lee, H. Noh, and B. U. Park, "Model selection via Bayesian information criterion for quantile regression models," *Journal of the American Statistical Association*, vol. 109, no. 505, pp. 216–229, 2014.
[39] L. Wang, Y. Kim, and R. Li, "Calibrating nonconvex penalized regression in ultra-high dimension," *The Annals of Statistics*, vol. 41, no. 5, pp. 2505–2536, 2013.
[40] Y. C. Wu and Y. F. Liu, "Variable selection in quantile regression," *Statistica Sinica*, vol. 19, pp. 801–817, 2009.

Hindawi
Mathematical Problems in Engineering
Volume 2020, Article ID 1835146, 14 pages
https://doi.org/10.1155/2020/1835146

Research Article

Stock Return Uncertainty and Life Insurance

Yang Dong, Hao Wang, and Lihong Zhang

Tsinghua University, School of Economics and Management, Beijing, China

Correspondence should be addressed to Yang Dong; dongy.17@sem.tsinghua.edu.cn

Received 3 June 2020; Accepted 19 June 2020; Published 10 July 2020

Guest Editor: Wenguang Yu

Knightian uncertainty embedded in stock returns causes rising demand for life insurance, as the uncertainty averse agent seeks alternative investment channels. Life insurance demand of middle-aged agent is more sensitive to the uncertainty. Stock return uncertainty reduces the agent's total wealth and subsequently the propensity of wealthy agent serving as an insurance seller. Rising demand and falling supply of life insurance imply that life insurance is more expensive in the presence of stock return uncertainty. Sensitivity of life insurance demand to the mortality rate and key stock return characteristics also changes with the uncertainty.

1. Introduction

Insurance market and stock market are closely connected in many ways [1–4]. Rational expectations models have been extensively used to study portfolio allocation and life insurance in equilibrium. These models assume that the agent possesses perfect knowledge about the probability law governing the stochastic asset return process. However, the true model is rarely known, so any specified probability law is subject to potential misspecification. Knightian uncertainty (henceforth, uncertainty) arises in the situation where the agent cannot develop a probability distribution to describe potential return misspecification. Stock returns are difficult to forecast [5–7] and are prone to such uncertainty. We in the paper formulate a continuous-time rational expectations model to examine the effects of stock return uncertainty on life insurance. The model admits uncertainty aversion as the agent suspects that stock return in the stochastic process is potentially misspecified. Following Hansen and Sargent [8], Anderson et al. [9], Uppal and Wang [10], and Maenhout [6], we impose an uncertainty penalty to the agent's objective function in reflecting his skeptical and conservative perspective. These years, many studies apply the model uncertainty to different models, for example, the stochastic interest rate [11], the insurer with reinsurance and investment problem [12], and the uncertainty about jump and diffusion risk [13].

We find that optimal insurance demand increases with the level of uncertainty. The agent shifts some of his investment in the stock to life insurance, confirming that the insurance market and the stock market, to some degree, substitute each other. Life insurance is used as a way to circumvent the uncertainty embedded in the stock. This effect is more prominent for the middle-aged agent. Younger agent's demand for life insurance is low in the first place. Elder agent consumes more, repressing demand for life insurance when it is close to the end of his financial planning horizon. As a result, the demand of younger and elder agents for life insurance is less sensitive to stock return uncertainty.

When the agent is endowed with a sufficiently high level of initial wealth, he optimally supplies insurance [14]. By reducing the agent's total wealth, stock return uncertainty decreases the propensity of wealthy agent serving as an insurance seller. The agent would act more conservatively in the insurance market facing stock return uncertainty. Agents would demand more insurance when the supply of insurance falls, implying that insurance premium would increase in equilibrium. We leave it to future research to develop an equilibrium model to explore such implications rigorously.

The sensitivity of insurance demand with respect to the mortality rate may change in the presence of stock return uncertainty. In the absence of uncertainty, an increase in the mortality rate leads to lower insurance demand. However, facing stock return uncertainty, the agent might demand more for insurance as the mortality rate increases. The rationale is that the mortality rate plays two roles in insurance decision making. On the one hand, it adversely affects the insurance payout ratio, so a higher mortality rate reduces the utility brought by life insurance. On the other hand, the mortality rate affects the probability of the agent obtaining life insurance payment within the financial planning horizon; thereby, the agent with a higher mortality rate is more willing to buy life insurance because there is a greater chance to receive the payment. When stock return uncertainty is low, the first effect dominates, while when the uncertainty is sufficiently high, the second effect is more prominent.

Our discoveries echo the phenomena found in empirical research, especially on the relationship between the stock market and the insurance market. Jawadi et al. [15] find a positive significant long-term relationship between insurance premium and stock price. Lamm-Tennant and Weiss [16] reveal that the insurance premium is significantly and negatively correlated to the stock index. Our findings are supportive of the supplementary relationship between the two markets. Uncertainty about stock returns reduces the stock market's attractiveness and boosts the relative competitiveness of insurance products.

Our work contributes uniquely to the life insurance literature [17–20]. Several works are closely related to ours. Among them, Merton [21] first models the dynamic asset price process and derives Hamilton–Jacobi–Bellman (HJB) equation to solve for optimal controls. Richard [14] combines life insurance and the rational expectations model developed by Merton [21] to investigate the optimal insurance demand problem. Pliska and Ye [22] study life insurance in a setting where the agent's lifetime is unbounded. Kwak and Lim [23], Huang et al. [24], and Pirvu and Zhang [25] examine inflation, stochastic labor income, and mean-reverting Sharpe ratio, respectively, under the Richard [14] framework. Recently, Huang et al. [26] considered stochastic mortality rate. Our work for the first time investigates the externality of stock return uncertainty on life insurance. Methodologically, modeling the dynamic wealth process illustrates age-dependent and wealth-path-contingent decision rules.

The remainder of the paper is organized as follows: Section 2 presents the model. Section 3 solves the general utility model and the CRRA utility model. Section 4 carries out the numerical analysis. Section 5 concludes the paper.

2. Model

This section introduces our model. It first describes the economy, followed by stock return uncertainty and the agent's objective function that admits stock return uncertainty.

2.1. Economy. Consider a simple continuous-time rational expectations model as in Merton [21], which involves one risk-free asset $R(t)$ and one stock $S(t)$. Let $T > 0$ be a finite financial planning horizon, and let $(\Omega, \mathcal{F}, P)$ be the probability space with information filtration $\{\mathcal{F}(t)\}_{t\in[0,T]}$. The prices of the two assets have the following processes:

$$\frac{\mathrm{d}R(t)}{R(t)} = r\,\mathrm{d}t, \tag{1}$$

$$\frac{\mathrm{d}S(t)}{S(t)} = \alpha\,\mathrm{d}t + \sigma\,\mathrm{d}z, \tag{2}$$

where α, σ, and r are constants, $\sigma > 0$, and $\alpha > r > 0$. Let $C(t)$ be the consumption rate at time t and $\omega(t)$ the fraction of wealth invested in the stock at time t, respectively. It is assumed that the consumption rate process $C(t)$ is nonnegative and $\mathcal{F}(t)$-progressively measurable, satisfying

$$\int_0^T C(t)\mathrm{d}t < \infty, \text{ almost surely (a.s.)}, \tag{3}$$

and, $\omega(t)$ is $\mathcal{F}(t)$-adapted, satisfying

$$\int_0^T \omega^2(t)\mathrm{d}t < \infty, \text{ (a.s.)}. \tag{4}$$

$\omega(t)$ can be negative without short-selling constraint.

Life insurance provides a lump sum payment when the agent deceases. Following Richard [14], we assume that the decease time is a nonnegative random variable τ independent of $z(t)$. Its distribution function and probability density function are given by

$$\begin{aligned} F(t) &= \Pr(\tau < t) = \int_0^t f(u)\mathrm{d}u, \\ f(t) &\geq 0, \quad \forall t \in [0, T]. \end{aligned} \tag{5}$$

We do not require $\int_0^T f(t)\mathrm{d}t = 1$, as the agent may still be alive at the end of the financial planning horizon. Let $\overline{F}(t)$ be the survival function at time t, so

$$\overline{F}(t) = \Pr(\tau \geq t) = 1 - F(t). \tag{6}$$

Based on the above expressions, the mortality rate is given by

$$\lambda(t) = \lim_{\Delta t \longrightarrow 0} \frac{\Pr(t \leq \tau < t + \Delta t \mid \tau \geq t)}{\Delta t} = \frac{f(t)}{\overline{F}(t)}. \tag{7}$$

Rewrite the mortality rate $\lambda(t)$ and $f(t)$ as

$$\begin{aligned} \lambda(t) &= -\frac{\mathrm{d}\ln\overline{F}(t)}{\mathrm{d}t}; \\ f(t) &= \lambda(t)\overline{F}(t) = \lambda(t)\exp\left[-\int_0^t \lambda(u)\mathrm{d}u\right]. \end{aligned} \tag{8}$$

The life insurance premium $P(t)$ is paid continuously. In return, when the agent deceases at t, the life insurance pays a lump sum amount of $P(t)/\mu(t)$, where $\mu(t)$ is a continuous and deterministic function of premium-insurance ratio. We assume $\mu(t) = \lambda(t) + \eta(t)$, where $\eta(t)$ represents the security loading.

2.2. Stock Return Uncertainty. Expected stock returns are difficult to estimate [6, 7], so the agent worries that α in equation (2) is potentially misspecified. Uncertainty arises as he cannot come up with a probability to describe such potential misspecification. To solve the problem, the agent considers a set of alternative models with probability measures P^Q, which are equivalent to the reference measure P^R. As in Anderson et al. [9] and Hansen and Sargent [8], the uncertainty averse agent optimizes his utility based on the worst-case alternative model. According to Girsanov's theorem, the relative entropy between P^Q and P^R is defined as

$$\frac{\mathrm{d}P^Q}{\mathrm{d}P^R} = \Gamma(t), \tag{9}$$

where

$$\Gamma(t) = \exp\left[-\int_0^t \frac{1}{\sigma}u(t)\mathrm{d}z - \frac{1}{2}\int_0^t \frac{1}{\sigma^2}u^2(t)\mathrm{d}s\right]. \tag{10}$$

Under Novikov's condition,

$$\mathbb{E}^P\left[\exp\left(\frac{1}{2}\int_0^T \frac{1}{\sigma^2}u^2(t)\mathrm{d}s\right)\right] < \infty. \tag{11}$$

$\Gamma(t)$ is the Radon–Nikodym derivative of P^Q with respect to P^R. Uncertainty aversion introduces an adjustment $u(t)$ to the expected stock return. In the alternative model, the stock price process follows

$$\frac{\mathrm{d}S(t)}{S(t)} = (\alpha - u(t))\mathrm{d}t + \sigma\,\mathrm{d}\tilde{z}. \tag{12}$$

The agent also receives labor income $y(t)$ during the time interval $[0, \min\{T,\tau\}]$. In decision making, the agent simultaneously chooses the fraction of wealth $\omega(t)$ invested in the risky asset, the consumption rate $C(t)$, and the amount of life insurance premium $P(t)$ at time t. His wealth process on $[0, \min\{T,\tau\}]$ satisfies

$$\begin{aligned}\mathrm{d}W_t &= (y(t) - C(t) - P(t))\mathrm{d}t\\ &\quad + \left(W_t\omega(t)(\alpha - u(t) - r) + W_t r\right)\mathrm{d}t\\ &\quad + W_t\omega(t)\sigma\,\mathrm{d}\tilde{z}.\end{aligned} \tag{13}$$

2.3. Objective Function. The agent's utility consists of two parts: utility $U(C(t),t)$ from consumption and bequest utility $B(Z(t),t)$ from legacy, where $Z(t)$ denotes the legacy left for future generations:

$$Z(t) = W_t + \frac{P(t)}{\mu(t)}. \tag{14}$$

The uncertainty averse agent optimizes his utility based on the worse-case alternative model by solving the following Max-Min problem:

$$\sup_{\{C,P,\omega\}}\inf_u \mathbb{E}\left[\int_0^T U(C(s),s)\mathrm{d}s + B(Z(T),T) + \int_0^T \frac{\phi(s)}{2\sigma^2}u^2(s)\mathrm{d}s\right]. \tag{15}$$

The third term of equation (15) is the uncertainty penalty function:

$$\Lambda(t) = \frac{\phi(t)}{2\sigma^2}u^2(t), \tag{16}$$

where $\phi(t)$ is a normalization function to transform the penalty function into the units of utility and $u(t)$ measures the "distance" between P^R and P^Q as the adjustment to α. $u^2(t)/2\sigma^2$ is the corresponding relative entropy. The selection of the special form of $\phi(t)$ should fulfill two purposes: reflecting agent's degree of uncertainty aversion and measuring the level of uncertainty, which can also be regarded as the agent's lack of confidence in the reference model. A larger $\phi(t)$ means the deviation of an alternative model from the reference model would be more heavily penalized, which means the agent highly trusts the reference model [10].

In the presence of stock return uncertainty, the agent's utility function is

$$\begin{aligned}&J(W,t;\omega,C,P,u)\\ &= \mathbb{E}_{t,W}\left[\int_t^{T\wedge\tau}\left(U(C(s),s) + \frac{\phi(s)}{2\sigma^2}u^2(s)\right)\mathrm{d}s + B(Z(\tau),\tau)\mathbb{I}(\tau\le T) + L(W_T,T)\mathbb{I}(\tau\ge T)\right]\\ &= \mathbb{E}_{t,W}\left[\int_t^T f(s,t)B(Z(s),s) + \overline{F}(s,t)\left(U(C(s),s) + \frac{\phi(s)}{2\sigma^2}u^2(s)\right)\mathrm{d}s + \overline{F}(T,t)L(W_T,T)\right],\end{aligned} \tag{17}$$

where $\mathbb{E}_{t,W}[\cdot]$ denotes the conditional expectation operator under the probability measure P^R; $T\wedge\tau = \min\{\tau,T\}$. $L(W_T,T)$ represents terminal wealth at time T if the agent survives beyond the time. $U(C(t),t)$ and $L(W_T,T)$ have the same functional form with respect to $C(t)$ and W_T, respectively. $f(s,t) = f(s)/\overline{F}(t)$ is the probability density function of the agent's decease at time s conditional on his survival at time t; $\overline{F}(s,t) = \overline{F}(s)/\overline{F}(t)$ is the agent's survival probability at time s conditional on his survival at time t; and $\mathbb{I}(\tau\le T)$ is an indicator function as

$$\mathbb{I}(\tau\le T) = \begin{cases}1, & \tau\le T,\\ 0, & \text{otherwise}.\end{cases} \tag{18}$$

Substituting equations (7) and (8) into (17) yields

$$J(W,t;\omega,C,P,u)=\int_t^T \lambda(s)e^{-\int_t^s \lambda(v)\mathrm{d}v}B(Z(s),s)+e^{-\int_t^s \lambda(v)\mathrm{d}v}\left[U(C(s),s)+\frac{\phi(s)}{2\sigma^2}u^2(s)\right]\mathrm{d}s+e^{-\int_t^T \lambda(v)\mathrm{d}v}L(W_T,T). \tag{19}$$

Let $\mathscr{A}=\{C(t),P(t),\omega(t)\}$; that is, $\mathscr{A}$ is the admissible set of consumption, insurance premium payment, and asset allocation controls. The objective of the agent is to choose the optimal control set $\mathscr{A}^*=\{C^*(t),P^*(t),\omega^*(t)\}$ to maximize the utility function in equation (19) based on the worst case of uncertainty-induced adjustment $u^*(t)$. Thus, the value function of this problem is

$$\begin{aligned}&V(W,t)=\sup_{\{C,P,\omega\}\in\mathscr{A}}\inf_u J(W,t;\omega,C,P,u)=J\left(t,W;\omega^*,C^*,P^*,u^*\right),\\&\text{subject to}\\&\mathrm{d}W_t=(y(t)-C(t)-P(t))\mathrm{d}t+\left(W_t\omega(t)(\alpha-u(t)-r)+W_tr\right)\mathrm{d}t+W_t\omega(t)\sigma\mathrm{d}\tilde{z};\\&Z(t)=W_t+\frac{P(t)}{\mu(t)}.\end{aligned} \tag{20}$$

3. Solutions

This section presents the solutions to the model with general utility and then the solutions to the CRRA utility model.

3.1. General Utility. We use the dynamic programming method to obtain the Hamilton–Jacobi–Bellman (HJB) equation. According to the optimality principle, the value function in equation (20) is expressed as

$$V(W,t)=\sup_{\{C,P,\omega\}\in\mathscr{A}}\inf_u \mathbb{E}_{t,W}\left[\int_t^{t+\Delta t} f(s,t)B(Z(s),s)+\overline{F}(s,t)\left(U(C(s),s)+\frac{\phi(s)}{2\sigma^2}u^2(s)\right)\mathrm{d}s+e^{-\int_t^{t+\Delta t}\lambda(v)\mathrm{d}v}V\left(W_{t+\Delta t},t+\Delta t\right)\right], \tag{21}$$

where $\Delta t\longrightarrow 0$ is the instantaneous moment. We have the following approximate relationship:

$$e^{-\int_t^{t+\Delta t}\lambda(v)\mathrm{d}v}=1-\lambda(t)\Delta t+o\left(\Delta t^2\right), \tag{22}$$

where $o(\Delta t^2)$ represents the higher-order infinitesimal of Δt. The relationship between $V(W_t,t)$ and $V(W_{t+\Delta t},t+\Delta t,)$ follows that

$$V\left(W_{t+\Delta t},t+\Delta t,\right)=V(W,t)+\mathscr{L}[V(W,t)]\Delta t, \tag{23}$$

where $\mathscr{L}[V(W,t)]=[\lim_{\Delta t\longrightarrow 0}V(W_{t+\Delta t},t+\Delta t,)-V(W,t)]/\Delta t$, which is also called the Dynkin operator. We substitute equations (22) and (23) into (21). Note $f(t,t)=\lambda(t)$ and $\overline{F}(t,t)=1$. Dividing both sides of the equation by Δt, we obtain

$$\begin{aligned}0=&\sup_{\{C,P,\omega\}\in\mathscr{A}}\inf_u \mathscr{L}[V(W,t)]-\lambda(t)V(W,t)\\&+\lambda(t)B(Z(t),t)+U(C(t),t)+\frac{\phi(t)}{2\sigma^2}u^2(t).\end{aligned} \tag{24}$$

By Ito's lemma, the Dynkin operator follows that

$$\begin{aligned}\mathscr{L}[V(W,t)]=&V_t+V_W[-C(t)-P(t)+y(t)\\&+W_t\omega(t)(\alpha-u(t)-r)+W_tr]\\&+\frac{1}{2}V_{WW}W_t^2\omega^2(t)\sigma^2,\end{aligned} \tag{25}$$

where V_t and V_W represent the first-order partial derivatives of $V(W,t)$ with respect to t and W, respectively. V_{WW} represents the second-order partial derivative of $V(W,t)$ with respect to W. Then, the HJB equation changes into

$$\begin{aligned}0=&\sup_{\{C,P,\omega\}\in\mathscr{A}}\inf_u -\lambda(t)V(W,t)+\lambda(t)B(Z(t),t)\\&+U(C(t),t)+V_t+V_W[-C(t)-P(t)+y(t)\\&+W_t\omega(\alpha-u-r)+W_tr]+\frac{1}{2}V_{WW}W_t^2\omega^2\sigma^2+\frac{\phi(t)}{2\sigma^2}u^2(t),\end{aligned} \tag{26}$$

with the boundary condition $V(W_T, T) = L(W_T, T)$. The last item of equation (26) is the uncertainty penalty function $\Lambda(t)$ in equation (16).

We first solve the minimization part of equation (26). Take the first-order condition with respect to $u(t)$ and obtain the worst-case uncertainty adjustment $u^*(t)$ as

$$-V_W W_t \omega + \frac{\phi(t)}{\sigma^2} u^*(t) = 0,$$
$$u^*(t) = \frac{1}{\phi(t)} V_W W_t \omega \sigma^2. \quad (27)$$

Substitute $u^*(t)$ back into equation (26) and take the first-order conditions with respect to $C(t), Z(t)$, and $\omega(t)$, respectively; we drive the optimal controls.

Proposition 1. *For an uncertainty averse agent with a general utility $U(C(t), t)$ and a bequest function $B(Z(t), t)$, the optimal controls are*

$$U_C(C^*(t), t) = V_W; \quad (28)$$

$$\frac{\lambda(t)}{\mu(t)} B_Z(Z^*(t), t) = V_W; \quad (29)$$

$$\omega^*(t) = \frac{V_W(\alpha - r)}{(1/\phi(t)) V_W^2 W_t - V_{WW} W_t \sigma^2}. \quad (30)$$

The optimal insurance demand $P^*(t)$ can be obtained with equations (14) and (29). The marginal ratio of consumption utility to bequest utility satisfies

$$\frac{U_C(C^*(t), t)}{B_Z(Z^*(t), t)} = \frac{\lambda(t)}{\mu(t)}. \quad (31)$$

The agent balances the optimal consumption $C^*(t)$ and optimal insurance demand $P^*(t)$ till $C^*(t)$ and the corresponding legacy $Z^*(t) = W_t + (P^*(t)/\mu(t))$ generate the same marginal utility of $\lambda(t)/\mu(t)$. The next section discusses the special case of CRRA utility, under which explicit optimal controls can be derived.

3.2. CRRA Utility. When the agent has a CRRA utility function, $U(C(t), t) = (e^{-\rho t}/\gamma) C^\gamma(t)$; $B(Z(t), t) = (e^{-\rho t}/\gamma) Z^\gamma(t)$; and $L(W_T, T) = (e^{-\rho T}/\gamma) W_T^\gamma$, where $1 - \gamma$ is the risk aversion coefficient, $\gamma < 1$ and $\gamma \neq 0$; ρ is the discount factor and $\rho > 0$. We follow Maenhout [6] to specify the normalization function $\phi(t)$ as

$$\phi(t) = \frac{\gamma}{\theta} V(W_t, t), \quad (32)$$

where θ represents the degree of uncertainty aversion. $\phi(t)$ is decreasing in the degree of uncertainty aversion—when the agent has a high degree of confidence in the reference model (with a small θ), a small deviation from the reference model will lead to a heavy penalty. According to equation (27), the worst-case adjustment $u^*(t)$ in this CRRA utility case is

$$u^*(t) = \frac{\theta}{\gamma V(W_t, t)} V_W W_t \omega \sigma^2. \quad (33)$$

Equation (33) shows that $u^*(t)$ is an increasing function of θ, implying that the more uncertainty averse the agent is, the greater the perceptional adjustment he will make. Substitute equation (33) into (16); we obtain

$$\Lambda(t) = \frac{\gamma u^2(t)}{2\theta\sigma^2} V(W_t, t) = \frac{\theta}{2\gamma V(W_t, t)} V_W^2 W_t^2 \omega^2 \sigma^2. \quad (34)$$

Substitute equations (32) and (33) into (26); we obtain the HJB function as

$$\begin{aligned} 0 = \max_{\{C,P,\omega\}\in\mathscr{A}} & \lambda(t) B(Z(t), t) + U(C(t), t) - \lambda(t) V + V_t \\ & + V_W[-C(t) - P(t) + y(t) + W_t \omega(t)(\alpha - r) + W_t r] \\ & + \frac{1}{2} V_{WW} W_t^2 \sigma^2 \omega^2(t) - \frac{\theta}{2\gamma V(W_t, t)} V_W^2 W_t^2 \omega^2(t) \sigma^2. \end{aligned} \quad (35)$$

We identify and distinguish three types of wealth: the current wealth, the labor wealth, and the total wealth. We will solve the problems above using these definitions. Denote

(i) $W(t)$ as the current wealth—the wealth the agent possesses at time t, whose process is specified in equation (13).

(ii) $b(t)$ as the labor wealth—the present value of the agent's future labor income. The discount rate applied to compute the present value equals the risk-free rate plus the insurance security loading that reflects the insurance market friction. Thus,

$$\begin{aligned} b(t) &= \int_t^{T\wedge\tau} y(s) \exp\left[-\int_t^s r + \eta(v) dv\right] ds \\ &= \int_t^T \overline{F}(s, t) y(s) \exp\left[-\int_t^s r + \eta(v) dv\right] ds \\ &= \int_t^T y(s) \exp\left[-\int_t^s r + \mu(v) dv\right] ds. \end{aligned} \quad (36)$$

(iii) $X(t)$ as the total wealth—the amount of wealth with which the agent uses for decision making. Thus,

$$X(t) = W_t + b(t). \quad (37)$$

At the end of the financial planning horizon, $b(T) = 0$ and $X(T) = W_T$.

The agent's current wealth W_t can be negative, implying that the agent is able to borrow against his future cash flows. However, the total wealth $X(t)$ is always positive as $b(t)$ is always positive, and the amount of borrowing cannot exceed $b(t)$.

We conjecture the objective function as

$$V(W, t) = \frac{e^{-\rho t} a(t)}{\gamma} [W_t + b(t)]^\gamma = \frac{e^{-\rho t} a(t)}{\gamma} X^\gamma(t), \quad (38)$$

where $a(t)$ is a time-varying function that captures the influence of stock return uncertainty. Its functional form is to be determined by the HJB function. Taking the partial derivatives of $V(W, t)$ with respect to W and t, respectively, we obtain

$$\begin{cases} V_W = e^{-\rho t} a(t) X^{\gamma-1}(t); \\ V_{WW} = e^{-\rho t}(\gamma-1) a(t) X^{\gamma-2}(t); \\ V_t = e^{-\rho t} a(t) b'(t) X^{\gamma-1}(t) + \dfrac{1}{\gamma}\left(e^{\rho t} a'(t) - \rho e^{-\rho t} a(t)\right) X^{\gamma}(t), \end{cases} \tag{39}$$

where $a'(t)$ and $b'(t)$ represent the first derivatives of $a(t)$ and $b(t)$ with respect to t, respectively. In particular, according to equation (36),

$$b'(t) = -y(t) + [r + \mu(t)] b(t). \tag{40}$$

Based on the above results, we have the following proposition.

Proposition 2. *For the uncertainty averse agent with CRRA utility* $U(C_t, t) = (e^{-\rho t}/\gamma) C^{\gamma}(t)$ *and bequest function* $B(Z(t), t) = (e^{-\rho t}/\gamma) Z^{\gamma}(t)$, *where* $\gamma < 1$ *and* $\gamma \neq 0$, *the optimal controls are*

$$C^*(t) = \left[\frac{1}{a(t)}\right]^{1/1-\gamma} X(t), \tag{41}$$

$$\omega^*(t) W_t = \frac{\alpha - r}{(\theta - \gamma + 1)\sigma^2} X(t), \tag{42}$$

$$P^*(t) = \mu(t)\left\{\left[\left(\frac{\lambda(t)}{\mu(t) a(t)}\right)^{1/1-\gamma} - 1\right] X(t) + b(t)\right\}. \tag{43}$$

The corresponding legacy is

$$Z^*(t) = W_t + \frac{P^*(t)}{\mu(t)} = \left(\frac{\lambda(t)}{\mu(t) a(t)}\right)^{1/1-\gamma} X(t), \tag{44}$$

where

$$a(t) = \left[e^{\int_t^T H(v)\mathrm{d}v} + \int_t^T K(s) e^{\int_t^s H(v)\mathrm{d}v}\mathrm{d}s\right]^{1-\gamma}, \tag{45}$$

$$H(t) = -\frac{\rho}{1-\gamma} + \frac{\gamma}{1-\gamma}\left[\mu(t) + r + \frac{1}{2}\frac{(\alpha - r)^2}{(\theta - \gamma + 1)\sigma^2}\right] - \frac{\lambda(t)}{1-\gamma}; \tag{46}$$

$$K(t) = 1 + \left(\frac{\lambda(t)}{\mu^{\gamma}(t)}\right)^{1/1-\gamma}. \tag{47}$$

Moreover, $a(t)$ is strictly positive.

Proof. Using $V(W, t)$ in equation (38) and the first-order conditions in Proposition 1, we obtain $C^*(t), \omega^*(t) W_t$, $Z^*(t)$, and $P^*(t)$ as in equations (41)–(43), respectively.

According to equation (33), the worst-case uncertainty adjustment satisfies

$$u^*(t) = \frac{\theta}{\gamma V(W_t, t)} V_W W_t \omega \sigma^2 = \frac{\theta(\alpha - r)}{\theta + 1 - \gamma}. \tag{48}$$

Substitute $C^*(t), \omega^*(t) W_t$, $Z^*(t)$, $P^*(t)$, and $u^*(t)$ into the HJB function in equation (35); we have the following:

$$\begin{aligned} 0 &= e^{-\rho t} a(t) b\prime(t) X^{\gamma-1}(t) + \frac{e^{-\rho t}}{\gamma} a\prime(t) X^{\gamma}(t) - \frac{\rho e^{-\rho t}}{\gamma} a(t) X^{\gamma}(t) - \frac{\lambda(t) e^{-\rho t}}{\gamma} a(t) X^{\gamma}(t) \\ &+ \frac{\lambda(t) e^{-\rho t}}{\gamma}\left[\frac{\lambda(t)}{\mu(t) a(t)}\right]^{\gamma/1-\gamma} X^{\gamma}(t) + \frac{e^{-\rho t}}{\gamma}\left[\frac{1}{a(t)}\right]^{\gamma/1-\gamma} X^{\gamma}(t) \\ &+ e^{-\rho t} a(t) X^{\gamma-1}(t)\left\{\frac{(\alpha - r)^2}{(\theta - \gamma + 1)\sigma^2} X(t) + W_t r + y(t) - \left[\frac{1}{a(t)}\right]^{1/1-\gamma} X(t) - \mu(t)\left[\left(\frac{\lambda(t)}{\mu(t) a(t)}\right)^{1/1-\gamma} X(t) - W_t\right]\right\} \\ &+ \frac{1}{2} e^{-\rho t} a(t) X^{\gamma}(t)\frac{(\alpha - r)^2(\gamma - 1)}{(\theta - \gamma + 1)^2\sigma^2} - \frac{1}{2} e^{-\rho t} a(t) X(t)\frac{\theta(\alpha - r)^2}{(\theta + 1 - \gamma)^2\sigma^2}. \end{aligned} \tag{49}$$

Given $X(t) = W_t + b(t)$, if we express W_t in $X(t)$, the above equation transforms into a homogeneous function of $e^{-\rho t} X(t)^{\gamma}$. Eliminating $e^{-\rho t} X(t)^{\gamma}$ turns equation (49) into an ordinary differential equation with $a(t)$:

$$\left(\frac{1}{\gamma} - 1\right)\left[1 + \left(\frac{\lambda(t)}{\mu^{\gamma}(t)}\right)^{1/1-\gamma}\right] a^{-(\gamma/1-\gamma)}(t) + \left[\mu(t) + r - \frac{\rho}{\gamma} - \frac{\lambda(t)}{\gamma} + \frac{1}{2}\frac{(\alpha - r)^2}{(\theta - \gamma + 1)\sigma^2}\right] a(t) + \frac{1}{\gamma} a\prime(t) = 0. \tag{50}$$

With $H(t)$ and $K(t)$ in equations (46) and (47), we can rewrite equation (50) as

$$(1-\gamma)K(t)a^{-(\gamma/1-\gamma)}(t)+(1-\gamma)H(t)a(t)+a\prime(t)=0, \quad (51)$$

which is a Bernoulli ordinary differential equation (ODE) that satisfies

$$\frac{\mathrm{d}a(t)}{\mathrm{d}t}=p(t)a(t)+q(t)a(t)^n, \quad (52)$$

where

$$\begin{aligned} p(t)&=(\gamma-1)H(t);\\ q(t)&=(\gamma-1)K(t);\\ n&=-\frac{\gamma}{1-\gamma}. \end{aligned} \quad (53)$$

This ODE has a general solution. The boundary condition that $V(T,W_T)=L(T,X_T)$ implies $a(T)=1$. Thus,

$$a(t)=\left[e^{\int_t^T H(v)\mathrm{d}v}+\int_t^T K(s)e^{\int_t^s H(v)\mathrm{d}v}\mathrm{d}s\right]. \quad (54)$$

Since $a(t)$ has a solution, $V(W_t,t)$ constitutes a solution to the HJB function. □

Note $u^*(t)=(\theta(\alpha-r)/\theta+1-\gamma)>0$ and note that $u^*(t)$ increases with the uncertainty level θ. The agent suspects that the reference model is potentially misspecified, and he negatively adjusts the expected stock returns in the decision rules. In particular, he perceives a lower expected stock return. Using $a(t)$ expressed in equation (45), we obtain the partial derivative of $a(t)$ with respect to θ:

$$\begin{aligned} \frac{\partial a(t)}{\partial\theta}&=-\frac{\gamma}{2}a^{-(\gamma/1-\gamma)}(t)\frac{(\alpha-r)^2}{(\theta+1-\gamma)^2\sigma^2}\\ &\quad\cdot\left\{(T-t)e^{\int_t^T H(v)\mathrm{d}v}+\int_t^T K(s)(s-t)e^{\int_t^s H(v)\mathrm{d}v}\mathrm{d}s\right\}. \end{aligned} \quad (55)$$

For the reasonable case of $\gamma<0$, $(\partial a(t)/\partial\theta)>0$. The sensitivity of $a(t)$ with respect to θ sheds light on the optimal insurance decision from the perspective of stock return uncertainty. The optimal insurance demand consists of a certainty part and an uncertainty part. The certainty part consists of wealth borrowed against future labor income, $\mu(t)b(t)$. This part has nothing to do with the uncertainty of stock returns. The other part is influenced by the agent's uncertainty aversion and equals $\mu(t)[(\lambda(t)/\mu(t)a(t))^{1/1-\gamma}-1]X(t)$. Stock return uncertainty not only changes the insurance investment strategy, that is, the proportion of the total wealth assigned to the insurance product $\mu(t)[(\lambda(t)/\mu(t)a(t))^{1/1-\gamma}-1]$ via $a(t)$, but also decreases the amount of total wealth $X(t)$. The next section examines the impact of stock return uncertainty on the total wealth.

3.3. Wealth Effect. To study the effect of uncertainty embedded in stock returns on insurance investment decisions at different ages, we consider the path-dependent wealth dynamics. According to equation (37), the process of $X(t)$ that admits stock return uncertainty is

$$\begin{aligned} \mathrm{d}X(t)&=\mathrm{d}W_t+b\prime(t)\mathrm{d}t\\ &=\left[(r+\mu(t))b(t)-C(t)+P(t)\right.\\ &\quad\left.+W_t\omega(t)(\alpha-u-r)+W_t r\right]\mathrm{d}t+W_t\omega(t)\sigma\,\mathrm{d}\tilde{z}. \end{aligned} \quad (56)$$

We obtain the following proposition.

Proposition 3. *The CRRA agent has the following wealth process:*

$$\begin{aligned} X(t)&=X(0)\left(\frac{a(t)e^{-\rho t}}{a(0)}\right)^{1/1-\gamma}\\ &\quad\cdot\exp\left\{\left[A\cdot\frac{(\alpha-r)^2}{2(\theta+1-\gamma)^2\sigma^2}+\frac{r}{1-\gamma}\right]t\right.\\ &\quad\left.+\frac{1}{1-\gamma}\int_0^t\eta(u)\mathrm{d}u+\frac{\alpha-r}{(\theta+1-\gamma)\sigma}\tilde{z}_t,\right. \end{aligned} \quad (57)$$

where $A=1-\gamma+\gamma\theta/(1-\gamma)$; *the initial wealth* $X(0)=W_0+b(0)$. *The expect total wealth at time t is expressed as*

$$\begin{aligned} \mathbb{E}(X(t))&=X(0)\left(\frac{a(t)e^{-\rho t}}{a(0)}\right)^{1/1-\gamma}\\ &\quad\cdot\exp\left\{\left[(A+1)\cdot\frac{(\alpha-r)^2}{2(\theta+1-\gamma)^2\sigma^2}+\frac{r}{1-\gamma}\right]t\right.\\ &\quad\left.+\frac{1}{1-\gamma}\int_0^t\eta(u)\mathrm{d}u\right\}. \end{aligned} \quad (58)$$

Proof. Substitute $C^*(t)$, $\omega^*(t)W_t, Z^*(t)$, and $u^*(t)$ into equation (56); we have

$$\begin{aligned} \frac{\mathrm{d}X(t)}{X(t)}&=\left[\mu(t)+r-\frac{K(t)}{a(t)^{1/1-\gamma}}+\frac{(\alpha-r)^2(1-\gamma)}{(\theta+1-\gamma)^2\sigma^2}\right]\mathrm{d}t\\ &\quad+\frac{\alpha-r}{(\theta-\gamma+1)\sigma}\mathrm{d}\tilde{z}. \end{aligned} \quad (59)$$

Since α, r, and σ are constants, equation (59) is a geometric Brown motion. We conjecture the solution to $X(t)$ as

$$\begin{aligned} X(t)&=X(0)\left(\frac{e^{-\rho t}a(t)}{a(0)}\right)^{1/1-\gamma}\\ &\quad\cdot\exp\left\{\left[A\cdot\frac{(\alpha-r)^2(1-\gamma)}{2(1-\gamma+\theta)^2\sigma^2}+\frac{r}{1-\gamma}\right]t\right.\\ &\quad\left.+\frac{1}{1-\gamma}\int_0^t\eta(u)\mathrm{d}u+\frac{\alpha-r}{(\theta+1-\gamma)\sigma}\tilde{z}_t\right\}, \end{aligned} \quad (60)$$

where A is a constant to be determined. Applying Ito's lemma to $X(t)$ gives

$$\frac{dX(t)}{X(t)} = \left[\frac{1}{(1-\gamma)a(t)}\cdot\frac{\partial a(t)}{\partial t} - \frac{\rho}{1-\gamma} + A\frac{(\alpha-r)^2(1-\gamma)}{2(1-\gamma+\theta)^2\sigma^2} + \frac{r}{1-\gamma} + \frac{1}{1-\gamma}\eta(t) + \frac{(\alpha-r)^2}{2(1-\gamma+\theta)^2\sigma^2}\right]dt + \frac{\alpha-r}{(1-\gamma+\theta)\sigma}d\tilde{z}. \quad (61)$$

Using equation (45), we derive $a(t)$ and

$$\frac{\partial a(t)}{\partial t} = -(1-\gamma)H(t)a(t) - (1-\gamma)a^{-(\gamma/1-\gamma)}(t)K(t). \quad (62)$$

Substituting equation (62) into (61) gives

$$\begin{aligned}\frac{dX(t)}{X(t)} &= \left[-\frac{K(t)}{a(t)^{1/1-\gamma}} - H(t) - \frac{1}{1-\gamma}\rho + A\frac{(\alpha-r)^2(1-\gamma)}{2(\theta+1-\gamma)^2\sigma^2} + \frac{(\alpha-r)^2}{2(\theta+1-\gamma)^2\sigma^2} + \frac{r}{1-\gamma} + \frac{\eta(t)}{1-\gamma}\right]dt + \frac{\alpha-r}{(1-\gamma+\theta)\sigma}d\tilde{z} \\ &= \left[\mu(t) + r - \frac{K(t)}{a^{1/1-\gamma}} + \frac{(\alpha-r)^2}{2(\theta+1-\gamma)^2\sigma^2}\left(-\frac{\gamma}{(1-\gamma)}(\theta+1-\gamma) + A(1-\gamma) + 1\right)\right]dt + \frac{\alpha-r}{(\theta+1-\gamma)\sigma}d\tilde{z}.\end{aligned} \quad (63)$$

Matching equation (63) to (59) gives

$$\frac{1}{2}\left(-\frac{\gamma}{1-\gamma}(\theta+1-\gamma) + A(1-\gamma) + 1\right) = 1-\gamma. \quad (64)$$

Thus,

$$A = 1 + \frac{\gamma\theta}{(1-\gamma)^2}. \quad (65)$$

We have proved that the solution to the total wealth satisfies the differential function in equation (56). Expressing the expectation of total wealth $X(t)$ with the standard Brown motion $\tilde{z}_t \sim N(0,t)$ gives

$$\mathbb{E}(X(t)) = X(0)\left(\frac{a(t)e^{-\rho t}}{a(0)}\right)^{1/1-\gamma}\exp\left\{\left[(A+1)\cdot\frac{(\alpha-r)^2}{2(\theta+1-\gamma)^2\sigma^2} + \frac{r}{1-\gamma}\right]t + \frac{1}{1-\gamma}\int_0^t \eta(u)du\right\}. \quad (66)$$

□

When $P^*(t)$ is negative, the agent chooses to supply insurance to the market. We examine the impact of stock return uncertainty on his demand/supply of life insurance. Let $P^*(t)$ be zero as the switch point between buying life insurance and selling life insurance; we obtain

$$X(t)|_{P^*(t)=0} = \frac{1}{1-(\lambda(t)/\mu(t)a(t))^{1/1-\gamma}}b(t). \quad (67)$$

Lemma 1. *If the agent's total wealth exceeds a certain threshold, that is,* $\mathbb{E}(X(t)) > X(t)|_{P^*(t)=0}$, *the agent provides life insurance to the market, that is,*

$$P^*(t) < 0 \Leftrightarrow \mathbb{E}(X(t)) > X(t)|_{P^*(t)=0}, \quad (68)$$

It is sensible that the agent does not leave a legacy $Z^*(t)$ greater than the total wealth $X(t)$; thereby, equation (44) implies

$$\zeta(t) = \left(\frac{\lambda(t)}{\mu(t)a(t)}\right)^{1/1-\gamma} < 1. \quad (69)$$

The decision to demand or supply life insurance depends on the expected total wealth $\mathbb{E}(X(t))$ relative to the labor wealth $b(t)$. Given $\zeta(t) < 1$, $\mathbb{E}(X(t))$ and the threshold $X(t)|_{P^*(t)=0}$ are decreasing in θ. According to Section 4, the magnitude of the decrease in $X(t)|_{P^*(t)=0}$ is much smaller compared to the magnitude of the decrease in $\mathbb{E}(X(t))$, given the same increase in θ. Additional numerical analysis is presented in Section 4.

3.4. Uncertainty-Induced Utility Loss. This section estimates wealth-measured utility loss when the agent follows a suboptimal strategy; that is, he applies the optimal strategy under the uncertainty-free model in the uncertainty aversion model. It provides a yardstick to measure the improvement in utility by undertaking robust optimal decisions. To more intuitively illustrate the utility loss, we use the indifference curve to transform the implied utility loss into percentage of wealth.

We solve equations (41)–(43) with $\theta = 0$ for the suboptimal decision set $\mathscr{A}^{\mathrm{Sub}}$. The agent exercises the following suboptimal controls:

$$\begin{aligned} C^{\mathrm{Sub}}(t) &= \left[\frac{1}{a^0(t)}\right]^{1/1-\gamma}(W_t + b(t)),\\ \omega^{\mathrm{Sub}}(t)W_t &= \frac{\alpha - r}{(1-\gamma)\sigma^2}(W_t + b(t)),\\ P^{\mathrm{Sub}}(t) &= \mu(t)\left\{\left[\left(\frac{\lambda(t)}{\mu(t)a^0(t)}\right)^{1/1-\gamma} - 1\right]X(t) + b(t)\right\}. \end{aligned} \tag{70}$$

The suboptimal control functions are used in the HJB function in equation (26), based on which $u(t)$ associated with the worst-case model is attained. The suboptimal objective function is conjectured as

$$V^{\mathrm{Sub}}(W,t) = \frac{a^{\mathrm{Sub}}(t)e^{-\rho t}}{\gamma}[X(t)]^{\gamma}. \tag{71}$$

Solving the model yields the worst-case adjustment to the expected stock return:

$$u^{\mathrm{Sub}}(t) = \frac{\theta}{\gamma V^{\mathrm{Sub}}(W,t)}V_W^{\mathrm{Sub}}W_t\omega^{\mathrm{Sub}}(t)\sigma^2; \tag{72}$$

$$a^{\mathrm{Sub}}(t) = \left[e^{\int_t^T H^{\mathrm{Sub}}(v)\mathrm{d}v} + \int_t^T K(s)e^{\int_s^t H^{\mathrm{Sub}}(v)\mathrm{d}v}\mathrm{d}s\right]^{1-\gamma}, \tag{73}$$

where $K(t)$ is as in equation (47) and $H(t)$ is expressed as

$$H^{\mathrm{Sub}}(t) = -\frac{\rho}{1-\gamma} + \frac{\gamma}{1-\gamma}\left(\mu(t) + r + \frac{(\alpha-r)^2(1-\gamma-\theta)}{2(1-\gamma)^2\sigma^2}\right) - \frac{\lambda(t)}{1-\gamma}. \tag{74}$$

Following Branger and Larsen [13], we transform the loss in utility into the percentage loss in wealth. Denote $\psi(t)$ as the percentage of initial wealth the agent gives up for robust decisions. The loss function can be expressed as

$$\begin{aligned} &V\left(X(t)(1-\psi(t)), t; C(t)^*, \omega^*(t), P^*(t)\right)\\ &\quad = V^{\mathrm{Sub}}\left(X(t), t; C^{\mathrm{Sub}}(t), \omega^{\mathrm{Sub}}(t), P^{\mathrm{Sub}}(t)\right). \end{aligned} \tag{75}$$

Using the definition of utility loss and equation (75), we compute the percentage loss in wealth as

$$\psi(t) = 1 - \sqrt[\gamma]{\frac{a^{\mathrm{Sub}}(t)}{a(t)}}, \tag{76}$$

where $a(t)$ and $a^{\mathrm{Sub}}(t)$ are given in equations (45) and (73), respectively.

4. Numerical Analysis

This section conducts numerical analysis to examine the qualitative implications of stock return uncertainty. The benchmark parameter values are given in Table 1. With a slight abuse of notation, we use θ to represent the level of uncertainty and set its values between zero and five.

Table 1: Benchmark parameter values.

Parameter	Value
$y(t)$	$1 \cdot e^{\rho t}$
α	0.1
$\lambda(t)$	$0.005 + 0.001125t$
$\mu(t)$	$0.005 + 0.001125t$
$\eta(t)$	0
r	0.04
σ	0.2
ρ	0.03
$1-\gamma$	4
T	80

The parameter values in Table 1 are also used in the previous literature, for example, Pliska and Ye [22] and Kwak et al. [27]. For simplicity, we set security loading $\eta(t) = 0$, so the insurance payout ratio equals $\lambda(t)$. We use a linear mortality rate to study the dynamic change in the optimal controls as the agent ages. Labor income growth is assumed to follow an exponential function, and we normalize the initial labor income to the unit of one. We normalize the initial wealth $W_0 = 10$.

4.1. Wealth. Figure 1 depicts $X(t)$, W_t, and $b(t)$ in the uncertainty-free model. The age-dependent wealth process sheds light on the agent's optimal decision rules at different ages. The agent's total wealth reaches the peak at the age around 65. The agent borrows against his future labor wealth to purchase stock and life insurance. W_t turns out to be negative at ages around 40–70. Figure 2 depicts the change in total wealth for different uncertainty levels at different ages. The total wealth decreases with stock return uncertainty. The pattern is, however, more apparent at an older age than at a younger age. Uncertainty aversion makes the agent allocate less wealth into risky assets as he becomes older. Moreover, the agent has less borrowing power as his future labor wealth diminishes.

4.2. Consumption and Investment. Figure 3 shows that consumption gradually and monotonically increases with the agent's age. The mortality rate is higher at an older age; thereby the agent rationally chooses to consume more and invest less compared to the younger him. However, the agent consumes less than an otherwise uncertainty-neutral agent, which is explained by the notion that the total wealth decreases with stock return uncertainty.

Figure 4 shows that investment in the stock decreases with the level of stock return uncertainty. Intuitively, return uncertainty reduces the attractiveness of stock relative to the life insurance product and the risk-free asset. Uncertainty aversion appears to change the pattern of investment in the stock at different ages. In the absence of uncertainty, the agent first increases his stock investment as he grows at young ages and then reverts to decrease investment in the

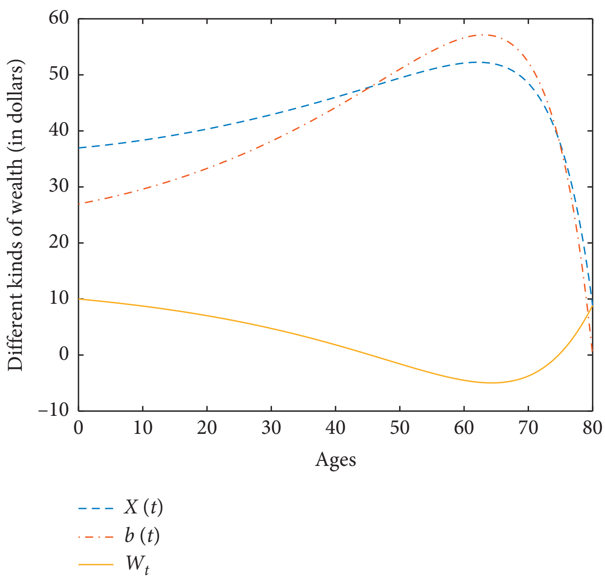

Figure 1: Total wealth at different ages.

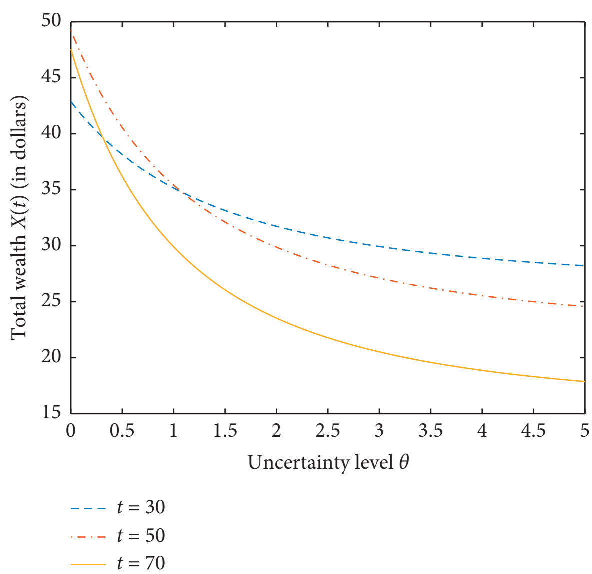

Figure 2: Change in total wealth with θ.

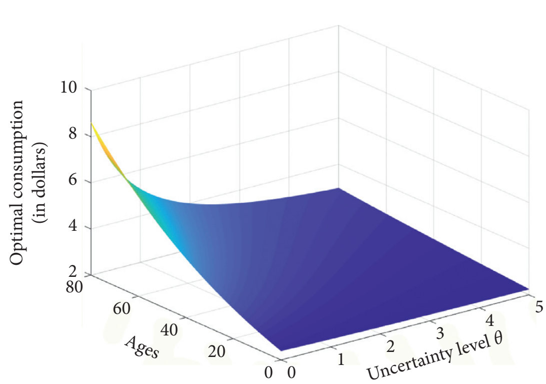

Figure 3: Optimal consumption.

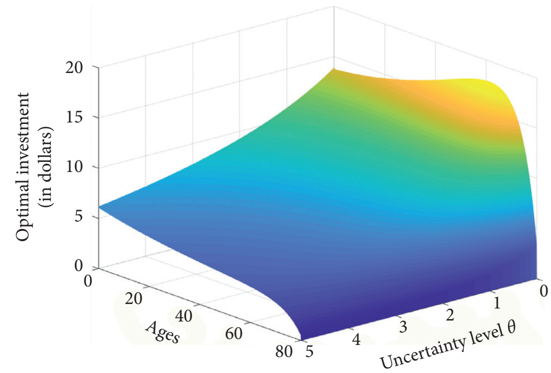

Figure 4: Optimal investment.

stock after a certain age. The peak appears around the age of 65 and drops towards zero as time passes by. This hump-shaped investment pattern, which can be traced to the hump-shaped wealth pattern, is consistent with that in Farhi and Panageas [28]. When $\theta = 5$, there is no investment peak as investment in the stock keeps decreasing as the agent ages. Uncertainty arising from the stock affects the agent's total wealth and subsequently alters his investment behavior. Shrinking wealth due to stock return uncertainty no longer supports increasing stock investment at younger ages, resulting in a monotonic declining pattern.

4.3. Life Insurance. Figure 5 shows that the optimal insurance demand increases with the level of uncertainty at all ages. The result implies that the agent shifts some investment in the stock to life insurance, confirming that the insurance market and the stock market, to some degree, substitute. Life insurance provides a way to hedge and evade the uncertainty embedded in the stock. This effect is more prominent for the middle-aged and elder agent. A young agent's demand for life insurance is low. When it is close to the end of the financial planning horizon, an elder agent consumes more, which represses demand for life insurance. As a result, the demand of younger and elder agents for life insurance is less sensitive to stock return uncertainty.

Figure 6 shows that, under different planning horizons, for example, $T = 60$ and $T = 100$, respectively, the patterns of demand for life insurance with respect to stock return uncertainty are in general the same. However, demand for life insurance is much less under a short planning horizon than under a long planning horizon. The result implies that people would demand more life insurance as they expect to live longer and plan financially for a longer horizon. Moreover, the increase in demand caused by the stock return uncertainty is also more significant within a longer planning horizon.

Lemma 1 shows that the agent becomes an insurance seller when his total wealth $\mathbb{E}(X(t))$ exceeds the threshold $X(t)|_{P^*(t)=0}$. Figure 7 shows that, for an agent at the age of 30 with initial wealth $W_0 = 20$, the agent is an insurance seller as $P^*(30) < 0$ in the absence of uncertainty. The expected total wealth drops sharply in the presence of uncertainty. The value of the threshold $X(t)|_{P^*(t)=0}$ also decreases, but at a much lower rate. When $\theta = 1.2$, the agent switches to buy

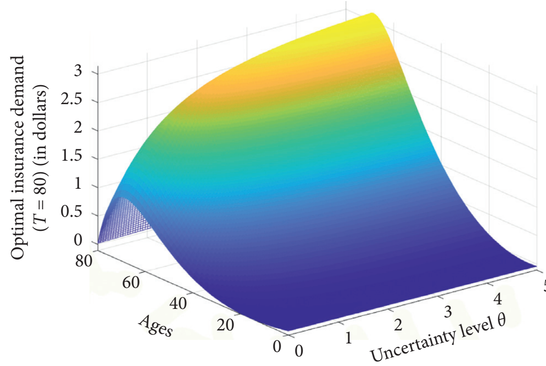

Figure 5: Demand of insurance at different levels of uncertainty.

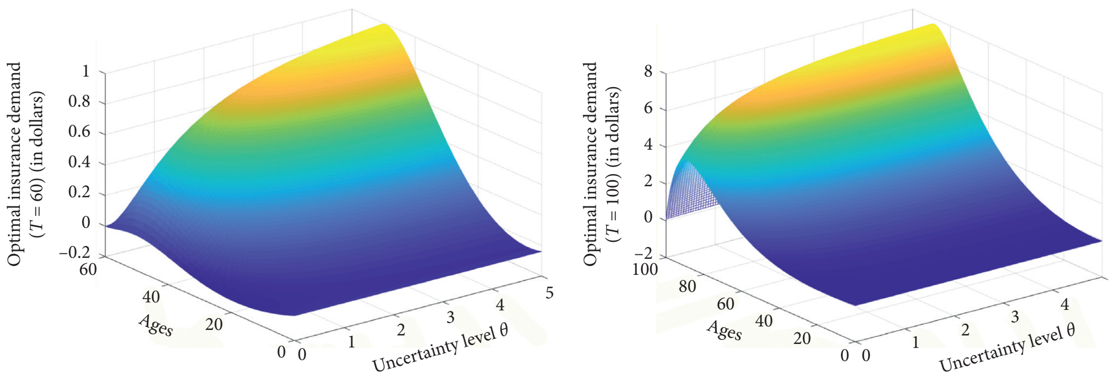

(a)

(b)

Figure 6: Demand of insurance for different financial planning horizons. (a) Insurance demand ($T = 60$). (b) Insurance demand ($T = 60$).

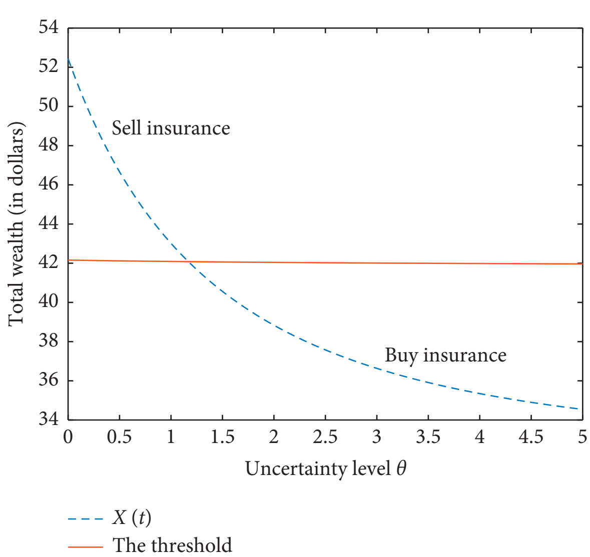

Figure 7: Buying vs. selling insurance.

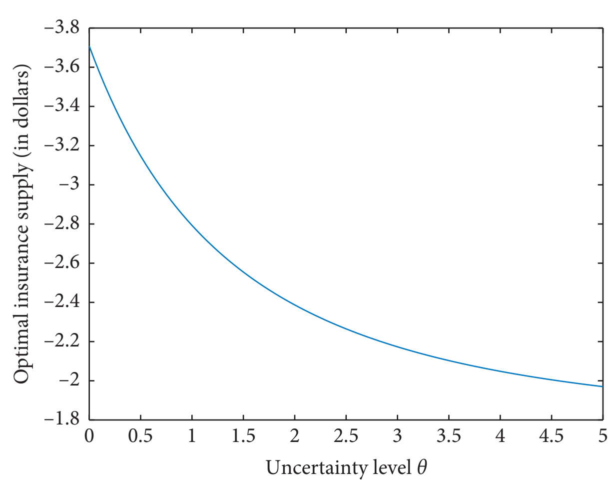

Figure 8: Supply of insurance and θ.

insurance as $\mathbb{E}(X(t))$ falls below the threshold $X(t)|_{P^*(t)=0}$. By reducing the agent's total wealth, the uncertainty decreases the propensity of the agent serving as an insurance seller.

Figure 8 shows that when the agent is endowed with an ultrahigh initial wealth, that is, $W_0 = 100$, this agent is wealthy enough to supply insurance even at a high level of uncertainty. The amount of supply, however, decreases with the level of uncertainty. Regardless of being an insurance buyer or supplier, the agent would be more conservative facing stock return uncertainty. In the insurance market, agents would demand more insurance, while the supply of insurance tends to fall, implying that insurance premium increases in equilibrium. Of course, an equilibrium model is required to explore such implication in a rigorous manner.

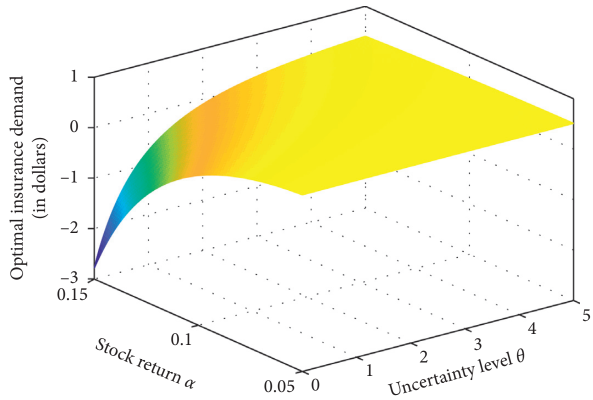

Figure 9: Insurance demand and α.

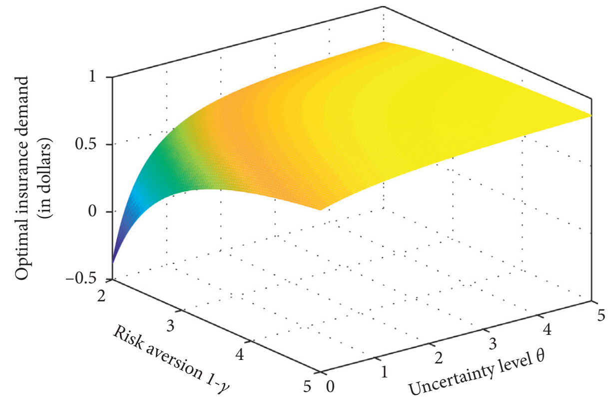

Figure 11: Insurance demand and γ.

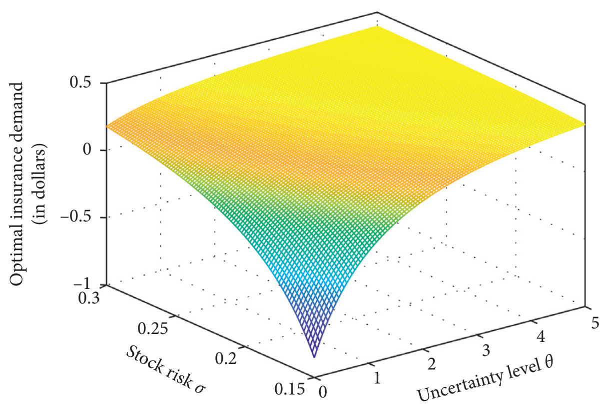

Figure 10: Insurance demand and σ.

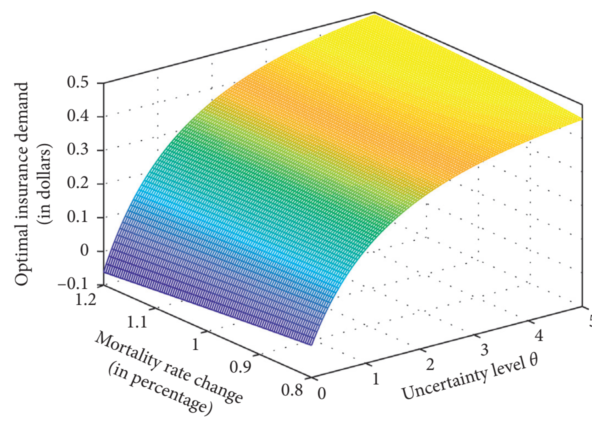

Figure 12: Insurance demand and $\lambda(t)$.

Stock market uncertainty also remarkably affects the relationships between the agent's life insurance decision and other structural factors. Figures 9 and 10 depict life insurance demand with respect to the expected stock return α and stock return volatility σ, respectively, assuming that the agent is 30 years old. The uncertainty tends to reduce the sensitivity of insurance demand with respect to these stock return characteristics. The findings are consistent with the previous result in that the agent tends to reduce investment in the stock when he is skeptical about the expected returns.

Figure 11 depicts life insurance demand with respect to the agent's risk/time preferences, $1-\gamma$, at different levels of uncertainty. For a CRRA agent, $1-\gamma$ also captures the time preferences of consumption. An agent with a higher $1-\gamma$ buys less insurance, as he values more current consumption relative to future consumption. The finding is consistent with those of Kwak and Lim [23] and Huang et al. [24]. Stock return uncertainty reduces the sensitivity of insurance demand to the agent's risk preferences.

Figure 12 shows that, in the absence of uncertainty, an increase in the mortality rate leads to a reduction in insurance demand. Stock return uncertainty could alter such a pattern, causing the agent's demand for insurance to increase with the mortality rate. The rationale is that the mortality rate plays two roles in insurance decision making. On the one hand, it adversely affects the insurance payout $P(t)/\lambda(t)$. Thus, higher $\lambda(t)$ reduces the utility brought by life insurance. On the other hand, the mortality rate increases the probability of obtaining life insurance compensation within the financial planning horizon—an agent with a higher mortality rate is more willing to buy insurance because there is a higher probability of receiving the insurance payment. When stock return uncertainty is low, the first effect dominates the second effect. However, when the level of uncertainty is sufficiently high, the agent values more the probability of receiving insurance compensation within the limited planning horizon than considering the amount of insurance payment.

4.4. Utility Loss. Figure 13 shows that utility loss due to uncertainty, $\psi(t)$, is increasing in the level of uncertainty, confirming that the agent is willing to give up a certain fraction of wealth for robust decision making. Such impact, however, decreases in age—the utility loss drops as the agent becomes older. A younger agent has a longer future horizon that is subject to stock return uncertain, so his optimal controls are more significantly shaped by the uncertainty.

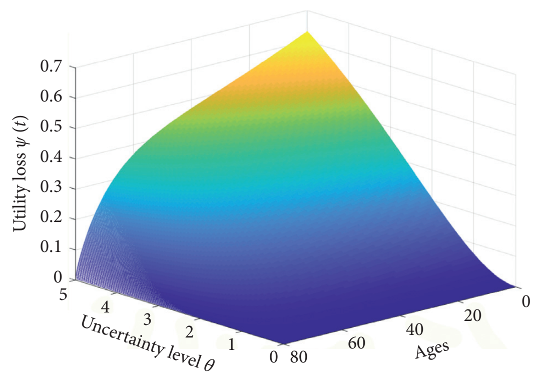

Figure 13: Uncertainty-induced utility loss.

5. Conclusion

This paper formulates a continuous-time rational expectations model to examine the effects of stock return uncertainty on life insurance. The model considers uncertainty aversion as the agent suspects that stock return in the stochastic process is potentially misspecified, and it imposes an uncertainty penalty to the objective function in reflecting his skeptical and conservative perspective. Facing stock return uncertainty, the agent shifts some of the investment in the stock to life insurance, confirming that the insurance market and the stock market are partially supplementary. Life insurance is used as a way to circumvent the uncertainty embedded in the stock. Overall, the agent would behave more conservatively in the insurance market facing stock return uncertainty. Agents would demand more insurance at a falling supply, implying that insurance premium might increase in equilibrium. We leave it to future research to develop an equilibrium model to explore such implications rigorously.

Data Availability

All data generated or analyzed during this study are included in this article.

Conflicts of Interest

The authors declare that they have no conflicts of interest.

Acknowledgments

The authors acknowledge financial supports from the National Natural Science Foundation of China (No. 71471099) and Tsinghua University Research Grant (No. 2019THZWLJ14).

References

[1] S. E. Harrington, "The financial crisis, systemic risk, and the future of insurance regulation," *Journal of Risk and Insurance*, vol. 76, no. 4, pp. 785–819, 2009.

[2] R. S. Headen and J. F. Lee, "Life insurance demand and household portfolio behavior," *The Journal of Risk and Insurance*, vol. 41, no. 4, pp. 685–698, 1974.

[3] J. H. Holsboer, "Repositioning of the insurance industry in the financial sector and its economic role," *Geneva Papers on Risk and Insurance - Issues and Practice*, vol. 24, no. 3, pp. 243–290, 1999.

[4] C.-C. Lee, W.-L. Huang, and C.-H. Yin, "The dynamic interactions among the stock, bond and insurance markets," *The North American Journal of Economics and Finance*, vol. 26, pp. 28–52, 2013.

[5] O. J. Blanchard, R. Shiller, and J. J. Siegel, "Movements in the equity premium," *Brookings Papers on Economic Activity*, vol. 1993, no. 2, pp. 75–138, 1993.

[6] P. J. Siegel, "Robust portfolio rules and asset pricing," *Review of Financial Studies*, vol. 17, no. 4, pp. 951–983, 2004.

[7] R. C. Merton, "On estimating the expected return on the market," *Journal of Financial Economics*, vol. 8, no. 4, pp. 323–361, 1980.

[8] L. P. Hansen and T. J. Sargent, "Robust control and model uncertainty," *American Economic Review*, vol. 91, no. 2, pp. 60–66, 2001.

[9] E. W. Anderson, L. P. Hansen, and T. J. Sargent, "A quartet of semigroups for model specification, robustness, prices of risk, and model detection," *Journal of the European Economic Association*, vol. 1, no. 1, pp. 68–123, 2003.

[10] R. Uppal and T. Wang, "Model misspecification and underdiversification," *The Journal of Finance*, vol. 58, no. 6, pp. 2465–2486, 2003.

[11] C. R. Flor, L. S. Larsen, and L. Sandris Larsen, "Robust portfolio choice with stochastic interest rates," *Annals of Finance*, vol. 10, no. 2, pp. 243–265, 2014.

[12] B. Yi, Z. Li, F. G. Viens, and Y. Zeng, "Robust optimal control for an insurer with reinsurance and investment under Heston's stochastic volatility model," *Insurance: Mathematics and Economics*, vol. 53, no. 3, pp. 601–614, 2013.

[13] N. Branger and L. S. Larsen, "Robust portfolio choice with uncertainty about jump and diffusion risk," *Journal of Banking & Finance*, vol. 37, no. 12, pp. 5036–5047, 2013.

[14] S. F. Richard, "Optimal consumption, portfolio and life insurance rules for an uncertain lived individual in a continuous time model," *Journal of Financial Economics*, vol. 2, no. 2, pp. 187–203, 1975.

[15] F. Jawadi, C. Bruneau, and N. Sghaier, "Nonlinear cointegration relationships between non-life insurance premiums and financial markets," *Journal of Risk and Insurance*, vol. 76, no. 3, pp. 753–783, 2009.

[16] J. Lamm-Tennant and M. A. Weiss, "International insurance cycles: rational expectations/institutional intervention," *The Journal of Risk and Insurance*, vol. 64, no. 3, pp. 415–439, 1997.

[17] R. A. Campbell, "The demand for life insurance: an application of the economics of uncertainty," *The Journal of Finance*, vol. 35, no. 5, pp. 1155–1172, 1980.

[18] S. Fischer, "A life cycle model of life insurance purchases," *International Economic Review*, vol. 14, no. 1, pp. 132–152, 1973.

[19] M. D. Hurd, "Mortality risk and bequests," *Econometrica*, vol. 57, no. 4, pp. 779–813, 1989.

[20] M. E. Yaari, "Uncertain lifetime, life insurance, and the theory of the consumer," *The Review of Economic Studies*, vol. 32, no. 2, pp. 137–150, 1965.

[21] R. C. Merton, "Optimum consumption and portfolio rules in a continuous-time model," *Journal of Economic Theory*, vol. 3, no. 4, pp. 373–413, 1971.

[22] S. R. Pliska and J. Ye, "Optimal life insurance purchase and consumption/investment under uncertain lifetime," *Journal of Banking & Finance*, vol. 31, no. 5, pp. 1307–1319, 2007.

[23] M. Kwak and B. H. Lim, "Optimal portfolio selection with life insurance under inflation risk," *Journal of Banking & Finance*, vol. 46, pp. 59–71, 2014.

[24] H. Huang, M. A. Milevsky, and J. Wang, "Portfolio choice and life insurance: the CRRA case," *Journal of Risk & Insurance*, vol. 75, no. 4, pp. 847–872, 2008.

[25] T. A. Pirvu and H. Zhang, "Optimal investment, consumption and life insurance under mean-reverting returns: the complete market solution," *Insurance: Mathematics and Economics*, vol. 51, no. 2, pp. 303–309, 2012.

[26] H. Huang, M. A. Milevsky, and T. S. Salisbury, "Optimal retirement consumption with a stochastic force of mortality," *Insurance: Mathematics and Economics*, vol. 51, no. 2, pp. 282–291, 2012.

[27] M. Kwak, Y. H. Shin, and U. J. Choi, "Optimal investment and consumption decision of a family with life insurance," *Insurance: Mathematics and Economics*, vol. 48, no. 2, pp. 176–188, 2011.

[28] E. Farhi and S. Panageas, "Saving and investing for early retirement: a theoretical analysis," *Journal of Financial Economics*, vol. 83, no. 1, pp. 87–121, 2007.

Hindawi
Mathematical Problems in Engineering
Volume 2020, Article ID 3239591, 10 pages
https://doi.org/10.1155/2020/3239591

Research Article

Modeling the Effect of Spending on Cyber Security by Using Surplus Process

Ciyu Nie,[1] Jingchao Li ,[2,3] and Shaun Wang[4]

[1]*Division of Banking and Finance, Nanyang Business School, Nanyang Technological University, 50 Nanyang Avenue, Singapore 639798*
[2]*College of Mathematics and Statistics, Shenzhen University, Nanhai Ave 3688, Shenzhen, Guangdong 518060, China*
[3]*Shenzhen Key Laboratory of Advanced Machine Learning and Applications, Shenzhen University, Shenzhen, Guangdong 518060, China*
[4]*Department of Finance, Southern University of Science and Technology, 1088 Xueyuan Avenue, Shenzhen, Guangdong 518055, China*

Correspondence should be addressed to Jingchao Li; jingchaoli@szu.edu.cn

Received 1 May 2020; Accepted 8 June 2020; Published 7 July 2020

Guest Editor: Wenguang Yu

In this paper, we assume the security level of a system is a quantifiable metric and apply the insurance company ruin theory in assessing the defense failure frequencies. The current security level of an information system can be viewed as the initial insurer surplus; defense investment can be viewed as premium income resulting in an increase in the security level; cyberattack arrivals follow a Poisson process, and the impact of attacks is modeled as losses on the security level. The occurrence of cyber breach is modeled as a ruin event. We use this framework to determine optimal investment in cyber security that minimizes the total cyber costs. We show by numerical examples that there is an optimal allocation of total cyber security budget to (1) IT security maintenance/upkeep spending versus (2) external cyber risk transfer.

1. Introduction

Cyber risk has become a hot topic given the ever-increasing cyber breaches and resulting losses of data and business disruptions. Cyber risk differs from traditional insurance risks in that they are very much driven by human behaviours in terms of attacks and defenses. What quantitative tools can actuaries imply to offer insights in measuring and managing cyber risks? In this paper, we apply traditional ruin theory in an innovative way to assess the stochastic changes in the level of cyber security and derived interesting insights from this theoretical framework.

Traditional actuarial ruin theory was developed in modeling of insurance capital solvency, whereas the level of capital is influenced by two opposing forces: the upward drift driven by a stream of insurance premium income and the random downward jump driven by insurance claims. During our literature review for cyber risk analysis (mostly from the computer science literature), we noticed that in many of the quantitative models, the security level of a system could be assumed as a quantifiable amount, which is primarily affected by the amount of investment in security development. In addition, it is commonly assumed that the probability and the loss severity of a defense failure (a cyber breach) depend on the security development and the damage control scheme.

In this paper, we assume the security level of a system is a quantifiable metric and apply the ruin theoretic framework in assessing the defense failure frequencies. We assume that the security level of a system changes over time due to attack and defense. The security level is then modeled by a modified surplus process: the current security level of an information system can be viewed as the initial surplus; defense investment resulting in an increase in the security level can be viewed as the premium income; the cyberattack arrivals are modeled as a Poisson process, and the impact of attacks is modeled as losses on the security level using an assumed loss distribution. A cyberattack succeeds (or the defense fails) when ruin occurs. In other words, we apply the risk process to model the frequency of the cyber failure. Once the defense failed, an independent financial loss amount is incurred depending on the nature of data being breached. Our goal of this paper is to provide a framework for analyzing the economical relationship between IT security investment and the associated cyber breach losses and to use this framework to make optimal IT security investment decisions.

In Section 2, we provide a detailed description of the model. We then derive the formula for the distribution of defense failure frequency, which is a function depending on security investments and attack arrivals. Assuming the distribution of the loss severity from a cyber breach is known, we show that the optimal investment amount can be solved by minimizing the expected total cyber costs. In Section 3, we use numerical calculations to provide insights on the changes in expected total cyber costs and the optimal amount of cyber investment, under different assumptions of loss severity, attack arrival as well as time horizon. We also provide a literature review on cyber risk modeling in Section 4 and comment on future research in Section 5.

To our knowledge, this paper is the first attempt to model cyber risk by applying the ruin theory in the literature. The goal of this paper is not to propose a new actuarial model for cyber losses (in terms of frequency and severity distributions), but instead, we apply the ruin theoretical framework to the level of cyber security over the course of time, under opposing forces of attackers and defenders. We then use the framework to draw insights about optimal allocation of cyber security budget.

2. Surplus Process for the Cyber Security Level over Time

2.1. Surplus Processes in the Classical Ruin Theory. We first review the classical insurance surplus process defined by

$$U_t = u + ct - \sum_{i=1}^{N_t} X_i, \tag{1}$$

where $u = U_0$ is the initial surplus, c is a constant rate of premium income per unit time, $\{N_t\}_{t\geq 0}$ is a counting process for the number of claims, and $\{X_i\}_{i=1}^{\infty}$ is a sequence of i.i.d. random variables representing individual claim amounts with probability density function (p.d.f.) $f(x)$ and cumulative distribution function (c.d.f.) $F(x)$. Let T_u be the time that surplus first falls below 0 given initial surplus u, and the ultimate ruin probability is defined as $\psi(u) = \Pr(T_u < \infty)$. Under the classical risk model, it is common to assume $ct > E(\sum_{i=1}^{N_t} X_i)$ to ensure $\psi(u)$ is not 1. Define $\omega_u(t)$ to be the defective density function of T_u and $\tilde{\omega}_u(s) = \int_0^{\infty} e^{-st}\omega_u(t)dt, s \geq 0$, as the Laplace transform of $\omega_u(t)$. The conditional density of $T_u | T_u < \infty$ is denoted as $\omega_u^c(t) = \omega_u(t)/\psi(u)$.

2.2. Cyber Security Level Model Description. Gordon and Loeb [1] defined a vulnerability term ν, as the probability that an attack being successful. The observation is that the vulnerability of a security system is not static over time and it depends on the maintenance effort of the system administrator through time.

Denote ν_t as the vulnerability level of a security system at time t. In addition, we define the strength level of a security system at time t as u_t, where $\nu_t = g(u_t)$ and $g(x) \in [0, 1], x \geq 0$, is a function that satisfies the following properties:

(1) $g'(x) < 0$, i.e., the higher the u_t is, the lower the vulnerability of the security system.

(2) When $x = 0$, $g(x) = 0$, i.e., when the strength level is 0, the probability of an attack being successful is 1.

(3) When $x \to \infty$, $g(x) \to 0$, i.e., when the strength level is extremely high, the probability of an attack being successful tends to 0. Here we assume that the security system cannot be completely protected; however, the system administrator manages it. There is always a probability of being breached.

One type of function that satisfies the above properties is where $g(x) = e^{-\alpha x}$, i.e., $\nu_t = e^{-\alpha u_t}$, where α is a parameter that transforms the strength level measurement u_t to a probability measurement ν_t.

We now apply some of the surplus process ideas to model the security strength level process of a firm's information system. Assume that process $\{u_t\}_{t\geq 0}$ represents the security strength at any time $t \geq 0$ of the system and that u_0 represents the system's current security level.

Let $\xi_t \geq 0$ denote the monetary (e.g., dollar) investment in security to protect the system. The result of such investment will create changes in security strength level u_t over time. For simplicity in our model, we assume that the investment is constant at ξ per unit of time and that the change in u_t is at $c = A(\xi)$ per unit of time, where $A(x)$ is a differentiable function with $A'(x) > 0$ and $A''(x) > 0$.

We assume that when $\xi_t = 0$, i.e., there is absolutely no effort in place on system maintenance, the process u_t will have a natural downward drift. We assume this downward drift to be a constant $-c', c' > 0$ until u_t hits 0. This is justified by common observations in security system management: if the system does not perform regular updates, scans, and inspections, the system becomes more and more vulnerable over time.

Let ξ' be the amount of investment that is needed to counter affect the downward drift c', and that the per unit time change in u_t caused by such investment is 0. If $\xi > \xi'$, then the per unit time change in u_t becomes c.

Mathematically, the above assumption can be summarized as the following conditions that need to be satisfied by function $A(x)$: $A(0) = -c'$, $A(x) = 0$ for $x = \xi'$, and $A(x) = c > 0$ for $x > \xi'$. The increase in the security level is justified by continuous effort on fixing known vulnerabilities, strengthening authentication and encryption, etc. References on over hundreds of defense methods can be found in Cohen [2].

The counting process $\{N_t\}_{t\geq 0}$ represents the number of attempted attacks during time $(0, t]$. When an attempted attack arrives at time t, we assume that the probability of that attack being successful is equal to $\nu_t = e^{-\alpha u_t}$. However, whether the i^{th} attempted attack is successful or not, we assume that the strength level of the system after the attempted attack will be damaged by a random variable X_i. During an attack event, the hacker may gain some information about the system mechanism and authentication methods and that a certain level of security strength is lost. This is modeled by losses $\{X_i\}_{i=1}^{\infty}$ in security level when attack arrives.

So far our security level process follows the fundamental works of a classical insurance surplus process. To further accommodate the modeling of cyber risks, we make two modifications on the process. First modification is that once ruin occurs, the surplus level returns to 0 immediately and the process continues. This implies that the security level does not remain at ruin state but restarts from 0 whenever a failure occurred. A realization of such process is shown in Figure 1. The reason for this is that it seems unrealistic to assume that the security level can remain negative. Even when a breach event occurs, the system engineers will continue to strengthen the system security over time by fixing exploited vulnerabilities and bugs.

Another modification is a loosening on the assumption for c such that the probability of ruin/breach event is not strictly less than 1 under our framework. More discussion on this modification can be found in Appendix A.

Table 1 provides a comparison between surplus process definitions under traditional ruin theory versus our cyber security framework. In reality, the cyber environment is characterized as an arms race between attackers and defenders. Perpetrators are actively searching for weak points and new methods and tools (e.g., malware) for attacking. The results of attackers are quantified by $\{X_i\}_{i=1}^{\infty}$ which emerges over time. Defenders must vigilantly monitor and constantly invest in cyber security in terms of time, knowledge, and measures. The defense spending of amount \$$\xi$ gives c as the continuous security development rate. Our focus is on the time dimension of the arms race between attackers and defenders. In this paper, we investigate how company spending in beefing up cyber security level can help maintain/achieve a desirable security level.

Let the counting process of the number of ruin events between time $(0,t]$ be $\{\mathrm{NR}_u(t)\}_{t\geq 0}$, with initial surplus u, under the modified surplus process. Let $T_{u,n}$ to be the time of n^{th} ruin event and $\omega_{u,n}(t)$ to be the probability density function of $T_{u,n}$. Define $W_{u,n}(t) = \int_0^t \omega_{u,n}(\tau)d\tau = \Pr(T_{u,n} \leq t)$, we can then derive the probability function for $\mathrm{NR}_u(t)$. For $n=0$, we have that

$$\Pr[\mathrm{NR}_u(t) = 0] = \Pr(T_u > t) = 1 - W_{u,1}(t). \tag{2}$$

Note that this also includes the probability that ruin never occurs and that by definition $W_{u,1}(t) = W_u(t)$. For $n \geq 1$,

$$\begin{aligned}\Pr[\mathrm{NR}_u(t) = n] &= \Pr\left(T_{u,n} \leq t < T_{u,n+1}\right) \\ &= \Pr\left(T_{u,n} \leq t\right) - \Pr\left(T_{u,n+1} \leq t\right) \\ &= W_{u,n}(t) - W_{u,n+1}(t).\end{aligned} \tag{3}$$

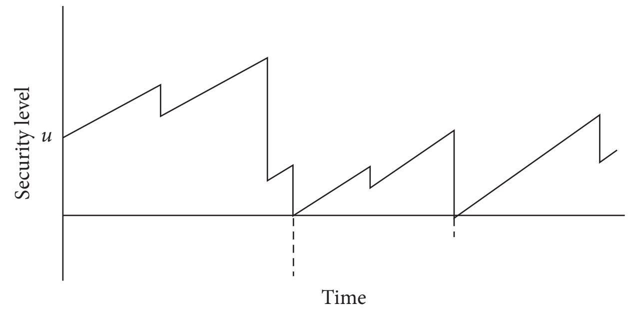

Figure 1: Security process.

Table 1: Traditional ruin theory and the proposed application on cyber security level modeling.

Notation	Traditional ruin theory	Apply to cyber security changes
U_t	Insurer's surplus level	Company's cyber security level
u	Initial surplus level	Initial level of cyber security
c	Continuous premium income	Continuous cyber security development derived from cyber security investment
N_t	Counting process of the number of claims	Counting process of the number of cyber attacks
X_i	Insurance claims	Damage to security level caused by the attacks
Ruin event	Insolvency	Cyber breach

Under our cyber risk model, we use $\mathrm{NR}_u(t)$ as the counting process for breach events. Furthermore, let $\{Y_i\}_{i=1}^{\infty}$ be independent and identically distributed random variables representing the severity of financial loss due to a security breach. We assume that $\{Y_i\}_{i=1}^{\infty}$ depends on the nature of data breached and is independent of U_t and $\mathrm{NR}_u(t)$. The total financial loss due to defense failure between time $(0,t]$ is then $\sum_{i=0}^{\mathrm{NR}_u(t)} Y_i$.

Since ξ is the amount of investment in cyber security per unit time, we denote $L(u,\xi,t)$ to be the total cyber cost between $(0,t]$ and we have

$$L(u,\xi,t) = \xi t + \sum_{i=1}^{\mathrm{NR}_u(t)} Y_i. \tag{4}$$

The expected total cyber costs between $(0,t]$ are then

$$E[L(u,\xi,t)] = \xi t + E[\mathrm{NR}_u(t)]E[Y_i], \tag{5}$$

where the expected number of breaches before t can be found as follows:

$$E[\mathrm{NR}_u(t)] = \sum_{n=1}^{\infty} n\left[W_{u,n}(t) - W_{u,n+1}(t)\right] = \sum_{n=1}^{\infty} W_{u,n}(t). \tag{6}$$

Taking the partial differentiation of $E[L(u,\xi,t)]$ with respect to ξ, we have

$$\frac{\partial E[L(u,\xi,t)]}{\partial \xi} = t + E(Y_i)A'(\xi)\sum_{n=0}^{\infty}\frac{\partial W_{u,n}(t)}{\partial c}. \quad (7)$$

Since $\partial W_0(t)/\partial c < 0$ and hence $\partial W_{u,n}(t)/\partial c < 0$, and that $A'(\xi) > 0$, we see that there exists an ξ^* such that $\partial E[L(u,\xi,t)]/\partial \xi = 0$.

Note that the expected loss $E[\mathrm{NR}_u(t)]E[Y_i]$ represents the net premium for cyber insurance cover for losses from cyber breach. The higher the IT security spending, the lower the resulting net premium of cyber insurance. There is an optimal amount of spending that minimizes the total cost to the firm. Using equation (5), firms can decide an optimal allocation of total cyber security budget to (1) IT security maintenance/upkeep spending versus (2) external cyber risk transfer. The total cyber cost function can be generalized to allow for expense loading of insurance covers. If the insurance premium is the expected financial loss $E[\mathrm{NR}_u(t)]E[Y_i]$ plus a loading θ under the expected value principle, the total cyber cost function then becomes

$$L(u,\xi,t) = \xi t + (1+\theta)E[\mathrm{NR}_u(t)]E[Y_i]. \quad (8)$$

3. Insights from the Framework

In this section, we assume a baseline scenario that $\{N_t\}_{t\geq 0}$ follows a Poisson process with parameter $\lambda = 1$, and $\{X_i\}_{i=1}^{\infty}$ follows an exponential distribution with parameter $\alpha = 1$. The initial security level is $u = U_0 = 3$. We also assume that the construction rate $c = A(\xi) = \ln(\xi + 1)$, where ξ is the amount of investment on security development. Note that under this assumption $A(0) = 0$, $A'(\xi) > 0$ and $A''(\xi) > 0$ for $\xi > 0$. The expected loss when breach occurs is assumed to be $E(Y_i) = \$20$ and the time horizon is $t = 2$. Some analytical results are given in Appendix B under these assumptions.

To further clarify the notation used, u, λ, α, and c are numerical metrics corresponding to the security level process, whereas ξ, $E(Y_i)$, and $E[L(u,\xi,t)]$ represent the monetary amounts associated with security investments and costs of cyber breaches.

In the following examples, we change various assumptions and study the impact on the expected total cyber cost $E[L(u,\xi,t)]$. Under each scenario, we find the optimal investment level ξ^* such that the expected cyber cost is minimized given the specific time horizon.

3.1. Impact of Loss Severity. In this example, we assume an alternative scenario with $E(Y_i) = \$40$. Clearly in our baseline scenario where $E(Y_i) = \$20$, the average severity of loss in an event of cyber breach is relatively low compared with $E(Y_i) = \$40$. Figure 2 shows how expected cyber costs change with respect to changes in ξ given the assumed $E(Y_i)$.

Under our baseline scenario, where $E(Y_i) = \$20$, if we invest nothing in security development such that $\xi = \$0$ and hence $c = 0$, the expected number of defense failures is 0.45. As ξ increases, we see that $E[L]$ firstly decreases until it reaches the minimum at $\xi^* = \$1.02$ with the minimized expected cyber cost at $E[L(3, 1.02, 2)]^* = \$7.22$. The expected number of defense failures given $\xi^* = \$1.02$ is 0.26. Note that with $\xi^* = \$1.02$, the corresponding $c = 0.70 < \lambda/\alpha$. This indicates that under the given conditions above, it is actually less optimal to maintain $c > \lambda/\alpha$, which is a condition needed for $\psi(u) < 1$.

For $E(Y_i) = \$40$, the minimum expected cost is \$11.65 with $\xi^* = \$1.94$. The optimal security investment is higher compared with the previous case. Table 2 provides a summary of the results above.

Insights: in the case of higher average loss severity, it is better to invest more in security defense to reduce the expected number of breach events.

3.2. Impact of Different Attack Arrivals. In this example, we look at the impact of different attack arrivals on expected cyber losses and optimal investment level ξ^*. We adopt the same baseline scenario such that $u = 3$, $\lambda = 1$ and $\alpha = 1$, $c = A(\xi) = \ln(\xi + 1)$, $t = 2$, and $E(Y_i) = \$20$. We assume two alternative sets of parameters for attack arrivals: for the first alternative scenario (scenario 2), we assume $\lambda = 0.5$ and $\alpha = 0.5$, which represents the case where the attack frequency is halved, but the expected impact is doubled due to more sophisticated attacks. For the second alternative scenario (scenario 3), we assume $\lambda = 10$ and $\alpha = 10$, which represents a high-frequency but low-impact (less sophisticated) attack for the attack arrivals.

Figure 3 shows the change in the expected number of breaches $E[\mathrm{NR}_3(2)]$ given ξ assuming different attack arrivals as above. We see that for scenario 3, $E[\mathrm{NR}_3(2)]$ decreases quickly with small increase in ξ. A small amount of investment can reduce the expected number of breaches significantly. For scenario 2, the investment is less efficient because $A''(\xi) < 0$ such that each additional unit spending of ξ causes smaller additional c and that high impact of the attacks overpowers the security improvement.

We then calculate the expected total cyber costs under the assumed three scenarios, and Figure 4 shows the changes in $E[L(3,\xi,2)]$ with respect to changes in ξ. The optimal investment ξ^* is then calculated for each scenario with corresponding results shown in Table 3.

For the baseline scenario, the optimal ξ^* is \$1.02 with the minimum expected cyber costs at \$7.22. For scenario 2, the optimal $\xi^* = \$0.38$ is smaller than the baseline scenario, with the minimum expected cyber costs higher at \$7.31. Under this scenario, the system manager actually opts to invest less due to the comparatively inefficient cyber investment. For scenario 3, the optimal $\xi^* = \$0.49$ is lower than the baseline scenario but higher than scenario 2. However, we see that the optimal expected cyber costs decreased significantly from \$7.22 and \$7.31, compared with the baseline scenario and scenario 2, respectively.

Insights: for a given expected loss amount as the product of frequency and severity, if a company's computer system is facing more frequent but less severe attacks, it is optimal for the company to invest less amount in security improvement.

3.3. Impact of Time Horizon. In previous sections, we assumed $t = 2$ for numerical illustrations. We now look at the impact of time horizon on the changes in the optimal

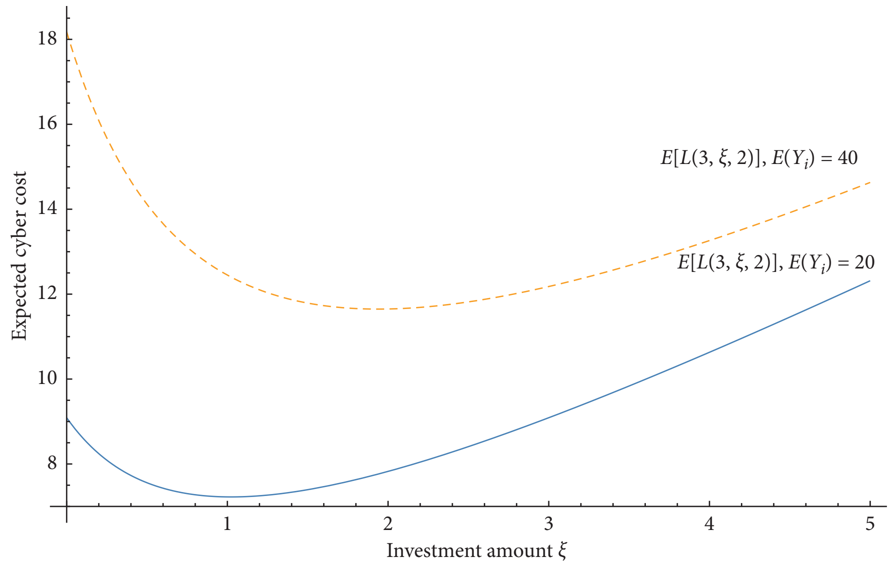

FIGURE 2: Total expected cyber cost with different $E(Y_i)$.

TABLE 2: Optimal ξ^* with different loss severity.

Expected loss per breach $E(Y_i)$	Optimal IT spending ξ^*	Insurance net premium $E[\mathrm{NR}_u(t)]E[Y_i]$	Expected cyber cost $E(L)^*$
\$20	\$1.02	\$6.20	\$7.22
\$40	\$1.94	\$9.71	\$11.65

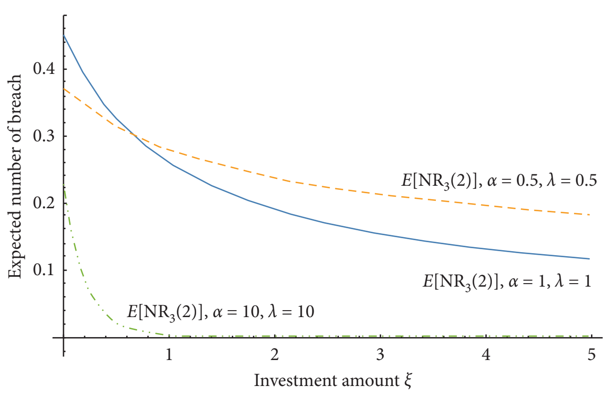

FIGURE 3: Expected number of breaches with different attack arrivals.

investment level ξ. We assume $u = 3$, $\lambda = 1$, $\alpha = 1$, $c = A(\xi) = \ln(\xi + 1)$, and $E(Y_i) = \$20$. Figure 5 illustrates the changes in $E[L(3, \xi, t)]$ with changes in ξ, assuming $t = 1$, $t = 2$, and $t = 5$, respectively.

Intuitively, as t increases, the expected total cyber cost shifts upward. Our interest lies in the changes in optimal investment amount when looking at different time horizons. Table 4 shows the optimal ξ^* for $t = 1$, $t = 2$, and $t = 5$, respectively. We also calculate the corresponding $E(L)^*/t$ and $E[\mathrm{NR}_3(t)]^*/t$, which represent the expected cyber cost and expected number of breaches per time unit, respectively, given ξ^*. There are a few observations from the results as follows. Firstly, as we look at longer time horizon, it is optimal to invest more in security development to reduce the total expected cyber costs. Next, the $E(L)^*$ is not linearly related to t as t changes. This is because at the end of one year, the security level may be lower or higher than the start of the year and the optimal level of investment will change accordingly for the next year. In addition, the optimal average expected number of breaches per time unit also changes when we consider different time horizons.

Insights: the choice of time horizon has important implications when deciding the optimal security spending.

3.4. Impact of Initial Security Level. In this example, we look at the impact of different initial security level u. We assume $\lambda = 1$, $\alpha = 1$, $c = A(\xi) = \ln(\xi + 1)$, $t = 2$, and $E(Y_i) = \$20$. Figure 6 illustrates the changes in $E[L(u, \xi, 2)]$ with changes in ξ, given $u = 1$, $u = 3$, and $u = 5$. We see that when ξ is small, the differences in expected cyber cost are relatively large when u changes. As ξ becomes larger, the gaps between the three lines become smaller and almost remain constant for large ξ.

In Table 5, we provide the optimal investment ξ^* and corresponding expected cyber costs. When $u = 1$, the optimal ξ^* is \$2.46 with minimum expected cyber costs at \$16.33. When $u = 5$, the optimal $\xi^* = \$0.16$ and the minimum expected cyber cost is \$2.87.

Assume we can invest ξ_a^b, $a < b$, to instantly increase U_t from a to b. We also assume that $\xi_a^b \geq A^{-1}(b - a)$. This implies that if we want to increase U_t from a to b instantly, it will cost more than develop U_t from a to b during 1 unit time. If at time $t = 0$ and $u = a$, the expected total cyber cost under previous settings will be $E[L(a, \xi, t)]$. Suppose we decide to invest ξ_a^b such that the initial u increases to b

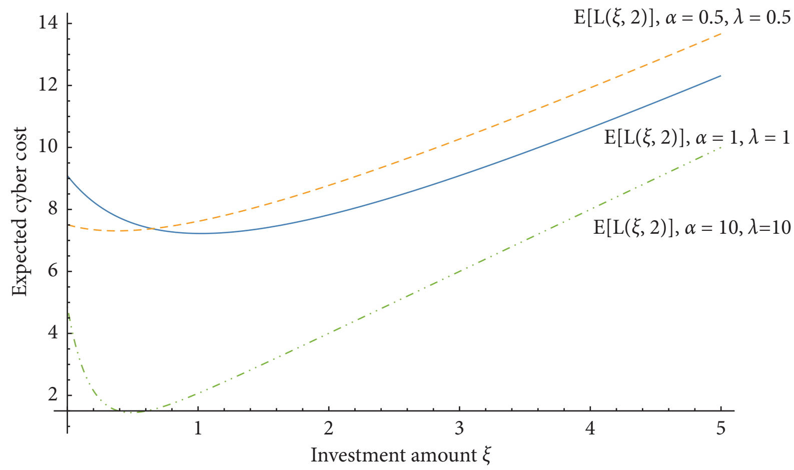

Figure 4: Total expected cyber cost with different attack arrivals.

Table 3: Optimal ξ with different attack arrivals.

Parameters	Expected cyber cost $E(L)^*$	Optimal IT spending ξ^*	Expected number of breaches $E[\mathrm{NR}_3(t)]^*$
$\lambda = 1,\ \alpha = 1$	\$7.22	\$1.02	0.26
$\lambda = 0.5,\ \alpha = 0.5$	\$7.31	\$0.38	0.33
$\lambda = 10,\ \alpha = 10$	\$1.45	\$0.49	0.02

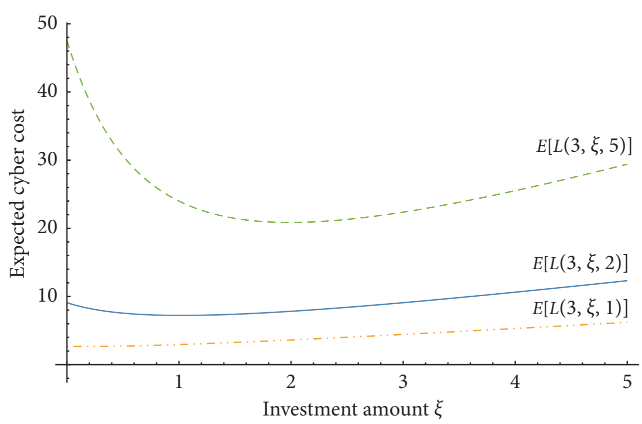

Figure 5: Total expected cyber cost with different t.

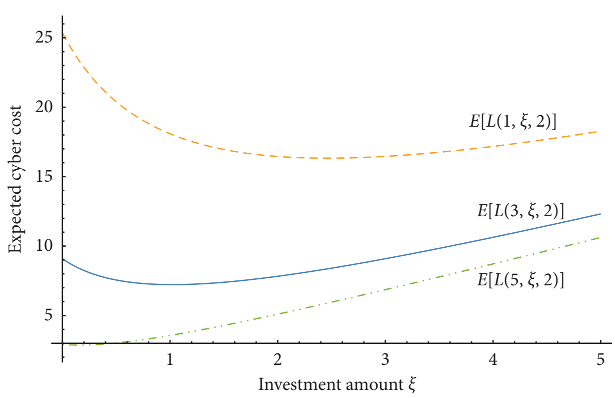

Figure 6: Total expected cyber cost with different u.

instantly and the process continues. The total cyber cost under this scenario is then $\xi_a^b + E[L(b, \xi, t)]$. From the table above, we see that $\xi_1^3 \geq \$6.39$. If $\xi_1^3 \leq \$9.11$, the firm can actually reduce the total expected cyber cost by a one-off investment to boost the initial security level from 1 to 3.

Insights: it may be worthwhile for a company to spend one-off investment from time to time to boost cyber security level to a desirable standard.

4. Literature Review on Cyber Risk Modeling

In this section, we provide a brief literature review on cyber risk modeling. The computer information system (CIS) risk had always been one of the key concerns for computer engineers. In the era of digitization, big data, and global connectivity, the requirements for cyber risks management escalate and become a key element in the risk management framework. In the computer science literature, the analysis of CIS risks has been split into development risks and security risks. Rigorous analysis methods and frameworks were designed to identify and manage critical risk factors in system development [3]. For security risks, the authors in [2, 4] provided extensive lists of potential attacks, defenses, threats, and consequences. With the effort to quantitatively analyze system security, network topology and graph are used together with epidemic models and become more popular in recent years. Li et al. [5] applied a stochastic model upon a complex network graph that includes sets of nodes and sets of edges over which direct attack can be carried out in the network. A stochastic abstraction of the interactions between the attacker and the defender in the network is considered to derive the probability that a

Table 4: Optimal ξ with different t.

Time	Expected cyber cost per time unit $E(L)^*/t$	Optimal IT spending ξ^*	Expected number of breaches per time unit $E[\mathrm{NR}_u(t)]^*/t$
$t = 1$	\$2.66	\$0.17	0.12
$t = 2$	\$3.61	\$1.02	0.13
$t = 5$	\$4.17	\$1.99	0.11

Table 5: Optimal ξ with different u.

Initial security level u	Optimal IT spending ξ^*	Insurance net premium $E[\mathrm{NR}_u(t)]E[Y_i]$	Expected cyber cost $E(L)^*$
$u = 1$	\$2.46	\$13.87	\$16.33
$u = 3$	\$1.02	\$6.20	\$7.22
$u = 5$	\$0.16	\$2.71	\$2.87

uniformly chosen node is compromised (or attacked) in the steady state. Xu and Xu [6] later extended this model by weakening some strong assumptions and provided analytical results for the desired steady-state probabilities. In 2015, Xu et al. [7] incorporated copulas in the cyber epidemic models to accommodate the dependences between the cyberattack events. Pastor-Satoras et al. [8] gave a detailed review of the vast research activity concerning cyber epidemic processes, detailing the successful theoretical approaches as well as making their limits and assumptions clear.

Another stream of research focused on economic models of security investments. For example, Gordon and Loeb [1] studied the optimal protection of information, which varies with the information set's vulnerability. Dillon and Pate-Cornell [9] developed a theoretical framework that uses a utility function to explicitly examine the tradeoffs between minimization of the probability of an IS project's failure and maximization of the expected benefits from its performance. Bohme and Moore [10] developed a dynamic model to reflect the interaction between a defender and an attacker and showed how the defender's knowledge about prospective attacks and the sunk costs incurred when upgrading defenses reactively affects the optimal security investment strategy. Many more literature studies can be found in Gordon and Loeb [11] and Wang [12]. In response to the escalating demands from companies to seek better cyber risk management, the market for insurance has emerged and evolved in recent years to provide covers on cyber-related losses. However, the industry has seen a slower pace in market expansion than anticipated due to a number of challenges. The first question is the insurability of cyber risks. Biener et al. [13] focused extensively on this matter by applying Berliner's [14] insurability framework together with empirical analysis. The first insurability criterion is the randomness of the loss occurrence and the conclusion is that it is problematic due to a number of reasons. Their paper also showed that the average loss in different industries differs due to different awareness levels and therefore different resources devoted to self-protection, and the nature of the asset being protected, for example, whether the data include sensitive personal information. The higher the expected loss, the more valuable the breached information must be and the higher the gain for the attacker. Higher frequency for attacks may be correlated to high potential loss. As a result, it may be optimal for a potential victim to spend more on security development, such that the expected total cyber cost is minimized.

Unlike traditional insured risks where the losses emerge from random events, the majority of known cyber loss events are usually consequences of failure in IS defense against intentional attacks. The losses from these attacks are quite profound, for example, the theft and leakage of SONY's internal data in 2014 caused an estimated USD 35 million loss. It is commonly believed that the company's investment on security development plays a key role in reducing the possibility of such loss [10]. Xu and Hua [15] developed a framework to model and price cyber security risk. Due to the constantly evolving technologies of both the attackers and defenders, the attempt to estimate the likelihood and severity of a cyber loss becomes even more challenging. Another obstacle for cyber insurance is the lack of historical loss data attributed to cyber losses that can be used to estimate probabilities of loss and calculate loss values [16]. The data scarcity problem has been addressed by the industry and there have been many attempts to pool relevant data for analytical purposes. Romanosky [17] used a unique dataset of over 12,000 cyber incidents recorded over the years 2004 and 2015 in the USA and examined the costs and causes of cyber incidents. It later went on to discuss the amount of capital a firm should spend on IT security.

Alternatively, one can possibly obtain data other than insurance losses for the purpose of studying cyber risks. Organizations usually have many sources of information about attacks that may be incident upon their networks [18]. One important source is firewall logs. Most, if not all, corporate networks will run a firewall that limits the traffic in and out of the corporate intranet according to some set of rules. Firewalls also log the network activity that they see, particularly the network traffic that is being dropped. Security teams examine firewall logs to get an indication of what attacks are occurring. The log files may show particular IP addresses that are running scans or particular network ports that are being attacked. A network intrusion detection system may be able to monitor and record abnormalities observed for future analysis of attack rates. Alternatively, some research studies focused on analyzing the honeypot-captured cyberattacks to better understand the attack behaviours, for example, Spitzner [19], Almotairi et al. [20], and Zhan et al. [21].

5. Conclusion and Future Research

In this paper, we assume the security level of a system is a quantifiable metric and apply the ruin theoretic framework in assessing the defense failure frequencies. We assume that the security level of a system changes over time due to attack and defense. The security level is then modeled by a modified surplus process: the current security level of an information system can be viewed as the initial surplus; defense investment resulting in an increase in the security level can be viewed as the premium income; the cyberattack arrivals are modeled as a Poisson process; and the impact of attacks is modeled as losses on the security level using an assumed loss distribution. A cyberattack succeeds (or the defense fails) when ruin occurs. In other words, we apply the risk process to model the frequency of the cyber failure. Once the defense failed, an independent financial loss amount is incurred depending on the nature of data being breached.

To our knowledge, this is the first attempt in the literature to apply the ruin theory on IT security investments and risk modeling. Instead of modeling cyber incidence directly, we assume that attacks can occur but unsuccessful if higher security level (strong defense) is in place. We also assume that the security level erodes even if unsuccessful attack happened. This is based on our assumption that the dark web (or cyber criminals) is capable of learning from their past attempts, which leads to a decrease in security level without active upgrading on the defense side. This paper is not meant to propose a new actuarial model for cyber risks, but instead using an actuarial ruin theory framework to gain insights about optimal allocation of cyber security budget.

One important insight derived from this theoretical framework is that there is an optimal allocation of total cyber security budget to (1) IT security maintenance/upkeep spending versus (2) external cyber risk transfer. This has an implication in insurance product design: insurers may consider offer a combination of IT risk management services and risk transfer. The IT risk management services can be jointly offered with or outsourced to IT security firms. The security level is modeled as a numerical level in this paper. In practice, one can develop extensive IT risk assessment framework to produce numeric ratings. However, this is beyond the scope of this paper. When modeling the security level, we used simple models for attack frequencies (Poisson arrivals) and severity (exponentially distributed), as well as the security construction rate (constant) which may be over simplifications of what the reality represents. However, our aim for this paper is to use a theoretical framework to derive insights on cyber security budgeting. A few possibilities to alter these assumptions for future research are listed as follows:

(1) The attacks may be modeled as nonhomogeneous Poisson process. IT security level could potentially also influence the attack behaviour. The attack frequencies might be high for a period of time and low if several attempts were unsuccessful. Alternatively, one can consider using a dependent risk process model to reflect some actual dependencies between attack frequencies and severity, and such model has been studied in the studies of Peng and Wang [22] and Hu and Zhang [23]. On the other hand, some more complicated risk models can be used to model the cyber risk, such as Markov-modulated risk model, Levy risk model, and MAP risk model. Many references can be found in the studies of Asmussen and Albrecher [24], Li et al. [25], Li et al. [26], Zhang et al. [27], Cheung and Feng [28], Yu et al. [29], etc.

(2) Instead of continuous observation of the process, the security officer may wish to adopt a periodic check-up strategy and place occasional boost-ups for the security level. This strategy can then be seen as a risk process that is periodically observed with some occasional capital injections (see Yu et al. [30] and Zhang et al. [31]).

(3) We assumed that the surplus level returns to 0 immediately after breach. Further research may alter this assumption since it may require some time to clear the virus or repair the equipment.

(4) Empirical calibration of model parameters using actual data.

Appendix

A. The Security Development Rate c

For the purpose of applying the surplus process to model the cyber security level, we made a loosening on the assumption for c. Under classical risk theory, it is typical to assume $ct > E(\sum_{i=1}^{N_t} X_i)$ to ensure that ultimate ruin probability is not 1. Under our cyber risk model, it may be unrealistic to assume the same for the security construction rate. Unlike the premium rates that are mainly determined by insurers, the system engineers are usually restrained by available resources and technology and may not have as much control over c. Also, it may be more appropriate to assume that given the same amount of investment, c should be lower when U_t is large and higher when U_t is low. This is due to the constraints on existing technologies and the higher the U_t is, the more difficult it is to strengthen it using existing methods. This will then correspond to a level-dependent risk process. Without newly developed technologies, ultimately $c \to 0$ as $U_t \to \infty$. Under this argument, the ruin probability will be 1 [24]. Some ruin theory discussions on surplus-dependent premiums can be found in Albrecher et al. [32]. Other relevant papers involving discussions on varying premiums may be found in Jasiulewicz [33], Li et al. [34], and Rong and Li [35]. However, most of these papers discussed ruin-related problem assuming $ct > E(\sum_{i=1}^{N_t} X_i)$. In this paper, we assume $c = A(\xi)$ to be a function of the security investment ξ but does not depend on the surplus level. As a result, the ultimate ruin probability $\psi(u)$ is 1 for some values of ξ.

B. Some Analytical Results

In this section, we derive some analytical results assuming that $\{N_t\}_{t\geq 0}$ follows a Poisson process with parameter λ, and $f(x)=\alpha e^{-\alpha x}$. It is a well-known result [36] that the Laplace transform of T_u is found as follows:

$$\tilde{\omega}_u(s)=\left(1-\frac{R_s}{\alpha}\right)e^{-R_s u}, \tag{B.1}$$

where $-R_s<0$ is a root of the characteristic equation:

$$x^2+\left(\alpha-\frac{\lambda+s}{c}\right)x-\frac{\alpha s}{c}=0. \tag{B.2}$$

Note that the derivation was done under the assumption that $c>\lambda E(X)$, but equation (B.1) is not affected if we relax this assumption. This is because $E[e^{-sT_u}I(T_u<\infty)]=E[e^{-sT_u}]=\tilde{\omega}_u(s)$, and that the derivation of $\tilde{\omega}_u(s)$ and $\omega_u(t)$ does not depend on the condition that $c>\lambda E(X)$. Dickson and Li [37] showed that the defective/proper density of T_u satisfies the following equation:

$$\omega_u(t)=\sum_{j=1}^{\infty}\omega_0^{j*}(t)\frac{(\alpha u)^{j-1}e^{-\alpha u}}{\Gamma(j)}, \tag{B.3}$$

where $\omega_0^{j*}(t)$ is the j-fold convolution of $\omega_0(t)$. From Nie et al. [38], we have

$$\omega_0^{j*}(t)=\frac{\lambda^j t^{j-1}e^{-(\lambda+\alpha c)t}}{\Gamma(j)}\,{}_0F_1\left(j+1;\alpha c\lambda t^2\right), \tag{B.4}$$

where

$$\begin{aligned}&{}_pF_q\left(B_1,B_2,\ldots,B_p,C_1,C_2,\ldots,C_q;Z\right)\\&\quad=\sum_{m=0}^{\infty}\frac{(B_1)_m(B_2)_m\ldots\left(B_p\right)_m}{(C_1)_m(C_2)_m\ldots\left(C_p\right)_m}\frac{Z^m}{m!},\end{aligned} \tag{B.5}$$

is the generalized hypergeometric function and $(a)_n=\Gamma(a+n)/\Gamma(a)$ is Pochhammer's symbol. Under the framework proposed in Section 2.2, we can derive the Laplace transform of $\omega_{u,n}(t)$ as follows:

$$\begin{aligned}\tilde{\omega}_{u,n}(s)&=\tilde{\omega}_u(s)\left[\tilde{\omega}_0(s)\right]^{n-1}\\&=\sum_{j=1}^{\infty}\frac{(\alpha u)^{j-1}e^{-\alpha u}}{\Gamma(j)}\left(1-\frac{R_s}{\alpha}\right)^{j+n-1}.\end{aligned} \tag{B.6}$$

The defective/proper density function of $T_{u,n}(t)$ is then

$$\begin{aligned}\omega_{u,n}(t)&=\omega_u*\omega_0^{n-1*}(t)\\&=\sum_{j=1}^{\infty}\omega_0^{j+n-1*}(t)\frac{(\alpha u)^{j-1}e^{-\alpha u}}{\Gamma(j)}\\&=\sum_{j=1}^{\infty}\frac{\lambda^{j+n-1}t^{j+n-2}e^{-(\lambda+\alpha c)t}}{\Gamma(j+n-1)}\,{}_0F_1\left(j+n;\alpha c\lambda t^2\right)\\&\quad\frac{(\alpha u)^{j-1}e^{-\alpha u}}{\Gamma(j)}.\end{aligned} \tag{B.7}$$

Note that for $c\leq\lambda E(x)$, $\Pr(T_{u,n}<\infty)=1$ and equation (B.7) becomes a proper density function. For $c>\lambda E(X)$, we have $\Pr(T_{u,n}<\infty)=\psi(u)\psi(0)^{n-1}$ and that the conditional density function of $T_{u,n}|T_{u,n}<\infty$ becomes $\omega_{u,n}(t)/\psi(u)\psi(0)^{n-1}$.

Data Availability

No real data were used in this manuscript.

Conflicts of Interest

The authors declare that they have no conflicts of interest.

Acknowledgments

Jingchao Li acknowledges the support from the National Natural Science Foundation of China (project no. 11601344), Shenzhen Peacock Program (project no. 000417), and Natural Science Foundation of Guangdong Province (project no. 2020A1515010372).

References

[1] L. A. Gordon and M. P. Loeb, "The economics of information security investment," *ACM Transactions on Information and System Security*, vol. 5, no. 4, pp. 438–457, 2002.
[2] F. Cohen, "Information system attacks: a preliminary classification scheme," *Computers & Securiy*, vol. 16, pp. 29–46, 1997a.
[3] J. L. Whitten and L. D. Bentley, *Systems Analysis and Design Methods*, Irwin McGraww-Hill, New York, NY, USA, 4th edition, 1998.
[4] F. Cohen, "Information system defences: a preliminary classification scheme," *Computers & Securiy*, vol. 16, pp. 94–114, 1997b.
[5] X. Li, T. Parker, and S. Xu, "A stochastic model for quantitative security analysis of networked systems," *IEEE Transactions on Dependable and Secure Computing*, vol. 8, no. 1, pp. 28–43, 2011.
[6] M. Xu and S. Xu, "An extended stochastic model for quantitative security analysis of networked systems," *Internet Mathematics*, vol. 8, no. 3, pp. 288–320, 2012.
[7] M. Xu, G. Da, and S. Xu, "Cyber epidemic models with dependence," *Internet Mathematics*, vol. 11, pp. 69–92, 2015.
[8] R. Pastor-Satorras, C. Castellano, P. V. Mieghem, and A. Vespignani, "Epidemic processes in complex networks," *Reviews of Modern Physics*, vol. 87, no. 3, pp. 925–979, 2015.
[9] R. L. Dillon and M. E. Pate-Cornell, "Including technical and security risks in the development of information systems: a programmatic risk management model," *Systems Engineering*, vol. 8, no. 1, pp. 15–28, 2008.
[10] R. Bohme and T. Moore, "The iterated weakest link: a model of adaptive security investment," in *Proceedings of the WEIS: 8th Workshop on the Economics of Information Security*, London, UK, June 2009.
[11] L. A. Gordon and M. P. Loeb, *Managing Cybersecurity Resources: A Cost-Benefit Analysis*, McGraw-Hill, New York, NY, USA, 2006.
[12] S. S. Wang, "Integrated framework for information security investment and cyber insurance," *Pacific-Basin Finance Journal*, vol. 57, p. 101173, 2019.

[13] C. Biener, M. Eling, and J. H. Wirfs, "Insurability of cyber risk: an empirical analysis," *Geneva Papers on Risk and Insurance-Issues and Practice*, vol. 40, no. 1, pp. 131–158, 2015.
[14] B. Berliner, *Limits of Insurability of Risks*, Prentice-Hall, Englewood Cliffs, NJ, USA, 1982.
[15] M. Xu and L. Hua, "Cybersecurity insurance: modeling and pricing," *North American Actuarial Journal*, vol. 23, no. 2, pp. 220–249, 2019.
[16] PwC, *Managing Cyber Risks with Insurance*, PwC, London, UK, 2014.
[17] S. Romanosky, "Examining the costs and causes of cyber incidents," *Journal of Cybersecurity*, vol. 2, no. 2, pp. 121–135, 2016.
[18] A. Baldwin, I. Cheyas, C. Ioannidis, D. Pym, and J. Williams, "Contagion in cybersecurity attacks," in *Proceedings of the WEIS: 11th Workshop on the Economics of Information Security*, Berlin, Germany, June 2012.
[19] L. Spitzner, *Honeypots: Tracking Hackers*, Addison-Wesley, Boston, MA, USA, 2003.
[20] S. Almotairi, A. Clark, G. Mohay, and J. Zimmermann, "A technique for detecting new attacks in low-interaction honeypot traffic," in *Proceedings of the Fourth International Conference on Internet Monitoring and Protection*, pp. 7–13, Venice, Italy, May 2009.
[21] Z. Zhan, M. Xu, and S. Xu, "Predicting cyber attack rates with extreme values," *IEEE Transactions on Information Forensics and Security*, vol. 10, no. 8, pp. 1666–1677, 2015.
[22] J. Peng and D. Wang, "Uniform asymptotics for ruin probabilities in a dependent renewal risk model with stochastic return on investments," *Stochastics An International Journal of Probability and Stochastic Processes*, vol. 90, no. 3, pp. 432–471, 2018.
[23] X. Hu and L. Zhang, "Ruin probability in a correlated aggregate claims model with common Poisson shocks: application to reinsurance," *Methodology and Computing in Applied Probability*, vol. 18, no. 3, pp. 675–689, 2016.
[24] S. Asmussen and H. Albrecher, *Ruin Probabilities*, World Scientific, Singapore, 2nd edition, 2010.
[25] J. Li, D. C. M. Dickson, and S. Li, "Some ruin problems for the MAP risk mode," *Insurance: Mathematics and Economics*, vol. 65, pp. 1–8, 2015.
[26] J. Li, D. C. M. Dickson, and S. Li, "Analysis of some ruin-related quantities in a Markov-modulated risk model," *Stochastic Models*, vol. 32, no. 3, pp. 351–365, 2016.
[27] Z. Zhang, Y. Yong, and W. Yu, "Valuing equity-linked death benefits in general exponential Levy models," *Journal of Computational and Applied Mathematics*, vol. 365, p. 112377, 2020.
[28] E. C. K. Cheung and R. Feng, "A unified analysis of claim costs up to ruin in a Markovian arrival risk model," *Insurance: Mathematics and Economics*, vol. 53, no. 1, pp. 98–109, 2013.
[29] W. Yu, Y. Yong, G. Guang, Y. Huang, W. Su, and C. Cui, "Valuing guaranteed minimum death benefits by cosine series expansion," *Mathematics*, vol. 7, no. 9, p. 835, 2019.
[30] W. Yu, P. Guo, Q. Wang et al., "On a periodic capital injection and barrier dividend strategy in the compound Poisson risk model," *Mathematics*, vol. 8, no. 4, p. 511, 2020.
[31] Z. Zhang, E. C. K. Cheung, and H. Yang, "On the compound Poisson risk model with periodic capital injections," *ASTIN Bulletin*, vol. 48, no. 1, pp. 435–477, 2017.
[32] H. Albrecher, C. Constantinescu, Z. Palmowski, G. Regensburger, and M. Rosenkranz, "Exact and asymptotic results for insurance risk models with surplus-dependent premiums," *SIAM Journal on Applied Mathematics*, vol. 73, no. 1, pp. p47–66, 2013.
[33] H. Jasiulewicz, "Probability of ruin with variable premium rate in a Markovian environment," *Insurance: Mathematics and Economics*, vol. 29, pp. 291–296, 2001.
[34] S. Li, D. Landriault, and C. Lemieux, "A risk model with varying premiums: its risk management implications," *Insurance: Mathematics and Economics*, vol. 60, pp. 38–46, 2014.
[35] W. Rong and W. Li, "The probability of ruin in a kind of cox risk model with variable premium rate," *Scandinavian Actuarial Journal*, vol. 2, pp. 121–132, 2004.
[36] D. C. M. Dickson, *Insurance Risk and Ruin*, Cambridge University Press, Cambridge, UK, 2005.
[37] D. C. M. Dickson and S. Li, "Finite time ruin problems for the Erlang(2) risk model," *Insurance: Mathematics and Economics*, vol. 46, pp. 12–18, 2010.
[38] C. Nie, D. C. M. Dickson, and S. Li, "The finite time ruin probability in a risk model with capital injections," *Scandinavian Actuarial Journal*, vol. 4, pp. 301–318, 2015.

Hindawi
Mathematical Problems in Engineering
Volume 2020, Article ID 3856323, 13 pages
https://doi.org/10.1155/2020/3856323

Research Article

An Uncertain Alternating Renewal Insurance Risk Model

Jia Zhai,[1] **Haitao Zheng**,[2] **Manying Bai**,[2] **and Yunyun Jiang**[3]

[1] *School of Economics, Beijing International Studies University, Beijing 100024, China*
[2] *School of Economics and Management, Beihang University, Beijing 100191, China*
[3] *School of Economics, Peking University, Beijing 100871, China*

Correspondence should be addressed to Haitao Zheng; zhenghaitao@buaa.edu.cn

Received 17 April 2020; Accepted 20 May 2020; Published 6 July 2020

Guest Editor: Wenguang Yu

The claim process in an insurance risk model with uncertainty is traditionally described by an uncertain renewal reward process. However, the claim process actually includes two processes, which are called the report process and the payment process, respectively. An alternative way is to describe the claim process by an uncertain alternating renewal reward process. Therefore, this paper proposes an insurance risk model under uncertain measure in which the claim process is supposed to be an alternating renewal reward process and the premium process is regarded as a renewal reward process. Then, the paper also gives the inverse uncertainty distribution of the insurance risk process. The expression of ruin index and the uncertainty distribution of the ruin time are derived which both have explicit expressions based on given uncertainty distributions. Finally, several examples are provided to illustrate the modeling ideas.

1. Introduction

The classical insurance risk models and their extended models generally assume that claim numbers and claim amounts are random variables. They also suppose that the time of the accident and the time of payment are consistent; that is, the insurance company immediately pays compensation to the insured when the accident occurs. Then, many types of insurance risk models are presented by means of stochastic process based on the probability theory; several scholars, for example, Dickson and Hipp [1], Li and Garrido [2], Dickson and Hipp [3], Chun [4], Gerber and Shiu [5], Sundt and Teugels [6], Paulsen and Gjessing [7], Albrecher and Hipp [8], and Yu et al. [9], extend the insurance risk model by considering inflation, dividend, and tax. Using Lévy process to model insurance risk processes and other insurance product has become popular, see, for example, Griffin [10], Biffis and Kyprianou [11], Zhang et al. [12], and Yu et al. [13].

However, for a new insurance product, it usually lacks historical data to estimate probability distributions. In this situation, we often use the belief degrees of the claim numbers and claim amounts estimated by some experienced domain experts to describe the indeterminacy. Kahneman and Tversky [14] find that humans tend to place too much emphasis on unlikely events. Thus, probability theory is difficult to model the belief degree unless we get enough historical data, and it is unreasonable to describe an insurance risk process with stochastic process. The research about the insurance risk process that is described by a stochastic process has been gradually challenged by many scholars. De Wit [15] first developed an insurance risk process under fuzzy theory. Then, the insurance risk processes with fuzziness are studied by Lemaire [16], Cummins and Derrig [17], Derrig and Ostaszewski [18], Yu [19], Shapiro [20], and Li et al. [21]. Furthermore, Huang et al. [22] and Shapiro [23] regard the claim amounts as fuzzy random variable and propose the fuzzy random risk model.

When the estimated distributions are not close enough to the real frequencies, Liu [24] invented the uncertainty theory, which is used to model human indeterminacy due to belief degrees. Now, the theory has been applied to construct insurance risk models. Considering the human uncertainty in running an insurance company, Li et al. [25] propose a premium principle under uncertain measure via the distortion function. To study the evolution of uncertain phenomenon over time, Liu [26] develops the concept of uncertain process. Meanwhile, Liu also presents the uncertain renewal process as a special and important case. After that, Liu [27] researches the uncertain renewal reward process. Yao and Relescu [28] apply the uncertain renewal process to analyze an age replacement policy. In addition, Yao [29] studies the uncertain calculus of the uncertain renewal process by proposing the integration and differentiation about the renewal process. Yao and Li [30] regard off-times and on-times as uncertain variables and propose an uncertain alternating renewal process. Zhang et al. [31] also show a delayed renewal process for uncertain interarrival times, where the first interarrival time is completely different from other times. Recently, Liu [32] provides an uncertain insurance risk model by applying the renewal reward process and derives the ruin index. In the uncertain insurance risk model, Liu assumes that the premium is a real function proportional to time and the claim amount obeys an uncertain renewal reward process. Based on Liu's insurance risk process, Yao and Zhou [33] further investigate the uncertainty distribution of the ruin time. Yao and Qin [34] point out that the premiums follow the renewal reward process in actual applications rather than a real function, so they propose an uncertain insurance risk process in which both the premiums and claims follow the uncertain renewal reward process. Liu et al. [35] extend Liu's model and discuss an uncertain insurance risk model with a variational lower limit. Liu and Yang [36] establish an uncertain insurance risk process considering an insurance company having multiple claims with uncertainty theory.

In the above studies, the claim process is regarded as a renewal process or a renewal reward process. In fact, the moment of the accident and the moment of the payment are not simultaneous, and in many types of insurance, the time interval between a claim event and the determination of the payment for the claim can be very long [37]. So, the claim process should include two processes: the report process and the payment process. The report process refers to the insured formally notifying the insurance company about an event. The payment process refers to the process whereby the insurer reviews the claim and sees whether the event or situation falls within the risks covered by the policy. That is to say, the insurer will need to determine that the claim meets the terms and conditions of the insurance policy. Obviously, the two processes should follow different uncertainty distributions. Therefore, it is more reasonable to view the claim process as an uncertain alternating renewal reward process. At present, few studies have considered the claim process in an insurance risk model as an uncertain alternating renewal process.

Inspired by the ideas we have reviewed, this paper proposes an insurance risk model in which the claims follow an uncertain alternating renewal reward process, while the premiums follow an uncertain renewal reward process. The inverse uncertainty distribution of insurance risk process, ruin index, and ruin time are derived. We also compare our model with Yao and Qin's model through numerical examples and explain the significance of describing the claim process by uncertain alternating renewal reward process.

The rest of the paper is organized as follows. Section 2 presents an uncertain alternating renewal insurance risk model and gives the expressions of ruin index and ruin time. In Section 3, several examples are provided to clarify the modeling idea of the insurance risk model. Finally, conclusions will be listed at the end.

2. An Uncertain Alternating Renewal Insurance Risk Model

Next, we study an insurance risk process in an uncertain environment. The premium process and the claim process are regarded as an uncertain renewal reward process and an uncertain alternating renewal reward process, respectively. In the following discussions, we give an assumption that the new claim event will not occur during the period of reviewing the current claim. Let the premium process be an uncertain renewal reward process:

$$R_{1t} = \sum_{i=1}^{N_{1t}} P_i, \tag{1}$$

where $P_1, P_2, \ldots$ are independent uncertain premium amounts, and

$$N_{1t} = \max_{n\geq 0}\{n \mid \xi_{11} + \xi_{12} + \cdots + \xi_{1n} \leq t\}, \tag{2}$$

is an uncertain renewal process with independent uncertain interarrival times $\xi_{11}, \xi_{12}, \ldots$.

The claim process is an uncertain alternating renewal reward process:

$$R_{2t} = \sum_{i=1}^{N_{2t}} C_i, \tag{3}$$

where $C_1, C_2, \ldots$ are independent uncertain claim amounts. Consider the claim process as an uncertain alternating renewal reward process, and the claim process can be described as the following process. The first event happens as well as the insured reports claim for an uncertain time ξ_{21}. After an uncertain time ξ_{21}, the insurer reviews your claim and provides a payout for an uncertain time η_{21} and at an uncertain claim amount C_1. Next, the second event happens and the insured reports claim for an uncertain time ξ_{22}. After an uncertain time ξ_{22}, the insurer reviews your claim and provides a payout for an uncertain time η_{22} and at an uncertain claim amount C_2. The process continues infinitely (see Figure 1). Then, let

$$\begin{aligned} N_{2t} &= \max_{n\geq 0}\{n \mid (\xi_{21} + \eta_{21}) + (\xi_{22} + \eta_{22}) + \cdots + (\xi_{2n} + \eta_{2n}) \leq t\} \\ &= \sup_{n\geq 0}\{n \mid 0 \leq (\xi_{21} + \eta_{21}) + (\xi_{22} + \eta_{22}) + \cdots + (\xi_{2n} + \eta_{2n}) \\ &\leq t < (\xi_{21} + \eta_{21}) + (\xi_{22} + \eta_{22}) + \cdots + (\xi_{2n} + \eta_{2n}) + \xi_{2n+1}\}, \end{aligned} \tag{4}$$

be an uncertain alternating renewal process, where $\xi_{21}, \xi_{22}, \ldots$ and $\eta_{21}, \eta_{22}, \ldots$ are independent uncertain

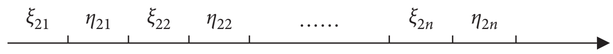

FIGURE 1: Alternating renewal process.

interarrival times. $S_n = (\xi_{21} + \eta_{21}) + (\xi_{22} + \eta_{22}) + \cdots + (\xi_{2n} + \eta_{2n})$ denotes the moment of the payment of the nth claim.

Let a be the initial capital, then the capital of an insurance company at time t is

$$Z_t = a + R_{1t} - R_{2t}. \tag{5}$$

The Z_t is an insurance risk model with an uncertain alternating renewal reward process. Apparently, once $Z_t < 0$, the insurance company faces the risk of ruin.

For an uncertain insurance risk model Z_t, in order to obtain some important theorems, the following notations will be used:

Φ: the uncertainty distribution of the premium amount P_1

Ψ: the uncertainty distribution of the claim amount C_1

μ_1: the uncertainty distribution of the interarrival time ξ_{11}

μ_2: the uncertainty distribution of the interarrival time ξ_{21}

λ: the uncertainty distribution of the interarrival time η_{21}

2.1. Ruin Index. The ruin index can be defined as the uncertain measure that the capital $Z_t < 0$ at time t. This section derives the explicit forms of the ruin index. Firstly, we get the inverse uncertainty distribution of an uncertain insurance risk process.

Theorem 1. *For an uncertain insurance risk process $Z_t = a + R_{1t} - R_{2t}$, the inverse uncertainty distribution of Z_t can be derived as*

$$\Upsilon_t^{-1}(\alpha) = a + \frac{\Phi^{-1}(\alpha)}{\mu_1^{-1}(1-\alpha)} t - \frac{\Psi^{-1}(\alpha)}{\mu_2^{-1}(\alpha) + \lambda^{-1}(\alpha)} t. \tag{6}$$

Proof. Note that, for any

$$\gamma \in \bigcup_{i=1}^{\infty} \left\{ \left(\xi_{1i} \geq \mu_1^{-1}(1-\alpha)\right) \cap \left(P_i \leq \Phi^{-1}(\alpha)\right) \cap \left(\xi_{2i} + \eta_{2i} \leq \mu_2^{-1}(\alpha) + \lambda_2^{-1}(\alpha)\right) \cap \left(C_i \geq \Psi^{-1}(1-\alpha)\right) \right\}, \tag{7}$$

we have

$$\begin{aligned}
Z_t(\gamma) &= a + \sum_{i=1}^{N_{1t}(\gamma)} P_i - \sum_{i=1}^{N_{2t}(\gamma)} C_i \\
&\leq a + \frac{\Phi^{-1}(\alpha)}{\mu_1^{-1}(1-\alpha)} t - \frac{\Psi^{-1}(\alpha)}{\mu_2^{-1}(\alpha) + \lambda^{-1}(\alpha)} t, \\
&\left\{ Z_t(\gamma) \leq a + \frac{\Phi^{-1}(\alpha)}{\mu_1^{-1}(1-\alpha)} t - \frac{\Psi^{-1}(\alpha)}{\mu_2^{-1}(\alpha) + \lambda^{-1}(\alpha)} t \right\} \\
&\supset \bigcup_{i=1}^{\infty} \left\{ \left(\xi_{1i} \geq \mu_1^{-1}(1-\alpha)\right) \cap \left(P_i \leq \Phi^{-1}(\alpha)\right) \cap \left(\xi_{2i} + \eta_{2i} \leq \mu_2^{-1}(\alpha) + \lambda_2^{-1}(\alpha)\right) \cap \left(C_i \geq \Psi^{-1}(1-\alpha)\right) \right\}.
\end{aligned} \tag{8}$$

Since the uncertain variables are independent and according to the property of uncertain measure, we can obtain

$$\begin{aligned}
&M\left\{ \bigcap_{i=1}^{\infty} \left(\xi_{1i} \geq \mu_1^{-1}(1-\alpha)\right) \cap \left(P_i \leq \Phi^{-1}(\alpha)\right) \cap \left(\xi_{2i} + \eta_{2i} \leq \mu_2^{-1}(\alpha) + \lambda_2^{-1}(\alpha)\right) \cap \left(C_i \geq \Psi^{-1}(1-\alpha)\right) \right\} \\
&= \bigwedge_{i=1}^{\infty} M\left\{\xi_{1i} \geq \mu_1^{-1}(1-\alpha)\right\} \wedge M\left\{P_i \leq \Phi^{-1}(\alpha)\right\} \wedge M\left\{\xi_{2i} + \eta_{2i} \leq \mu_2^{-1}(\alpha) + \lambda_2^{-1}(\alpha)\right\} \wedge M\left\{C_i \geq \Psi^{-1}(1-\alpha)\right\} \\
&= \bigwedge_{i=1}^{\infty} \alpha \wedge \alpha \wedge \alpha \wedge \alpha \\
&= \alpha.
\end{aligned} \tag{9}$$

Furthermore, it follows from the monotonicity of uncertain measure that

$$M\left\{Z_t(\gamma) \le a + \frac{\Phi^{-1}(\alpha)}{\mu_1^{-1}(1-\alpha)}t - \frac{\Psi^{-1}(\alpha)}{\mu_2^{-1}(\alpha)+\lambda^{-1}(\alpha)}t\right\} \ge \alpha. \quad (10)$$

In addition, since for any

$$\gamma \in \bigcap_{i=1}^{\infty}\left\{\left(\xi_{1i} < \mu_1^{-1}(1-\alpha)\right) \cap \left(P_i > \Phi^{-1}(\alpha)\right) \cap \left(\xi_{2i} + \eta_{2i} > \mu_2^{-1}(\alpha) + \lambda_2^{-1}(\alpha)\right) \cap \left(C_i < \Psi^{-1}(1-\alpha)\right)\right\}, \quad (11)$$

we have

$$\begin{aligned} Z_t(\gamma) &= a + \sum_{i=1}^{N_{1t}(\gamma)} P_i - \sum_{i=1}^{N_{2t}(\gamma)} C_i \\ &> a + \frac{\Phi^{-1}(\alpha)}{\mu_1^{-1}(1-\alpha)}t - \frac{\Psi^{-1}(\alpha)}{\mu_2^{-1}(\alpha)+\lambda^{-1}(\alpha)}t, \\ &\left\{Z_t(\gamma) > a + \frac{\Phi^{-1}(\alpha)}{\mu_1^{-1}(1-\alpha)}t - \frac{\Psi^{-1}(\alpha)}{\mu_2^{-1}(\alpha)+\lambda^{-1}(\alpha)}t\right\} \\ &\supset \bigcap_{i=1}^{\infty}\left\{\left(\xi_{1i} < \mu_1^{-1}(1-\alpha)\right) \cap \left(P_i > \Phi^{-1}(\alpha)\right) \cap \left(\xi_{2i} + \eta_{2i} > \mu_2^{-1}(\alpha) + \lambda_2^{-1}(\alpha)\right) \cap \left(C_i < \Psi^{-1}(1-\alpha)\right)\right\}. \end{aligned} \quad (12)$$

According to the independence of these uncertain variables again that

$$\begin{aligned} &M\left\{\bigcup_{i=1}^{\infty}\left(\xi_{1i} < \mu_1^{-1}(1-\alpha)\right) \cap \left(P_i > \Phi^{-1}(\alpha)\right) \cap \left(\xi_{2i} + \eta_{2i} > \mu_2^{-1}(\alpha) + \lambda_2^{-1}(\alpha)\right) \cap \left(C_i < \Psi^{-1}(1-\alpha)\right)\right\} \\ &= \bigwedge_{i=1}^{\infty} M\left\{\xi_{1i} < \mu_1^{-1}(1-\alpha)\right\} \wedge M\left\{P_i > \Phi^{-1}(\alpha)\right\} \wedge M\left\{\xi_{2i} + \eta_{2i} > \mu_2^{-1}(\alpha) + \lambda_2^{-1}(\alpha)\right\} \wedge M\left\{C_i < \Psi^{-1}(1-\alpha)\right\} \\ &= \bigwedge_{i=1}^{\infty} (1-\alpha) \wedge (1-\alpha) \wedge (1-\alpha) \wedge (1-\alpha) \\ &= 1-\alpha, \end{aligned} \quad (13)$$

we get

$$M\left\{Z_t(\gamma) > a + \frac{\Phi^{-1}(\alpha)}{\mu_1^{-1}(1-\alpha)}t - \frac{\Psi^{-1}(\alpha)}{\mu_2^{-1}(\alpha)+\lambda^{-1}(\alpha)}t\right\} \ge 1-\alpha, \quad (14)$$

which is equivalent to the following form (see duality of uncertain measure):

$$M\left\{Z_t(\gamma) \le a + \frac{\Phi^{-1}(\alpha)}{\mu_1^{-1}(1-\alpha)}t - \frac{\Psi^{-1}(\alpha)}{\mu_2^{-1}(\alpha)+\lambda^{-1}(\alpha)}t\right\} \le \alpha. \quad (15)$$

Above all, $M\{Z_t(\gamma) \le a + ((\Phi^{-1}(\alpha))/(\mu_1^{-1}(1-\alpha)))t - ((\Psi^{-1}(\alpha))/(\mu_2^{-1}(\alpha)+\lambda^{-1}(\alpha)))t\} = \alpha$.

Theorem 1 is proved. □

Theorem 2. *Let $Z_t = a + R_{1t} - R_{2t}$, the ruin index can be expressed as*

$$\text{ruin} = \max_{m\ge 0, n\ge 1} \alpha_{m,n}, \quad (16)$$

where m and n are nonnegative integers and

$$\alpha_{m,n} = \sup\left\{\alpha \in [0,1] \mid n\mu_2^{-1}(\alpha) + n\lambda^{-1}(\alpha) - (m+1)\mu_1^{-1}(1-\alpha) < 0, a + m\Phi^{-1}(\alpha) - n\Psi^{-1}(1-\alpha) < 0\right\}. \quad (17)$$

Proof. Obviously, the ruin risk can be calculated by

$$\left\{\inf_{t\geq 0} Z_t < 0\right\} = \bigcup_{m=0}^{\infty}\bigcup_{n=1}^{\infty}\left\{\left(\sum_{j=1}^{n}\left(\xi_{2j}+\eta_{2j}\right) < \sum_{i=1}^{m+1}\xi_{1i}\right)\cap\left(a+\sum_{i=1}^{m}P_i-\sum_{j=1}^{n}C_j<0\right)\right\}. \tag{18}$$

(1) For given nonnegative m and n,

$$\begin{aligned}&\left\{\left(\sum_{j=1}^{n}\left(\xi_{2j}+\eta_{2j}\right) < \sum_{i=1}^{m+1}\xi_{1i}\right)\cap\left(a+\sum_{i=1}^{m}P_i-\sum_{j=1}^{n}C_j<0\right)\right\}\\ &\supset \bigcap_{i=1}^{m+1}\left\{\xi_{1i}>\mu_1^{-1}\left(1-\alpha_{m,n}\right)\right\}\cap\bigcap_{i=1}^{m}\left\{P_i\leq\Phi^{-1}\left(\alpha_{m,n}\right)\right\}\cap\bigcap_{j=1}^{n}\left\{\left(\xi_{2j}+\eta_{2j}\leq\mu_2^{-1}\left(\alpha_{m,n}\right)+\lambda^{-1}\left(\alpha_{m,n}\right)\right)\cap\left(C_j>\Psi^{-1}\left(\alpha_{m,n}\right)\right)\right\}.\end{aligned} \tag{19}$$

Then, we have

$$\begin{aligned}&M\left\{\left(\sum_{j=1}^{n}\left(\xi_{2j}+\eta_{2j}\right) < \sum_{i=1}^{m+1}\xi_{1i}\right)\cap\left(a+\sum_{i=1}^{m}P_i-\sum_{j=1}^{n}C_j<0\right)\right\}\\ &\geq \bigcap_{i=1}^{m+1}\left\{\xi_{1i}>\mu_1^{-1}\left(1-\alpha_{m,n}\right)\right\}\cap\bigcap_{i=1}^{m}\left\{P_i\leq\Phi^{-1}\left(\alpha_{m,n}\right)\right\}\cap\bigcap_{j=1}^{n}\left\{\left(\xi_{2j}+\eta_{2j}\leq\mu_2^{-1}\left(\alpha_{m,n}\right)+\lambda^{-1}\left(\alpha_{m,n}\right)\right)\cap\left(C_j>\Psi^{-1}\left(\alpha_{m,n}\right)\right)\right\}\\ &\geq \bigwedge_{i=1}^{m+1}M\left\{\xi_{1i}>\mu_1^{-1}\left(1-\alpha_{m,n}\right)\right\}\wedge\bigwedge_{i=1}^{m}M\left\{P_i\leq\Phi^{-1}\left(\alpha_{m,n}\right)\right\}\wedge\bigwedge_{j=1}^{n}M\left\{\left(\xi_{2j}+\eta_{2j}\leq\mu_2^{-1}\left(\alpha_{m,n}\right)+\lambda^{-1}\left(\alpha_{m,n}\right)\right)\wedge\left(C_j>\Psi^{-1}\left(\alpha_{m,n}\right)\right)\right\}\\ &= \alpha_{m,n},\\ M&\left\{\inf_{t\geq 0} Z_t<0\right\} = M\left\{\bigcup_{m=0}^{\infty}\bigcup_{n=1}^{\infty}\left(\sum_{j=1}^{n}\left(\xi_{2j}+\eta_{2j}\right) < \sum_{i=1}^{m+1}\xi_{1i}\right)\cap\left(a+\sum_{i=1}^{m}P_i-\sum_{j=1}^{n}C_j<0\right)\right\}\\ &\geq \max_{m\geq 0,n\geq 1} M\left\{\left(\sum_{j=1}^{n}\left(\xi_{2j}+\eta_{2j}\right) < \sum_{i=1}^{m+1}\xi_{1i}\right)\cap\left(a+\sum_{i=1}^{m}P_i-\sum_{j=1}^{n}C_j<0\right)\right\}\\ &= \max_{m\geq 0,n\geq 1}\alpha_{m,n}.\end{aligned} \tag{20}$$

(2) For given nonnegative m and n,

$$\begin{aligned}&\left\{\left(\sum_{j=1}^{n}\left(\xi_{2j}+\eta_{2j}\right) < \sum_{i=1}^{m+1}\xi_{1i}\right)\cap\left(a+\sum_{i=1}^{m}P_i-\sum_{j=1}^{n}C_j<0\right)\right\}\\ &\subset \bigcup_{i=1}^{m+1}\left\{\xi_{1i}>\mu_1^{-1}\left(1-\alpha_{m,n}\right)\right\}\cup\bigcup_{i=1}^{m}\left\{P_i\leq\Phi^{-1}\left(\alpha_{m,n}\right)\right\}\cup\bigcup_{j=1}^{n}\left\{\left(\xi_{2j}+\eta_{2j}\leq\mu_2^{-1}\left(\alpha_{m,n}\right)+\lambda^{-1}\left(\alpha_{m,n}\right)\right)\cup\left(C_j>\Psi^{-1}\left(\alpha_{m,n}\right)\right)\right\}.\end{aligned} \tag{21}$$

Then, we also have

$$\begin{aligned}
&\bigcup_{m=0}^{\infty}\bigcup_{n=1}^{\infty}\left\{\left(\sum_{j=1}^{n}\left(\xi_{2j}+\eta_{2j}\right)<\sum_{i=1}^{m+1}\xi_{1i}\right)\cap\left(a+\sum_{i=1}^{m}P_i-\sum_{j=1}^{n}C_j<0\right)\right\}\\
&\subset\bigcup_{i=1}^{\infty}\bigcup_{n=1}^{\infty}\bigcup_{m=i-1}^{\infty}\left\{\xi_{1i}>\mu_1^{-1}\left(1-\alpha_{m,n}\right)\right\}\cup\bigcup_{i=1}^{\infty}\bigcup_{n=1}^{\infty}\bigcup_{m=i-1}^{\infty}\left\{P_i\le\Phi^{-1}\left(\alpha_{m,n}\right)\right\}\\
&\cup\bigcup_{j=1}^{\infty}\bigcup_{m=0}^{\infty}\bigcup_{n=j}^{\infty}\left\{\left(\xi_{2j}+\eta_{2j}\le\mu_2^{-1}\left(\alpha_{m,n}\right)+\lambda^{-1}\left(\alpha_{m,n}\right)\right)\cup\left(C_j>\Psi^{-1}\left(\alpha_{m,n}\right)\right)\right\}\\
&=\bigcup_{i=1}^{\infty}\left\{\xi_{1i}>\bigwedge_{n=1}^{\infty}\bigwedge_{m=i-1}^{\infty}\mu_1^{-1}\left(1-\alpha_{m,n}\right)\right\}\cup\bigcup_{i=1}^{\infty}\left\{P_i\le\bigvee_{n=1}^{\infty}\bigvee_{m=i-1}^{\infty}\Phi^{-1}\left(\alpha_{m,n}\right)\right\}\\
&\cup\bigcup_{j=1}^{\infty}\left\{\left(\xi_{2j}+\eta_{2j}\le\bigvee_{m=0}^{\infty}\bigvee_{n=j}^{\infty}\left(\mu_2^{-1}\left(\alpha_{m,n}\right)+\lambda^{-1}\left(\alpha_{m,n}\right)\right)\right)\cup\left(C_j>\bigwedge_{m=0}^{\infty}\bigwedge_{n=j}^{\infty}\Psi^{-1}\left(\alpha_{m,n}\right)\right)\right\}.
\end{aligned}\tag{22}$$

Similarly, it follows from definition of uncertain measure that

$$\begin{aligned}
&M\left\{\inf_{t\ge0}Z_t<0\right\}\le\bigvee_{i=1}^{\infty}M\left\{\xi_{1i}>\bigwedge_{n=1}^{\infty}\bigwedge_{m=i-1}^{\infty}\mu_1^{-1}\left(1-\alpha_{m,n}\right)\right\}\vee\bigvee_{i=1}^{\infty}M\left\{P_i\le\bigvee_{n=1}^{\infty}\bigvee_{m=i-1}^{\infty}\Phi^{-1}\left(\alpha_{m,n}\right)\right\}\\
&\quad\vee\bigvee_{j=1}^{\infty}M\left\{\xi_{2j}+\eta_{2j}\le\bigvee_{m=0}^{\infty}\bigvee_{n=j}^{\infty}\left(\mu_2^{-1}\left(\alpha_{m,n}\right)+\lambda^{-1}\left(\alpha_{m,n}\right)\right)\right\}\vee\bigvee_{j=1}^{\infty}M\left\{C_j>\bigwedge_{m=0}^{\infty}\bigwedge_{n=j}^{\infty}\Psi^{-1}\left(\alpha_{m,n}\right)\right\}\\
&=\max_{m,n\ge0}\alpha_{m,n}.
\end{aligned}\tag{23}$$

From (1) and (2), we can draw

$$M\left\{\inf_{t\ge0}Z_t<0\right\}=\max_{m,n\ge0}\alpha_{m,n}.\tag{24}$$

Theorem 2 is proved. □

Theorem 3. *Let $Z_t=a+R_{1t}-R_{2t}$ be an uncertain alternating renewal insurance risk process. Then, the ruin index can be calculated by the following form:*

$$\begin{aligned}
\text{ruin}=&\max_{m\ge0,n\ge1}\sup_{x,y\ge0}\left(1-\mu_1\left(\frac{x}{m+1}\right)\right)\wedge\mu_2\left(\frac{x}{2n}\right)\wedge\lambda\left(\frac{x}{2n}\right)\\
&\wedge\Phi\left(\frac{y}{m}\right)\wedge\left(1-\Psi\left(\frac{a+y}{n}\right)\right).
\end{aligned}\tag{25}$$

Proof. It is obvious that

$$\begin{aligned}
&M\left\{\left(\sum_{j=1}^{n}\left(\xi_{2j}+\eta_{2j}\right)<\sum_{i=1}^{m+1}\xi_{1i}\right)\cap\left(a+\sum_{i=1}^{m}P_i-\sum_{j=1}^{n}C_j<0\right)\right\}\\
&M\left\{\sum_{j=1}^{n}\left(\xi_{2j}+\eta_{2j}\right)<\sum_{i=1}^{m+1}\xi_{1i}\right\}\wedge M\left\{a+\sum_{i=1}^{m}P_i-\sum_{j=1}^{n}C_j<0\right\}.
\end{aligned}\tag{26}$$

Because we assume the uncertain interarrival times are independent, we have

$$\begin{aligned}
&M\left\{\sum_{j=1}^{n}\left(\xi_{2j}+\eta_{2j}\right)<\sum_{i=1}^{m+1}\xi_{1i}\right\}\\
&=M\left\{\sum_{j=1}^{n}\left(\xi_{2j}+\eta_{2j}\right)-\sum_{i=1}^{m+1}\xi_{1i}<0\right\}\\
&=\sup_{x\ge0}\left(1-\mu_1\left(\frac{x}{m+1}\right)\right)\wedge\mu_2\left(\frac{x}{2n}\right)\wedge\lambda\left(\frac{x}{2n}\right),\\
&M\left\{a+\sum_{i=1}^{m}P_i-\sum_{j=1}^{n}C_j<0\right\}\\
&=\sup_{y\ge0}\Phi\left(\frac{y}{m}\right)\wedge\left(1-\Psi\left(\frac{a+y}{n}\right)\right).
\end{aligned}\tag{27}$$

Hence,

$$\begin{aligned}
\text{ruin}=M\left\{\inf_{t\ge0}Z_t<0\right\}=&\max_{m\ge0,n\ge1}\sup_{x,y\ge0}\left(1-\mu_1\left(\frac{x}{m+1}\right)\right)\\
&\wedge\mu_2\left(\frac{x}{2n}\right)\wedge\lambda\left(\frac{x}{2n}\right)\wedge\Phi\left(\frac{y}{m}\right)\wedge\left(1-\Psi\left(\frac{a+y}{n}\right)\right).
\end{aligned}\tag{28}$$

Theorem 3 is proved. □

When uncertain variables P_1, ξ_{11}, C_1, ξ_{21}, and η_{22} have determinate uncertainty distributions and corresponding inverse uncertainty distributions exist, we can calculate the crisp expressions of ruin index through Theorem 3 and Theorem 2, respectively.

2.2. Ruin Time. In addition to the ruin index, ruin time can also be used to measure the risk of an insurance company. Next, the definition of ruin time will be given, and the uncertainty distribution of ruin time can be derived.

Let $Z_t = a + \sum_{i=1}^{N_{1t}} P_i - \sum_{j=1}^{N_{2t}} C_j$ be the uncertain alternating renewal insurance risk process of an insurance company. Then, the ruin time of the insurance company can be defined as

$$\tau = \inf\{t \geq 0 \mid Z_t < 0\}. \tag{29}$$

It is easy to know that $\tau = +\infty$ means that the insurance company will not ruin. Therefore, for any $t \geq 0$, the ruin index also can be expressed in the following form:

$$M\{\tau < +\infty\} = \lim_{t \longrightarrow \infty} M\{\tau \leq t\}, \tag{30}$$

where $M\{\tau \leq t\}$ denotes the uncertainty distribution of the ruin time.

We assume that the nth claim occurs at the instant $S_n = \sum_{i=1}^{n} (\xi_{2i} + \eta_{2i})$ and $N_{1t} = m$ at this time. Thus, the capital of the insurance company at the nth claim is

$$Y_{m,n} = a + \sum_{i=1}^{m} P_i - \sum_{j=1}^{n} C_j. \tag{31}$$

Then, we have

$$\{\tau \leq t\} = \left\{\inf_{0 \leq s \leq t} Z_s < 0\right\} = \bigcup_{m=0}^{\infty} \bigcup_{n=1}^{\infty} \left\{\sum_{i=1}^{m} \xi_{1i} \leq t, \sum_{j=1}^{n} \left(\xi_{2j} + \eta_{2j}\right) \leq t, Y_{m,n} < 0\right\}. \tag{32}$$

The uncertain event $\{\sum_{i=1}^{m} \xi_{1i} \leq t, \sum_{j=1}^{n} (\xi_{2j} + \eta_{2j}) \leq t, Y_{m,n} < 0\}$ means that the nth claim occurs before the instant t, and the capital of the insurance company is less than 0 at this time.

Theorem 4. *Suppose that the inverse uncertainty distributions of all the uncertain variables exist in the insurance risk process. Then,*

$$M\left\{\sum_{i=1}^{m} \xi_{1i} \leq t, \sum_{j=1}^{n} \left(\xi_{2j} + \eta_{2j}\right) \leq t, Y_{m,n} < 0\right\} = \alpha_{m,n}(t), \tag{33}$$

where

$$\begin{aligned} \alpha_{m,n}(t) = {} & \sup\left\{\alpha \in [0,1] \mid m\mu_1^{-1}(\alpha) \leq t\right\} \wedge \sup\left\{\alpha \in [0,1] \mid n\mu_2^{-1}(\alpha) + n\lambda^{-1}(\alpha) \leq t\right\} \\ & \wedge \sup\left\{\alpha \in [0,1] \mid a + m\Phi^{-1}(\alpha) - n\Psi^{-1}(1-\alpha) \leq 0\right\}. \end{aligned} \tag{34}$$

Proof. Since

$$\begin{aligned} & M\left\{\sum_{i=1}^{m} \xi_{1i} \leq t, \sum_{j=1}^{n} \left(\xi_{2j} + \eta_{2j}\right) \leq t, Y_{m,n} < 0\right\}, \\ & M\left\{\sum_{i=1}^{m} \xi_{1i} \leq t, \sum_{j=1}^{n} \left(\xi_{2j} + \eta_{2j}\right) \leq t, a + \sum_{i=1}^{m} P_i - \sum_{j=1}^{n} C_j < 0\right\}, \\ & \alpha_{m,n}(t) = \sup\left\{\alpha \in [0,1] \mid m\mu_1^{-1}(\alpha) \leq t\right\} \wedge \sup\left\{\alpha \in [0,1] \mid n\mu_2^{-1}(\alpha) + n\lambda^{-1}(\alpha) \leq t\right\} \\ & \qquad \wedge \sup\left\{\alpha \in [0,1] \mid a + m\Phi^{-1}(\alpha) - n\Psi^{-1}(1-\alpha) \leq 0\right\}, \end{aligned} \tag{35}$$

then, we have

$$\begin{aligned} & \left\{\sum_{i=1}^{m} \xi_{1i} \leq t, \sum_{j=1}^{n} \left(\xi_{2j} + \eta_{2j}\right) \leq t, Y_{m,n} < 0\right\}, \\ & \supset \bigcap_{i=1}^{m} \left\{\xi_{1i} \leq \mu_1^{-1}\left(\alpha_{m,n}(t)\right)\right\} \cap \bigcap_{j=1}^{n} \left\{\left(\xi_{2j} + \eta_{2j}\right) \leq \mu_2^{-1}\left(\alpha_{m,n}(t)\right) + \lambda^{-1}\left(\alpha_{m,n}(t)\right)\right\} \\ & \cap \bigcap_{i=1}^{m} \left\{P_i \leq \Phi^{-1}\left(\alpha_{m,n}(t)\right)\right\} \cap \bigcap_{j=1}^{n} \left\{C_j \geq \Psi^{-1}\left(1 - \alpha_{m,n}(t)\right)\right\}. \end{aligned} \tag{36}$$

According to the monotonicity of uncertain measure, it is obtained that

$$
\begin{aligned}
&M\left\{\sum_{i=1}^{m}\xi_{1i}\le t, \sum_{j=1}^{n}\left(\xi_{2j}+\eta_{2j}\right)\le t, a+\sum_{i=1}^{m}P_i-\sum_{j=1}^{n}C_j<0\right\}\\
&\ge \bigwedge_{i=1}^{m} M\left\{\xi_{1i}\le \mu_1^{-1}\left(\alpha_{m,n}(t)\right)\right\}\wedge \bigwedge_{j=1}^{n} M\left\{\left(\xi_{2j}+\eta_{2j}\right)\le \mu_2^{-1}\left(\alpha_{m,n}(t)\right)+\lambda^{-1}\left(\alpha_{m,n}(t)\right)\right\}\\
&\wedge \bigwedge_{i=1}^{m} M\left\{P_i\le \Phi^{-1}\left(\alpha_{m,n}(t)\right)\right\}\wedge \bigwedge_{j=1}^{n}\left\{C_j\ge \Psi^{-1}\left(1-\alpha_{m,n}(t)\right)\right\}\\
&=\alpha_{m,n}(t).
\end{aligned}
\tag{37}
$$

Additionally, we have

$$
\begin{aligned}
&\left\{\sum_{i=1}^{m}\xi_{1i}\le t, \sum_{j=1}^{n}\left(\xi_{2j}+\eta_{2j}\right)\le t, Y_{m,n}<0\right\}\\
&\subset \bigcup_{i=1}^{m}\left\{\xi_{1i}\le \mu_1^{-1}\left(\alpha_{m,n}(t)\right)\right\}\cup \bigcup_{j=1}^{n}\left\{\left(\xi_{2j}+\eta_{2j}\right)\le \mu_2^{-1}\left(\alpha_{m,n}(t)\right)+\lambda^{-1}\left(\alpha_{m,n}(t)\right)\right\}\\
&\cup \bigcup_{i=1}^{m}\left\{P_i\le \Phi^{-1}\left(\alpha_{m,n}(t)\right)\right\}\cup \bigcup_{j=1}^{n}\left\{C_j\ge \Psi^{-1}\left(1-\alpha_{m,n}(t)\right)\right\}.
\end{aligned}
\tag{38}
$$

Similarly, we can obtain

$$
\begin{aligned}
&M\left\{\sum_{i=1}^{m}\xi_{1i}\le t, \sum_{j=1}^{n}\left(\xi_{2j}+\eta_{2j}\right)\le t, a+\sum_{i=1}^{m}P_i-\sum_{j=1}^{n}C_j<0\right\}\\
&\le \bigvee_{i=1}^{m} M\left\{\xi_{1i}\le \mu_1^{-1}\left(\alpha_{m,n}(t)\right)\right\}\vee \bigvee_{j=1}^{n} M\left\{\left(\xi_{2j}+\eta_{2j}\right)\le \mu_2^{-1}\left(\alpha_{m,n}(t)\right)+\lambda^{-1}\left(\alpha_{m,n}(t)\right)\right\}\\
&\vee \bigvee_{i=1}^{m} M\left\{P_i\le \Phi^{-1}\left(\alpha_{m,n}(t)\right)\right\}\vee \bigvee_{j=1}^{n}\left\{C_j\ge \Psi^{-1}\left(1-\alpha_{m,n}(t)\right)\right\}\\
&=\alpha_{m,n}(t).
\end{aligned}
\tag{39}
$$

Above all, we get

$$
M\left\{\sum_{i=1}^{m}\xi_{1i}\le t, \sum_{j=1}^{n}\left(\xi_{2j}+\eta_{2j}\right)\le t, Y_{m,n}<0\right\}=\alpha_{m,n}(t).
\tag{40}
$$

Theorem 4 is proved. □

Theorem 5. *Suppose that the inverse uncertainty distributions of all the uncertain variables exist in the insurance risk process. Then, the ruin time* τ *has an uncertainty distribution:*

$$
M\{\tau\le t\}=\max_{m\ge 0,n\ge 1}\alpha_{m,n}(t),
\tag{41}
$$

where

$$
\begin{aligned}
\alpha_{m,n}(t)=&\sup\left\{\alpha\in[0,1]\mid m\mu_1^{-1}(\alpha)\le t\right\}\wedge\sup\left\{\alpha\in[0,1]\mid n\mu_2^{-1}(\alpha)+n\lambda^{-1}(\alpha)\le t\right\}\\
&\wedge\sup\left\{\alpha\in[0,]]\mid a+m\Phi^{-1}(\alpha)-n\Psi^{-1}(1-\alpha)\le 0\right\}.
\end{aligned}
\tag{42}
$$

Proof. Since

$$\{\tau \le t\} = \bigcup_{m=0}^{\infty}\bigcup_{n=1}^{\infty}\left\{\sum_{i=1}^{m}\xi_{1i} \le t, \sum_{j=1}^{n}\left(\xi_{2j}+\eta_{2j}\right) \le t, a + \sum_{i=1}^{m}P_i - \sum_{j=1}^{n}C_j < 0\right\}, \tag{43}$$

then, we have

$$\begin{aligned}
&\bigcup_{m=0}^{\infty}\bigcup_{n=1}^{\infty}\left\{\sum_{i=1}^{m}\xi_{1i} \le t, \sum_{j=1}^{n}\left(\xi_{2j}+\eta_{2j}\right) \le t, a + \sum_{i=1}^{m}P_i - \sum_{j=1}^{n}C_j < 0\right\}\\
&\supset \bigcup_{m=0}^{\infty}\bigcup_{n=1}^{\infty}\bigcap_{i=1}^{m}\left\{\xi_{1i} \le \mu_1^{-1}\left(\alpha_{m,n}(t)\right)\right\} \cap \bigcup_{m=0}^{\infty}\bigcup_{n=1}^{\infty}\bigcap_{j=1}^{n}\left\{\left(\xi_{2j}+\eta_{2j}\right) \le \mu_2^{-1}\left(\alpha_{m,n}(t)\right) + \lambda^{-1}\left(\alpha_{m,n}(t)\right)\right\}\\
&\cap \bigcup_{m=0}^{\infty}\bigcup_{n=1}^{\infty}\bigcap_{i=1}^{m}\left\{P_i \le \Phi^{-1}\left(\alpha_{m,n}(t)\right)\right\} \cap \bigcup_{m=0}^{\infty}\bigcup_{n=1}^{\infty}\bigcap_{j=1}^{n}\left\{C_j \ge \Psi^{-1}\left(1-\alpha_{m,n}(t)\right)\right\}.
\end{aligned} \tag{44}$$

According to the monotonicity of uncertain measure, it is obtained

$$\begin{aligned}
&M\{\tau \le t\}\\
&= M\left\{\bigcup_{m=0}^{\infty}\bigcup_{n=1}^{\infty}\left(\sum_{i=1}^{m}\xi_{1i} \le t, \sum_{j=1}^{n}\left(\xi_{2j}+\eta_{2j}\right) \le t, a + \sum_{i=1}^{m}P_i - \sum_{j=1}^{n}C_j < 0\right)\right\}\\
&\ge M\left\{\bigcup_{m=0}^{\infty}\bigcup_{n=1}^{\infty}\bigcap_{i=1}^{m}\left(\xi_{1i} \le \mu_1^{-1}\left(\alpha_{m,n}(t)\right)\right)\right\} \wedge M\left\{\bigcup_{m=0}^{\infty}\bigcup_{n=1}^{\infty}\bigcap_{j=1}^{n}\left\{\left(\left(\xi_{2j}+\eta_{2j}\right) \le \mu_2^{-1}\left(\alpha_{m,n}(t)\right) + \lambda^{-1}\left(\alpha_{m,n}(t)\right)\right)\right\}\right\}\\
&\wedge M\left\{\bigcup_{m=0}^{\infty}\bigcup_{n=1}^{\infty}\bigcap_{i=1}^{m}\left\{\left(P_i \le \Phi^{-1}\left(\alpha_{m,n}(t)\right)\right)\right\}\right\} \wedge M\left\{\bigcup_{m=0}^{\infty}\bigcup_{n=1}^{\infty}\bigcap_{j=1}^{n}\left(C_j \ge \Psi^{-1}\left(1-\alpha_{m,n}(t)\right)\right)\right\}\\
&= \bigvee_{m=0}^{\infty}\bigvee_{n=1}^{\infty}\bigwedge_{i=1}^{m} M\left\{\xi_{1i} \le \mu_1^{-1}\left(\alpha_{m,n}(t)\right)\right\} \wedge \bigvee_{m=0}^{\infty}\bigvee_{n=1}^{\infty}\bigwedge_{j=1}^{n} M\left\{\left(\xi_{2j}+\eta_{2j}\right) \le \mu_2^{-1}\left(\alpha_{m,n}(t)\right) + \lambda^{-1}\left(\alpha_{m,n}(t)\right)\right\}\\
&\wedge \bigvee_{m=0}^{\infty}\bigvee_{n=1}^{\infty}\bigwedge_{i=1}^{m} M\left\{P_i \le \Phi^{-1}\left(\alpha_{m,n}(t)\right)\right\} \wedge \bigvee_{m=0}^{\infty}\bigvee_{n=1}^{\infty}\bigwedge_{j=1}^{n} M\left\{C_j \ge \Psi^{-1}\left(1-\alpha_{m,n}(t)\right)\right\}\\
&= \bigvee_{m=0}^{\infty}\bigvee_{n=1}^{\infty}\alpha_{m,n}(t)\\
&= \max_{m\ge 0, n\ge 1}\alpha_{m,n}(t).
\end{aligned} \tag{45}$$

Also, since

$$\begin{aligned}
&\bigcup_{m=0}^{\infty}\bigcup_{n=1}^{\infty}\left\{\sum_{i=1}^{m}\xi_{1i} \le t, \sum_{j=1}^{n}\left(\xi_{2j}+\eta_{2j}\right) \le t, a + \sum_{i=1}^{m}P_i - \sum_{j=1}^{n}C_j < 0\right\}\\
&\subset \bigcup_{m=0}^{\infty}\bigcup_{n=1}^{\infty}\bigcup_{i=1}^{m}\left\{\xi_{1i} \le \mu_1^{-1}\left(\alpha_{m,n}(t)\right)\right\} \cup \bigcup_{m=0}^{\infty}\bigcup_{n=1}^{\infty}\bigcup_{j=1}^{n}\left\{\left(\xi_{2j}+\eta_{2j}\right) \le \mu_2^{-1}\left(\alpha_{m,n}(t)\right) + \lambda^{-1}\left(\alpha_{m,n}(t)\right)\right\}\\
&\cup \bigcup_{m=0}^{\infty}\bigcup_{n=1}^{\infty}\bigcup_{i=1}^{m}\left\{P_i \le \Phi^{-1}\left(\alpha_{m,n}(t)\right)\right\} \cup \bigcup_{m=0}^{\infty}\bigcup_{n=1}^{\infty}\bigcup_{j=1}^{n}\left\{C_j \ge \Psi^{-1}\left(1-\alpha_{m,n}(t)\right)\right\}\\
&= \bigcup_{i=1}^{\infty}\bigcup_{m=i}^{\infty}\bigcup_{n=1}^{m}\left\{\xi_{1i} \le \mu_1^{-1}\left(\alpha_{m,n}(t)\right)\right\} \cup \bigcup_{j=1}^{\infty}\bigcup_{n=j}^{\infty}\bigcup_{m=0}^{\infty}\left\{\left(\xi_{2j}+\eta_{2j}\right) \le \mu_2^{-1}\left(\alpha_{m,n}(t)\right) + \lambda^{-1}\left(\alpha_{m,n}(t)\right)\right\}\\
&\cup \bigcup_{i=1}^{\infty}\bigcup_{m=i}^{\infty}\bigcup_{n=1}^{m}\left\{P_i \le \Phi^{-1}\left(\alpha_{m,n}(t)\right)\right\} \cup \bigcup_{j=1}^{\infty}\bigcup_{n=j}^{\infty}\bigcup_{m=0}^{\infty}\left\{C_j \ge \Psi^{-1}\left(1-\alpha_{m,n}(t)\right)\right\}\\
&= \bigcup_{i=1}^{\infty}\left\{\xi_{1i} \le \bigvee_{m=i}^{\infty}\bigvee_{n=1}^{\infty}\mu_1^{-1}\left(\alpha_{m,n}(t)\right)\right\} \cup \bigcup_{j=1}^{\infty}\left\{\left(\xi_{2j}+\eta_{2j}\right) \le \bigvee_{n=j}^{\infty}\bigvee_{m=0}^{\infty}\left(\mu_2^{-1}\left(\alpha_{m,n}(t)\right)\right) + \lambda^{-1}\left(\alpha_{m,n}(t)\right)\right\}\\
&\cup \bigcup_{i=1}^{\infty}\left\{P_i \le \bigvee_{m=i}^{\infty}\bigvee_{n=1}^{\infty}\Phi^{-1}\left(\alpha_{m,n}(t)\right)\right\} \cup \bigcup_{j=1}^{\infty}\left\{C_j \ge \bigwedge_{n=j}^{\infty}\bigwedge_{m=0}^{\infty}\Psi^{-1}\left(1-\alpha_{m,n}(t)\right)\right\},
\end{aligned} \tag{46}$$

then, we have

$$\begin{aligned}
&M\{\tau\le t\}\\
&= M\left\{\bigcup_{m=0}^{\infty}\bigcup_{n=1}^{\infty}\left(\sum_{i=1}^{m}\xi_{1i}\le t,\sum_{j=1}^{n}\left(\xi_{2j}+\eta_{2j}\right)\le t, a+\sum_{i=1}^{m}P_i-\sum_{j=1}^{n}C_j<0\right)\right\}\\
&\le M\left\{\bigcup_{i=1}^{\infty}\left(\xi_{1i}\le\bigvee_{m=i}^{\infty}\bigvee_{n=1}^{\infty}\mu_1^{-1}\left(\alpha_{m,n}(t)\right)\right)\right\}\cup M\left\{\bigcup_{j=1}^{\infty}\left(\left(\xi_{2j}+\eta_{2j}\right)\le\bigvee_{n=j}^{\infty}\bigvee_{m=0}^{\infty}\left(\mu_2^{-1}\left(\alpha_{m,n}(t)\right)+\lambda^{-1}\left(\alpha_{m,n}(t)\right)\right)\right)\right\}\\
&\cup M\left\{\bigcup_{i=1}^{\infty}\left(P_i\le\bigvee_{m=i}^{\infty}\bigvee_{n=1}^{\infty}\Phi^{-1}\left(\alpha_{m,n}(t)\right)\right)\right\}\cup M\left\{\bigcup_{j=1}^{\infty}\left(C_j\ge\bigwedge_{n=j}^{\infty}\bigwedge_{m=0}^{\infty}\Psi^{-1}\left(1-\alpha_{m,n}(t)\right)\right)\right\}\\
&= \bigvee_{i=1}^{\infty}M\left\{\xi_{1i}\le\bigvee_{m=i}^{\infty}\bigvee_{n=1}^{\infty}\mu_1^{-1}\left(\alpha_{m,n}(t)\right)\right\}\vee\bigvee_{j=1}^{\infty}M\left\{\left(\xi_{2j}+\eta_{2j}\right)\le\bigvee_{n=j}^{\infty}\bigvee_{m=0}^{\infty}\left(\mu_2^{-1}\left(\alpha_{m,n}(t)\right)+\lambda^{-1}\left(\alpha_{m,n}(t)\right)\right)\right\}\\
&\vee\bigvee_{i=1}^{\infty}M\left\{P_i\le\bigvee_{m=i}^{\infty}\bigvee_{n=1}^{\infty}\Phi^{-1}\left(\alpha_{m,n}(t)\right)\right\}\vee\bigvee_{j=1}^{\infty}M\left\{C_j\ge\bigwedge_{n=j}^{\infty}\bigwedge_{m=0}^{\infty}\Psi^{-1}\left(1-\alpha_{m,n}(t)\right)\right\}\\
&= \bigvee_{i=1}^{\infty}\bigvee_{m=i}^{\infty}\bigvee_{n=1}^{\infty}\alpha_{m,n}(t)\vee\bigvee_{j=1}^{\infty}\bigvee_{n=j}^{\infty}\bigvee_{m=0}^{\infty}\alpha_{m,n}(t)\\
&= \max_{m\ge0,n\ge1}\alpha_{m,n}(t).
\end{aligned}\tag{47}$$

Thus, we get $M\{\tau\le t\}=\max_{m\ge0,n\ge1}\alpha_{m,n}(t)$.

Theorem 5 is proved. □

3. Numerical Examples

We will illustrate the above conclusions through the following five numerical examples and present how to calculate the ruin index and ruin time. Firstly, we compare our model with Yao and Qin's model [34] in Example 1 and compute the ruin index by inverse uncertainty distributions. Example 2 presents how to calculate the expected claim rate and the report rate according to the properties of uncertain renewal reward process [27] and uncertain alternating renewal process [30]. Example 3 and Example 4 give the uncertain measure that an insurance company ruins before time t. We compute the uncertainty distribution of ruin time in Example 5.

Example 1. Assume that $\mu_1=N(e_1,\sigma_1)$, $\mu_2=N(e_2,\sigma_2)$, $\lambda=N(e_3,\sigma_3)$, $\Phi=N(e_1',\sigma_1')$, and $\Psi=N(e_2',\sigma_2')$ follow normal uncertainty distributions. Then, we have

$$\begin{aligned}
&n\mu_2^{-1}(\alpha)+n\lambda^{-1}(\alpha)-(m+1)\mu_1^{-1}(1-\alpha)\\
&\quad= n\left(e_2+\frac{\sigma_2\sqrt{3}}{\pi}\ln\frac{\alpha}{1-\alpha}\right)+n\left(e_3+\frac{\sigma_3\sqrt{3}}{\pi}\ln\frac{\alpha}{1-\alpha}\right)-(m+1)\left(e_1+\frac{\sigma_1\sqrt{3}}{\pi}\ln\frac{\alpha}{1-\alpha}\right),\\
&a+m\Phi^{-1}(\alpha)-n\Psi^{-1}(1-\alpha)\\
&\quad= a+m\left(e_1'+\frac{\sigma_1'\sqrt{3}}{\pi}\ln\frac{\alpha}{1-\alpha}\right)-n\left(e_2'+\frac{\sigma_2'\sqrt{3}}{\pi}\ln\frac{1-\alpha}{\alpha}\right).
\end{aligned}\tag{48}$$

According to Theorem 2, we can obtain that

$$\begin{aligned}
\alpha_{m,n}=&\left(1+\exp\left(\frac{\pi}{\sqrt{3}}\cdot\frac{n(e_2+e_3)-(m+1)e_1}{n(\sigma_2+\sigma_3)+(m+1)\sigma_1}\right)\right)^{-1}\\
&\wedge\left(1+\exp\left(\frac{\pi}{\sqrt{3}}\cdot\frac{a+me_1'-ne_2'}{m\sigma_1'+n\sigma_2'}\right)\right)^{-1}.
\end{aligned}\tag{49}$$

Furthermore, the ruin index can be calculated as

$$\begin{aligned}
\text{ruin}=&\max_{m\ge0,n\ge1}\left(1+\exp\left(\frac{\pi}{\sqrt{3}}\cdot\frac{n(e_2+e_3)-(m+1)e_1}{n(\sigma_2+\sigma_3)+(m+1)\sigma_1}\right)\right)^{-1}\\
&\wedge\left(1+\exp\left(\frac{\pi}{\sqrt{3}}\cdot\frac{a+me_1'-ne_2'}{m\sigma_1'+n\sigma_2'}\right)\right)^{-1}.
\end{aligned}\tag{50}$$

We set $e_1=e_2=e_3=1$, $\sigma_1=\sigma_2=\sigma_3=1$, $e_1'=e_2'=3$, $\sigma_1'=\sigma_2'=3$, $a=1000$, and $m=n=80$ and calculate the risk index of the insurance company to be ruin = 0.0223. In addition, when the initial capital a varies from 0 to 1200, we calculate the ruin index and present the results in Figure 2. The results show that the ruin index falls from 0.3556 to 0.0106 when the initial capital a increases from 0 to 1200.

Note that if $e_3 = 0$ and $\sigma_3 = 0$ in Example 1, the ruin index degenerates into the ruin index of the modified insurance risk model proposed by Yao and Qin [34], that is, ruin $= \max_{m\geq 0, n\geq 1}(1+\exp((\pi/\sqrt{3})\cdot((ne_2-(m+1)e_1)/(n\sigma_2+(m+1)\sigma_1))))^{-1} \wedge (1+\exp((\pi/\sqrt{3})\cdot((a+me_1'-ne_2')/(m\sigma_1'+n\sigma_2'))))^{-1}$. When other parameters are fixed, $(1+\exp((\pi/\sqrt{3})\cdot(a+me_1'-ne_2'/m\sigma_1'+n\sigma_2')))^{-1}$ decreases as the initial capital a increases. The ruin index is equal to $\max_{m\geq 0, n\geq 1}(1+\exp((\pi/\sqrt{3})\cdot (a+me_1'-ne_2'/m\sigma_1'+n\sigma_2')))^{-1}$ when the initial capital a is large enough. We can analyze that, with the increase in initial capital a, the ruin index calculated by the uncertain alternating renewal insurance risk model will tend to be the same as that computed by the model proposed by Yao and Qin.

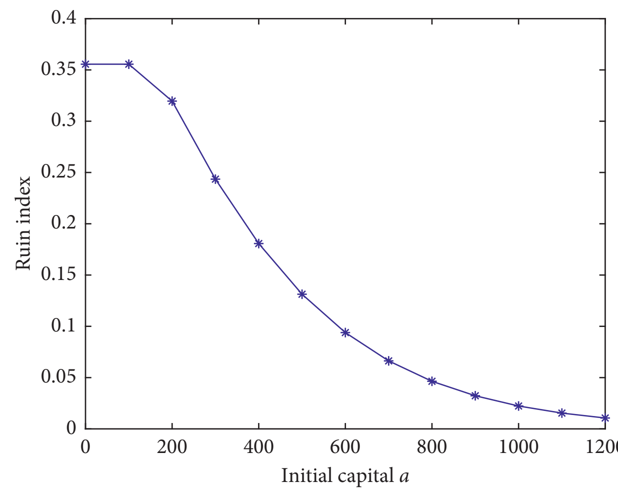

FIGURE 2: The ruin index with different initial capital a.

Example 2. Assume that $\mu_1 = L(0,1)$, $\mu_2 = L(1,4)$, $\lambda = L(2,3)$, $P_1 = L(0,10)$, and $C_1 = L(0,15)$ are linear uncertain variables. Thus, the expected claim rate is

$$\begin{aligned}\lim_{t\longrightarrow\infty}\frac{E[N_{2t}]}{t} &= E\left[\frac{1}{\xi_{21}+\eta_{21}}\right]\\ &= \int_0^1 \frac{1}{\mu_2^{-1}(\alpha)+\lambda^{-1}(\alpha)}\,\mathrm{d}\alpha \\ &= 0.212,\end{aligned}\tag{51}$$

and the report rate is

$$\begin{aligned}\lim_{t\longrightarrow\infty}\frac{E[A_t]}{t} &= E\left[\frac{\xi_{21}}{\xi_{21}+\eta_{21}}\right]\\ &= \int_0^1 \frac{\mu_2^{-1}(\alpha)}{\mu_2^{-1}(\alpha)+\lambda^{-1}(1-\alpha)}\,\mathrm{d}\alpha \\ &= 0.486.\end{aligned}\tag{52}$$

Example 3. Assume that $\mu_1 = L(0,1)$, $\mu_2 = L(1,4)$, $\lambda = L(2,3)$, $P_1 = L(0,10)$, $C_1 = L(0,15)$, the initial capital $a = 1000$, and premium amount $m = 80$. We calculate the company ruins with an uncertain measure 0.1 before the instant $t = 300$ at the $n = 80$th claim. Figure 3 shows the uncertain measure that the insurance company ruins before time t.

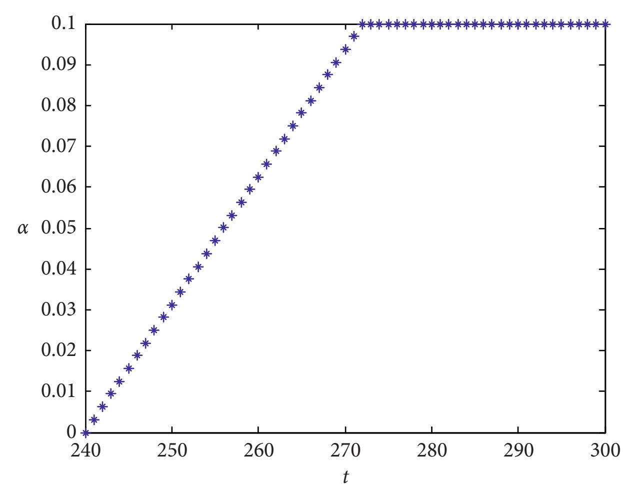

FIGURE 3: Risk measure of insurance company before the time t.

Example 4. Assume that $\mu_1 = L(0,1)$, $\mu_2 = L(1,4)$, $\lambda = L(2,3)$, $P_1 = L(0,10)$, and $C_1 = L(0,15)$ are linear uncertain variables. According to Theorem 5, if the initial capital a is 1000, then we can calculate that $M\{\tau \leq 300\} = 0.1524$; i.e., the insurance company ruins with an uncertain measure 0.1524 before the time $t = 300$.

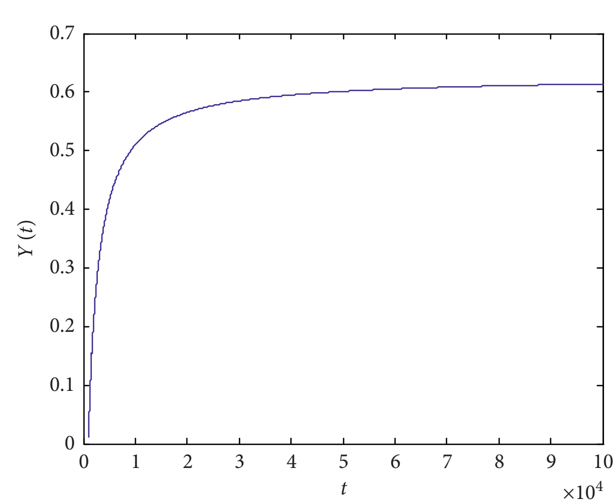

FIGURE 4: Uncertainty distribution of ruin time in Example 5.

Example 5. Similar to Example 4, we assume that $\mu_1 = \mathcal{L}(0,1)$, $\mu_2 = \mathcal{L}(1,4)$, $\lambda = \mathcal{L}(2,3)$, $P_1 = \mathcal{L}(0,10)$, and $C_1 = \mathcal{L}(0,15)$ are linear uncertain variables. According to Theorem 5, if the initial capital a is 5000, the uncertainty distribution of the ruin time τ is shown in Figure 4.

4. Conclusions

This paper extends an insurance risk model with an alternating renewal process in uncertain environment. We propose an uncertain insurance risk process in which the claim process is regarded as an uncertain alternating renewal reward process, and this process is more in line with the claim process in real life. Moreover, we provide the inverse uncertainty distribution of the uncertain insurance risk process and the ruin index. The explicit form of uncertainty distribution of ruin time is also derived. At last, several examples are provided to illustrate the proven results. In future research, some criteria such as inflation, dividend, and tax can be considered to further extend the uncertain insurance risk process.

Data Availability

The data presented in Examples 1–5 and Figures 2–4 in this paper, which are used to support the findings of this study, are included within the article.

Conflicts of Interest

The authors declare that they have no conflicts of interest.

Acknowledgments

This work was supported by the Beijing Natural Science Foundation (grant no. 9204024), National Natural Science Foundation of China (grant nos. 71873012 and 71571007), Humanities and Social Sciences Planning Fund of Ministry of Education (grant no. 17YJA790097), and Scientific Research Level Enhancement Funding Project of Beijing International Studies University.

References

[1] D. C. M. Dickson and C. Hipp, "Ruin probabilities for Erlang(2) risk processes," *Insurance: Mathematics and Economics*, vol. 22, no. 3, pp. 251–262, 1998.
[2] S. Li and J. Garrido, "On ruin for the Erlang(n) risk process," *Insurance: Mathematics and Economics*, vol. 34, no. 3, pp. 391–408, 2004.
[3] D. C. M. Dickson and C. Hipp, "On the time to ruin for Erlang(2) risk processes," *Insurance: Mathematics and Economics*, vol. 29, no. 3, pp. 333–344, 2001.
[4] Y. Chun, "Equivalence of axioms for bankruptcy problems," *International Journal of Game Theory*, vol. 28, no. 4, pp. 511–520, 1999.
[5] H. U. Gerber and E. S. W. Shiu, "On the time value of ruin," *North American Actuarial Journal*, vol. 2, no. 1, pp. 48–72, 1998.
[6] B. Sundt and J. L. Teugels, "Ruin estimates under interest force," *Insurance: Mathematics and Economics*, vol. 16, no. 1, pp. 7–22, 1995.
[7] J. Paulsen and H. K. Gjessing, "Optimal choice of dividend barriers for a risk process with stochastic return on investments," *Insurance: Mathematics and Economics*, vol. 20, no. 3, pp. 215–223, 1997.
[8] H. Albrecher and C. Hipp, "Lundberg's risk process with tax," *Blätter der DGVFM*, vol. 28, no. 1, pp. 13–28, 2007.
[9] W. Yu, P. Guo, Q. Wang et al., "On a periodic capital injection and barrier dividend strategy in the compound Poisson risk model," *Mathematics*, vol. 8, no. 4, p. 511, 2020.
[10] P. S. Griffin, "Sample path behavior of a Lévy insurance risk process approaching ruin, under the Cramér-Lundberg and convolution equivalent conditions," *The Annals of Applied Probability*, vol. 26, no. 1, pp. 360–401, 2016.
[11] E. Biffis and A. E. Kyprianou, "A note on scale functions and the time value of ruin for Lévy insurance risk processes," *Insurance: Mathematics and Economics*, vol. 46, no. 1, pp. 85–91, 2010.
[12] Z. Zhang, Y. Yong, and W. Yu, "Valuing equity-linked death benefits in general exponential Lévy models," *Journal of Computational and Applied Mathematics*, vol. 365, Article ID 112377, 2020.
[13] W. Yu, Y. Yong, G. Guan, Y. Huang, W. Su, and C. Cui, "Valuing guaranteed minimum death benefits by cosine series expansion," *Mathematics*, vol. 7, no. 9, p. 835, 2019.
[14] D. Kahneman and A. Tversky, "Prospect theory: an analysis of decision under risk," *Econometrica*, vol. 47, no. 2, pp. 263–292, 1979.
[15] G. W. De Wit, "Underwriting and uncertainty," *Insurance: Mathematics and Economics*, vol. 1, no. 4, pp. 277–285, 1982.
[16] J. Lemaire, "Fuzzy insurance," *ASTIN Bulletin*, vol. 20, no. 1, pp. 33–55, 1990.
[17] J. D. Cummins and R. A. Derrig, "Fuzzy trends in property-liability insurance claim costs," *The Journal of Risk and Insurance*, vol. 60, no. 3, pp. 429–465, 1993.
[18] R. A. Derrig and K. M. Ostaszewski, "Fuzzy techniques of pattern recognition in risk and claim classification," *The Journal of Risk and Insurance*, vol. 62, no. 3, pp. 447–482, 1995.
[19] W. Yu, F. Wang, Y. Huang, and H. Liu, "Social Optimal mean field control problem for population growth model," *Asian Journal of Control*, pp. 1–8, 2019.
[20] A. F. Shapiro, "Fuzzy logic in insurance," *Insurance: Mathematics and Economics*, vol. 35, no. 2, pp. 399–424, 2004.
[21] B. Li, W. Ni, and C. Constantinescu, "Risk models with premiums adjusted to claims number," *Insurance: Mathematics and Economics*, vol. 65, pp. 94–102, 2015.
[22] T. Huang, R. Zhao, and W. Tang, "Risk model with fuzzy random individual claim amount," *European Journal of Operational Research*, vol. 192, no. 3, pp. 879–890, 2009.
[23] A. F. Shapiro, "Modeling future lifetime as a fuzzy random variable," *Insurance: Mathematics and Economics*, vol. 53, no. 3, pp. 864–870, 2013.
[24] B. Liu, *Uncertainty Theory*, Springer, Berlin, Germany, 2007.
[25] S. Li, J. Peng, and B. Zhang, "The uncertain premium principle based on the distortion function," *Insurance: Mathematics and Economics*, vol. 53, no. 2, pp. 317–324, 2013.
[26] B. Liu, "Fuzzy process, hybrid process and uncertain process," *Journal of Uncertain Systems*, vol. 2, no. 1, pp. 3–16, 2008.
[27] B. Liu, *Uncertainty Theory: A Branch of Mathematics for Modeling Human Uncertainty*, Springer, Berlin, Germany, 2010.

[28] K. Yao and D. A. Relescu, "Age replacement policy in uncertain environment," *Iranian Journal of Fuzzy Systems*, vol. 10, no. 2, pp. 29–39, 2013.
[29] K. Yao, "Uncertain calculus with renewal process," *Fuzzy Optimization and Decision Making*, vol. 11, no. 3, pp. 285–297, 2012.
[30] K. Yao and X. Li, "Uncertain alternating renewal process and its application," *IEEE Transactions on Fuzzy Systems*, vol. 20, no. 6, pp. 1154–1160, 2012.
[31] X. Zhang, Y. Ning, and G. Meng, "Delayed renewal process with uncertain interarrival times," *Fuzzy Optimization and Decision Making*, vol. 1, pp. 279–287, 2013.
[32] B. Liu, "Extreme value theorems of uncertain process with application to insurance risk model," *Soft Computing*, vol. 17, no. 4, pp. 549–556, 2013.
[33] K. Yao and J. Zhou, "Ruin time of uncertain insurance risk process," *IEEE Transactions on Fuzzy Systems*, vol. 26, no. 1, pp. 19–28, 2018.
[34] K. Yao and Z. Qin, "A modified insurance risk process with uncertainty," *Insurance: Mathematics and Economics*, vol. 62, pp. 227–233, 2015.
[35] Y. Liu, X. Zhang, and W. Ma, "A new uncertain insurance model with variational lower limit," *Insurance: Mathematics and Economics*, vol. 74, pp. 164–169, 2017.
[36] Z. Liu and Y. Yang, "Uncertain insurance risk process with multiple classes of claims," *Applied Mathematical Modelling*, vol. 83, pp. 660–673, 2020.
[37] H. Lopes, J. Barcellos, J. Kubrusly, and C. Fernandes, "A nonparametric method for incurred but not reported claim reserve estimation," *International Journal for Uncertainty Quantification*, vol. 2, no. 1, pp. 39–51, 2012.

Hindawi
Mathematical Problems in Engineering
Volume 2020, Article ID 5349345, 9 pages
https://doi.org/10.1155/2020/5349345

Research Article

Pricing of Margin Call Stock Loan Based on the FMLS

Kaili Xiang,[1] Peng Hu [1,2] and Xiao Li [1]

[1]*School of Economic Mathematics, Southwestern University of Finance and economics, Chengdu, China*
[2]*College of Applied Mathematics, Chengdu University of Information Technology, Chengdu, China*

Correspondence should be addressed to Xiao Li; 471055395@qq.com

Received 22 April 2020; Accepted 8 June 2020; Published 27 June 2020

Guest Editor: Wenguang Yu

In common stock loan, lenders face the risk that their loans will not be repaid if the stock price falls below loan, which limits the issuance and circulation of stock loans. The empirical test suggests that the log-return series of stock price in the US market reject the normal distribution and admit instead a subclass of the asymmetric distribution. In this paper, we investigate the model of the margin call stock loan problem under the assumption that the return of stock follows the finite moment log-stable process (FMLS). In this case, the pricing model of the margin call stock loan can be described by a space-fractional partial differential equation with a time-varying free boundary condition. We transform the free boundary problem to a linear complementarity problem, and the fully-implicit finite difference method that we used is unconditionally stable in both the integer and fractional order. The numerical experiments are carried out to demonstrate differences of the margin call stock loan model under the FMLS and the standard normal distribution. Last, we analyze the impact of key parameters in our model on the margin call stock loan evaluation and give some reasonable explanation.

1. Introduction

Stock loan is a contract that the holders of securities take these securities as collateral to obtain loans from commercial banks. Xia et al. [1] quantified the stock loan, established the mathematical model of the stock loan with infinite maturity by assuming that the logarithm price of risk assets obeys geometric Brownian motion, and opened the door of research on the pricing of the stock loan.

The common stock loan does not have any restrictions on the borrower. When the total price of the stock runs below the loan, the rational borrower will default and the lender will bear the loss, which brings the risk to the lender and reduces the supply and circulation of the stock loan. In order to control the risk, Liang et al. [2] studied the infinite maturity stock loan with automatic termination clause, limit, and additional margin. They found that the unlimited stock loan would make the lender unable to obtain the maximum interest income, and the borrower could not borrow enough funds when he pledged the assets, so that the allocation efficiency of funds could not be maximized. Grasselli and Gómez [3] studied the trading restrictions on the stock holders in the incomplete market. According to the utility function of the fund borrower, the limited maturity stock loan is priced, and the limited maturity stock loan is priced according to the variational inequality. Wong [4] studied the optimal stop time problem of the infinite maturity stock loan similar to a permanent American option driven by the index Levy process and uses variational inequality to solve the problem. Cai and Sun [5] studied the infinite maturity and limited maturity stock loan models under the super index jump diffusion model. The accuracy of the solution is proved by numerical examples. Wong et al. [6] studied the case that stock volatility is a stochastic process. When the interest rate is negative, the optimal stop time of an American call option is considered.

Through the research and empirical test, scholars found that the classical B–S framework does not conform to the actual situation, and the logarithmic distribution of risk asset prices often has a "peak thick tail" phenomenon, which is consistent with the fact that the stock price is an autocorrelation process. Carr et al. [7] studied the volatility smile of asset prices through empirical research and found that the FMLS process model can better describe asset price changes.

As a special Levy process, the FMLS process can well reflect the large jump of risk asset price and the situation that the logarithm distribution of risk asset price is often biased. In the framework of FMLS, the α steady-state process is used as the driving process to describe the autocorrelation of asset price changes and ensure the stability. When $\alpha < 2$, the FMLS model is in good agreement with the phenomenon that the logarithm distribution of risk asset prices has thick tail. Because of its good properties, finite moment log steady state processes are more and more used to simulate asset price movement. Yu et al. [8] derived the equations and the boundary conditions satisfied by the Gerber–Shiu function, the expected discounted capital injection function and the expected discounted dividend function by assuming that the observation interval and claim amount are exponentially distributed, respectively. Yu et al. [9] considered a class of social optimal mean field control problem of the population growth model. Zhang et al. [10] focused on valuation of the products with guaranteed minimum death benefit (GMDB). The benefit amount is linked to the performance of the underlying asset, which is modeled by an exponential Levy process. Yu et al. [11] used the Fourier cosine series expansion (COS) method to value the guaranteed minimum death benefit (GMDB) products. Peng et al. [12] modeled the insurance company's surplus flow by a perturbed compound Poisson model.

Under the finite moment log-stable (FMLS) model, the partial differential equation of option pricing is not easy to get because of a fractional operator. Cartea [13] first gave the proper partial differential equation of European option pricing under the framework of FMLS by the Fourier transform. Chen et al. [14] gave the analytical solution of European option under the framework of FMLS through the Fourier integral transform on the basis of Cartea, and they studied the numerical solution of an American call option pricing under the framework of FMLS through the prediction correction method [15], in which the moving boundary problem was transformed into the fixed boundary problem through coordinate transformation. Zhang et al. [16] studied the numerical solution of European double barrier options driven by the Levy process, including FMLS, using the second-order implicit difference scheme. Chen [17] studied the second-order finite difference scheme and obtained the numerical solution of the American option in the form of penalty function.

Based on the previous research, we found that under the framework of FMLS, nobody studied the margin call stock loan. In the actual economic activities, the demand for the margin stock loan is increasing constantly.

The rest of this paper is arranged as follows. In the Section 2, we establish the mathematical model of the stock loan with margin call, transform the moving boundary problem into the fixed boundary problem through coordinate transformation, and finally transform it into the linear complementarity problem. In Section 3, we obtain the numerical solution of the linear complementarity problem by the finite difference method. In the Section 4, the validity of the numerical solution and the parameter analysis are verified by numerical examples. Finally, we draw the conclusion in the Section 5.

2. Pricing Model

The margin call stock loan: the borrower pledged stock S and got loan K from lender. The borrower can choose to repay the loan at any time. However, the borrower needs to pay a certain amount of interest while paying the loan K, so the borrower chooses the repayment amount at time t as $Ke^{\gamma t}$ when $S_t < Ke^{\gamma t}$; rational people will not repay, and his payment at time t is $(S_t - Ke^{\gamma t})^+$. In order to control the risk, the margin call stock loan has set a lower bound S_B; when the stock price S_t at t moment runs below S_B (generally $S_B = Ke^{\gamma t}$), the lender have the right to require the borrower to recover the funds of $\Delta Ke^{\gamma t_q}$, where Δ is the share to be recovered, and then, the remaining loan is $(1-\Delta)Ke^{\gamma t}$. After the payment is made, the margin call stock loan becomes a nonrecourse stock loan with a maturity of $T-t$; therefore, the value of the stock loan after recovery is $R(t) = V(x_B, 0; (1-\Delta)Ke^{\gamma t}) - \Delta Ke^{\gamma t}$, where $V$is the value of the nonrecourse stock loan with a maturity of $T - t_q$ and strike price of $(1-\Delta)Ke^{\gamma t}$.

The margin call stock loan stipulates a lower bound of the stock price. When the stock price reaches the lower bound, the stock loan is suspended, and the lender has the right to require the borrower to recover part of the loan. After the borrower recovers the loan, the stock loan with recourse is converted into a stock loan without recourse until the maturity date.

In conclusion, there are two stages in the margin call stock loan: the stage with recourse and the stage without recourse. This is similar to an American call option with a change barrier in the first stage and an American call option with a change strike price in the second stage, as shown in Figure 1.

The value of the margin call stock loan is V_{mc}(margin call [18]), where V is the nonrecourse stock loan. Let $x_t = \ln S_t$, and under the risk neutral measure, the stock price under the framework of FMLS obeys the following stochastic differential equation:

$$dx_t = (r - D - a)dt + \sigma dL_t^{\mathrm{FMLS}}, \tag{1}$$

where r is the risk-free interest rate, D is the continuous dividend rate of stock, σ is volatility, dL_t^{FMLS} is the α-steady state stochastic process, $dL_t^{\mathrm{FMLS}} \sim L^{\alpha}(0, dt^{1/\alpha}, -1)$, a is the convex adjustment, and $a = -\sigma^{\alpha}\sec(\alpha\pi/2)$. According to the above assumptions, the partial differential equation and boundary conditions of the pricing of the margin call stock loan can be obtained as

$$\begin{aligned}\frac{\partial V_{\mathrm{mc}}(x,t)}{\partial t} &= rV_{\mathrm{mc}}(x,t) - (r-D-a)\frac{\partial V_{\mathrm{mc}}(x,t)}{\partial x} \\ &\quad - a_{-\infty}D_x^{\alpha}V_{\mathrm{mc}}(x,t).\end{aligned} \tag{2}$$

Boundary condition 1: terminal condition.

$$V_{\mathrm{mc}}(x,T) = \left(e^{x_T} - Ke^{\gamma T}\right)^+. \tag{3}$$

Boundary condition 2: when $S_t = S_B = Ke^{\gamma t}$, i.e., $x_t = x_B$, the borrower needs to recover $\Delta Ke^{\gamma t}$, where

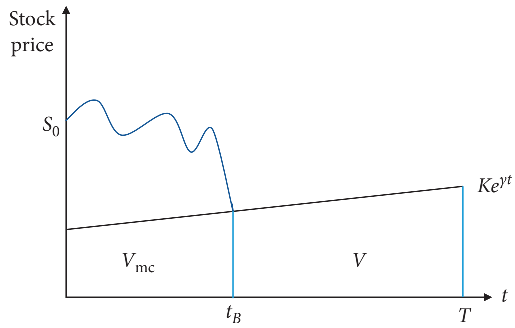

FIGURE 1: Two stages of the margin call stock loan.

V is the nonrecourse stock loan with the execution price of $(1-\Delta)Ke^{\gamma t}$ and the maturity date of $T-t_B$. So,

$$R(t)=V_{\mathrm{mc}}(x,t)=V\left(x,0;\,(1-\Delta)Ke^{\gamma t},T-t_B\right)-\Delta Ke^{\gamma t}. \tag{4}$$

In order to reduce the error of fractional order numerical calculation, take

$$R(x,t)=V_{\mathrm{mc}}(x,t)=V\left(x,0;\,(1-\Delta)Ke^{\gamma t},T-t_B\right)-\Delta Ke^{\gamma t},\quad x\in(-\infty,x_B). \tag{5}$$

When $\Delta=0$, the margin call stock loan becomes a stock loan without recourse.

Boundary condition 3: when the stock price approaches the free boundary,

$$V_{\mathrm{mc}}\left(x_f,t\right)=\left(e^{x_f}-Ke^{\gamma t}\right)^+. \tag{6}$$

Boundary condition 4: when the stock price approaches the free boundary, it should be kept smooth.

$$\frac{\partial V_{\mathrm{mc}}\left(x_f,t\right)}{\partial x}=e^{x_f}. \tag{7}$$

In conclusion, the partial differential equations and boundary conditions of the nonrecourse stock loan pricing with variable strike price under the framework of FMLS are as follows:

$$\begin{cases}\dfrac{\partial V_{\mathrm{mc}}(x,t)}{\partial t}=rV_{\mathrm{mc}}(x,t)-(r-D-a)\dfrac{\partial V_{\mathrm{mc}}(x,t)}{\partial x}-a_{-\infty}D_x^{\alpha}V_{\mathrm{mc}}(x,t), & x\in\left(-\infty,x_f\right), t\in[0,T], 1<\alpha<2,\\ V_{\mathrm{mc}}(x,t)=R(x,t), & x\in(-\infty,x_B),\\ V_{\mathrm{mc}}(x,T)=\left(e^{x_T}-Ke^{\gamma T}\right)^+, & \\ \dfrac{\partial V_{\mathrm{mc}}\left(x_f,t\right)}{\partial x}=e^{x_f}. & \end{cases} \tag{8}$$

Coordinate transformation for (8)

$$\begin{cases} y_t=x_t-\gamma t,\\ \tau=T-t,\\ \overline{V}(y,\tau)=e^{-\alpha t}V(x,t).\end{cases} \tag{9}$$

The final value problem with moving boundary is transformed into the initial boundary value problem with a fixed boundary.

First, the coordinate transformation of the fractional order operator is

$$\begin{aligned}{}_{-\infty}D_x^{\alpha}V_{\mathrm{mc}}(x,t)&=\frac{1}{\Gamma(n-\alpha)}\frac{\mathrm{d}^n}{\mathrm{d}x_t^n}\int_{-\infty}^{x_t}\frac{V_{\mathrm{mc}}(z,t)}{(x_t-z)^{\alpha-n+1}}\mathrm{d}z\\ &=\frac{1}{\Gamma(n-\alpha)}\frac{\mathrm{d}^n}{\mathrm{d}x_t^n}\int_{-\infty}^{x_t}\frac{e^{\alpha t}\overline{V}_{\mathrm{mc}}(y,\tau)}{(x_t-z)^{\alpha-n+1}}\mathrm{d}z\\ &=\frac{e^{\alpha t}}{\Gamma(n-\alpha)}\frac{\mathrm{d}^n}{\mathrm{d}(y_t+\gamma t)^n}\int_{-\infty}^{x}\frac{\overline{V}_{\mathrm{mc}}(y,\tau)}{(y_t+\gamma t-z)^{\alpha-n+1}}\mathrm{d}z\\ &=\frac{e^{\alpha t}}{\Gamma(n-\alpha)}\frac{\mathrm{d}^n}{\mathrm{d}y_t^n}\int_{-\infty}^{y_t}\frac{\overline{V}_{\mathrm{mc}}(y,\tau)}{(y_t-z)^{\alpha-n+1}}\mathrm{d}z,\end{aligned} \tag{10}$$

$$\begin{cases} \dfrac{\partial \overline{V}_{\mathrm{mc}}(y,\tau)}{\partial \tau} = (r-\gamma-D-a)\dfrac{\partial \overline{V}_{\mathrm{mc}}(y,\tau)}{\partial y} + a_{-\infty}D_y^{\alpha}\overline{V}_{\mathrm{mc}}(y,\tau) - (r-\gamma)\overline{V}_{\mathrm{mc}}(y,\tau), \quad y \in \left(-\infty, y_f\right], \tau \in [0,T], 1<\alpha<2, \\ \overline{V}_{\mathrm{mc}}(y,0) = (e^{y_0}-K)^+, \\ \overline{V}_{\mathrm{mc}}(y,\tau) = \overline{V}(y,\tau;(1-\Delta)K,\tau) - \Delta K, \quad y \in (-\infty, y_B], \\ \overline{V}_{\mathrm{mc}}\left(y_f,\tau\right) = (e^{y_f}-K)^+, \\ \dfrac{\partial \overline{V}_{\mathrm{mc}}\left(y_f,\tau\right)}{\partial y} = e^{y_f}. \end{cases} \tag{11}$$

Next, we transform (11) from the free boundary problem into a linear complementarity problem:

$$\begin{cases} \min\left(\dfrac{\partial \overline{V}_{\mathrm{mc}}}{\partial \tau} - L_y\overline{V}_{\mathrm{mc}}, \overline{V}_{\mathrm{mc}} - \left(e^y-K\right)^+\right) = 0, \\ \quad y \in R,\ \tau \in [0,T], \\ \overline{V}_{\mathrm{mc}}(y,0) = (e^{y_0}-K)^+, \quad y > y_B, \\ \overline{V}_{\mathrm{mc}}(y,\tau) = \overline{V}(y,\tau;(1-\Delta)K,\tau) - \Delta K, \\ \quad y \in \left(-\infty, y_B\right],\ \tau \in [0,T], \end{cases} \tag{12}$$

where

$$\begin{aligned} L_y\overline{V}_{\mathrm{mc}} &= (r-\gamma-D-a)\frac{\partial \overline{V}_{\mathrm{mc}}(y,\tau)}{\partial y} \\ &\quad + a_{-\infty}D_y^{\alpha}\overline{V}_{\mathrm{mc}}(y,\tau) - (r-\gamma)\overline{V}_{\mathrm{mc}}(y,\tau). \end{aligned} \tag{13}$$

So far, we derive the partial differential equations and boundary conditions for pricing contracts with recourse under the framework of FMLS, where the lower boundary is relatively special due to the limitation of recourse. Then, the final value problem with variable boundary is transformed into the initial value problem with fixed boundary by coordinate transformation. Finally, the free boundary problem is transformed into a linear complementarity problem, and a simpler and more convenient linear complementarity problem is obtained. In the next section, we will use the finite difference scheme to give the numerical solution of equation (12).

3. Numerical Format of the Model

Before numerical calculation, it is necessary to establish grid and approximate PDE. First, we divide the domain. Suppose y_B is the ordinate corresponding to the barrier price. Let $0 \le \tau = n\Delta\tau \le T$, $n = 0, 1, \ldots, N; L \le y \le R, \Delta y = (R - y_B/M), y_m = L + i\Delta y, \quad m = 0, 1, \ldots, M;$ and $\overline{V}_{\mathrm{mc}}^{\mathrm{n}} \approx \overline{V}_{\mathrm{mc}}(y_m, \tau_n, \alpha)$, and $y_B = L + b\Delta y$ is the ordinate corresponding to the margin call boundary.

The initial value and boundary conditions are as follows. Initial value condition:

$$\overline{V}_{\mathrm{mc}_m}^0 = \left(e^{y_m} - K\right)^+, \quad m = b, 1, \ldots, M. \tag{14}$$

Boundary condition 1:

$$\begin{aligned} \overline{V}_{\mathrm{mc}_m}^n &= \overline{V}\left(y_m, \tau_n; (1-\Delta)K, \tau_n\right) - \Delta K, \\ & n = 0, 1, \ldots, N,\ m = 0, 1, \ldots, b. \end{aligned} \tag{15}$$

Boundary condition 2:

$$\overline{V}_{\mathrm{mc}_M}^n = e^{y_m} - K, \quad n = 0, 1, \ldots, N. \tag{16}$$

We use the central difference scheme to approximate the first-order time and space partial derivatives:

$$\begin{aligned} \frac{\partial \overline{V}_{\mathrm{mc}}\left(y_m, \tau_n\right)}{\partial \tau} &= \frac{\overline{V}_{\mathrm{mc}_m}^{n+1} - \overline{V}_{\mathrm{mc}_{\mathrm{m}}}^{\mathrm{n}}}{\Delta\tau} + O(\Delta\tau), \\ \frac{\partial \overline{V}_{\mathrm{mc}}\left(y_m, \tau_n\right)}{\partial y} &= \frac{\overline{V}_{\mathrm{mc}_{m+1}}^{n+1} - \overline{V}_{m-1}^{n+1}}{2\Delta y} + O\left(\Delta y^2\right). \end{aligned} \tag{17}$$

We use the modified Grunwald–Letnikov formula to approximate the space-fractional derivative [19]:

$$_{-\infty}D_y^{\alpha}\overline{V}_{mc}\left(y_m, \tau_n\right) = \frac{1}{\Delta y^{\alpha}} \sum_{k=0}^{m+1} w_k^{(\alpha)} \overline{V}_{mc_{m-k+1}}^{n+1} + O\left(\Delta y^2\right), \tag{18}$$

where

$$\begin{aligned} w_k^{(\alpha)} = (-1)^k \begin{pmatrix} \alpha \\ k \end{pmatrix} &= \frac{(-1)^k \Gamma(\alpha+1)}{\Gamma(k+1)\Gamma(\alpha-k+1)} \\ &= \frac{\alpha(\alpha-1)\cdots(\alpha-k+1)}{k!}, \end{aligned} \tag{19}$$

is called the Grunwald–Letnikov coefficient. In numerical calculation, in order to save memory, the iterative algorithm is generally used to calculate $w_k^{(\alpha)}$. From the above formula, we found that the fractional derivative is related to all the values before $m+1$, which means the fractional derivative is a nonlocal operator, which can well explain that the underlying asset price movement is related to the previous historical price.

We get the implicit difference scheme of equation (11) based on the modified Grunwald–Letnikov formula approximation:

$$\begin{aligned}\frac{\overline{V}^{n+1}_{\mathrm{mc}_m}-\overline{V}^{n}_{\mathrm{mc}_m}}{\Delta\tau} &= \frac{1}{2}(r-\gamma-D-a)\left(\frac{\overline{V}^{n+1}_{\mathrm{mc}_{m+1}}-\overline{V}^{n+1}_{\mathrm{mc}_{m-1}}}{2\Delta y}+\frac{\overline{V}^{n+1}_{\mathrm{mc}_{m+1}}-V^{n+1}_{\mathrm{mc}_{m-1}}}{2\Delta y}\right)\\ &\quad+\frac{1}{2}a\left(\frac{1}{\Delta y^{\alpha}}\sum_{k=0}^{m+1}w_k^{(\alpha)}\overline{V}^{n+1}_{\mathrm{mc}_{m-k+1}}+\frac{1}{\Delta y^{\alpha}}\sum_{k=0}^{m+1}w_k^{(\alpha)}\overline{V}^{n+1}_{\mathrm{mc}_{m-k+1}}\right)\\ &\quad-\frac{1}{2}(r-\gamma)\left(\overline{V}^{n+1}_{\mathrm{mc}_m}+V^{n}_{\mathrm{mc}_m}\right).\end{aligned}\tag{20}$$

In reference [19], the scheme has been proved to be unconditionally stable. Equation (20) is sorted out as follows:

$$\begin{aligned}&-h_1\sum_{k=3}^{m+1}w_k^{(\alpha)}\overline{V}^{n+1}_{\mathrm{mc}_{m-k+1}}+\left(h_2-h_1w_2^{(\alpha)}\right)\overline{V}^{n+1}_{\mathrm{mc}_{m-1}}+\left(1-h_1w_1^{(\alpha)}+h_3\right)\overline{V}^{n+1}_{\mathrm{mc}_m}-\left(h_1w_0^{(\alpha)}+h_2\right)\overline{V}^{n+1}_{\mathrm{mc}_{m+1}}\\ &=h_1\sum_{k=3}^{m+1}w_k^{(\alpha)}\overline{V}^{n}_{\mathrm{mc}_{m-k+1}}+\left(h_1w_2^{(\alpha)}-h_2\right)\overline{V}^{n}_{\mathrm{mc}_{m-1}}+\left(1+h_1w_1^{(\alpha)}-h_3\right)\overline{V}^{n}_{\mathrm{mc}_m}+\left(h_1w_0^{(\alpha)}+h_2\right)\overline{V}^{n}_{\mathrm{mc}_{m+1}},\end{aligned}\tag{21}$$

where

$$\begin{aligned}h_1&=\frac{1}{2}\frac{a\Delta\tau}{\Delta y^{\alpha}},\\ h_2&=\frac{1}{4}(r-\gamma-D-a)\frac{\Delta\tau}{\Delta y},\\ h_3&=\frac{1}{2}(r-\gamma)\Delta\tau.\end{aligned}\tag{22}$$

Write (21) in matrix:

$$\mathbf{A}\overline{V}^{\mathbf{n+1}}_{\mathrm{mc}}=\mathbf{B}\overline{V}^{\mathbf{n}}_{\mathrm{mc}},\tag{23}$$

where

$$\mathbf{A}=\begin{bmatrix}1-h_1w_1^{(\alpha)}+h_3 & -\left(h_1w_0^{(\alpha)}+h_2\right) & 0 & \cdots & 0 & 0\\ h_2-h_1w_2^{(\alpha)} & 1-h_1w_1^{(\alpha)}+h_3 & -\left(h_1w_0^{(\alpha)}+h_2\right) & \cdots & 0 & 0\\ -h_1w_3^{(\alpha)} & h_2-h_1w_2^{(\alpha)} & 1-h_1w_1^{(\alpha)}+h_3 & \cdots & 0 & 0\\ \vdots & \vdots & \vdots & \ddots & \vdots & \vdots\\ -h_1w_M^{(\alpha)} & -h_1w_{M-1}^{(\alpha)} & -h_1w_{M-2}^{(\alpha)} & \cdots & 1-h_1w_1^{(\alpha)}+h_3 & -\left(h_1w_0^{(\alpha)}+h_2\right)\\ -h_1w_{M+1}^{(\alpha)} & -h_1w_M^{(\alpha)} & -h_1w_{M-1}^{(\alpha)} & \cdots & h_2-h_1w_2^{(\alpha)} & 1-h_1w_1^{(\alpha)}+h_3\end{bmatrix},$$

$$\mathbf{B}=\begin{bmatrix} 1+h_1w_1^{(\alpha)}-h_3 & h_1w_0^{(\alpha)}+h_2 & 0 & \cdots & 0 & 0 \\ h_1w_2^{(\alpha)}-h_2 & 1+h_1w_1^{(\alpha)}-h_3 & h_1w_0^{(\alpha)}+h_2 & \cdots & 0 & 0 \\ h_1w_3^{(\alpha)} & h_1w_2^{(\alpha)}-h_2 & 1+h_1w_1^{(\alpha)}-h_3 & \cdots & 0 & 0 \\ \vdots & \vdots & \vdots & \ddots & \vdots & \vdots \\ h_1w_M^{(\alpha)} & h_1w_{M-1}^{(\alpha)} & h_1w_{M-2}^{(\alpha)} & \cdots & 1+h_1w_1^{(\alpha)}-h_3 & h_1w_0^{(\alpha)}+h_2 \\ h_1w_{M+1}^{(\alpha)} & h_1w_M^{(\alpha)} & h_1w_{M-1}^{(\alpha)} & \cdots & h_1w_2^{(\alpha)}-h_2 & 1+h_1w_1^{(\alpha)}-h_3 \end{bmatrix},$$
$$\overline{V}_{mc}^{n+1}=\left[\overline{V}_0^{n+1},\overline{V}_1^{n+1},\overline{V}_2^{n+1},\ldots,\overline{V}_M^{n+1}\right],$$
$$\overline{V}_{mc}^{n}=\left[\overline{V}_0^{n},\overline{V}_1^{n},\overline{V}_2^{n},\ldots,\overline{V}_M^{n}\right]. \tag{24}$$

Since $B\overline{V}_{\mathrm{mc}}^n$ is known in numerical calculation, we can make $q^n=B\overline{V}_{\mathrm{mc}}^n$, that is, $A\overline{V}_{\mathrm{mc}}^{n+1}=q^n$. It can be obtained by Gauss elimination $[\mathbf{A}\,|\,\mathbf{q}^n]\longrightarrow[\mathbf{A}'\,|\,\mathbf{q}^{n'}]$, where $[\mathbf{A}'\,|\,\mathbf{q}^{n'}]$ is the simplest step matrix, so we get

$$\begin{cases} \overline{V}_{\mathrm{mc}_m}^{n+1}=\dfrac{q_m^{n'}}{A'_{m,m}}, & m=M, \\ \overline{V}_{\mathrm{mc}_m}^{n+1}=\dfrac{q_m^{n'}-A'_{m,m+1}\overline{V}_{m+1}^{n+1}}{A'_{m,m}}, & m=M-1,\,M-2,\ldots,b. \end{cases} \tag{25}$$

Formula (12) and the stock loan have their own characteristics. Formula (20), (21), and (25) are equivalent, and they are only established in area $m=0,1,\ldots,m_f$, where m_f is the point corresponding to the asset price closest to the free boundary. Obviously, m_f is a positive integer less than M. Due to the fact that the stock loan can be repaid at any time, obviously $\overline{V}_m^{n+1}$ should be greater than or equal to $(e^{y_f}-K)^+$. Therefore, the value of the stock loan on each approximation grid point should be expressed as

$$\begin{cases} \overline{V}_{\mathrm{mc}_m}^{n+1}=\max\left(\dfrac{q_m^{n'}-A'_{m,m+1}\overline{V}_{m+1}^{n+1}}{A'_{m,m}},e^{y_f}-K,0\right), \\ m=M-1,\,M-2,\ldots,0, \\ \overline{V}_{\mathrm{mc}_m}^{n+1}=\max\left(\dfrac{q_m^{n'}}{A'_{m,m}},e^{y_m}-K,0\right), \quad m=M. \end{cases} \tag{26}$$

According to the conclusion of reference [20], backward calculation $\overline{V}_{\mathrm{mc}_m}^{n+1}$ in (26), it will be more accurate to calculate the value of the stock loan from M. Because backward calculation defaults $\overline{V}_{\mathrm{mc}_m}^{n+1}=(e^{y_m}-K)^+$ when $m\geq m_f$. When $m<m_f$, the value of stock loan is determined by partial differential equation (11).

4. Numerical Example

4.1. Model Validation. Generally, the pledge rate of the stock loan is less than 0.6. We set the parameters of stock loans with recourse as follows: initial stock price $S_0=100$, loan $K=60$, expiration date $T=3$, risk free interest rate $r=0.05$, dividend rate $D=0.1$, volatility $\gamma=0.1$, tail index $\alpha=1.5$, and recovery factor $\Delta=0.4$, and let $S_{\max}=150$, $S_B=Ke^{\gamma t}$. Due to $y_t=\ln S_t-\gamma t$, $S_t=e^{y_t+\gamma t}$, corresponding $y_{\max}=5$ and $y_B=4.094$. If S_t is used as the boundary, it will cause the boundary moving, so we use the final result $\overline{V}_{mc}$ of model (11) as the inverse coordinate transformation to get V, $V_{\mathrm{mc}}(x,t)=e^{\alpha(T-t)}\overline{V}_{\mathrm{mc}}(y,\tau)$, and $e^{\alpha(T-\tau)}$ is always bigger than 1.

Figure 2 shows that the margin call stock loan is cut off at the barrier price y_B. It can be seen from the lower boundary, the longer the maturity, the greater the value of the non-recourse stock loan, and the greater the value of barrier y_B, the higher the corresponding function image. Under the price of y_B, the margin call stock loan is transformed into a stock loan without recourse. In this paper, we mainly discuss the nature of the margin call stock loan through numerical experiments.

Figure 3 shows that when the pledge rate $\Delta=0$, margin call stock loans equals no recourse stock loans.

4.2. Parameter Analysis. The risk of the margin call stock loan is more controllable for the lender, so the lender is more willing to improve the pledge rate to borrow more money and obtain more interest. With the increase of pledge rate, the borrower also gets more funds in the controllable range, which improves the allocation efficiency of funds.

Figure 4 shows the impact of different recourse shares Δ on the value of the margin call stock loan. The right side of the

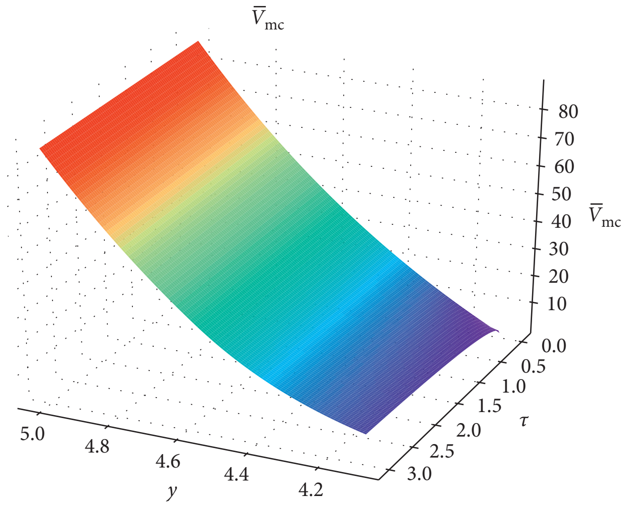

FIGURE 2: The value of $\overline{V}_{mc}$.

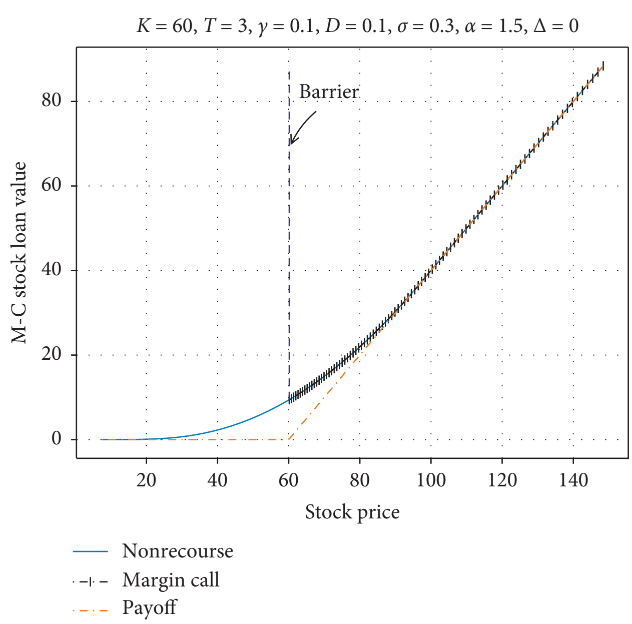

FIGURE 3: When $\Delta = 0$, V_{mc} coincides with V.

barrier indicates the contract value of the margin call stock loan. The left side of the obstacle is $V(x, 0; (1-\Delta)K, T) - \Delta K$, which means, the value of the nonrecourse stock loan with a maturity of $T$and loan amount of $(1-\Delta)K$ minus the value of recourse currency at time 0. Figure shows that the lower the share of recourse, the higher the contract value of the stock pledge loan with recourse, which is confirmed by the actual economic activities. And from formula (4), no matter how high the recourse share Δ is, the contract value of the margin call stock loan is always bigger than zero at the obstacle.

Figure 5 shows the effect of different loan interest rates γ on the contract value of the margin call stock loan under the condition that other parameters remain unchanged. We found that the higher the loan interest rate γ is, the lower the contract value of the margin call stock loan is because in practice, the higher the loan interest rate is, the higher the interest the borrower needs to pay and the faster the barrier

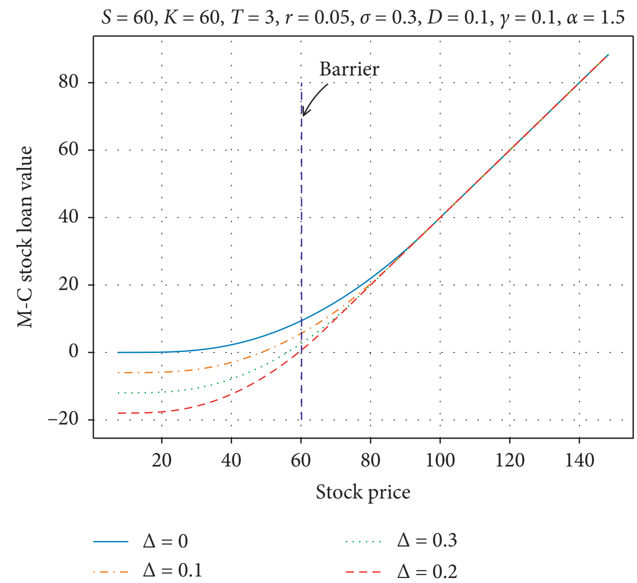

FIGURE 4: Effect of different recourse shares Δ on V_{mc}.

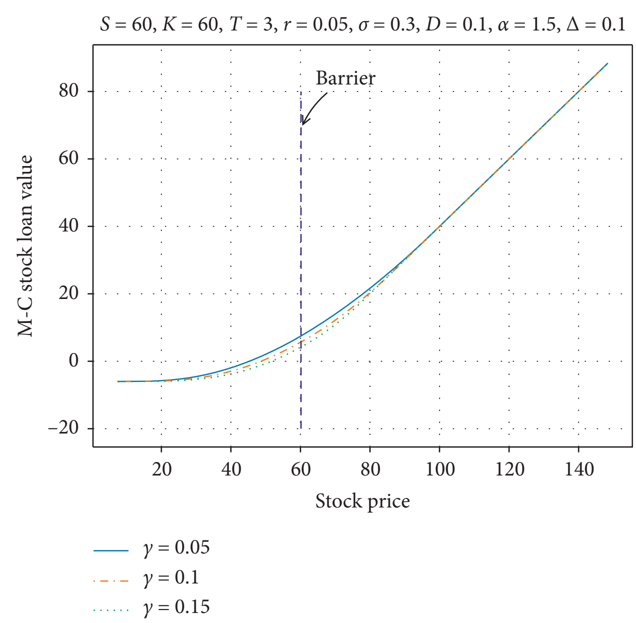

FIGURE 5: Effect of different loan interest rates γ on V_{mc}.

price will rise, so the corresponding contract value of the margin call stock loan will be lower.

Figure 6 shows the effect of different maturity dates T on the contract value of the margin call stock loan under the condition that other parameters remain unchanged. This is because in the actual economic activities, on the one hand, due to the existence of volatility, the longer the time is, the higher the stock price is likely to reach; on the other hand, the loan interest rate and dividend rate are greater than the risk-free interest rate, so the longer the time is, the greater the risk the fund lender bears. In conclusion, the longer the maturity T is, the higher the value of the margin call stock loan is.

Figure 7 shows the effect of different volatility σ on the margin call stock loan under the condition that other

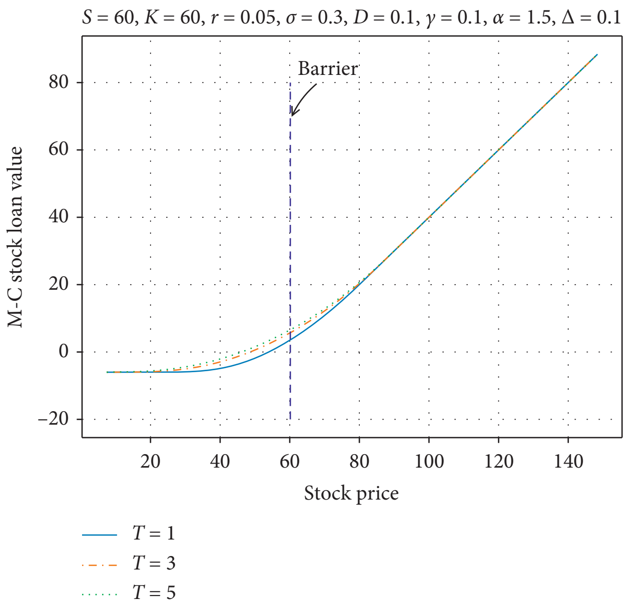

Figure 6: Effect of different maturity dates T on V_{mc}.

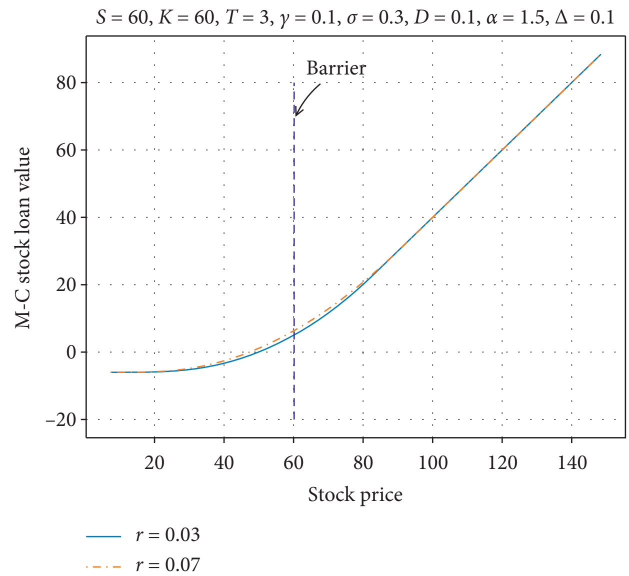

Figure 8: Effect of different risk-free interest rates r on V_{mc}.

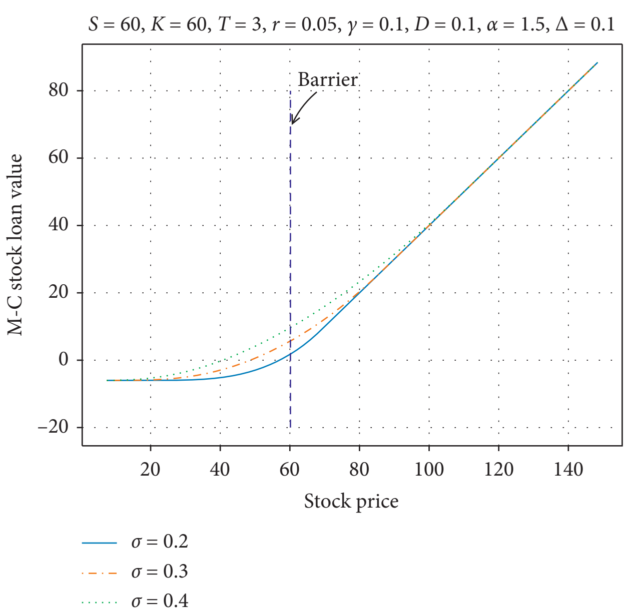

Figure 7: Effect of different volatility σ on V_{mc}.

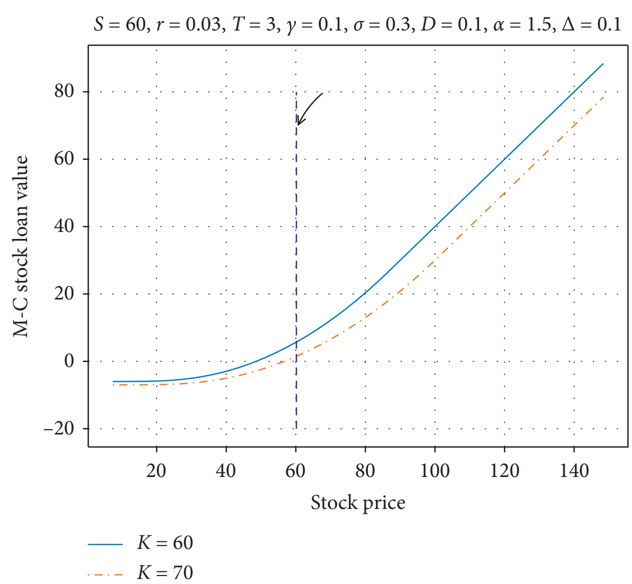

Figure 9: Effect of different loan amounts K on V_{mc}.

parameters are unchanged. It can be seen from the figure that the margin call stock loan increases with the volatility σ because the nonrecourse stock loan is similar to an American option. Due to the increase in the value of the American option with the increase of volatility σ, the increase of volatility σ will give a higher initial value to the recourse stock loan. On the other hand, the margin call stock loan is similar to an American barrier option, and the larger the volatility σ, the higher the value of the margin call stock loan.

Figure 8 shows the effect of different risk-free interest rates r on the contract value of the margin call stock loan under the condition that other parameters remain unchanged. The figure shows that the value of the margin call stock loan increases with the increase of the risk-free interest rate r. Which means the higher the risk-free interest rate is, the higher the contract value of the margin call stock loan is.

Because the risk of the margin call stock loan is more controllable for the lender, in order to obtain more interest income, the lender is willing to increase the pledge rate, which means to provide more loans. Figure 9 shows the effect of different loan amounts K on the contract value of the margin call stock loan. Because the higher the loan amount is, the easier the stock price is to reach the lower bound, the lower the contract value of the corresponding margin call stock loan is.

5. Conclusion

In this paper, we analyze the pricing process of the margin call stock loan under the framework of FMLS. We take the value of the nonrecourse stock loan as a boundary condition of the barrier of the recourse stock loan and study the pricing of the recourse stock loan. The partial differential equations and boundary conditions for the pricing of the margin call stock loan are obtained, and then, the unconditionally stable numerical scheme for the linear complementarity problem is given. And through numerical experiments, we verify the nature of the margin call stock loan, especially when the recourse share $\Delta = 0$, and the margin call stock loan is equivalent to the stock loan without recourse. Finally, we give the influence of different parameters on the stock loan with recourse through numerical experiments, especially the influence of different recourse shares Δ, which are unique to the stock loan with recourse, and explain the economic significance behind it.

Data Availability

The numerical simulation data used to support the findings of this study are included within the article.

Conflicts of Interest

The authors declare that there are no conflicts of interest regarding the publication of this paper.

Acknowledgments

The work in this paper was supported by the Ministry of Education of China Project of Humanities and Social Science (No. 19YJA790094), the National Natural Science Foundation of China (No. 11801463), and the Fundamental Research Funds for the Central Universities (JBK2003005).

References

[1] J. Xia and X. Y. Zhou, "Stock loans," *Mathematical Finance*, vol. 17, no. 2, pp. 307–317, 2007.
[2] Z. Liang, W. Wu, and S. Jiang, "Stock loan with automatic termination clause, cap, and margin," *Computers & Mathematics with Applications*, vol. 60, no. 12, pp. 3160–3176, 2010.
[3] M. R. Grasselli and C. Gómez, "Stock loans in incomplete markets," *Applied Mathematical Finance*, vol. 20, no. 2, pp. 118–136, 2013.
[4] T. W. Wong and H. Y. Wong, "Valuation of stock loans using exponential phase-type Lévy models," *Applied Mathematics and Computation*, vol. 222, pp. 275–289, 2013.
[5] N. Cai and L. Sun, "Valuation of stock loans with jump risk," *Journal of Economic Dynamics and Control*, vol. 40, pp. 213–241, 2014.
[6] T. W. Wong and H. Y. Wong, "Stochastic volatility asymptotics of stock loans: valuation and optimal stopping," *Journal of Mathematical Analysis and Applications*, vol. 394, no. 1, pp. 337–346, 2012.
[7] P. Carr and L. Wu, "The finite moment log stable process and option pricing," *The Journal of Finance*, vol. 58, no. 2, pp. 753–777, 2003.
[8] W. Yu, P. Guo, Q. Wang et al., "On a periodic capital injection and barrier dividend strategy in the compound Poisson risk model," *Mathematics*, vol. 8, no. 4, p. 511, 2020.
[9] W. Yu, F. Wang, Y. Huang, and H. Liu, "Social optimal mean field control problem for the population growth model," *Asian Journal of Control*, pp. 1–8, 2019.
[10] Z. Zhang, Y. Yong, and W. Yu, "Valuing equity-linked death benefits in general exponential Lévy models," *Journal of Computational and Applied Mathematics*, vol. 365, Article ID 112377, 2020.
[11] W. Yu, Y. Yong, G. Guan, Y. Huang, W. Su, and C. Cui, "Valuing guaranteed minimum death benefits by cosine series expansion," *Mathematics*, vol. 7, no. 9, p. 835, 2019.
[12] X. Peng, W. Su, W. Su, and Z. Zhang, "On a perturbed compound Poisson risk model under a periodic threshold-type dividend strategy," *Journal of Industrial & Management Optimization*, vol. 16, no. 4, pp. 1967–1986, 2020.
[13] Á. Cartea, "Dynamic hedging of financial instruments when the underlying follows a non-Gaussian process," *SSRN Electronic Journal*, 2005.
[14] W. Chen, X. Xu, and S.-P. Zhu, "Analytically pricing European-style options under the modified black-scholes equation with a spatial-fractional derivative," *Quarterly of Applied Mathematics*, vol. 72, no. 3, pp. 597–611, 2014.
[15] W. Chen, X. Xu, and S.-P. Zhu, "A predictor-corrector approach for pricing American options under the finite moment log-stable model," *Applied Numerical Mathematics*, vol. 97, pp. 15–29, 2015.
[16] H. Zhang, F. Liu, I. Turner, and S. Chen, "The numerical simulation of the tempered fractional Black–Scholes equation for European double barrier option," *Applied Mathematical Modelling*, vol. 40, no. 11-12, pp. 5819–5834, 2016.
[17] W. Chen, *Numerical methods for fractional Black–Scholes equations and variational inequalities governing option pricing*, Ph.D. thesis, The University of Western, London, Canada, 2014.
[18] X. Lu and E. R. M. Putri, "Finite maturity margin call stock loans," *Operations Research Letters*, vol. 44, no. 1, pp. 12–18, 2016.
[19] B. L. Guo, X. K. Pu, F. H. Huang, Fractional Partial Differential Equations and Their Numerical Solutions, 2015.
[20] Y. L. Zhu, *Derivative Securities and Difference Methods*, Springer, Berlin, Germany, 2004.

Hindawi
Mathematical Problems in Engineering
Volume 2020, Article ID 3518961, 10 pages
https://doi.org/10.1155/2020/3518961

Research Article

Partially Observed Nonzero-Sum Differential Game of BSDEs with Delay and Applications

Qiguang An[1] and Qingfeng Zhu [1,2]

[1]*School of Mathematics and Quantitative Economics and Shandong Key Laboratory of Blockchain Finance, Shandong University of Finance and Economics, Jinan 250014, China*
[2]*Institute for Financial Studies and School of Mathematics, Shandong University, Jinan 250100, China*

Correspondence should be addressed to Qingfeng Zhu; zhuqf508@sohu.com

Received 26 April 2020; Accepted 1 June 2020; Published 19 June 2020

Guest Editor: Zhimin Zhang

A class of partially observed nonzero-sum differential games for backward stochastic differential equations with time delays is studied, in which both game system and cost functional involve the time delays of state variables and control variables under each participant with different observation equations. A necessary condition (maximum principle) for the Nash equilibrium point to this kind of partially observed game is established, and a sufficient condition (verification theorem) for the Nash equilibrium point is given. A partially observed linear quadratic game is taken as an example to illustrate the application of the maximum principle.

1. Introduction

Game theory has penetrated into many fields of economics and attracted more and more attention. A series of studies on game theory was given by [1–9]. There have been many papers about the differential games driven by backward stochastic differential equations (BSDEs), such as [10, 11]. The prospective progress of many systems relies as much on their past history as on their current state. The optimal control problem of stochastic systems with time delays is studied by [12–22]. The game problem of stochastic systems with the time-delayed generator is discussed by [23–25].

Nevertheless, in the aforementioned control and game problems, it is assumed that the information is fully observed. This does not make sense in real life. In general, only partial information is available for controllers in most cases. The latest research studies on the partially observed optimal control issues of stochastic differential systems were given by [26–32]. The partially observed game issues of stochastic systems were studied by [33–36].

As far as we know, the results in regard to partially observed differential games corresponding to backward stochastic systems with time delays (BSDDE) are few. This problem will be investigated in this paper. Comparing the above results, our work differs in several aspects. Firstly, we research such a kind of partially observed differential game problem corresponding to the BSDDE, which enriches the game theory of backward stochastic systems. Secondly, under the circumstance of different observation equations for each participant, our controlled systems and utility functions include the delays of state variables and control variables. Thirdly, we study a class of linear quadratic (LQ) game corresponding to backward stochastic systems with the time-delayed generator and give the specific expression of the Nash equilibrium point.

The outline of this article is as follows. We present the main hypotheses and the partially observed differential game problem of BSDDE in Section 2. In Section 3, we obtain the necessary optimality conditions of the partially observed game of BSDDE. Section 4 is devoted to the sufficient maximum principle. In Section 5, we take a partially observed LQ game as an example to illustrate the application of our maximum principle. Section 6 is the conclusion of this paper.

2. Statement of the Problems

Throughout our article, $(\Omega, \mathscr{F}, \{\mathscr{F}_t\}_{t\geq 0}, \mathbb{P})$ is a complete filtered probability space, on which three mutually independent one-dimensional standard Brownian motions $W(t), Y_1(t)$, and $Y_2(t)$ are defined. Let $\mathscr{F}_t^W, \mathscr{F}_t^1$, and $\mathscr{F}_t^2$ be the natural filtrations generated by $W(\cdot), Y_1(\cdot)$, and $Y_2(\cdot)$, respectively. We set $\mathscr{F}_t = \mathscr{F}_t^W \otimes \mathscr{F}_t^1 \otimes \mathscr{F}_t^2$. For all $t \in [-\delta, 0]$, $\mathscr{F}_t \equiv \mathscr{F}_0$, which is the trivial σ-field, and $\mathscr{F} := \mathscr{F}_{T+\delta}$. Set $\mathscr{F}_t^i = \sigma\{Y_i(s); 0 \leq s \leq t\}$, $(i = 1, 2)$ and $\mathscr{F}_t^i \equiv \mathscr{F}_0^i \neq \phi$, $\forall t \in [-\delta, 0]$. The finite time duration is defined by $T > 0$, and the constant time delays are defined by $0 < \delta, \delta_1, \delta_2 < T$, respectively. The expectation on $(\Omega, \mathscr{F}, P)$ is denoted by $\mathbb{E}$, and the conditional expectation under $\mathscr{F}_t$ is denoted by $\mathbb{E}^{\mathscr{F}_t} := \mathbb{E}[.|\mathscr{F}_t]$. In $\mathbb{R}$ and $\mathbb{R}^{n\times d}$, $\langle\cdot,\cdot\rangle$ is the usual inner product and $|\cdot|$ is the Euclidean norm. The symbol "$\top$" that appears in the superscript represents the transpose of the matrix. In this article, all of the equalities and inequalities are in the sense of $\mathrm{d}t \times \mathrm{d}\mathbb{P}$ almost surely on $[0, T] \times \Omega$.

We introduce the following notations:

$$
\begin{aligned}
&L^2(\mathscr{F}_T; \mathbb{R}) = \left\{\xi\colon \xi \text{ is an } \mathbb{R}-\text{valued, } \mathscr{F}_T - \text{measurable random variable satisfying } \mathbb{E}|\xi|^2 < \infty\right\}, \\
&L^2_{\mathscr{F}}(s, r; \mathbb{R}) = \left\{v(t), s \leq t \leq r\colon v(t) \text{ is an } \mathbb{R}-\text{valued, } \mathscr{F}_t - \text{adapted process satisfying } \mathbb{E}\int_s^r |v(t)|^2 \mathrm{d}t < \infty\right\}.
\end{aligned} \tag{1}
$$

Let the nonempty set $U_i \in \mathbb{R}\,(i = 1, 2)$ be convex and the admissible control set be defined as the following:

$$
\mathscr{U}_i[0, T] = \left\{v_i\colon [0, T] \times \Omega \to U_i \,\middle|\, v_i \text{ is } \mathscr{F}_t^i - \text{adapted, } \mathbb{E}\int_0^T \left|v_i(t)\right|^4 \mathrm{d}t < \infty\right\}, \quad (i = 1, 2). \tag{2}
$$

Every element in $\mathscr{U}_i$ is known as an admissible control to Player $i\,(i = 1, 2)$. And $\mathscr{U}_1 \times \mathscr{U}_2$ is known as the admissible control set to the players.

This work pays attention to a kind of partially observed games of BSDDE, which stems from some attractive financial scenarios. Now let us elaborate on the problem. Take into account the following BSDDE:

$$
\begin{cases}
-\mathrm{d}y^{v_1,v_2}(t) = f(\Theta^{v_1,v_2}(t))\mathrm{d}t - z^{v_1,v_2}(t)\mathrm{d}W(t), & t \in [0, T], \\
y^{v_1,v_2}(T) = \xi,\ y^{v_1,v_2}(t) = \psi_0(t), & t \in [-\delta, 0], \\
v_1(t) = \psi_1(t), & t \in [-\delta_1, 0], \\
v_2(t) = \psi_2(t), & t \in [-\delta_2, 0],
\end{cases} \tag{3}
$$

where

$$
\begin{aligned}
\Theta^{v_1,v_2}(t) = \big(&t, y^{v_1,v_2}(t), y^{v_1,v_2}(t-\delta), z^{v_1,v_2}(t), v_1(t), \\
&v_1(t-\delta_1), v_2(t), v_2(t-\delta_2)\big),
\end{aligned} \tag{4}
$$

and $f\colon [0, T] \times \mathbb{R} \times \mathbb{R} \times \mathbb{R} \times \mathbb{R} \times \mathbb{R} \times \mathbb{R} \times \mathbb{R} \longrightarrow \mathbb{R}$, $\xi \in L^2(\mathscr{F}_T; \mathbb{R})$, and $\psi_0(\cdot) \in L^2_{\mathscr{F}}(-\delta, 0; \mathbb{R})$, $\psi_1(\cdot) \in L^2_{\mathscr{F}}(-\delta_1, 0; \mathbb{R})$, and $\psi_2(\cdot) \in L^2_{\mathscr{F}}(-\delta_2, 0; \mathbb{R})$ are the initial paths of y, v_1, andv_2, respectively. We suppose that $\psi_1(t) \in \mathscr{F}_0^1$ and $\psi_2(t) \in \mathscr{F}_0^2$ are measurable continuous functions such that $\mathbb{E}\int_0^T |\psi_1(t)|^4 \mathrm{d}t < \infty$ and $\mathbb{E}\int_0^T |\psi_2(t)|^4 \mathrm{d}t < \infty$. The control processes for Player 1 and Player 2 are $v_1(\cdot)$ and $v_2(\cdot)$, and $v(\cdot) = (v_1(\cdot), v_2(\cdot))$. Subscript 1 presents the variables to Player 1, and subscript 2 presents the variables to Player 2, respectively. BSDDE game system (3) means that the two players complete a common target ξ in the end time T.

Suppose that the two participants cannot directly observe the state processes $y^{v_1,v_2}(\cdot)$, but they can be aware of related noisy processes $Y_1(\cdot)$ and $Y_2(\cdot)$ of $y^{v_1,v_2}(\cdot)$, which are described as follows:

$$
\begin{cases}
\mathrm{d}Y_i(t) = h_i\big(t, y^{v_1,v_2}(t), y^{v_1,v_2}(t-\delta), z^{v_1,v_2}(t), v_1(t), v_2(t)\big)\mathrm{d}t + \mathrm{d}W_i(t), \\
Y_i(0) = 0, \quad (i = 1, 2),
\end{cases} \tag{5}
$$

where $W_1(\cdot)$ and $W_2(\cdot)$ are $\mathbb{R}$-valued stochastic processes depending on $v_1(\cdot)$ and $v_2(\cdot)$ and $h_i\colon [0, T] \times \mathbb{R} \times \mathbb{R} \times \mathbb{R} \times \mathbb{R} \times \mathbb{R} \longrightarrow \mathbb{R}$, $i = 1, 2$, are continuous functions.

We assume

$(H1)$ (i) f and $h_i, i = 1, 2$, are continuously differentiable with respect to $(y, y_\delta, z, v_1, v_{1\delta}, v_2, v_{2\delta})$

(ii) $f_y, f_{y_\delta}, f_z, f_{v_1}, f_{v_{1\delta}}, f_{v_2}, f_{v_{2\delta}}, h_{iy}, h_{iy_\delta}, h_{iz}, h_{iv_1}, h_{iv_2}, i = 1, 2$, are bounded by $c > 0$

Now, if $(H1)$ is true and both $v_1(\cdot)$ and $v_2(\cdot)$ are admissible controls, then BSDDE (3) has a unique solution $(y^{v_1,v_2}(\cdot), z^{v_1,v_2}(\cdot)) \in L^2_{\mathscr{F}}(-\delta,T;\mathbb{R}) \times L^2_{\mathscr{F}}(-\delta,T;\mathbb{R})$ (see [14]).

Define $\mathrm{d}\mathbb{P}^{v_1,v_2} \doteq Z^{v_1,v_2}(t)\mathrm{d}\mathbb{P}$, where

$$Z^{v_1,v_2}(t) = \exp\left\{\sum_{j=1}^{2}\int_0^t h_j(s, y^{v_1,v_2}(s), y^{v_1,v_2}(s-\delta), z^{v_1,v_2}(s), v_1(s), v_2(s))\mathrm{d}Y_j(s) - \frac{1}{2}\sum_{j=1}^{2}\int_0^t \left|h_j(s, y^{v_1,v_2}(s), y^{v_1,v_2}(s-\delta), z^{v_1,v_2}(s), v_1(s), v_2(s))\right|^2 \mathrm{d}s\right\}. \tag{6}$$

Obviously, $Z^{v_1,v_2}(t)$ satisfies the subsequent SDE:

$$\begin{cases} \mathrm{d}Z^{v_1,v_2}(t) = \sum_{j=1}^{2} h_j(t, y^{v_1,v_2}(t), y^{v_1,v_2}(t-\delta), z^{v_1,v_2}(t), v_1(t), v_2(t))Z^{v_1,v_2}(t)\mathrm{d}Y_j(t), \\ Z^{v_1,v_2}(0) = 1. \end{cases} \tag{7}$$

Hence, by $(H1)$ and Girsanov's theorem, we obtain a three-dimensional Brownian motion $(W(\cdot), W_1(\cdot), W_2(\cdot))$ built on the probability space $(\Omega, \mathscr{F}, \mathbb{P}^{v_1,v_2})$, in which $\mathbb{P}^{v_1,v_2}$ is a probability measure.

Making sure to accomplish the target ξ, each player owns his individual interest, which is the cost functional as follows:

$$J_i(v_1(\cdot), v_2(\cdot)) = \mathbb{E}^{v_1,v_2}\left\{\int_0^T l_i(\Theta^{v_1,v_2}(t))\mathrm{d}t + \Phi_i(y^{v_1,v_2}(0))\right\}, \quad (i=1,2), \tag{8}$$

where $\mathbb{E}^{v_1,v_2}$ is the expectation on $(\Omega, \mathscr{F}, \mathbb{P}^{v_1,v_2})$ and

$$\begin{aligned} l_i\colon f\colon [0,T]\times\mathbb{R}\times\mathbb{R}\times\mathbb{R}\times\mathbb{R}\times\mathbb{R}\times\mathbb{R}\times\mathbb{R} &\longrightarrow \mathbb{R}, \\ \Phi_i\colon \mathbb{R} &\longrightarrow \mathbb{R}, \quad (i=1,2). \end{aligned} \tag{9}$$

We also assume for $i = 1, 2$,

$(H2)$ (i) l_i are continuously differentiable with respect to $(y, y_\delta, z, v_1, v_{1\delta}, v_2, v_{2\delta})$, and their partial derivatives are continuous in $(y, y_\delta, z, v_1, v_{1\delta}, v_2, v_{2\delta})$ and bounded by $c(1 + |y| + |y_\delta| + |z| + |v_1| + |v_{1\delta}| + |v_2| + |v_{2\delta}|)$

(ii) Φ_i are continuously differentiable, and Φ_{iy} are bounded by $c(1 + |y|)$

Assume that every player wants to minimize the cost functional $J_i(v_1(\cdot), v_2(\cdot))$ by picking the appropriate admissible control $v_i(\cdot)$ $(i = 1, 2)$. Then, our partially observed nonzero-sum stochastic differential game problem is to find out a pair of admissible controls $(u_1(\cdot), u_2(\cdot)) \in \mathscr{U}_1 \times \mathscr{U}_2$ such that

$$\begin{cases} J_1(u_1(\cdot), u_2(\cdot)) = \min\limits_{v_1(\cdot)\in\mathscr{U}_1} J_1(v_1(\cdot), u_2(\cdot)), \\ J_2(u_1(\cdot), u_2(\cdot)) = \min\limits_{v_2(\cdot)\in\mathscr{U}_2} J_2(u_1(\cdot), v_2(\cdot)). \end{cases} \tag{10}$$

Obviously, cost functional (8) can be converted to

$$J_i(v_1(\cdot), v_2(\cdot)) = \mathbb{E}\left\{\int_0^T Z^{v_1,v_2}(t) l_i(\Theta^{v_1,v_2}(t))\mathrm{d}t + \Phi_i(y^{v_1,v_2}(0))\right\}, \quad (i=1,2). \tag{11}$$

So, the original problem (10) is the same thing as minimizing (11) over $(v_1(\cdot), v_2(\cdot)) \in \mathscr{U}_1 \times \mathscr{U}_2$ subject to (3) and (7). For the sake of convenience, we refer to the above game problem as Problem (POBNZ). If an admissible control $u(\cdot) = (u_1(\cdot), u_2(\cdot))$ which satisfied (10) can be found, then it is called as an equilibrium point of Problem (POBNZ), and the corresponding state trajectory is denoted by $(y(\cdot), z(\cdot)) = (y^u(\cdot), z^u(\cdot))$.

3. A Partially Observed Necessary Maximum Principle

In the case of a convex admissible control set, the convex perturbation method is the classical method to obtain the necessary optimality condition. Let the equilibrium point of Problem (POBNZ) be $u(\cdot) = (u_1(\cdot), u_2(\cdot))$, and the corresponding optimal trajectory is $(y(\cdot), z(\cdot))$. Let $(\widetilde{v}_1(\cdot), \widetilde{v}_2(\cdot))$

be such that $(u_1(\cdot)+\widetilde{v}_1(\cdot), u_2(\cdot)+\widetilde{v}_2(\cdot)) \in \mathscr{U}_1 \times \mathscr{U}_2$. Since $\mathscr{U}_1$ and $\mathscr{U}_2$ are convex, for any $0 \le \rho \le 1$, $(u_1^\rho(\cdot), u_2^\rho(\cdot)) = (u_1(\cdot)+\rho\widetilde{v}_1(\cdot), u_2(\cdot)+\rho\widetilde{v}_2(\cdot))$ is also in $\mathscr{U}_1 \times \mathscr{U}_2$. For the controls $(u_1^\rho(\cdot), u_2(\cdot))$ and $(u_1(\cdot), u_2^\rho(\cdot))$, the corresponding state trajectories of game system (3) are denoted by $(y^{u_1^\rho}(\cdot), z^{u_1^\rho}(\cdot))$ and $(y^{u_2^\rho}(\cdot), z^{u_2^\rho}(\cdot))$.

We introduce the subsequent symbols:

$$\begin{aligned}
\varphi(t) &= \varphi(t, y(t), y(t-\delta), z(t), u_1(t), u_1(t-\delta_1), u_2(t), u_2(t-\delta_2)),\\
\varphi^{v_1,v_2}(t) &= \varphi(t, y(t), y(t-\delta), z(t), v_1(t), v_1(t-\delta_1), v_2(t), v_2(t-\delta_2)),\\
\varphi^{u_1^\rho,u_2}(t) &= \varphi(t, y(t), y(t-\delta), z(t), u_1^\rho(t), u_1^\rho(t-\delta_1), u_2(t), u_2(t-\delta_2)),\\
\varphi^{u_1,u_2^\rho}(t) &= \varphi(t, y(t), y(t-\delta), z(t), u_1(t), u_1(t-\delta_1), u_2^\rho(t), u_2^\rho(t-\delta_2)),
\end{aligned} \tag{12}$$

where φ denotes one of $f, l_i, i = 1, 2$, and

$$\begin{aligned}
h_i(t) &= h_i(t, y(t), y(t-\delta), z(t), u_1(t), u_2(t)),\\
h_i^{v_1,v_2}(t) &= h_i(t, y(t), y(t-\delta), z(t), v_1(t), v_2(t)),\\
h_i^{u_1^\rho,u_2}(t) &= h_i(t, y(t), y(t-\delta), z(t), u_1^\rho(t), u_2(t)),\\
h_i^{u_1,u_2^\rho}(t) &= h_i(t, y(t), y(t-\delta), z(t), u_1(t), u_2^\rho(t)),\\
&\qquad (i = 1, 2).
\end{aligned} \tag{13}$$

The variational equations are as follows:

$$\begin{cases}
-\mathrm{d}y_i^1(t) = \left[f_y(t)y_i^1(t) + f_{y_\delta}(t)y_i^1(t-\delta) + f_z(t)z_i^1(t) + f_{v_i}(t)\widetilde{v}_i(t) + f_{v_{i\delta}}(t)\widetilde{v}_i(t-\delta_i)\right]\mathrm{d}t - z_i^1(t)\mathrm{d}W(t), \quad t \in [0, T],\\
y_i^1(T) = 0,\ y_i^1(t) = 0, \quad t \in [-\delta, 0],\\
\widetilde{v}_1(t) = 0, \quad t \in [-\delta_1, 0],\\
\widetilde{v}_2(t) = 0, \quad t \in [-\delta_2, 0],\ (i = 1, 2),
\end{cases} \tag{14}$$

$$\begin{cases}
\mathrm{d}Z_i^1(t) = \sum_{j=1}^{2}\left[Z_i^1(t)h_j(t) + Z(t)\left(h_{jy}(t)y_i^1(t) + h_{jy_\delta}(t)y_i^1(t-\delta) + h_{jz}(t)z_i^1(t) + h_{jv_i}(t)\widetilde{v}_i(t)\right)\right]\mathrm{d}Y_j(t),\\
Z_i^1(0) = 0,\ (i = 1, 2).
\end{cases} \tag{15}$$

From $(H1)$, it is easy to see that (14) and (15) admit unique solutions $(y^{v_1,v_2}(\cdot), z^{v_1,v_2}(\cdot)) \in L^2_{\mathscr{F}}(-\delta, T; \mathbb{R}) \times L^2_{\mathscr{F}}(-\delta, T; \mathbb{R})$ and $Z^1(t) \in L^2_{\mathscr{F}}(0, T; \mathbb{R})$, respectively.

For $t \in [0, T]$ and $\rho > 0$, we set

$$\begin{aligned}
\widetilde{y}_i^\rho(t) &= \frac{y^{u_i^\rho}(t) - y(t)}{\rho} - y_i^1(t),\\
\widetilde{z}_i^\rho(t) &= \frac{z^{u_i^\rho}(t) - z(t)}{\rho} - z_i^1(t),\\
\widetilde{Z}_i^\rho(t) &= \frac{Z^{u_i^\rho}(t) - Z(t)}{\rho} - Z_i^1(t),\\
&\qquad (i = 1, 2).
\end{aligned} \tag{16}$$

Similar to the arguments in Lemmas 3.1 and 3.2 in [34], it is easy to obtain subsequent Lemmas 1 and 2. Thus, we omit the details for simplicity.

Lemma 1. *Assume (H1) and (H2) are true. Then,*

$$\begin{aligned}
&\lim_{\rho\to 0}\sup_{0\le t\le T}\mathbb{E}\left|\widetilde{y}_i^\rho(t)\right|^2 = 0,\\
&\lim_{\rho\to 0}\mathbb{E}\int_0^T\left|\widetilde{z}_i^\rho(t)\right|^2\mathrm{d}t = 0,\\
&\lim_{\rho\to 0}\sup_{0\le t\le T}\mathbb{E}\left|\widetilde{Z}_i^\rho(t)\right|^2 = 0,\\
&\qquad (i = 1, 2).
\end{aligned} \tag{17}$$

Since $(u_1(\cdot), u_2(\cdot))$ is a Nash equilibrium point, then

$$\begin{aligned}
&\rho^{-1}\left[J_1(u_1^\rho(\cdot), u_2(\cdot)) - J_1(u_1(\cdot), u_2(\cdot))\right] \ge 0,\\
&\rho^{-1}\left[J_2(u_1(\cdot), u_2^\rho(\cdot)) - J_2(u_1(\cdot), u_2(\cdot))\right] \ge 0.
\end{aligned} \tag{18}$$

Let $\Gamma_i(t) = Z^{-1}(t)Z_i^1(t)$, $i = 1, 2$. From Itô's formula, we deduce

$$\begin{cases} \mathrm{d}\Gamma_i(t) = \sum_{j=1}^{2}\left[h_{jy}(t)y_i^1(t) + h_{jz}(t)z_i^1(t) + h_{jv}(t)\widetilde{v}_i(t)\right]\mathrm{d}W_j(t), \\ \Gamma_i(0) = 0, \quad (i = 1, 2). \end{cases} \tag{19}$$

From this and Lemma 1, we have the following.

Lemma 2. *Assume (H1) and (H2) are true. Then, we get the following variational inequality:*

$$\begin{aligned} &\mathbb{E}^{u_1,u_2}\int_0^T\left[l_i(t)\Gamma_i(t) + l_{iy}(t)y_i^1(t) + l_{iy_\delta}(t)y_i^1(t-\delta) + l_{iz}(t)z_i^1(t) + l_{iv_i}(t)\widetilde{v}_i(t) + l_{iv_{i\delta}}(t)\widetilde{v}_i(t-\delta_i)\right]\mathrm{d}t \\ &\quad + \mathbb{E}^{u_1,u_2}\left[\Phi_{iy}(y(0))y_i^1(0)\right] \geq 0, \quad (i = 1, 2). \end{aligned} \tag{20}$$

Our Hamiltonian function H_i: $[0,T] \times \mathbb{R} \times \mathbb{R} \times \mathbb{R} \times \mathbb{R} \times \mathbb{R} \times \mathbb{R} \times \mathbb{R} \times \mathbb{R} \times \mathbb{R} \times \mathbb{R} \to \mathbb{R}$, $i = 1, 2$, is defined as follows:

$$\begin{aligned} H_i(t, y, y_\delta, z, v_1, v_{1\delta}, v_2, v_{2\delta}, p_i, Q_{1i}, Q_{2i}) &= -\langle p_i(t), f(t, y, y_\delta, z, v_1, v_{1\delta}, v_2, v_{2\delta})\rangle \\ &\quad + \sum_{j=1}^{2}\langle Q_{ji}(t), h_j(t, y, y_\delta, z, v_1, v_2)\rangle + l_i(t, y, y_\delta, z, v_1, v_{1\delta}, v_2, v_{2\delta}), \quad (i = 1, 2). \end{aligned} \tag{21}$$

Denote $H_i(t) \equiv H_i(t, y, y_\delta, z, v_1, v_{1\delta}, v_2, v_{2\delta}, p_i, Q_{1i}, Q_{2i})$ and its derivatives.

We note that the adjoint equation to (19) is a BSDE, whose solution is $(P_i(\cdot), Q_{1i}(\cdot), Q_{2i}(\cdot))$:

$$\begin{cases} -\mathrm{d}P_i(t) = l_i(t)\mathrm{d}t - \sum_{j=1}^{2} Q_{ji}(t)\mathrm{d}W_j(t), \\ P_i(T) = 0, \quad (i = 1, 2), \end{cases} \tag{22}$$

and the adjoint equation to (14) is an SDE, whose solution is $p_i(\cdot)$:

$$\begin{cases} \mathrm{d}p_i(t) = -\left\{H_{iy}(t) + \mathbb{E}^{\mathcal{F}_t}\left[H_{iy_\delta}(t+\delta)\right]\right\}\mathrm{d}t - H_{iz}(t)\mathrm{d}W(t), \\ p_i(0) = -\Phi_{iy}(y(0)), \quad (i = 1, 2). \end{cases} \tag{23}$$

Remark 1. It is easy to see that equation (23) is a linear anticipated SDE. Under $(H1)$ and $(H2)$, the unique solvability of equation (23) is assured by Theorem 2.2 in [14].

Based on variational inequality (20), we set out the main result of this section.

Theorem 1 (partially observed necessary maximum principle). *Assume (H1) and (H2) are true, an equilibrium point of Problem (POBNZ) is $(u_1(\cdot), u_2(\cdot))$, the optimal trajectory is $(y(\cdot), z(\cdot))$, and the solution of (7) is $Z(\cdot)$. Let $(P_i(\cdot), Q_{1i}(\cdot), Q_{2i}(\cdot))$, $i = 1, 2$, be the solution of (22) and $p_i(\cdot)$ be the solution of adjoint equation (23). Then, the following maximum principle*

$$\mathbb{E}^{u_1,u_2}\left[\left(H_{1v_1}(t) + \mathbb{E}^{u_1,u_2}\left[H_{1v_1}(t+\delta_1) \mid \mathcal{F}_t^1\right]\right)(v_1 - u_1(t)) \mid \mathcal{F}_t^1\right] \geq 0, \tag{24}$$

$$\mathbb{E}^{u_1,u_2}\left[\left(H_{2v_2}(t) + \mathbb{E}^{u_1,u_2}\left[H_{2v_2}(t+\delta_2) \mid \mathcal{F}_t^2\right]\right)(v_2 - u_2(t)) \mid \mathcal{F}_t^2\right] \geq 0, \tag{25}$$

for any $(v_1, v_2) \in U_1 \times U_2$, a.e., $t \in [0,T]$, in which the Hamiltonian function H is defined as (21).

Proof. For $i = 1$, using Itô's formula to $\langle y_1^1(t), p_1(t)\rangle + \langle\Gamma(t), P_1(t)\rangle$, from variational equations (14) and (15), variational inequality (20), and adjoint equations (22) and (23), we obtain

$$\begin{aligned}
&\mathbb{E}^{u_1,u_2}\int_0^T\left[l_1(t)\Gamma_1(t)+l_{1y}(t)y_1^1(t)+l_{1y_\delta}(t)y_1^1(t-\delta)+l_{1z}(t)z_1^1(t)+l_{1v_1}(t)\tilde{v}_1(t)+l_{1v_{1\delta}}(t)\tilde{v}_1(t-\delta_1)\right]\mathrm{d}t\\
&+\mathbb{E}^{u_1,u_2}\left[\Phi_{1y}(y(0))y_1^1(0)\right]\\
&=\mathbb{E}^{u_1,u_2}\int_0^T\langle f_{v_1}^\top(t)p_1(t)+\sum_{j=1}^2 h_{jv_1}^\top(t)Q_{j1}(t)+l_{1v_1}(t)\\
&\quad+\mathbb{E}^{u_1,u_2}\left[f_{v_1}^\top(t+\delta)p_1(t+\delta)+\sum_{j=1}^2 h_{jv_1}^\top(t+\delta)Q_{j1}(t+\delta)+l_{1v_1}(t+\delta)\,\middle|\,\mathscr{F}_t^1\right],\tilde{v}_1(t)\rangle\mathrm{d}t\\
&=\mathbb{E}^{u_1,u_2}\int_0^T\langle H_{1v_1}(t)+\mathbb{E}^{u_1,u_2}\left[H_{1v_1}(t+\delta_1)\,\middle|\,\mathscr{F}_t^1\right],\tilde{v}_1(t)\rangle\mathrm{d}t\\
&\geq 0.
\end{aligned}\tag{26}$$

Because $\tilde{v}_1(t)$ satisfies $u_1(t)+\tilde{v}_1(t)\in U_1$, we have

$$\mathbb{E}^{u_1,u_2}\int_0^T\langle H_{1v_1}(t)+\mathbb{E}^{u_1,u_2}\left[H_{1v_1}(t+\delta_1)\,\middle|\,\mathscr{F}_t^1\right],v_1-u_1(t)\rangle\mathrm{d}t\geq 0,\quad\forall v_1\in U_1.\tag{27}$$

This implies that

$$\mathbb{E}^{u_1,u_2}\langle H_{1v_1}(t)+\mathbb{E}^{u_1,u_2}\left[H_{1v_1}(t+\delta_1)\,\middle|\,\mathscr{F}_t^1\right],v_1-u_1(t)\rangle\geq 0,\quad\forall v_1\in U_1.\tag{28}$$

Now, assume that F is an arbitrary element of σ-algebra $\mathscr{F}_t^1$ and $v_1(t)\in U_1$ is a deterministic element. Let

$$w_1(t)=v_1(t)\mathbf{1}_F+u_1(t)\mathbf{1}_{\Omega-F}.\tag{29}$$

Obviously, w_1 is an admissible control.

Using the above inequality to w_1, we obtain

$$\mathbb{E}^{u_1,u_2}\left[\mathbf{1}_F\langle H_{1v_1}(t)+\mathbb{E}^{u_1,u_2}\left[H_{1v_1}(t+\delta_1)\,\middle|\,\mathscr{F}_t^1\right],v_1-u_1(t)\rangle\right]\geq 0,\quad\forall F\in\mathscr{F}_t^1,\tag{30}$$

which implies that

$$\mathbb{E}^{u_1,u_2}\left[\langle H_{1v_1}(t)+\mathbb{E}^{u_1,u_2}\left[H_{1v_1}(t+\delta_1)\,\middle|\,\mathscr{F}_t^1\right],v_1-u_1(t)\rangle\,\middle|\,\mathscr{F}_t^1\right]\geq 0,\quad\forall v_1\in U_1,\ \text{a.e.}\,t\in[0,T],\ \text{a.s.}\tag{31}$$

Similar to the aforementioned method, we can get the other inequality for any $v_2\in U_2$. The proof of Theorem 1 is completed. □

4. A Partially Observed Sufficient Maximum Principle

In this section, we explore a sufficient maximum principle to Problem (POBNZ). Let $(y(t),z(t),u_1(t),u_2(t))$ be a quintuple that satisfies (3), and assume that there is a solution $p_i(t)$ corresponding to adjoint SDE (23). We assume the following:

($H3$) For $i=1,2$, for all $t\in[0,T]$, $H_i(t,\cdot,\cdot,\cdot,\cdot,\cdot,\cdot,\cdot,p_i,Q_{1i},Q_{2i})$ is convex in $(y,y_\delta,z,v_1,v_{1\delta},v_2,v_{2\delta})$, and $\Phi_i(y)$ is convex in y

For $i=1,2$, let

$$\begin{aligned}
H_i(t)&=H_i(t,y(t),y(t-\delta),z(t),u_1(t),u_1(t-\delta),u_2(t),u_2(t-\delta),p_i(t),Q_{1i}(t),Q_{2i}(t)),\\
H_i^{v_1}(t)&=H_i(t,y(t),y(t-\delta),z(t),v_1(t),v_1(t-\delta_1),u_2(t),u_2(t-\delta_2),p_i(t),Q_{1i}(t),Q_{2i}(t)),\\
H_i^{v_2}(t)&=H_i(t,y(t),y(t-\delta),z(t),u_1(t),u_1(t-\delta_1),v_2(t),v_2(t-\delta_2),p_i(t),Q_{1i}(t),Q_{2i}(t)),\\
h_i(t)&=h_i(t,y(t),y(t-\delta),z(t),u_1(t),u_2(t)),\\
h_i^{v_1}(t)&=h_i(t,y(t),y(t-\delta),z(t),v_1(t),u_2(t)),\\
h_i^{v_2}(t)&=h_i(t,y(t),y(t-\delta),z(t),u_1(t),v_2(t)),\\
\varphi(t)&=\varphi(t,y(t),y_\delta(t),z(t),u_1(t),u_1(t-\delta_1),u_2(t),u_2(t-\delta_2)),\\
\varphi^{v_1}(t,\cdot)&=\varphi(t,y(t),y_\delta(t),z(t),v_1(t),v_1(t-\delta_1),u_2(t),u_2(t-\delta_2)),\\
\varphi^{v_2}(t,\cdot)&=\varphi(t,y(t),y_\delta(t),z(t),u_1(t),u_1(t-\delta_1),v_2(t),v_2(t-\delta_2)),
\end{aligned}\tag{32}$$

where $\varphi = f, l_i, i = 1, 2$.

Theorem 2 (partially observed sufficient maximum principle). *Assume (H1)–(H3) are true. Moreover, the maximum conditions (24) and (25) of the partial observation are true; then, $(u_1(\cdot), u_2(\cdot))$ is the equilibrium point to Problem (POBNZ).*

Proof. For any $v_1(\cdot) \in \mathcal{U}_1$, we consider

$$\begin{aligned} &J_1(v_1(\cdot), u_2(\cdot)) - J_1(u_1(\cdot), u_2(\cdot)) \\ &\quad = \mathbb{E}\int_0^T l_1(t)\left[Z^{v_1}(t) - Z(t)\right]dt + \mathbb{E}\left[\Phi_1(y^{v_1}(0)) - \Phi_1(y(0))\right] + \mathbb{E}^{v_1,u_2}\int_0^T \left[l_1^{v_1}(t) - l_1(t)\right]dt \\ &\quad = I_1 + I_2 + I_3. \end{aligned} \tag{33}$$

Using Itô's formula to $\langle P_1(t), Z^{v_1,u_2}(t) - Z(t)\rangle$ on $[0,T]$, we deduce

$$I_1 = \mathbb{E}^{v_1,u_2}\int_0^T \sum_{j=1}^{2} Q_{j1}(t)\left[h_j^{v_1}(t) - h_j(t)\right]dt. \tag{34}$$

Using Itô's formula to $\langle p_1(t), y^{v_1}(t) - y(t)\rangle$ on $[0,T]$, from the convexity of Φ_1, we have

$$\begin{aligned} I_2 &\geq \mathbb{E}^{v_1,u_2}\langle \Phi_{1y}(y(0)), y^{v_1}(0) - y(0)\rangle \\ &= -\mathbb{E}^{v_1,u_2}\int_0^T \langle y^{v_1}(t) - y(t), H_{1y}(t) + \mathbb{E}^{\mathcal{F}_t}\left[H_{1y_\delta}(t+\delta)\right]\rangle dt \\ &\quad - \mathbb{E}^{v_1,u_2}\int_0^T \langle z^{v_1}(t) - z(t), H_{1z}(t)\rangle dt + \mathbb{E}^{v_1,u_2}\int_0^T \langle p_1(t), f^{v_1}(t) - f(t)\rangle dt. \end{aligned} \tag{35}$$

Then, we have

$$\begin{aligned} &J_1(v_1(\cdot), u_2(\cdot)) - J_1(u_1(\cdot), u_2(\cdot)) \\ &\geq \mathbb{E}\int_0^T \left[H_1^{v_1}(t) - H_1(t)\right]dt - \mathbb{E}\int_0^T \langle y^{v_1}(t) - y(t), H_{1y}(t) + \mathbb{E}^{\mathcal{F}_t}\left[H_{1y_\delta}(t+\delta)\right]\rangle dt - \mathbb{E}\int_0^T \langle z^{v_1}(t) - z(t), H_{1z}(t)\rangle dt. \end{aligned} \tag{36}$$

By the virtue of convexity of H_1 to $(y, y_\delta, z, v_1, v_{1\delta}, v_2, v_{2\delta})$, we deduce

$$\begin{aligned} H_1^{v_1}(t) - H_1(t) &\geq \langle y^{v_1}(t) - y(t), H_{1y}(t)\rangle + \langle y_\delta^{v_1}(t) - y_\delta(t), H_{1y_\delta}(t)\rangle \\ &\quad + \langle z^{v_1}(t) - z(t), H_{1z}(t)\rangle + \langle v_1(t) - u_1(t), H_{1v_1}(t)\rangle + \langle v_{1\delta}(t) - u_{1\delta}(t), H_{1v_{1\delta}}(t)\rangle. \end{aligned} \tag{37}$$

Notice the truth that

$$\begin{aligned} &\mathbb{E}\int_0^T \langle y_\delta^{v_1}(t) - y_\delta(t), H_{1y_\delta}(t)\rangle dt - \mathbb{E}\int_0^T \langle y^{v_1}(t) - y(t), \mathbb{E}^{\mathcal{F}_t}\left[H_{1y_\delta}(t+\delta)\right]\rangle dt \\ &\quad = \mathbb{E}\int_0^T \langle y_\delta^{v_1}(t) - y_\delta(t), H_{1y_\delta}(t)\rangle dt - \mathbb{E}\int_\delta^{T+\delta} \langle y_\delta^{v_1}(t) - y_\delta(t), H_{1y_\delta}(t)\rangle dt \\ &\quad = \mathbb{E}\int_0^\delta \langle y_\delta^{v_1}(t) - y_\delta(t), H_{1y_\delta}(t)\rangle dt - \mathbb{E}\int_T^{T+\delta} \langle y_\delta^{v_1}(t) - y_\delta(t), H_{1y_\delta}(t)\rangle dt \\ &\quad = 0. \end{aligned} \tag{38}$$

Then, we get

$$J_1(v_1(\cdot),u_2(\cdot)) - J_1(u_1(\cdot),u_2(\cdot)) \geq \mathbb{E}\int_0^T \langle H_{1v_1}(t) + \mathbb{E}^{\mathcal{F}_t}\left[H_{1v_{1\delta}}(t+\delta)\right], v_1(t)-u_1(t)\rangle \mathrm{d}t. \tag{39}$$

Finally, by necessary optimality conditions (24), we obtain

$$J_1(v_1(\cdot),u_2(\cdot)) - J_1(u_1(\cdot),u_2(\cdot)) \geq 0. \tag{40}$$

Then, it implies

$$J_1(u_1(\cdot),u_2(\cdot)) = \min_{v_1(\cdot)\in\mathcal{U}_1} J_1(v_1(\cdot),u_2(\cdot)). \tag{41}$$

In the same way,

$$J_2(u_1(\cdot),u_2(\cdot)) = \min_{v_2(\cdot)\in\mathcal{U}_2} J_2(u_1(\cdot),v_2(\cdot)). \tag{42}$$

So, we come to the expected conclusion. The proof is completed. □

5. Application

In this section, we construct a partially observed LQ differential game with regard to backward stochastic systems with time delays. Using the classical filtering theory and the aforementioned theoretical results, we attempt to give a specific expression of the Nash equilibrium point. Let us think about the subsequent linear BSDDE:

$$\begin{cases} -\mathrm{d}y^{v_1,v_2}(t) = \left(A(t)y^{v_1,v_2}(t) + \overline{A}(t)y^{v_1,v_2}(t-\delta) + B(t)z^{v_1,v_2}(t) + C_1(t)v_1(t) + C_2(t)v_2(t)\right)\mathrm{d}t - z^{v_1,v_2}(t)\mathrm{d}W(t), & t\in[0,T],\\ y^{v_1,v_2}(T) = \xi,\ y^{v_1,v_2}(t) = \psi(t), & t\in[-\delta,0], \end{cases} \tag{43}$$

and the observation

$$\begin{aligned} \mathrm{d}Y_i(t) &= D_i(t)\mathrm{d}t + \mathrm{d}W_i(t),\\ Y_i^{v_1,v_2}(0) &= 0,\\ &(i=1,2). \end{aligned} \tag{44}$$

We introduce the following cost functional:

$$J_i(v_1(\cdot),v_2(\cdot)) = \frac{1}{2}\mathbb{E}^{v_1,v_2}\left[\int_0^T M_i(t)v_i^2(t)\mathrm{d}t + N_i\left(y^v(0)\right)^2\right], \quad (i=1,2), \tag{45}$$

where constant $N_i\geq 0$, functions $A(\cdot),\overline{A}(\cdot),B(\cdot)$, $C_i(\cdot),D_i(\cdot),M_i(\cdot)$, $i=1,2$, are deterministic and bounded, and $M_i^{-1}(\cdot)$ is bounded. Our partially observed nonzero-sum LQ differential game is to find out a pair of admissible controls $(u_1(\cdot),u_2(\cdot))\in\mathcal{U}_1\times\mathcal{U}_2$ satisfying

$$\begin{cases} J_1(u_1(\cdot),u_2(\cdot)) = \min\limits_{v_1(\cdot)\in\mathcal{U}_1} J_1(v_1(\cdot),u_2(\cdot)),\\ J_2(u_1(\cdot),u_2(\cdot)) = \min\limits_{v_2(\cdot)\in\mathcal{U}_2} J_2(u_1(\cdot),v_2(\cdot)). \end{cases} \tag{46}$$

Similarly to [34], with the help of the necessary maximum principle (Theorem 1), we have the explicit expression to a Nash equilibrium point with regard to the above LQ game problem.

Theorem 3. *For the above LQ game, we find out a Nash equilibrium point as*

$$\begin{aligned}(u_1(t),u_2(t)) = \Big(&M_1^{-1}(t)C_1^\top(t)\mathbb{E}^{v_1,v_2}\left[p_1(t)\,\middle|\,\mathcal{F}_t^1\right],\\ &M_2^{-1}(t)C_2^\top(t)\mathbb{E}^{v_1,v_2}\left[p_2(t)\,\middle|\,\mathcal{F}_t^2\right]\Big), \quad t\in[0,T],\end{aligned} \tag{47}$$

in which $(y(t),z(t),p_1(t),p_2(t))$ satisfy the general FBSDE:

$$\begin{cases} -\mathrm{d}y^{v_1,v_2}(t) = \Big(A(t)y^{v_1,v_2}(t) + \overline{A}(t)y^{v_1,v_2}(t-\delta) + B(t)z^{v_1,v_2}(t) + C_1(t)M_1^{-1}(t)C_1^\top(t)\mathbb{E}^{v_1,v_2}\left[p_1(t)\,\middle|\,\mathcal{F}_t^1\right]\\ \quad + C_2(t)M_2^{-1}(t)C_2^\top(t)\mathbb{E}^{v_1,v_2}\left[p_2(t)\,\middle|\,\mathcal{F}_t^2\right]\Big)\mathrm{d}t - z^{v_1,v_2}(t)\mathrm{d}W(t), \quad t\in[0,T],\\ \mathrm{d}p_i(t) = \left\{A^\top(t)p_i(t) + \mathbb{E}^{\mathcal{F}_t}\left[\overline{A}^\top(t)p_{i\delta+}(t)\right]\right\}\mathrm{d}t + B^\top(t)p_i(t)\mathrm{d}W(t), \quad t\in[0,T],\ (i=1,2),\\ y^{v_1,v_2}(T) = \xi,\ y^{v_1,v_2}(t) = \psi(t), \quad t\in[-\delta,0],\\ p_i(0) = N_i y(0),\ p_i(t) = 0, \quad t\in[T,T+\delta],\ (i=1,2). \end{cases} \tag{48}$$

6. Conclusion

In this research, we have explored a class of partially observed game problem of the backward stochastic system with delay. More specially, based on the convex variational method, we establish the necessary and sufficient conditions with regard to Nash equilibrium in our game issue. The theoretical results of this paper are applied to an LQ game, for which the unique equilibrium point is expressed explicitly. On account of that the LQ model is usually used to depict many financial and economic phenomena, we expect that our LQ game result of BSDDEs can be widely used in these fields. As far as we know, the partially observed nonzero-sum backward game problem with the time-delay generator is firstly investigated in our paper.

Notwithstanding that we are committed to the above game problem, we are likewise able to progress some consequences of optimal control for BSDDEs, for example, [14, 34].

Data Availability

No data were used to support this study.

Conflicts of Interest

The authors declare that there are no conflicts of interest regarding the publication of this paper.

Acknowledgments

This work was supported by National Key R&D Program of China (2018YFA0703900), the National Natural Science Foundation of China (11871309, 11671229, 11371226, and 11301298), the Natural Science Foundation of Shandong Province of China (ZR2019MA013 and ZR2018MG002), Special Funds of Taishan Scholar Project (tsqn20161041), Humanities and Social Sciences Project of the Ministry Education of China (19YJA910002), and Fostering Project of Dominant Discipline and Talent Team of Shandong Province Higher Education Institutions.

References

[1] J. Von Neumann and O. Morgenstern, *The Theory of Games and Economic Behavior*, Princeton University Press, Princeton, NJ, USA, 1944.

[2] J. Nash, "Non-cooperative games," *The Annals of Mathematics*, vol. 54, no. 2, pp. 286–295, 1951.

[3] W. Yu, Y. Huang, and C. Cui, "The absolute ruin insurance risk model with a threshold dividend strategy," *Symmetry*, vol. 10, no. 9, p. 377, 2018.

[4] W. Yu, Y. Yong, G. Guan, Y. Huang, W. Su, and C. Cui, "Valuing guaranteed minimum death benefits by cosine series expansion," *Mathematics*, vol. 7, no. 9, p. 835, 2019.

[5] W. Yu, F. Wang, Y. Huang, and H. Liu, "Social optimal mean field control problem for population growth model," *Asian Journal of Control*, pp. 1–8, 2019.

[6] Q. Zhu, Y. Shi, and B. Teng, "Forward-backward doubly stochastic differential equations with random jumps and related games," *Asian Journal of Control*, pp. 1–16, 2020.

[7] W. Yu, P. Guo, Q. Wang et al., "On a periodic capital injection and barrier dividend strategy in the compound Poisson risk model," *Mathematics*, vol. 8, no. 4, p. 511, 2020.

[8] Z. Zhang, Y. Yong, and W. Yu, "Valuing equity-linked death benefits in general exponential Lévy models," *Journal of Computational and Applied Mathematics*, vol. 365, Article ID 112377, 2020.

[9] X. Peng, W. Su, W. Su, and Z. Zhang, "On a perturbed compound Poisson risk model under a periodic threshold-type dividend strategy," *Journal of Industrial & Management Optimization*, vol. 16, no. 4, pp. 1967–1986, 2020.

[10] Z. Yu and S. Ji, "Linear-quadratic non-zero sum differential game of backward stochstic differential equations," in *Proceedings of the 27th Chinese Control Conference*, Kunming, China, July 2008.

[11] G. Wang and Z. Yu, "A Pontryagin's maximum principle for nonzero sum differential games of BSDEs with applications," *IEEE Transactions on Automatic Control*, vol. 55, pp. 1742–1747, 2010.

[12] L. Chen and Z. Wu, "Maximum principle for the stochastic optimal control problem with delay and application," *Automatica*, vol. 46, no. 6, pp. 1074–1080, 2010.

[13] L. Chen and Z. Wu, "A type of general forward-backward stochastic differential equations and applications," *Chinese Annals of Mathematics, Series B*, vol. 32, no. 2, pp. 279–292, 2011.

[14] L. Chen and J. Huang, "Stochastic maximum principle for controlled backward delayed system via advanced stochastic differential equation," *Journal of Optimization Theory and Applications*, vol. 167, no. 3, pp. 1112–1135, 2015.

[15] M. Tang and Q. Zhang, "Optimal variational principle for backward stochastic control systems associated with Lévy processes," *Science China Mathematics*, vol. 55, no. 4, pp. 745–761, 2012.

[16] Q. Meng and P. Shi, "Stochastic optimal control for backward stochastic partial differential systems," *Journal of Mathematical Analysis and Applications*, vol. 402, no. 2, pp. 758–771, 2013.

[17] Y. Shen, Q. Meng, and P. Shi, "Maximum principle for mean-field jump-diffusion stochastic delay differential equations and its application to finance," *Automatica*, vol. 50, no. 6, pp. 1565–1579, 2014.

[18] Q. Meng and Y. Shen, "Optimal control of mean-field jump-diffusion systems with delay: a stochastic maximum principle approach," *Journal of Computational and Applied Mathematics*, vol. 279, pp. 13–30, 2015.

[19] Q. Meng and Y. Shen, "Optimal control for stochastic delay evolution equations," *Applied Mathematics & Optimization*, vol. 74, no. 1, pp. 53–89, 2016.

[20] M. Tang and Q. Meng, "Linear-quadratic optimal control problems for mean-field stochastic differential equations with jumps," *Asian Journal of Control*, vol. 21, pp. 1–15, 2019.

[21] Y. Dong and Q. Meng, "Second-order necessary conditions for optimal control with recursive utilities," *Journal of Optimization Theory and Applications*, vol. 182, no. 2, pp. 494–524, 2019.

[22] J. Xu, "Stochastic maximum principle for delayed doubly stochastic control systems and their applications," *International Journal of Control*, vol. 93, no. 6, pp. 1371–1380, 2020.

[23] L. Chen and Z. Yu, "Maximum principle for nonzero-sum stochastic differential game with delays," *IEEE Transactions on Automatic Control*, vol. 60, no. 5, pp. 1422–1426, 2015.

[24] J. Shi and G. Wang, "A nonzero sum differential game of BSDE with time-delayed generator and applications," *IEEE Transactions on Automatic Control*, vol. 61, no. 7, pp. 1959–1964, 2016.

[25] Y. Zhuang, "Non-zero sum differential games of anticipated forward-backward stochastic differential delayed equations under partial information and application," *Advances in Difference Equations*, vol. 2017, no. 1, p. 383, 2017.

[26] Z. Wu, "A maximum principle for partially observed optimal control of forward-backward stochastic control systems," *Science China Information Sciences*, vol. 53, no. 11, pp. 2205–2214, 2010.

[27] J. T. Shi and Z. Wu, "Maximum principle for partially-observed optimal control of fully-coupled forward-backward stochastic systems," *Journal of Optimization Theory and Applications*, vol. 145, no. 3, pp. 543–578, 2010.

[28] G. Wang and Z. Wu, "The maximum principle for stochastic recursive optimal control problems under partial information," *IEEE Transactions on Automatic Control*, vol. 54, pp. 1230–1242, 2009.

[29] G. C. Wang and Z. Wu, "General maximum principles for partially observed risk-sensitive optimal control problems and applications to finance," *Journal of Optimization Theory and Applications*, vol. 141, no. 3, pp. 677–700, 2009.

[30] H. Xiao, "The maximum principle for partially observed optimal control of forward-backward stochastic systems with random jumps," *Journal of Systems Science and Complexity*, vol. 24, no. 6, pp. 1083–1099, 2011.

[31] G. Wang, Z. Wu, and J. Xiong, "Maximum principles for forward-backward stochastic control systems with correlated state and observation noises," *SIAM Journal on Control and Optimization*, vol. 51, no. 1, pp. 491–524, 2013.

[32] Y. Shi and Q. Zhu, "Partially observed optimal controls of forward-backward doubly stochastic systems," *ESAIM: Control, Optimisation and Calculus of Variations*, vol. 19, no. 3, pp. 828–843, 2013.

[33] G. Wang and Z. Yu, "A partial information non-zero sum differential game of backward stochastic differential equations with applications," *Automatica*, vol. 48, no. 2, pp. 342–352, 2012.

[34] S. Wu and L. Shu, "Non-zero sum differential games of backward stochastic differential delay equations under partial information," *Asian Journal of Control*, vol. 19, no. 1, pp. 316–324, 2017.

[35] B. Yang, T. Guo, and J. Wu, "A partially observed nonzero-sum stochastic differential game with delays and its application to finance," *Asian Journal of Control*, vol. 21, pp. 1–12, 2019.

[36] J. Xiong, S. Zhang, and Y. Zhuang, "A partially observed non-zero sum differential game of forward-backward stochastic differential equations and its application in finance," *Mathematical Control & Related Fields*, vol. 9, no. 2, pp. 257–276, 2019.

Hindawi
Mathematical Problems in Engineering
Volume 2020, Article ID 2359135, 14 pages
https://doi.org/10.1155/2020/2359135

Research Article

Robust Time-Consistent Portfolio Selection for an Investor under CEV Model with Inflation Influence

Peng Yang [1,2]

[1] *School of Science, Xijing University, Xi'an 710123, China*
[2] *School of Mathematics and Statistics, Xi'an Jiaotong University, Xi'an 710049, China*

Correspondence should be addressed to Peng Yang; yangpeng511@163.com

Received 6 May 2020; Accepted 29 May 2020; Published 17 June 2020

Guest Editor: Wenguang Yu

A robust time-consistent optimal investment strategy selection problem under inflation influence is investigated in this article. The investor may invest his wealth in a financial market, with the aim of increasing wealth. The financial market includes one risk-free asset, one risky asset, and one inflation-indexed bond. The price process of the risky asset is governed by a constant elasticity of variance (CEV) model. The investor is ambiguity-averse; he doubts about the model setting under the original probability measure. To dispel this concern, he seeks a set of alternative probability measures, which are absolutely continuous to the original probability measure. The objective of the investor is to seek a time-consistent strategy so as to maximize his expected terminal wealth meanwhile minimizing his variance of the terminal wealth in the worst-case scenario. By using the stochastic optimal control technique, we derive closed-form solutions for the optimal time-consistent investment strategy, the probability scenario, and the value function. Finally, the influences of model parameters on the optimal investment strategy and utility loss function are examined through numerical experiments.

1. Introduction

Nowadays, portfolio selection is a very important research topic in mathematical finance. As we all know, Markowitz [1] pioneered this research topic. He measured the investment gain and risk by expectation and variance, respectively. Nowadays, scholars call this method as the mean-variance (MV) criterion. Li and Ng [2] and Zhou and Li [3], respectively, pioneered the multiperiod and the continuous-time MV problem, where the explicit solutions were obtained. Dai et al. [4] studied the continuous-time MV problem with transaction costs. Recently, Sun et al. [5, 6] studied the MV problem for an insurer.

The aforementioned work under the MV criterion is time inconsistency. That is to say, the optimal strategy made at time t may not be optimal at time s, $s > t$. However, time consistency of strategy is an important and a rational requirement in many practice scenarios. For example, a few years ago, the Chinese government decided to get rid of poverty by 2020. Naturally, they hope to get rid of poverty at 2020. To the best of our knowledge, Strotz [7] first formally treated time inconsistency. He proposed a game theoretic approach and sought an equilibrium strategy. Thus, the equilibrium strategy is time-consistent. Nowadays, this method becomes a mainstream way to deal with time-inconsistency. Ekeland et al. [8] first proposed the rigorous definition of the equilibrium strategy in a continuous-time framework. Björk and Murgoci [9] studied the time-consistent investment strategy, where the model parameters are controlled by a common Markov process. Li et al. [10] considered the optimal time-consistent MV problem under the Heston model. Yang [11] studied the similar problem, where the aggregate claim and the price are shocked by a common Poisson process. Zeng et al. [12] studied the robust time-consistent strategy under the MV framework. Furthermore, Yang et al. [13] extended the time-consistent MV problem to a new interaction mechanism. For more other detailed and related studies, one can refer to Björk et al. [14], Czichowsky [15], and Kronborg and Steffensen [16].

However, most of the aforementioned papers ignore the inflation risk and assume that the risky asset follows a geometric Brownian motion, which is usually contrary to practice investment activities according to many empirical studies. Brennan and Xia [17] studied the asset distribution problem under inflation influence. Han and Huang [18] considered the defined-contribution (DC) pension problem under inflation influence. Kwak and Lim [19] studied the optimal consumption-investment problem under inflation influence. Li et al. [20] studied the time-consistent investment strategy selection problem for a DC pension under partial information and inflation influence.

On the contrary, the CEV model has become popular among academia and practitioners since proposed by Cox and Ross [21]. Gao [22] investigated the DC pension investment problem under the CEV model. Gu et al. [23], Lin and Li [24], and Liang et al. [25] investigated the optimal reinsurance and investment strategy selection problem under the CEV model. Lin and Qian [26] studied the similar problem, where the strategy is time-consistent. For more other detailed and related studies about the CEV model, readers can refer to Li et al. [27] and Zheng et al. [28].

Bearing in mind the aforementioned state of the art, in this article, we will investigate the time-consistent investment strategy under the CEV model with inflation influence. The financial market includes one risk-free asset, one risky asset, and one inflation-indexed bond. The price process of the risky asset is governed by the CEV model. We assume that the investor is ambiguity-averse and worries about uncertainty in model setting. To dispel this concern, he seeks a set of alternative probability measures, which are absolutely continuous to the original probability measure. Then, the new model setting is obtained under the new probability measure. The objective of the investor is to find a time-consistent strategy so as to maximize his expected terminal wealth meanwhile minimizing his variance of the terminal wealth in the worst-case scenario. The problem's solving steps are as follows: first, we provide an extended HJB equation and a verification theorem. Second, by using the stochastic optimal control technique, we derive analytically the optimal time-consistent investment strategy, the probability scenario, and the value function. Finally, the influences of model parameters on the optimal investment strategy and utility loss function are examined through numerical experiments.

Compared with some related current research studies, our main contributions are given as follows:

(i) We consider a general financial market, which includes one risk-free asset, one risky asset, and one inflation-indexed bond. The price process of the risky asset is governed by the CEV model.

(ii) We study the time-consistent investment problem under inflation influence.

(iii) Closed-form solutions for the optimal time-consistent robust investment strategy, optimal probability scenario, and value function are derived.

(iv) The influences of model parameters on the optimal time-consistent investment strategy and utility loss function are systematically examined through numerical experiments.

The remainder of this article is arranged as follows. In Section 2, we describe the model setup. In Section 3, an optimal robust time-consistent investment strategy selection problem is formulated. In Section 4, the closed-form solutions for the time-consistent optimal investment strategy and optimal probability scenario are derived. In Section 5, the influences of model parameters on the optimal time-consistent investment strategy and utility loss function are examined through numerical experiments. The final section summarizes this article.

2. Model Setup

We construct a financial model and present some basic assumptions in this section. All stochastic processes and random variables, mentioned later, are defined on a filtered complete probability space $(\Omega, \mathcal{F}, \mathcal{F}_t, P)$. We assume that $\mathcal{F} := \{\mathcal{F}_t, t \geq 0\}$ is right-continuous and is complete with respect to P. $\mathcal{F}_t$ stands for the information acquired by the investor up to time t. We assume that there are no market frictions in trading.

2.1. Financial Market. A financial market with the inflation risk is given in this section. To the best of our knowledge, consumer price index (CPI) is often used to describe the inflation rate in economics and academic research. CPI can be seen as a price level process. In this article, the inflation price level $P_0(t)$ satisfies the following process:

$$\mathrm{d}P_0(t) = P_0(t)\left[\mu_1 \mathrm{d}t + \sigma_1 \mathrm{d}W_1(t)\right], \tag{1}$$

where $\mu_1 > 0$ represents the instantaneous expected rate of the inflation, $\sigma_1 > 0$ stands for the volatility of the inflation, and $W_1(t)$ stands for a standard Brownian motion.

We assume that there are three assets available for the investor: one risk-free asset, one risky asset, and one inflation-indexed bond. The price process $P_1(t)$ of the risk-free asset is given by

$$\mathrm{d}P_1(t) = r_1 P_1(t)\mathrm{d}t. \tag{2}$$

Here, $r_1 > 0$ represents the interest rate of the risk-free asset. The price process $S(t)$ of the risky asset satisfies the following CEV model:

$$\mathrm{d}S(t) = S(t)\left[\mu_2 \mathrm{d}t + \sigma_2 S^{\beta}(t)\mathrm{d}W_2(t)\right], \; S(0) = s_0. \tag{3}$$

Here, $\mu_2 \geq r_1$ stands for the appreciation rate, $\sigma_2 > 0$ represents the price volatility, $W_2(t)$ represents a standard Brownian motion, and β is the constant elasticity parameter. We assume $W_1(t)$ and $W_2(t)$ are mutually independent.

Remark 1. The parameter β can take all real numbers. Obviously, if $\beta = 0$, the CEV model will degenerate to a geometric Brownian motion. When the CEV model is proposed, β is assumed to be negative. Emanuel and Macbeth [29] proved that β can also be assumed to be positive. The CEV model has no jump, i.e., we do not consider the jump risk in this article. We can also consider the price process with the jump. Then, the exponential Lévy model is a good choice. For the exponential Lévy model, readers can refer to Yu et al. [30] and Zhang et al. [31].

The third asset to invest in is the inflation-indexed bond. Similar to Kwak and Lim [19], the price $P(t)$ of the inflation-indexed bond is given by

$$\frac{\mathrm{d}P(t)}{P(t)} = \left[r_2 \mathrm{d}t + \frac{\mathrm{d}P_0(t)}{P_0(t)}\right] = (r_2 + \mu_1)\mathrm{d}t + \sigma_1 \mathrm{d}W_1(t). \quad (4)$$

Here, $r_2 > 0$ represents the real interest rate, and $r_2 + \mu_1 > r_1$ stands for the appreciation rate.

2.2. Inflation-Adjusted Wealth Process. Let $u_1(t)$ and $u_2(t)$, respectively, denote the proportions of the wealth invested in the risky asset and the inflation-indexed bond at time t, and the remainder of the proportion is invested in the risk-free asset. At time t, the investor (here, we only consider an investor. To reflect the general situation, one can consider n investors. For example, Yang et al. [13], Espinosa and Touzi [32], and Yu et al. [33] studied the optimal control problem for n agents) can choose the proportions $u_1(t)$ and $u_2(t)$ as control strategies; we denote them as $u(t) = (u_1(t), u_2(t))$. For each strategy $u(t)$, the wealth process R_t^u can be described as

$$\begin{aligned}\frac{\mathrm{d}R_t^u}{R_t^u} &= [1 - u_1(t) - u_2(t)]\frac{\mathrm{d}P_1(t)}{P_1(t)} + u_1(t)\frac{\mathrm{d}S(t)}{S(t)} + u_2(t)\frac{\mathrm{d}P(t)}{P(t)} \\ &= [r_1 + u_1(t)(\mu_2 - r_1) + u_2(t)(r_2 + \mu_1 - r_1)]\mathrm{d}t \\ &\quad + u_1(t)\sigma_2 S^\beta(t)\mathrm{d}W_2(t) + u_2(t)\sigma_1 \mathrm{d}W_1(t).\end{aligned} \quad (5)$$

Denote

$$X_t^u = \frac{R_t^u}{P_0(t)}. \quad (6)$$

By applying Itô's formula, X_t^u can be described as

$$\begin{aligned}\mathrm{d}X_t^u &= \frac{1}{P_0(t)}\mathrm{d}R_t^u + R_t^u \mathrm{d}\frac{1}{P_0(t)} + d\left\langle R_t^u, \frac{1}{P_0(t)}\right\rangle \\ &= X_t^u\Big\{\big[r_1 + \sigma_1^2 - \mu_1 + u_1(t)(\mu_2 - r_1) \\ &\quad + u_2(t)\big(r_2 + \mu_1 - r_1 - \sigma_1^2\big)\big]\mathrm{d}t \\ &\quad + u_1(t)\sigma_2 S^\beta(t)\mathrm{d}W_2(t) + (u_2(t) - 1)\sigma_1(t)\mathrm{d}W_1(t)\Big\}.\end{aligned} \quad (7)$$

Here, X_t^u is the real wealth with stripping out inflation.

To facilitate solving the optimization problem in Section 3, we define the following notations:

$$\begin{cases}\pi_1(t) = u_1(t)X_t^u, \pi_2(t) = [u_2(t) - 1]X_t^u, & \pi(t) = (\pi_1(t), \pi_2(t)), \\ \widetilde{r}_1 = r_1 + \sigma_1^2 - \mu_1, \widetilde{r}_2 = r_2 + \mu_1 - r_1 - \sigma_1^2, & \widetilde{r} = \widetilde{r}_1 + \widetilde{r}_2.\end{cases} \quad (8)$$

Then, the real wealth X_t^π can be described as

$$\begin{aligned}\mathrm{d}X_t^\pi &= [\widetilde{r}X_t^\pi + \pi_1(t)(\mu_2 - r_1) + \pi_2(t)\widetilde{r}_2]\mathrm{d}t \\ &\quad + \pi_1(t)\sigma_2 S^\beta(t)\mathrm{d}W_2(t) + \pi_2(t)\sigma_1 \mathrm{d}W_1(t).\end{aligned} \quad (9)$$

3. Problem Formulation

MV investment strategy selection problem as a classic optimization problem can be given as follows:

$$\sup_\pi\left\{E_{0,x_0,s_0}[X_T^\pi], -\mathrm{Var}_{0,x_0,s_0}[X_T^\pi]\right\}. \quad (10)$$

Here, $E_{0,x_0,s_0}[\cdot] = E[X_0^\pi = x_0, S(0) = s_0]$, $\mathrm{Var}_{0,x_0,s_0}[\cdot] = \mathrm{Var}[X_0^\pi = x_0, S(0) = s_0]$, x_0 is the investor's initial wealth, and T is the termination time of the investment. Obviously, the objective of the investor is to find an investment strategy so as to maximize his expected terminal wealth meanwhile minimizing his variance of the terminal wealth. It is well known that this problem is equivalent to the following problem:

$$\sup_\pi\left\{E_{0,x_0,s_0}[X_T^\pi] - \frac{\gamma}{2}\mathrm{Var}_{0,x_0,s_0}[X_T^\pi]\right\}, \quad (11)$$

where $\gamma > 0$ represents the risk-aversion parameter. According to Björk and Murgoci [9] and Kronborg and Steffensen [16], we know that the optimal strategy of (11) is a precommitment strategy, which is time-inconsistent.

As we explained in the introduction, one usually takes into account the time-consistent strategy. Similar to Yang [11], Lin and Qian [26], and other related papers, we consider the following problem:

$$\sup_\pi\left\{E_{t,x,s}[X_T^\pi] - \frac{\gamma}{2}\mathrm{Var}_{t,x,s}[X_T^\pi]\right\}, \quad (12)$$

where $E_{t,x,s}[\cdot] = E[X_t^\pi = x, S(t) = s]$ and $\mathrm{Var}_{t,x,s}[\cdot] = \mathrm{Var}[X_t^\pi = x, S(t) = s]$. The target is to develop the corresponding equilibrium investment strategy, which is time-consistent.

Problem (12) is the traditional MV problem, where the investor is ambiguity-neutral. That is, he fully believes in the model defined under the probability measure P. In the actual economic activities, the investor often is ambiguity-averse and wants to protect himself against worst-case scenarios. Similar to Zeng et al. [12], Maenhout [34, 35], Chen and Yang [36], and other papers, we incorporate ambiguity aversion into MV problem (12). Since the investor is ambiguity-averse, he may doubt the model defined under the probability measure P. Hence, we defined an alternative probability measure Q, which is absolutely continuous to P. All such Q are denoted by $\mathcal{Q}$, that is,

$$\mathcal{Q} := \{Q \mid Q \sim P\}. \tag{13}$$

Now, we define an admissible strategy.

Definition 1. For any fixed $t \in [0,T]$, an investment strategy $\pi(t) = (\pi_1(t), \pi_2(t))$ is called an admissible strategy for the ambiguity-averse investor (AAI) if it satisfies the following:

(i) $\pi_1(t)$ and $\pi_2(t)$ are progressively measurable with respect to $\mathcal{F}_t$

(ii) $E^{Q^*}_{t,x,s}[\int_0^T \pi_1^2(t) S^{2\beta} dt] < \infty$ and $E^{Q^*}_{t,x,s}[\int_0^T \pi_2^2(t) dt] < \infty$, where Q^* is the probability measure under the worst-case scenario and $E^{Q^*}_{t,x,s}[\cdot] = E^{Q^*}_{t,x,s}[\cdot \mid X_t^\pi = x, S(t) = s]$

(iii) Equation (9) with respect to $\pi(t)$ has a unique strong solution

We denote all such admissible investment strategies on the time interval $[0,T]$ as Π.

To transform model (9) from the probability measure P to the probability measure Q, we define a process $\{\theta(t) = (\theta_1(t), \theta_2(t)) \mid t \in [0,T]\}$, which satisfies the following:

(i) $\theta_1(t)$ and $\theta_2(t)$ are progressively measurable with respect to $\mathcal{F}_t$

(ii) $E[\exp\{(1/2)\int_0^T [\theta_1^2(t) + \theta_2^2(t)] dt\}] < \infty$

All such $\theta(t)$ on the time interval $[0,T]$ are denoted by Θ. For any $\theta \in \Theta$, we define a real-valued process $\{Z^\theta(t) \mid t \in [0,T]\}$ on $(\Omega, \mathcal{F}, \mathcal{F}_t, P)$ as

$$\begin{aligned} Z^\theta(t) := \exp\bigg\{ &\int_0^t \theta_1(s) dW_1(s) + \int_0^t \theta_2(s) dW_2(s) \\ &- \frac{1}{2}\int_0^t \theta_1^2(s) ds - \frac{1}{2}\int_0^t \theta_2^2(s) ds \bigg\}. \end{aligned} \tag{14}$$

Then, $Z^\theta(t)$ is a martingale with respect to P. In the following, we define a new probability measure Q, which is given by

$$\left.\frac{dQ}{dP}\right|_{\mathcal{F}_T} := Z^\theta(T). \tag{15}$$

From the definition of Q, it is clear that Q is absolutely continuous to P.

For any $\theta \in \Theta$, we, respectively, define two new processes $W_1^Q(t)$ and $W_2^Q(t)$ by

$$\begin{aligned} dW_1^Q(t) &= dW_1(t) - \theta_1(t) dt, \\ dW_2^Q(t) &= dW_2(t) - \theta_2(t) dt. \end{aligned} \tag{16}$$

According to Girsanov's theorem, $W_1^Q(t)$ and $W_2^Q(t)$ are standard Brownian motions with respect to Q. Furthermore, the wealth process (9) under Q can be rewritten as

$$\begin{aligned} dX_t^\pi = &\left[\tilde{r} X_t^\pi + \pi_1(t)(\mu_2 - r_1) + \pi_2(t)\tilde{r}_2 \right. \\ &\left. + \pi_1(t)\theta_2(t)\sigma_2 S^\beta + \pi_2(t)\theta_1(t)\sigma_1\right] dt \\ &+ \pi_1(t)\sigma_2 S^\beta dW_2^Q(t) + \pi_2(t)\sigma_1 dW_1^Q(t), \end{aligned} \tag{17}$$

and corresponding CEV model (3) becomes

$$dS(t) = S(t)\left[\left(\mu_2 + \theta_2(t)\sigma_2 S^\beta(t)\right) dt + \sigma_2 S^\beta(t) dW_2^Q(t)\right]. \tag{18}$$

In the following, we modify MV problem (12) under the worst-case scenario. Through modifying MV problem (12), we shall deal with a robust time-consistent MV strategy selection problem as follows:

$$\sup_{\pi\in\Pi} V^\pi(t,x,s) = \sup_{\pi\in\Pi}\left\{\inf_{Q\in\mathcal{Q}} \widehat{V}^{\pi,Q}(t,x,s)\right\}. \tag{19}$$

Here,

$$\begin{aligned} \widehat{V}^{\pi,Q}(t,x,s) = &E^Q_{t,x,s}\left\{\int_t^T \left[\frac{(\theta_1(v))^2}{2\phi_1(v)} + \frac{(\theta_2(v))^2}{2\phi_2(v)}\right] dv\right\} \\ &+ E^Q_{t,x,s}[X_T^\pi] - \frac{\gamma}{2}\mathrm{Var}^Q_{t,x,s}[X_T^\pi], \end{aligned} \tag{20}$$

$$V^\pi(t,x,s) = \inf_{Q\in\mathcal{Q}} \widehat{V}^{\pi,Q}(t,x,s), \tag{21}$$

where $\phi_1(t)$ and $\phi_2(t)$ are nonnegative and stand for the investor's ambiguity aversion with respect to the model under P. The larger $\phi_1(t)$ and $\phi_2(t)$ are, the more the model under Q will deviate from the model under P. Therefore, AAI's ambiguity aversion is an increasing function of $\phi_1(t)$ and $\phi_2(t)$. To embody some good properties of the model under P, AAI deviation from P is penalized by the first two terms in (20). The penalty terms depend on the relative entropy. The increase in relative entropy from t to $t + dt$ equals

$$\frac{1}{2}\left[(\theta_1(t))^2 + (\theta_2(t))^2\right] dt. \tag{22}$$

The proof of (22) is similar to that in Appendix A in Zeng et al. [12]; we omit it here.

To obtain the time-consistent investment strategy, we present the definition of the equilibrium strategy.

Definition 2. For $\forall (t,x,s) \in [0,T] \times R \times R^+$, we choose an admissible strategy $\pi^*(t,x,s) \in \Pi$. Then, through choosing three real numbers $\tilde{a} \in R^+$, $\tilde{b} \in R$, and $\varsigma > 0$, we define a new strategy by

$$\pi^\varsigma(l,\tilde{x},\tilde{s}) = \begin{cases} (\tilde{a},\tilde{b}) & \text{for } (l,\tilde{x},s) \in [t, t+\varsigma) \times R \times R^+, \\ \pi^*(l,\tilde{x},s), & \text{for } (l,\tilde{x},s) \in [t+\varsigma, T] \times R \times R^+. \end{cases} \tag{23}$$

If for any $(\tilde{a},\tilde{b}) \in R^+ \times R$ and $(t,x,s) \in [0,T] \times R \times R^+$, we have

$$\liminf_{\varsigma\longrightarrow 0} \frac{V^{\pi^*}(t,x,s) - V^{\pi^\varsigma}(t,x,s)}{\varsigma} \geq 0, \tag{24}$$

which holds; then, $\pi^*(t,x,s)$ is called an equilibrium strategy, and the equilibrium value function $V(t,x,s)$ is given by

$$V(t,x,s) = V^{\pi^*}(t,x,s). \tag{25}$$

As evidenced by many references such as Björk and Murgoci [9] and Yang et al. [13], the equilibrium strategy defined by Definition 2 is time-consistent. Therefore, in the following, we call the equilibrium strategy and the equilibrium value function as the optimal time-consistent strategy and the optimal value function. Thus, the AAI's aim is to find an optimal time-consistent investment strategy to solve robust optimization problem (19).

For convenience, we define two notations:

$$C^{1,2,2}\left([0,T]\times R\times R^{+}\right)=\{\varphi(t,x,s)\mid \text{for}\,\forall[0,T]\times R\times R^{+},\ \varphi_x(t,x,s),\varphi_{xx}(t,x,s),\varphi_s(t,x,s),\ \varphi_{ss}(t,x,s)\ \text{are continuous}\},\tag{26}$$

and the usual infinitesimal generator $\mathscr{A}^{\pi,\theta}$ for the wealth process (17) is given by

$$\begin{aligned}\mathscr{A}^{\pi,\theta}(\varphi(t,x,s)) &= \varphi_t(t,x,s)+\left[\tilde{r}x+\pi_1(t)(\mu_2-r_1)+\pi_2(t)\tilde{r}_2+\pi_2(t)\theta_1(t)\sigma_1+\pi_1(t)\theta_2(t)\sigma_2 s^{\beta}\right]\varphi_x(t,x,s)\\ &\quad+\frac{1}{2}\left[\pi_1^2(t)\sigma_2^2 s^{2\beta}+\pi_2^2(t)\sigma_1^2\right]\varphi_{xx}(t,x,s)+\left[\mu_2 s+\theta_2(t)\sigma_2 s^{\beta+1}\right]\varphi_s(t,x,s)+\frac{1}{2}\sigma_2^2 s^{2\beta+2}\varphi_{ss}+\pi_1(t)\sigma_2^2(t)s^{2\beta+1}\varphi_{sx}(t,x,s),\end{aligned}\tag{27}$$

where $\varphi(t,x,s)\in C^{1,2,2}([0,T]\times R\times R^{+})$, $\pi\in\Pi$, and $\theta\in\Theta$.

To ensure the strategy obtained from robust MV problem (19) is optimal, we present the following verification theorem. The proof of this theorem is similar to that in Theorem 7.1 of Björk and Murgoci [9], Theorem 4.1 of Yang et al. [13], and other papers, so we omit it here.

Theorem 1. *For robust MV problem (19), if there exist two functions $W(t,x,s)$ and $g(t,x,s)$ satisfying the following extended HJB equation*

$$\sup_{\pi\in\Pi}\inf_{Q\in\mathcal{Q}}\left\{\mathscr{A}^{\pi,\theta}(W(t,x,s))-\mathscr{A}^{\pi,\theta}\left(\frac{\gamma}{2}g^2(t,x,s)\right)+\gamma g(t,x,s)\mathscr{A}^{\pi,\theta}(g(t,x,s))+\frac{(\theta_1(t))^2}{2\phi_1(t)}+\frac{(\theta_2(t))^2}{2\phi_2(t)}\right\}=0,\ W(T,x,s)=x,\tag{28}$$

$$\mathscr{A}^{\pi^*,\theta^*}(g(t,x,s))=0,\ g(T,x,s)=x,\tag{29}$$

$$(\pi^*,\theta^*)=\operatorname{argsup}_{\pi\in\Pi}\inf_{Q\in\mathcal{Q}}\left\{\mathscr{A}^{\pi,\theta}(W(t,x,s))-\mathscr{A}^{\pi,\theta}\left(\frac{\gamma}{2}g^2(t,x,s)\right)+\gamma g(t,x,s)\mathscr{A}^{\pi,\theta}(g(t,x,s))+\frac{(\theta_1(t))^2}{2\phi_1(t)}+\frac{(\theta_2(t))^2}{2\phi_2(t)}\right\},\tag{30}$$

then $V(t,x,s)=W(t,x,s)$, $E^{Q}_{t,x,s}[X^{\pi^*}_T]=g(t,x,s)$, π^* is the optimal robust time-consistent investment strategy for AAI, and θ^* is the optimal probability scenario for the market.

4. The Solution to the Robust MV Problem

This section is devoted to solve robust MV problem (19). By solving HJB equations (28) and (29), we can derive the solution to robust MV problem (19). To solve robust MV problem (19), similar to Maenhout [34, 35] and Chen and Yang [36], this article assumes that $\phi_1(t)=\alpha_1$ and $\phi_2(t)=\alpha_2$, where α_1 and α_1 are nonnegative.

Now, we give an explicit expression for HJB equation (28).

According to (27), we obtain

$$\begin{aligned}\mathscr{A}^{\pi,\theta}\left(\frac{\gamma}{2}g^2(t,x,s)\right) &= \gamma g g_t+\left[\tilde{r}x+\pi_1(t)(\mu_2-r_1)+\pi_2(t)\tilde{r}_2+\pi_2(t)\theta_1(t)\sigma_1+\pi_1(t)\theta_2(t)\sigma_2 s^{\beta}\right]\gamma g g_x\\ &\quad+\frac{1}{2}\left[\pi_1^2(t)\sigma_2^2 s^{2\beta}+\pi_2^2(t)\sigma_1^2\right]\left(\gamma g_x^2+\gamma g g_{xx}\right)+\mu_2 s\gamma g g_s+\frac{1}{2}\sigma_2^2 s^{2\beta+2}\left[\gamma g_s^2+\gamma g g_{ss}\right]\\ &\quad+\pi_1(t)\sigma_2^2 s^{2\beta+1}\left[\gamma g_s g_x+\gamma g g_{sx}\right],\\ \gamma g(t,x,s)\mathscr{A}^{\pi,\theta}(g(t,x,s)) &= \gamma g g_t+\left[\tilde{r}x+\pi_1(t)(\mu_2-r_1)+\pi_2(t)\tilde{r}_2+\pi_2(t)\theta_1(t)\sigma_1+\pi_1(t)\theta_2(t)\sigma_2 s^{\beta}\right]\gamma g g_x\\ &\quad+\frac{1}{2}\left[\pi_1^2(t)\sigma_2^2 s^{2\beta}+\pi_2^2(t)\sigma_1^2\right]\gamma g g_{xx}+\mu_2 s\gamma g g_s+\frac{1}{2}\sigma_2^2 s^{2\beta+2}\gamma g g_{ss}+\pi_1(t)\sigma_2^2(t)s^{2\beta+1}\gamma g g_{sx},\end{aligned}\tag{31}$$

where $g(t,x,s)$ is abbreviated as g and g_t, g_x, g_{xx}, g_s, g_{ss}, and g_{sx} are the partial derivatives of g with respect to the corresponding variables.

Then, HJB equation (28) can be more explicitly expressed as

$$\begin{aligned}&\sup_{\pi\in\Pi}\inf_{Q\in\mathcal{Q}}\Big\{W_t+\big[\tilde{r}x+\pi_1(t)(\mu_2-r_1)+\pi_2(t)\tilde{r}_2+\pi_2(t)\theta_1(t)\sigma+\pi_1(t)\theta_2(t)\sigma_2 s^{\beta}\big]W_x\\&+\frac{1}{2}\big[\pi_1^2(t)\sigma_2^2 s^{2\beta}+\pi_2^2(t)\sigma_1^2\big]\big(W_{xx}-\gamma g_x^2\big)+\big[\mu_2 s+\theta_2(t)\sigma_2 s^{\beta+1}\big]W_s\\&+\frac{1}{2}\sigma_2^2 s^{2\beta+2}\big(W_{ss}-\gamma g_s^2\big)+\pi_1(t)\sigma_2^2 s^{2\beta+1}\big(W_{sx}-\gamma g_s g_x\big)+\frac{\theta_1^2(t)}{2\alpha_1}+\frac{\theta_2^2(t)}{2\alpha_2}\Big\}=0,\end{aligned}\tag{32}$$

where $W(t,x,s)$ is abbreviated as W and W_t, W_x, W_{xx}, W_s, W_{ss}, and W_{sx} are the partial derivatives of W with respect to the corresponding variables.

Theorem 2. *For robust MV problem (19), the optimal robust time-consistent investment strategies are given by*

$$\pi_1^*(t)=\frac{(\mu_2-r_1)+2\gamma\beta\sigma_2^2\overline{B}(t)+2\alpha_2\beta\sigma_2^2B(t)}{(\alpha_2+\gamma)\sigma_2^2 s^{2\beta}}e^{-\tilde{r}(T-t)},\tag{33}$$

$$\pi_2^*(t)=\frac{\tilde{r}_2}{(\alpha_1+\gamma)\sigma_1^2}e^{-\tilde{r}(T-t)}.\tag{34}$$

The optimal probability scenarios for the market are given by

$$\theta_1^*(t)=-\frac{\alpha_1\tilde{r}_2}{(\alpha_1+\gamma)\sigma_1},\tag{35}$$

$$\theta_2^*(t)=\frac{2\beta\alpha_2\sigma_2B(t)}{s^{\beta}}-\frac{\alpha_2\big[(\mu_2-r_1)+2\gamma\beta\sigma_2^2\overline{B}(t)+2\alpha_2\beta\sigma_2^2B(t)\big]}{(\alpha_2+\gamma)\sigma_2 s^{\beta}}.\tag{36}$$

The optimal value function is given by

$$W(t,x,s)=xe^{\tilde{r}(T-t)}+B(t)s^{-2\beta}+C(t),\tag{37}$$

where $C(t)$ is given by (60), and $\overline{B}(t)$ and $B(t)$ are determined by the following ordinary differential equations (ODEs):

$$\begin{cases}B'(t)-2\mu_2\beta B(t)-2\sigma_2^2\gamma\beta^2\overline{B}^2-2\alpha_2\beta^2\sigma_2^2B^2(t)+\dfrac{\big[\mu_2-r_1+2\beta\sigma_2^2\big(\gamma\overline{B}(t)+\alpha_2B(t)\big)\big]^2}{2(\alpha_2+\gamma)\sigma_2^2}=0,\\ \overline{B}'(t)-2\overline{B}(t)\big[\mu_2\beta+4\alpha_2\beta^2\sigma_2^2B(t)\big]+\dfrac{1}{(\alpha_2+\gamma)\sigma_2^2}\Big\{\big[\mu_2-r_1+2\sigma_2^2\alpha_2\beta\big(\overline{B}(t)+B(t)\big)\big]\times\big[\mu_2-r_1+2\beta\sigma_2^2\big(\gamma\overline{B}(t)+\alpha_2B(t)\big)\big]\Big\}\\ -\dfrac{\alpha_2\big[\mu_2-r_1+2\beta\sigma_2^2\big(\gamma\overline{B}(t)+\alpha_2B(t)\big)\big]^2}{(\alpha_2+\gamma)^2\sigma_2^2}=0,\end{cases}\tag{38}$$

with boundary conditions $B(T)=0$ and $\overline{B}(T)=0$.

Proof. According to the structure of the wealth dynamics (17) and the boundary conditions $W(T,x,s)=g(T,x,s)=x$, we will seek the solution to HJB equations (28) and (29) with the following parametric form:

$$W(t,x,s)=A(t)x+B(t)s^{-2\beta}+C(t),\tag{39}$$

with boundary conditions

$$\begin{aligned}&A(T)=1,B(T)=0,C(T)=0,\\&g(t,x,s)=\overline{A}(t)x+\overline{B}(t)s^{-2\beta}+\overline{C}(t),\end{aligned}\tag{40}$$

with boundary conditions

$$\overline{A}(T)=1,\overline{B}(T)=0,\overline{C}(T)=0.\tag{41}$$

Then, the partial derivatives of $W(t,x,s)$ and $g(t,x,s)$ are given by

$$\begin{cases}W_t=A'(t)x+B'(t)s^{-2\beta}+C'(t),W_x=A(t),W_{xx}=0,\\ W_s=-2\beta B(t)s^{-2\beta-1},W_{ss}=2\beta(2\beta+1)B(t)s^{-2\beta-2},W_{sx}=0,\\ g_t=\overline{A}'(t)x+\overline{B}'(t)s^{-2\beta}+\overline{C}'(t),g_x=\overline{A}(t),g_{xx}=0,\\ g_s=-2\beta\overline{B}(t)s^{-2\beta-1},g_{ss}=2\beta(2\beta+1)\overline{B}(t)s^{-2\beta-2},g_{sx}=0.\end{cases}\tag{42}$$

Substituting equations (39)–(42) into equation (32), we obtain

$$
\begin{aligned}
&\left[A'(t)+\widetilde{r}A(t)\right]x+\left[B'(t)-2\mu_2\beta B(t)-2\sigma_2^2\gamma\beta^2\overline{B}^2\right]s^{-2\beta}+C'(t)\\
&+\sigma_2^2\beta(2\beta+1)B(t)+\sup_{\pi\in\Pi}\inf_{Q\in\mathbb{Q}}\left\{\frac{\theta_2^2(t)}{2\alpha_2}+\theta_2(t)\left[\pi_1(t)\sigma_2 s^{\beta}A(t)-2\sigma_2\beta B(t)s^{-\beta}\right]\right.\\
&+\frac{\theta_1^2(t)}{2\alpha_1}+\pi_2\theta_1(t)\sigma_1 A(t)-\frac{1}{2}\pi_1^2(t)\gamma\sigma_2^2 s^{2\beta}\overline{A}^2(t)+\pi_1(t)\left[(\mu_2-r_1)A(t)+2\gamma\sigma_2^2\beta\overline{A}(t)\overline{B}(t)\right]\\
&\left.-\frac{1}{2}\pi_2^2(t)\gamma\sigma_1^2\overline{A}^2(t)+\pi_2(t)\widetilde{r}_2A(t)\right\}=0.
\end{aligned}
\tag{43}
$$

According to the first-order optimality condition, $\theta_1(t)$ and $\theta_2(t)$, solving the minimization problem in equation (43), we obtain

$$\theta_1^*(t)=-\sigma_1\alpha_1\pi_2(t)A(t), \tag{44}$$

$$\theta_2^*(t)=-\sigma_2\alpha_2\pi_1(t)s^{\beta}A(t)+2\alpha_2\beta\sigma_2 s^{-\beta}B(t). \tag{45}$$

Plugging (44) and (45) into equation (43) yields

$$
\begin{aligned}
&\left[A'(t)+\widetilde{r}A(t)\right]x+\left[B'(t)-2\mu_2\beta B(t)-2\sigma_2^2\gamma\beta^2\overline{B}^2-2\alpha_2\beta^2\sigma_2^2B^2(t)\right]s^{-2\beta}+C'(t)+\sigma_2^2\beta(2\beta+1)B(t)+\sup_{\pi\in\Pi}\\
&\left\{-\frac{1}{2}\pi_1^2\left[\alpha_2A^2(t)+\gamma\overline{A}^2(t)\right]\sigma_2^2s^{2\beta}+\pi_1(t)\left[(\mu_2-r_1)A(t)+2\gamma\sigma_2^2\beta\overline{A}(t)\overline{B}(t)+2\alpha_2\sigma_2^2\beta A(t)B(t)\right]\right.\\
&\left.-\frac{1}{2}\pi_2^2\left[\alpha_1A^2(t)+\gamma\overline{A}^2(t)\right]\sigma_1^2+\pi_2(t)\widetilde{r}_2A(t)\right\}=0.
\end{aligned}
\tag{46}
$$

According to the first-order optimality condition, $\pi_1^*(t)$ and $\pi_2^*(t)$, solving the maximization problem in equation (46), we obtain

$$\pi_1^*(t)=\frac{(\mu_2-r_1)A(t)+2\gamma\beta\sigma_2^2\overline{A}(t)\overline{B}(t)+2\alpha_2\sigma_2^2\beta A(t)B(t)}{\left[\alpha_2A^2(t)+\gamma\overline{A}^2(t)\right]\sigma_2^2(t)s^{2\beta}}, \tag{47}$$

$$\pi_2^*(t)=\frac{\widetilde{r}_2A(t)}{\left[\alpha_1A^2(t)+\gamma\overline{A}^2(t)\right]\sigma_1^2(t)}. \tag{48}$$

Inserting (47) and (48) into equation (46) and after simplifying give

$$
\begin{aligned}
&\left[A'(t)+\widetilde{r}A(t)\right]x+\left\{B'(t)-2\mu_2\beta B(t)-2\sigma_2^2\gamma\beta^2\overline{B}^2-2\alpha_2\beta^2\sigma_2^2B^2(t)+\frac{\left[(\mu_2-r_1)A(t)+2\gamma\beta\sigma_2^2\overline{A}(t)\overline{B}(t)+2\alpha_2\sigma_2^2\beta A(t)B(t)\right]^2}{2\left[\alpha_2A^2(t)+\gamma\overline{A}^2(t)\right]\sigma_2^2}\right\}s^{-2\beta}\\
&+\left\{C'(t)+\sigma_2^2\beta(2\beta+1)B(t)+\frac{\widetilde{r}_2^2A^2(t)}{2\left[\alpha_1A^2(t)+\gamma\overline{A}^2(t)\right]\sigma_1^2}\right\}=0.
\end{aligned}
\tag{49}
$$

By substituting (40), (42), (44), (45), (47), and (48) into equation (29) yields

$$
\begin{aligned}
&\left[\overline{A}'(t)+\tilde{r}\overline{A}(t)\right]x+\Big\{\overline{B}'(t)-2\mu_2\beta\overline{B}(t)-4\alpha_2\beta^2\sigma_2^2B(t)\overline{B}(t)\\
&+\frac{1}{\left[\alpha_2A^2(t)+\gamma\overline{A}^2(t)\right]\sigma_2^2}\left[\left[(\mu_2-r_1)\overline{A}(t)+2\sigma_2^2\alpha_2\beta\left(A(t)\overline{B}(t)+\overline{A}(t)B(t)\right)\right]\right.\\
&\times\left.\left[(\mu_2-r_1)A(t)+2\gamma\beta\sigma_2^2\overline{A}(t)\overline{B}(t)+2\alpha_2\sigma_2^2\beta A(t)B(t)\right]\right]\\
&-\frac{\alpha_2A(t)\overline{A}(t)\left[(\mu_2-r_1)A(t)+2\gamma\beta\sigma_2^2\overline{A}(t)\overline{B}(t)+2\alpha_2\sigma_2^2\beta A(t)B(t)\right]^2}{\left[\alpha_2A^2(t)+\gamma\overline{A}^2(t)\right]^2\sigma_2^2}\Big\}s^{-2\beta}\\
&+\left\{\overline{C}'(t)+\sigma_2^2\beta(2\beta+1)\overline{B}(t)+\frac{\tilde{r}_2^2A(t)\overline{A}(t)}{\left[\alpha_1A^2(t)+\gamma\overline{A}^2(t)\right]\sigma_1^2}-\frac{\alpha_1\tilde{r}_2^2A^3(t)\overline{A}(t)}{\left[\alpha_1A^2(t)+\gamma\overline{A}^2(t)\right]^2\sigma_1^2}\right\}=0.
\end{aligned}
\tag{50}
$$

Thus, we must solve the following ODEs:

$$A'(t)+\tilde{r}A(t)=0,\ A(T)=1, \tag{51}$$

$$
\begin{aligned}
&B'(t)-2\mu_2\beta B(t)-2\sigma_2^2\gamma\beta^2\overline{B}^2-2\alpha_2\beta^2\sigma_2^2B^2(t)\\
&\quad+\frac{\left[(\mu_2-r_1)A(t)+2\gamma\beta\sigma_2^2\overline{A}(t)\overline{B}(t)+2\alpha_2\sigma_2^2\beta A(t)B(t)\right]^2}{2\left[\alpha_2A^2(t)+\gamma\overline{A}^2(t)\right]\sigma_2^2}=0,\ B(T)=0,
\end{aligned}
\tag{52}
$$

$$C'(t)+\sigma_2^2\beta(2\beta+1)B(t)+\frac{\tilde{r}_2^2A^2(t)}{2\left[\alpha_1A^2(t)+\gamma\overline{A}^2(t)\right]\sigma_1^2}=0,\ C(T)=0, \tag{53}$$

$$\overline{A}'(t)+\tilde{r}\overline{A}(t)=0,\ \overline{A}(T)=1, \tag{54}$$

$$
\begin{aligned}
&\overline{B}'(t)-2\mu_2\beta\overline{B}(t)-4\alpha_2\beta^2\sigma_2^2B(t)\overline{B}(t)\\
&\quad+\frac{1}{\left[\alpha_2A^2(t)+\gamma\overline{A}^2(t)\right]\sigma_2^2}\left[\left[(\mu_2-r_1)\overline{A}(t)+2\sigma_2^2\alpha_2\beta\left(A(t)\overline{B}(t)+\overline{A}(t)B(t)\right)\right]\right.\\
&\quad\times\left.\left[(\mu_2-r_1)A(t)+2\gamma\beta\sigma_2^2\overline{A}(t)\overline{B}(t)+2\alpha_2\sigma_2^2\beta A(t)B(t)\right]\right]\\
&\quad-\frac{\alpha_2A(t)\overline{A}(t)\left[(\mu_2-r_1)A(t)+2\gamma\beta\sigma_2^2\overline{A}(t)\overline{B}(t)+2\alpha_2\sigma_2^2\beta A(t)B(t)\right]^2}{\left[\alpha_2A^2(t)+\gamma\overline{A}^2(t)\right]^2\sigma_2^2}=0,\ \overline{B}(T)=0,
\end{aligned}
\tag{55}
$$

$$\overline{C}'(t)+\sigma_2^2\beta(2\beta+1)\overline{B}(t)+\frac{\tilde{r}_2^2A(t)\overline{A}(t)}{\left[\alpha_1A^2(t)+\gamma\overline{A}^2(t)\right]\sigma_1^2}-\frac{\alpha_1\tilde{r}_2^2A^3(t)\overline{A}(t)}{\left[\alpha_1A^2(t)+\gamma\overline{A}^2(t)\right]^2\sigma_1^2}=0,\overline{C}(T)=0. \tag{56}$$

First, solving equations (51) and (54), respectively, we obtain

$$A(t)=e^{\tilde{r}(T-t)}, \tag{57}$$

$$\overline{A}(t)=e^{\tilde{r}(T-t)}. \tag{58}$$

By substituting (57) and (58) into (52) and (55), we can obtain $B(t)$ and $\overline{B}(t)$ which are the solutions of ODEs (38).

Inserting (57), (58), and $\overline{B}(t)$ into equation (56), we obtain the solution to equation (56) which is given by

$$\overline{C}(t) = \frac{\gamma \widetilde{r}_2^2 (T-t)}{(\alpha_1+\gamma)^2 \sigma_1^2} + \sigma_2^2 \beta (2\beta+1) \int_t^T \overline{B}(s) ds. \quad (59)$$

By substituting (57), (58), and $B(t)$ into equation (53), and solving it, we obtain

$$C(t) = \frac{\widetilde{r}_2^2}{2(\alpha_1+\gamma)\sigma_1^2}(T-t) + \sigma_2^2 \beta (2\beta+1) \int_t^T B(s) ds. \quad (60)$$

Inserting (57), (58), $B(t)$, and $\overline{B}(t)$ into (47), we can obtain (33). By substituting (57) and (58) into (48), we can obtain (34). Plugging (33) into (45) and (34) into (44), we yield (36) and (35), respectively.

Based on Theorem 2 and the notation setting (8), we have the following theorem. □

Theorem 3. *For the wealth process (7), the optimal robust time-consistent investment strategies to robust MV problem (19) are given by*

$$u_1^*(t) = \frac{(\mu_2 - r_1) + 2\gamma\beta\sigma_2^2 \overline{B}(t) + 2\alpha_2 \beta \sigma_2^2 B(t)}{x(\alpha_2+\gamma)\sigma_2^2 s^{2\beta}} e^{-\widetilde{r}(T-t)}, \quad (61)$$

$$u_2^*(t) = \frac{\widetilde{r}_2}{x(\alpha_1+\gamma)\sigma_1^2} e^{-\widetilde{r}(T-t)} + 1. \quad (62)$$

Remark 2. From the expressions of optimal robust time-consistent investment strategies (61) and (62), we note that $u_1^*(t)$ is related to the appreciation rate μ_2 and price volatility σ_2 of the risky asset and the current wealth x, whereas $u_2^*(t)$ is related to the parameters μ_1 and σ_1 of the inflation level and the current wealth x. This difference between $u_1^*(t)$ and $u_2^*(t)$ is mainly because the inflation price process and the risky asset price process are independent in our model assumption.

5. Numerical Experiments

This section is devoted to providing the influences of model parameters on the optimal time-consistent investment strategy and utility loss function by numerical experiments. In the following, unless otherwise stated, we choose the basic parameter setting as given in Table 1.

5.1. The Influences of the Parameters on $u_1^*(t)$. We first present the effects of model parameters on $u_1^*(t)$, where $u_1^*(t)$ is determined by (61).

Let $s \in [2, 10]$; Figure 1 shows the effect of s on $u_1^*(t)$. From Figure 1, it is evident that $u_1^*(t)$ is a decreasing function of s, which describes the price of the risky asset. Form the meaning of s, we know that larger s implies that the investment risk becomes greater. Therefore, as s increases, the AAI will wish to invest less in the risky asset.

Figure 2 presents two curves about the effect of β on $u_1^*(t)$, where parameter $\beta \in [0.1, 0.6]$. From Figure 2, we can see that when $s = 2$, $u_1^*(t)$ is a decreasing function in β, while

Table 1: Values of model parameters.

μ_1	σ_1	r_1	μ_2	σ_2	r_2	γ	x	T	t	β	s	α_1	α_2
0.05	0.3	0.03	0.08	0.25	0.02	2	10	10	9	0.1	2	2	1

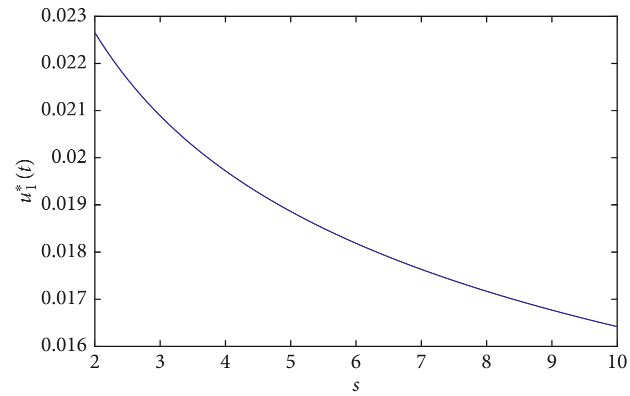

Figure 1: Effect of s on $u_1^*(t)$.

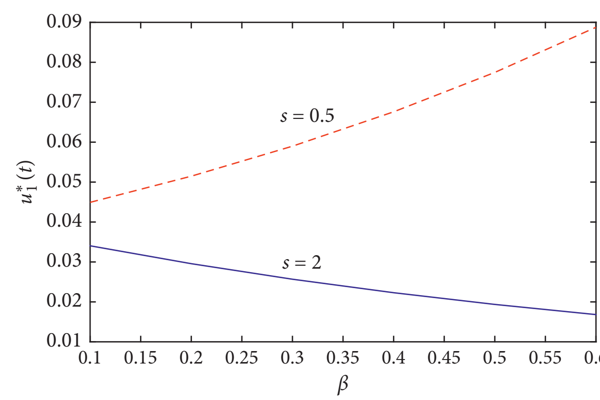

Figure 2: Effect of β on $u_1^*(t)$.

if $s = 0.5$, $u_1^*(t)$ is an increasing function in β. When $s = 2$ ($s = 0.5$), the larger β is, the greater (less) s^β will be and hence the greater (less) the risk will be; thus, the AAI will wish to invest less (greater) in the risky asset.

Let $\mu_2 \in [0.05, 0.1]$; we present the effect of μ_2 on $u_1^*(t)$ in Figure 3. From Figure 3, it is clear that $u_1^*(t)$ is increasing with respect to μ_2, which is the appreciation rate of the risky asset. Larger μ_2 implies that the expected income of the risky asset becomes greater. As a result, the AAI will wish to invest more in the risky asset.

Let $\sigma_2 \in [0.2, 0.6]$; Figure 4 displays the effect of σ_2 on $u_1^*(t)$. From Figure 4, we can observe that $u_1^*(t)$ is a decreasing function of σ_2. Recall that σ_2 is the price volatility; therefore, with the increase of σ_2, the investment risk will increase. Thus, the AAI will wish to invest less in the risky asset.

Figure 5 illustrates the effect of the risk-free interest rate r_1 on $u_1^*(t)$, where $r_1 \in [0.02, 0.06]$. This figure shows that $u_1^*(t)$ is a decreasing function with respect to r_1. Larger r_1 implies that the expected income of the risk-free asset

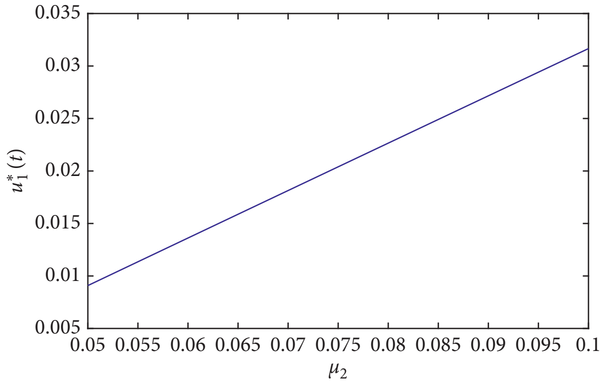

Figure 3: Effect of μ_2 on $u_1^*(t)$.

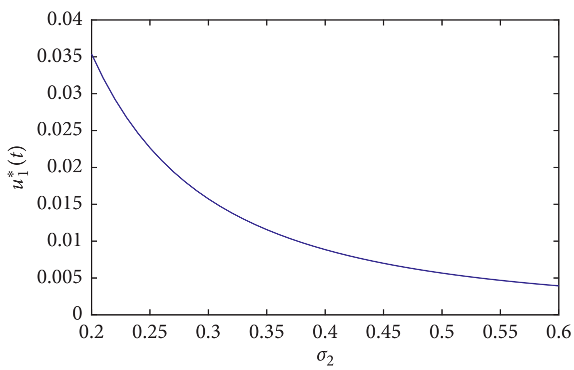

Figure 4: Effect of σ_2 on $u_1^*(t)$.

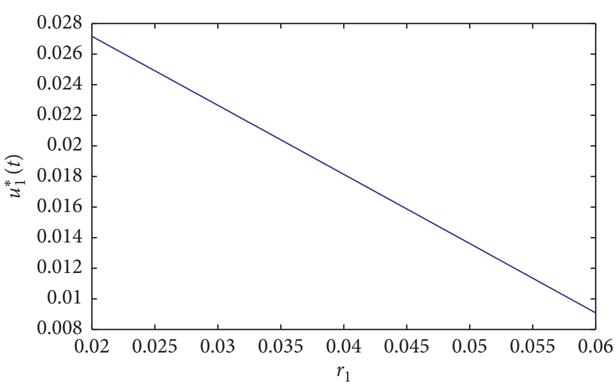

Figure 5: Effect of r_1 on $u_1^*(t)$.

becomes greater. A natural result is that the AAI will invest more in the risk-free asset. That is to say, the AAI will invest less in the risky asset.

Figure 6 discloses that $u_1^*(t)$ is a decreasing function of α_2, where $\alpha_2 \in [1, 6]$. Recall that α_2 stands for the AAI's ambiguity aversion. Larger α_2 implies that the model uncertainty becomes greater. Hence, the AAI will invest less in the risky asset.

Figure 7 shows the effect of γ on $u_1^*(t)$, where $\gamma \in [2, 8]$. From Figure 7, we see that $u_1^*(t)$ is a decreasing function with respect to γ. This is obvious. Since γ is the risk-aversion parameter, larger γ implies that the less aggressive the AAI will be. Therefore, the AAI will invest less in the risky asset.

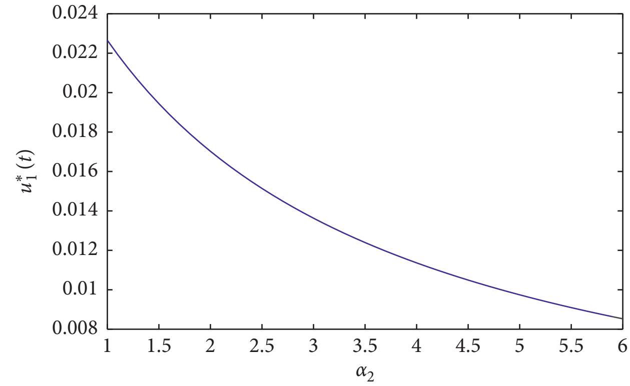

Figure 6: Effect of α_2 on $u_1^*(t)$.

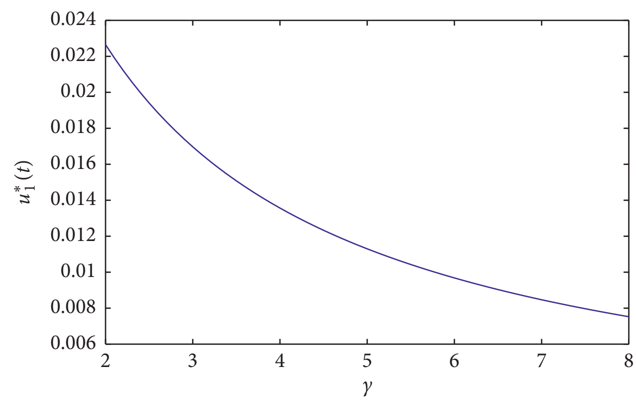

Figure 7: Effect of γ on $u_1^*(t)$.

Figure 8 reveals that $u_1^*(t)$ is increasing with respect to t, where $t \in [2, 9]$. This implies that, as the termination time of the investment approaches, the AAI will invest more in the risky assets.

5.2. The Influences of the Parameters on $u_2^*(t)$. Now, we illustrate the effects of model parameters on the optimal robust time-consistent investment strategy $u_2^*(t)$, where $u_2^*(t)$ is determined by (62).

Differentiating (62) with respect to μ_1, we obtain

$$\frac{\partial u_2^*(t)}{\partial \mu_1} = \frac{1}{x(\alpha_1 + \gamma)\sigma_1^2} e^{-\widetilde{r}(T-t)} > 0, \tag{63}$$

that is, $u_2^*(t)$ is increasing with respect to μ_1. This implies that, as the interest rate of the inflation-indexed bond increases, the AAI should retain more investments in the inflation-indexed bond.

Differentiating (62) with respect to σ_1, we have

$$\frac{\partial u_2^*(t)}{\partial \sigma_1} = -\frac{2(r_2 + \mu_1 - r_1)}{x(\alpha_1 + \gamma)\sigma_1^3} e^{-\widetilde{r}(T-t)} < 0, \tag{64}$$

so we know that $u_2^*(t)$ is decreasing with respect to σ_1. Recall that σ_1 is the volatility of the inflation-indexed bond. Therefore, larger σ_1 implies that the investment risk in the inflation-indexed bond becomes larger. Hence, the AAI retains less investments in the inflation-indexed bond.

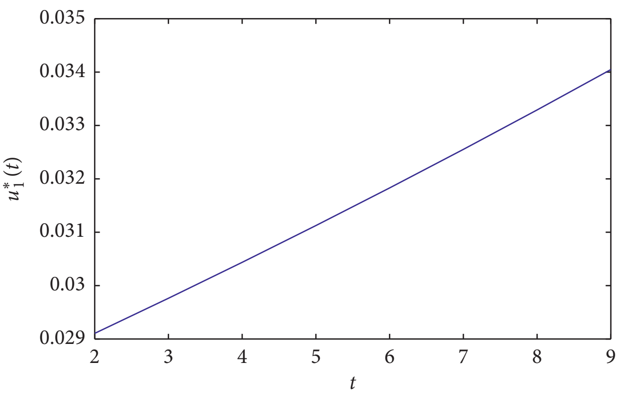

Figure 8: Effect of t on $u_1^*(t)$.

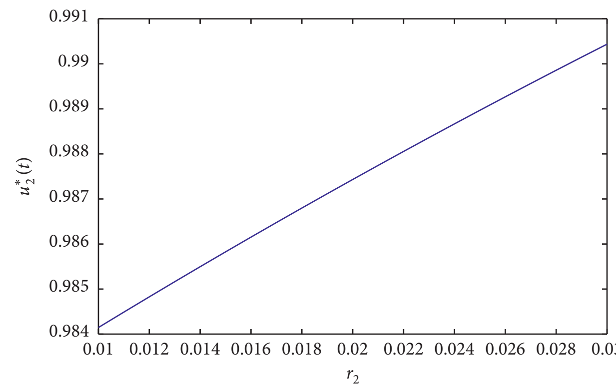

Figure 9: Effect of r_2 on $u_2^*(t)$.

Differentiating (62) with respect to r_1, we obtain

$$\frac{\partial u_2^*(t)}{\partial r_1} = -\frac{1}{x(\alpha_1+\gamma)\sigma_1^2}e^{-\tilde{r}(T-t)} < 0, \tag{65}$$

which implies that $u_2^*(t)$ is decreasing with respect to r_1. The reason is similar to what we have explained in Figure 5.

In the following, we analyze the effect of r_2 on $u_2^*(t)$ by the numerical experiment. We set $\mu_1 = 0.02, \sigma_1 = 0.04, \alpha_1 = 10$, $\gamma = 2, x = 10, T = 10, t = 5, r_2 \in [0.01, 0.03]$, and the result is shown in Figure 9. From Figure 9, we can observe that $u_2^*(t)$ is an increasing function with respect to r_2. Recall that r_2 stands for the real interest rate of the inflation-indexed bond. Hence, the larger r_2 is, the more the AAI will invest in the inflation-indexed bond.

5.3. The Influences of Model Parameters on Utility Loss Function. In Sections 5.1 and 5.2, we studied the case under the robust model. This part uses numerical experiments to investigate the influences of model parameters on utility loss function.

First, we give some results under the ambiguity-neutral case.

For an ambiguity-neutral optimization problem, all admissible investment strategies $\overline{\pi}(t)$ are denoted by $\overline{\Pi}$. Then, the wealth process becomes

$$\begin{aligned} dX_t^{\overline{\pi}} &= \left[\tilde{r}X_t^{\overline{\pi}} + \overline{\pi}_1(t)(\mu_2 - r_1) + \overline{\pi}_2(t)\tilde{r}_2\right]dt \\ &\quad + \overline{\pi}_1(t)\sigma_2 S^{\beta}(t)dW_2(t) + \overline{\pi}_2(t)\sigma_1 dW_1(t), \end{aligned} \tag{66}$$

and the objective function is as follows:

$$\sup_{\overline{\pi}\in\overline{\Pi}}\left\{E_{t,x,s}\left[X_T^{\overline{\pi}}\right] - \frac{\gamma}{2}\text{Var}_{t,x,s}\left[X_T^{\overline{\pi}}\right]\right\}. \tag{67}$$

Similar to what we have proved in Theorem 2, we can obtain the following theorem.

Theorem 4. *For problem (67), the optimal time-consistent investment strategies are given by*

$$\overline{\pi}_1^*(t) = \frac{(\mu_2 - r_1) + 2\gamma\beta\sigma_2^2 B_2(t)}{\gamma\sigma_2^2 s^{2\beta}}e^{-\tilde{r}(T-t)}, \tag{68}$$

$$\overline{\pi}_2^*(t) = \frac{\tilde{r}_2}{\gamma\sigma_1^2}e^{-\tilde{r}(T-t)}. \tag{69}$$

Furthermore, the optimal value function is given by

$$W_1(t,x,s) = xe^{\tilde{r}(T-t)} + B_1(t)s^{-2\beta} + C_1(t), \tag{70}$$

where

$$\begin{aligned} B_1(t) &= e^{-2\mu_2\beta(T-t)}\int_t^T f_1(s)e^{2\mu_2\beta(T-s)}ds, \\ B_2(t) &= \frac{(\mu_2 - r_1)^2}{2r_1\beta\gamma\sigma_2^2}\left[1 - e^{-2r_1\beta(T-t)}\right], \\ f_1(t) &= 2\beta(\mu_2 - r_1)B_2(t) + \frac{(\mu_2 - r_1)^2}{2\gamma\sigma_2^2}, \\ C_1(t) &= \frac{\tilde{r}_2^2}{2\gamma\sigma_1^2}(T-t) + \sigma_2^2\beta(2\beta+1)\int_t^T B_1(s)ds. \end{aligned} \tag{71}$$

Based on Theorems 2 and 4, we can define the utility loss function as

$$L(t) = 1 - \frac{W_1(t,x,s)}{W(t,x,s)}. \tag{72}$$

In the following, we investigate the effects of model parameters on $L(t)$.

(i) *The influence of ambiguity aversion on the utility loss: Let $\alpha_2 = 4$ and $\alpha_1 = 2,3,4,5,6,7,8$; we can obtain $W_1(t,x,s) = 10.2370$. The values of $W(t,x,s)$ and $L(t)$ are presented in Table 2. From Table 2, we know that the utility loss function is a decreasing function in α_1, where α_1 stands for the ambiguity aversion which arises from the inflation-indexed bond. By comparing the AAI's utility loss at different α_1, we find that the more ambiguity averse the AAI is, the less conservative investment strategy the AAI will be (because $W(t,x,s)$ is decreasing in α_1). Because AAI's*

Table 2: Effect of α_1 on $W(t,x,s)$ and $L(t)$.

α_1	2	3	4	5	6	7	8
$W(t,x,s)$	11.7217	11.7212	11.7209	11.7207	11.7205	11.7204	11.7202
$L(t)$	0.12666	0.12663	0.1266	0.12658	0.12657	0.12656	0.12655

Table 3: Effect of α_2 on $W(t,x,s)$ and $L(t)$.

α_2	2	3	4	5	6	7	8
$W(t,x,s)$	11.0307	11.0386	11.0429	11.0455	11.0472	11.0484	11.0492
$L(t)$	0.0719	0.0726	0.0730	0.0732	0.0733	0.0734	0.0735

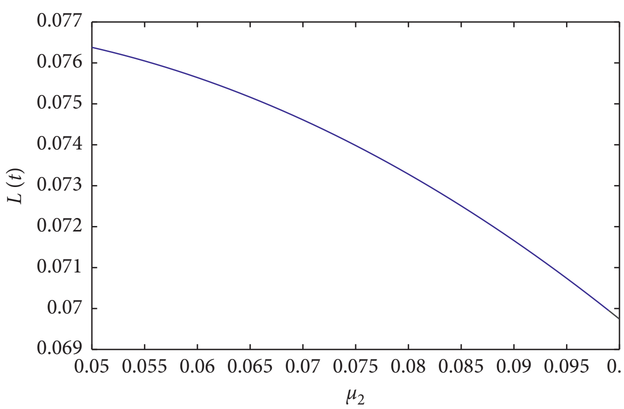

Figure 10: Effect of μ_2 on $L(t)$.

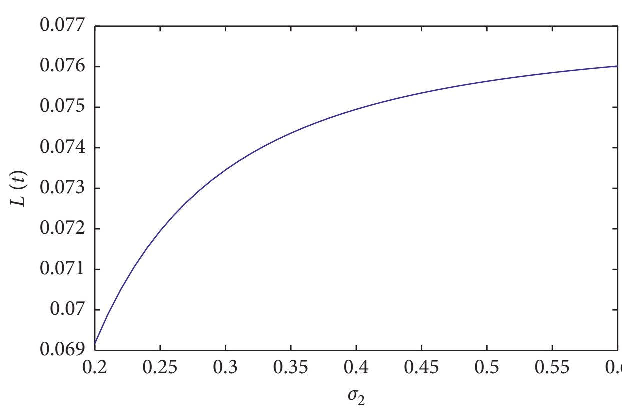

Figure 11: Effect of σ_2 on $L(t)$.

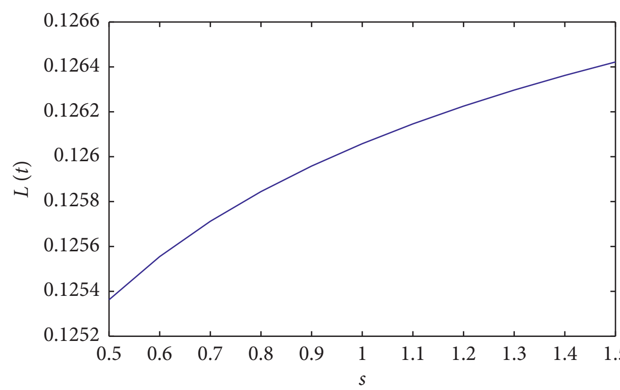

Figure 12: Effect of s on $L(t)$.

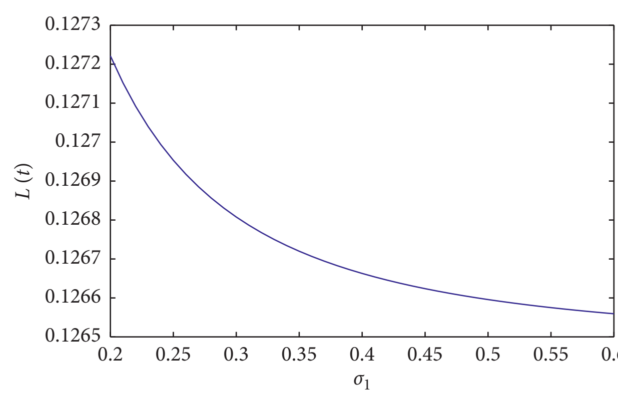

Figure 13: Effect of σ_1 on $L(t)$.

investment is robust, he will invest more money in the risk-free asset, so AAI will suffer less utility loss.

Let $\alpha_1 = 4$ and $\alpha_2 = 2,3,4,5,6,7,8$; we have $W_1(t,x,s) = 10.2370$. The values of $W(t,x,s)$ and $L(t)$ are presented in Table 3. From Table 3, it is evident that the utility loss function is an increasing function in α_2, where α_2 stands for the ambiguity aversion which arises from the risky asset.

(ii) The influence of market parameters on the utility loss:

Figure 10 discloses that $L(t)$ is a decreasing function with respect to μ_2, where $\mu_2 \in [0.05, 0.1]$. This indicates that the utility loss increases as the appreciation rate of the risky asset diminishes.

Figure 11 reveals that $L(t)$ is an increasing function with regard to σ_2, where $\sigma_2 \in [0.2, 0.6]$. Larger σ_2 implies that the investment risk becomes greater, and thus, the AAI will suffer from more utility losses.

Let $s \in [0.5, 1.5]$; Figure 12 gives the influence of parameter s on the utility loss. From Figure 12, we can observe that $L(t)$ is an increasing function of s. The larger the s is, the larger the price volatility will be, that is, the greater the risk will be, and hence, the AAI will suffer from more utility losses.

Let $\sigma_1 \in [0.2, 0.6]$; Figure 13 shows that the utility loss is a decreasing function of σ_1. Comparing Figures 11 with 13, it is clear that the effect of the volatilities of *the risky asset and the inflation on the utility loss is opposite.*

6. Conclusions

We have investigated a robust time-consistent MV strategy selection under the inflation risk for an AAI. The AAI doubts the model setting under the original probability measure. Then, he seeks a set of alternative probability measures, which are absolutely continuous to the original probability measure. Furthermore, we modify the model setting under the alternative probability measures. We form the AAI's objective under the framework of the robust MV criterion. As we all know, this problem is time-inconsistent. To solve this time-inconsistent problem, we seek the equilibrium strategy from the game framework. The equilibrium strategy is time-consistent. By using the stochastic optimal control technique, we derive the closed-form solutions for the optimal time-consistent investment strategy and the optimal value function. Finally, the influences of model parameters on the optimal time-consistent investment strategy and utility loss function are examined through numerical experiments.

Compared with Zeng et al. [12], Zheng et al. [28], Maenhout [34, 35], and other studies about the robust MV problem, the inflation risk and the CEV model are simultaneously introduced in this article. In addition, the influence of the model parameters of the inflation on the optimal time-consistent investment strategy and the utility loss are systematic analysis by numerical experiments.

It may be interesting to extend the current framework to that with dividend and state-dependent risk-aversion function or that in a partial information market in the future research. For these future research topics, we may need to adopt the methods used in Bjök et al. [14], Yu et al. [37], and Raychaudhury and Pal [38].

Data Availability

The data used to support the findings of this study are available upon request to the author.

Conflicts of Interest

The author declares that there are no conflicts of interest regarding the publication of this paper.

References

[1] H. Markowitz, "Portfolio selection," *The Journal of Finance*, vol. 7, no. 1, pp. 77–91, 1952.

[2] D. Li and W.-L. Ng, "Optimal dynamic portfolio selection: multiperiod mean-variance formulation," *Mathematical Finance*, vol. 10, no. 3, pp. 387–406, 2000.

[3] X. Y. Zhou and D. Li, "Continuous-time mean-variance portfolio selection: a stochastic LQ framework," *Applied Mathematics and Optimization*, vol. 42, no. 1, pp. 19–33, 2000.

[4] M. Dai, Z. Q. Xu, and X. Y. Zhou, "Continuous-time markowitz's model with transaction costs," *SIAM Journal on Financial Mathematics*, vol. 1, no. 1, pp. 96–125, 2010.

[5] Z. Sun, K. C. Yuen, and J. Guo, "A BSDE approach to a class of dependent risk model of mean-variance insurers with stochastic volatility and no-short selling," *Journal of Computational and Applied Mathematics*, vol. 366, Article ID 112413, 2020.

[6] Z. Sun, X. Zhang, and K. C. Yuen, "Mean-variance asset-liability management with affine diffusion factor process and a reinsurance option," *Scandinavian Actuarial Journal*, vol. 2020, no. 3, pp. 218–244, 2020.

[7] R. H. Strotz, "Myopia and inconsistency in dynamic utility maximization," *The Review of Economic Studies*, vol. 23, no. 3, pp. 165–180, 1955.

[8] I. Ekeland, O. Mbodji, and T. A. Pirvu, "Time-consistent portfolio management," *SIAM Journal on Financial Mathematics*, vol. 3, no. 1, pp. 1–32, 2012.

[9] T. Björk and A. Murgoci, "A general theory of Markovian time inconsistent stochastic control problems," in *Working Paper*, Stockholm School of Economics, Stockholm, Sweden, 2010.

[10] Z. Li, Y. Zeng, and Y. Lai, "Optimal time-consistent investment and reinsurance strategies for insurers under Heston's SV model," *Insurance: Mathematics and Economics*, vol. 51, no. 1, pp. 191–203, 2012.

[11] P. Yang, "Time-consistent mean-variance reinsurance-investment in a jump-diffusion financial market," *Optimization*, vol. 66, no. 5, pp. 737–758, 2017.

[12] Y. Zeng, D. Li, and A. Gu, "Robust equilibrium reinsurance-investment strategy for a mean-variance insurer in a model with jumps," *Insurance: Mathematics and Economics*, vol. 66, pp. 138–152, 2016.

[13] P. Yang, Z. Chen, and Y. Xu, "Time-consistent equilibrium reinsurance-investment strategy for n competitive insurers under a new interaction mechanism and a general investment framework," *Journal of Computational and Applied Mathematics*, vol. 374, Article ID 112769, 2020.

[14] T. Björk, A. Murgoci, and X. Zhou, "Mean variance portfolio optimization with state dependent risk aversion," *Math Finance*, vol. 24, no. 1, pp. 1–24, 2014.

[15] C. Czichowsky, "Time-consistent mean-variance portfolio selection in discrete and continuous time," *Finance and Stochastics*, vol. 17, no. 2, pp. 227–271, 2013.

[16] M. T. Kronborg and M. Steffensen, "Inconsistent investment and consumption problems," *Applied Mathematics & Optimization*, vol. 71, no. 3, pp. 473–515, 2015.

[17] M. J. Brennan and Y. Xia, "Dynamic asset allocation under inflation," *The Journal of Finance*, vol. 57, no. 3, pp. 1201–1238, 2002.

[18] N.-W. Han and M.-W. Hung, "Optimal asset allocation for DC pension plans under inflation," *Insurance: Mathematics and Economics*, vol. 51, no. 1, pp. 172–181, 2012.

[19] M. Kwak and B. H. Lim, "Optimal portfolio selection with life insurance under inflation risk," *Journal of Banking & Finance*, vol. 46, pp. 59–71, 2014.

[20] Y. Li, S. Wang, Y. Zeng, and H. Qiao, "Equilibrium investment strategy for a DC plan with partial information and mean-variance criterion," *IEEE Systems Journal*, vol. 11, no. 3, pp. 1492–1504, 2016.

[21] J. C. Cox and S. A. Ross, "The valuation of options for alternative stochastic processes," *Journal of Financial Economics*, vol. 3, no. 1-2, pp. 145–166, 1976.

[22] J. Gao, "Optimal investment strategy for annuity contracts under the constant elasticity of variance (CEV) model," *Insurance: Mathematics and Economics*, vol. 45, no. 1, pp. 9–18, 2009.

[23] M. Gu, Y. Yang, S. Li, and J. Zhang, "Constant elasticity of variance model for proportional reinsurance and investment strategies," *Insurance: Mathematics and Economics*, vol. 46, no. 3, pp. 580–587, 2010.
[24] X. Lin and Y. Li, "Optimal reinsurance and investment for a jump diffusion risk process under the CEV model," *North American Actuarial Journal*, vol. 15, no. 3, pp. 417–431, 2011.
[25] Z. Liang, K. C. Yuen, and K. C. Cheung, "Optimal reinsurance-investment problem in a constant elasticity of variance stock market for jump-diffusion risk model," *Applied Stochastic Models in Business and Industry*, vol. 28, no. 6, pp. 585–597, 2012.
[26] X. Lin and Y. Qian, "Time-consistent mean-variance reinsurance-investment strategy for insurers under CEV model," *Scandinavian Actuarial Journal*, vol. 2016, no. 7, pp. 646–671, 2016.
[27] D. Li, R. Chen, and C. Li, "Optimal reinsurance-investmentproblem under a CEV model: stochastic differential game formulation," *Mathematical Problems in Engineering*, vol. 2020, Article ID 7265121, 19 pages, 2020.
[28] X. Zheng, J. Zhou, and Z. Sun, "Robust optimal portfolio and proportional reinsurance for an insurer under a CEV model," *Insurance: Mathematics and Economics*, vol. 67, pp. 77–87, 2016.
[29] D. C. Emanuel and J. D. Macbeth, "Further results on the constant elasticity of variance call option pricing model," *The Journal of Financial and Quantitative Analysis*, vol. 17, no. 4, pp. 533–554, 1982.
[30] W. Yu, Y. Yong, G. Guan, Y. Huang, W. Su, and C. Cui, "Valuing guaranteed minimum death benefits by cosine series expansion," *Mathematics*, vol. 7, no. 9, p. 835, 2019.
[31] Z. Zhang, Y. Yong, and W. Yu, "Valuing equity-linked death benefits in general exponential Lévy models," *Journal of Computational and Applied Mathematics*, vol. 365, Article ID 112377, 2020.
[32] G.-E. Espinosa and N. Touzi, "Optimal investment under relative performance concerns," *Mathematical Finance*, vol. 25, no. 2, pp. 221–257, 2015.
[33] W. Yu, F. Wang, Y. Huang, and H. Liu, "Social optimal mean field control problem for population growth model," *Asian Journal of Control*, pp. 1–8, 2019.
[34] P. J. Maenhout, "Robust portfolio rules and asset pricing," *Review of Financial Studies*, vol. 17, no. 4, pp. 951–983, 2004.
[35] P. J. Maenhout, "Robust portfolio rules and detection-error probabilities for a mean-reverting risk premium," *Journal of Economic Theory*, vol. 128, no. 1, pp. 136–163, 2006.
[36] Z. Chen and P. Yang, "Robust optimal reinsurance-investment strategy with price jumps and correlated claims," *Insurance: Mathematics and Economics*, vol. 92, pp. 27–46, 2020.
[37] W. Yu, P. Guo, Q. Wang et al., "On a periodic capital injection and barrier dividend strategy in the compound Poisson risk model," *Mathematics*, vol. 8, no. 4, p. 511, 2020.
[38] C. Raychaudhury and D. Pal, "Usefulness of graph vertex complexity and class partial information content in explaining gas phase thermal entropy of chemical compounds," *Journal of Mathematical Chemistry*, vol. 58, no. 5, pp. 887–892, 2020.

Hindawi
Mathematical Problems in Engineering
Volume 2020, Article ID 2759580, 10 pages
https://doi.org/10.1155/2020/2759580

Research Article

The Delayed Doubly Stochastic Linear Quadratic Optimal Control Problem

Yan Chen[1,2] and Jie Xu[3]

[1]*Department of Mathematics, Jilin University, Changchun 130012, China*
[2]*School of Mathematics, Changchun Normal University, Changchun 130032, China*
[3]*College of Science, Jilin Institute of Chemical Technology, Jilin 132022, China*

Correspondence should be addressed to Jie Xu; aqie990132@126.com

Received 9 April 2020; Accepted 14 May 2020; Published 6 June 2020

Guest Editor: Wenguang Yu

In this paper, the delayed doubly stochastic linear quadratic optimal control problem is discussed. It deduces the expression of the optimal control for the general delayed doubly stochastic control system which contained time delay both in the state variable and in the control variable at the same time and proves its uniqueness by using the classical parallelogram rule. The paper is concerned with the generalized matrix value Riccati equation for a special delayed doubly stochastic linear quadratic control system and aims to give the expression of optimal control and value function by the solution of the Riccati equation.

1. Introduction

As is known to all, the stochastic differential equation and stochastic analysis have developed rapidly. The theory of the stochastic differential equation is widely used in economy, biology, physics, financial mathematics, and other fields. The latest research on the insurance model was given in [1–3]. The social optimal mean field control problem was discussed in [4]. In order to provide a probabilistic interpretation for the solution of a kind of partial differential equations, Pardoux and Peng [5] first introduced the backward doubly stochastic differential equations and proved the existence and uniqueness of this kind of differential. Then, people began to study doubly stochastic differential equations. Zhu and Shi [6, 7] were concerned with a class of partial information control problems for backward doubly stochastic systems and gave the maximum principle and its applications for the system. Recently, Shi and Zhu [8] studied a type of forward-backward doubly stochastic differential equations driven by Brownian motions and the Poisson process and applied the result to backward doubly stochastic linear quadratic nonzero sum differential games with random jumps to get the explicit form of the open-loop Nash equilibrium point by the solution of this kind of equation. With the deepening of research, people gradually realized that many problems are not only affected by the current situation, but also by their past history. This kind of problem is called the delay problem. The equation describing this kind of problem is called the delay equation. Due to the fact that time delay widely exists in the practical systems, it will cause the change in system performance. Therefore, it can increase the control difficulty of the system. Delayed problems have become the focus of scholar's research studies. Chen and Wu [9] considered the delayed backward system and obtained the maximum principle for these problems. Wu and Wang [10] studied the optimal control problem of the backward stochastic differential delay equation under partial information. Lv et al. [11] considered the maximum principle for optimal control of anticipated forward-backward stochastic delayed systems with regime switching. Wang and Wu [12] were concerned with the optimal control problems of forward-backward delay systems involving impulse controls and established the stochastic maximum principle for this kind of systems. Yu [13] investigated the maximum principle for stochastic optimal control problems of delay systems with random coefficients involving both continuous and impulse controls.

Linear quadratic (LQ) optimal control problem is the theoretical basis for many problems. When delay variables exist in the doubly stochastic control system, the LQ problem becomes more complex and interesting. Chen and Wu [14] considered the LQ problem with delay in which the state depended on the past time but not the control in the system. Tang and Wu [15] were concerned with the linear stochastic system with Lévy processes. Huang et al. [16] were concerned with one kind of delayed forward-backward linear quadratic stochastic control problems and derived the explicit form of the optimal control. However, to our best knowledge, there is little work on the doubly stochastic LQ problem with delay. Based on the abundant literature, we want to discuss the delayed doubly stochastic LQ problem. When the LQ control system contains time delay, some important characteristic changes have taken place in research. The system contains a delayed doubly stochastic differential equation and a new kind of equation called the anticipated backward doubly stochastic differential equation which was discussed in [17, 18]. Inspired by the idea of the maximum principle for the delayed doubly stochastic control system [19, 20], we studied the general LQ system in which both the state variable and the control variable contain time delay at the same time. As is known to all, it is the key to find out the feedback control of the LQ problem. We deduce the explicit expression of the optimal control for the delayed doubly stochastic LQ problem. We consider the matrix Riccati equation for a class of the LQ problem. We deduced the solution of the LQ system by the solution corresponding to the Riccati equation, which was introduced originally by Peng [21]. We hope that our research can better describe the optimal feedback control of the delayed doubly stochastic LQ problem.

The rest of our paper is organized as follows. First, we introduce preliminary results and some necessary notations. In Section 3, we give the explicit expression of optimal control and prove its uniqueness by using the classical parallelogram rule. And then, we discuss a special kind of the control system, in which the time delay is contained only in the control variables. We try to introduce the generalized matrix value Riccati equation corresponding to the system. And then, we use the solution of the Riccati equation to show the optimal control for the delayed doubly stochastic LQ problem. At the same time, we indicate the objective function by the solution of the Riccati equation and the initial value of the state variable.

2. Preliminaries

First, let us introduce the common notations in this paper. Let $(\Omega, \mathcal{F}, P)$ be a probability space. Assume $\{W(t)\colon 0 \le t \le T\}$ and $\{B(t)\colon 0 \le t \le T\}$ be two mutually independent standard Brownian motions defined on $(\Omega, \mathcal{F}, P)$, with values, respectively, in R^m and in R^d. Note the integral with respect to $\{W(t)\}$ as the forward Itô's integral and $\{B(t)\}$ as the backward Itô's integral. Let N denote the class of P null sets of $\mathcal{F}$. We define $\mathcal{F}_t^w = \mathrm{N} \vee \sigma\{W(r) - W(0)\colon 0 \le r \le t\}$, $\mathcal{F}_{t,T}^B = \mathrm{N} \vee \sigma\{B(r) - B(t)\colon t \le r \le T\}$, and $\mathcal{F}_t = \mathcal{F}_t^w \vee \mathcal{F}_{t,T}^B$ for each $t \in [0, T]$. We denote $M^2(0, T; R^n)$ the set of all classes of ($dt \times dP$ a.e. equal) $\mathcal{F}_t$ measurable stochastic process $\varphi(t)$ satisfying $E \int_0^T |\varphi(t)|^2 dt < +\infty$. Similarly, $S^2(0, T; R^n)$ denotes the set of continuous n-dimensional $\mathcal{F}_t$ measurable stochastic process $\varphi(t)$ satisfying $E\sup_{t\in[0,T]} |\varphi(t)|^2 < +\infty$. $E^{\mathcal{F}_t}[\cdot] = E[\mathcal{F}_t]$ denotes the conditional expectation under filtration $\mathcal{F}_t$. $\langle \cdot, \cdot \rangle$ denotes the scalar product, and $\top$ in the superscripts means the transpose of the matrix.

In this paper, we mainly investigate the delayed doubly stochastic linear quadratic control system:

$$
\begin{cases}
dx(t) = [A_1(t)x(t) + B_1(t)x_\delta(t) + C_1(t)y(t) + D_1(t)y_\delta(t) + E_1(t)u(t) + F_1(t)u_\delta(t)]dt \\
+[A_2(t)x(t) + B_2(t)x_\delta(t) + C_2(t)y(t) + D_2(t)y_\delta(t) + E_2(t)u(t) + F_2(t)u_\delta(t)], \\
\overrightarrow{dW(t)} - y(t)d\overleftarrow{B}(t), \quad t \in [0, T], \\
x(t) = \varphi(t), \quad t \in [-\delta, 0], \\
y(t) = \psi(t), \quad t \in [-\delta, 0], \\
u(t) = 0, \quad t \in [-\delta, 0],
\end{cases}
\tag{1}
$$

where the notation $x_\delta(t) = x(t - \delta)$, $y_\delta(t) = y(t - \delta)$, and $u_\delta(t) = u(t - \delta)$.

Remark 1. In this delayed doubly stochastic control system, the state and control variables contain time delay at the same time. Time delay exists all the time in the system. But, we do nothing before the initial time. So, we give the assumption that $u(t) = 0$ when time t belongs to the interval before the control intervenes.

The cost functional is written as

$$
J(u(\cdot)) = \frac{1}{2} E\left\{ \int_0^T [\langle K(t)x(t), x(t)\rangle + \langle R(t)y(t), y(t)\rangle + \langle S(t)u(t), u(t)\rangle] dt + \langle Qx(T), x(T)\rangle \right\}. \tag{2}
$$

For a convex subset $U \subset R^k$, we define $U[0,T]$ as follows:

$$U[0,T] := \left\{ u:\ [0,T] \times \Omega \longrightarrow U, E\int_0^T |u(t)|^2 \mathrm{d}t < +\infty \right\}. \tag{3}$$

Our optimal control problem can be stated as minimizing the cost functional over $U[0,T]$. For optimal control $u^*(\cdot)$ satisfying

$$J(u^*(\cdot)) = \inf_{u(\cdot)\in U[0,T]} J(u(\cdot)), \tag{4}$$

the corresponding $(x^*(\cdot), y^*(\cdot), u^*(\cdot))$ is called an optimal triple.

The corresponding adjoint equation becomes

$$\begin{cases} -\mathrm{d}p(t) = \{A_1^{\top}(t)p(t) + E^{\mathscr{F}_t}[B_1^{\top}(t+\delta)p(t+\delta)] + A_2^{\top}(t)q(t) - K(t)x(t) + E^{\mathscr{F}_t}[B_2^{\top}(t+\delta)q(t+\delta)]\}\mathrm{d}t \\ +\left\{R(t)y(t) - C_1^{\top}(t)p(t) - C_2^{\top}(t)q(t) - E^{\mathscr{F}_t}[D_1^{\top}(t+\delta)p(t+\delta)] - E^{\mathscr{F}_t}[D_2^{\top}(t+\delta)q(t+\delta)]\right\}\mathrm{d}\overleftarrow{B}(t), \\ -q(t)\overrightarrow{\mathrm{d}W(t)}, \quad t \in [0,T], \\ p(T) = -Qx(T), \\ p(t) = 0, \quad t \in (T, T+\delta], \\ q(t) = 0, \quad t \in (T, T+\delta]. \end{cases} \tag{5}$$

We assume that the following conditions hold:

(A1) Assume that the coefficient matrices A_i, B_i, C_i, D_i, E_i, and F_i $(i = 1, 2)$ are the matrix process with a proper dimension

(A2) The random matrix Q: $\Omega \longrightarrow R^{n\times n}$ is the nonnegatively bounded symmetric $\mathscr{F}_t$ adapt matrix

(A3) All the functions of t are bounded, $K(t)$, $R(t)$, and Q are symmetric nonnegative definite, and $S(t)$ is symmetric uniformly positive definite

3. Main Results

Theorem 1. *The function*

$$\begin{aligned} u^*(t) = S^{-1}(t)\{&E_1^{\top}(t)p(t) + E_2^{\top}(t)q(t) \\ &+ E^{\mathscr{F}_t}\left[F_1^{\top}(t+\delta)p(t+\delta) + F_2^{\top}(t+\delta)q(t+\delta)\right]\}, \end{aligned} \tag{6}$$

$t \in [0,T]$, is the unique optimal control for the delayed doubly stochastic linear quadratic optimal control problem, where $(x^*(\cdot), y^*(\cdot), p(\cdot), q(\cdot))$ is the solution of the following system:

$$\begin{cases} \mathrm{d}x(t) = [A_1(t)x(t) + B_1(t)x_\delta(t) + C_1(t)y(t) + D_1(t)y_\delta(t) + E_1(t)u(t) + F_1(t)u_\delta(t)]\mathrm{d}t \\ +[A_2(t)x(t) + B_2(t)x_\delta(t) + C_2(t)y(t) + D_2(t)y_\delta(t) + E_2(t)u(t) + F_2(t)u_\delta(t)] \\ \overrightarrow{\mathrm{d}W(t)} - y(t)\mathrm{d}\overleftarrow{B}(t), \quad t \in [0,T], \\ -\mathrm{d}p(t) = \{A_1^{\top}(t)p(t) + E^{\mathscr{F}_t}[B_1^{\top}(t+\delta)p(t+\delta)] + A_2^{\top}(t)q(t) - K(t)x(t) + E^{\mathscr{F}_t}[B_2^{\top}(t+\delta)q(t+\delta)]\}\mathrm{d}t \\ +\{R(t)y(t) - C_1^{\top}(t)p(t) - C_2^{\top}(t)q(t) - E^{\mathscr{F}_t}[D_1^{\top}(t+\delta)p(t+\delta)] - E^{\mathscr{F}_t}[D_2^{\top}(t+\delta)q(t+\delta)]\}\mathrm{d}\overleftarrow{B}(t) - q(t)\overrightarrow{\mathrm{d}W(t)}, \quad t \in [0,T], \\ x(t) = \varphi(t), \quad t \in [-\delta, 0], \\ y(t) = \psi(t), \quad t \in [-\delta, 0], \\ u(t) = 0, \quad t \in [-\delta, 0], \\ p(T) = -Qx(T), \\ p(t) = 0, \quad t \in (T, T+\delta], \\ q(t) = 0, \quad t \in (T, T+\delta]. \end{cases} \tag{7}$$

Proof. The existence and uniqueness of the solution for equation (1) can be guaranteed by Theorem 3.1 in [20] under the assumptions (A1)–(A3). Equation (5) is an anticipated backward doubly stochastic differential equation. Its existence and uniqueness can be deduced by Theorem 3.2 in [18]. Now, we prove that $u^*(t)$ is the optimal control. For all $v(\cdot) \in U[0,T]$, let $(x^*(\cdot), y^*(\cdot))$ and $(x^v(\cdot), y^v(\cdot))$ be the trajectory of the system corresponding to $u^*(t)$ and $v(t)$, respectively.

Then,

$$\begin{aligned}
&J(v(\cdot)) - J(u^*(\cdot)) \\
&= \frac{1}{2}E\bigg[\int_0^T (\langle K(t)x^v(t), x^v(t)\rangle - \langle K(t)x^*(t), x^*(t)\rangle + \langle R(t)y^v(t), y^v(t)\rangle \\
&\quad - \langle R(t)y^*(t), y^*\rangle + \langle S(t)v(t), v(t)\rangle - \langle S(t)u^*(t), u^*(t)\rangle)\mathrm{d}t \\
&\quad + \langle Qx^v(T), x^v(T)\rangle - \langle Qx^*(T), x^*(T)\rangle\bigg], \\
&= \frac{1}{2}E\bigg[\int_0^T (\langle K(t)(x^v(t) - x^*(t)), x^v(t) - x^*(t)\rangle + \langle S(t)(v(t) - u^*(t)), v(t) - u^*(t)\rangle \\
&\quad + \langle R(t)(y^v(t) - y^*(t)), y^v(t) - y^*(t)\rangle + 2\langle K(t)x^*(t), x^v(t) - x^*(t)\rangle \\
&\quad + 2\langle R(t)y^*(t), y^v(t) - y^*(t)\rangle + 2\langle S(t)u^*(t), v(t) - u^*(t)\rangle)\mathrm{d}t \\
&\quad + \langle Q(x^v(T) - x^*(T)), x^v(T) - x^*(T)\rangle + 2\langle Qx^*(T), x^v(T) - x^*(T)\rangle\bigg].
\end{aligned} \tag{8}$$

From the definitions of $K(t)$, $R(t)$, $S(t)$, and Q, we know $K(t)$, $R(t)$, and Q are symmetric nonnegative definite and $S(t)$ is symmetric uniformly positive definite. So, we have

$$\begin{aligned}
&J(v(\cdot)) - J(u^*(\cdot)) \\
&\geq E\bigg\{\int_0^T [\langle K(t)x^*(t), x^v(t) - x^*(t)\rangle + \langle S(t)u^*(t), v(t) - u^*(t)\rangle \\
&\quad + \langle R(t)y^*(t), y^v(t) - y^*(t)\rangle]\mathrm{d}t + \langle Qx^*(T), x^v(T) - x^*(T)\rangle\bigg\}.
\end{aligned} \tag{9}$$

Applying the Itô–Doeblin formula to

$$\langle Qx^*(T), x^v(T) - x^*(T)\rangle = \langle -p(T), x^v(T) - x^*(T)\rangle, \tag{10}$$

and paying attention to the initial condition and the terminal condition, we have

$$\begin{aligned}
&E\langle p(T), x^v(T) - x^*(T)\rangle \\
&= E\bigg[\int_0^T \langle p(t), A_1(t)(x^v(t) - x^*(t)) + B_1(t)(x^v_\delta(t) - x^*_\delta(t)) + C_1(t)(y^v(t) - y^*(t)) \\
&\quad + D_1(t)(y^v_\delta(t) - y^*_\delta(t)) + E_1(t)(v(t) - u^*(t)) + F_1(t)(v_\delta(t) - u^*_\delta(t))\rangle\mathrm{d}t \\
&\quad - \int_0^T \langle A_1^\top(t)p(t) + A_2^\top(t)q(t) - K(t)x^*(t) + E^{\mathscr{F}_t}\left[B_1^\top(t+\delta)p(t+\delta)\right] \\
&\quad + E^{\mathscr{F}_t}\left[B_2^\top(t+\delta)q(t+\delta)\right], x^v(t) - x^*(t)\rangle\mathrm{d}t \\
&\quad + \int_0^T \langle q(t), A_2(t)(x^v(t) - x^*(t)) + B_2(t)(x^v_\delta(t) - x^*_\delta(t)) + C_2(t)(y^v(t) - y^*(t)) \\
&\quad + D_2(t)(y^v_\delta(t) - y^*_\delta(t)) + E_2(t)(v(t) - u^*(t)) + F_2(t)(v_\delta(t) - u^*_\delta(t))\rangle\mathrm{d}t \\
&\quad + \int_0^T \langle R(t)y^*(t) - C_1^\top(t)p(t) - C_2^\top(t)q(t) - E^{\mathscr{F}_t}\left[D_1^\top(t+\delta)p(t+\delta)\right] \\
&\quad - E^{\mathscr{F}_t}\left[D_2^\top(t+\delta)q(t+\delta)\right], y^v(t) - y^*(t)\rangle\mathrm{d}t\bigg].
\end{aligned} \tag{11}$$

In fact, we have

$$\begin{aligned}
&E\int_0^T\left[\langle p(t),B_1(t)(x_\delta^v(t)-x_\delta^*(t))\rangle-\langle E^{\mathscr{F}_t}\left[B_1^\top(t+\delta)p(t+\delta)\right],x^v(t)-x^*(t)\rangle\right]\mathrm{d}t\\
&=E\int_0^T\langle p(t),B_1(t)(x_\delta^v(t)-x_\delta^*(t))\rangle\mathrm{d}t-\int_\delta^{T+\delta}\langle B_1^\top(t)p(t),x_\delta^v(t)-x_\delta^*(t)\rangle\mathrm{d}t\\
&=E\int_0^\delta\langle p(t),B_1(t)(x_\delta^v(t)-x_\delta^*(t))\rangle\mathrm{d}t-\int_T^{T+\delta}\langle B_1^\top(t)p(t),x_\delta^v(t)-x_\delta^*(t)\rangle\mathrm{d}t\\
&=0.
\end{aligned} \tag{12}$$

So, we have

$$\begin{aligned}
&E\langle -p(T),x^v(T)-x^*(T)\rangle\\
&=E\int_0^T[\langle -K(t)x^*(t),x^v(t)-x^*(t)\rangle+\langle -R(t)y^*(t),y^v(t)-y^*(t)\rangle\\
&\quad+\langle -p(t),E_1(t)(v(t)-u^*(t))+F_1(t)(v_\delta(t)-u_\delta^*(t))\rangle\\
&\quad+\langle -q(t),E_2(t)(v(t)-u^*(t))+F_2(t)(v_\delta(t)-u_\delta^*(t))\rangle]\mathrm{d}t.
\end{aligned} \tag{13}$$

Then,

$$\begin{aligned}
&J(v(\cdot))-J(u^*(\cdot))\ge E\int_0^T[\langle S(t)u^*(t),v(t)-u^*(t)\rangle+\langle -p(t),E_1(t)(v(t)-u^*(t))\\
&\quad+F_1(t)(v_\delta(t)-u_\delta^*(t))\rangle+\langle -q(t),E_2(t)(v(t)-u^*(t))\\
&\quad+F_2(t)(v_\delta(t)-u_\delta^*(t))\rangle]\mathrm{d}t.
\end{aligned} \tag{14}$$

So from the definition of $u^*(t)$, we have

$$J(v(\cdot))-J(u^*(\cdot))\ge 0, \tag{15}$$

for any $v(\cdot)\in U[0,T]$. This shows that $u^*(t)$ is the optimal control.

Next, we will prove the uniqueness. Assume that $u_1(\cdot)$ and $u_2(\cdot)$ are both optimal controls. $(x_1(\cdot),y_1(\cdot))$ and $(x_2(\cdot),y_2(\cdot))$ are the trajectories corresponding to $u_1(\cdot)$ and $u_2(\cdot)$, respectively. Equation (5) is a new type of the anticipated backward doubly stochastic differential equation. The existence and uniqueness of the solution for the equation can be guaranteed by Theorem 3.2 in [18]. By the uniqueness of the solution of the equation, we know that $((x_1(\cdot)+x_2(\cdot)/2),(y_1(\cdot)+y_2(\cdot)/2))$ is the trajectory corresponding to $(u_1(\cdot)+u_2(\cdot)/2)$. From the definition of $K(t)$, $R(t)$, $S(t)$, and Q, we know $J(u^1(\cdot))=J(u^2(\cdot))=\alpha\ge 0$.

Then,

$$\begin{aligned}
2\alpha&=J(u_1(\cdot))+J(u_2(\cdot))\\
&=J\left(\frac{u_1(\cdot)+u_2(\cdot)}{2}\right)\\
&\quad+E\int_0^T\left[\left\langle S(t)\frac{u_1(t)-u_2(t)}{2},\frac{u_1(t)-u_2(t)}{2}\right\rangle\right.\\
&\quad+\left\langle K(t)\frac{x_1(t)-x_2(t)}{2},\frac{x_1(t)-x_2(t)}{2}\right\rangle\\
&\quad+\left.\left\langle R(t)\frac{y_1(t)-y_2(t)}{2},\frac{y_1(t)-y_2(t)}{2}\right\rangle\right]\mathrm{d}t\\
&\quad+\left\langle Q\frac{x_1(T)-x_2(T)}{2},\frac{x_1(T)-x_2(T)}{2}\right\rangle\\
&\ge 2\alpha+E\int_0^T\left\langle S(t)\frac{u_1(t)-u_2(t)}{2},\frac{u_1(t)-u_2(t)}{2}\right\rangle\mathrm{d}t.
\end{aligned} \tag{16}$$

From the definition of $S(t)$, we have $u_1(\cdot) = u_2(\cdot)$.
We complete the proof of Theorem 1. □

Next, we study a special class of the delayed doubly stochastic LQ problem. We discuss the case that only the control contained the delayed variable, and the initial value of the state variable η is deterministic. The delayed system can be written as

$$\begin{cases} \mathrm{d}x(t) = [A_1(t)x(t) + C_1(t)y(t) + F_1(t)u_\delta(t)]\mathrm{d}t + [A_2(t)x(t) \\ +C_2(t)y(t) + F_2(t)u_\delta(t)]\overrightarrow{\mathrm{d}W(t)} - y(t)\mathrm{d}\overleftarrow{B}(t), \quad t \in [0,T], \\ -\mathrm{d}p(t) = [A_1^\top(t)p(t) + A_2^\top(t)q(t) - K(t)x(t)]\mathrm{d}t + [R(t)y(t) \\ -C_1^\top(t)p(t) - C_2^\top(t)q(t)]\mathrm{d}\overleftarrow{B}(t) \ - q(t)\overrightarrow{\mathrm{d}W(t)}, \quad t \in [0,T], \\ x(0) = \eta, \\ u(t) = 0, \quad t \in [-\delta, 0], \\ p(T) = -Qx(T), \\ p(t) = 0, \quad t \in (T, T+\delta], \\ q(t) = 0, \quad t \in (T, T+\delta]. \end{cases} \tag{17}$$

We also consider the optimal control problem (4) under the classical quadratic index (4).

From Theorem 1, we can deduce the optimal control directly:

$$u^*(t) = S^{-1}(t)E^{\mathcal{F}_t}\left[F_1^\top(t+\delta)p(t+\delta) + F_2^\top(t+\delta)q(t+\delta)\right], \quad t \in [0,T]. \tag{18}$$

Peng [21] gave the solution of a kind of stochastic Hamiltonian systems by the Riccati equation corresponding to the system. Following this way, we want to use the solution of the Riccati equation to introduce the optimal control for the delayed doubly stochastic LQ problem. First, we give the generalized matrix Riccati equation:

$$\begin{cases} -\dot{M}(t) = M(t)A_1(t) + A_1^\top(t)M(t) + M(t)C_1(t)G(t) + A_2^\top(t)N(t) \\ -K(t) + M(t)F_1(t)S^{-1}(t-\delta)[F_1^\top(t)M(t) + F_2^\top(t)N(t)], \\ M(t)G(t) = R(t)G(t) - C_1^\top(t)M(t) - C_2^\top(t)N(t), \\ N(t) = M(t)A_2(t) + M(t)F_2(t)S^{-1}(t-\delta)[F_1^\top(t)M(t) + F_2^\top(t)N(t)] \\ +M(t)C_2(t)G(t). \end{cases} \tag{19}$$

Theorem 2. *Let the assumptions (A1)–(A3) be satisfied. If the Riccati equation has a solution $(G(\cdot), M(\cdot), N(\cdot))$, then system (17) has a unique solution:*

$$(x(t), y(t), p(t), q(t)) = (x(t), G(t)x(t), M(t)x(t), N(t)x(t)), \tag{20}$$

where $x(t)$ is solved by

$$\begin{cases} \mathrm{d}x(t) = \{A_1(t) + C_1(t)G(t) + F_1(t)S^{-1}(t-\delta)E^{\mathcal{F}_{t-\delta}}[F_1^\top(t)p(t) \\ +F_2^\top(t)q(t)]\}x(t)\mathrm{d}t + \{A_2(t) + C_2(t)G(t) + F_2(t)S^{-1}(t-\delta) \\ E^{\mathcal{F}_{t-\delta}}[F_1^\top(t)p(t) + F_2^\top(t)q(t)]\}x(t)\overrightarrow{\mathrm{d}W(t)} - y(t)\mathrm{d}\overleftarrow{B}(t), \quad t \in [0,T], \\ x(0) = \eta, \\ u(t) = 0, \quad t \in [-\delta, 0]. \end{cases} \tag{21}$$

Proof. We apply Itô's formula to $M(t)x(t)$ and compare the coefficient with $p(t)$, then we can deduce the conclusion directly. Next, we will prove the uniqueness.

Assume that $(x(t), y(t), p(t), q(t))$ is a solution of system (17), with the conditions $x(0) = \eta$ and $P(T) = -Qx(T)$.

We set $\overline{y}(t) = G(t)x(t)$, $\overline{p}(t) = M(t)x(t)$, and $\overline{q}(t) = N(t)x(t)$. By differentiating $\overline{p}(t)$, we have

$$\begin{aligned}\mathrm{d}\overline{p}(t) &= \dot{M}(t)x(t)\mathrm{d}t + M(t)\mathrm{d}x(t)\\ &= \dot{M}(t)x(t)\mathrm{d}t + M(t)\left[A_1(t)x(t) + C_1(t)y(t) + F_1(t)u_\delta(t)\right]\mathrm{d}t\\ &\quad + M(t)\left[A_2(t)x(t) + C_2(t)y(t) + F_2(t)u_\delta(t)\right]\overrightarrow{\mathrm{d}W(t)} - M(t)y(t)\mathrm{d}\overleftarrow{B}(t).\end{aligned} \tag{22}$$

Substituting the first and the second equality of the Riccati equation (19) into (22), we have

$$\begin{aligned}\mathrm{d}\overline{p}(t) &= -\left[A_1^\top(t)\overline{p}(t) + M(t)C_1(t)(\overline{y}(t) - y(t)) + A_2^\top(t)\overline{q}(t) - K(t)x(t)\right]\mathrm{d}t\\ &\quad + \left[\overline{q}(t) - M(t)C_2(t)(\overline{y}(t) - y(t))\right]\overrightarrow{\mathrm{d}W(t)} - M(t)y(t)\mathrm{d}\overleftarrow{B}(t).\end{aligned} \tag{23}$$

On the other hand, from the Riccati equation (19), we have

$$\begin{aligned}M(t)y(t) &= M(t)\{\overline{y}(t) - [\overline{y}(t) - y(t)]\}\\ &= M(t)G(t)x(t) - M(t)[\overline{y}(t) - y(t)]\\ &= \left[R(t)G(t) - C_1^\top(t)M(t) - C_2^\top(t)N(t)\right]x(t) - M(t)[\overline{y}(t) - y(t)]\\ &= R(t)\overline{y}(t) - C_1^\top(t)\overline{p}(t) - C_2^\top(t)\overline{q}(t) - M(t)[\overline{y}(t) - y(t)].\end{aligned} \tag{24}$$

Then, equality (23) can be written as

$$\begin{aligned}\mathrm{d}\overline{p}(t) &= -\left[A_1^\top(t)\overline{p}(t) + M(t)C_1(t)(\overline{y}(t) - y(t)) + A_2^\top(t)\overline{q}(t) - K(t)x(t)\right]\mathrm{d}t\\ &\quad + \left[\overline{q}(t) - M(t)C_2(t)(\overline{y}(t) - y(t))\right]\overrightarrow{\mathrm{d}W(t)}\\ &\quad - \left[R(t)\overline{y}(t) - C_1^\top(t)\overline{p}(t) - C_2^\top(t)\overline{q}(t) - M(t)(\overline{y}(t) - y(t))\right]\mathrm{d}\overleftarrow{B}(t).\end{aligned} \tag{25}$$

We denote $(\widehat{y}(t), \widehat{p}(t), \widehat{q}(t)) = (\overline{y}(t) - y(t), \overline{p}(t) - p(t), \overline{q}(t) - q(t))$, then we have

$$\begin{aligned}-\mathrm{d}\widehat{p}(t) &= -\mathrm{d}\overline{p}(t) - (-\mathrm{d}p(t))\\ &= \left[A_1^\top(t)\widehat{p}(t) + A_2^\top(t)\widehat{q}(t) + M(t)C_1(t)\widehat{y}(t)\right]\mathrm{d}t\\ &\quad + \left[R(t)\widehat{y}(t) - C_1^\top(t)\widehat{p}(t) - C_2^\top(t)\widehat{q}(t) - M(t)\widehat{y}(t)\right]\mathrm{d}\overleftarrow{B}(t)\\ &\quad - \left[\widehat{q}(t) - M(t)C_2(t)\widehat{y}(t)\right]\overrightarrow{\mathrm{d}W(t)}.\end{aligned} \tag{26}$$

Now, we set $\widehat{q}(t) - M(t)C_2(t)\widehat{y}(t) = q\prime(t)$, that is, $\widehat{q}(t) = M(t)C_2(t)\widehat{y}(t) + q\prime(t)$, then equation (26) can be written as

$$\begin{aligned}-\mathrm{d}\widehat{p}(t) &= \left\{A_1^\top(t)\widehat{p}(t) + \left[M(t)C_1(t) + A_2^\top(t)M(t)C_2(t)\right]\widehat{y}(t) + A_2^\top(t)q\prime(t)\right\}\mathrm{d}t\\ &\quad + \left\{\left[R(t) - C_2^\top(t)M(t)C_2(t) - M(t)\right]\widehat{y}(t) - C_1^\top(t)\widehat{p}(t)\right.\\ &\quad \left. - C_2^\top(t)q\prime(t)\right\}\mathrm{d}\overleftarrow{B}(t) - q\prime(t)\overrightarrow{\mathrm{d}W(t)}.\end{aligned} \tag{27}$$

This is a linear backward doubly stochastic differential equation. This is a unique solution $(\hat{y}(t), \hat{p}(t), q\prime(t)) \equiv (0,0,0)$, that is, $(\hat{y}(t), \hat{p}(t), \hat{q}(t)) \equiv (0,0,0)$. So, we have $y(t) = G(t)x(t)$, $p(t) = M(t)x(t)$, and $q(t) = N(t)x(t)$.

We complete the proof of Theorem 2. □

Theorem 3. *Let the assumptions (A1)–(A3) be satisfied. Assume that $(G(\cdot), M(\cdot), N(\cdot))$ satisfies the generalized Riccati equation, then the optimal control of the delayed doubly stochastic linear quadratic optimal control problem has the following form:*

$$u^*(t) = S^{-1}(t)E^{\mathscr{F}_t}\left[F_1^\top(t+\delta)M(t+\delta) + F_2^\top(t+\delta)N(t+\delta)\right]x(t+\delta), \tag{28}$$

$$J(u^*) = -\frac{1}{2}\langle M(0)\eta, \eta\rangle. \tag{29}$$

Proof. From the assumption that $(G(\cdot), M(\cdot), N(\cdot))$ is the solution of the Riccati equation (19) set $y(t) = G(t)x(t)$, $p(t) = M(t)x(t)$, and $q(t) = N(t)x(t)$. Applying Itô's formula to $p(t)$, we have

$$\begin{aligned} dp(t) = {} & \left[\dot{M}(t)x(t) + M(t)A_1(t)x(t) + M(t)C_1(t)y(t) + M(t)F_1(t)u_\delta(t)\right]dt \\ & + \left[M(t)A_2(t)x(t) + M(t)C_2(t)y(t) + M(t)F_2(t)u_\delta(t)\right]\overrightarrow{dW(t)} \\ & - M(t)y(t)d\overleftarrow{B}(t), \quad t \in [0,T]. \end{aligned} \tag{30}$$

From the definition of the matrix Riccati equation (19), we have

$$\begin{aligned} dp(t) = {} & \Big\{-\big[A_1^\top(t)M(t) + M(t)A_1(t) + M(t)C_1(t)G(t) + A_2^\top(t)N(t) \\ & -K(t) + M(t)F_1(t)S^{-1}(t-\delta)\left(F_1^\top(t)M(t) + F_2^\top(t)N(t)\right)\big]x(t) \\ & +M(t)A_1(t)x(t) + M(t)C_1(t)y(t) + M(t)F_1(t)u_\delta(t)\Big\}dt \\ & +\Big\{\big[N(t) - M(t)C_2(t)G(t) - M(t)F_2(t)S^{-1}(t-\delta)\big(F_1^\top(t)M(t) \\ & +F_2^\top(t)N(t)\big)\big]x(t) + M(t)C_2(t)y(t) + M(t)F_2(t)u_\delta(t)\Big\}\overrightarrow{dW(t)} \\ & -\left[R(t)G(t) - C_1^\top(t)M(t) - C_2^\top(t)N(t)\right]x(t)d\overleftarrow{B}(t), \quad t \in [0,T]. \end{aligned} \tag{31}$$

That is,

$$\begin{aligned} -dp(t) = {} & \left[A_1^\top(t)p(t) + A_2^\top(t)q(t) - K(t)x(t)\right]dt + [R(t)y(t) \\ & -C_1^\top(t)p(t) - C_2^\top(t)q(t)\big]d\overleftarrow{B}(t) - q(t)\overrightarrow{dW(t)}, \quad t \in [0,T]. \end{aligned} \tag{32}$$

So, we know that the solution of system (17) satisfied the formula $y(t) = G(t)x(t)$, $p(t) = M(t)x(t)$, and $q(t) = N(t)x(t)$. Then, the optimal control can be written as (28).

Next, we deduce the objective function $J(u^*(\cdot))$ by the solution of the Riccati equation and the initial value of the state variable.

Applying Itô's formula to $\langle x(t), p(t)\rangle$ and taking expectation, we have

$$E[\langle x(T), p(T)\rangle - \langle x(0), p(0)\rangle] = E[\langle x(T), -Qx(T)\rangle - \langle \eta, M(0)\eta\rangle], \tag{33}$$

$$\begin{aligned} E[\langle x(T), p(T)\rangle - \langle x(0), p(0)\rangle] &= E\int_0^T [\langle K(t)x(t), x(t)\rangle + \langle R(t)y(t), y(t)\rangle + \langle F_1(t)u_\delta(t), p(t)\rangle + \langle F_2(t)u_\delta(t), q(t)\rangle]dt \\ &= E\int_0^T \big[E^{\mathscr{F}_t}\langle F_1(t+\delta)u(t), p(t+\delta)\rangle + E^{\mathscr{F}_t}\langle F_2(t+\delta)u(t), q(t+\delta)\rangle + \langle K(t)x(t), x(t)\rangle \\ &\quad + \langle R(t)y(t), y(t)\rangle]dt. \end{aligned} \tag{34}$$

Substituting equalities (33) and (34) into the function $J(u(\cdot))$, we can deduce

$$\begin{aligned} J(u(\cdot)) &= \frac{1}{2}\left\{E\int_0^T [\langle K(t)x(t), x(t)\rangle + \langle R(t)y(t), y(t)\rangle \right.\\ &\quad + \langle S(t)u(t), u(t)\rangle]\mathrm{d}t \\ &\quad \left. + \langle Qx(T), x(T)\rangle\right\} \\ &= -\frac{1}{2}\langle M(0)\eta, \eta\rangle. \end{aligned} \tag{35}$$

We complete the proof of Theorem 3. □

4. Applications

Case 1. For the general delayed doubly stochastic LQ system (1), when the coefficients are

$$B_i(t) = D_i(t) = F_i(t) = 0, \quad i = 1, 2, \tag{36}$$

this is the system without time delay. The optimal control deduced by Theorem 1 is consistent with the results in [22].

Case 2. When $F_i(t) = 0\,(i = 1, 2)$ in system (1), this is the case that the system does not contain time delay variables in control variables. The optimal control deduced by Theorem 1 is

$$u^*(t) = S^{-1}(t)\left[E_1^\top(t)p(t) + E_2^\top(t)q(t)\right]. \tag{37}$$

This is consistent with the result in [20]. From the expression of the optimal control, the factors affecting the optimal control are the same as that in [22].

Case 3. For the delayed doubly stochastic LQ system (17), when the optimal control deduced from Theorem 3 is

$$u^*(t) = S^{-1}(t)\left[F_1^\top(t)M(t) + F_2^\top(t)N(t)\right]x(t), \tag{38}$$

the optimal control is derived from the solution of the matrix Riccati equation. This is consistent with the result in [21].

In this paper, we are mainly concerned about the delayed doubly stochastic LQ system in which all the variables contained time delay. We deduced the explicit form of the optimal control for the general case. The results of this paper extend our previous work and enrich the content of the delayed doubly stochastic LQ problem. But, from the conclusion of the article, there are still some contents that need further study. We only discuss the matrix-valued Riccati equation corresponding to the special cases. For a more general Riccati equation of the delayed doubly stochastic LQ system, we will work hard to increase the research on this part in our future work.

Data Availability

No data were used to support this study.

Conflicts of Interest

The authors declare that there are no conflicts of interest regarding the publication of this paper.

Acknowledgments

The authors would like to thank Professor Yuecai Han for valuable suggestions and guidance on this article. This work was supported by science and technology research projects of the Jilin Province Education Department (JJKH20200235KJ) and the National Natural Science Foundation of China (grant number 11871244).

References

[1] W. Yu, P. Guo, Q. Wang et al., "On a periodic capital injection and barrier dividend strategy in the compound Poisson risk model," *Mathematics*, vol. 8, no. 4, p. 511, 2020.

[2] W. Yu, Y. Yong, G. Guan, Y. Huang, W. Su, and C. Cui, "Valuing guaranteed minimum death benefits by cosine series expansion," *Mathematics*, vol. 7, no. 9, p. 835, 2019.

[3] Z. Zhang, Y. Yong, and W. Yu, "Valuing equity-linked death benefits in general exponential Lévy models," *Journal of Computational and Applied Mathematics*, vol. 365, Article ID 112377, 2020.

[4] W. Yu, F. Wang, Y. Huang, and H. Liu, "Social optimal mean field control problem for population growth model," *Asian Journal of Control*, pp. 1–8, 2019.

[5] E. Pardoux and S. Peng, "Backward doubly stochastic differential equations and systems of quasilinear SPDEs," *Probability Theory and Related Fields*, vol. 98, no. 2, pp. 209–227, 1994.

[6] Y. Shi and Q. Zhu, "Partially observed optimal controls of forward-backward doubly stochastic systems," *ESAIM: Control, Optimisation and Calculus of Variations*, vol. 19, no. 3, pp. 828–843, 2013.

[7] Q. Zhu and Y. Shi, "Optimal control of backward doubly stochastic systems with partial information," *IEEE Transactions on Automatic Control*, vol. 60, no. 1, pp. 173–178, 2015.

[8] Q. Zhu, Y. Shi, and B. Teng, "Forward-backward doubly stochastic differential equations with random jumps and related games," *Asian Journal of Control*, 2020.

[9] L. Chen and Z. Wu, "Maximum principle for the stochastic optimal control problem with delay and application," *Automatica*, vol. 46, no. 6, pp. 1074–1080, 2010.

[10] S. Wu and G. Wang, "Optimal control problem of backward stochastic differential delay equation under partial information," *Systems & Control Letters*, vol. 82, no. 6, pp. 71–78, 2015.

[11] S. Lv, R. Tao, and Z. Wu, "Maximum principle for optimal control of anticipated forward-backward stochastic differential delayed systems with regime switching," *Optimal Control Applications and Methods*, vol. 37, no. 1, pp. 154–175, 2016.

[12] S. Wang and Z. Wu, "Stochastic maximum principle for optimal control problems of forward backward delay systems involving impulse controls," *Journal of Systems Science and Complexity*, vol. 30, no. 2, pp. 32–58, 2017.

[13] Z. Yu, "The stochastic maximum principle for optimal control problems of delay systems involving continuous and impulse controls," *Automatica*, vol. 48, no. 10, pp. 2420–2432, 2012.

[14] L. Chen and Z. Wu, "A type of general forward-backward stochastic differential equations and applications," *Chinese*

Annals of Mathematics, Series B, vol. 32, no. 2, pp. 279–292, 2011.

[15] H. Tang and Z. Wu, "Stochastic differential equations and stochastic linear quadratic optimal control problem with Lévy processes," *Journal of Systems Science and Complexity*, vol. 22, no. 1, pp. 122–136, 2009.

[16] J. Huang, X. Li, and J. Shi, "Forward-backward linear quadratic stochastic optimal control problem with delay," *Systems & Control Letters*, vol. 61, no. 5, pp. 623–630, 2012.

[17] S. Peng and Z. Yang, "Anticipated backward stochastic differential equations," *The Annals of Probability*, vol. 37, no. 3, pp. 877–902, 2009.

[18] X. Xu, "Anticipated backward doubly stochastic differential equations," *Applied Mathematics and Computation*, vol. 220, no. 4, pp. 53–62, 2013.

[19] J. Xu and Y. Han, "Stochastic maximum principle for delayed backward doubly stochastic control systems," *The Journal of Nonlinear Sciences and Applications*, vol. 10, no. 1, pp. 215–226, 2017.

[20] J. Xu, "Stochastic maximum principle for delayed doubly stochastic control systems and their applications," *International Journal of Control*, vol. 93, no. 6, pp. 1371–1380, 2018.

[21] S. Peng, "Problem of eigenvalues of stochastic Hamiltonian systems with boundary conditions," *Stochastic Processes and Their Applications*, vol. 88, no. 2, pp. 259–290, 2000.

[22] Y. Han, S. Peng, and Z. Wu, "Maximum principle for backward doubly stochastic control systems with applications," *SIAM Journal on Control and Optimization*, vol. 48, no. 7, pp. 4224–4241, 2010.

Hindawi
Mathematical Problems in Engineering
Volume 2020, Article ID 2743676, 13 pages
https://doi.org/10.1155/2020/2743676

Research Article

Option Pricing under Double Stochastic Volatility Model with Stochastic Interest Rates and Double Exponential Jumps with Stochastic Intensity

Ying Chang and Yiming Wang

School of Economics, Peking University, Beijing 100871, China

Correspondence should be addressed to Yiming Wang; wangyiming@pku.edu.cn

Received 22 January 2020; Revised 26 March 2020; Accepted 18 April 2020; Published 25 May 2020

Guest Editor: Wenguang Yu

We present option pricing under the double stochastic volatility model with stochastic interest rates and double exponential jumps with stochastic intensity in this article. We make two contributions based on the existing literature. First, we add double stochastic volatility to the option pricing model combining stochastic interest rates and jumps with stochastic intensity, and we are the first to fill this gap. Second, the stochastic interest rate process is presented in the Hull–White model. Some authors have concentrated on hybrid models based on various asset classes in recent years. Therefore, we build a multifactor model with the term structure of stochastic interest rates. We also approximated the pricing formula for European call options by applying the COS method and fast Fourier transform (FFT). Numerical results display that FFT and the COS method are much faster than the numerical integration approach used for obtaining the semi-closed form prices. The COS method shows higher accuracy, efficiency, and stability than FFT. Therefore, we use the COS method to investigate the impact of the parameters in the stochastic jump intensity process and the existence of the process on the call option prices. We also use it to examine the impact of the parameters in the interest rate process on the call option prices.

1. Introduction

An abundance of empirical studies show the existence of the asymmetric leptokurtic features and the volatility smile after Black and Scholes [1] did some experimental and pioneering work in European option pricing. Allowing the volatility and the interest rate to change, allowing for the existence of jumps, and the change of the jump intensity over time represent reasonable dynamics of the asset returns.

Stochastic volatility models have been playing a significant part in European option modelling since volatility should be a random variable based on extensive empirical studies. Some authors proposed several representative stochastic volatility models [2–5]. Heston [6] specified the variance (the square of volatility) with a Cox–Ingersoll–Ross (CIR) process which is more proper for application than other models. He contributed to the existing literature mainly by modelling the variance with the CIR process which displays mean-reverting and nonnegative properties, deriving the formulae for the characteristic functions with PDE approach and applying the Fourier transform for obtaining the closed-form valuation formula for European options since the density function is expressed with the characteristic function using inverse Fourier transform. Schöbel and Zhu [7] developed a model with stochastic volatility which is also proper for application. The volatility follows an Ornstein–Uhlenbeck process in their model with the asset returns, and its volatility being correlated with each other. They contributed to the existing literature mainly by using the expectation approach for deriving the formulae for the characteristic functions instead of PDE approach. Lewis [8] developed a stochastic variance model that the variance follows a 3/2 nonaffine stochastic process because the option prices under this model are local martingales instead of martingales, and 3/2 process is not stationary and it is improper for application. Grasselli [9] proposed that the variance follows a 4/2 process which is a mix of the 1/2 and the 3/2 terms. Since they quoted that the 4/2 model shares the same properties as the 3/2 model, so it is not proper for practical application as well. Christoffersen et al. [10] modelled the variance with a two-factor mean-reverting square root process that provides more flexibility than the Heston model. Their empirical study shows that their model works better than the one-factor model. Based on the existing forms of processes used to describe the dynamics of the volatility, we decide to study option pricing under two-factor stochastic volatility in this article since it is more applicable for practical application.

The interest rate is also time varying in the real economy. Meanwhile, stochastic interest rate models have a longer history than stochastic volatility models. They are initially used to study the zero-coupon bond and interest rate options and derive the formulae for them for application. There are four typical stochastic interest rate models. Vasicek [11] modelled the interest rate with an Ornstein–Uhlenbeck process for describing the change of it. Cox et al. [12] modelled the interest rate with mean-reverting square root process; henceforth, it was applied for reference to develop the stochastic volatility model. They contributed to the existing literature by expanding Vasicek's model that they added a term to the diffusion coefficient, and it maintains the mean-reverting and nonnegative properties that make it more proper for application than Vasicek's model. Since then, this model has been a benchmark to specify the dynamic change of the variance and the interest rate for decades. Longstaff [13] proposed a mean-reverting double square root model, and compared to the one square root model, it has some special features that it requires the parameters in the model to satisfy a specific condition. Since the dynamic change of the variance and the interest rate shares some common features, Zhu [14] expanded Longstaff's model to the stochastic variance model that they modelled the variance with double square root process. Hull and White [15] proposed a special process to specify the change of the interest rate with all the parameters in the model being time varying. Since this model cannot capture the market shapes very well in reality, they noted that the calibration of this model needs to be carefully dealt with. To make it perform better for practical application, Hull and White [16] improved their model to be a more reliable and applicable one that only one parameter in the process is time varying. It can be transformed to another form which is generally called the Hull–White interest rate process [17].

Because of the contribution of the authors who developed the stochastic interest rate models, some authors began to introduce the stochastic interest rate processes into European option pricing models to make them more reasonable for practical application. Their empirical work supports the significant improvement of stochastic interest rates [18, 19]. Meanwhile, several authors focused on option pricing combining stochastic volatility and interest rates to build hybrid models. CIR and Hull–White models are generally used to display the dynamics of the interest rate. Grzelak and Oosterlee [20] proposed an option pricing model with stochastic volatility and stochastic interest rates. The interest rate follows Hull–White and CIR processes in their model. Grzelak et al. [21] proposed option pricing combining stochastic volatility with Schöbel–Zhu and CIR processes and stochastic interest rate with Hull–White process, and they used some techniques for obtaining the formula for discounted characteristic function.

Jumps are used to describe the discontinuous behavior of the asset returns, and adding jumps to the option pricing model is also an extension. Merton [22] added the lognormal jumps to the option pricing model since he mentioned that the changes in stock prices appear to be jumps. However, the volatility is still a constant parameter in his model. Kou [23] proposed a double exponential jump-diffusion model for capturing discontinuous nature that the asset returns have; jump size is double exponentially distributed in his paper, and it can capture the leptokurtic feature and the volatility smile. Empirical studies also support the improvement of the option pricing model with jumps. Bates [24] established a model combining stochastic volatility and lognormal jumps, and his empirical work shows that his model can improve on fitting option prices. Bakshi et al. [25] also found that adding jumps to the option pricing model with stochastic volatility can improve the performance on pricing options, especially for short time to maturity.

Some authors also make some expansions that they focused on the option pricing modelling combining stochastic volatility, stochastic interest rates, and jumps, and several authors think that this kind of model is more reasonable and appropriate for application. Scott [26] supported better performance of this kind of the option pricing model. Jiang [27] also indicated that though their empirical study demonstrates that the dynamics of the interest rate has little impact on option pricing, option pricing modelling combining the three factors is still robust over time. Besides assuming the interest rate follows a CIR process, the Hull–White interest rate process also deserves studying [28].

In addition, empirical studies also support the existence of the change in the jump intensity over time. Santa-Clara and Yan [29] proposed that the volatility and the jump intensity change over time in their model. Their empirical results show that the volatility varies over time, and the jump intensity varies much wider than the former. Chang et al. [30] used ten years of stock returns data to affirm the existence of the change in the jump intensity over time and capture the switching of the jump intensity. Huang et al. [31] proposed a model combing stochastic volatility and jumps with stochastic intensity. They derived the characteristic function and did some numerical study based on it by applying FFT. Several authors presented models combing stochastic volatility, stochastic interest rates, and jumps with stochastic intensity [32, 33].

We present option pricing combining double stochastic volatility, stochastic interest rates, and double exponential jumps with stochastic intensity in this article. We derive the semi-closed form pricing formula and use it as the benchmark to examine some properties of two numerical approaches generally used to approximate the pricing formula for European options. Fast Fourier transform (FFT) and the COS method are two accurate and efficient numerical approaches generally used to approximate the formula for European option prices. Carr and Madan [34] developed a straightforward and efficient expression for the Fourier transform and used FFT to approximate the pricing formula for the options numerically. It makes computation simple and efficient and has a significant reduction in computation time. Fang and Oosterlee [35] developed the COS method for approximating the pricing formula for European options. Since the density function is expressed with the characteristic function via inverse Fourier transform, they used the Fourier cosine series to replace it for approximating the pricing formula. Their numerical results show that it is a highly efficient approach. In the numerical analysis part, we use FFT and the COS method to approximate the formula for European call option prices and compare the computation speed, the accuracy, the efficiency, and the stability between the two approaches. We examine the impact of the parameters in the jump intensity process and the existence of the process on call option prices. We also examine the impact of the parameters in the interest rate process on the call option prices.

We make two contributions based on the existing literature. First, we add double stochastic volatility to the option pricing model combining stochastic interest rates and jumps with stochastic intensity since the double stochastic volatility model is more applicable for practical application than the one-factor stochastic volatility model [10], and we are the first to fill this gap. Second, the stochastic interest rate process is presented in the Hull–White model. In recent years, some authors have concentrated on hybrid models based on various asset classes [20, 21], and the option pricing model with all these features have the possibility to develop more proper option prices [21]. Therefore, we build a multifactor model with the term structure of stochastic interest rates. It is an extension of the work by Grzelak et al. [21]. Since our model is in the class of the affine jump-diffusion (AJD) process which was introduced by Duffie et al. [36], we use their results to obtain the formula for the discounted characteristic function. Duffie et al. [36] did the pioneering research on the AJD process, the securities were modelled under an equivalent martingale measure, they extended the Heston model to be a multidimensional model, and the Fourier transform of the security price is in closed form which means that the coefficients in the expression of the Fourier form need to satisfy some ordinary differential equations by applying the Feynman–Kac theorem [36].

We form the structure of this article with the following sections. We develop option pricing modelling combining double stochastic volatility, stochastic interest rates, and double exponential jumps with stochastic intensity and derive the semiclosed form pricing formula in Section 2. In Section 3, we discuss and investigate some stochastic differential equations relevant to the Hull–White interest rate process and derive the discounted characteristic function. In Section 4, we do some numerical work. Section 5 provides the conclusion.

2. The Model and Semi-Closed Form Formula

Let $(\Omega, \mathscr{F}, (\mathscr{F}_t)_{t\in[0,T]}, \mathbb{Q})$be a complete probability space with a filtration and $\mathbb{Q}$ presents a risk-neutral measure. The stock price S_t is expressed by the following dynamic system:

$$\begin{cases} \dfrac{\mathrm{d}S_t}{S_t} = \left(r_t - \lambda_t \mu_J\right)\mathrm{d}t + \sqrt{V_{1t}}\,\mathrm{d}W_{1t}^S + \sqrt{V_{2t}}\,\mathrm{d}W_{2t}^S + (J-1)\mathrm{d}N_t, \\ \mathrm{d}V_{1t} = \kappa_1\left(\theta_1 - V_{1t}\right)\mathrm{d}t + \sigma_1\sqrt{V_{1t}}\,\mathrm{d}W_{1t}^V, \\ \mathrm{d}V_{2t} = \kappa_2\left(\theta_2 - V_{2t}\right)\mathrm{d}t + \sigma_2\sqrt{V_{2t}}\,\mathrm{d}W_{2t}^V, \\ \mathrm{d}r_t = \delta\left(\vartheta_t - r_t\right)\mathrm{d}t + \eta\,\mathrm{d}W_t^r, \\ \mathrm{d}\lambda_t = \kappa_\lambda\left(\theta_\lambda - \lambda_t\right)\mathrm{d}t + \sigma_\lambda\sqrt{\lambda_t}\,\mathrm{d}W_t^\lambda, \end{cases} \tag{1}$$

where W_{1t}^S, W_{2t}^S, W_{1t}^V, W_{2t}^V, ${W_t}^r$, and W_t^λ are the standard Brownian motions. We assume that W_{1t}^S is correlated with W_{1t}^V, $\mathrm{d}W_{1t}^S \cdot \mathrm{d}W_{1t}^V = \rho_1\mathrm{d}t$ and W_{2t}^S is correlated with W_{2t}^V, $\mathrm{d}W_{2t}^S \cdot \mathrm{d}W_{2t}^V = \rho_2\mathrm{d}t$. Any other Brownian motions are pairwise independent.

$V_{jt} = v_{jt}^2$, $j = 1, 2$, v_{jt} is the volatility, V_{jt} is its square which is called the variance, and λ_t is the jump intensity. θ_j and θ_λ are their mean-reversion levels, κ_j and κ_λ are their mean-reversion rates, and σ_j and σ_λ are their volatilities, respectively. r_t is the instantaneous spot interest rate, δ is its mean-reversion speed, η is its volatility, and ϑ_t is a time-varying drift term, and it is used to match the initial term structure of the interest rates.

N_t represents Poisson process with intensity λ_t and J represents the jump size, and we assume that $\ln J$ has an asymmetric double exponential distribution with density function $pdf_u(z)$:

$$pdf_u(z) = p\eta_1 e^{-\eta_1 z} 1_{\{z\geq 0\}} + q\eta_2 e^{\eta_2 z} 1_{\{z<0\}}, \tag{2}$$

where $\eta_1 > 1$, $\eta_2 > 0$, $p, q > 0$, and $p + q = 1$, where p and q represent the probabilities for positive and negative jumps, respectively; therefore, we can obtain that $\mu_J = \mathbb{E}^{\mathbb{Q}}(J-1) = (p\eta_1/\eta_1 - 1) + (q\eta_2/\eta_2 + 1) - 1$.

We set $X_t = \ln S_t$, $\tau = T - t$, $Y = \ln J$, and $k = \ln K$, where T is the maturity date, τ is the time to maturity, and K is the strike price. Under the risk-neutral measure $\mathbb{Q}$, the price of a call option $C(S, V_1, V_2, r, \lambda, t)$ at time $t \in [0, T]$ with strike price K and maturity date T is given by

$$C\left(S, V_1, V_2, r, \lambda, t\right) = \mathbb{E}^{\mathbb{Q}}\left(e^{-\int_t^T r_s \mathrm{d}s}\max\left(S_T - K, 0\right)\middle|\mathscr{F}_t\right), \tag{3}$$

we can rewrite it as

$$C(S,V_1,V_2,r,\lambda,t) = \mathbb{E}^{\mathbb{Q}}\left(e^{-\int_t^T r_s \mathrm{d}s} S_T 1_{\{X_T > k\}} \middle| F_t\right) - K\mathbb{E}^{\mathbb{Q}}\left(e^{-\int_t^T r_s \mathrm{d}s} 1_{\{X_T > k\}} \middle| \mathscr{F}_t\right). \quad (4)$$

The derivation of the semi-closed form formula is presented by applying Radon–Nikodym derivatives. We consider switching $\mathbb{Q}$ to the measure $\mathbb{Q}^S$ and the T forward measure $\mathbb{Q}^T$ for the first and second expectation parts respectively in (4). We give the following Radon–Nikodym derivatives:

$$\frac{\mathrm{d}\mathbb{Q}}{\mathrm{d}\mathbb{Q}^S} = \frac{e^X}{e^{-\int_t^T r_s \mathrm{d}s + X_T}}, \qquad \frac{\mathrm{d}\mathbb{Q}}{\mathrm{d}\mathbb{Q}^T} = \frac{P(t,T)}{e^{-\int_t^T r_s \mathrm{d}s}}, \quad (5)$$

where

$$S = e^X = \mathbb{E}^{\mathbb{Q}}\left(e^{-\int_t^T r_s \mathrm{d}s + X_T} \middle| \mathscr{F}_t\right), \quad (6)$$

$P(t,T) := \mathbb{E}^{\mathbb{Q}}(e^{-\int_t^T r_s \mathrm{d}s} | \mathscr{F}_t)$ is the price at time t of a zero-coupon bond which matures at time T.

Then, (4) can be rewritten as

$$C(S,V_1,V_2,r,\lambda,t) = S\mathbb{E}^{\mathbb{Q}^S}\left(1_{\{X_T > k\}} \middle| \mathscr{F}_t\right) \text{\&9;} \quad -KP(t,T)\mathbb{E}^{\mathbb{Q}^T}\left(1_{\{X_T > k\}} \middle| \mathscr{F}_t\right). \quad (7)$$

Since the density function $f(x)$ and the characteristic function $\widehat{f}(u)$ form a Fourier pair,

$$\widehat{f}(u) = \int_{\mathbb{R}} e^{iux} f(x)\mathrm{d}x, \qquad f(x) = \frac{1}{2\pi}\int_{\mathbb{R}} e^{-iux}\widehat{f}(u)\mathrm{d}u, \quad (8)$$

and we define

$$\varphi_S(u)\colon\ \varphi_S(u; X, V_1, V_2, r, \lambda, \tau) = \mathbb{E}^{\mathbb{Q}^S}\left(e^{iuX_T} \middle| \mathscr{F}_t\right), \quad (9)$$

$$\varphi_T(u)\colon\ \varphi_T(u; X, V_1, V_2, r, \lambda, \tau) = \mathbb{E}^{\mathbb{Q}^T}\left(e^{iuX_T} \middle| \mathscr{F}_t\right), \quad (10)$$

$$\varphi(u)\colon\ \varphi(u; X, V_1, V_2, r, \lambda, \tau) = \mathbb{E}^{\mathbb{Q}}\left(e^{-\int_t^T r_s \mathrm{d}s + iuX_T} \middle| \mathscr{F}_t\right), \quad (11)$$

where $\varphi_S(u)$ denotes the characteristic function under $\mathbb{Q}^S$, $\varphi_T(u)$ denotes the characteristic function under $\mathbb{Q}^T$, and $\varphi(u)$ denotes the discounted characteristic function under $\mathbb{Q}$.

We can obtain the following equations using Radon–Nikodym derivatives:

$$\varphi_S(u) = \mathbb{E}^{\mathbb{Q}^S}\left(\exp(iuX_T) \middle| \mathscr{F}_t\right) = \mathbb{E}^{\mathbb{Q}}\left(\frac{e^{-\int_t^T r_s \mathrm{d}s} e^{(iu+1)X_T}}{e^X} \middle| \mathscr{F}_t\right) = \frac{\varphi(u-i)}{\varphi(-i)}, \quad (12)$$

$$\varphi_T(u) = \mathbb{E}^{\mathbb{Q}^T}\left(\exp(iuX_T) \middle| \mathscr{F}_t\right) = \mathbb{E}^{\mathbb{Q}}\left(\frac{e^{-\int_t^T r_s \mathrm{d}s + iuX_T}}{P(t,T)} \middle| \mathscr{F}_t\right) = \frac{\varphi(u)}{P(t,T)}. \quad (13)$$

Then, (4) can be rewritten as

$$C(S,V_1,V_2,r,\lambda,t) = S\left(\frac{1}{2} + \frac{1}{\pi}\int_0^\infty R\left(\frac{e^{-iuk}\varphi(u-i)}{iu\varphi(-i)}\right)\mathrm{d}u\right) - KP(t,T)\left(\frac{1}{2} + \frac{1}{\pi}\int_0^\infty R\left(\frac{e^{-iuk}\varphi(u)}{iuP(t,T)}\right)\mathrm{d}u\right). \quad (14)$$

Therefore, we can get the semi-closed form formula once we obtain the formula for the discounted characteristic function $\varphi(u)$. The formula for $\varphi(u)$ is derived in the next section.

3. The Discounted Characteristic Function

The derivation of the formula for the discounted characteristic function is presented in this section. To be specific, first, we discuss and investigate some stochastic differential equations relevant to the Hull–White interest rate process, present the Hull–White decomposition, and enumerate some relevant formulae including the pricing formula for a zero-coupon bond. Second, we use the results given by Duffie et al. [36] to obtain the formula for the discounted characteristic function.

Applying Itô's lemma to the Hull–White model we obtain that

$$\mathrm{d}\left(e^{\delta t} r_t\right) = \delta e^{\delta t}\vartheta_t \mathrm{d}t + \eta e^{\delta t}\mathrm{d}W_t^r. \quad (15)$$

We integrate (15) to obtain that

$$r_T = r_t e^{-\delta(T-t)} + \delta\int_t^T e^{-\delta(T-u)}\vartheta_u \mathrm{d}u + \eta\int_t^T e^{-\delta(T-u)}\mathrm{d}W_u^r. \quad (16)$$

Therefore, r_T is a normally distributed conditional on $\mathscr{F}_t$ with

$$\mathbb{E}^{\mathbb{Q}}\left(r_T \middle| \mathscr{F}_t\right) = \mu_{HW} = r_t e^{-\delta(T-t)} + \delta\int_t^T e^{-\delta(T-u)}\vartheta_u \mathrm{d}u, \quad (17)$$

$$\mathrm{Var}^{\mathbb{Q}}\left(r_T \middle| \mathscr{F}_t\right) = \sigma_{\mathrm{HW}}^2 = \frac{\eta^2}{2\delta}\left(1 - e^{-2\delta(T-t)}\right). \quad (18)$$

The interest rate process in (1) can be decomposed into $r_t = \widetilde{r}_t + \psi_t$, and this is well known as the Hull–White decomposition. ψ_t and $\widetilde{r}_t$ are given by

$$\psi_t = \mathbb{E}^{\mathbb{Q}}\left(r_t \middle| \mathcal{F}_0\right) = r_0 e^{-\delta t} + \delta \int_0^t e^{-\delta(t-u)} \vartheta_u \mathrm{d}u, \tag{19}$$

$$\widetilde{r}_t = \eta \int_0^t e^{-\delta(t-u)} \mathrm{d}W_u^r. \tag{20}$$

We can obtain the following stochastic differential equation using Itô's lemma:

$$\mathrm{d}\widetilde{r}_t = -\delta \widetilde{r}_t \mathrm{d}t + \eta \mathrm{d}W_t^r, \quad \text{with } \widetilde{r}_0 = 0. \tag{21}$$

Theorem 1. *If the dynamics of $\widetilde{r}_t$ is given by the stochastic process (21), we define $f(t,T,\widetilde{r})$: $= \mathbb{E}^{\mathbb{Q}}(e^{-\int_t^T \widetilde{r}_u du} \mid \mathcal{F}_t)$, and it takes the following form:*

$$f(t,T,\widetilde{r}) = e^{C(t,T)-D(t,T)\widetilde{r}}, \tag{22}$$

where

$$C(t,T) = \frac{\eta^2}{2\delta^2}\left((T-t) - \frac{2}{\delta}\left(1-e^{-\delta(T-t)}\right) + \frac{1}{2\delta}\left(1-e^{-2\delta(T-t)}\right)\right)$$

%

$$D(t,T) = \frac{1-e^{-\delta(T-t)}}{\delta}. \tag{23}$$

Proof. Since (21) is an Ornstein–Uhlenbeck process and it possesses an affine term structure, we conjecture that

$$f(t,T,\widetilde{r}) = e^{C(t,T)-D(t,T)\widetilde{r}}, \tag{24}$$

where $f(t,T,\widetilde{r})$ satisfies a partial differential equation by applying the Feynman–Kac theorem [36]:

$$\frac{\partial f}{\partial t} - \delta \widetilde{r} \frac{\partial f}{\partial \widetilde{r}} + \frac{1}{2}\eta^2 \frac{\partial^2 f}{\partial \widetilde{r}^2} - \widetilde{r} f = 0, \tag{25}$$

with boundary condition $f(T,T,\widetilde{r}) = 1$.

We can obtain two ordinary differential equations by rearranging (25) in terms of (24)

$$\begin{cases} C_t(t,T) + \frac{1}{2}\eta^2 D^2(t,T) = 0, \\ D_t(t,T) - \delta D(t,T) + 1 = 0, \end{cases} \tag{26}$$

with boundary conditions $C(T,T) = 0$ and $D(T,T) = 0$.

We can obtain the solutions for $C(t,T)$ and $D(t,T)$ by solving the above two ordinary differential equations, thus the proof is complete.

Therefore, we can obtain the pricing formula for $P(0,T)$:

$$P(0,T) = e^{-\int_0^T \psi_u \mathrm{d}u + C(0,T)}. \tag{27}$$

Thus, ψ_T can be given by

$$\psi_T = -\frac{\partial \ln P(0,T)}{\partial T} + \frac{\partial C(0,T)}{\partial T} = f(0,T) + \frac{\eta^2}{2\delta^2}\left(1-e^{-\delta T}\right)^2, \tag{28}$$

where $f(0,T) = -(\partial \ln P(0,T)/\partial T)$, and we denote $f(0,T)$ as the instantaneous forward interest rate. According to (19), ϑ_t can be expressed as $\vartheta_t = (1/\delta)(\partial \psi_t/\partial t) + \psi_t$, and substituting (28) into it yields

$$\vartheta_t = f(0,t) + \frac{1}{\delta}\frac{\partial f(0,t)}{\partial t} + \frac{\eta^2}{2\delta^2}\left(1-e^{-2\delta t}\right). \tag{29}$$

Setting $f(0,T) = f^M(0,T)$, where $f^M(0,T)$ is the market instantaneous forward rates, the superscript M represents that the value is calculated according to a set yield curve [37]. □

Lemma 1. *If the dynamics of $\widetilde{r}_t$ is governed by the stochastic process (21), we can have the following equation:*

$$\int_t^T \widetilde{r} \mathrm{d}u = \frac{1-e^{-\delta(T-t)}}{\delta}\widetilde{r} + \frac{\eta}{\delta}\int_t^T \left(1-e^{-\delta(T-u)}\right)\mathrm{d}W_u^r. \tag{30}$$

Proof. The proof of Lemma 1 is in Appendix A. □

Theorem 2. *Since r_T is a normally distributed conditional on $\mathcal{F}_t$, $t \le T$, the integrated interest rate process $R_{t,T} = \int_t^T r_u du$ is normally distributed with*

$$\mathbb{E}^{\mathbb{Q}}\left(R_{t,T} \mid \mathcal{F}_t\right) = \mu_R = D(t,T)\left(r_t - \psi_t\right) + \ln \frac{P^M(0,t)}{P^M(0,T)} + (C(0,T) - C(0,t)), \tag{31}$$

$$\mathrm{Var}^{\mathbb{Q}}\left(R_{t,T} \mid \mathcal{F}_t\right) = \sigma_R^2 = 2C(t,T). \tag{32}$$

Proof. The Hull–White decomposition leads to

$$R_{t,T} = \int_t^T \widetilde{r} \mathrm{d}u + \int_t^T \psi_u \mathrm{d}u. \tag{33}$$

We can obtain the formula for the first integral part in (33) by using Lemma 1, and we only need to derive the formula for the second integral part to obtain mean μ_R and variance σ_R^2.

According to (27), we can express $P^M(0,T)$ as

$$P^M(0,T) = e^{-\int_0^T \psi_u \mathrm{d}u + C(0,T)}. \tag{34}$$

Therefore, we can obtain that

$$e^{-\int_t^T \psi_u \mathrm{d}u} = \frac{P^M(0,T)e^{-C(0,T)}}{P^M(0,t)e^{-C(0,t)}}, \tag{35}$$

which leads to

$$\int_t^T \psi_u \mathrm{d}u = \ln \frac{P^M(0,t)}{P^M(0,T)} + (C(0,T) - C(0,t)). \tag{36}$$

Therefore, we can obtain that

$$R_{t,T} = \int_t^T \widetilde{r}\mathrm{d}u + \int_t^T \psi_u \mathrm{d}u = \frac{\left(1-e^{-\delta(T-t)}\right)}{\delta}\widetilde{r}_t + \frac{\eta}{\delta}\int_t^T \left(1-e^{-\delta(T-u)}\right)\mathrm{d}W_u^r + \ln\frac{P^M(0,t)}{P^M(0,T)} + (C(0,T)-C(0,t)). \tag{37}$$

We can get equations (31) and (32) by simple calculation. The proof is complete. □

Theorem 3. *If the dynamics of the interest rate r_t is expressed as the stochastic process in system (1), the pricing formula for a zero-coupon bond $P(t,T) = \mathbb{E}^{\mathbb{Q}}(e^{-\int_t^T r_u du} \mid \mathcal{F}_t)$ takes the form*

$$P(t,T) = e^{\widetilde{C}(t,T) - D(t,T)r}, \tag{38}$$

where

$$\widetilde{C}(t,T) = D(t,T) f^M(0,t) + \ln\frac{P^M(0,T)}{P^M(0,t)} - \frac{\eta^2}{4\delta}\left(1-e^{-2\delta t}\right)D^2(t,T), \quad r = r_t. \tag{39}$$

Proof. Theorem 2 can lead us to the following equation:

$$P(t,T) = e^{C(t,T) - D(t,T)(r-\psi) + \ln P^M(0,T)/P^M(0,t) - (C(0,T)-C(0,t))}, \tag{40}$$

where $\psi = \psi_t$. We can obtain (38) by rearranging the above equation. The proof is complete. □

Theorem 4. *If the asset price is governed by the dynamic system (1), the discounted characteristic function $\varphi(u; X, V_1, V_2, r, \lambda, \tau)$ takes the following form:*

$$\varphi(u; X, V_1, V_2, r, \lambda, \tau) = e^{\widetilde{C}_A(u,\tau) + D_X(u,\tau)X + D_{V_1}(u,\tau)V_1 + D_{V_2}(u,\tau)V_2 + D_r(u,\tau)(r-\psi) + D_\lambda(u,\tau)\lambda}, \tag{41}$$

where

$$\begin{aligned}
\widetilde{C}_A(u,\tau) &= C_A(u,\tau) + \Lambda(u,t,T), \\
C_A(u,\tau) &= \sum_{j=1}^{2}\frac{2\kappa_j\theta_j}{\sigma_j^2}\left(\frac{\left(\kappa_j - iu\rho_j\sigma_j - \zeta_j\right)\tau}{2} + \ln\frac{2\zeta_j}{2\zeta_j + \left(\kappa_j - iu\rho_j\sigma_j - \zeta_j\right)\left(1-e^{-\zeta_j\tau}\right)}\right) \\
&\quad + \frac{2\kappa_\lambda\theta_\lambda}{\sigma_\lambda^3}\left(\frac{(\kappa_\lambda - \zeta_\lambda)\tau}{2} + \ln\left(\frac{2\zeta_\lambda}{2\zeta_\lambda + (\kappa_\lambda - \zeta_\lambda)(1-e^{-\zeta_\lambda\tau})}\right)\right) + (iu-1)^2 C(t,T), \\
\Lambda(u,t,T) &= (iu-1)\left(\ln\frac{P^M(0,t)}{P^M(0,T)} + (C(0,T)-C(0,t))\right), \\
D_X(u,\tau) &= iu, \\
D_{V_j}(u,\tau) &= \left((iu)^2 - iu\right)\frac{1-e^{-\zeta_j\tau}}{2\zeta_j + \left(\kappa_j - iu\rho_j\sigma_j - \zeta_j\right)\left(1-e^{-\zeta_j\tau}\right)}, \\
D_r(u,\tau) &= \frac{(iu-1)}{\delta}\left(1-e^{-\delta(T-t)}\right), \\
D_\lambda(u,\tau) &= 2\Pi(u)\frac{1-e^{-\zeta_\lambda\tau}}{2\zeta_\lambda + (\kappa_\lambda - \zeta_\lambda)(1-e^{-\zeta_\lambda\tau})}, \\
\zeta_j &= \sqrt{\left(\kappa_j - iu\rho_j\sigma_j\right)^2 - \sigma_j^2\left((iu)^2 - iu\right)}, \\
\zeta_\lambda &= \sqrt{\kappa_\lambda^2 - 2\sigma_\lambda^2\Pi(u)}, \\
M(u) &= \frac{p\eta_1}{\eta_1 - iu} + \frac{q\eta_2}{\eta_2 + iu} - 1, \\
\Pi(u) &= M(u) - iu\mu_J.
\end{aligned} \tag{42}$$

Proof. Although our model is in the class of the AJD process, we still need to separate X_t into two parts and use the Hull–White decomposition before using the results given by Duffie et al. [36]. According to Grzelak et al. [21], we define $X_t: = \widetilde{X}_t + \Psi_t$, with $\Psi_t = \int_0^t \psi_s ds$, and then we can obtain the following system by using the Hull–White decomposition $r_t = \widetilde{r}_t + \psi_t$:

$$\begin{cases} d\widetilde{X}_t = \left(\widetilde{r}_t - \lambda_t \mu_J - \frac{1}{2}(V_{1t} + V_{2t})\right)dt \\ \quad + \sqrt{V_{1t}}\, dW_{1t}^S + \sqrt{V_{2t}}\, dW_{2t}^S + Y dN_t, \\ dV_{1t} = \kappa_1(\theta_1 - V_{1t})dt + \sigma_1\sqrt{V_{1t}}\, dW_{1t}^V, \\ dV_{2t} = \kappa_2(\theta_2 - V_{2t})dt + \sigma_2\sqrt{V_t}\, dW_{2t}^V, \\ d\widetilde{r}_t = -\delta\widetilde{r}_t dt + \eta dW_t^r, \\ d\lambda_t = \kappa_\lambda(\theta_\lambda - \lambda_t)dt + \sigma_\lambda\sqrt{\lambda_t}\, dW_t^\lambda. \end{cases} \tag{43}$$

Then, we use the results given by Duffie et al. [36] to derive the discounted characteristic function.

We define

$$\widetilde{\varphi}(u; \widetilde{X}, V_1, V_2, \widetilde{r}, \lambda, \tau) := \mathbb{E}^{\mathbb{Q}}\left(e^{-\int_t^T \widetilde{r}_s ds + iu\widetilde{X}_T} \middle| \mathcal{F}_t\right), \tag{44}$$

where$\widetilde{\varphi}(u; \widetilde{X}, V_1, V_2, \widetilde{r}, \lambda, \tau)$ is the discounted characteristic function of $\widetilde{X}_t$ in system (43) under the risk-neutral measure $\mathbb{Q}$.

$\widetilde{\varphi}(u; \widetilde{X}, V_1, V_2, \widetilde{r}, \lambda, \tau)$ satisfies a PIDE by applying the Feynman–Kac theorem [36]:

$$\begin{aligned} &-\frac{\partial\widetilde{\varphi}}{\partial\tau} + \left(\widetilde{r} - \lambda\mu_J - \frac{1}{2}(V_1 + V_2)\right)\frac{\partial\widetilde{\varphi}}{\partial\widetilde{X}} + \frac{1}{2}(V_1 + V_2)\frac{\partial^2\widetilde{\varphi}}{\partial\widetilde{X}^2} \\ &+ \sum_{j=1}^{2}\left(\rho_j\sigma_j V_j\frac{\partial^2\widetilde{\varphi}}{\partial\widetilde{X}\partial V_j} + \kappa_j\left(\theta_j - V_j\right)\frac{\partial\widetilde{\varphi}}{\partial V_j} + \frac{1}{2}\sigma_j^2 V_j\frac{\partial^2\widetilde{\varphi}}{\partial V_j^2}\right) \\ &- \delta\widetilde{r}\frac{\partial\widetilde{\varphi}}{\partial\widetilde{r}} + \frac{1}{2}\eta^2\frac{\partial^2\widetilde{\varphi}}{\partial\widetilde{r}^2} + \kappa_\lambda(\theta_\lambda - \lambda)\frac{\partial\widetilde{\varphi}}{\partial\lambda} + \frac{1}{2}\sigma_\lambda^2\lambda\frac{\partial^2\widetilde{\varphi}}{\partial\lambda^2} \\ &+ \lambda\int_{-\infty}^{\infty}(\widetilde{\varphi}(\widetilde{X} + Y) - \widetilde{\varphi}(\widetilde{X}))f(Y)dY - \widetilde{r}\widetilde{\varphi} = 0. \end{aligned} \tag{45}$$

We conjecture $\widetilde{\varphi}(u; \widetilde{X}, V_1, V_2, \widetilde{r}, \lambda, \tau)$ has the following form:

$$\begin{aligned} &\widetilde{\varphi}(u; \widetilde{X}, V_1, V_2, \widetilde{r}, \lambda, \tau) \\ &\quad = e^{C_A(u,\tau) + D_X(u,\tau)\widetilde{X} + D_{V_1}(u,\tau)V_1 + D_{V_2}(u,\tau)V_2 + D_r(u,\tau)\widetilde{r} + D_\lambda(u,\tau)\lambda}, \end{aligned} \tag{46}$$

with boundary conditions $C_A(u,0) = 0$, $D_X(u,0) = iu$, $D_{V_j}(u,0) = 0$, $D_r(u,0) = 0$ and $D_\lambda(u,0) = 0$.

We simplify the integral term in (45) as

$$\lambda\int_{-\infty}^{\infty}(\widetilde{\varphi}(\widetilde{X} + Y) - \widetilde{\varphi}(\widetilde{X}))f(Y)dY = \lambda\widetilde{\varphi}(u)M(u), \tag{47}$$

where $M(u) = (p\eta_1/\eta_1 - iu) + (q\eta_2/\eta_2 + iu) - 1$.

We can get a system of six ordinary differential equations by rearranging (45) in terms of (46) and (47):

$$\begin{cases} \frac{dC_A}{d\tau} = \kappa_1\theta_1 D_{V_1} + \kappa_2\theta_2 D_{V_2} + \frac{1}{2}\eta^2 D_r^2 + \kappa_\lambda\theta_\lambda D_\lambda, \\ \frac{dD_X}{d\tau} = 0, \\ \frac{dD_{V_1}}{d\tau} = \frac{1}{2}\sigma_1^2 D_{V_1}^2 + (\rho_1\sigma_1 D_X - \kappa_1)D_{V_1} + \frac{1}{2}\left(D_X^2 - D_X\right), \\ \frac{dD_{V_2}}{d\tau} = \frac{1}{2}\sigma_2^2 D_{V_2}^2 + (\rho_2\sigma_2 D_X - \kappa_2)D_{V_2} + \frac{1}{2}\left(D_X^2 - D_X\right), \\ \frac{dD_r}{d\tau} = -\delta D_r + (D_X - 1), \\ \frac{dD_\lambda}{d\tau} = \frac{1}{2}\sigma_\lambda^2 D_\lambda^2 - \kappa_\lambda D_\lambda + M(u) - \mu_J D_X. \end{cases} \tag{48}$$

We can obtain the formulae for $C_A(u,\tau)$, $D_X(u,\tau)$, $D_{V_j}(u,\tau)$, $D_r(u,\tau)$, and $D_\lambda(u,\tau)$ by solving the above ordinary differential equations, and thus we can obtain the formula for $\widetilde{\varphi}(u; \widetilde{X}, V_1, V_2, \widetilde{r}, \lambda, \tau)$.

The discounted characteristic function $\varphi(u; X, V_1, V_2, r, \lambda, \tau)$ can be expressed as the following form:

$$\begin{aligned} \varphi(u; X, V_1, V_2, r, \lambda, \tau) &= \mathbb{E}^{\mathbb{Q}}\left(e^{-\int_t^T r_s ds + iuX_T} \middle| \mathcal{F}_t\right) \\ &= e^{-\int_t^T \psi_s ds + iu\Psi_T}\mathbb{E}^{\mathbb{Q}}\left(e^{-\int_t^T \widetilde{r}_s ds + iu\widetilde{X}_T} \middle| \mathcal{F}_t\right) \\ &= e^{-\int_t^T \psi_s ds + iu\Psi_T} \cdot \widetilde{\varphi}(u; \widetilde{X}, V_1, V_2, \widetilde{r}, \lambda, \tau). \end{aligned} \tag{49}$$

According to (36), we can obtain that

$$e^{(iu-1)\int_t^T \psi_s ds} = \exp\left((iu-1)\left(\ln\frac{P^M(0,t)}{P^M(0,T)} + (C(0,T) - C(0,t))\right)\right). \tag{50}$$

Hence, we can obtain the formula for $\varphi(u; X, V_1, V_2, r, \lambda, \tau)$:

$$\begin{aligned} &\varphi(u; X, V_1, V_2, \widetilde{r}, \lambda, \tau) \\ &\quad = e^{\widetilde{C}_A(u,\tau) + D_X(u,\tau)X + D_{V_1}(u,\tau)V_1 + D_{V_2}(u,\tau)V_2 + D_r(u,\tau)(r-\psi) + D_\lambda(u,\tau)\lambda}. \end{aligned} \tag{51}$$

The proof is complete. □

4. Numerical Discussion

The approximated pricing formula for the call options using the COS method is derived in this section. We use it to do some numerical analyses to compare the computation speed, the accuracy, the efficiency, and the stability between FFT and the COS method. We also investigate the impact of the parameters in the jump intensity process and the interest rate process and the existence of the jump intensity process on the call option prices.

Theorem 5. *The pricing formula for the call options with the COS method $V(t,x)$ at time $t \in [0,T]$ is approximated on a bounded interval $[a,b]$:*

$$V(t,x) \approx P(t,T) \sum_{k=0}^{N-1}{}' R\left\{\phi\left(\frac{k\pi}{b-a}; x\right) e^{-ik\pi(a/b-a)}\right\} W_k, \quad (52)$$

where the apostrophe on the right side of the summation symbol means that the first item is weighted by 1/2, $R(\cdot)$ is the real part, $x = ln(S/K)$, and $\phi(u;x)$ is the characteristic function of x, and it satisfies the following equation [35, 38]: $\phi(u;x) = \varphi_T(u; x, V_1, V_2, r, \lambda, \tau)$, a and b are specific constants that satisfy a<b, and W_k are the cosine series coefficients of the call option payoff.

Proof. The pricing formula under the T forward measure $\mathbb{Q}^T$ is given by

$$\begin{aligned} V(t,x) &= P(t,T)\mathbb{E}^{\mathbb{Q}^T}\left(V(T,y)|\mathcal{F}_t\right) \\ &= P(t,T)\int_{-\infty}^{\infty} V(T,y) f(y|x)\mathrm{d}y, \end{aligned} \quad (53)$$

where $f(y|x)$ is the density function of y given x with respect to $\mathbb{Q}^T$, $y = \ln(S_T/K)$, and $V(T,y)$ is the call option payoff.

According to Fang and Oosterlee [35], $f(y \mid x)$ decays fast to zero as $y \longrightarrow \pm\infty$, so we can truncate the integration to make the difference between the true value and approximation negligible by choosing a specific interval $[a,b]$, thus its approximation can be given by

$$V(t,x) \approx P(t,T)\int_a^b V(T,y) f(y \mid x)\mathrm{d}y. \quad (54)$$

Since $f(y \mid x)$ decays fast, we can approximate the characteristic function $\phi(u;x)$ on the interval $[a,b]$:

$$\phi(u;x) \approx \int_a^b e^{iuy} f(y \mid x)\mathrm{d}y. \quad (55)$$

To find an analytical approximation formula for $f(y \mid x)$, we can express it with the following Fourier cosine series expansion:

$$\begin{aligned} f(y \mid x) &= \sum_{k=0}^{\infty}{}' A_k \cos\left(k\pi\frac{y-a}{b-a}\right), \\ \text{with } A_k &= \frac{2}{b-a}\int_a^b f(y \mid x)\cos\left(k\pi\frac{y-a}{b-a}\right)\mathrm{d}y, \end{aligned} \quad (56)$$

then A_k can be given by

$$\begin{aligned} A_k &= \frac{2}{b-a}\int_a^b f(y \mid x) R\left(e^{ik\pi(y-a/b-a)}\right)\mathrm{d}y \\ &\approx \frac{2}{b-a} R\left(\phi\left(\frac{k\pi}{b-a}; x\right)e^{-ik\pi(a/b-a)}\right), \end{aligned} \quad (57)$$

thus the approximated pricing formula can be rewritten by

$$V(t,x) \approx P(t,T)\sum_{k=0}^{\infty}{}' R\left(\phi\left(\frac{k\pi}{b-a}; x\right)e^{-ik\pi(a/b-a)}\right) W_k, \quad (58)$$

where the cosine coefficient W_k is given by

$$W_k = \frac{2}{b-a}\int_a^b V(T,y)\cos\left(k\pi\frac{y-a}{b-a}\right)\mathrm{d}y. \quad (59)$$

Since the coefficients decay fast, the summation can be truncated to obtain that

$$V(t,x) \approx P(t,T)\sum_{k=0}^{N-1}{}' R\left(\phi\left(\frac{k\pi}{b-a}; x\right)e^{-ik\pi(a/b-a)}\right) W_k. \quad (60)$$

The call option payoff is given by

$$V(T,y) = \max(S_T - K, 0) = \max(K(e^y - 1), 0), \quad (61)$$

then W_k can be rewritten by

$$\begin{aligned} W_k &= \frac{2}{b-a}\int_a^b V(T,y)\cos\left(k\pi\frac{y-a}{b-a}\right)\mathrm{d}y \\ &= \frac{2}{b-a}K\left(\int_0^b e^y\cos\left(k\pi\frac{y-a}{b-a}\right)\mathrm{d}y - \int_0^b \cos\left(k\pi\frac{y-a}{b-a}\right)\mathrm{d}y\right). \end{aligned} \quad (62)$$

Using the basic integration rules straightforward, we can obtain that

$$W_k = \frac{2}{b-a}K\left(\chi_k(0,b) - \psi_k(0,b)\right), \quad (63)$$

where

$$\begin{aligned} \chi_k(0,b) &= \int_0^b e^y\cos\left(k\pi\frac{y-a}{b-a}\right)\mathrm{d}y \\ &= \frac{1}{1+(k\pi/b-a)^2}\left\{\cos(k\pi)e^b - \cos\left(-\frac{ak\pi}{b-a}\right)\right. \\ &\quad \left. + \frac{k\pi}{b-a}\left[\sin(k\pi)e^b - \sin\left(-\frac{ak\pi}{b-a}\right)\right]\right\}, \\ \psi_k(0,b) &= \int_0^b 1\cdot\cos\left(k\pi\frac{y-a}{b-a}\right)\mathrm{d}y \\ &= \begin{cases} \dfrac{b-a}{k\pi}\left[\sin(k\pi) - \sin\left(-\dfrac{ak\pi}{b-a}\right)\right], & k > 0, \\ b, k = 0. \end{cases} \end{aligned} \quad (64)$$

The proof is complete. □

To make the difference between the true value and approximation negligible, we need to determine the interval $[a, b]$ appropriately, and the range of interval $[a, b]$ is determined by [35]

$$[a, b] = \left[c_1 - L\sqrt{|c_2| + \sqrt{|c_4|}}, c_1 + L\sqrt{|c_2| + \sqrt{|c_4|}} \right], \quad (65)$$

where $c_n (n = 1, \ldots, 4)$ are the n-th cumulant of $\ln(S_T/K)$ and L is the truncation parameter. c_n can be given by

$$c_n = \left. \frac{\partial^n (\ln(\phi(u)))}{\partial u^n} \right|_{u=0}. \quad (66)$$

Since we cannot obtain the cumulants directly under the condition that the interest rate follows the Hull–White process, we use some specific and suitable range for approximation according to Grzelak et al. [21]:

$$[a, b] = [0 - L\sqrt{\tau}, 0 + L\sqrt{\tau}]. \quad (67)$$

We use the formulae derived above and set the values of the parameters to do some numerical analyses. The parameters are given in Table 1.

Table 2 shows the numerical results. We use the integration approach to calculate the semi-closed form prices obtained by (14), and it takes a large amount of time for calculation. The COS method and FFT are much faster than the integration approach which means that the two approaches make big improvement in computation speed. The numerical results demonstrate that the price differences between the COS method and semi-closed form prices are negligible compared to the price differences between FFT and semi-closed form prices which means that the COS method shows higher accuracy than FFT.

We compare the error convergence between the COS method and FFT with different grid points. We set the semi-closed form price as the benchmark, the values of the grid points with $N = 2^n (6, \ldots 10)$, the strike price $K = 80, 100$, and 120, $T = 1$, and Table 3 shows the result. The differences between the semi-closed form price and the prices computed by applying the COS method are negligible, and the COS method converges much faster than FFT which means that the COS method shows higher efficiency than FFT.

We examine the relative differences of the call option prices with different grid points to compare the COS method and FFT in terms of the stability. We set the value of grid points $N = 2^n (n = 15)$ as the benchmark, grid points with $N = 2^n (6, \ldots 10)$, the strike prices $K = 80, 100$, and 120, $T = 1$, and Table 4 shows the result. The relative differences computed using the COS method are lower than those computed using FFT for all the chosen values of grid points, respectively. It demonstrates that the COS method is more stable than FFT which means that the COS method shows higher stability than FFT.

Since the COS method is more accurate, efficient, and stable than FFT to approximate the option prices, we use it for approximation to investigate the impact of the parameters in the jump intensity process and the interest rate process and the existence of the jump intensity process on the call option prices.

Table 1: Values of parameters.

Parameter	Value	Parameter	Value
T	1	S	100
κ_1	1.5	κ_2	0.9
θ_1	0.08	θ_2	0.1
σ_1	0.15	σ_2	0.12
V_1	0.06	V_2	0.1
ρ_1	−0.5	ρ_2	−0.3
κ_λ	3	ρ_λ	0.5
θ_λ	0.3	λ	0.6
δ	0.1	r	0.04
η	0.02	p	0.5
η_1	5	ρ_2	5
N	1024	L	10

Table 2: Comparisons of European call option prices by applying the COS method and FFT.

Strike	Semi-closed form price	COS price	FFT price
80	29.1910	29.1910	29.2104
85	26.1354	26.1354	26.1695
90	23.3359	23.3359	23.3876
95	20.7865	20.7865	20.8192
100	18.4776	18.4776	18.566
105	16.3968	16.3968	16.4227
110	14.5297	14.5297	14.6222
115	12.8608	12.8608	12.9601
120	11.3742	11.3742	11.3798
Computation time (s)	1575.7674	0.0248	0.0175

Figure 1 illustrates that the change of the mean-reversion rate κ_λ has little impact on call option prices, and the change of the mean-reversion level θ_λ has important impact on call option prices. As θ_λ increases, call option price also increases, and the change of the call option price is an increasing function of θ_λ. The reason that this phenomenon happens is possibly when the mean level of the jump intensity is high and the cost of investing stocks becomes higher; therefore, the investors tend to buy call options to lower the cost of their investment which makes the call option price become higher.

We investigate the impact of the existence of the jump intensity process on the call option prices, and Figure 2 shows the result. It illustrates that the call option prices with stochastic jump intensity are higher than the call option prices with constant jump intensity. The reason that this phenomenon happens is possibly when the jump intensity changes over time, and there is a great opportunity that the cost of investing stocks becomes higher; therefore, the investors tend to buy call options to lower the cost of their investment which makes the call option price become higher.

We investigate the impact of the parameters in the interest rate process on the call option prices, and Figure 3 shows the result. It illustrates that the change of the mean-reversion rate δ has little impact on call option prices and the

Table 3: Comparisons of error convergence between the COS method and FFT.

K	n	6	7	8	9	10
80	COS	−0.2799	$-1.2E-09$	$-7.3E-10$	$-7.3E-10$	$-7.3E-10$
	FFT	−10.1215	−2.2598	0.0265	−0.0249	−0.0194
100	COS	0.5234	$6.91E-10$	$-2.4E-10$	$-2.4E-10$	$-2.4E-10$
	FFT	−14.9982	−2.9451	−1.4132	−0.2262	−0.0883
120	COS	−0.1211	$-4.1E-10$	$3.31E-10$	$3.31E-10$	$3.31E-10$
	FFT	−17.3328	−1.8551	−1.2309	−0.4625	−0.0056

Table 4: Relative differences of the call option prices computed by applying the COS method and FFT.

K	n	6	7	8	9	10
80	COS	−0.2799	$-4.5E-10$	0	0	0
	FFT	−10.1215	−2.2598	0.0266	−0.0248	−0.0194
100	COS	0.5234	$9.31E-10$	0	0	0
	FFT	−14.9982	−2.9451	−1.4132	−0.2261	−0.0883
120	COS	−0.1211	$-7.4E-10$	0	0	0
	FFT	−17.3327	−1.8550	−1.2308	−0.4624	−0.0055

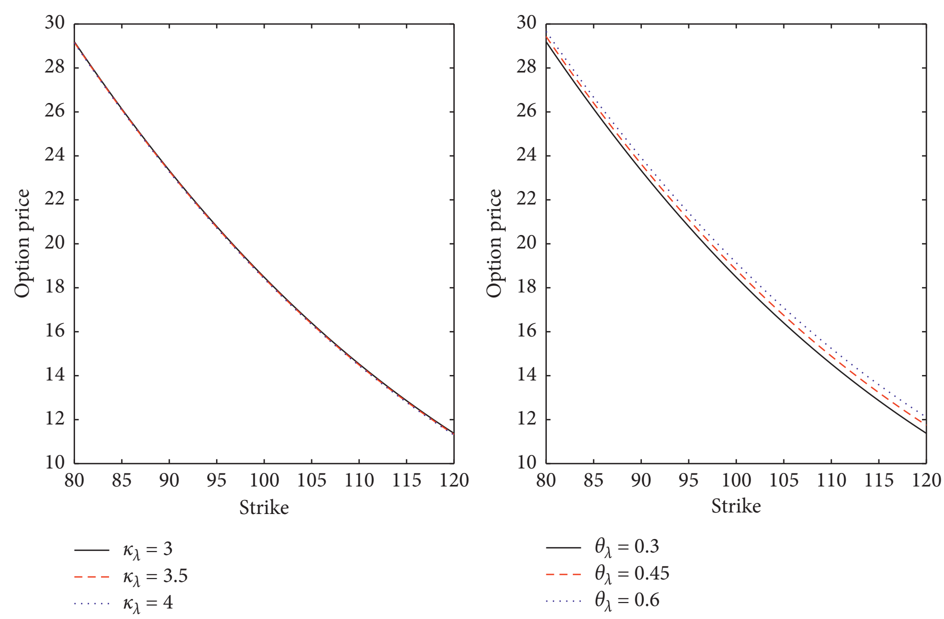

Figure 1: The impact of κ_λ and θ_λ on call option prices for $T = 1$.

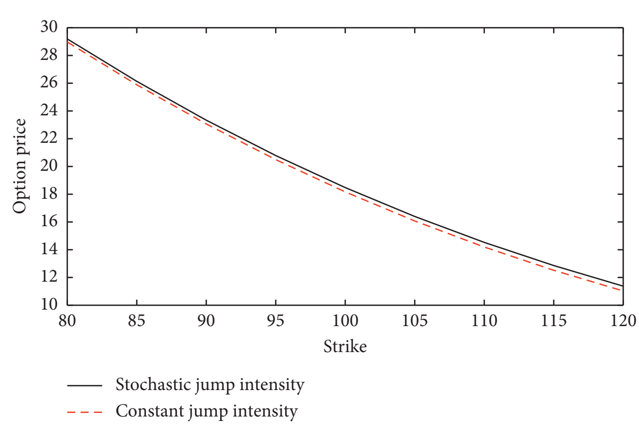

Figure 2: The impact of the existence of the jump intensity process on call option prices for $T = 1$.

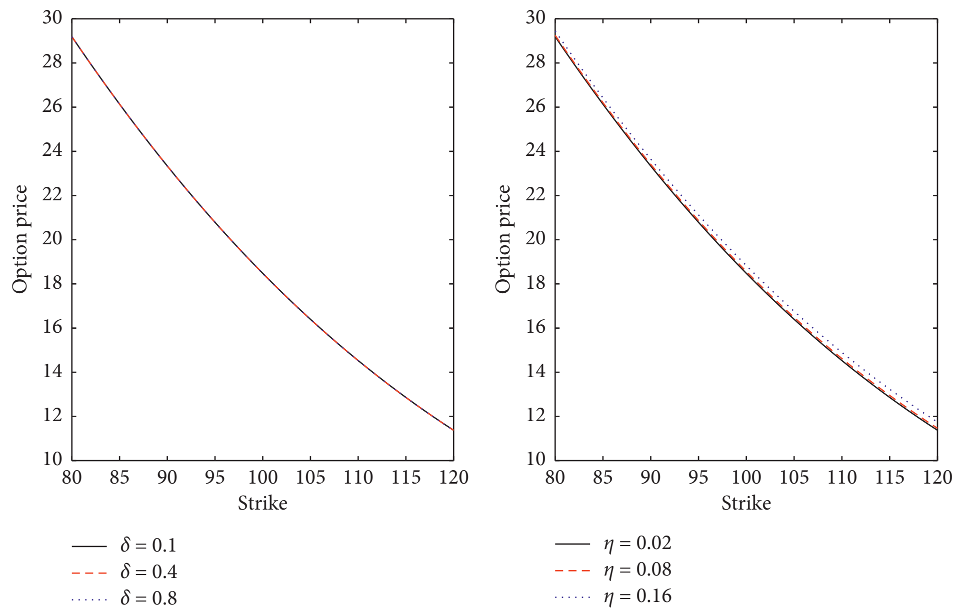

Figure 3: The impact of δ and η on call option prices for $T = 1$.

change of the volatility η has important impact on call option prices. As η increases, call option price also increases, and the change of call option price is an increasing function of η. The possible reason that this phenomenon happens is that greater volatility of the interest rate means a greater opportunity of the increase of it. The interest rate is the opportunity cost of the investment in stocks, options, and other financial products. When the interest rates increase, the cost of investing stocks becomes higher; therefore, the investors tend to buy call options to lower the cost of their investment which makes the call option price become higher. The investors can obtain the same profits by investing in the call options instead of investing in the stocks.

5. Conclusion

We addressed European option pricing under a double stochastic volatility model with stochastic interest rates and double exponential jumps with stochastic intensity in this article.

In theoretical part, we used Radon–Nikodym derivatives to derive the semi-closed form valuation formula with the expression of the discounted characteristic function which means we only need to derive the formula for the discounted characteristic function for obtaining the semi-closed form valuation formula. We used the results given by Duffie et al. [36] to derive the discounted characteristic function.

In the numerical analysis part, we derived the approximated pricing formula by applying the COS method and FFT and compared the calculation speed, the accuracy, the efficiency, and the stability between the COS method and FFT. The numerical results demonstrate that it takes a large amount of time to calculate the semi-closed form prices using the integration approach. Both the COS method and FFT takes less time, and they improve in computation speed. The price differences between the COS method and semi-closed form prices are negligible compared to the price differences between FFT and semi-closed form prices which means that the COS method shows higher accuracy than FFT. We compare the COS method and FFT in terms of the convergence, and it demonstrates that the COS method shows higher efficiency than FFT. We examined the relative differences of call option prices with different grid points to compare the COS method and FFT in terms of the stability. The result demonstrates that the COS method shows higher stability than FFT. Because of the higher accuracy, efficiency, and stability of the COS method, we use it to investigate the impact of the parameters in the jump intensity process on call option prices. The numerical results illustrate that the change of the mean-reversion rate has little impact on call option prices and the change of the mean-reversion level has important impact on call option prices. We examine the impact of the existence of the jump intensity on the call option prices with the COS method, and it illustrates that the call option prices with stochastic jump intensity are higher than the call option prices with constant jump intensity. We also investigate the impact of the parameters in the interest rate process on the call option prices with the COS method. It illustrates that the change of the mean-reversion rate has little impact on call option prices, and the change of the volatility has important impact on call option prices.

Appendix

A. Proof of Lemma 1

In this appendix, we derive Lemma 1, using the method initially presented by Brigo and Mercurio [39].

We can get the following equation by applying stochastic integration by parts:

$$\int_t^T \tilde{r}_u \mathrm{d}u = \int_t^T (T-u)\mathrm{d}\tilde{r}_u + (T-t)\tilde{r}_t. \tag{A.1}$$

According to (21), the integral in the right-hand side of (A.1) can be rewritten as

$$\int_t^T (T-u)d\tilde{r}_u = -\delta \int_t^T (T-u)\tilde{r}_u \mathrm{d}u + \eta \int_t^T (T-u)\mathrm{d}W_u^r. \tag{A.2}$$

According to (20) and (21), we have

$$\tilde{r}_u = \tilde{r}_t e^{-\delta(u-t)} + \eta \int_t^u e^{-\delta(u-s)}\mathrm{d}W_s^r. \tag{A.3}$$

Therefore, the first part in the right-hand side of (A.2) can be expressed as

$$\begin{aligned} -\delta \int_t^T (T-u)\tilde{r}_u \mathrm{d}u &= -\delta\tilde{r}_t \int_t^T (T-u)e^{-\delta(u-t)}\mathrm{d}u \\ &\quad - \delta\eta \int_t^T (T-u)\int_t^u e^{-\delta(u-s)}\mathrm{d}W_s^r \mathrm{d}u. \end{aligned} \tag{A.4}$$

The first part in the right-hand side of (A.4) can be expressed by the following equation using simple calculation:

$$-\delta\tilde{r}_t \int_t^T (T-u)e^{-\delta(u-t)}\mathrm{d}u = -(T-t)\tilde{r}_t + \frac{1-e^{-\delta(T-t)}}{\delta}\tilde{r}_t. \tag{A.5}$$

The second part in the right-hand side of (A.4) can be expressed by the following equation:

$$\begin{aligned} &- \delta\eta \int_t^T (T-u)\int_t^u e^{-\delta(u-s)}\mathrm{d}W_s^r \mathrm{d}u \\ &= -\delta\eta \int_t^T \left(\int_t^u e^{\delta s}\mathrm{d}W_s^r\right)\mathrm{d}_u\left(\int_t^u (T-v)e^{-\delta v}\mathrm{d}v\right) \\ &= -\delta\eta\left[\left(\int_t^T e^{\delta u}\mathrm{d}W_u^r\right)\left(\int_t^T (T-v)e^{-\delta v}\mathrm{d}v\right)\right. \\ &\quad \left. - \int_t^T \left(\int_t^u (T-v)e^{-\delta v}\mathrm{d}v\right)e^{\delta u}\mathrm{d}W_u^r\right] \\ &= -\delta\eta \int_t^T \left(\int_u^T (T-v)e^{-\delta v}\mathrm{d}v\right)e^{\delta u}\mathrm{d}W_u^r \\ &= -\eta \int_t^T \left((T-u) + \frac{e^{-\delta(T-u)}-1}{\delta}\right)\mathrm{d}W_u^r. \end{aligned} \tag{A.6}$$

Therefore, we can obtain that

$$\begin{aligned} \int_t^T (T-u)\mathrm{d}\tilde{r}_u &= -(T-t)\tilde{r}_t + \frac{\left(1-e^{-\delta(T-t)}\right)}{\delta}\tilde{r}_t \\ &\quad + \frac{\eta}{\delta}\int_t^T \left(1-e^{-\delta(T-u)}\right)\mathrm{d}W_u^r. \end{aligned} \tag{A.7}$$

Substituting (A.7) into (A.1), we can obtain (30); therefore, the proof is complete.

Data Availability

The data used to support the findings of this study are available from the corresponding author upon request.

Conflicts of Interest

The authors declare that they have no conflicts of interest.

References

[1] F. Black and M. Scholes, "The pricing of options and corporate liabilities," *Journal of Political Economy*, vol. 81, no. 3, pp. 637–654, 1973.

[2] J. Hull and A. White, "The pricing of options on assets with stochastic volatilities," *The Journal of Finance*, vol. 42, no. 2, pp. 281–300, 1987.

[3] L. O. Scott, "Option pricing when the variance changes randomly: theory, estimation, and an application," *The Journal of Financial and Quantitative Analysis*, vol. 22, no. 4, pp. 419–438, 1987.

[4] J. B. Wiggins, "Option values under stochastic volatility: theory and empirical estimates," *Journal of Financial Economics*, vol. 19, no. 2, pp. 351–372, 1987.

[5] E. M. Stein and J. C. Stein, "Stock price distributions with stochastic volatility: an analytic approach," *Review of Financial Studies*, vol. 4, no. 4, pp. 727–752, 1991.

[6] S. L. Heston, "A closed-form solution for options with stochastic volatility with applications to bond and currency options," *Review of Financial Studies*, vol. 6, no. 2, pp. 327–343, 1993.

[7] R. Schöbel and J. Zhu, "Stochastic volatility with an Ornstein-Uhlenbeck process: an extension," *Review of Finance*, vol. 3, no. 1, pp. 23–46, 1999.

[8] A. Lewis, *Option Valuation under Stochastic Volatility*, Finance Press, Los Altos, CA, USA, 2000.

[9] M. Grasselli, "The 4/2 stochastic volatility model: a unified approach for the Heston and the 3/2 model," *Mathematical Finance*, vol. 27, no. 4, pp. 1013–1034, 2017.

[10] P. Christoffersen, S. Heston, and K. Jacobs, "The shape and term structure of the index option smirk: why multifactor stochastic volatility models work so well," *Management Science*, vol. 55, no. 12, pp. 1914–1932, 2009.

[11] O. Vasicek, "An equilibrium characterization of the term structure," *Journal of Financial Economics*, vol. 5, no. 2, pp. 177–188, 1977.

[12] J. C. Cox, J. E. Ingersoll, and S. A. Ross, "A theory of the term structure of interest rates," *Econometrica*, vol. 53, no. 2, pp. 385–407, 1985.

[13] F. A. Longstaff, "A nonlinear general equilibrium model of the term structure of interest rates," *Journal of Financial Economics*, vol. 23, no. 2, pp. 195–224, 1989.

[14] J. W. Zhu, *Applications of Fourier Transform to Smile Modeling—Theroy and Implementation*, Springer, Berlin, Heidelberg, 2010.

[15] J. Hull and A. White, "Pricing interest-rate-derivative securities," *Review of Financial Studies*, vol. 3, no. 4, pp. 573–592, 1990.

[16] J. Hull and A. White, "One-factor interest-rate models and the valuation of interest-rate derivative securities," *The Journal of Financial and Quantitative Analysis*, vol. 28, no. 2, pp. 235–254, 1993.

[17] J. C. Hull and A. D. White, "Using Hull-White interest rate trees," *The Journal of Derivatives*, vol. 3, no. 3, pp. 26–36, 1996.

[18] K. Rindell, "Pricing of index options when interest rates are stochastic: an empirical test," *Journal of Banking & Finance*, vol. 19, no. 5, pp. 785–802, 1995.

[19] M. Abudy and Y. Izhakian, "Pricing stock options with stochastic interest rate," *SSRN Electronic Journal*, vol. 1, no. 3, 2011.

[20] L. A. Grzelak and C. W. Oosterlee, "On the Heston model with stochastic interest rates," *SIAM Journal on Financial Mathematics*, vol. 2, no. 1, pp. 255–286, 2011.

[21] L. A. Grzelak, C. W. Oosterlee, and S. Van Weeren, "Extension of stochastic volatility equity models with the Hull-White interest rate process," *Quantitative Finance*, vol. 12, no. 1, pp. 89–105, 2012.

[22] R. Merton, "Option pricing when underlying stock returns are discontinuous," *Journal of Financial Economics*, vol. 3, no. 1-2, pp. 125–144, 1976.

[23] S. G. Kou, "A jump-diffusion model for option pricing," *Management Science*, vol. 48, no. 8, pp. 1086–1101, 2002.

[24] D. S. Bates, "Jumps and stochastic volatility: exchange rate processes implicit in deutsche mark options," *Review of Financial Studies*, vol. 9, no. 1, pp. 69–107, 1996.

[25] G. Bakshi, C. Cao, and Z. Chen, "Empirical performance of alternative option pricing models," *The Journal of Finance*, vol. 52, no. 5, pp. 2003–2049, 1997.

[26] L. O. Scott, "Pricing stock options in a jump-diffusion model with stochastic volatility and interest rates: applications of Fourier inversion methods," *Mathematical Finance*, vol. 7, no. 4, pp. 413–426, 1997.

[27] G. J. Jiang, "Testing option pricing models with stochastic volatility, random jumps and stochastic interest rates," *International Review of Finance*, vol. 3, no. 3-4, pp. 233–272, 2002.

[28] J. Kienitz and D. Wetterau, *Financial Modelling: Theory, Implementation and Practice with Matlab Source*, John Wiley & Sons, Hoboken, NJ, USA, 2012.

[29] S. Yan and P. Santa-Clara, "Crashes, volatility, and the equity premium: lessons from S&P 500 options," *The Review of Economics and Statistics*, vol. 92, no. 2, pp. 435–451, 2010.

[30] C. Chang, C.-D. Fuh, and S.-K. Lin, "A tale of two regimes: theory and empirical evidence for a Markov-modulated jump diffusion model of equity returns and derivative pricing implications," *Journal of Banking & Finance*, vol. 37, no. 8, pp. 3204–3217, 2013.

[31] J. Huang, W. Zhu, and X. Ruan, "Option pricing using the fast Fourier transform under the double exponential jump model with stochastic volatility and stochastic intensity," *Journal of Computational and Applied Mathematics*, vol. 263, pp. 152–159, 2014.

[32] J. Huang, W. Zhu, and X. Ruan, "Fast Fourier transform based power option pricing with stochastic interest rate, volatility, and jump intensity," *Journal of Applied Mathematics*, vol. 2013, Article ID 875606, 7 pages, 2013.

[33] J. Y. Sang, N. Zhang, and M. Jian, "European option pricing under the double exponential jump model with stochastic interest rate, stochastic volatility and stochastic intensity," *Applied Mechanics and Materials*, vol. 631-632, pp. 1325–1328, 2014.

[34] P. Carr and D. Madan, "Option valuation using the fast Fourier transform," *The Journal of Computational Finance*, vol. 2, no. 4, pp. 61–73, 1999.

[35] F. Fang and C. W. Oosterlee, "A novel pricing method for European option based on Fourier-cosine series expansions," *SIAM Journal on Scientific Computing*, vol. 31, no. 2, pp. 826–848, 2008.

[36] D. Duffie, J. Pan, and K. Singleton, "Transform analysis and asset pricing for affine jump-diffusions," *Econometrica*, vol. 68, no. 6, pp. 1343–1376, 2000.

[37] H. Kammeyer and J. Kienitz, "The Heston-Hull-White model Part I: finance and analytics," *Wilmott*, vol. 2012, no. 57, pp. 46–53, 2012.

[38] S. Maze, *Efficient Implementation of the Heston-Hull & White Model*, University of Cape Town, Cape Town, South Africa, Masters dissertation, 2014.

[39] D. Brigo and F. Mercurio, *Interest Rate Models-Theory and Practice*, Springer, Berlin, Heidelberg, 2006.

Hindawi
Mathematical Problems in Engineering
Volume 2020, Article ID 3898191, 7 pages
https://doi.org/10.1155/2020/3898191

Research Article

Research on the Pricing of Global Drought Catastrophe Bonds

Guoqu Deng,[1] Shiqiang Liu,[1] Li Li,[1] and Chushi Deng[2]

[1]*School of Management, Henan University of Science and Technology, Luoyang 471003, China*
[2]*Business School, Deakin University, Melbourne, Victoria 3125, Australia*

Correspondence should be addressed to Guoqu Deng; dengguoqu@haust.edu.cn

Received 29 February 2020; Accepted 7 April 2020; Published 23 May 2020

Guest Editor: Wenguang Yu

The rapid development of catastrophe bonds provides a new idea for catastrophe risk dispersion, since its traditional means fail to afford the economic losses caused by the global drought catastrophe. With the deepening of the concept of the community with a shared future for mankind, there is an opportunity to issue global drought catastrophe bonds through international cooperation. Based on the data of global drought catastrophe losses from 1900 to 2018, this paper selects 21 countries as the primary participants of international cooperation and studies the pricing of drought catastrophe bonds by the POT model and high quantile estimation. The results show that the first-class bond has a 10% occurrence probability with the trigger point of $252.54 million, and the second-class one has a 35% occurrence probability with the trigger point being $117.13 million. In line with high quartile estimates, the one-year principal-protected catastrophe bonds with a face value of $1,000 are valued at $957.14 and $939.29, respectively. Besides, the principal portion of the lost bonds is $912.50 and $783.04, while the total of it is $867.86 and $626.79, respectively.

1. Introduction

According to a report by the CRED (Center for Research on Environmental Decisions), 347 droughts were recorded between 1998 and 2017, resulting in economic losses of about $124 billion; droughts affected the lives of around 1.5 billion people worldwide, accounting for 33 percent of the people affected by all disasters. At the same time, China is one of the most severely affected countries in the world. In 2017 alone, the drought caused a direct economic loss of 37.5 billion yuan, which is 12.4% of China's annual economic losses. It is very serious to issue catastrophe financial derivatives, such as catastrophe insurance and the catastrophe bond, owing to the limited affordability of the traditional insurance industry, as well as undersupply in government relief and social contribution.

Recent years witness a relatively significant increase in both the global issuance of catastrophe bonds and the annual aggregate trading volume. Even under the circumstances of the 2008 financial crisis, the issuance of global catastrophe bonds has also been comparatively unscathed. With the vital function of dispersing catastrophe risk, catastrophe financial derivatives such as catastrophe bonds have been integrated into the mainstream financial market, turning into an effective tool for catastrophe risk management and capital market investment. In January 2011, Swiss Re reached an agreement with Successor X Ltd. ("Successor X") by integrating earthquake risks in Australia with those in the United States. Besides, catastrophe risks in Australia, North Atlantic hurricanes and California earthquakes have been comprehensively covered, which has set an example of cooperation among different countries with various disasters. With the wide acceptance of the community of human destiny, the cooperation among countries in related fields is deepening, and international cooperation in the field of catastrophe is bound to become a part of it.

Through the collation of relevant literature, the related research of catastrophe bonds mainly focuses on three aspects: The first is the catastrophe bond pricing model. In terms of catastrophe bonds, Papaioannou and Pantelous [1] deduced the pricing formula by the Markov process, and Nowak and Romaniuk [2] proved the valuation formula with the generalized structure suitable for different yield functions by using the multifactor CIR model. He et al. [3] used the flood loss data in China to fit the model. Compared with other models, the POT model has better fitting effect and precision based on the results. To establish the pricing model, the catastrophe bond and convertible bond are combined into the catastrophe convertible bond by Wang [4]. The second is the influence of related factors on the price of the catastrophe bond. Lee and Yu [5] proved that moral hazard and basis risk can remarkably reduce the price of catastrophe bonds by introducing them into the ISR model. Kang and Xing [6] analyzed that efficacious asset-liability management can lower the impact of morals, default, and the basis on the catastrophe bond price, while Ma et al. [7] simulated the impact of interest rate risk on the catastrophe bond price. The third is the application research of the catastrophe bond. Shao et al. [8] priced California earthquake catastrophe bonds in line with neural network financial structure and equilibrium pricing theory. For the pricing of agricultural charity catastrophe bonds, Deng et al. [9] used the modified Wang two-factor model. Based on extreme value theory, Wu et al. [10] adopted the POT model to design typhoon catastrophe bonds. The latest application research has focused on Fourier transform by Yu et al. [11–13] and Zhang et al. [14].

According to the existing research results, there are theoretical research and application research for catastrophe bonds. The former mainly focuses on various pricing models and factors affecting pricing; the latter involves practical application pricing of flood, earthquake, and typhoon catastrophe bonds. However, no intersection about the catastrophe bond and the drought catastrophe risk has been discovered in the literature. Based on the abovementioned analysis, this paper applies the POT pricing model and attempts to price the drought catastrophe bonds using the global drought catastrophe loss data. This is the first time that catastrophe bond pricing has been applied to drought and catastrophe, with the research horizon based on global losses. Through the study on the pricing of drought catastrophe bonds, we hope to provide a new idea and means for the global drought catastrophe risk dispersion.

2. Definition of Catastrophic Drought Disaster and Loss in the World

At present, there lacks a special consistent standard of drought catastrophe at home and abroad. Zhang et al. [15] put forward five conditions: the direct economic loss of a single disaster exceeds 100 billion yuan; the proportion of disaster-causing crops exceeds 60%; the area of disaster-affected crops exceeds 50000 km^2, the disaster-affected population exceeds 50 million, and the population in need of relief exceeds 30%. When any three of the five conditions are met, the situation can be considered as having reached the level of drought catastrophe. For Swiss Re [16], a single loss of more than \$97.6 million is called a catastrophe. Deng et al. [17] defined the criteria for catastrophic disasters from different subjects. For disaster-bearing farmers, agricultural insurance brokers and the government, we can call it an agricultural catastrophe when the cumulative losses from a disaster exceed 40,800 yuan, 141.51 million yuan and 1% of the GDP of the year, respectively. As the second-largest reinsurance company in the world, Swiss Re has the classification standard generally accepted by the industry. That is to say, if the direct economic losses resulted from a single drought reach up to \$97.6 million, we can perceive it as a drought catastrophe.

From 1900 to 2018, there were 633 severe droughts in the world, resulting in more than \$167 billion in economic losses. In terms of regional distribution, Asia with 149 disasters suffered the most, bringing out economic losses of \$56.54 billion; North America ranked the second because of \$48.91 billion losses in the economy, with a single and largest average loss of \$740 million; Europe ranks the third with less frequent economic losses of \$26.6 billion. For Oceania, there were 19 times of disasters that generate a total economic loss of \$12.79 billion; for Africa, and it had 282 times of droughts and catastrophes, which is the highest number that far exceeds other regions, but economic losses amounted to only \$5.24 billion; the Caribbean region had the lowest disaster losses, with 17 disasters costing merely \$350 million (Figure 1).

The number of drought catastrophes and economic losses in various countries around the world are calculated, with the top 10 countries shown in Table 1. China had the highest number of droughts, namely, 39, far beyond that in other countries and twice as many as that in Brazil. In terms of economic losses, the United States ranked the first with a combined loss of \$41635 million, followed by China and Brazil (Table 1).

3. Pricing Model of Drought Catastrophe Bonds

The classical pricing models of catastrophe bonds include the Kreps model, the POT model, and the Wang transformation model. As the first model is mainly applied to actuarial insurance, it fails to reflect the tail characteristics of catastrophe risk effectively. While the Wang transformation model assumes that the risk probability model is known, the POT model based on extreme value theory is more propitious to the pricing when the probability of drought and catastrophe risk is unknown. In regard of pricing catastrophe bonds, the threshold, term structure of the interest rate, and the catastrophe loss model are the key factors.

3.1. Threshold Value. The threshold value (marked as U) is the key to the determination of bond prices. To determine the threshold value, domestic scholars normally use the graph of the average out-of-quantity function, which is a relative range instead of an exact value. With the simple and explicit process, the Kurtosis method proposed by Pieere Patie is more significant to determine the threshold of the loss probability distribution model. After repeated elimination of the data, the Kurtosis of the new sample data is less than 3, and then the maximum value of the new sample data can be used as the threshold value. The Kurtosis is calculated as follows:

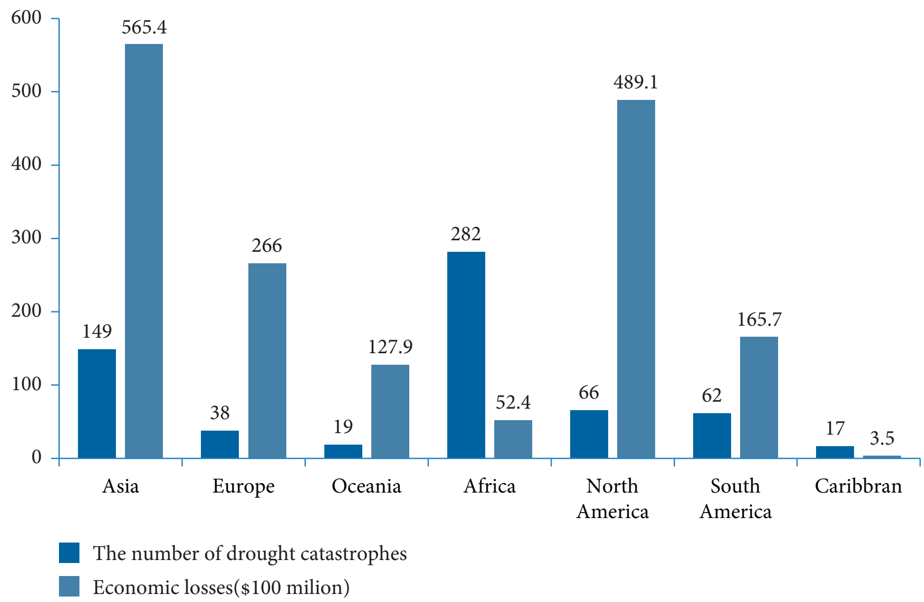

Figure 1: The number of drought catastrophes and economic losses in the world from 1900 to 2018.

Table 1: Top 10 countries for frequency of drought catastrophes and economic losses from 1900 to 2018.

Rank	Number of disasters countries	Economic losses (million)			
		Number	Rank	Countries	Losses
1	China	39	1	United States	41635
2	Brazil	18	2	China	35346.4
3	Ethiopia	16	3	Brazil	10183.1
4	United States	15	4	Spain	9660
5	India	15	5	Vietnam	7399.1
6	Kenya	15	6	India	5441.1
7	Somalia	15	7	Canada	4810
8	Niger	15	8	Italy	4290
9	Mauritania	14	9	Thailand	3725.5
10	Mozambique, Burkina Faso, Bolivia	13	10	Argentina	3520

$$K_n = \frac{(1/n)\sum_{i=1}^{n}\left(X_i - \overline{X}\right)^4}{\left(S_n^2\right)^2}, (2) \quad (1)$$

3.2. Term Structure of Interest Rates. Generally, the maturity of catastrophe bonds is short term (three years, even one year). As the interest rate will not vary much during the bond cycle, we use a relatively simple static term structure of interest rates in this paper.

3.3. Catastrophe Loss Model. The coupon-free catastrophe bond with a face value of 1 is payable when it matures in the following structure:

$$P_{\text{cat}}(T) = \begin{cases} 1, & L_T < U, \\ p, & L_T > U. \end{cases} \quad (3)$$

Among them, L_T is the total amount of loss in the bond term, with the bond term between each loss being independent and identically distributed; U denotes the threshold; and p represents the proportion paid by investors when the trigger level is reached.

Assuming that the number of catastrophes at time t obeys Poisson distribution of strength, X_i signifies that the losses at time X_i are independent and follow GPD distribution. Then, L_i, the total loss of the catastrophe, obeys Poisson distribution and can be expressed as follows:

$$L_i = X_1 + X_2 + \cdots + X_{N_t} = \sum_{i=1}^{N_t} X_i. \quad (4)$$

The probability that the catastrophe loss is less than the threshold U is

$$P\left(L_t < U\right) = \sum_{j=0}^{\infty} e^{-\lambda T}\frac{(\lambda T)^j}{j!}F^j(U). \quad (5)$$

Among them, $F^j(U) = P\left(X_1 + X_2 + \cdots + X_j \le U\right)$ is the j convolution of catastrophe loss.

4. Price Calculation of the Drought Catastrophe Bonds

4.1. Data Source. The following data are obtained from the EM-DAT (https://www.emdat.be/) and the database (1900–2018). Based on the Swiss Re catastrophe, the criteria is $97.6 million for a single loss; based on Disaster Management Index INFORM[1], the drought risk rating should be medium or higher. Countries having a land area of more than 300,000 square kilometers or meeting the above-mentioned conditions will be the subjects of international cooperation. The final group of 21 countries will be Vietnam, Zimbabwe, Bolivia, China, Thailand, India, Brazil, Philippines, Italy, Mexico, Ethiopia, Spain, Russia, Mauritania, Peru, Canada, Namibia, Argentina, South Africa, the United States, and Australia. A total of 82 drought events reached the catastrophic level, with effective years from 1968 to 2018. Due to the large time span, the CPI in 2018 is deemed as the benchmark 100 to adjust the losses of all previous drought catastrophes.

4.2. Descriptive Statistics. First of all, the data obtained are descriptive statistics. In the period of 1968–2018, there were 36 years of drought catastrophes and 15 years of a catastrophe. As the most frequently affected year, 2015 witnessed 9 times of catastrophic events, and the cumulative loss was $18.04 billion. In 2012, the cumulative economic loss was the largest on record at $21.75 billion.

Poisson distribution is suitable for the number of random events in decimal unit time. Many scholars used Poisson distribution to predict the number of natural disasters, such as Liu [18] and Xie Zhuolun [19]. Supposing that the frequency of drought disasters obeys Poisson distribution in this paper, Poisson intensity can be calculated from the frequency statistics λ:

$$\lambda = \frac{\sum N_i * x_i}{\sum x_i}, \tag{6}$$

where N_i represents the number of drought and x_i denotes frequency of occurrences. According to Table 2, the calculation result is $\lambda \approx 2.28$.

As can be seen from Table 3, the average loss from a single drought catastrophe was $145 million, with a maximum value of $1828.66 million. The whole sample data skewness is 4.63, which has the obvious right-skewness characteristic. Nevertheless, the Kurtosis is more than 3, with the apparent peak feature. From the sample data normal probability chart (Figure 2), the sample data are the right-skewness peak thick tail data, thus conforming to the traits of catastrophe risk distribution.

The frequency histogram and the empirical loss function of the catastrophic loss concerning drought disaster are plotted, based on which Figures 3 and 4 are obtained. According to the comprehensive statistical description analysis table and the normal probability graph of sample data, the sample data is right-biased thick-tailed data, which can meet the data characteristics of extreme value theory analysis and catastrophe data.

4.3. Loss Distribution Function of Drought Catastrophe. Since the threshold value calculated by the Kurtosis method is 115.3512, we selected 117.13, which is the nearest from 115.3512, as the threshold value. Finally, 52 data are eliminated from the sample data, and there are 30 data exceeding the threshold value, which are used as the tail parameter estimation data of the GPD distribution.

When we fit the GPD distribution data, the oversize distribution function is constructed as follows:

$$F_u = P(X < u + y \mid X > u), \quad X \geq 0, \tag{7}$$

where u is the threshold and $y = x - u$ represents excess value. After transformation, we obtain

$$F_u(y) = \frac{F(y+u) - F(u)}{1 - F(u)} = \frac{F(x) - F(u)}{1 - F(u)}. \tag{8}$$

According to the Pickands-Balkema-Haan theorem, when the threshold is large enough, there exists a nondegenerate distribution function $H_{\xi,\sigma}$ for a class of conditional overdistributions of F_u:

$$F_u(y) = H_{\xi,\sigma}(y), \quad u \longrightarrow \infty, \tag{9}$$

$$H_{\xi,\sigma}(y) = \begin{cases} 1 - \left(1 + \frac{\xi}{\sigma} y\right)^{-(1/\xi)}, & \xi \neq 0, \\ 1 - e^{-(y/\sigma)}, & \xi = 0. \end{cases} \tag{10}$$

In this case, $H_{\xi,\sigma}$ represents the generalized Pareto Distribution; ξ denotes the shape parameter; and σ represents the scale parameter.

If $y = x - u$ is transformed to $x = y + u$, the GPD function can be expressed as follows:

$$H_{\xi,\sigma}(x) = \begin{cases} 1 - \left(1 + \frac{\xi}{\sigma}(x-u)\right)^{-(1/\xi)}, & \xi \neq 0, \\ 1 - e^{-(x-u/\sigma)}, & \xi = 0. \end{cases} \tag{11}$$

If N_u represents the number that loss exceeds u, namely $x > u$, we can obtain

$$F_u(x) = H_{\xi,\sigma}(x) = \begin{cases} 1 - \dfrac{N_u}{N}\left(1 + \dfrac{\xi}{\sigma}(x-u)\right)^{-(1/\xi)}, & \xi \neq 0, \\ 1 - \dfrac{N_u}{N} e^{-(x-u/\sigma)}, & \xi = 0. \end{cases} \tag{12}$$

When the Lagrangian is applied to the maximum likelihood function of the GPD function, the shape and scale parameters can be derived to estimate the parameters of the GPD $\xi = 0.519$, $\sigma = 73.619$, and the position parameters theta $= (\sigma/\xi) = 141.848$. At that time, the maximum likelihood of the extremum is regular, and the asymptotic properties (consistency, asymptotic effectiveness, and asymptotic normality) of the criteria are satisfied, and thus the parameters can be estimated by the use of the standard asymptotic likelihood conclusion.

Table 2: The annual number of drought catastrophic statistics from 1968 to 2018.

Number of droughts	1	2	3	4	5	6	9
Frequency of occurrence (in years)	15	9	6	4	0	1	1

Table 3: Descriptive statistics of drought catastrophes losses from 1968 to 2018.

Min	Max	Mean	Standard deviation	Extreme bad	Degree of deviation	Kurtosis
9.8	1828.66	145	241.26	1825.36	4.63	30.34

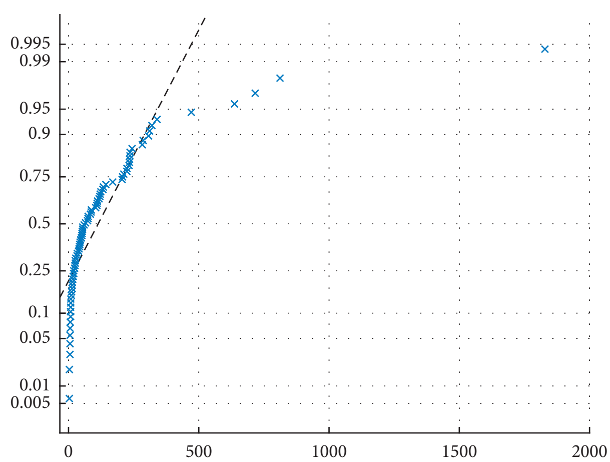

Figure 2: Normal probability chart of sample data.

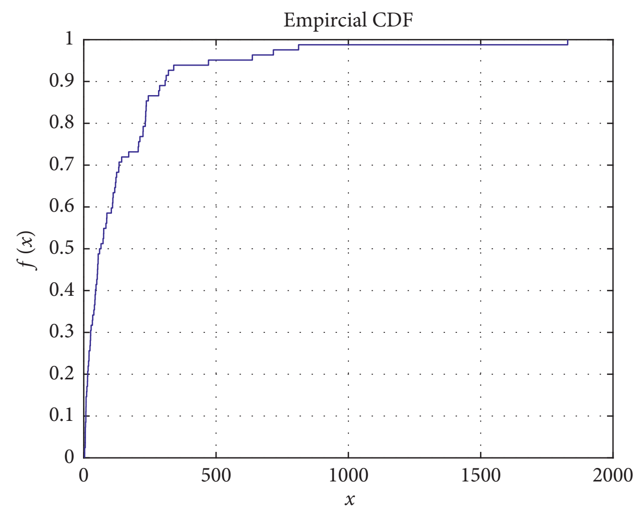

Figure 4: Empirical distribution function diagram of drought catastrophe loss.

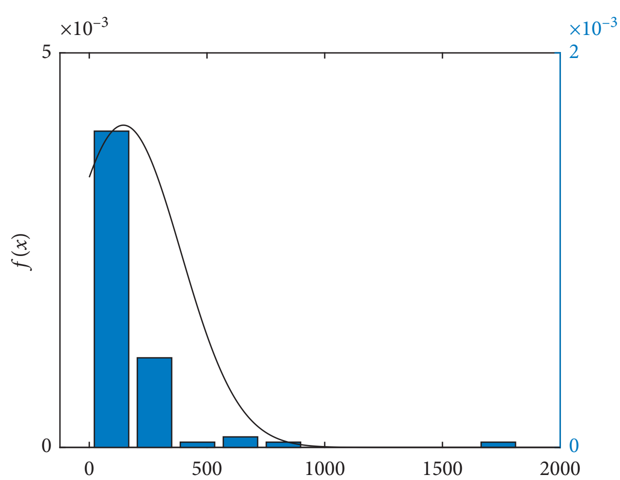

Figure 3: Histogram frequency of drought catastrophe loss.

Once the relevant parameters have been determined, a generalized Pareto distribution function can be acquired:

$$H_{\xi,\sigma}(x) = 1 - \left(1 + \frac{0.519}{73.619}(x - 117.13)\right)^{-(1/0.519)}, \quad x > 117.13. \tag{13}$$

The distribution function of the losses regarding drought catastrophic disasters is

$$F(x) = 1 - \frac{30}{82}\left(1 + \frac{0.519}{73.619}(x - 117.13)\right)^{-(1/0.519)}, \quad x > 117.13. \tag{14}$$

4.4. High Quantile and Price Estimation. Formula (9) can be used for the estimation of the high quantile of the loss resulted from drought catastrophic disaster. If the value of the quantile is p, the formula for estimating the high quantile is as follows:

$$x_p = u + \frac{\sigma}{\xi}\left(\left(\frac{n}{N_u}(1-p)\right)^{-\xi} - 1\right). \tag{15}$$

From the above, we can obtain $u = 117.13$, $\sigma = 73.169$, $\xi = 0.519$, $n = 82$, and $N_u = 30$. The given values of p are 90%, 95%, 99%, and 99.5%, respectively. Moreover, the high scores of drought catastrophic losses are calculated, as shown in Table 4.

From the results, the likelihood that the global drought catastrophe loss will be less than \$252.54 million will be 90%. When global drought catastrophe loss is less than \$372.20 million and \$889.24 million, the probability will be 95% and 99%, respectively. Besides, the probability when the loss reaches up to \$1,284.58 million or less is 99.5%. In terms of national losses, the United States and China each suffered

Table 4: High percentile statistical table of drought catastrophe losses.

U	N_u	σ	ξ	90%	95%	99%	99.5%
117.13	30	73.169	0.519	252.54	372.2	889.24	1284.58

three single losses of more than $252.54 million, while Brazil, Argentina, Vietnam, Thailand, and India each suffered one drought calamity of over $252.54 million.

When the drought catastrophic losses were $117.13 million, the quantile was 65 percent. To enhance the appeal of drought catastrophe bond design, the bond price is designed in accordance with different loss levels. In this regard, the trigger value of the first bond is designed as (252.54, 10%), and that of the secondary bond is (117.13, 35%). Suppose the bond has a face value of $1,000, a coupon of 8 percent, a risk-free interest rate of 12 percent, and a maturity of one year:

(1) The price of the drought catastrophe bond of the principal-protected type: if the drought catastrophe does not occur or does not meet the set trigger conditions, the investor may recover the principal and interest at the end of the period; otherwise, the SPV will no longer pay interest to the investor, who will only get their money back.

The issue price of the first bond is $P = (1080 * 90\% + 1000 * 10\%/1 + 12\%) = 957.14$.
The issue price of the secondary bond is $P = (1080 * 65\% + 1000 * 35\%/1 + 12\%) = 939.29$.

(2) The price of the drought catastrophe bond of the principal partial loss type: during the payment period, the SPV will charge the investor interest and part of the principal, with the loss rate of the principal being 50%:

The issue price of the first bond is $P = (1080 * 90\% + 1000 * 10\% * (1 - 50\%)/1 + 12\%) = 912.5$.
The issue price of the secondary bond is $P = (1080 * 65\% + 1000 * 35\% * (1 - 50\%)/1 + 12\%) = 783.04$.

(3) The price of the drought catastrophe bond with the total loss of principal type: during the payment period, if the drought event reaches the trigger condition, the investor loses all the principal and interest; otherwise, the SPV will pay the investor all the principal and interest.

The issue price of the first bond is $P = (1080*90\% + 1000*10\%* (1 - 100\%)/1 + 12\%) = 867.86$.
The issue price of the secondary bond is $P = (1080*65\% + 1000*35\%* (1 - 100\%)/1 + 12\%) = 626.79$.

According to the analysis of the data, the loss of drought catastrophic disaster has the right-off peak and tail. Besides, the distribution function of loss obeys the generalized Vilfredo Pareto's GPD function, which means issuing one-year drought catastrophe bonds with fixed interest rate term structure. Based on the high quartile estimation, the issuing price of the drought catastrophe bonds with a face value of $1000 is as follows: (1) for the principal principal-protected type, the price of the first- and second-order drought catastrophe bonds is $957.14 and $939.29, respectively; (2) for partial loss of principal type with a loss rate of 50%, the price is $912.50 for first-degree drought catastrophe bonds and $783.04 for second-degree ones; (3) for total loss of principal type, the price are $867.86 and $626.79 for first- and second-degree drought catastrophe bonds, respectively. The yield level of the bond is significantly higher than that of treasury bonds in the same period, which largely appeals to investors.

5. Conclusion

In this paper, dissimilar trigger points and various principal loss are designed, which can provide various options for investors with different preferences. Results show that the issuance price of low-loss and high-probability types of bonds is low. The higher risk means higher return. The high yield stimulus will attract a mass of investors to buy investments. Since the drought catastrophe bond is designed for the first time, the term structure of the fixed interest rate is used for the study to simplify the calculation. Nonetheless, in the actual market operation, the bond price interest rate is in dynamic change. Therefore, we can combine our future research with the actual situation more closely, using the dynamic term structure of the interest rate to price the drought catastrophe bond.

Data Availability

The data used to support the findings of this study are available from the corresponding author upon request.

Conflicts of Interest

The authors declare that they have no conflicts of interest.

Acknowledgments

This work was sponsored by the Key Program of National Social Science Foundation of China (No. 15AGL013), Major policy theoretical and practical issues of China Earthquake Bureau (CEAZY2019JZ09), Risk management innovation and public policy soft science research base of Henan Provincial Science and Technology Department, and Social Science Planning Project of Henan Province (2019BJJ030).

References

[1] A. D. Papaioannou and A. A. Pantelous, "Pricing and simulating catastrophe risk bonds in a markov-dependent environment," *Applied Mathematics and Computation*, vol. 309, pp. 68–84, Elsevier, Amsterdam, Netherlands, 2017.
[2] P. Nowak and M. Romaniuk, "Valuing catastrophe bonds involving correlation and CIR interest rate model," *Computational and Applied Mathematics*, vol. 37, no. 1, pp. 365–394, 2018.

[3] S. He, D. Wu, and S. Wang, “Study on flood disaster loss model based on extreme value theory,” *Journal of Yunnan Nationalities University*, vol. 23, no. 1, pp. 62–65, 2014.
[4] Li Wang, “Research on the pricing model of the convertible bond,” *Insurance Journal Research*, vol. 6, pp. 58–67, 2018.
[5] J.-P. Lee and M.-T. Yu, “Valuation of catastrophe reinsurance with catastrophe bonds,” *Insurance: Mathematics and Economics*, vol. 41, no. 2, pp. 264–278, 2007.
[6] H. Kang and T. Xing, “Research on catastrophe bond pricing in China considering multi-risk factors,” *Insurance Journal Research*, vol. 8, pp. 96–108, 2013.
[7] Z. Ma, X. Zou, and C. Ma, “Pricing and numerical simulation of catastrophe bonds under double stochastic compound poisson loss,” *China Management Science*, vol. 24, no. 10, pp. 35–43, 2016.
[8] J. Shao, A. Pantelous, and A. D. Papaioannou, “Catastrophe risk bonds with applications to earthquakes,” *European Actuarial Journal*, vol. 5, no. 1, pp. 113–138, 2015.
[9] G. Deng, W. Yan, and X. Zhu, “A study on the pricing of agricultural catastrophe bonds in China: a case study of Henan province flood catastrophe bonds,” *Financial Theory and Practice*, vol. 5, pp. 91–94, 2016.
[10] Y. Wu, S. Jiang, and X. Wu, “Study on loss distribution and financial countermeasures of typhoon disaster in Guangdong province based on extreme value theory,” *Seismology*, vol. 32, p. 131, 2017.
[11] W. Yu, Y. Yong, G. Guan, W. Y. Huang, S. Su, and C. Cui, “Valuing guaranteed minimum death benefits by cosine series expansion,” *Mathematics*, vol. 7, no. 9, p. 835, 2019.
[12] W. Yu, F. Wang, Y. Huang, and H. Liu, “Social optimal mean field control problem for population growth model,” *Asian Journal of Control*, pp. 1–8, 2019.
[13] W. Yu, P. Guo, Q. Wang et al., “On a periodic capital injection and barrier dividend strategy in the compound poisson risk model,” *Mathematics*, vol. 8, no. 4, p. 511, 2020.
[14] Z. Zhang, W. Y. Yong, and W. Yu, “Valuing equity-linked death benefits in general exponential lévy models,” *Journal of Computational and Applied Mathematics*, vol. 365, 2020.
[15] W. Zhang, P. Shi, and H. Zhou, “A study on the definition and classification of catastrophe—an analysis of typical disaster cases in the world in recent years,” *Disaster Science*, vol. 1, pp. 17–24, 2013.
[16] Swiss Reinsurance Economic Research, “Natural and man-made disasters in 2014: convective storms and winter storms cause the most damage,” *Swiss Re Sigma*, vol. 2, p. 46, 2015.
[17] G. Deng, H. Han, S. Kang, and J. Liu, *Exploring the Mechanism of Agricultural Catastrophe Risk, Risk Dispersion and Symbiosis in China*, China Social Sciences Press, Beijing, China, 2015.
[18] J. Liu and Y. Li, “Study on earthquake loss distribution and catastrophe bond pricing in China,” *Financial and Trade Studies*, vol. 6, pp. 82–88, 2009.
[19] Z. Xie, J. Chen, and Ye Lu, “Distribution fitting of earthquake catastrophe risk and bond, pricing in mainland China,” *Journal of Zhejiang Sci-Tech University*, vol. 42, no. 1, pp. 10–19, 2019.

Hindawi
Mathematical Problems in Engineering
Volume 2020, Article ID 2015845, 8 pages
https://doi.org/10.1155/2020/2015845

Research Article

European Spread Option Pricing with the Floating Interest Rate for Uncertain Financial Market

Lidong Zhang[1,2] **Yanmei Sun**,[3] **and Xiangbo Meng**[1]

[1]*School of Science, Tianjin University of Science & Technology, Tianjin 300457, China*
[2]*Center for Financial Engineering and Risk Management, Tianjin University of Science & Technology, Tianjin 300222, China*
[3]*College of Economics & Management, Tianjin University of Science & Technology, Tianjin 300222, China*

Correspondence should be addressed to Lidong Zhang; zhanglidong1999@126.com

Received 15 April 2020; Accepted 5 May 2020; Published 21 May 2020

Guest Editor: Wenguang Yu

In this paper, we investigate the pricing problems of European spread options with the floating interest rate. In this model, uncertain differential equation and stochastic differential equation are used to describe the fluctuation of stock price and the floating interest rate, respectively. We derive the pricing formulas for spread options including the European spread call option and the European spread put option. Finally, numerical algorithms are provided to illustrate our results.

1. Introduction

Since financial derivatives have the function of hedging and risk aversion, they are widely used in the financial market. Options are special financial derivatives, and they are used not only in the adjustment of the national debt but also in the leveraged investment of enterprises and the hedging of commodities. The value of an option depends not only on the price of its underlying asset but also on other factors such as the interest rate. Since Black and Scholes [1] established the B-S model, option pricing has become an important issue in financial mathematical research.

However, the expected return of a stock is different from the assumption of the B-S model in the financial market. In order to better match with the real market, scholars have improved the B-S model. Merton [2] proposed a jump-diffusion model and gave the European option pricing formula. Hull and White [3] studied the pricing problem for the European option under stochastic volatility. Heston [4] investigated the option pricing under stochastic interest rate and studied the pricing problems of the bond and currency option. Stock prices are easily affected by the social environment and investor belief degrees, but the existing models and theories are difficult to give a reasonable explanation. For dealing with the uncertainty of human behavior, Liu [5] founded the uncertainty theory based on normality, duality, subadditivity, and product axioms. To describe uncertain dynamic systems, Liu [6] introduced the concept of uncertain processes and proposed uncertain differential equations driven by canonical Liu process. Liu [7] proposed an uncertain stock model in which stock price was described by an uncertain differential equation. Subsequently, Chen [8] and Zhang and Liu [9] gave the pricing formulas for the European option, American option, and geometric Asian option, respectively. Considering the uncertain fluctuations of the interest rate, Chen and Gao [10] firstly studied the term structure of the uncertain interest rate. Yao [11] proposed an uncertain stock model with floating interest rate. Zhang et al. [12] derived the pricing formulas of interest rate ceiling and interest rate floor. Sun and Su [13] studied the pricing problems for the European and American option under the mean-reverting stock model. Gao et al. [14] discussed the pricing formulas of lookback options based on the uncertain exponential Ornstein–Uhlenbeck model. The latest research on the applications of uncertainty theory and probability theory was given by Gao [15], Lu and Zhu [16], Li et al. [17], Yu et al. [18, 19], and Zhang and Sun [20].

In this paper, we investigate the pricing problems for European spread options. It is well known that spread options are path-dependent exotic options whose returns depend on the spread of two or more assets. Although spread options are widely traded in different financial markets, it is still difficult to price such options. At present, there are relatively few research studies on the pricing of spread options. It is well known that interest rate is an important factor influencing the price of financial derivatives, and it is often fluctuated by stochastic factors such as economy and policy. Two stocks issued newly are considered in this paper, so the lack of historical data leads to the unsuccessful investigation on the price of spread options based on probability theory. Thus, basing uncertainty theory and probability theory (so-called chance theory), we study the pricing of spread options with a stochastic interest rate under uncertain environment. We introduce some basic knowledge of uncertainty theory and chance theory in Section 2. Then, we derive European spread call option and put option pricing formulas with stochastic interest rates and also give some numerical algorithms to calculate the prices in Section 3. Finally, a brief conclusion is given in Section 4.

2. Preliminaries

This section mainly introduces uncertainty theory and chance theory. Uncertainty theory is an effective tool for dealing with reliability issues related to human uncertainty, while chance theory is a basic tool to deal with complex systems with randomness and uncertainty. This section provides some basic definitions and results on uncertainty theory and chance theory. For more details, please see Liu's latest book [21].

2.1. Uncertainty Theory

2.1.1. Uncertain Variable

Definition 1 (see Liu [5, 7]). Let L be a σ-algebra on a nonempty set Γ. A set function $M\colon L \longrightarrow [0,1]$ is called an uncertain measure if it satisfies the following axioms:

Axiom 1 (normality axiom): $M\{\Gamma\} = 1$ for the universal set Γ.

Axiom 2 (duality axiom): $M\{\Lambda\} + M\{\Lambda^c\} = 1$ for any event Λ.

Axiom 3 (subadditivity axiom): for every countable sequence of events $\Lambda_1, \Lambda_2, \ldots$, we have

$$M\left\{\bigcup_{i=1}^{\infty}\Lambda_i\right\} \le \sum_{i=1}^{\infty} M\{\Lambda_i\}. \tag{1}$$

Axiom 4 (product axiom): let (Γ_k, L_k, M_k) be uncertainty spaces for $k = 1, 2, \ldots$. The product uncertain measure M is an uncertain measure satisfying

$$M\left\{\prod_{k=1}^{\infty}\Lambda_k\right\} = \bigwedge_{k=1}^{\infty} M_k\{\Lambda_k\}, \tag{2}$$

where Λ_k are arbitrarily chosen events from L_k for $k = 1, 2, \ldots$, respectively.

Definition 2 (see Liu [5]). An uncertain variable is a function from an uncertainty space (Γ, L, M) to the set of real numbers; for any Borel set B of real numbers, the set

$$\{\xi \in B\} = \{\gamma \in \Gamma \mid \xi(\gamma) \in B\}, \tag{3}$$

is an event.

The uncertainty distribution $\Phi(x)$ of an uncertain variable ξ is defined by $\Phi(x) = M\{\xi \le x\}$ for any real number x. An uncertainty distribution $\Phi(x)$ is said to be regular if it is a continuous and strictly increasing function with respect to x at which $0 < \Phi(x) < 1$, and

$$\begin{aligned} &\lim_{x \longrightarrow -\infty} \Phi(x) = 0, \\ &\lim_{x \longrightarrow +\infty} \Phi(x) = 1. \end{aligned} \tag{4}$$

If ξ has a regular uncertainty distribution $\Phi(x)$, then the inverse function $\Phi^{-1}(\alpha)$ is called the inverse uncertainty distribution of ξ.

Definition 3 (see Liu [7]). The uncertain variables $\xi_1, \xi_2, \ldots, \xi_m$ are said to be independent if

$$M\left\{\bigcap_{i=1}^{m}\{\xi_i \in B_i\}\right\} = \bigwedge_{i=1}^{m} M\{\xi_i \in B_i\}, \tag{5}$$

for any Borel sets $B_1, B_2, \ldots, B_m$ of real numbers.

Liu [22] proposed the operation law of uncertain variables and calculated the inverse uncertainty distribution of strictly monotone function of uncertain variables.

Theorem 1 (see Liu [22]). *Let $\xi_1, \xi_2, \ldots, \xi_n$ be independent uncertain variables with uncertainty distributions $\Phi_1, \Phi_2, \ldots, \Phi_n$. If the function $f(x_1, x_2, \ldots, x_n)$ is strictly increasing with respect to $x_1, x_2, \ldots, x_m$ and strictly decreasing with $x_{m+1}, x_{m+2}, \ldots, x_n$, then*

$$\xi = f(\xi_1, \xi_2, \ldots, \xi_m, \xi_{m+1}, \xi_{m+2}, \ldots, \xi_n), \tag{6}$$

is an uncertain variable with inverse uncertainty distribution

$$\Psi^{-1}(\alpha) = f\left(\Phi_1^{-1}(\alpha), \ldots, \Phi_m^{-1}(\alpha), \Phi_{m+1}^{-1}(1-\alpha), \ldots, \Phi_n^{-1}(1-\alpha)\right). \tag{7}$$

Definition 4 (see Liu [5]). The expected value of an uncertain variable ξ is defined by

$$E[\xi] = \int_0^{+\infty} M\{\xi \ge x\}\mathrm{d}x - \int_{-\infty}^{0} M\{\xi \le x\}\mathrm{d}x, \tag{8}$$

provided that at least one of the two integrals exists.

For an uncertain variable ξ with an uncertainty distribution $\Phi(x)$, if its expected value exists, Liu [5] showed that

$$E[\xi] = \int_0^{+\infty} (1 - \Phi(x))\mathrm{d}x - \int_{-\infty}^{0} \Phi(x)\mathrm{d}x. \tag{9}$$

Theorem 2 (see Liu [22]). *Assume the uncertain variable ξ has a regular uncertainty distribution Φ; then,*

$$E[\xi] = \int_0^1 \Phi^{-1}(\alpha)\mathrm{d}\alpha. \tag{10}$$

2.1.2. Uncertain Differential Equations. Liu [6] proposed the concept of uncertain process and defined the time integral of uncertain process.

Definition 5 (see Liu [6]). Let T be an index set, and let (Γ, L, M) be an uncertainty space. An uncertain process is a measurable function from $T \times (\Gamma, L, M)$ to the set of real numbers; for each $t \in T$ and any Borel set B,

$$\{X_t \in B\} = \{\gamma \in \Gamma \mid X_t(\gamma) \in B\}, \tag{11}$$

is an event.

An uncertain process X_t is said to have independent increments if $X_{t_0}, X_{t_1} - X_{t_0}, X_{t_2} - X_{t_1}, \ldots, X_{t_k} - X_{t_{k-1}}$ are independent uncertain variables, where t_0 is the initial time and $t_1, t_2, \ldots, t_k$ are any times with $t_0 < t_1 < \cdots < t_k$. An uncertain process X_t is said to have stationary increments if for any given $t > 0$, the increments $X_{s+t} - X_s$ are identically distributed uncertain variables for all $s > 0$.

Definition 6 (see Liu [7]). An uncertain process C_t is said to be a Liu process if

(i) $C_t = 0$, and almost all sample paths are Lipschitz continuous.

(ii) C_t has stationary and independent increments.

(iii) Every increment $C_{s+t} - C_s$ is a normal uncertain variable with expected value 0 and variance t^2, whose uncertainty distribution is

$$\Phi_t(x) = \left(1 + \exp\left(\frac{-\pi x}{\sqrt{3}t}\right)\right)^{-1}, \quad x \in \mathfrak{R}. \tag{12}$$

Definition 7 (see Liu [5]). Let X_t be an uncertain process, and let C_t be a Liu process. For any partition of closed interval $[a, b]$ with $a = t_1 < t_2 < \cdots < t_{k+1} = b$, the mesh is written as

$$\Delta = \max_{1\le i\le k}\left|t_{i+1} - t_i\right|. \tag{13}$$

Then, Liu integral of X_t with respect to C_t is defined as

$$\int_a^b X_t \mathrm{d}C_t = \lim_{\Delta\longrightarrow 0}\sum_{i=1}^{k} X_t \cdot \left(C_{t_{i+1}} - C_{t_i}\right), \tag{14}$$

provided that the limit exists almost surely and is finite. In this case, the uncertain process is said to be integrable.

Definition 8 (see Liu [6]). Suppose C_t is a Liu process, and f and g are two functions. Then,

$$\mathrm{d}X_t = f(t, X_t)\mathrm{d}t + g(t, X_t)\mathrm{d}C_t, \tag{15}$$

is called an uncertain differential equation. A solution is an uncertain process X_t that satisfies the equation identically in t.

Definition 9 (see Yao and Chen [23]). Let α be a number with $0 < \alpha < 1$. An uncertain differential equation

$$\mathrm{d}X_t = f(t, X_t)\mathrm{d}t + g(t, X_t)\mathrm{d}C_t, \tag{16}$$

is said to have an α-path X_t^α if it solves the corresponding ordinary differential equation:

$$\mathrm{d}X_t^\alpha = f(t, X_t^\alpha)\mathrm{d}t + \left|g(t, X_t^\alpha)\right|\Phi^{-1}(\alpha)\mathrm{d}t, \tag{17}$$

where $\Phi^{-1}(\alpha)$ is the inverse uncertainty distribution of the standard normal uncertain variable

$$\Phi^{-1}(\alpha) = \frac{\sqrt{3}}{\pi}\ln\frac{\alpha}{1-\alpha}. \tag{18}$$

Theorem 3 (see Yao and Chen [23]). *Let X_t and X_t^α be the solution and α-path of the uncertain differential equation*

$$\mathrm{d}X_t = f(t, X_t)\mathrm{d}t + g(t, X_t)\mathrm{d}C_t, \tag{19}$$

respectively. Then,

$$\begin{aligned} M\{X_t \le X_t^\alpha, \forall t\} &= \alpha, \\ M\{X_t > X_t^\alpha, \forall t\} &= 1 - \alpha. \end{aligned} \tag{20}$$

2.2. Chance Theory

Definition 10. Let (Γ, L, M) be an uncertainty space, and let $(\Omega, \mathscr{F}, \mathrm{P})$ be a probability space. Then, the product $(\Gamma, L, M) \times (\Omega, \mathscr{F}, P)$ is called a chance space.

Definition 11 (see Liu [24]). Let $(\Gamma, L, M) \times (\Omega, \mathscr{F}, P)$ be a chance space, and let $\Theta \in L \times \mathscr{F}$ be an event. Then, the chance measure of Θ is defined as

$$Ch\{\Theta\} = \int_0^1 P\{\omega \in \Omega | M\{\gamma \in \Gamma | (\gamma, \omega) \in \Theta\} \ge x\}\mathrm{d}x. \tag{21}$$

Theorem 4 (see Liu [24]). *Let ξ be an uncertain random variable on the chance space $(\Gamma, L, M) \times (\Omega, \mathscr{F}, P)$, and let B be a Borel set of real numbers. Then, $\{\xi \in B\}$ is an uncertain random event with chance measure*

$$Ch\{\xi \in B\} = \int_0^1 P\{\omega \in \Omega | M\{\gamma \in \Gamma | (\gamma, \omega) \in B\} \ge x\}\mathrm{d}x. \tag{22}$$

Definition 12 (see Liu [24]). Let ξ be an uncertain random variable. Then, its chance distribution is defined by

$$\Phi(x) = Ch\{\xi \le x\}, \tag{23}$$

for any $x \in R$.

Theorem 5 (see Liu [25]). *Let $\eta_1, \eta_2, \ldots, \eta_m$ be independent random variables with probability distributions $\Psi_1, \Psi_2, \ldots, \Psi_m$, and let $\tau_1, \tau_2, \ldots, \tau_n$ be independent uncertain variables with uncertainty distributions $\Upsilon_1, \Upsilon_2, \ldots, \Upsilon_n$, respectively. If f is a measurable function, then the uncertain random variable*

$$\xi = f(\eta_1, \eta_2, \ldots, \eta_m, \tau_1, \tau_2, \ldots, \tau_n), \tag{24}$$

has a chance distribution

$$\Phi(x) = \int_{R^m} F(x; y_1, y_2, \ldots, y_m) \mathrm{d}\Psi_1(y_1) \mathrm{d}\Psi_2(y_2) \ldots \mathrm{d}\Psi_m(y_m), \tag{25}$$

where

$$F(x; y_1, y_2, \ldots, y_m) = M\{f(y_1, y_2, \ldots, y_m, \tau_1, \tau_2, \ldots, \tau_n) \leq x\} \tag{26}$$

is the uncertainty distribution of $f(y_1, y_2, \ldots, y_m, \tau_1, \tau_2, \ldots, \tau_n)$ for any real numbers $y_1, y_2, \ldots, y_m$ and is determined by $\Upsilon_1, \Upsilon_2, \ldots, \Upsilon_n$.

Definition 13 (see Liu [24]). Let ξ be an uncertain random variable. Then, its expected value is defined by

$$E[\xi] = \int_0^{+\infty} Ch\{\xi \geq x\} \mathrm{d}x - \int_{-\infty}^0 Ch\{\xi \leq x\} \mathrm{d}x, \tag{27}$$

provided that at least one of the two integrals is finite.

Theorem 6 (see Liu [24]). *Let ξ be an uncertain random variable with chance distribution Φ. Then,*

$$E[\xi] = \int_{-\infty}^{+\infty} x \mathrm{d}\Phi(x). \tag{28}$$

Theorem 7 (see Liu [25]). *Let $\eta_1, \eta_2, \ldots, \eta_m$ be independent random variables with probability distributions $\Psi_1, \Psi_2, \ldots, \Psi_m$, and let $\tau_1, \tau_2, \ldots, \tau_n$ be independent uncertain variables with uncertainty distributions $\Upsilon_1, \Upsilon_2, \ldots, \Upsilon_n$, respectively. If f is a measurable function, then the uncertain random variable*

$$\xi = f(\eta_1, \eta_2, \ldots, \eta_m, \tau_1, \tau_2, \ldots, \tau_n) \tag{29}$$

has an expected value

$$E(\xi) = \int_{R^m} G(y_1, y_2, \ldots, y_m) \mathrm{d}\Psi_1(y_1) \mathrm{d}\Psi_2(y_2) \ldots \mathrm{d}\Psi_m(y_m), \tag{30}$$

where

$$G(y_1, y_2, \ldots, y_m) = E[f(y_1, y_2, \ldots, y_m, \tau_1, \tau_2, \ldots, \tau_n)] \tag{31}$$

is the uncertainty distribution of $f(y_1, y_2, \ldots, y_m, \tau_1, \tau_2, \ldots, \tau_n)$ for any real numbers $y_1, y_2, \ldots, y_m$ and is determined by $\Upsilon_1, \Upsilon_2, \ldots, \Upsilon_n$.

Corollary 1. *Let $\eta_1, \eta_2, \ldots, \eta_m$ be independent random variables with probability distributions $\Psi_1, \Psi_2, \ldots, \Psi_m$, and let $\tau_1, \tau_2, \ldots, \tau_n$ be independent uncertain variables with uncertainty distributions $\Upsilon_1, \Upsilon_2, \ldots, \Upsilon_n$, respectively. If f and g are measurable functions, then the uncertain random variable*

$$\xi = f(\eta_1, \eta_2, \ldots, \eta_m) \times g(\tau_1, \tau_2, \ldots, \tau_n), \tag{32}$$

has an expected value

$$E(\xi) = E[f(\eta_1, \eta_2, \ldots, \eta_m)] \times E[g(\tau_1, \tau_2, \ldots, \tau_n)]. \tag{33}$$

Proof. From Theorem 7, the expectation of the uncertain random variable ξ can be given by the following equation:

$$\begin{aligned}
E(\xi) &= \int_{R^m} E[f(y_1, y_2, \ldots, y_m) \times g(\tau_1, \tau_2, \ldots, \tau_n)] \\
&\quad \mathrm{d}\Psi_1(y_1) \mathrm{d}\Psi_2(y_2) \ldots d\Psi_m(y_m) \\
&= \int_{R^m} f(y_1, y_2, \ldots, y_m) \times E[g(\tau_1, \tau_2, \ldots, \tau_n)] \\
&\quad \mathrm{d}\Psi_1(y_1) \mathrm{d}\Psi_2(y_2) \ldots \mathrm{d}\Psi_m(y_m) \\
&= \int_{R^m} f(y_1, y_2, \ldots, y_m) \mathrm{d}\Psi_1(y_1) \mathrm{d}\Psi_2(y_2) \ldots \mathrm{d}\Psi_m(y_m) \\
&\quad \times E[g(\tau_1, \tau_2, \ldots, \tau_n)] \\
&= E[f(\eta_1, \eta_2, \ldots, \eta_m)] \times E[g(\tau_1, \tau_2, \ldots, \tau_n)].
\end{aligned} \tag{34}$$

□

3. European Spread Option Pricing Formulas

In this section, we discuss the pricing of spread options under the stochastic interest rate environment where stock prices follow uncertain exponential Ornstein–Uhlenbeck process and uncertain log-normal process, respectively. Firstly, we assume interest rate r, one stock price X, and another stock price Y which satisfy the following differential equation, respectively:

$$\begin{cases}
\mathrm{d}r_t = a(b - r_t)\mathrm{d}t + \sigma_0 \sqrt{r_t}\, \mathrm{d}W_t, \\
\mathrm{d}X_t = \mu_1 (1 - c \ln X_t) X_t \mathrm{d}t + \sigma_1 X_t \mathrm{d}C_{1t}, \\
\mathrm{d}Y_t = \mu_2 Y_t \mathrm{d}t + \sigma_2 Y_t \mathrm{d}C_{2t},
\end{cases} \tag{35}$$

where $a, b, \sigma_0, \mu_1, c, \sigma_1, \mu_2, \sigma_2$ are some positive real numbers, W_t is a Brownian motion, and C_{1t} and C_{2t} are independent canonical Liu processes.

Then, the inverse uncertainty distribution of X_t, Y_t is given by Dai et al. [26] and Yao and Chen [23]. The specific form is as follows:

$$\begin{aligned}
X_t^{-1}(\alpha) = \exp\Bigg(&\exp(-\mu_1 ct) \ln X_0 + \frac{1 - \exp(-\mu_1 ct)}{c} \\
&\left(1 + \frac{\sqrt{3}\sigma_1}{\mu_1 \pi} \ln \frac{\alpha}{1 - \alpha}\right)\Bigg),
\end{aligned} \tag{36}$$

$$Y_t^{-1}(\alpha) = Y_0 \exp\left(\mu_2 t + \frac{\sqrt{3}\sigma_2}{\pi} t \ln \frac{\alpha}{1 - \alpha}\right). \tag{37}$$

In the next sections, the pricing formulas of the European spread call option and the European spread put option are derived.

3.1. European Spread Call Option. Suppose X_t and Y_t are two asset price processes. Then, the European spread call option with maturity date T and strike price K is the contract that pays

$$(X_T - Y_T - K)^+. \tag{38}$$

Considering time value of the stock return, the present value of the payoff is

$$\exp\left(-\int_0^T r_t \mathrm{d}t\right)(X_T - Y_T - K)^+. \tag{39}$$

European spread call option should be the expectation of the discounted value of the stock return. So, the European spread call option has a price

$$f_{Ecall} = E\left[\exp\left(-\int_0^T r_t \mathrm{d}t\right)(X_T - Y_T - K)^+\right]. \tag{40}$$

Theorem 8. *Suppose that the European spread call option for the stock model (35) has a strike price K and an expiration time T. Then, the European spread call option pricing formula is*

$$f_{Ecall} = E\left[\exp\left(-\int_0^T r_t \mathrm{d}t\right)\right]\int_0^1 \left(X_T^{-1}(\alpha) - Y_T^{-1}(1-\alpha) - K\right)^+ \mathrm{d}\alpha. \tag{41}$$

Proof. According to Corollary 1, European spread call option is given by the following form:

$$f_{Ecall} = E\left[\exp\left(-\int_0^T r_t \mathrm{d}t\right)\right]E\left[(X_T - Y_T - K)^+\right]. \tag{42}$$

Since X_t, Y_t are independent uncertain processes, their α-path are, respectively, given by formulas (36) and (37). According to Theorem 1, the value of investor's return difference at the maturity date T,

$$(X_T - Y_T - K)^+, \tag{43}$$

has the α-path

$$\left(X_T^{-1}(\alpha) - Y_T^{-1}(1-\alpha) - K\right)^+. \tag{44}$$

So, the expectation of the uncertain variable $(X_T - Y_T - K)^+$ can be derived easily:

$$E\left[(X_T - Y_T - K)^+\right] = \int_0^1 \left(X_T^{-1}(\alpha) - Y_T^{-1}(1-\alpha) - K\right)^+ \mathrm{d}\alpha. \tag{45}$$

Thus, the price of the European spread call option is

$$f_{Ecall} = E\left[\exp\left(-\int_0^T r_t \mathrm{d}t\right)\right]\int_0^1 \left(X_T^{-1}(\alpha) - Y_T^{-1}(1-\alpha) - K\right)^+ \mathrm{d}\alpha. \tag{46}$$

The pricing formula of the European spread call option is derived.

From Theorem 8, the algorithm designed for calculating European spread call option price is divided by two parts. In the first procedure, $E[\exp(-\int_0^T r_t dt)]$ is calculated by Monte Carlo simulation. In the second procedure, $E[(X_T - Y_T - K)^+]$ can be calculated by using the property of inverse distribution. In the final procedure, European spread call option price is derived by virtue of Theorem 8.

In the first procedure, we will calculate $E[\exp(-\int_0^T r_t dt)]$. We will first generate some sample trajectories by stochastic simulations and calculate the average of the terminal trajectories.

Step 0: set $t_j = jT/M$, $k = 1, 2, \ldots, L$, $j = 1, 2, \ldots, M$, where L and M are two large numbers.

Step 1: set $k = 0$.

Step 2: set $k \longleftarrow k + 1$.

Step 3: set $j = 0$.

Step 4: set $j \longleftarrow j + 1$.

Step 5: calculate the value of the stochastic interest rate at the time t_j:

$$r_{t_j}^k = r_{t_{j-1}}^k + a\left(b - r_{t_{j-1}}^k\right)\left(t_j - t_{j-1}\right) + \sigma_0\sqrt{r_{t_{j-1}}^k}\sqrt{t_j - t_{j-1}}\varepsilon_j^k, \tag{47}$$

where $\varepsilon_j^k \sim N(0,1)$ are generated by stochastic simulations.

Step 6: calculate the discount rate:

$$\exp\left(-\int_0^T r_t^k \mathrm{d}t\right) \longleftarrow \exp\left(-\frac{T}{M}\sum_{j=1}^{M} r_{t_j}^k\right). \tag{48}$$

Step 7: calculate the approximated value of $E[\exp(-\int_0^T r_t dt)]$:

$$E\left[\exp\left(-\int_0^T r_t \mathrm{d}t\right)\right] \longleftarrow \frac{1}{L}\sum_{k=1}^{L}\exp\left(-\frac{T}{M}\sum_{j=1}^{M} r_{t_j}^k\right). \tag{49}$$

In the second procedure, we will calculate $E[(X_T - Y_T - K)^+]$.

Step 0: set $\alpha_i = i/N$, $i = 1, 2, \ldots, N-1$, where N is a large number.

Step 1: set $i = 0$.

Step 2: set $i \longleftarrow i + 1$.

Step 3: calculate the inverse uncertainty distribution of the stock processes:

$$X_T^{-1}(\alpha_i) = \exp\left(\exp(-\mu_1 cT)\ln X_0 + \frac{1}{c}(1-\exp(-\mu_1 cT))\left(1+\frac{\sqrt{3}\sigma_1}{\mu_1\pi}\ln\frac{\alpha_i}{1-\alpha_i}\right)\right),$$
$$Y_T^{-1}(1-\alpha_i) = Y_0 \times \exp\left(\mu_2 T + \frac{\sqrt{3}\sigma_2}{\pi}T\ln\frac{1-\alpha_i}{\alpha_i}\right). \tag{50}$$

Step 4: set

$$\beta^{\alpha_i} \longleftarrow \max\left(X_T^{-1}(\alpha_i) - Y_T^{-1}(1-\alpha_i) - K, 0\right). \tag{51}$$

If $i < N-1$, then return to Step 2.

Step 5: calculate the expectation of $(X_T - Y_T - K)^+$:

$$E\left[(X_T - Y_T - K)^+\right] \longleftarrow \frac{1}{N-1}\sum_{i=1}^{N-1}\beta^{\alpha_i}. \tag{52}$$

In the final procedure, the price of the European spread call option is derived by using Theorem 8. □

Example 1. Assume that the parameters of interest rate are $r_0 = 0.08, a = 0.05, \sigma_0 = 0.04, b = 2$, the parameters of stock price X are $X_0 = 5, \mu_1 = \sqrt{3}, \sigma_1 = 0.3, c = 0.3$, and the parameters of stock price Y are $Y_0 = 4, \mu_2 = 1, \sigma_2 = 0.2$. Then, the price of the European spread call option with maturity date $T = 1$ and strike price $K = 1$ is $f_{\text{Ecall}} = 2.0372$.

3.2. European Spread Put Option. Suppose X_t and Y_t are two asset price processes. Then, the European spread put option with maturity date T and strike price K is the contract that pays

$$(K - (X_T - Y_T))^+. \tag{53}$$

Considering time value of the stock return, the present value of the payoff is

$$\exp\left(-\int_0^T r_t \mathrm{d}t\right)(K - (X_T - Y_T))^+. \tag{54}$$

European spread put option should be the expectation of the discounted value of the stock return. So, the European spread put option has a price

$$f_{\text{Eput}} = E\left[\exp\left(-\int_0^T r_t \mathrm{d}t\right)(K - (X_T - Y_T))^+\right]. \tag{55}$$

Theorem 9. *Suppose that the European spread put option for the stock model (35) has a strike price K and an expiration time T. Then, the European spread put option pricing formula is*

$$f_{\text{Eput}} = E\left[\exp\left(-\int_0^T r_t \mathrm{d}t\right)\right]\int_0^1\left(K - \left(X_T^{-1}(1-\alpha) - Y_T^{-1}(\alpha)\right)\right)^+ \mathrm{d}\alpha. \tag{56}$$

Proof. According to Corollary 1, the European spread put option can be given in the following form:

$$f_{\text{Eput}} = E\left[\exp\left(-\int_0^T r_t \mathrm{d}t\right)\right]E\left[(K - (X_T - Y_T))^+\right]. \tag{57}$$

Since X_t, Y_t are independent uncertain processes, their α-path are, respectively, given by formulas (36) and (37). According to Theorem 1, the uncertain variable

$$(K - (X_T - Y_T))^+, \tag{58}$$

has the α-path

$$\left(K - \left(X_T^{-1}(1-\alpha) - Y_T^{-1}(\alpha)\right)\right)^+. \tag{59}$$

So, the expectation of the uncertain variable $(K - (X_T - Y_T))^+$ is given by the following equation:

$$E\left[(K - (X_T - Y_T))^+\right] = \int_0^1\left(K - \left(X_T^{-1}(1-\alpha) - Y_T^{-1}(\alpha)\right)\right)^+ \mathrm{d}\alpha. \tag{60}$$

Thus, the price of the European spread put option is

$$f_{\text{Eput}} = E\left[\exp\left(-\int_0^T r_t \mathrm{d}t\right)\right]\int_0^1\left(K - \left(X_T^{-1}(1-\alpha) - Y_T^{-1}(\alpha)\right)\right)^+ \mathrm{d}\alpha. \tag{61}$$

The pricing formula of the European spread put option is also derived.

From Theorem 9, the algorithm designed for calculating European spread put option price is the same as the procedure for calculating European spread call option price. Now, we will list the main procedures to calculate European spread put option price. First, we will calculate the expectation of $\exp(-\int_0^T r_t \mathrm{d}t)$.

Step 0: set $t_j = jT/M$, $k = 1, 2, \ldots, L$, $j = 1, 2, \ldots, M$, where L and M are two large numbers.

Step 1: set $k = 0$.

Step 2: set $k \longleftarrow k + 1$.

Step 3: set $j = 0$.

Step 4: set $j \longleftarrow j + 1$.

Step 5: calculate the value of the stochastic interest rate at the time t_j:

$$r_{t_j}^k = r_{t_{j-1}}^k + a\left(b - r_{t_{j-1}}^k\right)\left(t_j - t_{j-1}\right) + \sigma_0\sqrt{r_{t_{j-1}}^k}\sqrt{t_j - t_{j-1}}\varepsilon_j^k, \tag{62}$$

where $\varepsilon_j^k \sim N(0,1)$ are generated by stochastic simulations.

Step 6: calculate the discount rate:

$$\exp\left(-\int_0^T r_t^k \mathrm{d}t\right) \longleftarrow \exp\left(-\frac{T}{M}\sum_{j=1}^{M} r_{t_j}^k\right). \tag{63}$$

Step 7: calculate the approximated value of $E[\exp(-\int_0^T r_t \mathrm{d}t)]$:

$$E\left[\exp\left(-\int_0^T r_t \mathrm{d}t\right)\right] \longleftarrow \frac{1}{L}\sum_{k=1}^{L}\exp\left(-\frac{T}{M}\sum_{j=1}^{M} r_{t_j}^{k}\right). \quad (64)$$

Second, we will calculate $E[(K-(X_T-Y_T))^+]$.

Step 0: set $\alpha_i = i/N$, $i = 1, 2, \ldots, N-1$, where N is a large number.

Step 1: set $i = 0$.

Step 2: set $i \longleftarrow i+1$.

Step 3: calculate the inverse uncertainty distribution of the stock processes:

$$\begin{aligned} X_T^{-1}(1-\alpha_i) &= \exp\left(\exp(-\mu_1 cT)\ln X_0 + \frac{1}{c}(1-\exp(-\mu_1 cT))\right. \\ &\quad \left.\left(1+\frac{\sqrt{3}\,\sigma_1}{\mu_1\pi}\ln\frac{1-\alpha_i}{\alpha_i}\right)\right), \\ Y_T^{-1}(\alpha_i) &= Y_0\exp\left(\mu_2 T + \frac{\sqrt{3}\,\sigma_2}{\pi}T\ln\frac{\alpha_i}{1-\alpha_i}\right). \end{aligned} \quad (65)$$

Step 4: set

$$\gamma^{\alpha_i} \longleftarrow \max\left(K - \left(X_T^{-1}(1-\alpha_i) - Y_T^{-1}(\alpha_i)\right), 0\right). \quad (66)$$

If $i < N-1$, then return to Step 2.

Step 5: calculate the expectation of $(K-(X_T-Y_T))^+$:

$$E[(K-(X_T-Y_T))^+] \longleftarrow \frac{1}{N-1}\sum_{i=1}^{N-1}\gamma^{\alpha_i}. \quad (67)$$

In the final procedure, the price of the European spread put option is derived by using Theorem 9.

□

Example 2. Assume that the parameters of interest rate are $r_0 = 0.08, a = 0.05, \sigma_0 = 0.04, b = 2$, the parameters of stock price X are $X_0 = 5, \mu_1 = \sqrt{3}, \sigma_1 = 0.3, c = 0.3$, and the parameters of stock price Y are $Y_0 = 4, \mu_2 = 1, \sigma_2 = 0.2$. Then, the price of the European spread put option with maturity date $T = 1$ and strike price $K = 1$ is $f_{\mathrm{Eput}} = 1.9059$.

4. Conclusions

In this paper, we discuss the pricing of European spread options with the floating interest rate by chance theory. Some numerical algorithms are designed to calculate the price, and numerical simulations of spread options are given. Future research can think about some other multiasset option pricing problems.

Data Availability

All data used to support the findings of this study are included within this article.

Conflicts of Interest

The authors declare that they have no conflicts of interest.

Acknowledgments

This research was funded by the Youth Project of Humanities and Social Sciences of Ministry of Education (Grant nos. 19YJCZH251 and 20YJCZH245) and the Scientific Research Program of Tianjin Education Commission (Grant no. 2018KJ113).

References

[1] F. Black and M. Scholes, "The pricing of options and corporate liabilities," *Journal of Political Economy*, vol. 81, no. 3, pp. 637–654, 1973.

[2] R. C. Merton, "Theory of rational option pricing," *The Bell Journal of Economics and Management Science*, vol. 4, no. 1, pp. 141–183, 1973.

[3] J. Hull and A. White, "The pricing of options on assets with stochastic volatilities," *The Journal of Finance*, vol. 42, no. 2, pp. 281–300, 1987.

[4] S. L. Heston, "A closed-form solution for options with stochastic volatility with applications to bond and currency options," *Review of Financial Studies*, vol. 6, no. 2, pp. 327–343, 1993.

[5] B. Liu, *Uncertainty Theory*, Springer, Berlin, Germany, 2007.

[6] B. Liu, "Fuzzy process, hybrid process and uncertain process," *Journal of Uncertain Systems*, vol. 2, no. 1, pp. 3–16, 2008.

[7] B. Liu, "Some research problems in uncertainty theory," *Journal of Uncertain Systems*, vol. 3, no. 1, pp. 3–10, 2009.

[8] X. Chen, "American option pricing formula for uncertain financial market," *International Journal of Operations Research*, vol. 8, no. 2, pp. 32–37, 2011.

[9] Z. Zhang and W. Liu, "Geometric average Asian option pricing for uncertain financial market," *Journal of Uncertain Systems*, vol. 8, no. 4, pp. 317–320, 2014.

[10] X. Chen and J. Gao, "Uncertain term structure model of interest rate," *Soft Computing*, vol. 17, no. 4, pp. 597–604, 2013.

[11] K. Yao, "A no-arbitrage theorem for uncertain stock model," *Fuzzy Optimization and Decision Making*, vol. 14, no. 2, pp. 227–242, 2015.

[12] Z. Zhang, D. A. Ralescu, and W. Liu, "Valuation of interest rate ceiling and floor in uncertain financial market," *Fuzzy Optimization and Decision Making*, vol. 15, no. 2, pp. 139–154, 2016.

[13] Y. Sun and T. Su, "Mean-reverting stock model with floating interest rate in uncertain environment," *Fuzzy Optimization and Decision Making*, vol. 16, no. 2, pp. 235–255, 2017.

[14] Y. Gao, X. Yang, and Z. Fu, "Lookback option pricing problem of uncertain exponential Ornstein-Uhlenbeck model," *Soft Computing*, vol. 22, no. 17, pp. 5647–5654, 2018.

[15] R. Gao, "Stability in mean for uncertain differential equation with jumps," *Applied Mathematics and Computation*, vol. 346, pp. 15–22, 2019.

[16] Z. Lu and Y. Zhu, "Numerical approach for solution to an uncertain fractional differential equation," *Applied Mathematics and Computation*, vol. 343, pp. 137–148, 2019.

[17] Z. Li, Y.-J. Liu, and W.-G. Zhang, "Quasi-closed-form solution and numerical method for currency option with uncertain volatility model," *Soft Computing*, pp. 1–17, 2020.

[18] W. Yu, P. Guo, Q. Wang et al., "On a periodic capital injection and barrier dividend strategy in the compound Poisson risk model," *Mathematics*, vol. 8, no. 4, p. 511, 2020.
[19] W. Yu, F. Wang, Y. Huang, and H. Liu, "Social optimal mean field control problem for population growth model," *Asian Journal of Control*, vol. 21, no. 4, pp. 1–8, 2019.
[20] L. Zhang and Y. Sun, "Power options pricing in uncertain environment," *Acta Scientiarum Naturalium Universitatis Nankaiensis*, vol. 53, no. 2, pp. 1–6, 2020.
[21] B. Liu, *Uncertainty Theory*, Springer, Berlin, Germany, 2015.
[22] B. Liu, *Uncertainty Theory: A Branch of Mathematics for Modeling Human Uncertainty*, Springer, Berlin, Germany, 2010.
[23] K. Yao and X. Chen, "A numerical method for solving uncertain differential equations," *Journal of Intelligent & Fuzzy Systems*, vol. 25, no. 3, pp. 825–832, 2013.
[24] Y. Liu, "Uncertain random variables: a mixture of uncertainty and randomness," *Soft Computing*, vol. 17, no. 4, pp. 625–634, 2013.
[25] Y. Liu, "Uncertain random programming with applications," *Fuzzy Optimization and Decision Making*, vol. 12, no. 2, pp. 153–169, 2013.
[26] L. Dai, Z. Fu, and Z. Huang, "Option pricing formulas for uncertain financial market based on the exponential Ornstein-Uhlenbeck model," *Journal of Intelligent Manufacturing*, vol. 28, no. 3, pp. 597–604, 2017.

Hindawi
Mathematical Problems in Engineering
Volume 2020, Article ID 3143840, 10 pages
https://doi.org/10.1155/2020/3143840

Research Article

Optimal Investment Policy for Insurers under the Constant Elasticity of Variance Model with a Correlated Random Risk Process

Xiaotao Liu and Hailong Liu

Antai College of Economics and Management, Shanghai Jiao Tong University, Shanghai 200030, China

Correspondence should be addressed to Xiaotao Liu; manager@sjtu.edu.cn

Received 9 March 2020; Accepted 7 April 2020; Published 20 May 2020

Guest Editor: Wenguang Yu

This paper investigates the optimal portfolio choice problem for a large insurer with negative exponential utility over terminal wealth under the constant elasticity of variance (CEV) model. The surplus process is assumed to follow a diffusion approximation model with the Brownian motion in which is correlated with that driving the price of the risky asset. We first derive the corresponding Hamilton–Jacobi–Bellman (HJB) equation and then obtain explicit solutions to the value function as well as the optimal control by applying a variable change technique and the Feynman–Kac formula. Finally, we discuss the economic implications of the optimal policy.

1. Introduction

Since the seminal work of Browne [1], there is a growing literature investigating the dynamic portfolio choice problems for insurers under the stochastic optimal control framework. However, Browne [1] assumes that the risky asset's price is driven by geometric Brownian motions (GBMs), which implies that the expected instantaneous return and volatility of the risky asset are constant and deterministic. To be more empirical, nowadays, there has been a series of works analyzing the insurer's portfolio optimization problems with different variants of stochastic market settings, such as the stochastic interest rate model (e.g., Guan and Liang [2]), stochastic return model (e.g., Li et al. [3]), and stochastic volatility model (e.g., Li et al. [4] and Gu et al. [5]).

As a special stochastic volatility model, the constant elasticity of variance (CEV) model is widely used in finance theory and practice. The CEV model is a generalization of the GBM of which the variance elasticity parameter equals to zero and has been successfully employed in the option pricing literature to model the empirical observed pattern of stock prices with heavy tail (e.g., Schroder [6], Boyle and Tian [7], Davydov and Linetsky [8], and Park and Kim [9]). Moreover, the CEV model helps explain volatility smiles (Cox and Ross [10] and Cox [11]). Jones [12] further suggested that compared to Heston's stochastic volatility model, the equity index return data are better represented by a stochastic variance model in the CEV class.

Recently, due to the empirical advantage and mathematical tractability, considerable research efforts have been devoted to considering optimal investment problems under the CEV model. The most commonly selected objectives include maximizing expected utility and mean-variance criterion. For the objective of maximizing expected utility, the traditional portfolio selection problems (e.g., Zhao and Rong [13], Bakkaloglu et al. [14], and Josa-Fombellida et al. [15]), the optimal investment problem for pension plans with different classes of hyperbolic absolute risk aversion (HARA) utility functions (e.g., Xiao et al. [16], Gao [17, 18], and Jung and Kim [19]), and the optimal investment and reinsurance problem (e.g., Gu et al. [5], Gu et al. [20], Lin and Li [21], Li et al. [22], Zheng et al. [23], K. Wu and W. Wu [24], Chunxiang et al. [25], and Wang et al. [26]) are extensively investigated under the CEV model. For the objective of mean-variance criterion, Basak and Chabakauri [27] derived the closed-form optimal time-consistent investment policy for a self-financing portfolio, and lately, Shen et al. [28] discussed the corresponding precommitment solution; Li et al. [29] and Zhao et al. [30] studied the time-consistent reinsurance-investment strategy for an insurance portfolio. Li et al. [31] investigated the time-consistent investment strategy for a defined contribution (DC) pension plan. Zhang and Chen [32] also explored the asset-liability management (ALM) problem.

Even though the optimal investment problem for an insurer is more fundamental than the optimal investment-reinsurance problem, it is still worthy to be considered under the CEV model. In practice, because the reinsurance service is not cheap, large insurers with adequate risk tolerance may prefer an investment-only policy to an investment-reinsurance policy. Moreover, most of the aforementioned works specialize the assumptions to that the uncertainty source in the insurer's surplus process is perfectly uncorrelated with that in the risky asset's price process described by the CEV model, which implies that the insurance market is independent of the financial market. As a result, the optimal investment strategy derived is independent of the insurer's surplus model (see Gu et al. [20], Lin and Li [21], Gu et al. [5], and Chunxiang et al. [25]). But, some literature goes to another extreme case by assuming that the two processes are perfectly correlated and obtain the explicit solution only in the case of special variance elasticity parameters (see Wang et al. [26]); meanwhile, they show that the diffusion part of the surplus has an effect on the optimal investment policy. Yuan and Lai [33] also adopted similar assumptions in Wang et al. [26] to study the optimal investment strategy of a family with a random household expenditure, and they only derive the approximate numerical solutions.

However, in reality, besides the idiosyncratic risk, the insurer's surplus process and the risky asset's price process are affected by the systematic risk, which leads to a dependence between the two uncertainty sources. To the best of our knowledge, Browne [1] considered the correlation between the risk of the insurer's surplus process and that of the risky asset's price process under the GBMs in the investment problem of an insurer, while there has been no literature focusing on the similar problems under the CEV or other stochastic market models so far.

In this paper, we focus on the correlation that occurs between Brownian motions in the insurer's surplus process and those in the risky asset's price process, which represents the common uncertainty between the insurance and financial markets. By extending the price model of the risky asset to the CEV model, we reconsider the negative exponential utility maximizing problem of Browne [1]. The surplus process is described by the diffusion approximation model, and particularly, the Brownian motion driving price process of the risky asset is correlated with that driving the surplus process. By the stochastic optimal control theory, we first establish a three-dimensional Hamilton–Jacobi–Bellman (HJB) equation for the optimization problem and then simplify it into two parabolic partial differential equations (pdes) via a variable change technique. By the Feynman–Kac formula, we solve the two pdes and obtain the explicit expressions of value function as well as the optimal investment strategy. Finally, we compare the result with that of Browne [1] and Gu et al. [5], respectively, which are special cases of our model.

Due to the consideration of the correlation, the corresponding HJB equation becomes more difficult to solve. Specifically, the Legendre dual transformation technique introduced by Xiao et al. [16] and then heavily used in many of the aforementioned works (see Gao [17, 18] and Jung and Kim [19]) to reduce the HJB equation into a linear pde cannot be directly adapted to models with general correlation. For example, following the way, Wang et al. [26] and Yuan and Lai [33] assumed that the correlation equals to ± 1 to remove the nonlinear parts of the HJB equation. In this paper, instead of that method, we directly conjecture the functional form of the value function and by which the HJB equation can be directly simplified into two parabolic pdes. Moreover, we relax the perfect correlation restrictions. So, obtaining the explicit solution of the investment strategy in the case of imperfectly correlated uncertainty sources is a technique contribution of our paper.

Moreover, another contribution of our paper is that many interesting implications are obtained after introducing the correlation. We find that the optimal investment strategy can be separated into four independent components: the myopic, dynamic, static, and delta hedging demands. The myopic demands, also known as the Kelly criterion, are to optimize over the next instant; the dynamical hedging demands are to hedge against the fluctuations of the instantaneous volatility; the static hedging demands are to hedge against the hedgeable risk of the surplus; and the delta hedging demands are to hedge the fluctuations risk of the static hedged portfolio. In particular, both static and delta demands vanish, and our results reduce to that of Gu et al. [5] if the correlation vanishes. Asymptotic analysis further shows that, as the variance elasticity parameters approach to zero, the dynamic and delta hedging demands both vanish, and the results are equivalent to those of Browne [1].

The remainder of the article is organized as follows. In Section 2, the insurer's optimal investment problem is formulated. In Section 3, the explicit solution of the value function as well as the optimal investment policy are derived. In Section 4, the economic interpretation of the optimal investment policy is provided. Section 5 concludes this paper. The details to derive the optimal investment strategy are postponed to Appendix.

2. Problem Formulation

In this section, we will give some basic assumptions and then formulate the insurer's portfolio choice problem.

We consider a continuous-time Markovian economy with a fixed and finite time horizon $[t, T]$. Uncertainty is represented by a filtered probability space $(\Omega, \mathcal{F}, \{\mathcal{F}_s\}_{t\le s\le T}, \mathbb{P})$ satisfying the usual conditions, where $\mathcal{F}_s = \sigma((Z_1(s) \times Z_2(s)); t \le s \le T)$ is the information available until time s and $Z_1(s), Z_2(s)$ are two independent standard winner processes under measure $\mathbb{P}$. In that follows, we also assume that all stochastic processes and random variables are adapted to $\{\mathcal{F}_s\}_{t\le s\le T}$, and their moments introduced are well defined, without explicitly stating the regular conditions. Meanwhile, we also assume that trading takes place continuously over time, no transaction costs or taxes are involved in the trading, and there is no difference between lending and borrowing rate.

Without loss of generality, we assume the insurer can invest in a risk-free asset (the bank account) and a risky asset (stock). The price of the bond is given by

$$\frac{\mathrm{d}B(s)}{B(s)} = r\mathrm{d}s, \quad B(t) = 1, \tag{1}$$

where $r > 0$ is the risk-free rate. The stock price, S, follows the CEV model:

$$\frac{\mathrm{d}S(s)}{S(s)} = \mu\mathrm{d}s + \sigma S(s)^{\alpha}\mathrm{d}Z_1(s), \quad S(t) = S > 0, \tag{2}$$

where $\mu > r$ is the stock mean return; σ is a positive constant; 2α is the variance elasticity parameter; and $\sigma S(s)^{\alpha}$ is the instantaneous volatility. We also assume that $\alpha \geq 0$ as in Gu et al. [5], Li et al. [31], and Emanuel and Macbeth [34] for that the price may reach 0 for some negative α, which is also supported by the empirical estimations in Jones [12]. Since $S(s)$ is stochastic, the instantaneous volatility is also stochastic so that the insurer faces time-varying investment opportunities.

As in Browne [1], without investment, the wealth of the insurer follows a Brownian motion with drift, i.e., the diffusion limit of the classic Cramer-Lundberg risk model

$$\mathrm{d}R(s) = \mu_m\mathrm{d}s + \sigma_m\left(\rho\mathrm{d}Z_1(s) + \sqrt{1-\rho^2}\,\mathrm{d}Z_2(s)\right), \quad R(t) = 0, \tag{3}$$

where μ_m, σ_m, and ρ are all constants. As pointed out in Promislow and Young [35], when the parameters satisfy that (μ_m/σ_m) is big enough (at least 3), one will want to use this model in actuarial practice. We note that, under this setup, the market is incomplete as trading in the risky assets and bond cannot perfectly hedge against the surplus risk. However, in the special cases of perfect correlation between the stock return and risk process, $\rho = \pm 1$, dynamic market completeness is obtained.

A large insurer with adequate risk tolerance in this economy is endowed at time t with an initial wealth of W. The insurer chooses an investment policy w_s, where $w_s W(s)$ denotes the total money amount invested in the stock at time s and the remaining $1 - w_s$ portion of the wealth is invested in the risk-free asset. Thus, under policy w_s and with the initial wealth W, the wealth process $W(s)$ becomes

$$\begin{aligned}\mathrm{d}W(s) &= \frac{\mathrm{d}B(s)\left((1-w_s)W(s)\right)}{B(s)} + \frac{w_s W(s)\mathrm{d}S(s)}{S(s)} + \mathrm{d}R(s)\\ &= \left(\mu_m - r w_s W(s) + rW(s) + \mu w_s W(s)\right)\mathrm{d}s\\ &\quad + \left(\rho\sigma_m + \sigma w_s W(s)S(s)^{\alpha}\right)\mathrm{d}Z_1(s)\\ &\quad + \sqrt{1-\rho^2}\sigma_m\mathrm{d}Z_2(s).\end{aligned} \tag{4}$$

A control policy is said to be admissible if $\forall s \in [t,T], w_s$ is $\mathcal{F}_s$ progressively measurable, (4) has a unique strong solution, and $E_t[\int_t^T (w_s W(s)S(s)^{\alpha})^2\mathrm{d}s] < \infty$. Denote by $\mathcal{A}$ the collection of all admissible policies. Given the initial wealth $W(t) = W$ and spot price $S(t) = S$, the insurer aims to maximize the expected utility over terminal wealth $W(T)$, i.e.,

$$\max_{w_s\in\mathcal{A}} \mathbb{E}\left[U(W_T)\,\middle|\,W(t) = W, S(t) = S\right], \tag{5}$$

where $U(\cdot)$ is utility function satisfying $U\prime(W) > 0, U''(W) < 0$. In this paper, we specialize our setting that the insurer is guided by a constant absolute risk aversion (CARA) preference

$$U(W) = \frac{-e^{-\gamma W}}{\gamma}, \tag{6}$$

where $\gamma = -(U''(W)/U'(W)) > 0$ is the absolute risk aversion coefficient. Note that this function plays a vital role in actuarial mathematics and insurance practice for that it is the unique utility function under the principle of "zero utility" giving a fair premium that is independent of the level of reserves of insurers.

Remark 1. If $\alpha = 0$, the CEV model turns into the geometric Brownian motion process; then, our problem is equivalent to the utility maximizing problem in Browne [1].

Remark 2. If $\rho = 0$, our problem degenerates into the optimal investment-only problem in Gu et al. [5].

3. Problem Solution

In this section, we first provide the general framework for optimization problems (4) and (5) by using the classical tools of stochastic optimal control and then try to simplify the corresponding Hamilton–Jacobi–Bellman (HJB) equation into two parabolic pdes via a variable change technique. Finally, we solve the two parabolic pdes by the Feynman–Kac formula and obtain the value function as well as the optimal investment policy.

3.1. General Framework. For portfolio choice problem (5) with dynamic budget constrain (4), since the wealth process $W(s)$ contains two state variables $S(s), W(s)$, we can write the value function as

$$J(t,W,S) = \max_{w\in\mathcal{A}} \mathbb{E}\left[U(W_T)\,\middle|\,W(t) = W, S(t) = S\right]. \tag{7}$$

According to the classical dynamic programming principle, $J(t,W,S)$ satisfies the following HJB equation:

$$0 = \max_{w \in \mathscr{A}} \mathscr{A}^w J(t, W, S), \tag{8a}$$

$$\begin{aligned}\mathscr{A}^w f(t, W, S) = {} & f_W (\mu_m - r(w-1)W + \mu w W) \\ & + f_{WS}\left(\rho\sigma\sigma_m S^{\alpha+1} + \sigma^2 w W S^{2\alpha+1}\right) \\ & + f_{WW}\left(\frac{\sigma_m^2}{2} + \rho\sigma w W \sigma_m S^{\alpha} + \frac{1}{2}\sigma^2 w^2 W^2 S^{2\alpha}\right) \\ & + \frac{1}{2}\sigma^2 f_{SS} S^{2\alpha+2} + \mu S f_S + f_t,\end{aligned} \tag{8b}$$

$$J(T, W, S) = U(W), \quad \forall S, \tag{8c}$$

where $\mathscr{A}^w f(t, W, S)$ is the infinitesimal generator for w controlled stochastic process (4). Assuming there exists a sufficiently smooth solution $J(t, W, S)$ to the HJB equation, differentiating (8a)–(8c) with respect to w gives the first-order condition:

$$w^* = \frac{J_W (r-\mu) S^{-2\alpha}}{\sigma^2 W J_{WW}} - \frac{S J_{WS}}{W J_{WW}} - \frac{\rho\sigma_m S^{-\alpha}}{\sigma W}, \tag{9}$$

while the second-order condition is $\sigma^2 W^2 S^{2\alpha} J_{SS} \leq 0$, which, in other words, says that $J(t, W, S)$ must be concave as a function of W. Inserting first-order condition (9) into (8a)–(8c) yields after some routine manipulations the following two-dimensional nonlinear parabolic pde:

$$\begin{aligned}0 = {} & J_W\left(\frac{S J_{WS}(r-\mu)}{J_{WW}} + \mu_m + \frac{\rho\sigma_m (r-\mu) S^{-\alpha}}{\sigma} + rW\right) \\ & - \frac{1}{2}\left(\rho^2 - 1\right) J_{WW} \sigma_m^2 \\ & - \frac{J_W^2 (r-\mu)^2 S^{-2\alpha}}{2\sigma^2 J_{WW}} + \frac{1}{2}\sigma^2 J_{SS} S^{2\alpha+2} - \frac{\sigma^2 J_{WS}^2 S^{2\alpha+2}}{2 J_{WW}} \\ & + \mu S J_S + J_t,\end{aligned} \tag{10}$$

with boundary condition (8c).

Here, we notice that the optimal portfolio choice problem has been transformed into a nonlinear pde. The goal now is to construct an explicit solution to (10) and then incorporate the solution in (9) and obtain the optimal investment policy. However, as it stands, it is difficult to solve (10). Therefore, we shall first reduce the dimension and remove the nonlinearity of HJB equation (10).

3.2. Simplifying the Nonlinear PDE. Inspired by Browne [1], Gu et al. [5], and Gao [18], we try to conjecture a solution to (10) taking the following functional form:

$$J(t, W, S) = -\frac{\exp(g(t, S)) \exp(-\gamma \exp(r(T-t))(h(t, S) + W))}{\gamma}. \tag{11}$$

Then, we have

$$\left(\frac{J_S}{J}\right) = g_S - \gamma h_S e^{r(T-t)}, \tag{12a}$$

$$\left(\frac{J_{SS}}{J}\right) = -\gamma e^{r(T-t)}\left(2 g_S h_S + h_{SS}\right) + g_S^2 + g_{SS} + \gamma^2 h_S^2 e^{2r(T-t)}, \tag{12b}$$

$$\left(\frac{J_W}{J}\right) = \gamma\left(-e^{r(T-t)}\right), \tag{12c}$$

$$\left(\frac{J_{WS}}{J}\right) = \gamma e^{r(T-t)}\left(\gamma h_S e^{r(T-t)} - g_S\right), \tag{12d}$$

$$\left(\frac{J_{WW}}{J}\right) = \gamma^2 e^{2r(T-t)}, \tag{12e}$$

$$\left(\frac{J_t}{J}\right) = g_t + \gamma e^{r(T-t)}\left(r(h+W) - h_t\right). \tag{12f}$$

Incorporating these partial derivatives in (10) and after some simplifications, we obtain

$$\begin{aligned}0 = {} & rSg_S + \frac{1}{2}\sigma^2 g_{SS} S^{2\alpha+2} + g_t - \frac{(r-\mu)^2 S^{-2\alpha}}{2\sigma^2} \\ & - \gamma e^{r(T-t)}\left(rSh_S - hr + \frac{1}{2}\sigma^2 h_{SS} S^{2\alpha+2} + h_t\right. \\ & \left. + \mu_m + \frac{\rho\sigma_m (r-\mu) S^{-\alpha}}{\sigma} + \frac{1}{2}\gamma\left(\rho^2 - 1\right)\sigma_m^2 e^{r(T-t)}\right).\end{aligned} \tag{13}$$

We can decompose (13) into two independent linear parabolic pdes (14) and (16), and also by (6), we have boundary conditions (15) and (17):

$$0 = rSg_S + \frac{1}{2}\sigma^2 g_{SS} S^{2\alpha+2} + g_t - \frac{(r-\mu)^2 S^{-2\alpha}}{2\sigma^2}, \tag{14}$$

$$0 = g(T, S), \quad \forall S, \tag{15}$$

$$\begin{aligned}0 = {} & rSh_S - hr + \frac{1}{2}\sigma^2 h_{SS} S^{2\alpha+2} + h_t + \mu_m \\ & + \frac{\rho\sigma_m (r-\mu) S^{-\alpha}}{\sigma} + \frac{1}{2}\gamma\left(\rho^2 - 1\right)\sigma_m^2 e^{r(T-t)},\end{aligned} \tag{16}$$

$$0 = h(T, S), \quad \forall S. \tag{17}$$

Here, we have simplified the nonlinear pde to two linear parabolic pdes; the problem now is to solve (14) and (16) and replace the solutions in (11) and (9) so as to find the optimal investment policy.

3.3. Explicit Solution for the Insurer's Optimal Investment Problem. Since the problem for $\alpha = 0$ has been investigated in Browne [1], we, here, mainly focus on the solutions for $\alpha > 0$. By the techniques of stochastic analysis, we can obtain explicit solutions to (14) and (16), and we have the following theorem.

Theorem 1. *For portfolio choice problem (5), a solution to HJB equation (8a)–(8c) with terminal condition (10) is given by $J(t,W,S)$, and the corresponding optimal investment policy is given by w^* in feedback form if $\alpha > 0$, where*

$$J(t,W,S) = -\frac{\exp(g(t,S))\exp(-\gamma\exp(r(T-t))(h(t,S)+W))}{\gamma}, \tag{18}$$

$$\begin{aligned} w^* &= \frac{S^{-2\alpha}e^{r(t-T)}(\mu - r - 2\alpha\sigma^2 f_1(t))}{\gamma\sigma^2 W} - \frac{\rho\sigma_m S^{-\alpha}}{\sigma W} - \frac{Sh_S}{W} \\ &= \frac{S^{-2\alpha}e^{r(t-T)}(\mu - r - 2\alpha\sigma^2 f_1(t))}{\gamma\sigma^2 W} - \frac{\rho\sigma_m S^{-\alpha}}{\sigma W} \\ &\quad - \frac{\rho\sigma_m S(r-\mu)\left(\int_t^T e^{-r(s-t)}Dl(s,S)\mathrm{d}s\right)}{\sigma W}, \end{aligned} \tag{19}$$

$$\begin{aligned} g(t,S) &= f_1(t)S^{-2\alpha} + f_0(t), \\ f_1(t) &= \frac{(r-\mu)^2(e^{-2\alpha r(T-t)} - 1)}{4\alpha r\sigma^2}, \\ f_0(t) &= \frac{(2\alpha+1)(r-\mu)^2((2\alpha r(t-T)+1) - e^{-2\alpha r(t-T)})}{8\alpha r^2}, \\ h(t,S) &= \frac{\rho\sigma_m(r-\mu)}{\sigma}\int_t^T e^{-r(s-t)}l(s,S)\mathrm{d}s + \frac{\mu_m(1-e^{-r(t-T)})}{r} - \frac{\gamma(\rho^2-1)\sigma_m^2\sinh(r(t-T))}{2r}, \\ l(s,S) &= \frac{\Gamma((3/2)+(1/2\alpha))e^{\alpha(-r)(s-t)}{}_1F_1(-(1/2);\,(2\alpha+1/2\alpha);\,-S^{-2\alpha}M(s))}{\Gamma(1+(1/2\alpha))\sqrt{M(s)}}, \\ Dl(s,S) &= -\frac{\alpha\Gamma((3/2)+(1/2\alpha))\sqrt{M(s)}S^{-2\alpha-1}e^{\alpha r(t-s)}{}_1F_1((1/2);\,2+(1/2\alpha);\,-S^{-2\alpha}M(s))}{\Gamma(2+(1/2\alpha))}, \\ M(s) &= \frac{r}{\alpha\sigma^2(e^{2\alpha r(s-t)}-1)}. \end{aligned} \tag{20}$$

Here, $\Gamma(\cdot)$ is the gamma function and ${}_1F_1(a;b;z)$ denotes the confluent hypergeometric function, which is defined as follows:

$${}_1F_1(a;b;z) = \frac{\Gamma(b)}{\Gamma(a)\Gamma(b-a)}\int_0^1 t^{a-1}(1-t)^{b-a-1}\exp(zt)\mathrm{d}t. \tag{21}$$

Proof. The solution for $g(t,S), h(t,S)$ can be seen from Appendix. Inserting (18) into (9) yields (19). □

Remark 3. Obviously, Theorem 3 of Gu et al. [5] is the special case of our results as $\rho = 0$. Furthermore, let $\sigma_m = 0$, and the optimal investment policy also reduces to the results of Gao [17, 18].

Remark 4. According to Theorem 1, we find that the dollar amount invested in the risky asset, w^*W, is independent of the insurer's current wealth W, which results from the property of CARA utility function and is consistent with the results of Gu et al. [5], Gao [17, 18], and Gu et al. [20].

Remark 5. $h(t,S)$ is the indifference pricing of the surplus, which is an analog of equation (80) in Browne [1]. In general, indifference pricing depends on the instantaneous volatility of the risky assets. Consequently, the indifference pricing under the CEV model must be function of S unless $\alpha = 0$. However, as $\alpha \longrightarrow 0^+$, $h(t,S)$ would reduce to equation (80) in Browne [1], which will be shown later in (34).

4. Discussion

In this section, we discuss the economic interpretation of the optimal investment policy by decomposing it in different parts.

4.1. Economic Interpretation of the Optimal Investment Policy. It is easy to write the optimal investment policy w^* as the following structure:

$$w^* = w_{\text{myopic}}(t) + w_{\text{dhedge}}(t) + w_{\text{shedge}}(t) + w_{\text{deltahedge}}(t), \tag{22}$$

where

$$\begin{aligned}
w_{\text{myopic}}(t) &= \frac{(\mu - r)S^{-2\alpha}e^{-r(T-t)}}{\gamma\sigma^2 W},\\
w_{\text{dhedge}}(t) &= -\frac{2\alpha f_1(t)S^{-2\alpha}e^{r(t-T)}}{\gamma W},\\
w_{\text{shedge}}(t) &= -\frac{\rho\sigma_m S^{-\alpha}}{\sigma W},\\
w_{\text{deltahedge}}(t) &= -\frac{\rho\sigma_m S^{-\alpha}}{\sigma W}.
\end{aligned} \tag{23}$$

To gain a detailed insight on the optimal investment policy, we first consider the results for special model parameters.

Corollary 1. *If $\mu_m = 0$ and $\sigma_m = 0$, then $h(t,S) = 0$, $w_{shedge}(t) = 0$, and $w_{deltahedge}(t) = 0$, and the value function $J(t,W,S)$ is given by*

$$J(t,W,S) = -\frac{\exp(g(t,S))\exp(-\gamma\exp(r(T-t))W)}{\gamma}, \tag{24}$$

and the corresponding investment policy reduces to

$$w^* = w_{\text{myopic}}(t) + w_{\text{dhedge}}(t). \tag{25}$$

Note that if $\mu_m = 0$ and $\sigma_m = 0$, the surplus process of the insurer vanishes, and the portfolio is self-financing. If the insurer invests all the wealth in the risk-free asset, the expected utility at time T would be $J(t,W,S) = -(e^{-\gamma W e^{r(T-t)}}/\gamma)$. However, by taking an optimal investment policy on both risk-free asset and risky asset, the value function is modified by a factor $e^{g(t,S)}$. Since $g(t,S) < 0, \forall t < T, S > 0$, the insurer's welfare is always improved by investment in the risky asset.

The optimal investment policy given by (25) consists of the myopic demands and the dynamic hedging demands. The myopic demands, $w_{\text{myopic}}(t)$, also known as the Kelly criterion, would be the investment policy for an insurer who optimizes over the next instant, not accounting for her future investment. The dynamical hedging demands, $w_{\text{dhedge}}(t)$, arise due to the need to hedge against the fluctuations in the investment opportunities because of the stochastic volatility.

Different from the strategy in Gu et al. [5], besides the myopic and dynamic hedging parts, there exist another two terms in the optimal investment strategy in our model. We denote $w_{\text{shedge}}(t)$ and $-(Sh_S/W)$ as static hedging demands and delta hedging demands, respectively. To investigate the role of static hedging demands, suppose that the insurer adopts a policy by investing $w_{\text{shedge}}W = -(\rho\sigma_m S(s)^{-\alpha}/\sigma)$ dollar amount of money in the risky asset at time s; then, the dynamics of the wealth, $W_c(s)$, would be

$$\begin{aligned}
\mathrm{d}W_c(s) &= -\frac{\rho\sigma_m S(s)^{-\alpha}}{\sigma}(\mathrm{d}S(s)/S(s)) + \mathrm{d}R(s) + r\frac{\rho\sigma_m S(s)^{-\alpha}}{\sigma}\mathrm{d}s\\
&= \left(\mu_m - \frac{(\mu - r)\rho\sigma_m S(s)^{-\alpha}}{\sigma}\right)\mathrm{d}s + \sqrt{1-\rho^2}\sigma_m \mathrm{d}Z_2(s).
\end{aligned} \tag{26}$$

Note that (26) contains only $\mathrm{d}Z_2(s)$, the unhedgeable part of risk of the surplus, while the hedgeable risk $\mathrm{d}Z_1(s)$ vanishes, which implies that static hedging demands w_{shedge} perfectly hedge the hedgeable risk of the surplus. For special case of complete market, i.e., $\rho = \pm 1$, the unhedgeable risk also vanishes.

However, unless $\alpha = 0$, the wealth of the insurer in (26) is still stochastic as the drift term contains $S(s)$, which results in the delta hedging demands. The delta hedge demands can also be understood in the viewpoint of derivative pricing. Recall $h(t,S)$ is the indifference pricing of the surplus; by Ito's lemma, the dynamics for the portfolio $(h(t,S), -Sh_S(t,S))$ become

$$\begin{aligned}
&\mathrm{d}h(s,S(s)) - S(s)h_{SS}(s,S(s))(\mathrm{d}S(s) - r)\\
&= \mathrm{d}s\left(rS(s)h_{SS} + \frac{1}{2}\sigma^2 S(s)^{2\alpha+2}h_{SS}(s,S(s)) + h_t(s,S(s))\right),
\end{aligned} \tag{27}$$

which implies that the portfolio is free of risk. Therefore, we call $-(Sh_S/W)$ the delta hedge demands.

Corollary 2. *If $\rho\sigma_m = 0$, investment policy is given by*

$$w^* = w_{\text{myopic}}(t) + w_{\text{dhedge}}(t). \tag{28}$$

On the one hand, if $\rho = 0$, i.e., the risk of the financial market is perfectly uncorrelated with that of the surplus, taking positions in the risky asset does not help to reduce the surplus risk so that the static hedging demands vanish. Moreover, the surplus is independent of risk asset states, which leads to the delta hedge demands vanishing as well. On the other hand, if $\sigma_m = 0$, the surplus is equivalent to an annuity contract with continuous-time payoff μ_m, and $h(t,S) = (\mu_m(1 - e^{-r(T-t)})/r)$ is exactly its present value. Both static and delta hedge demands vanish for that the surplus and its indifference pricing are deterministic, and there is no need to hedging.

In addition to the parameters of the surplus, the variance elasticity parameter, α, is also worthy of discussing. Obviously, the optimal investment policy given by Theorem 1 is not well defined at $\alpha = 0$; instead, we are interested in its asymptotic behavior as $\alpha \longrightarrow 0^+$ and obtain the following corollary.

Corollary 3.

$$\lim_{\alpha \longrightarrow 0^+} w^* = \frac{(\mu - r)e^{r(t-T)}}{\gamma\sigma^2 W} - \frac{\rho\sigma_m}{\sigma W}. \tag{29}$$

Proof. As $\alpha \longrightarrow 0^+$, we have

$$\begin{aligned}
\lim_{\alpha \longrightarrow 0^+} f_1(t) &= \frac{(r-\mu)^2(t-T)}{2\sigma^2},\\
\lim_{\alpha \longrightarrow 0^+} f_0(t) &= 0.
\end{aligned} \tag{30}$$

Henceforth,

Table 1: Four parts of the optimal investment policy versus the parameters of the surplus and elasticity variance.

	Myopic	Dynamic	Static	Delta	Related works
$\alpha = 0, \rho\sigma_m = 0$	√				Special cases of Browne [1]
$\alpha \neq 0, \rho\sigma_m = 0$	√	√			Gu et al. [5] and Gao [17, 18]
$\alpha = 0, \rho\sigma_m \neq 0$	√		√		Browne [1]
$\alpha \neq 0, \rho\sigma_m \neq 0$	√	√	√	√	This paper

$$\lim_{\alpha \longrightarrow 0^+} g(t,S) = \frac{(r-\mu)^2(t-T)}{2\sigma^2}. \tag{31}$$

As

$$\begin{aligned} -\frac{r(\coth(\alpha r\tau)-1)}{2\alpha\sigma^2} &= -\frac{1}{2\alpha^2(\sigma^2\tau)} + \frac{r}{2\alpha\sigma^2} - \frac{r^2\tau}{6\sigma^2} \\ &\quad + \frac{\alpha^2 r^4\tau^3}{90\sigma^2} + O(\alpha^4), \\ {}_1F_1(a;b;z) &= \frac{\Gamma(b)}{\Gamma(b-a)}(-z)^{-a}(1+O(1/z)) \\ &\quad + \frac{\Gamma(b)}{\Gamma(a)}e^z z^{a-b}(1+O(1/z)), \\ &\quad \text{if } (|z| \longrightarrow \infty), \end{aligned} \tag{32}$$

we have

$$\begin{aligned} \lim_{\alpha \longrightarrow 0^+} l(s,S) &= 1, \\ \lim_{\alpha \longrightarrow 0^+} Dl(s,S) &= 0. \end{aligned} \tag{33}$$

Thus,

$$\begin{aligned} \lim_{\alpha \longrightarrow 0^+} h(t,S) &= -\frac{\gamma(\rho^2-1)\sigma_m^2 \sinh(r(t-T))}{2r} \\ &\quad - \frac{\rho\sigma_m(r-\mu)(e^{r(t-T)}-1)}{r\sigma} \\ &\quad - \frac{\mu_m(e^{r(t-T)}-1)}{r}, \end{aligned} \tag{34}$$

and the corresponding investment policy is (29). □

Remark 6. The CEV model with $\alpha = 0$ reduces to the GMBs, and our results in (29) is the same as those in Theorem 5 of Browne [1], which implies that the optimal investment policy is right continuous at $\alpha = 0$.

Note that if $\alpha = 0$, the investment opportunities are constant so that the dynamical hedging demands disappear. Meanwhile, the dynamics of $W_c(s)$ given by (29) become to

$$\mathrm{d}W_c(s) = \left(\mu_m - \frac{(\mu-r)\rho\sigma_m}{\sigma}\right)\mathrm{d}s + \sqrt{1-\rho^2}\sigma_m \mathrm{d}Z_2(s), \tag{35}$$

which implies that the static hedged portfolio is independent of the market states S. As a result, the delta hedge demands also vanish.

In total, we summarize the results of the above corollaries in Table 1.

5. Conclusion

We had investigated the optimal portfolio choice problem for a large insurer with negative exponential utility over terminal wealth. In particular, we applied the constant elasticity of variance (CEV) model to describe the price dynamics of the risky asset and allowed the Brownian motion driving the price process which was correlated with the Brownian motion driving the surplus process. By adopting a stochastic control approach, variable change technique, and the Feynman–Kac formula, we had obtained the explicit form expressions for the value function as well as the optimal investment policy. We had decomposed the optimal investment policy into four independent parts and discussed the effects of each component.

In future research concerning the optimal portfolio choice under the CEV model, it would be very interesting to extend our analysis to the case of more sophisticated surplus model, such as the classic Cramér–Lundberg risk models, jump-diffusion models, perturbed compound Poisson risk model (e.g., Peng et al. [36] and Yu et al. [37]), absolute ruin insurance risk model (e.g., Yu et al. [38]), and Lévy process (e.g., Huang et al. [39] and Zhang et al. [40]). Besides the negative exponential utility, optimal investment problems in terms of other utilities or even other objectives such as minimizing the ruin probability and the mean-variance criterion are also worthy of being investigated. Moreover, other stochastic optimal control or actuarial problems with the geometric Brownian motion settings (e.g., Yu et al. [41, 42]) can also be extended to the CEV model.

Appendix

We give some technical lemmas that are used in the proof of the main results in the paper.

Lemma 1. *If $S(s)$ follows the constant elasticity of variance process*

$$\frac{\mathrm{d}S(s)}{S(s)} = r\mathrm{d}s + \sigma S(s)^\alpha \mathrm{d}Z_1(s), \quad S(t) = S > 0, \tag{A.1}$$

with $\alpha \geq 0$, then $S(s)^{-2\alpha}$ follows the Cox–Ingersoll–Ross (CIR) model and admits a unique strong solution.

Proof. By Ito's lemma, we have

$$\begin{aligned} \mathrm{d}S(s)^{-2\alpha} &= \alpha\Big((2\alpha+1)\sigma^2 - 2rS(s)^{-2\alpha}\Big)\mathrm{d}s - 2\alpha\sigma S(s)^{-\alpha}\mathrm{d}Z_1(s) \\ &= \kappa\Big(\lambda - S(s)^{-2\alpha}\Big)\mathrm{d}s + \theta\sqrt{S(s)^{-2\alpha}}\mathrm{d}Z_1(s), \end{aligned} \tag{A.2}$$

where $\kappa = 2\alpha r, \lambda = ((2\alpha+1)\sigma^2/2r), \theta = -2\alpha\sigma$. Feller's square root condition $2\kappa\lambda - \theta^2 = 2\alpha\sigma^2 \geq 0$ is satisfied for all $\alpha \geq 0$; henceforth, $S(s)^{-2\alpha}$ admits a unique strong solution and is positive for all $s \in [t, T]$. □

Lemma 2. *If $X(s)$ is described by the Cox–Ingersoll–Ross (CIR) process*

$$\mathrm{d}X(s) = \kappa(\lambda - X(s))\mathrm{d}s + \theta\sqrt{X(s)}\mathrm{d}Z_1(s), \quad X(t) = X, \tag{A.3}$$

then

$$\mathbb{E}\left[X(s)^p \mid X(t) = X\right] = \frac{e^{\kappa(-p)\tau}\Big(2\kappa/\theta^2\left(e^{\kappa\tau}-1\right)\Big)^{-p}\Gamma\Big(p + \big(2\kappa\lambda/\theta^2\big)\Big)\,{}_1F_1\Big(-p; \big(2\kappa\lambda/\theta^2\big); -\big(2\kappa/\theta^2\big)\left(X/\left(e^{\kappa\tau}-1\right)\right)\Big)}{\Gamma\big(2\kappa\lambda/\theta^2\big)}, \tag{A.4}$$

for all $p > 0$, where $\tau = s - t > 0, \Gamma(\cdot)$ is the gamma function and ${}_1F_1(a; b; z)$ denotes the confluent hypergeometric function.

Proof. See Section 3 of Dereich et al. [43]. □

Proof of Theorem 1. □

Proof. We will first solve $g(t, S)$. By the Feynman–Kac formula (cf. Theorem 1 of Appendix E in Duffie [44]), $g(t, S)$ can be expressed as a conditional expectation:

$$g(t,S) = -\widetilde{\mathbb{E}}\left[\int_t^T \left(\frac{(r-\mu)^2\widetilde{S}(s)^{-2\alpha}}{2\sigma^2}\right)\mathrm{d}s \Big| \widetilde{S}(t) = S\right], \quad \forall t < T, \tag{A.5}$$

where $\widetilde{\mathbb{E}}[\widetilde{S}(t) = S]$ denotes the expectation under a new probability measure $\widetilde{\mathbb{P}}$, and $\widetilde{S}(s)$ follows dynamics:

$$\frac{\mathrm{d}\widetilde{S}(s)}{\widetilde{S}(s)} = r\mathrm{d}s + \sigma\widetilde{S}(s)^{\alpha}\mathrm{d}\widetilde{Z}(s), \quad \widetilde{S}(t) = S. \tag{A.6}$$

Here, $\widetilde{Z}(s)$ is a $\widetilde{\mathbb{P}}$-measure standard Brownian motion. By Lemma 1, $\widetilde{S}(s)^{-2\alpha}$ follows the Cox–Ingersoll–Ross model, and by Lemma 2, the conditional expectation is given by

$$\begin{aligned} \widetilde{\mathbb{E}}_t\left[\widetilde{S}(s)^{-2\alpha}\right] &= \widetilde{\mathbb{E}}[\widetilde{X}(s) \mid \widetilde{X}(t) = S] \\ &= \frac{(2\alpha+1)\sigma^2}{2r} + e^{-2\alpha r(s-t)}\left(S^{-2\alpha} - \frac{(2\alpha+1)\sigma^2}{2r}\right). \end{aligned} \tag{A.7}$$

Inserting (A.7) into (A.5) and after some manipulation yield

$$g(t,S) = f_1(t)S^{-2\alpha} + f_0(t), \tag{A.8}$$

where

$$\begin{aligned} f_1(t) &= \frac{(r-\mu)^2\left(e^{-2\alpha r(T-t)} - 1\right)}{4\alpha r\sigma^2}, \\ f_0(t) &= \frac{(2\alpha+1)(r-\mu)^2\left((2\alpha r(t-T)+1) - e^{-2\alpha r(T-t)}\right)}{8\alpha r^2}. \end{aligned} \tag{A.9}$$

Note that since $\alpha > 0$, we have $f_1(t) < 0, f_0(t) < 0, \forall t < T$. Henceforth, $g(t, S) < 0, \forall S > 0, t < T$.

For (18), by the Feynman–Kac theorem, $h(t, S)$ can also be expressed as a conditional expectation:

$$\begin{aligned} h(t,S) &= \widetilde{\mathbb{E}}\left[\int_t^T e^{-r(s-t)}\left(\frac{\rho\sigma_m(r-\mu)\widetilde{S}(s)^{-\alpha}}{\sigma} \right.\right. \\ &\quad \left.\left. + \mu_m - \frac{1}{2}\gamma\left(1-\rho^2\right)\sigma_m^2 e^{r(T-s)}\right)\mathrm{d}s \mid \widetilde{S}(t) = S\right] \\ &= \int_t^T e^{-r(s-t)}\widetilde{\mathbb{E}}\left[\left(\frac{\rho\sigma_m(r-\mu)\widetilde{S}(s)^{-\alpha}}{\sigma}\right) \mid \widetilde{S}(t) = S\right]\mathrm{d}s + A(t) \\ &= \frac{\rho\sigma_m(r-\mu)}{\sigma}\int_t^T e^{-r(s-t)}l(s,S)\mathrm{d}s + A(t), \end{aligned} \tag{A.10}$$

where

$$\begin{aligned} A(t) &= \frac{\mu_m\left(1 - e^{-r(T-t)}\right)}{r} - \frac{\gamma\left(\rho^2-1\right)\sigma_m^2\sinh(r(t-T))}{2r}, \\ l(s,S) &= \widetilde{\mathbb{E}}\left[\widetilde{S}(s)^{-\alpha} \,\Big|\, \widetilde{S}(t) = S\right]. \end{aligned} \tag{A.11}$$

Also, together by Lemmas 1 and 2, we have

$$\begin{aligned} l(s,S) &= \widetilde{\mathbb{E}}\left[\widetilde{X}(s)^{(1/2)} \,\Big|\, \widetilde{X}(t) = S^{-2\alpha}\right] \\ &= \frac{\Gamma((3/2)+(1/2\alpha))e^{\alpha(-r)\tau}\,{}_1F_1\left(-(1/2); (2\alpha+1/2\alpha); -S^{-2\alpha}M(\tau)\right)}{\Gamma(1+(1/2\alpha))\sqrt{M(\tau)}}, \end{aligned} \tag{A.12}$$

where $\tau = s - t, M(\tau) = \left(r/\alpha\sigma^2\left(e^{2\alpha r\tau} - 1\right)\right)$. □

Data Availability

No data were used to support this study.

Conflicts of Interest

The authors declare that they have no conflicts of interest.

Acknowledgments

This work was supported by the National Natural Science Foundation of China (grant no. 71873088).

References

[1] S. Browne, "Optimal investment policies for a firm with a random risk process: exponential utility and minimizing the probability of ruin," *Mathematics of Operations Research*, vol. 20, no. 4, pp. 937–958, 1995.

[2] G. Guan and Z. Liang, "Optimal reinsurance and investment strategies for insurer under interest rate and inflation risks," *Insurance: Mathematics and Economics*, vol. 55, pp. 105–115, 2014.

[3] Y. Li, H. Qiao, S. Wang, and L. Zhang, "Time-consistent investment strategy under partial information," *Insurance: Mathematics and Economics*, vol. 65, pp. 187–197, 2015.

[4] Z. Li, Y. Zeng, and Y. Lai, "Optimal time-consistent investment and reinsurance strategies for insurers under Heston's SV model," *Insurance: Mathematics and Economics*, vol. 51, no. 1, pp. 191–203, 2012.

[5] A. Gu, X. Guo, Z. Li, and Y. Zeng, "Optimal control of excess-of-loss reinsurance and investment for insurers under a CEV model," *Insurance: Mathematics and Economics*, vol. 51, no. 3, pp. 674–684, 2012.

[6] M. Schroder, "Computing the constant elasticity of variance option pricing formula," *The Journal of Finance*, vol. 44, no. 1, pp. 211–219, 1989.

[7] P. P. Boyle and Y. S. Tian, "Pricing lookback and barrier options under the CEV process," *The Journal of Financial and Quantitative Analysis*, vol. 34, no. 2, pp. 241–264, 1999.

[8] D. Davydov and V. Linetsky, "Pricing and hedging path-dependent options under the CEV process," *Management Science*, vol. 47, no. 7, pp. 949–965, 2001.

[9] S.-H. Park and J.-H. Kim, "Asymptotic option pricing under the CEV diffusion," *Journal of Mathematical Analysis and Applications*, vol. 375, no. 2, pp. 490–501, 2011.

[10] J. C. Cox and S. A. Ross, "The valuation of options for alternative stochastic processes," *Journal of Financial Economics*, vol. 3, no. 1-2, pp. 145–166, 1976.

[11] J. C. Cox, "The constant elasticity of variance option pricing model," *The Journal of Portfolio Management*, vol. 23, no. 5, pp. 15–17, 1996.

[12] C. S. Jones, "The dynamics of stochastic volatility: evidence from underlying and options markets," *Journal of Econometrics*, vol. 116, no. 1-2, pp. 181–224, 2003.

[13] H. Zhao and X. Rong, "Portfolio selection problem with multiple risky assets under the constant elasticity of variance model," *Insurance: Mathematics and Economics*, vol. 50, no. 1, pp. 179–190, 2012.

[14] A. Bakkaloglu, T. Aziz, A. Fatima, F. M. Mahomed, and C. M. Khalique, "Invariant approach to optimal investment-consumption problem: the constant elasticity of variance (CEV) model," *Mathematical Methods in the Applied Sciences*, vol. 40, no. 5, pp. 1382–1395, 2017.

[15] R. Josa-Fombellida, P. López-Casado, and J. P. Rincón-Zapatero, "Portfolio optimization in a defined benefit pension plan where the risky assets are processes with constant elasticity of variance," *Insurance: Mathematics and Economics*, vol. 82, pp. 73–86, 2018.

[16] J. Xiao, Z. Hong, and C. Qin, "The constant elasticity of variance (CEV) model and the Legendre transform-dual solution for annuity contracts," *Insurance: Mathematics and Economics*, vol. 40, no. 2, pp. 302–310, 2007.

[17] J. Gao, "Optimal investment strategy for annuity contracts under the constant elasticity of variance (CEV) model," *Insurance: Mathematics and Economics*, vol. 45, no. 1, pp. 9–18, 2009.

[18] J. Gao, "Optimal portfolios for DC pension plans under a CEV model," *Insurance: Mathematics and Economics*, vol. 44, no. 3, pp. 479–490, 2009.

[19] E. J. Jung and J. H. Kim, "Optimal investment strategies for the HARA utility under the constant elasticity of variance model," *Insurance: Mathematics and Economics*, vol. 51, no. 3, pp. 667–673, 2012.

[20] M. Gu, Y. Yang, S. Li, and J. Zhang, "Constant elasticity of variance model for proportional reinsurance and investment strategies," *Insurance: Mathematics and Economics*, vol. 46, no. 3, pp. 580–587, 2010.

[21] X. Lin and Y. Li, "Optimal reinsurance and investment for a jump diffusion risk process under the CEV model," *North American Actuarial Journal*, vol. 15, no. 3, pp. 417–431, 2011.

[22] Q. Li, M. Gu, and Z. Liang, "Optimal excess-of-loss reinsurance and investment polices under the CEV model," *Annals of Operations Research*, vol. 223, no. 1, pp. 273–290, 2014.

[23] X. Zheng, J. Zhou, and Z. Sun, "Robust optimal portfolio and proportional reinsurance for an insurer under a CEV model," *Insurance: Mathematics and Economics*, vol. 67, pp. 77–87, 2016.

[24] K. Wu and W. Wu, "Optimal controls for a large insurance under a CEV model: based on the Legendre transform-dual method," *Journal of Quantitative Economics*, vol. 14, no. 2, pp. 167–178, 2016.

[25] A. Chunxiang, Y. Lai, and Y. Shao, "Optimal excess-of-loss reinsurance and investment problem with delay and jump-diffusion risk process under the CEV model," *Journal of Computational and Applied Mathematics*, vol. 342, pp. 317–336, 2018.

[26] Y. Wang, X. Rong, and H. Zhao, "Optimal investment strategies for an insurer and a reinsurer with a jump diffusion risk process under the CEV model," *Journal of Computational and Applied Mathematics*, vol. 328, pp. 414–431, 2018.

[27] S. Basak and G. Chabakauri, "Dynamic mean-variance asset allocation," *Review of Financial Studies*, vol. 23, no. 8, pp. 2970–3016, 2010.

[28] Y. Shen, X. Zhang, and T. K. Siu, "Mean-variance portfolio selection under a constant elasticity of variance model," *Operations Research Letters*, vol. 42, no. 5, pp. 337–342, 2014.

[29] D. Li, X. Rong, and H. Zhao, "Time-consistent reinsurance-investment strategy for an insurer and a reinsurer with mean-variance criterion under the CEV model," *Journal of Computational and Applied Mathematics*, vol. 283, pp. 142–162, 2015.

[30] H. Zhao, C. Weng, Y. Shen, and Y. Zeng, "Time-consistent investment-reinsurance strategies towards joint interests of the insurer and the reinsurer under CEV models," *Science China Mathematics*, vol. 60, no. 2, pp. 317–344, 2017.

[31] D. Li, X. Rong, H. Zhao, and B. Yi, "Equilibrium investment strategy for DC pension plan with default risk and return of premiums clauses under CEV model," *Insurance: Mathematics and Economics*, vol. 72, pp. 6–20, 2017.

[32] M. Zhang and P. Chen, "Mean-variance asset-liability management under constant elasticity of variance process," *Insurance: Mathematics and Economics*, vol. 70, pp. 11–18, 2016.

[33] W. Yuan and S. Lai, "Family optimal investment strategy for a random household expenditure under the CEV model," *Journal of Computational and Applied Mathematics*, vol. 354, pp. 1–14, 2019.

[34] D. C. Emanuel and J. D. Macbeth, "Further results on the constant elasticity of variance call option pricing model," *The Journal of Financial and Quantitative Analysis*, vol. 17, no. 4, pp. 533–554, 1982.

[35] S. D. Promislow and V. R. Young, "Minimizing the probability of ruin when claims follow Brownian motion with drift," *North American Actuarial Journal*, vol. 9, no. 3, pp. 109–128, 2005.

[36] X. Peng, W. Su, and Z. Zhang, "On a perturbed compound Poisson risk model under a periodic threshold-type dividend strategy," *Journal of Industrial & Management Optimization*, vol. 13, no. 5, pp. 1–20, 2017.

[37] W. Yu, P. Guo, Q. Wang et al., "On a periodic capital injection and barrier dividend strategy in the compound Poisson risk model," *Mathematics*, vol. 8, no. 4, p. 511, 2020.

[38] W. Yu, Y. Huang, and C. Cui, "The absolute ruin insurance risk model with a threshold dividend strategy," *Symmetry*, vol. 10, no. 9, p. 377, 2018.

[39] Y. Huang, W. Yu, Y. Pan, and C. Cui, "Estimating the Gerber-Shiu expected discounted penalty function for Lévy risk model," *Discrete Dynamics in Nature and Society*, vol. 2019, Article ID 3607201, 15 pages, 2019.

[40] Z. Zhang, Y. Yong, and W. Yu, "Valuing equity-linked death benefits in general exponential Lévy models," *Journal of Computational and Applied Mathematics*, vol. 365, p. 112377, 2020.

[41] W. Yu, Y. Yong, G. Guan, Y. Huang, W. Su, and C. Cui, "Valuing guaranteed minimum death benefits by cosine series expansion," *Mathematics*, vol. 7, no. 9, p. 835, 2019.

[42] W. Yu, F. Wang, Y. Huang, and H. Liu, "Social optimal mean field control problem for population growth model," *Asian Journal of Control*, pp. 1–8, 2019.

[43] S. Dereich, A. Neuenkirch, and L. Szpruch, "An Euler-type method for the strong approximation of the Cox–Ingersoll–Ross process," *Proceedings of the Royal Society A: Mathematical, Physical and Engineering Sciences*, vol. 468, no. 2140, pp. 1105–1115, 2012.

[44] D. Duffie, *Dynamic Asset Pricing Theory*, Princeton University Press, Princeton, NJ, USA, 2010.

Hindawi
Mathematical Problems in Engineering
Volume 2020, Article ID 5145848, 14 pages
https://doi.org/10.1155/2020/5145848

Research Article

Optimal Investment of DC Pension Plan under Incentive Schemes and Loss Aversion

Yinghui Dong, Wenxin Lv, Siyuan Wei, and Yeyang Gong

Department of Mathematics and Physics, Suzhou University of Science and Technology, Suzhou 215009, China

Correspondence should be addressed to Yinghui Dong; dongyinghui1030@163.com

Received 17 April 2020; Accepted 4 May 2020; Published 18 May 2020

Guest Editor: Wenguang Yu

We investigate the DC pension manager's portfolio problem when the manager is remunerated through two schemes for DC pension managerial compensation under loss aversion and minimum guarantee. We apply the concavification technique and a static Lagrangian technique to solve the problem and derive the closed-form representation of the optimal wealth and portfolio processes. Theoretical and numerical results show that the incentive schemes can significantly impact the distribution of the optimal terminal wealth.

1. Introduction

As special financial institutions, risk management of insurance companies is the important guarantee of business security. In the existing references, some focus on the pricing aspect, see Dong [1], Yu et al. [2], and Zhang et al. [3], while others focus on the optimal problems, see Dong et al. [4], Dong and Zheng [5, 6], Sun et al. [7], and Yu et al. [8]. The objective of the present paper is to develop optimal asset management strategies for the DC pension plan.

Due to declining mortality and low interest rates, the literature on the asset allocation of defined contribution (DC) pension plans has grown up significantly in recent years. In a DC plan, the member contributes part of the salary to the pension account and upon retirement, the member can receive regular income from the pension account. The problem of optimal allocation during the accumulation phase for the DC pension plan has attracted a lot of attention, see Boulier et al. [9], Chen et al. [10], Zeng et al. [11], and Wang et al. [12].

The impact of the performance of a fund with respect to a benchmark on the asset management has been extensively investigated recently. The managers are often paid by an incentive scheme that depends on the performance of the fund they manage in order to inspire them to greater efforts. Such a scheme is made up of two components: a management fee, which is proportional to the fund wealth, and an incentive fee which is composed of a combination of some options on the fund, see, for example, Basek et al. [13, 14], Carpenter [15], Basak et al. [16], and Chen and Pennacchi [17]. Incentive schemes of the manager significantly affect the investment strategy. It has been believed that the asset manager may be motivated to take risk in excess by incentive schemes. However, little focuses on the performance fee schemes in DC pension plan management, since people argue that the performance fee may trigger managers to take excessive risk, which may lead to heavy losses in DC pension plans. A typical fee structure of defined contribution (DC) pension plan is an asset-based single management fee. However, managers typically perform poorly and cannot keep up with benchmarks under a scheme with lower incentives. It is widely believed that a performance-based and option-like fee may create greater incentives for a manager to exert more efforts in terms of investment.

As pointed out by He et al. [18], in the late 1990s, a performance-based fee structure was approved as a managerial incentive in DC pension plan management. However, the performance fee could induce managers to gamble at the expense of DC pension members. The purpose of a DC pension plan is to provide an adequate income for a DC member after retirement. Hence, to ensure safety of a DC pension, the performance fee scheme has not been implemented in most DC pension funds. He et al. [18] consider the optimal allocation of the DC pension fund for a manager under two fee structures: the single management fee and the mixed scheme of both management and performance fees. They compare the utilities of both fund managers and members under the two schemes and they state the win-win situation of implementing performance-based incentives in DC pension plan management. Furthermore, He et al. [18] consider the PI constraint, which can well protect the members' benefits by keeping the optimal terminal wealth always above the minimum guarantee, see Basek and Shapiro [13].

Prospect theory (PT), proposed by Kahneman and Tversky [19] and by Tversky and Kahneman [20], is one of the most notable theories in behavioral economics. With the framework of PT, investors base decisions on comparisons with a certain predefined reference point (also known as benchmark) rather than evaluating absolute level of total wealth itself. PT also suggests that individuals tend to be loss averse, that is, to be more sensitive to a loss than to a gain of the same amount. This loss aversion and risk-seeking behaviour is described in [20] by an asymmetric S-shaped utility function, convex in the domain of losses and concave in the domain of gains. In this paper, we extend the findings by He et al. [18] by incorporating loss aversion into modelling, which makes our optimization problem much more complex than that of [18]. We employ the martingale approach and the concavification technique to derive the optimal wealth and portfolio processes under a PI constraint and loss aversion. Although Dong and Zheng [5, 6] and Guan and Liang [21] also investigated the optimal allocation of the DC pension plan under loss aversion, they do not consider the remuneration schemes of DC pension.

The main contribution of this paper is that we have solved an optimization problem of a DC plan under two different kinds of remuneration schemes with the framework of PT. The rest of the paper is organized as follows. In Section 2, we formulate a DC investment problem under loss aversion and two different types of remuneration schemes. In Section 3, we apply the concavification technique and the martingale method to solve the optimization problem and derive closed-form expressions for the optimal wealth process and optimal control. In Section 4, we perform some numerical analysis and discuss the impacts of loss aversion and remuneration schemes on the distribution of the optimal terminal wealth. Section 5 concludes the paper.

2. The Model

Let $(\Omega, \mathcal{F}, \mathbb{F}, P)$ be a filtered complete probability space with the filtration $\mathbb{F} := \{\mathcal{F}_t \mid 0 \le t \le T\}$ being the natural filtration generated by a standard Brownian motion $\{W(t)\}_{0\le t\le T}$ and satisfying the usual conditions. Assume that all random variables and stochastic processes in this paper are well defined in this probability space. The DC pension fund starts at time 0, and the retirement time is T.

Let the financial market consist of one riskless savings account $S_0(t)$ and one risky asset $S_1(t)$.

The price of the risk-free asset $\{S_0(t)\}_{t\ge 0}$ satisfies the following differential equation:

$$\mathrm{d}S_0(t) = rS_0(t)\mathrm{d}t, \tag{1}$$

where r is a riskless interest rate. The price of the risky asset $\{S_1(t)\}_{t\ge 0}$ is modelled by the following stochastic differential equation (SDE):

$$\begin{aligned} \mathrm{d}S_1(t) &= S_1(t)(\mu\,\mathrm{d}t + \sigma \mathrm{d}W(t)) \\ &= S_1(t)(r\,\mathrm{d}t + \sigma(\mathrm{d}W(t) + \vartheta\,\mathrm{d}t)), \end{aligned} \tag{2}$$

where $\mu > r$ is the expected return of the risky asset, $\sigma > 0$ is the volatility of the risky asset, and $\vartheta = (\mu - r)^{\sigma}$ is the market price of risk.

In a DC plan, the pension members contribute continuously to the pension plan before retirement time T. Let $c(t) > 0$ denote the aggregated amount of money contributed at time t of a cohort of fund participants. As explained in [6], individual members' contribution rates may be random over the time, but the accumulated cash income of a large pension fund is in general deterministic and stable. We therefore, for simplicity, assume $c(t) \equiv c$ is a constant. Assume that there are no transaction costs or taxes in the financial market. The pension account is endowed with an initial endowment $x_0 \ge 0$.

Let $\pi(t)$ be the total amount allocated to the risky asset at time $t \in [0, T]$. Then, the wealth process $\{X^{\pi}(t)\}_{0\le t\le T}$ with the initial value $X^{\pi}(0) = 0$ satisfies the following controlled SDE:

$$\mathrm{d}X^{\pi}(t) = rX^{\pi}(t)\,\mathrm{d}t + \pi(t)\sigma(\mathrm{d}W(t) + \vartheta\,\mathrm{d}t) + c\,\mathrm{d}t. \tag{3}$$

Let $H(t)$ be the discounted value at time t of total pension contribution from t to T, where

$$H(t) = c\int_t^T e^{-r(s-t)}\mathrm{d}s = \frac{c}{r}\left(1 - e^{-r(T-t)}\right). \tag{4}$$

Traditionally, the fund manager charges a management fee as a reward, which is a fixed proportion of terminal fund wealth. More specifically, under this single management fee scheme, the payoff to the DC pension manager is

$$\Psi_1\left(X^{\pi}(T)\right) = k_1 X^{\pi}(T), \tag{5}$$

where $k_1 > 0$ is the rate of the management fee.

It is well known that the performance fee may lead to a greater incentive for the fund manager. Following [18], we consider an option-like incentive scheme (also called mixed scheme) and let $M(T)$ be the benchmark for the availability of the performance fee. Assume that $M(T)$ is the expected accumulation of contributions until time T under the reasonable accumulation rate:

$$M := M(T) = x_0 e^{\overline{r}T} + \frac{c}{\overline{r}}\left(e^{\overline{r}T} - 1\right), \tag{6}$$

where $\overline{r}$ is the accumulation rate. Under the mixed scheme, the payoff to the DC pension manager is

$$\Psi_2(X^\pi(T)) = \begin{cases} k_2 X^\pi(T), & X^\pi(T) < M, \\ k_2 X^\pi(T) + k_3(X^\pi(T) - M), & X^\pi(T) \geq M, \end{cases} \tag{7}$$

where $0 < k_2 \leq k_1$ is the rate of the management fee under the mixed scheme and $k_3 > 0$ is the rate of the performance fee. It is obvious that the manager receives a fixed proportion of terminal wealth and a variable component only in case the DC pension fund outperforms the benchmark M at time T.

The DC pension fund is supposed to meet DC members' elementary needs. Therefore, a downside protection $\overline{M}$ should be included in DC pension fund management. We next define the set of admissible trading strategies.

Definition 1. A portfolio strategy $\{\pi = \pi(t): t \in [0,T]\}$ is said to be admissible if, for all $t \in [0,T], \pi(t) \in \mathcal{F}_t$, with $\int_0^T \pi^2(t)dt < +\infty$, a.s., and $X^\pi(T)$ satisfies (3), $X^\pi(T) \geq \overline{M}$. We denote the set of admissible portfolio strategies by $\mathcal{A}$.

Consider a utility function defined by

$$U(x) = \begin{cases} -B(\theta - x)^{\gamma_1}, & 0 \leq x < \theta, \\ (x-\theta)^{\gamma_2}, & x \geq \theta, \end{cases} \tag{8}$$

where $\theta > 0$ is a reference point, $B > 1$ is called the loss aversion degree, $0 < \gamma_1 < 1, 0 < \gamma_2 < 1$ are the constants, γ_1 characterizes the degree of loss aversion, and γ_2 characterizes the degree of risk aversion, respectively.

For each $i = 1, 2$, we consider the following optimization problem with minimum guarantee:

$$\begin{cases} \max\limits_{\pi \in \mathcal{A}} & E[U(\Psi_i(X^\pi(T)))] \\ \text{s.t.} & X^\pi(T) \text{ satisfies (3) with } X^\pi(T) \geq \overline{M}, \text{a.s}\ldots \end{cases} \tag{9}$$

Since the market is complete, the unique pricing kernel is as follows:

$$\xi(t) = e^{-(r+(\vartheta^2/2))t - \vartheta W(t)}, \quad \xi(0) = 1, 0 \leq t \leq T, \tag{10}$$

where $\xi(t)$ is the Arrow–Debreu value per probability unit of a security which pays out 1 at time t if the scenario ω happens, and 0 else. As this value is high in a recession and low in prosperous times, $\xi(t)$ directly reflects the overall state of the economy.

Note that the shapes of $U(\Psi_1(\cdot))$ and $U(\Psi_2(\cdot))$ depend on the relationship of the parameters k_1, k_2, M, and $\overline{M}$. For simplicity, here we assume that $k_1\overline{M} \leq \theta \leq k_2 M$. For other cases, the analysis is similar.

Let

$$G_1(x) \doteq U(\Psi_1(x)) = \begin{cases} -B(\theta - k_1 x)^{\gamma_1}, & 0 \leq x < \dfrac{\theta}{k_1}, \\ (k_1 x - \theta)^{\gamma_2}, & x \geq \dfrac{\theta}{k_1}, \end{cases}$$

$$G_2(x) \doteq U(\Psi_2(x)) = \begin{cases} -B(\theta - k_2 x)^{\gamma_1}, & 0 \leq x < \dfrac{\theta}{k_2}, \\ (k_2 x - \theta)^{\gamma_2}, & \dfrac{\theta}{k_2} \leq x < M, \\ (k_2 x + k_3(x - M) - \theta)^{\gamma_2}, & x \geq M. \end{cases} \tag{11}$$

In the complete market, problem (9) can be rewritten as follows:

$$\begin{cases} \max\limits_{X^\pi(T)} & E[G_i(X^\pi(T))] \\ \text{s.t.} & E[\xi(T)X^\pi(T)] \leq x_0, X^\pi(T) \geq \overline{M}, \text{a.s}\ldots \end{cases} \tag{12}$$

3. Optimal Trading Strategy under Loss Aversion

In this section, we will solve the optimization problem (9) and derive the optimal wealth and portfolio processes.

Denote by

$$k = \frac{G_2(M) - G_2(\overline{M})}{M - \overline{M}}, \tag{13}$$

the slope of the straight line linking points $(\overline{M}, G_2(\overline{M}))$ and $(M, G_2(M))$.

Lemma 1

(1) For $k_1\overline{M} \leq \theta$, there exists a unique solution $(\theta/k_1) < z < \infty$ to the equation:

$$G_1(x) - (x - \overline{M})G_1'(x) - G_1(\overline{M}) = 0. \tag{14}$$

(2) Let k be defined by (13). For $k \geq G_2'(M-)$, there exists a unique $(\theta/k_2) < \overline{z} \leq M$ satisfying

$$G_2(\overline{z}) - G_2(\overline{M}) - G_2'(\overline{z})(\overline{z} - \overline{M}) = 0. \tag{15}$$

(3) For $k \leq G_2'(M+)$, there exists a unique $\tilde{z} \geq M$ satisfying

$$G_2(\tilde{z}) - G_2(\overline{M}) - G_2'(\tilde{z})(\tilde{z} - \overline{M}) = 0. \tag{16}$$

Proof. We first prove the first part. Denote $f(x) = G_1(x) - (x - \overline{M})G_1'(x) - G_1(\overline{M})$. It is easy to check that $f(x)$ is a decreasing, continuous function in $((\theta/k_1), \infty)$

and $f(\theta/k_1) < 0$, $\lim_{x\longrightarrow\infty} f(x) = \infty$. Therefore, there exists unique $(\theta/k_1) < z < \infty$ such that $f(z) = 0$ (see Figure 1), which concludes the proof of the first part. Similarly, we can prove the second and the third parts (see Figures 2 and 3). Here, we omit the details. □

Lemma 2. *For $G_2'(M-) < G_2'(M+)$, there exists a unique pair (z_1, z_2) with $(\theta/k_2) < z_1 < M < z_2$ satisfying*

$$\frac{G_2(z_2) - G_2(z_1)}{z_2 - z_1} = G_2'(z_1) = G_2'(z_2). \quad (17)$$

Proof. Note that $G_2'(x)$ is continuous and strictly decreasing on $((k_2/\theta), M)$ and (M, ∞), respectively. Furthermore,

$$G_2'(M-) < G_2'(M+), \quad \lim_{x\longrightarrow(\theta/k_2)+} G_2'(x) = +\infty, \quad \lim_{x\longrightarrow+\infty} G_2'(x) = 0. \quad (18)$$

Therefore, $G_2'(x)$ on $((k_2/\theta), M)$ and $G_2'(x)$ on (M, ∞) have strictly decreasing inverse functions and there must exist unique $(\theta/k_2) < \eta_1 < M$ and $\eta_2 > M$, such that

$$\begin{aligned} G_2'(\eta_1) &= G_2'(M+), \\ G_2'(\eta_2) &= G_2'(M-). \end{aligned} \quad (19)$$

For any $y \in [G_2'(M-), G_2'(M+)]$, we define $(\theta/k_2) < c_1(y) \le M \le c_2(y)$ as

$$G_2'(c_1(y)) = G_2'(c_2(y)) = y. \quad (20)$$

It is obvious that $c_1(y)$ and $c_2(y)$ are strictly decreasing and continuous on $[G_2'(M-), G_2'(M+)]$ and

$$\begin{aligned} \lim_{y\longrightarrow G_2'(M-)} c_1(y) &= M, \\ \lim_{y\longrightarrow G_2'(M-)} c_2(y) &= \eta_2, \\ \lim_{y\longrightarrow G_2'(M+)} c_1(y) &= \eta_1, \\ \lim_{y\longrightarrow G_2'(M+)} c_2(y) &= M. \end{aligned} \quad (21)$$

Define

$$\mathscr{K}(y) = \frac{G_2(c_2(y)) - G_2(c_1(y))}{c_2(y) - c_1(y)}. \quad (22)$$

It is easy to check that $\mathscr{K}(y)$ is continuous on $[G_2'(M-), G_2'(M+)]$. Using the concave inequalities, we have

$$\begin{aligned} G_2'(M+)(c_2(y) - M) &> G_2(c_2(y)) - G_2(M) \\ &> G_2'(c_2(y))(c_2(y) - M) \\ &\ge G_2'(M-)(c_2(y) - M), \\ G_2'(M+)(M - c_1(y)) &\ge G_2'(c_1(y))(M - c_1(y)) \\ &> G_2(M) - G_2(c_1(y)) \\ &> G_2'(M-)(M - c_1(y)). \end{aligned} \quad (23)$$

It follows from the above two inequalities that

$$G'(M+) > \mathscr{K}(y) > G'(M-). \quad (24)$$

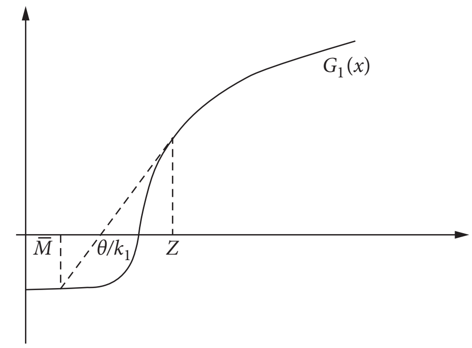

Figure 1: The root to equation (14).

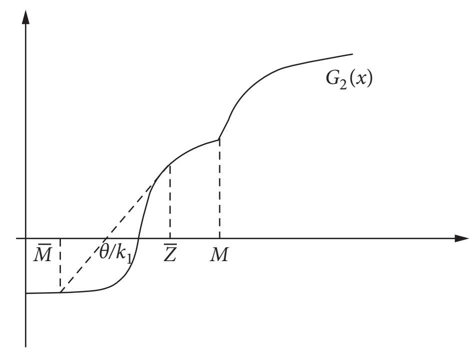

Figure 2: The root to equation (15).

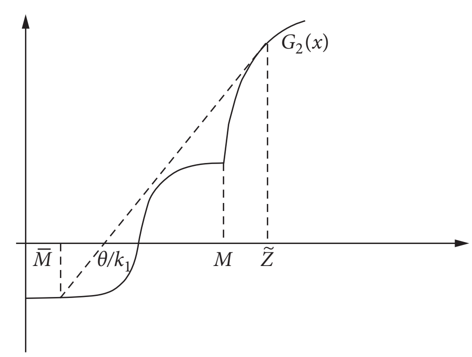

Figure 3: The root to equation (16).

In particular,

$$\begin{aligned} \mathscr{K}(G'(M-)) &> G'(M-), \\ \mathscr{K}(G'(M+)) &< G'(M+). \end{aligned} \quad (25)$$

Then, there must exist $G'(M-) < y_0 < G'(M+)$ such that $\mathscr{K}(y_0) = y_0$. Define $(k_2/\theta) < z_1 < M, z_2 > M$ by the relation $G_2'(z_1) = G_2'(z_2) = y_0$, which concludes the existence of z_1, z_2. Additionally, we can conclude that the linear interpolation between $G_2(z_1)$ and $G_2(z_2)$ has to be higher than $G_2(\cdot)$ on (z_1, z_2), that is,

$$G_2(x) < G_2(z_2) + G_2'(z_2)(x - z_2), \quad z_1 < x < z_2. \quad (26)$$

Now, we turn to the uniqueness of z_1, z_2. Assume there exists another pair $(\hat{z}_1, \hat{z}_2)$ with $(\theta/k_2) < \hat{z}_1 < M < \hat{z}_2$ satisfying

$$G_2(\widehat{z}_2) - G_2(\widehat{z}_1) = G_2'(\widehat{z}_1)(\widehat{z}_2 - \widehat{z}_1) = G_2'(\widehat{z}_2)(\widehat{z}_2 - \widehat{z}_1). \tag{27}$$

Without loss of generality, we assume that $\widehat{z}_1 > z_1$. From (26), we have $G_2(\widehat{z}_1) < G_2(z_2) + G_2'(z_2)(\widehat{z}_1 - z_2)$. So, for $z_2 \in (\widehat{z}_1, \widehat{z}_2)$,

$$G_2(z_2) > G_2(\widehat{z}_1) + G_2'(z_2)(z_2 - \widehat{z}_1) > G_2(\widehat{z}_1) + G_2'(\widehat{z}_1)(z_2 - \widehat{z}_1). \tag{28}$$

However, the linear interpolation between $G_2(\widehat{z}_1)$ and $G_2(\widehat{z}_2)$ has to be higher than $G_2(\cdot)$ on $(\widehat{z}_1, \widehat{z}_2)$, that is,

$$G_2(z_2) < G_2(\widehat{z}_1) + G_2'(\widehat{z}_1)(z_2 - \widehat{z}_1), \tag{29}$$

which leads to a contradiction. □ □

Proposition 1. *Assume $x_0 \geq \overline{M}e^{-rT} - H(0)$. Let $z, \overline{z}, \widetilde{z}$ and z_1, z_2 be determined by (14)–(17), respectively. Then, for the optimization problem (9), the optimal terminal wealth $X^{\pi^*,\beta^*}(T)$ is as follows with the multiplier $\beta^* > 0$ satisfying $E[\xi(T)X^{\pi^*,\beta^*}(T)] = x_0 + H(0)$.*

Under the single management fee scheme,

$$X^{\pi^*,\beta^*}(T) = \begin{cases} \overline{M}, & \xi(T) \geq \dfrac{G_1'(z)}{\beta^*}, \\ \dfrac{1}{k_1}\left(\left(\dfrac{\beta^*\xi(T)}{k_1\gamma_2}\right)^{(1/\gamma_2 - 1)} + \theta\right), & \xi(T) < \dfrac{G_1'(z)}{\beta^*}. \end{cases} \tag{30}$$

Under the mixed scheme,

Case A. If $k \geq G_2'(M-)$, then

(I) For $z_1 < \overline{z}$,

$$X^{\pi^*,\beta^*}(T) = \begin{cases} \overline{M}, & \xi(T) \geq \dfrac{G_2'(\widetilde{z})}{\beta^*}, \\ \dfrac{1}{k_2 + k_3}\left(\left(\dfrac{\beta^*\xi(T)}{\gamma_2(k_2 + k_3)}\right)^{(1/\gamma_2 - 1)} + k_3M + \theta\right), & \xi(T) < \dfrac{G_2'(\widetilde{z})}{\beta^*}. \end{cases} \tag{31}$$

(II) For $z_1 \geq \overline{z}$,

$$X^{\pi^*,\beta^*}(T) = \begin{cases} \overline{M}, & \xi(T) \geq \dfrac{G_2'(\overline{z})}{\beta^*}, \\ \dfrac{1}{k_2}\left(\theta + \left(\dfrac{\beta^*\xi(T)}{k_2\gamma_2}\right)^{(1/\gamma_2 - 1)}\right), & \dfrac{G_2'(z_1)}{\beta^*} \leq \xi(T) < \dfrac{G_2'(\overline{z})}{\beta^*}, \\ \dfrac{1}{k_2 + k_3}\left(\left(\dfrac{\beta^*\xi(T)}{\gamma_2(k_2 + k_3)}\right)^{(1/\gamma_2 - 1)} + k_3M + \theta\right), & \xi(T) < \dfrac{G_2'(z_1)}{\beta^*}. \end{cases} \tag{32}$$

Case B. If $k < G_2'(M-)$, then $X^{\pi^*,\beta^*}(T)$ is given by (31).

Proof. To solve problem (12), we define the Lagrangian of problem (12) as follows:

$$\mathscr{L}_i(X(T), \beta) = E[G_i(X(T)) - \beta\xi(T)X(T)], \tag{33}$$

where $\beta > 0$ is a Lagrange multiplier. Note that $G_i(\cdot)$ is not concave, so we first derive the concave envelope of $G_i(\cdot)$.

Under the single management fee scheme, we let z be the tangent point of the line starting at $(\overline{M}, G_1(\overline{M}))$ to the curve $G_1(x), x > (\theta/k_1)$. Then, the concave envelope of G_1 is given by (see Figure 4)

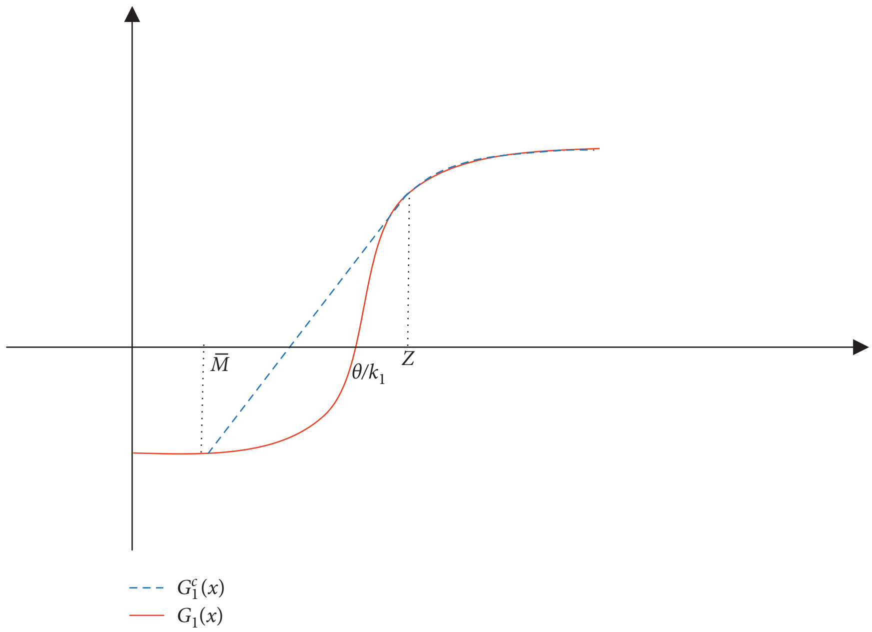

FIGURE 4: Concave envelope of G_1.

$$G_1^c(x) = \begin{cases} G_1(\overline{M}) + G_1'(z)(x - \overline{M}), & \overline{M} \le x < z, \\ (k_1 x - \theta)^{\gamma_2}, & x \ge z. \end{cases} \quad (34)$$

It is easy to verify that for $y > 0$,

$$x^*(y) \mathrel{\hat{=}} \arg\max_{x \ge \overline{M}} \{G_1^c(x) - xy\} = \begin{cases} \dfrac{1}{k_1}\left(\left(\dfrac{y}{k_1\gamma_2}\right)^{(1/\gamma_2 - 1)} + \theta\right), & 0 < y < G_1'(z), \\ \{\overline{M}, z\}, & y = G_1'(z), \\ \overline{M}, & y > G_1'(z). \end{cases} \quad (35)$$

Under the mixed fee scheme, Lemma 2 states that there exists a common tangent line with tangent point pair (z_1, z_2) to the curve $G_2(\cdot)$, $(\theta/k_2) < x < M$ and $G_2(\cdot)$, $x > M$.

Case A. For $k \ge G_2(M-)$, we let $\overline{z}$ be the tangent point of the line starting at $(\overline{M}, G_2(\overline{M}))$ to the curve $G_2(x)$, $(\theta/k_2) < x < M$.

(I) For $z_1 < \overline{z}$, it can be verified that there exists a unique tangent point $\tilde{z} > M$ of the line starting at $(\overline{M}, G_2(\overline{M}))$ to the curve $G_2(x), x > M$. Then, the concave envelope of G_2 is given by (see Figure 5)

$$G_2^c(x) = \begin{cases} G_2(\overline{M}) + G_1'(\tilde{z})(x - \overline{M}), & \overline{M} \le x < \tilde{z}, \\ G_2(x), & x \ge \tilde{z}. \end{cases} \quad (36)$$

Similar to deriving (35), we can obtain that

$$x^*(y) \mathrel{\hat{=}} \arg\max_{x \ge \overline{M}} \{G_2^c(x) - xy\} = \begin{cases} \dfrac{1}{k_2 + k_3}\left(\left(\dfrac{y}{\gamma_2(k_2 + k_3)}\right)^{(1/\gamma_2)} + k_3 M + \theta\right), & 0 < y < G_1'(z), \\ \{\overline{M}, \tilde{z}\}, & y = G_2'(\tilde{z}), \\ \overline{M}, & y > G_2'(\tilde{z}). \end{cases} \quad (37)$$

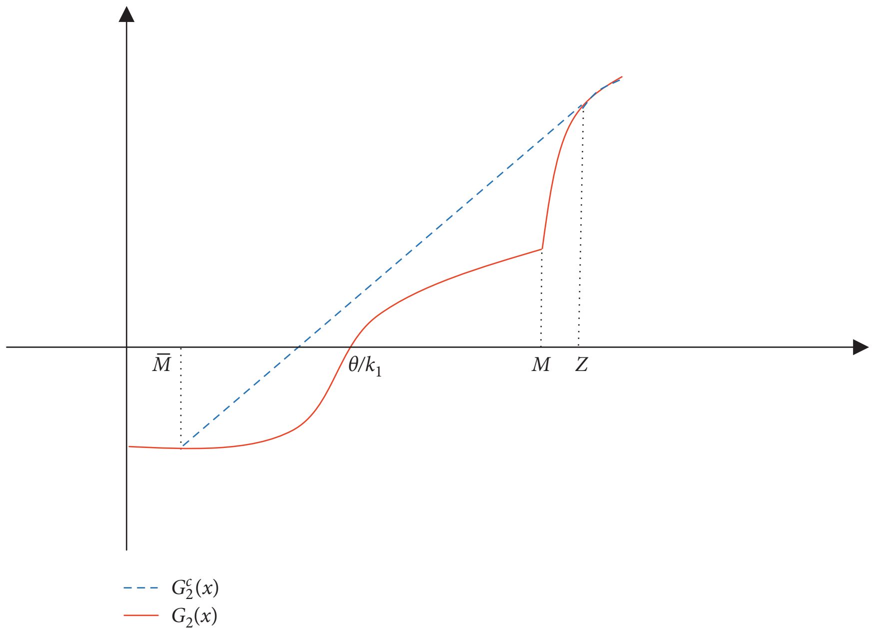

FIGURE 5: Concave envelope of G_2 for $k \geq G_2(M-), z_1 < \overline{z}$.

(II) For $z_1 \geq \overline{z}$, the concave envelope of G_2 is given by (see Figure 6)

$$G_2^c(x) = \begin{cases} G_2(\overline{M}) + G_2'(\overline{z})(x - \overline{M}), & \overline{M} \leq x < \overline{z}, \\ G_2(x), & \overline{z} \leq x < z_1, \\ G_2(z_1) + G_2'(z_1)(x - z_1), & z_1 \leq x < z_2, \\ G_2(x), & x \geq z_2. \end{cases} \quad (38)$$

So, we have

$$x^*(y) \widehat{=} \arg\max_{x \geq \overline{M}} \{G_2^c(x) - xy\} = \begin{cases} \dfrac{1}{k_2 + k_3}\left(\left(\dfrac{y}{\gamma_2(k_2 + k_3)}\right)^{(1/\gamma_2)} + k_3 M + \theta\right), & 0 < y < G_2'(z_2), \\ \{z_1, z_2\}, & y = G_2'(z_2), \\ \dfrac{1}{k_2}\left(\theta + \left(\dfrac{y}{k_2\gamma_2}\right)^{(1/\gamma_2 - 1)}\right), & G_2'(z_2) < y < G_2'(\overline{z}), \\ \{\overline{M}, z_1\}, & y = G_2'(\overline{z}), \\ \overline{M}, & y > G_2'(\overline{z}). \end{cases} \quad (39)$$

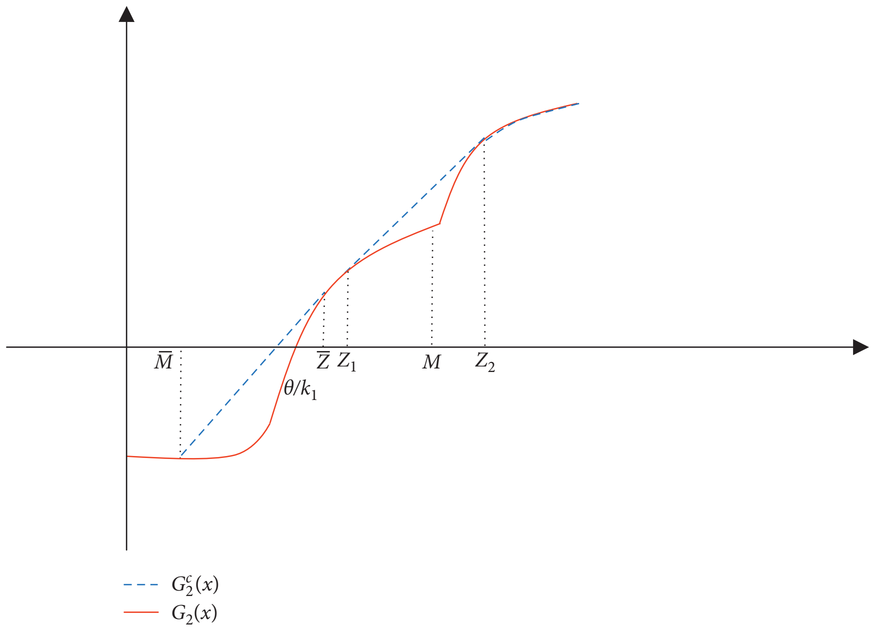

Figure 6: Concave envelope of G_2 for $k \geq G_2(M-), z_1 \geq \overline{z}$.

Case B. For $k < G_2(M-)$, we let $\tilde{z}$ be the tangent point of the line starting at $(\overline{M}, G_2(\overline{M}))$ to the curve $G_2(x)$, $(\theta/k_2) < x < M$ (see Figure 7). Then, the concave envelope of G_2 and $x^*(y)$ is given by (36) and (37), respectively.

According to the standard approach to portfolio selection problems, the original problem (12) is equivalent to the following problem:

$$\begin{cases} \inf\limits_{\beta>0} \max\limits_{X(T)} & \mathscr{L}_i(X(T), \beta) \\ \text{s.t.} & X(T) \geq \overline{M}, \text{a.s..} \end{cases} \tag{40}$$

To solve the above problem, we first consider the following problem:

$$\begin{cases} \max\limits_{X(T)} & \mathscr{L}_i(X(T), \beta) \\ \text{s.t.} & X(T) \geq \overline{M}, \text{a.s . . .} \end{cases} \tag{41}$$

It can be verified that for each $\beta > 0$, an optimal solution to (41) is

$$X^{\pi^*,\beta}(T) = x^*(\beta\xi(T)). \tag{42}$$

Secondly, it remains to solve an optimization problem w.r.t β:

$$\inf_{\beta>0} \mathscr{L}_i\left(X^{\pi^*,\beta}(T), \beta\right). \tag{43}$$

By the complementary slackness condition, the optimal solution $\beta^* > 0$ to problem (43) can be directly obtained from the following equation:

$$E\left[\xi(T)X^{\pi^*,\beta^*}(T)\right] = x_0 + H(0), \tag{44}$$

which yields the optimal solution $X^{\pi^*,\beta^*}(T)$ to problem (12).

It is easy to see that in each case, $V(\beta) = E[\xi(T)X^{\pi^*,\beta}(T)]$ is continuous and strictly decreasing in β. Furthermore, $\lim_{\beta \longrightarrow 0^+} V(\beta) = \infty$ and $\lim_{\beta \longrightarrow \infty} V(\beta) = \overline{M}e^{-rT}$. Thus, there exists a unique β^* satisfying condition (44), which implies that $X^{\pi^*,\beta^*}(T)$ is feasible to (12). We next show $X^{\pi^*,\beta^*}(T)$ is indeed the optimal terminal wealth to problem (12). Let $X(T)$ be an arbitrary terminal wealth satisfying the budget constraint in problem (12). Then, we have

$$\begin{aligned} E\left[G_i\left(X^{\pi^*,\beta^*}(T)\right)\right] - E[G_i(X(T))] \geq E\left[G_i\left(X^{\pi^*,\beta^*}(T)\right) - \beta^*\xi(T)X^{\pi^*,\beta^*}(T)\right] + \beta^*(x_0 + H(0)) \\ - \left(E[G_i(X(T)) - \beta^*\xi(T)X(T)] + \beta^*(x_0 + H(0))\right) \geq 0, \end{aligned} \tag{45}$$

where the first equality holds since the budget constraint holds with equality for $X^{\pi^*,\beta^*}(T)$ while with inequality for $X(T)$ and the second equality follows from the fact that $X^{\pi^*,\beta^*}(T)$ solves (41) for the multiplier β^*. □

Remark 1. Note that if $\overline{M} = 0$, then the loss aversion states a risk-seeking preference for the loss states, and therefore the terminal wealth equals to 0, which implies in the case of no regulation there is a moral hazard problem due to loss

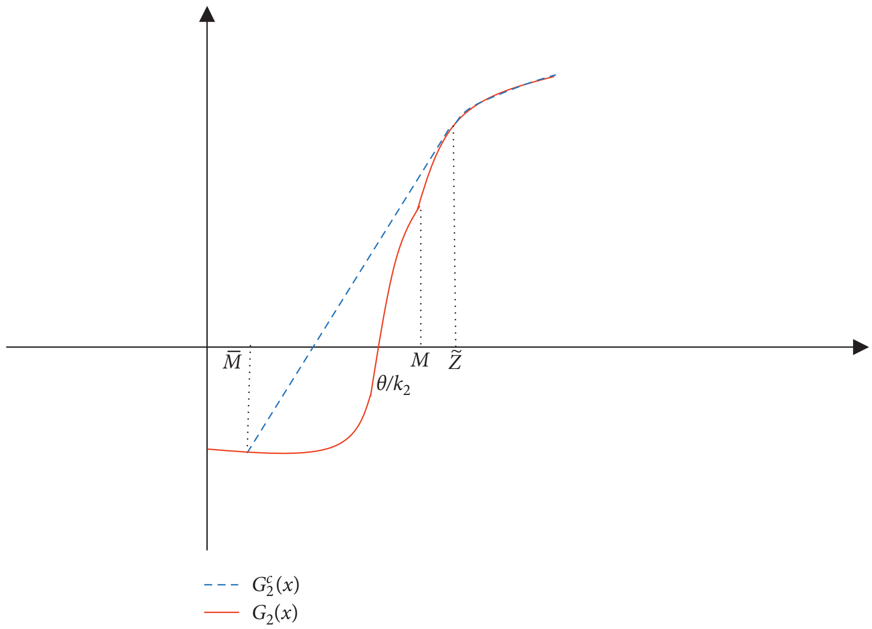

FIGURE 7: Concave envelope of G_2 for $k < G_2(M-)$.

aversion. In contrast to the unconstrained optimal terminal wealth, the optimal terminal wealth under the PI constraint in bad market scenarios is kept at the level $\overline{M}$ in order to satisfy the PI constraint while the unconstrained terminal wealth is always 0. Therefore, the PI constraint well protects the DC member's benefits in bad market scenarios.

Remark 2. Different from the derived results under the concave utility in [18], the linear envelope exists both under the single and the mixed fee schemes due to loss aversion. The optimal terminal wealth $X^{\pi^*,\beta^*}(T)$ is a function of the state price density at maturity $\xi(T)$ and the multiplier β^*. Under the single incentive scheme, the optimal terminal wealth takes a two-region form. When the state price density $\xi(T)$ is relatively low, the optimal terminal wealth $X^{\pi^*,\beta^*}(T)$ is similar to the smooth utility; when $\xi(T)$ increases above the boundary point of the bad-state region, $(G_1'(z)/\beta^*)$, the optimal terminal wealth drops to $\overline{M}$ due to the risk-seeking preference in the the domain of losses. Under the mixed incentive scheme, $X^{\pi^*,\beta^*}(T)$ takes a two-region form for $k < G_2'(M-)$ and may take a two- or three-region form for $k \geq G_2'(M-)$ according to the the relative position of the values of z_1 and $\overline{z}$. In all cases, the optimal terminal wealth is determined by the utility changing points and ends with the minimum guarantee $\overline{M}$ when the state price density at maturity $\xi(T)$ increases above the boundary point of the bad-state region.

After obtaining the optimal terminal wealth, we can derive the closed-form expression for the optimal investment strategy given in the following result.

Proposition 2. *Assume that $x_0 \geq \overline{M}e^{-rT} - H(0)$. Then, for the optimization problem (12), the optimal wealth process and the optimal strategy are given as follows with the multiplier $\beta^* > 0$ satisfying $E[\xi(T)X^{\pi^*,\beta^*}(T)] = x_0 + H(0)$.*

Under the single management fee scheme, the optimal wealth process at time t is given by

$$X^{\pi^*,\beta^*}(t) = A_1(\xi(t),t) - H(t), \tag{46}$$

where

$$\begin{aligned} A_1(\xi(t),t) = e^{-r(T-t)}\Big(&\overline{M}\Phi\big(\mathrm{d}_{1,t}(G_1'(z))\big) \\ &+ \frac{\theta}{k_1}\Big(1-\Phi\big(\mathrm{d}_{1,t}(G_1'(z))\big)\Big) \\ &+ \chi(z)\frac{\Phi'\big(\mathrm{d}_{1,t}(G_1'(z))\big)}{\Phi'\big(\mathrm{d}_{2,t}(G_1'(z))\big)}\Phi\big(\mathrm{d}_{2,t}(G_1'(z))\big)\Big), \end{aligned} \tag{47}$$

with Φ being the standard normal cumulative distribution function and

$$\begin{aligned} \mathrm{d}_{1,t}(x) &= \frac{\ln(x/\xi(t)\beta^*) + \big(r-(\vartheta^2/2)\big)(T-t)}{-\vartheta\sqrt{T-t}}, \\ \mathrm{d}_{2,t}(x) &= -\mathrm{d}_{1,t}(x) + \frac{\vartheta\sqrt{T-t}}{1-\gamma_2}, \\ \chi(x) &= \frac{k_1x-\theta}{k_1}. \end{aligned} \tag{48}$$

The percentage of wealth invested in the risky assets is given by

$$\pi^{*,\beta^*}(t) = \frac{\vartheta}{\sigma(1-\gamma_2)}\left(\underbrace{X^{\pi^*,\beta^*}(t)+H(t)}_{\text{total wealth}} \underbrace{- e^{-r(T-t)}\left(\Phi\left(\mathrm{d}_{1,t}(G_1'(z))\right)\overline{M} + \frac{\theta}{k_1}\left(1-\Phi\left(\mathrm{d}_{1,t}(G_1'(z))\right)\right)\right)}_{\text{deposit term}} \right.$$
$$\left. + \underbrace{(1-\gamma_2)\Phi'\left(\mathrm{d}_{1,t}(G_1'(z))\right)\frac{e^{-r(T-t)}}{\vartheta\sqrt{T-t}}(z-\overline{M})}_{\text{risk seeking term}}\right). \tag{49}$$

Under the mixed scheme,

Case A. If $k \geq G_2'(M-)$, then

(I) For $z_1 < \overline{z}$, the optimal wealth process at time t is given by

$$X^{\pi^*,\beta^*}(t) = \overline{A}_1(\xi(t),t) - H(t), \tag{50}$$

where

$$\overline{A}_1(\xi(t),t) = e^{-r(T-t)}\left(\overline{M}\Phi\left(\mathrm{d}_{1,t}(G_2'(\overline{z}))\right) + \frac{k_3M+\theta}{k_2+k_3}\left(1-\Phi\left(\mathrm{d}_{1,t}(G_2'(\overline{z}))\right)\right)\right.$$
$$\left. + \eta(\overline{z})\frac{\Phi'\left(\mathrm{d}_{1,t}(G_2'(\overline{z}))\right)}{\Phi'\left(\mathrm{d}_{2,t}(G_2'(\overline{z}))\right)}\Phi\left(\mathrm{d}_{2,t}(G_2'(\overline{z}))\right)\right), \tag{51}$$

with

$$\eta(x) = \frac{(k_2+k_3)x - k_3M - \theta}{k_2+k_3}. \tag{52}$$

The percentage of wealth invested in the risky assets is given by

$$\pi^{*,\beta^*}(t) = \frac{\vartheta}{\sigma(1-\gamma_2)}\left(\underbrace{X^{\pi^*,\beta^*}(t)+H(t)}_{\text{total wealth}}\right.$$
$$\underbrace{- e^{-r(T-t)}\left(\Phi\left(\mathrm{d}_{1,t}(G_2'(\overline{z}))\right)\overline{M} + \frac{k_3M+\theta}{k_2+k_3}\left(1-\Phi\left(\mathrm{d}_{1,t}(G_2'(\overline{z}))\right)\right)\right)}_{\text{deposit term}}$$
$$\left. + \underbrace{(1-\gamma_2)\Phi\prime\left(\mathrm{d}_{1,t}(G_2'(\overline{z}))\right)\frac{e^{-r(T-t)}}{\vartheta\sqrt{T-t}}(\overline{z}-\overline{M})}_{\text{risk-seeking term}}\right). \tag{53}$$

(II) For $z_1 \geq \overline{z}$, the optimal wealth process at time t is given by

$$X^{\pi^*,\beta^*}(t) = \overline{A}_2(\xi(t),t) - H(t), \tag{54}$$

where

$$\overline{A}_2(\xi(t),t) = e^{-r(T-t)}\left(\left(\overline{M}-\frac{\theta}{k_2}\right)\Phi\left(d_{1,t}(G_2'(\overline{z}))\right)+\frac{\theta}{k_2}\Phi\left(d_{1,t}(G_2'(z_1))\right)+\frac{k_2\overline{z}-\theta}{k_2}\frac{\Phi\prime\left(d_{1,t}(G_2'(\overline{z}))\right)}{\Phi\prime\left(d_{2,t}(G_2'(\overline{z}))\right)}\Phi\left(d_{2,t}(G_2'(\overline{z}))\right)\right.$$
$$\left.+\,left\psi(z_1)\frac{\Phi\prime\left(d_{1,t}(G_2'(z_1))\right)}{\Phi\prime\left(d_{2,t}(G_2'(z_1))\right)}\Phi\left(d_{2,t}(G_2'(z_1))\right)\right), \tag{55}$$

with

$$\psi(x) = \left(\left(\frac{k_2+k_3}{k_2}\right)^{(\gamma_2/1-\gamma_2)}\right)\frac{k_2x-\theta}{k_2}. \tag{56}$$

The percentage of wealth invested in the risky assets is given by

$$\pi^{*,\beta^*}(t) = \frac{\vartheta}{\sigma(1-\gamma_2)}\left(\underbrace{X^{\pi^*,\beta^*}(t)+H(t)}_{\text{total wealth}}\right.$$
$$\underbrace{-\,e^{-r(T-t)}\left(\frac{k_2\overline{M}-\theta}{k_2}\Phi\left(d_{1,t}(G_2'(\overline{z}))\right)+\frac{\theta}{k_2}\Phi\left(d_{1,t}(G_2'(z_1))\right)\right)}_{\text{deposit term}}$$
$$\left.\underbrace{+\,(1-\gamma_2)\left(\frac{\overline{z}-\overline{M}}{\vartheta\sqrt{T-t}}\Phi\prime\left(d_{1,t}(G_2'(\overline{z}))\right)+\frac{k_2\psi(z_1)-\theta}{k_2\vartheta\sqrt{T-t}}\Phi\prime\left(d_{1,t}(G_2'(z_1))\right)\right)}_{\text{risk-seeking term}}\right). \tag{57}$$

Case B. If $k < G_2'(M-)$, then the optimal wealth process at time t and the percentage of wealth invested in the risky assets are given by (50) and (53), respectively.

Proof. The price of $X^{\pi^*,\beta^*}(T)$ at t is calculated as follows:

$$X^{\pi^*,\beta^*}(t) = \frac{1}{\xi(t)}E\left[\xi(T)X^{\pi^*,\beta^*}(T)\,\middle|\,\mathcal{F}_t\right]-H(t). \tag{58}$$

Note that $\log(\xi(T))$ is a normal distribution. By substituting the expressions for $X^{\pi^*,\beta^*}(T)$ given in Proposition 1 into (58), we can easily obtain the formula for $X^{\pi^*,\beta^*}(t)$ by some straightforward calculations.

Let $X^{\pi^*,\beta^*}(t) = A(\xi(t),t)$. Then,

$$dX^{\pi^*,\beta^*}(t) = I(t,H(t))dt+\frac{\partial A}{\partial \xi}(-\xi(t)\vartheta dW(t)), \tag{59}$$

for some $I(t,H(t))$, and we are only interested in the diffusion part. Comparing it with (3), we have

$$\pi^{*,\beta^*}(t) = -\frac{\vartheta}{\sigma}\frac{\partial A}{\partial \xi}\xi(t). \tag{60}$$

Some simple calculations yield the results. □

Remark 3. Note that, under the concave utility in [18], a risk-seeking term only exists in the optimal policy under the mixed incentive scheme generated by the incentive of the performance fee. However, with the framework of PT, there exists a risk-seeking term both under the single and the mixed incentive schemes due to loss aversion. Therefore, the potential gambling risk-taking policy exists both under the single and the mixed incentive schemes.

4. Numerical Analysis

In this section, we do some numerical calculations to investigate the influence of incentive schemes on the optimal terminal wealth.

For all numerical computations, unless specified otherwise, the benchmark data used are as follows: $r = 0.03, \mu = 0.07, \sigma = 0.2, c = 1, B = 2.25, \gamma_1 = 0.2, \gamma_2 = 0.3, k_1 = 0.05, k_2 = 0.04, k_3 = 0.1, \theta = 10, \overline{r} = 0.06, x_0 = 20, \overline{M} = 50$, and $T = 40$.

Figure 8 presents the optimal terminal value $X^{\pi^*,\beta^*}(T)$ versus $\xi(T)$ for different θ. It is observed that there exists H^*, such that for $\xi(T) \geq H^*$, the optimal terminal value under the mixed incentive scheme is dominated by $X^{\pi^*,\beta^*}(T)$ under

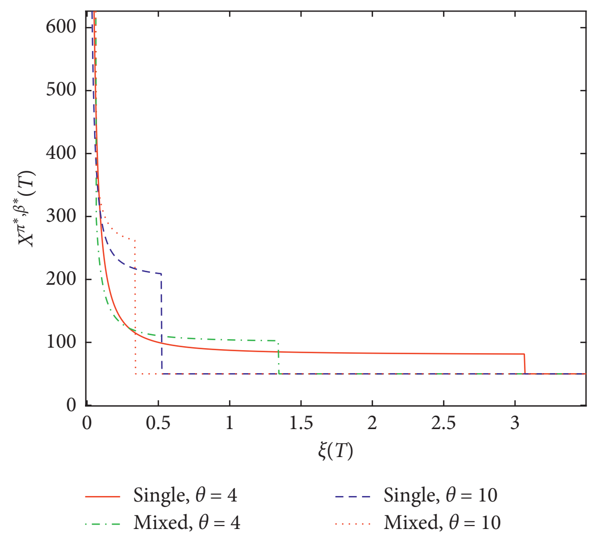

Figure 8: $X^{\pi^*,\beta^*}(T)$ versus $\xi(T)$ for different θ.

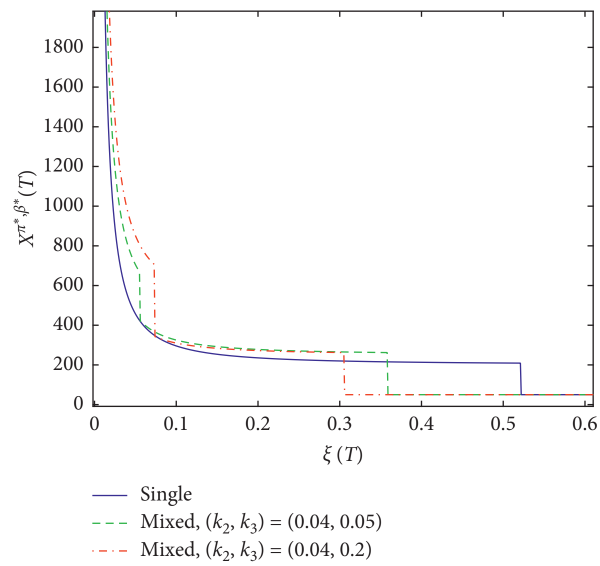

Figure 10: $X^{\pi^*,\beta^*}(T)$ versus $\xi(T)$ for different k_3.

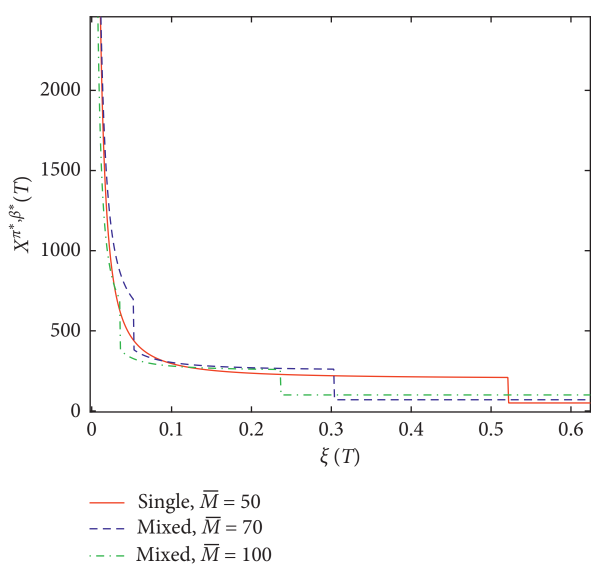

Figure 9: $X^{\pi^*,\beta^*}(T)$ versus $\xi(T)$ for different $\overline{M}$ under mixed incentive scheme.

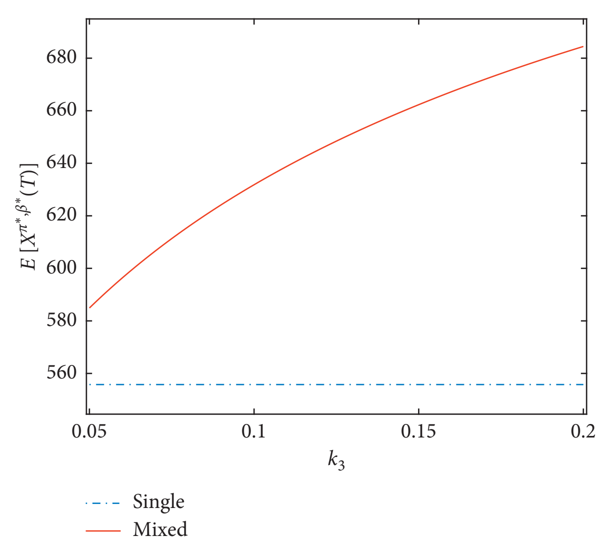

Figure 11: $E[X^{\pi^*,\beta^*}(T)]$ versus k_3.

the single fee scheme. This is consistent with the intuition that the manger will take more risky strategy to attain the performance fee, which leads to a higher left-tail risk. Furthermore, the mixed incentive scheme also leads to an increase in the optimal terminal wealth of good economic states. We can also note that with the reference point θ increasing, the bad-state region enlarges. This is because the manager is risk seeking towards the terminal wealth. To achieve a higher reference point, the manager invests much more money in the risky asset, which results in a higher left-tail risk.

Figure 9 shows the optimal terminal value $X^{\pi^*,\beta^*}(T)$ versus $\xi(T)$ under two incentive schemes with different minimum guarantee $\overline{M}$. From it, we can see that a higher left-tail risk under the mixed incentive scheme can be improved by increasing the minimum guarantee. Therefore, we can control the left-tail risk triggered by the mixed incentive scheme via a stricter PI constraint.

Figure 10 represents the optimal terminal value $X^{\pi^*,\beta^*}(T)$ versus $\xi(T)$ for different k_3. We can see that a higher performance fee rate k_3 leads to enlargement of the bad-state region and increase in the optimal terminal wealth in the good-state region. This is due to the fact that in order to attain the performance fee, the manager takes more risky strategies such that $X^{\pi^*,\varepsilon}(T)$ becomes more volatile.

Figure 11 plots the expectation of the optimal terminal value $E[X^{\pi^*,\beta^*}(T)]$ versus k_3. We can see that the expectation of the optimal terminal value $E[X^{\pi^*,\beta^*}(T)]$ under the mixed incentive scheme is greater than that under the single incentive scheme, and $E[X^{\pi^*,\beta^*}(T)]$ under the mixed incentive scheme increases with k_3. As pointed out in Figure 10, to achieve the performance fee, the manager invests

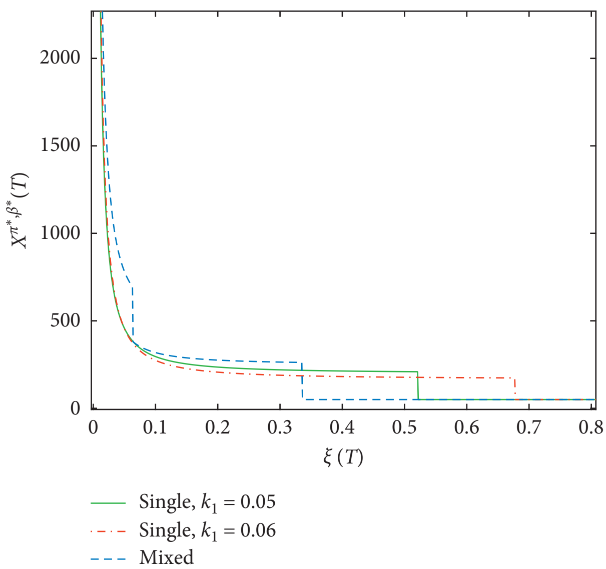

FIGURE 12: $X^{\pi^*,\beta^*}(T)$ versus $\xi(T)$ for different k_1.

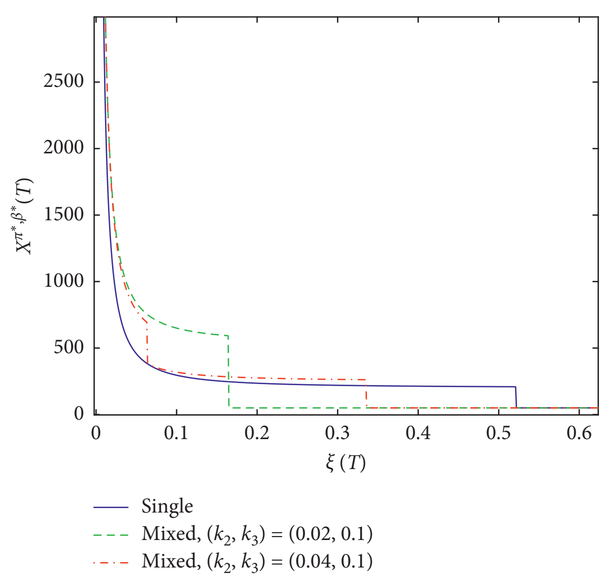

FIGURE 13: $X^{\pi^*,\beta^*}(T)$ versus $\xi(T)$ for different k_2.

much more money in the risky asset, which results in a higher expectation.

Figure 12 shows the optimal terminal value $X^{\pi^*,\beta^*}(T)$ versus $\xi(T)$ for different k_1. We can see that with k_1 increasing, the bad-state region shrinks and the optimal terminal wealth in the good-state region decreases. This is because that as k_1 increases, the manager is paid much more management fee and then the manager takes more prudent strategies such that $X^{\pi^*,\beta^*}(T)$ becomes less volatile. Therefore, a single incentive scheme with a higher management fee rate cannot provide incentive for a manager to increase the optimal terminal wealth.

Figure 13 plots the optimal terminal value $X^{\pi^*,\beta^*}(T)$ versus $\xi(T)$ for different k_2. It is seen that a higher fee rate k_2 leads to shrinkage in the bad-state region shrinks and decrease in the optimal terminal wealth in the good-state region. As explained in Figure 12, with k_2 increasing, the manager can receive much more management fee and then chooses to take more prudent strategies.

5. Conclusions

In this paper, we investigate the optimal portfolio selection problem for a DC plan manager with an S-shaped utility under a single fee scheme and a mixed fee scheme, respectively. We use a concavification technique and a Lagrange dual method to derive closed-form optimal wealth and portfolio processes of the DC pension fund. Due to loss aversion, the potential gambling risk-taking policy exists both under the single and the mixed incentive schemes. In particular, the mixed incentive scheme can induce the manager to take much more risky strategies to achieve a higher optimal terminal value. Financial regulation such as PI constraint can be used to prevent gambling when the performance deteriorates.

Data Availability

No data were used to support this study.

Conflicts of Interest

The authors declare that they have no conflicts of interest.

Acknowledgments

The research was supported by Humanities and Social Science Research Projects in the Ministry of Education (Grant no. 20YJAZH025), the NSF of Jiangsu Province (Grant no. BK20170064), the NNSF of China (Grant no. 11771320), and the QingLan Project of Jiangsu Province.

References

[1] Y. H. Dong, "Fair valuation of life insurance contract under a correlated jump diffusion model," *ASTIN Bull*, vol. 41, no. 2, pp. 429–447, 2011.

[2] W. Yu, Y. Yong, G. Guan, Y. Huang, W. Su, and C. Cui, "Valuing guaranteed minimum death benefits by cosine series expansion," *Mathematics*, vol. 7, no. 9, p. 835, 2019.

[3] Z. M. Zhang, Y. D. Yong, and W. G. Yu, "Valuing equity-linked death benefits in general exponential Lévy models," *Journal of Computational and Applied Mathematics*, vol. 365, 2020.

[4] Y. Dong, S. Wu, W. Lv, and G. Wang, "Optimal asset allocation for participating contracts under the VaR and PI constraint," *Scandinavian Actuarial Journal*, vol. 2020, no. 2, pp. 84–109, 2020.

[5] Y. Dong and H. Zheng, "Optimal investment of DC pension plan under short-selling constraints and portfolio insurance," *Insurance: Mathematics and Economics*, vol. 85, pp. 47–59, 2019.

[6] Y. Dong and H. Zheng, "Optimal investment with S-shaped utility and trading and value at risk constraints: an application to defined contribution pension plan," *European Journal of Operational Research*, vol. 281, no. 2, pp. 341–356, 2020.

[7] J. Y. Sun, Y. J. Li, and L. Zhang, "Robust portfolio choice for a defined contribution pension plan with stochastic income and

interest rate," *Communications in Statistics-Theory and Methods*, vol. 47, pp. 4095–4105, 2018.
[8] W. Yu, P. Guo, Q. Wang et al., "On a periodic capital injection and barrier dividend strategy in the compound Poisson risk model," *Mathematics*, vol. 8, no. 4, p. 511, 2020.
[9] J.-F. Boulier, S. Huang, and G. Taillard, "Optimal management under stochastic interest rates: the case of a protected defined contribution pension fund," *Insurance: Mathematics and Economics*, vol. 28, no. 2, pp. 173–189, 2001.
[10] Z. Chen, Z. Li, Y. Zeng, and J. Sun, "Asset allocation under loss aversion and minimum performance constraint in a DC pension plan with inflation risk," *Insurance: Mathematics and Economics*, vol. 75, pp. 137–150, 2017.
[11] Y. Zeng, D. Li, Z. Chen, and Z. Yang, "Ambiguity aversion and optimal derivative-based pension investment with stochastic income and volatility," *Journal of Economic Dynamics and Control*, vol. 88, pp. 70–103, 2018.
[12] S. Wang, X. Rong, and H. Zhao, "Optimal investment and benefit payment strategy under loss aversion for target benefit pension plans," *Applied Mathematics and Computation*, vol. 346, pp. 205–218, 2019.
[13] S. Basak and A. Shapiro, "Value-at-risk-based risk management: optimal policies and asset prices," *Review of Financial Studies*, vol. 14, no. 2, pp. 371–405, 2001.
[14] S. Basak, A. Pavlova, and A. Shapiro, "Optimal asset allocation and risk shifting in money management," *Review of Financial Studies*, vol. 20, no. 5, pp. 1583–1621, 2007.
[15] J. N. Carpenter, "Does option compensation increase managerial risk appetite?" *The Journal of Finance*, vol. 55, no. 5, pp. 2311–2331, 2000.
[16] S. Basak, A. Pavlova, and A. Shapiro, "Offsetting the implicit incentives: benefits of benchmarking in money management," *Journal of Banking & Finance*, vol. 32, no. 9, pp. 1883–1893, 2008.
[17] H.-L. Chen and G. G. Pennacchi, "Does prior performance affect a mutual fund's choice of risk? Theory and further empirical evidence," *Journal of Financial and Quantitative Analysis*, vol. 44, no. 4, pp. 745–775, 2009.
[18] L. He, Z. Liang, Y. Liu, and M. Ma, "Optimal control of DC pension plan management under two incentive schemes," *North American Actuarial Journal*, vol. 23, no. 1, pp. 120–141, 2019.
[19] D. Kahneman and A. Tversky, "Prospect theory: an analysis of decision under risk," *Econometrica*, vol. 47, no. 2, pp. 263–292, 1979.
[20] A. Tversky and D. Kahneman, "Advances in prospect theory: cumulative representation of uncertainty," *Journal of Risk and Uncertainty*, vol. 5, no. 4, pp. 297–323, 1992.
[21] G. Guan and Z. Liang, "Optimal management of DC pension plan under loss aversion and value-at-risk constraints," *Insurance: Mathematics and Economics*, vol. 69, pp. 224–237, 2016.

Hindawi
Mathematical Problems in Engineering
Volume 2020, Article ID 2127374, 21 pages
https://doi.org/10.1155/2020/2127374

Research Article

An Improved Hilbert Spectral Representation Method for Synthesizing Spatially Correlated Earthquake Ground Motions and Its Error Assessment

Luhua Zhu[1] and Erlei Yao[1,2]

[1]*School of Civil Engineering and Mechanics, Huazhong University of Science and Technology, Wuhan 430074, China*
[2]*Changjiang River Scientific Research Institute, Wuhan 430010, China*

Correspondence should be addressed to Erlei Yao; xiaoleiip@163.com

Received 26 February 2020; Accepted 5 May 2020; Published 16 May 2020

Guest Editor: Zhimin Zhang

This paper is an extension of the random amplitude-based improved Hilbert spectral representation method (IHSRM) that the authors developed previously for the simulation of spatially correlated earthquake ground motions (SCEGMs) possessing the nonstationary characteristics of the natural earthquake record. In fact, depending on the fundamental types (random phase method and random amplitude method) and matrix decomposition methods (Cholesky decomposition, root decomposition, and eigendecomposition), the IHSRM possesses various types. To evaluate the influence of different types of this method on the statistic errors, i.e., bias errors and stochastic errors, an error assessment for this method was conducted. First, the random phase-based IHSRM was derived, and its reliability was proven by theoretical deduction. Unified formulas were given for random phase- and random amplitude-based IHSRMs, respectively. Then, the closed-form solutions of statistic errors of simulated seismic motions were derived. The validness of the proposed closed-form solutions was proven by comparing the closed-form solutions with estimated values. At last, the stochastic errors of covariance (i.e., variance and cross-covariance) for different types of IHSRMs were compared, and the results showed that (1) the proposed IHSRM is not ergodic; (2) the random amplitude-based IHSRMs possessed higher stochastic errors of covariance than the random phase-based IHSRMs; and (3) the value of the stochastic error of covariance for the random phase-based IHSRM is dependent on the matrix decomposition method, while that for the random amplitude-based one is not.

1. Introduction

The spectral representation method (SRM) proposed by Rice [1] and then extended by Shinozuka and Jan [2–4] is the most widely used method to simulate random processes due to its accuracy and being easy to application [5, 6]. However, the random processes simulated by SRM are not always ergodic; in other words, the temporal statistics estimated from one SRM-simulated sample may be different from the targets [7]. The differences are errors. Besides, to reduce the calculation time and cost involved in the time-history analysis of complex or extended structures, only few samples or a set of random processes (e.g., seismic ground motion) would be generated and used in practice. Because the generated realizations that are utilized as inputs in time domain analysis of structures have great influence on the results [8–12], the rational estimation of these errors is necessary.

The difference between the estimated statistics and the target can be evaluated by the bias and stochastic errors. Hu et al. [13] assessed the errors produced by both the Cholesky decomposition-based SRM and the eigendecomposition-based SRM and found that the latter one produced smaller stochastic errors. Gao et al. [14] compared the bias errors and the stochastic errors of the random process simulated by the random amplitude-based SRM with those by the random phase-based SRM. Gao et al. [7] systematically investigated the bias errors and stochastic errors of the random process simulated by the coherency matrix-based SRM and compared them with the errors of the PSD matrix-based SRM. Hu et al. [15, 16] studied the statistical errors in the simulation of spatially varying seismic ground motions modeled by evolutionary Gaussian vector processes and simulated by the SRM. They indicated that the SRM implementation scheme involving both random amplitudes and phase angles would cause larger stochastic errors. Wu et al. [17] conducted the error assessment of multivariate random processes simulated by a conditional simulation method.

In accordance with the Hilbert spectral representation model proposed by Wen and Gu [18] and the Hilbert–Huang transform (HHT) [19], the authors had developed a random amplitude-based IHSRM [20] to simulate SCEGMs having natural nonstationary characteristics. To optimize and supplement the IHSRM aforementioned, the random phase-based IHSRM was developed in this paper. More importantly, a series of deduction around the random phase-based IHSRM was then conducted to verify the reliability of this method. Then, considering the fundamental types (random phase method and random amplitude method) and different matrix decomposition methods (Cholesky decomposition, root decomposition, and eigendecomposition) that may be used in the IHSRM, an error assessment was conducted to evaluate the temporal statistic errors of the IHSRM-simulated process. The unified formulas for random phase- and random amplitude-based IHSRMs were presented. Two types of statistical errors were prescribed, and then the closed-form solutions of statistical errors of seismic motions simulated by different types of IHSRMs were derived. The validness of the proposed closed-form solutions was verified by numerical examples. At last but not the least important, the optimal form of IHSRM was found.

2. Theoretical Background

2.1. The Hilbert Spectral Representation Model. A time series can be decomposed into a few intrinsic mode functions (IMFs) using HHT. The extraction of IMFs from a time series entails a repeated "sifting" procedure called empirical mode decomposition (EMD) [19]. After EMD, the original time series $X(t)$ can be expressed in terms of IMFs as follows:

$$X(t) = \sum_{j=1}^{N} I_j(t) + r(t), \tag{1}$$

where N is the number of the IMFs, $I_j(t)$ denotes the jth IMF, and $r(t)$ indicates the residual function. In general, $r(t)$ is too small to be of any consequence, or it becomes a monotonic function from which no IMF can be extracted anymore. Performing the Hilbert transform on $I_j(t)$ yields

$$Q_j(t) = H\left[I_j(t)\right] = \frac{1}{\pi} P \int_{-\infty}^{\infty} \frac{I_j(\tau)}{t-\tau} \mathrm{d}\tau, \tag{2}$$

where P denotes the Cauchy principal value. An analytical function can be formulated as follows:

$$Z_j(t) = I_j(t) + iQ_j(t) = a_j(t) e^{i\theta_j(t)}, \tag{3}$$

where time functions $a_j(t)$ and $\theta_j(t)$ are called instantaneous amplitude and instantaneous phase functions, respectively, and $i^2 = -1$. The instantaneous frequency of the jth IMF is given by

$$\omega_j(t) = \frac{\mathrm{d}\theta_j(t)}{\mathrm{d}t}. \tag{4}$$

$a_j(t)$ and $\omega_j(t)$ $(j = 1, 2, \ldots, N)$ define the Hilbert amplitude spectrum, or simply Hilbert spectrum. Then, the original time series can be represented as follows:

$$X(t) = \mathrm{Re}\left\{ \sum_{j=1}^{N} a_j(t) e^{i\theta_j(t)} \right\} + r(t). \tag{5}$$

Based on the above derivation, Wen and Gu [18] constructed the underlying random process model corresponding to an observational record by introducing a random element as follows:

$$X(t) = \mathrm{Re}\left\{ \sum_{j=1}^{N} a_j(t) e^{i\left[\theta_j(t)+\varphi_j\right]} \right\} + r(t), \tag{6}$$

where φ_j's are independent random phase angles that are uniformly distributed between 0 and 2π. The mean and variance of the process are as follows:

$$\mu_x(t) = \mathrm{Re}\left\{ \sum_{j=1}^{N} a_j(t) e^{i\theta_j(t)} E\left[e^{i\varphi_j}\right] \right\} + r(t) = r(t), \tag{7}$$

$$\sigma_x^2(t) = E\left\{\left[X(t) - \mu_x(t)\right]^2\right\} = \frac{1}{2} \sum_{j=1}^{N} a_j^2(t). \tag{8}$$

Then, the mean and variance of each component of $X(t)$ can be expressed as

$$\mu_{x,j}(t) = \mathrm{Re}\left\{a_j(t) e^{i\theta_j(t)} E\left[e^{i\varphi_j}\right]\right\} = 0, \quad j = 1, 2, \ldots, N, \tag{9}$$

$$\sigma_{x,j}^2(t) = E\left\{\left[X_j(t) - \mu_{x,j}(t)\right]^2\right\} = \frac{1}{2} a_j^2(t). \tag{10}$$

The Hilbert spectrum of each simulated sample is the same as that of the record; in other words, the ground motion simulated by using this method is ergodic in the sense of Hilbert spectrum. Thus, the ensemble average of the simulated Hilbert spectra is also identical with the target.

2.2. Random Amplitude-Based Improved Hilbert Spectral Representation Method. Based on the IMFs obtained from the underlying random process corresponding to a real earthquake record, SCEGMs possessing natural nonstationary characteristics can be simulated by means of a prescribed spatial correlation model [20]. The simulation procedure of the IHSRM is shown in Figure 1, where the N-S

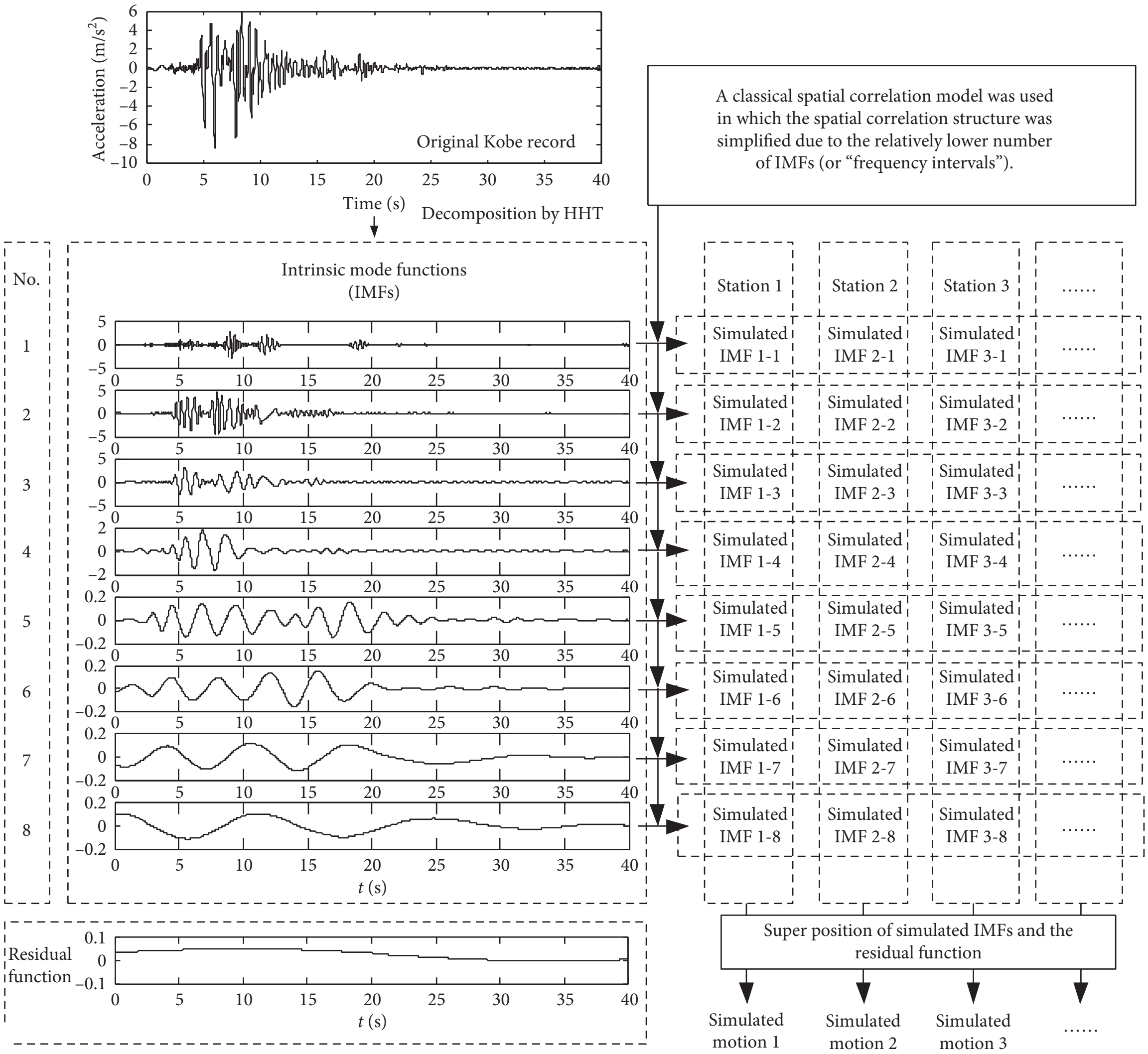

Figure 1: Simulation procedure of the IHSRM.

component of the 1995 Kobe earthquake is taken as an example.

Considering the correlation relations at the predominant frequency of each reference IMF and the Cholesky decomposition, the ground motion simulated by the random amplitude-based IHSRM at the mth station can be expressed as

$$x_m(t) = \sum_{k=1}^{m}\sum_{j=1}^{N}\sigma_j(t)D_{km,j}\left\{A_{kj}\cos\left[\theta_j(t)+\Phi_{km,j}\right]\right.$$
$$\left.+B_{kj}\sin\left[\theta_j(t)+\Phi_{km,j}\right]\right\}+r(t),\tag{11}$$
$$\Phi_{km,j} = -\frac{\omega_j \boldsymbol{\eta}_{km}}{V},$$

where $\sigma_j(t)$ is the ensemble variance of the jth IMF of the underlying random process, $D_{km,j}$ is an element of the decomposed spatial covariance matrix, $\boldsymbol{\eta}_{km}$ denotes the separation distance vector, and V is the apparent wave velocity in the medium; A_{kj} and B_{kj} denote independent and normally distributed zero-mean numbers with unit variance, obeying the following orthogonal relationships [21]:

$$\begin{aligned}E\left(A_{k1j1}A_{k2j2}\right) &= \delta_{k1k2}\delta_{j1j2},\\ E\left(B_{k1j1}B_{k2j2}\right) &= \delta_{k1k2}\delta_{j1j2},\\ E\left(A_{k1j1}B_{k2j2}\right) &= 0,\end{aligned}\tag{12}$$

where δ_{kj} is the Kronecker delta function. The ensemble averages of mean and variance of seismic motions simulated by the random amplitude-based IHSRM had been proved to be equal to the targets which were derived using equations (7)–(10); the ensemble averaged Hilbert spectra of generated motions are also identical with the target (detailed derivation processes can be found in [20]). In the present procedure, the frequency dependence of the spatial correlation function is simplified so that only the correlation at the predominant frequency of each IMF is taken into consideration. Thus, the number of frequency intervals is extremely lower than that in the classical SRM. The double summation and matrix decomposition in the proposed formula are quite simplified.

In addition, the decomposition of a real correlation coefficient matrix is relatively faster. Therefore, the proposed method facilitates the generation of ground motions with higher efficiency.

3. Random Phase-Based Improved Hilbert Spectral Representation Method

The simulated and target IMFs of the same order are assumed to have the same standard variance σ and instantaneous frequency, which is a reasonable approach when the focus of an earthquake is located at a large distance from the site compared with the site dimension [22]. To facilitate the derivation, the predictable wave propagation effect is assumed to have been removed temporally and that the spatial correlation structures are known a priori [20]. The covariance matrix **COV** can be expressed in terms of variance σ^2 and the spatial correlation coefficient matrix **C** as given by

$$\mathbf{COV} = \sigma^2 \mathbf{C} = \sigma^2 \begin{bmatrix} 1 & C_{12} & \cdots & C_{1L} \\ C_{L1} & 1 & \cdots & C_{2L} \\ \vdots & \vdots & \ddots & \vdots \\ C_{L1} & C_{L2} & \cdots & 1 \end{bmatrix}_{(L\times L)}, \tag{13}$$

where C_{mn} (m, $n = 1, 2, \ldots, L$) is typically a real function of frequency and separation distance and L is the number of simulation stations.

To make the generated ground motions compatible with the individual function in **COV**, the ground motion at the mth station is assumed to be

$$x_m(t) = \mathrm{Re}\left\{ \sum_{k=1}^{L} \sum_{j=1}^{N} A_{km,j}(t) e^{i\left[\theta_j(t)+\varphi_{k,j}\right]} \right\} + r(t), \quad m = 1, 2, \ldots, L, \tag{14}$$

where $A_{km,j}(t)$ denotes the instantaneous amplitude of the component IMF of the jth order by considering the correlations specified in equation (13). $A_{km,j}(t)$ can be determined by using the following algorithm.

The jth component IMF at the mth station can be expressed as

$$x_{m,j}(t) = \mathrm{Re}\left\{ \sum_{k=1}^{L} A_{km,j}(t) e^{i\left[\theta_j(t)+\varphi_{k,j}\right]} \right\}, \quad j = 1, 2, \ldots, N. \tag{15}$$

Then, the cross-covariance between $x_{m,j}(t)$ and $x_{n,j}(t)$ is

$$\mathrm{Cov}\left[x_{m,j}(t), x_{n,j}(t)\right] = E\left\{ \sum_{k=1}^{L} \mathrm{Re}\left\{A_{km,j}(t) e^{i\left[\theta_j(t)+\varphi_{k,j}\right]}\right\} \sum_{p=1}^{L} \mathrm{Re}\left\{A_{pn,j}(t) e^{i\left[\theta_j(t)+\varphi_{p,j}\right]}\right\} \right\}. \tag{16}$$

When $k \neq p$, the cross-covariance vanishes because $\varphi_{k,j}$ and $\varphi_{p,j}$ are statistically independent in such cases. Therefore,

$$\begin{aligned} \mathrm{Cov}\left[x_{m,j}(t), x_{n,j}(t)\right] &= E\left\{ \sum_{k=1}^{L} \mathrm{Re}\left\{A_{km,j}(t) e^{i\left[\theta_j(t)+\varphi_{k,j}\right]}\right\} \mathrm{Re}\left\{A_{kn,j}(t) e^{i\left[\theta_j(t)+\varphi_{k,j}\right]}\right\} \right\} \\ &= \sum_{k=1}^{L} \frac{1}{2} A_{km,j}(t) A_{kn,j}(t) E\left[\cos\left(2\theta_j(t) + 2\varphi_{k,j}\right) + \cos(0)\right] \\ &= \sum_{k=1}^{L} \frac{1}{2} A_{km,j}(t) A_{kn,j}(t). \end{aligned} \tag{17}$$

In accordance with equations (10) and (13), the preceding cross-covariance at the jth order can also be expressed in terms of the spatial correlation coefficients in the following form:

$$\mathrm{Cov}\left[x_{m,j}(t), x_{n,j}(t)\right] = \sigma_j^2(t) C_{mn,j}, \tag{18}$$

where $\sigma_j^2(t)$ denotes the ensemble variance of the jth target IMF and $C_{mn,j}$ represents the spatial correlation coefficient between the mth and nth motions that corresponds to the predominant frequency of the jth target IMF, ω_j.

Matrix $\mathbf{C}_j$ is usually symmetric and positive defined; therefore, it can usually be decomposed into the multiplication of two identical and symmetric matrices by utilizing the root decomposition process proposed by Wu et al. [23–25], which is described as follows:

$$\sigma_j^2(t)\mathbf{C}_j = \sigma_j^2(t)\mathbf{D}_j\mathbf{D}_j^T, \quad (19)$$

$$\sigma_j^2(t)C_{mn,j} = \sigma_j^2(t)\sum_{k=1}^{L} D_{km,j}D_{kn,j}, \quad (20)$$

where T indicates the transpose of a matrix.

Then, the following formula can be obtained:

$$\sum_{k=1}^{L}\frac{1}{2}A_{km,j}(t)A_{kn,j}(t) = \sigma_j^2(t)C_{mn,j} = \sigma_j^2(t)\sum_{k=1}^{L} D_{km,j}D_{kn,j}. \quad (21)$$

Comparing the corresponding terms on both sides of equation (21) yields

$$A_{km,j}(t) = \sqrt{2\sigma_j^2(t)}D_{km,j} = a_j(t)D_{km,j}. \quad (22)$$

Then, the SCEGMs that consider the wave propagation effect can be obtained as follows:

$$x_m(t) = \sum_{k=1}^{L}\sum_{j=1}^{N}\sqrt{2\sigma_j^2(t)}D_{km,j}\cos\left[\theta_j(t) + \Phi_{km,j} + \varphi_{k,j}\right] + r(t), \quad (23)$$

$$\Phi_{km,j} = -\frac{\omega_j\left|\boldsymbol{\eta}_{km}\right|}{V}. \quad (24)$$

To summarize the procedure as presented, the simulation of SCEGMs consists of the following steps: (i) $A_{km,j}(t)$ is computed using equations (13)–(22) based on a spatial correlation model for "phase-aligned" ground motions; (ii) the SCEGM for each simulation station is obtained using equations (23) and (24) by considering the wave propagation effect and the summation of simulated IMFs and the original residual function.

To construct the spatial covariance matrix shown in equation (13), the isotropic frequency-dependent correlation coefficient model used by Vanmarcke et al. [26, 27] and Zerva and Shinozuka [28] to simulate "phase-aligned" earthquake ground motions can be adopted:

$$C\left(\boldsymbol{\eta}_{mn}\right) = \exp\left[-\frac{\omega\left|\boldsymbol{\eta}_{mn}\right|}{2\pi V d}\right], \quad (25)$$

where d is the correlation distance, and $d > 0$. A large d value is expected to demonstrate high correlation between points of the random field. The covariance function for the jth components can be expressed as

$$\mathrm{COV}_{mn,j} = \sigma_j^2(t)C_j\left(\boldsymbol{\eta}_{mn}\right) = \sigma_j^2(t)\exp\left[-\frac{\omega_j\left|\boldsymbol{\eta}_{mn}\right|}{2\pi V d}\right]. \quad (26)$$

The ensemble averages of the mean and variance of $x_m(t)$ and $x_{m,j}(t)$ are determined to be identical with those of the target underlying random process and the jth reference IMF, respectively (see Appendix A). The Hilbert spectra of the sample realizations of this model differ, but $C_{mm,j} = 1$ ensures that the ensemble average of the Hilbert spectra of the samples is the same as the target Hilbert spectrum, which is also proven in Appendix A. Note that since only the predominant frequencies of reference IMFs were considered, the IHSRM-simulated random processes are not periodic.

Taking the E-W component of the 2011 Niigata earthquake in Japan as the reference, a group of SCEGMs are simulated for three locations to demonstrate the reliability of the present method, in which $d = 100$, and the spacing distance is set to 100 m. The original record and the corresponding generated ground motions are shown in Figure 2. It can be found that the waveform of the simulated motions is significantly close to the target motion. The acceleration response spectra of the original record and simulated motions are compared in Figure 3, and good match can be observed. In addition, the ensemble average correlation coefficients between simulated ground motions derived from 2,000 simulations are compared with the corresponding target values as shown in Figure 4. The simulation values of correlation coefficients are approximately identical with the targets, which verifies the validness of the proposed method.

4. Error Assessment

The decomposition of the spatial correlation coefficient matrix involved in the IHSRM can usually be carried out by Cholesky decomposition, root decomposition, or eigendecomposition. Thus, different combinations of the simulation formulas with the decomposition methods yield a distinction between these six types of IHSRMs: random phase formula and Cholesky decomposition-based IHSRM (RP-CIHSRM); random phase formula and root decomposition-based IHSRM (RP-RIHSRM); random phase formula and eigendecomposition-based IHSRM (RP-EIHSRM); random amplitude formula and Cholesky decomposition-based IHSRM (RA-CIHSRM); random amplitude formula and root decomposition-based IHSRM (RA-RIHSRM); and random amplitude formula and eigendecomposition-based IHSRM (RA-EIHSRM). Despite the difference among the three different decomposition methods, the formulas for these IHSRMs can be unified as follows.

For RP-IHSRM,

$$x_m(t) = \sum_{k=1}^{L}\sum_{j=1}^{N} a_j(t)D_{km,j}\cos\left[\theta_j(t) + \Phi_{km,j} + \varphi_{k,j}\right] + r(t). \quad (27)$$

For RA-IHSRM,

$$x_m(t) = \sum_{k=1}^{L}\sum_{j=1}^{N}\sigma_j(t)D_{km,j}\left\{A_{kj}\cos\left[\theta_j(t) + \Phi_{km,j}\right] + B_{kj}\sin\left[\theta_j(t) + \Phi_{km,j}\right]\right\} + r(t). \quad (28)$$

When different decomposition methods are employed, only $D_{km,j}$'s are different.

In this section, the N-S component of the 1995 Kobe earthquake in Japan was selected as the reference motion, and SCEGMs will be generated for three locations spaced at 100 m intervals (0, 100, and 200 m) along the direction of

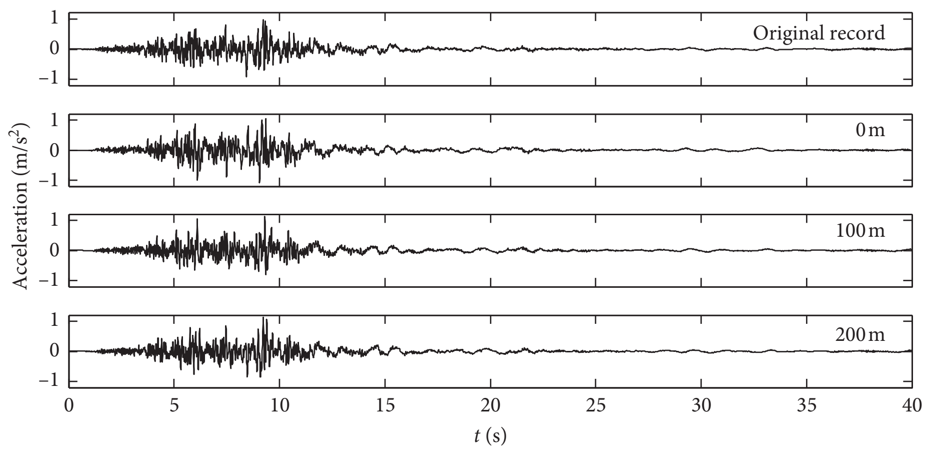

Figure 2: Comparison of acceleration-time histories of simulated ground motions with the original record.

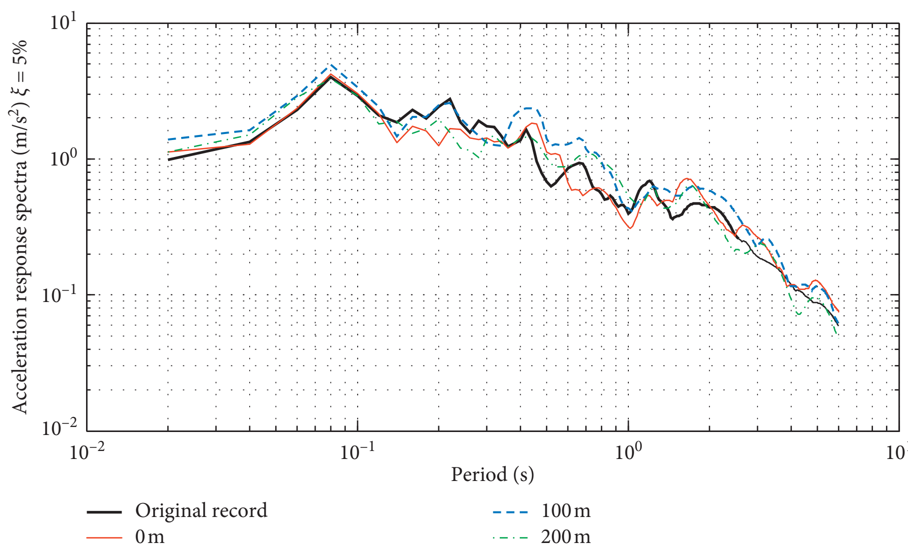

Figure 3: The acceleration response spectra of simulated ground motions and the original record.

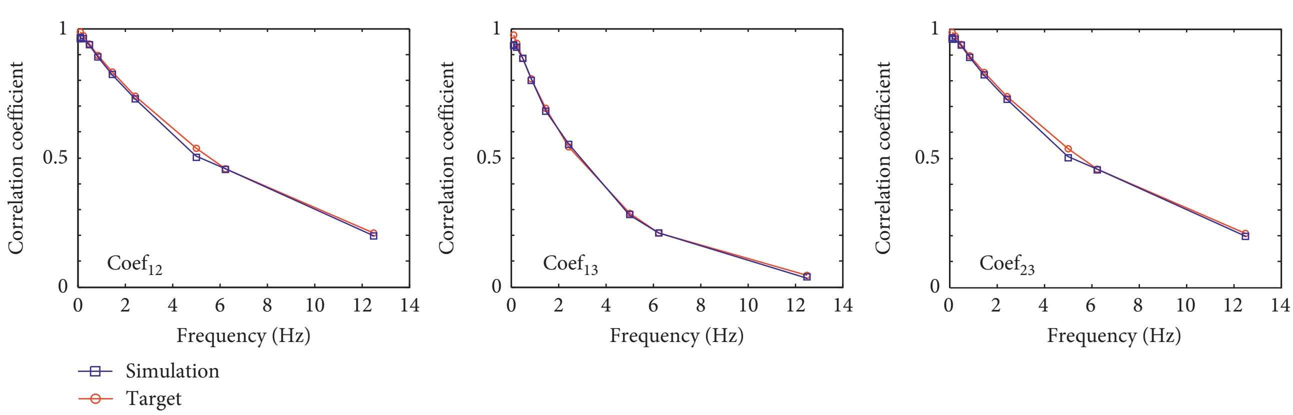

(a)

Figure 4: Continued.

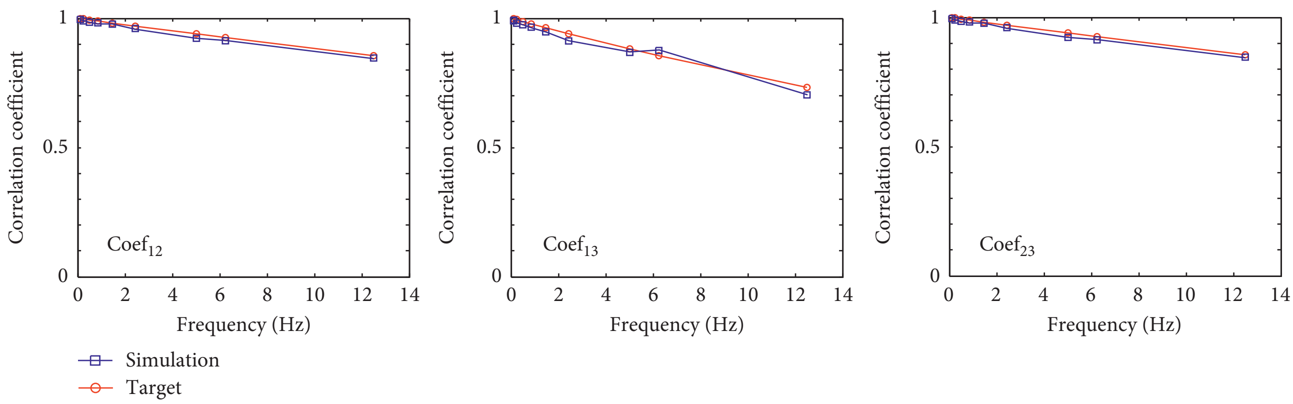

(b)

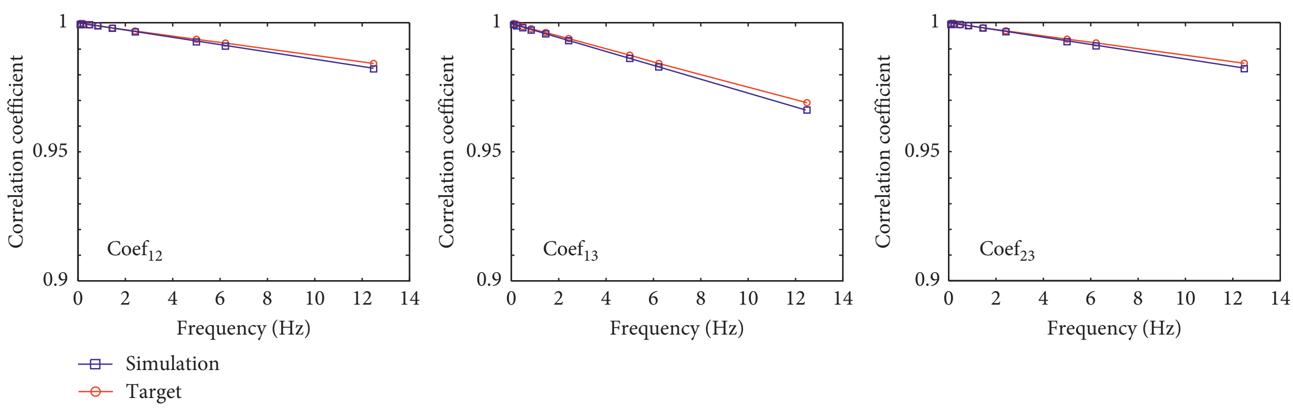

(c)

FIGURE 4: Comparison of the ensemble average correlation coefficients between simulated ground motions with targets: (a) $d = 1$; (b) $d = 10$; (c) $d = 100$.

wave propagation to proceed with the error assessment. Then, based on the unified simulation formulas, an error analysis of random processes simulated by the aforementioned IHSRMs is conducted, and the results are compared to facilitate the selection of the optimal type of IHSRM.

4.1. Definition of Errors. The bias error $b(\cdot)$ and the stochastic error $\sigma(\cdot)$ [29] were adopted to proceed with the error assessment which are shown as follows:

$$b\left(\vartheta^T\right) = E\left(\vartheta^T\right) - \vartheta^0, \tag{29}$$

$$\sigma\left(\vartheta^T\right) = \sqrt{E\left(\vartheta^T\right)^2 - E^2\left(\vartheta^T\right)} = \sqrt{E\left[\vartheta^T - E\left(\vartheta^T\right)\right]^2}, \tag{30}$$

where ϑ denotes one type of the temporal statistic of the simulated process and superscript T represents that the temporal statistic is obtained by estimating over the entire time duration; superscript 0 is the target value. The bias error can measure the degree that the ensemble average of the temporal estimation deviates from the corresponding target. By contrast, the stochastic error can measure the degree that the temporal estimation fluctuates around its ensemble average.

4.2. Bias Error and Stochastic Error of the Mean. Note that the ensemble average of mean, variance, and Hilbert spectra of seismic motions simulated by the RA-IHSRM had been proved to be equal to the target [20]. Appendix A has proved that the ensemble average of mean of $x_m(t)$ for the random phase method equates to the target. Therefore, the bias errors of mean of the component $x_m(t)$ are zero for these six types of formulas. For the random phase formulas, the stochastic error of mean of $x_m(t)$ can be expressed as

$$\begin{aligned}\sigma[\mu_m(t)] &= \sqrt{E[\mu_m(t)]^2 - E^2[\mu_m(t)]} \\ &= \sqrt{E\left\{\left\{\sum_{k1=1}^{L}\sum_{j1=1}^{N} a_{j1}(t)D_{k1m,j1}\cos\left[\theta_{j1}(t)+\varphi_{k1,j1}\right]+r(t)\right\}\cdot\left\{\sum_{k2=1}^{L}\sum_{j2=1}^{N} a_{j2}(t)D_{k2m,j2}\cos\left[\theta_{j2}(t)+\varphi_{k2,j2}\right]+r(t)\right\}\right\} - [r(t)]^2} \\ &= \sqrt{\sum_{k=1}^{L}\sum_{j=1}^{N}\frac{1}{2}a_j^2(t)D_{km,j}^2} \\ &= \sqrt{\sum_{j=1}^{N}\frac{1}{2}a_j^2(t)}.\end{aligned} \tag{31}$$

For the random amplitude formulas, the stochastic error of mean of $x_m(t)$ can be expressed as

$$\begin{aligned}\sigma[\mu_m(t)] &= \sqrt{E[\mu_m(t)]^2 - E^2[\mu_m(t)]} \\ &= \sqrt{E\left\{\left\{\sum_{k1=1}^{L}\sum_{j1=1}^{N} \sigma_{j1}(t)D_{k1m,j1}\left\{A_{k1j1}\cos\left[\theta_{j1}(t)\right]+B_{k1j1}\sin\left[\theta_{j1}(t)\right]\right\}+r(t)\right\}\cdot\left\{\sum_{k2=1}^{L}\sum_{j2=1}^{N} \sigma_{j2}(t)D_{k2m,j2}\left\{A_{k2j2}\cos\left[\theta_{j2}(t)\right]+B_{k2j2}\sin\left[\theta_{j2}(t)\right]\right\}+r(t)\right\}\right\} - [r(t)]^2} \\ &= \sqrt{\sum_{k=1}^{L}\sum_{j=1}^{N}\frac{1}{2}a_j^2(t)D_{km,j}^2} \\ &= \sqrt{\sum_{j=1}^{N}\frac{1}{2}a_j^2(t)}.\end{aligned} \tag{32}$$

From the stochastic errors presented above, it can be concluded that the IHSRM is not ergodic in terms of temporal mean.

4.3. Bias Error and Stochastic Error of the Variance. According to Appendix A and [20], the bias errors of variance of the component $x_m(t)$ simulated by random phase- and random amplitude-based IHSRMs are also zero.

For random phase formulas, the raw estimate of variance of $x_m(t)$ is

$$\hat{\sigma}_m^2(t) = \left\{\sum_{k1=1}^{L}\sum_{j1=1}^{N} a_{j1}(t)D_{k1m,j1}\cos\left[\theta_{j1}(t)+\varphi_{k1,j1}\right]\right\}\cdot\left\{\sum_{k2=1}^{L}\sum_{j2=1}^{N} a_{j2}(t)D_{k2m,j2}\cos\left[\theta_{k2}(t)+\varphi_{k2,j2}\right]\right\}. \tag{33}$$

Then, for random phase formulas, the stochastic error of variance of $x_m(t)$ can be derived as follows:

$$\begin{aligned}\sigma\left[\widehat{\sigma}_m^2(t)\right] &= \left\{E\left\{\left\{\sum_{k1=1}^{L}\sum_{j1=1}^{N} a_{j1}(t)D_{k1m,j1}\cos\left[\theta_{j1}(t)+\varphi_{k1,j1}\right]\right\}\cdot\left\{\sum_{k2=1}^{L}\sum_{j2=1}^{N} a_{j2}(t)D_{k2m,j2}\cos\left[\theta_{j2}(t)+\varphi_{k2,j2}\right]\right\}\right\}^2-\left[\sum_{j=1}^{N}\frac{1}{2}a_j^2(t)\right]^2\right\}^{1/2} \\ &= \left\{\sum_{k=1}^{L}\sum_{j=1}^{N}\frac{3}{8}a_j^4(t)D_{km,j}^4+\sum_{k=1}^{L}\sum_{\substack{p=1\\p\neq k}}^{L}\sum_{j=1}^{N}\sum_{\substack{q=1\\q\neq j}}^{N}\frac{3}{4}a_j^2(t)a_q^2(t)D_{km,j}^2D_{pm,q}^2-\left[\sum_{j=1}^{N}\frac{1}{2}a_j^2(t)\right]^2\right\}^{1/2}.\end{aligned} \tag{34}$$

For random amplitude formulas, the stochastic error of variance of $x_m(t)$ can be derived as follows:

$$\begin{aligned}\sigma\left[\widehat{\sigma}_m^2(t)\right] &= \left\{E\left\{\left\{\sum_{k1=1}^{L}\sum_{j1=1}^{N}\sigma_{j1}(t)D_{k1m,j1}\left\{A_{k1j1}\cos\left[\theta_{j1}(t)\right]+B_{k1j1}\sin\left[\theta_{j1}(t)\right]\right\}+r(t)\right\}\cdot\left\{\sum_{k2=1}^{L}\sum_{j2=1}^{N}\sigma_{j2}(t)D_{k2m,j2}\left\{A_{k2j2}\cos\left[\theta_{j2}(t)\right]+B_{k2j2}\sin\left[\theta_{j2}(t)\right]\right\}+r(t)\right\}\right\}^2-\left[\sum_{j=1}^{N}\frac{1}{2}a_j^2(t)\right]^2\right\}^{1/2} \\ &= \left\{\sum_{k=1}^{L}\sum_{j=1}^{N}\frac{3}{4}a_j^4(t)D_{km,j}^4+\sum_{k=1}^{L}\sum_{\substack{p=1\\p\neq k}}^{L}\sum_{j=1}^{N}\sum_{\substack{q=1\\q\neq j}}^{N}\frac{3}{4}a_j^2(t)a_q^2(t)D_{km,j}^2D_{pm,q}^2-\left[\sum_{j=1}^{N}\frac{1}{2}a_j^2(t)\right]^2\right\}^{1/2}.\end{aligned} \tag{35}$$

The specific derivation process is shown in Appendix B.

4.4. Bias Error and Stochastic Error of the Cross-Covariance. Taking equations (8) and (10) and the property of cross-covariance into account, the target cross-covariance between $x_m(t)$ and $x_n(t)$ can be expressed as

$$\mathrm{COV}_{mn}^0(t)=\sum_{j=1}^{N}\mathrm{COV}_{mn,j}^0(t)=\sum_{j=1}^{N}\frac{1}{2}a_j^2(t)C_{mn,j}. \tag{36}$$

For random phase- and random amplitude-based IHSRMs, the raw estimates of cross-covariance between $x_m(t)$ and $x_n(t)$ $(m,\ n=1,\ 2,\ 3)$ are

$$\begin{aligned}\widehat{\mathrm{COV}}_{mn}(t) &= \left\{\sum_{k1=1}^{L}\sum_{j1=1}^{N}a_{j1}(t)D_{k1m,j1}\cos\left[\theta_{j1}(t)+\varphi_{k1,j1}\right]\right\}\cdot\left\{\sum_{k2=1}^{L}\sum_{j2=1}^{N}a_{j2}(t)D_{k2n,j2}\cos\left[\theta_{j2}(t)+\varphi_{k2,j2}\right]\right\}, \\ \widehat{\mathrm{COV}}_{mn}(t) &= \left\{\sum_{k1=1}^{L}\sum_{j1=1}^{N}\sigma_{j1}(t)D_{k1m,j1}\left\{A_{k1j1}\cos\left[\theta_{j1}(t)\right]+B_{k1j1}\sin\left[\theta_{j1}(t)\right]\right\}\right\}\cdot\left\{\sum_{k2=1}^{L}\sum_{j2=1}^{N}\sigma_{j2}(t)D_{k2n,j2}\left\{A_{k2j2}\cos\left[\theta_{j2}(t)\right]\right.\right. \\ &\quad \left.\left.+B_{k2j2}\sin\left[\theta_{j2}(t)\right]\right\}\right\}.\end{aligned} \tag{37}$$

Performing mathematical expectation on $\widehat{\mathrm{COV}}_{mn}(t)$'s yields

$$E\left[\widehat{\mathrm{COV}}_{mn}(t)\right] = E\left\{\left\{\sum_{k=1}^{L}\sum_{j=1}^{N}\sqrt{2\sigma_j^2(t)}\,D_{km,j}\cos\left[\theta_j(t)+\varphi_{k,j}\right]\right\}\cdot\left\{\sum_{p=1}^{L}\sum_{q=1}^{N}\sqrt{2\sigma_q^2(t)}\,D_{pn,q}\cos\left[\theta_q(t)+\varphi_{p,q}\right]\right\}\right\}$$
$$= \sum_{j=1}^{N}\frac{1}{2}a_j^2(t)C_{mn,j}, \tag{38}$$

$$E\left[\widehat{\mathrm{COV}}_{mn}(t)\right] = E\left\{\left\{\sum_{k1=1}^{L}\sum_{j1=1}^{N}\sigma_{j1}(t)D_{k1m,j1}\left\{A_{k1j1}\cos\left[\theta_{j1}(t)\right]+B_{k1j1}\sin\left[\theta_{j1}(t)\right]\right\}\right\}\cdot\left\{\sum_{k2=1}^{L}\sum_{j2=1}^{N}\sigma_{j2}(t)D_{k2m,j2}\left\{A_{k2j2}\cos\left[\theta_{j2}(t)\right]\right.\right.\right.$$
$$\left.\left.\left.+B_{k2j2}\sin\left[\theta_{j2}(t)\right]\right\}\right\}\right\}$$
$$= \sum_{j=1}^{N}\frac{1}{2}a_j^2C_{mn,j}. \tag{39}$$

Thus, the bias errors of cross-covariance for both random phase- and random amplitude-based IHSRMs can be expressed as

$$b\left[\widehat{\mathrm{COV}}_{mn}(t)\right] = E\left[\widehat{\mathrm{COV}}_{mn}(t)\right] - \mathrm{COV}_{mn}^0(t) = 0. \tag{40}$$

The stochastic errors of cross-covariance for random phase and random amplitude formulas can be derived as follows (see Appendix C for a detailed proof):

$$\sigma\left[\widehat{\mathrm{COV}}_{mn}(t)\right] = \left\{E\left\{\left\{\sum_{k1=1}^{L}\sum_{j1=1}^{N}a_{j1}(t)D_{k1m,j1}\cos\left[\theta_{j1}(t)+\varphi_{k1,j1}\right]\right\}\cdot\left\{\sum_{k2=1}^{L}\sum_{j2=1}^{N}a_{j2}(t)D_{k2n,j2}\cos\left[\theta_{j2}(t)+\varphi_{k2,j2}\right]\right\}\right\}^2 - \left[\sum_{j=1}^{N}\frac{1}{2}a_j^2(t)C_{mn,j}\right]^2\right\}^{1/2}$$
$$= \left\{\sum_{k=1}^{L}\sum_{j=1}^{N}\frac{3}{8}a_j^4(t)D_{km,j}^2D_{kn,j}^2 + 2\sum_{k=1}^{L}\sum_{\substack{p=1\\p\neq k}}^{L}\sum_{j=1}^{N}\sum_{\substack{q=1\\q\neq j}}^{N}\frac{1}{4}a_j^2(t)a_q^2(t)D_{km,j}D_{kn,j}D_{pm,q}D_{pn,q} + \sum_{k=1}^{L}\sum_{\substack{p=1\\p\neq k}}^{L}\sum_{j=1}^{N}\sum_{\substack{q=1\\q\neq j}}^{N}\frac{1}{4}a_j^2(t)a_q^2(t)D_{km,j}^2D_{pn,q}^2 - \left[\sum_{j=1}^{N}\frac{1}{2}a_j^2(t)C_{mn,j}\right]^2\right\}^{1/2}, \tag{41}$$

$$\sigma\left[\widehat{COV}_{mn}(t)\right] = \left\{E\left\{\left\{\sum_{k1=1}^{L}\sum_{j1=1}^{N}\sigma_{j1}(t)D_{k1m,j1}\left\{A_{k1j1}\cos\left[\theta_{j1}(t)\right]+B_{k1j1}\sin\left[\theta_{j1}(t)\right]\right\}+r(t)\right\}\right.\right.$$
$$\left.\left.\cdot\left\{\sum_{k2=1}^{L}\sum_{j2=1}^{N}\sigma_{j2}(t)D_{k2n,j2}\left\{A_{k2j2}\cos\left[\theta_{j2}(t)\right]+B_{k2j2}\sin\left[\theta_{j2}(t)\right]\right\}+r(t)\right\}\right\}^2 - \left[\sum_{j=1}^{N}\frac{1}{2}a_j^2(t)C_{mn,j}\right]^2\right\}^{1/2}$$
$$= \left\{\sum_{k=1}^{L}\sum_{j=1}^{N}\frac{3}{4}a_j^4(t)D_{km,j}^2D_{kn,j}^2 + 2\sum_{k=1}^{L}\sum_{\substack{p=1\\p\neq k}}^{L}\sum_{j=1}^{N}\sum_{\substack{q=1\\q\neq j}}^{N}\frac{1}{4}a_j^2(t)a_q^2(t)D_{km,j}D_{kn,j}D_{pm,q}D_{pn,q}\right.$$
$$\left.+\sum_{k=1}^{L}\sum_{\substack{p=1\\p\neq k}}^{L}\sum_{j=1}^{N}\sum_{\substack{q=1\\q\neq j}}^{N}\frac{1}{4}a_j^2(t)a_q^2(t)D_{km,j}^2D_{pn,q}^2 - \left[\sum_{j=1}^{N}\frac{1}{2}a_j^2(t)C_{mn,j}\right]^2\right\}^{1/2} \tag{42}$$

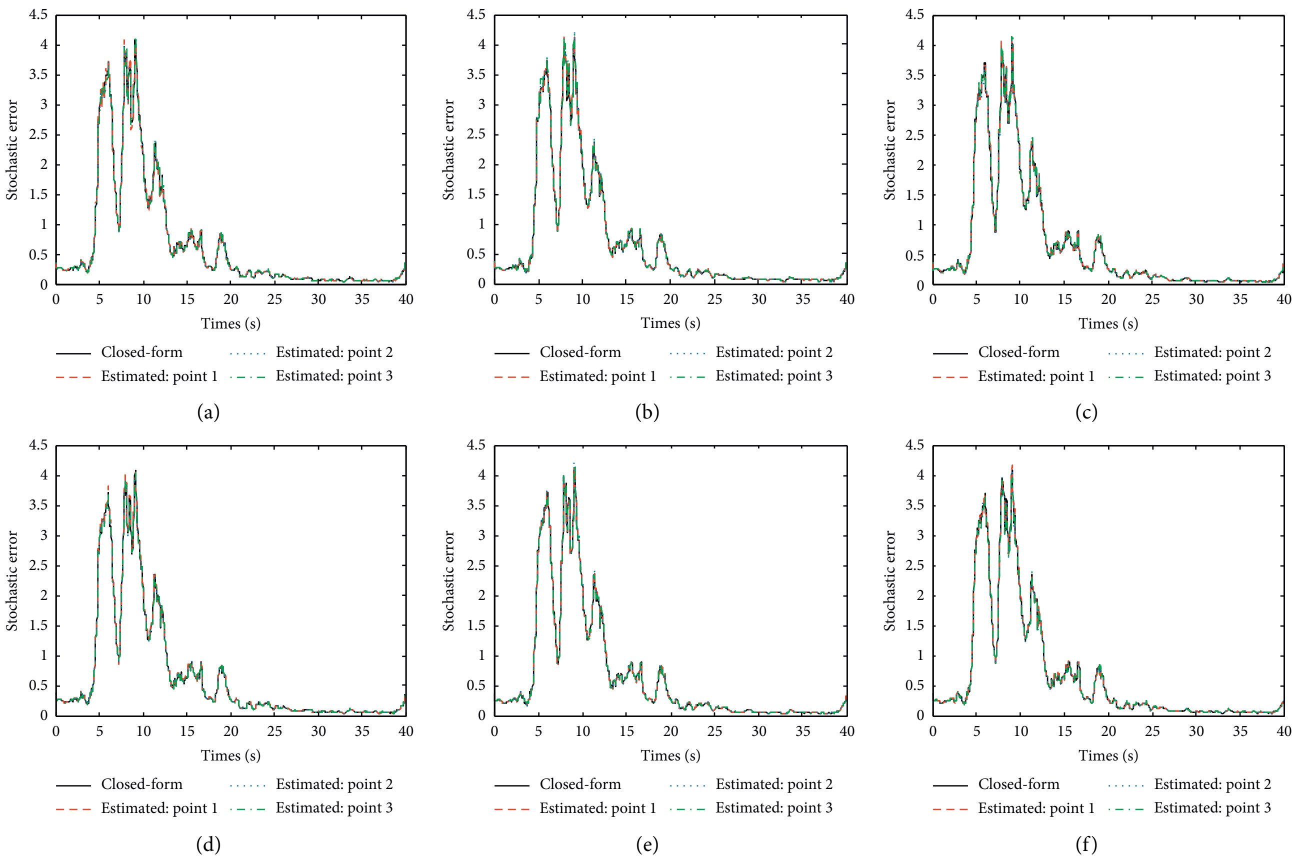

Figure 5: Comparison between the closed-form and estimated stochastic errors of temporal mean among the six types of methods: (a) RP-CIHSRM; (b) RP-RIHSRM; and (c) RP-EIHSRM; (d) RA-CIHSRM; (e) RA-RIHSRM; and (f) RA-EIHSRM.

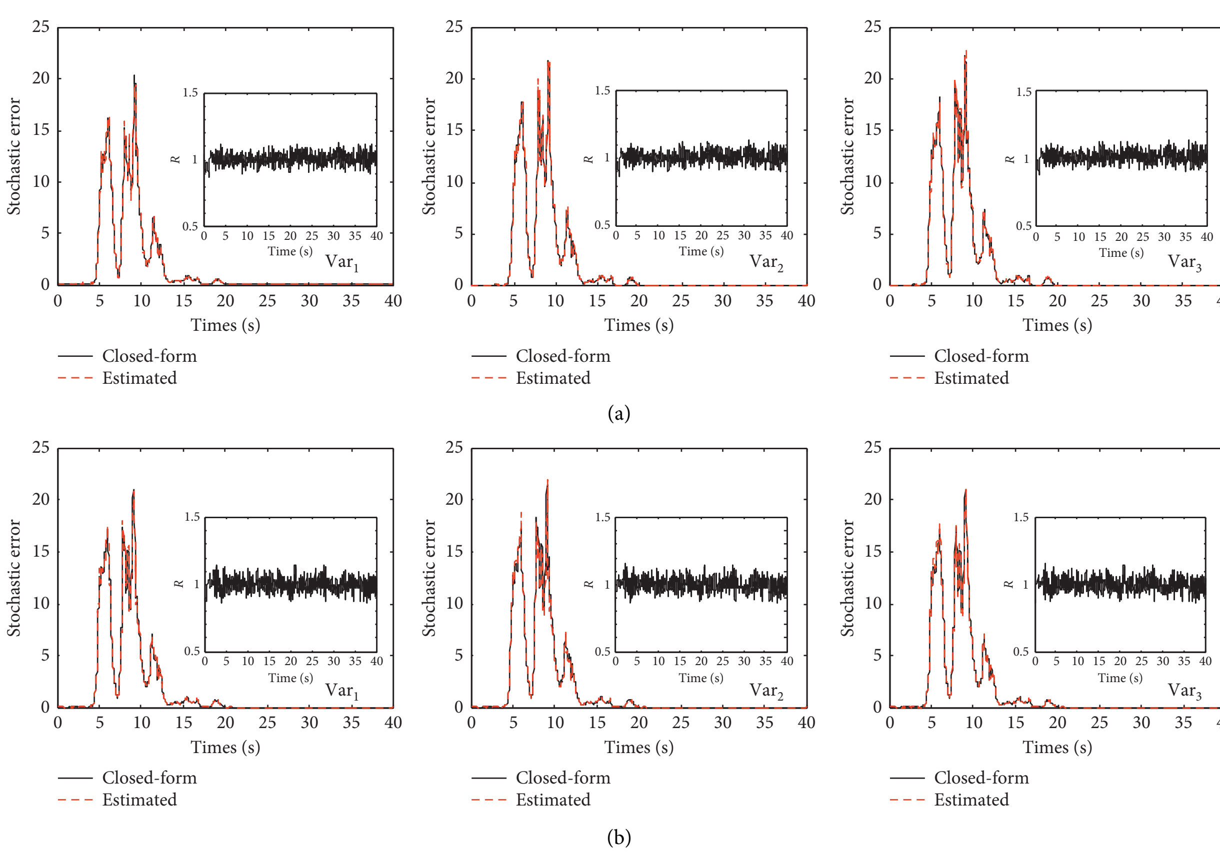

Figure 6: Continued.

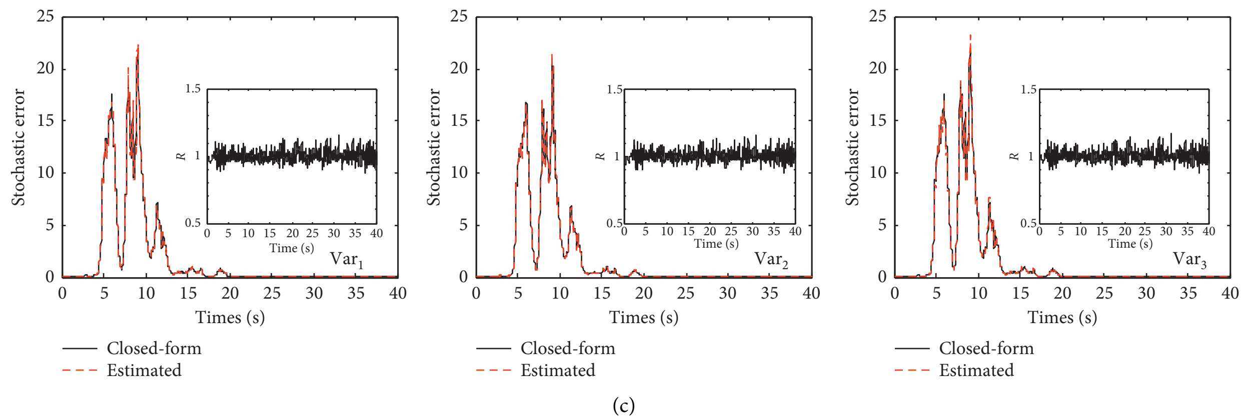

Figure 6: Comparison between the closed-form and estimated stochastic errors of temporal variance: (a) RP-CIHSRM; (b) RP-RIHSRM; (c) RP-EIHSRM.

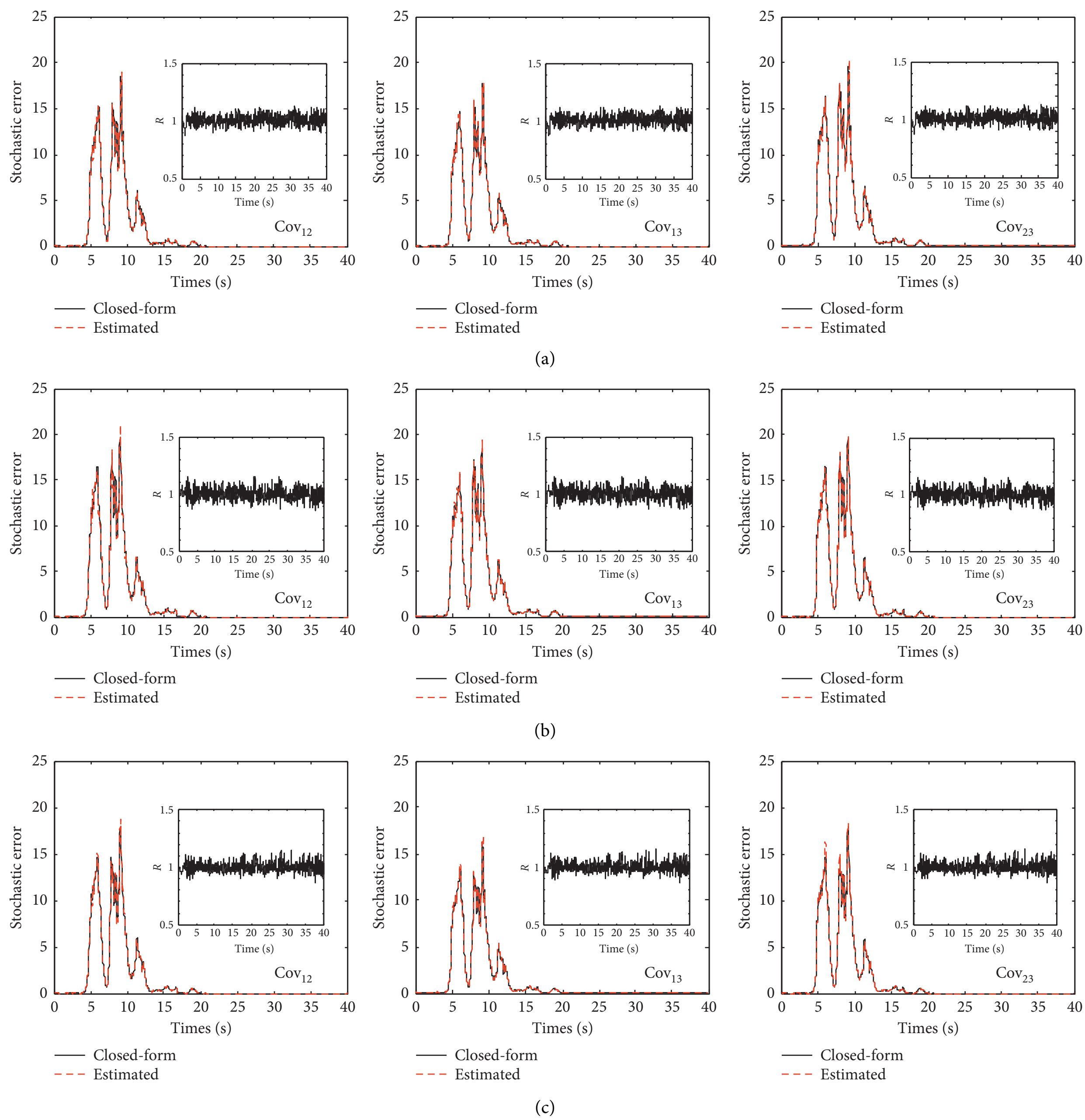

Figure 7: Comparison between the closed-form and estimated stochastic errors of temporal cross-covariance: (a) RP-CIHSRM; (b) RP-RIHSRM; (c) RP-EIHSRM.

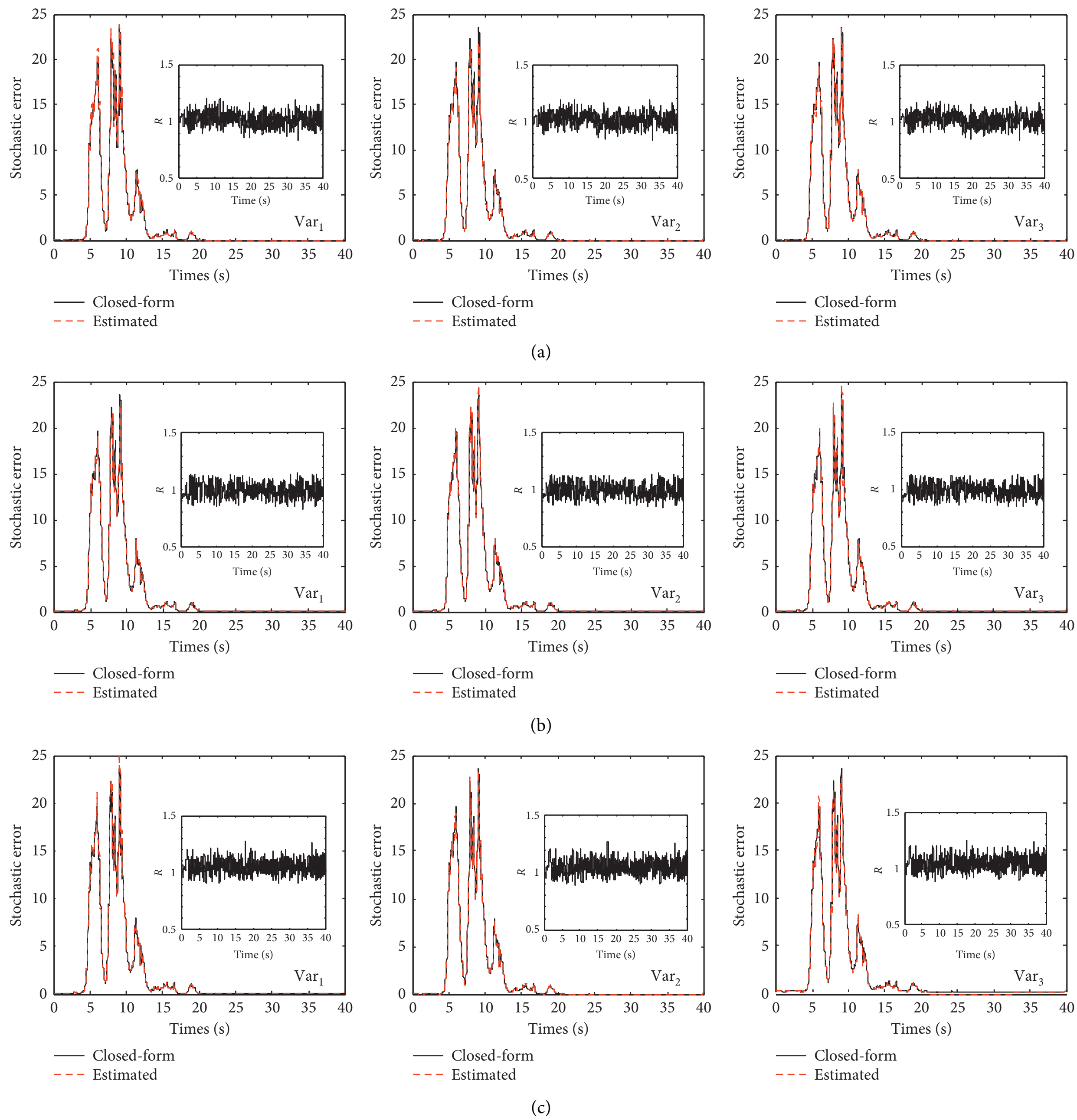

Figure 8: Comparison between the closed-form and estimated stochastic errors of temporal variance: (a) RA-CIHSRM; (b) RA-RIHSRM; (c) RA-EIHSRM.

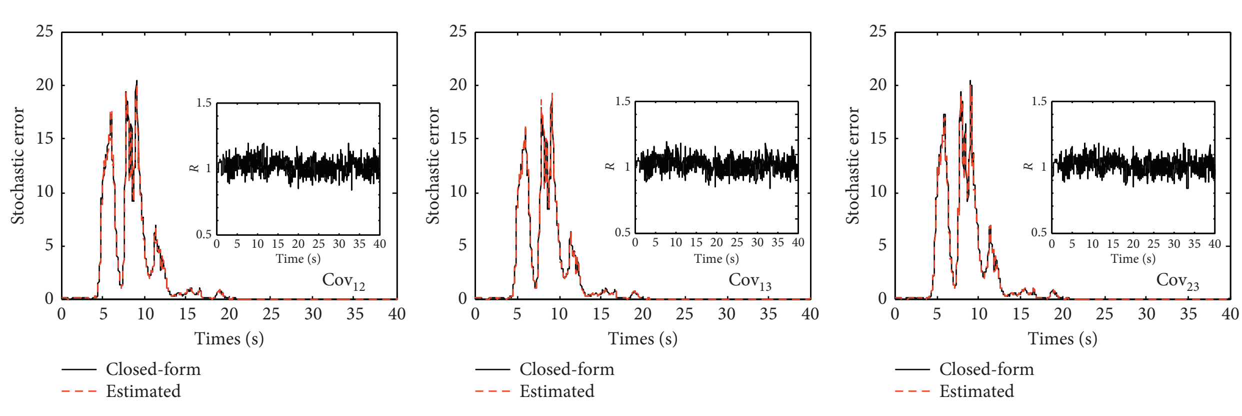

Figure 9: Continued.

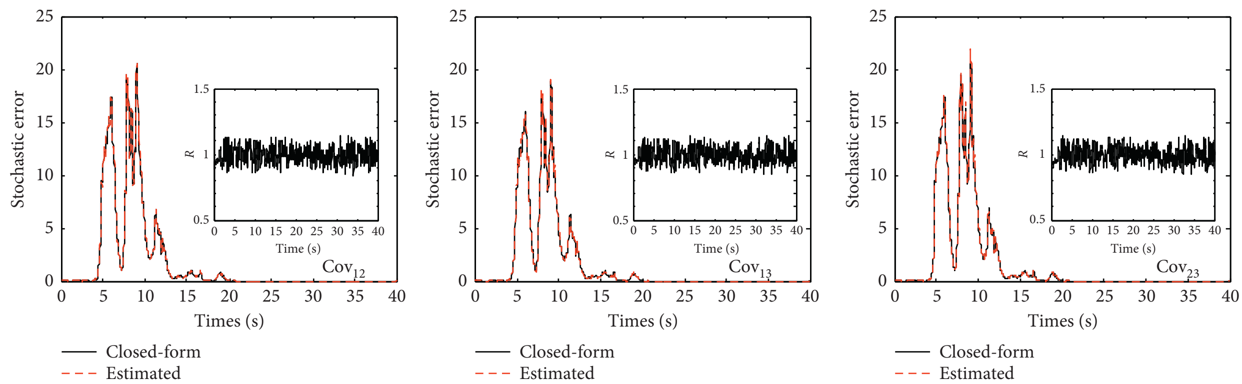

(b)

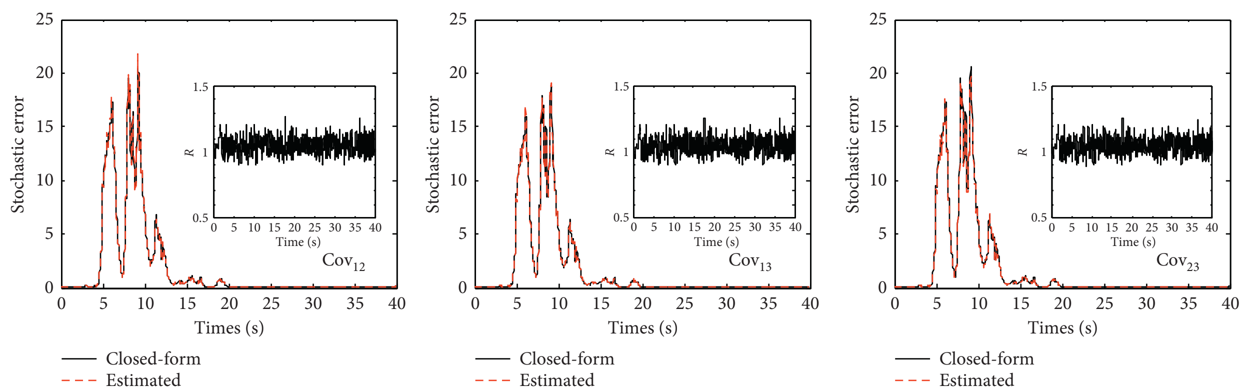

(c)

Figure 9: Comparison between the closed-form and estimated stochastic errors of temporal cross-covariance: (a) RA-CIHSRM; (b) RA-RIHSRM; (c) RA-EIHSRM.

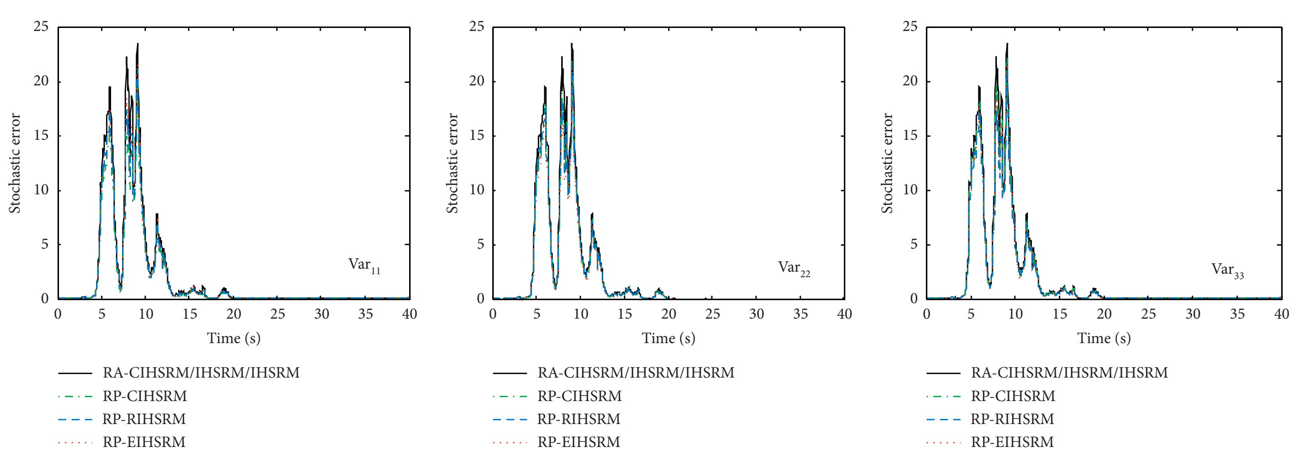

(a) (b) (c)

Figure 10: Continued.

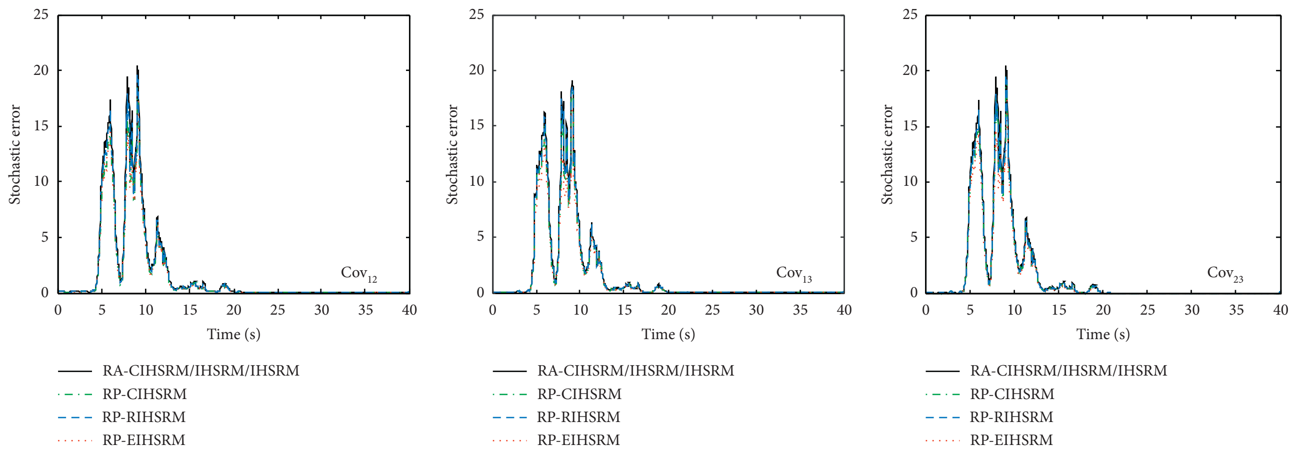

(d) (e) (f)

Figure 10: Comparison of the closed-form stochastic errors of temporal covariance among the six types of methods: (a) Var11; (b) Var22; and (c) Var33; (d) Cov12; (e) Cov13; and (f) Cov23.

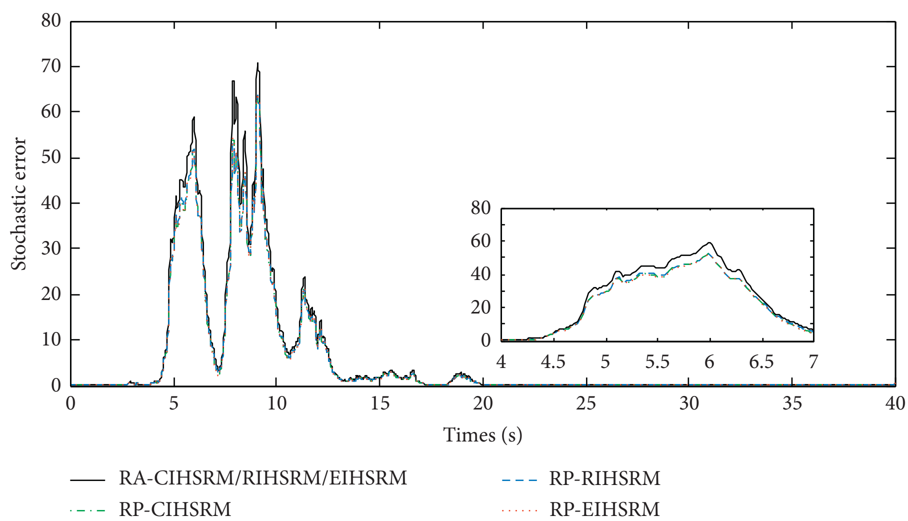

Figure 11: Sum of the stochastic errors of variance for different methods.

4.5. Verification and Discussion. To verify the closed-form stochastic errors of the temporal mean, variance, and cross-covariance, 2,000 sample processes were simulated for each of these six types of IHSRMs aforementioned. The estimated stochastic errors of mean for the six types of IHSRMs are compared with the corresponding closed-form ones in Figure 5. The estimated stochastic errors of variance and cross-covariance in comparison with the corresponding closed-form ones for RP-IHSRMs are shown in Figures 6 and 7, respectively. For RA-IHSRMs, the comparison between the estimated and closed-form stochastic errors of variance and cross-covariance is shown in Figures 8 and 9, respectively. In Figures 6–9, R denotes the ratio between closed-form and estimated stochastic errors. It can be found that the estimated temporal errors for each decomposition method match the corresponding closed-form ones very well, which verifies the validness of the derived closed-form solutions. Simultaneously, for all the six types of IHSRMs, the closed-form and estimated stochastic errors of cross-covariance between points 1 and 3 are slightly lower than those between points 1 and 2 and those between points 2 and 3 due to the loss of spatial correlation.

Figure 10 shows the comparison of the closed-form stochastic errors of temporal covariance (including variance and cross-covariance) among the six types of methods. For the three RA-IHSRMs, the closed-form stochastic errors of temporal covariance are identical, which demonstrates that the stochastic error of temporal covariance produced by RA-IHSRMs is independent of the matrix decomposition method. By contrast, the closed-form stochastic errors of temporal covariance produced by RP-IHSRMs are slightly different from each other. In addition, the stochastic errors of RA-IHSRMs are mildly higher than those of RP-IHSRMs.

The sum of stochastic errors of variance and that of cross-covariance are investigated, and the results are pictured in Figures 11 and 12, respectively, to further compare

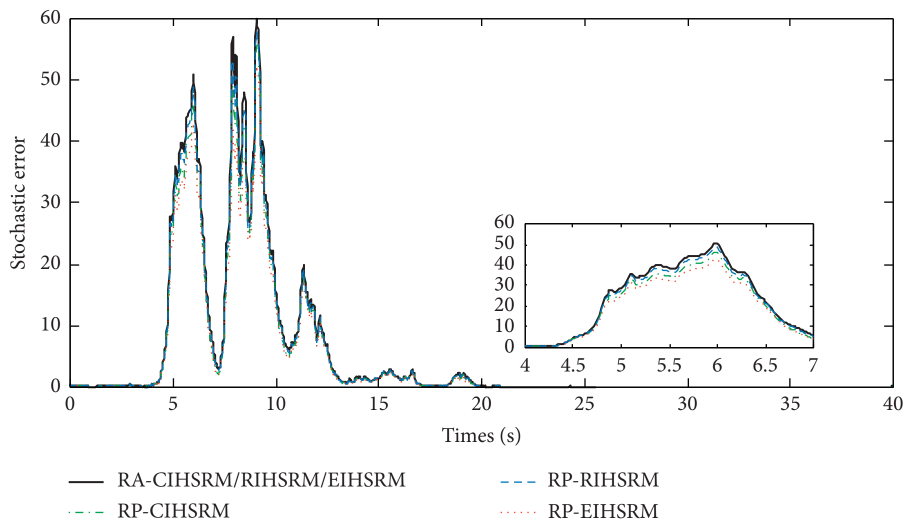

FIGURE 12: Sum of the stochastic errors of cross-covariance for different methods.

the stochastic errors of covariance for the six types of IHSRMs. As can be seen, the sum values of the variance stochastic errors for RP-IHSRMs are approximately the same. However, taking only the RP-IHSRMs into consideration, the sum value of the stochastic error of cross-covariance for the RP-RIHSRM is the largest, while that for the RP-EIHSRM is the lowest, despite that the differences are slight.

5. Conclusion

A random phase-based IHSRM is proposed to facilitate the simulation of SCEGMs possessing the nonstationary characteristics of the natural record, and a series of deduction and one numerical example are used to verify the validness of the proposed method. Besides, this paper presents an error assessment for the IHSRM. The closed-form solutions of predefined statistic errors were derived for the temporal mean, variance, and cross-covariance of the process simulated by six types of IHSRMs. The validness of the derived closed-form statistic errors was proven by a set of comparisons. The error analyses showed that the proposed method is not ergodic. The stochastic errors of temporal covariance produced by RP-IHSRMs are dependent on the matrix decomposition method, while those produced by the RA-IHSRMs are not. The RA-IHSRMs possess higher stochastic errors of temporal covariance than the RP-IHSRMs. Among RP-IHSRMs, the RP-EIHSRM exhibits the smallest stochastic error, while the RP-RIHSRM possesses the largest, but the difference is slight.

Appendix

A. Relation between the Ensemble Averages of the Mean, Variance, and Hilbert Spectrum of the Generated Ground Motions and Those of the Target

The ensemble averages of the mean and variance of $x_m(t)$ and $x_{m,j}(t)$ can be calculated using

$$\mu_m(t) = E[x_m(t)] = E\left\{\mathrm{Re}\left\{\sum_{k=1}^{L}\sum_{j=1}^{N} A_{km,j}(t)e^{i\left[\theta_j(t)+\Phi_{km,j}+\varphi_{k,j}\right]}\right\}\right\} + r(t) = r(t), \tag{A.1}$$

$$\begin{aligned}\sigma_m^2(t) &= E\left\{\left[x_m(t) - r(t)\right]^2\right\}\\ &= E\left\{\sum_{k=1}^{L}\sum_{j=1}^{N} A_{km,j}^2(t)\cos^2\left[\theta_j(t) + \Phi_{km,j} + \varphi_{k,j}\right]\right\}\\ &= \frac{1}{2}\sum_{k=1}^{L}\sum_{j=1}^{N} A_{km,j}^2(t) = \sum_{k=1}^{L}\sum_{j=1}^{N}\sigma_j^2(t)D_{km,j}^2 = \frac{1}{2}\sum_{j=1}^{N} a_j^2(t),\end{aligned} \tag{A.2}$$

$$\mu_{m,j}(t) = E\left[x_{m,j}(t)\right] = \mathrm{Re}\left\{\sum_{k=1}^{L} A_{km,j}(t)e^{i\left[\theta_j(t)+\Phi_{km,j}\right]}E\left[e^{i\varphi_{k,j}}\right]\right\} = 0, \tag{A.3}$$

$$\begin{aligned}\sigma_{m,j}^2(t) &= \mathrm{Var}\left[x_{m,j}(t)\right]\\ &= \sum_{k=1}^{L} A_{km,j}^2(t)\cos^2\left[\theta_j(t) + \Phi_{km,j} + \varphi_{k,j}\right]\\ &= \frac{1}{2}\sum_{k=1}^{L} A_{km,j}^2(t) = \sigma_j^2(t)\sum_{k=1}^{L} D_{km,j}^2 = \sigma_j^2(t)C_{mm,j} = \frac{1}{2}a_j^2(t).\end{aligned} \tag{A.4}$$

Therefore, considering equations (7)–(10), the ensemble averages of the mean and variance of $x_m(t)$ and $x_{m,j}(t)$ are evidently identical with those of the target underlying random process and the jth reference IMF, respectively.

In the present study, the instantaneous frequency of $x_{m,j}(t)$ is still clearly ω_j despite the existence of $\Phi_{km,j}$ and $\varphi_{k,j}$. Furthermore, the square of the amplitude of $\left\{\sum_{k=1}^{L} A_{km,j}(t)e^{i[\theta_j(t)+\Phi_{km,j}+\varphi_{k,j}]}\right\}$ can be expressed as

$$\begin{aligned}\mathrm{Amp}^2 &= \left\{\sum_{k=1}^{L} a_j(t)D_{km,j}\cos\left[\theta_j(t) + \Phi_{km,j} + \varphi_{k,j}\right]\right\}^2 + \left\{\sum_{k=1}^{L} a_j(t)D_{km,j}\sin\left[\theta_j(t) + \Phi_{km,j} + \varphi_{k,j}\right]\right\}^2\\ &= \sum_{k=1}^{L} a_j^2(t)D_{km,j}^2 + \sum_{p=1}^{L}\sum_{\substack{q=1\\ q\neq p}}^{L} a_j^2(t)D_{pm,j}D_{qm,j}\cos\left[\Phi_{pm,j} + \varphi_{p,j} - \Phi_{qm,j} - \varphi_{q,j}\right]\\ &= a_j^2(t)C_{mm,j} + \sum_{p=1}^{L}\sum_{\substack{q=1\\ q\neq p}}^{L} a_j^2(t)D_{pm,j}D_{qm,j}\cos\left[\Phi_{pm,j} + \varphi_{p,j} - \Phi_{qm,j} - \varphi_{q,j}\right]\\ &= a_j^2(t) + \sum_{p=1}^{L}\sum_{\substack{q=1\\ q\neq p}}^{L} a_j^2(t)D_{pm,j}D_{qm,j}\cos\left[\Phi_{pm,j} + \varphi_{p,j} - \Phi_{qm,j} - \varphi_{q,j}\right].\end{aligned} \tag{A.5}$$

Due to $E(\cos[\varphi_{p,j} - \varphi_{q,j}]) = 0$, the ensemble average of Amp^2 equates to

$$\begin{aligned}E\left(\mathrm{Amp}^2\right) &= a_j^2(t) + \sum_{p=1}^{L}\sum_{\substack{q=1\\ q\neq p}}^{L} a_j^2(t)D_{pm,j}D_{qm,j}E\left\{\cos\left[\Phi_{pm,j} + \varphi_{p,j} - \Phi_{qm,j} - \varphi_{q,j}\right]\right\}\\ &= a_j^2(t).\end{aligned} \tag{A.6}$$

Then, the ensemble average of the amplitude of $\left\{\sum_{k=1}^{L} A_{km,j}(t)e^{i[\theta_j(t)+\Phi_{km,j}+\varphi_{k,j}]}\right\}$ is $a_j(t)$, which is equal to the amplitude of the analytical function of the jth target IMF. Therefore, the ensemble average of the Hilbert spectrum of $x_m(t)$

is identical with that of the target underlying random process and, consequently, equates to the Hilbert spectrum of the record.

B. Proof of Equations (34) and (35)

For random phase formulas, the square of the raw estimation of variance of $x_m(t)$ can be expressed as

$$\begin{aligned}\left[\widehat{\sigma}_m^2(t)\right]^2 &= \left\{\left\{\sum_{k1=1}^{L}\sum_{j1=1}^{N} a_{j1}(t) D_{k1m,j1}\cos\left[\theta_{j1}(t)+\varphi_{k1,j1}\right]\right\}\cdot\left\{\sum_{k2=1}^{L}\sum_{j2=1}^{N} a_{j2}(t) D_{k2m,j2}\cos\left[\theta_{k2}(t)+\varphi_{k2,j2}\right]\right\}\right\}^2 \\ &= \sum_{k1=1}^{L}\sum_{j1=1}^{N}\sum_{p1=1}^{L}\sum_{q1=1}^{N}\sum_{k2=1}^{L}\sum_{j2=1}^{N}\sum_{p2=1}^{L}\sum_{q2=1}^{N} a_{j1}(t)a_{j2}(t)a_{q1}(t)a_{q2}(t)\cdot D_{k1m,j1}D_{p1m,q1}D_{k2m,j2}D_{p2m,q2}\cdot\cos\left[\theta_{j1}(t)+\varphi_{k1,j1}\right] \\ &\quad \cos\left[\theta_{q1}(t)+\varphi_{p1,q1}\right]\cos\left[\theta_{j2}(t)+\varphi_{k2,j2}\right]\cos\left[\theta_{q2}(t)+\varphi_{p2,q2}\right].\end{aligned} \tag{B.1}$$

If $k1 = p1 = k2 = p2 = k$ and $j1 = q1 = j2 = q2 = j$,

$$E\left[\widehat{\sigma}_m^2(t)\right]^2 = \sum_{k=1}^{L}\sum_{j=1}^{N}\frac{3}{8}a_j^4(t)D_{km,j}^4. \tag{B.2}$$

If $k1 = p1 = k \neq k2 = p2 = p$ and $j1 = q1 = j \neq j2 = q2 = q$ or $k1 = k2 = k \neq p1 = p2 = p$ and $j1 = j2 = j \neq q1 = q2 = q$ or $k1 = p2 = k \neq k2 = p1 = p$ and $j1 = q2 = j \neq j2 = q1 = q$,

$$E\left[\widehat{\sigma}_m^2(t)\right]^2 = \sum_{k=1}^{L}\sum_{j=1}^{N}\sum_{\substack{p=1\\p\neq k}}^{L}\sum_{\substack{q=1\\q\neq j}}^{N}\frac{1}{4}a_j^2(t)a_q^2(t)D_{km,j}^2D_{pm,q}^2. \tag{B.3}$$

Therefore, synthesizing equations (30), (A.2), and (B.1)–(B.3) will yield equation (34). By using the same derivation process, the proof of equation (35) can be conducted by

$$\begin{aligned}\left[\widehat{\sigma}_m^2(t)\right]^2 &= \left\{\left\{\sum_{k1=1}^{L}\sum_{j1=1}^{N}\sigma_{j1}(t)D_{k1m,j1}\left\{A_{k1j1}\cos\left[\theta_{j1}(t)\right]+B_{k1j1}\sin\left[\theta_{j1}(t)\right]\right\}+r(t)\right\}\right. \\ &\quad \left.\cdot\left\{\sum_{k2=1}^{L}\sum_{j2=1}^{N}\sigma_{j2}(t)D_{k2m,j2}\left\{A_{k2j2}\cos\left[\theta_{j2}(t)\right]+B_{k2j2}\sin\left[\theta_{j2}(t)\right]\right\}+r(t)\right\}\right\}^2 \\ &= \sum_{k1=1}^{L}\sum_{j1=1}^{N}\sum_{p1=1}^{L}\sum_{q1=1}^{N}\sum_{k2=1}^{L}\sum_{j2=1}^{N}\sum_{p2=1}^{L}\sum_{q2=1}^{N}\sigma_{j1}(t)\sigma_{j2}(t)\sigma_{q1}(t)\sigma_{q2}(t)\cdot D_{k1m,j1}D_{p1m,q1}D_{k2m,j2}D_{p2m,q2} \\ &\quad \cdot\left\{A_{k1j1}\cos\left[\theta_{j1}(t)\right]+B_{k1j1}\sin\left[\theta_{j1}(t)\right]\right\}\cdot\left\{A_{p1q1}\cos\left[\theta_{q1}(t)\right]+B_{p1q1}\sin\left[\theta_{q1}(t)\right]\right\} \\ &\quad \cdot\left\{A_{k2j2}\cos\left[\theta_{j2}(t)\right]+B_{k2j2}\sin\left[\theta_{j2}(t)\right]\right\}\cdot\left\{A_{p2q2}\cos\left[\theta_{q2}(t)\right]+B_{p2q2}\sin\left[\theta_{q2}(t)\right]\right\}.\end{aligned} \tag{B.4}$$

If $k1 = p1 = k2 = p2 = k$ and $j1 = q1 = j2 = q2 = j$,

$$E\left[\widehat{\sigma}_m^2(t)\right]^2 = \sum_{k=1}^{L}\sum_{j=1}^{N}\frac{3}{4}a_j^4(t)D_{km,j}^4. \tag{B.5}$$

If $k1 = p1 = k \neq k2 = p2 = p$ and $j1 = q1 = j \neq j2 = q2 = q$ or $k1 = k2 = k \neq p1 = p2 = p$ and $j1 = j2 = j \neq q1 = q2 = q$ or $k1 = p2 = k \neq k2 = p1 = p$ and $j1 = q2 = j \neq j2 = q1 = q$,

$$E\left[\widehat{\sigma}_m^2(t)\right]^2 = \sum_{k=1}^{L}\sum_{j=1}^{N}\sum_{\substack{p=1\\p\neq k}}^{L}\sum_{\substack{q=1\\q\neq j}}^{N}\frac{1}{4}a_j^2(t)a_q^2(t)D_{km,j}^2D_{pm,q}^2. \tag{B.6}$$

Therefore, synthesizing equations (30) and (B.4)–(B.6) will yield equation (35).

C. Proof of Equations (41) and (42)

For random phase formulas, the square of the raw estimation of cross-covariance between $x_m(t)$ and $x_n(t)$ can be expressed as

$$\begin{aligned}\left[\widehat{\mathrm{COV}}_{mn}(t)\right]^2 &= \left\{\left\{\sum_{k1=1}^{L}\sum_{j1=1}^{N} a_{j1}(t)D_{k1m,j1}\cos\left[\theta_{j1}(t)+\varphi_{k1,j1}\right]\right\}\cdot\left\{\sum_{k2=1}^{L}\sum_{j2=1}^{N} a_{j2}(t)D_{k2n,j2}\cos\left[\theta_{j2}(t)+\varphi_{k2,j2}\right]\right\}\right\}^2 \\ &= \sum_{k1=1}^{L}\sum_{j1=1}^{N}\sum_{p1=1}^{L}\sum_{q1=1}^{N}\sum_{k2=1}^{L}\sum_{j2=1}^{N}\sum_{p2=1}^{L}\sum_{q2=1}^{N} a_{j1}(t)a_{q1}(t)a_{j2}(t)a_{q2}(t)\cdot D_{k1m,j1}D_{p1n,q1}D_{k2m,j2}D_{p2n,q2}\cdot\cos\left[\theta_{j1}(t)+\varphi_{k1,j1}\right] \\ &\quad\cdot\cos\left[\theta_{q1}(t)+\varphi_{p1,q1}\right]\cdot\cos\left[\theta_{j2}(t)+\varphi_{k2,j2}\right]\cos\left[\theta_{q2}(t)+\varphi_{p2,q2}\right].\end{aligned} \tag{C.1}$$

If $k1=p1=k2=p2=k$ and $j1=q1=j2=q2=j$,

$$E\left[\widehat{\mathrm{COV}}_{mn}(t)\right]^2 = \sum_{k=1}^{L}\sum_{j=1}^{N}\frac{3}{8}a_j^4(t)D_{km,j}^2D_{kn,j}^2. \tag{C.2}$$

If $k1=p1=k\neq k2=p2=p$ and $j1=q1=j\neq j2=q2=q$ or $k1=p2=k\neq k2=p1=p$ and $j1=q2=j\neq j2=q1=q$,

$$E\left[\widehat{\mathrm{COV}}_{mn}(t)\right]^2 = \sum_{k=1}^{L}\sum_{j=1}^{N}\sum_{\substack{p=1\\p\neq k}}^{L}\sum_{\substack{q=1\\q\neq j}}^{N}\frac{1}{4}a_j^2(t)a_q^2(t)D_{km,j}D_{kn,j}D_{pm,q}D_{pn,q}. \tag{C.3}$$

If $k1=k2=k\neq p1=p2=p$ and $j1=j2=j\neq q1=q2=q$,

$$E\left[\widehat{\mathrm{COV}}_{mn}(t)\right]^2 = \sum_{k=1}^{L}\sum_{j=1}^{N}\sum_{\substack{p=1\\p\neq k}}^{L}\sum_{\substack{q=1\\q\neq j}}^{N}\frac{1}{4}a_j^2(t)a_q^2(t)D_{km,j}^2D_{pn,q}^2. \tag{C.4}$$

Therefore, synthesizing equations (30), (38), and (C.1)–(C.4) will yield equation (41).

For random amplitude formulas,

$$\begin{aligned}\left[\widehat{\mathrm{COV}}_{mn}(t)\right]^2 &= \left\{\left\{\sum_{k1=1}^{L}\sum_{j1=1}^{N}\sigma_{j1}(t)D_{k1m,j1}\left\{A_{k1j1}\cos\left[\theta_{j1}(t)\right]+B_{k1j1}\sin\left[\theta_{j1}(t)\right]\right\}+r(t)\right\}\right. \\ &\quad\left.\cdot\left\{\sum_{k2=1}^{L}\sum_{j2=1}^{N}\sigma_{j2}(t)D_{k2n,j2}\left\{A_{k2j2}\cos\left[\theta_{j2}(t)\right]+B_{k2j2}\sin\left[\theta_{j2}(t)\right]\right\}+r(t)\right\}\right\}^2 \\ &= \sum_{k1=1}^{L}\sum_{j1=1}^{N}\sum_{p1=1}^{L}\sum_{q1=1}^{N}\sum_{k2=1}^{L}\sum_{j2=1}^{N}\sum_{p2=1}^{L}\sum_{q2=1}^{N}\sigma_{j1}(t)\sigma_{j2}(t)\sigma_{q1}(t)\sigma_{q2}(t)\cdot D_{k1m,j1}D_{p1n,q1}D_{k2m,j2}D_{p2n,q2} \\ &\quad\cdot\left\{A_{k1j1}\cos\left[\theta_{j1}(t)\right]+B_{k1j1}\sin\left[\theta_{j1}(t)\right]\right\}\cdot\left\{A_{p1q1}\cos\left[\theta_{q1}(t)\right]+B_{p1q1}\sin\left[\theta_{q1}(t)\right]\right\} \\ &\quad\cdot\left\{A_{k2j2}\cos\left[\theta_{j2}(t)\right]+B_{k2j2}\sin\left[\theta_{j2}(t)\right]\right\}\cdot\left\{A_{p2q2}\cos\left[\theta_{q2}(t)\right]+B_{p2q2}\sin\left[\theta_{q2}(t)\right]\right\}.\end{aligned} \tag{C.5}$$

If $k1=p1=k2=p2=k$ and $j1=q1=j2=q2=j$,

$$E\left[\widehat{\mathrm{COV}}_{mn}(t)\right]^2 = \sum_{k=1}^{L}\sum_{j=1}^{N}\frac{3}{4}a_j^4(t)D_{km,j}^2D_{kn,j}^2. \tag{C.6}$$

If $k1=p1=k\neq k2=p2=p$ and $j1=q1=j\neq j2=q2=q$ or $k1=p2=k\neq k2=p1=p$ and $j1=q2=j\neq j2=q1=q$,

$$E\left[\widehat{\mathrm{COV}}_{mn}(t)\right]^2 = \sum_{k=1}^{L}\sum_{j=1}^{N}\sum_{\substack{p=1\\p\neq k}}^{L}\sum_{\substack{q=1\\q\neq j}}^{N}\frac{1}{4}a_j^2(t)a_q^2(t)D_{km,j}D_{kn,j}D_{pm,q}D_{pn,q}. \tag{C.7}$$

If $k1=k2=k\neq p1=p2=p$ and $j1=j2=j\neq q1=q2=q$,

$$E\left[\hat{\mathrm{COV}}_{mn}(t)\right]^2 = \sum_{k=1}^{L}\sum_{j=1}^{N}\sum_{\substack{p=1\\p\neq k}}^{L}\sum_{\substack{q=1\\q\neq j}}^{N}\frac{1}{4}a_j^2(t)a_q^2(t)D_{km,j}^2D_{pn,q}^2. \tag{C.8}$$

Therefore, synthesizing equations (30), (39), and (C.5)–(C.8) will yield equation (42).

Data Availability

All the data supporting the conclusions of this study are presented in the figures and tables of the article. The code and details involved in this paper are available upon request from the corresponding author.

Conflicts of Interest

The authors declare that there are no conflicts of interest regarding the publication of this paper.

Acknowledgments

This study was financially supported by the National Natural Science Foundation of China (no. 51908236), the China Postdoctoral Science Foundation (2019M652649), and the Basic Operating Expenses of the Central Level Public Welfare Research Institutes (CKSF2019193/YT and CKSF2019477/YT).

References

[1] S. O. Rice, *Mathematical Analysis of Random Noise. Selected Papers on Noise and Stochastic Processes*, Dover Publications., New York, NY, USA, 1954.

[2] M. Shinozuka, “Simulation of multivariate and multidimensional random processes,” *The Journal of the Acoustical Society of America*, vol. 49, no. 1B, pp. 357–368, 1971.

[3] M. Shinozuka, “Monte Carlo solution of structural dynamics,” *Computers and Structures*, vol. 2, no. 5-6, pp. 855–874, 1972.

[4] M. Shinozuka and C.-M. Jan, “Digital simulation of random processes and its applications,” *Journal of Sound and Vibration*, vol. 25, no. 1, pp. 111–128, 1972.

[5] G. Huang, “An efficient simulation approach for multivariate nonstationary process: hybrid of wavelet and spectral representation method,” *Probabilistic Engineering Mechanics*, vol. 37, no. 10, pp. 74–83, 2014.

[6] J. Liang, S. R. Chaudhuri, and M. Shinozuka, “Simulation of nonstationary stochastic processes by spectral representation,” *Journal of Engineering Mechanics*, vol. 133, no. 6, pp. 616–627, 2007.

[7] Y. Gao, Y. Wu, D. Li, Y. Cai, H. Liu, and N. Zhang, “Error assessment for the coherency matrix-based spectral representation method in multivariate random processes simulation,” *Journal of Engineering Mechanics*, vol. 139, no. 9, pp. 1294–1299, 2013.

[8] J. Liang, Z. Liu, L. Huang, and G. Yang, “The indirect boundary integral equation method for the broadband scattering of plane P, SV and Rayleigh waves by a hill topography,” *Engineering Analysis with Boundary Elements*, vol. 98, pp. 184–202, 2019.

[9] L. Huang, Z. Liu, C. Wu, and J. Liang, “The scattering of plane P, SV waves by twin lining tunnels with imperfect interfaces embedded in an elastic half-space,” *Tunnelling and Underground Space Technology*, vol. 85, pp. 319–330, 2019.

[10] E. Yao, Y. Miao, S. Wang, and X. Long, “Simulation of fully nonstationary spatially variable ground motions on a canyon site,” *Soil Dynamics and Earthquake Engineering*, vol. 115, pp. 198–204, 2018.

[11] E. Yao, S. Wang, B. Ruan, Y. Miao, and L. Zhu, “Numerical study on site response considering ground motion spatial variation,” *Soil Dynamics and Earthquake Engineering*, vol. 127, Article ID 105836, 2019.

[12] E. Yao, S. Wang, Y. Miao, L. Ye, and L. Zhu, “Simulation of fully non-stationary spatially varying ground motions considering nonlinear soil behavior,” *Soil Dynamics and Earthquake Engineering*, vol. 129, Article ID 105954, 2020.

[13] L. Hu, L. Li, and M. Gu, “Error assessment for spectral representation method in wind velocity field simulation,” *Journal of Engineering Mechanics*, vol. 136, no. 9, pp. 1090–1104, 2010.

[14] Y. Gao, Y. Wu, Y. Cai, H. Liu, D. Li, and N. Zhang, “Error assessment for spectral representation method in random field simulation,” *Journal of Engineering Mechanics*, vol. 138, no. 6, pp. 711–715, 2012.

[15] L. Hu, Z. F. Xu, Y. L. Xu et al., “Error analysis of spatially varying seismic ground motion simulation by spectral representation method,” *Journal of Engineering Mechanics, ASCE*, vol. 143, no. 9, Article ID 04017083, 2017.

[16] Z. F. Xu, L. Li, and L. Hu, “Estimation of evolutionary spectra of monitored seismic ground motions by transformation of correlation functions,” *Shock and Vibration*, vol. 2015, Article ID 846943, 9 pages, 2015.

[17] Y. X. Wu, Y. F. Gao, and D. Y. Li, “Error assessment of multivariate random processes simulated by a conditional-simulation method,” *Journal of Engineering Mechanics, ASCE*, vol. 141, no. 5, Article ID 04014155, 2014.

[18] Y. K. Wen and P. Gu, “Description and simulation of nonstationary processes based on Hilbert spectra,” *Journal of Engineering Mechanics*, vol. 130, no. 8, pp. 942–951, 2004.

[19] N. E. Huang, Z. Shen, S. R. Long et al., “The empirical mode decomposition and the Hilbert spectrum for nonlinear and non-stationary time series analysis,” *Proceedings of the Royal Society of London. Series A: Mathematical, Physical and Engineering Sciences*, vol. 454, no. 1971, pp. 903–995, 1998.

[20] Y. Miao, E. Yao, B. Ruan, H. Zhuang, G. Chen, and X. Long, “Improved hilbert spectral representation method and its application to seismic analysis of shield tunnel subjected to spatially correlated ground motions,” *Soil Dynamics and Earthquake Engineering*, vol. 111, pp. 119–130, 2018.

[21] M. Di Paola and M. Zingales, “Digital simulation of multivariate earthquake ground motions,” *Earthquake Engineering & Structural Dynamics*, vol. 29, no. 7, pp. 1011–1027, 2000.

[22] H. Hao, C. S. Oliveira, and J. Penzien, “Multiple-station ground motion processing and simulation based on smart-1 array data,” *Nuclear Engineering and Design*, vol. 111, no. 3, pp. 293–310, 1989.

[23] Y. X. Wu, Y. F. Gao, N. Zhang et al., “Simulation of spatially varying non–Gaussian and nonstationary seismic ground motions by the spectral representation method,” *Journal of Engineering Mechanics, ASCE*, vol. 144, no. 1, Article ID 04017143, 2018.

[24] Y. Wu and Y. Gao, “A modified spectral representation method to simulate non-Gaussian random vector process

considering wave-passage effect," *Engineering Structures*, vol. 201, Article ID 109587, 2019.

[25] Y. Wu, Y. Gao, L. Zhang, and J. Yang, "How the distribution characteristics of soil property affect probabilistic foundation settlement: from the view of the first four statistical moments," *Canadian Geotechnical Journal*, vol. 57, no. 4, pp. 595–607, 2020.

[26] E. H. Vanmarcke and G. A. Fenton, "Conditioned simulation of local fields of earthquake ground motion," *Structural Safety*, vol. 10, no. 1–3, pp. 247–264, 1991.

[27] E. H. Vanmarcke, E. Heredia-Zavoni, and G. A. Fenton, "Conditional simulation of spatially correlated earthquake ground motion," *Journal of Engineering Mechanics*, vol. 119, no. 11, pp. 2333–2352, 1993.

[28] A. Zerva and M. Shinozuka, "Stochastic differential ground motion," *Structural Safety*, vol. 10, no. 1-3, pp. 129–143, 1991.

[29] J. S. Bendat and A. G. Piersol, *Random Data: Analysis and Measurement Procedures*, Wiley, New York, NY, USA, 1986.

Hindawi
Mathematical Problems in Engineering
Volume 2020, Article ID 3596384, 12 pages
https://doi.org/10.1155/2020/3596384

Research Article

The New Fertility Policy and the Actuarial Balance of China Urban Employee Basic Endowment Insurance Fund Based on Stochastic Mortality Model

Yuantao Xie[1], **Xinzhu Zhang**[1], **Huijuan Lv**[1], **and Xiaojing Guo**[2]

[1]*School of Insurance and Economics, University of International Business and Economics, Beijing 100029, China*
[2]*Zhongtai Securities, Beijing 100032, China*

Correspondence should be addressed to Yuantao Xie; xieyuantao@uibe.edu.cn and Xiaojing Guo; 942005285@qq.com

Received 15 March 2020; Accepted 21 April 2020; Published 14 May 2020

Guest Editor: Wenguang Yu

This study aims to investigate the impact of China's new fertility policy on the actuarial balance of its Urban Employee Basic Endowment Insurance (UEBEI) fund, with stochastic mortality model included to address the longevity risk. Combined with the latest UEBEI policy, this paper constructs an actuarial balance model and introduces the growth rate of wage, the age of employment and the age of retirement, the rate of payment, the rate of replacement, the annual rate of pension adjustment, and the population in terms of age into the model, which arise from the rate of payment, average wage, and personal and social factors. This study uses the sixth population census data by age group and gender to employ empirical analysis. The sensitivity analysis of China's basic pension insurance fund balance is made. It is concluded that the increase in the growth rate of wage caused by social factors, the increase of fund investment returns, the delay of retirement, and the increase in the fund collection rate are all conducive to the sustainability of the UEBEI fund.

1. Introduction

Pension fund gap is one of the most urgent and important problems that China's pension system has to face. As early as 2014, the shortage of China's pension fund has begun to show gaps in about 23 provinces. According to "the 2016 Annual Report on the Development of Social Insurance in China" prepared by the social security management center of the Ministry of Human Resources and Social Security (http://www.mohrss.gov.cn/SYrlzyhshbzb/dongtaixinwen/buneiyaowen/201711/t20171124_282237.html), many provinces are suffering from gap in the current period, including Heilongjiang, Liaoning, Hebei, Jilin, Inner Mongolia, Hubei, and Qinghai. In 2016, Heilongjiang's pension gap reached 23.2 billion yuan, and Guangzhou's gap was 1.2 billion yuan. In 2018, the deficit gap of social security fund reached 450.4 billion RMB. As a matter of fact, the deficit gap of pension fund accounts for 70% of the deficit gap of social security fund (Ren et al. [1]). According to the World Bank, if China does not change its current pension insurance operation model, by 2065, the revenue and expenditure gap of China's pension insurance fund will reach 9 trillion yuan (World Bank [2]).

Freedman and Zhang [3] also believe that if the pension gap in the future is only fully covered by the pension fund, then the assets will be exhausted in about 2036. If we want the Pension Reserve to fully cover the pension gap, the annual growth rate will be as high as 30.5% (Tang et al. [4]).

The Urban Employee Basic Endowment Insurance (UEBEI) fund is an important part of pension fund and an important pillar to protect people's livelihood and maintain social stability. According to Figure 1, it can be seen that the revenue, expenditure, and balance of the UEBMI fund are still on the rise at present. However, we can also see that the growth rate of the cumulative balance has declined from 52.55% in 2002 to −0.06% in 2019. In fact, once there is a

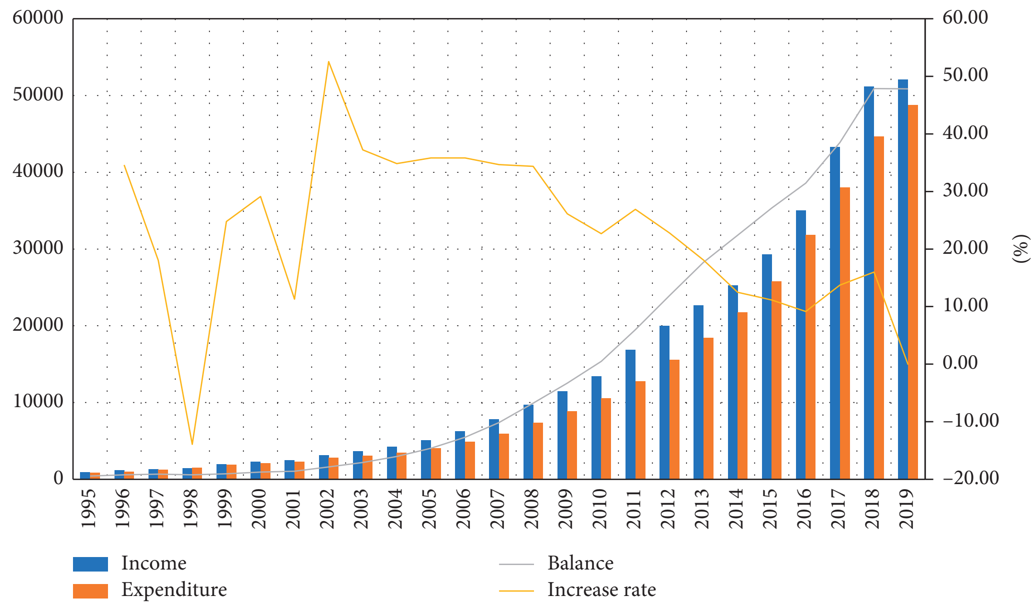

Figure 1: Revenue, expenditure, and balance of China's UEBEI fund (unit: 100 million RMB). Source: CEI net statistics database, http://202.204.164.23:91. Accessed on Feb. 18th, 2020.

fund gap in a province, the state and the province will use finance to subsidize the gap. After eliminating the financial subsidy from the fund income, the gap will be much higher than the figure on the chart.

The UEBEI fund has been affected by the problems associated with its demographic structure, such as low fertility and population aging. An increase in the aging population in the future may lead to a sharp increase in expenditure, and given the pay-as-you-go features of the UEBMI system, there might also be a huge deficit. According to the estimation results of "China's National Balance Sheet" prepared by the Chinese Academy of Social Sciences (http://ie.cass.cn/achievements/academic_works/201812/t20181227_4801661.html), the population over 60 years of age will reach 19.3% by 2020, and it will reach 38.6% by 2050; the dependency ratio of China's employee pension insurance will be 2.94 : 1 in 2020, and it will drop to 1.3 : 1 by 2050. There will be a fund gap in UEBEI nationwide by 2023 if we continue to implement the existing pension system; the accumulated balance of endowment insurance will be exhausted by 2029.

The UEBEI gap brings great pressure on the national finance. As of 2016, Shanghai's municipal financial revenue has reached a total of 17 billion yuan. According to the "China Pension Development Report 2019" compiled by the Chinese Academy of Social Sciences (http://www.cisscass.org/yanjiucglist.aspx?classid=1, http://mini.eastday.com/bdmip/190225130456273.html#), the transfer payment subsidies to the UEBEI reached 227.2 billion yuan in 2019, and the accumulated financial subsidies reached 1.2526 trillion yuan. According to "Resolving the Medium- and Long-Term Risks of National Assets and Liabilities" (http://misc.caijing.com.cn/chargeFullNews.jsp?id=111886697&time=2012-06-11&cl=106), the gap of the UEBEI fund will reach more than 20% of the fiscal expenditure in one year by 2050.

The government hopes to alleviate the problem of population aging by raising the birth rate, thereby relieving the pressure on pension payments. The eighteenth meeting of the Twelfth National Congress passed the decision on the revision of the population and family planning law, which means the coming of the era of universal two children. The state hopes to alleviate the problem of population aging by increasing the birth rate, so as to relieve the pressure of pension payment. In this context, this paper seeks to address the issue of increasing payment pressure on pension funds in the future. At present, there is not much research on the management of the provincial endowment insurance fund. In particular, there is not enough quantitative research on actuarial modeling of pension funds, actuarial balance, and financial sustainability. Under this background, this article seeks the solution of the problem of increasing pressure of basic pension insurance fund payment in the future. This article focuses on the management of the UEBEI fund and proposes reasonable and practical policy proposals as a timely solution to the development dilemma by using figures and suggestions.

2. Literature Review

There have been many studies in the literature on the revenue and expenditure balance of the UEBEI fund. Some scholars consider the issue from the perspective of the fund's expenditure. They hold the belief that population aging will lead to a rapid increase in UEBEI expenses. For the quantitative analysis of longevity risk, a good idea is to model mortality as random. The model of stochastic mortality has more advantages in the study of population structure. The classic model is Lee–Carter model (Carter and Lee [5]), which is a very influential model because of its simplicity and high accuracy. Renshaw and Haberman [6] improved the

Lee–Carter model and established the R-H model, which could model and analyze the cohort effect and period effect of the specific age at the same time. In addition, the more famous model in academic circles is the age-period-cohort model (APC model) (for example, Reither et al. [7]). Hainaut [8] studied the general features of multifactor Lee–Carter models, with switching regime time components, to combine population structure with prices of life and death insurances, applying to fit 2-dimension, 2-state model to the French population. Some scholars have expanded the model; for example, Bell [9] extended it to the multilevel APC model. To deal with the longevity risk and to get better pricing results for annuity and pension, three British scholars, Cairns et al. [10], first proposed a CBD model of two-factor mortality in the form of logistic, which was especially used to predict mortality for the elderly. Cairns et al. [11, 12] then quantitatively compared the current influential models based on the mortality data of the UK, Wales, and the United States. After that, they analyzed 8 random mortality models and evaluated them qualitatively and quantitatively according to the historical data. Finally, the results of 6 models were found to be pretty good, and some suggestions on the model evaluation methods were given. Since then, the improvement and practice of CBD model, APC model, and Lee–Carter model have been continuing. Hainaut [8] used an adjustable death process to vary the variables related to time, thus constructing a multiple Lee–Carter model to analyze the population divided by gender in France from 1946 to 2007. Carfora et al. [13] discussed the comparison of models. Chernyavskiy et al. [14] expanded the traditional APC model to include quadratic age, period, and cohort terms and introduce stratum-specific random effects as well to find a unified methodology for the analysis of multiple strata (see also Xie and Li [15]). Basnayake and Nawarathna [16] used the Singular Value Decomposition (SVD) approach for estimating the parameters of Lee–Carter model and the Autoregressive Integrated Moving Average (ARIMA) time-series model for forecasting the mortality values to fit and forecast the mortality rate of Norway. Giacometti et al. [17] compared the performance of the Lee–Carter model and an AR(1)-ARCH(1) model with respect to forecasting age-specific mortality in Italy.

Under the new birth policy, changes in population structure and scale will predictably affect the actuarial balance of pension funds. Zhu and Yang [18] incorporated birth, infant mortality, and mortality into Leslie matrix, applying Leslie matrix grey forecasting model to predict population. Xie et al. [19] used Leslie model applicable to universal two-child policy for analysis and prediction of the population of different ages.

Some scholars also measure the sustainability of the UEBEI funds through actuarial balance; for example, Mircea et al. [20] developed some models for mortality rates and pricing considering the longevity risk; they also expanded some models for the securitization of longevity bonds or loans to increase the sustainability of pension funds from the perspective of longevity risk (Mircea et al. [20]; Lin and Tsai [21]; Yu et al. [22]). Metzger [23] analyzed the medium-term sustainability of the Swiss old-age pension scheme by estimating a "Swedish" actuarial balance sheet, which compares pension liabilities with the explicit and implicit assets of the pension scheme. Meyricke and Sherris [24] assess the costs of longevity risk management using longevity swaps compared to costs of holding capital under Solvency II (Meyricke and Sherris [24]). Bosnjak [25] for the first time made projections of dependency ratio of pension and disability insurance fund of Republic of Srpska using the actuarial projection technique. Belolipetskii and Lepskaya [26] specified eight factors such as the mortality rate and financial indicators as random variables to calculate the probability of ruin of a pension fund on a finite time interval based on the standard Cramer–Lundberg model.

In China, Luo et al. [27] established the models of Population Prediction and the Basic Old-Age Insurance Fund's payments and emphatically considered the influence of the demographic change on the balance of revenue and expenditure model. Therefore, the population urbanization rate and the population birth rate factors were added to the population forecasting model, which showed that improving the birth rate and delaying the retirement will be helpful to the balance of China's basic pension insurance in the future (see also Yu et al. [28]). Wang et al. [29] focused on the influence of "comprehensive two-child" policy and delayed retirement policy on the fund balance of urban workers' basic old-age insurance; they found that the adjustment of fertility policy and retirement policy could postpone the beginning of short-term and long-term pension fund deficits to 2053 and after 2060, respectively. Cong and Jin [30] analyzed the long-term balance of pension fund from the perspective of contribution mechanism. The previous literature mainly used the traditional model to analyze the actuarial balance, and the application of the stochastic mortality model (for example, He and Liu [31] formulated a state-space framework and used the Kalman filtering technique to estimate the joint model of the fitting and forecasting stages of traditional CBD method) will be more fully analyzed in the actuarial equilibrium analysis. Wang and Huang [32] used Bayesian information criterion and likelihood ratio test on several popular stochastic mortality models and considered that CBD model had the best fit for Chinese data, and the impact of longevity risk on the gap of individual account fund in China was studied by using CBD model. Yuan and Pan [33] predicted the mortality rates from 2014 to 2050 and classified them by gender and age based on the Lee–Carter model. Cui et al. [34, 35] analyzed it from the view of income mobility, tax burden, and dynamic equilibrium of income distribution.

Lots of the researches on the pension funds start with the analysis of the influencing factors. Raising the retirement age may quickly entail the least political cost to get a great short-term budgetary effect by setting a variety of reform scenarios (Meyricke and Sherris [24]; Mircea et al. [20]), but reforms neglecting the interactions between the social security and the labor market are likely to fail. Zeng et al. [36] evaluated the effects of extending the retirement age in terms of fertility pattern and population structure by gender and workers categories. For more Chinese researches, see Zhao et al. [37]. Abdessalem and Cherni [38] developed a general equilibrium overlapping generations' model to evaluate the effects of different pension reforms: contribution rate increase, pensions' level reduction, the rise of the retirement age, and finally the introduction of a complementary fully funded system. Müller and Wagner [39] analyzed the impact of pension funding mechanisms on the solvency situation, including surplus distributions and remediation measures, and found that insurers and pension funds will profit from a cautious surplus distribution policy.

By establishing the actuarial model and using the stochastic mortality model to predict the population structure, this paper makes an empirical analysis on the balance of income and expenditure of the endowment insurance fund and the gap of funds in China by combining the real wage growth rate and the pension replacement rate. Through the study of the establishment and reform of the endowment insurance system in OECD countries, we compare the differences of that between OECD countries and China to find what can be used for reform in China. Under the background of population aging, this paper studies the financial balance of China's UEBEI fund in terms of actuarial science. At the same time, the CBD stochastic mortality model is introduced for the mortality forecast to get a better prediction than the life table.

This study explores the issue of the change in the fertility policy on the balance of China's UEBMI fund. This study establishes an actuarial model to predict the population structure based on the birth pattern under the second-child policy. It considers factors such as the actual wage growth rate and the replacement rate of pensions in China and conducts an empirical analysis of the balance of revenue and expenditure, fund gap, and other issues of China's pension funds. Overall, this paper studies the financial balance of China's pension fund from the point of view of actuarial aging under the background of population aging to address the longevity risk.

3. Methodology

Prior to the prediction of the dynamic balance of the UEBMI fund, we first need to predict the population structure under the two-child policy. Therefore, this paper adopts a two-stage research method. The first stage involves predicting the population structure under the universal two-child policy, and the second stage uses the predicted population structure to explore its impact on the balance of the UEBMI fund. In this study, the UEBMI refers to employees working in cities, including those with urban hukou, as well as those with rural hukou but working in cities. Therefore, the whole sample in the population analysis is adopted to examine the primary issue in this study.

3.1. Methods of Forecasting the Population Structure. It is assumed that the effect of migration is not taken into account, and no major natural disasters or wars will occur during the predicted time period in the future. That is, the population will change smoothly. Considering the corresponding mortality rate, the total number of x-age groups that can survive to the next year can be expressed as

$$N_{x+1}(t+1) = (1 - d_x(t)) \times N_x(t), \tag{1}$$

where $N_x(t)$ is the total number of people aged between x and $x+1$ in the year t and $d_x(t)$ is the death rate of x-age groups in a year t.

The number of newborns in the year t should be

$$N_{\text{newborn}}(t) = \sum_{x_i=x_1}^{x_i=x_2} b_{x_i}(t) \times \delta_{x_i}(t) \times N_x(t). \tag{2}$$

Among them, $b_{x_i}(t)$ represents the fertility rate of women in x_i-age groups in the year t, $x_i \in [x_1, x_2]$, and $\delta_{x_i}(t)$ represents the female ratio of the total population in x_i-age groups in a year t.

Suppose $d_{00}(t)$ is the t-year neonatal mortality rate; then the number of newborns in the year t who can survive to the next age group is

$$N_1(t+1) = (1 - d_{00}(t)) \times (1 - d_0(t)) \times N_{\text{newborn}}(t). \tag{3}$$

Let $B_{x_i}(t)$ be fertility pattern of childbearing women, and $\sum_{x_i=x_1}^{x_i=x_2} B_{x_i}(t) = 1$. Suppose $b_{x_i}(t) = \beta(t) \times B_{x_i}(t)$, where $\beta(t)$ is the total fertility rate in a year. Substitute into equation (3); that is,

$$N_1(t+1) = (1 - d_{00}(t))(1 - d_0(t)) \sum_{x_i=x_1}^{x_i=x_2} \beta(t) B_{x_i}(t) \delta_{x_i}(t) N_x(t). \tag{4}$$

Since $(1 - d_{00}(t))$, $(1 - d_0(t))$ and $\beta(t)$ are irrelevant to i, so let $\sum_{x_i=x_1}^{x_2} (1 - d_{00}(t))(1 - d_0(t)) B_{x_i}(t) \delta_{x_i}(t) = B'_{x_i}(t)$; then,

$$N_1(t+1) = \beta(t) \sum_{x_i=x_1}^{x_2} B'_{x_i}(t) N_x(t). \tag{5}$$

The next year's population vector can be deduced as

$$N(t+1) = L(t) \cdot N(t) + \beta(t) \cdot \Delta(t) \cdot N(t), \tag{6}$$

where $N(t) = [N_{\text{newborn}}(t), N_1(t), \ldots, N_{w-1}(t)]^T$ is the population vector in the initial year and survival rate matrix and fertility rate matrix can be shown as

$$L(t) = \begin{bmatrix} 0 & 0 & \cdots & 0 & 0 \\ 1 - d_1(t) & 0 & \cdots & 0 & 0 \\ 0 & 1 - d_2(t) & \cdots & 0 & 0 \\ & \vdots & \vdots & \vdots & \vdots \\ 0 & 0 & \cdots & 1 - d_{w-1}(t) & 0 \end{bmatrix},$$
$$\Delta(t) = \begin{bmatrix} 0 & \cdots & 0 & B'_{x_1}(t) & \cdots & B'_{x_2}(t) & 0 & \cdots & 0 \\ 0 & \cdots & 0 & 0 & \cdots & 0 & 0 & \cdots & 0 \\ \vdots & & \vdots & \vdots & & \vdots & \vdots & & \vdots \\ 0 & \cdots & 0 & 0 & \cdots & 0 & 0 & \cdots & 0 \end{bmatrix}. \tag{7}$$

Among them, $d_x(t)$ and $B_{x_i}(t)$ are not divided into different age group and gender, but the sixth population census is only divided by age group and gender; we use the Lee–Carter model for interpolation and then come to estimations of mortality and fertility pattern among different age group and gender:

$$\log \frac{d_x(t)}{1-d_x(t)} = A_1(t+1) + A_2(t+1)(x+t) + \varepsilon_x(t) \quad (8)$$

where $\log(d_x(t)/(1-d_x(t)))$ is log-normalized mortality odds ratio. $A_1(\cdot)$ and $A_2(\cdot)$ are period effect impact factors, which indicate that the mortality rate will change over time. $\varepsilon_x(t)$ is disturbance.

To predict the distribution of$A_1(\cdot)$ and $A_2(\cdot)$, we can model it as a random walk with a drift term:

$$\begin{pmatrix} A_1(t+1) \\ A_2(t+1) \end{pmatrix} = \begin{pmatrix} A_1(t) \\ A_2(t) \end{pmatrix} + \begin{pmatrix} d_1 \\ d_2 \end{pmatrix} + C\begin{pmatrix} z_1(t+1) \\ z_2(t+1) \end{pmatrix}, \quad (9)$$

where d_1 and d_2 are the drift terms, C is a constant upper triangular matrix, and $\begin{pmatrix} z_1(t+1) \\ z_2(t+1) \end{pmatrix}$ is a two-dimensional standard normal random variable. The OLS estimation of the drift term is relatively easy to obtain:

$$\widehat{d}_i = \frac{\widehat{A}_i(T) - \widehat{A}_i(1)}{T-1}, \quad i = 1, 2, \quad (10)$$

The estimation of C is as follows:

$$\widehat{C}\widehat{C}' = \begin{pmatrix} \widehat{\sigma}_1^2 & \widehat{\sigma}_{12} \\ \widehat{\sigma}_{12} & \widehat{\sigma}_2^2 \end{pmatrix}, \quad (11)$$

where

$$\widehat{\sigma}_i^2 = \frac{1}{T-1}\sum_{t=2}^{T}\left(\widehat{A}_i(t) - \widehat{A}_i(t-1) - \widehat{d}_i\right)^2, \quad i = 1, 2,$$

$$\widehat{\sigma}_{12} = \frac{1}{T-1}\sum_{s=1}^{T-1}\sum_{t=1}^{T-1}\left(\widehat{A}_1(s+1) - \widehat{A}_1(s) - \widehat{d}_1\right)\left(\widehat{A}_2(t+1) - \widehat{A}_2(t) - \widehat{d}_2\right). \quad (12)$$

3.2. Methods of Forecasting the Balance of China's UEBEI Fund. First of all, we need to determine a few assumptions.

Hypothesis 1. Only the workers' payment is considered in the income model of the fund, but the government's financial subsidies are not included temporarily. Otherwise, the expenditures of fund are not used for management expenses, and so forth, as they are used only for the pension for the insured retirees.

Hypothesis 2. The inflation factor is not considered in this model.

The factors that affect the income of the fund are the number of insured workers, the contribution rate, the collection rate, the UEBEI coverage rate and the workers' salary level, and growth rate; the factors that affect the fund expenditure are the number of retirees insured, the wage replacement rate of the UEBEI, and annual pension adjustment rate.

3.2.1. Income Model. First, we establish the actuarial model of the UEBEI fund's income in years as follows:

$$I(t) = C_r \cdot \sum_{x=\alpha}^{\beta-1}\left[\overline{W_{\alpha,1}} \cdot (1+g_1)^{x-\alpha}(1+g_2)^{t-1} \cdot L_x(t)\right] \cdot b(t), \quad (13)$$

where C_r is the contribution rate of the UEBEI, α is the working age of employees, β is the retirement age of employees, $\overline{W_{\alpha,1}}$ is the average wage of employees aged α in the first year of measurement period, g_1 is the wage growth rate caused by personal factors, g_2 is the wage growth rate caused by social factors, $L_x(t)$ is the number of insured workers aged x in year t, and $b(t)$ is the premium collection rate of the UEBEI. Suppose the workers covered in UEBEI are a fixed portion, which can be conducted from $N(t)$ by age x.

According to the annual basic pension insurance fund's income $I(t)$ and the fund yield r, we can get the accumulation value of the UEBEI fund income at the end of the forecast period n as follows:

$$I = \sum_{t=1}^{n} I(t) \cdot (1+r)^{n-t}, \quad (14)$$

where n denotes the year number during measurement period.

Substitute formula (13) for $I(t)$; then we have

$$I = \sum_{t=1}^{n}(1+r)^{n-t}\left\{C_r \cdot \sum_{x=\alpha}^{\beta-1}\left[\overline{W_{\alpha,1}} \cdot (1+g_1)^{x-\alpha}(1+g_2)^{t-1} \cdot L_x(t)\right] \cdot b_t\right\}. \quad (15)$$

3.2.2. Expenditure Model. The amount of the pension received by retirees is connected with the personal wage replacement rate. More specifically, the pension in the first year of retirement is the product of replacement rate and salary in the year prior to retirement. Let $\overline{W_\alpha(t-x+\alpha)}$ denote the average salary of employees aged α in year $t-x+\alpha$, that is, the average salary of one year prior to retirement for the employees aged x in years $t-x+\alpha$. Then, the salary of one year prior to retirement for workers aged x in years $t-x+\alpha$ is

$$\overline{W_\alpha(t-x+\alpha)} \cdot \left[(1+g_1)(1+g_2)\right]^{\beta-\alpha-1}, \quad (16)$$

and we have the following equation:

$$\begin{aligned}\overline{W_\alpha(t-x+\alpha)} &= \overline{W_\alpha(1)} \cdot (1+g_2)^{t-x+\alpha-1} \\ &= \overline{W_\alpha(1)} \cdot \frac{(1+g_2)^{t-1}}{(1+g_2)^{x-\alpha}}.\end{aligned} \quad (17)$$

As a result, the UEBEI fund expenditure in year t is

$$O(t) = T_i \sum_{x=\beta}^{w} \overline{W_\alpha(1)} \cdot \left[(1+g_1)(1+g_2)\right]^{\beta-\alpha-1}(1+g_2)^{t-1} \cdot \frac{(1+k)^{x-\beta} \cdot P_x(t)}{(1+g_2)^{x-\alpha}}, \quad (18)$$

where T_i is the wage replacement rate, k is the annual pension adjustment rate, which shows that the pension increases with the retirement age, and $P_x(t)$ is the number of retired workers aged x in years. Then the cumulative expenditure of the UEBEI fund at the end of the target test period is

$$\begin{aligned} O &= \sum_{s=1}^{n} O(t)\cdot(1+r)^{n-s} \\ &= \sum_{t=1}^{n}(1+r)^{n-t}\left\{T_i\sum_{x=\beta}^{w}\overline{W_\alpha(1)}\cdot\left[(1+g_1)(1+g_2)\right]^{\beta-\alpha-1}(1+g_2)^{t-1}\frac{(1+k)^{x-\beta}\cdot P_x(t)}{(1+g_2)^{x-\alpha}}\right\}. \end{aligned} \tag{19}$$

3.2.3. Actuarial Balance of the UEBEI Fund. Actuarial Balance of the UEBEI fund is

$$\Delta E = I(t) - O(t), \tag{20}$$

where ΔE is the cumulative balance; $\Delta E = 0$ shows the UEBEI fund income and expenditure balance in year t. $\Delta E > 0$ shows that the UEBEI fund current income is greater than the expenditure. $\Delta E < 0$ shows that the UEBEI fund expenditure in the current year is greater than income. This model, combined with the partial accumulation of the UEBEI system in China, can better predict the income and expenditure of the UEBEI fund in the future.

3.3. Parameter Setting

3.3.1. Population Structure Parameters. Leslie population prediction model is used to establish a discrete matrix by gender and age to predict the population and population structure of the UEBEI in the future. Based on the population census data by age in China in 2010, we input the population data of different age group in 2010 to get $N(t)$. The resulting fertility matrix and survival matrix, both of which are regular matrices, are substituted into equation (6). Table 1 shows the data by age group and gender about population composition, fertility rate, and fertility pattern as of 2015.

3.3.2. Parametric Assumptions of the Actuarial Balance Model

(1) Contribution rate C_r

The contribution rate represents the proportion of total endowment insurance paid by employees and employers to personal wages. According to the contents of the "decisions" published in 2005 and 2015, the company contribution accounts for 20% and individual contribution accounts for 8%. So, in this paper, we assume that the contribution rate C_r is 28%.

(2) Collection rate $b(t)$

The collection rate of endowment insurance is the rate of how many persons are covered in the endowment insurance. It reflects the collection enforcement of a national pension. In 1995, the contribution rate of Chinese endowment insurance was above 90%, but it has been declining gradually in recent years. However, taking into account the fact that the national collection system will be gradually improved, the average collection rate of endowment insurance premiums for the target period, that is $b(t)$, here is set to be 85%.

(3) The average wage level $\overline{W_\alpha(1)}$ and the growth rate of g_1, g_2

According to statistics on average wages and growth rates of Chinese workers from 2000 to 2014, we can get an average growth rate of 13.63% for workers' average money wages and 11.21% for real wages excluding price changes (according to the statistics released by the National Bureau of Statistics from 2007 to 2015, with the slowdown of China's economic development, the average wage growth rate of employees has exhibited a downward trend). In recent years, the rate of wage growth in China tends to slow down. Therefore, taking into account situations in last few years, this paper assumes that the actual rate of wage growth is 8%. In addition, because the influence factor of wage increase includes personal and social factors, this paper assumes that the annual average wage growth rate g_1 caused by personal factors is 2% and that the annual average annual wage growth rate g_2 caused by social factors is 6%.

Based on the assumed growth rate of 8%, the average wage in 2015 can be calculated as 60,868.8 yuan. From the actual situation, the wage of newly employed workers in China $\overline{W_\alpha(1)}$ is equivalent to 65% of the average social wage.

(4) Replacement rate T_i

The replacement rate of China's UEBEI system is set as 60%, so this paper assumes that the basic pension insurance salary substitution rate T_i of the retired workers is 60%.

(5) Annual adjustment rate of basic pension k

The base of the basic pension plan for retirees will be adjusted as the average wage increases, but the increase should not be higher than 60% of the average wage growth in the previous year. Therefore, this

Table 1: Population composition, fertility rate, and fertility pattern by age group and gender in 2015.

Age	Average proportion of childbearing women (%)	Births proportion (%)	Fertility rate of childbearing women (‰)	Fertility rate 1st birth (‰)	Fertility rate of 2nd birth (‰)	Fertility rate of 3rd birth and above (‰)
15–19	10.18	3.03	9.19	7.99	1.12	0.08
20–24	13.54	24.05	54.96	40.17	13.39	1.41
25–29	16.89	40.59	74.31	41.55	28.80	3.96
30–34	13.62	19.95	45.31	14.98	25.42	4.91
35–39	13.19	7.93	18.60	4.63	10.96	3.01
40–44	16.14	2.80	5.37	1.85	2.45	1.07
45–49	16.44	1.65	3.11	1.25	1.23	0.63
Total	100	100	30.93	16.43	12.30	2.21

Source: the authors performed calculation based on the data released by National Bureau of Statistics, http://data.stats.gov.cn/easyquery.htm?cn=C01.

paper assumes that the adjustment level of basic pension for retirees is 60% of the average wage growth rate for employees; that is, the annual adjustment rate of basic pension k is 4.8%.

(6) Fund yield r

According to the announcement issued by the Council of Social Security Fund in 2015, the total investment income of the social security fund was 139 billion and 209 million yuan in 2014, and the yield reached 11.43%, which was 9.43 percentage points higher than the inflation rate of the same period and also higher than the growth rate of the gross domestic product (GDP). From the establishment of the social security foundation to the end of 2014, the average annual rate of return on investment reached 8.36%. In 2015, the return of 1 trillion and 800 billion assets of the social security fund was 15.14%. At present, in addition to the traditional investment channels such as fixed deposits, long-term bonds and stocks, futures, and other investment approaches traded publicly, Chinese social security fund also aims at some "offbeat investment" channels, including private equity, venture capital, leveraged buyout, and many other varieties, and has got good results, showing a good developing tendency of the insurance funds investment, so this paper assumes that the yield r is 10%.

(7) Employment age α and retirement age β

The survey data from the Ministry of Human Resources and Social Security shows that the employment age is generally around 20 to 22 but starts from 16. For convenience of calculation, this paper assumes that the age of initial employment for employees is 16. In China, according to the provisions of the law on retirement age, except for special circumstances, male unified retirement age is 60, female workers' retirement age is 50, and female cadres' retirement age is 55. While taking into account the Chinese policy to postpone retirement age, possibly published in the future, our model sets the average retirement age for men and women β as 57. So, the average working length $\beta - \alpha$ is 36 years.

3.4. Research Limitations. Owing to data limitation, this study has made many strong but necessary assumptions. However, some strong assumptions are based on literature, for example, contribution rate, collection rate, the average wage level and the growth rate, replacement rate, annual adjustment rate of basic pension, and fund yield.

Although some of these strong assumptions regarding parameters have been relaxed by using factors analysis on the Balance of Revenue and Expenditure in the Model as shown in Section 4.3, some strong assumptions still exist due to data limitation. For example, the interest rate is constant during forecasting period, the demographic structure of the population participating in the UEBEI system is consistent with the demographic structure of the population in China, and the population of those insured consists entirely of those who are more than 20 years old. Nevertheless, all these assumptions are necessary and reasonable as the forecasting is conducted.

4. Empirical Analysis

4.1. The Estimation of Population System Covered by UEBEI. According to the population data from 1997 to 2019, the values of $\widehat{A}_1(t)$ and $\widehat{A}_2(t)$ can be obtained. Combined with formula (10), the drift term $\widehat{d}_i$ can be calculated. Then, according to formula (12) and formula (11), we can obtain C.

So, for this random walk model, we can estimate

$$\widehat{d}_i = \begin{pmatrix} \widehat{d}_1 \\ \widehat{d}_2 \end{pmatrix} = \begin{pmatrix} -2.1762 \\ 0.0018 \end{pmatrix},$$
$$\widehat{C}\widehat{C}' = \begin{pmatrix} \widehat{\sigma}_1^2 & \widehat{\sigma}_{12} \\ \widehat{\sigma}_{12} & \widehat{\sigma}_2^2 \end{pmatrix} = \begin{pmatrix} 123.1348 & 0.0224 \\ 0.0224 & 0.00369 \end{pmatrix}. \quad (21)$$

So far, we can get random walk models for $A_1(t)$ and $A_2(t)$, and then we can get the estimates of $A_1(t)$ and $A_2(t)$ for every year until 2030, and using those estimates, future annual mortality curves can be obtained, and the age-specific mortality rate for people over 60 years of age can be calculated, as shown in Figure 2.

Figure 2 shows a total of 21 mortality curves. From the figure, we can get the following aspects of information: (1) the mortality rate is accelerating as the age increases; (2) mortality rate in future years is obviously lower than the current year; (3) the mortality rate gradually approaches one

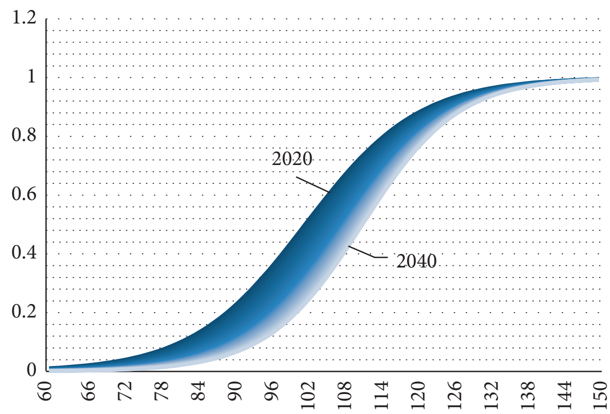

Figure 2: Estimated mortality probabilities for people over 60 years of age from 2020 to 2040. Source: the authors performed calculation based on the model.

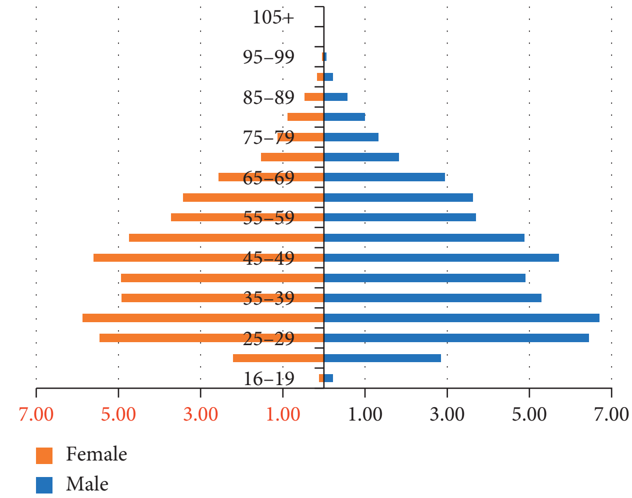

Figure 3: The population pyramid of the UEBEI in 2040. Source: the authors performed calculation based on the model.

around 150 years of age, which shows a longevity risk. Meanwhile, at present, the insurance industry generally adopts 105 as the ultimate survival age. Previously, the study on gap of pension insurance annuity also generally adopted 90 as the ultimate survival age. The mortality rate estimated by CBD model is different from that obtained by actual statistics. Demographics are cut off directly at the age of 90, and the CBD model can be used to estimate the mortality rate of people over 90 years of age.

In order to match the data analysis and let the data be more scientific and accurate, this paper adopts the 2010 census data as the population data. By substituting census data, we can deduce the annual population structure from 2010 to 2035. According to the insured structure of the UEBEI, the population structure of the UEBEI from 2010 to 2035 can be deduced. Figure 3 is the new birth policy predicted UEBEI covered population (note that the UEBEI covered population is different from the population. One will be covered in UEBEI after 16 when he or she starts to work) pyramid of China in 2040 based on the sixth census data and the predicted mortality probabilities.

4.2. The Actuarial Balance of the UEBEI Fund. Figure 4 shows the fund balance's forecast from 2020 to 2035. As shown, according to current assumptions, the trend that the annual fund expenditure is greater than the fund's revenue will occur in the UEBEI fund in 2025, with a fund gap of 141 billion yuan in that year and a fund gap of 9138.6 billion yuan in 2035. However, the cumulative pension fund pension has remained positive but will begin to decrease after 2030, but by 2035 there should be still 32736.4 billion. However, if the annual fund gap continues, the accumulated surplus will eventually be overdrawn.

Figure 5 shows the forecast of the fund balance under the pressure test considering the increase of the pension replacement rate by 5%. According to this analysis, by 2021, a fund gap of 3.1 billion yuan will start to occur in 2021, and the fund gap will reach 237.46 billion yuan and a cumulative deficit will be 511.16 billion yuan in 2030.

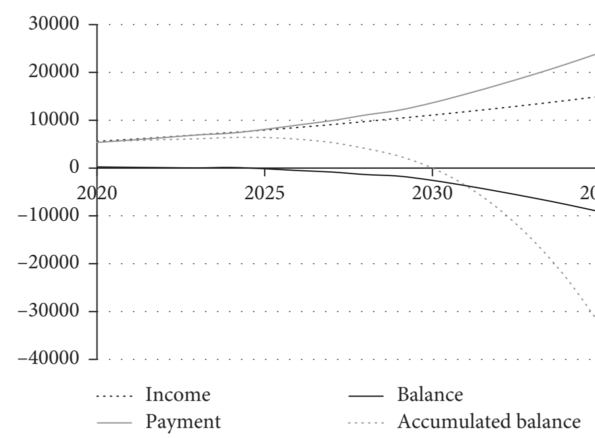

Figure 4: The forecast of the fund balance (in million yuan).

4.3. Analysis of the Factors Influencing the Balance of Revenue and Expenditure in the Model. Through the model analysis, we can see the influence of various factors on the balance of the model, as shown in Table 2.

Each variable in the model will affect the solvency of the insurance fund. There are several more important factors:

(1) Retirement age will affect how long people should work and how long retired workers can get their pension. Considering the impact on the pension fund's solvency, the higher the statutory retirement age is, the longer the employee's participation in UEBEI will be, the shorter the pension time will be, and the lesser the pressure on pension fund will be.

(2) The choice of pension replacement rate has a great impact on the operation of the UEBEI fund. Actually, this represents the "generosity" of the UEBEI system and measures the level of pension that retired workers receive.

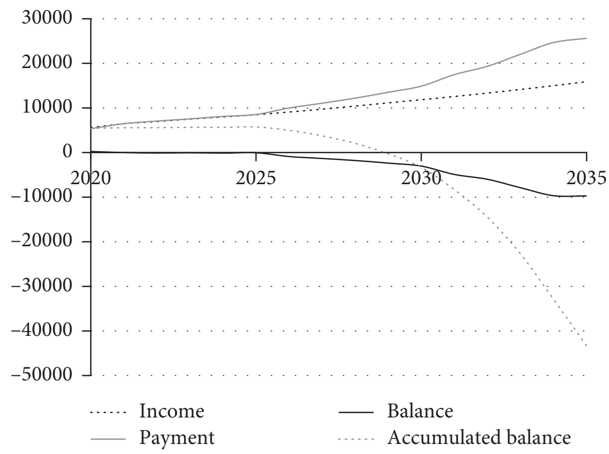

Figure 5: The forecast of the fund balance (the increase of the pension replacement rate by 5%).

Table 2: The influence of various factors on the balance of income and expenditure of the model.

	Collection rate	Investment yield	Payment rate	Substitution rate	Growth rate of wage	Age of retirement
Influence direction	+	+	+	−	+	+

Source: the authors draw the picture based on the results of the calculation of the changes in factors; "+" represents that an increase in the value of the factor can increase the fund balance; "−" represents that an increase in the value of the factor will reduce the fund balance.

(3) As the management of individual account in China adopts the fully accumulated model, the individual account funds are directly related to the solvency of pension funds. Only when the yield rate on investment of the UEBEI fund is at least higher than the inflation rate at the same time, the actual social purchasing power of the fund will not depreciate and then the UEBEI fund may be able to maintain its value. This is also a key for the individual account fund to maintain its financial sustainability.

(4) Social dependency rate refers to the ratio of the number of retired workers who meet the conditions for receiving pensions to the total number of people employed in the society. China has a high dependency rate and has more employees in the primary industry. However, employees in the primary industry do not belong to the coverage of the UEBEI. Therefore, the number of retired workers who meet the conditions of receiving pensions accounts for a low proportion of the total social employment.

As can be seen from the scenario simulation, if the pension replacement rate increases by 5%, the fund investment rate of return increases by 1%, the collection rate increases by 10%, the contribution rate increases by 1%, the average retirement age is extended to 60 (Figure 6), or the fertility rate increases by 10% (Figure 7); the cumulative balance of pension funds can keep increasing and does not fall. However, all the annual balances will be negative in the future. That is to say, with the limited adjustment, the gap of the UEBEI fund in the future is inevitable. The influence of these five factors on the UEBEI fund is different. The effect of a 10% increase in the collection rate and a 1% increase in the contribution rate is not as big as a 1% increase in wage and delaying retirement.

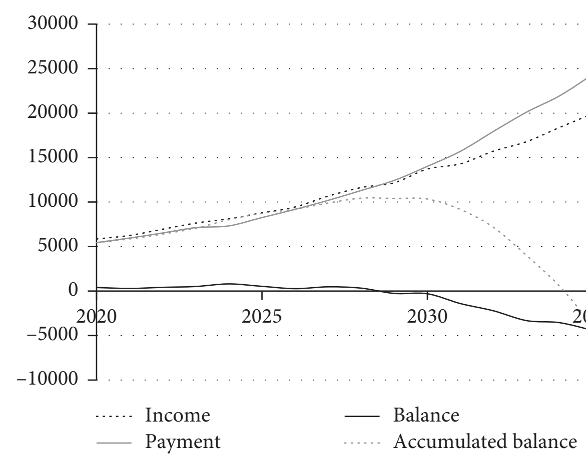

Figure 6: The forecast of the fund balance (the average retirement age is extended to 60).

The accumulated surplus gap is 3876 billion yuan by 2035 if retirement is delayed; the accumulated surplus gap is 22055 billion yuan by 2035 if the birth rate increases by 10%. Thus, delayed retirement has a huge impact on the sustainable development of the accumulated surplus of the UEBEI. The effect of the fertility rate policy has been slowed down, but the effect of the delayed retirement has been very rapid.

As for substitution rate, raising the replacement rate by 5% will obviously make the revenue and expenditure of the UEBEI worse, and the fund expenditure will be significantly faster than the fund's revenue. The annual surplus will begin

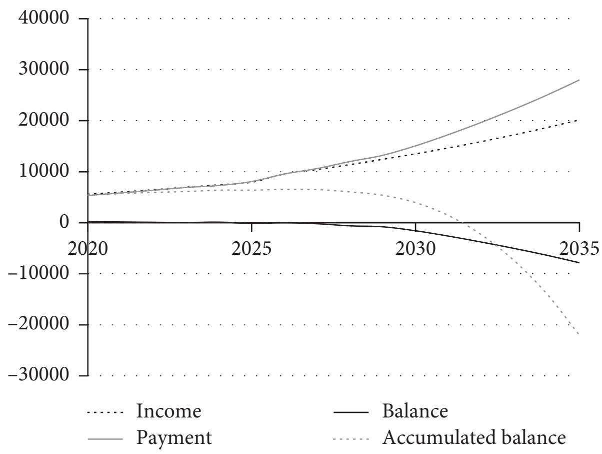

Figure 7: The forecast of the fund balance (the fertility rate increases by 10%).

to have a negative value in 2022, and the accumulated surplus will also decrease at a faster rate after 2029, finally reaching 43162 billion yuan by 2035. In view of this, in the future, if we want to improve the treatment of retirees, it is very likely that state finances will fail to provide pensions. Retirees who want to maintain their quality of life after retirement will probably have to rely on their own ways.

5. Concluding Remarks

5.1. Conclusions. Based on the partial accumulation system of China's basic pension insurance fund, this paper constructs an actuarial balance model and then makes assumptions about each parameter in the model combined with the actual situation in China. Then, for people over 60, the most important population in the future demographic structure, we use the CBD model to make predictions. This is an innovation in this paper. Since the CBD model used in this paper constructs a dynamic mortality formula, it can predict the population structure of the super-elderly group and does not require the usage of truncated populations for older people. For example, for the pension insurance revenue and expenditure model, it is generally assumed that the ultimate survival age is 90 years. In this paper, in the dynamic mortality model, the mortality rate reaches 1 in the age of 150, which is also different from the situation that the insurance industry directly cuts off at the age of 105, and sets the mortality rate of the 105-year-old population as 1. Moreover, through deductions of actual demographic data, China's ultimate survival age by 2030 can reach 113. The introduction of the CBD model has solved the problem of super-elderly population structure and improved the accuracy of estimation.

According to the calculation of this paper, China's UEBEI fund income will begin to be less than the expenditure in the year of 2024. After that, the annual fund gap will have been continuing to increase to 2 trillion and 520 billion in 2030. The cumulative surplus of the fund will maintain a rapid growth firstly, up to 17 trillion and 970 billion. However, from 2029, the accumulated balance of the fund will begin to decrease from growth, which will decline to 16 trillion and 600 billion in 2030, and the trend of the further decline is obvious.

In addition, the paper also analyzes the factors that affect the balance of basic pension insurance. The increase of the wage growth rate due to social factors, the increase of fund investment yield, the delay of retirement, the increase of fund collection rate, and the reduction of pension replacement rate are all beneficial to the sustainability of the basic old-age insurance fund.

5.2. Policy Recommendations. From 1990s, since the World Bank has put forward the "three-pillar" model of the endowment insurance system, the upsurge of endowment insurance system reform has been raised worldwide. The reform can be divided into two aspects, structural reform and parametric reform. Structural reform refers to a fundamental change in the framework of the three-pillar model. Parameter reform means adjusting the factors affecting the endowment insurance system.

The decision made in 2015 has required Chinese institutions to establish occupational pension system, which is a compulsory payment item. However, its coverage is only 40 million public officers. It seems that China still needs to improve the establishment of enterprise annuity because private pension scheme has taken the leading position in many OECD countries. It has become the primary source of income for the elderly in some countries.

Over the past decade, almost all OECD countries have adjusted the relevant parameters of the pension system. Unlike the structural reform that has two significant stages, parametric reform has time continuity and content diversity.

From the perspective of the system of China's endowment insurance, the location and function of social mutual assistance programs and personal accounts in the first pillar of the UEBEI still need to be clarified. At present, there are no clear dividing lines for the use of the two account funds in China, and they can be adjusted with each other. In the new situation of population aging, the indicators related to individual accounts and projects of social mutual assistance programs, such as the rate of substitution and the rate of payment, still need to be further adjusted.

As for the second pillar, the enterprise annuity, according to the actual situation in China, the basic old-age insurance system security level is not limited to its original function of preventing the elderly from poverty. For many people, the basic pension insurance for the first pillar is the guarantee of their old life. The development of China's enterprise annuity has lagged behind, and the coverage and protection level have not been greatly improved. It has not played a role in raising the living standard of the elderly. At the same time, this situation restrains that the level of the basic pension insurance, as the first pillar, cannot be reduced, which will lead to too much financial burden on the government. Moreover, as the population aging situation intensifies, the financial burden of the government will increase further.

Because of the early establishment of the OECD countries' public pension systems, they have been fully developed. So many OECD countries in this period mainly want to increase the coverage of private pension, and a few countries are committed to improving the coverage of compulsory pension insurance. As for China, although the coverage rate of enterprise annuity is very low, the top priority is to increase the coverage of basic pension insurance. The coverage rate of the UEBEI in China is about 63%; that is, nearly 40% of the workers are not involved in basic pension insurance. In this aspect, Switzerland can be taken as an example, which has reduced the threshold of the pension plan to ensure that more part-time and low-income workers are included in the pension system.

Because China is a typical economic transition country, the present old-age security system is not perfect enough. Many urban and rural people who do not have formal jobs and some low-income groups have not been absorbed into the old-age insurance system. Expanding the coverage of pension insurance is conducive to increasing the income of endowment insurance fund, and the social insurance is based on the law of large numbers; the more the number of participants, the lower the risk, and the funds raised will also increase, which will help to dissolve the pressure of the rapid growth of the endowment insurance fund.

In the process of economic development, the retirement age in China has been unchanged for more than 50 years. In many countries, the retirement age is 5 years higher than that of China. The current retirement policy of China is obviously not suitable for the current economic development, and it will bring negative impact on the balance of pension fund.

In the case of increasing life expectancy in China, it is feasible to raise the retirement age, and it can also be seen from the calculation of the fifth chapter that the delay of retirement is very beneficial to the balance of the UEBEI fund. Compared with other OECD countries, China's current retirement age has a large space to be improved, and it can be implemented in a phased and gradual way.

5.3. Shortages and Prospects. The CBD model has better prediction results for the elderly population over 60 years of age, while for the population below 60 years of age, it is not ideal, so the empirical life table of China's insurance industry in 2003 is still used to predict the population structure between the ages of 21 and 59, while the data of this experience table may not reflect the current situation in China. In addition, this article does not study the population structure in terms of gender, which may lead to a certain error.

Therefore, it is hoped that there will be a better model to fit the mortality rate of the Chinese people in terms of age in the future, so that the future population structure of China can be better predicted. In addition, the current changes of the fertility policy in China will have a significant impact on the future fund balance. However, this article only studies the years to 2030, and the change of fertility policy will not affect the population structure of people taking part in work before 2030, but, in a longer period of time, the fertility policy will show its influence, so the follow-up study can be carried out in this aspect.

Data Availability

All data are available from National Bureau of Statistics at http://data.stats.gov.cn/easyquery.htm?cn=C01.

Conflicts of Interest

The authors declare that they have no conflicts of interest.

Acknowledgments

This study was financially supported by the National Social Science Fund of China "research on the redistribution function of social security system: research on the national social security fund's intervention in pension insurance payment" and "the Fundamental Research Funds for the Central Universities" in UIBE (CXTD9-04).

References

[1] Z. Ren, Z. Luo, and W. Sun, *China financial Report 2019: who will afford our retirement?*, Evergrande Research Institute, Beijing, China, 2019, in Chinese.

[2] World Bank, *Averting the Old Age Crisis-Policies to Protect the Old and Promote Growth*, World Bank, Washington, DC, USA, 1994.

[3] J. Freedman and Y. Zhang, "China's pension paradoxes: challenges to creating an equitable and stable pension scheme," *China: An International Journal*, vol. 14, no. 3, pp. 153–166, 2016.

[4] Y. Tang, Y. Ruan, Y. Xu, and Y. Li, "Feedback analysis of population, economy and pension: moderate scale of China's pension strategic reserve," *Physica A-Statistical Mechanics and Its Applications*, vol. 12, pp. 40–43, 2020.

[5] L. R. Carter and R. D. Lee, "Modeling and forecasting US sex differentials in mortality," *International Journal of Forecasting*, vol. 8, no. 3, pp. 393–411, 1992.

[6] A. E. Renshaw and S. Haberman, "A cohort-based extension to the Lee-Carter model for mortality reduction factors," *Insurance: Mathematics and Economics*, vol. 38, no. 3, pp. 556–570, 2006.

[7] E. N. Reither, R. K. Masters, Y. C. Yang, D. A. Powers, H. Zheng, and K. C. Land, "Should age-period-cohort studies return to the methodologies of the 1970s?" *Social Science & Medicine*, vol. 128, pp. 356–365, 2015.

[8] D. Hainaut, "Multidimensional Lee-Carter model with switching mortality processes," *Insurance: Mathematics and Economics*, vol. 50, no. 2, pp. 236–246, 2012.

[9] A. Bell, "Life-course and cohort trajectories of mental health in the UK, 1991-2008 - a multilevel age-period-cohort analysis," *Social Science & Medicine*, vol. 120, pp. 21–30, 2014.

[10] A. J. G. Cairns, D. Blake, and K. Dowd, "A two-factor model for stochastic mortality with parameter uncertainty: theory and calibration," *Journal of Risk & Insurance*, vol. 73, no. 4, pp. 687–718, 2006.

[11] A. J. G. Cairns, D. Blake, K. Dowd, G. Coughlan, and D. Epstein, "A quantitative comparison of stochastic mortality models using data from England & Wales and the United

States," *North American Actuarial Journal*, vol. 13, no. 1, pp. 1–35, 2007.
[12] A. J. G. Cairns, D. Blake, K. Dowd, G. D. Coughlan, D. Epstein, and M. Khalaf-Allah, "Mortality density forecasts: an analysis of six stochastic mortality models," *Insurance: Mathematics and Economics*, vol. 48, no. 3, pp. 355–367, 2011.
[13] M. F. Carfora, L. Cutillo, and A. Orlando, "A quantitative comparison of stochastic mortality models on Italian population data," *Computational Statistics & Data Analysis*, vol. 112, pp. 198–214, 2017.
[14] P. Chernyavskiy, M. P. Little, and P. S. Rosenberg, "A unified approach for assessing heterogeneity in age-period-cohort model parameters using random effects," *Statistical Methods in Medical Research*, vol. 28, no. 1, pp. 20–34, 2019.
[15] Y. T. Xie and Z. X. Li, "Extension of bonus-malus factor based on joint pricing models," *Statistics & Information Forum*, vol. 30, no. 6, pp. 33–39, 2015, in Chinese.
[16] S. Basnayake and L. Nawarathna, "Modeling and forecasting Norway mortality rates using the Lee-carter model," *Journal of Biometrics & Biostatistics*, vol. 6, no. 1, 2017.
[17] R. Giacometti, M. Bertocchi, S. T. Rachev, and F. J. Fabozzi, "A comparison of the Lee-carter model and AR-ARCH model for forecasting mortality rates," *Insurance: Mathematics and Economics*, vol. 50, no. 1, pp. 85–93, 2012.
[18] F. Zhu and Y. Yang, "Based on the improved Leslie matrix gray model of the population precast," *Information Technology*, vol. 5, pp. 12–15, 2016.
[19] Y. Xie, H. Yu, X. Lei, and A. Lin, "The impact of fertility policy on the actuarial balance of China's urban employee basic medical insurance fund—the selective two-child policy vs. the universal two-child policy," *North American Journal of Economics and Finance*, 2020.
[20] I. Mircea, M. Covrig, and R. Serban, "Some mathematical models for longevity risk in the annuity market and pension funds," *Procedia Economics and Finance*, vol. 15, pp. 115–122, 2014.
[21] T. Lin and C. C.-L. Tsai, "On the mortality/longevity risk hedging with mortality immunization," *Insurance: Mathematics and Economics*, vol. 53, no. 3, pp. 580–596, 2013.
[22] W. Yu, P. Guo, Q. Wang et al., "On a periodic capital injection and barrier dividend strategy in the compound Poisson risk model," *Mathematics*, vol. 8, no. 4, p. 511, 2020.
[23] C. Metzger, "An actuarial balance sheet of the Swiss old-age pension scheme," *International Social Security Review*, vol. 71, no. 1, pp. 25–49, 2018.
[24] R. Meyricke and M. Sherris, "Longevity risk, cost of capital and hedging for life insurers under Solvency II," *Insurance: Mathematics and Economics*, vol. 55, no. 1, pp. 147–155, 2014.
[25] N. Bosnjak, "The actuarial projection method for pension fund's dependency ratio in case of Pension and Disability Insurance Fund of Republic of Srpska," *New Challenges of Official and Applied Statistics in European Union*, vol. 1, no. 1, pp. 72–78, 2016.
[26] A. A. Belolipetskii and M. A. Lepskaya, "A mathematical model of pension fund operation and methods of fund stability analysis," *Computational Mathematics and Modeling*, vol. 29, no. 2, pp. 233–243, 2018.
[27] Z. Q. Luo, Z. Y. Chen, and A. Lu, "A study on the effects of population factors on the payment balance of basic pension insurance funds in China," *Forecasting*, vol. 29, no. 2, pp. 42–46, 2010.
[28] W. Yu, F. Wang, Y. Huang, and H. Liu, "Social optimal mean field control problem for population growth model," *Asian Journal of Control*, vol. 2019, pp. 1–8, 2019.
[29] C. Q. Wang, Y. Tian, and H. Y. Xue, "Calculation on the fund balance of urban workers' basic old-age insurance: 2016–2060—based on the dual study of fertility policy adjustments and delaying retirement," *Reform of Economic System*, vol. 2017, no. 4, pp. 27–34, 2017.
[30] C. Cong and W. Jin, "The primary endowment insurance contribution mechanism: research on the effect of the long-term balance of endowment insurance fund," *Social Security Studies*, vol. 4, pp. 3–13, 2017.
[31] Y. Y. He and G. C. Liu, "A two factor state-space model for stochastic mortality and longevity risk measurement," *Theory & Practice of Finance & Economic*, vol. 35, no. 5, pp. 24–28, 2014.
[32] X. J. Wang and S. L. Huang, "Comparison and selection of stochastic mortality models in China," *Population & Economics*, vol. 1, pp. 82–86, 2011.
[33] L. Yuan and H. Pan, "Research on measurement of longevity risk of pension system: a projection of the population mortality in China based on Lee-carter model," *Labor Economic Review*, vol. 9, no. 2, pp. 70–84, 2016.
[34] J. H. Cui and Y. T. Xie, "Regional income mobility of urban households, tax burden, and dynamic equilibrium of income distribution," *Journal of Finance and Economics*, vol. 43, no. 8, pp. 43–55, 2017.
[35] J. H. Cui, W. F. Li, and Y. T. Xie, "Does decision-making of grassroots fiscal expenditure favour the poor? Evidence from tracking investigation of the Chinese countryside families," *Finance & Trade Economics*, vol. 39, no. 2, pp. 21–35, 2018.
[36] Y. Zeng, C. R. Ren, and Q. Liu, "Will extending the retirement age improve the solvency of China's pension insurance? Simulation analysis based on actuarial models," *Economic Management Journal*, vol. 35, no. 5, pp. 108–117, 2013.
[37] Y. Q. Zhao, M. Y. Bai, Y. L. Liu, and J. Z. Hao, "Quantitative analyses of transition pension liabilities and solvency sustainability in China," *Sustainability*, vol. 9, no. 12, pp. 22–52, 2017.
[38] T. Abdessalem and H. Chekki Cherni, "Macroeconomic effects of pension reforms in the context of aging populations: overlapping generations model simulations for Tunisia," *Middle East Development Journal*, vol. 8, no. 1, pp. 84–108, 2016.
[39] P. Müller and J. Wagner, "The impact of pension funding mechanisms on the stability and payoff from Swiss DC pension schemes: a sensitivity analysis," *The Geneva Papers on Risk and Insurance - Issues and Practice*, vol. 42, no. 3, pp. 423–452, 2017.

Hindawi
Mathematical Problems in Engineering
Volume 2020, Article ID 6197506, 15 pages
https://doi.org/10.1155/2020/6197506

Research Article

Pricing Catastrophe Equity Put Options in a Mixed Fractional Brownian Motion Environment

Guohe Deng

College of Mathematics and Statistics, Guangxi Normal University, Guilin 541004, China

Correspondence should be addressed to Guohe Deng; dengguohe@mailbox.gxnu.edu.cn

Received 25 March 2020; Accepted 23 April 2020; Published 11 May 2020

Guest Editor: Wenguang Yu

This paper considers the pricing of the CatEPut option (catastrophe equity put option) in a mixed fractional model in which the stock price is governed by a mixed fractional Brownian motion (mfBM model), which manifests long-range correlation and fluctuations from the financial market. Using the conditional expectation and the change of measure technique, we obtain an analytical pricing formula for the CatEPut option when the short interest rate is a deterministic and time-dependent function. Furthermore, we also derive analytical pricing formulas for the catastrophe put option and the influence of the Hurst index when the short interest rate follows an extended Vasicek model governed by another mixed fractional Brownian motion so that the environment captures the long-range dependence of the short interest rate. Based on the numerical experiments, we analyze quantitatively the impacts of different parameters from the mfBM model on the option price and hedging parameters. Numerical results show that the mfBM model is more close to the realistic market environment, and the CatEPut option price is evaluated accurately.

1. Introduction

As European put options, catastrophe equity put option (hereafter referred to as the CatEPut option) provides the insurance company the right to sell a specified amount of its stock to investors at a predetermined price at the expiration date of the option in case the total accumulated losses of the insured surpass a given trigger level of losses during the life time of the option. The CatEPut option is a catastrophe risk management tool and is firstly issued by RLI Corporation in 1996 to cover the potential losses caused by catastrophes such as typhoons, hurricanes, storms, waves, and earthquakes. Conceptually, CatEPut options and European put options are similar in that the two contractual financial instruments allow the holder special rights to sell securities. However, a CatEPut option differs from a European put option in two ways. One difference is that the CatEPut option is a sort of double trigger option. When the total accumulated losses surpass a given trigger level of losses during the lifetime of option, the CatEPut option is only exercisable. Other difference is that CatEPut options usually have five years or more to maturity. Consequently, the pricing mechanism for the CatEPut option is more complex.

There are few studies on pricing the CatEPut option in recent years. Cox et al. [1] first applied arbitrage-free approach to obtain a closed-form solution for the price of this option when the underlying asset price process satisfies the famous Black–Scholes model with the aggregate catastrophe losses of an insurance company following a Poisson process. Besides, they assumed that only the event of a catastrophe affects the underlying asset price, while the size of the catastrophe is irrelevant. Jaimungal and Wang [2] extended the work of Cox et al. [1] to analyze the pricing and hedging of the CatEPut option in a stochastic interest rate framework suggested by Vasicek [3] and assumed that the aggregate catastrophe losses followed a compound Poisson process and the underlying asset price process depended on the total loss level rather than on only the total number of losses. Furthermore, the underlying asset price process is modeled through a jump-diffusion process which is correlated to the loss process. Chang and Hung [4] supposed that the underlying asset price process was driven by a Lévy process with finite activity, and log jump sizes were independent identically distributed random variables with negative exponential density function and extended works of Cox et al. [1] and Jaimungal and Wang [2]. Lin et al. [5] considered different effects of catastrophe events and adopted a double Poisson process with log-normal intensity to model the number of catastrophe losses and derived the general pricing formula for contingent capital. Lin and Wang [6] applied a mixture of Erlangs as the distribution of the amounts for catastrophe losses and provided a pricing formula for the perpetual American CatEPut options using a penalty function approach. In addition, the pricing models for the CatEPut options with default risk have recently been studied (see Jiang et al. [7]; Jin and Zhong [8]; Koo and Kim [9] and Xu and Wang [10] for examples).

Recently, some researchers have adopted the stochastic volatility model or jump-diffusion model to describe the underlying asset price process. Kim et al. [11] extended the work of Lin and Wang [6] to the stochastic volatility model suggested by Heston [12] and investigated the value of the CatEPut options. Wang [13] presented CatEPut options with target variance which represents the insurance company's expectation of future realized variance under Heston's [12] model with stochastic interest rate and log-normal intensity of Poisson process. Wang et al. [14] considered pricing and hedging for the CatEPut options under a Markov-modulated jump-diffusion process with a Markov regime switching compensator. Kim et al. [15] provided a CatEPut option pricing model in which stock prices follow an additional jump term being moderately correlated with catastrophe losses and obtained a pricing formula for the perpetual American CatEPut options. Yu [16] and Yu et al. [17] studied pricing of the CatEPut options with double compound Poisson processes in which all jump terms are assumed to be independent mutually. The latest research studies on the valuing death benefits and population growth model were given by Yu et al. [18, 19] and Zhang et al. [20].

The aforementioned works have made significant contributions to the study of pricing catastrophe derivatives. However, none of the above works takes account of self-similarity and long-range dependence. A large number of empirical studies have shown that the distributions of the logarithm returns of the financial assets generally exhibit features of self-similarity and long-range dependence with heavy tails and volatility clustering in the real world (e.g., see Lo [21], Willinger et al. [22], Cont [23], Kang and Yoon [24], Kang et al. [25], and Huang et al. [26]). To incorporate this issue, the fractional Brownian motion (fBM) is introduced, which can capture the long-range dependence of the asset returns and produce burstiness in its sample path. Unfortunately, the fBM is neither a Markov nor a semimartingale and may, in some cases, still lead to implementable naive arbitrage opportunities (e.g., see Kuznetsov [27]; Bjork and Hult [28]). To get around this problem while taking into account the features of self-similarity and long-range dependence, the mixed fractional Brownian motion (mfBM) is suggested, which is a linear combination of a Brownian motion (BM) and an fBM with Hurst index $H \in (1/2, 1)$, to depict the underlying dynamics of the financial assets, and hence, it is arbitrage-free (see Cheridito [29, 30]). Recently, there has been considerable interest in applications of the mfBM environment on the pricing of various derivatives. One can refer to Deng and Xi [31]; Prakasa Rao [32]; Sun [33]; Xiao et al. [34, 35]; Zhang et al. [36]; He and Chen [37]; and Mehrdoust et al. [38] and the references therein. On the contrary, long-range dependence in bond market is a stylized fact that has been empirically studied by McCarthy et al. [39], Gil-Alana [40], Tabaka and Cajueiro [41], Cajueiro and Tabak [42], and Cajueiro and Tabak [43]. In this case, it is important to infer that there exists the long-range dependence in stochastic interest rates. Motivated by these results mentioned above, to make pricing models of financial derivatives more realistic, it is natural to replace the BM with the mfBM in stochastic interest rate models (see Xiao et al. [35]; Zhou et al. [44]).

In this paper, to price the CatEPut options under the stochastic interest rate framework and to capture the long-range dependence of both the underlying asset price and the short interest rate, we consider the pricing problem of this option in the mixed fractional Brownian motion environment with the mixed fractional Vasicek interest rate model. The contribution of this paper is two-fold. First, using the fractional Girsanov transform approach and the fractional Ito formula, we proposed the pricing models for the CatEPut options with constant or stochastic interest rates driven by the mixed fractional Vasicek model. Second, to assess the performance of our model, we apply the proposed model to compare the pricing results with those obtaining from traditional models, such as the famous Black–Scholes model and the fBM model.

The outline of this paper is as follows. Section 2 introduces the model for the mfBM, the underlying asset, and the catastrophe losses. Section 3 derives the explicit pricing formulas for the CatEPut options with constant or stochastic interest rates driven by the fractional Vasicek model. In Section 4, we provide some numerical examples of option prices to compare the pricing results with those obtaining from the famous Black–Scholes and fBM models and to observe effects of model parameters. Section 5 presents the dynamical hedging strategies for the CatEPut options. Section 6 summarizes this paper and discusses possible directions for future research.

2. The Model

In the section, we briefly review some background concerning the mixed fractional Brownian motion and describe a mixed fractional Brownian motion with the jump environment.

Let $(\Omega, \mathscr{F}, Q)$ be a complete probability space equipped with a filtration $(\mathscr{F}_t)_{t\geq 0}$ satisfying the usual conditions. All the random processes in this paper are defined on this given probability space. A mfBM M_t^H of parameters α, β, and H is defined by a linear combination of a standard Brownian motion W_t and an independent standard fractional Brownian motion W_t^H with Hurst index $H\,(0 < H < 1)$, that is, $M_t^H = \alpha W_t + \beta W_t^H$, where α and β are some real constants, not both are zero.

According to the definition above, it is clear that the mfBM M_t^H nests some popular processes in the literature. The mfBM degenerates to the fBM with $\alpha = 0$ and the BM with $\beta = 0$. The process M_t^H is a centered Gaussian process with $M_0^H = 0$ and with mean 0 for all $t \geq 0$ and covariation function $\mathrm{Cov}(M_t^H, M_s^H) = \alpha^2 \min\{t, s\} + \beta^2/2\,(|t|^{2H} + |s|^{2H} - |t-s|^{2H})$, for all $s, t \geq 0$. The increments of M_t^H are positively correlated if $H \in ((1/2), 1)$, uncorrelated if $H = 1/2$, and negatively correlated if $H \in (0, (1/2))$. It is remarkable that the mfBM M_t^H is the standard BM if $H = 1/2$, the increments of M_t^H are long-range dependent if and only if $H \in ((1/2), 1)$, and a self-similar process.

In order to ensure the market environment being arbitrage-free, we assume in this paper that the Hurst index $H \in ((3/4), 1)$, which leads to the mfBM being equivalent to a Wiener process (see Cheridito [29]). Now, consider a frictionless and arbitrage-free financial market where information arrives both continuously and discontinuously, and there exists a underlying stock S_t and a money market account B_t, which are traded continuously over a finite time interval $[0, T]$. Let r_t be the instantaneous interest rate process and L_t represent the total loss process of the insured over the time interval $[0, t]$, which is assumed to follow a compound Poisson process. Under the probability measure Q, the processes of S_t, B_t, and L_t can be expressed as follows:

$$\begin{cases} S_t = S_0 \exp\{-\mu L_t + \lambda\kappa t + X_t\}, \\ L_t = \sum_{i=1}^{N_t} Y_i, \\ B_t = B_0 e^{\int_0^t r_u \mathrm{d}u}, \quad B_0 = 1, \\ \mathrm{d}X_t = \left[r_t - \frac{1}{2}\sigma_s^2\left(\alpha^2 + 2\beta^2 H t^{2H-1}\right)\right]\mathrm{d}t + \sigma_s \mathrm{d}M_t^H, \end{cases} \tag{1}$$

where μ is a positive constant factor which denotes the percentage drop in the share value per unit loss, N_t is a Poisson process with constant intensity λ, $\{Y_i\}_{i=1}^{\infty}$ denote the size of i-th catastrophe loss and form a sequence of independent identically distributed random variables with probability density function $f_Y(y)$, and σ_s is the instantaneous volatility of the stock and is assumed to be constant. Additionally, all sources of randomness including the mfBM M_t^H, the Poisson process N_t, and the loss size sequence $(\{Y_i\}_{i=1}^{\infty})$ are assumed to be mutually independent. We also define the filtration $\mathscr{F}_t$ generated by $\mathscr{F}_t = \mathscr{F}_t^S$, where $\mathscr{F}_t^S = \sigma(S_u, u \leq t)$ is the natural filtration generated by S_t.

Since the share price of the underlying stock specified in (1) follows the compound Poisson process, the financial market is incomplete, and there is no unique equivalent martingale measure. We assume in this paper that the probability measure Q is a risk-neutral probability measure provided by the agents, and the jump risk presents the nonsystematic and diversifiable risk (see, e.g., Cox et al. [1]; Jaimungal and Wang [2]). Hence, in order to ensure the discounted stock price is a Q-martingale, the parameter κ satisfies $E(e^{-\mu L_t + \lambda\kappa t}) = 1$; here, $E(\cdot)$ denotes the quasi-expectation under measure Q.

Remark 1. $E(e^{-\mu L_t + \lambda\kappa t}) = 1 \Longrightarrow \kappa = \int_0^{+\infty}(1 - e^{-\mu y}) f_Y(y)\mathrm{d}y$.

From (1), it is easy to know that

$$S_T = S_t \exp\left\{\int_t^T r_u \mathrm{d}u - \mu(L_T - L_t) + \lambda\kappa(T-t) - \frac{1}{2}\sigma_s^2\left[\alpha^2(T-t) + \beta^2\left(T^{2H} - t^{2H}\right)\right] + \sigma_s\left(M_T^H - M_t^H\right)\right\}. \tag{2}$$

This implies that the stock price S_T is log-normally distributed with $\ln S_T \sim N(m, \nu^2)$ under r_t and L_t known on the time interval $[t, T]$, where $m = \ln S_t + \int_t^T r_u \mathrm{d}u - \mu(L_T - L_t) + \lambda\kappa\,(T-t) - (1/2)\sigma_s^2[\alpha^2(T-t) + \beta^2\,(T^{2H} - t^{2H})]$, $\nu^2 = \sigma_s^2(\alpha^2(T-t) + \beta^2(T^{2H} - t^{2H}))$, and $N(m, \nu^2)$ denotes the Gaussian distribution with mean m and variance ν^2.

3. Pricing the CatEPut Option

In this section, we shall first calculate the price of the CatEPut option when the short interest rate is a time-dependent and deterministic function. Second, we also derive a closed-form analytical expression for the price of the CatEPut option with the short interest rate following extended Vasicek's model in which the Brownian motion is replaced by a mfBM to capture the long-range dependence of the short-term interest rate.

The catastrophe put option is similar to a European put option, but it is termed a "double trigger" option, and its payoff at maturity T is given by

$$\text{payoff} = (K - S_T)^+ 1_{\left(L_T - L_{t_0} > L\right)}, \tag{3}$$

where $x^+ = \max\{x, 0\}$, K is the strike price, $L_T - L_{t_0}$ is the total accumulated losses of the insured over time period $(t_0, T]$, L is the trigger level of losses, and $1_{(\cdot)}$ denotes the indicator function. Let $P_{\mathrm{cat}}(t, t_0)$ denote the CatEPut option price at time t, which was signed at time $t_0 < t$ and matures at time $T > t$. In terms of the derivative pricing theory, we know that

$$P_{\mathrm{cat}}(t, t_0) = E\left[e^{-\int_t^T r_u \mathrm{d}u}(K - S_T)^+ 1_{\left(L_T - L_{t_0} > L\right)} \,\middle|\, \mathscr{F}_t\right]. \tag{4}$$

Proposition 1. *Let the dynamics processes S_t and L_t be given by (1). When the short interest rate r_t is a time-dependent and deterministic function, then the analytical pricing formula of the CatEPut option is*

$$P_{\mathrm{cat}}(t, t_0) \sum_{n=1}^{\infty} \frac{[\lambda(T-t)]^n e^{-\lambda(T-t)}}{n!} \int_{\widetilde{L}}^{+\infty} \Psi(y) f_Y^{(n)}(y)\mathrm{d}y, \tag{5}$$

where $\widetilde{L} = \max\left\{0, L + L_{t_0} - L_t\right\}$,

$$\Psi(y) = Ke^{-\int_t^T r_u \mathrm{d}u}\Phi(-d_2(y)) - S_t e^{-\mu y + \lambda\kappa(T-t)}\Phi(-d_1(y)),$$

$$d_1(y) = \frac{\ln(S_t/K) - \mu y + \lambda\kappa(T-t) + \int_t^T r_u \mathrm{d}u + 1/2\sigma_s^2\left[\alpha^2(T-t) + \beta^2(T^{2H} - t^{2H})\right]}{\sigma_s\sqrt{\alpha^2(T-t) + \beta^2(T^{2H} - t^{2H})}}, \tag{6}$$

$$d_2(y) = d_1(y) - \sigma_s\sqrt{\alpha^2(T-t) + \beta^2(T^{2H} - t^{2H})},$$

and $f_Y^{(n)}(y)$ is the n-fold convolution of the loss probability density function $f_Y(y)$ and $\Phi(\cdot)$ denotes the cumulated standard normal distribution function.

Proof. See Appendix A.

Since the life time of the CatEPut option can be 5 years or more, we generalize the price formula obtained above to the stochastic interest rate framework. Jaimungal and Wang [2], Jiang et al. [7], Yu [16], Wang [13], Koo and Kim [9], and Xu and Wang [10] extend the results in Cox et al. [1] by incorporating stochastic interest rate, which is assumed to satisfy Vasicek's model in which the driving process is supposed to be a Brownian motion. Note that a substantial amount of empirical evidence suggests that the process of the short interest rate may exhibit long-memory and self-similarity behaviors. Similar to Xiao et al. [35] and Zhou et al. [44], we assume that the short interest rate is controlled by the following process under the risk-neutral pricing measure Q:

$$\mathrm{d}r_t = a(b - r_t)\mathrm{d}t + \sigma_r \mathrm{d}Z_t^H, \tag{7}$$

where a denotes the mean-reversion rate, b represents the long-run mean of the interest rate, σ_r is the instantaneous volatility of the interest rate, and $Z_t^H = \alpha B_t + \beta B_t^H$ is another mfBM with parameters α, β, and H defined on the probability space $(\Omega, \mathcal{F}, Q)$ and is independent of the catastrophe loss process L_t. Moreover, the mfBM Z_t^H is correlated to the mfBM M_t^H with correlation coefficient $\rho \in [-1, 1]$, which is given by $\mathrm{d}M_t^H \mathrm{d}Z_t^H = \rho(\alpha^2 \mathrm{d}t + \beta^2 \mathrm{d}t^{2H})$. Additionally, we assume that a, b, σ_r, ρ and the initial value r_0 of r_t are real constants, standard Brownian motions, $W_t$and B_t, are independent of the fractional Brownian motions, W_t^H, B_t^H, and the filtration $\mathcal{F}_t$ generated by $\mathcal{F}_t = \mathcal{F}_t^S \vee \mathcal{F}_t^r$, where $\mathcal{F}_t^r = \sigma(r_u, u \le t)$ is the natural filtration generated by r_t.

Now, let us consider a zero-coupon bond that pays 1 unit of cash at maturity T. According to the risk-neutral pricing formula, the value of this bond at time $t \in [0, T]$, denoted by $P(t, T)$, is

$$P(t, T) = E\left[e^{-\int_t^T r_u \mathrm{d}u} \,\middle|\, \mathcal{F}_t^r\right]. \tag{8}$$

Using the fractional Ito formula (see Hu and Oksendal [45]), we have

$$\frac{\mathrm{d}P(t,T)}{P(t,T)} = r_t \mathrm{d}t + \sigma_r \frac{\partial P/\partial r}{P(t,T)} \mathrm{d}Z_t^H. \tag{9}$$

Moreover, $P(t, T)$ satisfies the following P.D.E.:

$$\begin{cases} \dfrac{\partial P}{\partial t} + \dfrac{1}{2}\sigma_r^2\left(\alpha^2 + 2\beta^2 H t^{2H-1}\right)\dfrac{\partial^2 P}{\partial r^2} + a(b-r)\dfrac{\partial P}{\partial r} - rP = 0, \\ P(T,T) = 1. \end{cases} \tag{10}$$

Similar to Xiao et al. [35], we obtain the following. □

Corollary 1. *When the short interest rate follows (7), the price of the zero-coupon bond is given by*

$$P(t,T) = \exp\{A(t,T) - B(t,T)r_t\}, \tag{11}$$

where $B(t,T) = 1 - e^{-a(T-t)}/a$ *and* $A(t,T) = (b - (\alpha^2\sigma_r^2/2a^2))[B(t,T) - (T-t)] - (\alpha^2\sigma_r^2/4a)B^2(t,T) + H\beta^2\sigma_r^2 \int_t^T u^{2H-1}B^2(u,T)du$.

Now, we introduce the Radon–Nikodym derivative as follows:

$$\begin{aligned} \left.\frac{\mathrm{d}Q^T}{\mathrm{d}Q}\right|_{\mathcal{F}_T} &= \frac{e^{-\int_t^T r_u \mathrm{d}u}}{P(t,T)} \\ &= \exp\left\{-\frac{1}{2}\int_t^T \sigma_r^2 B^2(u,T)\left(\alpha^2 + 2H\beta^2 u^{2H-1}\right)\mathrm{d}u \right. \\ &\quad \left. - \int_t^T \sigma_r B(u,T)\mathrm{d}Z_u^H\right\}. \end{aligned} \tag{12}$$

Using the fractional Girsanov theorem (see Hu and Oksendal [45]), then $\widehat{M}_t^H = \alpha\widehat{W}_t + \beta\widehat{W}_t^H, \widehat{Z}_t^H = \alpha\widehat{Z}_t + \beta\widehat{Z}_t^H$ defined by

$$\begin{aligned} \widehat{M}_t^H &= M_t^H + \int_0^t \rho\sigma_r B(u,T)\left(\alpha^2 + 2H\beta^2 u^{2H-1}\right)\mathrm{d}u, \\ \widehat{Z}_t^H &= Z_t^H + \int_0^t \sigma_r B(u,T)\left(\alpha^2 + 2H\beta^2 u^{2H-1}\right)\mathrm{d}u, \end{aligned} \tag{13}$$

are Q^T-mfBMs with the correlation coefficient ρ, and under Q^T,

$$\ln S_T = \ln \frac{S_t}{P(t,T)} - \mu\left(L_T - L_t\right) + \lambda\kappa(T-t) - \frac{1}{2}\sigma^2(u) + \int_t^T \sigma_s \mathrm{d}\widehat{M}_t^H + \int_t^T \sigma_r B(u,T)\mathrm{d}\widehat{Z}_t^H, \tag{14}$$

$$\int_t^T \sigma_s \mathrm{d}\widehat{M}_t^H + \int_t^T \sigma_r B(u,T)\mathrm{d}\widehat{Z}_t^H \sim N\left(0,\theta^2(t,T)\right), \tag{15}$$

where $\theta^2(t,T) = \int_t^T \widetilde{B}(u,T)(\alpha^2 + 2H\beta^2 u^{2H-1})\mathrm{d}u$ and $\widetilde{B}(u,T) = \sigma_s^2 + 2\rho\sigma_s\sigma_r B(u,T) + \sigma_r^2 B^2(u,T)$. Therefore, (4) can be rewritten as

$$P_{\text{cat}}(t,t_0) = P(t,T)E^T\left\{1_{\left(L_T - L_{t_0} > L\right)}\left(K - S_T\right)^+ \middle| \mathcal{F}_t\right\}, \tag{16}$$

where $E^T[\mathcal{F}_t]$ denotes the quasi-conditional expectation under the T-forward measure Q^T.

Proposition 2. *Let the dynamics processes S_t, L_t, and r_t be given by (1) and (7); then, the analytical pricing formula of the CatEPut option is*

$$P_{\text{cat}}(t,t_0) = \sum_{n=1}^{\infty} \frac{[\lambda(T-t)]^n e^{-\lambda(T-t)}}{n!}\int_{\widetilde{L}}^{+\infty} \widetilde{\Psi}(y) f_Y^{(n)}(y)\mathrm{d}y, \tag{17}$$

where $\widetilde{L} = \max\left\{0, L + L_{t_0} - L_t\right\}$,

$$\widetilde{\Psi}(y) = \mathrm{KP}(t,T)\Phi\left(-\widetilde{d}_2(y)\right) - S_t e^{-\mu y + \lambda\kappa(T-t)}\Phi\left(-\widetilde{d}_1(y)\right),$$

$$\widetilde{d}_1(y) = \frac{\ln\left(S_t/KP(t,T)\right) - \mu y + \lambda\kappa(T-t) + 1/2\theta^2(t,T)}{\theta(t,T)},$$

$$\widetilde{d}_2(y) = \widetilde{d}_1(y) - \theta(t,T). \tag{18}$$

Proof. See Appendix A.

Remark 2. When $(\alpha,\beta) = (1,0)$, then the result of Proposition 2 reduces to that of Jaimungal and Wang [2]. When $(\alpha,\beta) = (0,1)$, then the result of Proposition 2 is provided in the fBM environment. Therefore, the JW and fBM models are special cases of the mfBM model in this paper.

Remark 3. The integrations in the pricing model of equation (17), such as $\theta^2(t,T) = \int_t^T \widetilde{B}(u,T)(\alpha^2 + 2H\beta^2 u^{2H-1})\mathrm{d}u$, can be calculated using the Riemann integral.

Cox et al. [1] considered that the loss size conditional on a loss is fixed at l and the trigger level is an integer multiple of the loss size, i.e., $L = cl$. The parameter c, here labeled the trigger ratio level, represents the ratio of the trigger level to the total expected loss. The probability density function $f_Y(y)$ od loss size Y_i in this fixed loss case is a Dirac density $f_Y(y) = \delta(y-l)$, and then the following corollary is given.

Corollary 2. *If the loss size Y_i follows a Dirac density $f_Y(y) = \delta(y-l)$, the price function in (17) can be rewritten as follows:*

$$P_{\text{cat}}(t,t_0) = \sum_{n=\widehat{N}+1}^{\infty} \frac{[\lambda(T-t)]^n e^{-\lambda(T-t)}}{n!}\left[KP(t,T)\Phi\left(-\widehat{\mathrm{d}}_2(n)\right) - S_t e^{-\mu n l + \lambda\kappa(T-t)}\Phi\left(-\widehat{\mathrm{d}}_1(n)\right)\right], \tag{19}$$

where $\widetilde{N} = \max\left\{0, c + N_{t_0} - N_t\right\}$ *and*

$$\widehat{d}_1(n) = \frac{\ln\left(S_t/KP(t,T)\right) - \mu n l + \lambda\kappa(T-t) + (1/2)\theta^2(t,T)}{\theta(t,T)},$$

$$\widehat{d}_2(n) = \widehat{d}_1(n) - \theta(t,T). \tag{20}$$

It is clear that pricing model (17) depends on Hurst parameter H. Hence, we present the influence of this parameter based on price formulas (17) in the following proposition.

Proposition 3. *The influence of the Hurst parameter H is given by*

$$\frac{\partial P_{\text{cat}}(t,t_0)}{\partial H} = KP(t,T)\beta^2 \sum_{n=1}^{\infty} \frac{[\lambda(T-t)]^n e^{-\lambda(T-t)}}{n!}\int_{\widetilde{L}}^{+\infty}\int_t^T \cdot\left[\sigma_r^2\Phi\left(-\widetilde{d}_2(y)\right)B^2(u,T) + \frac{\widetilde{B}(u,T)e^{-\left(\widetilde{d}_2^2(y)/2\right)}}{\sqrt{2\pi}\,\theta(t,T)}\right] \cdot\left[u + H(2H-1)\right]u^{2H-2} f_Y^{(n)}(y)\mathrm{d}u\,\mathrm{d}y\Bigg]. \tag{21}$$

Moreover, we have $(\partial P_{cat}(t,t_0)/\partial H) > 0$ for fixed $t \in [0,T]$.

Proof. We get from (17) that

$$\frac{\partial P_{\text{cat}}(t,t_0)}{\partial H} = \sum_{n=1}^{\infty} \frac{[\lambda(T-t)]^n e^{-\lambda(T-t)}}{n!}\int_{\widetilde{L}}^{+\infty} \frac{\partial\widetilde{\Psi}(y)}{\partial H} f_Y^{(n)}(y)\mathrm{d}y. \tag{22}$$

Since

$$\frac{\partial\widetilde{\Psi}(y)}{\partial H} = K\frac{\partial P(t,T)}{\partial H}\Phi\left(-\widetilde{d}_2(y)\right) - KP(t,T)\Phi'\left(-\widetilde{d}_2(y)\right)\frac{\partial\widetilde{d}_2(y)}{\partial H} + S_t e^{-\mu y+\lambda\kappa(T-t)}\Phi'\left(-\widetilde{d}_1(y)\right)\frac{\partial\widetilde{d}_1(y)}{\partial H},$$

$$\begin{aligned}\frac{\partial P(t,T)}{\partial H} &= P(t,T)\frac{\partial A(t,T)}{\partial H},\\ &= P(t,T)\beta^2\sigma_r^2\int_t^T [u+H(2H-1)]B^2(u,T)u^{2H-2}\mathrm{d}u,\end{aligned} \tag{23}$$

$$\frac{\partial\widetilde{d}_2(y)}{\partial H} = \frac{\partial\widetilde{d}_1(y)}{\partial H} - \frac{\partial\theta(t,T)}{\partial H}.$$

On the contrary, we have

$$\begin{aligned}\frac{\partial\widetilde{d}_1(y)}{\partial H} &= \frac{[-(1/P(t,T))(\partial P(t,T)/\partial H) + \theta(t,T)(\partial\theta(t,T)/\partial H)] - \widetilde{d}_1(y)(\partial\theta(t,T)/\partial H)}{\theta(t,T)},\\ \frac{\partial\theta(t,T)}{\partial H} &= \beta^2\int_t^T \widetilde{B}(u,T)[\frac{u+tHn(2H-))]u^{2H-2}\mathrm{d}u}{\theta(t,T).}\end{aligned} \tag{24}$$

With tedious calculation, we obtain that

$$\begin{aligned}\frac{\partial\widetilde{\Psi}(y)}{\partial H} &= KP(t,T)\beta^2\int_t^T\left[\sigma_r^2\Phi\left(-\widetilde{d}_2(y)\right)B^2(u,T)\right.\\ &\quad\left.+\frac{\widetilde{B}(u,T)e^{-\widetilde{d}_2^2(y)/2}}{\sqrt{2\pi}\,\theta(t,T)}[u+H(2H-1)]u^{2H-2}\mathrm{d}u\right]\\ &\quad+\frac{\beta^2}{\sqrt{2\pi}}\left[S_t e^{-\mu y+\lambda\kappa(T-t)}e^{-\left(\widetilde{d}_1^2(y)/2\right)} - KP(t,T)e^{-\left(\widetilde{d}_1^2(y)/2\right)}\right]\\ &\quad\cdot\int_t^T\left[-\sigma_r^2B^2(u,T)+\left(1-\frac{\widetilde{d}_1(y)}{\theta(t,T)}\right)\widetilde{B}(u,T)\right]\\ &\quad\cdot[u+H(2H-1)]u^{2H-2}\mathrm{d}u.\end{aligned} \tag{25}$$

Note that $e^{-(\widetilde{d}_2^2(y)/2)} = e^{-(\widetilde{d}_1^2(y)/2)+\widetilde{d}_1^2(y)\theta(t,T)-(\theta^2(t,T)/2)} = (S_t/KP(t,T))e^{-\mu y+\lambda\kappa(T-t)}e^{-\widetilde{d}_1^2(y)/2}$; then, (25) can be rewritten as

$$\begin{aligned}\frac{\partial\widetilde{\Psi}(y)}{\partial H} &= KP(t,T)\beta^2\int_t^T\left[\sigma_r^2\Phi\left(-\widetilde{d}_2(y)\right)B^2(u,T)\right]\\ &\quad+\frac{\widetilde{B}(u,T)e^{-\widetilde{d}_2(y)/2}}{\sqrt{2\pi}\theta(t,T)}[u+H(2H-1)]u^{2H-2}\mathrm{d}u.\end{aligned} \tag{26}$$

Substituting (26) into (22) leads to finish the proof.

Corollary 4. *The risk-neutral probability that the CatEPut option ends in the money under the dynamics processes S_t, L_t, and r_t given by (1) and (7) is*

$$\begin{aligned}Q\left(S_T<K, L_T-L_{t_0}>L\,\middle|\,\mathcal{F}_{t_0}\right) &= \sum_{n=1}^{\infty}\frac{[\lambda(T-t_0)]^n e^{-\lambda(T-t_0)}}{n!}\\ &\quad\int_L^{+\infty}\Phi(-h(y))f_Y^{(n)}(y)\mathrm{d}y,\end{aligned} \tag{27}$$

where $h(y) = (\ln(S_{t_0}/KP(t_0,T)) - \mu y + \lambda\kappa(T-t_0) - 1/2\theta^2(t_0,T))/(\theta(t_0,T))$.

Proof. Similar to the proof of $\widehat{I}_1$ in (B.2), it is obvious to obtain (27).

Although it appears that the pricing formula in (17) involves infinite sum, in practice, it is not necessary. In the following, we will prove that numerically, only the first few terms in the series are needed when the jump intensity rate λ is small. Similar to the argument of Jaimungal and Wang [2], we let

$$P_{\text{cat}}(t,t_0;M) = \sum_{n=1}^{M}\frac{[\lambda(T-t)]^n e^{-\lambda(T-t)}}{n!}\int_{\widetilde{L}}^{+\infty}\widetilde{\Psi}(y)f_Y^{(n)}(y)\mathrm{d}y. \tag{28}$$

Then, by (17), we have

$$\begin{aligned}
\left|P_{\text{cat}}(t,t_0)-P_{\text{cat}}(t,t_0;M)\right| &= \sum_{n=M+1}^{\infty}\frac{[\lambda(T-t)]^n e^{-\lambda(T-t)}}{n!}\int_{\widetilde{L}}^{+\infty}\widetilde{\Psi}(y) f_Y^{(n)}(y)\mathrm{d}y \\
&\le \sum_{n=M+1}^{\infty}\frac{[\lambda(T-t)]^n e^{-\lambda(T-t)}}{n!}\int_{\widetilde{L}}^{+\infty} KP(t,T)\Phi\left(-\widetilde{d}_2(y)\right) f_Y^{(n)}(y)\mathrm{d}y \\
&\le \sum_{n=M+1}^{\infty}\frac{[\lambda(T-t)]^n e^{-\lambda(T-t)}}{n!} KP(t,T) \\
&\le KP(t,T)\left\{\frac{[\lambda(T-t)]^M}{M!}\left(1-e^{-\lambda(T-t)}\right)\right\}.
\end{aligned} \tag{29}$$

Consequently, the relative error in the price can be made very small by choosing M appropriately. For example, if $\lambda = 0.5$ and choosing $M = 20$, an accuracy of 0.4% can be obtained.

4. Numerical Results

In this section, we analyze numerically the proposed model by considering the stochastic interest rate environment. First, we clarify the effectiveness of the proposed model by making comparison with the results of Jaimungal and Wang [2] and the fBM model. Second, we present a sensitivity analysis for the CatEPut option prices under alternative parameter values. In particular, we examine the effects of two parameters of the claim size on the option price and the risk-neutral probability.

In the next numerical experiments, we consider the CatEPut option with maturity $T = 5$ year and show some parameter values in Table 1 if there is no special instruction. The loss size in this paper follows the gamma distribution with mean μ_l and standard deviation σ_l, that is, $f_Y(y) = (((\mu_l/\sigma_l^2)^{(\mu_l^2/\sigma_l^2)})/(\Gamma(\mu_l^2/\sigma_l^2)))y^{(\mu_l^2/\sigma_l^2)-1}e^{-(\mu_l/\sigma_l^2)y}, y>0,$ in which case, the n-fold convolution of the losses is given by

$$f_Y^{(n)}(y) = \frac{(\mu_l/\sigma_l^2)^{(n\mu_l^2/\sigma_l^2)}}{\Gamma\left(n\mu_l^2/\sigma_l^2\right)} y^{(n\mu_l^2/\sigma_l^2)-1} e^{-(\mu_l/\sigma_l^2)y}, \quad y>0 \tag{30}$$

where $\Gamma(\cdot)$ is the gamma function. The trigger level of losses L is defined by $c\lambda(T-t)\mu_l$ which denotes a multiple c of the expected losses. According to Remark 1, the parameter κ in this case is $\kappa = 1-(\mu_l/(\mu_l+\mu\sigma_l^2))^{(\mu_l^2/\sigma_l^2)}$. The parameter c denotes the real-valued trigger ratio level. Moreover, we also assume $L_t - L_{t_0} = 0$ and $(\alpha,\beta) = (1,1)$ for the mfBM.

Figure 1 displays all values of the CatEPut option against different values of S_0 with the trigger ratio level of $c = 1$ and $c = 2$ for three different models, including the JW (Jaimungal and Wang [2]), fBM, and mfBM models in the stochastic interest rate framework.

As can be seen from Figure 1, the curvature of all option price curves with the trigger ratio level $c = 1$ and $c = 2$ for the three models is significantly decreased as the stock price increases. This shows that the value of S_0 has a negative effect on the value of the CatEPut option. In addition, the option prices for the JW model are lower than the corresponding prices for the fBM and mfBM models. We point that the difference is caused by the existence of the long-range dependence. It implies that the proposed model can not only exhibit the long-range dependence but also produce closer results to the JW model in which BM has been used traditionally as the driving force for modeling the stock price.

Table 2 reports the option prices for the in-the-money ($S_0 = 60$), at-the-money ($S_0 = 80$), and out-of-the-money ($S_0 = 100$) CatEPut option under the constant/stochastic interest rate framework. As shown in Table 1, we know that the option price under stochastic interest rate is lower than the corresponding price under constant interest rate. This is reasonable because the introduction of stochastic interest rate reduces the variance of the return on the underlying stock compared with the situation with constant interest rate. No matter what the strike is, the price of the CatEPut option increases as the Hurst index H and the stock's volatility σ_s increase. One possible reason for this phenomenon is that the Hurst index represents the long-range dependency property. So, the bigger the Hurst index is, i.e., the stronger the long-memory property is, the higher the option price is. However, the option price decreases as the trigger ratio level c increases, which is obvious. In addition, the CatEPut option's price decreases from in-the-money to out-of-the-money.

Next, we examine how the option price is affected by the model parameter values of the spot interest rate process for a trigger ratio level $c = 1$. We focus on investigating the effects of two parameters σ_r and correlation coefficient ρ on the option price. The results are plotted in Figure 2.

Figure 2(a) indicates that the effect on option price is remarkable if the volatility of the spot interest rate is higher. This may be due to two facts: the uncertainty effect and the long-range dependence in the real world. The larger volatilities induce more uncertainty, and the long-range dependence produces burstiness in the sample path of asset returns, and these push the option prices upward. In Figure 2(b), we compare the option price with different

Table 1: The parameter values used in numerical examples.

Parameter	Value
K	80
r_0	0.02
σ_r	0.05
μ_l	25
λ	0.5
a	0.2
ρ	−0.1
σ_l	20
σ_s	0.2
b	0.3
μ	0.01
H	0.8

correlation coefficients ρ, which illustrates that the option prices decrease when the correlation coefficients ρ increase. By the light of nature, this is correct. The reason is if the asset price is strongly negatively correlated to the spot interest rates, the higher the asset price is, the lower the spot interest rates are and the higher the option price is. However, the changes in ρ do not affect the option prices as significantly as changes in the volatility.

In Figure 3, we illustrate how the option prices are affected by the mean μ_l and standard deviation σ_l of the claim size for two different trigger ratio levels of $c = 1$ and $c = 2$, respectively. For the trigger ratio level of $c = 2$, the option price decreases as the mean of the claim sizes increases, while for the trigger ratio level of $c = 1$, the option price increases as the mean of the claim sizes increases. This result is explained by exploring the risk-neutral probability in Figure 4(a) that the option is exercised. In Figure 4(a), the probability of exercising the option is an increasing function of the mean for smaller trigger ratio levels, while it is generally a constant function of the mean for larger trigger ratio levels. In addition, the probability of exercising the option for smaller trigger ratio levels is greater than that for larger ones. In Figure 3, we also find that, for the trigger ratio level of $c = 2$, the option price increases as the standard deviation of the claim sizes increases, while for the trigger ratio level of $c = 1$, the option price increases when the standard deviation of the claim sizes becomes smaller. However, after a certain value of σ_l and then onward, the option price decreases as σ_l increases. This reason is that, for reasonably small σ_l and the trigger ratio level of c, the option price is dominated by the risk-neutral probability, which is monotonically decreasing with σ_l, as shown in Figure 4(b).

5. Dynamically Hedging the CatEPut Option

A reinsurance company provides a CatEPut option to an insurance company, and they need to hedge risk for this contract to avoid taking on very large losses. In this section, we present how to hedge against stock price risk and interest rate risk. In a perfect market, delta-gamma hedging techniques are used to measure the sensitivity of the option's price to underlying asset price movements at the first and second order. Jaimungal and Wang [2] further used the delta-gamma-rho hedging strategy to measure the price risk of the stock price and interest rate. Here, we also use this technique to measure the price risk and compute various Greek values. The Greek letters are described as follows.

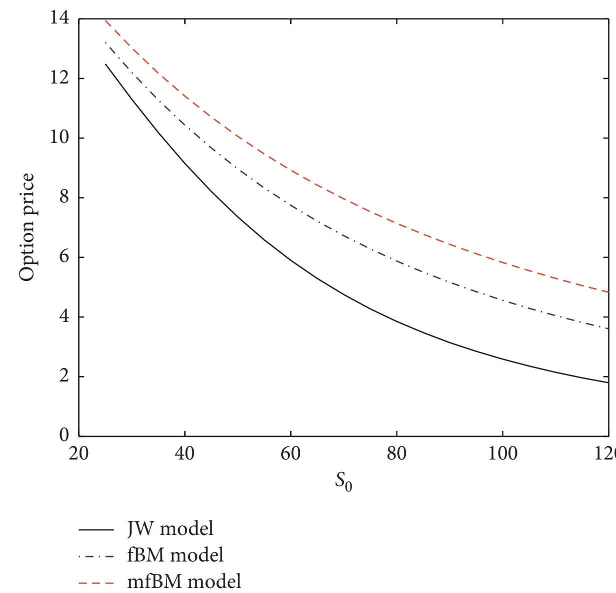

(a)

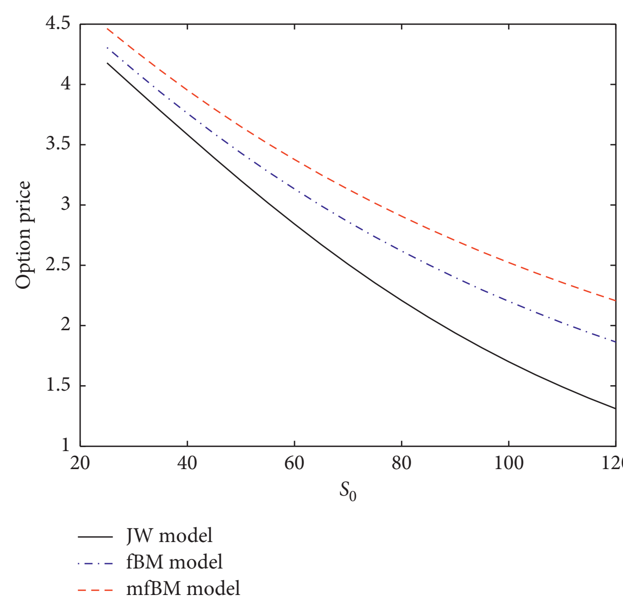

(b)

Figure 1: CatEPut option value for two trigger ratio levels $c = 1$ and $c = 2$ under the three specifications, JW, fBM, and mfBM models. (a) $c = 1$. (b) $c = 2$.

Proposition 4. *Under the dynamics processes S_t, L_t, and r_t modeled by (1) and (7), delta, gamma, and rho of the CatEPut option given in (17) are calculated as the following expressions:*

Table 2: Option prices under constant/stochastic interest rate.

S_0	Constant interest rate			Stochastic interest rate		
	$c = 1$	$c = 2$	$c = 3$	$c = 1$	$c = 2$	$c = 3$
$H = 0.8$						
60	17.7834	6.19015	1.45349	8.92275	3.37690	0.849746
80	14.9291	5.56540	1.37039	7.14182	2.90722	0.776963
100	12.6302	5.01053	1.29149	5.82774	2.52269	0.711669
$H = 0.9$						
60	18.3864	6.25808	1.45731	9.72182	3.53258	0.870091
80	15.7647	5.67737	1.37779	8.03146	3.09770	0.802079
100	13.6421	5.16633	1.30325	6.75448	2.73960	0.741522
$H = 0.98$						
60	18.9851	6.33379	1.46235	10.4918	3.68761	0.891346
80	16.5656	5.79439	1.38677	8.88816	3.2833	0.827782
100	14.5964	5.3226	1.31667	7.6544	2.94864	0.771475
$\sigma_s = 0.2$						
60	17.7834	6.19015	1.45349	8.92275	3.37690	0.849746
80	14.9291	5.56540	1.37039	7.14182	2.90722	0.776963
100	12.6302	5.01053	1.29149	5.82774	2.52269	0.711669
$\sigma_s = 0.25$						
60	18.9757	6.33639	1.46282	10.0168	3.55346	0.864323
80	16.5352	5.79539	1.38735	8.43109	3.14982	0.800556
100	14.5444	5.32101	1.31725	7.21853	2.81694	0.74415
$\sigma_s = 0.5$						
60	24.6637	7.27578	1.56092	14.8864	4.45694	0.969254
80	23.5855	7.03926	1.52517	14.1160	4.27946	0.941041
100	22.6716	6.83390	1.49338	13.4775	4.12875	0.916482

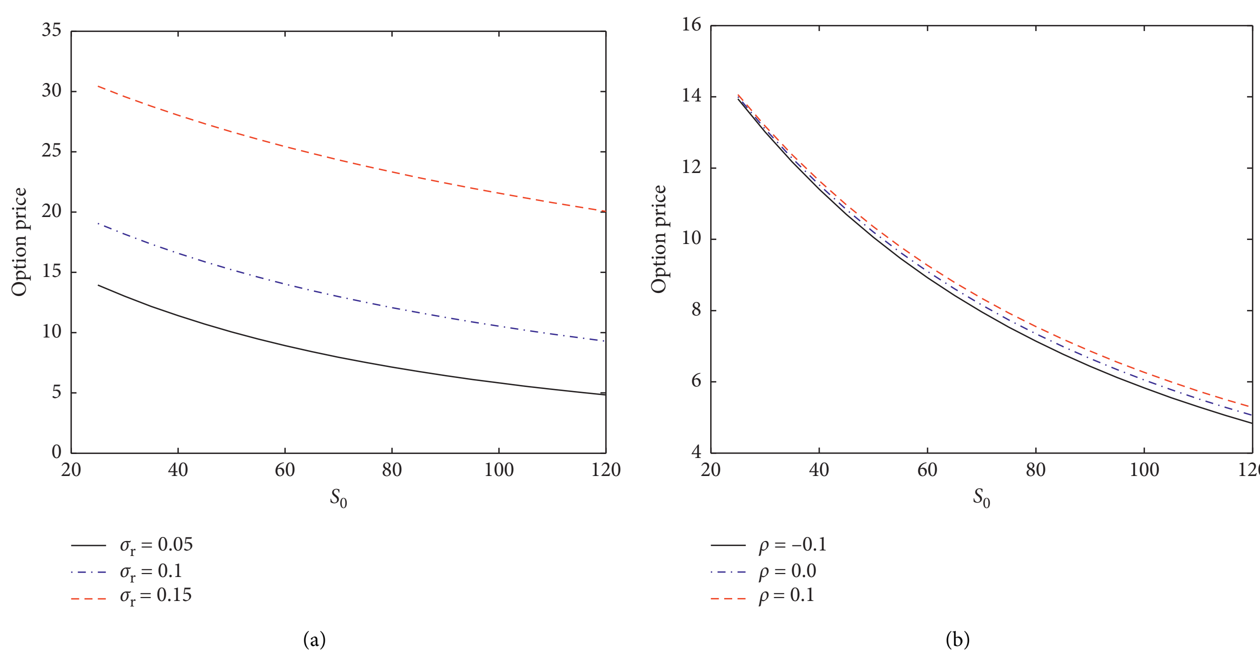

Figure 2: Option price for several parameter values of the interest rate. (a) Volatility levels. (b) Correlation coefficients.

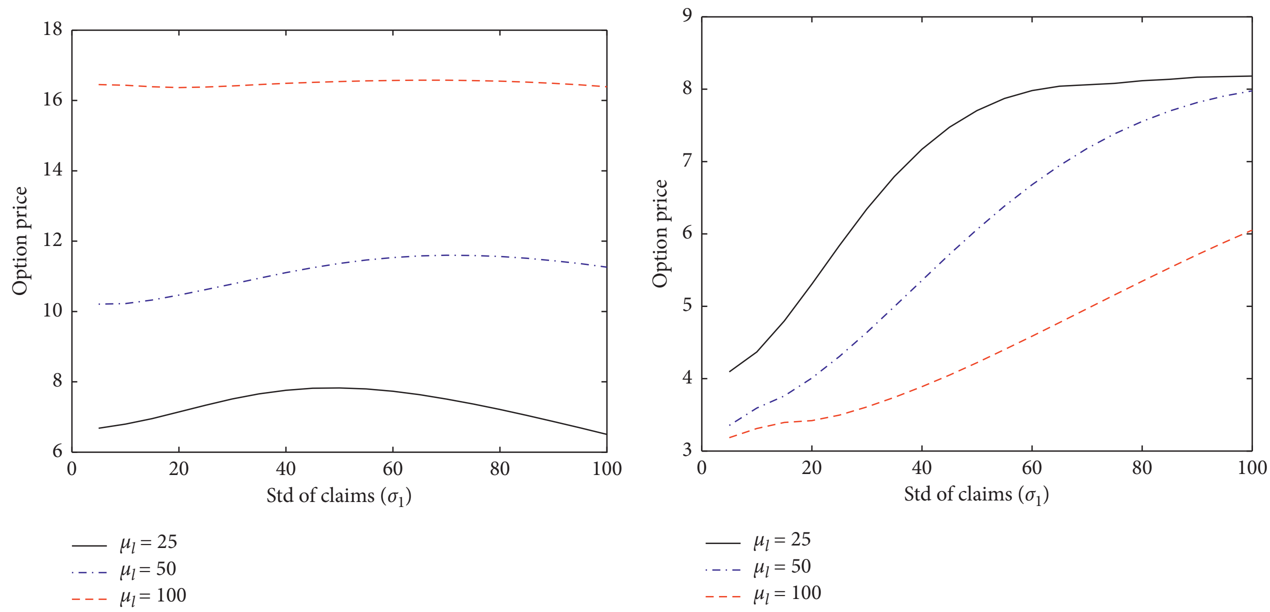

(a) (b)

Figure 3: The effect of σ_l on option price with different μ_l. (a) $c = 1$. (b) $c = 2$.

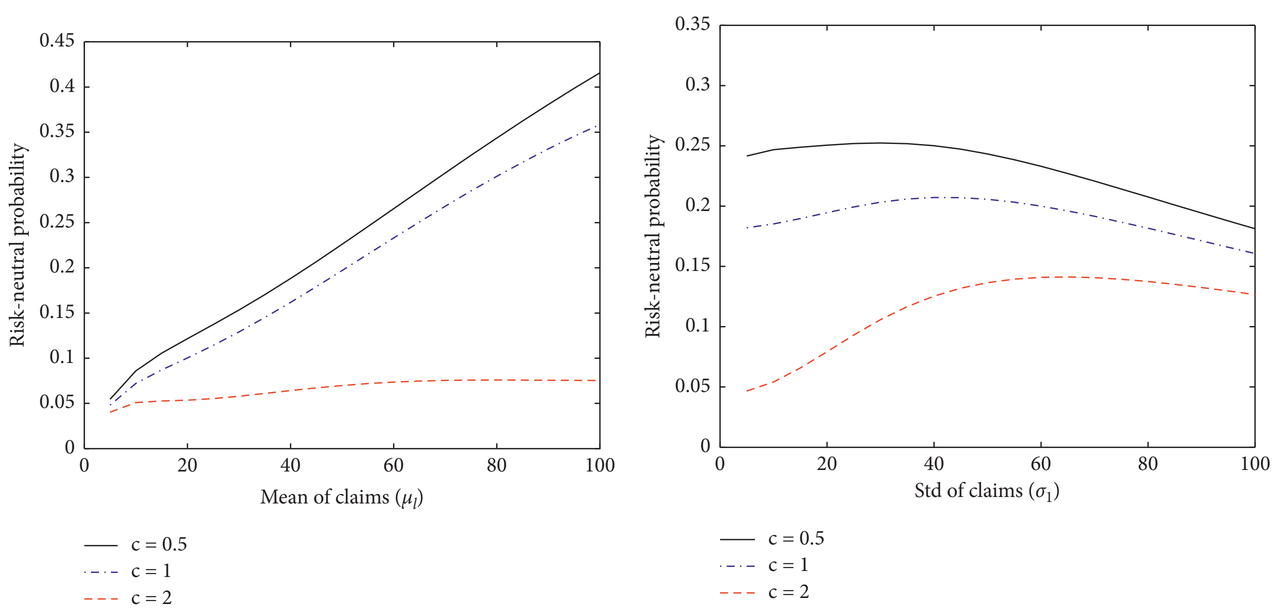

(a) (b)

Figure 4: The effects of μ_l and σ_l on risk-neutral probability of ending in-the-money for several trigger ratio levels of c. (a) Mean of claims μ_l. (b) Std of claims σ_l.

Table 3: Values of delta, gamma, and rho under JW and mfBM models.

S_0	JW model			mfBM model		
	60	80	100	60	80	100
$c = 1$						
$\Delta_S(t, t_0)$	−0.12908	−0.07965	−0.05676	−0.10417	−0.07585	−0.04934
$\Gamma_S(t, t_0)$	0.00303	0.00194	0.00116	0.00173	0.00115	0.00078
$\rho(t, t_0)$	−72.3660	−54.2121	−39.8832	−80.4577	−70.0462	−61.0020
$c = 2$						
$\Delta_S(t, t_0)$	−0.03472	−0.02853	−0.02229	−0.02596	−0.02119	−0.01741
$\Gamma_S(t, t_0)$	0.00032	0.00029	0.00028	0.00027	0.00021	0.00017
$\rho(t, t_0)$	−26.1142	−23.8098	−20.8363	−26.1645	−24.4051	−22.6102

$$\begin{aligned}
\Delta_S(t, t_0) &= \frac{\partial P_{\text{cat}}(t, t_0)}{\partial S_t} = -\sum_{n=1}^{\infty} \frac{[\lambda(T-t)]^n e^{\lambda(\kappa-1)(T-t)}}{n!} \\
&\quad \cdot \int_{\widetilde{L}}^{+\infty} e^{-\mu y} \Phi\left(-\widetilde{d}_1(y)\right) f_Y^{(n)}(y) \mathrm{d}y, \\
\Gamma_S(t, t_0) &= \frac{\partial^2 P_{\text{cat}}(t, t_0)}{\partial S_t^2} = \sum_{n=1}^{\infty} \frac{[\lambda(T-t)]^n e^{\lambda(\kappa-1)(T-t)}}{n!} \\
&\quad \cdot \frac{1}{\sqrt{2\pi} S_t \theta(t, T)} \int_{\widetilde{L}}^{+\infty} e^{-\mu y - \widetilde{d}_1^2(y)/2} f_Y^{(n)}(y) \mathrm{d}y, \\
\rho(t, t_0) &= \frac{\partial P_{\text{cat}}(t, t_0)}{\partial r_t} = \frac{\partial P_{\text{cat}}(t, t_0)}{\partial P(t, T)} \cdot \frac{\partial P(t, T)}{\partial r_t} \\
&= -KB(t, T) P(t, T) \cdot \sum_{n=1}^{\infty} \frac{[\lambda(T-t)]^n e^{\lambda(\kappa-1)(T-t)}}{n!} \\
&\quad \int_{\widetilde{L}}^{+\infty} \Phi\left(-\widetilde{d}_2(y)\right) f_Y^{(n)}(y) \mathrm{d}y.
\end{aligned} \tag{31}$$

Table 3 reports the values of delta, gamma, and rho for the in-the-money, at-the-money, and out-of-the-money CatEPut option under JW and mfBM models with two different trigger ratio levels of $c = 1$ and $c = 2$. First, the values of delta and gamma under the JW model are greater than those of the mfBM model. However, the values of rho under the JW model are smaller than those of the mfBM model. These findings are consistent with the results in Figure 1 since higher option's price leads to lower the values of delta and gamma and higher the values of rho.

Second, the values of delta, gamma, and rho for the CatEPut option decrease from in-the-money to out-of-the-money. Finally, the values of delta, gamma, and rho for the CatEPut option are sensitive to the trigger ratio level c and are decreasing with the trigger ratio level c.

6. Conclusion

This paper extends the analysis of Jaimungal and Wang [2] to make it more realistic by introducing the mfBM model, which includes the fBM model and the BM model in the literature as its special cases, to represent the underlying asset price and interest rate changes. A closed-form analytical expression for the price of the CatEPut option is then derived in the case of deterministic and stochastic interest rates based on the fractional Girsanov formula. Finally, through numerical experiments, the quantitative impacts of different parameters on the option price and hedging parameters of the CatEPut option are discussed.

Some possible extensions should be considered in future research. Firstly, the proposed model can be tested empirically by using the catastrophic data from PCS (Property Claim Service). For example, we can estimate the parameters of catastrophe arrival rate λ and the Hurst index H using the maximum likelihood estimation method. Secondly, the proposed model can also be extended by taking the counterparty risk into account and evaluating other catastrophe-linked financial options.

Appendix

A. The Proof of Proposition 1

Using the risk-neutral pricing theory and the law of iterated conditional expectation, we have

$$\begin{aligned}
P_{\text{cat}}(t, t_0) &= E\left\{ 1_{\left(L_T - L_{t_0} > L\right)} E\left[e^{-\int_t^T r_u \mathrm{d}u} (K - S_T)^+ \,\middle|\, L_T - L_t = \sum_{i=1}^{N_{T-t}} Y_i \right] \middle| \mathscr{F}_t \right\} \\
&= I_1 - I_2,
\end{aligned} \tag{A.1}$$

where

$$\begin{aligned} I_1 &= Ke^{-\int_t^T r_u \mathrm{d}u} E\left\{ 1_{\left(L_T - L_t > L + L_{t_0} - L_t\right)} E\left[1_{(S_T \le K)} \,\middle|\, L_T - L_t = \sum_{i=1}^{N_{T-t}} Y_i \right] \middle| \mathscr{F}_t \right\} \\ &= Ke^{-\int_t^T r_u \mathrm{d}u} E\left\{ 1_{\left(\sum_{i=1}^{N_{T-t}} Y_i > L + L_{t_0} - L_t\right)} Q\left(S_T \le K \,\middle|\, \sum_{i=1}^{N_{T-t}} Y_i \right) \middle| \mathscr{F}_t \right\}, \end{aligned} \tag{A.2}$$

$$\begin{aligned} I_2 &= E\left\{ 1_{\left(L_T - L_t > L + L_{t_0} - L_t\right)} E\left[S_T e^{-\int_t^T r_u \mathrm{d}u} 1_{(S_T \le K)} \,\middle|\, L_T - L_t = \sum_{i=1}^{N_{T-t}} Y_i \right] \middle| \mathscr{F}_t \right\}, \\ &= E\left\{ 1_{\left(\sum_{i=1}^{N_{T-t}} Y_i > L + L_{t_0} - L_t\right)} E\left[S_T e^{-\int_t^T r_u \mathrm{d}u} 1_{(S_T \le K)} \,\middle|\, \sum_{i=1}^{N_{T-t}} Y_i \right] \middle| \mathscr{F}_t \right\}. \end{aligned} \tag{A.3}$$

From (2), thus, formula I_1 in (A.2) can be rewritten as

$$\begin{aligned} I_1 &= Ke^{-\int_t^T r_u \mathrm{d}u} \sum_{n=1}^{\infty} \frac{[\lambda (T-t)]^n e^{-\lambda (T-t)}}{n!} E\left\{ 1_{\left(\sum_{i=1}^{n} Y_i > L + L_{t_0} - L_t\right)} \cdot Q\left(\ln S_T \le \ln K \,\middle|\, \sum_{i=1}^{n} Y_i \right) \middle| \mathscr{F}_t \right\} \\ &= Ke^{-\int_t^T r_u \mathrm{d}u} \sum_{n=1}^{\infty} \frac{[\lambda (T-t)]^n e^{-\lambda (T-t)}}{n!} E\Bigg\{ 1_{\left(\sum_{i=1}^{n} Y_i > L + L_{t_0} - L_t\right)} \cdot Q\Big(\sigma_s \left(M_T^H - M_t^H \right) \\ &\quad \le -\left[\ln \frac{S_t}{K} - \mu \sum_{i=1}^{n} Y_i + \lambda \kappa (T-t) + \int_t^T r_u \mathrm{d}u - \frac{1}{2}\sigma_s^2 \left[\alpha^2 (T-t) + \beta^2 \left(T^{2H} - t^{2H} \right) \right] \right] \Big| \sum_{i=1}^{n} Y_i \Big) \Bigg| \mathscr{F}_t \Bigg\} \\ &= \sum_{n=1}^{\infty} \frac{[\lambda (T-t)]^n e^{-\lambda (T-t)}}{n!} \int_{\widetilde{L}}^{+\infty} Ke^{-\int_t^T r_u \mathrm{d}u} \Phi(-d_2(y)) f_Y^{(n)}(y) \mathrm{d}y. \end{aligned} \tag{A.4}$$

Similarly, we rewrite (A.3) as

$$\begin{aligned} I_2 &= S_t E\left\{ 1_{\left(\sum_{i=1}^{N_{T-t}} Y_i > L + L_{t_0} - L_t\right)} E\left[\frac{S_T e^{-\int_t^T r_u \mathrm{d}u}}{S_t} 1_{(S_T \le K)} \,\middle|\, \sum_{i=1}^{N_{T-t}} Y_i \right] \middle| \mathscr{F}_t \right\} \\ &= S_t \widetilde{E}\left\{ 1_{\left(\sum_{i=1}^{N_{T-t}} Y_i > L + L_{t_0} - L_t\right)} \widetilde{Q}\left(\ln S_T \le \ln K \,\middle|\, \sum_{i=1}^{N_{T-t}} Y_i \right) \middle| \mathscr{F}_t \right\}, \end{aligned} \tag{A.5}$$

where $\widetilde{E}[\mathscr{F}_t]$ denotes the quasi-conditional expectation with respect to the probability measure $\widetilde{Q}$ which is equivalent to Q, and the Radon–Nikodym derivative which induced the measure change from Q to $\widetilde{Q}$ is given by the formula

$$\left.\frac{\mathrm{d}\widetilde{Q}}{\mathrm{d}Q}\right|_{\mathscr{F}_T} = \frac{S_T e^{-\int_0^T r_u \mathrm{d}u}}{S_0} = \exp\left\{ -\frac{1}{2}\left[\alpha^2 T + \beta^2 T^{2H} \right] + \sigma_s M_T^H \right\}. \tag{A.6}$$

Let $\widetilde{M}_t^H = \alpha \widetilde{W}_t + \beta \widetilde{W}_t^H = M_t^H - \sigma_s (\alpha^2 t + \beta^2 t^{2H})$; using the fractional Girsanov theorem (see Hu and Oksendal [45]), then $\widetilde{M}_t^H$ is also a mfBM with parameters α, β, and H under the new probability measure $\widetilde{Q}$. Hence, we can rewrite (2) as

$$\begin{aligned} \ln S_T = \ln S_t &+ \left\{ \int_t^T r_u \mathrm{d}u - \mu \left(L_T - L_t \right) + \lambda \kappa (T-t) \right. \\ &\left. + \frac{1}{2}\sigma_s^2 \left[\alpha^2 (T-t) + \beta^2 \left(T^{2H} - t^{2H} \right) \right] + \sigma_s \left(\widetilde{M}_T^H - \widetilde{M}_t^H \right) \right\}. \end{aligned} \tag{A.7}$$

under $\widetilde{Q}$ and obtain that

$$\begin{aligned} I_2 &= S_t \sum_{n=1}^{\infty} \frac{[\lambda(T-t)]^n e^{-\lambda(T-t)}}{n!} E\Big\{ 1_{\left(\sum_{i=1}^n Y_i > L + L_{t_0} - L_t\right)} e^{-\mu \sum_{i=1}^n Y_i + \lambda\kappa(T-t)} \cdot \widetilde{Q}\Big(\sigma_s \big(M_T^H - M_t^H \big) \\ &\le - \Big[\ln \frac{S_t}{K} - \mu \sum_{i=1}^n Y_i + \lambda\kappa(T-t) + \int_t^T r_u \mathrm{d}u \frac{1}{2}\sigma_s^2 \big[\alpha^2 (T-t) + \beta^2 \big(T^{2H} - t^{2H} \big) \big] \Big] \Big| \sum_{i=1}^n Y_i \Big) \Big| \mathscr{F}_t \Big\} \\ &= \sum_{n=1}^{\infty} \frac{[\lambda(T-t)]^n e^{-\lambda(T-t)}}{n!} \int_{\widetilde{L}}^{+\infty} S_t e^{-\mu y + \lambda\kappa(T-t)} \Phi(-d_1(y)) f_Y^{(n)}(y) \mathrm{d}y. \end{aligned} \tag{A.8}$$

From (A.4) and (A.8), the proof is completed.

B. The Proof of Proposition 2

From (16), we write $P_{\mathrm{cat}}(t, t_0)$ as a sum of two terms $\widehat{I}_1$ and $\widehat{I}_2$:

$$\begin{aligned} \widehat{I}_1 &= KP(t,T) E^T \left[1_{\left(L_T - L_t > L + L_{t_0} - L_t\right)} 1_{(\ln S_T \le \ln K)} \Big| \mathscr{F}_t \right], \\ \widehat{I}_2 &= P(t,T) E^T \left[1_{\left(L_T - L_t > L + L_{t_0} - L_t\right)} S_T 1_{(\ln S_T \le \ln K)} \Big| \mathscr{F}_t \right]. \end{aligned} \tag{B.1}$$

We denote $\gamma = -[\ln(S_t/KP(t,T)) - \mu \sum_{i=1}^n Y_i + \lambda\kappa(T-t) - (1/2)\theta^2(t,T)]$ and firstly calculate the term $\widehat{I}_1$. By using (14), we have

$$\begin{aligned} \widehat{I}_1 &= KP(t,T) E^T \left[1_{\left(L_T - L_t > L + L_{t_0} - L_t\right)} 1_{(\ln S_T \le \ln K)} \Big| \mathscr{F}_t \right] \\ &= KP(t,T) E^T \left[1_{\left(L_T - L_t > L + L_{t_0} - L_t\right)} E^T \left\{ 1_{(\ln S_T \le \ln K)} \big| L_T - L_t \right\} \Big| \mathscr{F}_t \right] \\ &= KP(t,T) \sum_{n=1}^{\infty} \frac{[\lambda(T-t)]^n e^{-\lambda(T-t)}}{n!} E\left\{ 1_{\left(\sum_{i=1}^n Y_i > L + L_{t_0} - L_t\right)} \cdot Q^T \left(\ln S_T \le \ln K \,\Big|\, \sum_{i=1}^n Y_i \right) \Big| \mathscr{F}_t \right\} \\ &= KP(t,T) \sum_{n=1}^{\infty} \frac{[\lambda(T-t)]^n e^{-\lambda(T-t)}}{n!} E\left\{ 1_{\sum_{i=1}^n Y_i > L + L_{t_0} - L_t} \cdot Q^T \left(\int_t^T \sigma_s \mathrm{d}\widehat{M}_t^H + \int_t^T \sigma_r B(u,T) \mathrm{d}\widehat{Z}_t^H \le \gamma \,\Big|\, \sum_{i=1}^n Y_i \right) \Big| \mathscr{F}_t \right\} \\ &= \sum_{n=1}^{\infty} \frac{[\lambda(T-t)]^n e^{-\lambda(T-t)}}{n!} \int_{\widetilde{L}}^{+\infty} KP(t,T) \Phi\big(-\widehat{d}_2(y)\big) f_Y^{(n)}(y) \mathrm{d}y. \end{aligned} \tag{B.2}$$

Similarly, we have

$$\begin{aligned} \widehat{I}_2 &= P(t,T) E^T \left[1_{\left(L_T - L_t > L + L_{t_0} - L_t\right)} S_T 1_{(\ln S_T \le \ln K)} \Big| \mathscr{F}_t \right] \\ &= P(t,T) E^T \left[1_{\left(L_T - L_t > L + L_{t_0} - L_t\right)} E^T \left\{ e^{\ln S_T} 1_{(\ln S_T \le \ln K)} \big| L_T - L_t \right\} \Big| \mathscr{F}_t \right] \\ &= S_t \sum_{n=1}^{\infty} \frac{[\lambda(T-t)]^n e^{-\lambda(T-t)}}{n!} E^T \Big\{ 1_{\left(\sum_{i=1}^n Y_i > L + L_{t_0} - L_t\right)} e^{-\mu \sum_{i=1}^n Y_i + \lambda\kappa(T-t) - (1/2)\theta^2(t,T)} \cdot E^T \\ &\quad \cdot \left[e^{\int_t^T \sigma_s \mathrm{d}\widehat{M}_t^H + \int_t^T \sigma_r B(u,T) \mathrm{d}\widehat{Z}_t^H} 1_{\left(\int_t^T \sigma_s \mathrm{d}\widehat{M}_t^H + \int_t^T \sigma_r B(u,T) \mathrm{d}\widehat{Z}_t^H \le \gamma\right)} \,\Big|\, \sum_{i=1}^n Y_i \right] \Big| \mathscr{F}_t \Big\}. \end{aligned} \tag{B.3}$$

Using the fact that $E[e^X 1_{(X<\gamma)}] = e^{\delta^2/2}\Phi((\gamma+\delta)/\delta)$ when $X \sim N(0,\delta^2)$, then

$$\begin{aligned}\widehat{I}_2 &= S_t \sum_{n=1}^{\infty} \frac{[\lambda(T-t)]^n e^{-\lambda(T-t)}}{n!} E^T\left\{ 1_{\left(\sum_{i=1}^n Y_i > L+L_{t_0}-L_t\right)} \cdot e^{-\mu\sum_{i=1}^n Y_i + \lambda\kappa(T-t)} \Phi\left(\frac{\gamma+\theta(t,T)}{\theta(t,T)}\right) \middle| \mathscr{F}_t \right\} \\ &= \sum_{n=1}^{\infty} \frac{[\lambda(T-t)]^n e^{-\lambda(T-t)}}{n!} \int_{\widetilde{L}}^{+\infty} S_t e^{-\mu y + \lambda\kappa(T-t)} \Phi\left(-\widehat{d}_2(y)\right) f_Y^{(n)}(y)\mathrm{d}y.\end{aligned} \tag{B.4}$$

Hence, (B.2) and (B.4) yield (17).

Data Availability

All data used to support the findings of this study are included within this article.

Conflicts of Interest

The author declares that there are no conflicts of interest regarding the publication of this paper.

Acknowledgments

This research was supported by the NSF of China (grant no. 11461008) and the Guangxi Natural Science Foundation (grant no. 2018GXNSFAA281016).

References

[1] S. H. Cox, J. R. Fairchild, and H. W. Pedersen, "Valuation of structured risk management products," *Insurance: Mathematics and Economics*, vol. 34, no. 2, pp. 259–272, 2004.

[2] S. Jaimungal and T. Wang, "Catastrophe options with stochastic interest rates and compound Poisson losses," *Insurance: Mathematics and Economics*, vol. 38, no. 3, pp. 469–483, 2006.

[3] O. Vasicek, "An equilibrium characterization of the term structure," *Journal of Financial Economics*, vol. 5, no. 2, pp. 177–188, 1977.

[4] L.-F. Chang and M.-W. Hung, "Analytical valuation of catastrophe equity options with negative exponential jumps," *Insurance: Mathematics and Economics*, vol. 44, no. 1, pp. 59–69, 2009.

[5] S.-K. Lin, C.-C. Chang, and M. R. Powers, "The valuation of contingent capital with catastrophe risks," *Insurance: Mathematics and Economics*, vol. 45, no. 1, pp. 65–73, 2009.

[6] X. S. Lin and T. Wang, "Pricing perpetual American catastrophe put options: a penalty function approach," *Insurance: Mathematics and Economics*, vol. 44, no. 2, pp. 287–295, 2009.

[7] I.-M. Jiang, S.-Y. Yang, Y.-H. Liu, and A. T. Wang, "Valuation of double trigger catastrophe options with counterparty risk," *The North American Journal of Economics and Finance*, vol. 25, pp. 226–242, 2013.

[8] Y. Jin and S. Zhong, "New explicit closed form formulae for the prices of catastrophe options," *International Journal of Financial Engineering*, vol. 2, pp. 1–16, 2015.

[9] E. Koo and G. Kim, "Explicit formula for the valuation of catastrophe put option with exponential jump and default risk," *Chaos, Solitons & Fractals*, vol. 101, pp. 1–7, 2017.

[10] Y. Xu and G. Wang, "Pricing catastrophe options with counterparty credit risk in a reduced form model," *Acta Mathematica Scientia*, vol. 38, no. 1, pp. 347–360, 2018.

[11] H.-S. Kim, B. Kim, and J. Kim, "Catastrophe equity put options under stochastic volatility and catastrophe-dependent jumps," *Journal of Industrial & Management Optimization*, vol. 10, no. 1, pp. 41–55, 2014.

[12] S. L. Heston, "A closed-form solution for options with stochastic volatility with applications to bond and currency options," *Review of Financial Studies*, vol. 6, no. 2, pp. 327–343, 1993.

[13] X. Wang, "Catastrophe equity put options with target variance," *Insurance: Mathematics and Economics*, vol. 71, pp. 79–86, 2016.

[14] W. Wang, L. Qian, and X. Su, "Pricing and hedging catastrophe equity put options under a Markov-modulated jump diffusion model," *Journal of Industrial & Management Optimization*, vol. 11, no. 2, pp. 493–514, 2015.

[15] H.-S. Kim, B. Kim, and J. Kim, "Pricing perpetual American CatEPut options when stock prices are correlated with catastrophe losses," *Economic Modelling*, vol. 41, pp. 15–22, 2014b.

[16] J. Yu, "Catastrophe options with double compound Poisson processes," *Economic Modelling*, vol. 50, pp. 291–297, 2015.

[17] W. Yu, P. Guo, Q. Wang et al., "On a periodic capital injection and barrier dividend strategy in the compound Poisson risk model," *Mathematics*, vol. 8, no. 4, pp. 511–531, 2020.

[18] W. Yu, Y. Yong, G. Guan, Y. Huang, W. Su, and C. Cui, "Valuing guaranteed minimum death benefits by cosine series expansion," *Mathematics*, vol. 7, no. 9, pp. 835–849, 2019.

[19] W. Yu, F. Wang, Y. Huang, and H. Liu, "Social optimal mean field control problem for population growth model," *Asian Journal of Control*, vol. 21, no. 4, pp. 1–8, 2019.

[20] Z. Zhang, Y. Yong, and W. Yu, "Valuing equity-linked death benefits in general exponential Lévy models," *Journal of Computational and Applied Mathematics*, vol. 365, Article ID 112377, 2020.

[21] A. W. Lo, "Long-term memory in stock market prices," *Econometrica*, vol. 59, no. 5, pp. 1279–1313, 1991.

[22] W. Willinger, M. S. Taqqu, and V. Teverovsky, "Stock market prices and long-range dependence," *Finance and Stochastics*, vol. 3, no. 1, pp. 1–13, 1999.

[23] R. Cont, "Empirical properties of asset returns: stylized facts and statistical issues," *Quantitative Finance*, vol. 1, no. 2, pp. 223–236, 2001.

[24] S. H. Kang and S.-M. Yoon, "Long memory features in the high frequency data of the Korean stock market," *Physica A:*

Statistical Mechanics and Its Applications, vol. 387, no. 21, pp. 5189–5196, 2008.

[25] S. H. Kang, C. Cheong, and S.-M. Yoon, “Long memory volatility in Chinese stock markets,” *Physica A: Statistical Mechanics and Its Applications*, vol. 389, no. 7, pp. 1425–1433, 2010.

[26] T.-C. Huang, Y.-C. Tu, and H.-C. Chou, “Long memory and the relation between options and stock prices,” *Finance Research Letters*, vol. 12, pp. 77–91, 2015.

[27] Y. A. Kuznetsov, “The absence of arbitrage in a model with fractal Brownian motion,” *Russian Mathematical Surveys*, vol. 54, no. 4, pp. 847-848, 1999.

[28] T. Bjork and H. Hult, “A note on wick products and the fractional Black-Scholes model,” *Finance and Stochastics*, vol. 9, no. 2, pp. 197–209, 2005.

[29] P. Cheridito, “Mixed fractional Brownian motion,” *Bernoulli*, vol. 7, no. 6, pp. 913–934, 2001.

[30] P. Cheridito, “Arbitrage in fractional Brownian motion models,” *Finance and Stochastics*, vol. 7, no. 4, pp. 533–553, 2003.

[31] G. Deng and H. Xi, “Pricing reset option in a fractional Brownian motion market,” in *Proceedings of the 30th Chinese Control Conference*, pp. 5727–5731, Yantai, China, July 2011.

[32] B. L. S. Prakasa Rao, “Pricing geometric Asian power options under mixed fractional Brownian motion environment,” *Physica A: Statistical Mechanics and Its Applications*, vol. 446, pp. 92–99, 2016.

[33] L. Sun, “Pricing currency options in the mixed fractional Brownian motion,” *Physica A: Statistical Mechanics and Its Applications*, vol. 392, no. 16, pp. 3441–3458, 2013.

[34] W.-L. Xiao, W.-G. Zhang, X. Zhang, and X. Zhang, “Pricing model for equity warrants in a mixed fractional Brownian environment and its algorithm,” *Physica A: Statistical Mechanics and Its Applications*, vol. 391, no. 24, pp. 6418–6431, 2012.

[35] W. Xiao, W. Zhang, X. Zhang, and X. Chen, “The valuation of equity warrants under the fractional Vasicek process of the short-term interest rate,” *Physica A: Statistical Mechanics and Its Applications*, vol. 394, pp. 320–337, 2014.

[36] W.-G. Zhang, Z. Li, and Y.-J. Liu, “Analytical pricing of geometric Asian power options on an underlying driven by a mixed fractional Brownian motion,” *Physica A: Statistical Mechanics and Its Applications*, vol. 490, pp. 402–418, 2018.

[37] X. He and W. Chen, “The pricing of credit default swaps under a generalized mixed fractional Brownian motion,” *Physica A: Statistical Mechanics and Its Applications*, vol. 404, pp. 26–33, 2014.

[38] F. Mehrdoust, A. R. Najafi, S. Fallah, and O. Samimi, “Mixed fractional Heston model and the pricing of American options,” *Journal of Computational and Applied Mathematics*, vol. 330, pp. 141–154, 2018.

[39] J. McCarthy, R. DiSario, H. Saraoglu, and H. Li, “Tests of long-range dependence in interest rates using wavelets,” *The Quarterly Review of Economics and Finance*, vol. 44, pp. 180–189, 2004.

[40] L. A. Gil-Alana, “Long memory in the interest rates in some Asian countries,” *International Advances in Economic Research*, vol. 9, no. 4, pp. 257–267, 2003.

[41] B. M. Tabak and D. O. Cajueiro, “The long-range dependence behavior of the term structure of interest rates in Japan,” *Physica A: Statistical Mechanics and Its Applications*, vol. 350, no. 2–4, pp. 418–426, 2005.

[42] D. O. Cajueiro and B. M. Tabak, “Long-range dependence and multifractality in the term structure of LIBOR interest rates,” *Physica A: Statistical Mechanics and Its Applications*, vol. 373, pp. 603–614, 2007.

[43] D. O. Cajueiro and B. M. Tabak, “Testing for long-range dependence in the Brazilian term structure of interest rates,” *Chaos, Solitons & Fractals*, vol. 40, no. 4, pp. 1559–1573, 2009.

[44] Q. Zhou, Q. Wang, and W. Wu, “Pricing of defaultable securities associated with recovery rate under the stochastic interest rate driven by fractional Brownian motion,” *Journal of Systems Science and Complexity*, vol. 32, no. 2, pp. 657–680, 2019.

[45] Y. Hu and B. Øksendal, “Fractional white noise calculus and applications to finance,” *Infinite Dimensional Analysis, Quantum Probability and Related Topics*, vol. 6, no. 1, pp. 1–32, 2003.

Hindawi
Mathematical Problems in Engineering
Volume 2020, Article ID 8175723, 11 pages
https://doi.org/10.1155/2020/8175723

Research Article

The Limit Theorems for Function of Markov Chains in the Environment of Single Infinite Markovian Systems

Zhanfeng Li,[1] Min Huang,[1,2] Xiaohua Meng,[3] and Xiangyu Ge [1]

[1]*School of Statistics and Mathematics, Zhongnan University of Economics and Law, Wuhan 430073, China*
[2]*Faculty of Information and Engineering, Wuhan College, Wuhan 430212, China*
[3]*Institute of Information Management and Statistics, Hubei University of Economics, Wuhan 430205, China*

Correspondence should be addressed to Xiangyu Ge; xiangyu_ge@163.com

Received 6 March 2020; Accepted 15 April 2020; Published 5 May 2020

Guest Editor: Wenguang Yu

This paper is intended to study the limit theorem of Markov chain function in the environment of single infinite Markovian systems. Moreover, the problem of the strong law of large numbers in the infinite environment is presented by means of constructing martingale differential sequence for the measurement under some different sufficient conditions. If the sequence of even functions $\{g_n(x), n \geq 0\}$ satisfies different conditions when the value ranges of x are different, we have obtained SLLN for function of Markov chain in the environment of single infinite Markovian systems. In addition, the paper studies the strong convergence of the weighted sums of function for finite state Markov Chains in single infinitely Markovian environments. Although the similar conclusions have been carried out, the difference results performed by previous scholars are that we give weaker different sufficient conditions of the strong convergence of weighted sums compared with the previous conclusions.

1. Introduction

The definition and properties of limit theorems have been studied for some time, especially for functions of Markov chain, which becomes one of the most popular research areas in the field of stochastic processes. In a random process model, the theory of Markov chain describes the change from one system state to another system state, and also the advent of quantitative analysis is explored according to the real system situations. In effect, the theory of Markov chain is not only widely used in scientific research but also used in the economic field. Recently, emphasis is placed on the application to explain many systemic problems of economic phenomena, and the interpretation of most economic phenomena can be realized under the framework of Markov chain.

Over the course of the past 40 years, a comprehensive study of the Markov chains has been undertaken. In the early 1980s, Cogburn [1] introduced the definition of Markov chain in the environment of random systems and discussed the state classification of Markov chain in the environment of Markovian systems. A relevant paper was published by Nawrotzki [2, 3], which discussed the state of classification about the Markov chain with feedback, based on other systems, namely, the single infinitely stable Markovian systems, and established the general theory of the topic. Subsequently, a further study on Markov chains under the condition of random environment has been reported by Cogburn [4] who have made a great contribution in this area. In random environments, Cogburn proposed a generic theory about the function of Markov chains and developed a lot of profound results with the theory of Hopf-Markov chain and some further studies of limit theories for function of Markov chain have been conducted. For instance, Cogburn [5, 6] discussed the convergence of the transfer probability, periodicity, and conditions for the establishment of the central limit theorem under the special circumstances, which are in the environment of the bi-infinite stable, as well as listing the connection with these theories. Orey [7] has studied the Markov chain in stochastic environment in depth based on Cogburn's study and put forward a series of problems, which attracted the attention of many probability scholars. Liu and Liu [8, 9] have investigated a series of limit properties of the random variables sequences with Lebesgue's theorem and then gave limit properties with the similar method for nonhomogeneous Markov chain.

The general theory about the function of Markov chain in the environment of random systems has become a popular research direction. As known, the limit theorem has been a hot topic in the study of classical Markov chain theory. Subsequently, a lot of scholars have conducted in-depth research in this field and achieved a series of profound and rich results. Various research theories about the function of Markov chain in Markovian environments have been proposed, called MCME for short (see [10–15]), and the same as theories about the function of Markov chain in random environments, which are called MCRE for short (see [16–18]). Exactly, the random environments can be catalogued into different situations, such as in space-time random environments (see [19]), in bi-infinite random environments (see [20]), and in single infinite random environments (see [21]).

Currently, a lot of research literatures on the strong limit theory for function of Markov chains in the environment of random systems or in the environment of Markovian systems have been found. The strong law of large numbers about the function of Markov chains in the environment of Markovian systems with discrete parameter was proposed by Wan [22] who obtained the sufficient conditions. Besides, Guo [16] also put forward the sufficient conditions, which are different from Wan [22], and the difference is mainly to prove this theorem in the case of the random environments. On the basis of existing research, Li [23] indicated the sufficient conditions established in the case of countable states for this theorem. Furthermore, for complete and imprecise knowledge of Markov chains, Li et al. [14] have developed a strong limit theorem of the Markov chain quaternion function in the environment of Markovian systems and extended the Shannon theorem in this environment. It becomes apparent that Markovian environments can be classified into different catalogues, such as in bi-infinite environments (see [24, 25]) and in single infinite environments (see [26]).

To the best of our knowledge, along with the increasing development of Markov chains in decision-making state of financial market, they have been widely used in financial insurance theory. Recently, statistical estimation of ruin related functions has become a popular topic in risk theory. However, some of the scholars proposed different estimators for the ruin probability in the classical risk. For example, a study by Yang and Yuen [27] offered a comprehensive analysis of two-dimensional delayed renewal risk model with a constant interest. They derived some asymptotic formulas for the finite-time and infinite-time ruin probabilities in the presence of heavy-tailed claim sizes. In addition, Yang et al. [28] constructed by the two-dimensional Fourier cosine series expansion to estimate the discounted density of the deficit at ruin. Similarly, with method of the Fourier cosine series expansion, one study by Yu et al. [29] valued the guaranteed minimum death benefit products. On valuation of the products with guaranteed minimum death benefit, Zhang et al. [30] applied a projection method combined with Fast Fourier Transform. Recently, a qualitative study by Yang et al. [31] described a discrete-time insurance risk model with insurance and financial risks. Then, a key study is that of Yu et al. [32], which proposed a new risk model called compound Poisson risk model by introducing a periodic capital injection strategy and a barrier dividend strategy into the classical risk model. Furthermore, the risk model can be further extended and applied to a wider range of practical problems. An example can be made by the optimal control problem (see [33]). Above all, most of existing studies failed to deal with the practical problems; it is necessary for us to study the limit theorems for function of Markov chains deeply.

Therefore, this paper set out to advance the research on the limit theory of a class of Markov chain functions, aiming to provide clarity understanding of the limit theorem for function of Markov chain in environment of single infinite Markovian systems. Based on the results of Li [17] and Wan [18], we have found two lemmas and derive the results of almost sure convergence with the finding of the lemmas. The results of the analysis of the strong law of large numbers in single infinite environment are presented to be an extension of the conclusion in the inference [34] on different sufficient conditions. Also, in single infinite Markovian environments, we come to the conclusions about the strong convergence and present the weighted sums for function of Markov chains. Driven by LLN (law of large numbers), the strong convergence of the weighted sum is also discussed when considering the compatibility of the least squares estimates of linear models. Although we prove similar conclusions, the difference from results obtained by previous scholars can be made based on weaker different sufficient conditions of the strong convergence of weighted sums provided [26].

The subsequent structure of our paper is as follows. A description of some basic notations, fundamental definitions, and lemmas is shown briefly in Section 2. Details under the condition of the environment of single infinite Markovian systems are discussed in Section 3 and Section 4. Section 3 is about SLLN (strong law of large numbers) for function of Markov chain in the environment of the setting of this paper. Section 4 derives the strong convergence of weighted sum for function of Markov chain in the environment of the setting of this paper. A series of sufficient conditions for the limit theorem are obtained in Sections 3 and 4, and specific proof process of theorem and corollary is considered, respectively. This paper concludes with a discussion in Section 5.

2. Fundamental Preliminaries

At first, we begin to introduce some basic notations which shall be used in the following sections. Let N represent an integer set and $(\Omega, \mathscr{F}, P)$ represent a probability space; both $(X, \mathscr{A})$ and $(\Theta, \mathscr{B})$are arbitrary measurable spaces. Respectively, let $\overrightarrow{\xi}_0^{\infty} = \{\xi_n\colon n \geq 0\}$ and $\overrightarrow{X} = \{X_n\colon n \geq 0\}$ be two random sequences defined on $(\Omega, \mathscr{F}, P)$ with value on set of Θ and X. Assume a family of transition function $\{P(\theta)\colon \theta \in \Theta\}$ defined on arbitrary measurable spaces of $(X, \mathscr{A})$. For any $A \in \mathscr{A}$, we suppose $P(\cdot;\cdot, A)$ is measurable regarding $\mathscr{B} \times \mathscr{A}$. Given a family of one-step transition probability function $\{K_n(\cdot,\cdot)\}$ defined on arbitrary measurable spaces of $(\Theta, \mathscr{B})$, where we assume that $K_n(\cdot, B)$ is measurable about $\mathscr{B}$ for any $B \in \mathscr{B}$. For arbitrary sequence of $\overrightarrow{\eta} = \{\eta_n\colon n \geq 0\}$, we denote $\overrightarrow{\eta}_k^r = \{\eta_n\colon 0 \leq n \leq r \leq \infty\}$.

If, for any of $A \in \mathscr{A}$ and $n \geq 0$, at the same time we have

$$P\left(X_0 \in A \,\middle|\, \overrightarrow{\xi}_0^{\infty}\right) = P\left(X_0 \in A \mid \xi_0\right),$$
$$P\left(X_{n+1} \in A \,\middle|\, \overrightarrow{X}_0^{n}, \overrightarrow{\xi}_0^{\infty}\right) = P\left(\xi_n; X_n, A\right), \tag{1}$$

then random variable sequence of $\overrightarrow{X}$ is called the Markov chain in the random system of $\overrightarrow{\xi}_0^{\infty}$; here $\overrightarrow{\xi}_0^{\infty}$ is a sequence in single infinite random environments. In other words, if $\overrightarrow{\xi}_0^{\infty}$ is a Markov sequence, $\overrightarrow{X}$ is called the Markov chain in the environment of single infinite Markovian systems.

Given a random variable sequence $\{X_n, n \geq 0\}$ on $(\Omega, \mathscr{F}, P)$, the following statement is satisfied. If, for arbitrary $x > 0$ and $n \geq 0$, there exists $P(|X_n| > x) \leq CP(V > x)$, where V represents a nonnegative random variable, C appearing here represents a constant and is greater than zero. Thus we call $\{X_n, n \geq 0\}$ the tail probability uniformly bounded by V and denote it as $\{X_n\} < V$. This paper always sets $\overrightarrow{X}$ as the Markov chain in single infinite Markovian environments. We assume that C appearing in this paper represents a positive constant that represents different values in different positions. The indicative function of the set of A is denoted as I_A.

The purpose of the study is to propose limit theorems for function of Markov chain in analysis of the environment of single infinite Markovian systems and to conclude some different sufficient conditions for the almost sure convergence by means of constructing martingale differential sequence. In addition, we derive the similar conclusion about strong convergence of the weighted sums in the given environment in terms of some weaker sufficient conditions.

Two specific contributions have been included as follows, which are both built on the environment of single infinite Markovian systems. Firstly, this study will offer a fresh insight into the following Theorem 1 and Theorem 2 and Corollaries 1 and 2 to show Markov chain's SLLN (strong law of large numbers) in the given environment. Secondly, this study will provide an important opportunity to advance the understanding of Markov chain strong convergence of weighted sum in the given environment. The results are given by Theorem 3 and Corollary 3.

To prove the main theorems, the following deformation lemmas are needed.

Lemma 1 (see, e.g., Conclusion 1 in [17]). *Given a Markov chain $\overrightarrow{X}$ in the environment of single infinite Markovian systems $\overrightarrow{\xi}_0^{\infty}$, the random variable sequence of $\{(X_n, \xi_n)\colon n \geq 0\}$ is the Markovian chain in double. In particular, if the one-step transition function in the single infinite Markovian environments $\overrightarrow{\xi}_0^{\infty}$ is $K_n(\theta, B)$, the one-step transition probability of $\{(X_n, \xi_n)\colon n \geq 0\}$ is*

$$Q_n(x, \theta; A \times B) = K_n(\theta, B) P(\theta; x, A). \tag{2}$$

If $\overrightarrow{\xi}_0^{\infty}$ is time-homogeneous, then $\{(X_n, \xi_n)\colon n \geq 0\}$ is time-homogeneous too.

Lemma 2 (see Lemma 2 in [18]). *Assume that X is a random variable; for any $x > 0$, there exists $P(|X| > x) \leq CP(V > x)$, where V is a nonnegative random variable and $C > 0$ is a constant, such that, for any $x > 0$ and $q > 0$, we have*

$$E|X|^q I_{\{|X| \leq x\}} \leq Cx^q P(V > x) + CEV^q I_{\{V \leq x\}}. \tag{3}$$

3. SLLN in the Environment of Single Infinite Markovian Systems

To begin with, we use Lemmas 1 and 2 to investigate SLLN for function of Markov chain in the environment of single infinite Markovian systems. A series of sufficient conditions for SLLN are given for function of Markov Chains in the environment of single infinite Markovian systems. The relevant results are in accordance with the following major Theorems 1 and 2, as well as Corollaries 1 and 2.

Theorem 1. *Given the probability space of $(\Omega, \mathscr{F}, P)$ with values on set of $X \times \Theta$, we assume that $\{(X_n, \xi_n)\colon n \geq 0\}$ is a Markov chain, $\{F_n(X_n, \xi_n)\colon n \geq 0\}$ is a sequence of measurable functions defined on $(X \times \Theta, \mathscr{A} \times \mathscr{B})$, and $\{g_n(x), n \geq 0\}$ is a sequence of even functions defined on set of R which is taking a positive value on the interval of $(0, \infty)$. For any $n \geq 0$, there always exists a value of $\lambda > 0$, if one of the following conditions holds:*

(i) $g_n(x)$ is monotonically nondecreasing on the interval of $(0, \infty)$. When $0 < x \leq 1$, there is $g_n(x) \geq \lambda x^{\theta}$ $(0 < \theta \leq 1)$, and $E(F_n(X_n, \xi_n)) = 0$, $n \geq 0$;

(ii) $g_n(x) \geq \begin{cases} \lambda x^{\alpha}\,(0 < \alpha \leq 2), & 0 < x \leq 1, \\ \lambda x^{\beta}\,(\beta \geq 1), & x > 1. \end{cases}$

At the same time, for positive constant sequences of $\{a_n, n \geq 0\}$ where $a_n \uparrow \infty$ is satisfied, if there exist

$$\sum_{m=0}^{\infty} E g_m\left(\frac{F_m(X_m, \xi_m)}{a_m}\right) < \infty, \tag{4}$$

then, for any $k \geq 1$, we get the following series, which are convergent almost surely:

$$\sum_{m=0}^{\infty} \frac{F_m(X_m, \xi_m) - E\left(F_m(X_m, \xi_m) \mid X_{m-k}, \xi_{m-k}\right)}{a_m} \tag{5}$$
$$\cdot \text{ a.s.convergence,}$$

and consequently we have the following formula, which is true almost surely:

$$\lim_{n\longrightarrow\infty}\frac{1}{a_n}\sum_{m=0}^{n}\left(F_m(X_m,\xi_m)\right.$$
$$\left.-E\left(F_m(X_m,\xi_m)\mid X_{m-k},\xi_{m-k}\right)\right)=0\text{ a.s.}. \tag{6}$$

Here, we agree $X_{-k}\equiv 0$ and $\xi_{-k}\equiv 0$ for any $k\geq 1$.

According to the derivation of Theorem 1, we can further generalize Corollary 1 as follows.

Corollary 1. *Assume a Markov chain $\{(X_n,\xi_n): n\geq 0\}$ which is defined on probability space of $(\Omega,\mathcal{F},P)$ with values on set of $X\times\Theta$. $\{F_n(X_n,\xi_n): n\geq 0\}$ is a sequence of measurable functions defined on $(X\times\Theta,\mathcal{A}\times\mathcal{B})$. For the positive constant sequences of $\{a_n,n\geq 0\}$, satisfying $a_n\uparrow\infty$, if one of the following two conditions holds:*

(iii) $\sum_{m=0}^{\infty}E(|F_m(X_m,\xi_m)|^r/(|a_m|^r+|F_m(X_m,\xi_m)|^r))<\infty$, where $0<r<1$ and $E(F_n(X_n,\xi_n))=0,n\geq 0$;

(iv) $\sum_{m=0}^{\infty}E((|F_m(X_m,\xi_m)|^r)/(|a_m|^r+a_m|F_m(X_m,\xi_m)|^{r-1}))<\infty$, where $1\leq r\leq 2$, then (5) and (6) hold.

Proof of Theorem 1. Let us now prove the above Theorem 1. In the process of proof, we discuss two situations. One situation is $k=1$, and the other situation is $k>1$.

Firstly, we consider the situation of $k=1$.

Under condition (i), there satisfies $|F_n(X_n,\xi_n)|>a_n$, that is, $(|F_n(X_n,\xi_n)|/a_n)>1$. We know from the condition that $g_n(x)$ is monotonically nondecreasing on the interval of $(0,\infty)$, and we can get $g_n(1)\geq\lambda$ when condition (i) is satisfied. Thus, we can get the inequality $g_n(|F_n(X_n,\xi_n)|/a_n)\geq Cg_n(1)$ which will be used in the following derivation. Next, let us give the detailed process of the derivation of inequalities (7) and (8) by using Lemma 2. The derivation of inequality is as follows:

$$\begin{aligned}\sum_{m=0}^{\infty}P\left(\left|F_m(X_m,\xi_m)\right|>a_m\right)&\leq C\sum_{m=1}^{\infty}Eg_m(1)I_{\{|F_m(X_m,\xi_m)|>a_m\}}\\&\leq C\sum_{m=1}^{\infty}Eg_m\left(\frac{\left|F_m(X_m,\xi_m)\right|}{a_m}\right)I_{\{|F_m(X_m,\xi_m)|>a_m\}}\\&\leq C\sum_{m=1}^{\infty}Eg_m\left(\frac{\left|F_m(X_m,\xi_m)\right|}{a_m}\right)<\infty,\end{aligned} \tag{7}$$

$$\begin{aligned}&E\left(\sum_{m=0}^{\infty}\left|E\left(\frac{F_m(X_m,\xi_m)}{a_m}I_{\{|F_m(X_m,\xi_m)|>a_m\}}\mid X_{m-1},\xi_{m-1}\right)\right|\right)\\&=E\left(\sum_{m=0}^{\infty}\left|E\left(\frac{F_m(X_m,\xi_m)}{a_m}I_{\{|F_m(X_m,\xi_m)|\leq a_m\}}\mid X_{m-1},\xi_{m-1}\right)\right|\right)\\&\leq\sum_{m=0}^{\infty}E\left(\frac{\left|F_m(X_m,\xi_m)\right|}{a_m}I_{\{|F_m(X_m,\xi_m)|\leq a_m\}}\right)\\&\leq\sum_{m=0}^{\infty}E\left(\frac{\left|F_m(X_m,\xi_m)\right|^{\theta}}{a_m^{\theta}}\right)I_{\{|F_m(X_m,\xi_m)|\leq a_m\}}\\&\leq C\sum_{m=0}^{\infty}Eg_m\left(\frac{\left|F_m(X_m,\xi_m)\right|}{a_m}\right)I_{\{|F_m(X_m,\xi_m)|\leq a_m\}}\\&\leq C\sum_{m=0}^{\infty}Eg_m\left(\frac{\left|F_m(X_m,\xi_m)\right|}{a_m}\right)<\infty.\end{aligned} \tag{8}$$

Under condition (ii), when $|F_n(X_n, \xi_n)| > a_n$ is satisfied at the same time, we use the second case of condition (ii) $g_n(x) \geq \lambda x^\beta$ $(\beta \geq 1, x > 1)$ to get the inequality $g_n(|F_n(X_n, \xi_n)|/a_n) \geq C(|F_n(X_n, \xi_n)|^\beta / a_n^\beta)$ which will be used in the following derivation. Next, let us give the detailed process of the derivation of inequalities (9) and (10). The derivation of inequality is as follows:

$$\begin{aligned}\sum_{m=0}^{\infty} P\left(\left|F_m(X_m, \xi_m)\right| > a_m\right) &\leq C \sum_{m=0}^{\infty} E\left(\frac{\left|F_m(X_m, \xi_m)\right|^\beta}{a_m^\beta}\right) I_{\{|F_m(X_m, \xi_m)| > a_m\}} \\ &\leq C \sum_{m=0}^{\infty} E g_m\left(\frac{\left|F_m(X_m, \xi_m)\right|}{a_m}\right) < \infty,\end{aligned} \tag{9}$$

$$\begin{aligned}&E\left(\sum_{m=0}^{\infty}\left|E\left(\frac{F_m(X_m, \xi_m)}{a_m} I_{\{|F_m(X_m, \xi_m)| > a_m\}} \mid X_{m-1}, \xi_{m-1}\right)\right|\right) \\ &\leq \sum_{m=0}^{\infty} E\left(\frac{\left|F_m(X_m, \xi_m)\right|}{a_m} I_{\{|F_m(X_m, \xi_m)| > a_m\}}\right) \\ &\leq \sum_{m=0}^{\infty} E\left(\frac{\left|F_m(X_m, \xi_m)\right|^\beta}{a_m^\beta}\right) I_{\{|F_m(X_m, \xi_m)| > a_m\}} \\ &\leq C \sum_{m=0}^{\infty} E g_m\left(\frac{\left|F_m(X_m, \xi_m)\right|}{a_m}\right) < \infty.\end{aligned} \tag{10}$$

Obviously, by using formulas (7) and (9), it is obvious that the result below is established almost surely:

$$\sum_{m=0}^{\infty} I_{\{|F_m(X_m, \xi_m)| > a_m\}} < \infty \text{ a.s..} \tag{11}$$

Because $P(|F_m(X_m, \xi_m)| > a_m\text{: i.o.}) = 0$, consequently we can get that the following series are convergent almost surely:

$$\sum_{m=0}^{\infty} \frac{F_m(X_m, \xi_m)}{a_m} I_{\{|F_m(X_m, \xi_m)| > a_m\}} \text{ a.s.convergence.} \tag{12}$$

At the same time, by using formulas (8) and (10), we can get that the following series are convergent almost surely:

$$\sum_{m=0}^{\infty} E\left(\frac{F_m(X_m, \xi_m)}{a_m} I_{\{|F_m(X_m, \xi_m)| > a_m\}} \mid X_{m-1}, \xi_{m-1}\right) \text{ a.s.convergence.} \tag{13}$$

Note that

$$\begin{aligned}Z_n &= \frac{F_n(X_n, \xi_n) I_{\{|F_n(X_n, \xi_n)| \leq a_n\}}}{a_n} \\ &\quad - \frac{E\left(F_n(X_n, \xi_n) I_{\{|F_n(X_n, \xi_n)| \leq a_n\}} \mid X_{n-1}, \xi_{n-1}\right)}{a_n},\end{aligned} \tag{14}$$

$$\mathscr{B}_n = \sigma\left(\overrightarrow{X}_0^n, \overrightarrow{\xi}_0^n\right).$$

$\{Z_n, \mathscr{B}_n, n \geq 0\}$ is known as a martingale difference sequence by the nature of function of Markov chain of $\{(X_n, \xi_n), n \geq 0\}$. Under condition (i), the following results can be derived by the orthogonality of martingale difference sequence:

$$\begin{aligned}E\left|\sum_{m=0}^{n} Z_m\right|^2 &= \sum_{m=0}^{n} E Z_m^2 \\ &\leq C \sum_{m=0}^{n} E\left(\frac{\left|F_m(X_m, \xi_m)\right|^2}{a_m^2} I_{\{|F_m(X_m, \xi_m)| \leq a_m\}}\right) \\ &\leq C \sum_{m=0}^{n} E\left(\frac{\left|F_m(X_m, \xi_m)\right|^\theta}{a_m^\theta} I_{\{|F_m(X_m, \xi_m)| \leq a_m\}}\right) \\ &\leq C \sum_{m=0}^{\infty} E g_m\left(\frac{\left|F_m(X_m, \xi_m)\right|}{a_m}\right) I_{\{|F_m(X_m, \xi_m)| \leq a_m\}} \\ &\leq C \sum_{m=0}^{\infty} E g_m\left(\frac{\left|F_m(X_m, \xi_m)\right|}{a_m}\right).\end{aligned} \tag{15}$$

Also, under condition (ii), the inequality is derived as follows:

$$\begin{aligned}E\left|\sum_{m=0}^{n} Z_m\right|^2 &= \sum_{m=0}^{n} E Z_m^2 \\ &\leq C \sum_{m=0}^{n} E\left(\frac{\left|F_m(X_m, \xi_m)\right|^2}{a_m^2} I_{\{|F_m(X_m, \xi_m)| \leq a_m\}}\right) \\ &\leq C \sum_{m=0}^{n} E\left(\frac{\left|F_m(X_m, \xi_m)\right|^\alpha}{a_m^\alpha} I_{\{|F_m(X_m, \xi_m)| \leq a_m\}}\right) \\ &\leq C \sum_{m=0}^{\infty} E g_m\left(\frac{\left|F_m(X_m, \xi_m)\right|}{a_m}\right).\end{aligned} \tag{16}$$

By formula (4), we know that $\sup_{n \geq 0} E|\sum_{m=0}^{n} Z_m|^2 < \infty$, which means $\{\sum_{m=0}^{n} Z_m, \mathscr{B}_n, n \geq 0\}$ is bounded martingale on

L^2. Thus, we can get that the series $\sum_{m=0}^{\infty} Z_m$ are convergent almost surely. Then, by combining formulas (12) and (13), we can see that formula (5) holds, and it is also easy to know that formula (6) holds by Kronecker's Lemma.

Secondly, we consider the other situation of $k > 1$.

By the nature of function of the Markov chain $\{(X_n, \xi_n)\colon n \geq 0\}$, it is known that $\{(X_{mk+n}, Y_{mk+n})\colon m \geq 0\}$ is a Markov chain for any $n = 1, 2, 3, \ldots, k-1$. It is easy to derive the following result regarding convergence by using formula (4):

$$\sum_{m=0}^{\infty} Eg_{mk+n}\left(\frac{F_{mk+n}(X_{mk+n}, \xi_{mk+n})}{a_{mk+n}}\right) < \infty. \tag{17}$$

Therefore, for any $n = 1, 2, 3, \ldots, k-1$, we have the series of almost sure convergence as follows:

$$\sum_{m=0}^{\infty} \frac{F_{mk+n}(X_{mk+n}, \xi_{mk+n}) - E\left(F_{mk+n}(X_{mk+n}, \xi_{mk+n}) \mid X_{mk+n-k}, \xi_{mk+n-k}\right)}{a_{mk+n}} \text{ a.s.convergence.} \tag{18}$$

Thus, the following results of convergence almost surely can be derived:

$$\begin{aligned}
&\sum_{m=0}^{\infty} \frac{F_m(X_m, \xi_m) - E\left(F_m(X_m, \xi_m) \mid X_{m-k}, Y_{m-k}\right)}{a_m} \\
&\quad = \sum_{m=0}^{\infty} \sum_{n=0}^{k-1} \frac{F_{mk+n}(X_{mk+n}, \xi_{mk+n}) - E\left(F_{mk+n}(X_{mk+n}, \xi_{mk+n}) \mid X_{mk+n-k}, \xi_{mk+n-k}\right)}{a_{mk+n}} \\
&\quad = \sum_{n=0}^{k-1} \sum_{m=0}^{\infty} \frac{F_{mk+n}(X_{mk+n}, \xi_{mk+n}) - E\left(F_{mk+n}(X_{mk+n}, \xi_{mk+n}) \mid X_{mk+n-k}, \xi_{mk+n-k}\right)}{a_{mk+n}},
\end{aligned} \tag{19}$$

where, for the situation of $k > 1$, formula (6) is true. Obviously, by Kronecker's Lemma, formula (7) also holds for the situation of $k > 1$.

Now, the conclusions on convergence have been demonstrated and proven completely. The method of using constructing martingale differential sequence to implement different sufficient conditions of the strong limit theorems is different from the evidence from previous observations. Our paper advances the research on the limit theory of a class of Markov chain functions by using different sufficient conditions. □

Remark 1. Both Theorem 1 and Lemma 4 in literature [24] give the sufficient conditions for SLLN of Markov chain, but the preconditions in the two theorems are different.

From Theorem 1, we can see that the sequence of even functions $\{g_n(x), n \geq 0\}$ satisfies different conditions when the value ranges of x are different. In condition (i), when $0 < x \leq 1$ and $0 < \theta \leq 1$, $g_n(x)$ needs to be monotonically nondecreasing and $E(F_n(X_n, \xi_n)) = 0$ with $n \geq 0$. However, in condition (ii), these conditions are not required to approach limit but only to obtain the segment $g_n(x)$ and also a range of values are satisfied. From these two different sufficient conditions, we have obtained SLLN for function of Markov chain in the environment of single infinite Markovian systems. On the basis of Theorem 1, Corollary 1 shows that SLLN can be obtained by assigning different functional forms to $g_n(x)$, which generalize the previous conclusions.

Proof of Corollary 1. At first, when condition (iii) is established, there exists $g_n(x) = |x|^r/(1 + |x|^r)$, where the range of value of r is $0 < r < 1$. When condition (iv) is established, there is $g_n'(x) = |x|^r/(1 + |x|^{r-1})$, where the range of value of r is $1 \leq r \leq 2$. Then, for any $n \geq 0$, $g_n(x)$ and $g_n'(x)$ are both even nondecreasing functions, taking a positive value on interval of $(0, \infty)$. At the same time, respectively, there are the following formulas:

$$\begin{aligned}
&g_n(x) \geq \frac{1}{2}x^r, \quad 0 < x \leq 1,\ 0 < r < 1, \\
&g_n'(x) \geq \begin{cases} \frac{1}{2}x^r, & 0 < x \leq 1, \quad 1 \leq r \leq 2, \\ \frac{1}{2}x, & x > 1. \end{cases}
\end{aligned} \tag{20}$$

If condition (iii) is satisfied, we have

$$\sum_{m=0}^{\infty} Eg_n\left(\frac{F_m(X_m, \xi_m)}{a_m}\right) = \sum_{m=0}^{\infty} E\left(\frac{|F_m(X_m, \xi_m)|^r}{|a_m|^r + |F_m(X_m, \xi_m)|^r}\right) < \infty. \tag{21}$$

If condition (iv) is satisfied, we have

$$\sum_{m=0}^{\infty} Eg_m'\left(\frac{F_m(X_m, \xi_m)}{a_m}\right) = \sum_{m=0}^{\infty} E\left(\frac{|F_m(X_m, \xi_m)|^r}{|a_m|^r + a_m|F_m(X_m, \xi_m)|^{r-1}}\right) < \infty. \tag{22}$$

From the above results, it can be seen that both condition (i) and condition (ii) under Theorem 1 are satisfied, so we can obtain that Corollary 1 holds by Theorem 1.

The sample frequency as a significant part of information theory plays a very important role in statistical hypothesis testing and coding theory. Based on the above results, a class of SLLN on the frequency of occurrence of the state are obtained for function of Markov chain in the environment of single infinite Markovian systems. Meanwhile, the relationship between the frequency of occurrence of state (x, θ) and the product of corresponding one-step transition probability function can be seen from the following Theorem 2. In particular, we can use the initial state to describe the frequency of occurrence of the state when the time-homogeneity is satisfied. Under the certain environment of the single infinite Markovian systems, we have concluded Corollary 2, which can be extended to a class of SLLN on the frequency of occurrence of the state for function of Markov chain. □

Theorem 2. *Assume that a Markov chain X is in the environment of the single infinite Markovian systems $\overrightarrow{\xi_0^\infty}$. $S_n(x,\theta)$ represents the frequency where (x,θ) appears in the sequence of $(X_1,\xi_1), (X_2,\xi_2), \ldots, (X_n,\xi_n)$; if $\sum_{m=0}^{\infty} a_m^{-r} < \infty$, when $1 < r \le 2$, we then have*

$$\lim_{n\longrightarrow\infty}\left(\frac{S_n(x,\theta)}{a_n} - \frac{1}{a_n}\sum_{m=0}^{n} K_m(\xi_{m-1},\theta)P(\xi_{m-1}; X_{m-1}, x)\right) = 0 \text{ a.s.}. \tag{23}$$

In particular, when $\overrightarrow{\xi_0^\infty}$ is time-homogeneous and $\lim_{n\longrightarrow\infty}(n/a_n) = C$, then we have

$$\lim_{n\longrightarrow\infty}\frac{S_n(x,\theta)}{a_n} = CK(\xi_0,\theta)P(\xi_0; X_0, x) \text{ a.s.}. \tag{24}$$

Corollary 2. *Assume that a Markov chain X is in the environment of the single infinite Markovian systems $\overrightarrow{\xi_0^\infty}$. $S_n(x)$ represents the frequency where x appears in the sequence of $X_1, X_2, \ldots, X_n$; if $\sum_{m=0}^{\infty} a_m^{-r} < \infty$, when $1 < r \le 2$, then we have*

$$\lim_{n\longrightarrow\infty}\left(\frac{S_n(x)}{a_n} - \frac{1}{n}\sum_{m=0}^{n} P(\xi_{m-1}; X_{m-1}, x)\right) = 0 \text{ a.s.}. \tag{25}$$

In particular, when $\overrightarrow{\xi_0^\infty}$ is time-homogeneous and $\lim_{n\longrightarrow\infty}(n/a_n) = C$, we have

$$\lim_{n\longrightarrow\infty}\frac{S_n(x)}{a_n} = CP(\xi_0; X_0, x) \text{ a.s.}. \tag{26}$$

Proof of Theorem 2. Given $F_n(X_n,\xi_n) = \delta_x(X_n)\delta_\theta(\xi_n)$, we have $S_n(x,\theta) = \sum_{m=1}^{n} F_m(X_m,\xi_m)$. Then the following inequality can be derived through equation (10) above:

$$\sum_{m=0}^{\infty} E\frac{|F_m(X_m,\xi_m)|^r}{a_m|F_m(X_m,\xi_m)|^{r-1} + a_m^r} \le \sum_{m=0}^{\infty} a_m^{-r} < \infty. \tag{27}$$

So we can get from the above formula that the series is convergent.

Obviously, it is known that the following limit holds almost surely by Corollary 1:

$$\lim_{n\longrightarrow\infty}\frac{1}{a_n}\sum_{m=0}^{n}\left(F_m(X_m,\xi_m) - E\left(F_m(X_m,\xi_m) \mid X_{m-1},\xi_{m-1}\right)\right) = 0 \text{ a.s.}. \tag{28}$$

Then, by the combination of the formula $\sum_{m=0}^{n} F_m(X_m,\xi_m) = S_n(x,\theta) + \delta_x(X_0)\delta_\theta(\xi_0)$ and Lemma 1, we can get the results below.

$$\begin{aligned} E\left(F_n(X_n,\xi_n) \mid X_{n-1},\xi_{n-1}\right) &= E\left(\delta_x(X_n)\delta_\theta(\xi_n) \mid X_{n-1},\xi_{n-1}\right) \\ &= Q_n(X_{n-1},\xi_{n-1}; x,\theta) \\ &= K_n(\xi_{n-1},\theta)P(\xi_{n-1}; X_{n-1}, x). \end{aligned} \tag{29}$$

Substituting the above formula into the formula limitation equation (28), we can get formula (23).

If $\overrightarrow{\xi_0^\infty}$ is time-homogeneous, it is known that $\{(X_n,\xi_n)\colon n \ge 0\}$ is also time-homogeneous by Lemma 1, and hence $Q_n(X_{n-1},\xi_{n-1}; x,\theta) = Q(X_0,\xi_0; x,\theta) = K(\xi_0,\theta)P(\xi_0; X_0, x)$. So we can get formula (24) by using formula (23). Therefore, Theorem 2 has been proven. □

Proof of Corollary 2. Given the formula $F_n(X_n,\xi_n) = \delta_x(X_n)$, we have the formula $S_n(x) + \delta_x(X_0) = \sum_{m=0}^{n} F_m(X_m,\xi_m) = \sum_{m=0}^{n}\delta_x(X_m)$. By combining these conditions and Lemma 1, we obtain the following results:

$$E\left(F_n(X_n,\xi_n) \mid X_{n-1},\xi_{n-1}\right) = E\left(\delta_x(X_m) \mid X_{n-1},\xi_{n-1}\right) = P(\xi_{n-1}; X_{n-1}, x), \tag{30}$$

and, therefore, Corollary 2 can be proven by using the method which is similar to that used in the Proof of Theorem 2. □

4. The Strong Convergence of Weighted Sums in the Environment of Single Infinite Markovian Systems

In this section, we use Lemmas 1 and 2 to study the strong convergence of weighted sum for the function of Markov chain in the environment of the single infinite Markovian systems. Some sufficient conditions for the strong convergence of weighted sum for the function of Markov Chains are obtained. The relevant results will be obtained from the analysis of Theorem 3 and Corollary 3.

Theorem 3. *Assume that a Markov chain $\{(X_n,\xi_n)\colon n \ge 0\}$ is defined on $(\Omega,\mathscr{F},P)$ with values on set of $X\times\Theta$. $\{F_n(X_n,\xi_n)\colon n\ge 0\}$ is a sequence of measurable functions defined on $(X\times\Theta,\mathscr{A}\times\mathscr{B})$. $\{a_n, n\ge 0\}$ and $\{b_n, n\ge 0\}$ are arbitrary sequences of positive real numbers, respectively, and we denote $c_n = b_n/a_n, b_n\uparrow\infty$, if the following conditions both hold:*

(a) $\sum_{m=1}^{\infty} c_m^{-1} E|F_m(X_m,\xi_m)| I_{\{|F_m(X_m,\xi_m)|>c_m\}} < \infty$;

(b) $\sum_{m=1}^{\infty} c_m^{-p} E|F_m(X_m,\xi_m)|^p I_{\{|F_m(X_m,\xi_m)|\le c_m\}} < \infty$, *where there is* $1 \le p \le 2$,

such that, for any $k \geq 1$, we can get that the following series are convergent almost surely:

$$\sum_{m=0}^{\infty} \frac{F_m(X_m, \xi_m) - E\big(F_m(X_m, \xi_m) \mid X_{m-k}, \xi_{m-k}\big)}{c_n} \cdot \text{a.s.convergence,} \tag{31}$$

and we have

$$\lim_{n\longrightarrow\infty} \frac{1}{b_n} \sum_{m=0}^{n} a_m \big(F_m(X_m, \xi_m) - E\big(F_m(X_m, \xi_m) \mid X_{m-k}, \xi_{m-k}\big)\big) = 0 \text{ a.s..} \tag{32}$$

Consequently, we get Corollary 3 as follows.

Corollary 3. *Assume that a Markov chain $\{(X_n, \xi_n): n \geq 0\}$ is defined on $(\Omega, \mathcal{F}, P)$ with values on set of $X \times \Theta$. $\{F_n(X_n, \xi_n): n \geq 0\}$ is a sequence of measurable functions defined on $(X \times \Theta, \mathcal{A} \times \mathcal{B})$, and it satisfies $\{F_n(X_n, \xi_n)\} < V$. $\{a_n, n \geq 0\}$ and $\{b_n, n \geq 0\}$ are arbitrary sequences of positive real numbers, respectively, and we denote $c_n = b_n/a_n$, $b_n \uparrow \infty$. For arbitrary $x > 0$, we denote $N(x) = Card\{n: c_n \leq x\}$, if V satisfies the following two conditions:*

(c) $EN(V) < \infty$;

(d) $\int_1^{\infty} EN(V/t)dt < \infty$.

In addition, one of the following conditions is satisfied:

(e) $\int_0^{\infty} t^{p-1} P(V > t) \int_t^{\infty} N(y)/y^{p+1} dy dt < \infty$, where there is $1 \leq p \leq 2$;

(f) $\max_{0\leq j\leq n} c_j^p \sum_{m=n}^{\infty} c_m^{-p} = O(n)$, where there is $1 \leq p \leq 2$;

(g) $\int_0^1 EN(V/t^{1/p})dt < \infty$, where there is $1 \leq p \leq 2$, and, for any $k \geq 1$, both (31) and (32) hold.

Proof of Theorem 3. In a similar way to Theorem 1, we also discuss two situations in the process of proof. One situation is $k = 1$; the other situation is $k > 1$.

We consider the first situation of $k = 1$. For any $m \geq 0$, we denote that

$$Z_m = \frac{F_m(X_m, \xi_m) I_{\{|F_m(X_m,\xi_m)| \leq c_m\}}}{c_m} - \frac{E\Big(F_m(X_m, \xi_m) I_{\{|F_m(X_m,\xi_m)| \leq c_m\}} \mid X_{m-1}, \xi_{m-1}\Big)}{c_m};$$
$$Z_m' = \frac{F_m(X_m, \xi_m) I_{\{|F_m(X_m,\xi_m)| > c_m\}}}{c_m}. \tag{33}$$

Under condition (a), it is known that the following series are absolute convergent almost surely:

$$\sum_{m=0}^{\infty} \left|Z_m'\right| < \infty \text{ a.s..} \tag{34}$$

Hence, the following series are convergent almost surely:

$$\sum_{m=0}^{\infty} Z_m' \text{ a.s..} \tag{35}$$

Meanwhile, the following series of conditional expectation are convergent almost surely:

$$\sum_{m=0}^{\infty} E\big(Z_m' \mid X_{m-1}, \xi_{m-1}\big) \text{ a.s..} \tag{36}$$

Then, due to the orthogonal properties of the martingale difference sequence, it is known that, for any $1 \leq p \leq 2$, we can get

$$E\left|\sum_{m=0}^{n} Z_m\right|^2 = \sum_{m=0}^{n} EZ_m^2 \leq C \sum_{m=0}^{n} \frac{1}{c_m^p} E\left|F_m(X_m, \xi_m)\right|^p I_{\{|F_m(X_m,\xi_m)| \leq c_m\}}. \tag{37}$$

Through the combination of condition (b) and formula (37), we have the formula $\sup_{n\geq 0} E|\sum_{m=0}^{n} Z_m|^2 < \infty$. In other words, this formula shows that the result of $\{\sum_{m=0}^{n} Z_m, \sigma_n, n \geq 0\}$ is a bounded martingale on L^2. Thus, we have that the series $\sum_{m=0}^{\infty} Z_m$ are convergent almost surely, which is the weighted sum mentioned in the previous section.

The joint two formulas (35) and (36) on almost sure convergence show that formula (31) holds for the situation of $k = 1$, and formula (32) for the situation of $k = 1$ is also true by Kronecker's Lemma.

Finally, the proof of the other situation of $k > 1$ is similar to Theorem 1, so it is omitted.

Here Theorem 3 has been proven regarding the strong convergence of weighted sums. We proved the similar conclusions, but it was from a different viewpoint compared to previous research. □

Remark 2. Both Theorem 3 and Theorem 2.1 in literature [25] give the sufficient conditions for strong convergence of weighted sums of Markov chains, which is unlike the preconditions in these two theorems. Furthermore, the results of the strong convergence of weighted sums can be demonstrated under weaker sufficient conditions compared with Theorem 1 in literature [26].

Proof of Corollary 3. Firstly, if V satisfies conditions (c), (d), and (e), for any $k \geq 1$, then both (31) and (32) hold. Now let us show this proof process as follows.

It is only necessary to verify that condition (a) and condition (b) of Theorem 3 are immediately available. As we have the inequality

$$\sum_{m=1}^{\infty} P\left(\left|F_m\left(X_m, \xi_m\right)\right| > c_m\right) \leq C \sum_{m=1}^{\infty} P\left(V > c_m\right) \leq CEN(V), \tag{38}$$

we can derive the following inequality:

$$\begin{aligned}
&\sum_{m=1}^{\infty} c_m^{-1} E\left|F_m\left(X_m, \xi_m\right)\right| I_{\{|F_m(X_m,\xi_m)|>c_m\}} \\
&\leq C \sum_{m=1}^{\infty} \frac{1}{c_m} \int_{c_m}^{\infty} P\left(\left|F_m\left(X_m, \xi_m\right)\right| > t\right) \mathrm{d}t \\
&\leq C \sum_{m=1}^{\infty} \frac{1}{c_m}\left(c_m P\left(\left|F_m\left(X_m, \xi_m\right)\right| > c_m\right)\right. \\
&\left.+ \int_{c_m}^{\infty} P\left(\left|F_m\left(X_m, \xi_m\right)\right| > t\right) \mathrm{d}t\right) \\
&\leq C\left(\sum_{m=1}^{\infty} P\left(V > c_m\right) + \sum_{m=1}^{\infty} \int_1^{\infty} P\left(V > t c_m\right) \mathrm{d}t\right) \\
&\leq C\left(EN(V) + \int_1^{\infty} EN\left(\frac{V}{t}\right) \mathrm{d}t\right),
\end{aligned} \tag{39}$$

and, from conditions (c) and (d) of this corollary, we can see that condition (a) of Theorem 3 holds.

By Lemma 2, we have the inequality

$$\begin{aligned}
&\sum_{m=1}^{\infty} c_m^{-p} E\left|F_m\left(X_m, \xi_m\right)\right|^p I_{\{|F_m(X_m,\xi_m)|\leq c_m\}} \\
&\leq C \sum_{m=1}^{\infty} P\left(V > c_m\right) + C \sum_{m=1}^{\infty} c_m^{-p} EV^p I_{\{V\leq c_m\}} \\
&\leq CEN(V) + C \sum_{m=1}^{\infty} c_m^{-p} EV^p I_{\{V\leq c_m\}},
\end{aligned} \tag{40}$$

as well as the inequality

$$\begin{aligned}
\sum_{m=1}^{\infty} c_m^{-p} E|V|^p I_{\{|V|\leq c_m\}} &\leq C \sum_{m=1}^{\infty} c_m^{-p} \int_0^{c_m} t^{p-1} P(|V| > t) \mathrm{d}t \\
&= C \int_0^{\infty} t^{p-1} P(V > t) \sum\nolimits_{\{m:\, c_m > t\}} c_m^{-p} \mathrm{d}t \\
&\leq C \int_0^{\infty} t^{p-1} P(V > t) \int_t^{\infty} \frac{N(y)}{y^{p+1}} \mathrm{d}y \mathrm{d}t.
\end{aligned} \tag{41}$$

The last inequality above is established based on the facts that

$$\begin{aligned}
&\sum_{\{m:\, c_m>t\}} c_m^{-p} = \lim_{s\longrightarrow\infty} \sum_{\{m:\, t<c_m<s\}} c_m^{-p} = \lim_{s\longrightarrow\infty} \int_t^s y^{-p} \mathrm{d}N(y) \\
&= \lim_{s\longrightarrow\infty}\left(s^{-p}N(s) - t^{-p}N(t) + p\int_{t<y\leq s} N\frac{(y)}{y^{p+1}} \mathrm{d}y\right); \\
&s^{-p}N(s) \leq p\int_s^{\infty} N\frac{(y)}{y^{p+1}} \mathrm{d}y \longrightarrow 0, \\
&\qquad s \longrightarrow \infty.
\end{aligned} \tag{42}$$

Then, by the combination of formula (40), formula (41), condition (c), and condition (e), we know that condition (b) of Theorem 3 holds. Therefore, the proof is completed when conditions (c), (d), and (e) are satisfied.

Secondly, if V satisfies conditions (c), (d), and (f), for any $k \geq 1$, we can get the same conclusions. The proof process is as follows.

Following the proof of Corollary 3 by using formula (40), we only need to prove

$$\sum_{m=1}^{\infty} c_m^{-p} EV^p I_{\{V\leq c_m\}} < \infty. \tag{43}$$

In fact, given some particular values $d_0 = 0$, $d_n = \max_{1\leq m\leq n} c_m$, combining the two conditions of (c) and (f), we have

$$\begin{aligned}\sum_{m=1}^{\infty} c_m^{-p} EV^p I_{\{V\le c_m\}} &\le \sum_{m=1}^{\infty} c_m^{-p} EV^p I_{\{V\le d_m\}}\\ &= \sum_{m=1}^{\infty}\sum_{j=1}^{m} c_m^{-p} EV^p I_{\{d_{j-1}<V\le d_j\}} = \sum_{j=1}^{\infty} EV^p I_{\{d_{j-1}<V\le d_j\}} \sum_{m=j}^{\infty} c_m^{-p}\\ &\le \sum_{j=1}^{\infty} P\left(d_{j-1}<V\le d_j\right) d_j^p \sum_{m=j}^{\infty} c_m^{-p} \le C\sum_{j=1}^{\infty} jP\left(d_{j-1}<V\le d_j\right)\\ &= C\sum_{j=1}^{\infty}\sum_{m=1}^{j} P\left(d_{j-1}<V\le d_j\right) \le C\sum_{m=1}^{\infty}\sum_{j=m}^{\infty} P\left(d_{j-1}<V\le d_j\right)\\ &= C\sum_{m=1}^{\infty} P\left(V>d_{m-1}\right) \le C\left(\sum_{m=1}^{\infty} P\left(V>c_m\right)+1\right)<\infty.\end{aligned} \tag{44}$$

Therefore, the proof is completed when conditions (c), (d), and (f) are satisfied.

Thirdly, if V satisfies conditions (c), (d), and (g), for any $k \ge 1$, we can also have formulas (31) and (32). The proof process is as follows.

Given $s = m^p t$, we use the similar proof method of the first case by condition (g); then we have

$$\begin{aligned}\sum_{m=1}^{\infty} c_m^{-p} EV^p I_{\{V\le c_m\}} &\le C\sum_{m=0}^{\infty} \frac{1}{c_m^p}\int_0^{c_m^p} P\left(V^p > s\right)\mathrm{d}s\\ &\le \int_0^1 EN\left(\frac{V}{t^{1/p}}\right)\mathrm{d}t<\infty.\end{aligned} \tag{45}$$

Therefore, the proof is completed when conditions (c), (d), and (g) are satisfied. □

Remark 3. The sufficient conditions of Corollary 3 are similar to those of Theorem 2.1 and Theorem 2.2 in literature [25], which shows that the conditions are applicable to the single infinite environment or double infinite environment.

5. Conclusions

From the above discussion, this study confirms that a series of limit theorems for the function of Markov chains in the environment of single infinite Markovian systems are proven. Furthermore, consistent with the literature, the study has found the sufficient conditions for convergence. Moreover, the results of strong law of large numbers and strong convergence of the weighted sums in the infinite environment are given by constructing martingale differential sequence. The finding of preconditions used in this research is broadly different from the previous observations. Although there are similarities between conclusions, they can be expressed by more sufficient conditions of the limit theorems, which are simpler than the analytical techniques proposed earlier. For the further research work, it may be extended to the limit theory related to the function of Markov chain in the environment of double infinite Markovian systems on finite state space.

Data Availability

No data were used to support this study.

Conflicts of Interest

The authors declare that there are no conflicts of interest regarding the publication of this paper.

Acknowledgments

This work was supported by the National Natural Science Foundation of China (NSFC) (no. 71974204) and the "Fundamental Research Funds for the Central Universities," Zhongnan University of Economics and Law (no. 2722020JX005).

References

[1] R. Cogburn, "Markov chains in random environments: the case of Markovian environments," *The Annals of Probability*, vol. 8, no. 5, pp. 908–916, 1980.
[2] K. Nawrotzki, "Ergodic theorem for random-processes with embedded homogeneous flow," *Theory of Probability and Its Applications*, vol. 26, no. 2, pp. 388–392, 1981.
[3] K. Nawrotzki, "Discrete open systems of Markov chains in random environment II," *Elektron Informationsverarb. Kybernet*, vol. 18, pp. 569–599, 1982.
[4] R. Cogburn, "The ergodic theory of Markov chains in random environments," *Zeitschrift für Wahrscheinlichkeitstheorie und Verwandte Gebiete*, vol. 66, no. 1, pp. 109–128, 1984.
[5] R. Cogburn, "On direct convergence and periodicity for transition probabilities of Markov chains in random environments," *The Annals of Probability*, vol. 18, no. 2, pp. 642–654, 1990.
[6] R. Cogburn, "On the central limit theorem for Markov chains in random environments," *The Annals of Probability*, vol. 19, no. 2, pp. 587–604, 1991.
[7] S. Orey, "Markov chains with stochastically stationary transition probabilities," *The Annals of Probability*, vol. 19, no. 3, pp. 907–928, 1991.
[8] W. Liu, "Relative entropy densities and a class of limit theorems of seqence of m-valued random variables," *The Annals of Probability*, vol. 18, no. 2, pp. 829–839, 1990.

[9] G. X. Liu and W. Liu, "Some strong limit theorems relative to the geometric average of random transition probabilities of arbitrary finite nonhomogeneous Markov chain," *Statistics & Probability Letters*, vol. 21, pp. 77–83, 1994.

[10] H. X. Wang and Y. L. Dai, "Poisson's limit law of Markov chain in Markov environment," *Journal of Mathematics*, vol. 40, pp. 265–270, 1997.

[11] Y. Q. Li, "Some notes on Markov chain in Markov environment," *Advances in Mathematics*, vol. 28, pp. 358–360, 1999.

[12] D. F. Fang, "The Shannon-McMillan-Breiman theorem of the Markov chain in the Markov environment," *Application Probability and Statistics*, vol. 16, pp. 295–298, 2000.

[13] D. F. Fang, H. X. Wang, and M. N. Tang, "Possion limit theorem for countable Markov chain in Markovian environments," *Applied Mathematics and Mechanics*, vol. 24, no. 3, pp. 298–306, 2003.

[14] Y. Q. Li, S. M. Wang, and Y. L. Hu, "A class of strong limit theorem of Markov chain in Markov environment," *Advances in Mathematics*, vol. 37, pp. 539–550, 2008.

[15] Z. Z. Wang, "A kind of asymptotic properties of moving averages for Markov chains in Markovian environments," *Communications in Statistics-Theory and Methods*, vol. 46, no. 22, pp. 10926–10940, 2017.

[16] M. L. Guo, "The strong law of large numbers for function of Markov chain in random environment," *Application Probability and Statistics*, vol. 12, pp. 154–160, 2004.

[17] Y. Q. Li, "Interrelation between Markov chain and Markov double chain in random environment," *Journal of Mathematics*, vol. 49, pp. 1373–1380, 2006.

[18] C. G. Wan, "The limit theorem of Markov chain function in random environment," *Mathematica Applicata*, vol. 23, pp. 618–624, 2010.

[19] D. H. Hu and X. Y. Hu, "On Markov chains in space-time random environments," *Acta Mathematica Scientia*, vol. 29, no. 1, pp. 1–10, 2009.

[20] W. Liu, C. Ma, Y. Li, and S. Wang, "A strong limit theorem for the average of ternary functions of Markov chains in bi-infinite random environments," *Statistics & Probability Letters*, vol. 100, pp. 12–18, 2015.

[21] Z. Shi, D. Bao, Y. Fan, and B. Wu, "The asymptotic equipartition property of Markov chains in single infinite Markovian environment on countable state space," *Stochastics*, vol. 91, no. 6, pp. 945–957, 2019.

[22] C. G. Wan, "The strong law of large numbers for function of Markov chain in Markovian environment," *Application Probability and Statistics*, vol. 19, pp. 1545–2160, 2003.

[23] Y. Q. Li, "The strong law of large numbers for function of Markov chain in Markovian environment with countable state," *Journal of Mathematics*, vol. 23, pp. 484–490, 2003.

[24] M. L. Guo, "The strong law of large numbers for Markov chain in double infinite environments," *Mathematica Applicata*, vol. 18, pp. 174–180, 2005.

[25] L. Liu and C. G. Wan, "Strong convergence for weighted sums of Markov chains in bi-infinite environments," *Journal of Applied Probability and Statistics*, vol. 28, pp. 12–20, 2012.

[26] C. G. Wan, "The strong convergence of weighted sums of function for finite state Markov chains in single infinitely Markovian environments," *Journal of Applied Probability and Statistics*, vol. 29, pp. 633–641, 2013.

[27] Y. Yang and K. C. Yuen, "Finite-time and infinite-time ruin probabilities in a two-dimensional delayed renewal risk model with Sarmanov dependent claims," *Journal of Mathematical Analysis and Applications*, vol. 442, no. 2, pp. 600–626, 2016.

[28] Y. Yang, W. Su, and Z. Zhang, "Estimating the discounted density of the deficit at ruin by Fourier cosine series expansion," *Statistics & Probability Letters*, vol. 146, pp. 147–155, 2019.

[29] W. Yu, Y. Yong, G. Guan, Y. Huang, W. Su, and C. Cui, "Valuing guaranteed minimum death benefits by cosine series expansion," *Mathematics*, vol. 7, no. 9, p. 835, 2019.

[30] Z. M. Zhang, Y. D. Yong, and W. G. Yu, "Valuing equity-linked death benefits in general exponential Lévy models," *Journal of Computational and Applied Mathematics*, vol. 365, Article ID 112377, 2020.

[31] Y. Yang, T. Jiang, K. Wang, and K. C. Yuen, "Interplay of financial and insurance risks in dependent discrete-time risk models," *Statistics and Probability Letters*, vol. 162, Article ID 108752, 2020.

[32] W. Yu, P. Guo, Q. Wang et al., "On a periodic capital injection and barrier dividend strategy in the compound Poisson risk model," *Mathematics*, vol. 8, no. 4, p. 511, 2020.

[33] W. G. Yu, F. Wang, Y. J. Huang, and H. D. Liu, "Social optimal mean field control problem for population growth model," *Asian Journal of Control*, pp. 1–8, 2019.

[34] Y. L. Wu and X. T. Wu, "The strong law of large numbers for function of Markov chain in Markovian environment," *Journal of Mathematics*, vol. 27, pp. 579–586, 2013.

Hindawi
Mathematical Problems in Engineering
Volume 2020, Article ID 9489612, 8 pages
https://doi.org/10.1155/2020/9489612

Research Article

Ruin Problems of Multidimensional Risk Models under Constant Interest Rates and Dependent Risks with Heavy Tails

Xinmei Shen , Meng Yuan, and Dawei Lu

School of Mathematical Sciences, Dalian University of Technology, Dalian 116024, China

Correspondence should be addressed to Xinmei Shen; xshen@dlut.edu.cn

Received 10 February 2020; Accepted 16 March 2020; Published 27 April 2020

Guest Editor: Wenguang Yu

Consider a discrete-time multidimensional risk model with constant interest rates where capital transfers between lines are partially allowed over each period. By assuming a large initial capital and regularly varying distributions for the losses, we derive asymptotic estimates for the ruin probability under some dependence structure and study the optimal allocation of the initial reserve. Some numerical simulations are provided to illuminate our main results.

1. Introduction

Consider an insurer with multiple business lines against catastrophic risks (e.g., earthquakes, floods, hurricane, or terrorist attacks). The eventual occurrence of these events usually has a substantial effect on some lines of business simultaneously. Thus, the statistical dependence among claims in these business lines should be considered. Moreover, the insurer may allow restricted capital transfers to reduce the risk of ruin in insurance practice. Particularly, the surplus of those profitable lines is partially allowed to be transferred to cover the total deficit of the other lines in deficit.

The reserve of the insurer can be described as the following multidimensional discrete-time risk model:

$$\mathbf{U}_0 = \begin{pmatrix} ub_1 \\ ub_2 \\ \vdots \\ ub_d \end{pmatrix},$$
$$\mathbf{U}_l = \begin{pmatrix} U_{1,l} \\ U_{2,l} \\ \vdots \\ U_{d,l} \end{pmatrix} = \begin{pmatrix} \left(U_{1,l-1} + e_{1,l-1}\right)\left(1+\rho_l\right) - Z_{1,l} \\ \left(U_{2,l-1} + e_{2,l-1}\right)\left(1+\rho_l\right) - Z_{2,l} \\ \vdots \\ \left(U_{d,l-1} + e_{d,l-1}\right)\left(1+\rho_l\right) - Z_{d,l} \end{pmatrix}, \quad l = 1, 2, \ldots, \tag{1}$$

where $u \geq 0$ is the global initial reserve, $b_i \in [0,1]$ is the proportion of capital allocated to the i-th business line so that $\sum_{i=1}^{d} b_i = 1$, and the constant interest rate over the l-th period is denoted by $\rho_l\,(\rho_l > -1)$ and $\rho_0 = 0$. For an insurer with $d\,(d \geq 2)$ lines of business, suppose now that the claim size with finite mean is denoted by $Z_{i,l}$ and the constant premium income is $e_{i,l-1}\,(e_{i,l-1} = (1+\lambda)EZ_{i,l}, \lambda > 0)$ from the i-th business line over the l-th period, that is, the claims are paid at the end of each period while the premiums are paid at the beginning of each period.

Throughout this paper, for the conciseness in expression, we shall mainly formulate our problems in a vector notation. Unless otherwise stated, random vectors and real vectors will be written as bold letters and will be assumed to be d-dimensional. For example, $\mathbf{X} = (X_1, \ldots, X_d)^T$ and the L_1 norm $\|\mathbf{X}\| = |X_1| + \cdots + |X_d|$. Particularly, we also use a bold Arabic number to stand for the vector with all components being that number, e.g., $\mathbf{1} = (1, \ldots, 1)^T$, $\mathbf{0} = (0, \ldots, 0)^T$. For two vectors $\mathbf{a}$ and $\mathbf{b}$ of the same dimension, we understand relations such as $\mathbf{a} \geq \mathbf{b}$ and $\mathbf{a} \pm \mathbf{b}$ as componentwise. Additionally, the scalar multiplication is defined as usual, i.e., $y\mathbf{a} = (ya_1, \ldots, ya_d)^T$ with y being a real number. Furthermore, for a set K and any real number u, $uK = \{u\mathbf{x}\colon \mathbf{x} \in K\}$.

Let

$$y_l = \prod_{k=0}^{l} \left(1+\rho_k\right)^{-1}, \quad l = 0, 1, \ldots, \tag{2}$$

which stand for the discount factors. With the above conventions, multidimensional risk model (1) can be rewritten as

$$\mathbf{U}_l = y_l^{-1}\left(u\mathbf{b} - \sum_{k=1}^{l}\left(\mathbf{Z}_k y_k - \mathbf{e}_{k-1} y_{k-1}\right)\right), \quad l = 1, 2, \ldots. \tag{3}$$

Ruin theory is a hot topic in risk theory and has been widely studied, for example, valuing death benefits of a Lévy model was studied by Yu et al. [1] and Zhang et al. [2]; the compound Poisson risk model with threshold dividend strategy was considered by Peng et al. [3] and Yu et al. [4]; and the compound Poisson risk model with discounted penalty function was considered by Ruan et al. [5]. In the classical risk theory, ruin probabilities with respect to the unidimensional risk process have been intensively investigated in the past decades. However, the unidimensional risk models cannot provide the whole picture for assessing the solvency ability of an insurer with multiple business lines, and the study on ruin probabilities of the multidimensional risk model has become a hot topic recently. Compared to fruitful results on the study of the unidimensional risk model, the investigation for the multidimensional risk model is quite limited. During the few works, Collamore [6, 7] addressed the multidimensional ruin problems with the general ruin set and studied the sampling techniques in a light-tailed case. Picard et al. [8] introduced a multidimensional discrete-time model and developed a sample recursive method for numerical evaluation of the corresponding ruin probability. Hult et al. [9] firstly studied the ruin probability for multidimensional heavy-tailed processes. Subsequently, under the assumption that the claim size vectors have multivariate regularly varying distribution, Hult and Lindskog [10] derived the asymptotic decay of the ruin probability as the initial capital tends to infinity and analysed the impact of rules for capital transfer on ruin probability. Biard et al. [11] extended some asymptotic results on finite-time probabilities with heavy-tailed claim sizes for the renewal risk model, in which the assumption of independence and stationarity was relaxed. Recently, Huang et al. [12] considered a discrete-time multidimensional risk model with the assumption of regularly varying distribution for net losses and established asymptotic estimates for finite-time ruin probabilities in terms of the upper tail dependence function. Under the framework of heavy-tailed and non-identically distributed claim sizes with some dependence structure, Li et al. [13] focused on the finite-time ruin probability of the continuous-time multidimensional model in which capital transfers were partially allowed, and they studied the optimal allocation of the initial reserve. For more recent studies on bidimensional risk models with heavy-tailed distribution about the ruin problem, see Yang and Yuen [14]; Yang et al. [15]; Chen and Yang [16]; Chen et al. [17]; Cheng and Yu [18], and Yang et al. [19], among many others.

Motivated by Li et al. [13], we consider the following ruin probability that the total surplus of a fraction of each profitable line fails to cover the total deficit of the others over n periods and the fraction can be different by lines:

$$\psi_{\boldsymbol{\omega}}(u,n) = \mathrm{P}\left(\mathbf{U}_l \in \Gamma_{\boldsymbol{\omega}} \text{ for some } l = 1, \ldots, n \,\middle|\, \mathbf{U}_0 = u\mathbf{b}\right), \tag{4}$$

where the ruin set is defined as follows:

$$\Gamma_{\boldsymbol{\omega}} = \left\{\mathbf{x}\colon \sum_{k=1}^{d} \omega_k (x_k)_+ < \sum_{k=1}^{d} (-x_k)_+\right\}, \tag{5}$$

for some $\boldsymbol{\omega} = (\omega_1, \omega_2, \ldots, \omega_d)^T \in [0,1]^d$, $\mathbf{b} = (b_1, b_2, \ldots, b_d)^T$, and $(x)_+ = \max\{x, 0\}$. The ruin set $\Gamma_{\boldsymbol{\omega}}$ denotes all possible events that the sum of some portions of the corresponding positive lines fails to cover the sum of the negative position of other lines. Particularly, for $\boldsymbol{\omega} = 0$, no transfer is allowed, and the corresponding ruin set $\Gamma_{\mathbf{0}} = \left\{\mathbf{x}\colon \sum_{k=1}^{d}(-x_k)_+ > 0\right\}$ denotes that the surplus of some business lines becomes negative. For $\boldsymbol{\omega} = 1$, the corresponding ruin set $\Gamma_{\mathbf{1}} = \left\{\mathbf{x}\colon \sum_{k=1}^{d} x_k < 0\right\}$ denotes the total surplus of all lines becomes negative.

The present paper focuses on establishing asymptotic estimates for ruin probability in a discrete-time model with constant interest rates. Under the assumption that the claim size vector follows a multivariate regularly varying distribution, capital transfers between business lines are partially allowed with different fractions $\{\omega_i \in [0,1], i = 1, \ldots, d\}$ for each line. Furthermore, the obtained asymptotic formula for ruin probability can be used to study the optimal allocation of the initial reserve in order to minimize the ruin probability.

The paper proceeds as follows. After introducing the concepts of multivariate regular variation, Section 2 states the main results for the multidimensional discrete-time risk model and then shows some specific examples for which the underlying dependence assumptions are satisfied. Section 3 proposes applications of the study to obtain the initial reserve allocation. Some numerical simulations on the ruin probability are presented to illuminate the main results in Section 4.

2. Multidimensional Finite-Time Ruin Probability

2.1. Preliminaries. We first recall the concept of regular variation. A positive measurable function $L(\cdot)$ on $[0,\infty)$ is said to be regularly varying at ∞ with regularity index $\rho \in \mathbb{R}$, written as $L \in RV_\rho(\infty)$, if it holds

$$\lim_{t\longrightarrow\infty} \frac{L(tx)}{L(t)} = x^{-\rho}, \quad x > 0. \tag{6}$$

We often suppress the argument ∞ in $RV_\rho(\infty)$ if there is no confusion in the context. Particularly, if $\rho = 0$, then L is said to be slowly varying.

Definition 1. A random vector $\mathbf{X}$ is said to be multivariate regularly varying (MRV) if there exists a nonzero Radon measure μ called intensity measure on $\overline{\mathbb{R}}^d \backslash \{\mathbf{0}\}$ such that

$$\lim_{t \longrightarrow \infty} \frac{P(\mathbf{X} \in tA)}{P(\|\mathbf{X}\| > t)} = \mu(A), \tag{7}$$

for every Borel set $A \subset \overline{\mathbb{R}}^d/\{\mathbf{0}\}$ with $\mu(\partial A) = 0$.

By Theorem 1.14 of Lindskog [20], for such a Radon measure μ, there exists $\alpha > 0$ such that $\mu(tA) = t^{-\alpha}\mu(A)$ holds for any $t > 0$, and each Borel set $A \subseteq \overline{\mathbb{R}}^d \backslash \{\mathbf{0}\}$ with $\mu(\partial A) = 0$. Hence, $\mathbf{X}$ is said to be regularly varying with index α and limiting measure μ meanwhile denoted by $\mathbf{X} \in MRV_{\alpha,\mu}$. The detailed discussions on multivariate regular variation including equivalent statements of MRV and its various applications can be found in Resnick's study [21].

2.2. Assumptions. In the present paper, we focus on risk vectors with MRV tails, comparable marginal tails, and asymptotic independence. Before giving the following assumptions, we have the setting that the claim sizes $\{\mathbf{Z}_l := (Z_{1,l}, \ldots, Z_{d,l})^T, l \geq 1\}$ are independent and identically distributed (i.i.d.) as a generic random vector $\mathbf{Z} = (Z_1, \ldots, Z_d)^T$. For a distribution function $F(x)$, let $\overline{F}(x) = 1 - F(x)$.

Assumption 1. The random vector $\mathbf{Z} \in MRV_{\alpha,\mu}$ for some $\alpha > 1$.

Assumption 2. The random vector $\mathbf{Z}$ has the univariate marginal distributions $F_1, \ldots, F_d$ satisfying $\overline{F}_1(x) \in RV_{-\alpha}$ for some $\alpha > 1$ and

$$\lim_{x \longrightarrow \infty} \frac{\overline{F}_i(x)}{\overline{F}_1(x)} = c_i, \tag{8}$$

for some $0 \leq c_i < \infty, i = 2, \ldots, d$ and $c_1 = 1$.

Remark 1. According to Section 6.5.6 of Resnick [21], if $\mathbf{Z} \in MRV_{\alpha,\mu}$ with univariate marginal distributions $F_1, \ldots, F_d$, then

$$\lim_{x \longrightarrow \infty} \frac{\overline{F}_i(x)}{\overline{F}_j(x)} = \frac{\lambda_i}{\lambda_j}, \tag{9}$$

for some $0 \leq \lambda_i \leq \infty, i = 1, 2, \ldots, d$, which means $\mathbf{Z}$ has comparable marginal tails. Particularly, the case that $\lambda_i = 0$ or ∞ for some $i = 1, 2, \ldots, d$ means some marginal tails are heavier than the others, so the index α of marginal tails may not be the same. But, with some transformation, we can bring it to the standard case of Theorem 6.1 of Resnick [21]. Throughout the paper, without loss of generality, suppose that $0 \leq c_i < \infty, i = 2, \ldots, d$ and $c_1 = 1$ in Assumption 2 which is a special case of the above relation (9). Moreover, $\alpha > 1$ is assumed such that $E(\mathbf{Z})$ can be well defined.

Assumption 3. The components of the random vector $\mathbf{Z}$ are bivariate asymptotically independent, that is,

$$\lim_{x \longrightarrow \infty} P\left(Z_i > x \,\middle|\, Z_j > x\right) = 0, \quad i \neq j. \tag{10}$$

It is well known that the Clayton family of Archimedean copulas with generator $\varphi(u) = (1/\theta)(u^{-\theta} - 1)$ is asymptotically independent for each $\theta > 0$. Other important families of copulas which are asymptotically independent include Gaussian copulas, and Farlie–Gumbel–Morgenstern copulas.

2.3. Main Results. We consider the d-dimensional discrete-time risk model $\mathbf{U}_l$ shown by (3) with the same constant interest rates over one period for all business lines. Due to the impact of interest rates in the above model, some results of the i.i.d. random vector sequence cannot be used directly to derive the asymptotic relation of the ruin probability. Under the assumption that the claim sizes follow a general MRV structure with capital transfer, the following Theorem 1 derives the asymptotic estimate of $\psi_{\boldsymbol{\omega}}(u, n)$.

Theorem 1. *Suppose that the multidimensional risk model $\mathbf{U}_l$ shown by (3) satisfies Assumption 1. Then, for any fixed integer $n \in \mathbb{N}$,*

$$\lim_{u \longrightarrow \infty} \frac{\psi_{\boldsymbol{\omega}}(u, n)}{P(\|\mathbf{Z}\| > u)} = \sum_{m=1}^{n} y_m^{\alpha} \mu(\mathbf{b} - \Gamma_{\boldsymbol{\omega}}). \tag{11}$$

Proof. Note that $u\Gamma_{\boldsymbol{\omega}} = \Gamma_{\boldsymbol{\omega}}$ for every real number $u > 0$, and we obtain

$$\begin{aligned}\psi_{\boldsymbol{\omega}}(u, n) &= P\left(\mathbf{U}_l \in \Gamma_{\boldsymbol{\omega}} \text{ for some } l = 1, \ldots, n \,\middle|\, \mathbf{U}_0 = u\mathbf{b}\right) \\ &\geq P\left(\mathbf{U}_n \in \Gamma_{\boldsymbol{\omega}} \,\middle|\, \mathbf{U}_0 = u\mathbf{b}\right) \\ &= P\left(\sum_{i=1}^{n} (\mathbf{Z}_i y_i - \mathbf{e}_{i-1} y_{i-1}) \in u(\mathbf{b} - \Gamma_{\boldsymbol{\omega}})\right),\end{aligned} \tag{12}$$

where

$$\{\mathbf{b} - \Gamma_{\boldsymbol{\omega}}\} = \left\{\mathbf{x}\colon \sum_{k=1}^{d} \omega_k (b_k - x_k)_+ < \sum_{k=1}^{d} (x_k - b_k)_+\right\}. \tag{13}$$

Since $\mathbf{Z} \in MRV_{\alpha,\mu}$, we have that $\mathbf{Z} - \mathbf{M} \in \mathbb{R}^d$ follows the same $MRV_{\alpha,\mu}$ structure where $\mathbf{M}$ is a constant vector. Note that $\mu(\partial\{\mathbf{b} - \Gamma_{\boldsymbol{\omega}}\}) = 0$. Then, we shall apply Proposition A.1 of Hult and Lindskog [22] to obtain

$$\begin{aligned}&\liminf_{u \longrightarrow \infty} \frac{\psi_{\boldsymbol{\omega}}(u, n)}{P(\sum_{i=1}^{n} \mathbf{Z}_i y_i \in u(\mathbf{b} - \Gamma_{\boldsymbol{\omega}}))} \\ &\quad \geq \liminf_{u \longrightarrow \infty} \frac{P(\sum_{i=1}^{n} (\mathbf{Z}_i y_i - \mathbf{e}_{i-1} y_{i-1}) \in u(\mathbf{b} - \Gamma_{\boldsymbol{\omega}}))}{P(\sum_{i=1}^{n} \mathbf{Z}_i y_i \in u(\mathbf{b} - \Gamma_{\boldsymbol{\omega}}))} = 1.\end{aligned} \tag{14}$$

On the contrary, denote

$$\widetilde{U}_l = y_l^{-1}\left(u\mathbf{b} - \sum_{k=1}^{l} \mathbf{Z}_k y_k\right), \quad l = 1, 2, \ldots, n. \tag{15}$$

Now, we have

$$\psi_{\boldsymbol{\omega}}(u, n) \leq P\left(\widetilde{U}_l \in \Gamma_{\boldsymbol{\omega}} \text{ for some } l = 1, \ldots, n \,\middle|\, \mathbf{U}_0 = u\mathbf{b}\right). \tag{16}$$

Note that $\{\widetilde{U}_i \in \Gamma_{\boldsymbol{\omega}}, i = 1, 2, \ldots, n\}$ is a nondecreasing sequence of events. Then, we have

$$\begin{aligned}\psi_{\boldsymbol{\omega}}(u, n) &\leq P\left(\widetilde{U}_n \in \Gamma_{\boldsymbol{\omega}} \,\middle|\, \mathbf{U}_0 = u\mathbf{b}\right) \\ &= P\left(\sum_{i=1}^{n} \mathbf{Z}_i y_i \in u\left(\mathbf{b} - \Gamma_{\boldsymbol{\omega}}\right)\right).\end{aligned} \tag{17}$$

Therefore,

$$\limsup_{u\longrightarrow\infty} \frac{\psi_{\boldsymbol{\omega}}(u, n)}{P\left(\sum_{i=1}^{n} \mathbf{Z}_i y_i \in u\left(\mathbf{b} - \Gamma_{\boldsymbol{\omega}}\right)\right)} \leq 1. \tag{18}$$

Combining (14) and (18) implies that

$$\lim_{u\longrightarrow\infty} \frac{\psi_{\boldsymbol{\omega}}(u, n)}{P\left(\sum_{i=1}^{n} \mathbf{Z}_i y_i \in u\left(\mathbf{b} - \Gamma_{\boldsymbol{\omega}}\right)\right)} = 1. \tag{19}$$

Finally, we apply Proposition A.1 of Hult and Lindskog [22] to derive that, for $u \longrightarrow \infty$,

$$\begin{aligned}\lim_{u\longrightarrow\infty} \frac{\psi_{\boldsymbol{\omega}}(u, n)}{P(\|\mathbf{Z}\| > u)} &= \lim_{u\longrightarrow\infty} \frac{P\left(\sum_{i=1}^{n} \mathbf{Z}_i y_i \in u\left(\mathbf{b} - \Gamma_{\boldsymbol{\omega}}\right)\right)}{P(\|\mathbf{Z}\| > u)} \\ &= \sum_{i=1}^{n} y_i^{\alpha} \mu\left(\mathbf{b} - \Gamma_{\boldsymbol{\omega}}\right).\end{aligned} \tag{20}$$

We obtain the desired result. ☐

Next, under the assumptions of asymptotic independence and comparable marginal tails, the following Proposition 1 gives a more explicit asymptotic estimate of the ruin probability.

Proposition 1. *Suppose that the multidimensional risk model* $\mathbf{U}_l$ *shown by (3) satisfies Assumptions 2 and 3. Then, for any fixed integer* $n \in \mathbb{N}$,

$$\lim_{u\longrightarrow\infty} \frac{\psi_{\boldsymbol{\omega}}(u, n)}{\overline{F}_1(u)} = \sum_{m=1}^{n} y_m^{\alpha} \sum_{i=1}^{d} c_i \left(b_i + \sum_{k\neq i}^{d} \omega_k b_k \right)^{-\alpha}. \tag{21}$$

Proof. Firstly, going along the same lines of the proofs of Lemma 3.2 of Li et al. [13] but with some modifications due to Assumption 2, by the inclusion-exclusion principle and Assumption 3, for any $\mathbf{x} > \mathbf{0}$,

$$\lim_{t\longrightarrow\infty} \frac{P\left(\mathbf{X}/t \in [\mathbf{0}, \mathbf{x}]^c\right)}{P\left(\mathbf{X}/t \in [\mathbf{0}, \mathbf{1}]^c\right)} = \lim_{t\longrightarrow\infty} \frac{P\left(\cup_{i=1}^{d} \{X_i > t x_i\}\right)}{P\left(\cup_{i=1}^{d} \{X_i > t\}\right)} = \frac{\sum_{i=1}^{n} c_i x_i^{-\alpha}}{\sum_{i=1}^{n} c_i}. \tag{22}$$

Then, by Theorem 6.1 of Resnick [21], we have $\mathbf{Z} \in MRV_{\alpha,\mu}$.

Next, according to Resnick [21], Assumption 3 means that μ puts zero mass in the interior of the positive quadrant, that is, the measure μ is concentrated on each axis. Thus,

$$\begin{aligned}\mu\left(\mathbf{b} - \Gamma_{\boldsymbol{\omega}}\right) &= \mu\left(\left\{ \mathbf{x}\colon \sum_{k=1}^{d} \omega_k \left(b_k - x_k\right)_+ < \sum_{k=1}^{d} \left(x_k - b_k\right)_+ \right\} \right) \\ &= \mu\left(\left\{ \mathbf{x}\colon \bigcup_{i=1}^{d} \left\{ x_i > b_i + \sum_{k\neq i}^{d} \omega_k b_k \right\} \right\} \right).\end{aligned} \tag{23}$$

Then, we shall apply Assumption 2 in the third step of the following display to obtain

$$\begin{aligned}\mu\left(\mathbf{b} - \Gamma_{\boldsymbol{\omega}}\right) &= \sum_{i=1}^{d} \mu\left(\left\{ \mathbf{x}\colon x_i > b_i + \sum_{k\neq i}^{d} \omega_k b_k \right\} \right) \\ &= \sum_{i=1}^{d} \lim_{u\longrightarrow\infty} \frac{P\left(Z_i > u\left(b_i + \sum_{k\neq i}^{d} \omega_k b_k\right)\right)}{P(\|\mathbf{Z}\| > u)} \\ &= \sum_{i=1}^{d} c_i \left(b_i + \sum_{k\neq i}^{d} \omega_k b_k \right)^{-\alpha} \lim_{u\longrightarrow\infty} \frac{\overline{F}_1(u)}{P(\|\mathbf{Z}\| > u)}.\end{aligned} \tag{24}$$

Combining Theorem 1 and (24), we obtain the desired result. ☐

2.4. Examples. In this section, we propose to use a copula to model the dependence among the components of the claim size vector with a continuous joint distribution. The following two examples take the form of excess of loss ratio reinsurance and proportional reinsurance policy, respectively.

Example 1. Suppose that an insurer with d lines of business purchases a proportional reinsurance policy, and the reinsurer takes a stated percentage share of each policy that the insurer issues. Particularly, under quota share arrangement, a fixed proportion of each business line is reinsured, that is, the insurer retains proportion $\boldsymbol{\eta} = (\eta_1, \eta_2, \ldots, \eta_d)^T \in (0, 1)^d$ of the claim sizes. Suppose the claim size vectors are i.i.d. as a generic random vector $\mathbf{Z} = (Z_1, \ldots, Z_d)^T$ which meets the following conditions:

(1) The components of $\mathbf{Z}$ follow the Pareto distribution for shape parameter $\alpha > 1$ and especially $Z_i \sim$ Pareto (γ_i, α) for some $\gamma_i > 0$, $i = 1, \ldots, d$, that is,

$$F_i(x_i) = \begin{cases} 0, & x_i < \gamma_i, \\ 1 - \left(\dfrac{\gamma_i}{x_i}\right)^{\alpha}, & x_i \geq \gamma_i. \end{cases} \tag{25}$$

(2) The underlying copula of $\mathbf{Z}$ is a Clayton copula with generator $\varphi(u) = (1/2)(u^{-2} - 1)$.

It is easy to verify that $\mathbf{Z}$ has the joint distribution

$$G(\mathbf{x}) = \left(1 - d + \sum_{i=1}^{d} F_i^{-2}(x_i) \right)^{-(1/2)}, \quad x_i > 0,\ i = 1, \ldots, d, \tag{26}$$

and the components of $\mathbf{Z}$ are tail equivalent and bivariate asymptotically independent. Let $\widetilde{Z} = (\eta_1 Z_1, \eta_2 Z_2, \ldots, \eta_d Z_d)^T$. Under the reinsurance policy, the claim sizes that the insurer should pay are i.i.d. as the random vector $\widetilde{Z}$. The distributions of the components of $\widetilde{Z}$ are still tail equivalent, and the dependence structure of $\widetilde{Z}$ is the same as $\mathbf{Z}$. Thus, according to Proposition 1, when the initial reserve u is large enough, the asymptotic estimate of ruin probability of the insurer under quota share arrangement is

$$\psi_{\boldsymbol{\omega}}(u,n) \sim \sum_{m=1}^{n} y_m^{\alpha} \sum_{i=1}^{d} \gamma_i^{\alpha} \eta_i^{\alpha} \left(b_i + \sum_{k\neq i}^{d} \omega_k b_k \right)^{-\alpha} u^{-\alpha}. \quad (27)$$

Similarly, the asymptotic estimate of ruin probability of the reinsurer under quota share arrangement is

$$\psi_{\widetilde{\omega}}(\widetilde{u},n) \sim \sum_{m=1}^{n} y_m^{\alpha} \sum_{i=1}^{d} \gamma_i^{\alpha} (1-\eta_i)^{\alpha} \left(\widetilde{b}_i + \sum_{k\neq i}^{d} \widetilde{\omega}_k \widetilde{b}_k \right)^{-\alpha} \widetilde{u}^{-\alpha}, \quad (28)$$

where $\widetilde{u}$, $\widetilde{\omega} = (\widetilde{\omega}_1, \widetilde{\omega}_2, \ldots, \widetilde{\omega}_d)^T$, and $\widetilde{b} = (\widetilde{b}_1, \widetilde{b}_2, \ldots, \widetilde{b}_d)^T$ are the initial reserve, the capital transfer ratio vector, and the allocation vector for the reinsurer, respectively.

Example 2. Suppose that the reinsurer sells an excess of loss ratio reinsurance policy to an insurer with d lines of business. The reinsurer only pays out if the total claims suffered by the insurer in a given period exceed a predetermined loss ratio $\boldsymbol{\eta} = (\eta_1, \eta_2, \ldots, \eta_d)^T \in (0,1)^d$ of the premium $\mathbf{e} = (e_1, e_2, \ldots, e_d)^T$ collected by the insurer, that is, the reinsurer has agreed to bear any balance so that the insurer's gross loss ratio is maintained at $\boldsymbol{\eta}$. Suppose the claim size vectors are i.i.d. as a generic random vector $\mathbf{Z} = (Z_1, \ldots, Z_d)^T$ with $Z_i \sim \text{Pareto}(\gamma_i, \alpha)$ for some $\gamma_i > 0$, $i = 1, \ldots, d$, and $\mathbf{Z}$ has the joint distribution

$$G(\mathbf{x}) = \left(1 + \theta \prod_{i=1}^{d} \overline{F}_i(x_i) \right) \prod_{i=1}^{d} F_i(x_i), \quad \theta \in [-1,1], \quad (29)$$

which implies that the underlying copula of $\mathbf{Z}$ is a Farlie–Gumbel–Morgenstern copula. It is clear that the components of $\mathbf{Z}$ are tail equivalent and bivariate asymptotically independent. So, the claim sizes that the reinsurer affords are i.i.d. as $\widetilde{Z} = ((Z_1 - \eta_1 e_1)_+, (Z_2 - \eta_2 e_2)_+, \ldots, (Z_d - \eta_d e_d)_+)^T$. The distributions of the components of $\widetilde{Z}$ are still tail equivalent, and the dependence structure of $\widetilde{Z}$ is the same as $\mathbf{Z}$. According to Proposition 1, when the initial reserve u is large enough, the asymptotic estimate of ruin probability of the reinsurer under excess of loss ratio reinsurance is

$$\psi_{\boldsymbol{\omega}}(u,n) \sim \sum_{m=1}^{n} y_m^{\alpha} \sum_{i=1}^{d} \gamma_i^{\alpha} \left(b_i + \sum_{k\neq i}^{d} \omega_k b_k \right)^{-\alpha} u^{-\alpha}. \quad (30)$$

From the above formula, we can observe that the excess of loss ratio $\boldsymbol{\eta}$ has no effect on reducing risk for the reinsurer, and they may turn to the other types of reinsurance such as quota share arrangement or design the capital transfer ratio $\boldsymbol{\omega}$ and the allocation $\mathbf{b}$.

3. Initial Reserve Allocation

In this section, the optimal allocation of the initial reserve is investigated. For some similar discussions on the optimization problem in insurance, see Biard [23]; Li et al. [13]; and Yu et al. [24], among many others. Suppose that the insurer owns a global initial reserve u to allocate to d lines of business. Let $b_i \in [0,1]$ be the proportion of capital allocated to the i-th business line. To minimize the asymptotic finite-time ruin probability, we have to find the optimal allocation of the initial reserve u. The problem can be formulated as the computation of the following optimization problem:

$$\min_{\mathbf{b}\in[0,1]^d} \psi_{\boldsymbol{\omega}(u,n)} \quad \text{s.t.} \sum_{i=1}^{d} b_i = 1. \quad (31)$$

According to Proposition 1, when the initial reserve u is large enough,

$$\psi_{\boldsymbol{\omega}}(u,n) \sim \overline{F}_1(u) \left(\sum_{m=1}^{n} y_m^{\alpha} \sum_{i=1}^{d} c_i \left(b_i + \sum_{k\neq i}^{d} \omega_k b_k \right)^{-\alpha} \right). \quad (32)$$

Given $\boldsymbol{\omega} = (\omega_1, \ldots, \omega_d)^T \in [0,1]^d$, it is sufficient to find the minimizer in $[0,1]^d$ of the following function

$$f(b_1, \ldots, b_d) = \sum_{i=1}^{d} c_i \left(b_i + \sum_{k\neq i}^{d} \omega_k b_k \right)^{-\alpha}, \quad (33)$$

where $\sum_{i=1}^{d} b_i = 1$.

First, consider the case that the insurer owns only two business lines with the same interest rate over one period.

Proposition 2. *Suppose that the risk model*

$$\mathbf{U}_l = \begin{pmatrix} y_l^{-1}\left(ub_1 - \sum_{k=1}^{l} \left(Z_{1,k} y_k - e_{1,k-1} y_{k-1} \right) \right) \\ y_l^{-1}\left(ub_2 - \sum_{k=1}^{l} \left(Z_{2,k} y_k - e_{2,k-1} y_{k-1} \right) \right) \end{pmatrix}, \quad l = 1, 2, \ldots, \quad (34)$$

satisfies Assumptions 2 and 3. For $\omega_1, \omega_2 \in [0,1]$ and $\alpha > 1$,

(a) *If $\omega_2 = \omega_1 = 1$, then any $b_1 \in [0,1]$ is the optimal solution for the problem of (31).*

(b) *If $\omega_2 \neq 1$ or $\omega_1 \neq 1$, then the problem of (31) has the optimal solution*

$$b^* = \begin{cases} 0, & a > \dfrac{1}{\omega_2} \text{ or } \omega_2 = 1, \\ \dfrac{1 - a\omega_2}{1 - a\omega_2 + a - \omega_1}, & \omega_1 \le a \le \dfrac{1}{\omega_2}, \\ 1, & a < \omega_1 \text{ or } \omega_1 = 1, \end{cases} \quad (35)$$

with $a = (c_2(1-\omega_1)/c_1(1-\omega_2))^{(1/\alpha+1)}$.

Proof. By Proposition 1, it suffices to find the critical points in $[0,1]$ of the following function:

$$L(b_1) = c_1(b_1 + \omega_2 b_2)^{-\alpha} + c_2(b_2 + \omega_1 b_1)^{-\alpha}$$
$$= c_1(\omega_2 + (1-\omega_2)b_1)^{-\alpha} + c_2(1 + (\omega_1 - 1)b_1)^{-\alpha}. \tag{36}$$

Let $L(x) = c_1(\omega_2 + (1-\omega_2)x)^{-\alpha} + c_2(1 + (\omega_1 - 1)x)^{-\alpha}$; then, we have

$$\frac{\partial L(x)}{\partial x} = (-\alpha)\left[c_1(\omega_2 + (1-\omega_2)x)^{-\alpha-1}(1-\omega_2) + c_2(1 + (\omega_1 - 1)x)^{-\alpha-1}(\omega_1 - 1)\right]. \tag{37}$$

For $\omega_2 = \omega_1 = 1$, we have $L(x) = c_1 + c_2$; thus, any $x \in [0,1]$ is the optimal solution.

We now consider the case $\omega_1 \neq 1$ or $\omega_2 \neq 1$. Note that $a = (c_2(1-\omega_1)/c_1(1-\omega_2))^{(1/\alpha+1)}$.

For $a > (1/\omega_2)$ or $\omega_2 = 1$, the function $L(x)$ increases in $x \in [0,1]$ and takes minimum at $x = 0$.

For $\omega_1 \leq a \leq (1/\omega_2)$, we have $(\partial L(x)/\partial x) < 0$ in $x \in [0, x^*)$ and $(\partial L(x)/\partial x) > 0$ in $x \in (x^*, 1]$, where $x^* = (1 - a\omega_2/1 - a\omega_2 + a - \omega_1)$. Thus, the function $L(x)$ is minimized at x^*.

For $a < \omega_1$ or $\omega_1 = 1$, $L(x)$ decreases in $x \in [0,1]$ and takes minimum at $x = 1$. □

We now move forward to the general case. The optimal solution for the problem must exist because the Hessian matrix of $f(b_1, \ldots, b_d)$ can be expressed as $\alpha(\alpha+1)\mathbf{W}[\mathbf{C}\mathbf{H}^{-\alpha-2}]\mathbf{W}^T$ which is positively definite in $[0,1]^d$, where $h_i = b_i + \sum_{k\neq i}^d \omega_k b_k$, $i = 1, \ldots, d$ and

$$\mathbf{W} = \begin{pmatrix} 1 & \omega_1 & \omega_1 & \ldots & \omega_1 \\ \omega_2 & 1 & \omega_2 & \ldots & \omega_2 \\ \omega_3 & \omega_3 & 1 & \ldots & \omega_3 \\ \vdots & \vdots & \vdots & \ddots & \vdots \\ \omega_d & \omega_d & \omega_d & \ldots & 1 \end{pmatrix}_{d\times d},$$
$$\mathbf{C} = \begin{pmatrix} c_1 & 0 & \ldots & 0 \\ 0 & c_2 & \ldots & 0 \\ \vdots & \vdots & \ddots & \vdots \\ 0 & 0 & \ldots & c_d \end{pmatrix}_{d\times d}, \tag{38}$$
$$\mathbf{H} = \begin{pmatrix} h_1 & 0 & \ldots & 0 \\ 0 & h_2 & \ldots & 0 \\ \vdots & \vdots & \ddots & \vdots \\ 0 & 0 & \ldots & h_d \end{pmatrix}_{d\times d}.$$

Subject to the equality constraint $\sum_{i=1}^d b_i = 1$, the method of Lagrange multipliers is a good strategy to find the minimum of the function $f(b_1, \ldots, b_d)$. The optimal solution in $(0,1)^d$ for the general case is given in Proposition 3 in the following. See also Proposition 4.2 of Li et al. [13] for the similar result. The algorithm was sketched to reach the optimal solution of allocation $\mathbf{b}$ in Li et al. [13].

Proposition 3. *Under Assumptions 2 and 3, if* $(\mathbf{W}^T)^{-1}(\mathbf{C}^{-1}\mathbf{W}^{-1}\mathbf{1}^T)^{-(1/\alpha+1)} > \mathbf{0}$ *and* $\mathbf{C}^{-1}\mathbf{W}^{-1}\mathbf{1}^T > \mathbf{0}$, *then the optimal solution in* $(0,1)^d$ *for problem (31) can be expressed as*

$$\mathbf{b}^* = \frac{(\mathbf{W}^T)^{-1}(\mathbf{C}^{-1}\mathbf{W}^{-1}\mathbf{1}^T)^{-(1/\alpha+1)}}{\mathbf{1}(\mathbf{W}^T)^{-1}(\mathbf{C}^{-1}\mathbf{W}^{-1}\mathbf{1}^T)^{-(1/\alpha+1)}}. \tag{39}$$

Proof. Going along the same lines of the proofs of Proposition 4.2 of Li et al. [13] but with some obvious modifications, we can prove Proposition 3 immediately. Thus, we omit the details here. □

4. Numerical Studies

In this section, we conduct numerical studies to examine the accuracy of the asymptotic relations. We choose the Clayton copula with generator $\varphi(u) = (1/2)(u^{-2} - 1)$. Assume that the claim size vectors are i.i.d. as $\mathbf{Z}$ whose components follow the Pareto distribution for shape parameter $\alpha > 1$, and especially, $Z_1 \sim \text{Pareto}(1, 1.5)$. With the settings above, $\mathbf{Z}$ has the joint distribution

$$G(\mathbf{x}) = \left(-2 + \sum_{i=1}^{3} F_i^{-2}(x_i)\right)^{-1/2}, \quad x_i > 0,\ i = 1,2,3. \tag{40}$$

Various parameters are set to be $\boldsymbol{\omega} = (\omega_1, \omega_2, \omega_3)^T = (0.5, 0.5, 0.5)^T$, $\mathbf{b} = (b_1, b_2, b_3)^T = (0.3, 0.4, 0.3)^T$, $c_1 = 1$, $c_2 = 0.9$, and $c_3 = 1.3$. The premium charged is assumed to be $1.2E(Z_i)$, $i = 1,2,3$.

We generate samples in the R environment using the copula package, and the ruin probability is obtained by crude Mote Carlo simulation. Letting insurance period $n = 10$, we compare asymptotic estimate given by (21) and $\psi_{\boldsymbol{\omega}}(u, n)$ by a simulation of 1,000,000 rounds on the left and show their ratios on the right in Figure 1. As is seen, the asymptotic estimate and the ruin probability are relatively close on the left, and the ratios do converge to 1 on the right when u is less than 4000. However, the ratio of Figure 1 seems not to converge to 1 when u goes to infinity. Our explanation for the phenomenon is the limitation of crude Mote Carlo simulation since the ruin probability becomes too small as u goes to infinity. With the sample size being increased to 10,000,000 in Figure 2, the convergence of ratio is much improved compared with Figure 1. In conclusion, the convergence is stable, and this confirms the efficiency of the asymptotic estimate in Proposition 1.

Next, we turn to consider the optimal allocation of the initial reserve given $\boldsymbol{\omega} = (\omega_1, \omega_2, \omega_3)^T = (0.5, 0.5, 0.5)^T$ and $c_1 = c_2 = c_3 = 1$. Under different initial reserves with different allocations $\mathbf{b}$, Table 1 lists ruin probabilities by a simulation of 1,000,000 rounds of the case $n = 10$ and the case $n = 30$, respectively. It is easy to verify that $b^* = ((1/3), (1/3), (1/3))^T$ is the optimal allocation by Proposition 3. As is seen in Table 1, the ruin probability achieves the smallest value at b^* with different initial reserves u in both cases.

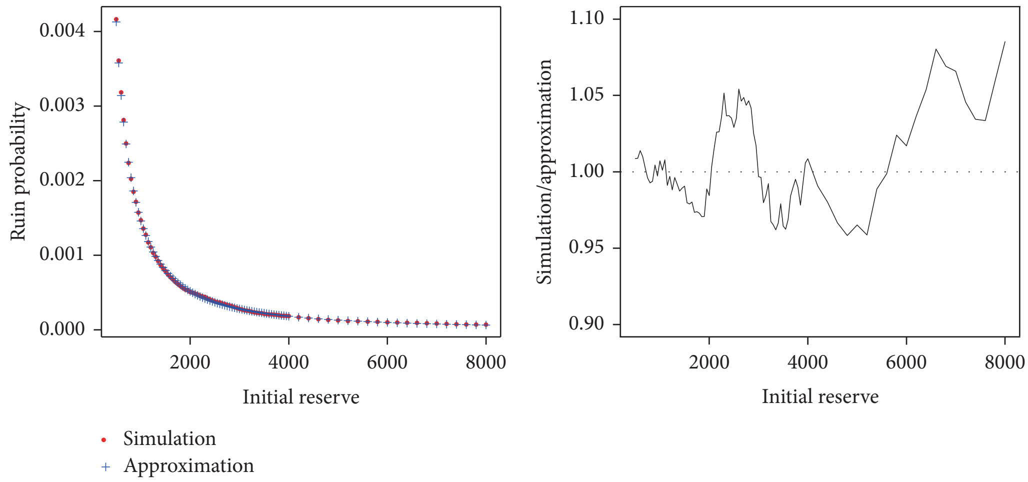

(a) (b)

Figure 1: Comparison of estimates and approximate of ruin probability ($n = 10$, 1,000,000 rounds).

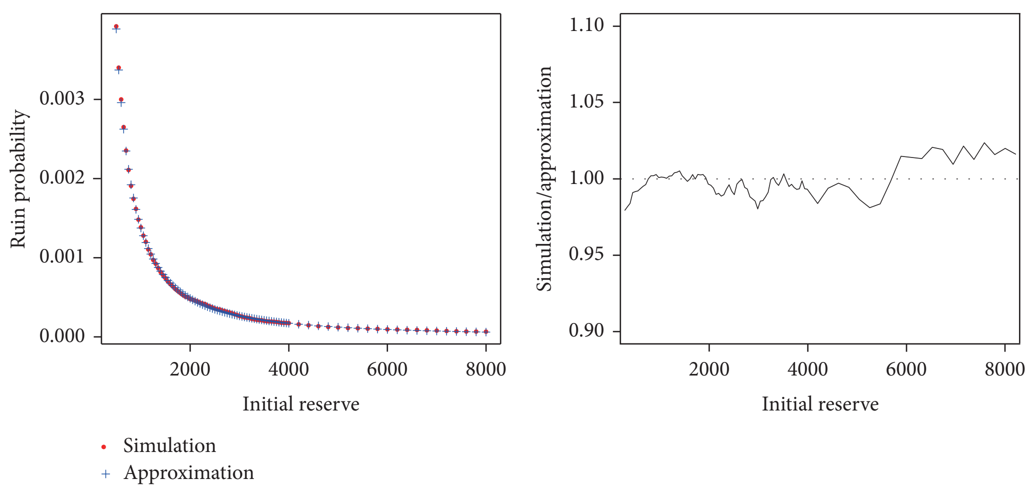

(a) (b)

Figure 2: Comparison of estimates and approximate of ruin probability ($n = 10$, 10,000,000 rounds).

Table 1: Ruin probability under allocation of **b**.

Insurance period	Initial reserve	Allocation of **b**				
		$((1/3), (1/3), (1/3))^T$	$(0.4, 0.3, 0.3)^T$	$(0.5, 0.2, 0.3)^T$	$(0.2, 0.6, 0.2)^T$	$(0.1, 0.4, 0.5)^T$
10	1000	0.001081	0.001092	0.001104	0.001110	0.001134
	3000	0.000192	0.000193	0.000198	0.000209	0.000204
	5000	0.000076	0.000076	0.000077	0.000078	0.000087
30	1000	0.001860	0.001877	0.001919	0.001914	0.001938
	3000	0.000379	0.000384	0.000382	0.000393	0.000385
	5000	0.000160	0.000161	0.000166	0.000168	0.000169

Data Availability

All data included in this study are available upon request by contact with the corresponding author.

Conflicts of Interest

The authors declare that they have no conflicts of interest.

Acknowledgments

This work was supported by the National Natural Science Foundation of China under Grant 11571058, by Humanities and Social Science Foundation of the Ministry of Education of China under Grant 17YJC910007, by Shanghai Municipal Science and Technology Major Project under Grant 2018SHZDZX01 and ZJLab, and by the Fundamental

Research Funds for the Central Universities under Grant DUT20LK27.

References

[1] W. Yu, Y. Yong, G. Guan, Y. Huang, W. Su, and C. Cui, "Valuing guaranteed minimum death benefits by cosine series expansion," *Mathematics*, vol. 7, no. 9, p. 835, 2019.

[2] Z. Zhang, Y. Yong, and W. Yu, "Valuing equity-linked death benefits in general exponential Lévy models," *Journal of Computational and Applied Mathematics*, vol. 365, p. 112377, 2020.

[3] X. Peng, W. Su, and Z. Zhang, "On a perturbed compound Poisson risk model under a periodic threshold-type dividend strategy," *Journal of Industrial & Management Optimization*, vol. 13, no. 5, pp. 1–20, 2017.

[4] W. Yu, Y. Huang, and C. Cui, "The absolute ruin insurance risk model with a threshold dividend strategy," *Symmetry*, vol. 10, no. 9, p. 377, 2018.

[5] J. Ruan, W. Yu, K. Song, Y. Sun, Y. Huang, and X. Yu, "A note on a generalized Gerber-Shiu discounted penalty function for a compound Poisson risk model," *Mathematics*, vol. 7, no. 10, p. 891, 2019.

[6] J. F. Collamore, "Hitting probabilities and large deviations," *The Annals of Probability*, vol. 24, no. 4, pp. 2065–2078, 1996.

[7] J. F. Collamore, "Importance sampling techniques for the multidimensional ruin problem for general Markov additive sequences of random vectors," *The Annals of Applied Probability*, vol. 12, no. 1, pp. 382–421, 2002.

[8] P. Picard, C. Lefèvre, and I. Coulibaly, "Multirisks model and finite-time ruin probabilities," *Methodology and Computing In Applied Probability*, vol. 5, no. 3, pp. 337–353, 2003.

[9] H. Hult, F. Lindskog, T. Mikosch, and G. Samorodnitsky, "Functional large deviations for multivariate regularly varying random walks," *The Annals of Applied Probability*, vol. 15, no. 4, pp. 2651–2680, 2005.

[10] H. Hult and F. Lindskog, "Heavy-tailed insurance protfolios: buffer capital and ruin probabilities," vol. 1441, School of ORIE, Cornall University, Ithaca, NY, USA, 2006, Technical report.

[11] R. Biard, C. Lefèvre, and S. Loisel, "Impact of correlation crises in risk theory: asymptotics of finite-time ruin probabilities for heavy-tailed claim amounts when some independence and stationarity assumptions are relaxed," *Insurance: Mathematics and Economics*, vol. 43, no. 3, pp. 412–421, 2008.

[12] W. Huang, C. Weng, and Y. Zhang, "Multivariate risk models under heavy-tailed risks," *Applied Stochastic Models in Business and Industry*, vol. 30, no. 3, pp. 341–360, 2014.

[13] X. Li, J. Wu, and J. Zhuang, "Asymptotic multivariate finite-time ruin probability with statistically dependent heavy-tailed claims," *Methodology and Computing in Applied Probability*, vol. 17, no. 2, pp. 463–477, 2015.

[14] Y. Yang and K. C. Yuen, "Finite-time and infinite-time ruin probabilities in a two-dimensional delayed renewal risk model with Sarmanov dependent claims," *Journal of Mathematical Analysis and Applications*, vol. 442, no. 2, pp. 600–626, 2016.

[15] Y. Yang, K. C. Yuen, and J.-F. Liu, "Asymptotics for ruin probabilities in Lévy-driven risk models with heavy-tailed claims," *Journal of Industrial & Management Optimization*, vol. 14, no. 1, pp. 231–247, 2018.

[16] Y. Chen and Y. Yang, "Bivariate regular variation among randomly weighted sums in general insurance," *European Actuarial Journal*, vol. 9, no. 1, pp. 301–322, 2019.

[17] Y. Chen, Y. Yang, and T. Jiang, "Uniform asymptotics for finite-time ruin probability of a bidimensional risk model," *Journal of Mathematical Analysis and Applications*, vol. 469, no. 2, pp. 525–536, 2019.

[18] D. Cheng and C. Yu, "Uniform asymptotics for the ruin probabilities in a bidimensional renewal risk model with strongly subexponential claims," *Stochastics*, vol. 91, no. 5, pp. 643–656, 2019.

[19] Y. Yang, K. Wang, J. Liu, and Z. Zhang, "Asymptotics for a bidimensional risk model with two geometric Lévy price processes," *Journal of Industrial & Management Optimization*, vol. 15, no. 2, pp. 481–505, 2019.

[20] F. Lindskog, *Multivariate Extremes and Regular Variation for Stochastic Processes*, Ph. D. thesis, Department of Mathematics, Swiss Federal Institute of Technology, Zurich, Switzerland, 2004.

[21] S. I. Resnick, *Heavy-Tail Phenomena: Probabilistic and Statistical Modeling*, Springer, New York, USA, 2007.

[22] H. Hult and F. Lindskog, "On regular variation for infinitely divisible random vectors and additive processes," *Advances in Applied Probability*, vol. 38, no. 1, pp. 134–148, 2006.

[23] R. Biard, "Asymptotic multivariate finite-time ruin probabilities with heavy-tailed claim amounts: impact of dependence and optimal reserve allocation," *Bulletin Français d'Actuariat, Institut des Actuaires*, vol. 13, no. 26, pp. 79–92, 2013.

[24] W. Yu, F. Wang, Y. Huang, and H. Liu, "Social optimal mean field control problem for population growth model," *Asian Journal of Control*, 2019.

Hindawi
Mathematical Problems in Engineering
Volume 2020, Article ID 7265121, 19 pages
https://doi.org/10.1155/2020/7265121

Research Article

Optimal Reinsurance-Investment Problem under a CEV Model: Stochastic Differential Game Formulation

Danping Li[1] **, Ruiqing Chen,**[1] **and Cunfang Li**[2]

[1] *Key Laboratory of Advanced Theory and Application, Statistics and Data Science-MOE, School of Statistics, East China Normal University, Shanghai 200062, China*
[2] *School of Business, Jiangsu Normal University, Xuzhou, Jiangsu 221000, China*

Correspondence should be addressed to Danping Li; dpli@fem.ecnu.edu.cn

Received 18 February 2020; Accepted 14 March 2020; Published 21 April 2020

Guest Editor: Wenguang Yu

This paper focuses on a stochastic differential game played between two insurance companies, a big one and a small one. In our model, the basic claim process is assumed to follow a Brownian motion with drift. Both of two insurance companies purchase the reinsurance, respectively. The big company has sufficient asset to invest in the risky asset which is described by the constant elasticity of variance (CEV) model and acquire new business like acting as a reinsurance company of other insurance companies, while the small company can invest in the risk-free asset and purchase reinsurance. The game studied here is zero-sum where there is a single exponential utility. The big company is trying to maximize the expected exponential utility of the terminal wealth to keep its advantage on surplus while simultaneously the small company is trying to minimize the same quantity to reduce its disadvantage. In this paper, we describe the Nash equilibrium of the game and prove a verification theorem for the exponential utility. By solving the corresponding Fleming-Bellman-Isaacs equations, we derive the optimal reinsurance and investment strategies. Furthermore, numerical examples are presented to show our results.

1. Introduction

Recently, most insurance companies manage their business by means of reinsurance and investment, which are effective way to spread risk and make profit. Therefore, these have inspired hundred researches. For instance, Schmidli [1], Promislow and Young [2], and Bai and Guo [3] investigated the optimal problems for an insurance company in the case of minimizing the ruin probability. Yang and Zhang [4], Wang [5], and Cao and Wan [6] studied the optimal reinsurance and investment problems of expected utility maximization. The latest researches on insurance and investment management problem can be referred to Yu et al. [7], Zhang et al. [8], Peng et al. [9], Yu et al. [10], Ruan et al. [11], Yu et al. [12], Huang et al. [13], Zeng et al. [14], Li et al. [15] and references therein.

However, most of the literature mentioned above only considered one insurance company, while there are many insurance companies in the market in reality and they compete with each other. Thus, two insurance companies, a big one and a small one, are focused on in this paper. This competition between the two insurance companies can be formulated as a stochastic differential game. In previous researches, Suijs et al. [16] showed that problems in non-life insurance and non-life reinsurance can be modeled as cooperative games. Zeng [17] discussed the competition between two companies and contrasted a single payoff function which depended on both insurance companies' surplus processes. Taksar and Zeng [18] investigated stochastic differential games between two insurance companies who employed the reinsurance to reduce risk exposure. Some papers focus on the relative performance of two insurance companies under a nonzero sum stochastic differential game framework, such as Bensoussan et al. [19], Meng et al. [20], Pun and Wong [21], and Siu et al. [22]. However, some literatures related to stochastic differential games ignore the problem of investment in insurance companies. Nowadays, investment plays a significant role in the insurance business, especially for those big insurance companies who have enough ability to invest in the risky asset for more profits.

Another aspect worthy to be further explored is that the price processes of risky assets in most of literature about the optimal reinsurance and investment problems in frameworks of stochastic differential games are assumed to follow a geometric Brownian motion (GBM), which implies that the volatilities of risky assets are constant and deterministic. This is contrary to practice according to the empirical results. Therefore, many works proposed various stochastic volatility models, such as constant elasticity of variance (CEV) model (Cox and Ross [23]), Stein-Stein model (Stein and Stein [24]), Heston model (Heston [25]) and so on. Among these stochastic volatility models, the CEV model is a natural extension of the GBM model and has the ability of capturing the implied volatility skew and explaining the volatility smile. There is a great deal of literature documenting the CEV model in assets' return for the optimal investment problem. For example, Gu et al. [26] considered the proportional reinsurance and investment problem for the diffusion risk model under the CEV model. Liang et al. [27] and Lin and Li [28] used the CEV model to study the proportional reinsurance and investment problem for an insurance company with the jump-diffusion risk model. Gu et al. [29] derived the excess-of-loss reinsurance and investment strategies with the risky asset's price following the CEV model. Zheng et al. [30] considered the robust optimal portfolio and proportional reinsurance for an insurer under a CEV model.

As far as we know, there is few research investigating more than one insurance company under the CEV model. Therefore, in this paper, we consider a stochastic differential game played between two insurance companies, a big one and a small one. In our model, the basic claim processes is assumed to follow a Brownian motion with drift. Both of two insurance companies purchase the reinsurance, respectively. The big insurance company has more initial surplus than the small one, so the big company has sufficient asset to invest in the risky asset which is described by the CEV model and acquire new business like acting as a reinsurance company of other insurance companies, while the small company can only invest in the risk-free asset and purchase reinsurance. The game studied here is zero-sum where there is a single exponential utility. The big company is trying to maximize the expected exponential utility of the terminal wealth to keep its advantage on surplus while simultaneously the small company is trying to minimize the same quantity to reduce its disadvantage. Firstly, we describe the Nash equilibrium of the game and prove a verification theorem for the exponential utility. By solving the corresponding Fleming-Bellman-Isaacs equations, we derive the optimal reinsurance and investment strategies. Finally, numerical simulation are proposed to illustrate the impacts of the model parameters on the strategies. Through this paper, we find that (1) for such a game the small insurance company takes extreme or trivial strategy, i.e., the optimal reinsurance strategy of the small company is either 1 or 0; (2) the optimal reinsurance and investment strategies of the big company are independent of the wealth process $X^{u_1,u_2}(t)$; (3) the effects of some model parameters on the big company's optimal reinsurance strategy are related to the correlation coefficient between the big and small companies' risk processes.

This paper proceeds as follows. In Section 2, we introduce the formulation of our model, describe the Nash equilibrium of the game, and prove a verification theorem for the exponential utility under the CEV model. Section 3 provides the optimal reinsurance and investment strategies of the big insurance company and the optimal reinsurance strategy of the small one in the stochastic differential game. In Section 4, numerical simulations are presented to illustrate our results. Section 5 concludes this paper.

2. Model Formulation

In this paper, we model the surplus process of the insurance company as

$$dR(t) = a dt + b dW(t), \tag{1}$$

where a, b are positive constants and $W(t)$ is a standard Brownian motion. To reduce the risk exposure, the insurance company is allowed to purchase the reinsurance and $p(t)$ represents the proportion of each claim paid by the insurance company. Assume $\lambda(1-p(t))$ is the rate at which the premiums are diverted to the reinsurance company. As usual, we have $\lambda \geq a$. Otherwise the insurance company will make a full reinsurance to receive a positive return with any risk. Considering the reinsurance, the surplus process of the insurance company becomes

$$dR(t) = (a-(1-p(t))\lambda)dt + bp(t)dW(t). \tag{2}$$

In this paper, we consider a stochastic differential game played between two insurance companies, a big one and a small one. The big insurance company has more initial surplus than the small one, so the big company has sufficient asset to invest in the risky asset and acquire new business like acting as a reinsurance company of other insurance companies, while the small company can only invest in the risk-free asset and purchase reinsurance, i.e., the reinsurance strategies of the big and small companies $p_1(t)$ and $p_2(t)$ satisfy $0 \leq p_1(t), 0 \leq p_2(t) \leq 1$. The game considered here is zero-sum where there is a single exponential utility. The big company is trying to maximize the expected exponential utility of the terminal wealth to keep its advantage on surplus while simultaneously the small company is trying to minimize the same quantity to reduce its disadvantage. One company's decision is assumed to be completely observed by its opponent.

Let $(\Omega, \mathcal{F}, (\mathcal{F}_t), P)$ be a complete probability space with filtration $(\mathcal{F}_t)$ and two standard Brownian motions $W_1(t)$ and $W_2(t)$, adapted to $(\mathcal{F}_t)$ with $\mathcal{F} = \mathcal{F}_T$, where T is a fixed and finite time horizon. The surplus processes of the two insurance companies associated with the proportional reinsurance $p_i(t), i = 1, 2$ are given by

$$dR_i(t) = \left(a_i\left(1-p_i(t)\right)\lambda_i\right)dt + b_i p_i(t)dW_i(t), \quad i = 1, 2, \tag{3}$$

where $\lambda_i \geq a_i > 0, b_i > 0, i = 1, 2$ are constants, $E[W_1(t)W_2(t)] = \rho_{12}t$.

In this paper, the big insurance company is allowed to invest in a risk-free asset whose price process satisfies

$$\mathrm{d}S_0(t) = r_0 S_0(t)\mathrm{d}t, \quad S_0(0) = 1, \tag{4}$$

and a risky asset whose price process is described by the CEV model (cf. Cox [31]):

$$\mathrm{d}S(t) = S(t)\left(\mu \mathrm{d}t + \sigma S^{\beta}(t)\mathrm{d}W_3(t)\right), \tag{5}$$

$S(0) = s_0$, where r_0 is the interest rate and μ, $\sigma S^{\beta}(t)$, and β are the appreciation rate, the instantaneous volatility, and the elasticity parameter of the risky asset. $W_3(t)$ is a standard Brownian motion independent of $W_1(t)$ and $W_2(t)$. As usual, we assume that $\mu > r_0$ and β satisfies the general condition $\beta \geq 0$. Meanwhile, the small one can invest in a risk-free asset to avoid risk. Strategies $u_1 := (\pi(t), p_1(t))$ and $u_2 := p_2(t)$ are said to be admissible if they are $(\mathcal{F}_t)$–progressively measurable and satisfy $(u_1, u_2) := ((\pi(t), p_1(t)), p_2(t)) \in \Pi$:

$$\Pi = \left\{(u_1, u_2) \colon E\left[\int_0^T \pi^2(t)\mathrm{d}t\right] < \infty,\ E\left[\int_0^T p_1^2(t)\mathrm{d}t\right] < \infty,\right.$$
$$\left. 0 \leq p_1(t),\ 0 \leq p_2(t) \leq 1\right\}, \tag{6}$$

where $\pi(t)$ represents the amount invested in the risky asset by the big insurance company at time t. Here Π is called the admissible set. Corresponding to an admissible strategy and the initial wealth $x_1 > x_2$, the wealth processes of the big and small insurance companies $X_1^{u_1}(t)$ and $X_2^{u_1}(t)$ are

$$\begin{cases} \mathrm{d}X_1^{u_1}(t) = \left[r_0 X_1^{u_1}(t) + \pi(t)\left(\mu - r_0\right) + a_1 - \left(1 - p_1(t)\right)\lambda_1\right]\mathrm{d}t + \pi(t)\sigma S^{\beta}(t)\mathrm{d}W_3(t) + b_1 p_1(t)\mathrm{d}W_1(t), \\ X_1^{u_1}(0) = x_1, \end{cases}$$
$$\begin{cases} \mathrm{d}X_2^{u_2}(t) = \left[r_0 X_2^{u_2}(t) + a_2 - \left(1 - p_2(t)\right)\lambda_2\right]\mathrm{d}t + b_2 p_2(t)\mathrm{d}W_2(t), \\ X_2^{u_2}(0) = x_2. \end{cases} \tag{7}$$

Let $X^{u_1,u_2}(t) = X_1^{u_1}(t) - X_2^{u_2}(t)$; then $X^{u_1,u_2}(t)$ follows the following stochastic differential equation:

$$\begin{cases} \mathrm{d}X^{u_1,u_2}(t) = \left[r_0 X^{u_1,u_2}(t) + \pi(t)\left(\mu - r_0\right) + D + p_1(t)\lambda_1 - p_2(t)\lambda_2\right]\mathrm{d}t + \pi(t)\sigma S^{\beta}(t)\mathrm{d}W_3(t) \\ \quad + b_1 p_1(t)\mathrm{d}W_1(t) - b_2 p_2(t)\mathrm{d}W_2(t), \\ X^{u_1,u_2}(0) = x_1 - x_2 = x, \end{cases} \tag{8}$$

where $D = a_1 - \lambda_1 - (a_2 - \lambda_2)$. Here, we usually assume $x > 0$, which describes that one of the two insurance companies is big, and the other is small. That is, this model is suitable for the case that x is positive and we can distinguish the big and small companies easily. If x is very small, we will choose the insurance company with larger initial wealth as the big one, and the other is the small one. If it is difficult to distinguish the big company and small company from the initial wealth, this framework may not be suitable.

Remark 1. If the elasticity parameter $\beta = 0$ in equation (1), the CEV model reduces to the GBM model.

In this paper, we consider the exponential utility which is given by

$$U(x) = -\frac{1}{\gamma}\mathrm{e}^{-\gamma x}, \tag{9}$$

where $\gamma > 0$. The exponential utility has the constant absolute risk aversion parameter γ, which plays an important role in insurance mathematics and actuarial practice.

Definition 1. Let

$$J^{u_1,u_2}(t,s,x) = \mathrm{E}\left[U\left(X^{u_1,u_2}(T)\right) \,\middle|\, S(t) = s, X^{u_1,u_2}(t) = x\right], \tag{10}$$

the strategy (u_1^*, u_2^*) is said to achieve a Nash equilibrium or equivalently a saddle point for the game, if the following inequalities are satisfied. For all $(u_1, u_2) \in \Pi$,

$$J^{u_1,u_2^*}(t,s,x) \leq J^{u_1^*,u_2^*}(t,s,x) \leq J^{u_1^*,u_2}(t,s,x). \tag{11}$$

In addition, let

$$\underline{J}(t,s,x) = \sup_{u_2\in\Pi}\inf_{u_2\in\Pi} J^{u_1,u_2}(t,s,x),$$
$$\overline{J}(t,s,x) = \inf_{u_2\in\Pi}\sup_{u_1\in\Pi} J^{u_1,u_2}(t,s,x), \tag{12}$$

denote the lower and upper values of the game respectively. If $\underline{J}(t,s,x) = \overline{J}(t,s,x)$, the value function of the game is given by $G(x) := \underline{J}(t,s,x) = \overline{J}(t,s,x)$.

In this paper, the goal of the big insurance company is to maximize the above expected exponential utility function while simultaneously the small one wants to minimize it. For convenience, we first provide some notations. Let $O_0 \subset \mathbb{R}^2$ be an open set and $O = [0,T] \times O_0$. Denote that

$$C^{1,2}(O) = \{\phi(t,s,x) \mid \phi(t,\cdot,\cdot) \text{ is once continuously differentiable on } [0,T] \text{ and } \phi(\cdot,s,x) \text{is twice continuously differentiable on } O_0\}, \tag{13}$$

and define a variation operator: for any $\phi(t,s,x) \in C^{1,2}(O)$, let

$$\begin{aligned}\mathscr{A}^{u_1,u_2}\phi(t,s,x) = {} & \phi_t + [r_0x + \pi(\mu - r_0) + D + p_1\lambda_1 - p_2\lambda_2]\phi_x + \frac{1}{2}\left[\pi^2\sigma^2 s^{2\beta} + p_1^2 b_1^2\right.\\ & \left. + p_2^2 b_2^2 - 2p_1p_2b_1b_2\rho_{12}\right]\phi_{xx} + \mu s\phi_s + \frac{1}{2}\sigma^2 s^{2\beta+2}\phi_{ss} + \pi\sigma^2 s^{2\beta+1}\phi_{xs}.\end{aligned} \tag{14}$$

For any given strategy u_2 by the small insurance company, let $\underline{V}^{u_2}(t,s,x)$ be the optimal expected exponential utility function of the big insurance company, i.e.,

$$\underline{V}^{u_2}(t,s,x) = \sup_{u_1\in\Pi} J^{u_1,u_2}(t,s,x). \tag{15}$$

Then $\underline{V}^{u_2}(t,s,x)$ satisfies the following Hamilton-Jacobi-Bellman (HJB) equation

$$\sup_{u_1\in\Pi} A^{u_1,u_2}\underline{V}^{u_2}(t,s,x) = 0, \quad 0 \le t \le T. \tag{16}$$

Similarly, let $\overline{V}^{u_1}(t,s,x)$ be the optimal expected exponential utility function of the small insurance company with any strategy u_1 given by the big insurance company, then $\overline{V}^{u_1}(t,s,x)$ satisfied another HJB equation

$$\inf_{u_2\in\Pi} \mathscr{A}^{u_1,u_2}\overline{V}^{u_1}(t,s,x) = 0, \quad 0 \le t \le T. \tag{17}$$

Denote

$$\begin{aligned}\widehat{u_1} &:= \arg\sup_{u_1\in\Pi} \mathscr{A}^{u_1,u_2}\underline{V}^{u_2}(t,s,x),\\ \widehat{u_2} &:= \arg\inf_{u_2\in\Pi} \mathscr{A}^{u_1,u_2}\overline{V}^{u_1}(t,s,x).\end{aligned} \tag{18}$$

Assume that a saddle point exits, then the game have a value function $V(t,s,x) = V^{u_1,u_2}(t,s,x) = V^{u_1,\widehat{u_2}}(t,s,x) = \underline{V}^{u_2}(t,s,x) = \overline{V}^{u_1}(t,s,x)$.

Let (u_1^*, u_2^*) be the solution to the following equations:

$$\begin{aligned}\widehat{u_1} &:= \arg\sup_{u_1\in\Pi} \mathscr{A}^{u_1,\widehat{u_2}}\underline{V}^{\widehat{u_2}}(t,s,x),\\ \widehat{u_2} &:= \arg\inf_{u_2\in\Pi} \mathscr{A}^{\widehat{u_1},u_2}\overline{V}^{\widehat{u_1}}(t,s,x),\end{aligned} \tag{19}$$

and substitute them into equations (16) and (17), respectively, we obtain the following equations:

$$\sup_{u_1\in\Pi} \mathscr{A}^{u_1,u_2^*}V^{u_1,u_2^*}(t,s,x) = 0, \quad 0 \le t \le T, \tag{20}$$

$$\inf_{u_2\in\Pi} \mathscr{A}^{u_1^*,u_2}V^{u_1^*,u_2}(t,s,x) = 0, \quad 0 \le t \le T, \tag{21}$$

with the boundary condition $V(T,s,x) = U(x)$.

Theorem 1 (Verification theorem). *If there exists a continuously differentiable function $H(t,s,x) \in C^{1,2}(O)$ and*

$$\begin{aligned}u_1^* &:= \arg\sup_{u_1\in\Pi} \mathscr{A}^{u_1,u_2^*}H^{u_1,u_2^*}(t,s,x),\\ u_2^* &:= \arg\inf_{u_2\in\Pi} \mathscr{A}^{u_1^*,u_2}H^{u_1^*,u_2}(t,s,x),\end{aligned} \tag{22}$$

satisfy equations (20) and (21) with the following moment properties

$$\begin{aligned}&\int_0^t E\left[H_s^2(\nu,s,x)\right]\mathrm{d}\nu < \infty,\\ &\int_0^t E\left[H_x^2[\nu,s,x]\right]\mathrm{d}\nu < \infty.\end{aligned} \tag{23}$$

In addition, the parameters satisfy one of the following conditions:

(a) $r_0 > (1 - (1/\sqrt{6}))\mu$;

(b) $r_0 < (1-(1/\sqrt{6}))\mu T < (1/(\beta\sqrt{6(\mu-r_0)^2-\mu^2}))\arctan(-((\sqrt{6(\mu_2-r_0)^2-\mu_2^2})/\mu_2))$, then (u_1^*, u_2^*) is the optimal strategy and the optimal value function is $V(t,s,x) = H(t,s,x)$.

Proof. See Appendix A.

The above theorem guarantees the solution to equations (20) and (21) is the value function for the game. □

3. Solution to the Model

In this section, we solve the game under the expected exponential utility. The big company is trying to maximize the expected exponential utility of the terminal wealth to keep its advantage on surplus while the small company is trying to minimize the same quantity to reduce its disadvantage, i.e.,

$$J^{u_1,u_2}(t,s,x) = E\left[U\left(X^{u_1,u_2}(T)\right) \,\middle|\, S(t)=s, X^{u_1,u_2}(t)=x\right]. \tag{24}$$

Assume the Nash equilibrium exits and let $H(t,s,x)$ satisfy

$$H(t,s,x) = \sup_{u_1\in\Pi}\inf_{u_2\in\Pi} J^{u_1,u_2}(t,s,x) = \inf_{u_2\in\Pi}\sup_{u_1\in\Pi} J^{u_1,u_2}(t,s,x), \tag{25}$$

then $H(t,s,x)$ is the solution to equations (20) and (21) with the boundary condition $H(T,s,x)=(x)$ and $H(t,s,x)$ is the optimal value function according to Theorem 1.

The following theorem gives the optimal reinsurance and investment strategies of the big company and the reinsurance strategy of the small company in the game under the CEV model with the expected exponential utility.

Theorem 2. *For the problem of maximizing the expected exponential utility for the big company while minimizing it for the small company under the CEV model, the optimal reinsurance and investment strategies are given as follows:*

(1) If $((\lambda_2 b_1 - \rho_{12}\lambda_1 b_2)/(b_1 b_2^2(1-\rho_{12}^2))) \geq -(\gamma/2)$ and $\rho_{12}\geq 0$, the optimal reinsurance and investment strategies of the big company and the reinsurance strategy of the small company are

$$\left(p_1^*(t), p_2^*(t)\right) = \left(\frac{\lambda_1}{\gamma b_1^2}e^{-r_0(T-t)} + \frac{b_2\rho_{12}}{b_1}, 1\right), \quad 0\leq t\leq T, \tag{26}$$

$$\pi^*(t) = \frac{(\mu - r_0)e^{-r_0(T-t)}}{\sigma^2 s^{2\beta}\gamma}\left[1 + \frac{\mu - r_0}{2r_0}\left(1 - e^{-2r_0\beta(T-t)}\right)\right], \quad 0\leq t\leq T. \tag{27}$$

The value function is given by equation (B.21).

(2) If $((\lambda_2 b_1 - \rho_{12}\lambda_1 b_2)/(b_1 b_2^2(1-\rho_{12}^2))) \geq -(\gamma/2)$, $\rho_{12} < 0$ and $-(\lambda_1/\gamma b_1 b_2\rho_{12})\leq 1$, the optimal reinsurance strategies of the big and small companies are

$$\left(p_1^*(t), p_2^*(t)\right) = (0,1), \quad 0\leq t\leq T, \tag{28}$$

while the optimal investment strategy of the big company is the same as that in equation (11) and the value function is given in equation (B.25).

(3) If $((\lambda_2 b_1 - \rho_{12}\lambda_1 b_2)/(b_1 b_2^2(1-\rho_{12}^2))) \geq -(\gamma/2)$, $\rho_{12} < 0$, $-(\lambda_1/\gamma b_1 b_2\rho_{12}) > 1$ and $e^{r_0 T} < -(\lambda_1/\gamma b_1 b_2 \rho_{12})$, the optimal reinsurance strategies of the big and small companies are the same as those in equation (26). The optimal investment strategy of the big company is expressed as that in equation (27) and the value function is given by equation (B.20).

(4) If $((\lambda_2 b_1 - \rho_{12}\lambda_1 b_2)/(b_1 b_2^2(1-\rho_{12}^2))) \geq -(\gamma/2)$, $\rho_{12} < 0$, $-(\lambda_1/\gamma b_1 b_2\rho_{12}) > 1$, and $e^{r_0 T} \geq -(\lambda_1/\gamma b_1 b_2\rho_{12})$, the optimal reinsurance strategies of the big and small companies are

$$\left(p_1^*(t), p_2^*(t)\right) = \begin{cases} (0,1), & 0\leq t\leq t_1, \\ \left(\dfrac{\lambda_1}{\gamma b_1^2}e^{-r_0(T-t)} + \dfrac{b_2\rho_{12}}{b_1}, 1\right), & t_1 < t\leq T, \end{cases} \tag{29}$$

while the optimal investment strategy of the big company is the same as that in equation (11) and the value function is given in equation (B.28).

(5) If $((\lambda_2 b_1 - \rho_{12}\lambda_1 b_2)/(b_1 b_2^2(1-\rho_{12}^2))) < -(\gamma/2)$ and $e^{r_0 T} < -(2(\lambda_2 b_1 - \rho_{12}\lambda_1 b_2)/(\gamma b_1 b_2^2(1-\rho_{12}^2)))$, the optimal reinsurance strategies of the big and small companies are

$$\left(p_1^*(t), p_2^*(t)\right) = \left(\frac{\lambda_1}{\gamma b_1^2}e^{-r_0(T-t)}, 0\right), \quad 0\leq t\leq T. \tag{30}$$

The optimal investment strategy of the big company is expressed as that in equation (11) and the value function is given by equation (B.32).

(6) If $((\lambda_2 b_1 - \rho_{12}\lambda_1 b_2)/(b_1 b_2^2(1-\rho_{12}^2))) < -(\gamma/2)$, $e^{r_0 T} \geq -(2(\lambda_2 b_1 - \rho_{12}\lambda_1 b_2)/(\gamma b_1 b_2^2(1-\rho_{12}^2)))$ and $\rho_{12}\geq 0$, the optimal reinsurance strategies of the big and small companies are

$$\left(p_1^*(t), p_2^*(t)\right) = \begin{cases} \left(\dfrac{\lambda_1}{\gamma b_1^2}e^{-r_0(T-t)} + \dfrac{b_2\rho_{12}}{b_1}, 1\right), & 0\leq t\leq t_2, \\ \left(\dfrac{\lambda_1}{\gamma b_1^2}e^{-r_0(T-t)}, 0\right), & t_2 < t\leq T, \end{cases} \tag{31}$$

while the optimal investment strategy of the big company is the same as that in equation (11) and the value function is given in equation (B.36).

(7) If $((\lambda_2 b_1 - \rho_{12}\lambda_1 b_2)/(b_1 b_2^2(1-\rho_{12}^2))) < -(\gamma/2)$, $e^{r_0 T} \geq -(2(\lambda_2 b_1 - \rho_{12}\lambda_1 b_2)/(\gamma b_1 b_2^2(1-\rho_{12}^2)))$, $\rho_{12} < 0$ and $-(\lambda_1/\gamma b_1 b_2\rho_{12})\leq 1$, the optimal reinsurance strategies of the big and small companies are

$$\left(p_1^*(t), p_2^*(t)\right) = \begin{cases} (0,1), & 0\leq t\leq t_2, \\ \left(\dfrac{\lambda_1}{\gamma b_1^2}e^{-r_0(T-t)}, 0\right), & t_2 < t\leq T. \end{cases} \tag{32}$$

Se optimal investment strategy of the big company is expressed as that in equation (11) and the value function is given by equation (B.39).

(8) If $((\lambda_2 b_1 - \rho_{12}\lambda_1 b_2)/(b_1 b_2^2(1-\rho_{12}^2))) < -(\gamma/2)$, $e^{r_0 T} \geq -(2(\lambda_2 b_1 - \rho_{12}\lambda_1 b_2)/(\gamma b_1 b_2^2(1-\rho_{12}^2)))$, $\rho_{12} < 0$, $-(\lambda_1/\gamma b_1 b_2\rho_{12}) > 1$, and $e^{r_0 T} < -(\lambda_1/\gamma b_1 b_2\rho_{12})$, the optimal reinsurance strategies of the big and small companies are the same as those in equation (29), while the optimal investment strategy of the big

company is the same as that in equation (27) and the value function is given in equation (B.39).

(9) If $((\lambda_2 b_1 - \rho_{12}\lambda_1 b_2)/(b_1 b_2^2(1-\rho_{12}^2))) < -(\gamma/2)$, $e^{r_0 T} \geq -(2(\lambda_2 b_1 - \rho_{12}\lambda_1 b_2)/(\gamma b_1 b_2^2(1-\rho_{12}^2)))$, $\rho_{12} < 0$, $-(\lambda_1/\gamma b_1 b_2 \rho_{12}) > 1$, and $e^{r_0 T} \geq -(\lambda_1/\gamma b_1\ b_2\rho_{12})$, the optimal reinsurance strategies of the big and small companies are

$$\left(p_1^*(t), p_2^*(t)\right) = \begin{cases} (0,1), & 0 \leq t \leq t_3, \\ \left(\dfrac{\lambda_1}{\gamma b_1^2} e^{-r_0(T-t)} + \dfrac{b_2\rho_{12}}{b_1}, 1\right), & t_3 < t \leq t_2, \\ \left(\dfrac{\lambda_1}{\gamma b_1^2} e^{-r_0(T-t)}, 0\right), & t_2 < t \leq T. \end{cases} \tag{33}$$

The optimal investment strategy of the big company is expressed as that in equation (11) and the value function is given by equation (B.42).

Proof. See Appendix B. □

Remark 2. From Theorem 2 we conclude that the wealth has no influence on the optimal investment strategy. This can be explained by the risk tolerance of the exponential utility function. The risk tolerance is $-U_x/U_{xx} = 1/\gamma$, which is independent of the wealth. Thus, the optimal strategy is independent of the wealth. In addition, the optimal reinsurance strategy of the big company is not related to the wealth as well and that of the small company is either 1 or 0, i.e., the small insurance company takes extreme or trivial strategy in this game.

Remark 3. In the case that the risky asset's price follows the GBM model, the optimal strategy of the big insurance company is

$$\pi^*(t) = \frac{(\mu - r_0)e^{-r_0(T-t)}}{\sigma^2\gamma}. \tag{34}$$

Compared with equation (34), we see that the optimal investment strategy under the CEV model can be decomposed into two parts. One is

$$M(t) = \frac{(\mu - r_0)e^{-r_0(T-t)}}{\sigma^2 s^{2\beta}\gamma}, \tag{35}$$

which is similar to the optimal strategy under the GBM model, but the volatility is stochastic. Thus, we call $M(t)$ as the moving GBM strategy. The other one is

$$N(t) = 1 + \frac{\mu - r_0}{2r_0}\left(1 - e^{-2r_0\beta(T-t)}\right), \tag{36}$$

which reflects the insurance company's decision to hedge the volatility risk and we regard it as a correction factor.

The following corollary discusses the property of the correction factor.

Corollary 1. *The correction factor $N(t)$ is a monotone decreasing function with respect to time t and satisfies*

$$1 \leq N(t) \leq 1 + \frac{\mu - r_0}{2r_0}\left[1 - e^{-2r_0\beta T}\right]. \tag{37}$$

Proof. According to $\mu > r_0$ and $\beta > 0$, we derive $N_t = -\beta(\mu - r_0)e^{-2r_0\beta(T-t)} < 0$. It implies that the correction factor is a monotone decreasing function with respect to time t. Since

$$N(0) = 1 + \frac{\mu - r_0}{2r_0}\left[1 - e^{-2r_0\beta}\right], \tag{38}$$

and $N(T) = 1$, we obtain inequality (37). □

Corollary 1 shows that the correction factor advises the big insurance company to invest more wealth in the risky asset at the beginning of the investment horizon and steadily decrease the amounts as time goes on.

Remark 4. We find that the optimal investment strategy is independent of the optimal reinsurance strategies. The main reason is that in this model, we assume that the financial market is not affected by the insurance market, which is used in a great deal of existing literature, such as Bai and Guo [3], Gu et al. [26], Gu et al. [29], and so on.

4. Numerical Examples

In this section, we provide some numerical simulations to illustrate our results. Because the optimal reinsurance strategy of the small company is either 1 or 0, we analyze the optimal reinsurance and investment strategies of the big company here. Throughout numerical analysis, unless otherwise stated, the basic parameters are given by $a_1 = 1.5$, $a_2 = 0.5$, $b_1 = 3$, $b_2 = 1$, $\lambda_1 = 2$, $\lambda_2 = 1$, $r_0 = 0.3$, $\mu = 0.5$, $\sigma = 1$, $\beta = 1$, $s = 67$, $\rho_{12} = \pm 0.5$, $\gamma = 0.5$, $T = 10$, and $t = 5$.

4.1. Numerical Simulations of the Big Company's Optimal Reinsurance Strategy. Figure 1 illustrates the influence of the risk averse coefficient γ on the optimal reinsurance strategy $p_1^*(t)$. The relationship between $p_1^*(t)$ and γ is negative. This can be attributed to the fact that a larger γ means the big insurance company is a more risk-averse individual. With the increase of γ, the big company wants to purchase more reinsurance to avoid risk and undertake less risk itself.

Figure 2 shows the effect of r_0 on the optimal reinsurance strategy $p_1^*(t)$. As r_0 increases, the big insurance company will obtain more profit from investment in the risk-free asset. Therefore, it has more money to purchase the reinsurance and bear less risk itself, so $p_1^*(t)$ decreases with r_0.

Figure 3 indicates the impact of λ_1 on the optimal reinsurance strategy $p_1^*(t)$. We can see that a greater λ_1 yields a greater reinsurance strategy. This is because that as λ_1 increases, the cost of reinsurance will become more expensive and the big insurance company prefers to maintain a stable revenue by purchasing less reinsurance and undertake more by itself.

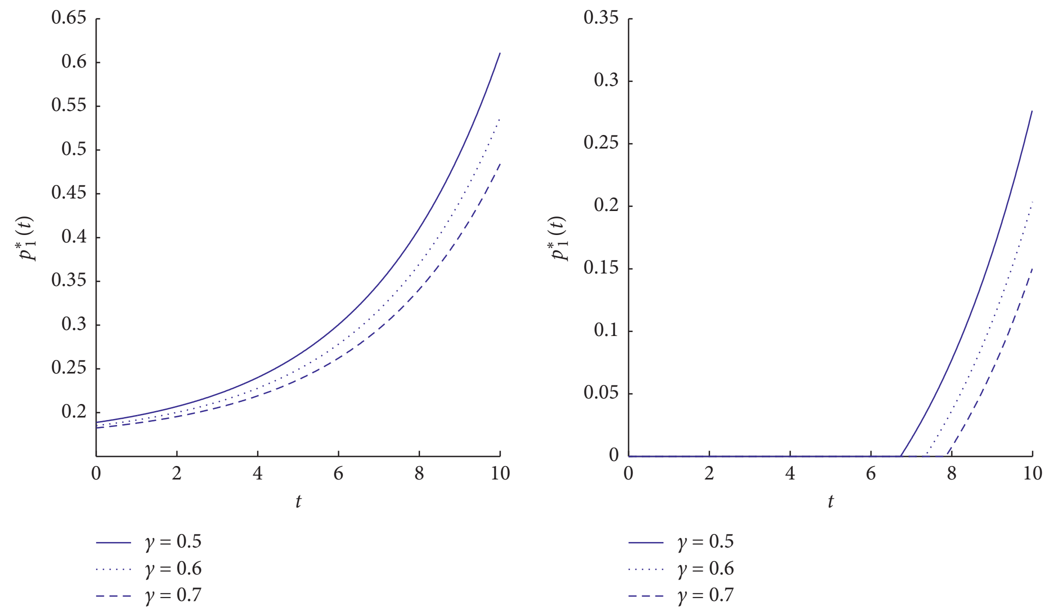

(a) (b)

FIGURE 1: (a) The effect of γ on the big company's optimal reinsurance strategy $p_1^*(t)$ when $\rho_{12} > 0$. (b) The effect of γ on the big company's optimal reinsurance strategy $p_1^*(t)$ when $\rho_{12} < 0$.

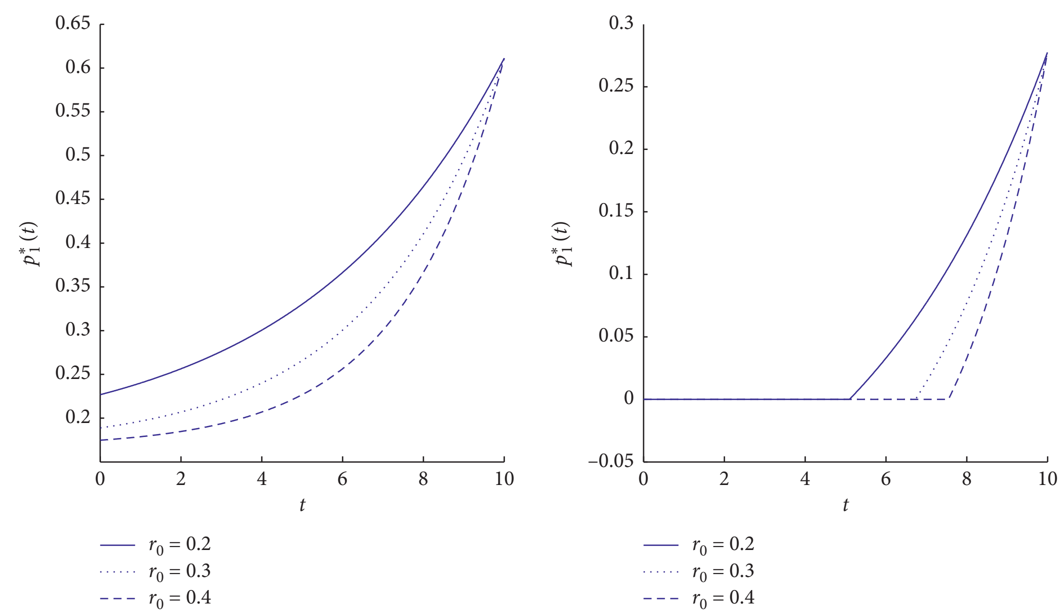

(a) (b)

FIGURE 2: (a) The effect of r_0 on the big company's optimal reinsurance strategy $p_1^*(t)$ when $\rho_{12} > 0$. (b) The effect of r_0 on the big company's optimal reinsurance strategy $p_1^*(t)$ when $\rho_{12} < 0$.

As is shown in Figure 4, we find that $p_1^*(t)$ is a decreasing function of b_1. This can be explained by that b_1 implies the fluctuation of the big insurance company's claim process. When b_1 increases, the insurance company wants to purchase more reinsurance while undertaking less risk by itself.

From Figure 5, we can see if $\rho_{12} > 0$, b_2 exerts a positive effect on the optimal reinsurance strategy $p_1^*(t)$ and if $\rho_{12} < 0$, the effect is opposite. This can be attributed to that the fluctuations of the big and small companies' claim processes are more serious with b_2 rising when $\rho_{12} > 0$. Therefore, the big company will take more risk, while when $\rho_{12} < 0$, the fluctuation of the big insurance company's claim process is weaker with the volatility of the small company becoming stronger. So the big company will face less risk.

In Figure 6, we demonstrate the effect of the correlation coefficient between the big and small insurance companies'

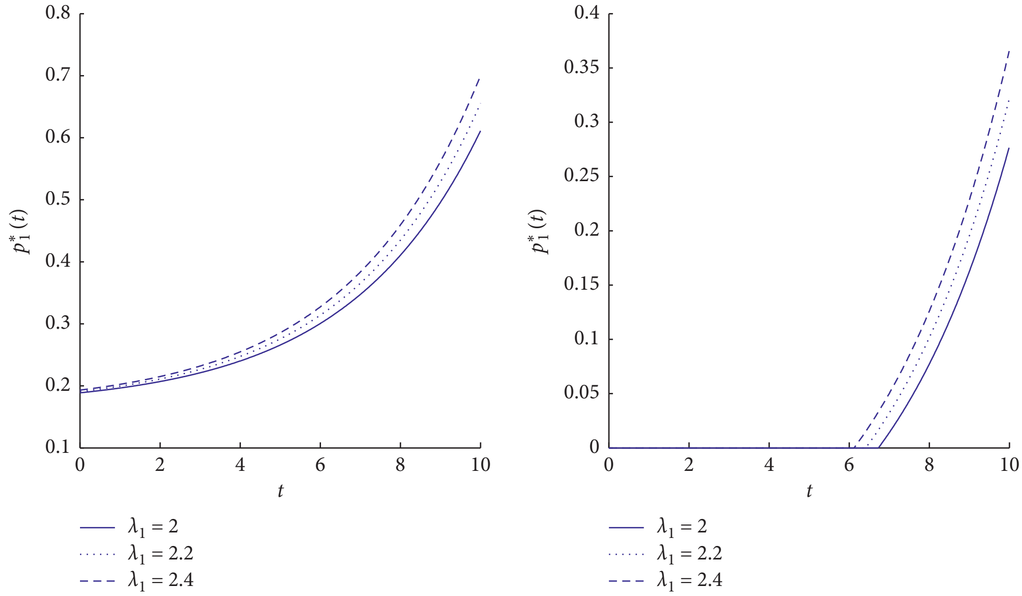

(a) (b)

Figure 3: (a) The effect of λ_1 on the big company's optimal reinsurance strategy $p_1^*(t)$ when $\rho_{12} > 0$. (b) The effect of λ_1 on the big company's optimal reinsurance strategy $p_1^*(t)$ when $\rho_{12} < 0$.

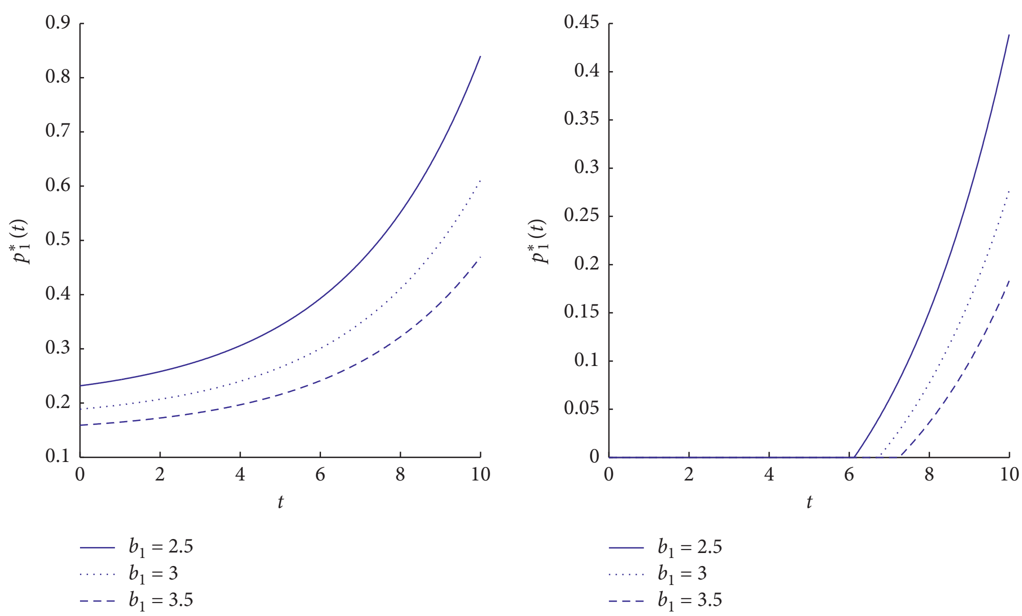

(a) (b)

Figure 4: (a) The effect of b_1 on the big company's optimal reinsurance strategy $p_1^*(t)$ when $\rho_{12} > 0$. (b) The effect of b_1 on the big company's optimal reinsurance strategy $p_1^*(t)$ when $\rho_{12} < 0$.

risk processes ρ_{12} on the optimal reinsurance strategy $p_1^*(t)$. We find that no matter ρ_{12} is positive or negative, the higher ρ_{12} is, the bigger $p_1^*(t)$ is. This is because that for the big company, the more relevant the relationship between two companies is, the greater the influence of the small company on the big company is. So the big company has to undertake more risk with ρ_{12} rising.

4.2. Numerical Simulations of the Big Insurance Company's Optimal Investment Strategy. Figure 7(a) plots the evolution of the risky asset's price over time under the CEV model. According to the change trend of the risky asset's price, we plot the dynamic behaviors of the optimal investment strategy of the big insurance company in Figure 7(b) and we can see that the change trend of the

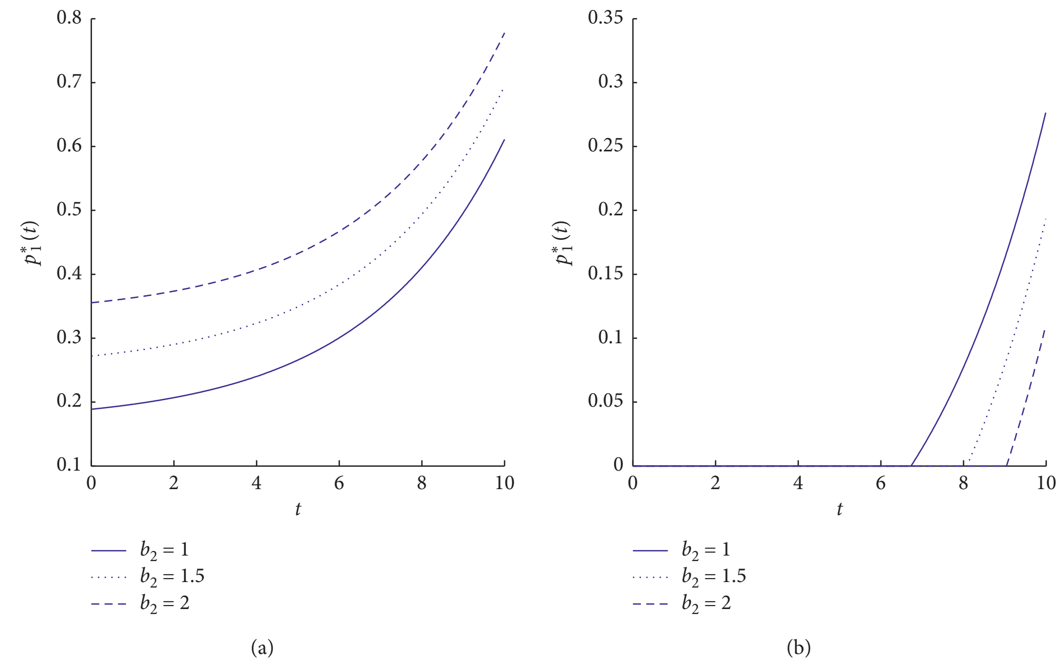

FIGURE 5: (a) The effect of b_2 on the big company's optimal reinsurance strategy $p_1^*(t)$ when $\rho_{12} > 0$. (b) The effect of b_2 on the big company's optimal reinsurance strategy $p_1^*(t)$ when $\rho_{12} < 0$.

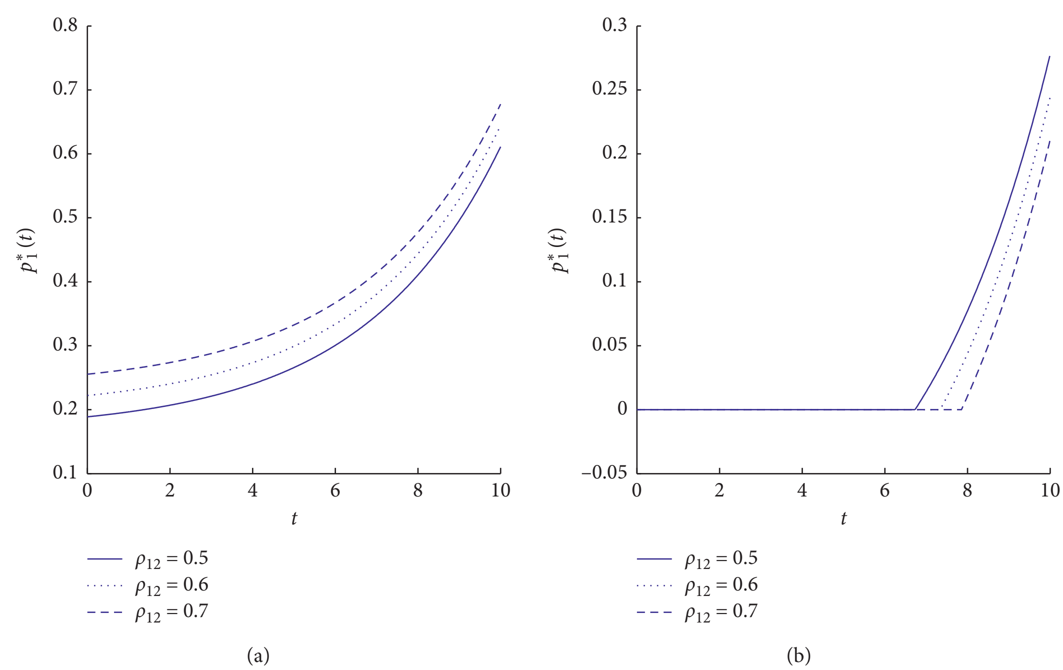

FIGURE 6: (a) The effect of ρ_{12} on the big company's optimal reinsurance strategy $p_1^*(t)$ when $\rho_{12} > 0$. (b) The effect of ρ_{12} on the big company's optimal reinsurance strategy $p_1^*(t)$ when $\rho_{12} < 0$.

optimal investment strategy is opposite to that of the risky asset's price, which can be attributed to the expression of the CEV model. When the price of risky asset is high, the big company should be cautious to invest, for the reason that the higher the risky asset's price is, the higher risk they will undertake.

In Figure 8(a), we find that the rate of the risky asset's return μ exerts positive effect on the optimal investment strategy $\pi^*(t)$. This is consistent with intuition. As μ increases, the big company will obtain more from investment. Therefore, it will increase the amounts invested in the risky asset. As shown in Figure 8(b), the optimal investment

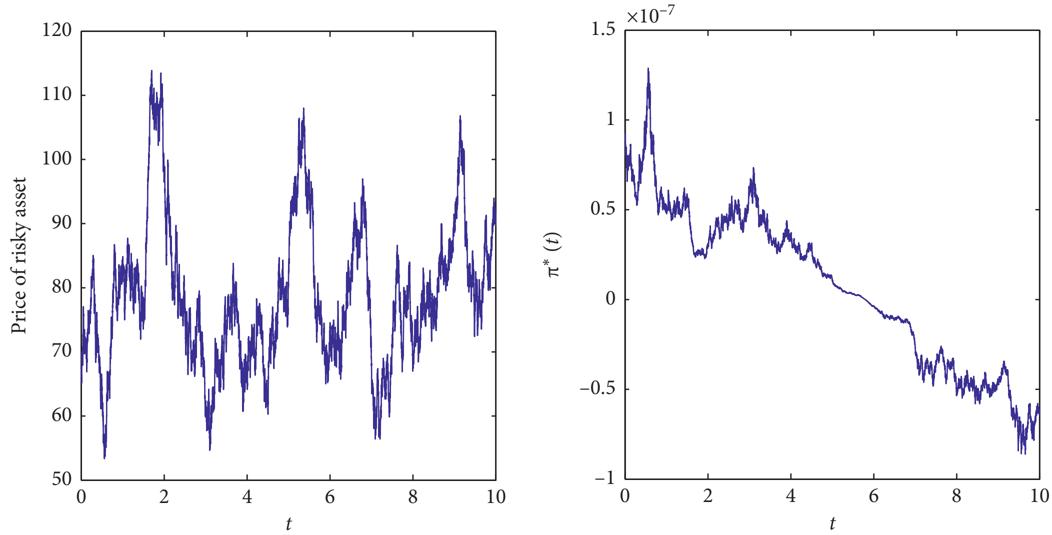

(a) (b)

Figure 7: (a) Evolution of risky asset's price over time. (b) Evolution of optimal investment strategy of the insurer $\pi^*(t)$ over time.

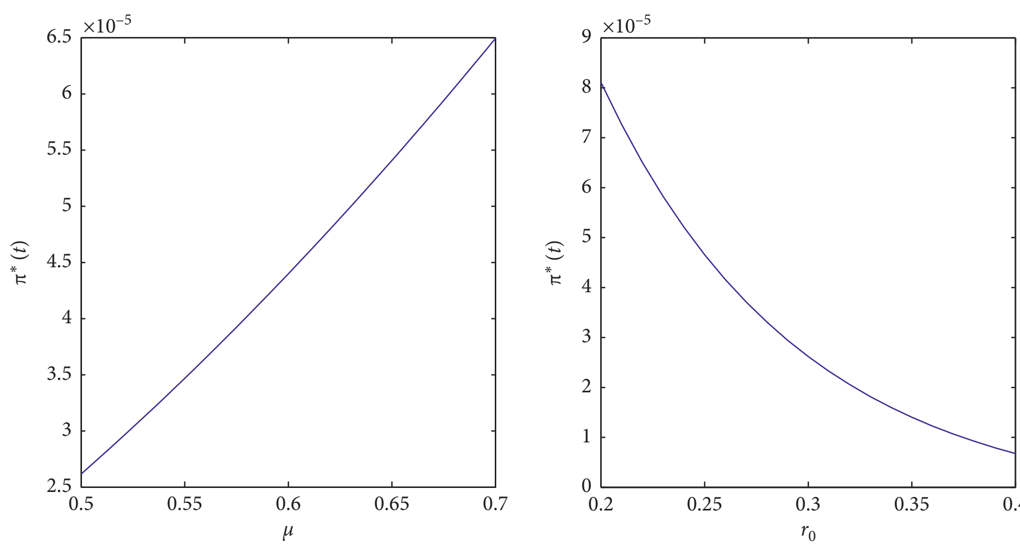

(a) (b)

Figure 8: (a) The effect of μ on the optimal investment strategy of the big insurance company $\pi^*(t)$. (b) The effect of r_0 on the optimal investment strategy of the big insurance company $\pi^*(t)$.

strategy $\pi^*(t)$ is a decreasing function of the interest rate r_0. When the interest rate r_0 increases, the risk-free asset is more attractive. Then the big company will invest more in the risk-free asset and reduce investment in the risky asset.

Figure 9(a) indicates the impact of the risk averse coefficient γ on the optimal investment strategy $\pi^*(t)$. We see that γ exerts negative effect on $\pi^*(t)$, which means that the big company with the higher risk averse level will invest less in the risky asset to avoid risk. Figure 9(b) illustrates the effect of the elasticity coefficient β on the optimal investment strategy $\pi^*(t)$. There is a negative relationship between $\pi^*(t)$ and β. This can be attributed to that a higher β leads to a larger expected drop in volatility and increased probability of a large adverse movement in the risky asset'a price. Thus,

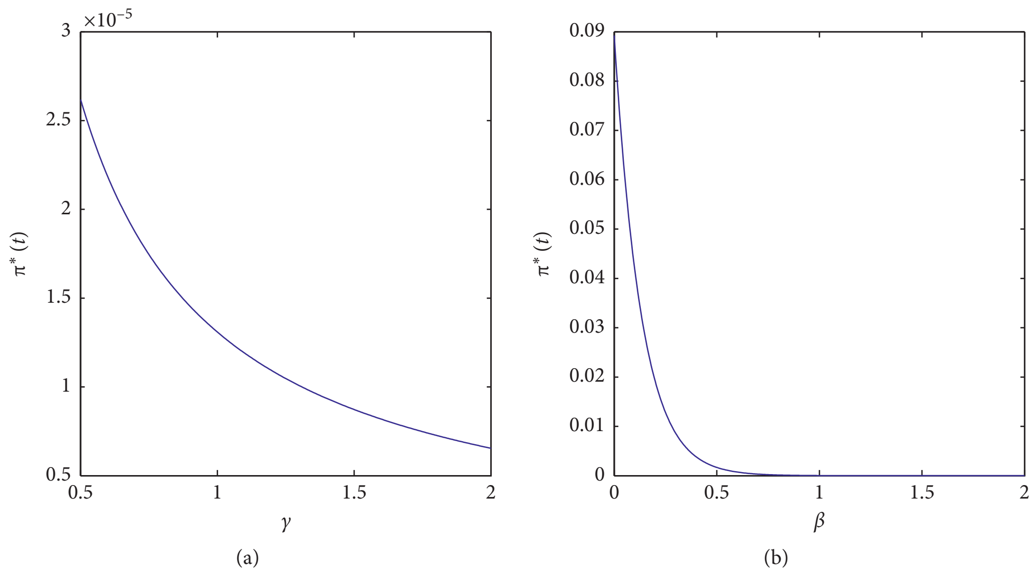

Figure 9: (a) The effect of γ on the optimal investment strategy of the big insurance company $\pi^*(t)$. (b) The effect of β on the optimal investment strategy of the big insurance company $\pi^*(t)$.

the big company will invest less in the risky asset as β increases to reduce the risk from the investment in the risky asset.

5. Conclusion

This paper considers a stochastic differential game played between two insurance companies, a big one and a small one. In our model, the basic claim process is assumed to follow a Brownian motion with drift. Both of two insurance companies purchase the reinsurance, respectively. The big insurance company has more initial surplus than the small one, so the big company has sufficient asset to invest in the risky asset which is described by the CEV model and acquire new business like acting as a reinsurance company of other insurance companies, while the small company can only invest in the risk-free asset and purchase reinsurance. The game studied here is zero-sum where there is a single exponential utility. The big company is trying to maximize the expected exponential utility of the terminal wealth to keep its advantage on surplus while simultaneously the small company is trying to minimize the same quantity to reduce its disadvantage. Firstly, we describe the Nash equilibrium of the game and prove a verification theorem for the exponential utility. By solving the corresponding Fleming-Bellman-Isaacs equations, we derive the optimal reinsurance and investment strategies. Finally, numerical simulation is proposed to illustrate the impacts of the model parameters on the strategies. Through this paper, we find that (1) for such a game, the small insurance company takes extreme or trivial strategy, i.e., the optimal reinsurance strategy of the small company is either 1 or 0; (2) the optimal reinsurance and investment strategies of the big company are independent of the wealth process $X^{u_1,u_2}(t)$; (3) the effects of some model parameters on the big company's optimal reinsurance strategy is related to the correlation coefficient between the big and small companies' risk processes. In future work, we will consider more complex models, such as both two insurers can invest in the risky asset, or n insurers will participate in the game.

Appendix

A. Proof of Theorem 1

Proof. By Itô's formula, we have

$$\begin{aligned} dH^{u_1,u_2}\left(t,S(t),X^{u_1,u_2}(t)\right) = {} & \mathscr{A}^{u_1,u_2}H^{u_1,u_2}\left(t,S(t),X^{u_1,u_2}(t)\right)dt \\ & + H_x^{u_1,u_2}\pi(t)\sigma S^{\beta}(t)dW_3(t) \\ & + H_x^{u_1,u_2}p_1(t)b_1dW_1(t) \\ & - H_x^{u_1,u_2}p_2(t)b_2dW_2(t) \\ & + H_s^{u_1,u_2}\sigma S^{\beta+1}(t)dW_3(t). \end{aligned} \tag{A.1}$$

Take a sequence of bounded open sets O_1, O_2, $O_3,\ldots$, with $O_i \subset O_{i+1} \subset O$, $i = 1,2,\ldots$, and $\cup_i O_i = O$. For $(s,x) \in O_1$, let τ_i be the exiting time of (s,x) from O_i. Then $\tau_i \wedge T \longrightarrow T$ when $i \longrightarrow \infty$. Integrating from two sides of equation (A.1), we have

$$\begin{aligned} &H^{u_1,u_2}\left(\tau_i\wedge T, S(\tau_i\wedge T), X^{u_1,u_2}(\tau_i\wedge T)\right)\\ &= H^{u_1,u_2}(0,s,x)+\int_0^{\tau_i\wedge T}\mathscr{A}^{u_1,u_2}H^{u_1,u_2}(\nu,S(\nu),X^{u_1,u_2}(\nu))\mathrm{d}\nu+\int_0^{\tau_i\wedge T}H_x^{u_1,u_2}\pi(\nu)\sigma S^{\beta}(\nu)\mathrm{d}W_3(\nu)\\ &\quad+\int_0^{\tau_i\wedge T}H_x^{u_1,u_2}p_1(\nu)b_1\mathrm{d}W_1(\nu)-\int_0^{\tau_i\wedge T}H_x^{u_1,u_2}p_2(\nu)b_2\mathrm{d}W_2(\nu)+\int_0^{\tau_i\wedge T}\sigma S^{\beta+1}(\nu)\mathrm{d}W_3(\nu), \end{aligned} \tag{A.2}$$

then

$$\begin{aligned} &H^{u_1,u_2^*}\left(\tau_i\wedge T, S(\tau_i\wedge T), X^{u_1,u_2^*}(\tau_i\wedge T)\right)\\ &= H^{u_1,u_2^*}(0,s,x)+\int_0^{\tau_i\wedge T}\mathscr{A}^{u_1,u_2^*}H^{u_1,u_2^*}\left(\nu,S(\nu),X^{u_1,u_2^*}(\nu)\right)\mathrm{d}\nu+\int_0^{\tau_i\wedge T}H_x^{u_1,u_2^*}\pi(\nu)\sigma S^{\beta}(\nu)\mathrm{d}W_3(\nu)\\ &\quad+\int_0^{\tau_i\wedge T}H_x^{u_1,u_2^*}p_1(\nu)b_1\mathrm{d}W_1(\nu)-\int_0^{\tau_i\wedge T}H_x^{u_1,u_2^*}p_2^*(\nu)b_2\mathrm{d}W_2(\nu)+\int_0^{\tau_i\wedge T}H_s^{u_1,u_2^*}\sigma S^{\beta+1}(\nu)\mathrm{d}W_3(\nu). \end{aligned} \tag{A.3}$$

Since the last five terms are square-integrable martingales with zero expectation, taking conditional expectation given (t,s,x) on both sides of the above formula and taking equation (21) into account results that

$$\begin{aligned} &\mathrm{E}\left[H^{u_1,u_2^*}\left(\tau_i\wedge T, S(\tau_i\wedge T), X^{u_1,u_2^*}(\tau_i\wedge T)\right)\Big| S(t)=s, X^{u_1,u_2^*}(t)=x\right]\\ &= H^{u_1,u_2^*}(0,s,x)+\mathrm{E}\left[\int_0^{\tau_i\wedge T}\mathscr{A}^{u_1,u_2^*}H^{u_1,u_2^*}\left(\nu,S(\nu),X^{u_1,u_2^*}(\nu)\right)\mathrm{d}\nu\Big| S(t)=s, X^{u_1,u_2^*}(t)=x\right]\\ &\leq H^{u_1,u_2^*}(0,s,x). \end{aligned} \tag{A.4}$$

By virtue of Lemma B.1, $H^{u_1,u_2^*}(\tau_i\wedge T, S(\tau_i\wedge T), X^{u_1,u_2^*}(\tau_i\wedge T))$, $i=1,2,..$ are uniformly integrable. It is easy to see that the equality holds for $u_1=u_1^*$. Thus, we have

$$\begin{aligned} V^{u_1,u_2^*}(t,s,x) &= \mathrm{E}\left[U\left(X^{u_1,u_2^*}(T)\right)\Big| S(t)=s, X^{u_1,u_2^*}(t)=x\right]\\ &= \lim_{i\longrightarrow\infty}\mathrm{E}\left[H^{u_1^*,u_2^*}\left(\tau_i\wedge T, S(\tau_i\wedge T), X^{u_1^*,u_2^*}(\tau_i\wedge T)\right)\Big| S(t)=s, X^{u_1,u_2^*}(t)=x\right]\leq H^{u_1,u_2^*}(0,s,x)\\ &= H^{u_1^*,u_2^*}(0,s,x)=\lim_{i\longrightarrow\infty}\mathrm{E}\left[H^{u_1^*,u_2^*}\left(\tau_i\wedge T, S(\tau_i\wedge T), X^{u_1^*,u_2^*}(\tau_i\wedge T)\right)\Big| S(t)=s, X^{u_1^*,u_2^*}(t)=x\right]\\ &= \mathrm{E}\left[U\left(X^{u_1^*,u_2^*}(T)\right)\Big| S(t)=s, X^{u_1^*,u_2^*}(t)=x\right]=V^{u_1^*,u_2^*}(t,s,x), \end{aligned} \tag{A.5}$$

i.e., $V^{u_1,u_2^*}(t,s,x)\leq V^{u_1^*,u_2^*}(t,s,x)$. Similarly, we can prove

$$V^{u_1^*,u_2^*}(t,s,x)\leq V^{u_1^*,u_2}(t,s,x). \tag{A.6}$$

Hence, (u_1^*, u_2^*) is a saddle point for the game by Definition 1 and according to

$$\begin{aligned}&E\left[H^{u_1,u_2^*}\left(\tau_i\wedge T, S(\tau_i\wedge T), X^{u_1,u_2^*}(\tau_i\wedge T)\right)\Big| S(t)=s, X^{u_1,u_2^*}(t)=x\right]\\&=H^{u_1,u_2^*}(t,s,x)+E\left[\int_t^{\tau_i\wedge T}\mathscr{A}^{u_1,u_2^*}H^{u_1,u_2^*}\left(\nu,S(\nu),X^{u_1,u_2^*}(\nu)\right)\mathrm{d}\nu\Big| S(t)=s, X^{u_1,u_2^*}(t)=x\right]\\&\leq H^{u_1,u_2^*}(t,s,x),\end{aligned}\tag{A.7}$$

we can derive

$$\begin{aligned}V^{u_1,u_2^*}(t,s,x)&=\mathrm{E}\left[U\left(X^{u_1,u_2^*}(T)\right)\Big| S(t)=s, X^{u_1,u_2^*}(t)=x\right]\\&=\lim_{i\longrightarrow\infty}\mathrm{E}\Big[H^{u_1,u_2^*}\left(\tau_i\wedge T, S(\tau_i\wedge T), X^{u_1,u_2^*}(\tau_i\wedge T)\right)\Big|\\&\qquad S(t)=s, X^{u_1,u_2^*}(t)=x\Big]\leq H^{u_1,u_2^*}(t,s,x).\end{aligned}\tag{A.8}$$

When $u_1=u_1^*$, the inequality in the above formula becomes an equality, i.e., $H(t,s,x)$ is the optimal value function. □

B. Proof of Theorem 2

Proof. According to the exponential utility described by equation (9), we try to find the optimal value function in the following way:

$$H(t,s,x)=-\frac{1}{\gamma}e^{-\gamma\left[e^{r_0(T-t)}(x-d(t))+g(t,s)\right]},\tag{B.1}$$

with the boundary condition given by $g(T)=1$. Then

$$\begin{aligned}&H_t=-\gamma\left[-r_0e^{r_0(T-t)}(x-d(t))-d_te^{r_0(T-t)}+g_t\right]H, H_s=-\gamma g_sH, H_{ss}=\left(\gamma^2g_s^2-\gamma g_{ss}\right)H,\\&H_x=-\gamma e^{r_0(T-t)}H, H_{xx}=\gamma^2e^{2r_0(T-t)}H, H_{sx}=\gamma^2e^{r_0(T-t)}g_sH.\end{aligned}\tag{B.2}$$

From equation (B.2), we obtain $H_{xx}<0$, the infumum in equation (21) is reached at $p_2^*(t)=0$ or $p_2^*(t)=1$. Let

$$\widehat{p}_2(t)=\frac{\lambda_2b_1-\rho_{12}\lambda_1b_2}{b_1b_2^2\left(1-\rho_{12}^2\right)}\cdot\frac{H_x}{H_{xx}}.\tag{B.3}$$

The first-order maximizing conditions for the optimal reinsurance and investment strategies of the big company give

$$\begin{aligned}p_1^*(t)&=-\frac{\lambda_1H_x}{b_1^2H_{xx}}+\frac{b_2\rho_{12}p_2^*(t)}{b_1},\\\pi^*(t)&=-\frac{(\mu-r_0)H_{xx}}{\sigma^2s^{2\beta}H_{xx}}-\frac{sH_{xs}}{H_{xx}}.\end{aligned}\tag{B.4}$$

Substituting $\pi^*(t)$, $p_1^*(t)$, and $p_2^*(t)$ into equations (20) and (21) yields

$$\begin{aligned}&H_t+r_0xH_x-\frac{(\mu-r_0)^2H_x^2}{2\sigma^2s^{2\beta}H_{xx}}+DH_x+\frac{1}{2}p_1^*(t)^2b_1^2H_{xx}+\frac{1}{2}p_2^*(t)^2b_2^2H_{xx}+p_1^*(t)\lambda_1H_x-p_2^*(t)\lambda_2H_x\\&-p_1^*(t)p_2^*(t)b_1b_2\rho_{12}H_{xx}+\mu sH_s+\frac{1}{2}\sigma^2s^{2\beta+2}H_{ss}-\frac{s(\mu-r_0)H_xH_{xs}}{H_{xx}}-\frac{\sigma^2s^{2\beta+2}H_{xs}^2}{2H_{xx}}=0.\end{aligned}\tag{B.5}$$

Inserting derivatives in equation (B.2) into equation (B.5), we obtain

$$\begin{aligned}&g_t+r_0sg_s+\frac{1}{2}\sigma^2s^{2\beta+2}g_{ss}+\frac{(\mu-r_0)^2}{2\gamma\sigma^2s^{2\beta}}+r_0e^{r_0(T-t)}d(t)-d_te^{r_0(T-t)}+De^{r_0(T-t)}+p_1^*(t)\lambda_1e^{r_0(T-t)}\\&-p_2^*(t)\lambda_2e^{r_0(T-t)}-\frac{1}{2}p_1^*(t)^2b_1^2\gamma e^{2r_0(T-t)}-\frac{1}{2}p_2^*(t)^2b_2^2\gamma e^{2r_0(T-t)}+p_1^*(t)p_2^*(t)b_1b_2\gamma e^{2r_0(T-t)}=0.\end{aligned}\tag{B.6}$$

In the following section, we try to find the solutions to equations (20) and (21) in the following cases. □

Case B.1. $((\lambda_2b_1-\rho_{12}\lambda_1b_2)/(b_1b_2^2(1-\rho_{12}^2)))\geq-(\gamma/2)$.

If $((\lambda_2 b_1 - \rho_{12}\lambda_1 b_2)/(b_1 b_2^2(1-\rho_{12}^2))) \geq -(\gamma/2)$, then $\widehat{p}_2(t) < (1/2)$. We have the optimal reinsurance strategies of the small and big company $p_2^*(t) = 1$ and

$$\widehat{p}_1(t) = \frac{\lambda_1}{\gamma b_1^2} e^{-r_0(T-t)} + \frac{b_2\rho_{12}}{b_1}. \tag{B.7}$$

Equation (B.7) shows that $\widehat{p}_1(t) \in (0, \infty)$ is equivalent to

$$t \geq t_1 = T - \frac{1}{r_0}\ln\left(-\frac{\lambda_1}{\gamma b_1 b_2 \rho_{12}}\right). \tag{B.8}$$

(1) If $\rho_{12} \geq 0$, we derive the optimal reinsurance strategies of the big and small companies

$$\left(p_1^*(t), p_2^*(t)\right) = \left(\frac{\lambda_1}{\gamma b_1^2} \mathrm{e}^{-r_0(T-t)} + \frac{b_2\rho_{12}}{b_1}, 1\right), \quad 0 \leq t \leq T. \tag{B.9}$$

Inputting equation (B.9) into equation (B.6) implies

$$\begin{aligned} & e^{r_0(T-t)}\left\{r_0 d(t) - d(t) + D - \lambda_2 + \frac{\lambda_1 b_2 \rho_{12}}{b_1} - \frac{1}{2} b_2^2 \gamma\left(1-\rho_{12}^2\right) e^{r_0(T-t)}\right\} \\ & \quad + g_t + r_0 s g_s + \frac{1}{2}\sigma^2 s^{2\beta+2} g_{ss} + \frac{(\mu - r_0)^2}{2\gamma\sigma^2 s^2 \beta} + \frac{\lambda_1^2}{2\gamma b_1^2} = 0. \end{aligned} \tag{B.10}$$

Equation (B.10) can be decomposed into two equations by separating variables

$$d_t - r_0 d(t) - D + \lambda_2 - \frac{\lambda_1 b_2 \rho_{12}}{b_1} + \frac{1}{2} b_2^2 \gamma\left(1-\rho_{12}^2\right) \mathrm{e}^{r_0(T-t)} = 0, \tag{B.11}$$

$$g_t + r_0 s g_s + \frac{1}{2}\sigma^2 s^{2\beta+2} g_{ss} + \frac{(\mu - r_0)^2}{2\gamma\sigma^2 s^{2\beta}} + \frac{\lambda_1^2}{2\gamma b_1^2} = 0. \tag{B.12}$$

Taking the boundary condition $d(T) = 0$ into account, the solution to equation (B.11) is

$$\begin{aligned} d(t) = & -\frac{1}{r_0}\left(D + \frac{\lambda_1 b_2 \rho_{12}}{b_1} - \lambda_2\right)\left(1 - e^{-r_0(T-t)}\right) \\ & + \frac{\gamma b_2^2 (1-\rho_{12}^2)}{4 r_0}\left(e^{r_0(T-t)} - e^{-r_0(T-t)}\right). \end{aligned} \tag{B.13}$$

In order to solve equation (B.12), we define

$$g(t, s) = m(t, v), \quad v = s^{-2\beta}, \tag{B.14}$$

and the boundary condition is $m(T, v) = 0$. Then

$$\begin{aligned} g_t &= m_t, \\ g_s &= -2\beta s^{-2\beta-1} m_v, \\ g_{ss} &= 2\beta(2\beta+1) s^{-2\beta-2} m_v + 4\beta^2 s^{-4\beta-2} m_{vv}. \end{aligned} \tag{B.15}$$

Substituting these derivatives into equation (B.15) yields

$$\begin{aligned} & m_t - 2r_0\beta v m_v + \beta(2\beta+1)\sigma^2 m_v + 2\beta^2\sigma^2 v m_{vv} \\ & \quad + \frac{(\mu - r_0)^2 v}{2\sigma^2\gamma} + \frac{\lambda_1^2}{2\gamma b_1^2} = 0. \end{aligned} \tag{B.16}$$

We try to find a solution to equation (B.16) with the following structure:

$$m(t, v) = A(t) + B(t) v, \tag{B.17}$$

and the boundary conditions are $A(T) = 0$ and $B(T) = 0$. Plugging equation (B.17) into equation (B.15), we derive

$$\begin{aligned} & A_t + \beta(2\beta+1)\sigma^2 B(t) + \frac{\lambda_1^2}{2\gamma b_1^2} \\ & \quad + v\left\{B_t - 2r_0\beta B(t) + \frac{(\mu - r_0)^2}{2\sigma^2\gamma}\right\} = 0. \end{aligned} \tag{B.18}$$

By matching coefficients, $A(t)$ and $B(t)$ satisfy the following equations:

$$\begin{aligned} & A_t + \beta(2\beta+1)\sigma^2 B(t) + \frac{\lambda_1^2}{2\gamma b_1^2} = 0, \\ & B_t - 2r_0\beta B(t) + \frac{(\mu - r_0)^2}{2\sigma^2\gamma} = 0. \end{aligned} \tag{B.19}$$

Considering the boundary conditions $A(T) = 0$ and $B(T) = 0$, the solutions to equation (B.19) are

$$\begin{aligned} A(t) &= \frac{\lambda_1^2}{2\gamma b_1^2}(T - t) + \beta(2\beta+1)\sigma^2 \int_t^T B(v)\mathrm{d}v, \\ B(t) &= \frac{(\mu - r_0)^2}{4\sigma^2\gamma r_0\beta}\left(1 - \mathrm{e}^{-2r_0\beta(T-t)}\right). \end{aligned} \tag{B.20}$$

Thus, we obtain

$$H(t,s,x) = -\frac{1}{\gamma}e^{-\gamma\left[e^{r_0(T-t)}\left(x-d_1(t)\right)+A_1(t)+B(t)s^{-2\beta}\right]}, \tag{B.21}$$

where

$$d_1(t) = -\frac{1}{r_0}\left(D + \frac{\lambda_1 b_2\rho_{12}}{b_1} - \lambda_2\right)\left(1 - e^{-r_0(T-t)}\right) + \frac{\gamma b_2^2\left(1-\rho_{12}^2\right)}{4r_0}\left(e^{r_0(T-t)} - e^{-r_0(T-t)}\right),$$
$$A_1(t) = \frac{\lambda_1^2}{2\gamma b_1^2}(T-t) + \beta(2\beta+1)\sigma^2\int_t^T B(\nu)\mathrm{d}\nu, \tag{B.22}$$

and $B(t)$ is given by equation (B.20).

(2) If $\rho_{12} < 0$ and $-(\lambda_1/\gamma b_1 b_2\rho_{12}) \le 1$, we have the optimal reinsurance strategies of the big and small companies

$$\left(p_1^*(t), p_2^*(t)\right) = (0,1), \quad 0 \le t \le T. \tag{B.23}$$

Putting equation (B.23) into equation (B.6), we derive

$$\mathrm{e}^{r_0(T-t)}\left\{r_0 d(t) - d_t + D - \lambda_2 - \frac{1}{2}b_2^2\gamma\mathrm{e}^{r_0(T-t)}\right\} + g_t + r_0 s g_s + \frac{1}{2}\sigma^2 s^{2\beta+2}g_{ss} + \frac{(\mu - r_0)^2}{2\gamma\sigma^2 s^{2\beta}} = 0. \tag{B.24}$$

We can solve equation (B.24) like Case B.1 (1) and get

$$H(t,s,x) = -\frac{1}{\gamma}e^{-\gamma\left[e^{r_0(T-t)}\left(x-d_2(t)\right)+A_2((t)+B(t)s^{-2\beta}\right]}, \tag{B.25}$$

where

$$d_2(t) = -\frac{1}{r_0}(D-\lambda_2)\left(1 - e^{-r_0(T-t)}\right) + \frac{\gamma b_2^2}{4r_0}\left(e^{r_0(T-t)} - e^{-r_0(T-t)}\right),$$
$$A_2(t) = \beta(2\beta+1)\sigma^2\int_t^T B(\nu)\mathrm{d}\nu, \tag{B.26}$$

with $B(t)$ given in equation (B.20).

(3) If $\rho_{12} < 0$, $-(\lambda_1/\gamma b_1 b_2\rho_{12}) > 1$ and $e^{r_0 T} < -(\lambda_1/\gamma b_1 b_2\rho_{12})$, the optimal reinsurance strategies of the big and small companies are the same as those in equation (B.9) and the expression of $H(t,s,x)$ is given by equation (B.21).

(4) If $\rho_{12} < 0$, $-(\lambda_1/\gamma b_1 b_2\rho_{12}) > 1$ and $e^{r_0 T} \ge -(\lambda_1/\gamma b_1 b_2\rho_{12})$, when $0 \le t \le t_1$, the optimal reinsurance strategies of the big and small companies are expressed as those in equation (B.23) and when $t_1 < t \le T$, $p_1^*(t)$ and $p_2^*(t)$ are the same as those in equation (B.9), i.e.,

$$\left(p_1^*(t), p_2^*(t)\right) = \begin{cases} (0,1), & 0 \le t \le t_1, \\ \left(\dfrac{\lambda_1}{\gamma b_1^2}e^{-r_0(T-t)} + \dfrac{b_2\rho_{12}}{b_1}, 1\right), & t_1 < t \le T. \end{cases} \tag{B.27}$$

By similar derivatives, noting that $H(t,s,x)$ is continuous at $t = t_1$ and taking the boundary conditions into account, we obtain

$$H(t,s,x) = \begin{cases} -\dfrac{1}{\gamma}e^{-\gamma\left[e^{r_0(T-t)}\left(x-d_3(t)\right)+A_3(t)+B(t)s^{-2\beta}\right]}, & 0 \le t \le t_1, \\ -\dfrac{1}{\gamma}e^{-\gamma\left[e^{r_0(T-t)}\left(x-d_1(t)\right)+A_1(t)+B(t)s^{-2\beta}\right]}, & t_1 < t \le T, \end{cases} \tag{B.28}$$

where

$$d_3(t) = -\frac{1}{r_0}(D-\lambda_2)\left(1 - e^{-r_0(t_1-t)}\right) - \frac{\lambda_1 b_2\rho_{12}}{r_0 b_1}\cdot\left(e^{-r_0(t_1-t)} - e^{-r_0(T-t)}\right) + \frac{\gamma b_2^2}{4r_0}\left(e^{r_0(T-t)} - e^{-r_0(T-t)}\right) - \frac{\gamma b_2^2\rho_{12}^2}{4r_0}\left(\mathrm{e}^{r_0(T+t-2t_1)} - \mathrm{e}^{-r_0(T-t)}\right),$$
$$A_3(t) = \frac{\lambda_1^2}{2\gamma b_1^2}(T-t_1) + \beta(2\beta+1)\sigma^2\int_t^T B(\nu)\mathrm{d}\nu, \tag{B.29}$$

and $B(t)$, $d_1(t)$ and $A_1(t)$ are given in equations (B.20) and (B.21).

Case B.2. $((\lambda_2 b_1 - \rho_{12}\lambda_1 b_2)/(b_1 b_2^2(1-\rho_{12}^2))) < -(\gamma/2)$ and $e^{r_0 T} < -(2(\lambda_2 b_1 - \rho_{12}\lambda_1 b_2)/\gamma b_1 b_2^2(1-\rho_{12}^2))$.

If $((\lambda_2 b_1 - \rho_{12}\lambda_1 b_2)/(b_1 b_2^2(1-\rho_{12}^2))) < -(\gamma/2)$ and $e^{r_0 T} < -(2(\lambda_2 b_1 - \rho_{12}\lambda_1 b_2)/\gamma b_1 b_2^2(1-\rho_{12}^2))$, then $\widehat{p}_2(t) \ge 1/2$. The optimal reinsurance strategies of the big and small companies are as following:

$$\left(p_1^*(t), p_2^*(t)\right) = \left(\frac{\lambda_1}{\gamma b_1^2}e^{-r_0(T-t)}, 0\right), \quad 0 \le t \le T, \tag{B.30}$$

and equation (B.6) is simplified into

$$e^{r_0(T-t)}\left\{r_0 d(t) - d_t + D\right\} + g_t + r_0 s g_s + \frac{1}{2}\sigma^2 s^{2\beta+2}g_{ss} + \frac{(\mu - r_0)^2}{2\gamma\sigma^2 s^{2\beta}} + \frac{\lambda_1^2}{2\gamma b_1^2} = 0. \tag{B.31}$$

Thus, $H(t,s,x)$ satisfies

$$H(t,s,x) = -\frac{1}{\gamma}e^{-\gamma\left[e^{r_0(T-t)}\left(x-d_4(t)\right)+A_4(t)+B(t)s^{-2\beta}\right]}, \tag{B.32}$$

where

$$d_4(t) = -\frac{D}{r_0}\left(1 - e^{-r_0(T-t)}\right),$$
$$A_4(t) = \frac{\lambda_1^2}{2\gamma b_1^2}(T-t) + \beta(2\beta+1)\sigma^2\int_t^T B(\nu)\mathrm{d}\nu, \tag{B.33}$$

with $B(t)$ given by equation (B.20).

Case B.3. $((\lambda_2 b_1 - \rho_{12}\lambda_1 b_2)/(b_1 b_2^2(1-\rho_{12}^2))) < -(\gamma/2)$ and $e^{r_0 T} \geq -(2(\lambda_2 b_1 - \rho_{12}\lambda_1 b_2)/\gamma b_1 b_2^2(1-\rho_{12}^2))$.

If $((\lambda_2 b_1 - \rho_{12}\lambda_1 b_2)/(b_1 b_2^2(1-\rho_{12}^2))) < -(\gamma/2)$ and $e^{r_0 T} \geq -(2(\lambda_2 b_1 - \rho_{12}\lambda_1 b_2)/\gamma b_1 b_2^2(1-\rho_{12}^2))$, we derive the optimal reinsurance strategy of the small company

$$p_2^*(t) = \begin{cases} 1, & 0 \leq t \leq t_2, \\ 0, & t_2 < t \leq T, \end{cases} \tag{B.34}$$

where $t_2 = T - (1/r_0)\ln(-(2(\lambda_2 b_1 - \rho_{12}\lambda_1 b_2)/\gamma b_1 b_2^2(1-\rho_{12}^2)))$. Let $t_3 = \min(t_1, t_2)$.

(1) If $\rho_{12} \geq 0$, when $0 \leq t \leq t_2$, the optimal reinsurance strategies of the big and small companies are expressed as those in equation (B.9) and when $t_2 < t \leq T$, $p_1^*(t)$ and $p_2^*(t)$ are the same as those in equation (B.30), i.e.,

$$\left(p_1^*(t), p_2^*(t)\right) = \begin{cases} \left(\frac{\lambda_1}{\gamma b_1^2}e^{-r_0(T-t)} + \frac{b_2\rho_{12}}{b_1}, 1\right), & 0 \leq t \leq t_2, \\ \left(\frac{\lambda_1}{\gamma b_1^2}e^{-r_0(T-t)}, 0\right), & t_2 < t \leq T. \end{cases} \tag{B.35}$$

Similarly, the expression of $H(t,s,x)$ is

$$H(t,s,x) = \begin{cases} -\frac{1}{\gamma}e^{-\gamma\left[e^{r_0(T-t)}\left(x - d_5(t)\right) + A_5(t) + B(t)s^{-2\beta}\right]}, & 0 \leq t \leq t_2, \\ -\frac{1}{\gamma}e^{-\gamma\left[e^{r_0(T-t)}\left(x - d_4(t)\right) + A_4(t) + B(t)s^{-2\beta}\right]}, & t_2 < t \leq T, \end{cases} \tag{B.36}$$

where

$$d_5(t) = -\frac{D}{r_0}\left(1 - e^{-r_0(T-t)}\right) - \frac{\lambda_1 b_2\rho_{12} - \lambda_2 b_1}{r_0 b_1}\left(1 - e^{-r_0(t_2-t)}\right) + \frac{\gamma b_2^2(1-\rho_{12}^2)}{4r_0}\left(e^{r_0(T-t)} - e^{r_0(T+t-2t_2)}\right),$$
$$A_5(t) = \frac{\lambda_1^2}{2\gamma b_1^2}(T-t) + \beta(2\beta+1)\sigma^2\int_t^T B(\nu)\mathrm{d}\nu, \tag{B.37}$$

and $B(t)$, $d_4(t)$, $A_4(t)$ are given in equations (B.20) and (B.33).

(2) If $\rho_{12} < 0$ and $-(\lambda_1/\gamma b_1 b_2\rho_{12}) \leq 1$, when $0 \leq t \leq t_2$, the optimal reinsurance strategies of the big and small companies are expressed as those in equation (B.23) and when $t_2 < t \leq T$, $p_1^*(t)$ and $p_2^*(t)$ are the same as those in equation (B.30), i.e.,

$$\left(p_1^*(t), p_2^*(t)\right) = \begin{cases} (0,1), & 0 \leq t \leq t_2, \\ \left(\frac{\lambda_1}{\gamma b_1^2}e^{-r_0(T-t)}, 0\right), & t_2 < t \leq T, \end{cases} \tag{B.38}$$

while $H(t,s,x)$ is

$$H(t,s,x) = \begin{cases} -\frac{1}{\gamma}e^{-\gamma\left[e^{r_0(T-t)}\left(x - d_6(t)\right) + A_6(t) + B(t)s^{-2\beta}\right]}, & 0 \leq t \leq t_2, \\ -\frac{1}{\gamma}e^{-\gamma\left[e^{r_0(T-t)}\left(x - d_4(t)\right) + A_4(t) + B(t)s^{-2\beta}\right]}, & t_2 < t \leq T, \end{cases} \tag{B.39}$$

where

$$d_6(t) = -\frac{D}{r_0}\left(1 - e^{-r_0(T-t)}\right) + \frac{\lambda_2}{r_0}\left(1 - e^{-r_0(t_2-t)}\right) + \frac{\gamma b_2^2}{4r_0}\left(e^{r_0(T-t)} - e^{r_0(T+t-2t_2)}\right),$$
$$A_6(t) = \frac{\lambda_1^2}{2\gamma b_1^2}(T-t_2) + \beta(2\beta+1)\sigma^2\int_t^T B(\nu)\mathrm{d}\nu, \tag{B.40}$$

with $B(t)$, $d_4(t)$ and $A_4(t)$ are given by equations (B.20) and (B.33).

(3) If $\rho_{12} < 0$, $-(\lambda_1/\gamma b_1 b_2\rho_{12}) > 1$ and $e^{r_0 T} < -(\lambda_1/\gamma b_1 b_2\rho_{12})$, the optimal reinsurance strategies of the big and small companies are expressed as those in equation (B.20) and $H(t,s,x)$ is given in equation (B.36).

(4) If $\rho_{12} < 0$, $-(\lambda_1/\gamma b_1 b_2\rho_{12}) > 1$ and $e^{r_0 T} \geq -(\lambda_1/\gamma b_1 b_2\rho_{12})$, when $0 \leq t \leq t_3$, the optimal reinsurance strategies of the big and small companies are the same as those in equation (B.23), when $t_3 < t \leq t_2$, $p_1^*(t)$ and $p_2^*(t)$ are expressed as those in equation (B.9) and when $t_2 < t \leq T$, $p_1^*(t)$ and $p_2^*(t)$ are shown in equation (B.30), i.e.,

$$\left(p_1^*(t), p_2^*(t)\right) = \begin{cases} (0,1), & 0 \leq t \leq t_3, \\ \left(\frac{\lambda_1}{\gamma b_1^2}e^{-r_0(T-t)} + \frac{b_2\rho_{12}}{b_1}, 1\right), & t_3 < t \leq t_2, \\ \left(\frac{\lambda_1}{\gamma b_1^2}e^{-r_0(T-t)}, 0\right), & t_2 < t \leq T. \end{cases} \tag{B.41}$$

Through the above derivatives, we obtain

$$H(t,s,x)=\begin{cases}-\frac{1}{\gamma}e^{-\gamma\left[e^{r_0(T-t)}\left(x-d_7(t)\right)+A_7(t)+B(t)s^{-2\beta}\right]}, & 0\le t\le t_3,\\ -\frac{1}{\gamma}e^{-\gamma\left[e^{r_0(T-t)}\left(x-d_5(t)\right)+A_5(t)+B(t)s^{-2\beta}\right]}, & t_3<t\le t_2,\\ -\frac{1}{\gamma}e^{-\gamma\left[e^{r_0(T-t)}\left(x-d_4(t)\right)+A_4(t)+B(t)s^{-2\beta}\right]}, & t_2<t\le T,\end{cases} \tag{B.42}$$

where

$$\begin{aligned} d_7(t)={}&-\frac{D}{r_0}\left(1-e^{-r_0(T-t)}\right)+\frac{\lambda_2}{r_0}\left(1-e^{-r_0(t_2-t)}\right)\\ &-\frac{\lambda_1 b_2\rho_{12}}{r_0 b_1}\left(e^{-r_0(t_3-t)}-e^{-r_0(t_2-t)}\right)\\ &+\frac{\gamma b_2^2}{4r_0}\left(e^{r_0(T-t)}-e^{r_0(T+t-2t_2)}\right)\\ &-\frac{\gamma b_2^2\rho_{12}^2}{4r_0}\left(e^{r_0(T+t-2t_3)}-e^{r_0(T+t-2t_2)}\right), \end{aligned} \tag{B.43}$$

$$A_7(t)=\frac{\lambda_1^2}{2\gamma b_1^2}(T-t_3)+\beta(2\beta+1)\sigma^2\int_t^T B(v)\mathrm{d}v,$$

with $B(t)$, $d_4(t)$, $A_4(t)$, $d_5(t)$, and $A_5(t)$ are given by equations (B.20), (B.33), and (B.39).

To proof Theorem 1, we first introduce a lemma. For convenience, denote $O := [0,+\infty)\times[0,+\infty)\times[0,+\infty)$.

Lemma B.1. *Take a sequence of bounded open sets O_1, O_2, $O_3,\ldots$, with $O_i\subset O_{i+1}\subset O$, $i=1,2,\ldots$ and $\cup_i O_i=O$. Let τ_i be the exiting time of $(X^{u_1^*,u_2^*}(t),S(t))$ from O_i. If one of the conditions (a) and (b) in Theorem 1 holds, then we have $E[H^{u_1^*,u_2^*}(\tau_i\wedge T,S(\tau_i\wedge T),X^{u_1^*,u_2^*}(\tau_i\wedge T))^2\mid S(t)=s,X^{u_1^*,u_2^*}(t)=x]<\infty$ for $i=1,2,\ldots$.*

Proof. We first denote $H^{u_1^*,u_2^*}(t)=H^{u_1^*,u_2^*}(t,S(t),X^{u_1^*,u_2^*}(t))$ for simplicity. Applying Itô's formula, we have

$$\begin{aligned} \mathrm{d}\left(H^{u_1^*,u_2^*}(t)\right)^2 ={}& 2H^{u_1^*,u_2^*}(t)\Big\{\left[H_x^{u_1^*,u_2^*}\pi^*(t)\sigma S^{\gamma_1}(t)+H_s^{u_1^*,u_2^*}\sigma S^{\beta+1}(t)\right]\mathrm{d}W_3(t)+H_x^{u_1^*,u_2^*}p_1^*(t)b_1\mathrm{d}W_1(t)\\ &-H_x^{u_1^*,u_2^*}p_2^*(t)b_2\mathrm{d}W_2(t)+\mathscr{A}^{u_1^*,u_2^*}H^{u_1^*,u_2^*}(t)\mathrm{d}t\Big\}+\Big\{\left(H_x^{u_1^*,u_2^*}\right)^2\left[(\pi^*(t))^2\sigma^2S^{2\beta}(t)+(p_1^*(t))^2b_1^2+(p_2^*(t))^2b_2^2\right]\\ &+\left(H_s^{u_1^*,u_2^*}\right)^2\sigma^2S^{2\beta+2}(t)+2H_x^{u_1^*,u_2^*}H_s^{u_1^*,u_2^*}\pi^*(t)\sigma^2S^{2\beta+1}(t)\Big\}\mathrm{d}t. \end{aligned} \tag{B.44}$$

Since u_1^*,u_2^* are the optimal strategies of equations (20) and (21), $\mathscr{A}^{\pi^*}H^{u_1^*,u_2^*}(t,s,x)=0$. Putting the expressions of H_x, H_s, $\pi^*(t)$, $p_1^*(t)$, and $p_2^*(t)$ into equation (B.44), we obtain

$$\begin{aligned} \frac{\mathrm{d}\left(H^{u_1^*,u_2^*}(t)\right)^2}{\left(H^{u_1^*,u_2^*}(t)\right)^2} ={}& -2\left[\frac{\mu-r_0}{\sigma}S^{-\beta}(t)\mathrm{d}W_3(t)+\gamma e^{r_0(T-t)}p_1^*(t)b_1\mathrm{d}W_1(t)-\gamma e^{r_0(T-t)}p_2^*(t)b_2\mathrm{d}W_2(t)\right]\\ &+\left[\frac{(\mu-r_0)^2}{\sigma^2}S^{-2\beta}(t)+\gamma^2e^{2r_0(T-t)}(p_1^*(t))^2b_1^2+\gamma^2e^{2r_0(T-t)}(p_2^*(t))^2b_2^2\right]\mathrm{d}t. \end{aligned} \tag{B.45}$$

The solution to the above equation is

$$\begin{aligned}\frac{\left(H^{u_1^*,u_2^*}(t)\right)^2}{\left(H^{u_1^*,u_2^*}(0)\right)^2} = \exp\Bigg\{&\int_0^t -\frac{2(\mu-r_0)}{\sigma}S^{-\beta}(\nu)\mathrm{d}W_3(\nu) - \frac{1}{2}\int_0^t \frac{4(\mu-r_0)^2}{\sigma^2}S^{-2\beta}(\nu)\mathrm{d}\nu \\ &+ \int_0^t -2\gamma e^{r_0(T-\nu)}p_1^*(\nu)b_1 dW_1(\nu) - \frac{1}{2}\int_0^t 4\gamma^2 e^{2r_0(T-\nu)}\left(p_1^*(\nu)\right)^2 b_1^2 \mathrm{d}\nu \\ &+ \int_0^t 2\gamma e^{r_0(T-\nu)}p_2^*(\nu)b_2 dW_2(\nu) - \frac{1}{2}\int_0^t 4\gamma^2 e^{2r_0(T-\nu)}\left(p_2^*(\nu)\right)^2 b_2^2 \mathrm{d}\nu \\ &+ \int_0^t \left(3\gamma^2 e^{2r_0(T-\nu)}\left(p_1^*(\nu)\right)^2 b_1^2 + 3\gamma^2 e^{2r_0(T-\nu)}\left(p_2^*(\nu)\right)^2 b_2^2 + \frac{3(\mu-r_0)^2}{\sigma^2}S^{-2\beta}(\nu)\right)\mathrm{d}\nu\Bigg\}.\end{aligned} \tag{B.46}$$

According to the expression of the CEV model and Itô's formula, we can derive

$$\mathrm{d}S(t)^{-2\beta} = \left(\beta(2\beta+1)\sigma^2 - 2\beta\mu S^{-2\beta}(t)\right)\mathrm{d}t - 2\beta\sigma\sqrt{S^{-2\beta}(t)}\mathrm{d}W_3(t). \tag{B.47}$$

By Zeng and Taksar [32], we know that

$$\exp\left\{\int_0^t -\frac{2(\mu-r_0)}{\sigma}S^{-\beta}(\nu)\mathrm{d}W_3(\nu) - \frac{1}{2}\int_0^t \frac{4(\mu-r_0)^2}{\sigma^2}S^{-2\beta}(\nu)\mathrm{d}\nu\right\}, \tag{B.48}$$

is martingales and

$$E\left[\exp\left\{\int_0^t \frac{3(\mu-r_0)^2}{\sigma^2}S^{-2\beta}(\nu)\mathrm{d}\nu\right\}\right] < \infty, \tag{B.49}$$

when one of the conditions (a) and (b) in Theorem 1 is satisfied. According to the expression of $p_1^*(t)$, $p_2^*(t)$, and Novikov's condition,

$$\begin{aligned}&\exp\left\{\int_0^t -2\gamma e^{r_0(T-\nu)}p_1^*(\nu)b_1\mathrm{d}W_1(\nu) - \frac{1}{2}\int_0^t 4\gamma^2 e^{2r_0(T-\nu)}\left(p_1^*(\nu)\right)^2 b_1^2\mathrm{d}\nu\right\}, \\ &\exp\left\{\int_0^t 2\gamma e^{r_0(T-\nu)}p_2^*(\nu)b_2\mathrm{d}W_2(\nu) - \frac{1}{2}4\int_0^t 2\gamma e^{r_0(T-\nu)}p_2^*(\nu)b_2^2\mathrm{d}\nu\right\},\end{aligned} \tag{B.50}$$

are martingales. Taking expectation from both sides of equation (B.46) yields

$$\begin{aligned}E\left[\left(H^{u_1^*,u_2^*}(t)\right)^2\right] = \left(H^{u_1^*,u_2^*}(0)\right)^2\Bigg[E\exp\Bigg\{&\int_0^t 3\gamma^2 \mathrm{e}^{2r_0(T-\nu)} \\ &\cdot \left(p_1^*(\nu)\right)^2 b_1^2 + 3\gamma^2 \mathrm{e}^{2r_0(T-\nu)}\left(p_2^*(\nu)\right)^2 b_2^2 \\ &+ \frac{3(\mu-r_0)^2}{\sigma^2}S^{-2\beta}(\nu)\mathrm{d}\nu\Bigg\}\Bigg] < \infty,\end{aligned} \tag{B.51}$$

i.e., $E[(H^{u_1^*,u_2^*}(t, S(t), X^{u_1^*,u_2^*}(t)))^2] < \infty$. So $E[(H^{u_1^*,u_2^*}(\tau_i \wedge T, S(\tau_i \wedge T), X^{u_1^*,u_2^*}(\tau_i \wedge T)))^2 \mid S(t) = s, X^{u_1^*,u_2^*}(t) = x] < \infty$ for $i = 1, 2, \ldots$. □

Data Availability

The data used to support the findings of this study are included within the article.

Conflicts of Interest

The authors declare that they have no conflicts of interest.

Acknowledgments

This research was supported by the National Natural Science Foundation of China (Nos. 11801179, 71573110, 71771220, 11971172, 71701084), the "Chenguang Program", Shanghai, China (No. 18CG26), the Fundamental Research Funds for the Central Universities (No. 2019ECNU-HWFW028), and the 111 Project, China (No. B14019).

References

[1] H. Schmidli, "On minimizing the ruin probability by investment and reinsurance," *The Annals of Applied Probability*, vol. 12, no. 3, pp. 890–907, 2002.

[2] D. S. Promislow and V. R. Young, "Minimizing the probability of ruin when claims follow Brownian motion with drift," *North American Actuarial Journal*, vol. 9, no. 3, pp. 109–128, 2005.

[3] L. Bai and J. Guo, "Optimal proportional reinsurance and investment with multiple risky assets and no-shorting constraint," *Insurance: Mathematics and Economics*, vol. 42, no. 3, pp. 968–975, 2008.
[4] H. Yang and L. Zhang, "Optimal investment for insurer with jump-diffusion risk process," *Insurance: Mathematics and Economics*, vol. 37, no. 3, pp. 615–634, 2005.
[5] N. Wang, "Optimal investment for an insurer with exponential utility preference," *Insurance: Mathematics and Economics*, vol. 40, no. 1, pp. 77–84, 2007.
[6] Y. Cao and N. Wan, "Optimal proportional reinsurance and investment based on Hamilton-Jacobi-Bellman equation," *Insurance: Mathematics and Economics*, vol. 45, no. 2, pp. 157–162, 2009.
[7] W. Yu, Y. Yong, G. Guan, Y. Huang, W. Su, and C. Cui, "Valuing guaranteed minimum death benefits by cosine series expansion," *Mathematics*, vol. 7, no. 9, p. 835, 2019.
[8] Z. Zhang, Y. Yong, and W. Yu, "Valuing equity-linked dealth benefits in general exponential Lévy models," *Journal of Computational and Applied Mathematics*, vol. 365, Article ID 112377, 2020.
[9] X. Peng, W. Su, and Z. Zhang, "On a perturbed compound Poisson risk model under a periodic threshold-type dividend strategy," *Journal of Industrial and Management Optimization*, vol. 13, no. 5, pp. 1–20, 2019.
[10] W. Yu, F. Wang, Y. Huan, and H. Liu, "Social optimal mean field control problem for population growth model," *Asian Journal of Control*, 2019.
[11] J. Ruan, W. Yu, K. Song, Y. Sun, Y. Huang, and X. Yu, "A note on a generalized Berber-Shiu discounted penalty function for a compound Poisson risk model," *Mathematics*, vol. 7, no. 10, p. 891, 2019.
[12] W. Yu, Y. Huan, and C. Cui, "The absolute ruin insurance risk model with a threshold dividend strategy," *Symmetry*, vol. 10, no. 9, p. 377, 2018.
[13] Y. Huang, W. Yu, Y. Pan, and C. Cui, "Estimating the gerber-shiu expected discounted penalty function for lévy risk model," *Discrete Dynamics in Nature and Society*, vol. 2019, Article ID 3607201, 15 pages, 2019.
[14] Y. Zeng, D. Li, and A. Gu, "Robust equilibrium reinsurance-investment strategy for a mean-variance insurer in a model with jumps," *Insurance: Mathematics and Economics*, vol. 66, pp. 138–152, 2016.
[15] D. Li, Y. Zeng, and H. Yang, "Robust optimal excess-of-loss reinsurance and investment strategy for an insurer in a model with jumps," *Scandinavian Actuarial Journal*, vol. 2018, no. 2, pp. 145–171, 2018.
[16] J. Suijs, A. De Waegenaere, and P. Borm, "Stochastic cooperative games in insurance," *Insurance: Mathematics and Economics*, vol. 22, no. 3, pp. 209–228, 1998.
[17] X. Zeng, "A stochastic differential reinsurance game," *Journal of Applied Probability*, vol. 47, no. 2, pp. 335–349, 2010.
[18] M. Taksar and X. Zeng, "Optimal non-proportional reinsurance control and stochastic differential games," *Insurance: Mathematics and Economics*, vol. 48, no. 1, pp. 64–71, 2011.
[19] A. Bensoussan, C. C. Siu, S. C. P. Yam, and H. Yang, "A class of non-zero-sum stochastic differential investment and reinsurance games," *Automatica*, vol. 50, no. 8, pp. 2025–2037, 2014.
[20] H. Meng, S. Li, and Z. Jin, "A reinsurance game between two insurance companies with nonlinear risk processes," *Insurance: Mathematics and Economics*, vol. 62, pp. 91–97, 2015.
[21] C. S. Pun and H. Y. Wong, "Robust non-zero-sum stochastic differential reinsurance game," *Insurance: Mathematics and Economics*, vol. 68, pp. 169–177, 2016.
[22] C. C. Siu, S. C. P. Yam, H. Yang, and H. Zhao, "A class of nonzero-sum investment and reinsurance games subject to systematic risks," *Scandinavian Actuarial Journal*, vol. 2017, no. 8, pp. 670–707, 2017.
[23] C. J. Cox and S. A. Ross, "The valuation of options for alternative stochastic processes," *Journal of Financial Economics*, vol. 4, no. 1-2, pp. 145–166, 1976.
[24] E. M. Stein and J. C. Stein, "Stock price distributions with stochastic volatility: an analytic approach," *Review of Financial Studies*, vol. 4, no. 4, pp. 727–752, 1991.
[25] S. L. Heston, "A closed-form solution for options with stochastic volatility with applications to bond and currency options," *Review of Financial Studies*, vol. 6, no. 2, pp. 327–343, 1993.
[26] M. Gu, Y. Yang, S. Li, and J. Zhang, "Constant elasticity of variance model for proportional reinsurance and investment strategies," *Insurance: Mathematics and Economics*, vol. 46, no. 3, pp. 580–587, 2010.
[27] Z. Liang, K. C. Yuen, and K. C. Cheung, "Optimal reinsurance-investment problem in a constant elasticity of variance stock market for jump-diffusion risk model," *Applied Stochastic Models in Business and Industry*, vol. 28, no. 6, pp. 585–597, 2012.
[28] X. Lin and Y. Li, "Optimal reinsurance and investment for a jump diffusion risk process under the CEV model," *North American Actuarial Journal*, vol. 15, no. 3, pp. 417–431, 2011.
[29] A. Gu, X. Guo, Z. Li, and Y. Zeng, "Optimal control of excess-of-loss reinsurance and investment for insurers under a CEV model," *Insurance: Mathematics and Economics*, vol. 51, no. 3, pp. 674–684, 2012.
[30] X. Zheng, J. Zhou, and Z. Sun, "Robust optimal portfolio and proportional reinsurance for an insurer under a CEV model," *Insurance: Mathematics and Economics*, vol. 67, pp. 77–87, 2016.
[31] J. C. Cox, "The constant elasticity of variance option pricing model," *The Journal of Portfolio Management*, vol. 23, no. 5, pp. 15–17, 1996.
[32] X. Zeng and M. Taksar, "A stochastic volatility model and optimal portfolio selection," *Quantitative Finance*, vol. 13, no. 10, pp. 1547–1558, 2013.

Hindawi
Mathematical Problems in Engineering
Volume 2020, Article ID 4758052, 10 pages
https://doi.org/10.1155/2020/4758052

Research Article

Asian Option Pricing under an Uncertain Volatility Model

Yuecai Han and Chunyang Liu

School of Mathematics, Jilin University, Changchun 130012, China

Correspondence should be addressed to Yuecai Han; hanyc@jlu.edu.cn and Chunyang Liu; liucy17@mails.jlu.edu.cn

Received 23 January 2020; Accepted 5 March 2020; Published 21 April 2020

Guest Editor: Zhimin Zhang

In this paper, we study the asymptotic behavior of Asian option prices in the worst-case scenario under an uncertain volatility model. We derive a procedure to approximate Asian option prices with a small volatility interval. By imposing additional conditions on the boundary condition and splitting the obtained Black–Scholes–Barenblatt equation into two Black–Scholes-like equations, we obtain an approximation method to solve a fully nonlinear PDE.

1. Introduction

An option on a traded account is a financial contract that allows the buyer of the contract the right to trade an underlying asset for a specified price, called the strike price, during the lifetime of the option. There are various options, such as European options, American options, Asian options and barrier options. The foundation for the modern analysis of options, the Black–Scholes–Merton pricing formula for European options, was introduced by Black and Scholes [1] and Merton [2]. The Black–Scholes–Merton model assumes constant volatility. However, constant volatility cannot explain the observed market prices for options.

After Black, Scholes and Merton's work, some scholars studied option pricing models with stochastic volatility. A series of papers introduced several models for stochastic volatility, such as the Hull–White stochastic volatility model [3] and the Heston stochastic volatility model [4].

The uncertain volatility model is another approach to describe nonconstant volatility. In 1995, Lyons [5] and Avellaneda et al. [6] introduced uncertain volatility models. In these models, volatility is assumed to lie within a range of values, so prices are no longer unique. We can only get the best-case and worst-case scenario prices. Several studies investigate problems with uncertain volatility. We can see these results in Lyons [5], Avellaneda et al. [6], Dokuchaev and Savkin [7], Zhou and Li [8], and Forsyth and Vetzal [9]. These papers show pricing in uncertain volatility models involving nonlinear partial differential equations. Vorbrink [10] and Epstein and Ji [11] generalized the no-arbitrage theory to financial markets with ambiguous volatility in the mathematically rigorous framework of G-Brownian motion. Method of approximating the valuation equations and the latest research on Fourier transform was given by Zhang et al. [12] and Yu et al. [13]. Pooley et al. [14] and Avellaneda et al. [6] propose some numerical methods.

In 2014, Fouque and Ren [15] studied the price of European derivatives in the worst-case scenario with the uncertain volatility model. They provide an approximate method of pricing the derivatives with a small volatility interval. In addition, the paper also shows that the solution reduces to a constant volatility problem for simple options with convex payoffs.

This study examines the pricing problem of Asian options. The payoff function is path dependent on risky asset price processes with the addition of another variable to solve the problem. The first problem in estimating the worst-case scenario Asian option prices is obtaining the Hamilton–Jacobi–Bellman (HJB) equation for the prices. The HJB equation is called the Black–Scholes–Barenblatt (BSB) equation in financial mathematics. We can obtain the BSB equation using stochastic control theory. The next difficulty is to prove the convergence of the estimation. To control the error term, we obtain its expectation form using the

Dynkin's formula and determine the conditions to impose on the payoff function through proof and deduction. Finally, we obtain the approximation procedure for the prices. Compared to Fouque and Ren's paper [15], we add an equation to the stochastic control system, which we can also reflect in the BSB equation. In terms of the dynamics of the risky asset price process, we provide an equation to describe the path dependence. When estimating the expectation form, we use the relationship between the two processes, in Section 4.4, we fix one of the two variables first to simplify the problem. We manage the two variables using another method that changes the form of the BSB equation.

The paper is organized as follows. In Section 2, we briefly describe Asian options under the uncertain volatility model and give the BSB equations for the option prices. In Section 3, we estimate the Asian option prices in the worst-case scenario, where the estimation relies on two Black–Scholes-like PDEs. Next, we propose the main result of this study, which shows the rationality of the estimation. In Section 4, we give the proof of the main result. Through the conditions imposed on the payoff function, we obtain the convergence of the error term. In the process, we obtain the expectation form of the error term, which we divide into three parts. We derive the control for each part using stochastic control theory and the properties of the worst-case scenario Asian option price process. Finally, we conclude the paper.

2. Asian Options under Uncertain Volatility Model

In this section, we introduce Asian options under the uncertain volatility model. Then, we provide the BSB equation of Asian option prices. Suppose that $\mathscr{X}$ is an Asian option written on a risky asset with maturity T and payoff $\varphi(\cdot)$. $\varphi(\cdot)$ is a nonconvex function and the result is identical to the Black–Scholes result under convex conditions. That is to say, this study results cover generalized Asian options. Here, generality means that the payoff function $\varphi(\cdot)$ can be in different forms, as long as it is nonconvex. Assume that the price process of the risky asset X_t solves the stochastic differential equation:

$$\mathrm{d}X_t = rX_t\mathrm{d}t + \sigma_t X_t \mathrm{d}W_t, \tag{1}$$

where r is the constant risk-free interest rate and W_t is a standard Brownian motion on the probability space $(\Omega, \mathfrak{F}, \mathbb{P})$. Let $\underline{\sigma}$ and $\overline{\sigma}$ are two constants and there is $\underline{\sigma} \leq \overline{\sigma}$. The volatility process $\sigma_t \in \mathscr{A}[\underline{\sigma}, \overline{\sigma}]$ for each $t \in [0, T]$, which is a family of progressively measurable and $[\underline{\sigma}, \overline{\sigma}]$-valued processes. By the abovementioned definition, we know that volatility in an uncertain volatility model is not a stochastic process with a probability distribution, but a family of stochastic processes with unknown prior information. Thus, we can use model ambiguity to distinguish between uncertain volatility models.

Due to the path dependence of risky asset price processes, we assume that $Y_{t,T}$ satisfies

$$Y_{t,T} = \frac{Y_T - Y_t}{T - t}, \tag{2}$$

where $Y_t = \int_0^t X_u \mathrm{d}u$. Then, we can obtain Asian option prices in the worst-case scenario at time $t < T$ as follows:

$$V(t, X_t, Y_t) = \exp(-r(T-t)) \operatorname*{esssup}_{\sigma\in\mathscr{A}[\underline{\sigma},\overline{\sigma}]} E\left[\varphi(Y_{0,T}) \,\middle|\, \mathfrak{F}_t\right], \tag{3}$$

where esssup is the essential supremum. By the ambiguity of the uncertain volatility model, we obtain the definition of price as equation (3). Obviously, the worst-case scenario price is for the option seller and is related to the coherent risk measure that quantifies the model risk induced by volatility uncertainty (see [16]). Moreover, model ambiguity in mathematical finance has captured the attention of many. Therefore, we should pay attention to the importance of the worst-case prices.

Through stochastic control theory (see [17]), $V(t, X_t, Y_t)$ satisfies the HJB (BSB) equation.

Lemma 1. *$V(t, X_t, Y_t)$ satisfies the following BSB equation:*

$$\begin{cases} \partial_t V + r(x\partial_x V - V) + x\partial_y V + \sup\limits_{\sigma\in\mathscr{A}[\underline{\sigma},\overline{\sigma}]} \left[\dfrac{1}{2}x^2\sigma^2\partial_{xx}^2 V\right] = 0, \\ 0 \leq t \leq T,\ x \geq 0,\ y \geq 0, \\ V(T, x, y) = \varphi\left(\dfrac{y}{T}\right), \quad x \geq 0,\ y \geq 0. \end{cases} \tag{4}$$

Proof. Note that the stochastic control system is

$$\begin{cases} \mathrm{d}X_t = rX_t\mathrm{d}t + \sigma_t X_t \mathrm{d}W_t, \quad \sigma_t \in \mathscr{A}[\underline{\sigma}, \overline{\sigma}], \\ \mathrm{d}Y_t = X_t \mathrm{d}t. \end{cases} \tag{5}$$

Then, for all $(s, x, y) \in [0, T] \times R^+ \times R^+$, we first establish the dynamic program frame:

$$\begin{cases} \mathrm{d}X_t = rX_t\mathrm{d}t + \sigma_t X_t \mathrm{d}W_t, \\ \mathrm{d}Y_t = X_t \mathrm{d}t, \\ X_s = x, \\ Y_s = y. \end{cases} \tag{6}$$

The cost function is

$$J(s, x, y; \sigma) = E_s\left[e^{-r(T-s)}\varphi(Y_{0,T})\right], \tag{7}$$

where $E_s[\cdot] = E[\cdot \mid \mathfrak{F}_s]$. The value function is

$$V(s, x, y) = \operatorname*{esssup}_{\sigma\in\mathscr{A}[\underline{\sigma},\overline{\sigma}]} J(s, x, y; \sigma). \tag{8}$$

For all $0 \leq s \leq \widehat{s} \leq T$, $\sigma \in \mathscr{A}[\underline{\sigma}, \overline{\sigma}]$, we have

$$\begin{aligned} V(s, x, y) &\geq E_s\left[e^{-r(T-s)}\varphi(Y_{0,T})\right] \\ &= E_s\left[\int_s^{\widehat{s}} -re^{-r(T-t)}\varphi \mathrm{d}t + e^{-r(T-\widehat{s})}\varphi\right]. \end{aligned} \tag{9}$$

Then, we obtain

$$0 \geq E_s\left[\int_s^{\widehat{s}} -re^{-r(T-t)}\varphi \mathrm{d}t\right] + V(\widehat{s}, x, y) - V(s, x, y). \quad (10)$$

Dividing both sides of the inequality by $\widehat{s} - s$, we have

$$0 \geq E_s\left[\frac{\int_s^{\widehat{s}} -re^{-r(T-t)}\varphi \mathrm{d}t}{\widehat{s} - s}\right] + \frac{V(\widehat{s}, x, y) - V(s, x, y)}{\widehat{s} - s}. \quad (11)$$

Here, we assume that φ is Lipschitz continuous. Then, according to It ô's formula and equation (6), we obtain

$$\begin{aligned} \mathrm{d}V &= V_t \mathrm{d}t + V_x \mathrm{d}X_t + V_y \mathrm{d}Y_t + \frac{1}{2}V_{xx}\mathrm{d}X_t\mathrm{d}X_t + \frac{1}{2}V_{yy}\mathrm{d}Y_t\mathrm{d}Y_t \\ &\quad + \frac{1}{2}V_{xy}\mathrm{d}X_t\mathrm{d}Y_t \\ &= \left(V_t + rX_tV_x + X_tV_y + \frac{1}{2}\sigma_t^2X_t^2V_{xx}\right)\mathrm{d}t + \sigma_t X_t V_x \mathrm{d}W_t. \end{aligned} \quad (12)$$

Let $\widehat{s} \longrightarrow s$. For all $\sigma \in \mathscr{A}[\underline{\sigma}, \overline{\sigma}]$, we have

$$\begin{aligned} 0 &\geq -rE_s\left[e^{-r(T-s)}\varphi\right] + V_t + rX_sV_x + X_sV_y + \frac{1}{2}\sigma_s^2X_s^2V_{xx} \\ &\geq -rV(s, x, y) + V_t(s, x, y) + rxV_x(s, x, y) + xV_y(s, x, y) \\ &\quad + \frac{1}{2}\sigma_s^2X_s^2V_{xx}(s, x, y), \end{aligned} \quad (13)$$

which is

$$0 \geq -rV + V_t + rxV_x + xV_y + \sup_{\sigma \in \mathscr{A}[\underline{\sigma}, \overline{\sigma}]} \frac{1}{2}\sigma^2x^2V_{xx}. \quad (14)$$

In contrast, for any $\varepsilon > 0$, there is a $\sigma(\varepsilon) \in \mathscr{A}[\underline{\sigma}, \overline{\sigma}]$ such that

$$\begin{aligned} V(s, x, y) - \varepsilon(\widehat{s} - s) &\leq E_s\left[e^{-r(T-s)}\varphi\right] \\ &= E_s\left[\int_s^{\widehat{s}} -re^{-r(T-t)}\varphi \mathrm{d}t\right] + E_s\left[e^{-r(T-\widehat{s})}\varphi\right]. \end{aligned} \quad (15)$$

Thus, we have

$$-\varepsilon \leq E_s\left[\frac{\int_s^{\widehat{s}} -re^{-r(T-t)}\varphi \mathrm{d}t}{\widehat{s} - s}\right] + \frac{V(\widehat{s}, x, y) - V(s, x, y)}{\widehat{s} - s}. \quad (16)$$

From the argument above, we obtain

$$0 \leq -rV + V_t + rxV_x + xV_y + \sup_{\sigma \in \mathscr{A}[\underline{\sigma}, \overline{\sigma}]} \frac{1}{2}\sigma^2x^2V_{xx}. \quad (17)$$

Combining (14) with (17), we have

$$0 = -rV + V_t + rxV_x + xV_y + \sup_{\sigma \in \mathscr{A}[\underline{\sigma}, \overline{\sigma}]} \frac{1}{2}\sigma^2x^2V_{xx}. \quad (18)$$

□

Remark 1. Here, adding variable Y into the dynamic system leads to a more complex stochastic control system, which adds the dimensionality of the BSB equation.

Remark 2. Note that (4) is a fully nonlinear PDE which has no solution, unlike the Black–Scholes equation. Thus, we solve the problem by reducing it to two Black–Scholes-like PDEs.

3. Black–Scholes-Like PDEs and Main Result

In this section, we first reparameterize the uncertain volatility model to study prices in the worst-case scenario. Assume that the risky asset price process satisfies the following SDE:

$$\begin{cases} \mathrm{d}X_t^\varepsilon = rX_t^\varepsilon \mathrm{d}t + \sigma_t X_t^\varepsilon \mathrm{d}W_t, \\ \mathrm{d}Y_t^\varepsilon = X_t^\varepsilon \mathrm{d}t, \end{cases} \quad (19)$$

where $\sigma_t \in \mathscr{A}^\varepsilon = \{\sigma_t | \sigma_t \text{ is a } [\sigma_0, \sigma_0 + \varepsilon]\text{–valued progressively measurable process}\}$ and $\sigma_0 \in [\underline{\sigma}, \overline{\sigma}]$. The cost function is

$$J^\varepsilon(t, x, y; \sigma) = e^{-r(T-t)}E_{txy}\left[\varphi\left(Y_{0,T}^\varepsilon\right)\right], \quad (20)$$

where $E_{txy}[\cdot]$ refers to the conditional expectation taken with respect to $X_t^\varepsilon = x$, $Y_t^\varepsilon = y$. The value function is

$$V^\varepsilon(t, x, y; \sigma) = \operatorname*{esssup}_{\sigma \in \mathscr{A}^\varepsilon}\left[J^\varepsilon(t, x, y; \sigma)\right]. \quad (21)$$

By Lemma 1, we obtain the following BSB equation for V^ε:

$$\begin{cases} \partial_t V^\varepsilon + r\left(x\partial_x V^\varepsilon - V^\varepsilon\right) + x\partial_y V^\varepsilon + \sup_{\sigma \in \mathscr{A}^\varepsilon} \frac{1}{2}x^2\sigma^2\partial_{xx}^2 V^\varepsilon = 0, \\ 0 \leq t \leq T,\ x \geq 0,\ y \geq 0, \\ V^\varepsilon(T, x, y) = \varphi\left(\frac{y}{T}\right), \quad x \geq 0,\ y \geq 0, \end{cases} \quad (22)$$

which is equivalent to

$$\begin{cases} \partial_t V^\varepsilon + r\left(x\partial_x V^\varepsilon - V^\varepsilon\right) + x\partial_y V^\varepsilon \\ \quad + \sup_{\gamma \in \mathscr{A}[0,1]} \frac{1}{2}x^2\left(\sigma_0 + \varepsilon\gamma\right)^2\partial_{xx}^2 V^\varepsilon = 0, \\ 0 \leq t \leq T,\ x \geq 0,\ y \geq 0, \\ V^\varepsilon(T, x, y) = \varphi\left(\frac{y}{T}\right), \quad x \geq 0,\ y \geq 0, \end{cases} \quad (23)$$

where $\mathscr{A}[0,1] = \{\gamma_t \mid \gamma_t \text{ is a } [0,1]\text{–valued progressively measurable process}\}$. It is obvious that the worst-case scenario price is higher than any Black–Scholes price with a constant volatility of $\sigma_0 \in [\underline{\sigma}, \overline{\sigma}]$. In the following section, we will show that the worst-case scenario price of Asian options will converge to its Black–Scholes price with constant volatility σ_0. In addition, we can obtain the rate of convergence of the Asian option prices as the volatility interval shrinks to a single point. Then, we can estimate prices through this result when the interval is sufficiently small.

Let V_0 be the Black–Scholes prices, $V^0 = V^\varepsilon|_{\varepsilon=0}$, $V_1 = \partial_\varepsilon V^\varepsilon|_{\varepsilon=0}$. Now, we suppose that V^ε is continuous with respect to ε. Then, by the continuity of V^ε and equation (3), we have $V_0 = V^0 = V^\varepsilon|_{\varepsilon=0}$. It is well known that V_0 satisfies the following partial differential equation:

$$\begin{cases} \partial_t V_0 + r\left(x\partial_x V_0 - V_0\right) + x\partial_y V_0 + \dfrac{1}{2}\sigma_0^2 x^2 \partial_{xx}^2 V_0 = 0, \\ 0 \le t \le T,\ x \ge 0,\ y \ge 0, \\ V_0(T, x, y) = \varphi\left(\dfrac{y}{T}\right), \quad x \ge 0,\ y \ge 0. \end{cases} \tag{24}$$

In contrast, we have $V_1 = \partial_\varepsilon V^\varepsilon|_{\varepsilon=0}$, which is the rate of convergence of the Asian option prices as ε approaches 0. To obtain the equation characterizing V_1, we differentiate both sides of equation (23) with respect to ε and let $\varepsilon = 0$, then we have

$$\begin{cases} \partial_t V_1 + r\left(x\partial_x V_1 - V_1\right) + x\partial_y V_1 + \dfrac{1}{2}\sigma_0^2 x^2 \partial_{xx}^2 V_1 \\ \quad + \sup\limits_{\gamma \in \mathscr{A}[0,1]} \gamma\sigma_0 x^2 \partial_{xx}^2 V_0 = 0, \\ 0 \le t \le T, x \ge 0, y \ge 0, \\ V_1(T, x, y) = 0, \quad x \ge 0,\ y \ge 0. \end{cases} \tag{25}$$

We now have two Black–Scholes-like PDEs. Next, we want to find the connection between V^ε and V_0, V_1. Then, we try to prove whether it is possible to impose additional conditions on the payoff function to make the error term $V^\varepsilon - (V_0 + \varepsilon V_1)$ be of order $o(\varepsilon)$. That is to say, the estimation of the worst-case scenario Asian option prices will approach the truth-value as the model ambiguity decreases. This will also provide a method to estimate the worst-case Asian option prices. By the deduction in Section 4, we obtain the following theorem, which is the main result of this study.

Theorem 1. *Assume that $\varphi \in \mathscr{C}_p^2(R^+)$ is Lipschitz continuous, the fourth derivative of φ exists and the second derivative of φ is continuous. Then,*

$$\lim_{\varepsilon \downarrow 0} \frac{V^\varepsilon - \left(V_0 + \varepsilon V_1\right)}{\varepsilon} = 0. \tag{26}$$

Here, $\varphi \in \mathscr{C}_p^2(R^+)$ means that its derivatives up to order 2 have polynomial growth.

Remark 3. There are some difficulties in proving Theorem 1. The first is how to convert the error term into an estimable form. Here, we obtain its expectation form and divide it into three parts in Section 4. The second difficulty is how to estimate the three parts. Here, we will use stochastic control theory, the zero set property of equation (33), the properties of sublinear expectation in [18], and the properties of the worst-case scenario Asian option price processes.

Remark 4. By Theorem 1, we can compute Asian option price $V^\varepsilon(t, X_t^\varepsilon, Y_t^\varepsilon)$ with its approximation, $V_0(t, X_t^\varepsilon, Y_t^\varepsilon) + \varepsilon V_1(t, X_t^\varepsilon, Y_t^\varepsilon)$, where $V_0(t, X_t^\varepsilon, Y_t^\varepsilon)$ is the Black–Scholes price of the Asian option and we can compute $V_1(t, X_t^\varepsilon, Y_t^\varepsilon)$ numerically by a simple difference scheme according to (25) (see [14]).

Remark 5. Note that (24) and (25) are independent of ε. Thus, when we compute V^ε with different ε, we only need to compute V_0 and V_1 once for all small values of ε by Theorem 1.

4. Proof of the Main Result

In this section, we try to control the error term to prove that we can compute V^ε with its estimation $V_0 + \varepsilon V_1$. Additionally, from the conditions imposed on φ mentioned in Theorem 1, we have the following process of proof. The following parts also reflect our thought process.

4.1. The Lipschitz Continuity of the Payoff Function. From Section 3, we know that only with the continuity of V^ε can we obtain the PDEs of $V_0 = (V^\varepsilon|_{\varepsilon=0})$ and $V_1 = (\partial_\varepsilon V^\varepsilon|_{\varepsilon=0})$. Thus, to obtain the continuity of V^ε, we suppose that φ is Lipschitz continuous. Then, there exists a constant K_1 such that

$$|\varphi(x) - \varphi(y)| \le K_1 |x - y|, \quad \text{for all } x \ne y,\ x, y \in R^+. \tag{27}$$

Thus, we have the following Lemma.

Lemma 2. *Assume that φ is Lipschitz continuous. Then, V^ε is continuous with respect to ε.*

Proof. Let $0 \le \varepsilon_0 \le \varepsilon < 1$. Note that

$$V^\varepsilon(t, x, y; \sigma) = \operatorname*{esssup}_{\sigma \in \mathscr{A}^\varepsilon} \left\{ e^{-r(T-t)} E_{txy}\left[\varphi\left(Y_{0,T}^\varepsilon\right)\right] \right\}. \tag{28}$$

We have

$$\begin{aligned} e^{r(T-t)} V^{\varepsilon_0}(t, x, y; \sigma) &= \operatorname*{esssup}_{\sigma \in \mathscr{A}^{\varepsilon_0}} E_{txy}\left[\varphi\left(Y_{0,T}^{\varepsilon_0}(\sigma)\right)\right] \\ &= \operatorname*{esssup}_{\sigma \in \mathscr{A}^{\varepsilon}} E_{txy}\left[\varphi\left(Y_{0,T}^{\varepsilon}\left(\sigma \wedge \left(\sigma_0 + \varepsilon_0\right)\right)\right)\right]. \end{aligned} \tag{29}$$

By the Lipschitz continuity of φ and equation (1), there is a constant K_1 such that

$$\begin{aligned}
&e^{r(T-t)}\left|V^{\varepsilon}(t,x,y;\sigma)-V^{\varepsilon_0}(t,x,y;\sigma)\right| \\
&\quad\leq \operatorname*{esssup}_{\sigma\in\mathscr{A}^{\varepsilon}}\left|E_{txy}\left[\varphi\left(Y^{\varepsilon}_{0,T}(\sigma)\right)\right]-E_{txy}\left[\varphi\left(Y^{\varepsilon}_{0,T}(\sigma\wedge(\sigma_0+\varepsilon_0))\right)\right]\right| \\
&\quad\leq K_1 \operatorname*{esssup}_{\sigma\in\mathscr{A}^{\varepsilon}}\left(E_{txy}\left|Y^{\varepsilon}_{0,T}(\sigma)-Y^{\varepsilon}_{0,T}(\sigma\wedge(\sigma_0+\varepsilon_0))\right|^2\right)^{(1/2)} \\
&\quad\leq (K_1/T) \operatorname*{esssup}_{\sigma\in\mathscr{A}^{\varepsilon}}\left(E_{txy}\int_0^T\left|X^{\varepsilon}_u(\sigma)-X^{\varepsilon}_u(\sigma\wedge(\sigma_0+\varepsilon_0))\right|^2\mathrm{d}u\right)^{(1/2)}.
\end{aligned} \tag{30}$$

With the estimates of the moments of solutions of the stochastic differential equations (Theorem 9 in Section 2.9 and Corollary 12 in Section 2.5 of [19]), we have the constants
$N=N(q,r,\sigma_0)$, $N'=N'(q,r,\sigma_0)$, and $C=\max\{NN',\ N+N\}'$ such that

$$\begin{aligned}
&E_{txy}\left[\sup_{s\leq u}\left|X^{\varepsilon}_s(\sigma)-X^{\varepsilon}_s(\sigma\wedge(\sigma_0+\varepsilon_0))\right|^{2q}\right] \\
&\quad\leq Nu^{q-1}e^{Nu}E_{txy}\left[\int_0^u\left|X^{\varepsilon}_s(\sigma)\right|^{2q}\cdot\left|\sigma_s-\sigma_s\wedge(\sigma_s+\varepsilon_0)\right|^{2q}\mathrm{d}s\right] \\
&\quad\leq Nu^{q-1}e^{Nu}N'e^{N'u}u\left(1+x^{2q}\right)\left|\varepsilon-\varepsilon_0\right|^{2q} \\
&\quad= Cu^q e^{Cu}\left(1+x^{2q}\right)\left|\varepsilon-\varepsilon_0\right|^{2q}.
\end{aligned} \tag{31}$$

Thus, we have

$$\begin{aligned}
&e^{r(T-t)}\left|V^{\varepsilon}(t,x,y)-V^{\varepsilon_0}(t,x,y)\right| \\
&\quad\leq\frac{K_1}{T}\operatorname*{esssup}_{\sigma\in\mathscr{A}^{\varepsilon}}\left(\int_0^T E_{txy}\sup_{s\in[0,u]}\left|X^{\varepsilon}_u(\sigma)-X^{\varepsilon}_u(\sigma\wedge(\sigma_0+\varepsilon_0))\right|^2\mathrm{d}u\right)^{(1/2)} \\
&\quad\leq\frac{K_1}{T}\operatorname*{esssup}_{\sigma\in\mathscr{A}^{\varepsilon}}\left(\int_0^T Cue^{Cu}\left(1+x^2\right)\left|\varepsilon-\varepsilon_0\right|^2\mathrm{d}u\right)^{(1/2)} \\
&\quad\leq K_1'\left(1+x^2\right)^{(1/2)}\left|\varepsilon-\varepsilon_0\right|,
\end{aligned} \tag{32}$$

where $K_1'=K_1'(K_1,C,T)$.

Let $\varepsilon\longrightarrow\varepsilon_0$. We have $\left|V^{\varepsilon}(t,x,y)-V^{\varepsilon_0}(t,x,y)\right|\longrightarrow 0$.

The continuity of V^{ε} with respect to ε can be proven similarly when $\varepsilon\leq\varepsilon_0$. □

4.2. Expectation Form of the Error Term. In this section, we analyze the error term and give its expectation form as preparation work before proving the convergence of $V_0+\varepsilon V_1$.

Let $\widehat{\sigma}_t$ be the worst-case scenario volatility process and $\widehat{X}^{\varepsilon}_t$ be the worst-case scenario risky asset process. Then, we can rewrite equation (19) as follows:

$$\begin{cases}\mathrm{d}\widehat{X}^{\varepsilon}_t=r\widehat{X}^{\varepsilon}_t\mathrm{d}t+\widehat{\sigma}_t\widehat{X}^{\varepsilon}_t\mathrm{d}W_t,\\ \mathrm{d}\widehat{Y}^{\varepsilon}_t=\widehat{X}^{\varepsilon}_t\mathrm{d}t.\end{cases} \tag{33}$$

We can obtain the expression of $\widehat{\sigma}$ by equation (23), and we have $\widehat{\sigma}(\varepsilon)=\sigma_0+\varepsilon\widehat{\gamma}$, where

$$\widehat{\gamma}(t,x,y;\varepsilon)=\begin{cases}1, & \partial^2_{xx}V^{\varepsilon}(t,x,y)\geq 0,\\ 0, & \partial^2_{xx}V^{\varepsilon}(t,x,y)<0.\end{cases} \tag{34}$$

Similarly, by solving equation (25) for V_1, we have the volatility process, $\overline{\sigma}(\varepsilon)=\sigma_0+\varepsilon\overline{\gamma}$, where

$$\overline{\gamma}(t,x,y)=\begin{cases}1, & \partial^2_{xx}V_0(t,x,y)\geq 0,\\ 0, & \partial^2_{xx}V_0(t,x,y)<0.\end{cases} \tag{35}$$

Here, we use the short notation $\widehat{\gamma}_t$ and $\overline{\gamma}_t$ for $\widehat{\gamma}(t,x,y;\varepsilon)$ and $\overline{\gamma}(t,x,y)$, respectively. Let $Z^{\varepsilon}=V^{\varepsilon}-(V_0+\varepsilon V_1)$. To estimate the error term Z^{ε}, we define the operator $L(\sigma)=\partial_t+rx\partial_x-r+(1/2)\sigma^2x^2\partial^2_{xx}+x\partial_y$. According to partial differential equations (22), (24) and (25), we have

$$\begin{aligned}
L(\widehat{\sigma}_t)Z^{\varepsilon}&=L(\widehat{\sigma}_t)\left(V^{\varepsilon}-(V_0+\varepsilon V_1)\right)\\
&=0-L(\widehat{\sigma}_t)(V_0+\varepsilon V_1)\\
&=-(L(\widehat{\sigma}_t)-L(\sigma_0))V_0-L(\sigma_0)V_0-\varepsilon(L(\widehat{\sigma}_t)\\
&\quad-L(\sigma_0))V_1-\varepsilon L(\sigma_0)V_1\\
&=\varepsilon(\overline{\gamma}_t-\widehat{\gamma}_t)\sigma_0x^2\partial^2_{xx}V_0-\frac{\varepsilon^2}{2}\left((\widehat{\gamma}_t)^2x^2\partial^2_{xx}V_0\right.\\
&\quad\left.+2\sigma_0\widehat{\gamma}_tx^2\partial^2_{xx}V_1\right)-\frac{\varepsilon^3}{2}(\widehat{\gamma}_t)^2x^2\partial^2_{xx}V_1\\
&=-f^{\varepsilon}(t,x,y),
\end{aligned} \tag{36}$$

with the boundary condition $Z^{\varepsilon}(T)=V^{\varepsilon}(T)-V_0(T)-\varepsilon V_1(T)=0$. We have the following expectation form of Z^{ε} by the Dynkin's formula:

$$\begin{aligned}
Z^{\varepsilon}&=E_{txy}\left[\int_t^T f^{\varepsilon}(s,x,y)\mathrm{d}s\right]\\
&=\varepsilon E_{txy}\left[\int_t^T(\widehat{\gamma}_s-\overline{\gamma}_s)\cdot\sigma_0\cdot\left(\widehat{X}^{\varepsilon}_s\right)^2\partial^2_{xx}V_0\left(s,\widehat{X}^{\varepsilon}_s,\widehat{Y}^{\varepsilon}_s\right)\mathrm{d}s\right]\\
&\quad+\varepsilon^2E_{txy}\left[\int_t^T\left\{\frac{1}{2}(\widehat{\gamma}_s)^2\left(\widehat{X}^{\varepsilon}_s\right)^2\partial^2_{xx}V_0\left(s,\widehat{X}^{\varepsilon}_s,\widehat{Y}^{\varepsilon}_s\right)\right.\right.\\
&\quad\left.\left.+\sigma_0(\widehat{\gamma}_s)\left(\widehat{X}^{\varepsilon}_s\right)^2\wp^2_{xx}V_1\left(s,\widehat{X}^{\varepsilon}_s,\widehat{Y}^{\varepsilon}_s\right)\right\}\mathrm{d}s\right]\\
&\quad+\varepsilon^3E_{txy}\left[\int_t^T\frac{1}{2}(\widehat{\gamma}_s)^2\left(\widehat{X}^{\varepsilon}_s\right)^2\partial^2_{xx}V_1\left(s,\widehat{X}^{\varepsilon}_s,\widehat{Y}^{\varepsilon}_s\right)\mathrm{d}s\right]\\
&=\varepsilon I_1+\varepsilon^2I_2+\varepsilon^3I_3,
\end{aligned} \tag{37}$$

where

$$I_1 = E_{txy}\left[\int_t^T (\widehat{\gamma}_s - \overline{\gamma}_s)\cdot\sigma_0\cdot\left(\widehat{X}_s^\varepsilon\right)^2\partial_{xx}^2 V_0\left(s,\widehat{X}_s^\varepsilon,\widehat{Y}_s^\varepsilon\right)\mathrm{d}s\right], \tag{38}$$

$$\begin{aligned}I_2 = E_{txy}\Bigg[\int_t^T \Big\{&\frac{1}{2}(\widehat{\gamma}_s)^2\left(\widehat{X}_s^\varepsilon\right)^2\partial_{xx}^2 V_0\left(s,\widehat{X}_s^\varepsilon,\widehat{Y}_s^\varepsilon\right)\\ &+\sigma_0(\widehat{\gamma}_s)\left(\widehat{X}_s^\varepsilon\right)^2\partial_{xx}^2 V_1\left(s,\widehat{X}_s^\varepsilon,\widehat{Y}_s^\varepsilon\right)\Big\}\mathrm{d}s\Bigg],\end{aligned} \tag{39}$$

$$I_3 = E_{txy}\left[\int_t^T \frac{1}{2}(\widehat{\gamma}_s)^2\left(\widehat{X}_s^\varepsilon\right)^2\partial_{xx}^2 V_1\left(s,\widehat{X}_s^\varepsilon,\widehat{Y}_s^\varepsilon\right)\mathrm{d}s\right]. \tag{40}$$

$$\left|Z^\varepsilon\right| \le \varepsilon\left|I_1\right| + \varepsilon^2\left|I_2\right| + \varepsilon^3\left|I_3\right|. \tag{41}$$

We can therefore estimate Z^ε by controlling $|I_1|$, $|I_2|$, and $|I_3|$.

4.3. The Polynomial Growth Condition of the Payoff Function. From Section 4.2, we know that to control the error term, we need to analyze the three parts. By (41), we have

$$\left|\frac{Z^\varepsilon}{\varepsilon}\right| \le \left|I_1\right| + \varepsilon\left(\left|I_2\right| + \varepsilon\left|I_3\right|\right). \tag{42}$$

Therefore, it is sufficient to prove

$$\lim_{\varepsilon\downarrow 0}\left|I_1\right| + \varepsilon\left(\left|I_2\right| + \varepsilon\left|I_3\right|\right) = 0. \tag{43}$$

Obviously, it is necessary to obtain controls of the terms $|I_2|$ and $|I_3|$. For $|I_1|$, we need to prove its convergence. We first consider controls of the terms $|I_2|$ and $|I_3|$.

By the expressions of I_2 and I_3, we can see that the partial derivatives of V_0 and V_1 are involved. Thus, we should consider estimating them before controlling I_2 and I_3. Next, we can obtain the expectation form of V_0 and V^ε by the classical result. When $\varepsilon = 0$, we have

$$X(u) = x\ \exp\left\{\left(r - \frac{\sigma_0^2}{2}\right)(u-t) + \sigma_0\left(W_u - W_t\right)\right\}. \tag{44}$$

Thus,

$$\begin{aligned}V_0(t,x,y) &= e^{-r(T-t)}E_{txy}\left[\varphi\left(Y_{0,T}\right)\right]\\ &= e^{-r(T-t)}E_{txy}\left[\varphi\left(\frac{1}{T}\int_0^T X(u)\mathrm{d}u\right)\right]\\ &= e^{-r(T-t)}E_{txy}\left[\varphi\left(\frac{1}{T}\cdot x\cdot\left(\int_0^T e^{(r-(\sigma_0^2/2))(u-t)+\sigma_0(W_u-W_t)}\mathrm{d}u\right)\right)\right]\\ &= e^{-r(T-t)}E_{txy}\left[\varphi(x\cdot H)\right],\end{aligned} \tag{45}$$

where $H(=(1/T)\int_0^T \exp\{(r-(\sigma_0^2/2))(u-t)+\sigma_0(W_u-W_t)\}\mathrm{d}u)$ is a random variable for fixed $t\in[0,T]$. Similarly, we have

$$\begin{aligned}V^\varepsilon(t,x,y) &= e^{-r(T-t)}\operatorname*{esssup}_{\sigma\in\mathscr{A}^\varepsilon}\left\{E_{txy}\left[\varphi\left(Y_{0,T}^\varepsilon\right)\right]\right\}\\ &= e^{-r(T-t)}E_{txy}\left[\varphi(x\cdot G)\right],\end{aligned} \tag{46}$$

where $G(=(1/T)\int_0^T \exp\{(r-(\widehat{\sigma}_u)^2/2)(u-t)-\widehat{\sigma}_u(W_u-W_t)\}\mathrm{d}u)$ is a random variable for a fixed $t\in[0,T]$.

By equations (45) and (46), we note that it is necessary to impose polynomial growth conditions on φ to control $\partial_{xx}^2 V_0$ and $\partial_{xx}^2 V^\varepsilon$. Then, we estimate $\partial_{xx}^2 V_0(t,x,y)$ and $\partial_{xx}^2 V^\varepsilon(t,x,y)$ in the following Lemma.

Lemma 3. *Suppose that the second derivative of the payoff function satisfies the polynomial growth condition, that is, there are constants K_2 and m such that $\varphi''(x)\le K_2(1+|x|^m)$. Then, we have constant K_3 such that*

$$\left|\partial_{xx}^2 V_0(t,x,y)\right| \le K_3\left(1+|x|^m\right), \tag{47}$$

where K_3 depends on T, t, $E_{txy}[|H|^2]$, $E_{txy}[|H|^{m+2}]$, and K_2. Moreover, there is a constant K_4 such that

$$\left|\partial_{xx}^2 V^\varepsilon(t,x,y)\right| \le K_4\left(1+|x|^m\right), \tag{48}$$

where K_4 depends on T, t, $E_{txy}[|G|^2]$, $E_{txy}[|G|^{m+2}]$, and K_2.

Proof. As the assumption of φ in the lemma, we have

$$\begin{aligned}\partial_{xx}^2 V_0(t,x,y) &= e^{-r(T-t)}E_{txy}\left[\varphi''(xH)H^2\right]\\ &\le e^{-r(T-t)}E_{txy}\left[K_2\left(1+|xH|^m\right)H^2\right]\\ &\le K_3\left(1+|x|^m\right).\end{aligned} \tag{49}$$

Here, K_3 depends on T, t, $E_{txy}[|H|^2]$, $E_{txy}[|H|^{m+2}]$, and K_2.

Indeed, for a constant $m>0$, we have

$$\begin{aligned}EH^m &= \frac{1}{(T)}^m E\left(\int_{-t}^{T-t}\exp\left\{\left(\frac{r-\sigma_0^2}{2}\right)u + \sigma_0 W_u\right\}\mathrm{d}u\right)^m\\ &\le \left(\frac{1}{T}\right)^m E\left(\int_{-t}^{T-t} e^{|r-\sigma_0^2/2|(T-t)+\sigma_0 W_u}\mathrm{d}u\right)^m\\ &\le \left(\frac{1}{T}\right)^m e^{m|r-\sigma_0^2/2|(T-t)}E\left(\sup_{s\in(-t,T-t)}\left\{e^{\sigma_0 W_s}\right\}\right)^m < +\infty.\end{aligned} \tag{50}$$

We obtain the control tial$^2_{xx}V^\varepsilon$ similarly. Then, there is a constant K_4 that depends on T, t, $E_{txy}[|G|^2]$, $E_{txy}[|G|^{m+2}]$, and K_2 such that

$$\left|\partial^2_{xx}V^\varepsilon(t,x,y)\right| \le K_4\left(1+|x|^m\right). \tag{51}$$

Now, by the following proposition, we can obtain controls of the terms $|I_2|$ and $|I_3|$. □

Proposition 1. *Assume that $\varphi \in \mathscr{C}^2_p(R^+)$ and the Lipschitz continuity condition holds. Then, there exist constants C_1 and p_1 such that I_2 and I_3 in equations (39) and (40) satisfy*

$$\left|I_2\right| + \left|I_3\right| \le C_1\left(1+|x|^{p_1}\right). \tag{52}$$

Proof. By Lemma 3, we have the following inequality from (23) and (48):

$$\begin{aligned}\left|\partial_t V^\varepsilon + r\left(x\partial_x V^\varepsilon - V^\varepsilon\right) + x\partial_y V^\varepsilon\right| &\le \left|\frac{1}{2}(\sigma_0+\varepsilon)^2 x^2\partial^2_{xx}V^\varepsilon\right| \\ &\le \left|\left(\frac{K_4}{2}\right)(\sigma_0+\varepsilon)^2\left(|x|^2+|x|^{m+2}\right)\right|.\end{aligned} \tag{53}$$

By the expression of V_1, it is true that

$$\left|\partial_t V_1 + r\left(x\partial_x V_1 - V_1\right) + x\partial_y V_1\right| \le \left|K_4\sigma_0\left(|x|^2+|x|^{m+2}\right)\right|. \tag{54}$$

By (25) and (47), we get the controls for $x^2\partial^2_{xx}V_1$:

$$\begin{aligned}\left|x^2\partial^2_{xx}V_1\right| &= \left|\partial_t V_1 + r\left(x\partial_x V_1 - V_1\right) + x\partial_y V_1 + \overline{g}_t\sigma_0 x^2\partial^2_{xx}V_0\right|\cdot\left(\frac{2}{\sigma_0^2}\right) \\ &\le \left(\left|\partial_t V_1 + r\left(x\partial_x V_1 - V_1\right) + x\partial_y V_1\right| + \left|\sigma_0 x^2\partial^2_{xx}V_0\right|\right)\cdot\left(\frac{2}{\sigma_0^2}\right) \\ &\le M_1\left(|x|^2+|x|^{m+2}\right),\end{aligned} \tag{55}$$

where M_1 depends on K_3, K_4, and σ_0. We can obtain the existence and uniqueness of $\widehat{X}^\varepsilon_t$ from Theorem 5.2.1 in [20]. Then, by the estimates of the moments of solutions of the stochastic differential equations (Corollary 12 in Section 2.5 of [19]), there is a constant $N_1(q)$ for a fixed $q>0$ such that

$$E_{txy}\left[\sup_{s\in[t,T]}\left|\widehat{X}^\varepsilon_s\right|^q\right] \le N_1(q)e^{N_1(q)(T-t)}\left(1+|x|^q\right). \tag{56}$$

By (40), (55), and (56), we have the following inequality:

$$\begin{aligned}\left|I_3\right| &= \left|E_{txy}\left[\int_t^T \frac{1}{2}(\widehat{\gamma}_s)^2\left(\widehat{X}^\varepsilon_s\right)^2\partial^2_{xx}V_1\left(s,\widehat{X}^\varepsilon_s,\widehat{Y}^\varepsilon_s\right)ds\right]\right| \\ &\le \left(\frac{M_1}{2}\right)E_{txy}\left[\int_t^T\left(\left|\widehat{X}^\varepsilon_s\right|^2+\left|\widehat{X}^\varepsilon_s\right|^{m+2}\right)ds\right] \le M_1'\left(1+|x|^{m+2}\right).\end{aligned} \tag{57}$$

Here, M_1' depends on T, t, $N_1(2)$, $N_1(m+2)$, and M_1.

By (39), (47), (55), and (56), we obtain the control of term $|I_2|$.

$$\begin{aligned}\left|I_2\right| &= \left|E_{txy}\left[\int_t^T \frac{1}{2}(\widehat{\gamma}_s)^2\left(\widehat{X}^\varepsilon_s\right)^2\partial^2_{xx}V_0 + \sigma_0(\widehat{\gamma}_s)\left(\widehat{X}^\varepsilon_s\right)^2\partial^2_{xx}V_1 ds\right]\right| \\ &\le \frac{K_3}{2}E_{txy}\left[\int_t^T\left(\widehat{X}^\varepsilon_s\right)^2+\left(\widehat{X}^\varepsilon_s\right)^{m+2}ds\right] \\ &\quad + M_1E_{txy}\left[\int_t^T\left(\widehat{X}^\varepsilon_s\right)^2+\left(\widehat{X}^\varepsilon_s\right)^{m+2}ds\right] \\ &\le M_2\left(1+|x|^{p_1}\right),\end{aligned} \tag{58}$$

where M_2 depends on T, t, M_1, K_3, $N_1(2)$, and $N_1(m+2)$, $p_1 \ge m+2$.Combining (57) and (58), we have a constant C_1 such that

$$\left|I_2\right| + \left|I_3\right| \le C_1\left(1+|x|^{p_1}\right). \tag{59}$$

□

4.4. The Continuity of the Second Derivative of the Payoff Function. By Proposition 1, we obtain controls of the terms $|I_2|$ and $|I_3|$. Next, for the fixed point $(t,x,y)\in[0,T]\times R^+\times R^+$, it suffices to prove that

$$\lim_{\varepsilon\downarrow 0}\left|I_1\right| = 0. \tag{60}$$

Note that if $\varphi \in \mathscr{C}^2_p(R^+)$ (i.e., its derivatives up to order 2 have polynomial growth), we can obtain the following inequality by (38), (47), (56), and Hölder inequality:

$$\begin{aligned}\left|I_1\right| &\le \left[E_{txy}\left[\int_t^T\left(\sigma_0\left(\widehat{X}^\varepsilon_s\right)^2\partial^2_{xx}V_0\right)^2 ds\right]\right]^{(1/2)} \\ &\quad\cdot\left[E_{txy}\left[\int_t^T\left(\widehat{\gamma}_s-\overline{\gamma}_s\right)^2 ds\right]\right]^{(1/2)} \\ &\le M_3\left(1+|x|^{p_2}\right)^{(1/2)}\left[E_{txy}\left[\int_t^T\left|\widehat{\gamma}_s-\overline{\gamma}_s\right|ds\right]\right]^{(1/2)}.\end{aligned} \tag{61}$$

Here, M_3 depends on K_3, T, t, σ_0, and $p_2 \ge 4+2m$. Moreover, M_3 is independent of ε.

Let $h^\varepsilon(t,x,y) = \widehat{\gamma}(t,x,y;\varepsilon) - \overline{\gamma}(t,x,y)$. By (34) and (35), we have

$$\left|h^\varepsilon(t,x,y)\right| = \begin{cases}1, & \partial^2_{xx}V^\varepsilon\partial^2_{xx}V_0 < 0,\\ 0, & \partial^2_{xx}V^\varepsilon\partial^2_{xx}V_0 \ge 0.\end{cases} \tag{62}$$

Thus, to prove $|I_1| \longrightarrow 0$ as $\varepsilon \longrightarrow 0$, it suffices to prove that

$$\lim_{\varepsilon\downarrow 0} E_{txy}\left[\int_t^T\left|h^\varepsilon\left(s,\widehat{X}^\varepsilon_s,\widehat{Y}^\varepsilon_s\right)\right|ds\right] = 0. \tag{63}$$

By the expression of h^ε, we should analyze the derivatives of V_0 and V^ε. Here, we find that the continuity of φ'' is necessary.

Lemma 4. *Assume that φ'' is continuous. Then, $\partial^2_{xx}V_0$ and $\partial^2_{xx}V^\varepsilon$ are continuous with respect to (x,y).*

Proof. By (45), we have $V_0(t,x,y) = e^{-r(T-t)}E_{txy}[\varphi(xH)]$ and $\partial^2_{xx}V_0(t,x,y) = e^{-r(T-t)}E_{txy}[\varphi''(xH)H^2]$. If φ'' is continuous, then for all $x_0 \in R^+$, $\delta > 0$, there is a constant $\xi = \xi(\delta, x_0)$ such that

$$\left|\varphi''(xH) - \varphi''(x_0H)\right| \le \delta, \tag{64}$$

for all $xH \in (x_0H - \xi, x_0H + \xi)$. So, for all $(x_0, y_0) \in R^+ \times R^+$, $xH \in (x_0H - \xi, x_0H + \xi)$, and $y \in (y_0 - \xi, y_0 + \xi)$, we have

$$\begin{aligned}\left|\partial^2_{xx}V_0(t,x,y) - \partial^2_{xx}V_0(t,x_0,y_0)\right| &= e^{-r(T-t)}\left|E_{txy}\left[\varphi''(xH)H^2 - \varphi''(x_0H)H^2\right]\right| \\ &\le e^{-r(T-t)}E_{txy}\left[H^2\left|\varphi''(xH) - \varphi''(x_0H)\right|\right] \\ &\le e^{-r(T-t)}\delta E_{txy}\left[H^2\right].\end{aligned} \tag{65}$$

Thus, we obtain

$$\lim_{(x,y)\longrightarrow(x_0,y_0)} \partial^2_{xx}V_0(t,x,y) = \partial^2_{xx}V_0(t,x_0,y_0). \tag{66}$$

Similarly, we can obtain the continuity of $\partial^2_{xx}V^\varepsilon$. □

Remark 6. Rationally, V^ε and its derivatives converge to V_0 and its corresponding derivatives as ε approaches 0 by Lemma 2.

Remark 7. To simplify the complexity brought by the variable Y, which is called path dependence, and to study the behavior of h^ε, we define

$$D^\lambda_{ty} = \left\{x \in R^+ \mid \partial^2_{xx}V^{\varepsilon_0}\partial^2_{xx}V_0 \le 0, \exists\varepsilon_0 > \lambda\right\}. \tag{67}$$

Let $D^0_{ty} = \lim_{\lambda\downarrow 0}D^\lambda_{ty}$. Then, we can obtain the following equation when $\partial^2_{xx}V^\varepsilon$ is continuous:

$$D^0_{ty} = \left\{x \in R^+ \mid \partial^2_{xx}V_0(t,x,y) = 0\right\}. \tag{68}$$

Remark 8. To control h^ε, we divide D^λ_{ty} into two parts. Let $\alpha(\rho) = [-\rho, \rho]$. We will discuss the characteristics of $D^\lambda_{ty} \cap \alpha(\rho)$ and $D^\lambda_{ty} \cap \alpha(\rho)^c$.

Lemma 5. *Assume that φ'' is continuous and the fourth derivative of φ exists. Then, we have*

$$P_{txy}\left(D^0_{sy_s} \cap \alpha(\rho)\right) = 0, \quad \text{for } s \in [t,T]. \tag{69}$$

Here, $P_{txy}(\cdot)$ refers to the conditional probability with respect to $X^\varepsilon_t = x$ and $Y^\varepsilon_t = y$.

Proof. By (33) and (24), we can obtain the equation

$$\begin{cases} 2\partial_t V_0 + r(x\partial_x V_0 - V_0) + \dfrac{1}{2}\sigma_0^2 x^2 \partial^2_{xx}V_0 = 0, \\ \\ V_0(T) = \varphi(xH). \end{cases} \tag{70}$$

Let $Q = \partial^2_{xx}V_0$. Then, by equation (70) and the existence of the fourth derivative of φ, we have

$$\begin{cases} 2\partial_t Q + (r + \sigma_0^2)Q + (r + 2\sigma_0^2)x\partial_x Q + \dfrac{1}{2}\sigma_0^2 x^2 \partial^2_{xx}Q = 0, \\ \\ Q(T) = \varphi''(xH)H^2. \end{cases} \tag{71}$$

Let $x = \log k$. Then, we have

$$\begin{cases} 2\partial_t Q + (r + \sigma_0^2)Q + (r + 2\sigma_0^2)\partial_k Q + \dfrac{1}{2}\sigma_0^2 \partial^2_k Q = 0, \\ \\ Q(T) = \varphi''((\log k)H)H^2. \end{cases} \tag{72}$$

Note that the coefficients in equation (72) are constants and Q is bounded on $D^0_{sy_s} \cap \alpha(\rho)$ by the continuity of φ'' and Lemma 4. Moreover, by equation (72), we find that y has no relationship with the equations. Then, by Theorem A of [21] and the remark below it, we find that the number of zero points of Q is only countable for all $(s, y_s) \in [t,T] \times R$. Thus, $\partial^2_{xx}V_0$ has only countable zero points. Hence, we have $P_{txy}(D^0_{sy_s} \cap \alpha(\rho)) = 0$ by Lemma 4.10 of [15] and then the proof of Lemma 5 is complete.

Based on the previous analysis, we will now prove (63). We split the expectation into two parts. By proving the convergence of each part, we can show the convergence of the expectation. □

Proposition 2. *Assume that $\varphi \in \mathscr{C}^2_p(R^+)$, φ'' is continuous, and the fourth derivative of φ exists. Then, we obtain equation (63).*

Proof. Let $\overline{D}^\lambda_{ty}$ be the closure of D^λ_{ty}, $\overline{D}^0_{ty} = \lim_{\lambda\downarrow 0}\overline{D}^\lambda_{ty}$, and $0 \le \lambda < \varepsilon < 1$.

By the definition of D^λ_{ty}, we have

$$\begin{aligned}
&E_{txy}\left[\int_t^T \left|h^\varepsilon\left(s,\widehat{X}_s^\varepsilon,\widehat{Y}_s^\varepsilon\right)\right|\mathrm{d}s\right]\\
&\leq E_{txy}\left[\int_t^T \mathbb{I}_{\overline{D}^\lambda_{\left(s\widehat{Y}_s^\varepsilon\right)}}\left(\widehat{X}_s^\varepsilon\right)\mathrm{d}s\right]\\
&= E_{txy}\left[\int_t^T \mathbb{I}_{\overline{D}^\lambda_{\left(s\widehat{Y}_s^\varepsilon\right)}\cap\alpha(\rho)}\left(\widehat{X}_s^\varepsilon\right)\mathrm{d}s\right]\\
&\quad + E_{txy}\left[\int_t^T \mathbb{I}_{\overline{D}^\lambda_{\left(s\widehat{Y}_s^\varepsilon\right)}\cap\alpha(\rho)^c}\left(\widehat{X}_s^\varepsilon\right)\mathrm{d}s\right]\\
&= \Phi_1 + \Phi_2.
\end{aligned} \tag{73}$$

Now, we consider the second part of (73) first. By (56) and Chebyshev's inequality,

$$\begin{aligned}
\Phi_2 &\leq E_{txy}\left[\int_t^T \mathbb{I}_{\alpha(\rho)^c}\left(\widehat{X}_s^\varepsilon\right)\mathrm{d}s\right]\\
&\leq \int_t^T P_{txy}\left(\sup_{s\in[t,T]}\left|\widehat{X}_s^\varepsilon\right|\geq\rho\right)\mathrm{d}s\\
&\leq \frac{T-t}{\rho}E_{txy}\left[\sup_{s\in[t,T]}\left|\widehat{X}_s^\varepsilon\right|\right]\\
&\leq \frac{(T-t)N_1(1)}{\rho}e^{N_1(1)(T-t)}(1+|x|).
\end{aligned} \tag{74}$$

Thus, we have

$$\lim_{\rho\longrightarrow\infty}\Phi_2 = 0. \tag{75}$$

For the first part, we note that

$$\Phi_1 = \int_t^T P_{txy}\left(\widehat{X}_s^\varepsilon \in \overline{D}^\lambda_{\left(s\widehat{Y}_s^\varepsilon\right)}\cap\alpha(\rho)\right)\mathrm{d}s. \tag{76}$$

Let $\theta(\Omega) = \sup_{\lambda\in[0,1]}P_{txy}(\Omega)$; then,

$$P_{txy}\left(\widehat{X}_s^\varepsilon \in \overline{D}^\lambda_{\left(s\widehat{Y}_s^\varepsilon\right)}\cap\alpha(\rho)\right) \leq \theta\left(\overline{D}^\lambda_{\left(s\widehat{Y}_s^\varepsilon\right)}\cap\alpha(\rho)\right). \tag{77}$$

Note that $\lambda<\varepsilon$. Then, $\overline{D}^\lambda_{sy}$ is a sequence of decreasing closed sets as $\varepsilon\downarrow 0$. Obviously, $\widehat{X}_s^\varepsilon$ converges weakly to X_s. Thus, $\{X_s\}$ is weakly compact. By Lemma 8 in [18], we can see that

$$\lim_{\varepsilon\downarrow 0}\theta\left(\overline{D}^\lambda_{\left(s\widehat{Y}_s^\varepsilon\right)}\cap\alpha(\rho)\right) = \theta\left(\overline{D}^0_{\left(s\widehat{Y}_s^0\right)}\cap\alpha(\rho)\right). \tag{78}$$

By Lemma 4, there is $\overline{D}^0_{sy} = D^0_{sy}$. Then, by Lemma 5, we have

$$P_{txy}\left(\widehat{X}_s^\varepsilon \in \overline{D}^0_{\left(s\widehat{Y}_s^\varepsilon\right)}\cap\alpha(\rho)\right) = 0, \quad \text{for } \varepsilon\geq 0. \tag{79}$$

Next, by the definition of $\theta(\Omega)$, we have

$$\theta\left(\overline{D}^0_{\left(s\widehat{Y}_s^0\right)}\cap\alpha(\rho)\right) = 0. \tag{80}$$

Thus,

$$\lim_{\varepsilon\downarrow 0}\theta\left(\overline{D}^\lambda_{\left(s\widehat{Y}_s^\varepsilon\right)}\cap\alpha(\rho)\right) = 0. \tag{81}$$

Then, we obtain

$$\lim_{\varepsilon\downarrow 0}\Phi_1 = \lim_{\varepsilon\downarrow 0}P_{txy}\left(\widehat{X}_s^\varepsilon \in \overline{D}^\lambda_{\left(s\widehat{Y}_s^\varepsilon\right)}\cap\alpha(\rho)\right) = 0. \tag{82}$$

By equations (75) and (82), for any $\delta>0$, there is $\rho_0 = \rho_0(t,x,y,\delta)>0$ such that

$$\Phi_2 < \frac{\delta}{2}, \quad \text{for all } \rho>\rho_0. \tag{83}$$

Next, for a given ρ_0 and δ, there is $\varepsilon_0 = \varepsilon_0(t,x,y,\delta,\rho_0(t,x,y,\delta))$ such that

$$\Phi_1 < \frac{\delta}{2}, \quad \text{for all } \varepsilon<\varepsilon_0. \tag{84}$$

Therefore, for any $\delta>0$, there is $\varepsilon_0 = \varepsilon_0(t,x,y,\delta)$ such that

$$\Phi_1+\Phi_2<\delta, \quad \text{for all } \varepsilon<\varepsilon_0, \tag{85}$$

i.e.,

$$\lim_{\varepsilon\downarrow 0}E_{txy}\left[\int_t^T \left|h^\varepsilon\left(s,\widehat{X}_s^\varepsilon,\widehat{Y}_s^\varepsilon\right)\right|\mathrm{d}s\right] = 0. \tag{86}$$

□

4.5. Proof of the Main Result. Now, from the analysis above, we can give the brief proof of Theorem 1.

By inequality (61) and Proposition 2, we have

$$\lim_{\varepsilon\downarrow 0}\left|I_1\right| = 0. \tag{87}$$

By inequality (41), we have

$$\left|\frac{V^\varepsilon-(V_0+\varepsilon V_1)}{\varepsilon}\right| \leq \left|I_1\right| + \varepsilon\left(\left|I_2\right|+\varepsilon\left|I_3\right|\right) = 0. \tag{88}$$

By Proposition 1 and equation (87), we obtain the theorem.

5. Conclusion

In this study, we analyze the behavior of Asian option prices in the worst-case scenario using an uncertain volatility model with volatility interval $[\sigma_0,\sigma_0+\varepsilon]$. As ε approaches 0, the ambiguity of the model vanishes. We can also see that the worst-case scenario prices of Asian options converge to its Black–Scholes prices with constant volatility as the interval shrinks. Additionally, this study provides an approach to estimate the worst-case scenario Asian option prices. At the same time, we also provide an estimation method to solve a fully nonlinear PDE (22) by imposing additional conditions on the boundary condition and splitting it into two Black–Scholes-like equations.

Data Availability

No data were used to support this study.

Conflicts of Interest

The authors declare that they have no conflicts of interest.

Acknowledgments

This paper was partially supported by NSFC (Grant nos. 11871244 and 11901233).

References

[1] F. Black and M. Scholes, "The pricing of options and corporate liabilities," *Journal of Political Economy*, vol. 81, no. 3, pp. 637–654, 1973.
[2] R. C. Merton, "Theory of rational option pricing," *The Bell Journal of Economics and Management Science*, vol. 4, no. 1, pp. 141–183, 1973.
[3] J. Hull and A. White, "The pricing of options on assets with stochastic volatilities," *The Journal of Finance*, vol. 42, no. 2, pp. 281–300, 1987.
[4] S. L. Heston, "A closed-form solution for options with stochastic volatility with applications to bond and currency options," *Review of Financial Studies*, vol. 6, no. 2, pp. 327–343, 1993.
[5] T. J. Lyons, "Uncertain volatility and the risk-free synthesis of derivatives," *Applied Mathematical Finance*, vol. 2, no. 2, pp. 117–133, 1995.
[6] M. Avellaneda, A. Levy, and A. ParÁS, "Pricing and hedging derivative securities in markets with uncertain volatilities," *Applied Mathematical Finance*, vol. 2, no. 2, pp. 73–88, 1995.
[7] N. G. Dokuchaev and A. V. Savkin, "The pricing of options in a financial market model with transaction costs and uncertain volatility," *Journal of Multinational Financial Management*, vol. 8, no. 2-3, pp. 353–364, 1998.
[8] Q. Zhou and X. Li, "Vulnerable options pricing under uncertain volatility model," *Journal of Inequalities and Applications*, vol. 2019, no. 1, p. 315, 2019.
[9] P. A. Forsyth and K. R. Vetzal, "Implicit solution of uncertain volatility/transaction cost option pricing models with discretely observed barriers," *Applied Numerical Mathematics*, vol. 36, no. 4, pp. 427–445, 2001.
[10] J. Vorbrink, "Financial markets with volatility uncertainty," *Journal of Mathematical Economics*, vol. 53, no. 8, pp. 64–78, 2014.
[11] L. G. Epstein and S. Ji, "Ambiguous volatility and asset pricing in continuous time," *Review of Financial Studies*, vol. 26, no. 7, pp. 1740–1786, 2013.
[12] Z. Zhang, Y. Yong, and W. Yu, "Valuing equity-linked death benefits in general exponential Lévy models," *Journal of Computational and Applied Mathematics*, vol. 365, Article ID 112377, 2020.
[13] W. Yu, Y. Yong, G. Guan, Y. Huang, W. Su, and C. Cui, "Valuing guaranteed minimum death benefits by cosine series expansion," *Mathematics*, vol. 7, no. 9, p. 835, 2019.
[14] D. M. Pooley, P. A. Forsyth, and K. R. Vetzal, "Numerical convergence properties of option pricing pdes with uncertain volatility," *IMA Journal of Numerical Analysis*, vol. 23, no. 2, pp. 241–267, 2003.
[15] J.-P. Fouque and B. Ren, "Approximation for option prices under uncertain volatility," *SIAM Journal on Financial Mathematics*, vol. 5, no. 1, pp. 360–383, 2014.
[16] R. Cont, "Model uncertainty and its impact on the pricing of derivative instruments," *Mathematical Finance*, vol. 16, no. 3, pp. 519–547, 2006.
[17] J. Yong and X. Zhou, *Stochastic Controls, Hamiltonian Systems and HJB Equations*, Springer, New York, NY, USA, 1999.
[18] L. Denis, M. Hu, and S. Peng, "Function spaces and capacity related to a sublinear expectation: application to G-Brownian motion paths," *Potential Analysis*, vol. 34, no. 2, pp. 139–161, 2011.
[19] N. Krylov, *Controlled Diffusion Processes*, Springer, Berlin, Germany, 1980.
[20] B. Øksendal, *Stochastic Differential Equations*, Springer, Berlin, Germany, 2003.
[21] S. Angenent, "The zero set of a solution of a parabolic equation," *Journal für die Reine und Angewandte Mathematik*, vol. 390, pp. 79–96, 1988.

Hindawi
Mathematical Problems in Engineering
Volume 2020, Article ID 1398476, 7 pages
https://doi.org/10.1155/2020/1398476

Research Article

The Properties of Generalized Collision Branching Processes

Juan Wang[1] **and Chunhao Cai**[2]

[1]*University of Shanghai for Science and Technology, Shanghai, China*
[2]*Shanghai University of Finance and Economics, Shanghai, China*

Correspondence should be addressed to Chunhao Cai; caichunhao@mail.shufe.edu.cn

Received 17 January 2020; Accepted 24 February 2020; Published 17 April 2020

Guest Editor: Wenguang Yu

We consider basic properties regarding uniqueness, extinction, and explosivity for the Generalized Collision Branching Processes (GCBP). Firstly, we investigate some important properties of the generating functions for GCB q-matrix in detail. Then for any given GCB q-matrix, we prove that there always exists exactly one GCBP. Next, we devote to the study of extinction behavior and hitting times. Some elegant and important results regarding extinction probabilities, the mean extinction times, and the conditional mean extinction times are presented. Moreover, the explosivity is also investigated and an explicit expression for mean explosion time is established.

1. Introduction

In this paper, we mainly consider extinction and explosivity for the Generalized Collision Branching Processes (GCBP). The particles in the system that evolves can be described as follows. Collisions between particles occur at random, and whenever m particles collide, they are removed and replaced by j "offsprings" with probability p_j $(j \geq 0)$, independently of other collisions. In any small time interval $(t, t+\Delta t)$, there is a positive probability $\theta\Delta t + o(\Delta t)$ that a collision occurs, and the chance of 2 or more collisions occurring in that time interval is $o(\Delta t)$.

Assume that there are i particles present at time t and all interactions are equally likely. Then, there will be j particles with probability $\binom{i}{m}\theta p_{j-i+m}\Delta t + o(\Delta t)$ after time Δt. In this paper, we take $X(t)$ be the number of particles present at time t and therefore $X(t)$ to be a continuous-time Markov chain with nonzero transition rates $q_{ij} = \binom{i}{m} b_{j-i+m}, j \geq i-m$, $i \geq m$, where $b_m = -\theta(1-p_m)$ and $b_j = \theta p_j$ for $j \neq m$.

This leads us to the following formal definition.

Definition 1. A q-matrix $Q = (q_{ij}; i, j \in \mathbb{Z}_+)$ is called a generalized collision branching q-matrix (henceforth referred to as a GCB q-matrix) if it takes the following form:

$$q_{ij} = \begin{cases} \binom{i}{m} b_{j-i+m}, & \text{if } i \geq m, j \geq i-m, \\ 0, & \text{otherwise}, \end{cases} \quad (1)$$

where

$$\begin{aligned} &b_j \geq 0 \, (j \neq m), \\ &\sum_{j=m+1}^{\infty} b_j > 0, \\ &0 < -b_m = \sum_{j \neq m} b_j < +\infty, \end{aligned} \quad (2)$$

together with $b_k > 0 (k = 0, 1, \ldots, m-1)$.

The conditions $b_0 > 0$ and $\sum_{j=m+1}^{\infty} b_j > 0$ are essential, while condition $b_k > 0 (k = 1, \ldots, m-1)$ is imposed for convenience; all our conclusions hold true with some minor and obvious adjustments if this latter condition is removed.

Guided by this fact, we formally define this generalized collision branching process as follows.

Definition 2. A generalized collision branching process (henceforth referred to simply as a GCBP) is a continuous-time

Markov chain, taking values in $\mathbb{Z}_+$, whose transition function $P(t) = (p_{ij}(t); i, j \in \mathbb{Z}_+)$ satisfies the forward equation

$$P'(t) = P(t)Q, \quad (3)$$

where Q is a GCB q-matrix as defined in (1) and (2).

In order to avoid discussing some trivial cases, we shall assume that $\mathbb{Z}_+$ is an irreducible class for our q-matrix Q as well as for the corresponding Feller minimal Q-function throughout this paper excepting where we consider the absorbing case.

Good references of Asmussen and Hering [1], Athreya and Jagers [2], Athreya and Ney [3], Chen et al. [4], Ezhov [5], Harris [6], Kalinkin [7], Li [8, 9], Li and Wang [10], Sevast'yanov [11] considered kinds of generalized branching models. Whilst for more other recent excellent developments, we can see Chen et al. [12, 13], Li [14] and Yu et al. [15–17], Ren et al. [18], Xiong and Yang [19], Zhang [20], Zhang [21] and Zhang et al. [22], and so on. In this paper, we consider a more challenging and practical meaning model, which involved $m > 2$ particles collision, and hence, investigating the properties of such model is of great significance. In such case, we assume that m is the smallest positive integer such that all states $\{m, m+1, \ldots,\}$ communicate; in other words, $G = \{m, m+1, \ldots,\}$ is an irreducible class for the GCB q-matrix Q. The more general jump rates will be discussed in subsequence papers.

The structure of this paper is as follows. Some preliminary results are obtained in Section 2. In Section 3, we show that there always exists exactly one GCBP for a given GCB q-matrix Q. And then the extinction behavior and hitting times are considered in the Section 4, where some elegant and important results regarding extinction probabilities and mean extinction times and explosion times are obtained.

2. Preliminaries

In order to investigate properties of GCBPs, we introduce the generating function $B(s)$ of the sequence $\{b_k; k \geq 0\}$ in (1) and (2) as

$$B(s) = \sum_{j=0}^{\infty} b_j s^j, \quad |s| \leq 1. \quad (4)$$

The function plays an extremely important role in the following discussion. It is easy to see that $B(0) = b_0 > 0$. Furthermore, $B(s)$ is well defined at least on $[-1, 1]$.

It is clear that $B'(1) > -\infty$. Moreover, the number of solutions to equation $B(s) = 0$ in $s \in [0, 1)$ is determined by the sign of $B'(1)$, and we will give the simple results in the following. However, their proofs are obvious and thus omitted in this paper.

Lemma 1. *The equation $B(s) = 0$ has at least m roots $q_0, q_1, \ldots, q_{m-1}$ in $[-1, 1]$, where $|q_k| \leq q_0$ and $0 < q_0 \leq 1$ is a positive root. Specially,*

(i) If $B'(1) \leq 0$, then $B(s) = 0$ has exactly m roots in $[-1, 1]$ with $q_0 = 1$ and $B(s) > 0$ for all $s \in [0, 1)$.

(ii) If $0 < B'(1) \leq +\infty$, then $B(s) = 0$ has exactly $m+1$ roots $1, q_0, q_1, \ldots, q_{m-1}$ in $[-1, 1]$ with $|q_k| \leq q_0$ and that $q_0 < 1$; moreover, $B(s) > 0$ for $s \in [0, q_0)$ and $B(s) < 0$ for $s \in (q_0, 1)$.

(iii) $B(s)$ can be expressed as

$$B(s) = (q_0 - s)(s - q_1)\cdots(s - q_{m-1}) \cdot \left(q_0 - \sum_{k=1}^{\infty} q_k s^k\right), \quad (5)$$

where q_0, $q_k \geq 0 (k \geq 1)$. Moreover, $\sum_{k=1}^{\infty} q_k \leq q_0$ if $B'(1) < 0$, while $\sum_{k=1}^{\infty} q_k = q_0$ if $B'(1) \geq 0$. Furthermore, if $\{m, m+1, \ldots,\}$ is irreducible for Q, then $q_1 > 0$.

Throughout this paper, we will always denote q_0 be the smallest nonnegative root of $B(s) = 0$ on $(0, 1]$. Moreover, it is easy to see that $q_0 = 1$ iff $B'(1) \leq 0$ from Lemma 1.

Lemma 2. *Suppose that Q is a GCB q-matrix as defined in (1) and (2) and let $P(t) = (p_{ij}(t); i, j \geq 0)$ and $\Phi(\lambda) = (\phi_{ij}(\lambda); i, j \geq 0)$ be the Feller minimal Q-function and its Q-resolvent, respectively. Then for any $i \geq 0$, $t \geq 0$, $\lambda > 0$, and $|s| < 1$, we have*

$$\frac{\partial F_i(s,t)}{\partial t} = \frac{1}{m!} B(s) \cdot \frac{\partial^m F_i(s,t)}{\partial s^m}, \quad (6)$$

or equivalently

$$\lambda \Phi_i(s,\lambda) - s^i = \frac{1}{m!} B(s) \cdot \frac{\partial^m \Phi_i(s,\lambda)}{\partial s^m}, \quad (7)$$

where $F_i(s,t) = \sum_{j=0}^{\infty} p_{ij}(t) s^j$ and $\Phi_i(s,\lambda) = \sum_{j=0}^{\infty} \phi_{ij}(\lambda) s^j$.

Proof. By the Kolmogorov forward equation (3), for any i, $j \geq 0$,

$$p'_{ij}(t) = \sum_{k=m}^{j+m} p_{ik}(t) \binom{k}{m} b_{j-k+m}. \quad (8)$$

Multiplying s^j on both sides of the above equality and summing over $j \in \mathbb{Z}_+$, we immediately obtain (6). Finally, (7) is the Laplace transform of (6).

3. Uniqueness

In this section, we mainly consider the uniqueness of GCBPs.

Lemma 3. *Let $(p_{ij}(t), i, j \in \mathbb{Z}_+)$ and $(\phi_{ij}(\lambda), i, j \in \mathbb{Z}_+)$ be the Feller minimal Q-function and Q-resolvent, respectively, where Q is a GCB q-matrix. Then for any $i \geq m$ and $|s| < 1$, we have*

(i) $\int_0^{\infty} p_{ij}(t)dt < +\infty (i, j \geq m)$ and thus $\lim_{t \longrightarrow \infty} p_{ij}(t) = 0 (i, j \geq m)$.

(ii) For any $i \geq m$ and $s \in [0, 1)$,

$$\sum_{j=m}^{\infty} p_{ij}(t)\binom{j}{m}\cdot s^{j-m} < +\infty, \tag{9}$$

$$\sum_{j=0}^{\infty} p'_{ij}(t)s^j = B(s)\sum_{j=m}^{\infty} p_{ij}(t)\binom{j}{m}\cdot s^{j-m}, \tag{10}$$

and

$$\sum_{j=m}^{\infty} \phi_{ij}(\lambda)\binom{j}{m}\cdot s^{j-m} < +\infty, \tag{11}$$

$$\lambda\sum_{j=0}^{\infty} \phi_{ij}(\lambda)s^j - s^i = B(s)\sum_{j=m}^{\infty} \phi_{ij}(\lambda)\binom{j}{m}\cdot s^{j-m}. \tag{12}$$

Proof. It is easily seen that all states $G = \{m, m+1, \ldots,\}$ are transient, and thus, (*i*) follows. This simple fact can also be easily obtained analytically. Indeed, by Kolmogorov forward equation, we have

$$p'_{i0}(t) = p_{im}(t)b_0, \quad i \ge m, \tag{13}$$

which implies that $\int_0^{\infty} p_{im}(t)dt < +\infty$ since $b_0 > 0$. Hence, by the irreducibility of all states $\{m, m+1, \ldots,\}$ we know that $\int_0^{\infty} p_{ij}(t)dt < +\infty$ for all $i, j \ge m$.

We now prove (9). Firstly, we know that the Feller minimal Q-resolvent can be obtained by the following (Laplace transform version) forward integral iteration:

$$\begin{cases} \phi_{ij}^{(0)}(\lambda) = \dfrac{\delta_{ij}}{\lambda + q_j}, \\ \phi_{ij}^{(n+1)}(\lambda) = \dfrac{\delta_{ij}}{\lambda + q_j} + \sum_{k\ne j}\phi_{ik}^{(n)}\cdot\dfrac{q_{kj}}{\lambda + q_j}, \quad n \ge 0, \end{cases} \tag{14}$$

and that $\phi_{ij}^{(n)}(\lambda) \uparrow \phi_{ij}(\lambda)$ as $n \longrightarrow \infty$ for all $i, j \in \mathbb{E}$.

Now, we consider our GCB q-matrix Q on $\mathbb{Z}_+$, and we still denote $\{\phi_{ij}^{(n)}(\lambda), i, j \in \mathbb{Z}_+\}$ to be the corresponding Feller minimal resolvent. Firstly, we claim that for any $n \ge 0$, $i \ge 0$ and $0 < s < 1$,

$$\sum_{j=m}^{\infty} \phi_{ij}^{(n)}(\lambda)\binom{j}{m}s^{j-m} < \infty. \tag{15}$$

For $j < m$, (15) is trivially true, so we assume $j \ge m$. We use mathematically induction on n to prove the conclusion. Obviously, it is true for $n = 0$.

Next, by (14), we can easily get that

$$\begin{aligned} &\sum_{j=0}^{\infty}\lambda\phi_{ij}^{(n+1)}(\lambda)s^j - \sum_{j=m}^{\infty}\binom{j}{m}b_m\phi_{ij}^{(n+1)}(\lambda)s^j \\ &\quad = s^i + \sum_{k=m}^{\infty}\phi_{ik}^{(n)}(\lambda)\binom{k}{m}s^{k-m}\cdot\left(\sum_{j\ne m}^{\infty} b_j s^j\right). \end{aligned} \tag{16}$$

Define $A_{ij}^{(n+1)}(\lambda) = \phi_{ij}^{(n+1)}(\lambda) - \phi_{ij}^{(n)}(\lambda)\,(n \ge 0)$, then $A_{ij}^{(n)}(\lambda) \ge 0$ and

$$\lim_{n\longrightarrow\infty} A_{ij}^{(n)}(\lambda) = 0, \quad \text{for all } i, j \in \mathbb{Z}_+. \tag{17}$$

Applying the notation, (16) can be rewritten as

$$\begin{aligned} \lambda\sum_{j=0}^{\infty}\phi_{ij}^{(n+1)}(\lambda)s^j &= s^i + B(s)\sum_{k=m}^{\infty}\phi_{ij}^{(n)}(\lambda)\binom{k}{m}s^{k-m} \\ &\quad + b_m s^m\sum_{j=m}^{\infty}A_{ij}^{(n+1)}(\lambda)\binom{j}{m}s^{j-m}. \end{aligned} \tag{18}$$

By (14), $A_{ij}^{(n+1)}(\lambda) = \sum_{k\ne j}A_{ik}^{(n)}(\lambda)q_{kj}/(\lambda + q_j)$, $n \ge 0$, then

$$\begin{aligned} \sum_{j=0}^{\infty}A_{ij}^{(n+1)}(\lambda)(\lambda + q_j)s^j &= \sum_{k=2}^{\infty}A_{ik}^{(n)}(\lambda)\binom{k}{m}s^{k-2} \\ &\quad \cdot\left(b_0 + b_1 s + \sum_{m=1}^{\infty}b_{m+2}s^{m+2}\right). \end{aligned} \tag{19}$$

It follows from the above two expressions that

$$\sum_{j=m}^{\infty}A_{ij}^{(n+1)}(\lambda)\binom{j}{m}s^{j-m} \le \frac{B(s) - b_m s^m}{-b_m s^m}\sum_{j=m}^{\infty}A_{ij}^{(n)}(\lambda)\binom{j}{m}s^{k-m}, \tag{20}$$

and so (15) follows from the induction principle.

Also, letting $s \uparrow 1$ in (20) yields that

$$\sum_{j=m}^{\infty}A_{ij}^{(n+1)}(\lambda)\binom{j}{m} \le \sum_{j=m}^{\infty}A_{ij}^{(n)}(\lambda)\binom{j}{m}, \quad n \ge 1. \tag{21}$$

However, it is easily seen that

$$\sum_{k=m}^{\infty}A_{ik}^{(1)}(\lambda)\binom{k}{m} \le -\frac{1}{b_m}, \quad n \ge 1, \tag{22}$$

and thus, by (18), we have

$$\sum_{k=m}^{\infty}A_{ik}^{(n)}(\lambda)\binom{k}{m} \le -\frac{1}{b_m}, \quad n \ge 1. \tag{23}$$

It follows from the Dominated Convergence Theorem and (20) yields that for $0 < s < 1$,

$$\lim_{n\longrightarrow\infty}\sum_{j=m}^{\infty}A_{ij}^{(n+1)}\binom{j}{m}s^{j-m} = 0. \tag{24}$$

Letting $n \longrightarrow \infty$ in (18) and applying the above equality leads to the conclusion that for $0 < s < 1$,

$$\lambda\sum_{j=0}^{\infty}\phi_{ij}(\lambda)s^j = s^i + B(s)\lim_{n\longrightarrow\infty}\sum_{k=m}^{\infty}\phi_{ik}^{(n)}(\lambda)\binom{k}{m}s^{k-m}. \tag{25}$$

However, for all $0 < 1 - \varepsilon \le s < 1$, we may find an $\varepsilon > 0$ such that $B(s) \ne 0$. Thus,

$$\lim_{n\longrightarrow\infty}\sum_{k=m}^{\infty}\phi_{ik}^{(n)}(\lambda)\binom{k}{m}s^{k-m}<\infty,\quad 1-\varepsilon\le s<1. \tag{26}$$

Applying the Monotone Convergence Theorem and Dominated Convergence Theorem yields

$$\sum_{k=m}^{\infty}\phi_{ik}(\lambda)\binom{k}{m}s^{k-m}=\lim_{n\longrightarrow\infty}\sum_{k=m}^{\infty}\phi_{ik}^{(n)}(\lambda)\binom{k}{m}s^{k-m}<\infty,\quad 1-\varepsilon\le s<1. \tag{27}$$

It easy to see that the above equality holds for all $0<s<1$. Thus, (12) yields from (25). Moreover, (10) is the Laplace transform of (12), which implies that (10) holds for almost all $t\ge 0$. Furthermore, note that the left-hand side of (11) is a continuous function of $t>0$; thus, (10) holds for all $t\ge 0$.

Theorem 1. *The GCB q-matrix is regular iff $B'(1)\le 0$.*

Proof. Firstly, we suppose that $B'(1)\le 0$ and let $P(t)=\{p_{ij}(t), i, j\ge 0\}$ be the minimal Q-transition function. Substituting (1) into (3) gives

$$p'_{ij}(t)=\sum_{k=m}^{j+m}p_{ik}(t)\binom{k}{m}b_{j-k+m},\quad i,j\ge 0. \tag{28}$$

It easily yields that for $0\le s<1$,

$$\sum_{j=0}^{\infty}p'_{ij}(t)s^j=B(s)\sum_{k=m}^{\infty}\binom{k}{m}p_{ik}(t)s^{k-m},\quad i\ge 0, \tag{29}$$

the right-hand side being strictly positive for $s\in(0,1)$ follows from the Lemma 1. Moreover, it is easy to dictate that for all $t\ge 0$,

$$\sum_{j=0}^{\infty}\left|p'_{ij}(t)\right|\le 2q_i, \tag{30}$$

where $q_i:=-q_{ii}=\binom{i}{m}b_m<\infty$. Therefore, the series $\sum_{j=0}^{\infty}p'_{ij}(t)s^j$ converges uniformly on $[0,\infty)$ for every $s\in[0,1)$, and since the derivatives $p'_{ij}(t)$ are all continuous, the derivative of $\sum_{j=0}^{\infty}p_{ij}(t)s^j$ exists and equals $\sum_{j=0}^{\infty}p_{ij}(t)s^j$. Thus, we may integrate (29) to obtain

$$\sum_{j=0}^{\infty}p_{ij}(t)s^j-s^i\ge 0,\quad i\ge 0, 0\le s<1. \tag{31}$$

Letting $s\uparrow 1$ in (31) yields $\sum_{j=0}^{\infty}p_{ij}(t)\ge 1$, which implies that the equality holds for all $i\ge 0$. Therefore, the minimal Q-transition function is honest, and hence, Q is regular.

Conversely, by the Theorem 3.6 of Li and Chen [9], it is easy to obtain the conclusion since $\sum_{k=m}^{\infty}1/\binom{k}{m}<\infty$. The proof is complete.

By Theorem 1, we can see that if $B'(1)\le 0$, then the GCBP is regular. In the sequel, we will prove that for any given GCB q-matrix Q, there always exists exactly one Q-process satisfying the Kolmogorov forward equation (3).

Theorem 2. *There exists exactly one GCBP.*

Proof. It follows from Theorem 1, we only need to consider the case $0<B'(1)\le+\infty$. In order to prove the uniqueness of the GCBP, we will verify Reuter's condition, i.e., we need to prove that the equation

$$\begin{cases} Y(\lambda I-Q)=0, & 0\le Y<+\infty,\\ \sum_{j\in\mathbb{Z}_+}y_j<+\infty, \end{cases} \tag{32}$$

has only the trivial solution, and then cover all $\lambda>0$.

Let $Y=(y_i;\, i\ge 0)$ be a nontrivial solution corresponding to $\lambda=1$, then $y_0>0$ and by (32),

$$\eta_j=\sum_{i=m}^{j+m}\eta_i\binom{i}{m}b_{j-i+m},\quad j\ge 0, \tag{33}$$

with

$$\begin{gathered}\eta_j\ge 0\,(j\ge 0),\\ \sum_{j=0}^{\infty}\eta_j<+\infty.\end{gathered} \tag{34}$$

It is clear that the nontriviality of the solution η implies that

$$\eta_j>0. \tag{35}$$

$\sum_{j=0}^{\infty}\eta_j$ is well defined for all $s\in[0,1]$ since (34) holds, which implies that

$$\eta_j=\sum_{i=m}^{\infty}\eta_j s^j<+\infty,\quad 0\le s<1, \tag{36}$$

because it follows from the root test, these series have the same radius of convergence. Applying Fubini's theorem together with (33) and (36) yields that

$$\sum_{j=0}^{\infty}\eta_j s^j=B(s)\sum_{i=m}^{\infty}\binom{i}{m}\eta_i s^{i-m},\quad 0\le s<1. \tag{37}$$

Therefore, $\sum_{j=0}^{\infty}\eta_j s^j$ and $\sum_{i=m}^{\infty}\binom{i}{m}\eta_i s^{i-m}$ are strictly positive for all $s\in(0,1)$ based on (33)–(36), and thus $B(s)>0$ for all $s\in(0,1)$, since $0<B'(1)\le+\infty$, which contradicts with Lemma 1.

4. Extinction and Explosion

From the previous section, we have obtained that the GCBP is uniquely determined by its q-matrix, so we will examine some of its properties in this section. Let $\{X(t), t\ge 0\}$ be the unique GCBP, and denote $P(t)=\{p_{ij}(t), i, j\ge 0\}$ be its transition function. Define the extinction times τ_k for $k=0, 1, \ldots, m-1$ as

$$\tau_k=\begin{cases}\inf\{t>0, X(t)=k\}, & \text{if } X(t)=k \text{ for some } t>0,\\ +\infty, & \text{if } X(t)\ne k \text{ for all } t>0,\end{cases} \tag{38}$$

and denote the corresponding extinction probabilities by

$$a_{ik} = P(\tau_k < +\infty \mid X(0) = i) = \lim_{t\longrightarrow\infty} p_{ik}(t), \tag{39}$$

and the overall extinction probability by $a_k = P(\tau < \infty \mid X(0) = i) = \sum_{k=0}^{m-1} a_{ik}$. Also let $E_i(\cdot)$ denote the expectation conditional on $X(0) = i$.

Theorem 3. *The extinction probabilities $a_{ik}(k = 0, 1, \ldots, m-1)$ satisfy*

$$a_{i0} + q_k a_{i1} + \cdots + q_k^{m-1} a_{im-1} = q_k^i, \quad k = 0, 1, \ldots, m-1. \tag{40}$$

More specifically,

$$a_{i0} + a_{i1} + \cdots + a_{im-1} = 1, \quad \text{if } B'(1) \le 0, \tag{41}$$

$$a_{i0} + q_k a_{i1} + \cdots + q_k^{m-1} a_{im-1} = q_k^i < 1, \quad \text{if } 0 < B'(1) \le +\infty. \tag{42}$$

Proof. Firstly, it is clear that all states $\{m, m+1, \ldots\}$ are transient. For all i, $k \ge m$, we have $\lim_{t\longrightarrow\infty} p_{ik}(t) = 0$ follows from $\int_0^\infty p_{ik}(t)dt < +\infty$. Thus, letting $t \longrightarrow \infty$ in (30) and using the Dominated Convergence Theorem, we obtain that $a_{i0} + qa_{i1} + \cdots + q^{m-1}a_{im-1} \ge s^i$ for $s \in [0, 1)$. Letting $s \uparrow 1$, we immediately obtain (41) since $a_{i0} + a_{i1} + \cdots + a_{im-1} \le 1$.

We now prove (42). It follows from Lemma 1 that we have $q < 1$ since $0 < B'(1) \le \infty$. Putting $s = q$ in (11) and noting that $B(q) = 0$, we discover that $\sum_{j=0}^\infty p'_{ij}(t)q^j = 0$ for any $t > 0$, implying that $\sum_{j=0}^\infty \int_0^t p'_{ij}(u)du \cdot q^j = 0$. Thus, for any $t > 0$,

$$\sum_{j=0}^\infty p_{ij}(t)q^j = q^i, \quad i \ge m. \tag{43}$$

Letting $t \longrightarrow \infty$, we have

$$\begin{aligned}&\lim_{t\longrightarrow\infty} p_{i0}(t) + q \cdot \lim_{t\longrightarrow\infty} p_{i1}(t) + \cdots + q^{m-1} \cdot \lim_{t\longrightarrow\infty} p_{im-1}(t) \\ &\quad + \lim_{t\longrightarrow\infty} \sum_{j=m}^\infty p_{ij}(t)q^j = q^i, \quad i \ge m.\end{aligned} \tag{44}$$

Noting that all of the limits exist, we may apply the Dominated Convergence Theorem in the last term on the left-hand side to obtain (42) since $q < 1$.

By Theorem 3, we know that the process is absorbed with probability less than 1 if $0 < B'(1) \le +\infty$. Our next result establishes that the process must explode if absorption does not occur in such cases.

Theorem 4. *For the Feller minimal GCBP,*

$$E_i(\tau) = m! \cdot \int_0^1 \frac{(1-y)^{m-1}(a_{i0} + a_{i1}y + \cdots + a_{im-1}y^{m-1} - y^i)}{B(y)} dy. \tag{45}$$

Therefore, $E_i(\tau)$ is finite for any $i \ge m$ iff

$$\int_0^1 \frac{a_{i0} + a_{i1}y + \cdots + a_{im-1}y^{m-1} - y^i}{B(y)} dy < \infty. \tag{46}$$

Proof. It follows from (10), for all $s \in [0, 1)$, we have

$$\frac{1}{B(s)} \sum_{j=0}^\infty p'_{ij}(t)s^j = \sum_{j=m}^\infty p_{ij}(t)\binom{j}{m} \cdot s^{j-m}, \tag{47}$$

i.e.,

$$\frac{\partial F_i(t,s)}{\partial t} = \frac{1}{m!} \cdot B(s) \cdot \frac{\partial^m F_i(t,s)}{\partial s^m}, \tag{48}$$

where $F'_i(t,s) = \sum_{j=0}^\infty p'_{ij}(t)s^j$. The apparent singularity at $s = q$ on the left-hand side is removable, because the series on the right-hand side certainly converges for all $s \in [0, 1)$. Moreover, the left-hand side is continuous and strictly positive (indeed increasing) on this interval. Therefore, integrating (48) with respect to s iteration m times and applying Fubini's theorem yields that for any $s \in [0, 1)$,

$$\begin{aligned}F_i(t,s) &= p_{i0}(t) + p_{i1}(t)s + \cdots + p_{im-1}(t)s^{m-1} \\ &\quad + m! \cdot \int_0^s \frac{(s-y)^{m-1}}{B(y)} \cdot F'_i(t,y)dy.\end{aligned} \tag{49}$$

Letting $s \uparrow 1$ in (49), we can get that the equality (49) also holds for $s = 1$, and

$$\sum_{j=m}^\infty p_{ij}(t) = m! \cdot \int_0^1 \frac{(1-y)^{m-1}}{B(y)} \cdot F'_i(t,y)dy. \tag{50}$$

Then the proof is complete if (46) holds since

$$\begin{aligned}E_i(\tau) &= \int_0^\infty \left(m! \cdot \int_0^1 \frac{(1-y)^{m-1}F'_i(t,y)}{B(y)}\right)dt \\ &= m! \cdot \int_0^1 \frac{(1-y)^{m-1}(a_{i0} + a_{i1}y + \cdots + a_{im-1}y^{m-1} - y^i)}{B(y)} dy.\end{aligned} \tag{51}$$

Lemma 4. *Let $(p_{ij}(t), i, j \in \mathbb{Z}_+)$ and $(\phi_{ij}(\lambda), i, j \in \mathbb{Z}_+)$ be the Feller minimal Q-function and Q-resolvent where Q is a GCB q-matrix.*

(i) For any i, $k \ge m$,

$$\int_0^\infty p_{ik}(t)dt = \frac{1}{\binom{k}{m}} \cdot \frac{G_i^{k-m}(0)}{(k-m)!}. \tag{52}$$

(ii) For any $i \ge m$,

$$\int_0^\infty \sum_{k=m}^\infty p_{ik}(t)\mathrm{d}t = \sum_{k=m}^\infty \frac{1}{\binom{k}{m}} \cdot \frac{G_i^{(k-m)}(0)}{(k-m)!} < \infty, \tag{53}$$

and hence, considering the integrand is nonnegative, we obtain that

$$\lim_{t\longrightarrow\infty} \sum_{k=m}^\infty p_{ik}(t) = 0. \tag{54}$$

Proof. By (10), we have

$$\sum_{j=0}^\infty p_{ij}(t)s^j - s^i = B(s) \cdot \sum_{k=m}^\infty \left(\int_0^t p_{ik}(u)\mathrm{d}u\right)\binom{k}{m} s^{k-m}. \tag{55}$$

Letting $t \longrightarrow \infty$ in the equality (55) for $s \in (-1, 1)$, applying the Dominated Convergence Theorem on the left-hand side and the Monotone Convergence Theorem on the right-hand side, we obtain (53) by the uniqueness of the Taylor expansion. Furthermore, (53) implies (54) is trivial, and hence, the proof is complete.

Theorem 5. *For the Feller minimal GCBP, $E_i(\tau)$ is finite for some (and for all) $i \geq m$ iff $B'(1) \leq 0$, and hence*

$$E_i(\tau) = \sum_{k=m}^\infty \frac{G_i^{(k-m)}(0)}{\binom{k}{m} \cdot (k-m)!}. \tag{56}$$

More specifically, if $0 < B'(1) \leq +\infty$, then $E_i(\tau) = +\infty$ for any $i \geq m$.

Proof. It is easily seen from Theroem 3 and Lemma 1 that if $0 < B'(1) \leq \infty$, then $\sum_{k=0}^{m-1} a_{ik} < 1$ which implies $E_i(\tau) = +\infty$, so let us assume that $B'(1) \leq 0$. For these latter cases, it follows from (55) and applying the Monotone Convergence Theorem yields

$$\begin{aligned} E_i[\tau] &= \int_0^\infty (1 - p_{i0}(t) - \cdots - p_{im-1}(t))\mathrm{d}t \\ &= \int_0^\infty \sum_{k=m}^\infty p_{ik}(t)\mathrm{d}t \\ &= \sum_{k=m}^\infty \frac{1}{\binom{k}{m}} \cdot \frac{G_i^{(k-m)}(0)}{(k-m)!}. \end{aligned} \tag{57}$$

Thus, the proof is complete.

It is easily seen that $E_i(\tau_k) = +\infty (i \geq m, k = 0, 1, \ldots, m-1)$ when the extinction is not certain. Under these circumstances, it is natural to consider the conditional expected extinction times, given by $E_i(\tau_k \mid \tau_k < \infty) = \mu_k / a_{ik}$, where $\mu_k = E_i(\tau_k I_{\{\tau_k < \infty\}})$.

Theorem 6. *For the Feller minimal GCBP starting in state $i (i \geq m)$, $E_i(\tau_k \mid \tau_k < \infty)(k = 0, 1, \ldots, m-1)$ are all finite, and moreover,*

$$E_i(\tau_k \mid \tau_k < \infty) = \frac{\mu_{ik}}{a_{ik}}, \quad k \leq m-1, i \geq m, \tag{58}$$

where $\mu_{ik}(k \leq m-1)$ satisfy the linear equations

$$\sum_{k=0}^{m-1} \mu_{ik} q_j^k = \sum_{k=m}^\infty \frac{1}{\binom{k}{m}} \cdot \frac{G_i^{(k-m)}(0)}{(k-m)!} \cdot q_j^k, \quad j = 0, 1, \ldots, m-1. \tag{59}$$

Proof. First we consider the case $0 < B'(1) \leq +\infty$, and thus, $0 < q_0 < 1$, and $|q_i| < 1$ for $j = 1, \ldots, m-1$, applying the Theorem 3 together with $\sum_{k=0} p_{ik}(t) q^k = q^i$ yields the expression

$$\sum_{k=0}^{m-1} (a_{ik} - p_{ik}(t)) q_j^k = \sum_{k=m} p_{ik}(t) q_j^k, \quad j = 0, 1, \ldots, m-1. \tag{60}$$

On integrating (60) and using $a_{ik} - p_{ik}(t) = P(t < \tau_k < \infty \mid X(0) = i)(k = 0, 1, \ldots, m-1)$, we obtain that

$$\begin{aligned} &q_j^k \cdot \int_0^\infty P(s < \tau_k < \infty \mid X(0) = i)\mathrm{d}s \\ &\quad = \sum_{k=m}^\infty \int_0^t p_{ik}(s)\mathrm{d}s \cdot q_j^k, \quad j = 0, 1, \ldots, m-1. \end{aligned} \tag{61}$$

Noting that $|q_j| < 1$ for $j = 1, \ldots, m-1$, letting $t \longrightarrow \infty$ and applying the monotone convergence theorem yields

$$\mu_{i0} + q_k \mu_{i1} + \cdots + q_k^{m-1} \mu_{im-1} = \sum_{k=m}^\infty \frac{G_i^{(k-m)}(0)}{(k-m)!} \cdot q_k^j. \tag{62}$$

On the other hand, by the definition of τ, $E_i(\tau I_{\{\tau<\infty\}}) = \sum_{k=0}^\infty E_i(\tau_k I_{\{\tau_k<\infty\}})$, and then all of the conclusions follow since $|q_i| < 1$ for $j = 1, \ldots, m-1$.

Next we consider the case $B'(1) \leq 0$, then we have $P(\tau < \infty \mid X(0) = i) = 1$. It follows from Theorem 3 that $a_i = a_{i0} + a_{i1} + \cdots + a_{im-1} = 1$, and hence, the ensuing honesty of the transition function allows us to deduce that

$$\sum_{k=0}^\infty (a_{ik} - p_{ik}(t)) = \sum_{k=m}^\infty p_{ik}(t). \tag{63}$$

Noting that $q_0 = 1$ and $|q_i| < 1$ for $j = 1, \ldots, m-1$, and letting $t \longrightarrow \infty$ again and applying the monotone convergence theorem yields

$$\mu_{i0} + q_k \mu_{i1} + \cdots + q_k^{m-1} \mu_{im-1} = \sum_{k=m}^\infty \frac{G_i^{(k-m)}(0)}{(k-m)!} \cdot q_k^j. \tag{64}$$

We know that (59) still holds for $j = 1, \ldots, m-1$ in this case. Hence, we have (40) with $q_0 = 1$. A similar argument yields the required conclusions.

From now on, we will consider the explosion probabilities and expected explosion times. By Theorem 1, we only need to consider the case that $0 < B'(1) \le \infty$. Denote τ_∞ be the explosion time and let $a_{i\infty} = P(\tau_\infty \mid X(0) = i)$ be the probability of explosion starting in state i. Since we are aiming at the minimal process, $p_{i\infty}(t) := 1 - \sum_{j=0}^{\infty} p_{ij}(t) = P(\tau_\infty \le t \mid X(0) = i)$ is the probability of explosion by time t starting in state i, and $p_{i\infty}(t) \longrightarrow a_{i\infty}$ as $t \longrightarrow \infty$.

Theorem 7. *For the minimal process starting in $i (i \ge m)$, we have the following statements.*

(i) If $B'(1) \le 0$, then $a_{i\infty} = 0$.

(ii) If $0 < B'(1) \le +\infty$, then

$$\sum_{k=0}^{m-1} a_{ik} E_i(\tau_k \mid \tau_k < \infty) + a_{i\infty} E_i(\tau_\infty \mid \tau_\infty < \infty) = \sum_{k=m}^{\infty} \frac{G_i^{(k-m)}(0)}{\binom{k}{m}(k-m)!}. \tag{65}$$

Proof. If $B'(1) \le 0$, then $a_{i\infty} = 0$ since the minimal process is honest. If $0 < B'(1) \le +\infty$, by Theorem 2 we know that the minimal process is dishonest, i.e., $p_{i\infty}(t) = 1 - \sum_{j=0}^{\infty} p_{ij}(t) > 0$. Letting $t \longrightarrow \infty$ and applying (30) together with Theorem 3 yields our expression for $a_{i\infty}$. Next we write $\sum_{k=0}^{m-1} (a_{ik} - p_{ik}(t)) + a_{i\infty} - p_{i\infty}(t) = \sum_{j=m}^{\infty} p_{ij}(t)$; then we obtain (65) by integrating this equality with respect to t, and noting that $P(\tau_\infty \le t \mid \tau_\infty < \infty, X(0) = i) = p_{i\infty}(t)/a_{i\infty}$.

Finally, we consider the time spent in each state over the lifetime of the process. Let T_k be the total time spent in state $k (k \ge m)$ and let $\mu_{ik} = E_i(T_k) (i \ge m)$. Then,

$$\mu_{ik} = E\left(\int_0^\infty I_{\{X(t)=k\}} \mathrm{d}t \mid X(0) = i\right) = \int_0^\infty p_{ik}(t) \mathrm{d}t. \tag{66}$$

This quantity was evaluated in (29). We have therefore the following result.

Theorem 8. *All of $\mu_{ik} (i \ge m, k \ge m)$ are finite and given by*

$$\mu_{ik} = \frac{G_i^{(k-m)}(0)}{\binom{k}{m} \cdot (k-m)!}. \tag{67}$$

Data Availability

Not applicable.

Conflicts of Interest

The authors declare that they have no conflicts of interest.

Acknowledgments

This work was substantially supported by the National Natural Sciences Foundation of China (No. 11901392).

References

[1] S. Asmussen and H. Hering, *Branching Processes*, Birkhauser, Boston, MA, USA, 1983.

[2] K. B. Athreya and P. Jagers, *Classical and Modern Branching Processes*, Springer, Berlin, Germany, 1972.

[3] K. B. Athreya and P. E. Ney, *Branching Processes*, Springer, Berlin, Germany, 1983.

[4] A. Chen, P. Pollett, H. Zhang, and J. Li, "The collision branching process," *Journal of Applied Probability*, vol. 41, no. 4, pp. 1033–1048, 2004.

[5] I. I. Ezhov, "Branching processes with group death," *Theory of Probability and Its Applications*, vol. 25, pp. 202-203, 1980.

[6] T. E. Harris, *The Theory of Branching Processes*, Springer, Berlin, Germany, 1963.

[7] A. V. Kalinkin, "Markov branching processes with interaction," *Russian Mathematical Surveys*, vol. 57, no. 2, pp. 241–304, 2002.

[8] J. Li, "Decay parameter and related properties of 2-type branching processes," *Science in China Series A: Mathematics*, vol. 52, no. 5, pp. 875–894, 2009.

[9] J. Li and A. Chen, "Generalized Markov interacting branching processes," *Science China Mathematics*, vol. 61, no. 3, pp. 545–562, 2018.

[10] J. Li and J. Wang, "Decay parameter and related properties of n-type branching processes," *Science China Mathematics*, vol. 55, no. 12, pp. 2535–2556, 2012.

[11] B. A. Sevast'yanov, "On certain types of Markov processes (in Russian)," *Uspekhi Matematicheskikh Nauk*, vol. 4, p. 194, 1949.

[12] D. Y. Chen, Y. Y. Hu, and S. Lin, "Resistance growth of branching random networks," *Electronic Journal of Probability*, vol. 23, no. 52, pp. 1–17, 2018.

[13] D. Chen, L. de Raphélis, and Y. Hu, "Favorite sites of randomly biased walks on a supercritical Galton-Watson tree," *Stochastic Processes and Their Applications*, vol. 128, no. 5, pp. 1525–1557, 2018.

[14] Z. Li, "Path-valued branching processes and nonlocal branching superprocesses," *The Annals of Probability*, vol. 42, no. 1, pp. 41–79, 2014.

[15] W. Yu, Y. Huang, and C. Cui, "The absolute ruin insurance risk model with a threshold dividend strategy," *Symmetry*, vol. 10, no. 9, p. 377, 2018.

[16] W. Yu, F. Wang, Y. Huang, and H. Liu, "Social optimal mean field control problem for population growth model," *Asian Journal of Control*, pp. 1–8, 2019.

[17] W. Yu, Y. Yong, G. Guan, Y. Huang, W. Su, and C. Cui, "Valuing guaranteed minimum death benefits by cosine series expansion," *Mathematics*, vol. 7, no. 9, p. 835, 2019.

[18] Y.-X. Ren, R. Song, and R. Zhang, "Central limit theorems for supercritical branching nonsymmetric Markov processes," *The Annals of Probability*, vol. 45, no. 1, pp. 564–623, 2017.

[19] J. Xiong and X. Yang, "Superprocesses with interaction and immigration," *Stochastic Processes and Their Applications*, vol. 126, no. 11, pp. 3377–3401, 2016.

[20] M. Zhang, "Central limit theorems for a super-diffusion over a stochastic flow," *Journal of Theoretical Probability*, vol. 24, no. 1, pp. 294–306, 2011.

[21] Y.-H. Zhang, "Strong ergodicity for single-birth processes," *Journal of Applied Probability*, vol. 38, no. 1, pp. 270–277, 2001.

[22] Z. Zhang, Y. Yong, and W. Yu, "Valuing equity-linked death benefits in general exponential Lévy models," *Journal of Computational and Applied Mathematics*, vol. 365, Article ID 112377, 2020.

Hindawi
Mathematical Problems in Engineering
Volume 2020, Article ID 3469486, 8 pages
https://doi.org/10.1155/2020/3469486

Research Article

A Quantitative Comparison of Multiple Population Mortality Model on Some East Asian Countries and Regions

Ming Zhao,[1] **Xiaojun Wang**,[2] **Yu Liu**,[1] **and Jiali Shen**[1]

[1]*School of Finance, Capital University of Economics and Business, Beijing 100070, China*
[2]*School of Statistics, Renmin University of China, Beijing 100872, China*

Correspondence should be addressed to Ming Zhao; zhaoming@cueb.edu.cn

Received 16 January 2020; Accepted 11 March 2020; Published 9 April 2020

Guest Editor: Ming Zhou

This paper reviews the progress of the multiple population mortality model and the defects in parameter estimation and proposes an effective method to improve the performance of the mortality model. We set up a multiple population group, using the data of mainland China, Hong Kong (China), and Japan, to test fitting performance and forecasting performance. Using the TSWLS and TSSVD methods in a multiple population stochastic mortality model has advantages in fitting performance and robustness. In addition, the forecasting value of mortality ratio between any two populations can converge to a fixed constant in a certain time period which obeys the regular of human biological characteristics.

1. Introduction

With the demographic dividend gradually disappearing worldwide, it is common for the elders to have fewer children. In the future, it will seriously change the age structure of the population and interfere with the country's formulation of certain strategic policies. Additionally, the acceleration of the life expectancy and the ageing of the population would lead to varying shocks to the national pension system, commercial insurance companies, and families, which makes a negative impact on the economic development for a country. Therefore, it is beneficial to take countermeasures in advance to help economic entities, using scientific methods to forecasting the population mortality and reasonably assessing the impact of longevity risk. The research on the method of forecasting of mortality has experienced the development from a single population model to multiple population model. Among them, some classical methods, such as the Lee–Carter model, APC model, and CBD model, have been verified for stability, which represent the frontier progress of the research on the stochastic mortality model.

The stochastic mortality model which is used for a single population group is first proposed by Lee and Carter in [1]. The Lee–Carter model assumes that the logarithmic mortality is composed of independent age and period effects, with fewer model parameters, simple fitting process, robust forecasting results, and other advantages, which has been widely used by scholars all over the world. The Lee–Carter model applies a two-stage method to estimate parameters. In the first stage, it uses the orthogonal least squares (OLS) method, the maximum likelihood estimate (MLE) method, or singular value decomposition (SVD) method to estimate static parameters. For the second stage, dynamic parameters are fitted by the time series model [2]. Scholars have made many improvements to the Lee–Carter model, including the improvement of the parameter estimation method [3] and model hypothesis [4]. Renshaw et al. [5] took the cohort effect of population mortality into consideration and further expanded it into the age-period-cohort (APC) model. Although the APC model is used in medicine for a long time, the idea of modelling stochastic mortality originated from the Lee–Carter model. Furthermore, due to the relatively small number of population exposures of old age, the Lee–Carter model and APC model are not well suitable for the mortality of the elders. However, it is found that the CBD model with two factors could cope with this problem [6]. The CBD mode with cohort effects is a prominent choice [7] for fitting mortality of the elders when both BIC information criterion and robustness of the parameters are considered. With the continuous development of population mortality models, there is an increasing number of shortcomings of single population stochastic mortality model exposed and there would be unreasonable crossover or deviation in mortality forecasting in a long time [8, 9]. Because the mortality modelling is a kind of systematic work, it only considers a single population group, which will cause different population mortality violating human biological laws over time. Therefore, it is necessary to promote the forecasting performance of mortality in the long term by combining with two or more populations in one model, which can make the mortality model have better fitting goodness and forecasting performance.

Carter and Lee [10] proposed the first multiple mortality model called the Joint-k model, which assumes that the mortality of multiple populations has the common period effect factor, and the gap among population groups reflects only in the individual age effect factor. Li and Lee [11] extended the age effect factor to a common factor based on the Joint-k model and then put forward the Li–Lee model, an augmented common factor model, which has common age and period effect factors plus the additional age and period effect factors that represent the mortality in a single population. Li and Hardy [12] proved that there is a cointegration relationship on the trend of the period effect factor among multiple populations and then established a linear time-effect factor model called the cointegrated Lee–Carter model. Kleinow [13] proposed a common age effect (CAE) model, using a common principal component analysis to estimate the parameter. The model is simple and has a better fitting performance. Enchev et al. [14] compared the above models with the MLE method to select which model has the best fitting performance. According to the result, the CAE model and Li–Lee model are more suitable for modelling on multiple population mortality, but there is a problem in converging of parameter estimation. Li and Liu [15] built a logistic two-population mortality projection model for the mortality at ages 80 to 100 of both sexes, applied this model and its extensions to high-quality old-age mortality data of Belgium, Sweden, Switzerland, and the UK, and produced a decent model performance in both mortality fitting and forecasting. Tsai and Zhang [16] proposed a nonparametric method to forecast the mortality of a multiple populations of the United States, the United Kingdom, and Japan.

According to current research, it is found that the multiple population stochastic mortality model has become the frontier progress, and there have been studies on the quantitative comparison of different types of multiple mortality models, but the quantitative comparison of parameter estimation methods is still blank. In addition, most of the data used to test the multiple population mortality models are European countries in the human mortality database, but few studies use data from statistical institutions in developing countries. As a country with a large population and rapid economic development, the mortality rate of mainland China is rapidly decreasing, but there are few studies on mortality forecasting based on the multiple population model. It is meaningful for mainland China to build a multiple mortality model with neighbouring countries or regions which not only have the lower values and higher quality mortality but also have much closer genes and habits that can affect mortality. Therefore, this paper selects East Asian countries and regions, including Hong kong (China) and Japan to build a multiple population model with mainland China to compare quantitatively the methods of parameter estimation.

The structure of this paper is as follows. Section 2 explains the rationale of the methods of parameter estimation for the multiple mortality model. Next, Section 3 describes the data features and research scheme. Following this, Section 4 inspects the fitting performance of the proposed methods. Section 5 examines the forecasting performance among the three population groups. Finally, Section 6 concludes the paper.

2. Mortality Models

2.1. Lee–Carter Model. Lee and Carter (1992) propose a logarithmic, linear stochastic mortality model as follows:

$$\ln m(x,t) = \alpha(x) + \beta(x) * k(t) + \varepsilon(x,t), \tag{1}$$

in which $m(x, t)$ is the crude mortality rate at the age x in the year t for a single population, $\alpha(x)$ and $\beta(x)$ are variables about the age x, while $\alpha(x)$ is the average of the logarithmic mortality in all years, $\beta(x)$ shows the age effect parameter which stands for the slope of the logarithmic mortality, $k(t)$ explains the period effect parameter that represents the slope of the logarithmic mortality in the year t, and $\varepsilon(x, t)$ is the normal error with i.i.d. There are three types of methods to estimate the parameters in the Lee–Carter model, including the OLS, SVD, and MLE method.

2.2. Li–Lee Model. While requiring the high quality of death data, the Lee–Carter model can only be used to forecast the mortality of a single population. To make up for the defects of the Lee–Carter model, Li and Lee proposed a mortality model from the perspective of multiple populations as follows:

$$\ln m(x,t,i) = \alpha(x,i) + B(x) * K(t) + \beta(x,i) * k(t,i) + \varepsilon(x,t,i), \tag{2}$$

in which $m(x, t, i)$ is the crude mortality rate at the age x in the year t in the population i and $\alpha(x, i)$ explains the average of logarithmic mortality at the age x in all years in the population i. The common age effect parameter $B(x)$ represents the slope of the logarithmic mortality at the age x for all population groups, $K(t)$ is period effect parameter which shows the slope of the logarithmic mortality in the year t for all population groups, the specific age effect parameter $\beta(x, i)$ is the slope of the logarithmic mortality at the age x in the population i, $k(t, i)$ is the specific period effect parameter that represents the slope of the logarithmic mortality in the year t in the population i, and $\varepsilon(x, t, i)$ is the normal error with i.i.d. Similar to the Lee–Carter model, the Li–Lee model also contains three methods to estimate the parameters that are SVD, OLS, and MLE.

Li and Lee used the SVD method to estimate the parameters of the multiple population mortality model. However, that experiment discovers the lack of suitability in the SVD method for certain deformation forms. Enchev et al. used the MLE method, which has an extensive range of applications to almost all types of multiple population mortality models, to estimate parameters. Nevertheless, the multiple population mortality models have more parameters, and there will be errors that the converging value is mistaken for the optimal local solution during the calculation process of the Newton–Raphson iterative algorithm. For the sake of solving the problems above, we propose two methods to estimate the parameter of the Li–Lee model, which are two-step weighted least squares (TSWLS) and two-step singular-value decomposition (TSSVD).

In what follows, we derive and implement constraints for the parameters that allow us to solve the identifiability issues. The constraints are as follows:

$$\begin{aligned}\sum_x B(x) &= 1,\\ \sum_t K(t) &= 0,\\ \sum_x \beta(x,i) &= 1,\\ \sum_t k(t,i) &= 0,\end{aligned} \tag{3}$$

in which we normalise the sums of the common age parameter to equate to unity. Additionally, the specific age parameters should also equate to unity for every population i. Furthermore, the common period parameter should sum to zero, and finally, the specific period parameters should sum to zero for each population i as well. The steps of TSWLS and TSSVD methods are as follows:

Step 1: using the Lee–Carter model, define

$$\ln(x,t,i) = \alpha(x,i) + B(x) * K(t) + \varepsilon(x,t,i), \tag{4}$$

and then estimate the parameters $\alpha(x, i)$, $B(x)$, and $K(t)$ for the combined dataset of all populations. Both the methods, TSWLS and TSSVD, have the same Step 1.

(1) Based on $\sum_t K(t) = 0$, get the estimation of $\alpha(x, i)$:t

$$\widehat{\alpha}_{x,i} = \frac{\sum_{t=t_L}^{t_U} \ln m_{x,t,i}}{t_U - t_L + 1}. \tag{5}$$

(2) Based on $\sum_x B(x) = 1$, get the estimation of $K(t)$:

$$\widehat{K}_t = \sum_{i=1}^{r}\sum_{x=x_L}^{x_U} w_i \times \left[\ln\left(m_{x,t,i}\right) - \widehat{\alpha}_{x,i}\right]. \tag{6}$$

in which $t = t_L, \ldots, t_U$, $i = 1, \ldots, r$, $x = x_L, \ldots, x_U$, and $i = 1, \ldots, r$; $w_i$is the weight of the group i, that is, $\sum_{i=1}^{r} w_i = 1$; in this article, the weight of every group is $w_i = 1/r$.

(3) Based on $[\ln(m_{x,t,i}) - \alpha_{x,i}]$, use WLS to obtain the estimation of $B(x)$:

$$\widehat{B}_x = \frac{\sum_{i=1}^{r}\sum_{t=t_L}^{t=t_U} w_i\left[\widehat{K}_t \times \left(\ln m_{x,t,i} - \widehat{\alpha}_{x,i}\right)\right]}{\sum_{t=t_L}^{t_U}\widehat{K}_t^2}. \tag{7}$$

Step 2: using the Li–Lee model, define

$$\ln m(x,t,i) = \widehat{\alpha}(x,i) + \widehat{B}(x) * \widehat{K}(t) + \beta(x,i) * k(t,i). \tag{8}$$

in which the estimated $\alpha(x, i)$, $B(x)$, and $K(t)$ are fixed as constant values.

(4) Based on $\sum_x B(x,i) = 1$, obtain the estimation of $k(t, i)$:

$$\widehat{k}_{t,i} = \sum_{x=x_L}^{x_U}\left[\ln\left(m_{x,t,i}\right) - \widehat{\alpha}_{x,i} - \widehat{B}_x \times \widehat{K}_t\right]. \tag{9}$$

(5) Based on $[\ln(m_{x,t,i}) - \widehat{\alpha}_{x,i} - \widehat{B}_x \times \widehat{K}_t]$, use OLS to obtain the estimation of $\beta(x, i)$:

$$\widehat{\beta}_{x,i} = \frac{\sum_{t=t_L}^{t_U}\left[\widehat{k}_{t,i} \times \left(\ln m_{x,t,i} - \widehat{\alpha}_{x,i}\right)\right] - \widehat{B}_x \sum_{t=t_L}^{t_U} K_t \widehat{k}_{t,i}}{\sum_{t=t_L}^{t_U}\widehat{k}_{t,i}^2}. \tag{10}$$

The above step is the parameter estimation process of the TSWLS method, and the process of the TSSVD method can be directly used by singular-value decomposition.

2.3. Mortality Graduation Method. Although the Li–Lee model, as Kang et al. [17] reveal, is one of the classical methods among the multiple population mortality models, the fluctuation of crude mortality data defects the fitting performance. Therefore, graduating the crude mortality data before fitting the model is necessary. In this paper, we apply the two-dimensional beta kernel density method, which can guarantee the reasonable smoothing results on both age and time dimensions, to graduate the crude mortality [18]. The two-dimensional beta kernel density method requires three steps, as follows:

Step 1: modelling two-dimensional beta kernel density:

(1) Define the distribution function of the numbers of death:

$$d(x,y) \sim \mathrm{Bin}[e(x,y), q(x,y)], \tag{11}$$

in which x is the age, y is the year, at the age x in the year y, $d(x, y)$ is the numbers of death satisfying the binomial distribution, $e(x, y)$ is the exposure, and $q(x, y)$ is the actual mortality.

(2) Define the function of two-dimensional beta kernel density:

$$k_{h_Z}(z;m_Z) = \left(z - a_Z + \frac{1}{2}\right)^{(m_Z - a_Z + (1/2))/(h_Z(c_Z+1))} \cdot \left(b_Z + \frac{1}{2} - z\right)^{(b_Z + (1/2) - m_Z)/(h_Z(c_Z+1))}, \quad z \in \mathcal{Z}, \tag{12}$$

in which Z is a two-dimensional random variable that has the value space of $\mathcal{Z} = \{a_Z, b_Z\}$, $c_Z = b_Z - a_Z$, and h_z is the bandwidth. The above formula can be standardized as

$$K_{h_Z}(z;m_Z) = \frac{k_{h_Z}(z;m_Z)}{\sum_{\omega\in Z} k_{h_Z}(\omega;m_Z)}, \quad z \in \mathcal{Z}. \tag{13}$$

(3) Estimate the crude mortality:

$$\widehat{q}(x,y) = \sum_{u\in\mathcal{X}}\sum_{v\in\mathcal{Y}} K_{h_X,h_Y}(u,v;m_X = x, m_Y = y)\dot{q}\,(u,v), \quad (x,y) \in \mathcal{X}\times\mathcal{Y}, \tag{14}$$

in which $\dot{q}(x,y)$ is defined as the crude mortality that is accord with the $q(x,y)$, $x \in \mathcal{X}$, and $y \in \mathcal{Y}$. Otherwise,

$$K_{h_X,h_Y}(x,y;m_X,m_Y) = K_{h_X}(x;m_X)K_{h_Y}(y;m_Y), \quad (x,y) \in \mathcal{X}\times\mathcal{Y}. \tag{15}$$

Step 2: setting the adaptive bandwidth:

The formula of bandwidth adaptation is

$$h_Z(z;s_Z) = h_Z[l_Z(z)]^{s_Z}, \quad z \in \mathcal{Z}, \tag{16}$$

in which $h_Z$stands for the global bandwidth factor and $s$is a sensitive parameter as the local bandwidth factor, $s \in [0,1]$. The reliability function $l_Z(z)$can determine the numerical ranges of the local bandwidth factor, and at the same time, reliability function is limited by the local bandwidth factor so that extreme values do not occur.

Mazza and Punzo used variation coefficient (VC) to measure $l_Z(z)$, which is as follows:

$$VC(z) = \frac{\sqrt{e(z)\widetilde{q}(z)[1-\widetilde{q}(z)]}}{e(z)\widetilde{q}(z)}, \quad z \in \mathcal{Z}. \tag{17}$$

When the reliability function satisfies the condition of $[l_Z(z)]^{s_Z} \in [0,1]$,

$$[l_Z(z)] = \frac{\mathrm{VC}(z)}{\sum_{\omega\in\mathcal{Z}}\mathrm{VC}(\omega)}, \quad z \in \mathcal{Z}. \tag{18}$$

Step 3: selection of sensitive parameters:

In the process of mortality graduation of the two-dimensional beta kernel, the selection of bandwidth is realised by minimizing CV statistics, whose formula is

$$\mathrm{CV}(h_Z) = \sum_{z\in\mathcal{Z}} \mathrm{res}^2[\dot{q}(z), \widehat{q}_{-z}(z)], \tag{19}$$

in which $\mathrm{res}[\dot{q}(z), \widehat{q}_{-z}(z)]$ is the residual in z and $\dot{q}(z)$is the rude mortality in z. The formula of $\widehat{q}_{-z}(z)$ can be expressed as

$$\widehat{q}_{-z}(z) = \sum_{\substack{v\in Z\\ v\neq zZ}} \frac{k_{h_Z}(v;m_Z = z)}{\sum_{\substack{w\in Z\\ w\neq z}} k_{h_Z}(w;m_Z = z)}\dot{q}(z). \tag{20}$$

Furthermore, the proportional difference form of residual in mortality graduation is commonly used, that is,

$$\mathrm{res}[\dot{q}(z), \widehat{q}_{-z}(z)] = \frac{\widehat{q}_{-z}(z)}{\dot{q}(z)} - 1. \tag{21}$$

2.4. Fitting and Forecasting. Before forecasting the mortality out-of-sample, it is necessary to test the fitting performance. The average absolute percentage error (MAPE) is used frequently [19] whose expression is

$$\mathrm{MAPE}_i = \frac{1}{x_U - x_L + 1}\frac{1}{t_U - t_L + 1}\sum_{x=x_L}^{x_U}\sum_{t=t_L}^{t_U}\left|\frac{\widehat{m}_{x,t,i} - m_{x,t,i}}{m_{x,t,i}}\right|. \tag{22}$$

Forecasting the mortality should model the time-effect factors first. The Li–Lee model includes both the common time-effect factor, $K(t)$, and the specific time-effect factor, $k(t, i)$. They are modeled as

$$\begin{aligned}\widehat{K}_t &= \theta + \widehat{K}_{t-1} + \varepsilon_t,\\ \widehat{k}_{t,i} &= \phi_0 + \phi_1\widehat{k}_{t-1,i} + \varepsilon_{t,i}.\end{aligned} \tag{23}$$

in which $K(t)$ is the processes of a random walk with drift and $k(t, i)$ explains the autoregressive process with one order. On this basis, we get the following mortality prediction formula:

$$\widehat{m}_{x,t,i} = \dot{m}_{x,s,i}\exp\left[\widehat{B}_x\left(\widehat{K}_t - K_s\right) + \widehat{\beta}_{x,i}\left(\widehat{k}_{t,i} - k_{s,i}\right)\right]. \tag{24}$$

The forecasting results can not only reflect the trend of mortality decline but also ensure the long-term consistency of mortality among different population groups.

3. Data and Research Scheme

We perform our analysis based on data obtained from public resources of the National Bureau of Statistics of China (BSC) and Human Mortality Database (HMD). The typical dataset consists of the numbers of deaths and the central exposure. The age period range considered is from 0 up to 100 years (101 consecutive ages in total) and from 1994 up to the year 2014 (21 years in total), respectively.

To compare advantages of methods used in this paper, we make the following designs: (1) due to the lower number of deaths, we select male mortality as the research samples; (2) in order to keep up with the standard of HMD data, we use two-dimensional beta kernel density method to graduate the mortality in mainland China; (3) we select the data from East Asian countries or regions of mainland China, Hong Kong (China), and Japan to compare our method with the Lee–Carter model; and (4) we test the robustness of our method by replacing the data of crude mortality with the graduated mortality.

4. Quantitative Comparison of Fitting Performance

In this paper, we compare models between the multiple population stochastic mortality model and single population Lee–Carter model, so do methods between the TSWLS method and the TSSVD method in the Li–Lee model, from the perspective of horizontal comparison. Because major research on mortality modelling of China uses the crude data, this paper first applies the same mortality data for analysis. Also, the MLE method cannot converge to a stable value all the time in the Li–Lee model, so it is not included in our study. Based on methods of the second part in this paper, we can calculate the MAPE values.

Table 1 shows the MAPE values of the three methods in mainland China, Hong Kong (China), and Japan, in which a smaller MAPE value indicates a better fitting performance. In general, the Li–Lee model with the TSSVD method has the lowest MAPE value of 20.22% in all the years from 1995 to 2014, while the Lee–Carter model has the highest MAPE value of 21.18%. Therefore, we can infer that the fitting performance of multiple population mortality model under the two methods for parameter estimation is better than that under the single population mortality model. Next, we plan to analyse the fitting performance of different population groups below. For mainland China, the Lee–Carter model gets the lowest MAPE value, while the Li–Lee model under the TSWLS method has the highest in all the years from 1995 to 2014. However, in most of the five-year periods, the Li–Lee model does better than the Lee–Carter model on fitting performance. For example, the Li–Lee model with TSSVD method has the best performance in the years of 1995~2000 and 2006~2010. By contrast, the Lee–Carter model only shows a surprisingly lowest MAPE value in the years of 2011~2014, which brings about the best fitting performance in the whole historical period. In Hong Kong (China), the Li–Lee model with TSSVD method always displays the lowest MAPE value during 1995 and 2014, and only in 1995~2000, it gets slightly higher value than the TSWLS method. As for Japan, the last population group, the Li–Lee model with TSSVD method is the one that has the best performance among any periods of years. In terms of numerical values, Japan's MAPE value ranges from 5% to 9%, while that in mainland China is from 27% to 49% and 18% to 25% in Hong Kong (China). From the above analysis, we can assume a preliminary conclusion that when the higher the smoothness is, the better fitting performance the mortality model will have.

Then, we use the two-dimensional beta kernel density method, aiming to derive mortality with higher smoothness in the dimension of the period, to graduate the data in mainland China. Although the mortality from the HMD database is graduated, the method is constrained within the dimension of age, which ignores the impact of the period trend. To not only test the robustness of the estimation but also explain whether the smoother population mortality data can improve the fitting performance of the model, we use the two-dimensional smoothing method for the population mortality in mainland China.

Table 2 shows the MAPE values of three methods in mainland China, Hong Kong (China), and Japan, respectively. From Table 2, we notice that the fitting mortality model based on the graduated data makes a considerable positive impact on mainland China, which reduces the MAPE value range from the 27%~49% to 9%~15% but has less effect on the fitting performance of Japan and Hong Kong (China). It means that the smoothness of the data can significantly improve the fitting effect of the Li–lee model, with both methods, and the Lee–Carter model. At the same time, we can observe that the three methods show a stable estimation effect in all populations. Consistent with Table 1, the Li–Lee model with TSSVD method gets the lowest MAPE value, while the Lee–Carter model has the highest MAPE value. Consequently, we can make advancement in model fitting performance by using the graduated mortality data and solving the multiple population mortality models with the TSSVD method, especially for forecasting of mortality in mainland China.

5. Quantitative Comparison of Forecasting Performance

According to equation (11), we can obtain the numerical values of out-of-sample mortality from 2015 to 2050. In this paper, we take the 30-year-old population as an example and then display the values in Table 3. All three types of methods could show a decreasing trend of population mortality in the future, but there are some differences in detail. From the perspective of different population groups, the mortality of the Lee–Carter model in mainland China declines rapidly from 0.97‰ in 2015 to 0.28‰ in 2050, while the forecasting values of the other two methods are very close to each other which decline from 1.00‰ in 2015 to 0.50‰ in 2050 together. For Hong Kong (China), the mortality forecasting results by all methods are similar, except the Li–Lee model with TSWLS, which has slightly higher values. Compared with that in mainland China, the future values of population mortality in Japan is also close under the two methods of the Li–Lee model, but the Lee–Carter model has higher forecasting values. The reason for the above situation is that the multiple population mortality model is systematic, which can consider the interrelationship between different population groups and make the expected results reasonable in the long term. Because the single population of the Lee–Carter model assumes that the mortality decreases with a fixed constant, the forecasting values of mortality among different population groups will cross or

Table 1: MAPE values of all the models on crude mortality data (%).

	1995~2000	2001~2005	2006~2010	2011~2014	All years
Mainland China					
Li–Lee model (TSWLS)	28.76	**27.45**	40.76	47.19	35.17
Li–Lee model (TSSVD)	**28.75**	27.61	40.03	45.91	34.77
Lee–Carter model	29.02	27.99	**39.32**	**44.24**	**34.42**
Hong Kong (China)					
Li–Lee model (TSWLS)	**23.61**	19.21	20.15	23.03	21.05
Li–Lee model (TSSVD)	23.64	**18.66**	**18.75**	**22.57**	**20.49**
Lee–Carter model	23.13	19.15	20.21	24.10	21.16
Japan					
Li–Lee model (TSWLS)	5.52	4.82	5.10	6.93	5.49
Li–Lee model (TSSVD)	**5.49**	**4.70**	**4.81**	**6.91**	**5.39**
Lee–Carter model	6.99	7.59	8.46	8.65	7.95
Sum of above					
Li–Lee model (TSWLS)	19.30	17.16	22.00	25.72	20.57
Li–Lee model (TSSVD)	**19.29**	**16.99**	**21.20**	**25.13**	**20.22**
Lee–Carter model	19.71	18.24	22.66	25.66	21.18

Table 2: MAPE values of all the models on graduated mortality data (%).

	1995~2000	2001~2005	2006~2010	2011~2014	All years
Mainland China					
Li–Lee model (TSWLS)	7.36	**6.26**	6.96	13.55	8.39
Li–Lee model (TSSVD)	7.76	6.62	7.41	**9.13**	**7.86**
Lee–Carter model	**7.35**	6.28	**6.89**	14.39	8.54
Hong Kong (China)					
Li–Lee model (TSWLS)	23.39	19.25	20.03	23.30	21.04
Li–Lee model (TSSVD)	23.53	**18.68**	**18.70**	**22.23**	**20.38**
Lee–Carter model	**23.13**	19.15	20.21	24.10	21.16
Japan					
Li–Lee model (TSWLS)	**5.50**	4.68	4.71	**6.88**	**5.36**
Li–Lee model (TSSVD)	5.55	**4.68**	**4.70**	6.98	5.38
Lee–Carter model	6.99	7.59	8.46	8.65	7.95
Sum of above					
Li–Lee model (TSWLS)	**12.08**	10.06	10.57	14.58	11.60
Li–Lee model (TSSVD)	12.28	**9.99**	**10.27**	**12.78**	**11.21**
Lee–Carter model	12.49	11.01	11.85	15.71	12.55

Table 3: Numerical values of out-of-sample mortality from 2015 to 2050 (‰).

	2015	2020	2025	2030	2035	2040	2045	2050
Mainland China								
Li–Lee model (TSWLS)	0.98	0.89	0.80	0.72	0.65	0.58	0.52	0.47
Li–Lee model (TSSVD)	1.00	0.91	0.82	0.73	0.66	0.59	0.53	0.48
Lee–Carter model	0.97	0.81	0.68	0.57	0.48	0.40	0.34	0.28
Hong Kong (China)								
Li–Lee model (TSWLS)	0.59	0.54	0.49	0.44	0.39	0.35	0.32	0.28
Li–Lee model (TSSVD)	0.58	0.52	0.46	0.42	0.37	0.33	0.30	0.27
Lee–Carter model	0.57	0.51	0.46	0.41	0.37	0.33	0.30	0.27
Japan								
Li–Lee model (TSWLS)	0.65	0.56	0.50	0.45	0.40	0.36	0.32	0.29
Li–Lee model (TSSVD)	0.67	0.60	0.53	0.48	0.43	0.39	0.35	0.31
Lee–Carter model	0.68	0.66	0.63	0.61	0.59	0.57	0.56	0.54

deviate abnormally in the long term. Therefore, the multiple population mortality model is more suitable for forecasting mortality than the single population mortality model in the long term, also effectively improves the reliability of the prediction value.

Next, we use three figures to show the forecasting performance vividly. From the perspective of different methods, we further analyse the evidence of rationality of the population mortality model. Figure 1 shows the trend of mortality in different populations under the Lee–Carter

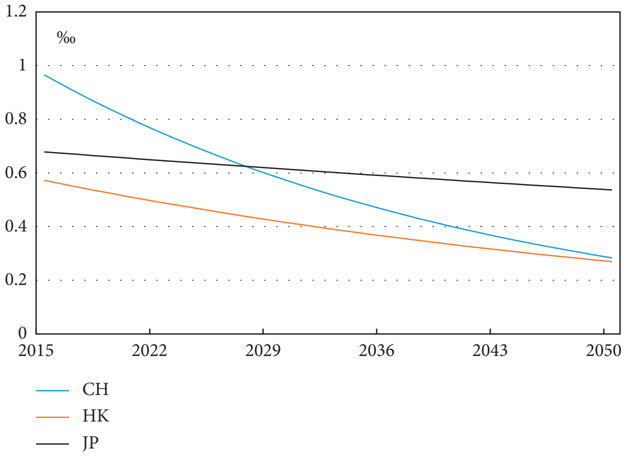

FIGURE 1: Trends in mortality based on the Lee–Carter model from 2015 to 2050.

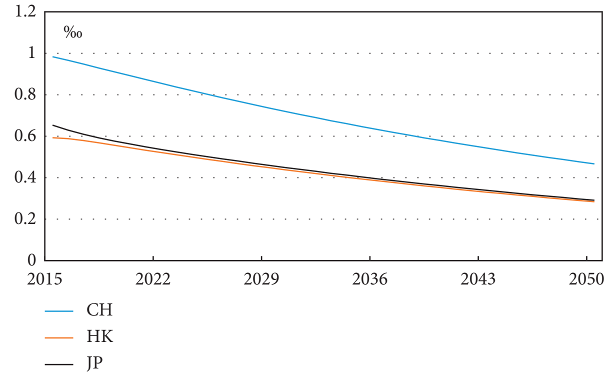

FIGURE 2: Trends in mortality based on the Li–Lee model with TSWLS from 2015 to 2050.

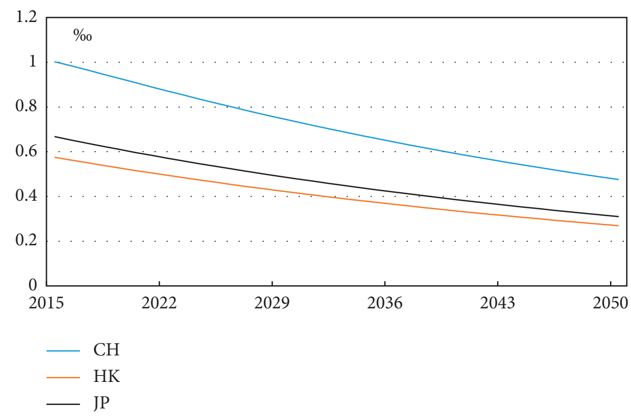

FIGURE 3: Trends in mortality based on the Li–Lee model with TSSVD from 2015 to 2050.

model in 2015–2050. We can find two unreasonable problems in Figure 1. Firstly, the curve of mortality trend of mainland China intersects with Japan in 2038. On the other hand, it keeps below that of Japan in the following years. The reason is that the Lee–Carter model only considers the velocity of single population mortality decline in historical data. Due to the higher level of mortality in mainland China, the velocity of mortality decline rate is faster than that of Japan, which has finished the historical stage of rapid decline of mortality. If the mortality rates of the two population groups continue to fall at the current speed, the life expectancy in mainland China will surpass that in Japan soon after, though it is contradicting to the biological law of human beings. As time goes by, the gap of mortality curves between Hong Kong (China) and Japan is gradually widening with a trumpet shape, which is also attributed to the defects in the hypothesis of a single mortality model.

Figure 2 demonstrates the forecasting values of mortality based on the Li–Lee model with the TSWLS method, the above problems in the single mortality model can be fixed through the multiple mortality model. The mortality of the three groups shows a consistent trend from 2015 to 2050 in Figure 2, similar to the historical experience of decline. Mortality of mainland China maintains a higher level than the others, and the gap is narrowing. However, there will be no crossing in the future. We can tell from Figure 2 that the mortality gap between Hong Kong (China) and Japan is relatively small and even overlapped in a short period, which is not accord with the current mortality relationship between the two populations.

How to address this issue can be found in Figure 3. Figure 3 witnesses forecasting values of mortality based on the Li–Lee model with the TSSVD method from 2015 to 2050, in which the forecasting values of mortality on mainland China is close to the values in Figure 2. Yet, the TSSVD method for forecasting the mortality of two population groups in Hong Kong (China) and Japan has more advantages, as reflecting the mortality gap decreasing over time but no crossing in the short term. Overall, we conclude that the multiple population model is better than the single population model in terms of forecasting of mortality, and the TSSVD method is more suitable for the multiple population model than the TSWLS method.

6. Conclusion

This paper reviews the progress of the multiple population stochastic mortality model and finds some defects in parameter estimation, so that it proposes an effective method to improve the parameter estimation. We set up multiple population groups, using the data of mainland China, Hong Kong (China), and Japan, to test fitting performance and forecasting performance, and draw the following conclusions: (1) for the parameter estimation method, TSWLS and TSSVD methods, in a multiple population stochastic mortality model, can avoid some problems, like maximum likelihood estimation is not converge, or the result is local optimal caused by the more parameters. The two methods are simple and easy to understand and are the tools for the application in the multiple population mortality model. (2) For fitting performance, the multiple population mortality model is robustness based on TSWLS and TSSVD methods. Additionally, the fitting performance can be significantly improved based on graduated data, which illustrates that the multiple population mortality model is more suitable for smooth mortality. (3) For forecasting performance, the multiple population stochastic mortality model with additional period effect factors can obtain consistent values among different population groups, and the mortality ratio between any two populations can converge to a fixed constant in a certain period which obeys the regular of human biological characteristics.

Data Availability

The data used to support the findings of this study are from the Human Mortality Database and China National Bureau of Statistics.

Conflicts of Interest

The authors declare that there are no conflicts of interest regarding the publication of this paper.

Acknowledgments

This work was supported by the Beijing Social Science Foundation of China (no. 19YJC042), the Special Foundation for Basic Scientific Research Business Expenses of Universities owned by the Municipal Government of Beijing of Capital University of Economics and Business, titled "Research on the Measurement of Longevity Risk of Pension System Considering the Change of Death Pattern."

References

[1] R. D. Lee and L. R. Carter, "Modeling and forecasting U.S. mortality," *Journal of the American Statistical Association*, vol. 45, no. 6, pp. 4–19, 1992.

[2] J. Bongaarts and G. Feeney, "How long do we live?" *Population and Development Review*, vol. 28, no. 1, pp. 13–29, 2002.

[3] J. R. Wilmoth, "Mortality projections for Japan: a comparison of four methods," in *Health and Mortality Among Elderly Populations*, G. Caselli and A. Lopez, Eds., pp. 266–287, Clarendon Press, Oxford, UK, 1996.

[4] N. Li, R. Lee, and S. Tuljapurkar, "Using the Lee–Carter method to forecast mortality for populations with limited data," *International Statistical Review*, vol. 72, no. 1, pp. 19–36, 2004.

[5] A. E. Renshaw, S. Haberman, J. Insmatheco et al., "A cohort-based extension to the Lee-Carter model for mortality reduction factors," *Insurance: Mathematics and Economics*, vol. 38, no. 3, pp. 556–570, 2006.

[6] A. J. G. Cairns, D. Blake, K. Dowd et al., "A quantitative comparison of stochastic mortality models using data from England and Wales and the United States," *North American Actuarial Journal*, vol. 13, no. 1, pp. 1–35, 2007.

[7] A. J. G. Cairns, D. Blake, K. Dowd, G. D. Coughlan, D. Epstein, and M. Khalaf-Allah, "Morality density forecasts: an analysis of six stochastic mortality models," *Insurance: Mathematics and Economics*, vol. 48, no. 3, pp. 355–367, 2011.

[8] W. Yu, Y. Yong, G. Guan, Y. Huang, W. Su, and C. Cui, "Valuing guaranteed minimum death benefits by cosine series expansion," *Mathematics*, vol. 7, no. 9, p. 835, 2019.

[9] Z. Zhang, Y. Yaodi, and W. Yu, "Valuing equity-linked death benefits in general exponential Lévy models," *Journal of Computational and Applied Mathematics*, vol. 365, Article ID 112377, 2020.

[10] L. R. Carter and R. D. Lee, "Modeling and forecasting US sex differentials in mortality," *International Journal of Forecasting*, vol. 8, no. 3, pp. 393–411, 1992.

[11] N. Li and R. D. Lee, "Coherent mortality forecasts for a group of populations: an extension of the Lee-Carter method," *Demography*, vol. 42, no. 3, pp. 575–594, 2005.

[12] J. S.-H. Li and M. R. Hardy, "Measuring basis risk in longevity hedges," *North American Actuarial Journal*, vol. 15, no. 2, pp. 177–200, 2011.

[13] T. Kleinow, "A common age effect model for the mortality of multiple populations," *Insurance: Mathematics and Economics*, vol. 63, pp. 147–152, 2015.

[14] V. Enchev, T. Kleinow, and A. J. G. Cairns, "Multi-population mortality models: fitting, forecasting and comparisons," *Scandinavian Actuarial Journal*, vol. 2017, no. 4, pp. 1–24, 2017.

[15] J. Li and J. Liu, "A logistic two-population mortality projection model for modelling mortality at advanced ages for both sexes," *Scandinavian Actuarial Journal*, vol. 2019, no. 2, pp. 97–112, 2019.

[16] C. C. L. Tsai and Y. Zhang, "A multi-dimensional Bühlmann credibility approach to modeling multiple population mortality rates," *Scandinavian Actuarial Journal*, vol. 2019, no. 1, pp. 406–443, 2019.

[17] M. Kang, Y. Liu, S. H. Li, and W. S. Chan, "Mortality forecasting for multiple populations: an augmented common factor model with a penalized log-likelihood," *Communications in Statistics: Case Studies, Data Analysis and Applications*, vol. 4, no. 3-4, pp. 118–141, 2019.

[18] A. Mazza and A. Punzo, *Graduation by Adaptive Discrete Beta Kernels, Classification and Data Mining*, Springer, Berlin, Germany, 2013.

[19] T. Lin, C.-W. Wang, and C. C.-L. Tsai, "Age-specific copula-AR-GARCH mortality models," *Insurance: Mathematics and Economics*, vol. 61, pp. 110–124, 2015.

Hindawi
Mathematical Problems in Engineering
Volume 2020, Article ID 3705325, 6 pages
https://doi.org/10.1155/2020/3705325

Research Article

Asymptotic Behaviors for Delay Lotka–Volterra Model Disturbed by *G*-Brownian Motion

Ping He,[1,2] **Yong Ren**,[1] **and Defei Zhang**[2]

[1]*Department of Mathematics, Anhui Normal University, Wuhu 241000, China*
[2]*Department of Mathematics, Honghe University, Mengzi 661199, China*

Correspondence should be addressed to Defei Zhang; zhdefei@163.com

Received 30 December 2019; Accepted 10 February 2020; Published 7 April 2020

Guest Editor: Wenguang Yu

In this paper, we propose the stochastic Lotka–Volterra model with delay disturbed by G-Brownian motion $\mathrm{d}x = \mathrm{diag}\,(x_1, x_2, \ldots, x_n)[(Ax(t-\tau)+b)d\langle B\rangle(t) + \sigma x \mathrm{d}B(t)]$. Under a natural assumption on noise, we study existence and uniqueness of the global positive solution for the system and its asymptotic pathwise moment behavior and prove that the solution does not explode to infinity in a finite time.

1. Introduction

Since the Lotka–Volterra model (LVM in short) was provided by Lotka [1] and Volterra [2], there were extensive works concerned with the dynamics of this system and global stability and the stochastic Lotka–Volterra population model, and in here, we only mention [3, 4] (for deterministic situation) and [5–8] (for stochastic situation). The well-known two-dimensional delay Lotka–Volterra ecological population model driven by Brownian motion is

$$\begin{cases} \mathrm{d}x_1 = x_1\left[(a_1 + b_{11}x_1(t-\tau) + b_{12}x_2(t-\tau))\mathrm{d}t \right. \\ \left. +(c_{11}x_1 + c_{12}x_2)\mathrm{d}W(t)\right], \\ \mathrm{d}x_2 = x_2\left[(a_2 + b_{21}x_1(t-\tau) + b_{22}x_2(t-\tau))\mathrm{d}t \right. \\ \left. +(c_{21}x_1 + c_{22}x_2)\mathrm{d}W(t)\right]. \end{cases} \tag{1}$$

Bahar and Mao in [9] proved that the solution of (1) is almost surely nonnegative and finite. Wu and Xu in [10] investigated stochastic LVM with infinite delay. Global asymptotic stability for a stochastic delay LVM was obtained in [11].

Peng first established the stochastic analysis theory under the G-expectation framework in references [12–14]. Peng's G-expectation space is an essential extension for probability measure space. Since then, many important theoretical results in this field are obtained, for example, SLL for sublinear expectations are obtained in [15], capacity theory results are discussed in [16] and [17–19], and other related technologies in [20–22]. Inspired by these results, we investigate a stochastic delay Lotka–Volterra model disturbed by G-Brownian motion:

$$\mathrm{d}x = \mathrm{diag}\,(x_1, x_2, \ldots, x_n)[(b + Ax(t-\tau))\mathrm{d}\langle B\rangle(t) + \sigma x \mathrm{d}B(t)], \tag{2}$$

with $\{x(s)\colon -\tau \le s \le 0\} \in C([-\tau, 0]; R_+^n)$, where $x = (x_1, \ldots, x_n)^T$ is a n-dimensional vector, $x_i(t)$ is the population size of species i at time $t (t \ge 0)$, $b = (b_1, b_2, \ldots, b_n)^T$, b_i is the species i's growth rate, $A = (a_{ij})_{n\times n}$ is a $n\times n$ community matrix, $a_{ij}(I \ne j)$ is the interspecific interaction effect, and a_{ii} is the intraspecific interaction effect. We assume that the interaction effect in this system was disturbed by a G-Brownian motion with $\hat{\mathbb{E}}[B(t)^2] = \overline{\sigma}^2 t$ and $\hat{\mathbb{E}}[-B(t)^2] = -\underline{\sigma}^2 t$, where $\sigma = (\sigma_{ij})_{n\times n}$ is a constant matrix, representing the total interference intensity matrix for the system; $B(t)$ has a variance-uncertainty but not mean-uncertainty; $\langle B\rangle(t)$ has a mean-uncertainty property. Therefore, $(\langle B\rangle, B)$ is used to characterise the disturbed growth rate, disturbed interspecific, or intraspecific interactions and interference intensity at the same time. We think the model (2) considers the stochastic interference from both mean-uncertainty and variance-uncertainty, but the traditional stochastic model cannot describe this property. Indeed, we prove the solution of (2) is quasi-surely nonnegative and finite. Some asymptotic pathwise moment estimations for the solutions of this system are presented.

2. Stochastic Delay Lotka–Volterra Model Driven by G-Brownian Motion

Definitions about sublinear expectations, G-Brownian motions, and quadratic variation process $\langle B\rangle\,(t)$ and notations, as well as more details can also be found in [12–14]. For a matrix A, we denote $|A| = \sqrt{(A^T A)}$ and $\|A\| = \sup\{|Ax|: |x| = 1\}$. $C([-\tau, 0]; R_+^n)$ denotes the family of continuous functions from $[-\tau, 0]$ to R_+^n. We assume the matrix σ satisfies the following assumption:

$$\text{(A)}\quad \begin{cases} \sigma_{ii} > 0, & i \in [1, n], \\ \sigma_{ij} \geq 0, & i \neq j \in [1, n]. \end{cases} \tag{3}$$

The assumption (A) was first assumed by Mao et al. in [5], and it is also necessary in our framework.

Theorem 1. *If the matrix σ in system (2) satisfies assumption (A), then $\forall A \in R^{n\times n}$, $b \in R^n$ and $\{x(s): s \in [-\tau, 0]\}$, then there exists a unique solution x of equation (2). Furthermore, $x(s) \in R_+^n$ for all $s \geq -\tau$ quasi-surely, namely, $\nu(\omega: x(s) \in R_+^n, s \in [-\tau, \infty)) = 1$.*

Proof. Because the coefficients of equation (2) are locally Lipschitz continuous, there exist a unique local solution $x(s)$ on $s \in [-\tau, \tau_e)$, where τ_e is called explosion time. To see it is also global, we must show $\tau_\infty = \infty$ q.s. Suppose $k_0(k_0 > 0)$ is large enough s.t. $x(t)(t \in [-\tau, 0])$ satisfies $1/k_0 < \min |x(t)|$, $\max |x(t)| < k_0$. For any $k(k \geq k_0)$, set $\tau_k = \inf\{s \in [0, \tau_e): x_i(s) \notin (1/k, k), 1 < i \leq n\}$, where $\inf \varnothing = \infty$. Noting that τ_k is increasing when $k \longrightarrow \infty$, let $\tau_\infty = \lim_{k\longrightarrow\infty}\tau_k$, then $\tau_\infty \leq \tau_e$ q.s. If we can prove $\tau_\infty = \infty$ q.s., then $\tau_e = \infty$ q.s. and $x(t) \in R_n^+$ q.s., $t \geq 0$. If $\tau_\infty \neq \infty$ q.s., then $\exists$ a constant $T > 0$ s.t. $V(\omega: \tau_\infty(\omega) \leq T) \geq \varepsilon$ for any $\varepsilon > 0$, namely, $\exists$ an integer $k_1(k_1 \geq k_0)$ s.t. $V(A_k) := V(\omega: \tau_k(\omega) \leq T) \geq \varepsilon$ for all $k \geq k_1$. Let $U: R_n^+ \longrightarrow R^+$ be $U(x) = \sum_{i=1}^n (\sqrt{x_i} - 0.5\log(x_i) - 1)$. Set $k \geq k_0$ and $T > 0$. Using the G-Itô lemma for $\check{V}(t, x) =: U(x) + \int_{t-\tau}^t |x(s)|^2 \mathrm{d}\langle B\rangle(s)$, $t \in [0, \tau_k \wedge T]$, we get

$$\begin{aligned} \mathrm{d}\check{V}(x, t) = {} & \sum_{i=1}^n \left\{ \left(0.5x_i^{0.5} - 0.5\right)\left(\sum_{j=1}^n a_{ij}x_j(t-\tau) + b_i\right)\mathrm{d}\langle B\rangle(t) + \left(-0.125x_i^{0.5} + 0.25\right)\left(\sum_{j=1}^n \sigma_{ij}x_j\right)^2 \mathrm{d}\langle B\rangle(t) \right\} \\ & + \sum_{i=1}^n \left(0.5x_i^{0.5} - 0.5\right)\sum_{j=1}^n \sigma_{ij}x_j \mathrm{d}B(t) + \left(|x|^2 - |x(t-\tau)|^2\right)\mathrm{d}\langle B\rangle(t), \end{aligned} \tag{4}$$

and noting that

$$\sum_{i=1}^n \left[\left(0.5x_i^{0.5} - 0.5\right)\left(b_i + \sum_{j=1}^n a_{ij}x_j(t-\tau)\right)\right] \leq \frac{1}{2}\sum_{i=1}^n \left(x_i^{0.5} - 1\right)b_i + |x(t-\tau)|^2 + \sum_{i=1}^n\sum_{j=1}^n \frac{na_{ij}^2}{16}\left(x_i^{0.5} - 1\right)^2, \tag{5}$$

and $\sum_{i=1}^n \left(\sum_{j=1}^n \sigma_{ij}x_j\right)^2 \leq \sum_{i=1}^n |\sigma|^2 x_i^2 = |\sigma|^2|x|^2$, as well as $\sum_{i=1}^n x_i^{0.5}\left(\sum_{j=1}^n \sigma_{ij}x_j\right)^2 \geq \sum_{i=1}^n \sigma_{ii}^2 x_i^{2.5}$ by the assumption (A). Thus,

$$\begin{aligned} \mathrm{d}\check{V}(t, x(t)) \leq {} & \left[\sum_{i=1}^n \frac{1}{2}\left(x_i^{0.5} - 1\right)b_i + |x(t)|^2 + \sum_{i=1}^n\sum_{j=1}^n \frac{na_{ij}^2}{16}\left(x_i^{0.5} - 1\right)^2\right]\mathrm{d}\langle B\rangle(t) + \left[-0.125\sum_{i=1}^n \sigma_{ii}^2 x_i^{2.5} + 0.25|\sigma|^2|x|^2\right]\mathrm{d}\langle B\rangle(t) \\ & + \sum_{i=1}^n \left(0.5x_i^{0.5} - 0.5\right)\sum_{j=1}^n \sigma_{ij}x_j \mathrm{d}B(t). \end{aligned} \tag{6}$$

Denote

$$f(x,a,b,\sigma) = \sum_{i=1}^{n} \frac{1}{2}\left(x_i^{0.5}-1\right)b_i + |x|^2\left(1+\frac{1}{4}|\sigma|^2\right) + \sum_{i=1}^{n}\sum_{j=1}^{n}\frac{na_{ij}^2}{16}\left(x_i^{0.5}-1\right)^2 - \frac{1}{8}\sum_{i=1}^{n}\sigma_{ii}^2 x_i^{2.5}, \quad (7)$$

since we note that there is K s.t. $f(x, a, b, \sigma)$ is bounded, namely, $f(x, a, b, \sigma) < K$, then

$$\hat{\mathbb{E}}\left[\int_{\tau_k\wedge T-\tau}^{T\wedge\tau_k} |x|^2 \mathrm{d}\langle B\rangle(s) + U\left(x\left(T\wedge\tau_k\right)\right)\right] \le \hat{\mathbb{E}}\left[\int_{-\tau}^{0}|x|^2\mathrm{d}\langle B\rangle(s)\right] + U\left(x_0\right) + K\overline{\sigma}^2\hat{\mathbb{E}}\left[T\wedge\tau_k\right] \le \overline{\sigma}^2\int_{-\tau}^{0}\hat{\mathbb{E}}\left[|x|^2\right]\mathrm{d}s + U\left(x_0\right) + K\overline{\sigma}^2\hat{\mathbb{E}}\left[T\wedge\tau_k\right], \quad (8)$$

then $\hat{\mathbb{E}}[U(x(\tau_k\wedge T))] \le U(x_0) + \overline{\sigma}^2\int_{-\tau}^{0}\hat{\mathbb{E}}[|x(s)|^2]\mathrm{d}s + K\overline{\sigma}^2 T < \infty$. From the definition of τ_k, we know $\forall\omega\in A_k$, $\exists$ some i s.t. $x_i(\tau_k, \omega)\notin(1/k, k)$, namely, $x_i(\tau_k)\le 1/k$, or $x_i(\tau_k)\ge k<\infty$. Noting that the function $U(x_i)$ is decreasing when $0<x_i\le 1$ and is increasing when $x_i>1$, hence $U(x(\tau_k))\ge U(1/k, \ldots, 1/k)$ and $U(x(\tau_k))\ge U(k, \ldots, k)$, namely, $U(x(\tau_k))\ge \max\left\{\sqrt{(1/k)} - 0.5\log(1/k) - 1, \sqrt{k} - 0.5\log(k) - 1\right\}$. Therefore, we have

$$\varepsilon C_k \le C_k V\left(A_k\right) \le \hat{\mathbb{E}}\left[I_{A_k}U\left(x\left(\tau_k\right)\right)\right] \le \hat{\mathbb{E}}\left[U\left(x\left(T\wedge\tau_k\right)\right)\right] \le U\left(x_0\right) + \overline{\sigma}^2\int_{-\tau}^{0}\hat{\mathbb{E}}\left[|x|^2\right]\mathrm{d}t + K\overline{\sigma}^2 T. \quad (9)$$

Setting $k\longrightarrow\infty$, we have the contradiction $\infty\le\hat{\mathbb{E}}[U(x(\tau_k\wedge T))]<\infty$; therefore, we have $\tau_\infty=\infty$ q.s., namely, $\tau_e=\infty$ q.s., so $\nu(\omega: x(t)\in R_+^n, t\ge 0) = 1$.

3. Asymptotic Behaviors of the Solution

Theorem 2. *Under the assumption (A), if* $\hat{\mathbb{E}}[B(1)^2] = \overline{\sigma}^2 \le 1$, *for any* $\beta\in(0, 1)$ *and* $\delta\in(0, 1)$, $\exists C_0 = C(\delta) > 0$ *s.t. the solution* $x(t)$ *of equation (2) is as follows:*

$$\limsup_{t\longrightarrow\infty} V\left(e^{\left(\langle B\rangle(t)-\overline{\sigma}^2 t\right)/\beta}|x(t)|\le C_0\right) \ge 1-\delta. \quad (10)$$

Proof. Let

$$U(x) = \sum_{i=1}^{n} x_i^{\beta}. \quad (11)$$

Using the G-Itô lemma for $U(x)$ and noting

$$\mathrm{d}x_i(t) = x_i\left[\left(\sum_{j=1}^{n}a_{ij}x_j(t-\tau) + b_i\right)\mathrm{d}\langle B\rangle(t) + \sum_{j=1}^{n}\sigma_{ij}x_j\mathrm{d}B(t)\right], \quad (12)$$

we have

$$\mathrm{d}U(x) = \sum_{i=1}^{n}\beta x_i^{\beta}\left[\left(b_i + \sum_{j=1}^{n}a_{ij}x_j(t-\tau)\right)\mathrm{d}\langle B\rangle(t) + \sum_{j=1}^{n}\sigma_{ij}x_j\mathrm{d}B(t)\right] + \frac{1}{2}\beta(\beta-1)\sum_{i=1}^{n}x_i^{\beta}\left[\sum_{j=1}^{n}\sigma_{ij}x_j\right]^2\mathrm{d}\langle B\rangle(t). \quad (13)$$

Since

$$\sum_{i=1}^{n}\sum_{j=1}^{n}\beta x_i^{\beta}a_{ij}x_j(t-\tau) \le \sum_{i=1}^{n}\sum_{j=1}^{n}\left[\frac{n}{4}\left(\beta a_{ij}x_i^{\beta}\right)^2 + \frac{x_j(t-\tau)^2}{n}\right], \quad (14)$$

and from equation (13), we get

$$\mathrm{d}U(x) \le \left[\sum_{i=1}^{n}\beta b_i x_i^{\beta} + \frac{n}{4}\sum_{i=1}^{n}\sum_{j=1}^{n}\left(\beta a_{ij}x_i^{\beta}\right)^2\right]\mathrm{d}\langle B\rangle(t) + \left[\frac{1}{2}\beta(\beta-1)\sum_{i=1}^{n}x_i^{\beta+2}\sigma_{ii}^2 + |x(t-\tau)|^2\right]\mathrm{d}\langle B\rangle(t) + \left(\sum_{i=1}^{n}\beta x_i^{\beta}\sum_{j=1}^{n}\sigma_{ij}x_j\right)\mathrm{d}B(t), \quad (15)$$

then

$$d\left(e^{\langle B\rangle(t)}U(x(t))\right) = e^{\langle B\rangle(t)}U(x(t))d\langle B\rangle(t) + e^{\langle B\rangle(t)}\mathrm{d}U(x(t))$$
$$\le e^{\langle B\rangle(t)}\left[\sum_{i=1}^{n}(\beta b_i+1)x_i^{\beta} + \frac{n}{4}\sum_{i=1}^{n}\sum_{j=1}^{n}\left(\beta a_{ij}x_i^{\beta}\right)^2\right]\mathrm{d}\langle B\rangle(t) + \exp(\langle B\rangle(t))\left[|x(t-\tau)|^2 + 0.5\beta(\beta-1)\sum_{i=1}^{n}x_i^{\beta+2}\sigma_{ii}^2\right]\mathrm{d}\langle B\rangle(t)$$
$$+ e^{\langle B\rangle(t)}\left(\sum_{i=1}^{n}\beta x_i^{\beta}\sum_{j=1}^{n}\sigma_{ij}x_j\right)\mathrm{d}B(t). \tag{16}$$

We set

$$F_1(x) = \sum_{i=1}^{n}(1+\beta b_i)x_i^{\beta} + \frac{n}{4}\sum_{i=1}^{n}\sum_{j=1}^{n}\left(\beta a_{ij}x_i^{\beta}\right)^2 + e^{\tau}|x|^2 - \frac{1}{2}\beta(1-\beta)\sum_{i=1}^{n}x_i^{\beta+2}\sigma_{ii}^2, \tag{17}$$

then $F_1(x)$ is bounded in R_+^n, say K_1, from (16),

$$d\left(e^{\langle B\rangle(t)}U(x(t))\right) \le e^{\langle B(t)\rangle}\left[K_1 - e^{\tau}|x(t)|^2 + |x(t-\tau)|^2\right]d\langle B\rangle(t) + e^{\langle B\rangle(t)}\left(\sum_{i=1}^{n}\beta x_i^{\beta}\sum_{j=1}^{n}\sigma_{ij}x_j\right)\mathrm{d}B(t), \tag{18}$$

namely,

$$\begin{aligned}
\hat{\mathbb{E}}\left[e^{\langle B\rangle(t)}U(x(t))\right] &\le U_0 + \hat{\mathbb{E}}\left[\int_0^t e^{\langle B\rangle(s)}\left(K_1 - e^{\tau}|x(s)|^2 + |x(s-\tau)|^2\right)\mathrm{d}\langle B\rangle(s)\right]\\
&\le U_0 + \hat{\mathbb{E}}\left[\int_0^t e^{\overline{\sigma}^2 s}\left(K_1 - e^{\tau}|x(s)|^2 + |x(s-\tau)|^2\right)\mathrm{d}\langle B\rangle(s)\right]\\
&\le U_0 + \overline{\sigma}^2\hat{\mathbb{E}}\left[\int_0^t e^{\overline{\sigma}^2 s}\left(K_1 - e^{\tau}|x(s)|^2 + |x(s-\tau)|^2\right)\mathrm{d}s\right]\\
&\le U_0 + K_1 e^{\overline{\sigma}^2 t} + \overline{\sigma}^2\hat{\mathbb{E}}\left[\int_0^t e^{\overline{\sigma}^2 s}|x(s-\tau)|^2 - e^{\overline{\sigma}^2 s+\tau}|x(s)|^2\mathrm{d}s\right]\\
&= U_0 + K_1 e^{\overline{\sigma}^2 t} + \overline{\sigma}^2\hat{\mathbb{E}}\left[\int_{-\tau}^{t-\tau} e^{\overline{\sigma}^2(s+\tau)}|x(s)|^2 - e^{\overline{\sigma}^2 s+\tau}|x(s)|^2\mathrm{d}s\right],
\end{aligned} \tag{19}$$

where $U_0 = U(x(0))$, and noting that $\overline{\sigma}^2$ satisfies $\overline{\sigma}^2 \le 1$, by (19), then

$$\hat{\mathbb{E}}\left[e^{\langle B\rangle(t)}U(x(t))\right] \le U_0 + K_1 e^{\overline{\sigma}^2 t} + \overline{\sigma}^2\hat{\mathbb{E}}\left[\int_{-\tau}^{0} e^{\overline{\sigma}^2(s+\tau)}|x(s)|^2\mathrm{d}s\right], \tag{20}$$

therefore,

$$\limsup_{t\longrightarrow\infty}\hat{\mathbb{E}}\left[e^{\langle B\rangle(t)-\overline{\sigma}^2 t}U(x(t))\right] \le K_1. \tag{21}$$

In addition, we note

$$|x|^{\beta} = \left(\sum_{i=1}^{n}x_i^2\right)^{\beta/2} \le n^{\beta/2}\max_{1\le i\le n}x_i^{\beta} \le n^{\beta/2}U(x), \tag{22}$$

so

$$\limsup_{t\longrightarrow\infty}\hat{\mathbb{E}}\left[e^{\langle B\rangle(t)-\overline{\sigma}^2 t}|x|^{\beta}\right] \le K_0, \tag{23}$$

$\forall\delta > 0$, let $C_0 = (K_0/\delta)^{1/\beta}$, then

$$v\left(\exp\left(\frac{\langle B\rangle(t)-\overline{\sigma}^2 t}{\beta}\right)|x| > C_0\right) \le \frac{\hat{\mathbb{E}}\left[\exp(\langle B\rangle(t)-\overline{\sigma}^2 t)|x|^{\beta}\right]}{C_0^{\beta}} \le \frac{K_0}{C_0^{\beta}} = \delta. \tag{24}$$

Hence,

$$\limsup_{t\longrightarrow\infty}V\left(e^{(\langle B\rangle(t)-\overline{\sigma}^2 t)/\beta}|x| \le C_0\right) \ge 1-\delta. \tag{25}$$

Theorem 3. *Suppose the (A) is true, and there exists $K(K>0)$ is independent of $\{x(s): s\in[-\tau, 0]\}$, then*

$$\limsup_{T\longrightarrow\infty}\frac{-1}{T}\widehat{\mathbb{E}}\left[\int_0^T -|x|^2\mathrm{d}\langle B\rangle(s)\right]\le K\overline{\sigma}^2. \tag{26}$$

Proof. Write (7) as $g(x,a,b,\sigma)=g_1(x,a,b,\sigma)-|x|^2$, where

$$\begin{aligned}g_1(x,a,b,\sigma) &:= \sum_{i=1}^n 0.5\left(x^{0.5}-1\right)b_i+\sum_{i=1}^n\sum_{j=1}^n\frac{na_{ij}^2}{16}\left(x^{0.5}-1\right)^2\\ &\quad -0.125\sum_{i=1}^n\sigma_{ii}^2x_i^{2.5}+|x|^2\left(2+0.25|\sigma|^2\right),\end{aligned} \tag{27}$$

then $g(x,a,b,\sigma)\le K-|x|^2$, where $K:=\max_{x\in R_+^n}g_1(x)<\infty$. Taking expectation from 0 to $\tau_k\wedge T$ on both sides of equation (6), we have

$$\begin{aligned}0&\le\widehat{\mathbb{E}}\left[\int_{-\tau}^0|x|^2\mathrm{d}\langle B\rangle(s)\right]+U(x_0)\\ &\quad+\widehat{\mathbb{E}}\left[\int_0^{\tau_k\wedge T}\left(K-|x|^2\right)\mathrm{d}\langle B\rangle(s)\right]\\ &\le\overline{\sigma}^2\int_{-\tau}^0\widehat{\mathbb{E}}\left[|x|^2\right]\mathrm{d}s+U(x_0)+K\overline{\sigma}^2\widehat{\mathbb{E}}[T\wedge\tau_k]\\ &\quad+\widehat{\mathbb{E}}\left[\int_0^{T\wedge\tau_k}-|x|^2\mathrm{d}\langle B\rangle(s)\right].\end{aligned} \tag{28}$$

Letting $k\longrightarrow\infty$ yields

$$-\widehat{\mathbb{E}}\left[\int_0^T -|x|^2\mathrm{d}\langle B\rangle(s)\right]\le\overline{\sigma}^2\int_{-\tau}^0\widehat{\mathbb{E}}\left[|x|^2\right]\mathrm{d}s+U(x_0)+K\overline{\sigma}^2T. \tag{29}$$

Therefore, setting $T\longrightarrow\infty$,

$$\limsup_{T\longrightarrow\infty}\frac{-1}{T}\widehat{\mathbb{E}}\left[\int_0^T -|x|^2\mathrm{d}\langle B\rangle(s)\right]\le K\overline{\sigma}^2. \tag{30}$$

4. Asymptotic Moment Estimations

Theorem 4. *If condition (A) is true, then* $\forall\ \{x(s): s\in[-\tau,0]\}$, *$x(t)$ in (2) satisfies*

$$\limsup_{t\longrightarrow\infty}\frac{1}{t}\widehat{\mathbb{E}}\left[\log\left(\frac{|x(t)|}{\sqrt{n}}\right)+\frac{\widehat{\sigma}^2}{4n}\int_0^t|x(s)|^2\mathrm{d}\langle B\rangle(s)\right]\le\overline{\sigma}^2K, \tag{31}$$

where $\widehat{\sigma}=\min_{1\le i\le n}\sigma_{ii}$.

Proof. Let $\widetilde{V}(x)=\sum_{i=1}^n x_i(t)$ for $x\in R_+^n$, then by G-Itô's lemma of Reference [13], we have

$$\begin{aligned}\log(\widetilde{V}(x)) &= C_0+\int_0^t\frac{x^T(s)}{V(x(s))}(b+Ax(s-\tau))\mathrm{d}\langle B\rangle(s)\\ &\quad+\int_0^t\frac{x^T(s)\sigma x(s)}{\widetilde{V}(x(s))}\mathrm{d}B(s)-\int_0^t\frac{\left|x^T(s)\sigma x(s)\right|^2}{2\widetilde{V}^2(x)}\mathrm{d}\langle B\rangle(s),\end{aligned} \tag{32}$$

where $C_0=\log(\tilde{V}(x(0)))$. Noting that

$$\left\langle\int_0^t\frac{x^T\sigma x}{\widetilde{V}(x)}\mathrm{d}B(s),\left|\int_0^t\frac{\left|x^T\sigma x\right|^2}{\widetilde{V}^2(x)}\right|\mathrm{d}\langle B\rangle(s)\right\rangle=\int_0^t\frac{\left|x^T\sigma x\right|^2}{\widetilde{V}^2(x)}\mathrm{d}\langle B\rangle(s), \tag{33}$$

$\forall\varepsilon\in(0,1/2)$, from Lemma 3.1 in reference [19], for any integer $k\ge1$, we have

$$V\left(\sup_{0\le t\le k}\left[\int_0^t\frac{x^T\sigma x}{\widetilde{V}(x)}\mathrm{d}B(s)-\frac{\varepsilon}{2}\int_0^t\frac{\left|x^T\sigma x\right|^2}{\widetilde{V}^2(x)}\mathrm{d}\langle B\rangle(s)\right]>\frac{2}{\varepsilon}\ln k\right)\le\frac{1}{k^2}, \tag{34}$$

so

$$\sum_{k=1}^\infty V\left(\sup_{0\le t\le k}\left[\int_0^t\frac{x^T\sigma x}{\widetilde{V}(x)}\mathrm{d}B(s)-\frac{\varepsilon}{2}\int_0^t\frac{\left|x^T\sigma x\right|^2}{\widetilde{V}^2(x)}\mathrm{d}\langle B\rangle(s)\right]>\frac{2}{\varepsilon}\ln k\right)<\infty, \tag{35}$$

applying Lemma 2 in [15], we know for all but finitely many k,

$$\sup_{0\le t\le k}\left[\int_0^t\frac{x^T\sigma x}{\widetilde{V}(x)}\mathrm{d}B(s)-\frac{\varepsilon}{2}\int_0^t\frac{\left|x^T\sigma x\right|^2}{\widetilde{V}^2(x)}\mathrm{d}\langle B\rangle(s)\right]\le\frac{\ln k^2}{\varepsilon}, \tag{36}$$

quasi-surely true, i.e., $\exists\Omega_i\subset\Omega$ $(v(\Omega i)=1)$ s.t. $\forall\omega\in\Omega_i$ and $k_i=k_i(\omega)$ s.t.

$$\int_0^t\frac{x^T(s)\sigma x}{\widetilde{V}(x)}\mathrm{d}B(s)-\frac{\varepsilon}{2}\int_0^t\frac{\left|x^T\sigma x\right|^2}{\widetilde{V}^2(x)}d\langle B\rangle(s)\le\frac{\ln k^2}{\varepsilon},\quad 0\le t\le k, \tag{37}$$

$k\ge k_i(\omega)$. From equation (32) and inequality (37),

$$\begin{aligned}\log(\widetilde{V}(x)) &\le C_0+\frac{\ln k^2}{\varepsilon}+\int_0^t\Big[\sqrt{n}\,(|x(s-\tau)|\|A\|+|b|)\\ &\quad-\widehat{\sigma}^2|x|^2\frac{(1-\varepsilon)}{2n}\Big]\mathrm{d}\langle B\rangle(s),\end{aligned} \tag{38}$$

$t\in[0,\ k_i(\omega)]$, $k\ge k_i(\omega)$, in other words,

$$\begin{aligned}&\log(\widetilde{V}(x))+\widehat{\sigma}^2\frac{(1-2\varepsilon)}{4n}\int_0^t|x|^2d\langle B\rangle(s)\\ &\le C_0+\frac{\ln k^2}{\varepsilon}+\int_0^t\left[\sqrt{n}\,(|x(s-\tau)|\|A\|+|b|)-|x|^2\frac{\widehat{\sigma}^2}{4n}\right]d\langle B\rangle(s),\end{aligned} \tag{39}$$

where $\widehat{\sigma}=\min\sigma_{ii}\ (i\in[1,n])$. Taking G-expectation $\widehat{\mathbb{E}}$ for (39), and then $\forall\omega\in\cap_{i=1}^n\Omega_i$, from (39), we get

$$\widehat{\mathbb{E}}\left[\widehat{\sigma}^2\frac{(1-2\varepsilon)}{4n}\int_0^t|x|^2\mathrm{d}\langle B\rangle(s)+\log(\widetilde{V}(x))\right]$$
$$\le\frac{\ln k^2}{\varepsilon}+\overline{\sigma}^2\widehat{\mathbb{E}}\left[\int_0^t(|x(s-\tau)|\|A\|+|b|)\sqrt{n}-\frac{\widehat{\sigma}^2}{4n}|x|^2\mathrm{d}s\right]+C_0$$
$$\le C_0+\frac{\ln k^2}{\varepsilon}+\sqrt{n}\|A\|\overline{\sigma}^2\widehat{\mathbb{E}}\left[\int_{-\tau}^0|x|\mathrm{d}s\right]$$
$$+\overline{\sigma}^2\widehat{\mathbb{E}}\left[\int_0^t\sqrt{n}\,(|b|+\|A\||x|)-\frac{\widehat{\sigma}^2}{4n}|x|^2\mathrm{d}s\right]$$
$$\le C_0+\frac{2\ln k}{\varepsilon}+\sqrt{n}\|A\|\overline{\sigma}^2\widehat{\mathbb{E}}\left[\int_{-\tau}^0|x|\mathrm{d}s\right]+\overline{\sigma}^2Kt, \tag{40}$$

where $\sqrt{n}(\|A\||x|+|b|)-(\widehat{\sigma}^2/4n)|x(s)|^2\le K$. Set $\max\{k_i(\omega), i\in[1,n]\}=k_0(\omega)$, then $\forall\omega\in\cap_{i=1}^n\Omega_i$, $t\in[k-1,k]$, $k\ge k_0(\omega)$, it gets from (40):

$$\limsup_{t\longrightarrow\infty}\frac{1}{t}\widehat{\mathbb{E}}\left[\log(\widetilde{V}(x))+\frac{\widehat{\sigma}^2(1-2\varepsilon)}{4n}\int_0^t|x|^2d\langle B\rangle(s)\right]\le\overline{\sigma}^2K. \tag{41}$$

Letting ε tend to zero and noting that $|x|\le\sqrt{n}V(x)$ yield

$$\limsup_{t\longrightarrow\infty}\frac{1}{t}\widehat{\mathbb{E}}\left[\log\left(\frac{|x(t)|}{\sqrt{n}}\right)+\frac{\widehat{\sigma}^2}{4n}\int_0^t|x(s)|^2d\langle B\rangle(s)\right]\le\overline{\sigma}^2K. \tag{42}$$

The proof is complete.

Data Availability

No data were used to support this study.

Conflicts of Interest

The authors declare that they have no conflicts of interest to this work.

Acknowledgments

This research was supported by the NSF-China (nos. 11761028 and 11501009), NSF-Anhui Province (1508085 JGD10), HTIT and RTFS-Yunnan Province, and Honghe University (nos. 2015HB061, 2014HB0204, and 2018JS480).

References

[1] A. J. Lotka, *Elements of Physical Biology*, William and Wilkins, Baltimore, MD, USA, 1925.
[2] V. Volterra, "Variazioni e fluttuazioni del numero dindividui in specie d'animani conviventi," *Mem. Acad. Lincei*, vol. 2, pp. 31–113, 1926.
[3] Y. Lou, S. Martínez, and P. Poláčik, "Loops and branches of coexistence states in a Lotka-Volterra competition model," *Journal of Differential Equations*, vol. 230, no. 2, pp. 720–742, 2006.
[4] Y. Zhang and M. Wang, "Bifurcation of Lotka-Volterra competition model with nonlinear boundary conditions," *Applied Mathematics Letters*, vol. 38, pp. 52–56, 2014.
[5] X. Mao, G. Marion, and E. Renshaw, "Environmental Brownian noise suppresses explosions in population dynamics," *Stochastic Processes and Their Applications*, vol. 97, no. 1, pp. 95–110, 2002.
[6] X. Mao, S. Sabanis, and E. Renshaw, "Asymptotic behaviour of the stochastic Lotka-Volterra model," *Journal of Mathematical Analysis and Applications*, vol. 287, no. 1, pp. 141–156, 2003.
[7] A. Hastings, "Global stability in Lotka-Volterra systems with diffusion," *Journal of Mathematical Biology*, vol. 6, no. 2, pp. 163–168, 1978.
[8] N. H. Du and V. H. Sam, "Dynamics of a stochastic Lotka-Volterra model perturbed by white noise," *Journal of Mathematical Analysis and Applications*, vol. 324, no. 1, pp. 82–97, 2006.
[9] A. Bahar and X. Mao, "Stochastic delay Lotka-Volterra model," *Journal of Mathematical Analysis and Applications*, vol. 292, no. 2, pp. 364–380, 2004.
[10] F. Wu and Y. Xu, "Stochastic Lotka-Volterra population dynamics with infinite delay," *SIAM Journal on Applied Mathematics*, vol. 70, no. 3, pp. 641–657, 2009.
[11] Y. Huang, Q. Liu, and Y. Liu, "Global asymptotic stability of a general stochastic Lotka-Volterra system with delays," *Applied Mathematics Letters*, vol. 26, no. 1, pp. 175–178, 2013.
[12] S. Peng, "*G*-expectation, *G*-brownian motion and related stochastic calculus of Itô type," in *Stochastic Analysis and Applications, Abel Symp. 2*, F. E. Benth, G. Di Nunno, T. Lindstrøm et al., Eds., pp. 541–567, Springer, Berlin, Germany, 2007.
[13] S. Peng, "Nonlinear expectations and stochastic calculus under uncertainty-with robust central limit theorem and *G*-Brownian motion," 2010, https://arxiv.org/abs/1002.4546.
[14] S. Peng, "Backward stochastic differential equation, nonlinear expectation and their applications," in *Proceedings of the International Congress of Mathematicians*, World Scientific, Singapore, pp. 393–432, 2010.
[15] Z. Chen, "Strong laws of large numbers for sub-linear expectations," *Science China Mathematics*, vol. 59, no. 5, pp. 945–954, 2016.
[16] L. Denis, M. Hu, and S. Peng, "Function spaces and capacity related to a sublinear expectation: application to *G*-brownian motion paths," *Potential Analysis*, vol. 34, no. 2, pp. 139–161, 2011.
[17] H. M. Soner, N. Touzi, and J. Zhang, "Martingale representation theorem for the *G*-expectation," *Stochastic Processes and Their Applications*, vol. 121, no. 2, pp. 265–287, 2011.
[18] F. Gao, "Pathwise properties and homeomorphic flows for stochastic differential equations driven by *G*-brownian motion," *Stochastic Processes and Their Applications*, vol. 119, pp. 3356–3382, 2009.
[19] D. Zhang and Z. Chen, "Exponential stability for stochastic differential equation driven by *G*-brownian motion," *Applied Mathematics Letters*, vol. 25, no. 11, pp. 1906–1910, 2012.
[20] W. Yu, Y. Yong, G. Guan, Y. Huang, W. Su, and C. Cui, "Valuing guaranteed minimum death benefits by cosine series expansion," *Mathematics*, vol. 7, no. 9, p. 835, 2019.
[21] Z. Zhang, Y. Yong, and W. Yu, "Valuing equity-linked death benefits in general exponential Lévy models," *Journal of Computational and Applied Mathematics*, vol. 365, Article ID 112377, 2020.
[22] W. Yu, F. Wang, Y. Huang, and H. Liu, "Social Optimal mean field control problem for population growth model," *Asian Journal of Control*, vol. 21, 2019.

Hindawi
Mathematical Problems in Engineering
Volume 2020, Article ID 6282869, 12 pages
https://doi.org/10.1155/2020/6282869

Research Article

A Lévy Risk Model with Ratcheting Dividend Strategy and Historic High-Related Stopping

Aili Zhang[1] and Zhang Liu[2,3]

[1]School of Statistics and Mathematics, Nanjing Audit University, Nanjing 211815, China
[2]School of Computer and Information Engineering, Jiangxi Agricultural University, Nanchang 330045, China
[3]School of Mathematics and Statistics, Wuhan University, Wuhan 430072, China

Correspondence should be addressed to Zhang Liu; liuzhang1006@163.com

Received 15 January 2020; Accepted 14 February 2020; Published 26 March 2020

Guest Editor: Wenguang Yu

This paper focuses on the De Finetti's dividend problem for the spectrally negative Lévy risk process, where the dividend is deducted from the surplus process according to the racheting dividend strategy which was firstly introduced in Albrecher et al. (2018). A major feature of the racheting strategy lies in which the dividend rate never decreases. Unlike the conventional studies, the closed form expression for the expected, accumulated, and discounted dividend payments until the draw-down time (rather than the ruin time) is obtained in terms of the scale functions corresponding to the underlying Lévy process. The optimal barrier for the ratcheting strategy is also studied, where the dividend rate can be increased. Finally, two special cases, where the scale functions are explicitly known, i.e., the Brownian motion with drift and the compound Poisson model, are considered to illustrate the main result.

1. Introduction

During the first half of the 20th century, the actuaries concentrated on assessing the stability of an insurance company via the probability of ruin. In the seminal paper of De Finetti [1], the drawbacks of this approach was pointed out and an alternative approach was proposed, say, the approach of the expected discounted accumulated dividend payments, laying the foundations of De Finetti's dividend problem which has become a flourishing research topic now. In addition, the classical work of Miller and Modigliani [2] also claimed that the value of the firm can be equated with the discounted accumulated value of the dividend payments up to the infinite horizon. Roughly speaking, the classical De Finetti's dividend problem is to optimize the time and amount of dividends paid to the shareholders under certain criterion. In [1], where the surplus dynamics followed a discrete time random walk, De Finetti showed that a barrier dividend strategy is the optimal dividend strategy because it produces the maximum firm value of the company. From then on, the optimality of the barrier dividend strategy has been proved for various risk models under suitable assumptions, see, for instance, Loeffen [3], Loeffen and Renaud [4], Yin and Wang [5], Yuen and Yin [6], Wang and Zhou [7], Yu et al. [8], and the references therein.

Once the barrier dividend strategy with barrier b is adopted by the controller of the company, all overflow part of the surplus above b shall be paid out as dividends, i.e., the rate dividends paid out can be infinite. However, this requires that the controller has unlimited ability to control, which is often obviously not feasible nor realistic in real-life implementation. In addition, although the barrier dividend strategy commonly turns out to be the optimal one in many existing works, its optimality can easily vanish due to a different choice of the parameters of the underlying process. For example, it is seen from Loeffen [3] that the optimality of the barrier dividend strategy may fail when the assumption of a completely monotone density of the underlying process fails. Furthermore, a risk process imposed with a barrier dividend strategy has an ultimate ruin probability 1 (see, Gerber and Shiu [9]), a scenario far from being acceptable. Therefore, it is reasonable to restrict ourselves in those dividend strategies that modify the underlying surplus process moderately, or, in those dividend strategies with bounded dividend rates.

A known subclass of dividend strategies with bounded dividend rates is the threshold dividend strategy; dividends are paid out at a constant rate whenever the surplus is above the dividend threshold (say, b), whereas no dividend is paid when the surplus is below b. To the best of our knowledge, the threshold dividend strategy, which is also known as the refracting dividend strategy, was firstly introduced by Jeanblanc-Picqué and Shiryaev [10] and Asmussen and Taksar [11] for the diffusion process, and by Gerber and Shiu [12], for the Cremér–Lundberg risk process. Recently, the periodic threshold dividend strategy under a perturbed compound Poisson model was studied in Peng et al. [13] and Liu et al. [14]. For original ideas and analogues of the threshold dividend strategy, the readers are referred to Gerber and Shiu [9] and Avanzi et al. [15]. It needs to be mentioned that, for De Finetti's dividend problems, where the dividend strategies are bounded from above in the dividend rates, the optimal dividend strategy yielding the largest expected discounted accumulated dividends is in many scenarios the threshold dividend strategy, see Jeanblanc-Picqué and Shiryaev [10], Asmussen and Taksar [11], Gerber and Shiu [12], Avanzi et al. [15], and the references therein.

Note that the rate of paying dividends obeying a threshold dividend strategy may decrease to 0 once the surplus drops from levels above b to levels below b. While, in practice, the practitioners are unwilling to accept a reduction in the rate of the dividend payment stream because a decrease in the rate of paying dividends may lead to negative psychological impacts on shareholders and the firm value of the company. Taking into account these considerations, Albrecher et al. [16] introduced a dividend strategy called ratcheting strategy, where the dividend rate would never decrease over time, but would increase once the underlying process hits some b and stay at this higher level until the time of ruin. The authors derived the corresponding formulas for the resulting expected accumulated discounted dividend payments until ruin. We believe that the ratcheting strategy represents another subclass of constrained dividend strategies (other than the threshold dividend strategies) that is comparatively more acceptable in the community of practitioners.

However, one may not ignore the issue that the ratcheting dividend strategy inevitably increases the risk of bankruptcy compared to the threshold dividend strategy because the former entails larger amount of modification to the underlying process. To address this issue, in this paper the draw-down stopping (see (6) for its definition) will be introduced into the Lévy risk process with dividends deducted according to the ratcheting dividend strategy. In fact, the classical ruin time is a reduced version of the draw-down stopping, with the latter being more reserve involved and more efficient in assessing the stability of the insurance company taking on risks. In addition, one can expect positive surplus at the termination of the business if the draw-down stopping is adopted rather than the ruin time. Therefore, the draw-down stopping allows the insurer to achieve a balance between dividend distribution and solvency and hence represents a nice solution to the issue of large bankruptcy risk associated with the ratcheting dividend strategy.

Actually, as a remarkable progress in risk measurement and management, the draw-down time has recently gained a lot of attention in actuarial sciences and many ruin-based results were extended to draw-down versions. To name a few, Avram et al. [17] generalized the results of Albrecher and Thonhauser [18] by considering a linear draw-down stopping. Wang and Zhou [19] defined a draw-down reflected process which can be used to characterise the risk process with capital injections and solved several fluctuation identities. More recently, Wang and Zhou [20] introduced the concept of draw-down Parisian ruin time for a spectrally negative Lévy risk process and obtained the kth moment of the discounted total dividends paid according to the barrier dividend strategy until the draw-down Parisian ruin time, which generalized a result of Czarna and Palmowski [21]. In addition, Wang and Zhou [7] solved a general draw-down version of De Finetti's optimal dividend problem. Wang and Zhang [22] studied the optimal loss-carry-forward tax problem with the general draw-down stopping. For application of the draw-down time in risk theory, we are referred to Wang and Ming [23], Wang et al. [24], Chen et al. [25], Avram et al. [17], Ruan et al. [26], Yu et al. [27], and Zhang et al. [28].

In this paper, motivated by Albrecher et al. [16], Wang and Zhou [7], Wang and Zhou [20], and Wang and Zhang [22], we are to introduce the general draw-down time into the Lévy risk process with dividends deducted according to the racheting dividend strategy and to generalize the ruin-involved results of Albrecher et al. [16] to the general draw-down-based version. The expressions of the expected accumulated discounted dividend payments until the general draw-down time are obtained. The optimal surplus level where the dividend rate can be increased is also studied. All results are expressed in terms of the scale functions. Finally, two special cases where the scale functions are explicitly known, i.e., the Brownian motion with drift and the compound Poisson model with exponential jumps, are considered. The contribution of this paper lies in which our results shall serve as a nice solution to the concern of large bankruptcy risk associated with the ratcheting dividend strategy, hence achieve a balance between dividend distribution and solvency. It should be mentioned that the results in Albrecher et al. [16] can be recovered when the draw-down functions are specified to be 0.

The rest of this paper is organized as follows. In Section 2, we review the spectrally negative Lévy processes, the associated scale functions, the draw-down time, and existing results of the exit problems for spectrally negative Lévy processes involving the general draw-down time. In Section 3, we derive the formula for the expected accumulated discounted dividend payments until draw-down time according the ratcheting dividend strategy and obtain a criterion for the optimal ratcheting barrier. Section 4 studies two special spectrally negative Lévy processes and obtains the corresponding explicit expressions for the expected discounted dividend payments.

2. Problem Formulation

Let $Y = \{Y_t; t \geq 0\}$ be a spectrally negative Lévy process defined on a filtered probability space $(\Omega, \{\mathcal{F}_t; t \geq 0\}, \mathbb{P})$ with the natural filtration $\{\mathcal{F}_t; t \geq 0\}$. Denote by $\mathbb{P}_x$ the conditional probability given $Y_0 = x$ and by $\mathcal{E}_x$ the associated conditional expectation. For notational convenience, we write $\mathbb{P}$ and $\mathcal{E}$ in place of $\mathbb{P}_0$ and $\mathcal{E}_0$, respectively. In this paper, the surplus process in the absence of dividends is expressed by $Y = \{Y_t; t \geq 0\}$. We shall assume that the company will pay dividends to its shareholders according to the ratcheting strategy introduced by Albrecher et al. [16]. Roughly speaking, dividends are paid constantly at rate $c_1 \geq 0$, and in certain periods at an increased rate $c_1 + c_2$ with $c_2 > 0$. To characterise the modified surplus processes, we introduce

$$\begin{aligned} X_t &= Y_t - c_1 t, \\ \widetilde{X}_t &= Y_t - (c_1 + c_2)t, \end{aligned} \tag{1}$$

for all $t \geq 0$. It should be mentioned that they are still spectrally negative Lévy processes.

The Laplace exponent of X is defined by

$$\psi(\theta) := \log \mathcal{E}_x\left[e^{\theta(X_1 - x)}\right], \quad \theta \geq 0, \tag{2}$$

which is strictly convex and infinitely differentiable.

Scale functions play a key role in analyzing spectrally negative Lévy processes. We now recall the definitions of the scale functions $W_q(x)$ and $Z_q(x)$ corresponding to X. For each $q \geq 0$, W_q: $[0, \infty) \longrightarrow [0, \infty)$ is the unique strictly increasing and continuous function with the Laplace transform:

$$\int_0^\infty e^{-\lambda x} \mathbb{W}_q(x) \mathrm{d}x = \frac{1}{\psi(\lambda) - q}, \quad \lambda > \Phi_q, \tag{3}$$

where Φ_q is the largest solution of the equation $\psi(\lambda) = q$ (there are at most two). For convenience, we extend the domain of $W_q(x)$ to the whole real line by setting $W_q(x) = 0$ for $x < 0$. Associated to the function W_q, the function Z_q is defined by

$$Z_q(x) = 1 + q\int_0^x \mathbb{W}_q(z) \mathrm{d}z, \quad x \geq 0. \tag{4}$$

Throughout the paper, we assume $W_q(x)$ is differentiable. It is known that when X has sample paths of unbounded variation or when X has sample paths of bounded variation and the Lévy measure has no atoms, the scale function $W_q(x)$ is continuously differentiable over $(0, \infty)$. The interested readers are referred Kuznetsov et al. [29] for more detailed discussions on the smoothness of scale functions. In addition, we define $\mathbb{W}_q(x)$ and $\mathbb{Z}_q(x)$ analogously for $\{\widetilde{X}_t; t \geq 0\}$.

Let $\overline{X}_t = \sup_{0 \leq s \leq t} X_s$ denote the running maximum process for X. A measurable function ξ defined on $\mathbb{R}$ is called a general draw-down function if $\xi(x) < x$ for all $x \in \mathbb{R}$. In the following, we define the first up-crossing time of the given process X for a fixed $b \geq 0$ and the general draw-down time of X with the draw-down function ξ, respectively, as

$$\tau_b^+ := \inf\{t \geq 0, X_t > b\}, \tag{5}$$

$$\tau_\xi := \inf\{t \geq 0, X_t < \xi(\overline{X}_t)\}, \tag{6}$$

with the convention that $\inf \varnothing = \infty$.

Remark 1. When $\xi \equiv 0$, τ_ξ reduces to the classical ruin time. When the draw-down function is linear, i.e., $\xi(\overline{X}_t) = k\overline{X}_t - d$ for $k < 1$, $X_t < \xi(\overline{X}_t)$ is identical to $k\overline{X}_t - X_t > d$; hence, τ_ξ refers for the first time the surplus process X_t drops more than d units below $k\overline{X}_t$. Examples of nonlinear forms of ξ can be found in Remark 2 of Avram et al. [17].

Remark 2. By definition, the draw-down time is the first time when a drop of the surplus process from the running maximum exceeds a certain surplus-related level. This nature of the draw-down time assures its feasibility of applying it in measuring and managing extreme risks. In practice, people can select the draw-down functions according to management needs and attitudes toward risks, for example, risk-averse insurer may choose larger draw-down function, vice versa. In addition, one can adjust the draw-down function so that the surplus remains positive at the draw-down time with positive probability, see Wang and Zhang [22] and Wang and Zhou [7]. The insurer may deem $\xi(\overline{X}_t)$ as a warning line (over time) for taking actions to avoid even worse situations, see Wang et al. [24]. Moreover, the draw-down function can also be chosen to be negative valued, in this case the draw-down time is also called the absolute ruin time, see Wang and Zhang [22] and Landriault et al. [30].

The following solution for the draw-down-based two-side exit problem is found in Proposition 3.1 of Li et al. [31] and Wang and Zhou [7], which will be used later on.

Lemma 1 (two-side exit problem involving draw-down). *For $b \in [0, \infty)$ and $x \in [0, b)$, we have*

$$\mathbb{E}_x\left(e^{-q\tau_b^+} 1_{\{\tau_b^+ < \tau_\xi\}}\right) = \exp\left(-\int_x^b \frac{\mathbb{W}_q'(\overline{\xi}(z))}{\mathbb{W}_q(\overline{\xi}(z))} \mathrm{d}z\right), \tag{7}$$

$$\begin{aligned} \mathbb{E}_x\left(e^{-q\tau_\xi} 1_{\{\tau_\xi < \tau_b^+\}}\right) = \int_x^b &\exp\left(-\int_x^z \frac{\mathbb{W}_q'(\overline{\xi}(w))}{\mathbb{W}_q(\overline{\xi}(w))} \mathrm{d}w\right) \\ &\times \left(\frac{\mathbb{W}_q'(\overline{\xi}(z))}{\mathbb{W}_q(\overline{\xi}(z))} Z_q(\overline{\xi}(z)) \right. \\ &\left. - q\mathbb{W}_q(\overline{\xi}(z))\right) \mathrm{d}z, \end{aligned} \tag{8}$$

where $\overline{\xi}(z) := z - \xi(z)$.

Remark 3. Letting $b \longrightarrow \infty$ in (8), we can obtain the Laplace transform of the general draw-down time of the Lévy risk process as follows:

$$\mathbb{E}_x\left(e^{-q\tau_\xi}\right) = \int_x^\infty \exp\left(-\int_x^z \frac{\mathbb{W}_q'(\bar{\xi}(w))}{\mathbb{W}_q(\bar{\xi}(w))}\mathrm{d}w\right) \cdot \left(\frac{\mathbb{W}_q'(\bar{\xi}(z))}{\mathbb{W}_q(\bar{\xi}(z))} Z_q(\bar{\xi}(z)) - q\mathbb{W}_q(\bar{\xi}(z))\right)\mathrm{d}z. \tag{9}$$

3. Problem Presentation and the Main Results

In this section, we consider the racheting dividend strategy with a general draw-down time and obtain our main results. Under the racheting strategy with barrier level b, dividends are paid at a fixed constant rate $c_1 \geq 0$ until the first time the surplus process hits a barrier b, and from then the dividend rate is increased (racheted) to $c_1 + c_2$ for a fixed constant $c_2 > 0$. The cumulative dividends paid out up to time t is represented by $D_t = \int_0^t (c_1 + c_2 1_{\{M_s \geq b\}})\mathrm{d}s$, where $M_t := \sup_{0\leq s\leq t} X_s$. The surplus process after the deduction of dividends is given by

$$U_t = Y_t - D_t = X_t - \int_0^t c_2 1_{\{M_s \geq b\}}\,\mathrm{d}s. \tag{10}$$

In order to balance the dividend optimization and solvency (see also paragraph 5 of Section 1), we consider the value function of the dividend strategy by the expected value of the accumulated discounted dividend payments until the draw-down time, instead of the ruin time. The draw-down time when the dividend payments are taken into account is defined by

$$\tau_\xi^u := \inf\{t \geq 0, U_t < \xi(\overline{U}_t)\}, \tag{11}$$

where $\bar{U}_t = \sup_{0\leq s\leq t} U_s$. The expected value of the accumulated discounted dividend payments until the draw-down time under the ratcheting strategy can be expressed by

$$V_\xi(x) = \mathbb{E}_x\left(\int_0^{\tau_\xi^u} e^{-qt}\left(c_1 + c_2 1_{\{M_t \geq b\}}\right)\mathrm{d}t\right), \tag{12}$$

where q is the force of interest for valuation. In this paper, our goal is to obtain the expression of the expected value of the accumulated discounted dividend payments until the draw-down time under the ratcheting strategy and find the optimal level b for the fixed c_1 and c_2.

The following Theorem 1 gives the expression of V_ξ in terms of the scale functions of X and $\widetilde{X}$.

Theorem 1. *The expected value of the accumulated discounted dividend payments until the draw-down time under the ratcheting strategy for the modified surplus process is given as follows.*

(1) For $x \in [b, \infty)$, we have

$$V_\xi(x) = \frac{c_1 + c_2}{q}\left[1 - \int_x^\infty \exp\left(-\int_x^z \frac{\mathbb{W}_q'(\bar{\xi}(w))}{\mathbb{W}_q(\bar{\xi}(w))}\mathrm{d}w\right) \times \left(\frac{\mathbb{W}_q'(\bar{\xi}(z))}{\mathbb{W}_q(\bar{\xi}(z))}\mathbb{Z}_q(\bar{\xi}(z)) - q\mathbb{W}_q(\bar{\xi}(z))\right)\mathrm{d}z\right]. \tag{13}$$

(2) For $x \in [0, b)$, we have

$$\begin{aligned} V_\xi(x) = {} & \frac{c_1}{q} - \frac{c_1}{q}\int_x^b \exp\left(-\int_x^z \frac{\mathbb{W}_q'(\bar{\xi}(w))}{\mathbb{W}_q(\bar{\xi}(w))}\mathrm{d}w\right) \cdot \left(\frac{\mathbb{W}_q'(\bar{\xi}(z))}{\mathbb{W}_q(\bar{\xi}(z))}Z_q(\bar{\xi}(z)) - q\mathbb{W}_q(\bar{\xi}(z))\right)\mathrm{d}z \\ & + \exp\left(-\int_x^b \frac{\mathbb{W}_q'(\bar{\xi}(z))}{\mathbb{W}_q(\bar{\xi}(z))}\mathrm{d}z\right)\left(V_\xi(b) - \frac{c_1}{q}\right). \end{aligned} \tag{14}$$

Proof.

(1) For $x \in [b, \infty)$, the dividends are paid out at the rate $c_1 + c_2$ from the beginning. In this case, the modified surplus process is given by $U_t = Y_t - \int_0^t (c_1 + c_2)\mathrm{d}s = \widetilde{X}_t$, and

$$\begin{aligned} V_\xi(x) &= (c_1 + c_2)\mathbb{E}_x\left(\int_0^{\tau_\xi^u} e^{-qt}\mathrm{d}t\right) \\ &= \frac{c_1 + c_2}{q}\mathbb{E}_x\left(1 - e^{-q\widetilde{\tau}_\xi}\right), \end{aligned} \tag{15}$$

where $\widetilde{\tau}_\xi := \inf\left\{t \geq 0, \widetilde{X}_t < \xi(\overline{\widetilde{X}}_t)\right\}$. Under the framework of $\widetilde{X}$, using Remark 3, we can get (13) immediately.

(2) For $x \in [0, b)$, we should consider whether the process will reach b before the first time of dropping across the level of the draw-down function of the running maximum. If the process touches the barrier b first, i.e., $\tau_b^+ < \tau_\xi^u$, the strong Markov property will be used at that point in time τ_b^+, and from which the dividend rate is ratcheted to $c_1 + c_2$. Hence,

$$\begin{aligned} V_\xi(x) = {} & c_1\mathbb{E}_x\left(1_{\{\tau_\xi^u < \tau_b^+\}}\int_0^{\tau_\xi^u} e^{-qt}\mathrm{d}t\right) \\ & + \left[c_1\mathbb{E}_x\left(1_{\{\tau_b^+ < \tau_\xi^u\}}\int_0^{\tau_b^+} e^{-qt}\mathrm{d}t\right) + \mathbb{E}_x\left(e^{-q\tau_b^+}1_{\{\tau_b^+ < \tau_\xi^u\}}\right)V_\xi(b)\right] \\ = {} & \frac{c_1}{q} - \frac{c_1}{q}\mathbb{E}_x\left(e^{-q\tau_\xi^u}1_{\{\tau_\xi^u < \tau_b^+\}}\right) - \left[\frac{c_1}{q}\mathbb{E}_x\left(e^{-q\tau_b^+}1_{\{\tau_b^+ < \tau_\xi^u\}}\right) - \mathbb{E}_x\left(e^{-q\tau_b^+}1_{\{\tau_b^+ < \tau_\xi^u\}}\right)V_\xi(b)\right] \\ = {} & \frac{c_1}{q} - \frac{c_1}{q}\mathbb{E}_x\left(e^{-q\tau_\xi}1_{\{\tau_\xi < \tau_b^+\}}\right) - \mathbb{E}_x\left(e^{-q\tau_b^+}1_{\{\tau_b^+ < \tau_\xi\}}\right) \left(V_\xi(b) - \frac{c_1}{q}\right), \end{aligned} \tag{16}$$

where $V_\xi(b)$ is given by (13). According to the formulations of the two-side exit problem involving dawn-down time in Lemma 1, we can obtain (14). □

The following corollaries will present the expressions of $V_\xi(x)$ with $\xi(x) = kx - a$.

Corollary 1. *For $k < 1$ and $a > 0$, we have, for $x \in [b, \infty)$,*

$$V_{kx-a}(x) = \frac{c_1 + c_2}{q}\left(1 - \mathbb{Z}_q((1-k)x + a) + qk\left(\mathbb{W}_q((1-k)x + a)\right)^{1/(1-k)} \times \int_x^\infty \left(\mathbb{W}_q((1-k)z + a)\right)^{-k/(1-k)} \mathrm{d}z\right), \tag{17}$$

and for $x \in [0, b)$,

$$V_{kx-a}(x) = \frac{c_1}{q}\left(1 - Z_q((1-k)x + a) + Z_q((1-k)b + a)\left(\frac{\mathbb{W}_q((1-k)x + a)}{\mathbb{W}_q((1-k)b + a)}\right)^{1/(1-k)} + qk\left(\mathbb{W}_q((1-k)x + a)\right)^{1/(1-k)} \cdot \int_x^b \left(\mathbb{W}_q((1-k)z + a)\right)^{1/(1-k)} \mathrm{d}z\right) + \left(\frac{\mathbb{W}_q((1-k)x + a)}{\mathbb{W}_q((1-k)b + a)}\right)^{1/(1-k)}\left(V_{kx-a}(b) - \frac{c_1}{q}\right). \tag{18}$$

Corollary 2. *For $k = 1$ and $a > 0$, we have, for $x \in [b, \infty)$,*

$$V_\xi(x) = \frac{c_1 + c_2}{q}\left(1 - \mathbb{Z}_q(a) + q\frac{1}{\mathbb{W}_q'(a)}\right), \tag{19}$$

and for $x \in [0, b)$,

$$\begin{aligned} V_\xi(x) &= \frac{c_1}{q}\left(1 - Z_q(a) + q\frac{1}{\mathbb{W}_q'(a)}\right) \\ &\quad - \left[\frac{c_1}{q}\left(1 - Z_q(a) + q\frac{1}{\mathbb{W}_q'(a)}\right) - \frac{c_1 + c_2}{q}\left(1 - \mathbb{Z}_q(a) + q\frac{1}{\mathbb{W}_q'(a)}\right)\right] \\ &\quad \exp\left(-\frac{\mathbb{W}_q'(a)}{\mathbb{W}_q(a)}(b - x)\right). \end{aligned} \tag{20}$$

Remark 4. If $\xi(x) \equiv 0$, the draw-down time $\tau_\xi^u = \inf\{t \geq 0, U_t < 0\}$ is the classical ruin time of U_t, and (13) and (14) reduce to that of Theorem 2.1 of Albrecher et al. [16].

Denote the right-hand side of (13) and (14) by $V_\xi^+(x)$ and $V_\xi^-(x, b)$, respectively. For fixed $x \in [0, \infty)$, define a function $V_\xi(x, b)$ of b and the largest global maximum point b^* of $V_\xi(x, b)$ as

$$\begin{aligned} V_\xi(x, b) &:= V_\xi^+(x) 1_{[0,x]}(b) + V_\xi^-(x, b) 1_{(x,\infty)}(b), \\ b^* &:= \sup\left\{b_0 \geq 0 \mid V_\xi(x, b_0) \geq V_\xi(x, b), \forall b \geq 0\right\}. \end{aligned} \tag{21}$$

Hence, b^* is the optimal barrier level that maximizes the expectation of the accumulated discounted dividends until the draw-down time. For the purpose of simplification, we shall define some auxiliary functions as

$$\iota_\xi(x) = \frac{\mathbb{W}_q'(\overline{\xi}(x))}{\mathbb{W}_q(\overline{\xi}(x))} Z_q(\overline{\xi}(x)) - q\mathbb{W}_q(\overline{\xi}(x)), \tag{22}$$

$$\varrho_\xi(x) = \frac{\mathbb{W}_q'(\overline{\xi}(x))}{\mathbb{W}_q(\overline{\xi}(x))}. \tag{23}$$

Similarly,

$$\widetilde{\iota}_\xi(x) = \frac{\mathbb{W}_q'(\overline{\xi}(x))}{\mathbb{W}_q(\overline{\xi}(x))} \mathbb{Z}_q(\overline{\xi}(x)) - q\mathbb{W}_q(\overline{\xi}(x)), \tag{24}$$

$$\widetilde{\varrho}_\xi(x) = \frac{\mathbb{W}_q'(\overline{\xi}(x))}{\mathbb{W}_q(\overline{\xi}(x))}. \tag{25}$$

Proposition 1. *Let b^* be given by (21) with fixed c_1, $c_2 > 0$ and $x \geq 0$. If $b^* \in (x, \infty)$, then b^* must be solution of*

$$c_1\left[\iota_\xi(b) + \varrho_\xi(b)\left(\frac{q}{c_1}V_\xi(b) - 1\right)\right] = \left(c_1 + c_2\right)\left[\widetilde{\iota}_\xi(b) + \widetilde{\varrho}_\xi(b)\left(\frac{q}{c_1 + c_2}V_\xi(b) - 1\right)\right]. \tag{26}$$

Proof. For fixed $x \in [0, \infty)$, it is seen by (21) that $V_\xi(x, b)$ is flat over $[0, x]$, i.e., $V_\xi(x, b) \equiv V_\xi^+(x)$ for all $b \in [0, x]$; hence, the optimal threshold level $b^* \in [x, \infty]$.

If $b^* \in (x, \infty)$, then by (21), one knows that b^* must be a zero of the equation $(\partial/\partial b)V_{\xi}^{-}(x,b) = 0$, i.e.,

$$
\begin{aligned}
0 = \frac{\partial}{\partial b}V_{\xi}^{-}(x,b) &= \exp\left(-\int_x^b \frac{\mathbb{W}_q'(\overline{\xi}(w))}{\mathbb{W}_q(\overline{\xi}(w))}\mathrm{d}w\right) \\
&\cdot\Bigg[-\frac{c_1}{q}\left(\frac{\mathbb{W}_q'(\overline{\xi}(b))}{\mathbb{W}_q(\overline{\xi}(b))}Z_q(\overline{\xi}(b)) - q\mathbb{W}_q(\overline{\xi}(b))\right) - \frac{\mathbb{W}_q'(\overline{\xi}(b))}{\mathbb{W}_q(\overline{\xi}(b))}\left(V_{\xi}^{+}(b) - \frac{c_1}{q}\right) + \frac{c_1+c_2}{q}\left(\frac{\mathbb{W}_q'(\overline{\xi}(b))}{\mathbb{W}_q(\overline{\xi}(b))}\mathbb{Z}_q(\overline{\xi}(b)) - q\mathbb{W}_q(\overline{\xi}(b))\right) \\
&-\frac{c_1+c_2}{q}\frac{\mathbb{W}_q'(\overline{\xi}(b))}{\mathbb{W}_q(\overline{\xi}(b))}\int_b^{\infty}\exp\left(-\int_b^z \frac{\mathbb{W}_q'(\overline{\xi}(w))}{\mathbb{W}_q(\overline{\xi}(w))}\mathrm{d}w\right)\times\left(\frac{\mathbb{W}_q'(\overline{\xi}(z))}{\mathbb{W}_q(\overline{\xi}(z))}\mathbb{Z}_q(\overline{\xi}(z)) - q\mathbb{W}_q(\overline{\xi}(z))\right)\mathrm{d}z\Bigg] \\
&= \exp\left(-\int_x^b \varrho_{\xi}(w)\mathrm{d}w\right)\left[-\frac{c_1}{q}\iota_{\xi}(b) - \varrho_{\xi}(b)\left(V_{\xi}(b) - \frac{c_1}{q}\right) + \frac{c_1+c_2}{q}\overline{\iota}_{\xi}(b) + \frac{c_1+c_2}{q}\widetilde{\varrho}_{\xi}(b)\left(\frac{q}{c_1+c_2}V_{\xi}(b) - 1\right)\right].
\end{aligned}
\tag{27}
$$

The proof is complete.

The following proposition characterizes the optimal barrier level b from the view of smoothness. □

Proposition 2. *In the ratcheting dividend problem, for the fixed c_1, $c_2 > 0$, the optimal barrier $b^* \in (x, \infty)$ coincides with the one which makes the $V_{\xi}(x)$ continuously differentiable.*

Proof. For $x \in [0, b)$, we have

$$
\begin{aligned}
\frac{\partial}{\partial x}V_{\xi}(x) &= \frac{c_1}{q}\left(\frac{\mathbb{W}_q'(\overline{\xi}(x))}{\mathbb{W}_q(\overline{\xi}(x))}Z_q(\overline{\xi}(x)) - q\mathbb{W}_q(\overline{\xi}(x))\right) \\
&+ \exp\left(-\int_x^b \frac{\mathbb{W}_q'(\overline{\xi}(w))}{\mathbb{W}_q(\overline{\xi}(w))}\mathrm{d}w\right)\frac{\mathbb{W}_q'(\overline{\xi}(x))}{\mathbb{W}_q(\overline{\xi}(x))}\left(V_{\xi}(b) - \frac{c_1}{q}\right) - \frac{c_1}{q}\frac{\mathbb{W}_q'(\overline{\xi}(x))}{\mathbb{W}_q(\overline{\xi}(x))}\int_x^b \exp\left(-\int_x^z \frac{\mathbb{W}_q'(\overline{\xi}(w))}{\mathbb{W}_q(\overline{\xi}(w))}\mathrm{d}w\right) \\
&\times\left(\frac{\mathbb{W}_q'(\overline{\xi}(z))}{\mathbb{W}_q(\overline{\xi}(z))}Z_q(\overline{\xi}(z)) - q\mathbb{W}_q(\overline{\xi}(z))\right)\mathrm{d}z \\
&= \frac{c_1}{q}\iota_{\xi}(x) + \exp\left(-\int_x^b \varrho_{\xi}(x)\mathrm{d}w\right)\varrho_{\xi}(x)\left(V_{\xi}(b) - \frac{c_1}{q}\right) \\
&- \frac{c_1}{q}\varrho_{\xi}(x)\int_x^b \exp\left(-\int_x^z \varrho_{\xi}(w)\mathrm{d}w\right)\iota_{\xi}(z)\mathrm{d}z,
\end{aligned}
\tag{28}
$$

and for $x \in [b, \infty)$, we can obtain

$$
\begin{aligned}
\frac{\partial}{\partial x}V_{\xi}(x) &= -\frac{c_1+c_2}{q}\frac{\mathbb{W}_q'(\overline{\xi}(x))}{\mathbb{W}_q(\overline{\xi}(x))}\int_x^{\infty}\exp\left(-\int_x^z \frac{\mathbb{W}_q'(\overline{\xi}(w))}{\mathbb{W}_q(\overline{\xi}(w))}\mathrm{d}w\right)\times\left(\frac{\mathbb{W}_q'(\overline{\xi}(z))}{\mathbb{W}_q(\overline{\xi}(z))}\mathbb{Z}_q(\overline{\xi}(z)) - q\mathbb{W}_q(\overline{\xi}(z))\right)\mathrm{d}z \\
&+ \frac{c_1+c_2}{q}\left(\frac{\mathbb{W}_q'(\overline{\xi}(x))}{\mathbb{W}_q(\overline{\xi}(x))}\mathbb{Z}_q(\overline{\xi}(x)) - q\mathbb{W}_q(\overline{\xi}(x))\right) \\
&= -\frac{c_1+c_2}{q}\widetilde{\varrho}_{\xi}(x)\int_x^{\infty}\exp\left(-\int_x^z \widetilde{\varrho}_{\xi}(w)\mathrm{d}w\right)\overline{\iota}_{\xi}(z)\mathrm{d}z + \frac{c_1+c_2}{q}\overline{\iota}_{\xi}(x).
\end{aligned}
\tag{29}
$$

Letting $x \uparrow b$ in (28) and $x \downarrow b$ in (29), respectively, gives rise to

$$V_\xi'(b-) = \frac{c_1}{q}\imath_\xi(b) + \varrho_\xi(b)\left(V_\xi(b) - \frac{c_1}{q}\right), \tag{30}$$

$$V_\xi'(b+) = -\frac{c_1+c_2}{q}\widetilde{\varrho}_\xi(b)\int_b^\infty \exp\left(-\int_b^z \widetilde{\varrho}_\xi(w)\mathrm{d}w\right)\widetilde{\imath}_\xi(z)\mathrm{d}z + \frac{c_1+c_2}{q}\widetilde{\imath}_\xi(b). \tag{31}$$

In addition, applying the auxiliary functions, (13) can be expressed as

$$\int_b^\infty \exp\left(-\int_b^z \widetilde{\varrho}_\xi(w)\mathrm{d}w\right)\widetilde{\imath}_\xi(z)\mathrm{d}z = 1 - \frac{q}{c_1+c_2}V_\xi(b). \tag{32}$$

Substitute (32) into (31) and then combine the yielding equation with (30), one can find that $V_\xi'(b-) = V_\xi'(b+)$ coincides with (26). □

4. Special Cases

In this section, we shall examine two special cases of our model, i.e., the Brownian motion with drift and the compound Poison process. Explicit results of the expected accumulated discounted dividend payments until the general draw-down time are obtained.

Example 1. Let $Y_t = x + \mu t + \sigma B_t$, $t \geq 0$ with $\mu > 0$, $\sigma > 0$, and $\{B_t;\ t \geq 0\}$ being a standard Brownian motion. In this case, the scale functions of X_t and $\widetilde{X}_t$ are given, respectively, by

$$\begin{aligned} \mathbb{W}_q(x) &= \kappa\left(e^{\theta_1 x} - e^{\theta_2 x}\right), \\ \mathbb{W}_q(x) &= \widetilde{\kappa}\left(e^{\widetilde{\theta}_1 x} - e^{\widetilde{\theta}_2 x}\right), \end{aligned} \tag{33}$$

where

$$\begin{aligned} \kappa &= \left(\left(\mu - c_1\right)^2 + 2\sigma^2 q\right)^{-(1/2)}, \\ \theta_1 &= \frac{c_1 - \mu + \sqrt{\left(\mu - c_1\right)^2 + 2\sigma^2 q}}{\sigma^2}, \\ \theta_2 &= \frac{c_1 - \mu - \sqrt{\left(\mu - c_1\right)^2 + 2\sigma^2 q}}{\sigma^2}, \\ \widetilde{\kappa} &= \left(\left(\mu - c_1 - c_2\right)^2 + 2\sigma^2 q\right)^{-(1/2)}, \\ \widetilde{\theta}_1 &= \frac{\left(c_1 + c_2\right) - \mu + \sqrt{\left(\mu - \left(c_1 + c_2\right)\right)^2 + 2\sigma^2 q}}{\sigma^2}, \\ \widetilde{\theta}_2 &= \frac{\left(c_1 + c_2\right) - \mu - \sqrt{\left(\mu - \left(c_1 + c_2\right)\right)^2 + 2\sigma^2 q}}{\sigma^2}. \end{aligned} \tag{34}$$

They are well-known results (see Wang and Zhang [22]).

For x, $q \geq 0$, by some algebraic manipulations, we have

$$\begin{aligned} Z_q(x) &= \frac{q}{\theta_1}\mathbb{W}_q(x) + e^{\theta_2 x}, \\ \mathbb{Z}_q(x) &= \frac{q}{\widetilde{\theta}_1}\mathbb{W}_q(x) + e^{\widetilde{\theta}_2 x}. \end{aligned} \tag{35}$$

By (33) and (35), we can verify that

$$\varrho_\xi(x) = \frac{\mathbb{W}_q'(\bar{\xi}(x))}{\mathbb{W}_q(\bar{\xi}(x))} = \frac{\theta_1 e^{\theta_1\bar{\xi}(x)} - \theta_2 e^{\theta_2\bar{\xi}(x)}}{e^{\theta_1\bar{\xi}(x)} - e^{\theta_2\bar{\xi}(x)}}, \tag{36}$$

$$\begin{aligned}\iota_\xi(x) &= \frac{\mathbb{W}_q'(\bar{\xi}(x))}{\mathbb{W}_q(\bar{\xi}(x))} Z_q(\bar{\xi}(x)) - q\mathbb{W}_q(\bar{\xi}(x)) \\ &= \frac{q}{\theta_1}\mathbb{W}_q'(\bar{\xi}(x)) + \frac{\mathbb{W}_q'(\bar{\xi}(x))}{\mathbb{W}_q(\bar{\xi}(x))} e^{\theta_2\bar{\xi}(x)} - q\mathbb{W}_q(\bar{\xi}(x)) \\ &= \frac{q}{\theta_1}\kappa\left(\theta_1 e^{\theta_1\bar{\xi}(x)} - \theta_2 e^{\theta_2\bar{\xi}(x)}\right) + \frac{\mathbb{W}_q'(\bar{\xi}(x))}{\mathbb{W}_q(\bar{\xi}(x))} e^{\theta_2\bar{\xi}(x)} \\ &\quad - q\kappa\left(e^{\theta_1\bar{\xi}(x)} - e^{\theta_2\bar{\xi}(x)}\right) \\ &= \frac{(\theta_1 - \theta_2) e^{(\theta_1+\theta_2)\bar{\xi}(x)}}{e^{\theta_1\bar{\xi}(x)} - e^{\theta_2\bar{\xi}(x)}}.\end{aligned} \tag{37}$$

Similarly, it can be verified that

$$\tilde{\varrho}_\xi(x) = \frac{\mathbb{W}_q'(\bar{\xi}(x))}{\mathbb{W}_q(\bar{\xi}(x))} = \frac{\tilde{\theta}_1 e^{\tilde{\theta}_1\bar{\xi}(x)} - \tilde{\theta}_2 e^{\tilde{\theta}_2\bar{\xi}(x)}}{e^{\tilde{\theta}_1\bar{\xi}(x)} - e^{\tilde{\theta}_2\bar{\xi}(x)}}, \tag{38}$$

$$\begin{aligned}\tilde{\iota}_\xi(x) &= \frac{\mathbb{W}_q'(\bar{\xi}(x))}{\mathbb{W}_q(\bar{\xi}(x))} Z_q(\bar{\xi}(x)) - q\mathbb{W}_q(\bar{\xi}(x)) \\ &= \frac{(\tilde{\theta}_1 - \tilde{\theta}_2) e^{(\tilde{\theta}_1+\tilde{\theta}_2)\bar{\xi}(x)}}{e^{\tilde{\theta}_1\bar{\xi}(x)} - e^{\tilde{\theta}_2\bar{\xi}(x)}}.\end{aligned} \tag{39}$$

Combining (36)–(39), for $x \in [b, \infty)$,

$$\begin{aligned}V_\xi(x) &= \frac{c_1 + c_2}{q}\left[1 - \int_x^\infty \exp\left(-\int_x^z \tilde{\varrho}_\xi(w)\mathrm{d}w\right)\tilde{\iota}_\xi(z)\mathrm{d}z\right] \\ &= \frac{c_1 + c_2}{q}\left[1 - \int_x^\infty \exp\left(-\int_x^z \frac{\tilde{\theta}_1 e^{\tilde{\theta}_1\bar{\xi}(w)} - \tilde{\theta}_2 e^{\tilde{\theta}_2\bar{\xi}(w)}}{e^{\tilde{\theta}_1\bar{\xi}(w)} - e^{\tilde{\theta}_2\bar{\xi}(w)}}\mathrm{d}w\right)\right. \\ &\quad \left.\frac{(\tilde{\theta}_1 - \tilde{\theta}_2) e^{(\tilde{\theta}_1+\tilde{\theta}_2)\bar{\xi}(z)}}{e^{\tilde{\theta}_1\bar{\xi}(z)} - e^{\tilde{\theta}_2\bar{\xi}(z)}}\mathrm{d}z\right],\end{aligned} \tag{40}$$

and for $x \in [0, b)$,

$$\begin{aligned}V_\xi(x) &= \frac{c_1}{q} - \frac{c_1}{q}\int_x^b \exp\left(-\int_x^z \varrho_\xi(w)\mathrm{d}w\right)\iota_\xi(z)\mathrm{d}z + \exp\left(-\int_x^b \varrho_\xi(z)\mathrm{d}z\right)\left(V_\xi(b) - \frac{c_1}{q}\right) \\ &= \frac{c_1}{q}\left[1 - \int_x^b \exp\left(-\int_x^z \frac{\theta_1 e^{\theta_1\bar{\xi}(w)} - \theta_2 e^{\theta_2\bar{\xi}(w)}}{e^{\theta_1\bar{\xi}(w)} - e^{\theta_2\bar{\xi}(w)}}\mathrm{d}w\right)\frac{(\theta_1 - \theta_2) e^{(\theta_1+\theta_2)\bar{\xi}(z)}}{e^{\theta_1\bar{\xi}(z)} - e^{\theta_2\bar{\xi}(z)}}\mathrm{d}z\right] \\ &\quad + \exp\left(-\int_x^b \frac{\theta_1 e^{\theta_1\bar{\xi}(z)} - \theta_2 e^{\theta_2\bar{\xi}(z)}}{e^{\theta_1\bar{\xi}(z)} - e^{\theta_2\bar{\xi}(z)}}\mathrm{d}z\right)\left(V_\xi(b) - \frac{c_1}{q}\right).\end{aligned} \tag{41}$$

Now, we give some numerical illustrations. Consider the following three draw-down functions: $\xi(x) = 0$, $\xi(x) = 0.2x - 0.2$, and $\xi(x) = 0.5x - 0.2$. As discussed in Remark 1, when $\xi = 0$, τ_ξ reduces to the classical ruin time, then case (a) can be regarded as the dividend problem until the classical ruin time. For the linear draw-down function $\xi(x) = 0.5x - 0.2$, we have that $X_t < \xi(\overline{X}_t) = 0.5\overline{X}_t - 0.2$ at the first draw-down time, which is equivalent to $0.5\overline{X}_t - X_t > 0.2$. This refers to the first time that the surplus process drops 0.2 units below 50% of its maximum to date. In practice, the risk manager can use it as a turning point of taking some actions, such as increasing the premium rate μ to avoid possible disasters.

We choose the parameters of the surplus process as follows: $\mu = 2$, $\sigma = 5$ and $q = 0.01$. For the values of c_1 and c_2 of the ratchet dividend strategy, we consider the following three cases: (a) $c_1 = 0$, $c_2 = 0.5$, (b) $c_1 = 0.1$, $c_2 = 0.5$, and (c) $c_1 = 0.1$, $c_2 = 1$. In Figure 1, for a fixed initial value $x = 1$, we depict the behaviors of V_ξ as a function of b for these three cases. Firstly, it is obvious to see the trends in Figure 1(a) that V_ξ is a decreasing function of b. Note that, in the case $c_1 = 0$, there is no dividend to be paid at the beginning of the surplus process (assume the threshold level $b > x = 1$); therefore, when the threshold b becomes larger, the surplus process has fewer chances of going above b, so the total expected dividend decreases. Secondly, in Figures 1(b) and 1(c), we can see that when $b > 1$, V_ξ first increases and then decreases in b, namely, V_ξ is a concave function of b. This phenomenon can be explained by the following two aspects. On the one hand, a smaller value of b means that more dividends may be paid in finite time, but the draw-down (ruin) time may come earlier due to the lower surplus of the process. On the other hand, when the value of b is larger, the surplus process is more difficult to exceed the threshold level b so as to obtain a larger dividend rate, and hence the total expected dividend until the draw-down (ruin) time may be less. The concavity of V_ξ in Figures 1(b) and 1(c) motivates us to find the optimal threshold (denote it by b^*). By (26), we can get the corresponding optimal threshold level b^* for different cases, as shown in Table 1.

Example 2. Let $Y_t = x + ct - \sum_{i=1}^{N_t} Z_i, t \geq 0$, where $N = \{N_t\}_{t\geq 0}$ is a Poisson process with intensity $\lambda > 0$ and Z_i are i.i.d. exponential random variables with parameter μ. In

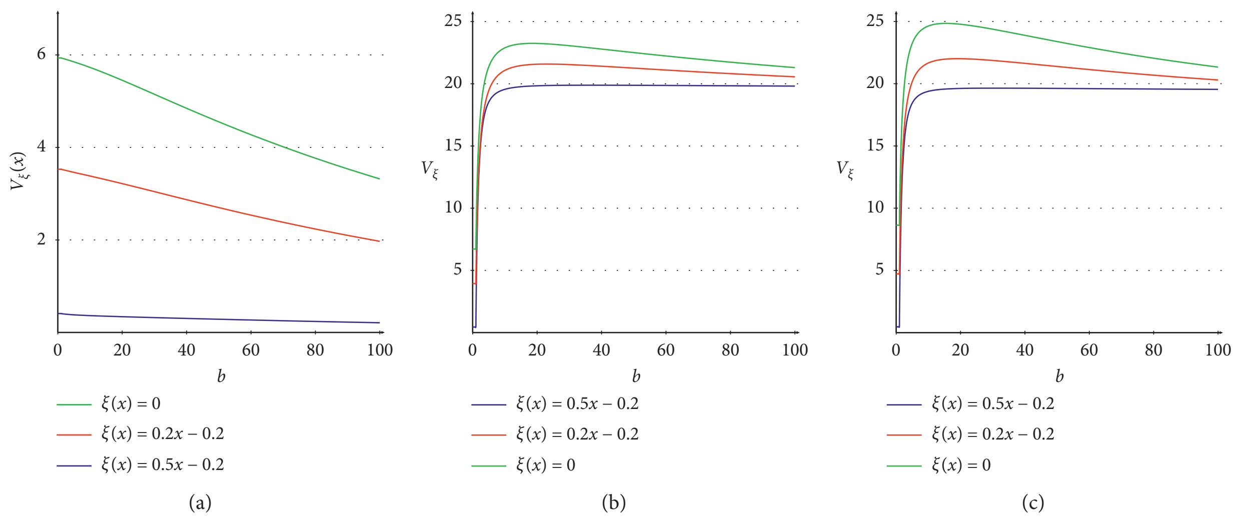

FIGURE 1: Plot of V_ξ as a function of b for the Brownian motion with drift with $q = 0.01$, $\sigma = 5$. (a) $c_1 = 0$, $c_2 = 0.5$, $c = 2$, (b) $c_1 = 0.1$, $c_2 = 0.5$, $\mu = 2$, and (c) $c_1 = 0.1$, $c_2 = 1$, $\mu = 2$.

TABLE 1: Exact values of b^* for the Brownian motion with drift.

The optimal b^*	$\xi(x) = 0$	$\xi(x) = 0.2x - 0.2$	$\xi(x) = 0.5x - 0.2$
$c_1 = 0.1$, $c_2 = 0.5$	18.53	22.92	36.70
$c_1 = 0.1$, $c_2 = 1$	15.46	19.15	30.26

addition, let $X_t = x + (c - c_1)t - \sum_{i=1}^{N_t} Z_i, t \geq 0$ and $\widetilde{X}_t = x + (c - c_1 - c_2)t - \sum_{i=1}^{N_t} Z_i, t \geq 0$. The scale functions associated with X and $\widetilde{X}$ are given, respectively, by

$$\begin{aligned} \mathbb{W}_q(x) &= \frac{A_1}{c - c_1} e^{\theta_1 x} - \frac{A_2}{c - c_1} e^{\theta_2 x}, \\ \mathbb{W}_q(x) &= \frac{\widetilde{A}_1}{c - c_1 - c_2} e^{\widetilde{\theta}_1 x} - \frac{\widetilde{A}_2}{c - c_1 - c_2} e^{\widetilde{\theta}_2 x}, \end{aligned} \tag{42}$$

where

$$\begin{aligned} A_1 &= \frac{\mu + \theta_1}{\theta_1 - \theta_2}, \\ A_2 &= \frac{\mu + \theta_2}{\theta_1 - \theta_2}, \\ \theta_1 &= \frac{\lambda + q - (c - c_1)\mu + K}{2(c - c_1)}, \\ \theta_2 &= \frac{\lambda + q - (c - c_1)\mu - K}{2(c - c_1)}, \\ K &= \sqrt{((c - c_1)\mu - \lambda - q)^2 + 4(c - c_1)q\mu}, \\ \widetilde{A}_1 &= \frac{\mu + \widetilde{\theta}_1}{\widetilde{\theta}_1 - \widetilde{\theta}_2}, \\ \widetilde{A}_2 &= \frac{\mu + \widetilde{\theta}_2}{\widetilde{\theta}_1 - \widetilde{\theta}_2}, \end{aligned}$$

$$\begin{aligned} \widetilde{\theta}_1 &= \frac{\lambda + q - (c - c_1 - c_2)\mu + \widetilde{K}}{2(c - c_1 - c_2)}, \\ \widetilde{\theta}_2 &= \frac{\lambda + q - (c - c_1 - c_2)\mu - \widetilde{K}}{2(c - c_1 - c_2)}, \\ \widetilde{K} &= \sqrt{((c - c_1 - c_2)\mu - \lambda - q)^2 + 4(c - c_1 - c_2)q\mu}. \\ \widetilde{A}_1 &= \frac{\mu + \widetilde{\theta}_1}{\widetilde{\theta}_1 - \widetilde{\theta}_2}, \\ \widetilde{A}_2 &= \frac{\mu + \widetilde{\theta}_2}{\widetilde{\theta}_1 - \widetilde{\theta}_2}, \\ \widetilde{\theta}_1 &= \frac{\lambda + q - (c - c_1 - c_2)\mu + \widetilde{K}}{2(c - c_1 - c_2)}, \\ \widetilde{\theta}_2 &= \frac{\lambda + q - (c - c_1 - c_2)\mu - \widetilde{K}}{2(c - c_1 - c_2)}, \\ \widetilde{K} &= \sqrt{((c - c_1 - c_2)\mu - \lambda - q)^2 + 4(c - c_1 - c_2)q\mu}. \end{aligned} \tag{43}$$

From (42), we have

$$\begin{aligned} Z_q(x) &= 1 + \frac{qA_1}{(c - c_1)\theta_1}\left(e^{\theta_1 x} - 1\right) \\ &\quad - \frac{qA_2}{(c - c_1)\theta_2}\left(e^{\theta_2 x} - 1\right), \quad \text{for } x, q \geq 0, \end{aligned} \tag{44}$$

$$\begin{aligned} \mathbb{Z}_q(x) &= 1 + \frac{q\widetilde{A}_1}{(c - c_1 - c_2)\widetilde{\theta}_1}\left(e^{\widetilde{\theta}_1 x} - 1\right) \\ &\quad - \frac{q\widetilde{A}_2}{(c - c_1 - c_2)\widetilde{\theta}_2}\left(e^{\widetilde{\theta}_2 x} - 1\right), \quad \text{for } x, q \geq 0. \end{aligned} \tag{45}$$

It follows from (42) and (44) that

$$\varrho_\xi(x)=\frac{\mathbb{W}_q'(\bar\xi(x))}{\mathbb{W}_q(\bar\xi(x))}=\frac{A_1\theta_1e^{\theta_1\bar\xi(x)}-A_2\theta_2e^{\theta_2\bar\xi(x)}}{A_1e^{\theta_1\bar\xi(x)}-A_2e^{\theta_2\bar\xi(x)}}, \tag{46}$$

$$\begin{aligned}\iota_\xi(x)&=\frac{\mathbb{W}_q'(\bar\xi(x))}{\mathbb{W}_q(\bar\xi(x))}Z_q(\bar\xi(x))-q\mathbb{W}_q(\bar\xi(x))\\&=\frac{A_1\theta_1e^{\theta_1\bar\xi(x)}-A_2\theta_2e^{\theta_2\bar\xi(x)}}{A_1e^{\theta_1\bar\xi(x)}-A_2e^{\theta_2\bar\xi(x)}}\\&\quad\left[1+\frac{qA_1}{(c-c_1)\theta_1}\left(e^{\theta_1\bar\xi(x)}-1\right)-\frac{qA_2}{(c-c_1)\theta_2}\left(e^{\theta_2\bar\xi(x)}-1\right)\right]\\&=\frac{1}{A_1e^{\theta_1\bar\xi(x)}-A_2e^{\theta_2\bar\xi(x)}}\\&\quad\left[\left(1-\frac{qA_1}{(c-c_1)\theta_1}+\frac{qA_2}{(c-c_1)\theta_2}\right)A_1\theta_1e^{\theta_1\bar\xi(x)}\right.\\&\quad-\left(1-\frac{qA_1}{(c-c_1)\theta_1}+\frac{qA_2}{(c-c_1)\theta_2}\right)A_2\theta_2e^{\theta_2\bar\xi(x)}\\&\quad\left.+\frac{qA_1A_2}{(c-c_1)}\left(2-\frac{\theta_1}{\theta_2}-\frac{\theta_2}{\theta_1}\right)e^{(\theta_1+\theta_2)\bar\xi(x)}\right].\end{aligned} \tag{47}$$

In addition, plugging (42) and (45) into (24) and (25) leads to

$$\widetilde\varrho_\xi(x)=\frac{\widetilde A_1\widetilde\theta_1e^{\widetilde\theta_1\bar\xi(x)}-\widetilde A_2\widetilde\theta_2e^{\widetilde\theta_2\bar\xi(x)}}{\widetilde A_1e^{\widetilde\theta_1\bar\xi(x)}-\widetilde A_2e^{\widetilde\theta_2\bar\xi(x)}}, \tag{48}$$

$$\begin{aligned}\widetilde\iota_\xi(x)&=\frac{1}{\widetilde A_1e^{\widetilde\theta_1\bar\xi(x)}-\widetilde A_2e^{\widetilde\theta_2\bar\xi(x)}}\left[\left(1-\frac{q\widetilde A_1}{(c-c_1-c_2)\widetilde\theta_1}\right.\right.\\&\quad\left.+\frac{q\widetilde A_2}{(c-c_1-c_2)\widetilde\theta_2}\right)\widetilde A_1\widetilde\theta_1e^{\widetilde\theta_1\bar\xi(x)}-\left(1-\frac{q\widetilde A_1}{(c-c_1-c_2)\widetilde\theta_1}\right.\\&\quad\left.+\frac{q\widetilde A_2}{(c-c_1-c_2)\widetilde\theta_2}\right)\widetilde A_2\widetilde\theta_2e^{\widetilde\theta_2\bar\xi(x)}+\frac{q\widetilde A_1\widetilde A_2}{(c-c_1-c_2)}\\&\quad\left.\left(2-\frac{\widetilde\theta_1}{\widetilde\theta_2}-\frac{\widetilde\theta_2}{\widetilde\theta_1}\right)e^{(\widetilde\theta_1+\widetilde\theta_2)\bar\xi(x)}\right].\end{aligned} \tag{49}$$

Combining (13), (14), and (46)–(49) yields

$$\begin{aligned}V_\xi(x)&=\frac{c_1+c_2}{q}\left(1-\int_x^\infty\exp\left(-\int_x^z\widetilde\varrho_\xi(w)\mathrm{d}w\right)\widetilde\iota_\xi(z)\mathrm{d}z\right)\\&=\frac{c_1+c_2}{q}\left\{1-\int_x^\infty\exp\left(-\int_x^z\frac{\widetilde A_1\widetilde\theta_1e^{\widetilde\theta_1\bar\xi(w)}-\widetilde A_2\widetilde\theta_2e^{\widetilde\theta_2\bar\xi(w)}}{\widetilde A_1e^{\widetilde\theta_1\bar\xi(w)}-\widetilde A_2e^{\widetilde\theta_2\bar\xi(w)}}\mathrm{d}w\right)\frac{1}{\widetilde A_1e^{\widetilde\theta_1\bar\xi(z)}-\widetilde A_2e^{\widetilde\theta_2\bar\xi(z)}}\right.\\&\quad\times\left[\left(1-\frac{q\widetilde A_1}{(c-c_1-c_2)\widetilde\theta_1}+\frac{q\widetilde A_2}{(c-c_1-c_2)\widetilde\theta_2}\right)\widetilde A_1\widetilde\theta_1e^{\widetilde\theta_1\bar\xi(z)}-\left(1-\frac{q\widetilde A_1}{(c-c_1-c_2)\widetilde\theta_1}+\frac{q\widetilde A_2}{(c-c_1-c_2)\widetilde\theta_2}\right)\widetilde A_2\widetilde\theta_2e^{\widetilde\theta_2\bar\xi(z)}\right.\\&\quad\left.\left.+\frac{q\widetilde A_1\widetilde A_2}{(c-c_1-c_2)}\left(2-\frac{\widetilde\theta_1}{\widetilde\theta_2}-\frac{\widetilde\theta_2}{\widetilde\theta_1}\right)e^{(\widetilde\theta_1+\widetilde\theta_2)\bar\xi(z)}\right]\mathrm{d}z\right\},\quad x\in[b,\infty),\\V_\xi(x)&=\frac{c_1}{q}-\frac{c_1}{q}\int_x^b\exp\left(-\int_x^z\varrho_\xi(w)\mathrm{d}w\right)\iota_\xi(z)\mathrm{d}z+\exp\left(-\int_x^b\varrho_\xi(z)\mathrm{d}z\right)\left(V_\xi(b)-\frac{c_1}{q}\right)\\&=\frac{c_1}{q}\left\{1-\int_x^b\exp\left(-\int_x^z\frac{A_1\theta_1e^{\theta_1\bar\xi(w)}-A_2\theta_2e^{\theta_2\bar\xi(w)}}{A_1e^{\theta_1\bar\xi(w)}-A_2e^{\theta_2\bar\xi(w)}}\mathrm{d}w\right)\frac{1}{A_1e^{\theta_1\bar\xi(z)}-A_2e^{\theta_2\bar\xi(z)}}\right.\\&\quad\left[\left(1-\frac{qA_1}{(c-c_1)\theta_1}+\frac{qA_2}{(c-c_1)\theta_2}\right)A_1\theta_1e^{\theta_1\bar\xi(z)}-\left(1-\frac{qA_1}{(c-c_1)\theta_1}+\frac{qA_2}{(c-c_1)\theta_2}\right)\times A_2\theta_2e^{\theta_2\bar\xi(z)}\right.\\&\quad\left.\left.+\frac{qA_1A_2}{(c-c_1)}\left(2-\frac{\theta_1}{\theta_2}-\frac{\theta_2}{\theta_1}\right)e^{(\theta_1+\theta_2)\bar\xi(z)}\right]\mathrm{d}z\right\}\\&\quad+\exp\left(-\int_x^b\frac{A_1\theta_1e^{\theta_1\bar\xi(z)}-A_2\theta_2e^{\theta_2\bar\xi(z)}}{A_1e^{\theta_1\bar\xi(z)}-A_2e^{\theta_2\bar\xi(z)}}\mathrm{d}z\right)\left(V_\xi(b)-\frac{c_1}{q}\right),\quad x\in[0,b).\end{aligned} \tag{50}$$

Now, we give some numerical illustrations for this example. We still consider these three draw-down functions as given in Example 1: $\xi(x)=0$, $\xi(x)=0.2x-0.2$, and $\xi(x)=0.5x-0.2$. We choose the parameters of the surplus process as follows: $c=2$, $\lambda=\mu=1$ and $q=0.01$. For the values of c_1 and c_2 of the ratchet dividend strategy we also consider the following three cases: (a) $c_1=0$, $c_2=0.5$, (b) $c_1=0.1$, $c_2=0.5$, and (c) $c_1=0.1$, $c_2=1$. In Figures 2(a)–2(c), for a

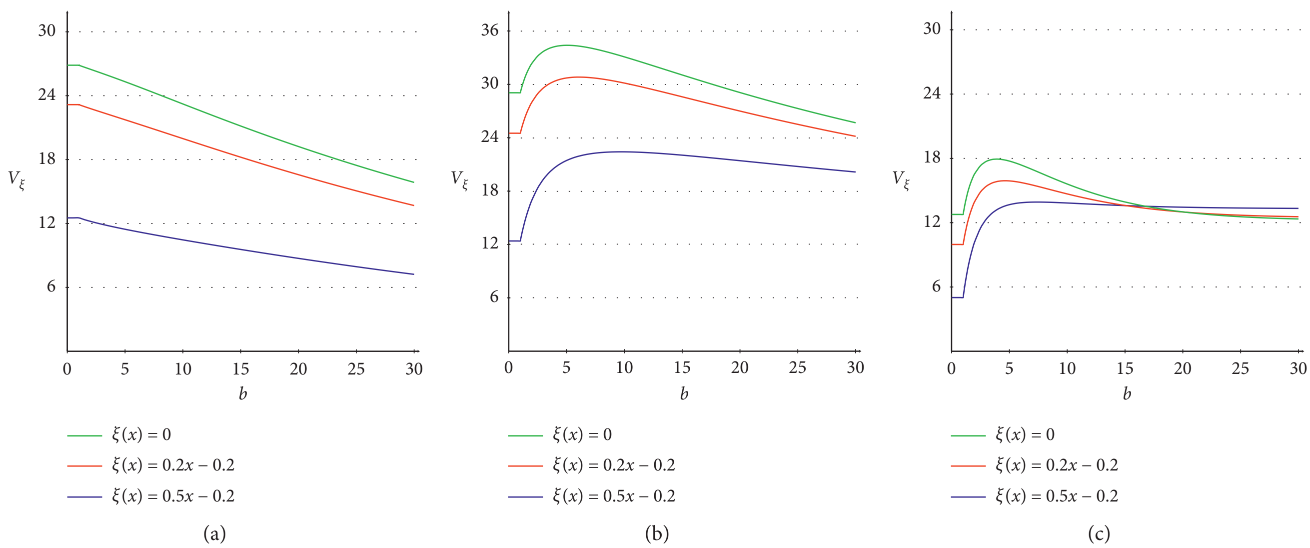

FIGURE 2: Plot of V_ξ as a function of b for the compound Poisson process with $\lambda = \mu = 1$, $q = 0.01$. (a) $c_1 = 0$, $c_2 = 0.5$, $c = 2$, (b) $c_1 = 0.1$, $c_2 = 0.5$, $c = 2$, and (c) $c_1 = 0.1$, $c_2 = 1$, $c = 2$.

TABLE 2: Exact values of b^* for the compound Poisson model.

The optimal b^*	$\xi(x) = 0$	$\xi(x) = 0.2x - 0.2$	$\xi(x) = 0.5x - 0.2$
$c_1 = 0.1,\ c_2 = 0.5$	5.06	6.09	9.72
$c_1 = 0.1,\ c_2 = 1$	3.90	4.63	7.41

fixed initial value $x = 1$, we depict the behaviors of V_ξ as a function of b for these three cases. The trends of V_ξ can be similarly explained, as in Example 1. Furthermore, by (26), we can also get the corresponding optimal threshold level b^* for the compound Poisson risk model, which is shown in Table 2.

Data Availability

The data used to support the results of this study are included within the supplementary information files.

Conflicts of Interest

The authors declare that they have no conflicts of interest.

Acknowledgments

This work was supported by the Science and Technology Planning Project of Jiangxi Provincial Education Department (no. GJJ180201).

Supplementary Materials

(1) Attachments 1 and 2 include the Matlab operation programs of case 1 (in Section 4: numerical illustrations for V_ξ (as a function of b) and for solving the optimal threshold level b^* (for the Brownian motion with drift) of this manuscript). (2) Attachments 3 and 4 include the Matlab operation programs of case 2 (in Section 4: numerical illustrations for V_ξ (as a function of b) and for solving the optimal threshold level b^* (for the compound Poison process) of this manuscript). (*Supplementary Materials*)

References

[1] B. De Finetti, "Su unimpostazione alternativa della teoria collettiva del rischio," *Transactions of the XVth International Congress of Actuaries*, vol. 2, no. 1, pp. 433–443, 1957.

[2] M. H. Miller and F. Modigliani, "Dividend policy, growth, and the valuation of shares," *The Journal of Business*, vol. 34, no. 4, pp. 411–433, 1961.

[3] R. L. Loeffen, "On optimality of the barrier strategy in de Finetti's dividend problem for spectrally negative lévy processes," *The Annals of Applied Probability*, vol. 18, no. 5, pp. 1669–1680, 2008.

[4] R. L. Loeffen and J.-F. Renaud, "De Finetti's optimal dividends problem with an affine penalty function at ruin," *Insurance: Mathematics and Economics*, vol. 46, no. 1, pp. 98–108, 2010.

[5] C. Yin and C. Wang, "Optimality of the barrier strategy in de Finetti's dividend problem for spectrally negative lévy processes: an alternative approach," *Journal of Computational and Applied Mathematics*, vol. 233, no. 2, pp. 482–491, 2009.

[6] K. C. Yuen and C. Yin, "On optimality of the barrier strategy for a general Lévy risk process," *Mathematical and Computer Modelling*, vol. 53, no. 9-10, pp. 1700–1707, 2011.

[7] W. Wang and X. Zhou, "General drawdown-based de Finetti optimization for spectrally negative lévy risk processes," *Journal of Applied Probability*, vol. 55, no. 2, pp. 513–542, 2018.

[8] W. Yu, F. Wang, Y. Huang, and H. Liu, "Social optimal mean field control problem for population growth model," *Asian Journal of Control*, pp. 1–8, 2019.

[9] H. U. Gerber and E. S. W. Shiu, "On optimal dividends: from reflection to refraction," *Journal of Computational and Applied Mathematics*, vol. 186, no. 1, pp. 4–22, 2006.

[10] M. Jeanblanc-Picqué and A. N. Shiryaev, "Optimization of the flow of dividends," *Uspekhi Matematicheskikh Nauk*, vol. 50, no. 2, pp. 25–46, 1995.

[11] S. Asmussen and M. Taksar, "Controlled diffusion models for optimal dividend pay-out," *Insurance: Mathematics and Economics*, vol. 20, no. 1, pp. 1–15, 1997.
[12] H. U. Gerber and E. S. W. Shiu, "On optimal dividend strategies in the compound Poisson model," *North American Actuarial Journal*, vol. 10, no. 2, pp. 76–93, 2006.
[13] X. Peng, W. Su, and Z. Zhang, "On a perturbed compound Poisson risk model under a periodic threshold-type dividend strategy," *Journal of Industrial & Management Optimization*, vol. 13, no. 5, pp. 1–20, 2017.
[14] Z. Liu, P. Chen, and Y. Hu, "On the dual risk model with diffusion under a mixed dividend strategy," *Applied Mathematics and Computation*, vol. 376, Article ID 125115, 2020.
[15] B. Avanzi, J.-L. Pérez, B. Wong, and K. Yamazaki, "On optimal joint reflective and refractive dividend strategies in spectrally positive lévy models," *Insurance: Mathematics and Economics*, vol. 72, pp. 148–162, 2017.
[16] H. Albrecher, N. Bäuerle, and M. Bladt, "Dividends: from refracting to ratcheting," *Insurance: Mathematics and Economics*, vol. 83, pp. 47–58, 2018.
[17] F. Avram, N. L. Vu, and X. Zhou, "On taxed spectrally negative lévy processes with draw-down stopping," *Insurance: Mathematics and Economics*, vol. 76, pp. 69–74, 2017.
[18] H. Albrecher and S. Thonhauser, "Optimality results for dividend problems in insurance. RACSAM-revista de la real academia de ciencias exactas, fisicasy naturales," *Revista de la Real Academia de Ciencias Exactas, Fisicas y Naturales. Serie A. Matematicas*, vol. 103, no. 2, pp. 295–320, 2009.
[19] W. Wang and X. Zhou, "A drawdown reflected spectrally negative lévy process," *Journal of Theoretical Probability*, pp. 1–24, 2019.
[20] W. Wang and X. Zhou, "Draw-down parisian ruin for spectrally negative lévy process," 2019, https://arxiv.org/abs/1904.03286.
[21] I. Czarna and Z. Palmowski, "Dividend problem with parisian delay for a spectrally negative lévy risk process," *Journal of Optimization Theory and Applications*, vol. 161, no. 1, pp. 239–256, 2014.
[22] W. Wang and Z. Zhang, "Optimal loss-carry-forward taxation for lévy risk processes stopped at general draw-down time," *Advances in Applied Probability*, vol. 51, no. 3, pp. 865–897, 2019.
[23] W. Wang and R. Ming, "Two-side exit problems for taxed lévy risk process involving the general draw-down time," *Statistics & Probability Letters*, vol. 138, pp. 66–74, 2018.
[24] W. Wang, P. Chen, and S. Li, "Generalized expected discounted penalty function at general drawdown for lévy risk processes. Insurance: mathematics and economics," 2020, https://arxiv.org/abs/1906.01449.
[25] X. Chen, D. Landriault, B. Li, and D. Li, "On minimizing drawdown risks of lifetime investments," *Insurance: Mathematics and Economics*, vol. 65, pp. 46–54, 2015.
[26] J. Ruan, W. Yu, K. Song, Y. Sun, Y. Huang, and X. Yu, "A note on a generalized Gerber-Shiu discounted penalty function for a compound Poisson risk model," *Mathematics*, vol. 7, no. 10, p. 891, 2019.
[27] W. Yu, Y. Yong, G. Guan, Y. Huang, W. Su, and C. Cui, "Valuing guaranteed minimum death benefits by cosine series expansion," *Mathematics*, vol. 7, no. 9, p. 835, 2019.
[28] Z. Zhang, Y. Yong, and W. Yu, "Valuing equity-linked death benefits in general exponential lévy models," *Journal of Computational and Applied Mathematics*, vol. 365, Article ID 112377, 2020.
[29] A. Kuznetsov, A. E. Kyprianou, and V. Rivero, "The theory of scale functions for spectrally negative Lévy processes," in *Lévy matters II*, pp. 97–186, Springer, Berlin, Germany, 2012.
[30] D. Landriault, B. Li, and H. Zhang, "On magnitude, asymptotics and duration of drawdowns for Lévy models," *Bernoulli*, vol. 23, no. 1, pp. 432–458, 2017.
[31] B. Li, N. L. Vu, and X. Zhou, "Exit problems for general drawdown times of spectrally negative lévy processes," *Journal of Applied Probability*, vol. 56, no. 2, pp. 441–457, 2019.

Hindawi
Mathematical Problems in Engineering
Volume 2020, Article ID 1450486, 7 pages
https://doi.org/10.1155/2020/1450486

Research Article

Egoroff's Theorem and Lusin's Theorem for Capacities in the Framework of g-Expectation

Zhaojun Zong,[1] **Feng Hu**,[1,2] **and Xiaoxin Tian**[1]

[1]*School of Statistics, Qufu Normal University, Qufu 273165, China*
[2]*Department of Statistics and Actuarial Science, The University of Hong Kong, Pokfulam Road, Hong Kong, China*

Correspondence should be addressed to Feng Hu; hufengqf@163.com

Received 26 December 2019; Accepted 28 January 2020; Published 20 March 2020

Guest Editor: Wenguang Yu

In the classical real analysis theory, Egoroff's theorem and Lusin's theorem are two of the most important theorems. The σ-additivity of measures plays a crucial role in the proofs of these theorems. Later, many researchers have carried out lots of studies on Egoroff's theorem and Lusin's theorem when the measure is monotone and nonadditive (see, e.g., Li and Yasuda (2004) and Li and Mesiar (2011)). In this paper, we study Egoroff's theorem and Lusin's theorem for capacities in the framework of g-expectation. We give some different assumptions that provide Egoroff's theorem and Lusin's theorem in the framework of g-expectation.

1. Introduction

In the classical real analysis theory, Egoroff's theorem and Lusin's theorem are two of the most important theorems. The σ-additivity of measures plays a crucial role in the proofs of these theorems. But in fact, the σ-additivity of measures has been abandoned in some areas because many uncertain phenomena cannot be well modelled by using additive measures.

The research studies on Egoroff's theorem in nonadditive measure theory were carried out by Wang and Klir [1]; Li [2]; Li and Yasuda [3]; and Murofushi et al. [4]. These results faithfully contribute to nonadditive measure theory. Li [2] introduced the concept of *condition (E)* of set function and proved an essential result: a necessary and sufficient condition that Egoroff's theorem remains valid for monotone set function is that the monotone set function fulfils *condition (E)*. Murofushi et al. [4] defined the concept of *Egoroff condition* and proved that it is a necessary and sufficient condition for Egoroff's theorem with respect to nonadditive measures. Li and Yasuda [3] studied Egoroff's theorem on finite monotone nonadditive measure space by using *condition (E)*.

In nonadditive measure theory, Lusin's theorem was generalized by Wu and Ha [5] under the conditions of continuity and autocontinuity. Further research on this matter was performed by Jiang and Suzuki [6]. Kawabe [7] investigated regularity and Lusin's theorem for Riesz space-valued fuzzy measures. Li and Mesiar [8] proved Lusin's theorem on monotone measure spaces, assuming that the monotone measure fulfils *condition (E)* and has $(p.g.p.)$ that was introduced by Dobrakov and Farkova [9].

The original motivation for studying nonlinear expectation and g-expectation comes from expected utility theory, which is the foundation of modern mathematical economics. Chen and Epstein [10] gave an application of dynamically consistent nonlinear expectation to recursive utility. Peng [11, 12] and Rosazza Gianin [13] investigated some applications of dynamically consistent nonlinear expectations and g-expectations to static and dynamic pricing mechanisms and risk measures. Hu et al. [14] studied Fubini's theorem for nonadditive measures in the framework of g-expectation.

In this paper, we study Egoroff's theorem and Lusin's theorem for capacities induced by g-expectation. We give the sufficient conditions that provide Egoroff's theorem and Lusin's theorem in the framework of g-expectation. The remainder of this paper is organized as follows: In Section 2, we introduce some notations, assumptions, notions, lemmas, and propositions that are used in this paper. In Section 3, we give Egoroff's theorem, Lusin's theorem, and continuous function approximation theorem in the framework of g-expectation including the proofs.

2. Preliminaries

In this section, we shall present some notations, assumptions, notions, lemmas, and propositions that are used in this paper.

Let $(\Omega, \mathcal{F}, P)$ be a complete probability space and $(W_t)_{t\geq 0}$ be a d-dimensional standard Brownian motion with respect to filtration $(\mathcal{F}_t)_{t\geq 0}$ generated by the Brownian motion and all P-null subsets, i.e.,

$$\mathcal{F}_t = \sigma\{W_s; s \leq t\} \vee \mathcal{N}, \tag{1}$$

where $\mathcal{N}$ is the set of all P-null subsets. Fix a real number $T > 0$.

Let us introduce the following spaces:

$L^2(\Omega, \mathcal{F}_T, P) = \{\xi\colon \xi$ is F_T − measurable random variable such that $E[|\xi|^2] < \infty\}$

$L^2(0, T; P; \mathbb{R}^d) = \{V\colon V_t$ is $\mathbb{R}^d$-valued and $\mathcal{F}_t$-adapted process such that $E[\int_0^T |V_t|^2 dt] < \infty\}$

$S^2(0, T; P; \mathbb{R}) = \{V\colon V_t$ is continuous process in $L^2(0, T; P; \mathbb{R})$ such that $E[\sup_{0\leq t\leq T} |V_t|^2] < \infty\}$

Now, we consider the following 1-dimensional backward stochastic differential equation (BSDE):

$$y_t = \xi + \int_t^T g(t, y_s, z_s) ds - \int_t^T z_s dW_s, \quad t \in [0, T]. \tag{2}$$

Let

$$g\colon \Omega \times [0, T] \times \mathbb{R} \times \mathbb{R}^d \longmapsto \mathbb{R}, \tag{3}$$

such that for any $(y, z) \in \mathbb{R} \times \mathbb{R}^d$, $g(\cdot, y, z)$ is $\mathcal{F}_t$-progressively measurable. We make the following assumptions:

(H1) $E[\int_0^T |g(t, 0, 0)|^2 dt] < \infty$.

(H2) There exists a constant $\mu > 0$ such that for any $\omega \in \Omega$, $t \in [0, T]$, y_1, $y_2 \in \mathbb{R}$ and $z_1, z_2 \in \mathbb{R}^d$,

$$|g(t, y_1, z_1) - g(t, y_2, z_2)| \leq \mu(|y_1 - y_2| + |z_1 - z_2|). \tag{4}$$

(H3) For any $\omega \in \Omega$, $t \in [0, T]$ and $y \in \mathbb{R}$, $g(t, y, 0) = 0$.

(H4) g is subadditive with respect to y and z, i.e., for any $\omega \in \Omega$, $t \in [0, T]$, y_1, $y_2 \in \mathbb{R}$ and $z_1, z_2 \in \mathbb{R}^d$,

$$g(t, y_1 + y_2, z_1 + z_2) \leq g(t, y_1, z_1) + g(t, y_2, z_2). \tag{5}$$

Lemma 1 (see Pardoux and Peng [15]). *Suppose that g satisfies (H1) and (H2). Then, for any $\xi \in L^2(\Omega, \mathcal{F}_T, P)$, BSDE (2) has a unique pair of adapted processes $(y_t, z_t) \in S^2(0, T; P; \mathbb{R}) \times L^2(0, T; P; \mathbb{R}^d)$.*

Definition 1 (g-expectation, see Peng [16]). Suppose that g satisfies (H2) and (H3). For any $\xi \in L^2(\Omega, \mathcal{F}_T, P)$, let (y_t, z_t) be the solution of BSDE (2) with terminal value ξ. Consider the mapping $\varepsilon_g[\cdot] : L^2(\Omega, \mathcal{F}_T, P) \longmapsto \mathbb{R}$, denoted by $\varepsilon_g[\xi] = y_0$. We call $\varepsilon_g[\xi]$ the g-expectation of ξ.

From Peng [16], we know that that g-expectation keeps many properties of mathematical expectation:

(i) $\varepsilon_g[c] = c$, if c is a constant

(ii) $\varepsilon_g[\xi_1] \geq \varepsilon_g[\xi_2]$, if $\xi_1 \geq \xi_2$

For more details of the properties of g-expectation, we can see Briand et al. [17]; Chen et al. [18, 19]; Jiang [20]; He et al. [21]; Hu [22]; Zong and Hu [23, 24]; and Zong et al. [25].

Proposition 1 (see Briand et al. *[17]). Suppose that g satisfies (H2) and (H3). For any $\xi, \eta \in L^2(\Omega, \mathcal{F}_T, P)$, there exists a positive constant C such that*

$$\left|\varepsilon_g[\xi] - \varepsilon_g[\eta]\right|^2 \leq CE\left[|\xi - \eta|^2\right]. \tag{6}$$

Definition 2 (see Choquet [26]). A capacity is a real-valued set function $V\colon \mathcal{F} \longmapsto [0, 1]$ satisfying

(1) $V(\varnothing) = 0$, $V(\Omega) = 1$

(2) $V(A) \leq V(B)$, whenever and $A, B \in \mathcal{F}$

Define the conjugate $\overline{V}$ of V by $\overline{V}(A) := 1 - V(\Omega \backslash A)$, $\forall A \in \mathcal{F}$. Obviously, $\overline{V}$ is also a capacity and $\overline{\overline{V}} = V$.

Definition 3. Suppose that V is a capacity. Then,

(i) Countably subadditive:

$$V\left(\bigcup_{n=1}^{\infty} A_n\right) \leq \sum_{n=1}^{\infty} V(A_n), \quad \forall A_n \in \mathcal{F}. \tag{7}$$

(ii) Continuity from above: for any A_n, $A \in \mathcal{F}$ $(n = 1, 2, \ldots)$, $\lim_{n\longrightarrow\infty} V(A_n) = V(A)$, whenever $A_n \searrow A$.

(iii) Continuity from below: for any A_n, $A \in \mathcal{F}$ $(n = 1, 2, \ldots)$, $\lim_{n\longrightarrow\infty} V(A_n) = V(A)$, whenever $A_n \nearrow A$.

(iv) Continuity: V is continuous from below and above.

Definition 4 (see Wang and Klir [1]). Let F be the class of all finite real-valued measurable functions on $(\Omega, \mathcal{F}, V)$, and let f, $f_n \in F$ $(n = 1, 2, \ldots)$:

(i) $\{f_n\}$ converges almost everywhere to f on Ω ($f_n \xrightarrow{\text{a.e.}} f$): there is a set $E \in \mathcal{F}$ such that $V(E) = 0$ and $f_n \longrightarrow f$ on $\Omega \backslash E$

(ii) $\{f_n\}$ converges pseudo almost everywhere to f on Ω ($f_n \xrightarrow{\text{p.a.e.}} f$): there is a set $Q \in \mathcal{F}$, such that $V(\Omega \backslash Q) = 1$ and $f_n \longrightarrow f$ on $\Omega \backslash Q$

(iii) $\{f_n\}$ converges almost uniformly to f on Ω ($f_n \xrightarrow{\text{a.u.}} f$): for any $\delta > 0$, there is a set $E_\delta \in \mathcal{F}$, such that $V(\Omega \backslash E_\delta) < \delta$ and f_n converges to f uniformly on E_δ

(iv) $\{f_n\}$ converges to f pseudo almost uniformly on Ω ($f_n \xrightarrow{\text{p.a.u.}} f$): there exists $\{Q_k\} \subset \mathcal{F}$ with $\lim_{k\longrightarrow\infty} V(\Omega\backslash Q_k) = 1$ such that f_n converges to f on $\Omega\backslash Q_k$ uniformly for any fixed $k = 1, 2, \ldots$

Remark 1. It is easy to prove that

(1) $f_n \xrightarrow{\text{a.e.}} f$ with respect to V if and only if $f_n \xrightarrow{\text{p.a.e.}} f$ with respect to $\overline{V}$

(2) $f_n \xrightarrow{\text{a.u.}} f$ with respect to V if and only if $f_n \xrightarrow{\text{p.a.u.}} f$ with respect to $\overline{V}$

Define

$$V_g(A) := \varepsilon_g[I_A], \quad \forall A \in \mathcal{F}_T. \tag{8}$$

It is easy to check that V_g is a capacity.

Remark 2. By Proposition 1, we can obtain that suppose g satisfies (H2) and (H3), $A_n, A \in \mathcal{F}_T$ $(n = 1, 2, \ldots)$; then

(1) $V_g(A_n) \searrow V_g(A)$, whenever $A_n \searrow A$

(2) $V_g(A_n) \nearrow V_g(A)$, whenever $A_n \nearrow A$

Thus, V_g is a continuous capacity. Similarly, $\overline{V_g}$ is a continuous capacity.

The following proposition is a special case of Corollary 3.5 by Peng [12].

Proposition 2. *Suppose that g satisfies (H2)–(H4). Then, $V_g(A_1 \cup A_2) \le V_g(A_1) + V_g(A_2)$ $\forall A_1, A_2 \in \mathcal{F}_T$.*

Remark 3. Suppose that g satisfies (H2)–(H4). By Remark 2 and Proposition 2, we have

$$\begin{aligned} V_g\left(\bigcup_{k=1}^{\infty} A_k\right) &= \lim_{n\longrightarrow\infty} V_g\left(\bigcup_{k=1}^{n} A_k\right) \le \lim_{n\longrightarrow\infty} \sum_{k=1}^{n} V_g(A_k) \\ &= \sum_{k=1}^{\infty} V_g(A_k). \end{aligned} \tag{9}$$

Thus, V_g is countably subadditive.

3. Main Results

In this section, we study Egoroff's theorem, Lusin's theorem, and continuous function approximation theorem in the framework of g-expectation.

Theorem 1 (Egoroff's Theorem). *Suppose that g satisfies (H2)–(H4), f_n and f are $\mathcal{F}_T$-measurable random variables. Then,*

(1) If $f_n \xrightarrow{a.e.} f$ with respect to V_g, then $f_n \xrightarrow{a.u.} f$ with respect to V_g

(2) If $f_n \xrightarrow{p.a.e.} f$ with respect to $\overline{V}_g$, then $f_n \xrightarrow{p.a.u.} f$ with respect to $\overline{V}_g$

Proof. Firstly, we prove Theorem 1 (1). Let D be the set of these points ω at which $\{f_n\}$ does not converge to f. Then,

$$D = \bigcup_{k=1}^{\infty} \bigcap_{N=1}^{\infty} \bigcup_{n=N}^{\infty} \left\{\omega : |f_n(\omega) - f(\omega)| \ge \frac{1}{k}\right\}. \tag{10}$$

Since $f_n \xrightarrow{\text{a.e.}} f$ with respect to V_g, we have $V_g(D) = 0$. Thus, for any fixed positive integer k,

$$V_g\left(\bigcap_{N=1}^{\infty} \bigcup_{n=N}^{\infty} \left\{\omega : |f_n(\omega) - f(\omega)| \ge \frac{1}{k}\right\}\right) = 0. \tag{11}$$

Noting the fact that

$$\bigcup_{n=N}^{\infty} \left\{\omega : |f_n(\omega) - f(\omega)| \ge \frac{1}{k}\right\} \searrow \bigcap_{N=1}^{\infty} \bigcup_{n=N}^{\infty} \left\{\omega : |f_n(\omega) - f(\omega)| \ge \frac{1}{k}\right\}, \tag{12}$$

and by Remark 2, we have

$$\begin{aligned} &\lim_{N\longrightarrow\infty} V_g\left(\bigcup_{n=N}^{\infty} \left\{\omega : |f_n(\omega) - f(\omega)| \ge \frac{1}{k}\right\}\right) \\ &\quad = V_g\left(\bigcap_{N=1}^{\infty} \bigcup_{n=N}^{\infty} \left\{\omega : |f_n(\omega) - f(\omega)| \ge \frac{1}{k}\right\}\right) \\ &\quad = 0. \end{aligned} \tag{13}$$

Therefore for any $\delta > 0$ and any positive integer k, there exists a positive integer N_k, such that

$$V_g\left(\bigcup_{n=N_k}^{\infty} \left\{\omega : |f_n(\omega) - f(\omega)| \ge \frac{1}{k}\right\}\right) < \frac{\delta}{2^k}. \tag{14}$$

Let

$$E_\delta := \bigcap_{k=1}^{\infty} \bigcap_{n=N_k}^{\infty} \left\{\omega : |f_n(\omega) - f(\omega)| < \frac{1}{k}\right\}. \tag{15}$$

By Remark 3, we have

$$\begin{aligned} V_g(\Omega\backslash E_\delta) &= V_g\left(\bigcup_{k=1}^{\infty} \bigcup_{n=N_k}^{\infty} \left\{\omega : |f_n(\omega) - f(\omega)| \ge \frac{1}{k}\right\}\right) \\ &\le \sum_{k=1}^{\infty} V_g\left(\bigcup_{n=N_k}^{\infty} \left\{\omega : |f_n(\omega) - f(\omega)| \ge \frac{1}{k}\right\}\right) \\ &< \sum_{k=1}^{\infty} \frac{\delta}{2^k} \\ &= \delta. \end{aligned} \tag{16}$$

Thus, f_n converges to f uniformly on E_δ. The proof of Theorem 1 (1) is complete.

From Theorem 1 (1) and by Remark 1, we can easily obtain Theorem 1 (2).

From now on, for studying Lusin's theorem, we consider the following path spaces: $\Omega = C_0^d(\mathbb{R}^+)$ is the space of all $\mathbb{R}^d$-valued continuous paths $(\omega_t)_{t\ge0}$ with $\omega_0 = 0$, equipped with the distance

$$\rho\left(\omega^1, \omega^2\right) := \sum_{n=1}^{\infty} 2^{-n}\left[\left(\max_{t\in[0,n]} \left|\omega_t^1 - \omega_t^2\right|\right) \wedge 1\right]. \tag{17}$$

We set $\Omega_T := \{\omega_{\cdot\wedge T} : \omega \in \Omega\}$. It is clear that (Ω, ρ) and (Ω_T, ρ) are both complete separable metric spaces. Let $\mathcal{O}$ and $\mathcal{C}$ be the classes of open sets and closed sets in (Ω, ρ), respectively. Similarly, $\mathcal{O}_T$ and $\mathcal{C}_T$ are the classes of open sets and closed sets in (Ω_T, ρ), respectively.

We consider the canonical process: $\omega_t = W_t(\omega)$, $t \in [0,\infty)$, for $\omega \in \Omega$. Let $\mathscr{F}$ be the smallest σ-algebra containing $\mathscr{O}$, and let $\mathscr{F}_T$ be the smallest σ-algebra containing $\mathscr{O}_T$. We can choose a probability measure $\widetilde{P}$ such that $(W_t)_{t\geq 0}$ is a d-dimensional standard Brownian motion under $(C_0^d(\mathbb{R}^+), \mathscr{F}, \widetilde{P})$. □

Definition 5 (see Wu and Ha [5]). A capacity V is called regular, if for every $A \in \mathscr{F}$ and $\delta > 0$, there exists a closed set F_δ and an open set G_δ of Ω, such that

$$\begin{gathered} F_\delta \subset A \subset G_\delta, \\ V(G_\delta \backslash F_\delta) < \delta. \end{gathered} \tag{18}$$

Lemma 2. *Suppose that g satisfies (H2)–(H4), then V_g is regular on $\mathscr{F}_T$.*

Proof. Let $\mathscr{A}$ be the class of all sets $A \in \mathscr{F}_T$ such that for any $\delta > 0$, there exists a closed set F_δ and an open set G_δ of Ω_T satisfying

$$\begin{gathered} F_\delta \subset A \subset G_\delta, \\ V_g(G_\delta \backslash F_\delta) < \delta. \end{gathered} \tag{19}$$

To prove this lemma, it is sufficient to show that $\mathscr{F}_T \subset \mathscr{A}$.

Firstly, we verify that $\mathscr{A}$ is an algebra. It is easy to know that $\Omega_T \in \mathscr{A}$. Suppose $A, B \in \mathscr{A}$, then for any $\delta > 0$, there exist closed sets $F_{1,\delta}, F_{2,\delta} \in \Omega_T$ and open sets $G_{1,\delta}, G_{2,\delta} \in \Omega_T$ such that

$$\begin{gathered} F_{1,\delta} \subset A \subset G_{1,\delta}, \\ V_g\left(G_{1,\delta} \backslash F_{1,\delta}\right) < \delta; \\ F_{2,\delta} \subset B \subset G_{2,\delta}, \\ V_g\left(G_{2,\delta} \backslash F_{2,\delta}\right) < \delta. \end{gathered} \tag{20}$$

So we have

$$F_{1,\delta} G_{2,\delta}^c \subset A \backslash B \subset G_{1,\delta} F_{2,\delta}^c. \tag{21}$$

$F_{1,\delta} G_{2,\delta}^c$ is a closed set of Ω_T, $G_{1,\delta} F_{2,\delta}^c$ is an open set of Ω_T, and

$$\begin{aligned} V_g\left(G_{1,\delta} F_{2,\delta}^c \backslash F_{1,\delta} G_{2,\delta}^c\right) &= V_g\left(G_{1,\delta} F_{2,\delta}^c F_{1,\delta}^c G_{2,\delta}\right) \\ &= V_g\left(\left(G_{1,\delta} \backslash F_{1,\delta}\right) \bigcap \left(G_{2,\delta} \backslash F_{2,\delta}\right)\right) \\ &\leq \min\left\{V_g\left(G_{1,\delta} \backslash F_{1,\delta}\right), V_g\left(G_{2,\delta} \backslash F_{2,\delta}\right)\right\} \\ &< \delta. \end{aligned} \tag{22}$$

That is, $A \backslash B \subset \mathscr{A}$. So $\mathscr{A}$ is an algebra of Ω_T.

Next, we prove that $\mathscr{A}$ is closed under the formation of pairwise disjoint countable unions. Let $\{A_n\}_{n=1}^\infty \subset \mathscr{A}$ be the sequence of pairwise disjoint set and $\delta > 0$ be given. From the definition of $\mathscr{A}$ and $A_n \in \mathscr{A}$, we know that for each given n, there exist an open set G_n and a closed set F_n of Ω_T such that

$$\begin{gathered} F_n \subset A_n \subset G_n, \\ V_g(G_n \backslash F_n) < \frac{\delta}{2^{n+1}}. \end{gathered} \tag{23}$$

Noting the fact that

$$\bigcup_{n=1}^\infty F_n \backslash \bigcup_{n=1}^k F_n \searrow \varnothing, \tag{24}$$

and by Remark 2, we have

$$\lim_{k\longrightarrow\infty} V_g\left(\bigcup_{n=1}^\infty F_n \backslash \bigcup_{n=1}^k F_n\right) = 0. \tag{25}$$

Thus, there exists a positive integer k_0 such that

$$V_g\left(\bigcup_{n=1}^\infty F_n \backslash \bigcup_{n=1}^k F_n\right) < \frac{\delta}{2}. \tag{26}$$

Denote $G_\delta := \bigcup_{n=1}^\infty G_n$ and $F_\delta := \bigcup_{n=1}^{k_0} F_n$; then, G_δ is an open set of Ω_T, F_δ is a closed set of Ω_T, and

$$F_\delta \subset \bigcup_{n=1}^\infty A_n \subset G_\delta. \tag{27}$$

By Remark 3, we have

$$\begin{aligned} V_g(G_\delta \backslash F_\delta) &= V_g\left(\bigcup_{n=1}^\infty F_n \backslash \bigcup_{n=1}^{k_0} F_n\right) \\ &\leq V_g\left(\left(\bigcup_{n=1}^\infty (G_n \backslash F_n)\right) \bigcup \left(\bigcup_{n=1}^\infty F_n \backslash \bigcup_{n=1}^{k_0} F_n\right)\right) \\ &\leq V_g\left(\bigcup_{n=1}^\infty (G_n \backslash F_n)\right) + V_g\left(\left(\bigcup_{n=1}^\infty F_n \backslash \bigcup_{n=1}^{k_0} F_n\right)\right) \\ &\leq \sum_{n=1}^\infty V_g(G_n \backslash F_n) + V_g\left(\left(\bigcup_{n=1}^\infty F_n \backslash \bigcup_{n=1}^{k_0} F_n\right)\right) \\ &< \delta. \end{aligned} \tag{28}$$

That is,

$$\bigcup_{n=1}^\infty A_n \in \mathscr{A}. \tag{29}$$

So $\mathscr{A}$ is a σ-algebra of Ω_T.

In real analysis theory, we know that for any closed set $F \in \mathscr{C}_T$, there exists a sequence of open sets $\{E_n\}_{n=1}^\infty$ such that

$$E_n \backslash F \searrow \varnothing, \quad \text{as } n \longrightarrow \infty. \tag{30}$$

Therefore, by Remark 2, we have $\lim_{n\longrightarrow\infty} V_g(E_n \backslash F) = 0$. Thus, $\mathscr{C}_T \subset \mathscr{A}$. Since $\mathscr{A}$ is closed under the formation of complements, we have $\mathscr{O}_T \subset \mathscr{A}$. This shows that $\mathscr{A}$ is a σ-algebra containing $\mathscr{O}_T$. So $\mathscr{F}_T \subset \mathscr{A}$. □

Remark 4. Suppose that g satisfies (H2)–(H4).

(1) By Lemma 2, we know that for any $A \in \mathscr{F}_T$, there exist an increasing sequence $\{F_n\}_{n=1}^\infty$ of closed sets

and a decreasing sequence $\{G_n\}_{n=1}^{\infty}$ of open sets such that for every $n = 1, 2, \ldots$, $F_n \subset A \subset G_m$,

$$\begin{aligned} V_g(G_n \backslash A) &< \frac{1}{n}, \\ V_g(A \backslash F_n) &< \frac{1}{n}. \end{aligned} \tag{31}$$

(2) By Theorem 1 (1) and Lemma 2, we know that if $f_n \xrightarrow{\text{a.e.}} f$ with respect to V_g, then for any $\delta > 0$, there exists a closed set $F_\delta \in \mathscr{C}_T$ such that $V_g(\Omega_T \backslash F_\delta) < \delta$ and f_n converges to f uniformly on F_δ.

(3) By Theorem 1 (1) and Lemma 2, we know that if $f_n \xrightarrow{\text{a.e.}} f$ with respect to V_g, then there exists an increasing sequence of closed sets $\{H_k\}_{k=1}^{\infty} \subset \mathscr{F}_T$ such that

$$V_g\left(\Omega_T \backslash \bigcup_{k=1}^{\infty} H_k\right) = 0, \tag{32}$$

and f_n converges to f on H_k uniformly for any fixed $k = 1, 2, \ldots$.

In the following, we present Lusin's theorem in the framework of g-expectation.

Theorem 2 (Lusin's Theorem). *Suppose that g satisfies (H2)–(H4) and f is an $\mathscr{F}_T$-measurable random variable. Then, for each $\delta > 0$, there exists a closed set $F_\delta \in \mathscr{C}_T$ such that $V_g(\Omega_T \backslash F_\delta) < \delta$ and f is continuous on F_δ.*

Proof. We prove this theorem stepwise in the following two situations.

(a) Suppose that f is a simple function, i.e., $f = \sum_{k=1}^{n} c_k \chi_{E_k}$, where χ_{E_k} is the characteristic function of E_k and $\Omega_T = \bigcup_{k=1}^{n} E_k$ (a disjoint finite union). For any $\delta > 0$, by Lemma 2, we know that for each k, there exists a closed set F_k of Ω_T such that $F_k \subset E_k$ and

$$V_g(E_k \backslash F_k) < \frac{\delta}{n}. \tag{33}$$

Let

$$F_\delta := \bigcup_{k=1}^{n} F_k. \tag{34}$$

Then, F_δ is a closed set. By Remark 3, we have

$$\begin{aligned} V_g(\Omega_T \backslash F_\delta) &= V_g\left(\bigcup_{k=1}^{n} E_k \backslash \bigcup_{k=1}^{n} F_k\right) \\ &\le V_g\left(\bigcup_{k=1}^{n} (E_k \backslash F_k)\right) \\ &\le \sum_{k=1}^{n} V_g(E_k \backslash F_k) \\ &< \delta. \end{aligned} \tag{35}$$

Obviously, f is continuous on F_δ.

(b) Let f be an $\mathscr{F}_T$-measurable random variable. Then, there exists a sequence $\{\varphi_n\}_{n=1}^{\infty}$ of simple functions such that $\varphi_n \longrightarrow f$ on Ω, as $n \longrightarrow \infty$. With the help of Remark 4 (3), we know that there exists an increasing sequence of closed sets $\{H_k\}_{k=1}^{\infty} \subset \mathscr{F}_T$ such that

$$V_g\left(\Omega_T \backslash \bigcup_{k=1}^{\infty} H_k\right) = 0, \tag{36}$$

and φ_n converges to f on H_k uniformly for any fixed $k = 1, 2, \ldots$. Applying (a), we can prove that for any fixed n, there exists a closed set $F_k^{(n)}$ of Ω_T satisfying that $F_k^{(n)} \subset H_k$ such that

$$V_g\left(H_k \backslash F_k^{(n)}\right) < \frac{\delta}{2^{n+k}}, \quad k = 1, 2, \ldots, \tag{37}$$

and φ_n is continuous on $F_k^{(n)}$. Let

$$F_\delta := \bigcap_{k=1}^{\infty} \bigcap_{n=1}^{\infty} F_k^{(n)}. \tag{38}$$

Then, F_δ is a closed set. By Remark 3, we have

$$\begin{aligned} V_g(\Omega_T \backslash F_\delta) &= V_g\left(\left(\Omega_T \backslash \bigcup_{k=1}^{\infty} H_k\right) \bigcup \left(\bigcup_{k=1}^{\infty} H_k \backslash \bigcap_{k=1}^{\infty} \bigcap_{n=1}^{\infty} F_k^{(n)}\right)\right) \\ &\le V_g\left(\Omega_T \backslash \bigcup_{k=1}^{\infty} H_k\right) + V_g\left(\bigcup_{k=1}^{\infty} H_k \backslash \bigcap_{k=1}^{\infty} \bigcap_{n=1}^{\infty} F_k^{(n)}\right) \\ &\le V_g\left(\bigcup_{n=1}^{\infty} \bigcup_{k=1}^{\infty} \left(H_k \backslash F_k^{(n)}\right)\right) \\ &\le \sum_{n=1}^{\infty} \sum_{k=1}^{\infty} V_g\left(H_k \backslash F_k^{(n)}\right) \\ &< \delta. \end{aligned} \tag{39}$$

At last, we show that f is continuous on F_δ. In fact, φ_n is continuous and converges to f uniformly on F_δ. So for any $\varepsilon > 0$ and any $\omega, \omega_0 \in F_\delta$, there exist a positive integer n_o and a positive constant ς such that

$$\begin{aligned} \left|\varphi_{n_0}(\omega) - f(\omega)\right| &< \frac{\varepsilon}{3}, \\ \left|\varphi_{n_0}(\omega) - \varphi_{n_0}(\omega_0)\right| &< \frac{\varepsilon}{3}, \end{aligned} \tag{40}$$

when $|\omega - \omega_0| < \varsigma$. Thus, we have

$$\begin{aligned} \left|f(\omega) - f(\omega_0)\right| &= \left|f(\omega) - \varphi_{n_0}(\omega) + \varphi_{n_0}(\omega) - \varphi_{n_0}(\omega_0)\right. \\ &\quad \left. + \varphi_{n_0}(\omega_0) - f(\omega_0)\right| \\ &\le \left|f(\omega) - \varphi_{n_0}(\omega)\right| + \left|\varphi_{n_0}(\omega) - \varphi_{n_0}(\omega_0)\right| \\ &\quad + \left|\varphi_{n_0}(\omega_0) - f(\omega_0)\right| \\ &< \varepsilon. \end{aligned} \tag{41}$$

So f is continuous on F_δ. □

Remark 5. Suppose that g satisfies (H2)–(H4). By Theorem 2 and Lemma 2, we know that for any fixed $n = 1, 2, \ldots$, there exists a closed sequence $\{F_n\}_{n=1}^{\infty} \subset \mathcal{F}_T$ such that f is continuous on F_n and

$$V_g(\Omega_T \backslash F_n) < \frac{1}{n}. \tag{42}$$

At last, we show continuous function approximation theorem in the framework of g-expectation.

Theorem 3 (Continuous Function Approximation Theorem). *Suppose that g satisfies (H2)–(H4) and f is an $\mathcal{F}_T$-measurable random variable. Then, there exists a continuous function sequence $\{\phi_n\}_{n=1}^{\infty}$ on Ω such that $\phi_n \xrightarrow{a.e.} f$ with respect to V_g. Furthermore, if $|f| \leq M$, then $|\phi_n| \leq M$ $(n = 1, 2, \ldots)$, where M is a positive constant.*

Proof. By Remark 5, we know that for every $k = 1, 2, \ldots$, there exists a closed set F_k of Ω_T such that f is continuous on F_k and $V_g(\Omega_T \backslash F_k) < (1/k)$ By Tietze's extension theorem in Royden [27], for every $k = 1, 2, \ldots$, there exists a continuous function ψ_k on Ω such that $\psi_k(\omega) = f(\omega)$, for $\omega \in F_k$. And if $|f| \leq M$, then $|\psi_k| \leq M$. Therefore, for any $\varepsilon > 0$, we have

$$\left\{\omega: \left|\psi_k(\omega) - f(\omega)\right| \geq \varepsilon\right\} \subset \Omega_T \backslash F_k, \tag{43}$$

And, hence, for any $k = 1, 2, \ldots$,

$$V_g\left(\left\{\omega: \left|\psi_k(\omega) - f(\omega)\right| \geq \varepsilon\right\}\right) \leq V_g(\Omega_T \backslash F_k) < \frac{1}{k}. \tag{44}$$

Thus, we have

$$\lim_{k \longrightarrow \infty} V_g\left(\left\{\omega: \left|\psi_k(\omega) - f(\omega)\right| \geq \varepsilon\right\}\right) = 0. \tag{45}$$

From the above fact, we can choose a subsequence $\{\psi_{k_n}\}_{n=1}^{\infty}$ of $\{\psi_k\}_{k=1}^{\infty}$ such that

$$V_g\left(\left\{\omega: \left|\psi_{k_n}(\omega) - f(\omega)\right| \geq \frac{1}{2^n}\right\}\right) < \frac{1}{2^n}. \tag{46}$$

Let

$$E_n := \left\{\omega: \left|\psi_{k_n}(\omega) - f(\omega)\right| \geq \frac{1}{2^n}\right\}. \tag{47}$$

Then,

$$\sum_{n=1}^{\infty} V_g(E_n) < \infty. \tag{48}$$

Next, we prove

$$V_g\left(\bigcap_{n=1}^{\infty} \bigcup_{\nu=1}^{\infty} \left\{\omega: \left|\psi_{k_{n+\nu}}(\omega) - f(\omega)\right| \geq \varepsilon\right\}\right) = 0. \tag{49}$$

Indeed, for any $\varepsilon > 0$, there exists a positive integer n_0 such that for any $n \geq n_0$, $(1 \backslash 2^n) < \varepsilon$ and

$$\begin{aligned} & V_g\left(\bigcap_{n=1}^{\infty} \bigcup_{\nu=1}^{\infty} \left\{\omega: \left|\psi_{k_{n+\nu}}(\omega) - f(\omega)\right| \geq \varepsilon\right\}\right) \\ & \leq \sum_{m=n}^{\infty} V_g\left(\left\{\omega: \left|\psi_{k_m}(\omega) - f(\omega)\right| \geq \varepsilon\right\}\right) \\ & \leq \sum_{m=n}^{\infty} V_g(E_m) \\ & \longrightarrow 0, \quad \text{as } n \longrightarrow \infty. \end{aligned} \tag{50}$$

That is, $\psi_{kn} \xrightarrow{\text{a.e.}} f$ with respect to V_g, we take $\phi_n = \psi_{k_n}$, $n = 1, 2, \ldots$. □

Data Availability

No data were used to support this study.

Conflicts of Interest

The authors declare that there are no conflicts of interest regarding the publication of this paper.

Acknowledgments

This work was supported partly by the National Natural Science Foundation of China (no. 11801307) and the Natural Science Foundation of Shandong Province of China (nos. ZR2016JL002 and ZR2017MA012).

References

[1] Z. Wang and G. J. Klir, *Fuzzy Measure Theory*, Plenum, New York, NY, USA, 1992.

[2] J. Li, "A further investigation for Egoroffs theorem with respect to monotone set functions," *Kybernetika*, vol. 39, no. 6, pp. 753–760, 2003.

[3] J. Li and M. Yasuda, "Egoroff's theorem on monotone non-additive measure spaces," *International Journal of Uncertainty, Fuzziness and Knowledge-Based Systems*, vol. 12, no. 1, pp. 61–68, 2004.

[4] T. Murofushi, K. Uchino, and S. Asahina, "Conditions for Egoroff's theorem in non-additive measure theory," *Fuzzy Sets and Systems*, vol. 146, no. 1, pp. 135–146, 2004.

[5] C. Wu and M. Ha, "On the regularity of the fuzzy measure on metric fuzzy measure spaces," *Fuzzy Sets and Systems*, vol. 66, no. 3, pp. 373–379, 1994.

[6] Q. Jiang and H. Suzuki, "Fuzzy measures on metric spaces," *Fuzzy Sets and Systems*, vol. 83, no. 1, pp. 99–106, 1996.

[7] J. Kawabe, "Regularity and Lusin's theorem for Riesz space-valued fuzzy measures," *Fuzzy Sets and Systems*, vol. 158, no. 8, pp. 895–903, 2007.

[8] J. Li and R. Mesiar, "Lusin's theorem on monotone measure spaces," *Fuzzy Sets and Systems*, vol. 175, no. 1, pp. 75–86, 2011.

[9] I. Dobrakov and J. Farkova, "On submeasures II," *Mathematica Slovaca*, vol. 30, pp. 65–81, 1980.

[10] Z. Chen and L. Epstein, "Ambiguity, risk, and asset returns in continuous time," *Econometrica*, vol. 70, no. 4, pp. 1403–1443, 2002.

[11] S. Peng, "Filtration consistent nonlinear expectations and evaluations of contingent claims," *Acta Mathematicae*

Applicatae Sinica, English Series, vol. 20, no. 2, pp. 191–214, 2004.

[12] S. Peng, "Modelling derivatives pricing mechanism with their generating functions," 2006, http://arxiv.org/abs/math.PR/0605599v1.

[13] E. Rosazza Gianin, "Risk measures via g-expectations," *Insurance: Mathematics and Economics*, vol. 39, no. 1, pp. 19–34, 2006.

[14] F. Hu, Z. Zong, and H. Wu, "Fubini theorem for non additive measures in the framework of g-expectation," *Communications in Statistics—Theory and Methods*, vol. 46, no. 23, pp. 11776–11785, 2017.

[15] E. Pardoux and S. G. Peng, "Adapted solution of a backward stochastic differential equation," *Systems & Control Letters*, vol. 14, no. 1, pp. 55–61, 1990.

[16] S. Peng, "Backward SDE and related g-expectation," in *Backward Stochastic Differential Equations*, N. El Karoui and L. Mazliak, Eds., vol. 364, Pitman Research Notes in Mathematics Series, pp. 141–159, Longman, 1997.

[17] P. Briand, F. Coquet, Y. Hu, J. Mémin, and S. Peng, "A converse comparison theorem for BSDEs and related properties of g-expectation," *Electronic Communications in Probability*, vol. 5, pp. 101–117, 2000.

[18] Z. Chen, T. Chen, and M. Davison, "Choquet expectation and Peng's g-expectation," *The Annals of Probability*, vol. 33, no. 3, pp. 1179–1199, 2005.

[19] Z. Chen, R. Kulperger, and L. Jiang, "Jensens inequality for g-expectation: part 1," *Comptes Rendus Mathematique*, vol. 337, no. 11, pp. 725–730, 2003.

[20] L. Jiang, "Convexity, translation invariance and subadditivity for g-expectations and related risk measures," *The Annals of Applied Probability*, vol. 18, no. 1, pp. 245–258, 2008.

[21] K. He, M. Hu, and Z. Chen, "The relationship between risk measures and choquet expectations in the framework of g-expectations," *Statistics & Probability Letters*, vol. 79, no. 4, pp. 508–512, 2009.

[22] F. Hu, "Dynamically consistent nonlinear evaluations with their generating functions in L^p," *Acta Mathematica Sinica, English Series*, vol. 29, no. 4, pp. 815–832, 2013.

[23] Z. Zong and F. Hu, "BSDEs under filtration-consistent nonlinear expectations and the corresponding decomposition theorem for ε-supermartingales in L^p," *Rocky Mountain Journal of Mathematics*, vol. 43, no. 2, pp. 677–695, 2013.

[24] Z. Zong and F. Hu, "L^p weak convergence method on BSDEs with non-uniformly Lipschitz coefficients and its applications," *Proceedings of the Indian Academy of Sciences-Mathematical Sciences*, vol. 126, no. 3, pp. 433–460, 2016.

[25] Z. Zong, F. Hu, C. Yin, and H. Wu, "On Jensen's inequality, Hölder's inequality and Minkowski's inequality for dynamically consistent nonlinear evaluations," *Journal of Inequalities and Applications*, vol. 2015, no. 152, p. 152, 2015.

[26] G. Choquet, "Theory of capacities," *Annales de I'nstitut Fourier (Grenoble)*, vol. 5, pp. 131–295, 1953.

[27] H. L. Royden, *Real Analysis*, Macmillan, New York, NY, USA, 1988.

Hindawi
Mathematical Problems in Engineering
Volume 2020, Article ID 6395717, 8 pages
https://doi.org/10.1155/2020/6395717

Research Article

On Periodic Dividends for the Classical Risk Model with Debit Interest

Hua Dong and Xianghua Zhao

School of Statistics, Qufu Normal University, Shandong 273165, China

Correspondence should be addressed to Hua Dong; sddh1978@126.com

Received 13 January 2020; Accepted 11 February 2020; Published 17 March 2020

Guest Editor: Zhimin Zhang

A periodic dividend problem is studied in this paper. We assume that dividend payments are made at a sequence of Poisson arrival times, and ruin is continuously monitored. First of all, three integro-differential equations for the expected discounted dividends are obtained. Then, we investigate the explicit expressions for the expected discounted dividends, and the optimal dividend barrier is given for exponential claims. A similar study on a generalized Gerber–Shiu function involving the absolute time is also performed. To demonstrate the existing results, we give some numerical examples.

1. Introduction

Suppose the dynamics of the surplus process of an insurance company at time t is defined as the solution to

$$\mathrm{d}R_t = \begin{cases} c\mathrm{d}t - \mathrm{d}S_t, & R_t \geq 0, \\ (c+\alpha R_t)\mathrm{d}t - \mathrm{d}S_t, & -\dfrac{c}{\alpha} \leq R_t < 0, \end{cases} \quad (1)$$

where $c > 0$ is the premium charged in the unit time and $\alpha > 0$ is the debit interest. $S_t = \sum_{i=1}^{N(t)} X_i$ is a compound Poisson process with intensity $\gamma > 0$ representing the total claim amounts until time t, and X_i is the $i-$th claim size. Suppose that the claim sizes are independent of each other and have common density function ς. We also assume that X_i and $N(t)$ are mutually independent.

Model (1) means that the insurer can make loans at the rate $\alpha > 0$ once the process R_t goes below zero. When $R(t) < -c/\alpha$, the insurer can be prohibited to run its business, i.e., the insurer is absolutely ruined. The absolute ruin risk models have been investigated extensively, see Gerber and Yang [1], Cai [2], Yuen et al. [3], Wang and Yin [4], and Cai and Yang [5], among others.

In recent years, the research problems in risk theory are more and more closely related to real life. The risk model with debit interest is a good example. The insurer cannot monitor the surplus continuously, and the dividend can be paid at some certain times. Because of its importance in real life, the topic of periodic dividends has become very popular in risk theory during the last twenty years. Considering dividends can only be made at some discrete times in practice, Albrecher et al. [6] put forward the periodic barrier dividends in this type of risk model. They assumed that both barrier dividends and ruin can only be observed at some randomized times. Considering the insurer monitors bankruptcy more closely than dividends, Avanzi et al. [7] investigated periodic dividend barrier strategy in the dual model where the solvency is monitored continuously. For those risk models with periodic dividends and bankruptcy, the reader can refer to Zhang and Cheung [8, 9], Avanzi et al. [10], Dong et al. [11], and Peng et al. [12], among others. Different to the papers mentioned above, the periodic dividend strategy in Peng et al. [12] is threshold strategy.

Now, we study surplus process (1) under periodic dividend strategy. We assume the ruin is continuously monitored as usual. Let $\{Z_i\}$ be the sequence of dividend observation times with $Z_0 = 0$ and $W_i = Z_i - Z_{i-1}\,(i = 1, 2, \ldots)$ be an exponentially random variable with $\mathbb{E}W_i = 1/\beta$. In addition, we assume that

$W_k\,(k=1,2,\ldots)$ are independent of $N(t)$ and X_i. Furthermore, we assume that no dividends are made at time 0. The modified surplus process is given by R_t^b with $b>0$ being the constant level of the dividend barrier. Denote by $T=\inf\{t>0\colon R_t^b<-(c/\alpha)\}$ the time of absolute ruin for R_t^b with the convention that $\inf\phi=\infty$.

Let

$$\nu(x,b)=\mathbb{E}_x\left[\sum_{Z_k\le T}e^{-\sigma Z_k}\left(R_{Z_k}^b-b\right)_+\right], \tag{2}$$

be the expected discounted dividend before time T, and $\sigma\ge 0$. The generalized Gerber–Shiu function is also our concern:

$$\Phi(x)=\mathbb{E}_x\left[e^{-\sigma T}s^{N(T)}\omega\left(R_{T-}^b,\left|R_T^b\right|\right)1_{\{T<\infty\}}\right],\quad 0<s\le 1, \tag{3}$$

where 1_A denotes the indicator function of event A. $\omega(x,y)\ge 0$ is a bounded measurable function of $x\ge-(c/\alpha)$, $y>(c/\alpha)$, R_{T-}^b is the surplus prior to time T, and $|R_T^b|$ is the deficit at time T. When $s=1,\Phi(x)$ is the Gerber–Shiu function proposed by Gerber and Shiu [13]. When $\omega(\cdot,\cdot)=1,\Phi(x)$ describes the joint distribution of the absolute time T and $N(T)$:

$$\phi(x)=\mathbb{E}_x\left[s^{N(T)}e^{-\sigma T}1_{\{T<\infty\}}\right]. \tag{4}$$

When $\omega(\cdot,\cdot)=1,\sigma=0,\Phi(x)$ is the probability generating function of $N(T)$. The topic on the number of claims has been studied by many scholars in various forms. Some scholars focus on some generalized Gerber–Shiu functions, see Li and Lu [14] and Wang et al. [15]; some only considered the Laplace transform, see Egidio dos Reis [16]; and some studied the density function, see Dickson [17] and Czarna et al. [18].

We arrange the paper as follows. In Section 2, we first derive a system of integro-differential equations for $\nu(x,b)$. For exponential claims, explicit results for $\nu(x,b)$ are given. The generalized Gerber–Shiu function is discussed in Section 3. In Section 4, some numerical results are shown to illustrate the given results.

2. Results for $\nu(x,b)$

2.1. Integro-differential Equations for $\nu(x,b)$. The integro-differential equation is a conventional method; we start this section with the expression for $\nu(x,b)$.

Theorem 1. *For $-(c/\alpha)\le x<0$, we have*

$$(\alpha x+c)\nu'(x,b)-(\sigma+\gamma)\nu(x,b)+\gamma\int_0^{x+c/\alpha}\nu(x-z,b)\varsigma(z)\mathrm{d}z=0, \tag{5}$$

for $0\le x<b$, we have

$$c\nu'(x,b)-(\sigma+\gamma)\nu(x,b)+\gamma\int_0^{x+c/\alpha}\nu(x-z,b)\varsigma(z)\mathrm{d}z=0, \tag{6}$$

and for $x>b$, we have

$$\begin{aligned}&c\nu'(x,b)-(\sigma+\beta+\gamma)\nu(x,b)+\beta(x-b)+\beta\nu(b,b)\\&\quad+\gamma\int_0^{x+c/\alpha}\nu(x-z,b)\varsigma(z)\mathrm{d}z=0.\end{aligned} \tag{7}$$

In addition, we have the following relations:

$$\nu(b-,b)=\nu(b+,b), \tag{8}$$

$$\nu'(b-,b)=\nu'(b+,b), \tag{9}$$

$$\nu(0-,b)=\nu(0+,b), \tag{10}$$

$$\nu'(0-,b)=\nu'(0+,b), \tag{11}$$

$$\nu\left(-\frac{c}{\alpha},b\right)=0. \tag{12}$$

Proof. A standard method is used here, see also Yuen et al. [3] and Albrecher et al. [6]. For a small interval $(0,s)$, all the possible events are taken into account. Then, we have

$$\begin{aligned}\nu(x,b)&=e^{-(\beta+\sigma+\gamma)s}\nu(x+cs,b)+\beta se^{-(\sigma+\gamma)s}\\&\quad\cdot[x+cs-b+\nu(b,b)]1_{\{x+cs>b\}}\\&\quad+\beta se^{-(\sigma+\gamma)s}\nu(x+cs,b)1_{\{0<x+cs<b\}}\\&\quad+\gamma se^{-(\sigma+\gamma)s}\int_0^{x+cs+c/\alpha}\nu(x+cs-y,b)\varsigma(y)\mathrm{d}y+o(s),\end{aligned} \tag{13}$$

for $x\ge 0$, and for $-(c/\alpha)\le x<0$,

$$\begin{aligned}\nu(x,b)&=e^{-(\beta+\sigma+\gamma)s}\nu(t_\alpha(s,x),b)+\beta se^{-(\sigma+\gamma)s}\nu(t_\alpha(s,x))\\&\quad+\gamma se^{-(\sigma+\beta)s}\int_0^{t_\alpha(s,x)+c/\alpha}\nu(t_\alpha(s,x)-y,b)\varsigma(y)\mathrm{d}y+o(s),\end{aligned} \tag{14}$$

where $t_\alpha(s,x)=xe^{\alpha s}+c(e^{\alpha s}-1)/\alpha$.

Taking derivative on s in (13) and letting $s\longrightarrow 0$, we arrive at (6) and (7). By a similar method, (5) can be obtained from (14).

Continuity condition (8) can be obtained from (13), and (10) can be obtained by comparing (13) with (14). (9) can be obtained by using (6) and (7), while (11) is derived by (5) and (6). Let $x=-c/\alpha$ in (5), and we have boundary condition (12). ☐

Remark 1. Obviously, (6) and (7) are the same as (2.1) and (2.2) in Yuen et al. [3], respectively.

2.2. Explicit Expressions of $v(x,b)$. In this section, the density function of claim sizes is supposed to be $f(x) = \mu e^{-\mu x}$, $x > 0$. Applying the operator $(d/dx + \mu)$ to (5), then we have

$$(\alpha x + c)v''(x,b) + (\alpha\mu x + c\mu + \alpha - \gamma - \sigma)v'(x,b) - \sigma\mu v(x,b) = 0, \tag{15}$$

for $(-c/\alpha) \le x < 0$.

By the transforms $v(x,b) = k(z)$ and $z = -\mu(x + c/\alpha)$, (15) is reduced to a confluent hypergeometric equation:

$$zk''(z) + \left(1 - \frac{\sigma+\gamma}{\alpha} - z\right)k'(z) + \frac{\sigma}{\alpha}k(z) = 0, \quad z < 0. \tag{16}$$

It follows from Abramowitz and Stegun [19] that $k(x)$ admits the following expression:

$$k(z) = C_1 e^z U\left(1 - \frac{\gamma}{\alpha}, 1 - \frac{\sigma+\gamma}{\alpha}, -z\right) + C_2 z^{(\sigma+\gamma/\alpha)} M \cdot \left(\frac{\gamma s}{\alpha}, 1 + \frac{\sigma+\gamma}{\alpha}, z\right), \tag{17}$$

where C_1 and C_2 are two constants, $M(a,b,z)$ is the first kind of confluent hypergeometric function, and $U(a,b,z)$ is the second kind of confluent hypergeometric function. Hence, the solution of (15) can be expressed as

$$\begin{aligned} v(x,b) &= C_1 e^{-\mu(x+c/\alpha)} U\left(1 - \frac{\gamma}{\alpha}, 1 - \frac{\sigma+\gamma}{\alpha}, \mu\left(x + \frac{c}{\alpha}\right)\right) \\ &\quad + C_2\left(-\mu\left(x + \frac{c}{\alpha}\right)\right)^{(\sigma+\gamma)/\alpha} M\left(\frac{\gamma}{\alpha}, 1 + \frac{\sigma+\gamma}{\alpha}, -\mu\left(x + \frac{c}{\alpha}\right)\right). \end{aligned} \tag{18}$$

Due to boundary condition (13), one immediately deduces $C_1 = 0$.

Using a similar procedure to (15), we deduce

$$cv''(x,b) - (\sigma + \gamma - c\mu)v'(x,b) - \sigma\mu v(x,b) = 0 \tag{19}$$

for $0 < x < b$ and

$$\begin{aligned} &cv''(x,b) - (\gamma + \beta + \sigma - c\mu)v'(x,b) - (\sigma+\beta)\mu v(x,b) \\ &\quad + \beta\mu[v(b,b) + x - b] + \beta = 0, \end{aligned} \tag{20}$$

for $x \ge b$. Solving (19) and (20) by the knowledge of the ordinary differential equation, one deduces

$$v(x,b) = C_3 e^{\rho_0 x} + C_4 e^{R_0 x}, \quad 0 \le x < b, \tag{21}$$

$$v(x,b) = D_1 e^{\rho_\beta x} + D_2 e^{R_\beta x} + D_3 x + D_4, \quad x \ge b, \tag{22}$$

where $\rho_\beta > 0$, $R_\beta < 0$ are roots of the equation

$$r^2 + \left(\mu - \frac{\sigma+\gamma+\beta}{c}\right)r - \frac{(\sigma+\beta)\mu}{c} = 0. \tag{23}$$

Clearly, $v(x,b)$ is bounded. Hence, $D_1 = 0$. By (18), (21), and (22) and (8)–(11), we get the following equations:

$$C_3 + C_4 = C_2\Delta_1, \tag{24}$$

$$C_3\rho_0 + C_4 R_0 = C_2\Delta_2, \tag{25}$$

$$D_2 e^{R_\beta b} + D_3 b + D_4 = C_3 e^{\rho_0 b} + C_4 e^{R_0 b}, \tag{26}$$

$$D_2 R_\beta e^{R_\beta b} + D_3 = C_3 \rho_0 e^{\rho_0 b} + C_4 R_0 e^{R_0 b}, \tag{27}$$

where

$$\begin{aligned} \Delta_1 &= \left(\frac{-c\mu}{\alpha}\right)^{(\sigma+\gamma)/\alpha} M\left(\frac{\gamma}{\alpha}, 1 + \frac{\sigma+\gamma}{\alpha}, -\frac{c\mu}{\alpha}\right), \\ \Delta_2 &= \frac{\sigma+\gamma}{c}\Delta_1 - \frac{\gamma\mu}{\sigma+\alpha+\gamma}\left(\frac{-c\mu}{\alpha}\right)^{(\sigma+\gamma)/\alpha} M\left(1 + \frac{\gamma}{\alpha}, 2 + \frac{\sigma+\gamma}{\alpha}, -\frac{c\mu}{\alpha}\right). \end{aligned} \tag{28}$$

Substituting (22) into (7) and equating the coefficients of x lead to

$$D_3 = \frac{\beta}{\beta+\sigma}, \tag{29}$$

and then equating the constant term yields

$$\beta D_2 e^{R_\beta b} - \sigma D_4 = \left(\frac{\gamma}{\mu - c - \beta b}\right) D_3 + \beta b. \tag{30}$$

Solving (24)–(30), we get

$$v(x,b) = \frac{(R_0 - \rho_0)h(\beta)(-\mu(x + (c/\alpha)))^{\sigma+\gamma/\alpha} M((\gamma/\alpha), 1 + (\sigma + \gamma/\alpha), -\mu(x + (c/\alpha)))}{H(\beta,b)}, \quad -\frac{c}{\alpha} < x < 0, \tag{31}$$

$$\begin{aligned} v(x,b) &= \frac{(R_0\Delta_1 - \Delta_2)h(\beta)}{H(\beta,b)}e^{\rho_0 x} + \frac{(\Delta_2 - \rho_0\Delta_1)h(\beta)}{H(\beta,b)}e^{R_0 x}, \quad 0 \le x \le b, \\ v(x,b) &= D_2 e^{R_\beta x} + D_3 x + D_4, \quad x > b, \end{aligned} \tag{32}$$

where

$$D_2 = \frac{\left[\rho_0 (R_0\Delta_1 - \Delta_2)e^{(\rho_0 - R_\beta)b} + R_0 (\Delta_2 - \rho_0\Delta_1)e^{(R_0 - R_\beta)b}\right]h(\beta)}{R_\beta H(\beta, b)} - \frac{\beta}{R_\beta(\beta+\sigma)}e^{-R_\beta b},$$

$$D_3 = \frac{\beta}{\beta+\sigma},$$

$$D_4 = \frac{\left[\left(1-(\rho_0/R_\beta)\right)(R_0\Delta_1 - \Delta_2)e^{\rho_0 b} + \left(1-(R_0/R_\beta)\right)(\Delta_2 - \rho_0\Delta_1)e^{R_0 b}\right]h(\beta)}{H(\beta, b)} - \frac{\beta}{\beta+\sigma}\left(b - \frac{1}{R_\beta}\right), \tag{33}$$

$$H(\beta, b) = \left[(\sigma+\beta)\rho_0 - \sigma R_\beta\right](\Delta_2 - R_0\Delta_1)e^{\rho_0 b} + \left[(\sigma+\beta)R_0 - \sigma R_\beta\right](\rho_0\Delta_1 - \Delta_2)e^{R_0 b},$$

$$h(\beta) = -\frac{\beta\left[\gamma R_\beta + \mu\left(\beta+\sigma - cR_\beta\right)\right]}{\mu(\beta+\sigma)}.$$

Remark 2. For $\beta \longrightarrow \infty$, it is easy to check that $R_\beta \longrightarrow -\mu$. Letting $\beta \longrightarrow \infty$ in (31) and (32) and noticing $\rho_0 + R_0 = -\mu + (\sigma+\gamma)/c$, we have

$$V_c(x, b) = \frac{(\rho_0 - R_0)(1 + (\alpha x/c))^{(\sigma+\gamma)/\alpha} M(\gamma/\alpha, 1 + (\sigma+\gamma/\alpha), -\mu(x + c/\alpha))}{(\rho_0+\mu)\Delta_1 - (\gamma\mu/\gamma+\alpha+\sigma)M(1+(\gamma/\alpha), 2+(\sigma+\gamma/\alpha), -c\mu/\alpha)}, \quad -\frac{c}{\alpha} < x < 0,$$

$$V_c(x, b) = \frac{(\Delta_2 - R_0\Delta_1)e^{\rho_0 x} + (\rho_0\Delta_1 - R_0)e^{R_0 x}}{(\rho_0+\mu)\Delta_1 - (\gamma\mu/\gamma+\alpha+\sigma)M(1+(\gamma/\alpha), 2+(\sigma+\gamma/\alpha), -(c\mu/\alpha))}, \quad 0 \le x \le b, \tag{34}$$

which are in accordance to (3.4) in Yuen et al. [3].

When the initial surplus $-c/\alpha < x \le b$, we can investigate the optimal dividend barrier b^* which can maximize $v(x, b)$ before absolute ruin. By (31) and (32), we identify that their numerators have nothing to do with the barrier b, and their denominators are $H(\beta, b)$. We also find that their numerators are bigger than 0. So, the optimal barrier b^* solves $H'(\beta, b^*) = 0$, i.e.,

$$b^* = \frac{1}{\rho_0 - R_0}\ln\frac{R_0\left[(\sigma+\beta)R_0 - \sigma R_\beta\right](\rho_0\Delta_1 - \Delta_2)}{\rho_0\left[(\sigma+\beta)\rho_0 - \sigma R_\beta\right](R_0\Delta_1 - \Delta_2)}. \tag{35}$$

When $\beta \longrightarrow \infty, b^* \longrightarrow (1/\rho_0 - R_0)\ln(R_0^2(\rho_0\Delta_1 - \Delta_2)/\rho_0^2(R_0\Delta_1 - \Delta_2))$, which is the same as (3.5) in Yuen et al. [3].

Remark 3. When the claim sizes are general distributions, e.g., Erlang(n) or mixture of exponential distribution, the explicit expression for $v(x, b)$ cannot be provided for $(-c/\alpha) < x < 0$. Then, some numerical methods will be helpful, e.g., Yu et al. [20] and Zhang et al. [21].

3. Results for $\Phi(x)$

Using a similar method for Theorem 1, we can obtain the following results for the generalized Gerber–Shiu function $\Phi(x)$.

Theorem 2. *The generalized Gerber–Shiu function $\Phi(x)$ admits the following expressions:*

$$c\Phi'(x) - (\gamma+\beta+\sigma)\Phi(x) + \beta\Phi(b) + \gamma s\int_0^{x+c/\alpha}\Phi(x-z)\varsigma(z)\mathrm{d}z + \gamma s\int_{x+c/x}^{\infty}\omega(x, z-x)\varsigma(z)\mathrm{d}z = 0, \quad x \ge b, \tag{36}$$

$$c\Phi'(x) - (\sigma+\gamma)\Phi(x) + \gamma s\int_0^{x+(c/\alpha)}\Phi(x-z)\varsigma(z)\mathrm{d}z + \gamma s\int_{x+(c/x)}^{\infty}\omega(x, z-x)\varsigma(z)\mathrm{d}z = 0, \quad 0 \le x < b, \tag{37}$$

$$(\alpha x + c)\Phi'(x) - (\sigma + \gamma)\Phi(x) + \gamma s \int_0^{x+(c/\alpha)} \Phi(x - z)\varsigma(z)\mathrm{d}z + \gamma s \int_{x+(c/x)}^{\infty} \omega(x, z - x)\varsigma(z)\mathrm{d}z = 0, \quad -\frac{c}{\alpha} \le x < 0, \tag{38}$$

with the following conditions:

$$\Phi(0+) = \Phi(0-), \tag{39}$$

$$\Phi(b+) = \Phi(b-), \tag{40}$$

$$\Phi'(b+) = \Phi'(b-), \tag{41}$$

$$\Phi'(0+) = \Phi'(0-), \tag{42}$$

$$\Phi\left(-\frac{c}{\alpha}\right) = \frac{\gamma s}{\gamma + \sigma} \int_0^{\infty} \omega\left(-\frac{c}{\alpha}, -\frac{c}{\alpha} - y\right)\varsigma(y)\mathrm{d}y. \tag{43}$$

3.1. Explicit Expressions of $\phi(x)$. We also assume that the claim sizes have the density function $f(x) = \mu e^{-\mu x}$ $(x > 0)$, similar to Section 2.2, and we have

$$\begin{gathered}(\alpha x + c)\phi''(x) + (\alpha\mu x + c\mu + \alpha - \gamma - \sigma)\phi'(x) + [\gamma\mu s - (\sigma + \gamma)\mu]\phi(x) = 0, \quad -\frac{c}{\alpha} < x < 0, \\ c\phi''(x) - (\sigma + \gamma - c\mu)\phi'(x) - [(\sigma + \gamma)\mu - \gamma\mu s]\phi(x) = 0, \quad 0 \le x < b, \\ c\phi''(x) + (c\mu - \gamma - \beta - \sigma)\phi'(x) - [(\gamma + \beta + \sigma)\mu - \gamma\mu s]\phi(x) + \beta\mu\phi(b) = 0, \quad x \ge b.\end{gathered} \tag{44}$$

Then, solving the above system of equations leads to

$$\begin{aligned}\phi(x) &= c_1 M_1(x, s) + c_2 M_2(x, s), \quad -\frac{c}{\alpha} \le x < 0, \\ \phi(x) &= c_3 e^{\rho_{0s} x} + c_4 e^{R_{0s} x}, \quad 0 \le x < b, \\ \phi(x) &= d_1 e^{\rho_{\beta s} x} + d_2 e^{R_{\beta s} x} + d_4, \quad x \ge b,\end{aligned} \tag{45}$$

where

$$\begin{aligned}M_1(x, s) &= e^{-\mu(x+(c/\alpha))} U\left(1 - \frac{\gamma s}{\alpha}, 1 - \frac{\sigma + \gamma}{\alpha}, \mu\left(x + \left(\frac{c}{\alpha}\right)\right)\right), \\ M_2(x, s) &= \left(-\mu\left(x + \left(\frac{c}{\alpha}\right)\right)\right)^{(\sigma+\gamma)/\alpha} M\left(\frac{\gamma s}{\alpha}, 1 + \frac{\sigma + \gamma}{\alpha}, -\mu \cdot \left(x + \left(\frac{c}{\alpha}\right)\right)\right),\end{aligned} \tag{46}$$

and $\rho_{\beta s} > 0, R_{\beta s} < 0$ are solutions of the equation

$$cr^2 + (\gamma + \beta + \sigma - cu)r - (\gamma + \beta + \sigma - \gamma s)\mu = 0. \tag{47}$$

Since $\phi(x)$ is a bounded function, then $d_1 = 0$. By conditions (40)–(43), we have

$$\frac{\Gamma(\sigma + \gamma/\alpha)}{\Gamma(\gamma + \alpha + \sigma - \gamma s/\alpha)} c_1 = \frac{\gamma s}{\sigma + \gamma}, \tag{48}$$

$$c_3 + c_4 = c_1 M_1(0, s) + c_2 M_2(0, s), \tag{49}$$

$$c_3 \rho_{0s} + c_4 R_{0s} = c_1 M_1'(0, s) + c_2 M_2'(0, s), \tag{50}$$

$$c_3 e^{\rho_{0s} b} + c_4 e^{R_{0s} b} = d_2 e^{R_{\beta s} b} + d_4, \tag{51}$$

$$c_3 \rho_{0s} e^{\rho_{0s} b} + c_4 R_{0s} e^{R_{0s} b} = d_2 R_{\beta s} e^{R_{\beta s} b}. \tag{52}$$

Inserting (45) into (36) and comparing the coefficients of constants yield

$$(\gamma s - \gamma - \sigma) d_4 + \beta d_2 e^{R_{\beta s} b} = 0. \tag{53}$$

Solving (48)–(53), one obtains

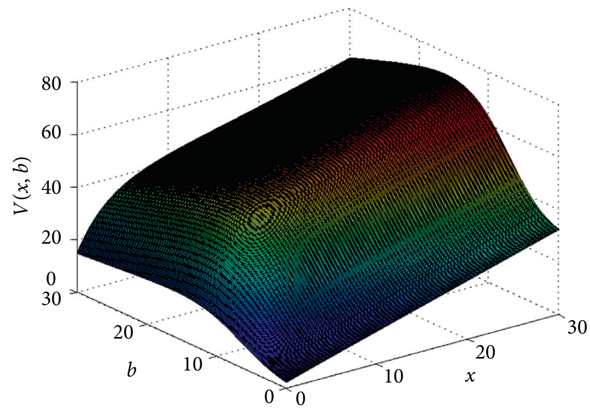

FIGURE 1: Influence of x and b on the expected discounted dividend $v(x,b)$.

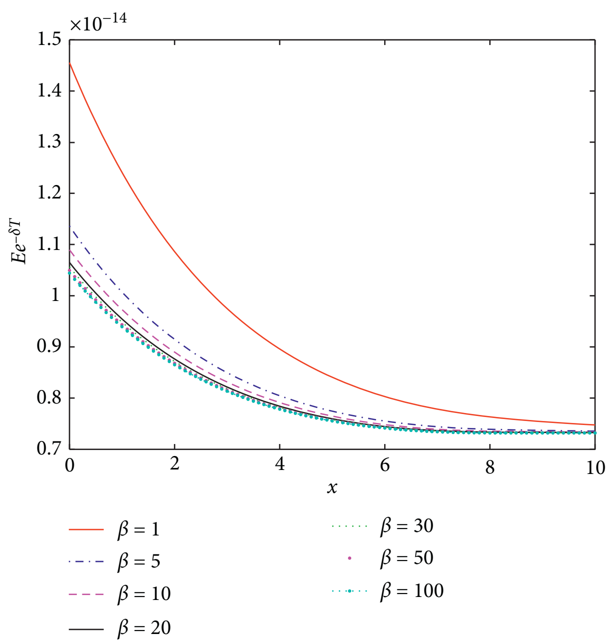

FIGURE 2: Influence of β on $\mathbb{E}_x[\exp - \sigma T]$.

$$\begin{aligned}
c_1 &= \frac{\gamma s \Gamma(\gamma+\alpha+\sigma-\gamma s/\alpha)}{(\sigma+\gamma)\Gamma(\sigma+\gamma/\alpha)},\\
c_2 &= \frac{\gamma s \Gamma(\gamma+\alpha+\sigma-\gamma s/\alpha)\left[(\ell_1+\ell_2)M_1'(0,s)+(\ell_1\rho_{0s}+\ell_2R_{0s})M_1(0,s)\right]}{(\sigma+\gamma)\Gamma(\sigma+\gamma/\alpha)\left[(\ell_1\rho_{0s}+\ell_2R_{0s})M_2(0,s)-(\ell_1+\ell_2)M_2'(0,s)\right]},\\
c_3 &= \frac{\gamma s \Gamma(\gamma+\alpha+\sigma-\gamma s/\alpha)\ell_1\left[M_1'(0,s)M_2(0,s)-M_1(0,s)M_2'(0,s)\right]}{(\sigma+\gamma)\Gamma(\sigma+\gamma/\alpha)\left[(\ell_1\rho_{0s}+\ell_2R_{0s})M_2(0,s)-(\ell_1+\ell_2)M_2'(0,s)\right]},\\
c_4 &= \frac{\gamma s \Gamma(\gamma+\alpha+\sigma-\gamma s/\alpha)\ell_2\left[M_1'(0,s)M_2(0,s)-M_1(0,s)M_2'(0,s)\right]}{(\sigma+\gamma)\Gamma(\sigma+\gamma/\alpha)\left[(\ell_1\rho_{0s}+\ell_2R_{0s})M_2(0,s)-(\ell_1+\ell_2)M_2'(0,s)\right]},\\
d_2 &= \frac{\gamma s \Gamma(\gamma+\alpha+\sigma-\gamma s/\alpha)(\sigma+\gamma-\gamma s)\left[M_1'(0,s)M_2(0,s)-M_1(0,s)M_2'(0,s)\right]}{(\sigma+\gamma)\Gamma(\sigma+\gamma/\alpha)\left[(\ell_1\rho_{0s}+\ell_2R_{0s})M_2(0,s)-(\ell_1+\ell_2)M_2'(0,s)\right]}e^{-R_{\beta s}b},\\
d_4 &= \frac{\beta\gamma s \Gamma(\gamma+\alpha+\sigma-\gamma s/\alpha)\left[M_1'(0,s)M_2(0,s)-M_1(0,s)M_2'(0,s)\right]}{(\sigma+\gamma)\Gamma(\sigma+\gamma/\alpha)\left[(\ell_1\rho_{0s}+\ell_2R_{0s})M_2(0,s)-(\ell_1+\ell_2)M_2'(0,s)\right]},
\end{aligned} \tag{54}$$

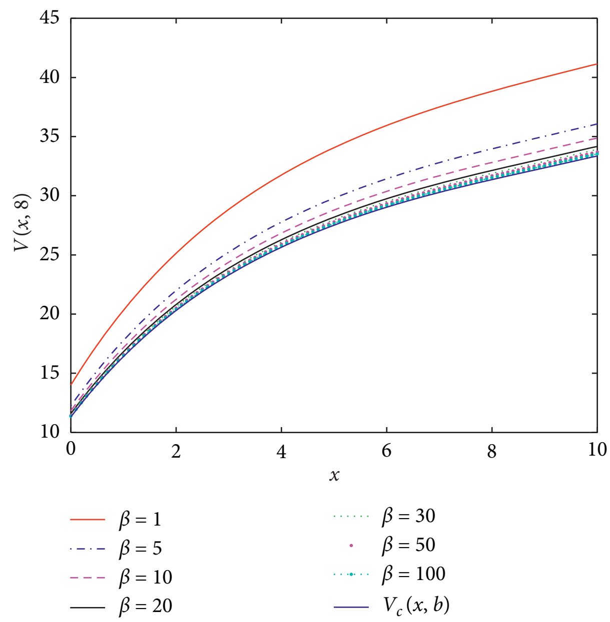

FIGURE 3: Influence of β on $v(x, b)$.

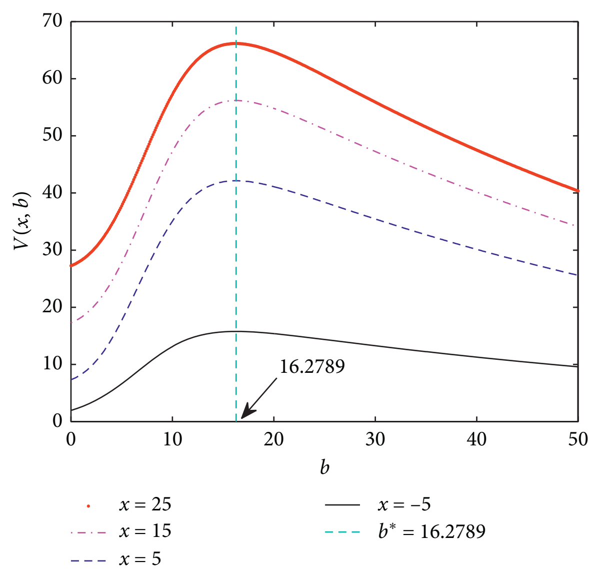

FIGURE 4: $v(x, b)$ as a function of b.

where

$$\ell_1 = \frac{\left(R_{0s} - R_{\beta s}\right)(\sigma + \gamma - \gamma s) + \beta R_{0s}}{R_{0s} - \rho_{0s}} e^{-\rho_{0s} b},$$
$$\ell_2 = \frac{\left(\rho_{0s} - R_{\beta s}\right)(\sigma + \gamma - \gamma s) + \beta \rho_{0s}}{\rho_{0s} - R_{0s}} e^{-R_{0s} b}. \qquad (55)$$

4. Numerical Examples

In this last section, we give some numerical examples to illustrate the results. In Figures 1–4, we assume that the claim size follows exponential distribution with mean 2, the premium rate $c = 4$, the Poisson intensity $\gamma = 0.8$, the discounted factor $\sigma = 0.04$, and the debit interest $\alpha = 0.06$. Figure 1 depicts the profiles of $v(x, b)$ for $(x, b) \in (0, 30) \times (0, 30)$. We find that $v(x, b)$ is not a monotone function of b. When $b = 8$, the curves of $\mathbb{E}_x[e^{-\sigma T} 1_{\{T<\infty\}}]$ and $v(x, b)$ are given in Figures 2 and 3 for several different β, respectively. It is shown that $v(x, b)$ is a decreasing function of β, while $\mathbb{E}_x[e^{-\sigma T} 1_{\{T<\infty\}}]$ is a increasing function of β. The bigger β means the more frequent observation, which can lead to the earlier ruin. By Figure 3, we also find that $v(x, b)$ is more and more close to $V_c(x, b)$ as β becomes more and more large. The profiles of $v(x, b)$ are given in Figure 4 for some different initial surplus x. By Figure 4, we know that the optimal barrier is $b^* = 16.2789$ which has nothing to do with the initial surplus.

Table 1: Impact of β and α on b^* when $c = 4$, $\gamma = 0.8$, $\mu = 0.5$, and $\sigma = 0.04$.

α	$\beta = 1$	$\beta = 5$	$\beta = 10$	$\beta = 20$	$\beta = 30$	$\beta = 50$	$\beta = 100$	$\beta \longrightarrow \infty$
0.04	14.4939	15.9856	16.2774	16.4446	16.5045	16.5541	16.5925	16.6320
0.06	14.4954	15.9870	16.2789	16.4460	16.5059	16.5556	16.5940	16.6335
0.07	14.4960	15.9877	16.2795	16.4467	16.5066	16.5563	16.5947	16.6341
0.084	14.5125	16.0042	16.2960	16.4632	16.5231	16.5727	16.6111	16.6506

The numerical results for b^* are given in Table 1 for various observation intensity β and debit interest α. The optimal dividend barrier b^* is an increasing function of β, which is also an increasing function of α. More frequent observation will give rise to more dividend payments in the initial stage and earlier absolute ruin. In order to avoid the earlier absolute ruin, a bigger dividend barrier will be needed to decrease the dividend payments at the beginning.

Data Availability

No data were used to support this study.

Conflicts of Interest

The authors declare that they have no conflicts of interest.

Acknowledgments

This work was supported by the National Natural Science Foundation of China (nos. 11701319 and 11571198) and Fuyang Municipal Government-Fuyang Normal College Horizontal Cooperation Projects in 2017 (no. XDHXTD201709).

References

[1] H. U. Gerber and H. Yang, "Absolute ruin probabilities in a jump diffusion risk model with investment," *North American Actuarial Journal*, vol. 11, no. 3, pp. 159–169, 2007.

[2] J. Cai, "On the time value of absolute ruin with debit interest," *Advances in Applied Probability*, vol. 39, no. 2, pp. 343–359, 2007.

[3] K.-C. Yuen, M. Zhou, and J. Guo, "On a risk model with debit interest and dividend payments," *Statistics & Probability Letters*, vol. 78, no. 15, pp. 2426–2432, 2008.

[4] C. Wang and C. Yin, "Dividend payments in the classical risk model under absolute ruin with debit interest," *Applied Stochastic Models in Business and Industry*, vol. 25, no. 3, pp. 247–262, 2009.

[5] J. Cai and H. Yang, "On the decomposition of the absolute ruin probability in a perturbed compound poisson surplus process with debit interest," *Annals of Operations Research*, vol. 212, no. 1, pp. 61–77, 2014.

[6] H. Albrecher, E. C. K. Cheung, and S. Thonhauser, "Randomized observation periods for the compound poisson risk model: dividends," *ASTIN Bulletin*, vol. 41, no. 2, pp. 645–672, 2011.

[7] B. Avanzi, E. C. K. Cheung, B. Wong, and J.-K. Woo, "On a periodic dividend barrier strategy in the dual model with continuous monitoring of solvency," *Insurance: Mathematics and Economics*, vol. 52, no. 1, pp. 98–113, 2013.

[8] Z. Zhang and E. C. K. Cheung, "The markov additive risk process under an erlangized dividend barrier strategy," *Methodology and Computing in Applied Probability*, vol. 18, no. 2, pp. 275–306, 2016.

[9] Z. Zhang and E. C. K. Cheung, "A note on a lévy insurance risk model under periodic dividend decisions," *Journal of Industrial and Management Optimization*, vol. 13, no. 2, pp. 36–46, 2018.

[10] B. Avanzi, V. Tu, and B. Wong, "On optimal periodic dividend strategies in the dual model with diffusion," *Insurance: Mathematics and Economics*, vol. 55, no. 1, pp. 210–224, 2014.

[11] H. Dong, C. Yin, and H. Dai, "Spectrally negative lévy risk model under erlangized barrier strategy," *Journal of Computational and Applied Mathematics*, vol. 351, pp. 101–116, 2019.

[12] X. Peng, W. Su, and Z. Zhang, "On a perturbed compound poisson risk model under a periodic threshold-type dividend strategy," *Journal of Industrial & Management Optimization*, vol. 13, no. 5, pp. 1–20, 2017.

[13] H. U. Gerber and E. S. W. Shiu, "On the time value of ruin," *North American Actuarial Journal*, vol. 2, no. 1, pp. 48–72, 1998.

[14] S. Li and Y. Lu, "On the time and the number of claims when the surplus drops below a certain level," *Scandinavian Actuarial Journal*, vol. 2016, no. 5, pp. 420–445, 2016.

[15] W. Wang, P. Chen, and S. Li, "Generalized expected discounted penalty function at general drawdown for lévy risk processes," *Insurance: Mathematics and Economics*, vol. 91, pp. 12–25, 2020.

[16] A. D. Egidio dos Reis, "How many claims does it take to get ruined and recovered?" *Insurance: Mathematics and Economics*, vol. 31, no. 2, pp. 235–248, 2002.

[17] D. C. M. Dickson, "The joint distribution of the time to ruin and the number of claims until ruin in the classical risk model," *Insurance: Mathematics and Economics*, vol. 50, no. 3, pp. 334–337, 2012.

[18] I. Czarna, Y. Li, Z. Palmowski, and C. Zhao, "The joint distribution of the parisian ruin time and the number of claims until parisian ruin in the classical risk model," *Journal of Computational and Applied Mathematics*, vol. 313, pp. 499–514, 2017.

[19] M. Abramowitz and I. A. Stegun, *Handbook of Mathematical Function: With Formulas, Graphs, and Mathematical Tables*, US Government Printing Office, Washington, DC, USA, 1972.

[20] W. Yu, Y. Yong, G. Guan, Y. Huang, W. Su, and C. Cui, "Valuing guaranteed minimum death benefits by cosine series expansion," *Mathematics*, vol. 7, no. 9, p. 835, 2019.

[21] Z. Zhang, Y. Yong, and W. Yu, "Valuing equity-linked death benefits in general exponential lévy models," *Journal of Computational and Applied Mathematics*, vol. 365, Article ID 112377, 2020.

Hindawi
Mathematical Problems in Engineering
Volume 2020, Article ID 4268196, 12 pages
https://doi.org/10.1155/2020/4268196

Research Article

Pricing of Power Exchange Option with Jumps under the Double Risk of Exchange and Default

Kaili Xiang,[1] Peng Hu ,[1,2] and Jie Shen[3]

[1]*School of Economic Mathematics, Southwestern University of Finance and Economics, Chengdu, China*
[2]*College of Applied Mathematics, Chengdu University of Information Technology, Chengdu, China*
[3]*Hexa Asset Management Co. Ltd., Shanghai, China*

Correspondence should be addressed to Peng Hu; alex_hp117@aliyun.com

Received 6 January 2020; Accepted 11 February 2020; Published 17 March 2020

Guest Editor: Zhimin Zhang

Power exchange option is an exotic option which combines power option and exchange option. In this paper, we consider the pricing of the power exchange option under exchange rate volatility risk and issuing company bankruptcy risk. Meanwhile, considering the major events between the two countries, we add the Poisson jump process to the option model in order to reflect the impact of sudden factors on the price of transnational derivatives in the international market. According to the no-arbitrage principle, a mathematical model for pricing such problems is established, and explicit solutions are obtained. The numerical examples show that the model established in this paper is effective.

1. Introduction

As the influence of fierce market competition and homogenization of financial products, the traditional European option or American option can no longer meet the needs of investors. Various types of overseas derivatives and risk management financial products have been designed by many financial institutions. Some of them are customized products which can cater to the special risk hedging needs of institutional investors. Power exchange option is an exotic option which is derived from exchange option and power option; both of them are powerful financial instruments for hedging nonlinear risks or incentive design of the executive stock option [1, 2], which are mainly traded in the OTC market. Compared with the traditional options, the application scenarios of power exchange options are more diversified, with better flexibility, innovation, and practicability. As the option is trade in the OTC market, the power exchange option is typically nonstandardized contracts. The elements are designed and adjusted on the basis of the specific needs of both parties, and there is no unified and standardized standard. On the one hand, the OTC option meets the needs of both buyers and sellers, so the volume of trading and the volume of trading far exceed the OTC option. On the other hand, different security firms or future companies have different pricing standards for royalties, and only the contracting parties can understand the content of the contract, let alone obtain market data, which leads to the almost opaque phenomenon of the OTC option. Because the exchange could not monitor whether the parties to the contract have fulfilled their obligations, when the issuing company is in bankruptcy, liquidation, etc., the counterparty would not be able to complete the payment according to the contract when the option expires; thus, a breach of contract occurred.

Many scholars have conducted in-depth research on the power exchange option and jump risk.

Margrabe [3] introduced the definition of exchange option firstly, which was a new option whose underlying assets are two risky assets. It allowed option holders to exchange the two risky assets at the maturity date. At the same time, Margrabe proposed that the value of American exchange options with short-term maturity was consistent with that of European exchange options with standard conditions. That is to say, American exchange options with early exercise rights were not superior to the European exchange options. Fischer [4] studied the pricing of an exchange option and explained that the exercise price was the price of untranslated assets.

Blenman and Clark [5] summarized the exchange option of Fischer-Margrabe [3, 4] and Tompkins [1] as the power exchange option, whose payoffs were $(\lambda_1 S_1^{\alpha_1}(T) - \lambda_2 S_2^{\alpha_2}(T))^+$. Under the risk-neutral probability, assumed that the values of underlying assets were controlled by geometric Brownian motion, they found the pricing formula of the European power exchange option:

$$\mathrm{PE}(t, S_1, S_2, \xi; T) = \gamma_1(t, S_1, \xi; T) N(d_1) - \gamma_2(t, S_2, \xi; T) N(d_2), \tag{1}$$

where

$$\begin{aligned}
d_1 &= \frac{\ln\left(\lambda_1 S_1^{\alpha_1}/\lambda_2 S_2^{\alpha_2}\right) + \left[\alpha_1(r-\delta_1) - \alpha_2(r-\delta_2) - \alpha_1(1-\alpha_1)\left(\sigma_1^2/2\right)\right] + \alpha_2(1-\alpha_2)\left(\sigma_2^2/2\right) + (1/2)v^2(T-t)}{v\sqrt{(T-t)}},\\
d_2 &= \frac{\ln\left(\lambda_1 S_1^{\alpha_1}/\lambda_2 S_2^{\alpha_2}\right) + \left[\alpha_1(r-\delta_1) - \alpha_2(r-\delta_2) - \alpha_1(1-\alpha_1)\left(\sigma_1^2/2\right) + \alpha_2(1-\alpha_2)\left(\sigma_2^2/2\right) - (1/2)v^2\right](T-t)}{v\sqrt{(T-t)}},\\
\Upsilon_1(t, S_1, \xi; T) &= \lambda_1 S_1^{\alpha_1} \exp\left\{\left[(\alpha_1 - 1)r - \alpha_1\delta_1 - \alpha_1(1-\alpha_1)\frac{\sigma_1^2}{2}\right](T-t)\right\},\\
\Upsilon_1(t, S_1, \xi; T) &= \lambda_1 S_1^{\alpha_1} \exp\left\{\left[(\alpha_1 - 1)r - \alpha_1\delta_1 - \alpha_1(1-\alpha_1)\frac{\sigma_1^2}{2}\right](T-t)\right\},
\end{aligned} \tag{2}$$

where $N(\cdot)$ denotes the cumulative normal density function.

With this formula, they proved that perfect hedging could be achieved by holding multiple positions of asset S_1 value $\alpha_1 N(d_1)\Upsilon_1$, short positions of asset S_2 value $\alpha_2 N(d_2)\Upsilon_2$, and buying or selling portfolios of riskless assets.

Blenman and Clark also proved the equivalence of American power exchange option and European power exchange option under certain conditions. For the American power exchange option with parameters $\xi = (r, \alpha_1, \alpha_2, \lambda_1, \lambda_2, \delta_1, \delta_2)$, if $\alpha_2 \le 1, \alpha_1(r-\delta_1) \ge r$ and $\alpha_2(r-\delta_2) \le r$, it is not optimal to exercise option rights early, and its value is the same as that of European options.

The appearance of new information in option pricing is likely to bring about discontinuous changes in asset prices. In order to capture discontinuous asset prices, Merton [6] based on Black–Scholes model by using underlying assets included a compound Poisson process to simulate discontinuous changes in stock prices. The pricing formulas of several kinds of exotic options in the jump process were given, which laid a foundation for further research.

By using the jump-diffusion model, Tian et al. [7] assumed that the dynamics of asset prices are controlled by jump-diffusion and that the two assets were interrelated, and a closed valuation formula for the fragile European option was calculated. It was proved that the price of the fragile call option was fragile. If there was no consideration of jump risk, the value of fragile options and stocks were calculated. Price may run counter to reality.

Wang [8] incorporated the discontinuous change of risky asset prices into the power-exchange option model. The jump-diffusion process was used to describe the dynamic change of asset prices. Not only the common jump time but also the jump strength and the difference of the impact of common jump components on asset prices were considered. The total jump risk was divided into special components and general jump risk, and the differences between special jump risk and general jump risk are considered. In addition, the correlation between two kinds of risky assets was included in both the continuous part and the discontinuous part, while the correlation between the discontinuous part was linked through a common jump process, which improved the pricing framework of the power exchange option of Blenman and Clark [5] and obtained a clear pricing formula of the power exchange option.

Owing to the fact that the exchange does not assume the responsibility of the over-the-counter (OTC) parties to fulfill their obligations, the holders of over-the-counter (OTC) contracts are vulnerable to the risk of counterparties, that is, the risk that one counterparty in a financial contract fails to meet the agreed terms. Hull and White [9] calculated the pricing formulas of defaultable European option and compared the pricing analytic formulas of defaultable European option, American option, and ordinary European option by numerical methods. Klein [10] put forward a more realistic assumption that the final payment of default depended on the final market value of assets and other companies with the same level of liability. Brigo and Mercurio [11] showed how to consider the event that counterparties may default in a risk-neutral valuation of financial returns.

Wang et al. [12] proposed a power-exchange option pricing model including default risk and jump risk. In their model, they not only included jump components in all asset price processes but also made these processes interrelated. In the calculation process, the pricing formulas of the power exchange option under counterparty risk and jump risk are obtained by using measure transformation technology.

Xu et al. [13] studied the pricing of power exchange options with default risk. They considered the possibility of bankruptcy and liquidation of the company at any time before the expiration of the option. That is to say, the time when the counterparty actually defaults was uncertain. Furthermore, the pricing formula of the power exchange option with uncertain default risk was given.

With the integration of the international financial environment, cross-trading of various types of asset securities is frequent, and various pricing problems between the two kinds of currency transactions have been considered. Reiner [14] linked foreign stock and currency risk on the premise that both underlying asset value and exchange rate fluctuations met the B-S equation. For the first time, the pricing model of dual-currency stock options in four cases was proposed, which progressively progressed according to the degree of complexity.

At present, the research on foreign exchange options has formed a relatively complete theoretical structure, while the deeper level of dual-currency options is still under continuous research. Kwok and Wong [15] gave the pricing formula of the singular option with dual-currency assets. Li and Zhou [16] studied the pricing of the power exchange option under the influence of exchange rate fluctuations. Gao and Wang [17], under the dual-currency model, used the method of measure transformation to give the European option pricing formula of asset price with jump process. Huang and He [18] studied the pricing theory of dual-currency European option and reset option under jump risk related to floating exchange rate. Furthermore, underlying asset can be considered drived by Lévy process. Yu et al. [19] modeled the price of the found by an exponential Lévy process. Zhang et al. [20] linked to the performance of the underlying asset, which is modeled by an exponential Lévy process.

According to the research path of the above literature studies, this paper comprehensively considers the power exchange option with the dual risk of exchange rate and default. Also, the Poisson jump process is added into the option to analyze the pricing of the power exchange options with dual currency with jump process.

2. Model Building

In recent years, financial market emergencies and important policies occur frequently, and the release of such major financial events and important policies has a seismic impact on the entire financial market. In order to reflect the unexpected and unpredictable major events in the market, we add the Poisson jump process to the basic assets, company value, and exchange rate, based on which we analyze the dual-currency power-exchange option model with default risk.

Assume that the probability space (Ω, F, P) represents an economic environment with uncertainty, where P is the risk-neutral probability measure. We define the market environment that includes two risky assets. At the expiration date T, the payoffs of European power exchange options are as follows:

$$V(S_1(T), S_2(T), T) = \left(\lambda_1 S_1^{\alpha_1}(T) - \lambda_2 S_2^{\alpha_2}(T)\right)^+, \qquad (3)$$

where $\lambda_i (i = 1, 2)$ and $\alpha_i (i = 1, 2)$ are positive constants. Especially, for $\lambda_1 = \lambda_2 = 1$ and $\alpha_1 = \alpha_2 = 1$, it simplifies to the standard exchange option.

According to Merton's [6] assumption, the jump risks common to the underlying assets are diversified in the market, and the risk premium is 0. We use the method of partial differential equation to research the pricing of dual-currency power exchange options with jump process.

With the risk-neutral probability measure P, according to the different combinations of stocks that investors hold, we divide the dual-currency power exchange options with jump process into two types for discussion.

Type 1. A domestic investor invests in a foreign stock and a domestic stock at the same time. Over the life of the investment, he will sell foreign stocks and buy domestic ones if they outperform the foreign ones. So, to reduce the transaction cost of switching the underlying asset, he bought a power exchange option that would exchange the two assets at maturity time.

Assume the underlying assets $S_i(t), i = 1, 2$ and the exchange rate $X(t)$ follow the following equations; each of these equations contains a jump representing a major event $N(t)$.

$$\begin{aligned}
\mathrm{d}S_1(t) &= \left(r_f - \rho_{1X}\sigma_1\sigma_X - k_1\lambda\right)S_1(t)\mathrm{d}t + \sigma_1 S_1(t)\mathrm{d}W_1(t) + \left(e^{Z_1(t-)} - 1\right)S_1(t)\mathrm{d}N(t),\\
\mathrm{d}S_2(t) &= (r_d - k_2\lambda)S_2(t)\mathrm{d}t + \sigma_2 S_2(t)\mathrm{d}W_2(t) + \left(e^{Z_2(t-)} - 1\right)S_2(t)\mathrm{d}N(t),\\
\mathrm{d}X(t) &= \left(r_d - r_f\right)X(t)\mathrm{d}t + \sigma_X X(t)\mathrm{d}W_X(t) + \left(e^{Z_X(t-)} - 1\right)X(t)\mathrm{d}N(t),
\end{aligned} \qquad (4)$$

where r_f is the foreign risk-free interest rate; r_d is the risk-free interest rate of the country; σ_1 and σ_2 are the instantaneous standard deviations of foreign stock return volatility and domestic stock return, respectively; σ_X is the instantaneous standard deviation of the exchange rate; $\rho_{1X} = \mathrm{Cov}(\mathrm{d}W_1(t), \mathrm{d}W_X(t))$ represents the instantaneous covariance of foreign stocks and exchange rates; and $W_1(t)$, $W_2(t)$, and $W_X(t)$ are standard Brownian motion under the measure, which meet $\mathrm{d}W_1(t)\cdot\mathrm{d}W_2(t) = \rho_{12}\mathrm{d}t$, $\mathrm{d}W_1(t)\cdot\mathrm{d}W_X(t) = \rho_{1X}\mathrm{d}t$, and $\mathrm{d}W_2(t)\cdot\mathrm{d}W_X(t) = \rho_{2X}\mathrm{d}t$. In addition, as described by Merton [6], $N(t)$ is a Poisson process with an intensity of λ, and it is independent of other Brownian motions. It is used to simulate the discontinuous changes of asset prices and affect the general changes of asset prices. If the general jump occurs at time t, then the jump of the asset is $S_i(t), i = 1, 2$ controlled by $Z_i(t)$, where $Z_i(t)$ is the normal distribution with mean μ_i and standard deviation $\gamma_i > 0$.

Type 2. A domestic investor is interested in two foreign stocks, so he buys foreign power exchange options which use the two stocks as the underlying asset. Since he buys in his own currency, he should exchange the option at the exchange rate. In this case, assume that the price of the underlying asset $S_i(t), i = 1, 2$ and the exchange rate $X(t)$ follow the following equations, where the parameters have the same meaning as those of Type 1.

$$\begin{aligned} dS_1(t) &= \left(r_f - \rho_{1X}\sigma_1\sigma_X - k_1\lambda\right)S_1(t)dt + \sigma_1 S_1(t)dW_1(t) + \left(e^{Z_1(t-)} - 1\right)S_1(t)dN(t), \\ dS_2(t) &= \left(r_f - \rho_{2X}\sigma_2\sigma_X - k_2\lambda\right)S_2(t)dt + \sigma_2 S_2(t)dW_2(t) + \left(e^{Z_2(t-)} - 1\right)S_2(t)dN(t), \\ dX(t) &= \left(r_d - r_f - k_X\lambda\right)X(t)dt + \sigma_X X(t)dW_X(t) + \left(e^{Z_X(t-)} - 1\right)X(t)dN(t). \end{aligned} \tag{5}$$

3. Explicit Solution of the Model

3.1. Solution of the Pricing Model of Type 1. According to the principle of no arbitrage and using ITO's lemma, we get the following conclusions for the first kind of the dual-currency power exchange option model.

Theorem 1. *Pricing formula of dual-currency power exchange options under the first kind of jump risk is*

$$\begin{aligned} C^* &= e^{-r_d T} E\left[\lambda_2 S_2^{\alpha_2}(\mathrm{T})\right] \cdot \sum_{n=0}^{\infty} \frac{\left(\lambda^Q T\right)^n e^{-\lambda^Q T}}{n!}\left(K_1 - K_2 + K_3 - K_4\right) \\ &= \lambda_2 e^{-r_d T} \cdot S_2^{\alpha_2}(0) \cdot \exp\left[\left(\alpha_2\left(r_d - \frac{\sigma_2^2}{2} - k_2\lambda\right) + \frac{\alpha_2^2\sigma_2^2}{2}\right)T\right] \cdot \exp\left[\lambda\left(e^{\alpha_2\mu_2 + (1/2)\alpha_2^2\gamma_2^2} - 1\right)T\right] \cdot \sum_{n=0}^{\infty} \frac{\left(\lambda^Q T\right)^n e^{-\lambda^Q T}}{n!}\left(K_1 - K_2 + K_3 - K_4\right), \end{aligned} \tag{6}$$

where

$$\begin{aligned} K_1 &= \frac{\lambda_1}{\lambda_2} e^{M_1 + (1/2)H_1} N_2\left(\frac{M_1 - \ln\left(\lambda_2/\lambda_1\right) + H_1}{\sqrt{H_1}}, \frac{M_2 - \ln L^* + \rho\sqrt{H_1}\sqrt{H_2}}{\sqrt{H_2}}, \rho\right), \\ K_2 &= N_2\left(\frac{M_1 - \ln\left(\lambda_2/\lambda_1\right)}{\sqrt{H_1}}, \frac{M_2 - \ln L^*}{\sqrt{H_2}}, \rho\right), \\ K_3 &= \frac{\lambda_1}{\lambda_2} \cdot \frac{(1-\alpha)}{L} \cdot e^{M_1 + M_2 + (1/2)H_1 + (1/2)H_2 + \rho\sqrt{H_1}\sqrt{H_2}} \cdot N_2 \\ &\quad \cdot \left(\frac{M_1 - \ln\left(\lambda_2/\lambda_1\right) + H_1 + \rho\sqrt{H_1}\sqrt{H_2}}{\sqrt{H_1}}, -\frac{\ln L^* - M_2 - \rho\sqrt{H_1}\sqrt{H_2} - H_2}{\sqrt{H_2}}, -\rho\right), \\ K_4 &= \frac{(1-\alpha)}{L} e^{M_2 + (1/2)H_2} N_2\left(\frac{M_1 - \ln\left(\lambda_2/\lambda_1\right) + \rho\sqrt{H_1}\sqrt{H_2}}{\sqrt{H_1}}, -\frac{M_2 - \ln L^* + H_2}{\sqrt{H_2}}, -\rho\right). \end{aligned} \tag{7}$$

Proof. Let $G(t) = X(t) \cdot S_1(t)$, so $G(t)$ satisfy the following random process:

$$\begin{aligned} dG(t) &= dX(t)S_1(t) = X(t)dS_1(t) + S_1(t)dX(t) + dS_1(t)dX(t) + \left(X(t)S_1(t) - X(t-)S_1(t-)\right)dN(t) \\ &= X(t)S_1(t)\left[\left(r_f - \rho_{1X}\sigma_1\sigma_X - k_1\lambda\right)dt + \sigma_1 dW_1(t)\right] + S_1(t)X(t)\left[\left(r_d - r_f - k_X\lambda\right)dt + \sigma_X dW_X(t)\right] + \sigma_1 S_1(t)\sigma_X X(t)dW_1 \\ &\quad \cdot (t)dW_X(t) + \left[\left(\left(e^{Z_X(t-)} - 1\right)X(t-) + X(t-)\right) \cdot \left(\left(e^{Z_1(t-)} - 1\right)S_1(t-) + S_1(t-)\right) - X(t-)S_1(t-)\right]dN(t) \\ &= G(t)\left(r_d - k_1\lambda - k_X\lambda\right)dt + G(t)\left[\sigma_1 dW_1(t) + \sigma_X dW_X(t)\right] + \left(e^{Z_X(t-) + Z_1(t-)} - 1\right)G(t-)dN(t) \\ &= \left(r_d - k_1\lambda - k_X\lambda\right)G(t)dt + \sigma_G G(t)dW_G(t) + \left(e^{Z_G(t-)} - 1\right)G(t-)dN(t), \end{aligned} \tag{8}$$

where $W_G(t)$ is the Brownian motion under risk-neutral measure and $\sigma_G^2 = \sigma_1^2 + \sigma_X^2 - 2\sigma_1\sigma_X\rho_{1X}$.

According to $\sigma_G\rho_{2G} = \sigma_1\rho_{12} + \sigma_X\rho_{2X}$, we have $\rho_{2G} = ((\sigma_1\rho_{12} + \sigma_X\rho_{2X})/\sigma_G)$. In the same way, according to $\sigma_G\rho_{GV} = \sigma_1\rho_{1V} + \sigma_X\rho_{VX}$, we have $\rho_{GV} = ((\sigma_1\rho_{1V} + \sigma_X\rho_{VX})/\sigma_G)$. On the contrary, $N(t)$ is still a Poisson process with intensity λ, and $Z_G(t) = Z_X(t) + Z_1(t)$ is a normal distribution with mean $\mu_X + \mu_1$ and variance $\gamma_X^2 + \gamma_1^2$.

By using the orthogonal transformation, we have

$$\begin{cases} dG(t) = (r_d - k_1\lambda - k_X\lambda)G(t)\mathrm{d}t + \sigma_G G(t)\mathrm{d}W_G(t) + \left(e^{Z_G(t-)} - 1\right)G(t-)\mathrm{d}N(t), \\ \mathrm{d}V(t) = (r_d - k_V\lambda)V(t)\mathrm{d}t + \sigma_V\rho_{GV}V(t)\mathrm{d}B_G(t) + \sigma_V\sqrt{1-\rho_{GV}^2}\,V(t)\mathrm{d}B_V(t) + \left(e^{Z_V(t-)} - 1\right)V(t-)\mathrm{d}N(t), \\ \mathrm{d}S_2(t) = (r_d - k_2\lambda)S_2(t)\mathrm{d}t + \sigma_2\rho_{2V}S_2(t)\left(\rho_{GV}\mathrm{d}B_G(t) + \sqrt{1-\rho_{GV}^2}\,\mathrm{d}B_V(t)\right) + \sigma_2\sqrt{1-\rho_{2V}^2}\,S_2(t)\mathrm{d}B_2(t) + \left(e^{Z_2(t-)} - 1\right)S_2(t-)\mathrm{d}N(t), \end{cases} \tag{9}$$

where $\mathrm{d}B_G(t)$, $\mathrm{d}B_2(t)$, and $\mathrm{d}B_V(t)$ are independent Brownian motions under the risk-neutral probability measure P.

Define a new probability measure Q, which is equivalent to a probability measure P.

$$\Delta(t) = \frac{\mathrm{d}Q}{\mathrm{d}P} = \frac{E_t^P\left[S_2^{\alpha_2}(T)\right]}{E\left[S_2^{\alpha_2}(T)\right]}. \tag{10}$$

From the driving equation of risk assets $S_2(t)$ (9), the following equation can be obtained by transformation:

$$\begin{aligned} \mathrm{d}\ln S_2(t) &= \frac{\mathrm{d}S_2(t)}{S_2(t)} - \frac{1}{2}\frac{1}{S_2^2(t)}\mathrm{d}S_2(t)\cdot\mathrm{d}S_2(t) + \left(\ln S_2(t) - \ln S_2(t-)\right)\mathrm{d}N(t) \\ &= \left(r_d - \frac{\sigma_2^2}{2} - k_2\lambda\right)\mathrm{d}t + \sigma_2\rho_{2v}\cdot\rho_{GV}\cdot\mathrm{d}B_G(t) + \sigma_2\rho_{2v}\sqrt{1-\rho_{GV}^2}\cdot\mathrm{d}B_V(t) + \sigma_2\sqrt{1-\rho_{2V}^2}\mathrm{d}B_2(t) \\ &\quad + \left[\ln\left(S_2(t-) + \left(e^{Z_2(t-)} - 1\right)S_2(t-)\right) - \ln S_2(t-)\right]\mathrm{d}N(t) \\ &= \left(r_d - \frac{\sigma_2^2}{2} - k_2\lambda\right)\mathrm{d}t + \sigma_2\rho_{2v}\rho_{GV}\mathrm{d}B_G(t) + \sigma_2\rho_{2v}\sqrt{1-\rho_{GV}^2}\cdot\mathrm{d}B_V(t) \\ &\quad + \sigma_2\sqrt{1-\rho_{2V}^2}\mathrm{d}B_2(t) + Z_2(t-)\mathrm{d}N(t). \end{aligned} \tag{11}$$

To integrate directly, we have

$$\begin{aligned} S_2^{\alpha_2}(t) = S_2^{\alpha_2}(0)\cdot\exp\Bigg\{&\alpha_2\left(r_d - \frac{\sigma_2^2}{2} - k_2\lambda\right)t + \alpha_2\sigma_2\rho_{2v}\rho_{GV}B_G(t) \\ &+ \alpha_2\sigma_2\rho_{2v}\sqrt{1-\rho_{GV}^2}\cdot B_V(t) + \alpha_2\sigma_2\sqrt{1-\rho_{2V}^2}\,B_2(t) \\ &+ \alpha_2\sum_k^{N(t)} Z_2(\tau(k))\Bigg\}. \end{aligned} \tag{12}$$

Then, to calculate its expectation, we have

$$\begin{aligned} E^P\left[S_2^{\alpha_2}(T)\right] = S_2^{\alpha_2}(0)\cdot\exp\Bigg[&\left(\alpha_2\left(r_d - \frac{\sigma_2^2}{2} - k_2\lambda\right) + \frac{\alpha_2^2\sigma_2^2}{2}\right) \\ &+ \lambda\left(e^{\alpha_2\mu_2 + (1/2)\alpha_2^2\gamma_2^2} - 1\right)\Bigg]T. \end{aligned} \tag{13}$$

Therefore, the new probability measure can be obtained:

$$\begin{aligned} \Delta(t) &= \frac{E_t^P\left[S_2^{\alpha_2}(T)\right]}{E\left[S_2^{\alpha_2}(T)\right]} = E^P\left[\frac{S_2^{\alpha_2}(T)}{E\left[S_2^{\alpha_2}(T)\right]}\,|\,F_t\right] \\ &= E\Bigg\{\exp\Bigg[-\frac{\alpha_2\sigma_2^2}{2}T + \alpha_2\sigma_2\rho_{2v}\cdot\rho_{GV}\cdot B_G(T) \\ &\quad + \alpha_2\sigma_2\rho_{2v}\sqrt{1-\rho_{GV}^2}\cdot B_V(T) + \alpha_2\sigma_2\sqrt{1-\rho_{2V}^2}\,B_2(T) \\ &\quad + \alpha_2\sum_k^{N(T)} Z_2(\tau(k)) - \lambda\left(e^{\alpha_2\mu_2 + (1/2)\alpha_2^2\gamma_2^2} - 1\right)T\Bigg]\,|\,F_t\Bigg\}. \end{aligned} \tag{14}$$

According to Girsanov theorem, $B_G^Q(t)$, $B_2^Q(t)$, and $B_V^Q(t)$ are Brownian motions under the probability measure Q, and

$$\begin{cases} B_G^Q(t) = B_G(t) - \alpha_2\sigma_2\rho_{2V}\rho_{GV}t, \\ B_2^Q(t) = B_2(t) - \alpha_2\sigma_2\sqrt{1-\rho_{2V}^2}\,t, \\ B_V^Q(t) = B_V(t) - \alpha_2\sigma_2\rho_{2V}\sqrt{1-\rho_{GV}^2}\,t. \end{cases} \quad (15)$$

On the contrary, after measure transformation, the discontinuity term also changes correspondingly, where $N^Q(t)$ is also the Poisson process, but its strength is $\lambda^Q = \lambda e^{\alpha_2\mu_2 + (1/2)\alpha_2^2\gamma_2^2}$, $Z_{2,k}^Q$ is normal distribution which has mean $\mu_2 + \alpha_2\gamma_2^2$ and variance γ_2^2, and $Z_{G,k}^Q$ and $Z_{V,k}^Q$ are normal distribution whose parameters are unchanged.

The value equation of the dual-currency power exchange options is

$$\begin{aligned} C^* &= e^{-rT}E\left[\left(\lambda_1 G^{\alpha_1}(T) - \lambda_2 S_2^{\alpha_2}(T)\right)^+\left(I_{\{V(T)\geq L^*\}} + (1-\alpha)\frac{V(T)}{L}I_{\{V(T)<L^*\}}\right)\right] \\ &= e^{-rT}E\left[\lambda_2 S_2^{\alpha_2}(T)\right]E\left[\frac{\lambda_2 S_2^{\alpha_2}(T)}{E\left[\lambda_2 S_2^{\alpha_2}(T)\right]}\left(\frac{\lambda_1 G^{\alpha_1}(T)}{\lambda_2 S_2^{\alpha_2}(T)} - 1\right)^+\left(I_{\{V(T)\geq L^*\}} + \frac{(1-\alpha)V(T)}{L}I_{\{V(T)<L^*\}}\right)\right]. \end{aligned} \quad (16)$$

That is to say,

$$\begin{aligned} C^* &= e^{-rT}E\left[\lambda_2 S_2^{\alpha_2}(T)\right]\cdot E^Q\left[\left(\frac{\lambda_1 G^{\alpha_1}(T)}{\lambda_2 S_2^{\alpha_2}(T)} - 1\right)^+\left(I_{\{V(T)\geq L^*\}} + (1-\alpha)\frac{V(T)}{L}I_{\{V(T)<L^*\}}\right)\right] \\ &= e^{-rT}E\left[\lambda_2 S_2^{\alpha_2}(T)\right]\cdot\sum_{n=0}^{\infty}E^Q\left[\left(\frac{\lambda_1 G^{\alpha_1}(T)}{\lambda_2 S_2^{\alpha_2}(T)} - 1\right)^+\left(I_{\{V(T)\geq L^*\}} + (1-\alpha)\frac{V(T)}{L}I_{\{V(T)<L^*\}}\right)\Big| N^Q(t) = n\right]\cdot P\left\{N^Q(t) = n\right\} \\ &= e^{-rT}E\left[\lambda_2 S_2^{\alpha_2}(T)\right]\cdot\sum_{n=0}^{\infty}\frac{(\widehat{\lambda}T)^n e^{-\widehat{\lambda}T}}{n!}E^Q\left[\left(\frac{\lambda_1 G^{\alpha_1}(T)}{\lambda_2 S_2^{\alpha_2}(T)} - 1\right)^+\cdot\left(I_{\{V(T)\geq L^*\}} + (1-\alpha)\frac{V(T)}{L}I_{\{V(T)<L^*\}}\right)\Big| Z^{(n)}\right] \\ &= e^{-rT}E\left[\lambda_2 S_2^{\alpha_2}(T)\right]\cdot\sum_{n=0}^{\infty}\frac{(\widehat{\lambda}T)^n e^{-\widehat{\lambda}T}}{n!}\cdot C_n, \end{aligned} \quad (17)$$

where C_n satisfy

$$\begin{aligned} C_n &= E^Q\left[\left(\frac{\lambda_1 G^{\alpha_1}(T,n)}{\lambda_2 S_2^{\alpha_2}(\mathrm{T},n)} - 1\right)\left(I_{\left\{\left(\lambda_1 G^{\alpha_1}(T,n)/\lambda_2 S_2^{\alpha_2}(\mathrm{T},n)\right)\geq 1, V(T,n)\geq L^*\right\}} + (1-\alpha)\frac{V(T,n)}{L}I_{\left\{\left(\lambda_1 G^{\alpha_1}(T,n)/\lambda_2 S_2^{\alpha_2}(\mathrm{T},n)\right)\geq 1, V(T,n)< L^*\right\}}\right)\right] \\ &= E^Q\left[\frac{\lambda_1 G^{\alpha_1}(T,n)}{\lambda_2 S_2^{\alpha_2}(\mathrm{T},n)}\cdot I_{\left\{\left(\lambda_1 G^{\alpha_1}(T,n)/\lambda_2 S_2^{\alpha_2}(\mathrm{T},n)\right)\geq 1, V(T,n)\geq L^*\right\}}\right] - E^Q\left[I_{\left\{\left(\lambda_1 G^{\alpha_1}(T,n)/\lambda_2 S_2^{\alpha_2}(\mathrm{T},n)\right)\geq 1, V(T,n)\geq L^*\right\}}\right] \\ &\quad + \frac{(1-\alpha)}{L}E^Q\left[\frac{\lambda_1 G^{\alpha_1}(T,n)}{\lambda_2 S_2^{\alpha_2}(\mathrm{T},n)}\cdot V(T,n)\cdot I_{\left\{\left(\lambda_1 G^{\alpha_1}(T,n)/\lambda_2 S_2^{\alpha_2}(\mathrm{T},n)\right)\geq 1, V(T,n)< L^*\right\}}\right] \\ &\quad - \frac{(1-\alpha)}{L}E^Q\left[V(T,n)\cdot I_{\left\{\left(\lambda_1 G^{\alpha_1}(T,n)/\lambda_2 S_2^{\alpha_2}(\mathrm{T},n)\right)\geq 1, V(T,n)< L^*\right\}}\right]. \end{aligned} \quad (18)$$

Next, the solutions of the three stochastic differential equations in (9) are calculated. According to the Girsanov theorem, the correlation between the $B_G^Q(t)$, $B_2^Q(t)$, and $B_V^Q(t)$ with the new probability measure Q and $B_G(t)$, $B_2(t)$, and $B_V(t)$ with the risk-neutral measure P is equation (15). By using the logarithmic transformation, we have

$$
\begin{aligned}
&\ln G(t,n) = \ln G(0) + \left(r_d - \frac{\sigma_G^2}{2} - k_1\lambda - k_X\lambda + \alpha_2\sigma_2\sigma_G\rho_{2V}\rho_{GV}\right)t + \sigma_G B_G^Q(t) + \sum_{k=1}^{n} Z_G^Q(\tau(k)),\\
&\ln V(t,n) = \ln V(0) + \left(r_d - \frac{\sigma_V^2}{2} - k_V\lambda + \alpha_2\sigma_V\sigma_2\rho_{2V}\right)t + \sigma_V\rho_{GV}B_G^Q(t) + \sigma_V\sqrt{1-\rho_{GV}^2}B_V^Q(t) + \sum_{k=1}^{n} Z_V^Q(\tau(k)),\\
&\ln S_2(t,n) = \ln S_2(0) + \left(r_d - \frac{\sigma_2^2}{2} - k_2\lambda + \alpha_2\sigma_2^2\right)t + \sigma_2\rho_{2V}\rho_{GV}B_G^Q(t) + \sigma_2\rho_{2V}\sqrt{1-\rho_{GV}^2}B_V^Q(t) + \sigma_2\sqrt{1-\rho_{2V}^2}B_2^Q(t) + \sum_{k=1}^{n} Z_2^Q(\tau(k)),\\
&\ln S_2(t,n) = \ln S_2(0) + \left(r_d - \frac{\sigma_2^2}{2} - k_2\lambda + \alpha_2\sigma_2^2\right)t + \sigma_2\rho_{2V}\rho_{GV}B_G^Q(t) + \sigma_2\rho_{2V}\sqrt{1-\rho_{GV}^2}B_V^Q(t) + \sigma_2\sqrt{1-\rho_{2V}^2}B_2^Q(t) + \sum_{k=1}^{n} Z_2^Q(\tau(k)),\\
&\ln\frac{G^{\alpha_1}(T,n)}{S_2^{\alpha_2}(T,n)} = \alpha_1\ln G(0) - \alpha_2\ln S_2(0) + \alpha_1\left(r_d - \frac{\sigma_G^2}{2} - k_1\lambda - k_X\lambda + \alpha_2\sigma_2\sigma_G\rho_{2V}\rho_{GV}\right)t - \alpha_2\left(r_d - \frac{\sigma_2^2}{2} - k_2\lambda + \alpha_2\sigma_2^2\right)t\\
&\qquad + \left(\alpha_1\sigma_G - \alpha_2\sigma_2\rho_{2V}\rho_{GV}\right)B_G^Q(t) - \alpha_2\sigma_2\rho_{2V}\sqrt{1-\rho_{GV}^2}B_V^Q(t)\\
&\qquad - \alpha_2\sigma_2\sqrt{1-\rho_{2V}^2}B_2^Q(t) + \alpha_1\sum_{k=1}^{n} Z_G^Q(\tau(k)) - \alpha_2\sum_{k=1}^{n} Z_2^Q(\tau(k)),
\end{aligned}
\tag{19}
$$

where the mathematical expectations of $\ln(G^{\alpha_1}(T,n)/S_2^{\alpha_2}(T,n))$ and $\ln V(T,n)$ are

$$
\begin{cases}
M_1 = E\left[\ln\dfrac{G^{\alpha_1}(T,n)}{S_2^{\alpha_2}(T,n)}\right] = \alpha_1\ln G(0) - \alpha_2\ln S_2(0) + \alpha_1\left(r_d - \dfrac{\sigma_G^2}{2} - k_1\lambda - k_X\lambda + \alpha_2\sigma_2\sigma_G\rho_{2V}\rho_{GV}\right)\cdot T - \alpha_2\\
\quad\cdot\left(r_d - \dfrac{\sigma_2^2}{2} - k_2\lambda + \alpha_2\sigma_2^2\right)\cdot T + n\alpha_1\mu_G - n\alpha_2\left(\mu_2 + \alpha_2\gamma_2^2\right),\\
M_2 = E[\ln V(T,n)] = \ln V(0) + \left(r_d - \dfrac{\sigma_V^2}{2} - k_V\lambda + \alpha_2\sigma_V\sigma_2\rho_{2V}\right)\cdot T + n\mu_V.
\end{cases}
\tag{20}
$$

Further, the variance and covariance of $\ln(G^{\alpha_1}(T,n)/S_2^{\alpha_2}(T,n))$ and $\ln V(T,n)$ are

$$
\begin{cases}
H_1 = \mathrm{Var}\left[\ln\dfrac{G^{\alpha_1}(T,n)}{S_2^{\alpha_2}(T,n)}\right] = \alpha_1^2\sigma_G^2T + \alpha_2^2\sigma_2^2T - 2\alpha_1\alpha_2\sigma_G\sigma_2\rho_{2V}\rho_{GV}T + n\alpha_1^2\gamma_G^2 + n\alpha_2^2\gamma_2^2,\\
H_2 = \mathrm{Var}[\ln V(T,n)] = \sigma_V^2\cdot T + n\gamma_V^2,\\
R_{12} = \mathrm{Cov}\left[\ln\dfrac{G^{\alpha_1}(T,n)}{S_2^{\alpha_2}(T,n)},\ \ln V(T,n)\right] = \left(\alpha_1\sigma_G\sigma_V\rho_{GV} - \alpha_2\sigma_2\sigma_V\rho_{2V}\right)\cdot T.
\end{cases}
\tag{21}
$$

Since $\ln(G^{\alpha_1}(T,n)/S_2^{\alpha_2}(T,n))$ and $\ln V(T,n)$ are two normal random variables with the above properties, for simplicity, it can be transformed into the following form:

$$\begin{cases} \ln \dfrac{G^{\alpha_1}(T,n)}{S_2^{\alpha_2}(T,n)} = M_1 + \sqrt{H_1}\,\xi_1, \\ \\ \ln V(T,n) = M_2 + \sqrt{H_2}\,\xi_2, \end{cases} \tag{22}$$

where (ξ_1, ξ_2) is a two-dimensional standard normally distributed random variable with correlation coefficient $\rho = (R_{12}/\sqrt{H_1} \cdot \sqrt{H_2})$. As a result,

$$\begin{aligned} K_1 &= E^Q\left[\frac{\lambda_1 G^{\alpha_1}(T,n)}{\lambda_2 S_2^{\alpha_2}(T,n)} \cdot I_{\{(\lambda_1 G^{\alpha_1}(T,n)/\lambda_2 S_2^{\alpha_2}(T,n))\ge 1, V(T,n)\ge L^*\}}\right] \\ &= \frac{\lambda_1}{\lambda_2} e^{M_1+(1/2)H_1} N_2\left(\frac{M_1 - \ln(\lambda_2/\lambda_1) + H_1}{\sqrt{H_1}}, \frac{M_2 - \ln L^* + \rho\sqrt{H_1}\sqrt{H_2}}{\sqrt{H_2}}, \rho\right), \\ K_2 &= E^Q\left[I_{\{(\lambda_1 G^{\alpha_1}(T,n)/\lambda_2 S_2^{\alpha_2}(T,n))\ge 1, V(T,n)\ge L^*\}}\right] = N_2\left(\frac{M_1 - \ln(\lambda_2/\lambda_1)}{\sqrt{H_1}}, \frac{M_2 - \ln L^*}{\sqrt{H_2}}, \rho\right), \\ K_3 &= \frac{(1-\alpha)}{L} E^Q\left[\frac{\lambda_1 G^{\alpha_1}(T,n)}{\lambda_2 S_2^{\alpha_2}(T,n)} \cdot V(T,n) \cdot I_{\{(\lambda_1 G^{\alpha_1}(T,n)/\lambda_2 S_2^{\alpha_2}(T,n))\ge 1, V(T,n)< L^*\}}\right] \\ &= \frac{\lambda_1}{\lambda_2} \cdot \frac{(1-\alpha)}{L} \cdot e^{M_1+M_2+(1/2)H_1+(1/2)H_2+\rho\sqrt{H_1}\sqrt{H_2}} \cdot N_2\left(\frac{M_1 - \ln(\lambda_2/\lambda_1) + H_1 + \rho\sqrt{H_1}\sqrt{H_2}}{\sqrt{H_1}}, -\frac{\ln L^* - M_2 - \rho\sqrt{H_1}\sqrt{H_2} - H_2}{\sqrt{H_2}}, -\rho\right). \end{aligned} \tag{23}$$

Similarly,

$$\begin{aligned} K_4 &= \frac{(1-\alpha)}{L} E^Q\left[V(T,n) \cdot I_{\{(\lambda_1 G^{\alpha_1}(T,n)/\lambda_2 S_2^{\alpha_2}(T,n))\ge 1, V(T,n)< L^*\}}\right] \\ &= \frac{(1-\alpha)}{L} e^{M_2+(1/2)H_2} N_2\left(\frac{M_1 - \ln(\lambda_2/\lambda_1) + \rho\sqrt{H_1}\sqrt{H_2}}{\sqrt{H_1}}, \right. \\ &\quad \left. -\frac{M_2 - \ln L^* + H_2}{\sqrt{H_2}}, -\rho\right), \end{aligned} \tag{24}$$

and finally, we get the pricing formula of the first kind of dual-currency power exchange options with jump risk. □

3.2. Solution of the Pricing Model of Type 2. For the power-exchange option model of the second kind of dual currency, the following conclusions can be obtained by applying the similar method.

Theorem 2. *Power exchange options with double risks of exchange rate and default under the second kind of jump risk have the following pricing formula:*

$$\begin{aligned} C^{**} &= e^{-r_d T} \lambda_2 E\left[X(T) S_2^{\alpha_2}(T)\right] \cdot \sum_{n=0}^{\infty} \frac{\left(\lambda^{\widehat{Q}} T\right)^n e^{-\lambda^{\widehat{Q}} T}}{n!} \\ &\quad \cdot \left(K_1' - K_2' + K_3' - K_4'\right) \\ &= \lambda_2 e^{-r_d T} \cdot X(0) S_2^{\alpha_2}(0) \cdot \exp\left\{\alpha_2\left(r_d - \frac{\sigma_X^2}{2} - \frac{\sigma_2^2}{2} \right.\right. \\ &\quad \left. - \rho_{2X}\sigma_2\sigma_X\right) T - \frac{1}{2}\alpha_2^2\left(\sigma_X^2 + 2\sigma_X\sigma_2\rho_{2V}\rho_{VX} + \sigma_2^2\right) T \\ &\quad + \alpha_2(-k_V\lambda - k_2\lambda) T + \lambda\left(e^{\mu_X + (1/2)\gamma_X^2} - 1\right) T \\ &\quad \left. + \lambda\left(e^{\alpha_2\mu_2 + (1/2)\alpha_2^2\gamma_2^2} - 1\right) T \right\} \\ &\quad \cdot \sum_{n=0}^{\infty} \frac{\left(\lambda^{\widehat{Q}} T\right)^n e^{-\lambda^{\widehat{Q}} T}}{n!} \cdot \left(K_1' - K_2' + K_3' - K_4'\right), \end{aligned} \tag{25}$$

where

$$K_1' = \frac{\lambda_1}{\lambda_2} e^{M_1' + (1/2) H_1'} N_2\left(\frac{M_1' - \ln(\lambda_2/\lambda_1) + H_1'}{\sqrt{H_1'}}, \frac{M_2' - \ln L^* + \rho\prime \sqrt{H_1'}\sqrt{H_2'}}{\sqrt{H_2'}}, \rho'\right),$$

$$K_2' = N_2\left(\frac{M_1' - \ln(\lambda_2/\lambda_1)}{\sqrt{H_1'}}, \frac{M_2' - \ln L^*}{\sqrt{H_2'}}, \rho\prime\right),$$

$$K_3' = \frac{\lambda_1}{\lambda_2} \cdot \frac{(1-\alpha)}{L} \cdot e^{M_1' + M_2' + (1/2) H_1' + (1/2) H_2' + \hat{\rho}\sqrt{H_1'}\sqrt{H_2'}} \cdot N_2\left(\frac{M_1' - \ln(\lambda_2/\lambda_1) + H_1' + \rho' \sqrt{H_1'}\sqrt{H_2'}}{\sqrt{H_1'}}, -\frac{\ln L^* - M_2' - \rho' \sqrt{H_1'}\sqrt{H_2'} - H_2'}{\sqrt{H_2'}}, -\rho'\right),$$

$$K_4' = \frac{(1-\alpha)}{L} \cdot e^{M_2' + (1/2) H_2'} \cdot N_2\left(\frac{M_1' - \ln(\lambda_2/\lambda_1) + \rho' \sqrt{H_1'}\sqrt{H_2'}}{\sqrt{H_1'}}, -\frac{M_2' - \ln L^* + H_2'}{\sqrt{H_2'}}, -\rho'\right). \tag{26}$$

4. Numerical Examples

According to the calculation results of two kinds of dual-currency power exchange options, we assign the related parameters in the pricing formula and simulate a numerical case to illustrate how some specific factors affect the price of power exchange options.

Firstly, we consider the first characteristic of power exchange options, the exponential factor of magnification, and analyze how the dual-currency power exchange options with exchange rate and default risk will react with the change of option time under the influence of exponential power. Secondly, in order to explore what kind of influence is taken by the jump risk, exchange rate risk, and default risk, respectively, we increase the special circumstances as the comparison sample: no jump risk fragile dual-currency power exchange option, without the fragility of the exchange rate risk jumping power exchange option, and without the risk of default dual-currency bouncing power exchange options, according to the two differences between them were analyzed and determine each factor's influence on power exchange option price direction and the amplitude of the influence. Finally, for the basic model of power exchange options with the dual risk of exchange rate and default with the jump process studied in this paper, the influence of the change of important parameters related to the jump process on the price of options is considered.

As a reference standard for numerical simulation test, Table 1 summarizes the assignment of selected basic parameters. The values of the following parameters are mainly derived from those of Wang et al. [12], which are commonly used in the literature by Bakshi et al. [21] and Christoffersen et al. [22]. Without loss of generality, we set the initial price of the underlying asset to be $S_1(0) = S_2(0) = 5.0$ and the domestic risk-free rate to be $r = 0.02$. Assume that the instantaneous volatility of the underlying asset to be $\sigma_1 = \sigma_2 = 0.15$ and the jump intensity to be $\lambda = 1$. Now, we should choose the parameters of the option seller's assets, and we assume instantaneous volatility $\sigma_V = 0.15$, the limit for a company to actually default is 3/4 of the initial value of the seller's assets $V(0)$; that is to say, in the following example, the default barrier $L^* = 7.5$, and Chen [23] found in the literature that the bond recovery rate of 9 different states was about 0.60, so we set the self-weight cost below to be $\alpha = 0.40$. Finally, the option expiration date is assumed to be $T = 1.0$. In Figures 1 and 2 and Table 1, we will change the parameter values accordingly to research the impact of exchange rate risk, counterparty risk, and jump risk on the option price. Other variables maintain the values listed in Table 1.

At the same time, to confirm the value of n, we should analyze the convergence of the series $\sum_{n=0}^{\infty}((\lambda^{\hat{Q}}T)^n/n!)$. By using MATLAB, the following calculation is chosen for accuracy 0.001.

Next, we analyze the exponential sensitivity of power exchange options. The basic operations are set the expiration time as a variable on the premise that the data in the above parameter table remain unchanged. Change index term of power exchange options under the triple risk of exchange rate, volatility risk, counterparty default risk, and jump risk. Specifically, the exponential coefficients are set to be $\alpha_1 = \alpha_2 = 1; 1.5; 2; 2.5$. Then, observe the relative position of the four curves.

Figures 1 and 2, respectively, represent the price changes of power exchange options with different index terms related to expiration time T in two types of dual-currency power exchange options. From the trend, the option price increases with the expiration time T. However, due to the difference in the magnification factor of the index term, when the option α becomes larger, it is more sensitive to the expiration time T, which is what we understand the function of leverage in economic terms. In a benign financial environment, index power changes the structure of returns and effectively hedges risks. However, in a vicious financial environment, the higher the leverage, the more losses will be multiplied. If not timely controlled, the single high-leverage behavior can even cause irreconcilable harm to the entire financial market.

By comparing Figures 1 and 2, no matter which index value is selected, we find that, at time 0, the price of the power exchange option of the first type of dual currency is higher than the price of the power exchange option of the second type of dual currency. However, the second kind of

Table 1: Parameter assignment table.

Parameter	Assignment
Initial price $S_1(0)$	5.0
Constant coefficient λ_1	1
Index coefficient α_1	2
Volatility σ_1	0.15
Domestic risk-free rate r_d r_d	0.02
Initial rate X	1
Initial asset V	10
Deadweight loss α	0.4
Material default limit L^*	7.5
Creditor's rights L	7.5
Correlation coefficient ρ_{1V}	0.5
Maturity date T	1
Intensity of jump λ	1
Step of jump μ_X	0
Standard deviation γ_1	0.1
Standard deviation γ_2	0.1
Initial price $S_2(0)$	5.0
Constant coefficient λ_2	1
Index coefficient α_2	2
Volatility σ_2	0.15
Foreign risk-free rate r_f	0.03
Volatility σ_X	0.15
Volatility σ_V	0.15
Correlation coefficient ρ_{1X}	0.5
Correlation coefficient ρ_{VX}	0.2
Correlation coefficient ρ_{2X}	0.5
Correlation coefficient ρ_{2V}	0.5
Step of jump μ_1	0
Step of jump μ_2	0
Step of jump μ_V	0
Standard deviation γ_X	0.1
Standard deviation γ_V	0.1

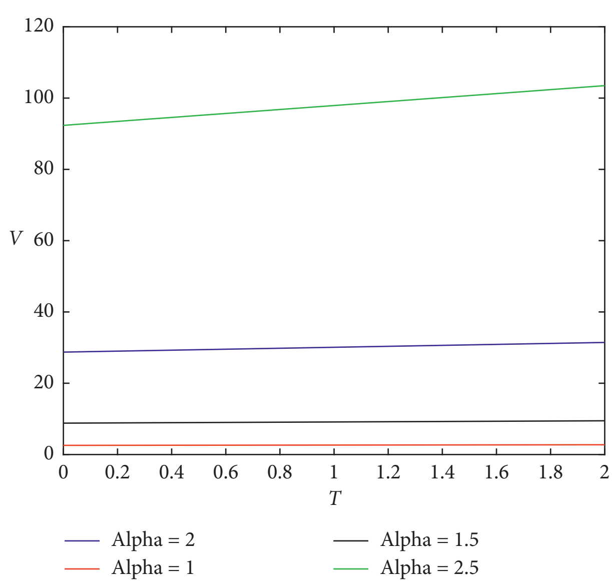

Figure 1: Exponential change of the first kind of dual-currency power exchange option price and expiration time.

the dual-currency power exchange option is more sensitive than the first kind of the dual-currency power exchange option.

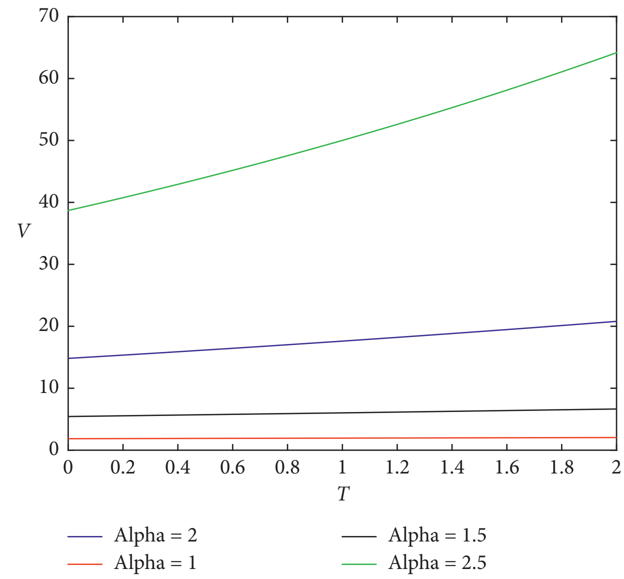

Figure 2: Exponential change of the second kind of dual-currency power exchange option price and expiration time.

Lines in Figures 3–6, black, green, red, and blue lines, represent the exchange rate, the risk of default, jumping, three kinds of standard power exchange option, no jump risk, power exchange option, without the risk of default power exchange option, and exchange rate risk of power exchange option of option value with the changing trend of related parameters.

Figures 3 and 4, respectively, represent the changing relationship between the value and expiration time of power swap options in two types of dual currencies. The overall trend is that, regardless of which of the three risks is removed, the option price increases with the expiration time.

In Figure 3, in the event of a market impact, compared with no jump risk, green line, black line, and red line, blue line all had greater growth, which is similar to our conjecture. As an example, in March 2018, when the trade war between China and the United States was launched, the market sentiment was depressed, and the global stock market fell, and the Shanghai stock index immediately fell below 3200. Many asset prices were suddenly impacted. Adding the same situation to our research when some unforeseen major events occur, it will not only cause the price of the underlying assets to soar or plummet but also take huge fluctuation to the value of the company, even cause frequent fluctuation of exchange rate. By the combined influence of these risk factors, the option price is bound to be higher than the option price without jump risk. A similar conclusion can be drawn from Figure 4, that is, the occurrence of major unexpected events will lead to the increase of option price.

Figures 5 and 6 show the impact of jump intensity λ on the option price. In terms of the overall trend, except for the nonjump risk model, the jump intensity all influences the other three models to some extent. However, despite the positive or negative impact of jump intensity on the option price, the impact range is almost zero. According to the

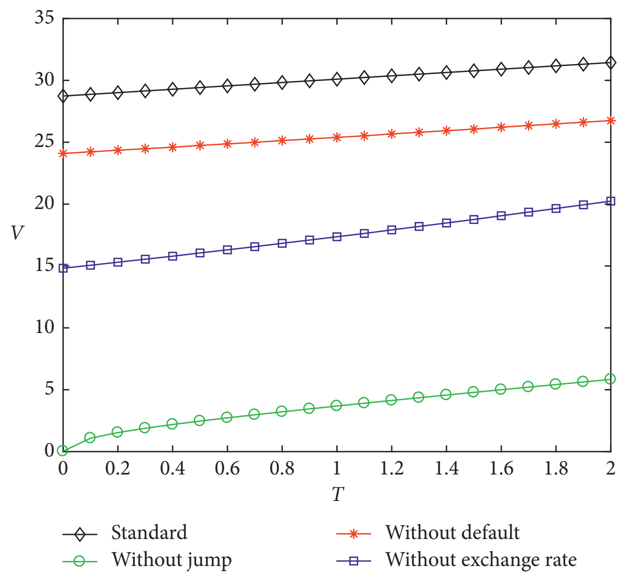

Figure 3: The relationship between the expiration time and the price of the power exchange option of the first kind in dual currency.

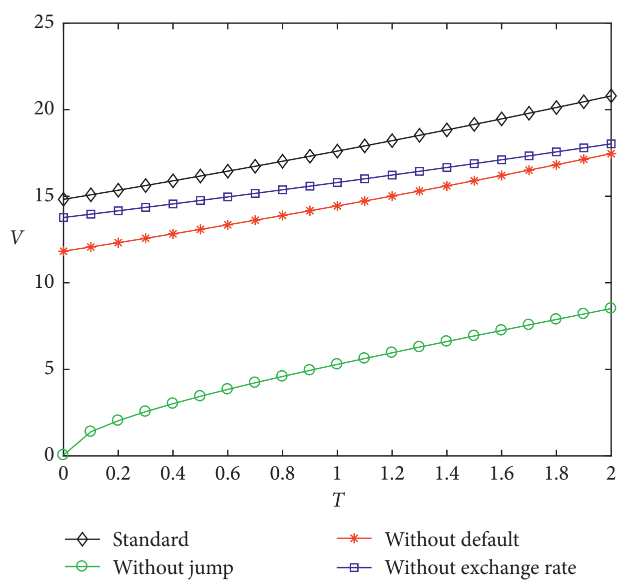

Figure 4: The relationship between the expiration time and the price of the power exchange option of the second kind in dual currency.

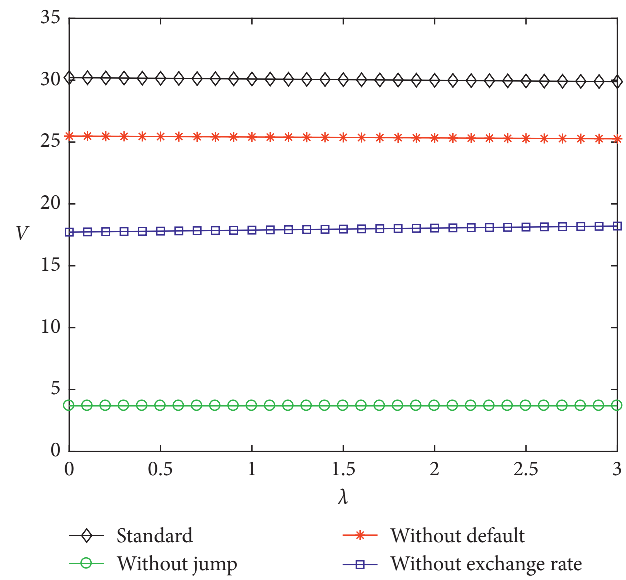

Figure 5: The relationship between jump strength and power exchange option price of the first kind in dual currency.

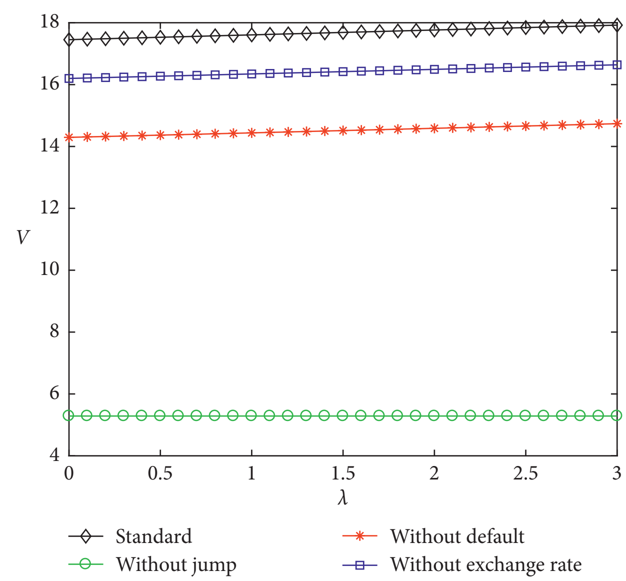

Figure 6: The relationship between jump strength and power exchange option price of the second kind in dual currency.

differences in Figures 5 and 6, for the first type of dual-currency option model, the jump intensity has a negative impact on the option price due to the change of exchange rate; for the second kind of dual-currency option model, the price of the power exchange option increases slightly with the increase of jump intensity.

To sum up, through numerical examples, we make some simple verification of the pricing formula and get the following conclusions:

(1) With the change of index term of power exchange option, the price of the power exchange option can more sensitively follow the change of relevant factors.

(2) Exchange rate risk, counterparty default risk, and jump risk all increase the price of power swap options, but their effects are different. The biggest impact is the jump risk, which is the impact of major events, which makes the price curve of power exchange options rise almost in parallel, which is consistent with the impact of major international relation events on cross-border transactions we analyzed.

(3) When other factors remain unchanged, the jump intensity makes the power exchange option price fluctuate up and down, but the fluctuation range is limited.

Data Availability

The numerical simulation data used to support the findings of this study are included within the article.

Conflicts of Interest

The authors declare that there are no conflicts of interest regarding the publication of this paper.

Authors' Contributions

The manuscript was written through the contributions of all authors. All authors read and approved the final manuscript.

Acknowledgments

This work was supported by the Ministry of Education of China Project of Humanities and Social Science (no. 19YJA790094) and the Fundamental Research Funds for the Central Universities, P.R. China (JBK2003005).

References

[1] R. Tompkins, "Power options: hedging nonlinear risks," *The Journal of Risk*, vol. 2, no. 2, pp. 29–45, 2000.

[2] S. A. Johnson and Y. S. Tian, "Indexed executive stock options," *Journal of Financial Economics*, vol. 57, no. 1, pp. 35–64, 2000.

[3] W. Margrabe, "The value of an option to exchange one asset for another," *The Journal of Finance*, vol. 33, no. 1, pp. 177–186, 1978.

[4] S. Fischer, "Call option pricing when the exercise price is uncertain, and the valuation of index bonds," *The Journal of Finance*, vol. 33, no. 1, pp. 169–176, 1978.

[5] L. P. Blenman and S. P. Clark, "Power exchange options," *Finance Research Letters*, vol. 2, no. 2, pp. 97–106, 2005.

[6] R. C. Merton, "Option prices when underlying stock returns are discontinuous," *Journal of Financial Economics*, vol. 3, no. 1-2, pp. 125–144, 1976.

[7] L. Tian, G. Wang, X. Wang, and Y. Wang, "Pricing vulnerable options with correlated credit risk under jump-diffusion processes," *Journal of Futures Markets*, vol. 34, no. 10, pp. 957–979, 2014.

[8] X. Wang, "Pricing power exchange options with correlated jump risk," *Finance Research Letters*, vol. 19, pp. 90–97, 2016.

[9] J. Hull and A. White, "The impact of default risk on the prices of options and other derivative securities," *Journal of Banking & Finance*, vol. 19, no. 11, pp. 3797–3801, 1995.

[10] P. Klein, "Pricing black-scholes options with correlated credit risk," *Journal of Banking & Finance*, vol. 20, no. 7, pp. 1211–1229, 1996.

[11] D. Brigo and F. Mercurio, "Interest rate models- theory and practice: with smile, inflation and credit," in *Springer Finance*, vol. 11, pp. 559–572, no. 4, Springer, Berlin, Germany, 2006.

[12] X. Wang, S. Song, and Y. Wang, "The valuation of power exchange options with counterparty risk and jump risk," *Journal of Futures Markets*, vol. 37, no. 5, pp. 499–521, 2017.

[13] G. L. Xu, X. J. Song, and X. C. Wang, "Analytical valuation of power exchange options with default risk," *Finance Research Letters*, vol. 28, pp. 265–274, 2019.

[14] E. Reiner, "Quanto mechanics," *Risk Magazine*, vol. 5, no. 3, pp. 59–63, 1992.

[15] Y.-K. Kwok and H.-Y. Wong, "Currency-translated foreign equity options with path dependent features and their multi-asset extensions," *International Journal of Theoretical and Applied Finance*, vol. 3, no. 2, pp. 257–278, 2000.

[16] W. Li and S. W. Zhou, "Quanto power-function exchange options pricing," *Journal of Xuzhou Istitute of Technology*, vol. 26, no. 3, pp. 35–38, 2011.

[17] H. Z. Gao and Y. W. Wang, "European option pricing model of the asset price with jump in double currency market," *Natural Science Journal of Harbin Normal University*, vol. 28, no. 6, pp. 14–16, 2012.

[18] Y. Y. Huang and J. N. He, "Research on double currency jump diffusion European option and double currency reset option based on floating exchange rate," *Finance Theory and Teaching*, vol. 3, pp. 21–26, 2017.

[19] W. Yu, Y. Yong, G. Guan, Y. Huang, W. Su, and C. Cui, "Valuing guaranteed minimum death benefits by cosine series expansion," *Mathematics*, vol. 7, no. 9, pp. 835–850, 2019.

[20] Z. Zhang, Y. Yong, and W. Yu, "Valuing equity-linked death benefits in general exponential Lévy models," *Journal of Computational and Applied Mathematics*, vol. 365, Article ID 112377, 2020.

[21] G. Bakshi, C. Cao, and Z. Chen, "Empirical performance of alternative option pricing models," *The Journal of Finance*, vol. 52, no. 5, pp. 2003–2049, 1997.

[22] P. Christoffersen, K. Jacobs, and C. Ornthanalai, "Dynamic jump intensities and risk premiums: evidence from S&P500 returns and options," *Journal of Financial Economics*, vol. 106, no. 3, pp. 447–472, 2012.

[23] H. Chen, "Macroeconomic conditions and the puzzles of credit spreads and capital structure," *Journal of Finance*, vol. 65, no. 6, pp. 2171–2212, 2010.

Hindawi
Mathematical Problems in Engineering
Volume 2020, Article ID 6207805, 26 pages
https://doi.org/10.1155/2020/6207805

Research Article

Optimal Strategies for an Ambiguity-Averse Insurer under a Jump-Diffusion Model and Defaultable Risk

Man Li,[1,2] Yingchun Deng,[1,3] Ya Huang ,[4] and Hui Ou[1,3]

[1]*LCSM, Ministry of Education, School of Mathematics and Statistics, Hunan Normal University, Changsha, Hunan 410081, China*
[2]*School of Mathematics and Physics, Nanyang Institute of Technology, Nanyang, Henan 473004, China*
[3]*Key Laboratory of Applied Statistics and Data Science, Hunan Normal University, College of Hunan Province, Changsha, Hunan 410081, China*
[4]*School of Business, Hunan Normal University, Changsha, Hunan 410081, China*

Correspondence should be addressed to Ya Huang; huangya0219@163.com

Received 24 December 2019; Accepted 4 February 2020; Published 11 March 2020

Guest Editor: Wenguang Yu

In this paper, we consider a robust optimal investment-reinsurance problem with a default risk. The ambiguity-averse insurer (AAI) may carry out transactions on a risk-free asset, a stock, and a defaultable corporate bond. The stock's price is described by a jump-diffusion process, and both the jump intensity and the distribution of jump amplitude are uncertain, i.e., the jump is ambiguous. The AAI's surplus process is assumed to follow an approximate diffusion process. In particular, the reinsurance premium is calculated according to the generalized mean-variance premium principle, and the reinsurance type has to follow a self-reinsurance function. In performing dynamic programming, both the predefault case and the postdefault case are analyzed, and the optimal strategies and the corresponding value functions are derived under the worst-case scenario. Moreover, we give a detailed proof of the verification theorem and give some special cases and numerical examples to illustrate our theoretical results.

1. Introduction

Investment is the most common way for the insurer to cope with the fierce competition in the insurance market and get higher returns, including risk-free investment (bank), risky investment (stock), and bond investment. The insurer can also transfer their risks by buying reinsurance. Therefore, the optimal investment-reinsurance problem of insurers has received extensive attention in the field of insurance and stochastic control. Browne [1] originally optimized the exponential utility of terminal wealth in order to obtain an optimal investment strategy for the insurer. Since then, a large number of works have been done concerning this topic (see Yang and Zhang [2], Bai and Guo [3], Huang et al. [4], Zhang et al. [5], Zeng et al. [6], Peng et al. [7], etc.).

For the stock's price process, some scholars have paid attention to the jump risk, such as Yu et al. [8] and Zhang et al. [9]. This is because in the face of serious events (natural disasters and serious large-scale diseases), the stock price may jump to a new level. Therefore, it is not suitable for the stock price to be described by a geometric Brownian motion (GBM) with the constant appreciation rate and volatility. Moreover, the optimal investment-reinsurance problem under the jump-diffusion model has drawn much attention, for example, Li et al. [10], Cao [11], Liang et al. [12], Lin et al. [13], Yang and Zhang [2], and Zhao et al. [14].

Recently, the investors/insurers have an increasing interest in the default risk of corporate bonds with high yield. Default risk (credit risk) refers to the risk that the security issuer will not be able to repay the principal and interest at the maturity of the security, which makes the investor suffer losses. Therefore, it is the purpose of investors to reduce credit risk and obtain higher returns. In fact, several scholars have addressed the portfolio optimization on corporate bonds in the last several decades. Bielecki and Jang [15] studied an optimal allocation problem associated with defaultable bond, and their goal was to maximize the expected utility of the terminal wealth. Bo et al. [16, 17] considered an investment-consumption problem for an investor who can invest in a defaultable market. For more results about default risk, see Capponi and Figueroa-López [18], Zhu et al. [19], Zhao et al. [20], and Deng et al. [21].

For the insurer, reinsurance is an important method to balance their risk and obtain higher profit via an optimal reinsurance strategy. The reinsurance includes the reinsurance premium and reinsurance type. In most of the above results, the reinsurance premium principle is calculated according to the expected value principle or variance principle, such as Liang and Bayraktar [22] and Sun et al. [23]. In previous conclusions, two types of reinsurance policies are most commonly studied in the literature. One policy is the proportional (quota-share) reinsurance (see Zhou et al. [24] and Shen and Zeng [25]), and the other policy is the excess-of-loss reinsurance (see [10, 14]). Recently, Zhang et al. [26] studied the optimal investment-insurance for insurers with the generalized mean-variance principle. In their article, a generalized mean-variance principle included two special cases: the expected value principle and the variance principle. The reinsurance policy was considered a self-reinsurance function, which included the proportional reinsurance and the excess-of-loss reinsurance.

Apart from the investment-reinsurance, recent advances are on the ambiguity aversion, the uncertainty associated with the model, and the risk aversion. In reality, it is a notorious fact that the return of risky assets is difficult to estimate accurately. Therefore, investors may consider some alternative models that are close to the estimated model to deal with portfolio selection in case of ambiguity. Anderson et al. [27] introduced the concept of ambiguity aversion and formulated a robust control problem for investors. Uppal and Wang [28] extended the results of Anderson et al. [27] under the model uncertainty robustness framework with different levels of ambiguity. For investors, Maenhout [29, 30] derived the closed-form solutions to robust optimal strategies by innovating a "homothetic robustness" framework. A lot of descendent researches of Maenhout [29, 30] concentrated on the influences of ambiguity in the field of finance or insurance, and the representative publications are Zhang and Siu [31], Yi et al. [32], Flor and Larsen [33], Pun and Wong [34], Zeng et al. [35], Zheng et al. [26], Zhang et al. [36], etc.

Moreover, the jump risk, especially that associated with disaster events, is more difficult to estimate accurately. So many scholars have paid attention to the ambiguity of jump risks. For the sake of explanation, the distribution of jump amplitude is assumed to be known and is restricted to be identical under the reference model's measure P and the alternative measure P^{ϕ}, but the jump intensity is uncertain. This topic was studied by some scholars, for example, Branger and Larsen [37], Zeng et al. [6], Sun et al. [23], and Li et al. [10]. But in most instances, the distribution of jump amplitude is unknown. Jin et al. [38] considered the dynamic portfolio choice problem with ambiguous jump risks in a multidimensional jump-diffusion framework. In their results, both the jump amplitude distribution and the jump intensity were assumed to be uncertain.

For these reasons, we choose a jump-diffusion process to describe the price of the stock and consider the robust model to find an optimal strategy in this paper. Moreover, the AAI is allowed to buy reinsurance and allocate his/her wealth among a risk-free asset, a stock, and a default corporate bond. According to Zhang et al. [5], we assume that the reinsurance premium is calculated about the generalized mean-variance principle, which is more general than that reported by Sun et al. [23] and Li et al. [10]. Specifically, in our model, the stock's price changes dramatically, while the parameters of the underlying jump processes are difficult to estimate accurately. Therefore, we assume that the stock's jump amplitude distribution and the jump intensity are uncertain, which are different from those reported by Sun et al. [23] and Li et al. [10]. The surplus of an AAI is described by an approximate diffusion process. In light of the principle of dynamic programming, the corresponding Hamilton–Jacobi–Bellman (HJB) equations are deduced for both the postdefault case and the predefault case. Using the variable change and variable separation techniques, we obtain the optimal reinsurance and investment strategies and the corresponding value functions. Our goal is to maximize the expected utility of terminal wealth under the worst-case scenario according to the max-min expected utility. Finally, we exemplify our deductions by some special cases and numerical cases, which verify our theoretical results.

Here, we arrange the remaining part of this paper as follows: Section 2 formulates the robust investment-reinsurance optimization regarding the default risk under the jump-diffusion model. In Section 3, we derive the closed-form expressions for the optimal strategies and the corresponding value functions under the predefault case and postdefault case, respectively. Section 4 provides a proof of the verification theorem. Section 5 provides some special cases. Numerical examples of our results are demonstrated in Section 6. Finally, conclusions are given in Section 7.

2. Model Formulation

In this article, we consider a complete probability space $(\Omega, \mathcal{F}, P)$. Let $\mathbb{F} := (\mathcal{F}_t)_{t\geq 0}$ be the right-continuous, P-complete filtration generated by two standard Brownian motions $\{W_1(t)\}$ and $\{W_2(t)\}$, a Poisson process $\{N(t)\}$, and two families of random variables $\{Y_i, i \geq 1\}$ and $\{Z_i, i \geq 1\}$. We assume that $\{W_1(t)\}, \{W_2(t)\}, \{N(t)\}$, $\{Y_i\}$, and $\{Z_i\}$ are mutually independent. Let $\mathbb{G}: = (\mathcal{G}_t)_{t\geq 0}$ be the enlarged filtration of $\mathbb{F}$ and $\mathbb{H}$, i.e., $\mathcal{G}_t: = \mathcal{F}_t \vee \mathcal{F}_t^H$, where the filtration $\mathbb{H} = (\mathcal{F}_t^H)_{t\geq 0}$ is generated by a default process $\{H(t)\}$. We assume that every $\mathbb{F}$-martingale is also a $\mathbb{G}$-martingale. The probability measure P is the real-world probability measure, and Q is the risk-neutral measure.

2.1. The Financial Market. In this section, we consider a financial market consisting of three types of securities: a risk-free asset, a stock, and a defaultable corporate bond. The price process of the risk-free asset under the measure P is described by

$$\mathrm{d}R(t) = rR(t)\mathrm{d}t, \tag{1}$$

where $r > 0$ is the risk-free interest rate. The price process $\{S(t)\}_{t\geq 0}$ of a stock is described by a jump-diffusion process:

$$\mathrm{d}S(t) = S(t-)\left[\mu\,\mathrm{d}t + \sigma\,\mathrm{d}W_1(t) + \mathrm{d}\sum_{i=1}^{N_1(t)} Y_i\right], \tag{2}$$

where $\mu > 0$ is the expected instantaneous rate of return of the stock; σ is a positive constant; $\{N_1(t)\}_{t\in[0,T]}$ is a homogeneous Poisson process with intensity λ_1, representing the number of a stock price's jumps during the time interval $[0,t]$; and Y_i is the ith jump amplitude of the stock's price, and $Y_1, Y_2, \ldots$, are i.i.d. random variables with the common distribution function $F_1(y)$, the first moment $E[Y_i] = \mu_Y$, and the second moment $E[Y_i^2] = \sigma_Y^2$. We assume that $P\{Y_i > -1 \text{ for all } i \geq 1\}$ to ensure that the stock's price remains positive. Generally, the expect return of the stock is larger than the risk-free interest rate, so we assume that $\mu + \lambda_1\mu_Y > r$.

Next, we consider that $N(\mathrm{d}t, \mathrm{d}y)$ is a Poisson random measure on $\Omega \times [0,T] \times (-1,\infty)$ and $v(\mathrm{d}t,\mathrm{d}y)$ is the compensator measure of $N(\mathrm{d}t,\mathrm{d}y)$. That is, $\widetilde{N}(\mathrm{d}t,\mathrm{d}y) = N(\mathrm{d}t,\mathrm{d}y) - v(\mathrm{d}t,\mathrm{d}y)$, and then

$$\mathrm{d}S(t) = S(t-)\left[\mu\,\mathrm{d}t + \sigma\,\mathrm{d}W_1(t) + \int_{-1}^{\infty} yN(\mathrm{d}t,\mathrm{d}y)\right], \tag{3}$$

where $v(\mathrm{d}t,\mathrm{d}y) = \lambda_1\mathrm{d}t\,\mathrm{d}F_1(y)$. By the definition of $\mathbb{F}$, for any $A \in \mathscr{B}((-1,\infty))$, $\{\widetilde{N}(t,A) \mid t \in [0,T]\}$ is a $(P,\mathbb{F})$-martingale.

Next, we consider the price process of the defaultable corporate bond by the intensity-based approach. Let τ be the time of default and τ represent the first jump time of a Poisson process with constant intensity $h^P > 0$ under P. A default indicator process is defined as $H(t) := I_{\{\tau\leq t\}}$ for each $t\geq 0$, and the value of the corporate bond is assumed to be zero after default. Let $\mathbb{H}$ be the filtration generated by the default process $H(t)$ and augmented in the usual way. By definition, τ is naturally an $\mathbb{H}$-stopping time and a $\mathbb{G}$-stopping time. Furthermore, the martingale default process is thus given by $M^P(t) = H(t) - \int_0^t (1 - H(u))h^P\mathrm{d}u$, which is a $(P,\mathbb{G})$-martingale. By Girsanov's theorem in Bielecki and Jang [15], under the chosen risk-neutral measure Q, the arrival intensity of default is given by $h^Q = h^P/\Delta$. We denote that $1/\Delta \geq 1$ is the default risk premium. We assume that there exists a defaultable zero coupon bond with a maturity date T_1, and the insurer can recover a fraction of the market value of the defaultable bond just prior to default. Now, for the positive interest rate r, the price dynamics of the defaultable bond under P is (see Deng et al. [21])

$$\begin{aligned}\mathrm{d}p(t,T_1) = p(t-,T_1)[r\,\mathrm{d}t + (1 - H(t))\delta(1-\Delta)\mathrm{d}t \\ - (1 - H(t-))\zeta\,\mathrm{d}M^P(t)\big],\end{aligned} \tag{4}$$

where $\delta := \zeta h^Q$ represents the risk-neutral credit spread and $0 < \zeta < 1$ denotes the loss rate of the bond when a default occurs.

2.2. Dynamics of Surplus Process. The insurer's surplus process $\{U_0(t)\}_{t\geq 0}$ is described by a jump-diffusion risk model:

$$\mathrm{d}U_0(t) = c\,\mathrm{d}t + \sigma_0\,\mathrm{d}W_2(t) - \mathrm{d}\sum_{i=1}^{N_2(t)} Z_i, \tag{5}$$

where c is the premium rate and $\sigma_0 \geq 0$ is a constant. $\sum_{i=1}^{N_2(t)} Z_i$ represents the aggregate claim amount up to time t, where $\{N_2(t)\}$ is a homogeneous Poisson process with intensity $\lambda_2 > 0$, and the individual claim sizes $Z_1, Z_2, \ldots$, independent of $\{N_2(t)\}$, are i.i.d. positive random variables with the common distribution function $F_2(z)$, the first moment $E[Z_i] = \mu_Z$, and the second moment $E[Z_i^2] = \sigma_Z^2$.

In addition, the insurance premium rate c under the expected value principle is given by $c = \lambda_2\mu_Z(1+\theta_0)$, where $\theta_0 > 0$ is the relative safety loading of the insurer. Suppose the insurer wants to reduce his/her risk by purchasing reinsurance. If there is a claim Z_i at time t, a proportion $\mathscr{H}(Z_i)$ (self-reinsurance function, see Schmidli [39]) is paid by the insurer, and the rest $Z_i - \mathscr{H}(Z_i)$ is paid by the reinsurer. $c^{\mathscr{H}}$ is the premium rate of the reinsurer and is calculated according to the generalized mean-variance principle [5]. So, the premium rate of the insurer is

$$c - c^{\mathscr{H}} = \lambda_2\left[(\theta_0 - \eta)\mu_Z + (1+\eta)\left(E\mathscr{H}(Z_i) - \theta_1 E(Z_i - \mathscr{H}(Z_i))^2\right)\right], \tag{6}$$

where $\eta \geq 0$ and $\theta_1 \geq 0$ is the relative safety loading of the reinsurer.

According to Grandell [40], the surplus process can be approximated by the following diffusion process:

$$\begin{aligned}\mathrm{d}U(t) = \lambda_2\big[(\theta_0 - \eta)\mu_Z + \eta E\mathscr{H}(Z_i) - (1+\eta)\theta_1 E \\ \cdot (Z_i - \mathscr{H}(Z_i))^2\big]\mathrm{d}t + \sigma_0\mathrm{d}W_2(t) \\ + \sqrt{\lambda_2 E(\mathscr{H}(Z_i))^2}\mathrm{d}W_3(t).\end{aligned} \tag{7}$$

While the self-reinsurance function $\mathscr{H}(\cdot)$ may take various forms, Zhang et al. [5] supposed that

$$\mathscr{H}(Z_i) = a(\eta + 2(1+\eta)\theta_1 Z_i) \wedge Z_i, \quad t \in [0,T], \tag{8}$$

where $a \in [0, (1/2(1+\eta)\theta_1)]$. Next, we will only consider reinsurance strategies given by (8). In this case, since $\mathscr{H}(Z_i)$ is uniquely characterized by the parameter a, we also rewrite $\mathscr{H}(Z_i)$ as $\mathscr{H}(a, Z_i)$ to emphasize the dependence on a and call a as the insurer's reinsurance strategy. That is, $\mathscr{H}(a, Z_i) = a(\eta + 2(1+\eta)\theta_1 Z_i) \wedge Z_i$. At any time t, with a larger a, the insurer reduces expenses on reinsurance and pays a larger proportion of each claim by himself/herself. Specially, when $a = 1/2(1+\eta)\theta_1$, $\mathscr{H}(a, Z_i) = Z_i$, that is, the insurer pays all of the claims by himself/herself; when $a = 0$, he/she transfers all of the claims to the reinsurer according to Chen et al. [41]. Then, the surplus process of the insurer under the retention $\mathscr{H}$ at time t is given by

$$\begin{aligned} dU^{\mathscr{H}}(t) &= \lambda_2\left[(\theta_0-\eta)\mu_Z+\eta E\mathscr{H}(a,Z_i)-(1+\eta)\theta_1 E\right.\\ &\quad \left.\cdot\left(Z_i-\mathscr{H}(a,Z_i)\right)^2\right]dt+\sigma_0 dW_2(t)\\ &\quad +\sqrt{\lambda_2 E\left(\mathscr{H}(a,Z_i)\right)^2}dW_3(t). \end{aligned} \tag{9}$$

Remark 1. If $\eta=0$, then $\mathscr{H}(Z_i)=2a\theta_1 Z_i$ becomes a proportional reinsurance type (see also Zhou et al. [24] and Zheng et al. [26]); if $\theta_1=0$, then $\mathscr{H}(Z_i)=(a\eta)\wedge Z_i$ becomes an excess-of-loss reinsurance type, the reinsurance premium under the mean principle (see also Zhao et al. [14] and Li et al. [10]). Therefore, proportional reinsurance and excess-of-loss reinsurance are special cases of (8).

2.3. The Wealth Process. In this section, we assume that the insurer is allowed to invest all his/her surplus in the financial market defined above. The insurer's trading strategy is $\pi(t)=(\pi_1(t),\pi_2(t),a)$, where $\pi_1(t)$ is the total amount of wealth invested in the risky asset (a stock) at time t, $\pi_2(t)$ is the amount of wealth invested in the defaultable corporate bond, and a is the insurer's reinsurance strategy. The remainder amount is invested in the risk-free asset. We assume that the corporate bond is not traded after default, and the investment horizon is $[0,T]$, where $T<T_1$. The reserve process subjected to this choice is denoted by $X^{\pi}(T)$. Thus, the wealth process can be presented as follows:

$$\begin{aligned} dX^{\pi}(t) &= \frac{X(t)-\pi_1(t)-\pi_2(t)}{R(t)}dR(t)+\frac{\pi_1(t)}{S(t-)}dS(t)+\frac{\pi_2(t)}{p(t-,T_1)}dp(t,T_1)+dU^{\mathscr{H}}(t)\\ &=\left\{rX(t)+(\mu-r)\pi_1(t)+\pi_2(t)(1-H(t))\delta+\lambda_2\left[(\theta_0-\eta)\mu_Z+\eta E\mathscr{H}(a,Z_i)-(1+\eta)\theta_1 E\left(Z_i-\mathscr{H}(a,Z_i)\right)^2\right]\right\}dt\\ &\quad +\pi_1(t)\sigma\, dW_1(t)+\pi_1(t)\int_{-1}^{\infty} yN(dt,dy)+\sigma_0 dW_2(t)+\sqrt{\lambda_2 E\left(\mathscr{H}(a,Z_i)\right)^2}dW_3(t)-\pi_2(t)(1-H(t-))\zeta\, dH(t). \end{aligned} \tag{10}$$

Suppose that the insurer has an exponential utility function defined by

$$U(x)=-\frac{1}{\alpha}e^{-\alpha x},\quad \alpha>0. \tag{11}$$

For an admissible control $\pi(t)$ and an initial value (x,h), we define the objective function as

$$\sup_{\pi\in\Pi} E\left[U\left(X^{\pi}(T)\right)\mid (X(t),H(t))=(x,h)\right]=\sup_{\pi\in\Pi} E\left[-\frac{1}{\alpha}e^{-\alpha X^{\pi}(T)}\,\middle|\,(X(t),H(t))=(x,h)\right]. \tag{12}$$

We denote the set of all admissible strategies by Π. Then, we have the following definition for the set of admissible strategies.

Definition 1. A trading strategy $\pi(t)=(\pi_1(t),\pi_2(t),a(t))$ is said to be admissible if

(i) $\pi(t)$ is $\mathbb{G}$-progressively measurable

(ii) $E^{P^{\phi}}[\int_0^T(\pi_1^2(t)+\pi_2^2(t)+a^2(t))dt]<\infty$

(iii) $\forall(\pi(t),X^{\pi}(t))$, the stochastic differential equation (10) has a pathwise unique solution $X^{\pi}(t)$ with $E^{P^{\phi}}[\exp(-\alpha X^{\pi}(t))]<\infty$, where P^{ϕ} is the chosen measure to describe the worst case and will be shown later

However, the AAI wants to guard himself/herself against worst-case scenarios. We assume that the knowledge of the AAI about ambiguity is described by probability P, namely, the reference probability (or model). But, he/she is skeptical about this reference model and hopes to consider alternative models, which are defined as a class of probability measures $\mathscr{P}:=\{P^{\phi}\mid P^{\phi}\sim P\}$ equivalent to P (Anderson et al. [27] and Zeng et al. [6]). At first, we define a process $\phi(t,y)=(\phi_1(t),\phi_2(t),\phi_3(t),\phi_4(t),\phi_5(t),\varphi(t,y))$ such that

(1) $\phi(t,y)$ is $\mathscr{G}_t$-measurable, for each $t\in[0,T]$

(2) $\phi_4(t)=\phi_4(t,\omega)>0$ and $\phi_5(t)\varphi(t,y)=\phi_5(t,\omega)\varphi(t,y,\omega)>0$ a.s. $(t,y,\omega)\in[0,T]\times(-1,\infty)\times\Omega$

(3) $\int_0^T[\phi_1^2(t)+\phi_2^2(t)+\phi_3^2(t)+\phi_4^2(t)]dt<\infty$ and $\int_0^T\int_{-1}^{\infty}\phi_5^2(t)\varphi^2(t,y)dF_1(y)dt<\infty$, P-a.s.

The alternative measures $\phi_1(t),\phi_2(t),\phi_3(t),\phi_4(t),\phi_5(t)$, and $\varphi(t,y)$ are positive stochastic processes. We write Σ for the space of all such processes ϕ. Note that P is the probability measure associated with the reference model. For every $\phi\in\Sigma$, each probability measure $P^{\phi}\in\mathscr{P}$ has a Radon–Nikodym derivative:

$$\left.\frac{dP^{\phi}}{dP}\right|_{\mathscr{G}_T}:=\Lambda^{\phi}(T), \tag{13}$$

with respect to P, where the process $\Lambda^{\phi}(t)$ is modelled by the stochastic differential equation (see Jin et al. [38])

$$\Lambda^{\phi}(t) := \exp\left\{\int_0^t \phi_1(u)\mathrm{d}W_1(u) - \frac{1}{2}\int_0^t \phi_1^2(u)\mathrm{d}u - \int_0^t \phi_2(u)\mathrm{d}W_2(u) - \frac{1}{2}\int_0^t \phi_2^2(u)\mathrm{d}u \right.$$
$$\left. - \int_0^t \phi_3(u)\mathrm{d}W_3(u) - \frac{1}{2}\int_0^t \phi_3^2(u)\mathrm{d}u + \int_0^t \ln\phi_4(u)\mathrm{d}H(u) + h^P\int_0^t (1-\phi_4(u))(1-H(u))\,\mathrm{d}u\right\} \tag{14}$$
$$+ \int_0^t\int_{-1}^{\infty} \ln(\phi_5(u)\varphi(u,y))N(\mathrm{d}u,\mathrm{d}y) + \int_0^t\int_{-1}^{\infty}(1-\phi_5(u)\varphi(u,y))v(\mathrm{d}u,\mathrm{d}y),$$

with $\Lambda^{\phi}(0) = 1$, P-a.s. By the Itô differentiation rule, we get

$$\mathrm{d}\Lambda^{\phi}(t) = \Lambda^{\phi}(t-) - \Big(\phi_1(t)\mathrm{d}W_1(t) - \phi_2(t)\mathrm{d}W_2(t)$$
$$- \phi_3(t)\mathrm{d}W_3(t) - (1-\phi_4(t))\mathrm{d}M^P(t)\Big) \tag{15}$$
$$- \int_{-1}^{\infty}(1-\phi_5(t)\varphi(t,y))\widetilde{N}(\mathrm{d}t,\mathrm{d}y).$$

Note that $\phi_5(t)$ and $\varphi(t,y)$ are positive stochastic processes, and $\varphi(t,y)$ satisfies the following relationship:

$$\int_{-1}^{\infty}\varphi(t,y)\mathrm{d}F_1(y) = 1. \tag{16}$$

The distribution of the stock's jump amplitude and the jump intensity is ambiguous, so the density function is not equal under P and P^{ϕ}. Under the probability measure P^{ϕ}, the jump intensity λ_1 and the density function $\mathrm{d}F_1(y)$ of the stock's price process are changed into $\phi_5(t)\lambda_1$ and $\varphi(t,y)\mathrm{d}F_1(y)$ in the alternative model. That is, $\lambda_1^{P^{\phi}}(t) = \phi_5(t)\lambda_1$, and $\widetilde{N}^{P^{\phi}}(\mathrm{d}t,\mathrm{d}y) := N(\mathrm{d}t,\mathrm{d}y) - \phi_5(t)\varphi(t,y)\lambda_1\mathrm{d}t\,\mathrm{d}F_1(y)$ is a compensated Poisson random measure. For the default indicator process $H(t): \;= H_{\{\tau\le t\}}$, $t\ge 0$, the intensity h^P of the jumps becomes $\phi_4(t)h^P$, and the jump size is always equal to 1, so the jump size distribution is identical under P and P^{ϕ}. For three standard Brownian motions, according to Girsanov's theorem, $\mathrm{d}W_i^{P^{\phi}}(t) = \mathrm{d}W_i(t) + \phi_i(t)\mathrm{d}t$, $i = 1,2,3$. Thus, the wealth process under P^{ϕ} becomes that

$$\mathrm{d}X^{\pi}(t) = \Big\{rX(t) + (\mu-r)\pi_1(t) + \pi_2(t)(1-H(t))\delta + \lambda_2\big[(\theta_0-\eta)\mu_Z + \eta E\mathscr{H}(a,Z_i) - (1+\eta)\theta_1 E(Z_i - \mathscr{H}(a,Z_i))^2\big]$$
$$-\phi_1(t)\pi_1(t)\sigma - \phi_3(t)\sqrt{\lambda_2 E(\mathscr{H}(a,Z_i))^2}\Big\}\mathrm{d}t \tag{17}$$
$$- \sigma_0\phi_2(t) + \pi_1(t)\sigma\,\mathrm{d}W_1^{P^{\phi}}(t) + \sigma_0\mathrm{d}W_2^{P^{\phi}}(t) + \sqrt{\lambda_2 E(\mathscr{H}(a,Z_i))^2}\,\mathrm{d}W_3^{P^{\phi}}(t)$$
$$+ \pi_1(t)\int_{-1}^{\infty} yN(\mathrm{d}t,\mathrm{d}y) - \pi_2(t)(1-H(t-))\zeta\,\mathrm{d}H(t).$$

To simplify further analysis, we define the following functions:

$$g_0(x) = \frac{\eta x}{1-2(1+\eta)\theta_1 x},$$
$$g(z) = \eta + 2(1+\eta)\theta_1 z,$$
$$h_1(a) := \eta h_3(a) - (1+\eta)\theta_1 h_4(a),$$
$$h_2(a) := E\big[\mathscr{H}(a,Z)^2\big] = 2\int_0^a x\left(\int_{g_0(x)}^{\infty} g^2(z)\mathrm{d}F_2(z)\right)\mathrm{d}x, \tag{18}$$
$$h_3(a) := E[\mathscr{H}(a,Z)] = \int_0^a\left(\int_{g_0(x)}^{\infty} g^2(z)\mathrm{d}F_2(z)\right)\mathrm{d}x,$$
$$h_4(a) := E\big[(Z-\mathscr{H}(a,Z))^2\big] = 2\int_a^{1/2(1+\eta)\theta_1}\left(\int_{g_0(x)}^{\infty}[z - xg(z)]g(z)\mathrm{d}F_2(z)\right)\mathrm{d}x.$$

Then, the dynamics of the wealth process under P^{ϕ} is

$$\begin{aligned}\mathrm{d}X^{\pi}(t) = \Big[& rX(t) + (\mu - r)\pi_1(t) + \pi_2(t)(1 - H(t))\delta + \lambda_2\left((\theta_0 - \eta)\mu_Z + h_1(a)\right) - \phi_1(t)\pi_1(t)\sigma - \sigma_0\phi_2(t) - \phi_3(t)\sqrt{\lambda_2 h_2(a)}\Big]\mathrm{d}t \\ & + \pi_1(t)\sigma\,\mathrm{d}W_1^{P^{\phi}}(t) + \sigma_0\mathrm{d}W_2^{P^{\phi}}(t) + \sqrt{\lambda_2 h_2(a)}\mathrm{d}W_3^{P^{\phi}}(t) + \pi_1(t)\int_{-1}^{\infty} yN(\mathrm{d}t, \mathrm{d}y) - \pi_2(t)(1 - H(t-))\zeta\,\mathrm{d}H(t).\end{aligned} \tag{19}$$

Next, we assume that the insurer determines a robust portfolio strategy which is the best choice in some worst-case models as Anderson et al. [42]. The insurer penalizes any deviation from this reference model and the penalty increases with this deviation. Then, we use relative entropy to measure the deviation between the reference measure P and an alternative measure P^{ϕ}. The increase in relative entropy from t to $t + \mathrm{d}t$ is shown by

$$\begin{aligned}&\frac{1}{2}\phi_1^2(t)\mathrm{d}t + \frac{1}{2}\phi_2^2(t)\mathrm{d}t + \frac{1}{2}\phi_3^2(t)\mathrm{d}t + \left(\phi_4(t)\ln\phi_4(t) - \phi_4(t) + 1\right)h^P(1 - h)\mathrm{d}t \\ &\quad + \int_{-1}^{\infty}\left[\phi_5(t)\varphi(t, y)\ln\left(\phi_5(t)\varphi(t, y)\right) - \phi_5(t)\varphi(t, y) + 1\right]\lambda_1\mathrm{d}F_1(y)\mathrm{d}t,\end{aligned} \tag{20}$$

with $h \in \{0, 1\}$. The increase is caused by three diffusion components and two jump components.

On the basis of Branger and Larsen [37], which allows the insurer's ambiguity aversion with respect to the diffusion risk and jump risk to differ from each other, we can modify problem (12) and define the value function as

$$V(t, x, h) := \sup_{\pi\in\Pi}\inf_{\phi\in\sum} E_{x,h}^{P^{\phi}}\left[-\frac{1}{\alpha}e^{-\alpha X^{\pi}(T)} + \int_t^T G(u, X^{\pi}(u), \phi(u))\mathrm{d}u\right], \tag{21}$$

where $E_{x,h}^{P^{\phi}}$ is calculated under the alternative measure P^{ϕ}, the initial values of the processes are given by $X^{\pi}(t) = x, H(t) = h$, and

$$\begin{aligned}G(t, X^{\pi}(t), \phi(t)) = & \frac{\phi_1^2(t)}{2\Psi_1(t, X^{\pi}(t), H(t))} + \frac{\phi_2^2(t)}{2\Psi_2(t, X^{\pi}(t), H(t))} + \frac{\phi_3^2(t)}{2\Psi_3(t, X^{\pi}(t), H(t))} \\ & + \frac{\left(\phi_4(t)\ln\phi_4(t) - \phi_4(t) + 1\right)h^P(1 - H(t))}{\Psi_4(t, X^{\pi}(t), H(t))} \\ & + \frac{\int_{-1}^{\infty}\left[\phi_5(t)\varphi(t, y)\ln\left(\phi_5(t)\varphi(t, y)\right) - \phi_5(t)\varphi(t, y) + 1\right]\lambda_1 dF_1(y)}{\Psi_5(t, X^{\pi}(t), H(t))}.\end{aligned} \tag{22}$$

The five terms in (22) are scaled by $\Psi_1 \geq 0, \Psi_2 \geq 0, \Psi_3 \geq 0, \Psi_4 \geq 0$, and $\Psi_5 \geq 0$, which are state-dependent. We follow Maenhout [29] and set

$$\begin{aligned}\Psi_1(t, x, h) &= -\frac{\beta_1}{\alpha V(t, x, h)}, \\ \Psi_2(t, x, h) &= -\frac{\beta_2}{\alpha V(t, x, h)}, \\ \Psi_3(t, x, h) &= -\frac{\beta_3}{\alpha V(t, x, h)}, \\ \Psi_4(t, x, h) &= -\frac{\beta_4}{\alpha V(t, x, h)}, \\ \Psi_5(t, x, h) &= -\frac{\beta_5}{\alpha V(t, x, h)},\end{aligned} \tag{23}$$

where $\beta_i \geq 0, i = 1, 2, 3, 4, 5$, is the ambiguity aversion coefficient with respect to three diffusion risks and two jump risks. The larger the values of $\Psi_1, \Psi_2, \Psi_3, \Psi_4$, and Ψ_5 are, the less a given deviation from the reference model is penalized, the less the faith of the insurer in the reference model, and the more the worst-case model will deviate from the reference model.

3. The Main Result

In this section, the goal is to find the optimal allocation pair $(\pi_1(t), \pi_2(t), a(t))$ under the worst-case scenario. According to the dynamic programming principle, the HJB equation can be derived as (Anderson et al. [42])

$$\sup_{\pi\in\Pi}\inf_{\phi\in\Sigma}\left\{\mathscr{A}^{\pi,\phi}V+G\left(t,X^{\pi}(t),\phi(t)\right)\right\}=0, \tag{24}$$

with the boundary condition $V(T,x,h)=-(1/\alpha)e^{-\alpha x}$, where $\mathscr{A}^{\pi,\phi}$ is the infinitesimal generator of (21) under P^{ϕ} and is defined by

$$\begin{aligned}\mathscr{A}^{\pi,\phi}V(t,x,h)={}&V_t+V_x\left\{rx+(\mu-r)\pi_1(t)+(1-h)\delta\pi_2(t)+\lambda_2\left[(\theta_0-\eta)\mu_Z+h_1(a)\right]-\sigma\phi_1(t)\pi_1(t)-\sigma_0\phi_2(t)-\phi_3(t)\sqrt{\lambda_2h_2(a)}\right\}\\&+\frac{1}{2}V_{xx}\left(\sigma^2\pi_1^2(t)+\sigma_0^2+\lambda_2h_2(a)\right)+\lambda_1E_{P\phi}\left[V\left(t,x+\pi_1(t)Y,h\right)-V(t,x,h)\right]\\&+h^P(1-h)\left(V\left(t,x-\pi_2(t)\zeta,1\right)-V(t,x,0)\right)\phi_4(t),\end{aligned} \tag{25}$$

where V_t,V_x, and V_{xx} represent the value function's partial derivatives with respect to the corresponding variables. We split equation (24) into two cases: the postdefault case ($h=1$) and the predefault case ($h=0$), and denote V as follows:

$$\begin{aligned}V(t,x,h)&=V(t,x,1)\\&=V(t,x,0).\end{aligned} \tag{26}$$

According to (26) and (21), the HJB equation (24) transforms into the following two forms:

$$\begin{aligned}0=\sup_{\pi\in\Pi}\inf_{\phi\in\Sigma}\Bigg\{&V_t(t,x,1)+V_x(t,x,1)\left[rx+(\mu-r)\pi_1(t)+\lambda_2\left[(\theta_0-\eta)\mu_Z+h_1(a)\right]-\sigma\phi_1(t)\pi_1(t)-\sigma_0\phi_2(t)-\phi_3(t)\sqrt{\lambda_2h_2(a)}\right]\\&+\frac{1}{2}V_{xx}(t,x,1)\left[\sigma^2\pi_1^2(t)+\sigma_0^2+\lambda_2h_2(a)\right]+E_{P\phi}\left[V\left(t,x+\pi_1(t)Y,1\right)-V(t,x,1)\right]\\&-\frac{\phi_1^2(t)\alpha}{2\beta_1}V(t,x,1)-\frac{\phi_2^2(t)\alpha}{2\beta_2}V(t,x,1)-\frac{\phi_3^2(t)\alpha}{2\beta_3}V(t,x,1)\\&-\frac{\int_{-1}^{\infty}\left(\phi_5\varphi(t,y)\ln\left(\phi_5(t)\varphi(t,y)\right)-\phi_5(t)\varphi(t,y)+1\right)\lambda_1\mathrm{d}F_1(y)}{\beta_5}\alpha V(t,x,1)\Bigg\},\end{aligned} \tag{27}$$

$$\begin{aligned}0=\sup_{\pi\in\Pi}\inf_{\phi\in\Sigma}\Bigg\{&V_t(t,x,0)+V_x(t,x,0)\Bigg[rx+(\mu-r)\pi_1(t)+\delta\pi_2(t)+\lambda_2\left[(\theta_0-\eta)\mu_Z+h_1(a)\right]-\sigma\phi_1(t)\pi_1(t)-\sigma_0\phi_2(t)-\phi_3(t)\\&\cdot\sqrt{\lambda_2h_2(a)}\Bigg]+\frac{1}{2}V_{xx}(t,x,0)\left(\sigma^2\pi_1^2(t)+\sigma_0^2+\lambda_2h_2(a)\right)+E_{P\phi}\left[V\left(t,x+\pi_1(t)Y,0\right)-V(t,x,0)\right]+h^P\phi_5(t)\left(V\left(t,x-\pi_2(t)\zeta,1\right)\right.\\&\left.-V(t,x,0)\right)-\frac{\phi_1^2(t)}{2\beta_1}\alpha V(t,x,0)-\frac{\phi_2^2(t)}{2\beta_2}\alpha V(t,x,0)-\frac{\phi_3^2(t)}{2\beta_3}\alpha V(t,x,0)\\&-\frac{\int_{-1}^{\infty}\left(\phi_5(t)\varphi(t,y)\ln\left(\phi_5(t)\varphi(t,y)\right)-\phi_5(t)\varphi(t,y)+1\right)\lambda_1\mathrm{d}F_1(y)}{\beta_5}\alpha V(t,x,0)-\frac{\left(\phi_4(t)\ln\phi_4(t)-\phi_4(t)+1\right)}{\beta_4}h^P\alpha V(t,x,0)\Bigg\}.\end{aligned} \tag{28}$$

In the following two sections, we derive the optimal reinsurance and investment strategies and corresponding value functions in the postdefault case and predefault case, respectively.

3.1. The Postdefault Case.

In this section, we will concentrate on the postdefault case, that is, HJB equation (27) for $V(t,x,1)$, and we conjecture that the value function has the following form:

$$V(t,x,1) = -\frac{1}{\alpha}\exp\left\{-\alpha x e^{r(T-t)}\right\} g_1(t), \tag{29}$$

where $g_1(t)$ is a deterministic function, with $g_1(T) = 1$. We get

$$\begin{cases} V_t(t,x,1) = \left[\dfrac{g_1'(t)}{g_1(t)} + r\alpha x e^{r(T-t)}\right] V(t,x,1), \\ V_x(t,x,1) = -\alpha e^{r(T-t)} V(t,x,1), \\ V_{xx}(t,x,1) = \alpha^2 e^{2r(T-t)} V(t,x,1), \\ E\left[V(t, x+\pi_1(t)Y, 1) - V(t,x,1)\right] = \lambda_1 \\ \displaystyle\int_{-1}^{\infty}\left(e^{-\alpha\pi_1(t)e^{r(T-t)}y} - 1\right)\phi_5(t)\varphi(t,y)dF_1(y)V(t,x,1). \end{cases} \tag{30}$$

Substituting these partial derivatives and $E[\cdot]$ into equation (27), we get

$$\begin{aligned} 0 = \inf_{\phi\in\Sigma}\sup_{\pi\in\Pi}\Bigg\{ & \frac{g_1'(t)}{g_1(t)} - \alpha e^{r(T-t)}\left[(\mu-r)\pi_1(t) - \sigma\phi_1(t)\pi_1(t) - \sigma_0\phi_2(t) + \lambda_2\left[(\theta_0-\eta)\mu_Z + h_1(a)\right] - \phi_3(t)\sqrt{\lambda_2 h_2(a)}\right] \\ & + \frac{1}{2}\alpha^2 e^{2r(T-t)}\left(\sigma^2\pi_1^2(t) + \sigma_0^2\right) + \frac{1}{2}\alpha^2 e^{2r(T-t)}\lambda_2 h_2(a) \\ & + \lambda_1\int_{-1}^{\infty}\left(e^{-\alpha\pi_1(t)e^{r(T-t)}y} - 1\right)\phi_4(t)\varphi(t,y)\mathrm{d}F_1(y) - \frac{\phi_1^2(t)}{2\beta_1}\alpha - \frac{\phi_2^2(t)}{2\beta_2}\alpha - \frac{\phi_3^2(t)}{2\beta_3}\alpha \\ & -\frac{\lambda_1\alpha}{\beta_5}\int_{-1}^{\infty}\left(\phi_5(t)\varphi(t,y)\ln\left(\phi_5(t)\varphi(t,y)\right) - \phi_5(t)\varphi(t,y) + 1\right)\mathrm{d}F_1(y)\Bigg\}. \end{aligned} \tag{31}$$

Fixing π and a and maximizing over ϕ yield the following first-order condition for the minimum point $\phi^* = (\phi_1^*, \phi_2^*, \phi_3^*, \phi_5^*, \varphi^*)$ (there is no ambiguity about the default jump risk after default):

$$\begin{aligned} \phi_1^*(t) &= \beta_1\sigma\pi_1(t)e^{r(T-t)}, \\ \phi_2^*(t) &= \beta_2\sigma_0 e^{r(T-t)}, \\ \phi_3^*(t) &= \beta_3\sqrt{\lambda_2 h_2(a)}e^{r(T-t)}, \\ \phi_5^*(t)\varphi^*(t,y) &= \exp\left\{\frac{\beta_5}{\alpha}\left(e^{-\alpha\pi_1(t)e^{r(T-t)}y} - 1\right)\right\}. \end{aligned} \tag{32}$$

Noting that $E[\varphi(t,Y)] = 1$ (formula (16)), we have

$$\begin{aligned} \varphi^*(t,y) &= \frac{1}{\phi_5^*(t)}\exp\left\{\frac{\beta_5}{\alpha}\left(e^{-\alpha\pi_1(t)e^{r(T-t)}y} - 1\right)\right\}, \\ \phi_5^*(t) &= E\left[\exp\left\{\frac{\beta_5}{\alpha}\left(e^{-\alpha\pi_1(t)e^{r(T-t)}Y} - 1\right)\right\}\right]. \end{aligned} \tag{33}$$

Lemma 1. *For any $t \in [0,T]$, the equation*

$$\pi_1(t) = \frac{e^{-r(T-t)}}{\sigma^2(\alpha+\beta_1)}\left[\mu - r + \lambda_1\int_{-1}^{\infty} y e^{-\alpha\pi_1(t)e^{r(T-t)}y}\exp\left\{\frac{\beta_5}{\alpha}\left(e^{-\alpha\pi_1(t)e^{r(T-t)}y} - 1\right)\right\}\mathrm{d}F_1(y)\right], \tag{34}$$

has a unique positive solution $\pi_1^*(t)$.

Proof. Suppose $W(t,\pi_1)=\mu-r+\lambda_1\int_{-1}^{\infty} ye^{-\alpha\pi_1(t)e^{r(T-t)}y}\exp\{(\beta_5/\alpha)(e^{-\alpha\pi_1(t)e^{r(T-t)}y}-1)\}\mathrm{d}F_1(y)-\sigma^2(\alpha+\beta_1)\pi_1(t)e^{r(T-t)}$, then we get

$$\begin{aligned}\frac{\partial W(t,\pi_1)}{\partial\pi_1}=&-\lambda_1\alpha e^{r(T-t)}\int_{-1}^{\infty}y^2e^{-\alpha\pi_1(t)e^{r(T-t)}y}\exp\left\{\frac{\beta_5}{\alpha}\left(e^{-\alpha\pi_1(t)e^{r(T-t)}y}-1\right)\right\}\mathrm{d}F_1(y)\\&-\sigma^2(\alpha+\beta_1)e^{r(T-t)}-\lambda_1\beta_5e^{r(T-t)}\int_{-1}^{\infty}y^2e^{-2\alpha\pi_1(t)e^{r(T-t)}y}\exp\left\{\frac{\beta_5}{\alpha}\left(e^{-\alpha\pi_1(t)e^{r(T-t)}y}-1\right)\right\}\mathrm{d}F_1(y)<0,\end{aligned}\tag{35}$$

which implies that $W(t,\pi_1)$ is a decreasing function w.r.t. π_1. Furthermore, we have $W(t,0)=\mu-r+\lambda_1\int_{-1}^{\infty}y\,\mathrm{d}F_1(y)=\mu-r+\lambda_1\mu_Y>0$. Also, we can find that if $\pi_1(t)>\mu-r+\lambda_1\mu_Y/\sigma^2(\alpha+\beta_1)e^{r(T-t)}>0$, we have $W(t,\pi_1)<0$. Therefore, equation (34) has a unique positive root $\pi_1^*(t)$. □

Lemma 2. *For the functions $h_i(a)$, $i=1,2,3,4$, defined above, we have the following relationship:*

$$\begin{aligned}h_1'(a)&=-\frac{h_2'(a)}{2}\left[2(1+\eta)\theta_1-\frac{1}{a}\right],\\h_1(a)&=-(1+\eta)\theta_1h_4(0)-\frac{h_2(a)}{2}\left[2(1+\eta)\theta_1-\frac{1}{a}\right]+\int_0^a\frac{h_2(x)}{2x^2}\mathrm{d}x,\\&=-(1+\eta)\theta_1h_4(0)-(1+\eta)\theta_1h_2(a)+\int_0^a\left(\int_{g_0(x)}^{\infty}g(z)\mathrm{d}F_2(z)\right)dx.\end{aligned}\tag{36}$$

Substituting ϕ^* into (31), according to the first-order condition and Lemmas 1 and 2, we can obtain the maximum point $\pi^*:=(\pi_1^*,\pi_2^*,a^*)$ given by

$$\begin{aligned}\pi_1^*(t)&=\frac{e^{-r(T-t)}}{\sigma^2(\alpha+\beta_1)}\left[\mu-r+\lambda_1\int_{-1}^{\infty}ye^{-\alpha\pi_1^*(t)e^{r(T-t)}y}\exp\left\{\frac{\beta_5}{\alpha}\left(e^{-\alpha\pi_1^*(t)e^{r(T-t)}y}-1\right)\right\}\mathrm{d}F_1(y)\right],\\\pi_2^*(t)&=0,\\a^*(t)&=\frac{1}{2(1+\eta)\theta_1+(\alpha+\beta_3)e^{r(T-t)}}.\end{aligned}\tag{37}$$

Substituting π^* and ϕ^* into (31), we get the equation

$$\begin{aligned}0=&\frac{g_1'(t)}{g_1(t)}+\frac{\alpha+\beta_2}{2}\alpha\sigma_0^2e^{2r(T-t)}-\alpha\lambda_2e^{r(T-t)}(\theta_0-\eta)\mu_Z-\frac{\lambda_1\alpha}{\beta_5}-\alpha e^{r(T-t)}(\mu-r)\pi_1^*(t)\\&+\frac{\alpha+\beta_1}{2}\alpha\sigma^2e^{2r(T-t)}(\pi_1^*(t))^2+\frac{\lambda_1\alpha}{\beta_5}\int_{-1}^{\infty}\exp\left\{\frac{\beta_5}{\alpha}\left(e^{-\alpha\pi_1^*(t)e^{r(T-t)}y}-1\right)\right\}\mathrm{d}F_1(y)\\&-\alpha\lambda_2e^{r(T-t)}\left[h_1(a^*(t))-\frac{\alpha+\beta_3}{2}h_2(a^*(t))e^{r(T-t)}\right].\end{aligned}\tag{38}$$

Therefore, we can derive the following theorem.

Theorem 1 (postdefault strategy). *The robust optimal reinsurance and investment strategies for the period after default are given as*

$$\begin{cases} \phi_1^*(t) = \beta_1 \sigma \pi_1(t) e^{r(T-t)}, \\ \phi_2^*(t) = \beta_2 \sigma_0 e^{r(T-t)}, \\ \phi_3^*(t) = \beta_3 \sqrt{\lambda_2 h_2(a)}\, e^{r(T-t)}, \\ \varphi^*(t,y) = \dfrac{1}{\phi_5^*} \exp\left\{\dfrac{\beta_5}{\alpha}\left(e^{-\alpha\pi_1(t)e^{r(T-t)}y} - 1\right)\right\}, \\ \phi_5^*(t) = E\left[\exp\left\{\dfrac{\beta_5}{\alpha}\left(e^{-\alpha\pi_1(t)e^{r(T-t)}Y} - 1\right)\right\}\right], \\ \pi_1^*(t) = \dfrac{e^{-r(T-t)}}{\sigma^2(\alpha+\beta_1)}\left[\mu - r + \lambda_1 \displaystyle\int_{-1}^{\infty} y e^{-\alpha\pi_1^*(t)e^{r(T-t)}y} \exp\left\{\dfrac{\beta_5}{\alpha}\left(e^{-\alpha\pi_1^*(t)e^{r(T-t)}y} - 1\right)\right\} \mathrm{d}F_1(y)\right], \\ \pi_2^*(t) = 0, \\ a^*(t) = \dfrac{1}{2(1+\eta)\theta_1 + (\alpha+\beta_3)e^{r(T-t)}}. \end{cases} \tag{39}$$

Furthermore, the postdefault value function is given by

$$V(t,x,1) = -\frac{1}{\alpha}\exp\left\{-\alpha x e^{r(T-t)}\right\} g_1(t), \tag{40}$$

where

$$\begin{aligned} g_1(t) = \exp\Bigg\{\int_t^T \Bigg\{ & \frac{\alpha+\beta_2}{2}\alpha\sigma_0^2 e^{2r(T-u)} - \alpha\lambda_2 e^{r(T-u)}(\theta_0 - \eta)\mu_Z - \frac{\lambda_1\alpha}{\beta_5} - \alpha e^{r(T-u)}(\mu - r)\pi_1^*(u) + \frac{\alpha+\beta_1}{2}\alpha\sigma^2 e^{2r(T-u)}\left(\pi_1^*(u)\right)^2 \\ & + \frac{\lambda_1\alpha}{\beta_5}\int_{-1}^{\infty}\exp\left\{\frac{\beta_5}{\alpha}\left(e^{-\alpha\pi_1^*(u)e^{r(T-u)}y} - 1\right)\right\}\mathrm{d}F_1(y) - \alpha\lambda_2 e^{r(T-u)}\left[h_1(a^*(u)) - \frac{\alpha+\beta_3}{2}h_2(a^*(u))e^{r(T-u)}\right]\Bigg\}\mathrm{d}u\Bigg\}. \end{aligned} \tag{41}$$

3.2. The Predefault Case. In this section, we will concentrate on the predefault case, that is, HJB equation (28) for $V(t,x,0)$, and we conjecture that the value function has the following form:

$$V(t,x,0) = -\frac{1}{\alpha}\exp\left\{-\alpha x e^{r(T-t)}\right\} g_2(t), \tag{42}$$

where $g_2(t)$ is a deterministic function, with $g_2(T) = 1$. We get

$$\begin{cases} V_t(t,x,0) = \left[\dfrac{g_2'(t)}{g_2(t)} + r\alpha x e^{r(T-t)}\right] V(t,x,0), \\ V_x(t,x,0) = -\alpha e^{r(T-t)} V(t,x,0), \\ V_{xx}(t,x,0) = \alpha^2 e^{2r(T-t)} V(t,x,0), \\ E\left[V(t, x+\pi_1(t)Y, 0) - V(t,x,0)\right] = \lambda_1 \displaystyle\int_{-1}^{\infty}\left(e^{-\alpha\pi_1(t)e^{r(T-t)}y} - 1\right)\phi_5(t)\varphi(t,y) dF_1(y) V(t,x,0), \\ V(t, x-\pi_2(t)\zeta, 1) - V(t,x,0) = \left(\dfrac{g_1(t)}{g_2(t)}\exp\left\{\alpha\zeta\pi_2(t)e^{r(T-t)}\right\} - 1\right) V(t,x,0). \end{cases} \tag{43}$$

Substituting these partial derivatives, $E[\cdot]$, and $V(\cdot,\cdot,1) - V(\cdot,\cdot,0)$ into equation (28), we get

$$\begin{aligned}
0 = \inf_{\phi\in\Sigma}\sup_{\pi\in\Pi}\Bigg\{&\frac{g_2'(t)}{g_2(t)} - \alpha e^{r(T-t)}\Big[(\mu-r)\pi_1(t) + \pi_2(t)\delta - \sigma\phi_1(t)\pi_1(t) - \sigma_0\phi_2(t) + \lambda_2\big((\theta_0-\eta)\mu_Z + h_1(a)\big) - \phi_3(t)\sqrt{\lambda_2 h_2(a)}\Big]\\
&+\frac{1}{2}\alpha^2 e^{2r(T-t)}\big(\sigma^2\pi_1^2(t) + \sigma_0^2 + \lambda_2 h_2(a)\big) - \frac{\phi_1^2(t)}{2\beta_1}\alpha\\
&-\frac{\phi_2^2(t)}{2\beta_2}\alpha - \frac{\phi_3^2(t)}{2\beta_3}\alpha + \lambda_1\int_{-1}^{\infty}\Big(e^{-\alpha\pi_1(t)e^{r(T-t)}y} - 1\Big)\phi_5(t)\varphi(t,y)\mathrm{d}F_1(y)\\
&+\phi_5(t)h^P\left(\frac{g_1(t)}{g_2(t)}\exp\big\{\alpha\zeta\pi_2(t)e^{r(T-t)}\big\} - 1\right) - \frac{\phi_4(t)\ln\phi_4(t) - \phi_4(t) + 1}{\beta_4}h^P\alpha\\
&-\frac{\lambda_1\alpha}{\beta_5}\int_{-1}^{\infty}\big(\phi_5(t)\varphi(t,y)\ln\big(\phi_5(t)\varphi(t,y)\big) - \phi_5(t)\varphi(t,y) + 1\big)\mathrm{d}F_1(y)\Bigg\}.
\end{aligned} \tag{44}$$

Fixing π and maximizing over ϕ yield the following first-order condition for the minimum point $\phi^{*'} = (\phi_1^{*'}, \phi_2^{*'}, \phi_3^{*'}, \phi_4^{*'}, \phi_5^{*'}, \varphi^{*'})$:

$$\begin{aligned}
\phi_1^{*'}(t) &= \beta_1\sigma\pi_1(t)e^{r(T-t)},\\
\phi_2^{*'}(t) &= \beta_2\sigma_0 e^{r(T-t)},\\
\phi_3^{*'}(t) &= \beta_3\sqrt{\lambda_2 h_2(a)}e^{r(T-t)},\\
\ln\phi_4^{*}(t) &= \frac{\beta_4}{\alpha}\left[\frac{g_1(t)}{g_2(t)}\exp\big\{\alpha\zeta\pi_2(t)e^{r(T-t)}\big\} - 1\right],\\
\phi_5^{*'}(t)\varphi^{*'}(t,y) &= \exp\left\{\frac{\beta_5}{\alpha}\left(e^{-\alpha\pi_1(t)e^{r(T-t)}y} - 1\right)\right\}.
\end{aligned} \tag{45}$$

Noting that $E[\varphi(t,Y)] = 1$, we have

$$\begin{aligned}
\varphi^{*'}(t,y) &= \frac{1}{\phi_5^{*'}(t)}\exp\left\{\frac{\beta_5}{\alpha}\left(e^{-\alpha\pi_1(t)e^{r(T-t)}y} - 1\right)\right\},\\
\phi_5^{*'}(t) &= E\left[\exp\left\{\frac{\beta_5}{\alpha}\left(e^{-\alpha\pi_1(t)e^{r(T-t)}Y} - 1\right)\right\}\right].
\end{aligned} \tag{46}$$

Substituting $\phi^{*'}$ into (44), according to the first-order condition, we can obtain the maximum point $\pi^{*'} := (\pi_1^{*'}, \pi_2^{*'}, a^{*'})$ given by

$$\pi_1^{*'}(t) = \frac{e^{-r(T-t)}}{\sigma^2(\alpha+\beta_1)}\left[\mu - r + \lambda_1\int_{-1}^{\infty} y e^{-\alpha\pi_1^{*'}(t)e^{r(T-t)}y}\exp\left\{\frac{\beta_5}{\alpha}\left(e^{-\alpha\pi_1^{*'}(t)e^{r(T-t)}y} - 1\right)\right\}\mathrm{d}F_1(y)\right], \tag{47}$$

$$\pi_2^{*'}(t) = \frac{e^{-r(T-t)}}{\alpha\zeta}\left[\ln\frac{g_2(t)}{\Delta\phi_4^{*}(t)g_1(t)}\right], \tag{48}$$

$$a^{*'}(t) = \frac{1}{2(1+\eta)\theta_1 + (\alpha+\beta_3)e^{r(T-t)}}. \tag{49}$$

Substituting $\pi_2^{*'}(t)$ into equation (45), we have $(\alpha h^P/\beta_4)\phi_4^{*}(t)\ln\phi_4^{*}(t) + h^P\phi_4^{*}(t) - (\delta/\zeta) = 0$, and this equation has a unique positive root by the following lemma.

Lemma 3. *Let* $\widetilde{W}(t,\phi_4) = (\alpha h^P/\beta_4)\phi_4(t)\ln\phi_4(t) + h^P\phi_4(t) - (\delta/\zeta)$, *then* $\widetilde{W}(t,\phi_4)$ *has a unique positive root* $\phi_4^{*}(t)$.

Proof. It is similar to the proof of Proposition 4.2 in the study of Sun et al. [23]. So we omit it.

According to (47) and (49), we obtain $a^{*'} = a^*$ and $\pi_1^{*'} = \pi_1^*$. Substituting $\pi^{*'}$ and $\phi^{*'}$ into (44), we get the equation

$$0 = \frac{g_2'(t)}{g_2(t)} - \frac{\delta}{\zeta}\ln g_2(t) + \frac{\alpha+\beta_2}{2}\alpha\sigma_0^2 e^{2r(T-t)} - \alpha\lambda_2 e^{r(T-t)} \cdot (\theta_0-\eta)\mu_Z - \alpha e^{r(T-t)}(\mu-r)\pi_1^*(t) + \frac{\alpha+\beta_1}{2}\alpha\sigma^2 e^{2r(T-t)}(\pi_1^*(t))^2 + \frac{\lambda_1\alpha}{\beta_5}\int_{-1}^{\infty} \cdot \exp\left\{\frac{\beta_5}{\alpha}\left(e^{-\alpha\pi_1^*(t)e^{r(T-t)}y}-1\right)\right\}\mathrm{d}F_1(y) - \frac{\lambda_1\alpha}{\beta_5} - \alpha\lambda_2 e^{r(T-t)}\left[h_1(a^*(t)) - \frac{\alpha+\beta_3}{2}h_2(a^*(t))e^{r(T-t)}\right] + \frac{\delta}{\zeta}\left(\ln\Delta\phi_4^*(t) + \ln g_1(t) + \frac{\phi_4^*(t)-1}{\beta_4}\alpha\Delta\right). \tag{50}$$

Note that $g_2(t)>0$; in order to get the expression for $g_2(t)$ with the boundary condition $g_2(T)=1$, we try the following form of $g_2(t) = e^{\overline{g}_2(t)}$:

$$0 = \overline{g}_2'(t) - \frac{\delta}{\zeta}\overline{g}_2(t) + \frac{\alpha+\beta_2}{2}\alpha\sigma_0^2 e^{2r(T-t)} - \alpha\lambda_2 e^{r(T-t)} \cdot (\theta_0-\eta)\mu_Z - \frac{\lambda_1\alpha}{\beta_5} - \alpha e^{r(T-t)}(\mu-r)\pi_1^*(t) + \frac{\alpha+\beta_1}{2}\alpha\sigma^2 e^{2r(T-t)}(\pi_1^*(t))^2 + \frac{\lambda_1\alpha}{\beta_5}\int_{-1}^{\infty} \cdot \exp\left\{\frac{\beta_5}{\alpha}\left(e^{-\alpha\pi_1^*(t)e^{r(T-t)}y}-1\right)\right\}dF_1(y) - \alpha\lambda_2 e^{r(T-t)}\left[h_1(a^*(t)) - \frac{\alpha+\beta_3}{2}h_2(a^*(t))e^{r(T-t)}\right] + \frac{\delta}{\zeta}\left(\ln\Delta\phi_4^*(t) + \ln g_1(t) + \frac{\phi_4^*(t)-1}{\beta_4}\alpha\Delta\right). \tag{51}$$

Therefore, we can derive the following theorem. □

Theorem 2 (predefault strategy). *The robust optimal reinsurance and investment strategies for the period before default are given as*

$$\begin{cases} \phi_1^{*'}(t) = \beta_1\sigma\pi_1(t)e^{r(T-t)} = \phi_1^*(t), \\ \phi_2^{*'}(t) = \beta_2\sigma_0 e^{r(T-t)} = \phi_2^*(t), \\ \phi_3^{*'}(t) = \beta_3\sqrt{\lambda_2 h_2(a)}\,e^{r(T-t)} = \phi_3^*(t), \\ \dfrac{\alpha h^P}{\beta_4}\phi_4^*(t)\ln\phi_4^*(t) + h^P\phi_4^*(t) - \dfrac{\delta}{\zeta} = 0, \\ \varphi^{*'}(t,y) = \dfrac{1}{\phi_5^*(t)}\exp\left\{\dfrac{\beta_5}{\alpha}\left(e^{-\alpha\pi_1(t)e^{r(T-t)}y}-1\right)\right\} = \varphi^*(t,y), \\ \phi_5^{*'}(t) = E\left[\exp\left\{\dfrac{\beta_5}{\alpha}\left(e^{-\alpha\pi_1(t)e^{r(T-t)}Y}-1\right)\right\}\right] = \phi_5^*(t), \\ \pi_1^{*'}(t) = \dfrac{e^{-r(T-t)}}{\sigma^2(\alpha+\beta_1)}\left[\mu - r + \lambda_1\displaystyle\int_{-1}^{\infty} y e^{-\alpha\pi_1^{*'}(t)e^{r(T-t)}y} \cdot \exp\left\{\dfrac{\beta_5}{\alpha}\left(e^{-\alpha\pi_1^{*'}(t)e^{r(T-t)}y}-1\right)\right\}dF_1(y)\right] = \pi_1^*(t), \\ \pi_2^{*'}(t) = \dfrac{e^{-r(T-t)}}{\alpha\zeta}\left[\ln\dfrac{g_2(t)}{\Delta\phi_4^*(t)g_1(t)}\right], \\ a^{*'}(t) = \dfrac{1}{2(1+\eta)\theta_1 + (\alpha+\beta_3)e^{r(T-t)}} = a^*(t). \end{cases} \tag{52}$$

Furthermore, the predefault value function is given by

$$V(t,x,0) = -\frac{1}{\alpha}\exp\left\{-\alpha x e^{r(T-t)}\right\}g_2(t), \tag{53}$$

where $g_2(t) = e^{\overline{g}_2(t)}$, in which

$$\overline{g}_2(t) = e^{-(\delta/\zeta)(T-t)}\int_t^T e^{(\delta/\zeta)(T-u)}\left\{\frac{\alpha+\beta_2}{2}\alpha\sigma_0^2 e^{2r(T-u)} - \alpha e^{r(T-u)}\left[\lambda_2(\theta_0-\eta)\mu_Z + (\mu-r)\pi_1^*(u)\right] + \frac{\alpha+\beta_1}{2}\alpha\sigma^2 e^{2r(T-u)}(\pi_1^*(u))^2 - \frac{\lambda_1\alpha}{\beta_5} + \frac{\lambda_1\alpha}{\beta_5}\int_{-1}^{\infty}\exp\left\{\frac{\beta_5}{\alpha}\left(e^{-\alpha\pi_1^*(u)e^{r(T-u)}y}-1\right)\right\}\mathrm{d}F_1(y) - \alpha\lambda_2 e^{r(T-u)}\left[h_1(a^*(u)) - \frac{\alpha+\beta_3}{2}h_2(a^*(u))e^{r(T-u)}\right] + \frac{\delta}{\zeta}\left(\ln\Delta\phi_4^*(u) + \ln g_1(u) + \frac{\phi_4^*(u)-1}{\beta_4}\alpha\Delta\right)\right\}\mathrm{d}u. \tag{54}$$

Next, putting the predefault and postdefault cases together, we have the following solution to the HJB equation (24) associated with the value function $V(t,x,h)$:

$$V(t,x,h) = (1-h)V(t,x,0) + hV(t,x,1), \quad \text{where } h = 0 \text{ or } 1. \tag{55}$$

Let us define the following processes which are candidate optimal strategies:

$$\begin{aligned}
\phi_1^*(t) &= \beta_1\sigma\pi_1(t)e^{r(T-t)}, \quad t \in [0,T], \\
\phi_2^*(t) &= \beta_2\sigma_0 e^{r(T-t)}, \quad t \in [0,T], \\
\phi_3^*(t) &= \beta_3\sqrt{\lambda_2 h_2(a)}e^{r(T-t)}, \quad t \in [0,T], \\
0 &= \frac{\alpha h^P}{\beta_4}\phi_4^*(t)\ln\phi_4^*(t) + h^P\phi_4^*(t) - \frac{\delta}{\zeta}, \quad t \in [0,T], \\
\varphi^*(t,y) &= \frac{1}{\phi_5^*(t)}\exp\left\{\frac{\beta_5}{\alpha}\left(e^{-\alpha\pi_1(t)e^{r(T-t)}y} - 1\right)\right\}, \quad t \in [0,T], \\
\phi_5^*(t) &= E\left[\exp\left\{\frac{\beta_5}{\alpha}\left(e^{-\alpha\pi_1(t)e^{r(T-t)}Y} - 1\right)\right\}\right], \quad t \in [0,T], \\
\pi_1^*(t) &= \frac{e^{-r(T-t)}}{\sigma^2(\alpha+\beta_1)}\left[\mu - r + \lambda_1\int_{-1}^{\infty} ye^{-\alpha\pi_1^*(t)e^{r(T-t)}y}\right. \\
&\quad \left.\cdot\exp\left\{\frac{\beta_5}{\alpha}\left(e^{-\alpha\pi_1^*(t)e^{r(T-t)}y} - 1\right)\right\}\mathrm{d}F_1(y)\right], \\
\pi_2^*(t) &= \begin{cases} \dfrac{1}{\alpha\zeta}e^{-r(T-t)}\left[\ln\dfrac{g_2(t)}{\Delta\phi_4^*(t)g_1(t)}\right], & t \in [0,T], \\ 0, & t \in [\tau\wedge T, T], \end{cases} \\
a^*(t) &= \frac{1}{2(1+\eta)\theta_1 + (\alpha+\beta_3)e^{r(T-t)}}, \quad t \in [0,T].
\end{aligned} \tag{56}$$

From the above expressions for $\phi_1^*, \phi_2^*, \phi_3^*, \phi_4^*, \phi_5^*$, *and* φ^*, it is easy to verify that the expression $\Lambda^{\phi}(t)$ with $\phi_1^*, \phi_2^*, \phi_3^*, \phi_4^*, \phi_5^*$, *and* φ^* instead of $\phi_1, \phi_2, \phi_3, \phi_4, \phi_5$, *and* φ is indeed a P-martingale, which ensures a well-defined P^{ϕ^*}.

In the next section, we shall show that the above stochastic control policies are indeed the optimal strategies and that the value function $\widehat{V}(t,x,h)$ is unique.

4. Verification Theorem

In order to verify the candidate optimal strategies π^* and ϕ^* are indeed optimal, and the candidate value function is (55), we give the verification theorem as follows.

Proposition 1. *Let $\mathcal{O} := (0,T)\times R\times\{0,1\}$ and $\overline{\mathcal{O}}$ denote the closure of $\mathcal{O}$. Suppose that there exist a function $\widehat{V} \in \mathcal{C}^{1,2,1}(\mathcal{O})\cap\mathcal{C}(\overline{\mathcal{O}})$ and a control $(\phi^*,\pi^*) \in \Sigma\times\Pi$ such that*

(1) $\mathcal{A}^{\phi,\pi^*}\widehat{V}(t,X^{\pi^*}(t),H(t)) + G(t,X^{\pi^*}(t),\phi(t)) \geq 0$, for all $\phi \in \Sigma$

(2) $\mathcal{A}^{\phi^*,\pi}\widehat{V}(t,X^{\pi}(t),H(t)) + G(t,X^{\pi}(t),\phi^*(t)) \leq 0$, for all $\pi \in \Pi$

(3) $\mathcal{A}^{\phi^*,\pi^*}\widehat{V}(t,X^{\pi^*}(t),H(t)) + G(t,X^{\pi^*}(t),\phi^*(t)) = 0$

(4) For all $(\phi,\pi) \in \Sigma\times\Pi$: $\lim_{t\longrightarrow T-}\widehat{V}(t,X^{\pi}(t),H(t)) = U(X^{\pi}(T))$

(5) $\{\widehat{V}(\tau,X^{\pi}(\tau),H(\tau))\}_{\tau\in\mathcal{T}}$ and $\{G(\tau,X^{\pi}(\tau),\phi(\tau))\}_{\tau\in\mathcal{T}}$ are uniformly integrable, where $\mathcal{T}$ denotes the set of stopping times $\tau \leq T$

Then, $\widehat{V}(t,x,h) = V(t,x,h)$ and (ϕ^*,π^*) are an optimal control.

Proof. According to $\widehat{V} \in \mathcal{C}^{1,2,1}(\mathcal{O})\cap\mathcal{C}(\overline{\mathcal{O}})$, choose $(\phi,\pi) \in \Sigma\times\Pi$, by the definition of $H(t)$, $\widehat{V}(\tau_n,X^{\pi}(\tau_n),H(\tau_n)) = \widehat{V}(\tau_n,X^{\pi}(\tau_n),1)$, and $\widehat{V}(\tau_n,X^{\pi}(\tau_n),H(\tau_n)) = \widehat{V}(\tau_n,X^{\pi}(\tau_n),0)$; therefore, the Itô formula can be applied to $\widehat{V}(\tau_n,X^{\pi}(\tau_n),0)$:

$$\begin{aligned}
\widehat{V}(\tau_n,X^{\pi}(\tau_n),0) &= \widehat{V}(t,x,0) + \int_t^{\tau_n}\mathcal{A}^{\phi,\pi}\widehat{V}(u,X^{\pi}(u),0)\mathrm{d}u \\
&\quad + \int_t^{\tau_n}\widehat{V}_x\pi_1(u)\sigma\,\mathrm{d}W_1^{P^{\phi}}(u) \\
&\quad + \int_t^{\tau_n}\widehat{V}_x\sigma_0\mathrm{d}W_2^{P^{\phi}}(u) \\
&\quad + \int_t^{\tau_n}\widehat{V}_x\sqrt{\lambda_2 h_2(a)}\mathrm{d}W_3^{P^{\phi}}(u) \\
&\quad + \int_t^{\tau_n}\widehat{V}\int_{-1}^{\infty}\pi_1(u)yN(\mathrm{d}u,\mathrm{d}y),
\end{aligned} \tag{57}$$

where $\tau_n = T\wedge n\wedge\inf\{u>t; |X^{\pi}(u)| \geq n\}$, for $n = 1,2,\ldots$, and $\widehat{V}_x = \widehat{V}_x(t,x,0)$ and $a = a(t)$ for short. Because the continuous function $\widehat{V}_x$ is bounded on the set $[t,\tau_n]\times R$, we obtain the following estimate with an appropriate constant $M > 0$:

$$\int_t^{\tau_n}\frac{1}{2}\widehat{V}_x^2\pi_1^2(u)\sigma^2\mathrm{d}u \leq M\int_t^{\tau_n}\pi_1^2(u)\sigma^2\mathrm{d}u. \tag{58}$$

Due to (ii) of Definition 1, it follows that

$$E_{t,x,0}^{P^{\phi}}\left[\int_t^{\tau_n}\frac{1}{2}\widehat{V}_x^2\pi_1^2(u)\sigma^2\mathrm{d}u\right] < \infty. \tag{59}$$

By the similar way as that in (59), we have

$$\begin{aligned}
&E_{t,x,0}^{P^{\phi}}\left[\int_t^{\tau_n}\frac{1}{2}\widehat{V}_x^2\sigma_0^2\mathrm{d}u\right] < \infty, E_{t,x,0}^{P^{\phi}}\left[\int_t^{\tau_n}\frac{1}{2}\widehat{V}_x^2\lambda_2 h_2(a)\mathrm{d}u\right] < \infty, \\
&E_{t,x,0}^{P^{\phi}}\left[\int_t^{\tau_n}\frac{1}{2}\widehat{V}_x^2\int_{-1}^{\infty}\pi_1(u)yN(\mathrm{d}u,\mathrm{d}y)\right] < \infty.
\end{aligned} \tag{60}$$

Therefore, taking expectations in (57) leads to

$$\widehat{V}(t,x,0)=E_{t,x,0}^{P^{\phi}}\left[\widehat{V}(\tau_n,X^{\pi}(\tau_n),0)-\int_t^{\tau_n}\mathscr{A}^{\phi,\pi}\widehat{V}(u,X^{\pi}(u),0)\mathrm{d}u\right]. \tag{61}$$

If we apply (61) to (ϕ,π^*) with $\phi\in\Sigma$ and use property 1, we get

$$\widehat{V}(t,x,0)\le E_{t,x,0}^{P^{\phi}}\left[\widehat{V}\left(\tau_n,X^{\pi^*}(\tau_n),0\right)+\int_t^{\tau_n}G\left(u,X^{\pi^*}(u),\phi(u)\right)\mathrm{d}u\right]. \tag{62}$$

Letting $n\longrightarrow\infty$ and using properties 4 and 5, we have

$$\widehat{V}(t,x,0)\le E_{t,x,0}^{P^{\phi}}\left[U\left(X^{\pi^*}(T)\right)+\int_t^{T}G\left(u,X^{\pi^*}(u),\phi(u)\right)\mathrm{d}u\right]. \tag{63}$$

Since this holds for all $\phi\in\Sigma$, we deduce that

$$\widehat{V}(t,x,0)\le \inf_{\phi\in\Sigma}E_{t,x,0}^{P^{\phi}}\left[U\left(X^{\pi^*}(T)\right)+\int_t^{T}G\left(u,X^{\pi^*}(u),\phi(u)\right)\right]. \tag{64}$$

Hence,

$$\widehat{V}(t,x,0)\le \sup_{\pi\in\Pi}\inf_{\phi\in\Sigma}E_{t,x,0}^{P^{\phi}}\left[U\left(X^{\pi}(T)\right)+\int_t^{\tau_n}G\left(u,X^{\pi}(u),\phi(u)\right)\mathrm{d}u\right]=V(t,x,0). \tag{65}$$

Next, if we apply (61) to (ϕ^*,π) with $\pi\in\Pi$ and use property 2, we get

$$\widehat{V}(t,x,0)\ge E_{t,x,0}^{P^{\phi}}\left[\widehat{V}(\tau_n,X^{\pi}(\tau_n),0)+\int_t^{\tau_n}G(u,X^{\pi}(u),\phi^*(u))\mathrm{d}u\right]. \tag{66}$$

Letting $n\longrightarrow\infty$ and using properties 4 and 5, we have

$$\begin{aligned}\widehat{V}(t,x,0)&\ge E_{t,x,0}^{P^{\phi}}\left[U(X^{\pi}(T))+\int_t^{T}G(u,X^{\pi}(u),\phi^*(u))\mathrm{d}u\right]\\&\ge \inf_{\phi\in\Sigma}E_{t,x,0}^{P^{\phi}}\left[U(X^{\pi}(T))+\int_t^{T}G(u,X^{\pi}(u),\phi(u))\mathrm{d}u\right].\end{aligned} \tag{67}$$

Since this holds for all $\pi\in\Pi$, we deduce that

$$\widehat{V}(t,x,0)\ge \sup_{\pi\in\Pi}\inf_{\phi\in\Sigma}E_{t,x,0}^{P^{\phi}}\left[U(X^{\pi}(T))+\int_t^{T}G(u,X^{\pi}(u),\phi(u))\mathrm{d}u\right]=V(t,x,0). \tag{68}$$

According to (65) and (68), we get $\widehat{V}(t,x,0)=V(t,x,0)$. Finally, we apply (61) to (ϕ^*,π^*) as the above process. Then,

$$\begin{aligned}\widehat{V}(t,x,0)&=E_{t,x,0}^{P^{\phi^*}}\left[U\left(X^{\pi^*}(T)\right)+\int_t^{T}G\left(u,X^{\pi^*}(u),\phi^*(u)\right)\mathrm{d}u\right]\\&=V(t,x,0).\end{aligned} \tag{69}$$

For $h=1$, we can obtain the following result by the similar method:

$$\begin{aligned}\widehat{V}(t,x,1)&=E_{t,x,1}^{P^{\phi^*}}\left[U\left(X^{\pi^*}(T)\right)+\int_t^{T}G\left(u,X^{\pi^*}(u),\phi^*(u)\right)\mathrm{d}u\right]\\&=V(t,x,1).\end{aligned} \tag{70}$$

Thus, (ϕ^*,π^*) is an optimal control strategy about (69)-(70), and $\widehat{V}(t,x,h)=V(t,x,h)$. □

Lemma 4. *The following integral is finite:*

$$\begin{aligned}I(T):=E\Bigg[\exp\Bigg\{\int_0^T\Bigg(&\frac{\alpha}{2\beta_1}\phi_1^*(t)^2+\frac{\alpha}{2\beta_2}\phi_2^*(t)^2+\frac{\alpha}{2\beta_3}\phi_3^*(t)^2+\frac{\phi_4^*(t)\ln\phi_4^*(t)-\phi_4^*(t)+1}{\beta_4}h^P\alpha\\&+\frac{\lambda\alpha\int_{-1}^{\infty}[\phi_5^*(t)\varphi^*(t,y)\ln(\phi_5^*(t)\varphi^*(t,y))-\phi_5^*(t)\varphi^*(t,y)+1]\mathrm{d}F_1(y)}{\beta_5}\Bigg)\mathrm{d}t\Bigg\}\Bigg]<\infty.\end{aligned} \tag{71}$$

Proof. Putting ϕ^* and π_1^* into (71), with an appropriate constant $M_1 > 0$, we have

$$\begin{aligned} I(T) &= E\left[\exp\left\{\int_0^T\left(\frac{\alpha}{2}e^{2r(T-t)}\left(\beta_1\sigma^2\pi_1^{*2}+\beta_2\sigma_0^2+\beta_3\lambda_2h_2(a^*)\right)+\frac{\phi_4^*(t)\ln\phi_4^*(t)-\phi_4^*(t)+1}{\beta_4}h^P\alpha\right.\right.\right.\\ &\quad\left.\left.\left.+\frac{\lambda\alpha\int_{-1}^{\infty}[\phi_5^*(t)\varphi^*(t,y)\ln(\phi_5^*(t)\varphi^*(t,y))-\phi_5^*(t)\varphi^*(t,y)+1]\mathrm{d}F_1(y)}{\beta_5}\right)\mathrm{d}t\right\}\right]\\ &\le M_1E\left[\exp\left\{\int_0^T\left(\frac{\phi_4^*(t)\ln\phi_4^*(t)-\phi_4^*(t)+1}{\beta_4}h^P\alpha+\frac{\lambda\alpha\int_{-1}^{\infty}(\phi_5^*(t)\varphi^*(t,y)\ln(\phi_5^*(t)\varphi^*(t,y))-\phi_5(t)\varphi^*(t,y)+1)\mathrm{d}F_1(y)}{\beta_5}\right)\mathrm{d}t\right\}\right]<\infty, \end{aligned} \tag{72}$$

where the inequality is established because π^* and ϕ^* are the deterministic and bound functions on $[0,T]$. □

Lemma 5. *For the optimal control problem (21) with the exponential utility function (11), if $\widehat{V}(t,x,h)$ is the solution of (24) with the boundary condition $\widehat{V}(T,x,h)=U(x)$, then we have*

$$\begin{aligned} &E^{P^{\phi^*}}\left(\sup_{t\in[0,T]}\left|\widehat{V}\left(t,X^{\pi^*}(t),H(t)\right)\right|^4\right)<\infty,\\ &E^{P^{\phi^*}}\left(\sup_{t\in[0,T]}\left|G\left(t,X^{\pi^*}(t),\phi^*(t)\right)\right|^2\right)<\infty. \end{aligned} \tag{73}$$

Proof. Substituting (π^*,ϕ^*) into (19), we have the wealth process under (π^*,ϕ^*):

$$\begin{aligned} X^{\pi^*}(t) &= e^{rt}X^{\pi^*}(0)+\int_0^t e^{-r(u-t)}\left[(\mu-r)\pi_1^*(u)+\pi_2^*(u)(1-H(u))\delta+\lambda_2\left((\theta_0-\eta)\mu_Z+h_1(a^*)\right)-\phi_1^*(u)\pi_1^*(u)\sigma-\sigma_0\phi_2^*(u)\right.\\ &\quad\left.-\phi_3^*(u)\sqrt{\lambda_2h_2(a^*)}\right]\mathrm{d}u+\int_0^t e^{-r(u-t)}\pi_1^*(u)\sigma\,\mathrm{d}W_1^{P^{\phi^*}}(u)\\ &\quad+\int_0^t e^{-r(u-t)}\sigma_0\mathrm{d}W_2^{P^{\phi^*}}(u)+\int_0^t e^{-r(u-t)}\sqrt{\lambda_2h_2(a^*)}\mathrm{d}W_3^{P^{\phi^*}}(u)\\ &\quad-\int_0^t e^{-r(u-t)}\pi_2^*(u)(1-H(u-))\zeta\,\mathrm{d}H(u)+\int_0^t\int_{-1}^{\infty}e^{-r(u-t)}\pi_1^*(u)y\widetilde{N}^{P^{\phi^*}}(\mathrm{d}u,\mathrm{d}y). \end{aligned} \tag{74}$$

For the candidate value function (21), we get

$$\begin{aligned} \left|\widehat{V}\left(t,X^{\pi^*}(t),H(t)\right)\right|^4 &= \left|(1-H(t))\widehat{V}\left(t,X^{\pi^*}(t),0\right)+H(t)\widehat{V}\left(t,X^{\pi^*}(t),1\right)\right|^4\\ &\le 4\left|\widehat{V}\left(t,X^{\pi^*}(t),0\right)\right|^4+4\left|\widehat{V}\left(t,X^{\pi^*}(t),1\right)\right|^4. \end{aligned} \tag{75}$$

At first, we prove $E^{P^{\phi^*}}(\sup_{t\in[0,T]}|\widehat{V}(t,X^{\pi^*}(t),0)|^4)<\infty$. π^*,ϕ^*, and $g_2(t)$ are deterministic continuous functions and are bounded on $[0,T]$. Substituting (75) into (48), there are two constants K_1 and K_2 satisfying $0<K_1<K_2$ such that

$$\begin{aligned}
\left|\widehat{V}\left(t, X^{\pi^*}(t), 0\right)\right|^4 = {} & \frac{g_2^4(t)}{\alpha^4}\exp\Bigg\{-4\alpha\Bigg[e^{rt}X^{\pi^*}(0) + \int_0^t e^{-r(u-t)}(\mu - r)\pi_1^*(u) + \pi_2^*(u)(1 - H(u))\delta + \lambda_2\left((\theta_0 - \eta)\mu_Z + h_1(a^*)\right) \\
& - \phi_1^*(u)\pi_1^*(u)\sigma - \sigma_0\phi_2^*(u) - \phi_3^*(u)\sqrt{\lambda_2 h_2(a^*)}\Bigg]du + \int_0^t e^{-r(u-t)}\pi_1^*(u)\sigma\, dW_1^{P^{\phi^*}}(u) \\
& + \int_0^t e^{-r(u-t)}\sigma_0\, dW_2^{P^{\phi^*}}(u) + \int_0^t e^{-r(u-t)}\sqrt{\lambda_2 h_2(a^*)}\, dW_3^{P^{\phi^*}}(u) - \int_0^t e^{-r(u-t)}\pi_2^*(u)(1 - H(u-))\zeta\, dH(u) \\
& + \int_0^t\int_{-1}^{\infty} e^{-r(u-t)}\pi_1^*(u)y\widetilde{N}^{P^{\phi^*}}(du, dy)\Bigg]\Bigg\} \\
\le {} & K_1\exp\Bigg\{-4\alpha\Bigg[\int_0^t e^{-r(u-t)}\pi_1^*(u)\sigma\, dW_1^{P^{\phi^*}}(u) + \int_0^t e^{-r(u-t)}\sigma_0 dW_2^{P^{\phi^*}}(u) + \int_0^t e^{-r(u-t)}\sqrt{\lambda_2 h_2(a^*)}\, dW_3^{P^{\phi^*}}(u) \\
& - \int_0^t e^{-r(u-t)}\pi_2^*(u)(1 - H(u-))\zeta\, dH(u) + \int_0^t\int_{-1}^{\infty} e^{-r(u-t)}\pi_1^*(u)y\widetilde{N}^{P^{\phi^*}}(du, dy)\Bigg]\Bigg\} \\
= {} & K_1\exp\Bigg\{4\alpha\int_0^t e^{-r(u-t)}\pi_2^*(u)(1 - H(u-))\zeta\, dH(u) + 32\alpha^2\int_0^t e^{-2r(u-t)}\left(\pi_1^{*2}(u)\sigma^2 + \sigma_0^2 + \lambda_2 h_2(a^*)\right)du \\
& - 32\alpha^2\int_0^t e^{-2r(u-t)}\pi_1^{*2}(u)\sigma^2 du - 4\alpha\int_0^t e^{-r(u-t)}\pi_1^*(u)\sigma\, dW_1^{P^{\phi^*}}(u) - 32\alpha^2\int_0^t e^{-2r(u-t)}\sigma_0^2 du \\
& - 4\alpha\int_0^t e^{-r(u-t)}\sigma_0 dW_2^{P^{\phi^*}}(u) - 32\alpha^2\int_0^t e^{-2r(u-t)}\lambda_2 h_2(a^*)\, du - 4\alpha\int_0^t e^{-r(u-t)}\sqrt{\lambda_2 h_2(a^*)}\, dW_3^{P^{\phi^*}}(u) \\
& - 4\alpha\int_0^t\int_{-1}^{\infty} e^{-r(u-t)}\pi_1^*(u)y\widetilde{N}^{P^{\phi^*}}(du, dy)\Bigg\} \\
\le {} & K_2\exp\Bigg\{-32\alpha^2\int_0^t e^{-2r(u-t)}\pi_1^{*2}(u)\sigma^2 du - 4\alpha\int_0^t e^{-r(u-t)}\pi_1^*(u)\sigma\, dW_1^{P^{\phi^*}}(u) - 32\alpha^2\int_0^t e^{-2r(u-t)}\sigma_0^2 du \\
& - 4\alpha\int_0^t e^{-r(u-t)}\sigma_0 dW_2^{P^{\phi^*}}(u) - 32\alpha^2\int_0^t e^{-2r(u-t)}\lambda_2 h_2(a^*)\, du - 4\alpha\int_0^t e^{-r(u-t)}\sqrt{\lambda_2 h_2(a^*)}\, dW_3^{P^{\phi^*}}(u) \\
& - 4\alpha\int_0^t\int_{-1}^{\infty} e^{-r(u-t)}\pi_1^*(u)y\widetilde{N}^{P^{\phi^*}}(du, dy)\Bigg\} \\
\triangleq {} & K_2\exp\{D_1(t) + D_2(t) + D_3(t) + D_4(t)\},
\end{aligned} \tag{76}$$

where

$$\begin{aligned}
D_1(t) &= -32\alpha^2\int_0^t e^{-2r(u-t)}\pi_1^{*2}(u)\sigma^2 du - 4\alpha\int_0^t e^{-r(u-t)}\pi_1^*(u)\sigma\, dW_1^{P^{\phi^*}}(u), \\
D_2(t) &= -32\alpha^2\int_0^t e^{-2r(u-t)}\sigma_0^2 du - 4\alpha\int_0^t e^{-r(u-t)}\sigma_0 dW_2^{P^{\phi^*}}(u), \\
D_3(t) &= -32\alpha^2\int_0^t e^{-2r(u-t)}\lambda_2 h_2(a^*)du - 4\alpha\int_0^t e^{-r(u-t)}\sqrt{\lambda_2 h_2(a^*)}dW_3^{P^{\phi^*}}(u), \\
D_4(t) &= -4\alpha\int_0^t\int_{-1}^{\infty} e^{-r(u-t)}\pi_1^*(u)y\widetilde{N}^{P^{\phi^*}}(du, dy),
\end{aligned} \tag{77}$$

where π^* and ϕ^* are deterministic continuous functions, which are bounded on $[0,T]$, and we get

$$E^{P^{\phi^*}}\left(\exp\{4D_4(t)\}\right) < E^{P^{\phi^*}}\left(\exp\left\{-16\alpha\int_0^t\int_{-1}^{\infty} e^{-r(u-t)}\pi_1^*(u)y\widetilde{N}^{P^{\phi^*}}(\mathrm{d}u,\mathrm{d}y)\right\}\right) < \infty. \tag{78}$$

Applying Lemma 5 in Zeng and Taksar [43], we know that $\exp\{4D_1(t)\}$, $\exp\{4D_2(t)\}$, and $\exp\{4D_3(t)\}$ are martingales; then,

$$E^{P^{\phi^*}}\left(\exp\{4D_1(t)\}\right) < \infty, \tag{79}$$

$$E^{P^{\phi^*}}\left(\exp\{4D_2(t)\}\right) < \infty, \tag{80}$$

$$E^{P^{\phi^*}}\left(\exp\{4D_3(t)\}\right) < \infty. \tag{81}$$

Applying (78)–(81) with an appropriate constant K_3 satisfying $K_3 > K_2$, we have

$$\begin{aligned}
E^{P^{\phi^*}}\left(\left|\widehat{V}\left(t, X^{\pi^*}(t), 0\right)\right|^4\right) &\le K_3 E^{P^{\phi^*}}\left[\exp\{D_1(t) + D_2(t) + D_3(t) + D_4(t)\}\right] \\
&\le K_3\left(E^{P^{\phi^*}}\left[\exp\{2D_3(t) + 2D_4(t)\}\right]E^{P^{\phi^*}}\left[\exp\{2D_1(t) + 2D_2(t)\}\right]\right)^{(1/2)} \\
&\le K_3\left(E^{P^{\phi^*}}\left[\exp\{4D_3(t)\}\right]E^{P^{\phi^*}}\left[\exp\{4D_4(t)\}\right] \times E^{P^{\phi^*}}\left[\exp\{4D_1(t)\}\right]E^{P^{\phi^*}}\left[\exp\{4D_2(t)\}\right]\right)^{(1/4)} < \infty.
\end{aligned} \tag{82}$$

Consequently, $E^{P^{\phi^*}}(\sup_{t\in[0,T]}|\widehat{V}(t, X^{\pi^*}(t), 0)|^4) < \infty$. Similarity, we can also prove

$$E^{P^{\phi^*}}\left(\sup_{t\in[0,T]}\left|\widehat{V}\left(t, X^{\pi^*}(t), 1\right)\right|^4\right) < \infty. \tag{83}$$

Then, the formula $E^{P^{\phi^*}}(\sup_{t\in[0,T]}|\widehat{V}(t, X^{\pi^*}(t), H(t))|^4) < \infty$ holds. The first part of Lemma 4 is proved.

Let

$$\begin{aligned}
f(t) &= \frac{\alpha}{2\beta_1}\phi_1^*(t)^2 + \frac{\alpha}{2\beta_2}\phi_2^*(t)^2 + \frac{\alpha}{2\beta_3}\phi_3^*(t)^2 + \frac{\phi_4^*(t)\ln\phi_4^*(t) - \phi_4^*(t) + 1}{\beta_4}h^P\alpha \\
&\quad + \frac{\lambda\alpha\int_{-1}^{\infty}\left(\phi_5^*(t)\varphi^*(t,y)\ln\left(\phi_5^*(t)\varphi^*(t,y)\right) - \phi_5^*(t)\varphi^*(t,y) + 1\right)\mathrm{d}F_1(y)}{\beta_5},
\end{aligned} \tag{84}$$

where $f(t)$ is obviously bounded, then we get

$$\begin{aligned}
E^{P^{\phi^*}}\left(\sup_{t\in[0,T]}\left|G\left(t, X^{\pi^*}(t), \phi^*(t)\right)\right|^2\right) &= E^{P^{\phi^*}}\left(\sup_{t\in[0,T]}|f(t)|^2\left|\widehat{V}\left(t, X^{\pi^*}(t), h\right)\right|^2\right) \\
&\le \left(E^{P^{\phi^*}}\sup_{t\in[0,T]}|f(t)|^4\right)^{1/2}\left(E^{P^{\phi^*}}\sup_{t\in[0,T]}\left|\widehat{H}\left(t, X^{\pi^*}(t), h\right)\right|^4\right)^{1/2} < \infty.
\end{aligned} \tag{85}$$

The first inequality follows from Cauchy–Schwarz inequality. The last inequality follows from (71). Lemma 5 is proved. □

Based on the discussion above, the main theorem is summarized as follows.

Theorem 3. *For the robust optimal control problem (21) with the exponential utility function (11), $\widehat{V}(t,x,h)$ is the solution of (24) with the boundary condition $\widehat{V}(T,x,h) = U(x)$, (π^*, ϕ^*) is an optimal strategy, and then $V(t,x,h) = \widehat{V}(t,x,h)$ is the corresponding value function.*

Proof. From Lemmas 1, 2, and 3 and Theorems 1 and 2, we can obtain properties 1–4 in Proposition 1. By Lemma 5, condition 5 in Proposition 1 also holds for $\widehat{V}(t,x,h)$. From Proposition 1, we can obtain the result of Theorem 3, (π^*,ϕ^*) is an optimal strategy, and $V(t,x,h)$ is the corresponding value function. □

5. Some Special Cases

In this section, we shall present some special cases of our results, such as the proportional reinsurance, the excess-of-loss reinsurance, and an ambiguity-neutral insurer of the insurance.

5.1. The Proportional Reinsurance. The parameter η satisfies $\eta=0$, and the insurer purchases reinsurance in the form of the proportional reinsurance, that is, $\mathscr{H}(a,Z)=2a\theta_1 Z$. The result is shown by corollary as follows.

Corollary 5.1. *If $\eta=0$, then the value function $V(t,x,h)=(1-h)V(t,x,0)+hV(t,x,1), h=0,1$, and the optimal strategies π^* and ϕ^* are given by*

$$\begin{aligned}
\phi_1^*(t) &= \beta_1\sigma\pi_1(t)e^{r(T-t)}, \quad t\in[0,T],\\
\phi_2^*(t) &= \beta_2\sigma_0 e^{r(T-t)}, \quad t\in[0,T],\\
\phi_3^*(t) &= 2\beta_3\sqrt{\lambda_2}a^*(t)\theta_1\sigma_Z e^{r(T-t)},\\
0 &= \frac{\alpha h^P}{\beta_4}\phi_4^*(t)\ln\phi_4^*(t)+h^P\phi_4^*(t)-\frac{\delta}{\zeta}, \quad t\in[0,T],\\
\varphi^*(t,y) &= \frac{1}{\phi_5^*(t)}\exp\left\{\frac{\beta_5}{\alpha}\left(e^{-\alpha\pi_1(t)e^{r(T-t)}y}-1\right)\right\}, \quad t\in[0,T],\\
\phi_5^*(t) &= E\left[\exp\left\{\frac{\beta_5}{\alpha}\left(e^{-\alpha\pi_1(t)e^{r(T-t)}Y}-1\right)\right\}\right], \quad t\in[0,T],\\
\pi_1^*(t) &= \frac{e^{-r(T-t)}}{\sigma^2(\alpha+\beta_1)}\left[\mu-r+\lambda_1\int_{-1}^{\infty}ye^{-\alpha\pi_1^*(t)e^{r(T-t)}y}\exp\left\{\frac{\beta_5}{\alpha}\left(e^{-\alpha\pi_1^*(t)e^{r(T-t)}y}-1\right)\right\}\mathrm{d}F_1(y)\right], \quad t\in[0,T],\\
\pi_2^*(t) &= \begin{cases}\dfrac{1}{\alpha\zeta}e^{-r(T-t)}\left[\ln\dfrac{g_2(t)}{\Delta\phi_4^*(t)g_1(t)}\right], & t\in[0,\tau\wedge T],\\[2ex] 0, & t\in[\tau\wedge T,T],\end{cases}\\
a^*(t) &= \frac{1}{2\theta_1+(\alpha+\beta_3)e^{r(T-t)}}, \quad t\in[0,T].
\end{aligned}\tag{86}$$

The optimal value function $V(t,x,h)$ is as follows:

$$V(t,x,1)=-\frac{1}{\alpha}\exp\left\{-\alpha xe^{r(T-t)}\right\}g_1(t),\text{and}\,V(t,x,0)=-\frac{1}{\alpha}\exp\left\{-\alpha xe^{r(T-t)}\right\}g_2(t),\tag{87}$$

where

$$\begin{aligned}
g_1(t) = \exp\Bigg\{\int_t^T\Bigg\{&\frac{\alpha+\beta_2}{2}\alpha\sigma_0^2e^{2r(T-u)}-\alpha\lambda_2e^{r(T-u)}(\theta_0-\eta)\mu_Z-\frac{\lambda_1\alpha}{\beta_5}-\alpha e^{r(T-u)}(\mu-r)\pi_1^*(u)+\frac{\alpha+\beta_1}{2}\alpha\sigma^2e^{2r(T-u)}(\pi_1^*(u))^2\\
&+\frac{\lambda_1\alpha}{\beta_5}\int_{-1}^{\infty}\exp\left\{\frac{\beta_5}{\alpha}\left(e^{-\alpha\pi_1^*(u)e^{r(T-u)}y}-1\right)\right\}\mathrm{d}F_1(y)-\alpha\lambda_2e^{r(T-u)}\left[-\theta_1(1-2a^*(u)\theta_1)^2\sigma_Z^2-2(\alpha+\beta_3)(a^*(u))^2\theta_1^2\sigma_Z^2e^{r(T-u)}\right]\Bigg\}\mathrm{d}u\Bigg\},
\end{aligned}\tag{88}$$

and $g_2(t) = e^{\overline{g}_2(t)}$, in which

$$\overline{g}_2(t) = e^{-(\delta/\zeta)(T-t)} \int_t^T e^{(\delta/\zeta)(T-u)} \left\{ \frac{\alpha+\beta_2}{2} \alpha\sigma_0^2 e^{2r(T-u)} - \alpha\lambda_2 e^{r(T-u)} (\theta_0 - \eta)\mu_Z - \alpha e^{r(T-u)} (\mu - r)\pi_1^*(u) \right.$$
$$+ \frac{\alpha+\beta_1}{2} \alpha\sigma^2 e^{2r(T-u)} (\pi_1^*(u))^2 - \frac{\lambda_1\alpha}{\beta_5} + \frac{\lambda_1\alpha}{\beta_5} \int_{-1}^{\infty} \exp\left\{ \frac{\beta_5}{\alpha} \left(e^{-\alpha\pi_1^*(u)e^{r(T-u)} y} - 1 \right) \right\} \mathrm{d}F_1(y) - \alpha\lambda_2 e^{r(T-u)} \tag{89}$$
$$\left. \cdot \left[-\theta_1 (1 - 2a^*(u)\theta_1)^2 \sigma_Z^2 - 2(\alpha+\beta_3)(a^*(u))^2 \theta_1^2 \sigma_Z^2 e^{r(T-u)} \right] + \frac{\delta}{\zeta} \left(\ln \Delta\phi_4^*(u) + \ln g_1(u) + \frac{\phi_4^*(u) - 1}{\beta_4} \alpha\Delta \right) \right\} \mathrm{d}u.$$

Proof. In this case, $\mathscr{H}(a, Z) = 2a\theta_1 Z$, and then the functions in our results are as follows:

$$\begin{aligned} h_1(a) &= \eta h_3(a) - (1+\eta)\theta_1 h_4(a) = -\theta_1 (1 - 2a\theta_1)^2 \sigma_Z^2, \\ h_2(a) &= E\left[\mathscr{H}(a, Z)^2\right] = 4a^2\theta_1^2\sigma_Z^2, \\ h_3(a) &= E[\mathscr{H}(a, Z)] = 2a\theta_1\mu_Z, \\ h_4(a) &= E\left[(Z - \mathscr{H}(a, Z))^2\right] = (1 - 2a^*\theta_1)^2 \sigma_Z^2. \end{aligned} \tag{90}$$

According to Theorems 3.3 and 3.5, we can obtain the result. □

Remark 2. If $\eta = 0$, and $2a\theta_1 = q$, then $\mathscr{H}(Z_i) = 2a\theta_1 Z_i = qZ_i$ becomes a proportional reinsurance type. There are similar studies, for example, Zhou et al. [24], Zheng et al. [26], and Wang et al. [44].

5.2. The Excess-of-Loss Reinsurance. The parameter θ_1 satisfies $\theta_1 = 0$, and the insurer purchases reinsurance in the form of the excess-of-loss reinsurance, that is, $\mathscr{H}(a, Z) = a\eta \wedge Z$. The result is shown by corollary as follows.

Corollary 5.3. *If $\theta_1 = 0$, then the optimal value function $V(t, x, h) = (1-h)V(t, x, 0) + hV(t, x, 1), h = 0, 1$, and the optimal strategies π^* and ϕ^* are given by*

$$\begin{aligned} \phi_1^*(t) &= \beta_1\sigma\pi_1(t)e^{r(T-t)}, \quad t \in [0, T], \\ \phi_2^*(t) &= \beta_2\sigma_0 e^{r(T-t)}, \quad t \in [0, T], \\ \phi_3^*(t) &= \beta_3\sqrt{\lambda_2 h_2(a)} e^{r(T-t)}, \\ 0 &= \frac{\alpha h^P}{\beta_4}\phi_4^*(t)\ln\phi_4^*(t) + h^P\phi_4^*(t) - \frac{\delta}{\zeta}, \quad t \in [0, T], \\ \varphi^*(t, y) &= \frac{1}{\phi_5^*(t)} \exp\left\{ \frac{\beta_5}{\alpha} \left(e^{-\alpha\pi_1(t)e^{r(T-t)} y} - 1 \right) \right\}, \quad t \in [0, T], \\ \phi_5^*(t) &= E\left[\exp\left\{ \frac{\beta_5}{\alpha} \left(e^{-\alpha\pi_1(t)e^{r(T-t)} Y} - 1 \right) \right\} \right], \quad t \in [0, T], \\ \pi_1^*(t) &= \frac{e^{-r(T-t)}}{\sigma^2(\alpha+\beta_1)} \left[\mu - r + \lambda_1 \int_{-1}^{\infty} y e^{-\alpha\pi_1^*(t)e^{r(T-t)} y} \exp\left\{ \frac{\beta_5}{\alpha} \left(e^{-\alpha\pi_1^*(t)e^{r(T-t)} y} - 1 \right) \right\} \mathrm{d}F_1(y) \right], \quad t \in [0, T], \\ \pi_2^*(t) &= \begin{cases} \dfrac{1}{\alpha\zeta} e^{-r(T-t)} \left[\ln \dfrac{g_2(t)}{\Delta\phi_4^*(t) g_1(t)} \right], & t \in [0, \tau \wedge T], \\ 0, & t \in [\tau \wedge T, T], \end{cases} \\ a^*(t) &= \frac{1}{(\alpha+\beta_3)e^{r(T-t)}}, \quad t \in [0, T] \end{aligned} \tag{91}$$

The optimal value function $V(t,x,h)$ is as follows:

$$V(t,x,1) = -\frac{1}{\alpha}\exp\left\{-\alpha x e^{r(T-t)}\right\} g_1(t),$$
$$V(t,x,0) = -\frac{1}{\alpha}\exp\left\{-\alpha x e^{r(T-t)}\right\} g_2(t), \tag{92}$$

where

$$g_1(t) = \exp\left\{\int_t^T \left\{\frac{\alpha+\beta_2}{2}\alpha\sigma_0^2 e^{2r(T-u)} - \alpha\lambda_2 e^{r(T-u)}(\theta_0-\eta)\mu_Z - \frac{\lambda_1\alpha}{\beta_5} - \alpha e^{r(T-u)}(\mu-r)\pi_1^*(u) + \frac{\alpha+\beta_1}{2}\alpha\sigma^2 e^{2r(T-u)}(\pi_1^*(u))^2 + \frac{\lambda_1\alpha}{\beta_5}\int_{-1}^{\infty}\exp\left\{\frac{\beta_5}{\alpha}\left(e^{-\alpha\pi_1^*(u)e^{r(T-u)}y}-1\right)\right\}\mathrm{d}F_1(y) - \alpha\lambda_2 e^{r(T-u)}\left[h_1(a^*(u)) - \frac{\alpha+\beta_3}{2}h_2(a^*(u))e^{r(T-u)}\right]\right\}\mathrm{d}u\right\}, \tag{93}$$

and $g_2(t) = e^{\overline{g}_2(t)}$, in which

$$\overline{g}_2(t) = e^{-(\delta/\zeta)(T-t)}\int_t^T e^{(\delta/\zeta)(T-u)}\left\{\frac{\alpha+\beta_2}{2}\alpha\sigma_0^2 e^{2r(T-u)} - \alpha\lambda_2 e^{r(T-u)}(\theta_0-\eta)\mu_Z - \alpha e^{r(T-u)}(\mu-r)\pi_1^*(u) + \frac{\alpha+\beta_1}{2}\alpha\sigma^2 e^{2r(T-u)}(\pi_1^*(u))^2 - \frac{\lambda_1\alpha}{\beta_5} + \frac{\lambda_1\alpha}{\beta_5}\int_{-1}^{\infty}\exp\left\{\frac{\beta_5}{\alpha}\left(e^{-\alpha\pi_1^*(u)e^{r(T-u)}y}-1\right)\right\}\mathrm{d}F_1(y) - \alpha\lambda_2 e^{r(T-u)} \cdot \left[h_1(a^*(u)) - \frac{\alpha+\beta_3}{2}h_2(a^*(u))e^{r(T-u)}\right] + \frac{\delta}{\zeta}\left(\ln\Delta\phi_4^*(u) + \ln g_1(u) + \frac{\phi_4^*(u)-1}{\beta_4}\alpha\Delta\right)\right\}\mathrm{d}u. \tag{94}$$

Proof. In this case, $\mathscr{H}(a,Z) = a\eta\wedge Z$, and then the functions in our results are as follows:

$$h_1(a) = \eta h_3(a) - (1+\eta)\theta_1 h_4(a) = \eta\int_0^{a\eta}(1-F_2(z))\mathrm{d}z,$$
$$h_2(a) = E\left[\mathscr{H}(a,Z)^2\right] = 2\int_0^{a\eta}(1-F_2(z))\mathrm{d}z,$$
$$h_3(a) = E[\mathscr{H}(a,Z)] = \int_0^{a\eta}(1-F_2(z))\mathrm{d}z. \tag{95}$$

According to Theorems 1 and 2, we can obtain the result. □

Remark 3. If $\theta_1 = 0$, then $\mathscr{H}(Z_i) = (a\eta)\wedge Z_i$ becomes an excess-of-loss reinsurance type. Without regard for the default bond, let $\eta = 1$, then the reinsurance strategy becomes the result of Li et al. [10].

5.3. Ambiguity-Neutral Insurer (ANI) Case. If the insurer is an ambiguity-neutral insurer, then the aversion ambiguity coefficient $\beta_i = 0$, $i = 1,2,3,4,5$. In this case, for an admissible control $(\check{a}(t), \check{\pi}_1(t), \check{\pi}_2(t))$ and an initial value (x,h), the objective function is described by

$$\check{V}(t,x,h) = \sup_{\pi\in\Pi} E\left[U\left(X^{\check{\pi}}(T)\right) \mid (X(t),H(t)) = (x,h)\right]. \tag{96}$$

The corresponding HJB equation is

$$0 = \sup_{\pi\in\Pi}\left\{\check{V}_t + \check{V}_x\{rx + (\mu-r)\pi_1(t) + (1-h)\delta\pi_2(t) + \lambda_2[(\theta_0-\eta)\mu_Z + h_1(a(t))]\} + \frac{1}{2}V_{xx}\left(\sigma^2\pi_1^2(t) + \sigma_0^2 + \lambda_2 h_2(a(t))\right) + \lambda_1 E_{P\phi} \cdot \left[\check{V}(t,x+\pi_1(t)Y,h) - \check{V}(t,x,h)\right] + h^P(1-h)\left(\check{V}(t,x-\pi_2(t)\zeta,1) - \check{V}(t,x,0)\right)\right\}. \tag{97}$$

From the value functions

$$V(t,x,1) = -\frac{1}{\alpha}\exp\left\{-\alpha x e^{r(T-t)}\right\} g_{10}(t),$$
$$V(t,x,0) = -\frac{1}{\alpha}\exp\left\{-\alpha x e^{r(T-t)}\right\} g_{20}(t), \tag{98}$$

we can get the following candidate optimal strategies by the same way:

$$\check{\pi}_2^*(t) = \frac{e^{-r(T-t)}}{\sigma^2\alpha}\left[\mu - r + \lambda_1 E\left[e^{-\alpha\check{\pi}_2^*(t)e^{r(T-t)Y}}\right]\right], \quad t \in [0,T],$$
$$\check{\pi}_2^*(t) = \begin{cases} \dfrac{1}{\alpha\zeta}e^{-r(T-t)}\left[\ln\dfrac{g_{20}(t)}{\Delta g_{10}(t)}\right] & t \in [0, \tau\wedge T], \\ 0, & t \in [\tau\wedge T, T], \end{cases}$$
$$\check{a}^*(t) = \frac{1}{2(1+\eta)\theta_1 + \alpha e^{r(T-t)}}, \quad t \in [0,T]. \tag{99}$$

where

$$g_{10}(t) = \exp\left\{\int_t^T \frac{\alpha^2}{2}e^{2r(T-u)}\left(\sigma^2\left(\pi_1^*(u)\right)2 + \sigma_0^2 + \lambda_2 h_2\left(a^*(u)\right)\right) - \alpha e^{r(T-u)}\left\{(\mu-r)\pi_1^*(u) + \lambda_2\left[(\theta_0-\eta)\mu_Z + h_1\left(a^*(u)\right)\right] + \lambda_1\left(E\left[e^{-\alpha\pi_1^*(u)e^{r(T-u)Y}}\right] - 1\right)\right\}du\right\}, \tag{100}$$

and $g_{20}(t) = e^{\overline{g}_{20}(t)}$, in which

$$\overline{g}_{20}(t) = e^{-(\delta/\zeta)(T-t)}\int_t^T e^{(\delta/\zeta)(T-u)}\left\{\frac{\alpha^2}{2}e^{2r(T-u)}\left(\sigma^2\left(\pi_1^*(u)\right)^2 + \sigma_0^2 + \lambda_2 h_2\left(a^*(u)\right)\right) + \frac{\delta}{\zeta}\left(\Delta - 1 - \frac{1}{\delta}\right) - \alpha e^{r(T-u)} \cdot \left\{(\mu-r)\pi_1^*(u) + \lambda_2\left[(\theta_0-\eta)\mu_Z + h_1\left(a^*(u)\right)\right]\right\} + \lambda_1\left(E\left[e^{-\alpha\pi_1^*(u)e^{r(T-u)Y}}\right] - 1\right)\right\}du. \tag{101}$$

Remark 4. If all of the ambiguity aversion coefficients equal 0, i.e., $\beta_i = 0, i = 1,2,3,4,5$, our model reduces to an optimization problem for an ambiguity-neutral insurer (ANI). For the ANI, the optimization investment-reinsurance is researched by Cao [11], Yang and Zhang [2], etc.

6. Sensitivity Analysis

In this section, we will give several numerical examples to illustrate the influences of the parameters on the optimal strategies and the optimal value functions. Unless otherwise stated, the basic parameters are given in Table 1.

TABLE 1: Model parameters.

μ	T	r	α	σ	σ_0	λ_1	λ_2	θ_1	θ_0	δ
0.1	1	0.05	1	0.15	0.5	2	2	2	1	0.2

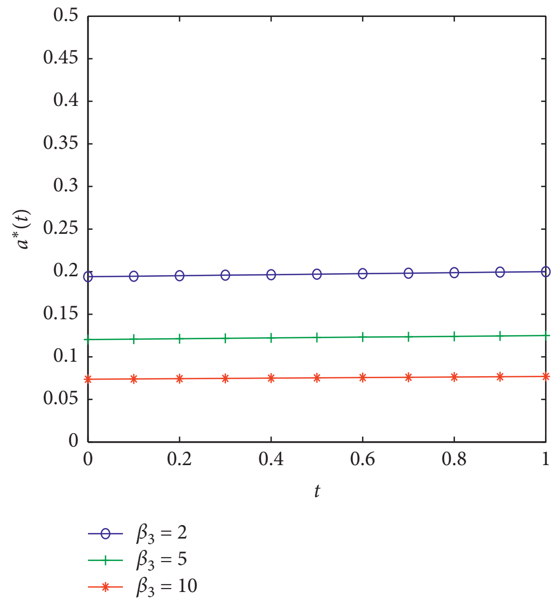

FIGURE 1: Effect of β_3 on $a^*(t)$.

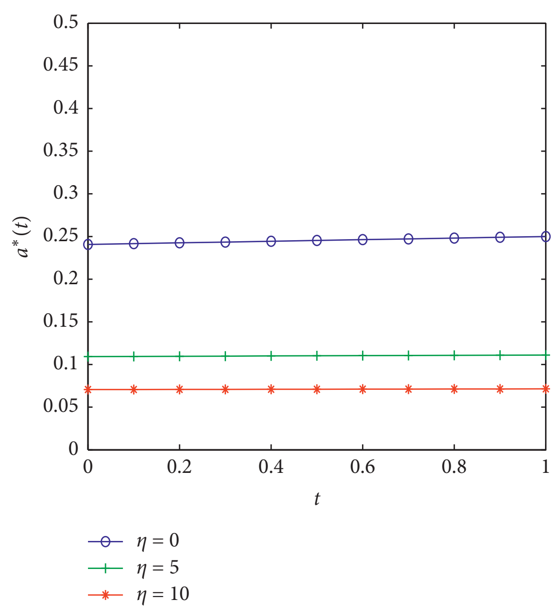

FIGURE 2: Effect of η on $a^*(t)$.

Some analyses of the optimal reinsurance strategy $a^*(t)$ are shown in Figures 1–4. β_3 is the ambiguity aversion coefficient of the AAI. From Figure 1, it is found that β_3 affects the reinsurance strategy of the insurer. As β_3 increases, the insurer has lower risk exposure in the insurance market, so less amount of money will be paid to purchase reinsurance. η and θ_1 are the relative safety loadings of the

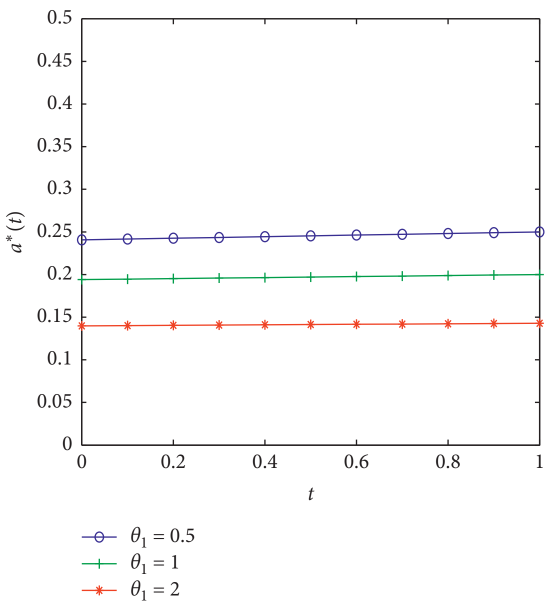

Figure 3: Effect of θ_1 on $a^*(t)$.

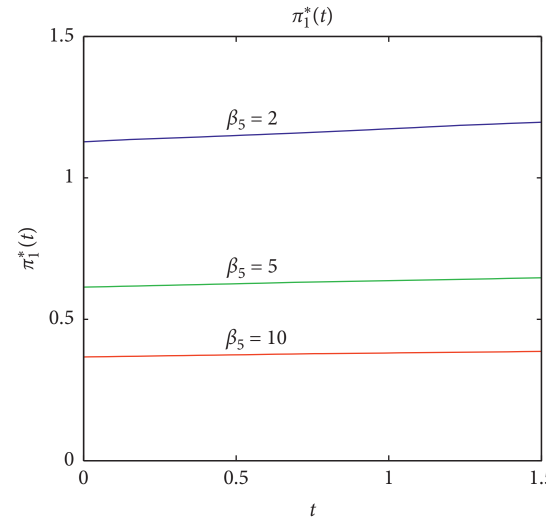

Figure 6: Effect of β_5 on $\pi_1^*(t)$.

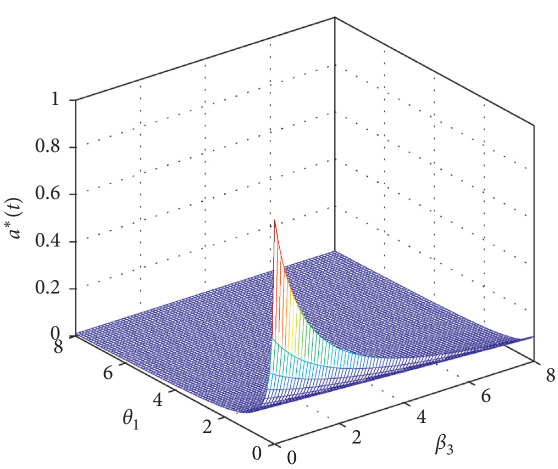

Figure 4: Effect of θ_1 and β_3 on $a^*(t)$.

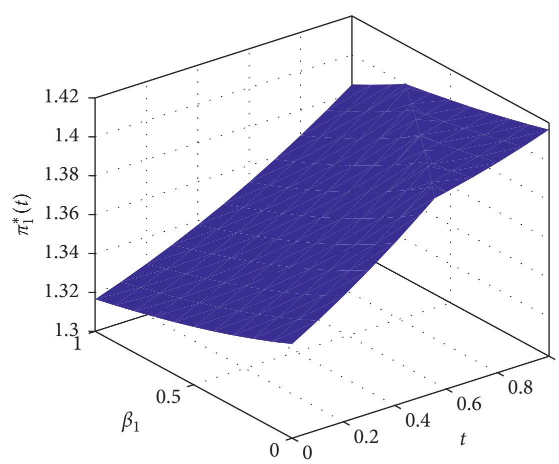

Figure 7: Effect of β_1 and the time t on $\pi_1^*(t)$.

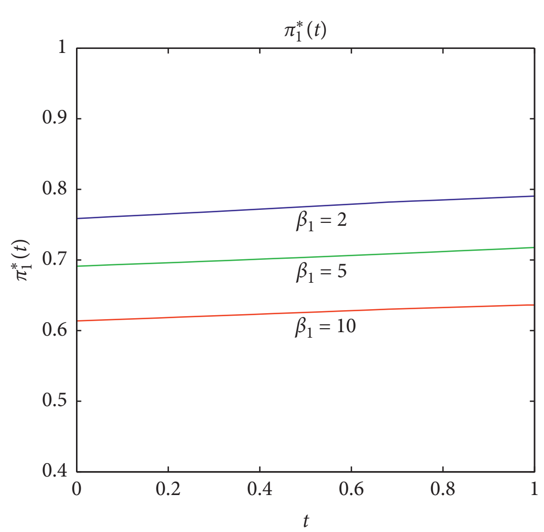

Figure 5: Effect of β_1 on $\pi_1^*(t)$.

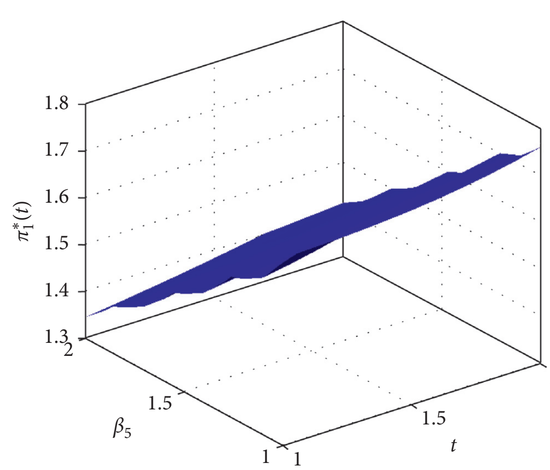

Figure 8: Effect of β_5 and the time t on $\pi_1^*(t)$.

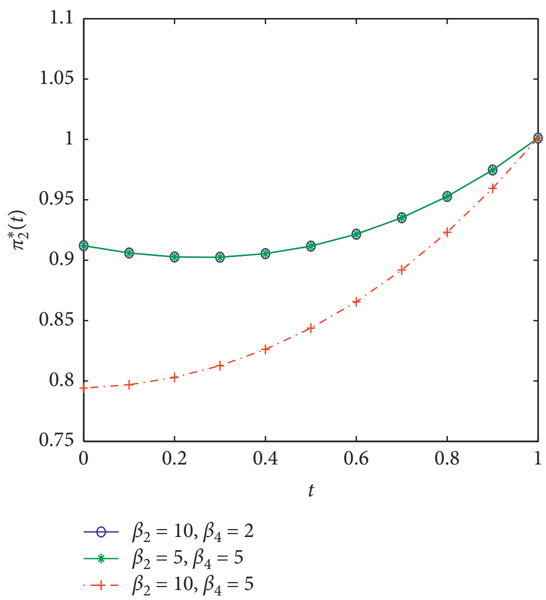

Figure 9: Effect of β_2 and β_4 on $\pi_2^*(t)$.

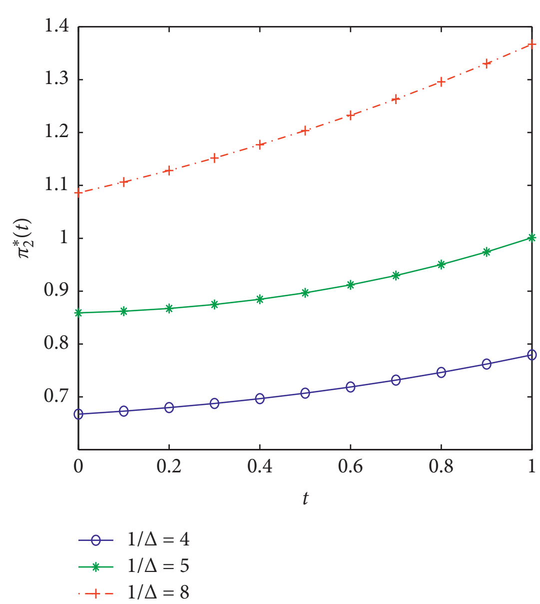

Figure 10: Effect of $1/\Delta$ on $\pi_2^*(t)$.

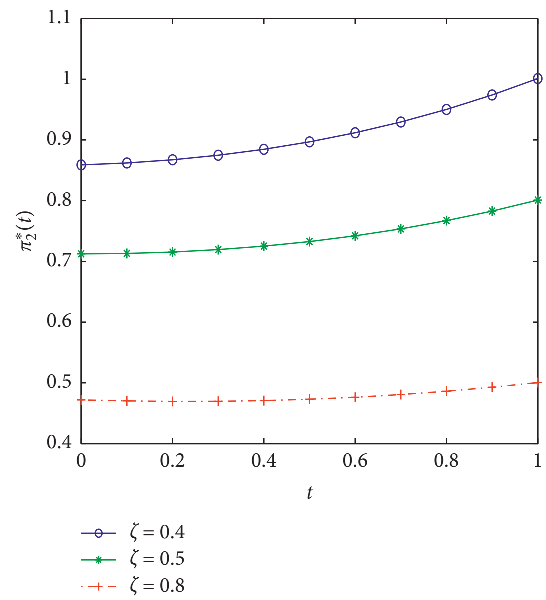

Figure 11: Effect of ζ on $\pi_2^*(t)$.

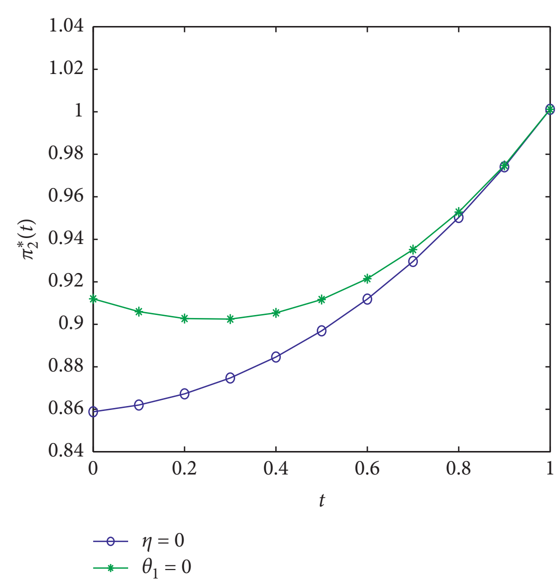

Figure 12: Effect of $\theta_1 = 0$ and $\eta = 0$ on $\pi_2^*(t)$.

reinsurer. Figures 2 and 3 show the effects of η or θ_1 on the insurer's reinsurance strategy. As η or θ_1 increases, the reinsurer pays more concern on his/her risk exposures and charges more for them. Consequently, the insurer decreases his/her demand for reinsurance and pays more claims by himself/herself. In Figure 4, we show the common effects of the safety loading θ_1 and the ambiguity aversion coefficient β_3 on $a^*(t)$.

In Figures 5–8, we illustrate the impacts of the ambiguity aversion coefficients β_1 and β_5 on the stock strategy $\pi_1^*(t)$. From Figures 5 and 6, we find that the AAI will reduce the wealth invested on the stock, when there is a higher ambiguity aversion coefficient. From Figures 7 and 8, we find that as the time t increases, the AAI increases the stock investment amount. These figures show that the robust optimal strategies can effectively reduce the sensitivity of $\pi_1^*(t)$ on the stock.

For the defaultable corporate bond, the value is assumed to be zero after default. In Figures 9–13, we show the numerical analysis of the defaultable corporate bond strategy $\pi_2^*(t)$ before default. β_2 and β_4 are the ambiguity aversion coefficients. As β_4 increases, the insurer will reduce the money on the defaultable corporate bond, but β_2 does not affect the investment, as shown in Figure 9. In Figure 10, the insurer will invest more amount of his/her money, if the defaultable corporate bond with a higher premium induces a

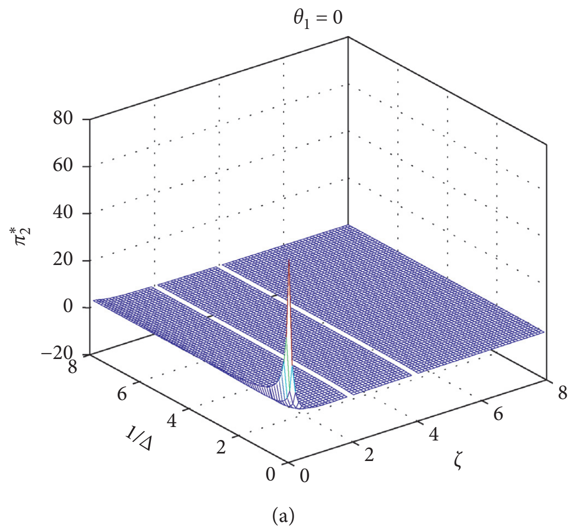

FIGURE 13: Effect of $1/\Delta$ and ζ on $\pi_2^*(t)$ with $\theta_1 = 0$ and $\eta = 0$.

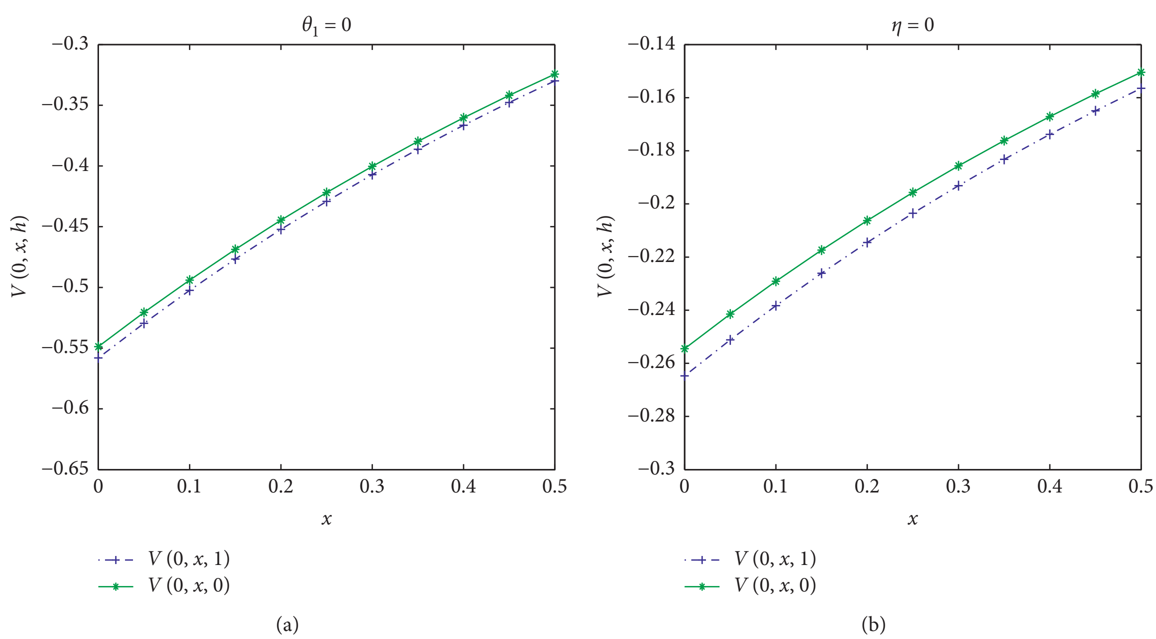

FIGURE 14: Value functions with respect to x when $\theta_1 = 0$ and $\eta = 0$.

higher potential yield. Contrary to the default risk premium $1/\Delta$, the accession of ζ reduces the insurer's investment on the defaultable bond, as shown in Figure 11. A higher loss rate ζ leads to a less recovery value, which implies a higher potential loss of the insurer. When $\eta = 0$, the reinsurance type is a proportional reinsurance, and when $\theta_1 = 0$, the reinsurance type becomes an excess-of-loss reinsurance. We show that the proportion reinsurance is always below the excess-of-loss reinsurance at the same time in Figure 12. Figure 13 provides a full description of $\pi_2^*(t)$ with respect to $1/\Delta$ and ζ with two different reinsurance types, respectively.

In Figure 14, we illustrate the predefault value function $V(0, x, 0)$ and the postdefault value function $V(0, x, 1)$ with respect to the initial wealth about a proportional reinsurance and an excess-of-loss reinsurance, respectively. We can see that the value functions of the insurer increase as the initial wealth increases and the predefault value function is always greater than or equal to the postdefault value function.

7. Conclusion

In this paper, we consider a robust optimal reinsurance-investment problem of an insurer under the generalized mean-variance premium principle and a defaultable market. The insurer can trade in a risk-free asset, a stock, and a defaultable corporate bond. The surplus of the AAI is described by an approximate diffusion process. The stock's price process is described by a jump-diffusion model. Using the dynamic programming approach, we study the predefault case and the postdefault case, respectively, and derive the optimal strategies and the corresponding value functions under the worst-case scenario. We give some sensitivity analysis to illustrate our theoretical results. In future research, we will consider some complex models, such as the robust optimal reinsurance-investment problem of stochastic differential games.

Data Availability

All data generated or analyzed during this study are included in this article.

Conflicts of Interest

The authors declare that they have no conflicts of interest.

Acknowledgments

This work was supported by the National Natural Science Foundation of China (grant nos. 71701068, 11701175, and 11671132), the Natural Science Foundation of Hunan Province, China (no. 2018JJ3360), and the Scientific Research Fund of Hunan Provincial Education Department, China (nos. 19B343, 17C1001, and 17K057).

References

[1] S. Browne, "Optimal investment policies for a firm with a random risk process: exponential utility and minimizing the probability of ruin," *Mathematics of Operations Research*, vol. 20, no. 4, pp. 937–958, 1995.

[2] H. Yang and L. Zhang, "Optimal investment for insurer with jump-diffusion risk process," *Insurance: Mathematics and Economics*, vol. 37, no. 3, pp. 615–634, 2005.

[3] L. Bai and J. Guo, "Optimal proportional reinsurance and investment with multiple risky assets and no-shorting constraint," *Insurance: Mathematics and Economics*, vol. 42, no. 3, pp. 968–975, 2008.

[4] Y. Huang, X. Yang, and J. Zhou, "Optimal investment and proportional reinsurance for a jump-diffusion risk model with constrained control variables," *Journal of Computational and Applied Mathematics*, vol. 296, pp. 443–461, 2016.

[5] X. Zhang, H. Meng, and Y. Zeng, "Optimal investment and reinsurance strategies for insurers with generalized mean-variance premium principle and no-short selling," *Insurance: Mathematics and Economics*, vol. 67, pp. 125–132, 2016.

[6] Y. Zeng, D. Li, and A. Gu, "Robust equilibrium reinsurance-investment strategy for a mean-variance insurer in a model with jumps," *Insurance: Mathematics and Economics*, vol. 66, pp. 138–152, 2016.

[7] X. H. Peng, W. Su, and Z. M. Zhang, "On a perturbed compound Poisson risk model under a periodic threshold-type dividend strategy," *Journal of Industrial and Management Optimization*, vol. 13, no. 5, pp. 1–20, 2017.

[8] W. Yu, Y. Yong, G. Guan, Y. Huang, W. Su, and C. Cui, "Valuing guaranteed minimum death benefits by cosine series expansion," *Mathematics*, vol. 7, no. 9, p. 835, 2019.

[9] Z. Zhang, Y. Yong, and W. Yu, "Valuing equity-linked death benefits in general exponential Lévy models," *Journal of Computational and Applied Mathematics*, vol. 365, Article ID 112377, 2020.

[10] D. Li, Y. Zeng, and H. Yang, "Robust optimal excess-of-loss reinsurance and investment strategy for an insurer in a model with jumps," *Scandinavian Actuarial Journal*, vol. 2018, no. 2, pp. 145–171, 2018.

[11] Y. Cao, "Optimal investment-reinsurance problem for an insurer with jump-diffusion risk process: correlated of Brownian motions," *Journal of Interdisciplinary Mathematics*, vol. 20, no. 2, pp. 497–511, 2017.

[12] Z. Liang, K. C. Yuen, and K. C. Cheung, "Optimal reinsurance-investment problem in a constant elasticity of variance stock market for jump-diffusion risk model," *Applied Stochastic Models in Business and Industry*, vol. 28, no. 6, pp. 585–597, 2012.

[13] X. Lin, C. Zhang, and T. K. Siu, "Stochastic differential portfolio games for an insurer in a jump-diffusion risk process," *Mathematical Methods of Operations Research*, vol. 75, no. 1, pp. 83–100, 2012.

[14] H. Zhao, X. Rong, and Y. Zhao, "Optimal excess-of-loss reinsurance and investment problem for an insurer with jump-diffusion risk process under the Heston model," *Insurance: Mathematics and Economics*, vol. 53, no. 3, pp. 504–514, 2013.

[15] T. R. Bielecki and I. Jang, "Portfolio optimization with a defaultable security," *Asia-Pacific Financial Markets*, vol. 13, no. 2, pp. 113–127, 2007.

[16] L. Bo, H. Liao, and X. Yu, "Risk sensitive portfolio optimization with default contagion and regime-switching," *SIAM Journal on Control and Optimization*, vol. 57, no. 1, pp. 366–401, 2019.

[17] L. Bo, Y. Wang, and X. Yang, "Stochastic portfolio optimization with default risk," *Journal of Mathematical Analysis and Applications*, vol. 397, no. 2, pp. 467–480, 2013.

[18] A. Capponi and J. E. Figueroa-López, "Dynamic portfolio optimization with a defaultable security and regime-switching," *Mathematical Finance*, vol. 24, no. 2, pp. 207–249, 2014.

[19] H. Zhu, C. Deng, S. Yue, and Y. Deng, "Optimal reinsurance and investment problem for an insurer with counterparty risk," *Insurance: Mathematics and Economics*, vol. 61, pp. 242–254, 2015.

[20] H. Zhao, Y. Shen, and Y. Zeng, "Time-consistent investment-reinsurance strategy for mean-variance insurers with a defaultable security," *Journal of Mathematical Analysis and Applications*, vol. 437, no. 2, pp. 1036–1057, 2016.

[21] C. Deng, X. Zeng, and H. Zhu, "Non-zero-sum stochastic differential reinsurance and investment games with default risk," *European Journal of Operational Research*, vol. 264, no. 3, pp. 1144–1158, 2018.

[22] Z. B. Liang and E. Bayraktar, "Optimal reinsurance and investment with unobservable claim size and intensity," *Insurance: Mathematics and Economics*, vol. 55, no. 2, pp. 156–166, 2014.

[23] Z. Sun, X. Zheng, and X. Zhang, "Robust optimal investment and reinsurance of an insurer under variance premium principle and default risk," *Journal of Mathematical Analysis and Applications*, vol. 446, no. 2, pp. 1666–1686, 2017.

[24] J. Zhou, Y. Deng, Y. Huang, and X. Yang, "Optimal proportional reinsurance and investment for a constant elasticity of variance model under variance principle," *Acta Mathematica Scientia*, vol. 35, no. 2, pp. 303–312, 2015.

[25] Y. Shen and Y. Zeng, "Optimal investment-reinsurance strategy for mean-variance insurers with square-root factor process," *Insurance: Mathematics and Economics*, vol. 62, pp. 118–137, 2015.

[26] X. Zheng, J. Zhou, and Z. Sun, "Robust optimal portfolio and proportional reinsurance for an insurer under a CEV model,"

Insurance: Mathematics and Economics, vol. 67, pp. 77–87, 2016.
[27] E. Anderson, L. P. Hansen, and T. J. Sargent, *Robustness Detection and the Price of Risk*, Working Paper, University of Chicago, Chicago, IL, USA, 1999.
[28] R. Uppal and T. Wang, "Model misspecification and underdiversification," *The Journal of Finance*, vol. 58, no. 6, pp. 2465–2486, 2003.
[29] P. J. Maenhout, "Robust portfolio rules and asset pricing," *Review of Financial Studies*, vol. 17, no. 4, pp. 951–983, 2004.
[30] P. J. Maenhout, "Robust portfolio rules and detection-error probabilities for a mean-reverting risk premium," *Journal of Economic Theory*, vol. 128, no. 1, pp. 136–163, 2006.
[31] X. Zhang and T. K. Siu, "Optimal investment and reinsurance of an insurer with model uncertainty," *Insurance: Mathematics and Economics*, vol. 45, no. 1, pp. 81–88, 2009.
[32] B. Yi, Z. Li, F. G. Viens, and Y. Zeng, "Robust optimal control for an insurer with reinsurance and investment under Heston's stochastic volatility model," *Insurance: Mathematics and Economics*, vol. 53, no. 3, pp. 601–614, 2013.
[33] C. R. Flor and L. S. Larsen, "Robust portfolio choice with stochastic interest rates," *Annals of Finance*, vol. 10, no. 2, pp. 243–265, 2014.
[34] C. S. Pun and H. Y. Wong, "Robust investment-reinsurance optimization with multiscale stochastic volatility," *Insurance: Mathematics and Economics*, vol. 62, pp. 245–256, 2015.
[35] Y. Zeng, D. Li, Z. Chen, and Z. Yang, "Ambiguity aversion and optimal derivative-based pension investment with stochastic income and volatility," *Journal of Economic Dynamics and Control*, vol. 88, pp. 70–103, 2018.
[36] X. Zhang, H. Meng, J. Xiong et al., "Robust optimal investment and reinsurance of an insurer under jump-diffusion models," *Mathematical Control & Related Fields*, vol. 9, no. 1, pp. 59–76, 2019.
[37] N. Branger and L. S. Larsen, "Robust portfolio choice with uncertainty about jump and diffusion risk," *Journal of Banking & Finance*, vol. 37, no. 12, pp. 5036–5047, 2013.
[38] X. Jin, D. Luo, and X. D. Zeng, "Dynamic asset allocation with uncertain jump risks: a pathwise optimization approach," *Mathematics of Operations Research*, vol. 43, no. 2, pp. 347–376, 2017.
[39] H. Schmidli, *Stochastic Control in Insurance*, Springer Science and Business Media, Berlin, Germany, 2007.
[40] J. Grandell, *Aspects of Risk Theory*, Springer Science and Business Media, Berlin, Germany, 2012.
[41] S. Chen, H. Yang, and Y. Zeng, "Stochastic differential games between two insurers with generalized mean-variance premium principle," *ASTIN Bulletin*, vol. 48, no. 1, pp. 413–434, 2018.
[42] E. W. Anderson, L. P. Hansen, and T. J. Sargent, "A quartet of semigroups for model specification, robustness, prices of risk, and model detection," *Journal of the European Economic Association*, vol. 1, no. 1, pp. 68–123, 2003.
[43] X. Zeng and M. Taksar, "A stochastic volatility model and optimal portfolio selection," *Quantitative Finance*, vol. 13, no. 10, pp. 1547–1558, 2013.
[44] Y. Wang, X. Rong, and H. Zhao, "Optimal investment strategies for an insurer and a reinsurer with a jump diffusion risk process under the CEV model," *Journal of Computational and Applied Mathematics*, vol. 328, pp. 414–431, 2018.

Hindawi
Mathematical Problems in Engineering
Volume 2020, Article ID 7130243, 5 pages
https://doi.org/10.1155/2020/7130243

Research Article

Estimates for the Finite-Time Ruin Probability of a Time-Dependent Risk Model with a Brownian Perturbation

Kaiyong Wang, Yongfang Cui, and Yanzhu Mao

School of Mathematics and Physics, Suzhou University of Science and Technology, Suzhou 215009, China

Correspondence should be addressed to Kaiyong Wang; beewky@vip.163.com

Received 10 January 2020; Accepted 30 January 2020; Published 18 February 2020

Guest Editor: Wenguang Yu

In this paper, we consider a time-dependent risk model with a Brownian perturbation. In this model, there is a dependence structure between the claim sizes and their corresponding interarrival times. Assuming the claim sizes have subexponential distributions, we obtain the asymptotic lower bound of the finite-time ruin probability. When the claim sizes have distributions from the class $L\cap D$, the asymptotic upper bound of the finite-time ruin probability has been presented. These results confirm that when the claim sizes are heavy-tailed, the asymptotics of the finite-time ruin probability of this time-dependent model are insensitive to the Brownian perturbation.

1. Introduction

This paper considers a dependent risk model with a constant force of interest and Brownian perturbation. In such a model, the claim sizes form a sequence of independent and identically distributed (i.i.d.) nonnegative random variables $X_n, n\geq 1$, with a distribution F and the interarrival times are also a sequence of i.i.d. nonnegative random variables $\theta_n, n\geq 1$, with a distribution G. In this paper, we consider there exists a dependence structure between the claim sizes $X_n, n\geq 1$, and their corresponding interarrival times $\theta_n, n\geq 1$. The claim arrival times are denoted by $\tau_n=\sum_{i=1}^{n}\theta_i, n\geq 1$. The renewal counting process

$$N(t)=\sup\{n\geq 1\colon\ \tau_n\leq t\},\quad t\geq 0,\tag{1}$$

is the number of claims by time t. Suppose that $N(t), t\geq 0$, has a finite mean:

$$\lambda(t)=\mathrm{EN}(t)=\sum_{n=1}^{\infty}P(\tau_n\leq t),\quad t\geq 0.\tag{2}$$

Then, the amount of aggregate claim sizes is $S(t)=\sum_{n=1}^{N(t)}X_n, t\geq 0$, where by convention, $\sum_{n=1}^{0}=0$. Suppose that, in this risk model, there is a constant force of interest $r\geq 0$. The discounted aggregate claim size by time t is

$$D(t)=\int_{0^-}^{t}e^{-\mathrm{ru}}S(\mathrm{du})=\sum_{n=1}^{\infty}X_n e^{-r\tau_n}1_{\{\tau_n\leq t\}},\quad t\geq 0,\tag{3}$$

where 1_A is the indicator function of an event A. Then, the insurer's surplus process of an insurance company by time t is

$$U(t)=e^{\mathrm{rt}}x+\int_0^t e^{r(t-s)}C(\mathrm{d}s)-e^{\mathrm{rt}}D(t)+\delta\int_0^t e^{r(t-s)}B(\mathrm{d}s),\quad t\geq 0,\tag{4}$$

where $x\geq 0$ is the initial surplus; $C(t)$ is the premium income up to time t, $t\geq 0$, which is a nondecreasing and nonnegative stochastic process satisfying $C(0)=0$ and $C(t)<\infty, 0<t<\infty$, almost surely; $B(t), t\geq 0$, is a diffusion perturbation which is a standard Brownian motion, and $\delta\geq 0$ is a volatility factor. Throughout the paper, we suppose that $\{C(t), t\geq 0\}$, $\{(X_n,\theta_n), n\geq 1\}$, and $\{B(t), t\geq 0\}$ are mutually independent. For every $0<t<\infty$, let $\widetilde{C}(t)=\int_0^t e^{-\mathrm{rs}}C(\mathrm{d}s)$. The finite-time ruin probability up to time t is defined as

$$\psi(x,t)=P\left(\inf_{0<s\leq t}U(s)<0\,\middle|\,U(0)=x\right),\quad t\geq 0.\tag{5}$$

This paper considers the asymptotics for $\psi(x,t)$ as x tends to ∞ under the heavy-tailed claim sizes.

When the claim sizes $X_n, n \geq 1$, and the interarrival time $\theta_n, n \geq 1$, are independent, there are many literatures to investigate ruin probabilities for claim sizes with independent/dependent structure (see, e.g., Asmussen [1], Chen and Ng [2], Hao and Tang [3], Kalashnikov and Konstantinides [4], Klüppelberg and Stadtmüller [5], Konstantinides et al. [6], Wang et al. [7], Dong et al. [8], Fu et al. [9], Li [10], Peng et al. [11], Peng and Wang [12, 13], Yang et al. [14], Yu et al. [15], and Zhang et al. [16]). However, in the last few years, many researchers have proposed some dependent risk models with various dependence structures modeling the dependence between the claim sizes and their corresponding interarrival times (see, e.g., Albrecher and Teugels [17], Boudreault et al. [18], Cossette et al. [19], Badescu et al. [20], and Asmussen et al. [21]).

In this paper, we use the dependence structure proposed by Asimit and Badescu [22]. Assume that $(X_n, \theta_n), n \geq 1$, are i.i.d. copies of a generic pair (X, θ) with dependent components X and θ satisfying

$$P(X > x \mid \theta = t) \sim \overline{F}(x)h(t), \tag{6}$$

holds uniformly for $t \geq 0$, where $h(\cdot)$: $[0,\infty)$ is a measurable function and the symbol $\sim$ means that the quotient of both sides tends to 1 as $x \longrightarrow \infty$. Asimit and Badescu [22] and Li et al. [23] have shown that (6) can be satisfied by many copulas, such as Ali-Mikhail-Haq copula, Farlie–Gumbel–Morgenstern copula, and Frank copula.

Using the uniformity of (6), we know that $\mathrm{Eh}(\theta) = 1$. Thus, we can define a random variable θ_1^*, which is independent of $\{X_n, n \geq 1\}$, $\{\theta_n, n \geq 1\}$, $\{C(t), t \geq 0\}$, and $\{B(t), t \geq 0\}$ and has the following distribution:

$$G^*(\mathrm{d}t) = h(t)G(\mathrm{d}t), \quad t \geq 0. \tag{7}$$

Define $\tau_1^* = \theta_1^*$ and $\tau_n^* = \theta_1^* + \sum_{i=2}^{n} \theta_i, n \geq 2$, which constitute a delayed renewal counting process

$$N^*(t) = \sup\{n \geq 1 : \tau_n^* \leq t\}, \quad t \geq 0, \tag{8}$$

with a mean function

$$\widetilde{\lambda}(t) = \mathrm{EN}^*(t) = \int_{0^-}^{t} (1 + \lambda(t-u))h(u)G(\mathrm{d}u), \quad t \geq 0. \tag{9}$$

For the risk model (4), when the claim sizes $X_n, n \geq 1$, and the interarrival times $\theta_n, n \geq 1$, are independent and the premium income process $C(t), t \geq 0$, is a linear process, Li [10] provided the asymptotics of the finite-time ruin probability for subexponential claim sizes. Wang et al. [24] considered a risk model with stochastic return. This paper considers there exists a dependence structure (6) between the claim sizes $X_n, n \geq 1$, and their corresponding interarrival times $\theta_n, n \geq 1$, and provides the estimates of the finite-time ruin probability of this model with heavy-tailed claim sizes.

In this paper, unless stated otherwise, all limits are for $x \longrightarrow \infty$. For two positive functions $u(\cdot)$ and $v(\cdot)$, if $\limsup u(x)/v(x) \leq 1$, then we write $u(x) \lesssim v(x)$; if $\liminf u(x)/v(x) \geq 1$, then we write $u(x) \gtrsim v(x)$; if $\lim u(x)/v(x) = 0$, then we write $u(x) = o(v(x))$; if $\limsup u(x)/v(x) < \infty$, then we write $u(x) = O(v(x))$. For a distribution V on $(-\infty,\infty)$, let $\overline{V}(x) = 1 - V(x)$, $x \in (-\infty,\infty)$, be its (right) tail.

For a distribution V on $[0,\infty)$, if $\int_0^\infty e^{\lambda y} V(\mathrm{d}y) = \infty$ for any $\lambda > 0$, then we say that V is heavy-tailed; otherwise, we say that V is light-tailed. In the following, we introduce some subclasses of heavy-tailed distribution class. Say that a distribution V on $[0,\infty)$ belongs to the subexponential distribution class S, if

$$\overline{V^{*n}}(x) \sim n\overline{V}(x), \tag{10}$$

holds for some (or equivalently for all) $n \geq 2$, where V^{*n} is the n-fold convolution of V. Lemma 1.3.5(b) of Embrechts et al. [25] shows that if $V \in \mathscr{S}$, then for any $\varepsilon > 0$,

$$e^{-\varepsilon x} = o(\overline{V}(x)). \tag{11}$$

Say that a distribution V on $[0,\infty)$ belongs to the long-tailed distribution class L, if for any $y > 0$,

$$\overline{V}(x+y) \sim \overline{V}(x). \tag{12}$$

By the uniform convergence theorem for slowly varying functions (Theorem A3.2 of Embrechts et al. [25]), this convergence also holds uniformly for every compact set of y. Say that a distribution V on $[0,\infty)$ belongs to the dominated varying distribution class D, if for any $0 < y < 1$,

$$\overline{V}(xy) = O(\overline{V}(x)). \tag{13}$$

The above distribution classes have the following proper relation:

$$L \cap D \subset S \subset L, \tag{14}$$

(see, e.g., Embrechts et al. [25] and Klüppelberg and Stadtmüller [5]). The following is the main result of this paper.

Theorem 1. *Consider the risk model (4). Assume that (X_n, θ_n), $n \geq 1$, are i.i.d. and satisfy (6).*

(1) If $F \in \mathscr{S}$, then for each $t > 0$,

$$\psi(x,t) \gtrsim \int_{0^-}^{t} \overline{F}(x e^{rs}) \widetilde{\lambda}(\mathrm{d}s). \tag{15}$$

(2) If $F \in \mathscr{L} \cap \mathscr{D}$, then for each $t > 0$,

$$\psi(x,t) \lesssim \int_{0^-}^{t} \overline{F}(x e^{rs}) \widetilde{\lambda}(\mathrm{d}s). \tag{16}$$

Because $L \cap D \subset S$, from Theorem 1, we can obtain the following corollary.

Corollary 1. *Consider the risk model (4). Assume that (X_n, θ_n), $n \geq 1$, are i.i.d. and satisfy (6). If $F \in \mathscr{L} \cap \mathscr{D}$, then for each $t > 0$,*

$$\psi(x,t) \sim \int_{0^-}^{t} \overline{F}(x e^{rs}) \widetilde{\lambda}(\mathrm{d}s). \tag{17}$$

Remark 1. When the claim sizes $X_n, n \geq 1$, and the interarrival times $\theta_n, n \geq 1$, are independent, Li [10] considered the risk model (4) for a linear premium income process $C(t), t \geq 0$, and subexponential claim sizes. He obtained

$$\psi(x,t) \sim \int_{0^-}^{t} \overline{F}(\mathrm{xe}^{\mathrm{rs}})\lambda(\mathrm{d}s), \tag{18}$$

holds uniformly for t in a finite-time interval. This result indicates that when the claim sizes are heavy-tailed, the asymptotics of the finite-time ruin probability is insensitive to a Brownian perturbation. Theorem 1 confirms that when there exists the dependence structure (6) between the claim sizes $X_n, n \geq 1$, and their corresponding interarrival times $\theta_n, n \geq 1$, the asymptotics of the finite-time ruin probability is also insensitive to a Brownian perturbation for heavy-tailed claim sizes.

2. Proof of the Main Result

Lemma 1. *Consider the risk model (4). Assume that* (X_n, θ_n), $n \geq 1$, *are i.i.d. and satisfy (6).*

(1) If $F \in S$, then for each $t > 0$,

$$P(D(t) > x) \sim \int_{0^-}^{t} \overline{F}(\mathrm{xe}^{\mathrm{rs}})\widetilde{\lambda}(\mathrm{d}s). \tag{19}$$

(2) If $F \in L \cap D$, then for each $t > 0$, the distribution of $D(t)$ belongs to the class $L \cap D$.

Proof. The result (1) is from Theorem 2.1 of Li et al. [23]. Now, we prove (2). Because $L \cap D \subset S$, for each $t > 0$, relation (19) holds.

For every $y > 0$ and any $0 \leq s \leq t$, $y \leq \mathrm{ye}^{\mathrm{rs}} \leq \mathrm{ye}^{\mathrm{rt}}$. Because $F \in L$, by the local uniformity of the class $\mathscr{L}$, it holds uniformly for $0 \leq s \leq t$ that

$$\overline{F}(x + \mathrm{ye}^{\mathrm{rs}}) \sim \overline{F}(x). \tag{20}$$

This means that, for any $\varepsilon > 0$, there exists $x_0 = x_0(\varepsilon, y, t) > 0$ such that for any $x > x_0$ and $0 \leq s \leq t$,

$$(1-\varepsilon)\overline{F}(x) \leq \overline{F}(x + \mathrm{ye}^{\mathrm{rs}}) \leq (1+\varepsilon)\overline{F}(x). \tag{21}$$

Hence, for any $x > x_0$ and $0 \leq s \leq t$,

$$(1-\varepsilon)\overline{F}(\mathrm{xe}^{\mathrm{rs}}) \leq \overline{F}((x+y)e^{\mathrm{rs}}) \leq (1+\varepsilon)\overline{F}(\mathrm{xe}^{\mathrm{rs}}). \tag{22}$$

By (22), it holds that

$$\begin{aligned}(1-\varepsilon)\int_{0^-}^{t} \overline{F}(\mathrm{xe}^{\mathrm{rs}})\widetilde{\lambda}(\mathrm{d}s) &\leq \int_{0^-}^{t} \overline{F}((x+y)e^{\mathrm{rs}})\widetilde{\lambda}(\mathrm{d}s) \\ &\leq (1+\varepsilon)\int_{0^-}^{t} \overline{F}(\mathrm{xe}^{\mathrm{rs}})\widetilde{\lambda}(\mathrm{d}s),\end{aligned} \tag{23}$$

that is,

$$\int_{0^-}^{t} \overline{F}((x+y)e^{\mathrm{rs}})\widetilde{\lambda}(\mathrm{d}s) \sim \int_{0^-}^{t} \overline{F}(\mathrm{xe}^{\mathrm{rs}})\widetilde{\lambda}(\mathrm{d}s). \tag{24}$$

By (19) and (24), we know that the distribution of $D(t)$ belongs to the class L. Next, we will prove the distribution of $D(t)$ belongs to the class D. Because $F \in D$, for every $0 < y < 1$, there exist constants $M > 0$ and $x_1 = x_1(y) > 0$ such that for any $x > x_1$ and $0 \leq s \leq t$,

$$\overline{F}(\mathrm{xye}^{\mathrm{rs}}) \leq M\overline{F}(\mathrm{xe}^{\mathrm{rs}}). \tag{25}$$

Here, for any $x > x_1$,

$$\int_{0^-}^{t} \overline{F}(\mathrm{xye}^{\mathrm{rs}})\widetilde{\lambda}(\mathrm{d}s) \leq M\int_{0^-}^{t} \overline{F}(\mathrm{xe}^{\mathrm{rs}})\widetilde{\lambda}(\mathrm{d}s). \tag{26}$$

By (19) and (26), for every $0 < y < 1$, it holds that

$$\limsup_{x \longrightarrow \infty} \frac{P(D(t) > xy)}{P(D(t) > x)} \leq M, \tag{27}$$

that is, the distribution of $D(t)$ belongs to the class D.

The next lemma is Lemma 4.2 of Li et al. [23]. □

Lemma 2. *Consider the risk model (4). Assume that (X_n, θ_n), $n \geq 1$, are i.i.d. and satisfy (6). If $F \in S$, then for every $n \geq 1$, it holds for each $t > 0$ that*

$$P\left(\sum_{i=1}^{n} X_i e^{-r\tau_i} > x, N(t) = n\right) \sim \sum_{i=1}^{n} P\left(X_i e^{-r\tau_i} > x, N(t) = n\right). \tag{28}$$

The following lemma slightly extends the above lemma.

Lemma 3. *Consider the risk model (4). Assume that (X_n, θ_n), $n \geq 1$, are i.i.d. and satisfy (6). Suppose that ξ is a nonnegative random variable and independent of other random variables. If $F \in S$, then for every $n \geq 1$ and each $t > 0$, it holds that*

$$P\left(\sum_{i=1}^{n} X_i e^{-r\tau_i} > x + \xi, N(t) = n\right) \sim \sum_{i=1}^{n} P\left(X_i e^{-r\tau_i} > x, N(t) = n\right). \tag{29}$$

Proof. Because ξ is nonnegative, by Lemma 2, for every $n \geq 1$ and each $t > 0$,

$$\begin{aligned}P\left(\sum_{i=1}^{n} X_i e^{-r\tau_i} > x + \xi, N(t) = n\right) &\leq P\left(\sum_{i=1}^{n} X_i e^{-r\tau_i} > x, N(t) = n\right) \\ &\sim \sum_{i=1}^{n} P\left(X_i e^{-r\tau_i} > x, N(t) = n\right).\end{aligned} \tag{30}$$

Next, we prove that, for every $n \geq 1$ and each $t > 0$,

$$P\left(\sum_{i=1}^{n} X_i e^{-r\tau_i} > x + \xi, N(t) = n\right) \gtrsim \sum_{i=1}^{n} P\left(X_i e^{-r\tau_i} > x, N(t) = n\right). \tag{31}$$

Because ξ is nonnegative and independent of other random variables, by Lemma 2, for every $n \geq 1$ and each $t > 0$,

$$\begin{aligned}&P\left(\sum_{i=1}^{n} X_i e^{-r\tau_i} > x + \xi, N(t) = n\right) \\ &\quad \sim \sum_{i=1}^{n} P\left(X_i e^{-r\tau_i} > x + \xi, N(t) = n\right).\end{aligned} \tag{32}$$

Because $F \in S \subset L$, by the dominated convergence theorem, for each $t > 0$, it holds uniformly for $1 \le i \le n$ that

$$\lim_{x\longrightarrow\infty} \frac{P(X_i > x + e^{rt}\xi)}{P(X_i > x)} = \int_{0^-}^{\infty} \lim_{x\longrightarrow\infty} \frac{\overline{F}(x + ye^{rt})}{\overline{F}(x)} P(\xi \in dy) = 1. \tag{33}$$

Hence, for any $\varepsilon > 0$, there exists a constant $x_3 = x_3(\varepsilon, t, n) > 0$ such that for any $x > x_3$ and $1 \le i \le n$,

$$P\left(X_i > x + e^{rt}\xi\right) \ge (1-\varepsilon) P(X_i > x). \tag{34}$$

For every $t > 0$ and $n \ge 1$, set $\Omega_n(t) = \{(s_1, \dots, s_n) \in [0,t]^n : t_n = \sum_{i=1}^n s_i \le t\}$. By (6), (32), and (34), for every $n \ge 1$, each $t > 0$, and $x > x_3$, it holds that

$$\begin{aligned}
&P\left(\sum_{i=1}^{n} X_i e^{-r\tau_i} > x + \xi, N(t) = n\right) \\
&\quad\sim \sum_{i=1}^{n} P\left(X_i e^{-r\tau_i} > x + \xi, N(t) = n\right) \\
&\quad= \sum_{i=1}^{n} P\left(X_i e^{-r\tau_i} > x + \xi, \tau_n \le t, \tau_{n+1} > t\right) \\
&= \sum_{i=1}^{n} \int \underset{\Omega_n(t)}{\cdots} \int P\left(X_i e^{-rt_i} > x + \xi \mid \theta_i = s_i\right) \overline{G}(t - t_n) \prod_{i=1}^{n} G(ds_i) \\
&\quad\sim \sum_{i=1}^{n} \int \underset{\Omega_n(t)}{\cdots} \int P\left(X_i e^{-rt_i} > x + \xi\right) h(s_i) \overline{G}(t - t_n) \prod_{i=1}^{n} G(ds_i) \\
&\quad\ge \sum_{i=1}^{n} \int \underset{\Omega_n(t)}{\cdots} \int P\left(X_i > xe^{rt_i} + e^{rt}\xi\right) h(s_i) \overline{G}(t - t_n) \prod_{i=1}^{n} G(ds_i) \\
&\quad\ge (1-\varepsilon) \sum_{i=1}^{n} \int \underset{\Omega_n(t)}{\cdots} \int P\left(X_i > xe^{rt_i}\right) h(s_i) \overline{G}(t - t_n) \prod_{i=1}^{n} G(ds_i) \\
&\quad\sim (1-\varepsilon) \sum_{i=1}^{n} P\left(X_i e^{-r\tau_i} > x, N(t) = n\right),
\end{aligned} \tag{35}$$

that is, (31) holds.

The following lemma is derived from Proposition 1(a) of Embrechts et al. [26]. □

Lemma 4. *Let $V_i, i = 1, 2$ be two distributions on $[0, \infty)$. If $V_1 \in \mathcal{S}$ and $\overline{V_2}(x) = o(\overline{V_1}(x))$, then*

$$\overline{V_1 * V_2}(x) \sim \overline{V_1}(x). \tag{36}$$

For the above risk model, write

$$p(t) = \delta \int_0^t e^{-rs} B(ds), \quad t \ge 0. \tag{37}$$

Let

$$\begin{aligned}
p_*(t) &= \inf_{0\le s\le t} p(s) \le 0, \quad t \ge 0, \\
p^*(t) &= \sup_{0\le s\le t} p(s) \ge 0, \quad t \ge 0.
\end{aligned} \tag{38}$$

The following lemma can be obtained from Theorem D.3 (ii) of Piterbarg [27].

Lemma 5. *For each $t > 0$,*

$$P\left(p_*(t) < -x\right) = P\left(p^*(t) > x\right) \sim 2\overline{\Phi}\left(\frac{\sqrt{2r}}{\delta\sqrt{1 - e^{-2rt}}} x\right), \tag{39}$$

where $\overline{\Phi}(x) \sim 1/\sqrt{2\pi} x e^{-x^2/2}$ is the tail of a standard normal distribution, and when $r = 0$, $\sqrt{2r}/\sqrt{1 - e^{-2rt}}$ is $1/\sqrt{t}$ (i.e., a limit as $r \longrightarrow 0$).

Proof of Theorem 1. By Lemma 3, for each $t > 0$ and any integer $m > 0$, it holds that

$$\begin{aligned}
\psi(x,t) &\ge P\left(\sum_{i=1}^{N(t)} X_i e^{-r\tau_i} - \widetilde{C}(t) - p^*(t) > x\right) \\
&\ge \sum_{n=1}^{m} P\left(\sum_{i=1}^{n} X_i e^{-r\tau_i} > x + \widetilde{C}(t) + p^*(t), N(t) = n\right) \\
&\sim \sum_{n=1}^{m} \sum_{i=1}^{n} P\left(X_i e^{-r\tau_i} > x, N(t) = n\right) \\
&= \left(\sum_{n=1}^{\infty} - \sum_{n=m+1}^{\infty}\right) \sum_{i=1}^{n} P\left(X_i e^{-r\tau_i} > x, N(t) = n\right) \\
&=: I_1 - I_2.
\end{aligned} \tag{40}$$

By (4.19) and (4.20) of Li et al. [23], we obtain for each $t > 0$,

$$\lim_{x\longrightarrow\infty} \frac{I_1}{\int_{0^-}^{t} \overline{F}(xe^{rs}) \widetilde{\lambda}(ds)} = 1, \tag{41}$$

$$\lim_{m\longrightarrow\infty} \lim_{x\longrightarrow\infty} \frac{I_2}{\int_{0^-}^{t} \overline{F}(xe^{rs}) \widetilde{\lambda}(ds)} = 0. \tag{42}$$

By (40)–(42), we obtain for each $t > 0$,

$$\psi(x,t) \gtrsim \int_{0^-}^{t} \overline{F}(xe^{rs}) \widetilde{\lambda}(ds). \tag{43}$$

For each $t > 0$ and $x > 0$, Lemma 5 implies

$$\begin{aligned}
\psi(x,t) &\le P\left(\sum_{i=1}^{N(t)} X_i e^{-r\tau_i} - p_*(t) > x\right) \\
&= P\left(\sum_{i=1}^{N(t)} X_i e^{-r\tau_i} + p^*(t) > x\right) \\
&= P\left(D(t) + p^*(t) > x\right).
\end{aligned} \tag{44}$$

By Lemma 1 (2), we know that the distribution of $D(t)$ belongs to the class $L \cap D$. Hence, by Lemmas 3 and 4, it holds that

$$P\left(p^*(t) > x\right) = o(P(D(t) > x)). \tag{45}$$

Hence, by (44), Lemmas 2 (1) and 4, we obtain

$$\begin{aligned}
\psi(x,t) &\lesssim P(D(t) > x) \\
&\sim \int_{0^-}^{t} \overline{F}(xe^{rs}) \widetilde{\lambda}(ds).
\end{aligned} \tag{46}$$

□

Data Availability

No data were used to support this study.

Conflicts of Interest

The authors declare that there are no conflicts of interest regarding the publication of this paper.

Acknowledgments

This work was supported by the National Natural Science Foundation of China (no. 11401418), the 333 Talent Training Project of Jiangsu Province, and the Jiangsu Province Key Discipline in the 13th Five-Year Plan.

References

[1] S. Asmussen, "Subexponential asymptotics for stochastic processes: extremal behavior, stationary distributions and first passage probabilities," *The Annals of Applied Probability*, vol. 8, no. 2, pp. 354–374, 1998.

[2] Y. Chen and K. W. Ng, "The ruin probability of the renewal model with constant interest force and negatively dependent heavy-tailed claims," *Insurance: Mathematics and Economics*, vol. 40, no. 3, pp. 415–423, 2007.

[3] X. Hao and Q. Tang, "A uniform asymptotic estimate for discounted aggregate claims with subexponential tails," *Insurance: Mathematics and Economics*, vol. 43, no. 1, pp. 116–120, 2008.

[4] V. Kalashnikov and D. Konstantinides, "Ruin under interest force and subexponential claims: a simple treatment," *Insurance: Mathematics and Economics*, vol. 27, no. 1, pp. 145–149, 2000.

[5] C. Klüppelberg and U. Stadtmüller, "Ruin probabilities in the presence of heavy-tails and interest rates," *Scandinavian Actuarial Journal*, vol. 1998, no. 1, pp. 49–58, 1998.

[6] D. Konstantinides, Q. Tang, and G. Tsitsiashvili, "Estimates for the ruin probability in the classical risk model with constant interest force in the presence of heavy tails," *Insurance: Mathematics and Economics*, vol. 31, no. 3, pp. 447–460, 2002.

[7] K. Wang, Y. Wang, and Q. Gao, "Uniform asymptotics for the finite-time ruin probability of a dependent risk model with a constant interest rate," *Methodology and Computing in Applied Probability*, vol. 15, no. 1, pp. 109–124, 2013.

[8] Y. Dong, K. C. Yues, and G. Wang, "Pricing credit derivatives under a correlated regime-switching hazard processes model," *Journal of Industrial & Management Optimization*, vol. 13, no. 3, pp. 1395–1415, 2017.

[9] Q. Fu, P.-P. Gu, and J.-R. Wu, "Decentralized iterative learning control for large-scale interconnected linear systems with fixed initial shifts," *International Journal of Control, Automation and Systems*, vol. 15, no. 5, pp. 1991–2000, 2017.

[10] J. Li, "A note on the finite-time ruin probability of a renewal risk model with Brownian perturbation," *Statistics & Probability Letters*, vol. 127, pp. 49–55, 2017.

[11] X. Peng, W. Su, and Z. Zhang, "On a perturbed compound poisson risk model under a periodic threshold-type dividend strategy," *Journal of Industrial & Management Optimization*, vol. 13, no. 5, pp. 1–20, 2017.

[12] J. Peng and D. Wang, "Asymptotics for ruin probabilities of a non-standard renewal risk model with dependence structures and exponential Lévy process investment returns," *Journal of Industrial & Management Optimization*, vol. 13, no. 1, pp. 155–185, 2017.

[13] J. Peng and D. Wang, "Uniform asymptotics for ruin probabilities in a dependent renewal risk model with stochastic return on investments," *Stochastics: An International Journal of Probability and Stochastic Processes*, vol. 90, no. 3, pp. 432–471, 2018.

[14] Y. Yang, K. Wang, J. Liu et al., "Asymptotics for a bidimensional risk model with two geometric Lévy price processes," *Journal of Industrial & Management Optimization*, vol. 15, no. 2, pp. 481–505, 2019.

[15] W. Yu, Y. Yong, G. Guan, Y. Huang, W. Su, and C. Cui, "Valuing guaranteed minimum death benefits by cosine series expansion," *Mathematics*, vol. 7, no. 9, p. 835, 2019.

[16] Z. Zhang, Y. Yong, and W. Yu, "Valuing equity-linked death benefits in general exponential Lévy models," *Journal of Computational and Applied Mathematics*, vol. 365, Article ID 112377, 2020.

[17] H. Albrecher and J. L. Teugels, "Exponential behavior in the presence of dependence in risk theory," *Journal of Applied Probability*, vol. 43, no. 1, pp. 257–273, 2006.

[18] M. Boudreault, H. Cossette, D. Landriault, and E. Marceau, "On a risk model with dependence between interclaim arrivals and claim sizes," *Scandinavian Actuarial Journal*, vol. 2006, no. 5, pp. 265–285, 2006.

[19] H. Cossette, E. Marceau, and F. Marri, "On the compound poisson risk model with dependence based on a generalized Farlie-Gumbel-Morgenstern copula," *Insurance: Mathematics and Economics*, vol. 43, no. 3, pp. 444–455, 2008.

[20] A. L. Badescu, E. C. K. Cheung, and D. Landriault, "Dependent risk models with bivariate phase-type distributions," *Journal of Applied Probability*, vol. 46, no. 1, pp. 113–131, 2009.

[21] S. Asmussen, H. Schmidli, and V. Schmidt, "Tail probabilities for non-standard risk and queueing processes with subexponential jumps," *Advances in Applied Probability*, vol. 31, no. 2, pp. 422–447, 1999.

[22] A. V. Asimit and A. L. Badescu, "Extremes on the discounted aggregate claims in a time dependent risk model," *Scandinavian Actuarial Journal*, vol. 2010, no. 2, pp. 93–104, 2010.

[23] J. Li, Q. Tang, and R. Wu, "Subexponential tails of discounted aggregate claims in a time-dependent renewal risk model," *Advances in Applied Probability*, vol. 42, no. 04, pp. 1126–1146, 2010.

[24] K. Wang, L. Chen, Y. Yang, and M. Gao, "The finite-time ruin probability of a risk model with stochastic return and brownian perturbation," *Japan Journal of Industrial and Applied Mathematics*, vol. 35, no. 3, pp. 1173–1189, 2018.

[25] P. Embrechts, C. Klüppelberg, and T. Mikosch, *Modelling Extremal Events for Insurance and Finance*, Springer, Berlin, Germany, 1997.

[26] P. Embrechts, C. M. Goldie, and N. l. Veraverbeke, "Subexponentiality and infinite divisibility," *Zeitschrift für Wahrscheinlichkeitstheorie und Verwandte Gebiete*, vol. 49, no. 3, pp. 335–347, 1979.

[27] V. I. Piterbarg, *Asymptotic Methods in the Theory of Gaussian Processes and Fields*, American Mathematical Society, Providence, RI, USA, 1996.